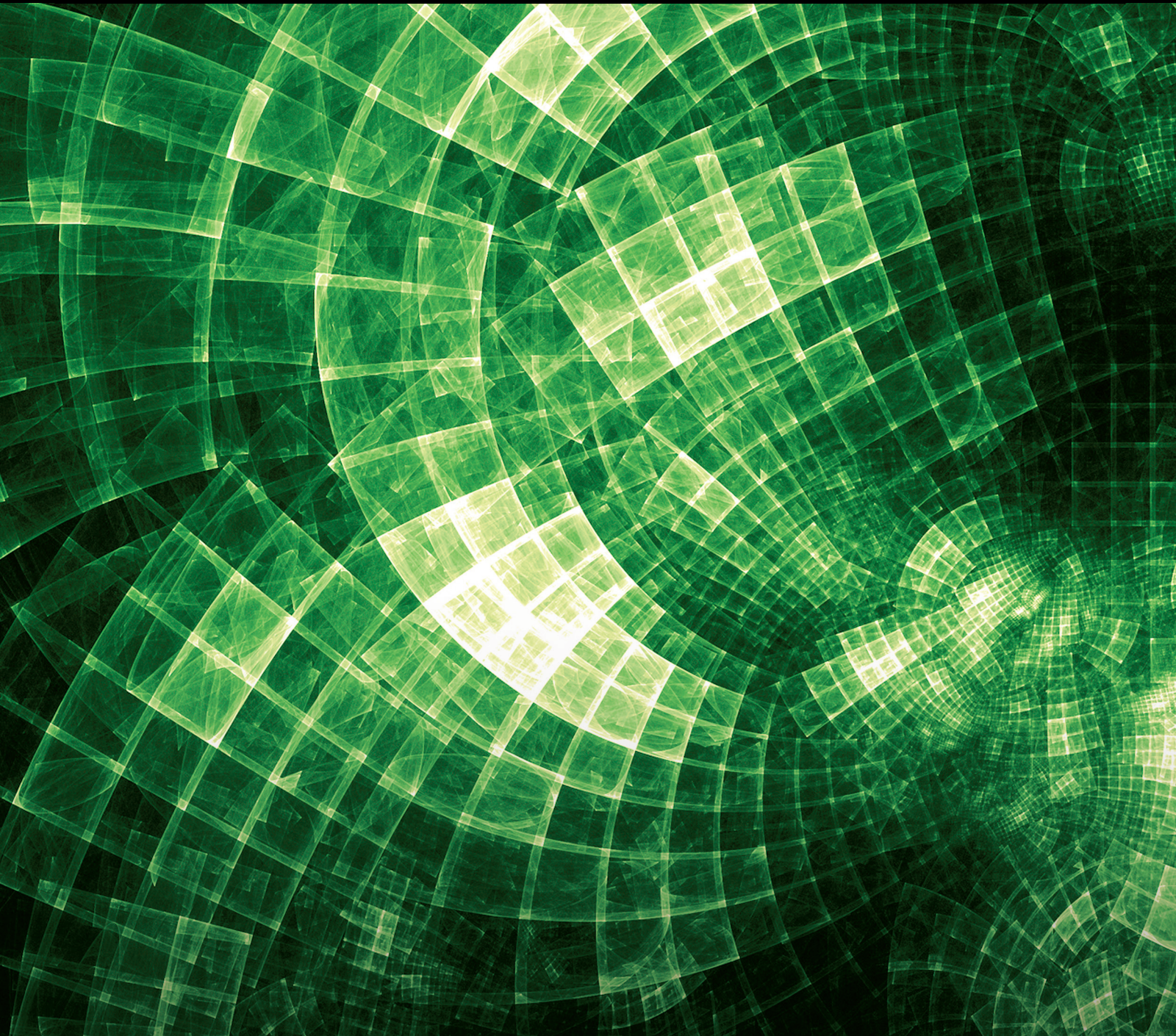


Advances in Graph Labeling

Lead Guest Editor: Ali Ahmad

Guest Editors: Tomas Vetrik, Syafrizal Sy, Rajarathinam Vadivel,
Muhammad Kamran Siddiqui, and Muhammad Imran





Advances in Graph Labeling

Journal of Mathematics

Advances in Graph Labeling

Lead Guest Editor: Ali Ahmad

Guest Editors: Tomas Vetrik, Syafrizal Sy,
Rajarathinam Vadivel, Muhammad Kamran
Siddiqui, and Muhammad Imran



Copyright © 2022 Hindawi Limited. All rights reserved.

This is a special issue published in "Journal of Mathematics." All articles are open access articles distributed under the Creative Commons Attribution License, which permits unrestricted use, distribution, and reproduction in any medium, provided the original work is properly cited.

Chief Editor

Jen-Chih Yao, Taiwan

Algebra

SEÇİL ÇEKEN , Turkey
Faranak Farshadifar , Iran
Marco Fontana , Italy
Genni Fragnelli , Italy
Xian-Ming Gu, China
Elena Guardo , Italy
Li Guo, USA
Shaofang Hong, China
Naihuan Jing , USA
Xiaogang Liu, China
Xuanlong Ma , China
Francisco Javier García Pacheco, Spain
Francesca Tartarone , Italy
Fernando Torres , Brazil
Zafar Ullah , Pakistan
Jiang Zeng , France

Geometry

Tareq Al-shami , Yemen
R.U. Gobithaasan , Malaysia
Erhan Güler , Turkey
Ljubisa Kocinac , Serbia
De-xing Kong , China
Antonio Masiello, Italy
Alfred Peris , Spain
Santi Spadaro, Italy

Logic and Set Theory

Ghous Ali , Pakistan
Kinkar Chandra Das, Republic of Korea
Jun Fan , Hong Kong
Carmelo Antonio Finocchiaro, Italy
Radomír Halaš, Czech Republic
Ali Jaballah , United Arab Emirates
Baoding Liu, China
G. Muhiuddin , Saudi Arabia
Basil K. Papadopoulos , Greece
Musavarah Sarwar, Pakistan
Anton Setzer , United Kingdom
R Sundareswaran, India
Xiangfeng Yang , China

Mathematical Analysis

Ammar Alsinai , India
M.M. Bhatti, China
Der-Chen Chang, USA
Phang Chang , Malaysia
Mengxin Chen, China
Genni Fragnelli , Italy
Willi Freeden, Germany
Yongqiang Fu , China
Ji Gao , USA
A. Ghareeb , Egypt
Victor Ginting, USA
Azhar Hussain, Pakistan
Azhar Hussain , Pakistan
Ömer Kişi , Turkey
Yi Li , USA
Stefan J. Linz , Germany
Ming-Sheng Liu , China
Dengfeng Lu, China
Xing Lü, China
Gaetano Luciano , Italy
Xiangyu Meng , USA
Dimitri Mugnai , Italy
A. M. Nagy , Kuwait
Valeri Obukhovskii, Russia
Humberto Rafeiro, United Arab Emirates
Luigi Rarità , Italy
Hegazy Rezk, Saudi Arabia
Nasser Saad , Canada
Mohammad W. Alomari, Jordan
Guotao Wang , China
Qiang Wu, USA
Çetin YILDIZ , Turkey
Wendong Yang , China
Jun Ye , China
Agacik Zafer, Kuwait

Operations Research

Ada Che , China
Nagarajan Deivanayagam Pillai, India
Sheng Du , China
Nan-Jing Huang , China
Chiranjibe Jana , India
Li Jin, United Kingdom
Mehmet Emir Koksal, Turkey
Palanivel M , India




Stanislaw Migorski , Poland
Predrag S. Stanimirović , Serbia
Balendu Bhooshan Upadhyay, India
Ching-Feng Wen , Taiwan
K.F.C. Yiu , Hong Kong
Liwei Zhang, China
Qing Kai Zhao, China

Probability and Statistics

Mario Abundo, Italy
Antonio Di Crescenzo , Italy
Jun Fan , Hong Kong
Jiancheng Jiang , USA
Markos Koutras , Greece
Fawang Liu , Australia
Barbara Martinucci , Italy
Yonghui Sun, China
Niansheng Tang , China
Efthymios G. Tsionas, United Kingdom
Bruce A. Watson , South Africa
Ding-Xuan Zhou , Hong Kong



Contents

On the Edge Resolvability of Double Generalized Petersen Graphs

Tanveer Iqbal , Muhammad Rafiq, Muhammad Naeem Azhar, Muhammad Salman , and Imran Khalid 



Research Article (14 pages), Article ID 6490698, Volume 2022 (2022)

Comparative Study of Generalized Sum Graphs via Degree-Based Topological Indices

Muhammad Javaid , Saira Javed, and Ebenezer Bonyah 




Research Article (15 pages), Article ID 9001167, Volume 2022 (2022)

On the Graphs of Minimum Degree At Least 3 Having Minimum Sum-Connectivity Index

Wael W. Mohammed, Shahzad Ahmed, Zahid Raza, Jia-Bao Liu , Farooq Ahmad, and Elsayed M. Elsayed 

Research Article (11 pages), Article ID 1203303, Volume 2022 (2022)

On Edge H -Irregularity Strength of Hexagonal and Octagonal Grid Graphs

Muhammad Ibrahim , Ana Gulzar, Muhammad Fazil , and Muhammad Naeem Azhar 

Research Article (10 pages), Article ID 6047926, Volume 2022 (2022)

Some Resolving Parameters in a Class of Cayley Graphs

Jia-Bao Liu  and Ali Zafari 


Research Article (5 pages), Article ID 9444579, Volume 2022 (2022)

Some Upper Bounds on the First General Zagreb Index

Muhammad Kamran Jamil , Aisha Javed, Ebenezer Bonyah , and Iqra Zaman



Research Article (4 pages), Article ID 8131346, Volume 2022 (2022)

A Novel Mathematical Model for Radio Mean Square Labeling Problem

Elsayed Badr , Shokry Nada, Mohammed M. Ali Al-Shamiri , Atef Abdel-Hay , and Ashraf ELrokh




Research Article (9 pages), Article ID 3303433, Volume 2022 (2022)

On the Sum of Degree-Based Topological Indices of Rhombus-Type Silicate and Oxide Structures

Rong Qi, Haidar Ali , Usman Babar, Jia-Bao Liu , and Parvez Ali



Research Article (16 pages), Article ID 1100024, Volume 2021 (2021)

Modular Irregular Labeling on Double-Star and Friendship Graphs

K. A. Sugeng , Z. Z. Barack, N. Hinding , and R. Simanjuntak 

Research Article (6 pages), Article ID 4746609, Volume 2021 (2021)

Research on Energy Efficiency Management of Forklift Based on Improved YOLOv5 Algorithm

Zhenyu Li, Ke Lu, Yanhui Zhang, Zongwei Li , and Jia-Bao Liu 



Research Article (9 pages), Article ID 5808221, Volume 2021 (2021)

Radio Labelings of Lexicographic Product of Some Graphs




Muhammad Shahbaz Aasi , Muhammad Asif , Tanveer Iqbal , and Muhammad Ibrahim 

Research Article (6 pages), Article ID 9177818, Volume 2021 (2021)


3-Total Edge Product Cordial Labeling for Stellation of Square Grid Graph

Rizwan Ullah, Gul Rahmat, Muhammad Numan, Kraidi Anoh Yannick , and Adnan Aslam 
Research Article (6 pages), Article ID 1724687, Volume 2021 (2021)



On the Exact Values of HZ-Index for the Graphs under Operations

Dalal Awadh Alrowaili , Saira Javed , and Muhammad Javaid 
Research Article (17 pages), Article ID 3304939, Volume 2021 (2021)






An Application of Sombor Index over a Special Class of Semigroup Graph

Seda Oğuz Ünal 
Research Article (6 pages), Article ID 3273117, Volume 2021 (2021)

Computing Gutman Connection Index of Thorn Graphs

Muhammad Javaid , Muhammad Khubab Siddique, and Ebenezer Bonyah 
Research Article (13 pages), Article ID 2289514, Volume 2021 (2021)




Edge Weight-Based Entropy of Magnesium Iodide Graph

Maryam Salem Alatawi , Ali Ahmad , Ali N. A. Koam , Sadia Husain , and Muhammad Azeem 
Research Article (7 pages), Article ID 4330498, Volume 2021 (2021)




Topological Indices of Pent-Heptagonal Nanosheets via M-Polynomials

Hafiza Bushra Mumtaz, Muhammad Javaid , Hafiz Muhammad Awais, and Ebenezer Bonyah 
Research Article (13 pages), Article ID 4863993, Volume 2021 (2021)

Bicyclic Graphs with the Second-Maximum and Third-Maximum Degree Resistance Distance

Wenjie Ning , Kun Wang , and Hassan Raza 
Research Article (11 pages), Article ID 8722383, Volume 2021 (2021)



On Some Properties of Multiplicative Topological Indices in Silicon-Carbon

Abid Mahboob , Sajid Mahboob, Mohammed M. M. Jaradat , Nigait Nigar, and Imran Siddique 
Research Article (10 pages), Article ID 4611199, Volume 2021 (2021)



On Computation of Edge Degree-Based Banhatti Indices of a Certain Molecular Network

Jiang-Hua Tang, Muhammad Abid, Kashif Ali, Asfand Fahad , Muhammad Anwar Chaudhry, Muhammad Imran Qureshi , and Jia-Bao Liu 
Research Article (7 pages), Article ID 5185270, Volume 2021 (2021)

New Results on the Forgotten Topological Index and Coindex



Akbar Jahanbani , Maryam Atapour , and Rana Khoeilar
Research Article (11 pages), Article ID 8700736, Volume 2021 (2021)

On the Number of Conjugate Classes of Derangements




Wen-Wei Li , Zhong-Lin Cheng, and Jia-Bao Liu 
Research Article (20 pages), Article ID 6023081, Volume 2021 (2021)

Contents




Characterization of the Congestion Lemma on Layout Computation

Jia-Bao Liu , Arul Jeya Shalini , Micheal Arockiaraj, and J. Nancy Delaila
Research Article (5 pages), Article ID 2984703, Volume 2021 (2021)



On the Connected Safe Number of Some Classes of Graphs

Rakib Iqbal, Muhammad Shoaib Sardar , Dalal Alrowaili , Sohail Zafar, and Imran Siddique 
Research Article (4 pages), Article ID 9483892, Volume 2021 (2021)


Computation of Edge Resolvability of Benzenoid Tripod Structure

Ali Ahmad , Sadia Husain, Muhammad Azeem , Kashif Elahi, and M. K. Siddiqui 
Research Article (8 pages), Article ID 9336540, Volume 2021 (2021)




Some Vertex/Edge-Degree-Based Topological Indices of r -Apex Trees

Akbar Ali , Waqas Iqbal, Zahid Raza, Ekram E. Ali, Jia-Bao Liu , Farooq Ahmad, and Qasim Ali Chaudhry
Research Article (8 pages), Article ID 4349074, Volume 2021 (2021)




Connectivity of Semicartesian Products

Metrose Metsidik  and Helin Gong
Research Article (6 pages), Article ID 6125053, Volume 2021 (2021)

On char $232(\wp, \wp - 1, \dots, 1)$ Labelings of Circulant Graphs

K. Mageshwaran, Ali Ahmad , Bundit Unyong, G. Kalaimurugan , and S. Gopinath 
Research Article (7 pages), Article ID 6578478, Volume 2021 (2021)



The Normalized Laplacians, Degree-Kirchhoff Index, and the Complexity of Möbius Graph of Linear Octagonal-Quadrilateral Networks

Jia-Bao Liu , Qian Zheng , and Sakander Hayat 
Research Article (25 pages), Article ID 2328940, Volume 2021 (2021)




Several Topological Indices of Two Kinds of Tetrahedral Networks

Jia-Bao Liu  and Lu-Lu Fang 
Research Article (10 pages), Article ID 9800246, Volume 2021 (2021)




On Locating-Dominating Set of Regular Graphs

Anuwar Kadir Abdul Gafur  and Suhadi Widodo Saputro 
Research Article (6 pages), Article ID 8147514, Volume 2021 (2021)

(k, l) -Anonymity in Wheel-Related Social Graphs Measured on the Base of k -Metric Antidimension


Jiang-Hua Tang, Tahira Noreen, Muhammad Salman , Masood Ur Rehman , and Jia-Bao Liu 
Research Article (13 pages), Article ID 8038253, Volume 2021 (2021)

New Cubic Trigonometric Bezier-Like Functions with Shape Parameter: Curvature and Its Spiral Segment

Abdul Majeed , Muhammad Abbas , Amna Abdul Sittar, Mohsin Kamran, Saba Tahseen, and Homan Emadifar 



Research Article (13 pages), Article ID 6330649, Volume 2021 (2021)

Distance-Based Polynomials and Topological Indices for Hierarchical Hypercube Networks

Tingmei Gao  and Iftikhar Ahmed


Research Article (11 pages), Article ID 5877593, Volume 2021 (2021)

Enumeration of the Edge Weights of Symmetrically Designed Graphs

Muhammad Javaid , Hafiz Usman Afzal, and Ebenezer Bonyah 


Research Article (15 pages), Article ID 8335054, Volume 2021 (2021)

Sharp Lower Bounds of the Sum-Connectivity Index of Unicyclic Graphs

Maryam Atapour 

Research Article (6 pages), Article ID 8391480, Volume 2021 (2021)

Total Face Irregularity Strength of Grid and Wheel Graph under K-Labeling of Type (1, 1, 0)

Aleem Mughal and Noshad Jamil 







Research Article (16 pages), Article ID 1311269, Volume 2021 (2021)

Minimum Partition of an r -Independence System

Zill-e-Shams, Muhammad Salman , Zafar Ullah , and Usman Ali 



Research Article (10 pages), Article ID 7163840, Volume 2021 (2021)

On Constant Metric Dimension of Some Generalized Convex Polytopes

Xuewu Zuo , Abid Ali , Gohar Ali , Muhammad Kamran Siddiqui , Muhammad Tariq Rahim , and Anton Asare-Tuah 




Research Article (7 pages), Article ID 6919858, Volume 2021 (2021)

Resistance Distance in Tensor and Strong Product of Path or Cycle Graphs Based on the Generalized Inverse Approach

Muhammad Shoab Sardar , Xiang-Feng Pan, Dalal Alrowaili , and Imran Siddique 




Research Article (10 pages), Article ID 1712685, Volume 2021 (2021)

Super H -Antimagic Total Covering for Generalized Antiprism and Toroidal Octagonal Map

Amir Taimur, Gohar Ali , Muhammad Numan, Adnan Aslam , and Kraidi Anoh Yannick 

Research Article (8 pages), Article ID 9680137, Volume 2021 (2021)




New Results on the Geometric-Arithmetic Index

Akbar Jahanbani , Maryam Atapour , and Zhibin Du 

Research Article (12 pages), Article ID 4901484, Volume 2021 (2021)


Contents

The Vertex-Edge Resolvability of Some Wheel-Related Graphs

Bao-Hua Xing, Sunny Kumar Sharma , Vijay Kumar Bhat , Hassan Raza, and Jia-Bao Liu 

Research Article (16 pages), Article ID 1859714, Volume 2021 (2021)

Metric Dimension of Crystal Cubic Carbon Structure

Xiujun Zhang  and Muhammad Naeem 

Research Article (8 pages), Article ID 3438611, Volume 2021 (2021)

Research Article

On the Edge Resolvability of Double Generalized Petersen Graphs

Tanveer Iqbal ¹, Muhammad Rafiq,² Muhammad Naeem Azhar,³ Muhammad Salman ,⁴
and Imran Khalid ⁵

¹Department of Mathematics, Emerson University, Multan 60700, Pakistan

²Department of Mathematics and Statistics, Institute of Southern Punjab, Multan 60800, Pakistan

³Department of Mathematics, Bahawalnagar Campus, The Islamia University of Bahawalpur, Multan 60800, Pakistan

⁴Department of Mathematics, The Islamia University of Bahawalpur, Bahawalpur, Pakistan

⁵Center for Advanced Studies in Pure and Applied Mathematics, Bahauddin Zakariya University, Multan 60800, Pakistan

Correspondence should be addressed to Muhammad Salman; muhhammad.salman@iub.edu.pk

Received 24 August 2021; Revised 4 October 2021; Accepted 23 December 2021; Published 22 April 2022

Academic Editor: Ali Ahmad

Copyright © 2022 Tanveer Iqbal et al. This is an open access article distributed under the Creative Commons Attribution License, which permits unrestricted use, distribution, and reproduction in any medium, provided the original work is properly cited.

For a connected graph $G = (V(G), E(G))$, let $v \in V(G)$ be a vertex and $e = uv \in E(G)$ be an edge. The distance between the vertex v and the edge e is given by $d_G(e, v) = \min\{d_G(u, v), d_G(w, v)\}$. A vertex $w \in V(G)$ distinguishes two edges $e_1, e_2 \in E(G)$ if $d_G(w, e_1) \neq d_G(w, e_2)$. A well-known graph invariant related to resolvability of graph edges, namely, the edge resolving set, is studied for a family of 3-regular graphs. A set S of vertices in a connected graph G is an edge metric generator for G if every two edges of G are distinguished by some vertex of S . The smallest cardinality of an edge metric generator for G is called the edge metric dimension and is denoted by $\beta_e(G)$. As a main result, we investigate the minimum number of vertices which works as the edge metric generator of double generalized Petersen graphs, $DGP(n, 1)$. We have proved that $\beta_e(DGP(n, 1)) = 4$ when $n \equiv 0, 1, 3 \pmod{4}$ and $\beta_e(DGP(n, 1)) = 3$ when $n \equiv 2 \pmod{4}$.

1. Introduction

The concept of the resolving set or the locating set was introduced by Slater [1] and then by Harary and Melter [2] separately. A resolving set R of a given graph is the subset of the vertex set of the given graph so that the vertices of the graph can be located at a unique location by the distances of them from the vertices of R . The cardinality of a such a smallest set R for G is called the metric dimension of G , denoted by $\beta(G)$ [1, 2]. Resolvability in graphs has diverse applications related to the navigation of robots in networks [3–5], pattern identification, and image processing. It has also many applications in pharmaceutical chemistry and drugs [6–8]. In [9], some interesting connections of metric generators of graphs with the mastermind game and coin weighing problem have been presented. This concept was used by Slater [1] to determine the location of an intruder in a network in a unique

way. However, if there is an intruder that cannot be accessed by its nodes or vertices rather by using the links between them called edges, then, in this case, the location of an intruder in a network need not to be identified. Thus, in this situation, there is need to define extra condition to overcome the problem.

For a simple, undirected, and connected graph G , the vertex set and edge set of G is denoted by $V(G)$ and $E(G)$, respectively. The vertices and the edges of G can be resolved or determined with the help of distance parameter. The distance between a vertex α and an edge $\beta = \alpha_1\alpha_2$ in a graph G is given by $d(\beta, \alpha) = \min\{d(\alpha_1, \alpha), d(\alpha_2, \alpha)\}$. Any two edges β_1 and β_2 are said to be resolved (identified) by a vertex α of G if and only if $d(\beta_1, \alpha) = d(\beta_2, \alpha)$ implies $\beta_1 = \beta_2$. A set of vertices $X \subseteq V(G)$ is an edge resolving set for G if and only if every two distinct edges of G are resolved by some vertex in X . The edge metric dimension of G is the cardinality of such a smallest set X , denoted by $\beta_e(G)$ [10].

2. Literature Review

Motivated by this, Kelenc et al. [10] recently defined the concept of edge resolvability in graphs and studied its different properties. In their work, they extended the study of the resolving set to the edge resolving set. There are several graphs for which the metric dimension is equal to the edge metric dimension, the metric dimension is less than the edge metric dimension, and the metric dimension is greater than the edge metric dimension [10]. Moreover, exact values for the edge metric dimension of many classes of graphs were computed, while the upper and lower bounds of many other graphs have been given. The results of the mixed metric dimensions and the edge metric dimensions for some families of graphs are given in [11, 12]. Peterin and Yero [13] computed exact formulae for different products of graphs. Zubrilina [14] categorized some properties of edge metric dimension of graphs. Moreover, we refer the reader to the work [15–19] where some related results on this topic can be found.

3. Double Generalized Petersen Graph

The double generalized Petersen graph $DGP(n, k)$ is a cubic graph, for $n \geq 3$ and $1 \leq k \leq n-1$, with vertex set $V(DGP(n, k)) = \{x_i, u_i, v_i, y_i : 1 \leq i \leq n\}$ and edge set $E(DGP) = \{x_i x_{i+1}, x_i u_i, u_i v_{i+k}, v_i u_{i+k}, v_i y_i, y_i y_{i+1} : 1 \leq i \leq n\}$. The exterior cycle of the $DGP(n, k)$ contains vertices $x_i, 1 \leq i \leq n$, in which every vertex x_i is adjacent to the vertex u_i to make spokes of type $x_i u_i; 1 \leq i \leq n$. Similarly, the inner cycle of the $DGP(n, k)$ contains the vertices $y_i, 1 \leq i \leq n$, in which every vertex y_i is adjacent to the vertex v_i to make spokes of type $v_i y_i; 1 \leq i \leq n$ [20]. Throughout the study, the indices will be taken under modulo n . For $n = 13$ and $k = 1$, the double generalized Petersen graph is shown in Figure 1.

4. Edge Metric Dimension of $DGP(n, 1)$

In this section, we investigate the edge metric dimension of $DGP(n, 1)$ by proving its upper and lower bounds.

4.1. Upper Bound. For a set $W = \{\alpha_1, \alpha_2, \dots, \alpha_k\} \subseteq V(G)$, the code of any edge $e \in E(G)$ is the k -vector:

$$c_W(e) = (d(e, \alpha_1), d(e, \alpha_2), \dots, d(e, \alpha_k)). \quad (1)$$

Equivalently, the set W is an edge resolving set for G if and only if each edge in G has the unique code with respect to W . That is, W is an edge metric for G if and only if two edges $e_1, e_2 \in E(G)$ and $c_W(e_1) = c_W(e_2)$ imply $e_1 = e_2$. Next, first four lemmas provide the upper bound for the edge metric dimension of $DGP(n, 1)$.

Lemma 1. For $n \geq 16$ and $n \equiv 0 \pmod{4}$, we have $\beta_e(DGP(n, 1)) \leq 4$.

Proof. Let $W = \{x_1, x_{n/2-2}, v_{n/2}, y_{n/2-2}\}$. Define $k_1 = n/2$ and $l = n/4$. Codes of all the edges of $DGP(n, 1)$ with respect to W are given in Tables 1–10.

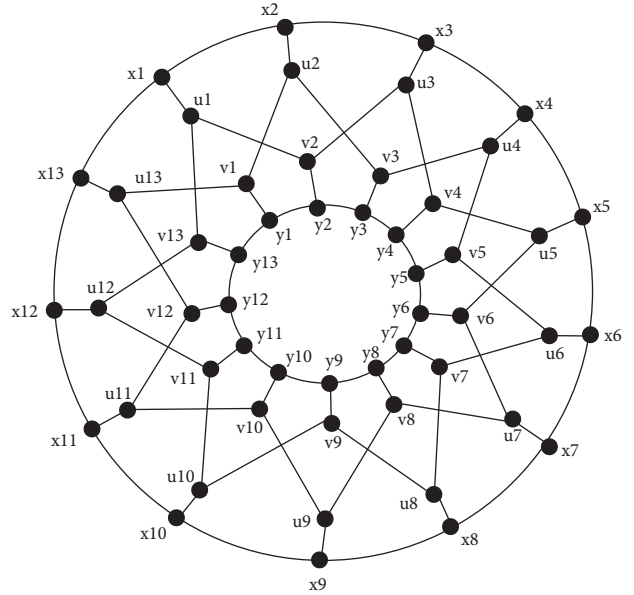


FIGURE 1: The graph of $DGP(13, 1)$.

TABLE 1: Codes of outermost edges, $e = x_c x_{c+1}$.

$c_W(e)$	x_1	$x_{n/2-2}$	$v_{n/2}$	$y_{n/2-2}$
$1 \leq c \leq k_1 - 4$	$c - 1$	$k_1 - c - 3$	$k_1 - c$	$k_1 - c - 1$
$c = k_1 - 3$	$c - 1$	0	3	3
$c = k_1 - 2$	$c - 1$	0	2	3
$k_1 - 1 \leq c \leq k_1$	$c - 1$	$c + 2 - k_1$	2	$c + 4 - k_1$
$k_1 + 1 \leq c \leq n - 3$	$n - c$	$c + 2 - k_1$	$c + 1 - k_1$	$c + 4 - k_1$
$n - 2 \leq c \leq n - 1$	$n - c$	$n - 3 + k_1 - c$	$c + 1 - k_1$	$n - c + k_1 - 1$
$c = n$	$n - c$	$n - 3 + k_1 - c$	k_1	$n - c + k_1 - 1$

From Tables 1–10, it can be seen that each edge of $DGP(n, 1)$ has the unique code w. r. t. W . So, W is an edge resolving set for $DGP(n, 1)$ and $\beta_e(DGP(n, 1)) \leq 4$. \square

Lemma 2. For $n \geq 13$ and $n \equiv 1 \pmod{4}$, we have $\beta_e(DGP(n, 1)) \leq 4$.

Proof. Let $W = \{x_1, x_{\lfloor n/2 \rfloor - 1}, v_{\lfloor n/2 \rfloor + 1}, y_{\lfloor n/2 \rfloor - 1}\}$. Define $k_1 = \lfloor n/2 \rfloor$ and $l = \lfloor n/4 \rfloor$. Codes of all the edges of $DGP(n, 1)$ with respect to W are given in Tables 11–20.

From Tables 11–20, it can be observed that each edge of $DGP(n, 1)$ has unique codes w. r. t. W . So, W is an edge resolving set for $DGP(n, 1)$ and $\beta_e(DGP(n, 1)) \leq 4$. \square

Lemma 3. For $n \geq 15$ and $n \equiv 3 \pmod{4}$, we have $\beta_e(DGP(n, 1)) \leq 4$.

Proof. Let $W = \{x_1, x_{\lfloor n/2 \rfloor - 1}, v_{\lfloor n/2 \rfloor + 1}, y_{\lfloor n/2 \rfloor - 1}\}$. Define $k_1 = \lfloor n/2 \rfloor$ and $l = \lfloor n/2 \rfloor$. Codes of all the edges in $DGP(n, 1)$ with respect to W are given in Tables 21–29.

From Tables 21–29, we observe that each edge of $DGP(n, 1)$ has unique code w. r. t. W . Hence, W is an edge resolving set for $DGP(n, 1)$ and $\beta_e(DGP(n, 1)) \leq 4$. \square

TABLE 2: Codes of edges, $e = x_c u_c$, when c is odd.

$c_W(e)$	x_1	$x_{n/2-2}$	$v_{n/2}$	$y_{n/2-2}$
$1 \leq c \leq k_1/2 - 1$	$2c - 2$	$k_1 - 2c - 1$	$k_1 + 1 - 2c$	$k_1 - 2c$
$k_1/2 \leq c \leq k_1/2 + 1$	$2c - 2$	$2c + 1 - k_1$	1	$2c + 2 - k_1$
$k_1/2 + 2 \leq c \leq k_1 - 1$	$n + 2 - 2c$	$2c + 1 - k_1$	$2c - k_1 - 1$	$2c + 2 - k_1$
$c = k_1$	2	$k_1 - 1$	$k_1 - 1$	k_1

TABLE 3: Codes of edges, $e = x_c u_c$, when c is even.

$c_W(e)$	x_1	$x_{n/2-2}$	$v_{n/2}$	$y_{n/2-2}$
$1 \leq c \leq k_1/2 - 2$	$2c - 1$	$k_1 - 2c - 2$	$k_1 + 1 - 2c$	$k_1 - 2c - 1$
$k_1/2 - 1 \leq c \leq k_1/2$	$2c - 1$	$2c + 2 - k_1$	3	3
$k_1/2 + 1 \leq c \leq k_1 - 1$	$n + 1 - 2c$	$2c + 2 - k_1$	$2c + 1 - k_1$	$2c + 3 - k_1$
$c = k_1$	1	$k_1 - 2$	$k_1 + 1$	$k_1 - 1$

TABLE 4: Codes of edges, $e = u_{2c-1} v_{2c}$.

$c_W(e)$	x_1	$x_{n/2-2}$	$v_{n/2}$	$y_{n/2-2}$
$1 \leq c \leq l - 2$	$2c - 1$	$k_1 - 2c - 1$	$k_1 - 2c$	$k_1 - 2c - 1$
$l - 1 \leq c \leq l$	$2c - 1$	2	$k_1 - 2c$	$c - l + 2$
$l + 1 \leq c \leq k_1 - 1$	$n + 2 - 2c$	$2c + 2 - k_1$	$2c - k_1 - 1$	$2c + 2 - k_1$
$c = k_1$	2	$k_1 - 1$	$k_1 - 1$	$k_1 - 1$

TABLE 5: Codes of edges, $e = u_{2c} v_{2c+1}$.

$c_W(e)$	x_1	$x_{n/2-2}$	$v_{n/2}$	$y_{n/2-2}$
$1 \leq c \leq l - 2$	$2c$	$k_1 - 2c - 2$	$k_1 + 1 - 2c$	$k_1 - 2c - 2$
$l - 1 \leq c \leq l$	$2c$	$2c + 3 - k_1$	3	$c - l + 3$
$l + 1 \leq c \leq k_1 - 2$	$n + 1 - 2c$	$2c - k_1 + 3$	$2c - k_1 + 2$	$2c + 3 - k_1$
$c = k_1 - 1$	$k_1 + 2 - c$	$n + k_1 - 2c - 2$	$c + 1$	$n + k_1 - 2c - 2$
$c = k_1$	$k_1 + 2 - c$	$n + k_1 - 2c - 2$	$c + 1$	$n + k_1 - 2c - 2$

TABLE 6: Codes of edges, $e = u_{2c} v_{2c-1}$.

$c_W(e)$	x_1	$x_{n/2-2}$	$v_{n/2}$	$y_{n/2-2}$
$c = 1$	2	$k_1 - 2c - 1$	$k_1 + 2 - 2c$	$k_1 - 2c - 1$
$2 \leq c \leq l - 2$	$2c - 1$	$k_1 - 2c - 1$	$k_1 + 2 - 2c$	$k_1 - 2c - 1$
$l - 1 \leq c \leq l$	$2c - 1$	$c + 2 - l$	$l + 3 - c$	2
$l + 1 \leq c \leq k_1 - 1$	$n + 2 - 2c$	$2c + 2 - k_1$	$2c + 1 - k_1$	$2c + 2 - k_1$
$c = k_1$	2	$k_1 - 1$	$k_1 + 1$	$k_1 - 1$
$u_1 v_n$	1	$k_1 - 2$	$k_1 - 1$	$k_1 - 2$

TABLE 7: Codes of edges, $e = u_{2c+1} v_{2c}$.

$c_W(e)$	x_1	$x_{n/2-2}$	$v_{n/2}$	$y_{n/2-2}$
$1 \leq c \leq l - 2$	$2c$	$k_1 - 2c - 2$	$k_1 - 1 - 2c$	$k_1 - 2c - 2$
$l - 1 \leq c \leq l$	$2c$	$c + 3 - l$	$l - c$	$2c + 3 - k_1$
$l + 1 \leq c \leq k_1 - 2$	$n + 1 - 2c$	$2c + 3 - k_1$	$2c - k_1$	$2c + 3 - k_1$
$c = k_1 - 1$	2	$k_1 - 1$	$k_1 + 1$	$k_1 - 1$

TABLE 8: Codes of edges, $e = v_{2c-1} y_{2c-1}$.

$c_W(e)$	x_1	$x_{n/2-2}$	$v_{n/2}$	$y_{n/2-2}$
$c = 1$	3	$k_1 - 2$	k_1	$k_1 - 3$
$2 \leq c \leq k_1/2 - 1$	$2c - 1$	$k_1 - 2c$	$k_1 + 2 - 2c$	$k_1 - 2c - 1$
$k_1/2 \leq c \leq k_1/2 + 1$	$2c - 1$	$2c + 2 - k_1$	2	$2c + 1 - k_1$
$k_1/2 + 2 \leq c \leq k_1 - 1$	$n + 3 - 2c$	$2c + 2 - k_1$	$2c - k_1$	$2c + 1 - k_1$
$c = k_1$	3	k_1	k_1	$k_1 - 1$

TABLE 9: Codes of edges, $e = v_{2c}y_{2c}$.

$c_W(e)$	x_1	$x_{n/2-2}$	$v_{n/2}$	$y_{n/2-2}$
$1 \leq c \leq k_1/2 - 2$	$2c$	$k_1 - 2c - 1$	$k_1 - 2c$	$k_1 - 2c - 2$
$k_1/2 - 1 \leq c \leq k_1/2$	$2c$	3	$k_1 - 2c$	$2c + 2 - k_1$
$k_1/2 + 1 \leq c \leq k_1 - 1$	$n + 2 - 2c$	$2c + 3 - k_1$	$2c - k_1$	$2c + 2 - k_1$
$c = k_1$	2	$k_1 - 1$	k_1	$k_1 - 2$

TABLE 10: Codes of edges, $e = y_c y_{c+1}$.

$c_W(e)$	x_1	$x_{n/2-2}$	$v_{n/2}$	$y_{n/2-2}$
$c = 1$	3	$k_1 - 2$	$k_1 - 1$	$k_1 - 4$
$2 \leq c \leq k_1 - 4$	$c + 1$	$k_1 - c - 1$	$k_1 - c$	$k_1 - c - 3$
$k_1 - 3 \leq c \leq k_1 - 2$	$c + 1$	3	$k_1 - c$	0
$k_1 - 1 \leq c \leq k_1$	$c + 1$	$c + 4 - k_1$	1	$c + 2 - k_1$
$k_1 + 1 \leq c \leq n - 3$	$n + 2 - c$	$c + 4 - k_1$	$c + 1 - k_1$	$c + 2 - k_1$
$n - 2 \leq c \leq n - 1$	$n + 2 - c$	$n - c + k - 1$	$c + 1 - k_1$	$k_1 + n - c - 3$
$c = n$	3	$k_1 - 1$	k_1	$k_1 - 3$

TABLE 11: Codes of outermost edges, $e = x_c x_{c+1}$.

$c_W(e)$	x_1	$x_{\lfloor n/2 \rfloor - 1}$	$v_{\lfloor n/2 \rfloor + 1}$	$y_{\lfloor n/2 \rfloor - 1}$
$1 \leq c \leq k_1 - 3$	$c - 1$	$k_1 - (c + 2)$	$k_1 + 1 - c$	$k_1 - c$
$c = k_1 - 2$	$c - 1$	0	3	3
$k_1 - 1 \leq c \leq k_1$	$c - 1$	$c + 1 - k_1$	2	3
$c = k_1 + 1$	k_1	2	2	4
$k_1 + 2 \leq c \leq n - 2$	$n - c$	$c + 1 - k_1$	$c - k_1$	$c + 3 - k_1$
$n - 1 \leq c \leq n$	$n - c$	$n - 2 + k_1 - c$	$c - k_1$	$n - c + k_1$

TABLE 12: Codes of edges, $e = x_c u_c$, when c is odd.

$c_W(e)$	x_1	$x_{\lfloor n/2 \rfloor - 1}$	$v_{\lfloor n/2 \rfloor + 1}$	$y_{\lfloor n/2 \rfloor - 1}$
$1 \leq c \leq k_1/2 - 1$	$2c - 2$	$k_1 - 2c$	$k_1 + 3 - 2c$	$k_1 + 1 - 2c$
$k_1/2 \leq c \leq k_1/2 + 1$	$2c - 2$	$2c - k_1$	3	3
$k_1/2 + 2 \leq c \leq k_1$	$n + 2 - 2c$	$2c - k_1$	$2c - k_1 - 1$	$2c + 1 - k_1$
$c = k_1 + 1$	1	$k_1 - 1$	$k_1 + 1$	k_1

TABLE 13: Codes of edges, $e = x_c u_c$, when c is even.

$c_W(e)$	x_1	$x_{\lfloor n/2 \rfloor - 1}$	$v_{\lfloor n/2 \rfloor + 1}$	$y_{\lfloor n/2 \rfloor - 1}$
$1 \leq c \leq k_1/2 - 1$	$2c - 1$	$k_1 - 2c - 1$	$k_1 + 1 - 2c$	$k_1 - 2c$
$c = k_1/2$	$2c - 1$	1	1	2
$k_1/2 + 1 \leq c \leq k_1 - 1$	$n + 1 - 2c$	$2c - k_1 + 1$	$2c - k_1 - 1$	$2c + 2 - k_1$
$c = k_1$	2	k_1	$k_1 - 1$	$k_1 + 1$

TABLE 14: Codes of edges, $e = v_c y_c$, when c is odd.

$c_W(e)$	x_1	$x_{\lfloor n/2 \rfloor - 1}$	$v_{\lfloor n/2 \rfloor + 1}$	$y_{\lfloor n/2 \rfloor - 1}$
$c = 1$	3	$k_1 + 1 - 2c$	$k_1 + 2 - 2c$	$k_1 - 2c$
$2 \leq c \leq k_1/2 - 1$	$2c - 1$	$k_1 + 1 - 2c$	$k_1 + 2 - 2c$	$k_1 - 2c$
$k_1/2 \leq c \leq k_1/2 + 1$	$2c - 1$	3	$k_1 + 2 - 2c$	$2c - k_1$
$k_1/2 + 2 \leq c \leq k_1$	$n + 3 - 2c$	$2c + 1 - k_1$	$2c - k_1 - 2$	$2c - k_1$
$c = k_1 + 1$	2	k_1	k_1	$k_1 - 1$

TABLE 15: Codes of edges, $e = v_c y_c$, when c is even.

$c_W(e)$	x_1	$x_{\lfloor n/2 \rfloor - 1}$	$v_{\lfloor n/2 \rfloor + 1}$	$y_{\lfloor n/2 \rfloor - 1}$
$1 \leq c \leq k_1/2 - 2$	$2c$	$k_1 - 2c$	$k_1 + 2 - 2c$	$k_1 - 2c - 1$
$k_1/2 - 1 \leq c \leq k_1/2$	$2c$	2	$k_1 + 2 - 2c$	1
$k_1/2 + 1 \leq c \leq k_1 - 1$	$n + 2 - 2c$	$2c + 2 - k_1$	$2c - k_1$	$2c + 1 - k_1$
$c = k_1$	3	$k_1 + 1$	k_1	k_1

TABLE 16: Codes of edges, $e = y_c y_{c+1}$.

$c_W(e)$	x_1	$x_{\lfloor n/2 \rfloor - 1}$	$v_{\lfloor n/2 \rfloor + 1}$	$y_{\lfloor n/2 \rfloor - 1}$
$c = 1$	3	$k_1 - 1$	k_1	$k_1 - 3$
$2 \leq c \leq k_1 - 3$	$c + 1$	$k_1 - i$	$k_1 + 1 - c$	$k_1 - c - 2$
$k_1 - 2 \leq c \leq k_1 - 1$	$c + 1$	3	$k_1 + 1 - c$	0
$k_1 \leq c \leq k_1 + 1$	$c + 1$	$c + 3 - k_1$	1	$c + 1 - k_1$
$k_1 + 2 \leq c \leq n - 2$	$n + 2 - c$	$c + 3 - k_1$	$c - k_1$	$c - k_1 + 1$
$n - 1 \leq c \leq n$	3	$n - c + k_1$	$c + 1 + k_1 - n$	$k_1 + n - c - 2$

TABLE 17: Codes of edges, $e = u_{2c-1} v_{2c}$.

$c_W(e)$	x_1	$x_{\lfloor n/2 \rfloor - 1}$	$v_{\lfloor n/2 \rfloor + 1}$	$y_{\lfloor n/2 \rfloor - 1}$
$1 \leq c \leq l - 2$	$2c - 1$	$k_1 - 2c$	$k_1 + 3 - 2c$	$k_1 - 2c$
$l - 1 \leq c \leq l$	$2c - 1$	$2c - k_1 + 1$	3	$c - l + 3$
$l + 1 \leq c \leq k_1$	$n + 2 - 2c$	$2c - k_1 + 1$	$2c - k_1$	$2c + 1 - k_1$
$u_n v_1$	2	$k_1 - 1$	k_1	$k_1 - 1$

TABLE 18: Codes of edges, $e = u_{2c} v_{2c+1}$.

$c_W(e)$	x_1	$x_{\lfloor n/2 \rfloor - 1}$	$v_{\lfloor n/2 \rfloor + 1}$	$y_{\lfloor n/2 \rfloor - 1}$
$1 \leq c \leq l - 3$	$2c$	$k_1 - 2c - 1$	$k_1 - 2c$	$k_1 - 2c - 1$
$l - 2 \leq c \leq l - 1$	$2c$	2	$k_1 - 2c$	$c - l + 3$
$l \leq c \leq k_1 - 1$	$n + 1 - 2c$	$2c - k_1 + 2$	$2c - k_1 - 1$	$2c + 2 - k_1$
$c = k_1$	2	k_1	$k_1 - 1$	k_1

TABLE 19: Codes of edges, $e = u_{2c} v_{2c-1}$.

$c_W(e)$	x_1	$x_{\lfloor n/2 \rfloor - 1}$	$v_{\lfloor n/2 \rfloor + 1}$	$y_{\lfloor n/2 \rfloor - 1}$
$1 \leq c \leq l - 3$	$c + 1$	$k_1 - 2c$	$k_1 - 2c + 1$	$k_1 - 2c$
$l - 2 \leq c \leq l - 1$	$2c - 1$	2	$k_1 - 2c + 1$	$l - c$
$l \leq c \leq k_1$	$n + 2 - 2c$	$2c + k_1 + 2 - n$	$2c + k_1 - n - 1$	$2c + 2 + k_1 - n$
$u_1 v_n$	1	$k_1 - 1$	k_1	$k_1 - 1$

TABLE 20: Codes of edges, $e = u_{2c+1} v_{2c}$.

$c_W(e)$	x_1	$x_{\lfloor n/2 \rfloor - 1}$	$v_{\lfloor n/2 \rfloor + 1}$	$y_{\lfloor n/2 \rfloor - 1}$
$1 \leq c \leq l - 3$	$2c$	$k - 2c - 1$	$k_1 + 2 - 2c$	$k_1 - 2c - 1$
$l - 2 \leq c \leq l - 1$	$2c$	$c - 2$	$l + 2 - c$	2
$l \leq c \leq k_1 - 1$	$n + 1 - 2c$	$2c + 2 - k_1$	$2c + 1 - k_1$	$2c + 2 - k_1$
$c = k_1$	2	k_1	$k_1 + 1$	k_1

TABLE 21: Codes of edges, $e = x_c u_c$, when c is odd.

$c_W(e)$	x_1	$x_{\lfloor n/2 \rfloor - 1}$	$v_{\lfloor n/2 \rfloor + 1}$	$y_{\lfloor n/2 \rfloor - 1}$
$1 \leq c \leq \lfloor k_1/2 \rfloor$	$2c - 2$	$k_1 - 2c$	$k_1 + 2 - 2c$	$k_1 + 1 - 2c$
$c = \lfloor k_1/2 \rfloor + 1$	$k_1 - 1$	1	1	2
$\lfloor k_1/2 \rfloor + 2 \leq c \leq k_1$	$n + 2 - 2c$	$2c - k_1$	$2c - k_1 - 2$	$2c + 1 - k_1$
$c = k_1 + 1$	1	$k_1 - 1$	k_1	k_1

TABLE 22: Codes of edges, $e = x_c u_c$, when c is even.

$c_W(e)$	x_1	$x_{\lfloor n/2 \rfloor - 1}$	$v_{\lfloor n/2 \rfloor + 1}$	$y_{\lfloor n/2 \rfloor - 1}$
$1 \leq c \leq \lfloor k_1/2 \rfloor - 1$	$2c - 1$	$k_1 - 2c - 1$	$k_1 + 2 - 2c$	$k_1 - 2c$
$\lfloor k_1/2 \rfloor \leq c \leq \lfloor k_1/2 \rfloor + 1$	$2c - 1$	$2c + 1 - k_1$	3	3
$\lfloor k_1/2 \rfloor + 2 \leq c \leq k_1 - 1$	$n + 1 - 2c$	$2c - k_1 + 1$	$2c - k_1$	$2c + 2 - k_1$
$c = k_1$	2	k_1	k_1	$k_1 + 1$

TABLE 23: Codes of edges, $e = v_c y_c$, when c is odd.

$c_W(e)$	x_1	$x_{\lfloor n/2 \rfloor - 1}$	$v_{\lfloor n/2 \rfloor + 1}$	$y_{\lfloor n/2 \rfloor - 1}$
$c = 1$	3	$k_1 + 1 - 2c$	$k_1 + 3 - 2c$	$k_1 - 2c$
$2 \leq c \leq l - 1$	$2c - 1$	$k_1 + 1 - 2c$	$k_1 + 3 - 2c$	$k_1 - 2c$
$l \leq c \leq l + 1$	$l + c - 1$	$2c - k_1 + 1$	2	$2c - k_1$
$l + 2 \leq c \leq k_1$	$n + 3 - 2c$	$2c + 1 - k_1$	$2c - k_1 - 1$	$2c - k_1$
$c = k_1$	2	k_1	$k_1 + 1$	$k_1 - 1$

TABLE 24: Codes of edges, $e = v_c y_c$, when c is even.

$c_W(e)$	x_1	$x_{\lfloor n/2 \rfloor - 1}$	$v_{\lfloor n/2 \rfloor + 1}$	$y_{\lfloor n/2 \rfloor - 1}$
$1 \leq c \leq l - 2$	$2c$	$k_1 - 2c$	$k_1 + 1 - 2c$	$k_1 - 2c - 1$
$l - 1 \leq c \leq l$	$2c$	3	$k_1 + 1 - 2c$	$2c + 1 - k_1$
$l + 1 \leq c \leq k_1 - 1$	$n + 2 - 2c$	$2c + 2 - k_1$	$2c - k_1 - 1$	$2c + 1 - k_1$
$c = k_1$	3	$k_1 + 1$	$k_1 - 1$	k_1

TABLE 25: Codes of edges, $e = y_c y_{c+1}$.

$c_W(e)$	x_1	$x_{\lfloor n/2 \rfloor - 1}$	$v_{\lfloor n/2 \rfloor + 1}$	$y_{\lfloor n/2 \rfloor - 1}$
$c = 1$	3	$k_1 - 1$	k_1	$k_1 - 2$
$2 \leq c \leq k_1 - 3$	$c + 1$	$k_1 - c$	$k_1 + 1 - c$	$k_1 - c - 2$
$k_1 - 2 \leq c \leq k_1 - 1$	$c + 1$	3	$k_1 + 1 - c$	0
$k_1 \leq c \leq k_1 + 1$	$c + 1$	$c + 3 - k_1$	1	$c + 1 - k_1$
$k_1 + 2 \leq c \leq n - 2$	$n + 2 - c$	$c + 3 - k_1$	$c - k_1$	$c - k_1 + 1$
$n - 1 \leq c \leq n$	3	$n - c + k_1$	$c + 1 + k_1 - n$	$k_1 + n - c - 2$

TABLE 26: Codes of edges, $e = u_{2c-1} v_{2c}$.

$c_W(e)$	x_1	$x_{\lfloor n/2 \rfloor - 1}$	$v_{\lfloor n/2 \rfloor + 1}$	$y_{\lfloor n/2 \rfloor - 1}$
$1 \leq c \leq l - 2$	$2c - 1$	$k_1 - 2c$	$k_1 + 1 - 2c$	$k_1 - 2c$
$l - 1 \leq c \leq l$	$2c - 1$	2	$k_1 + 1 - 2c$	$c - l - 2$
$l + 1 \leq c \leq k_1$	$n + 2 - 2c$	$2c + 2k_1 - n$	$2c + k_1 - n - 1$	$2c + 2 + k_1 - n$
$u_n v_1$:	2	$k_1 - 1$	k_1	$k_1 - 1$

TABLE 27: Codes of edges, $e = u_{2c} v_{2c+1}$.

$c_W(e)$	x_1	$x_{\lfloor n/2 \rfloor - 1}$	$v_{\lfloor n/2 \rfloor + 1}$	$y_{\lfloor n/2 \rfloor - 1}$
$1 \leq c \leq l - 2$	$2c$	$k_1 - 2c - 1$	$k_1 + 2 - 2c$	$k_1 - 2c - 1$
$l - 1 \leq c \leq l$	$2c$	$2c + 3 + k_1 - n$	3	$c - l + 3$
$l + 1 \leq c \leq k_1 - 1$	$n + 1 - 2c$	$2c - k_1 + 2$	$2c - k_1 + 1$	$2c + 2 - k_1$
$c = k_1$	$n + 1 - 2c$	k_1	$k_1 + 1$	k_1

TABLE 28: Codes of edges, $e = u_{2c}v_{2c-1}$.

$c_W(e)$	x_1	$x_{\lfloor n/2 \rfloor - 1}$	$v_{\lfloor n/2 \rfloor + 1}$	$y_{\lfloor n/2 \rfloor - 1}$
$c = l$	2	$k_1 - 2$	$k_1 + 1$	$k_1 - 2$
$2 \leq c \leq l - 2$	$2c - 1$	$k_1 - 2c$	$k_1 + 3 - 2c$	$k_1 - 2c$
$l - 1 \leq c \leq l$	$2c - 1$	$c + 2 - l$	$1 + 3 - c$	2
$l + 1 \leq c \leq k_1$	$n + 2 - 2c$	$2c + 2 + k_1 - n$	$2c + 1 + k_1 - n$	$2c + 2 + k_1 - n$
u_1v_n :	1	$k_1 - 1$	k_1	$k_1 - 1$

TABLE 29: Codes of edges, $e = u_{2c+1}v_{2c}$.

$c_W(e)$	x_1	$x_{\lfloor n/2 \rfloor - 1}$	$v_{\lfloor n/2 \rfloor + 1}$	$y_{\lfloor n/2 \rfloor - 1}$
$c = l$	2	$k_1 - 2$	$k_1 + 1$	$k_1 - 2$
$2 \leq c \leq l - 2$	$2c - 1$	$k_1 - 2c$	$k_1 + 3 - 2c$	$k_1 - 2c$
$l - 1 \leq c \leq l$	$2c - 1$	$c + 2 - l$	$1 + 3 - c$	2
$l + 1 \leq c \leq k_1$	$n + 2 - 2c$	$2c + 2 + k_1 - n$	$2c + 1 + k_1 - n$	$2c + 2 + k_1 - n$
u_1v_n :	1	$k_1 - 1$	k_1	$k_1 - 1$

TABLE 30: Codes of outermost edges, $e = x_cx_{c+1}$.

$c_W(e)$	x_1	$x_{n/2+2}$	$u_{n/2-3}$
$c = 1$	$c - 1$	$k_1 - 1$	$k_1 - 2c - 2$
$2 \leq c \leq k_1 - 4$	$c - 1$	$k_1 + 1 - c$	$k_1 - c - 3$
$k_1 - 3 \leq c \leq k_1$	$c - 1$	$k_1 + 1 - c$	$c + 4 - k_1$
$k_1 + 1 \leq c \leq k_1 + 2$	$n - c$	0	$c + 4 - k_1$
$k_1 + 3 \leq c \leq n - 4$	$n - c$	$c + k_1 - n - 2$	$c + 4 - k_1$
$n - 3 \leq c \leq n$	$n - c$	$k_1 + c - n - 2$	$n + k_1 - c - 3$

TABLE 31: Codes of edges, $e = v_{2c-1}y_{2c-1}$.

$c_W(e)$	x_1	$x_{n/2+2}$	$u_{n/2-3}$
$c = 1$	3	k_1	$k_1 - 2c - 2$
$2 \leq c \leq l - 2$	$2c - 1$	$k_1 + 4 - 2c$	$k_1 - 2 - 2c$
$c = l - 1$	$2c - 1$	$k_1 + 4 - 2c$	$k_1 - 2c$
$l \leq c \leq l + 1$	k_1	3	$2c + 2 - k_1$
$l + 2 \leq c \leq k_1 - 1$	$n + 3 - 2c$	$2c - k_1 - 2$	$2c + 2 - k_1$
$c = k_1$	$n + 3 - 2c$	$2c - k_1 - 2$	$k_1 - 2$

TABLE 32: Codes of edges, $e = v_{2c}y_{2c}$.

$c_W(e)$	x_1	$x_{n/2+2}$	$u_{n/2-3}$
$1 \leq c \leq l - 3$	$2c$	$k_1 - 2c + 3$	$k_1 - 2c - 2$
$c = l - 2$	$2c$	$k_1 + 3 - 2c$	3
$l - 1 \leq c \leq l$	$2c$	$k_1 + 3 - 2c$	$2c + 4 - k_1$
$l + 1 \leq c \leq k_1 - 2$	$n + 2 - 2c$	$2c - k_1 - 1$	$2c + 4 - k_1$
$k_1 - 1 \leq c \leq k_1$	$n + 2 - 2c$	$2c - k_1 - 1$	$n - 2c + k_1 - 2$

Lemma 4. For $n \geq 14$ and $n \equiv 2 \pmod{4}$, we have $\beta_e(DG P(n, 1)) \leq 3$.

Proof. Let $W = \{x_1, x_{n/2+2}, u_{n/2-3}\}$. Define $k_1 = \lfloor n/2 \rfloor$ and $l = \lceil n/4 \rceil$. Codes of outermost edges, inner edges, and spokes of DGP $(n, 1)$ with respect to W are given in Tables 30–39.

From Tables 30–39, we observe that each edge of DGP $(n, 1)$ has unique code w. r. t. W . Thus, W is an edge resolving set for DGP $(n, 1)$ and $\beta_e(DG P(n, 1)) \leq 3$. \square

4.2. Lower Bound. For all t -regular graphs, the following lower bound for the edge metric dimension of any connected graph was explored in [21].

Lemma 5 (see [21]). *If G is a connected t -regular graph, then $\beta_e(G) \geq 1 + \lceil \log_2 t \rceil$.*

As we know that DGP (n, k) are 3-regular graphs and $\lceil \log_2 3 \rceil = 2$, so the next result holds consequently.

TABLE 33: Codes of spokes, $e = x_c u_c$, when c is odd.

$C_W(e)$	x_1	$x_{n/2+2}$	$u_{n/2-3}$
$c = 1$	$2c - 2$	$k_1 - 1$	$k_1 - 1 - 2c$
$2 \leq c \leq l - 2$	$2c - 2$	$k_1 + 3 - 2c$	$k_1 - 2c - 1$
$l - 1 \leq c \leq l$	$2c - 2$	$k_1 + 3 - 2c$	$2c + 3 - k_1$
$l + 1 \leq c \leq k_1 - 1$	$n + 2 - 2c$	$2c - k_1 - 3$	$2c - k_1 + 3$
$c = k_1$	$n + 2 - 2c$	$2c - k_1 - 3$	$k_1 - 1$

TABLE 34: Codes of spokes, $e = x_c u_c$, when c is even.

$c_W(e)$	x_1	$x_{n/2+2}$	$u_{n/2-3}$
$1 \leq c \leq l - 2$	$2c - 1$	$k_1 + 2 - 2c$	$k_1 - 3 - 2c$
$l - 1 \leq c \leq l$	$2c - 1$	$k_1 + 2 - 2c$	$2c + 3 - k_1$
$l + 1 \leq c \leq k_1 - 2$	$n + 1 - 2c$	$2c - k_1 - 2$	$2c + 3 - k_1$
$k_1 - 1 \leq c \leq k_1$	$n + 1 - 2c$	$2c - k_1 - 2$	$n + k_1 - 2c - 3$

TABLE 35: Codes of edges, $e = y_c y_{c+1}$.

$c_W(e)$	x_1	$x_{n/2+2}$	$u_{n/2-3}$
$c = 1$	3	$k_1 + 1$	$k_1 - 2c - 2$
$2 \leq c \leq k_1 - 5$	$c + 1$	$k_1 + 3 - c$	$k_1 - c - 3$
$k_1 - 4 \leq c \leq k_1 - 2$	$c + 1$	$k_1 + 3 - c$	2
$k_1 - 1 \leq c \leq k_1$	$c + 1$	$k_1 + 3 - c$	$c + 4 - k_1$
$k_1 + 1 \leq c \leq k_1 + 2$	$n + 2 - c$	3	$c + 4 - k_1$
$k_1 + 3 \leq c \leq n - 4$	$n + 2 - c$	$c - k_1$	$c + 4 - k_1$
$n - 3 \leq c \leq n - 1$	$n + 2 - c$	$c + k_1 - n$	$n + 4 - c$
$y_n y_1$	3	k_1	$k_1 - 3$

TABLE 36: Codes of edges, $e = u_{2c-1} v_{2c}$.

$c_W(e)$	x_1	$x_{n/2+2}$	$u_{n/2-3}$
$1 \leq c \leq l - 3$	$2c$	$k_1 + 2 - 2c$	$k_1 - 2c - 2$
$c = l - 2$	$2c$	$k_1 + 2 - 2c$	3
$l - 1 \leq c \leq l$	$l + c - 1$	$k_1 + 2 - 2c$	$2c + 5 - k_1$
$l + 1 \leq c \leq k_1 - 1$	$n + 1 - 2c$	$2c - k_1 - 1$	$2c + 5 - k_1$
$c = k_1$	3	$k_1 - 3$	k_1

TABLE 37: Codes of edges, $e = u_{2c-1} v_{2c}$.

$c_W(e)$	x_1	$x_{n/2+2}$	$u_{n/2-3}$
$c = 1$	1	k_1	$k_1 + 1 - 4c$
$2 \leq c \leq l - 3$ (for $n \neq 14$)	$2c - 1$	$k_1 + 3 - 2c$	$k_1 - 2c - 1$
$l - 2 \leq c \leq l - 1$ (for $n = 14$)	$2c - 1$	$k_1 + 3 - 2c$	3
$l - 2 \leq c \leq l - 1$	$2c - 1$	$k_1 + 3 - 2c$	3
$c = l$	$2c - 1$	$k_1 + 3 - 2c$	5
$l + 1 \leq c \leq k_1 - 2$	$n + 2 - 2c$	$2c - k_1 - 2$	$2c + 4 - k_1$
$k_1 - 1 \leq c \leq k_1$	$n + 2 - 2c$	$2c - k_1 - 2$	$n + k_1 - 1 - 2c$

Lemma 6. For any double generalized Petersen graph $DGP(n, k)$, we have $\beta_e(DGP(n, k)) \geq 3$.

The next result provides the lower bound for the edge metric dimension of $DGP(n, 1)$ whenever $n \not\equiv 2 \pmod{4}$.

Lemma 7. For $n \geq 13$ and $n \equiv 0, 1, 3 \pmod{4}$, we have $\beta_e(DGP(n, 1)) \geq 4$.

Proof. We now prove that the cardinality of any minimum edge resolving set W is 4. On the contrary, suppose that the cardinality of W is 3, by Lemma 5. To prove that the existence of such edge resolving set W is not possible, we have the following claims. Define $k = n/2$, and let the vertex set of $DGP(n, 1)$ be $X \cup Y \cup U \cup V$, where $X = \{x_i; 1 \leq i \leq n\}$, $Y = \{y_i; 1 \leq i \leq n\}$, $U = \{u_i; 1 \leq i \leq n\}$, and $V = \{v_i; 1 \leq i \leq n\}$. \square

TABLE 38: Codes of edges, $e = u_{2c}v_{2c+1}$.

$c_W(e)$	x_1	$x_{n/2+2}$	$u_{n/2-3}$
$1 \leq c \leq l-3$	$2c$	$k_1 + 2 - 2c$	$k_1 - 4 - 2c$
$l-2 \leq c \leq l-1$	$2c$	$k_1 + 2 - 2c$	$2c + 3 - k_1$
$c = l$	$2c - 1$	2	4
$l+1 \leq c \leq k_1 - 2$	$n + 1 - 2c$	$2c - k_1 - 1$	$2c + 3 - k_1$
$c = k_1 - 1$	$n + 2 - k_1 - c$	$2c - k_1 - 1$	$n + k_1 - 2c - 4$
$u_n v_1$	$n + 2 - k_1 - c$	$2c - k_1 - 1$	$n + k_1 - 2c - 4$

TABLE 39: Codes of edges, $e = u_{2c}v_{2c-1}$.

$c_W(e)$	x_1	$x_{n/2+2}$	$u_{n/2-3}$
$c = 1$	$2c$	k_1	$k_1 - 2c - 3$
$2 \leq c \leq l-2$	$2c - 1$	$k_1 + 3 - 2c$	$k_1 - 2c - 3$
$l-1 \leq c \leq l$	$2c - 1$	$k_1 + 3 - 2c$	$2c + 2 - k_1$
$c = l + 1$	$k_1 - 1$	2	5
$l+2 \leq c \leq k_1 - 2$ (for $n \neq 14$)	$n + 2 - 2c$	$2c - k_1 - 2$	$2c + 2 - k_1$
$l+2 \leq c \leq k_1$ (for $n = 14$)	$n + 2 - 2c$	$2c - k_1 - 2$	$n + k_1 - 3 - 2c$
$k_1 - 1 \leq c \leq k_1$	$n + 2 - 2c$	$2c - k_1 - 2$	$n + k_1 - 3 - 2c$
$u_1 v_n$	1	$k_1 - 1$	$k_1 - 2$

Claim 1. The set W can contain at most one vertex from either X or Y . On contrary, let $x_1, x_i \in W$, then with out loss of generality, the third vertex of W is either from X or Y or U or V . Thus, we have following possibilities:

- (i) If $x_j \in W$, when $n \equiv 0, 1, 3 \pmod{4}$, then $c_W(u_{n-1}v_n) = c_W(u_n v_{n-1})$ when $2 \leq i \leq n-3, 3 \leq j \leq n-2$. For $n-3 \leq i \leq n-1, n-1 \leq j \leq n$, we have the following edges with same codes: $c_W(x_1 x_2) = c_W(x_1 u_1)$
- (ii) If $y_j \in W$, when $n \equiv 0, 1, 3 \pmod{4}$, then $c_W(u_{n-1}v_n) = c_W(u_n v_{n-1})$ when $2 \leq i \leq n-2, 1 \leq j \leq n-2$. For $n-1 \leq i \leq n, 1 \leq j \leq n-4$, the edges with same code: $c_W(u_{n-3}v_{n-2}) = c_W(u_{n-2}v_{n-3})$. Also when $n-1 \leq i \leq n, n-3 \leq j \leq n$, we have $c_W(u_2 v_3) = c_W(u_3 v_2)$.
- (iii) If $u_{2j-1} \in W$, when $n \equiv 0 \pmod{4}$ and $n \geq 16$, then $c_W(x_{n-1}x_n) = c_W(x_n u_n)$ when $2 \leq i \leq k-1, 1 \leq j \leq (k/2)$. For $2 \leq i \leq k-1, (k/2) + 1 \leq j \leq k, c_W(x_{k-1}u_{k-1}) = c_W(x_{k-1}x_k)$. When $i = k, 1 \leq j \leq (k/2)$, $c_W(x_k u_k) = c_W(x_k x_{k+1})$. $c_W(x_1 u_1) = c_W(x_n x_1)$ for $i = k, j = (k/2) + 1$. For $k \leq i \leq k+1, (k/2) + 2 \leq j \leq k$, we have $c_W(v_1 y_1) = c_W(y_1 y_2)$. For $i = k+1, j = 1$ and $j = (k/2) + 1$, we have $c_W(x_1 x_2) = c_W(x_n x_1)$. When $k+1 \leq i \leq n-1, 2 \leq j \leq (k/2)$, $c_W(v_1 y_1) = c_W(y_1 y_n)$. For $k+2 \leq i \leq n, (k/2) + 2 \leq j \leq k$ and $j = 1$, we have $c_W(x_{k+2}u_{k+2}) = c_W(x_{k+1}x_{k+2})$. When $i = k+2, j = (k/2) + 1$, the edges with same codes: $c_W(u_{k+1}v_k) = c_W(u_{k+1}v_{k+2})$. Also $c_W(x_{k+3}u_{k+3}) = c_W(x_{k+2}x_{k+3})$ when $k+3 \leq i \leq n, j = (k/2) + 1$.
- (iv) If $u_{2j} \in W$, when $n \equiv 0 \pmod{4}$ and $n \geq 16$, then $c_W(x_n x_1) = c_W(x_1 u_1)$ when $2 \leq i \leq k, 1 \leq j \leq (k/2)$. For $2 \leq i \leq k-1, (k/2) + 1 \leq j \leq k, c_W(x_{k+1}u_{k+1}) = c_W(u_{k+1}v_k)$. When $i = k, (k/2) + 1 \leq j \leq k, c_W(x_k$

$u_k) = c_W(x_{k+1}x_k)$. If $i = k+1, j = 1$, then $c_W(y_k y_{k+1}) = c_W(v_{k+1}y_{k+1})$. For $i = k+1, 2 \leq j \leq (k/2)$, the edges with same codes: $c_W(u_n v_1) = c_W(v_2 y_2)$. For $k+2 \leq i \leq n, 1 \leq j \leq (k/2)$ and $k+2 \leq i \leq n, (k/2) + 1 \leq j \leq k$, the edges having same codes: $c_W(x_{k+1}x_{k+2}) = c_W(x_{k+2}u_{k+2})$ and $c_W(x_1 x_2) = c_W(x_1 u_1)$ respectively.

- (v) If $v_{2j-1} \in W$, when $n \equiv 0 \pmod{4}$ and $n \geq 16$, then $c_W(v_{k+1}y_{k+1}) = c_W(y_k y_{k+1})$ for $2 \leq i \leq k-1, i = k+1, 1 \leq j \leq (k/2)$. When $2 \leq i \leq k-2, (k/2) + 1 \leq j \leq k, c_W(v_k y_k) = c_W(y_{k-1}y_k)$. If $3 \leq i \leq k+1, 2 \leq j \leq (k/2) + 1$, then $c_W(v_1 y_1) = c_W(y_1 y_2)$. For $k+3 \leq i \leq n, (k/2) + 2 \leq j \leq k$, the following edges have same codes: $c_W(v_{k+1}y_{k+1}) = c_W(y_{k+1}y_{k+2})$. If $k+2 \leq i \leq n, 2 \leq j \leq (k/2)$, then $c_W(x_{k+2}u_{k+2}) = c_W(x_{k+1}x_{k+2})$. When $k+2 \leq i \leq n-1, (k/2) + 1 \leq j \leq k$, then $c_W(v_1 y_1) = c_W(y_n y_1)$.
- (vi) If $v_{2j} \in W$, when $n \equiv 0 \pmod{4}$ and $n \geq 16$, then $c_W(u_{n-1}v_n) = c_W(v_n y_n)$ when $2 \leq i \leq k-1, 1 \leq j \leq (k/2) - 1$ and $j = k$. If $2 \leq i \leq k-1, 1 \leq j \leq (k/2)$, then $c_W(u_{k+1}v_k) = c_W(v_k y_k)$. For $2 \leq i \leq k-1, (k/2) \leq j \leq k-1$, we have $c_W(v_{n-1}y_{n-1}) = c_W(y_{n-1}y_n)$. If $2 \leq i \leq k, 1 \leq j \leq (k/2) - 1$, then $c_W(x_k u_k) = c_W(x_k x_{k+1})$. When $i = k, j = (k/2)$, the edges have same codes are: $c_W(u_{k-2}v_{k-1}) = c_W(x_{k+2}x_{k+3})$. If $3 \leq i \leq k+1, (k/2) + 1 \leq j \leq k$, then $c_W(v_1 y_1) = c_W(y_1 y_2)$. When $i = k+1$ and $k+3 \leq i \leq n, 1 \leq j \leq (k/2)$, then $c_W(v_{k+1}y_{k+1}) = c_W(y_{k+1}y_{k+2})$. For $k+1 \leq i \leq n-1, 1 \leq j \leq (k/2)$, $c_W(v_1 y_1) = c_W(y_1 y_n)$. If $i = k+2, j = (k/2) + 1$, then $c_W(x_{k-1}x_k) = c_W(u_{k+4}v_{k+3})$. For $k+2 \leq i \leq n, (k/2) + 2 \leq j \leq k$ and $k+3 \leq i \leq n, (k/2) + 1 \leq j \leq k$, the edges with same codes: $c_W(x_{k+1}x_{k+2}) = c_W(x_{k+2}u_{k+2})$ and $c_W(u_{k+1}v_{k+2}) = c_W(v_{k+2}y_{k+2})$, respectively.

Claim 2. The set W can contain at most one vertex either from U or V . Due to symmetry, it is enough to show that W contains at most one vertex from U . On contrary, let $u_1, u_j \in W$.

- (i) If $u_j \in W$, when $n \equiv 0, 1, 3 \pmod{4}$, then $c_W(x_{n-1}x_n) = c_W(y_{n-1}y_n)$ for $2 \leq i \leq n-3, 3 \leq j \leq n-2$. If $n-2 \leq i \leq n-1, n-1 \leq j \leq n$, then $c_W(x_2x_3) = c_W(y_2y_3)$.
- (ii) If $u_1, u_{2i-1}, y_j \in W$ and , when $n \equiv 0 \pmod{4}$ and $n \geq 16$, then $c_W(u_k v_{k+1}) = c_W(v_{k+1} y_{k+1})$ when $1 \leq i \leq (k/2) + 1, 1 \leq j \leq k-1$. If $1 \leq i \leq (k/2) + 1, 3 \leq j \leq k+1$, then $c_W(u_2 v_1) = c_W(v_1 y_1)$. If $1 \leq i \leq (k/2), k+2 \leq j \leq n$, then $c_W(x_k u_k) = c_W(x_k x_{k+1})$. When $(k/2) + 1 \leq i \leq k, k+1 \leq j \leq n-1$, then $c_W(u_n v_1) = c_W(y_1 v_1)$. For $i=1, (k/2) + 1 \leq i \leq k, j=1$ and $k+3 \leq j \leq n$, $c_W(u_{k+2} v_{k+1}) = c_W(v_{k+1} y_{k+1})$. If $(k/2) + 2 \leq i \leq k, 2 \leq j \leq k$, then $c_W(x_{k+2} u_{k+2}) = c_W(x_{k+1} x_{k+2})$.
- (iii) If $u_1, u_{2i}, y_j \in W$ and , when $n \equiv 0 \pmod{4}$ and $n \geq 16$, then $c_W(x_{k+1} x_{k+2}) = c_W(x_{k+1} u_{k+1})$ when $1 \leq i \leq (k/2), j=1$ and $k+3 \leq j \leq n$. If $1 \leq i \leq (k/2), 2 \leq j \leq k$, then $c_W(x_{k+1} u_{k+2}) = c_W(x_{k+2} u_{k+2})$. When $1 \leq i \leq (k/2) + 1, 4 \leq j \leq k+2$, then $c_W(v_2 y_2) = c_W(u_3 v_2)$. If $(k/2) + 1 \leq i \leq k, 1 \leq j \leq k-1$, then edges having same codes: $c_W(x_k x_{k+1}) = c_W(x_{k+1} u_{k+1})$. For $(k/2) + 1 \leq i \leq k, 3 \leq j \leq k+1$ and $(k/2) + 1 \leq i \leq k, k+2 \leq j \leq n$, then edges with same codes: $c_W(u_2 v_1) = c_W(v_1 y_1)$ and $c_W(x_k x_{k+1}) = c_W(x_k u_k)$, respectively.
- (iv) If $v_j \in W$, when $n \equiv 0, 1, 3 \pmod{4}$, then $c_W(x_{n-1} x_n) = c_W(y_n y_{n-1})$ for $2 \leq i \leq n-2, 1 \leq j \leq n-2$. If $n-1 \leq i \leq n, 1 \leq j \leq n-4$, then $c_W(x_{n-3} x_{n-2}) = c_W(y_{n-2} y_{n-3})$. For $n-2 \leq i \leq n, n-3 \leq j \leq n$, we have $c_W(x_2 x_3) = c_W(y_2 y_3)$.
- (v) If $u_1, u_{2i-1}, x_j \in W$ and when $n \equiv 0 \pmod{4}$ with $n \geq 16$, then $c_W(x_{n-1} x_n) = c_W(x_n u_n)$ when $2 \leq i \leq (k/2), 1 \leq j \leq k-1, j=n$. If $2 \leq i \leq (k/2), 1 \leq j \leq k$, then $c_W(x_k u_k) = c_W(x_k x_{k+1})$. For $2 \leq i \leq (k/2), k+1 \leq j \leq n-1$, we have $c_W(x_1 u_1) = c_W(u_1 v_n)$. If $(k/2) + 1 \leq i \leq k, 2 \leq j \leq k+1$, then edges with same codes: $c_W(u_n v_1) = c_W(v_1 y_1)$. For $2 \leq i \leq (k/2) + 1, k+2 \leq j \leq n$ and $(k/2) + 2 \leq i \leq k, j=1$ and $k+2 \leq j \leq n$, then we have $c_W(u_2 v_1) = c_W(v_1 y_1)$ and $c_W(x_{k+1} x_{k+2}) = c_W(x_{k+2} u_{k+2})$.
- (vi) If $u_1, u_{2i}, x_j \in W$, when $n \equiv 0 \pmod{4}$ and $n \geq 16$, then $c_W(u_{k+2} v_{k+3}) = c_W(x_k x_{k+1})$ for $i=1, j=1$ and $j=k+2$. If $1 \leq i \leq (k/2), 2 \leq j \leq k+1$, then $c_W(x_{k+1} u_{k+1}) = c_W(x_{k+1} x_{k+2})$. If $1 \leq i \leq (k/2), k+2 \leq j \leq n$, then the following edges have same codes: $c_W(x_{k+2} u_{k+2}) = c_W(x_{k+1} x_{k+2})$. For $2 \leq i \leq (k/2) + 1, 1 \leq j \leq 2, k+4 \leq j \leq n$, then $c_W(x_4 u_4) = c_W(u_4 v_3)$. If $(k/2) + 1 \leq i \leq k, 1 \leq j \leq k$, then $c_W(x_k u_k) = c_W(x_k x_{k+1})$. When $(k/2) + 1 \leq i \leq k, k+1 \leq j \leq n$, then $c_W(x_{k+1} u_{k+1}) = c_W(x_{k+1} x_k)$.

Claim 3. If $x_1, u_{2i-1}, y_j \in W$, when $n \equiv 0 \pmod{4}$ and $n \geq 16$, then $c_W(x_1 x_2) = c_W(x_1 x_n)$ for $i=1, 1 \leq j \leq 2$. If $i=1$ and $(k/2) + 2 \leq i \leq k, 2 \leq j \leq k$, then $c_W(y_{k+2} v_{k+2}) = c_W(u_{k+1} v_{k+2})$. If $i=1$ and $(k/2) + 3 \leq i \leq k, (k/2) \leq j \leq k+1$, then edges with same codes are: $c_W(x_{k+2} x_{k+3}) = c_W(u_{k+4} v_{k+3})$. When $1 \leq i \leq (k/2)$ and $k+2 \leq j \leq n$, then $c_W(v_k y_k) = c_W(u_{k+1} v_k)$. For $2 \leq i \leq (k/2), 1 \leq j \leq k$, we have $c_W(y_1 v_1) = c_W(y_n y_1)$. If $1 \leq i \leq (k/2), k \leq j \leq n-2$ and $j=n$, then $c_W(x_{n-1} x_n) = c_W(x_n u_n)$. Moreover, for $(k/2) + 1 \leq i \leq k, k+1 \leq j \leq n-1$ and $j=1$, $c_W(x_n x_1) = c_W(x_1 u_1)$, for $2 \leq i \leq (k/2) + 1, 2 \leq j \leq k$, $c_W(x_{k+1} u_{k+1}) = c_W(u_{k+1} v_{k+2})$ and for $(k/2) + 1 \leq i \leq k, k+2 \leq j \leq n$, $c_W(x_{k+1} u_{k+1}) = c_W(v_k u_{k+1})$.

- (i) If $x_1, u_{2i}, y_j \in W$, when $n \equiv 0 \pmod{4}$ and $n \geq 16$, then $c_W(x_n x_1) = c_W(x_1 u_1)$ for $1 \leq i \leq (k/2), k+1 \leq j \leq n-1$ and $j=1$. If $i=1, j=2$, the $c_W(u_2 v_1) = c_W(u_2 v_3)$. For $1 \leq i \leq (k/2) + 1, 3 \leq j \leq k+1$, we have following edges having same codes: $c_W(x_{k+2} u_{k+2}) = c_W(u_{k+2} v_{k+3})$. If $1 \leq i \leq (k/2) - 1, k+2 \leq j \leq n$, then $c_W(x_{k+1} u_{k+1}) = c_W(u_{k+1} v_k)$. If $2 \leq i \leq (k/2) + 1, 4 \leq j \leq k+2$ and $j=2$, then $c_W(x_2 x_3) = c_W(x_2 u_2)$. When $(k/2) \leq i \leq k-1, k \leq j \leq n-2$ and $j=n$, then $c_W(x_{n-1} x_n) = c_W(x_n u_n)$. For $(k/2) + 1 \leq i \leq k-1, 1 \leq j \leq k$, $c_W(v_1 y_1) = c_W(y_n y_1)$. If $(k/2) + 1 \leq i \leq k, k+2 \leq j \leq n$ and $j=k$, then $c_W(x_k u_k) = c_W(x_k x_{k+1})$. For $(k/2) + 1 \leq i \leq k, 3 \leq j \leq k+1$ and $j=1$, $c_W(x_1 x_2) = c_W(x_1 u_1)$ and for $(k/2) + 2 \leq i \leq k, 2 \leq j \leq k$, $c_W(x_{k+1} u_{k+1}) = c_W(u_{k+1} v_{k+2})$.
- (ii) If $u_1, v_{2i-1}, y_j \in W$, when $n \equiv 0 \pmod{4}$ and $n \geq 16$, then $c_W(u_1 v_n) = c_W(u_1 v_2)$ for $i=1$ and $j=1$. If $i=1$ and $(k/2) + 1 \leq i \leq k, 2 \leq j \leq k$, then $c_W(x_1 u_1) = c_W(u_1 v_n)$. For $i=1$ and $(k/2) + 2 \leq i \leq k, 3 \leq j \leq k+1$, the edges with same codes are: $c_W(u_2 v_1) = c_W(v_1 y_1)$. For $1 \leq i \leq (k/2) + 1$ and $k+2 \leq j \leq n$, $c_W(x_1 u_1) = c_W(u_1 v_2)$. When $2 \leq i \leq (k/2) + 1, k+3 \leq j \leq n$ and $j=1$, then $c_W(u_2 v_3) = c_W(v_3 y_3)$. For $2 \leq i \leq (k/2) + 2, 1 \leq j \leq 2$ and $k+4 \leq j \leq n$, we have $c_W(x_3 u_3) = c_W(u_3 v_4)$. If $2 \leq i \leq (k/2), 3 \leq j \leq k$, then $c_W(x_{k+1} x_{k+2}) = c_W(u_{k+2} v_{k+3})$. For $1 \leq i \leq (k/2), k+1 \leq j \leq n-1$, we have the following edges with same codes: $c_W(u_n v_1) = c_W(y_1 v_1)$. If $i=(k/2) + 1, j=k+1$, then $c_W(u_{k+1} v_k) = c_W(v_{k+2} u_{k+1})$. For $(k/2) + 2 \leq i \leq k, k+2 \leq j \leq n$, $c_W(v_k y_k) = c_W(u_{k+1} v_k)$ and for $(k/2) + 1 \leq i \leq k, 1 \leq j \leq k-1$, $c_W(u_k v_{k+1}) = c_W(y_{k+1} v_{k+1})$.
- (iii) If $u_1, v_{2i}, y_j \in W$, when $n \equiv 0 \pmod{4}$ and $n \geq 16$, then If $1 \leq i \leq (k/2) - 1$ and $i=k, 1 \leq j \leq k-2$ and $j=n$, then $c_W(x_{n-1} u_{n-1}) = c_W(u_{n-1} v_{n-2})$. For $1 \leq i \leq (k/2) - 1$ and $i=k, k \leq j \leq n-2$, we have $c_W(u_{n-1} v_n) = c_W(v_n y_n)$. When $1 \leq i \leq (k/2), k+2 \leq j \leq n$, then $c_W(v_k y_k) = c_W(u_{k+1} v_k)$. If $1 \leq i \leq (k/2), 2 \leq j \leq k$, then $c_W(x_1 u_1) = c_W(u_1 v_n)$. The edges $c_W(x_k x_{k+1}) = c_W(x_{k+1} x_{k+2})$ have same codes when $(k/2) \leq i \leq (k/2) + 1, j=1$. For $1 \leq i \leq (k/2)$ and $i=k+1 \leq j \leq n-1$, we have

- $c_W(x_k u_k) = c_W(u_k v_{k-1})$. If $(k/2) + 1 \leq i \leq k$, $2 \leq j \leq k$, then $c_W(v_{k+2} y_{k+2}) = c_W(u_{k+1} v_{k+2})$. For $i = (k/2) + 1$, $j = k + 1$, we have $c_W(x_{k-1} x_k) = c_W(u_{k+4} v_{k+3})$. When $(k/2) + 1 \leq i \leq k$, $k + 2 \leq j \leq n$, then $c_W(x_1 u_1) = c_W(u_1 v_2)$. For $(k/2) + 2 \leq i \leq k$ and $i = 1$, $1 \leq j \leq 2$ and $k + 4 \leq j \leq n$, $c_W(x_{k+3} u_{k+3}) = c_W(u_{k+3} v_{k+2})$ and for $(k/2) + 2 \leq i \leq k$ and $i = 1$, $4 \leq j \leq k + 2$, $c_W(u_3 v_2) = c_W(y_2 v_2)$.
- (iv) If $x_1, u_{2i-1}, v_{2j-1} \in W$, when $n \equiv 0 \pmod{4}$ and $n \geq 16$, then $c_W(x_2 u_2) = c_W(x_n u_n)$ when $i = j = 1$. If $(k/2) + 3 \leq i \leq k$, $i = 1$, $2 \leq j \leq (k/2)$, then $c_W(u_{k+1} v_{k+2}) = c_W(y_{k+2} y_{k+3})$. For $1 \leq i \leq (k/2)$, $(k/2) + 1 \leq j \leq k - 1$, we have $c_W(u_{n-1} v_n) = c_W(v_n y_n)$. The following edges $c_W(x_k u_k) = c_W(x_k x_{k+1})$ and $c_W(u_{n-2} v_{n-1}) = c_W(v_{n-1} y_{n-1})$ have same codes for $1 \leq i \leq (k/2)$, $(k/2) + 2 \leq j \leq k$ and when $i = j = k$, respectively.
- (v) If $x_1, u_{2i}, v_{2j} \in W$, when $n \equiv 0 \pmod{4}$ and $n \geq 16$, then $c_W(u_2 v_1) = c_W(u_2 v_3)$ for $i = j = 1$. If $(k/2) + 2 \leq i \leq k$ and $i = 1$, $2 \leq j \leq (k/2)$, then $c_W(x_{k+2} x_{k+3}) = c_W(x_{k+3} u_{k+3})$. When $1 \leq i \leq (k/2) + 1$, $(k/2) + 1 \leq j \leq k$, then $c_W(y_{k+2} v_{k+2}) = c_W(u_{k+1} v_{k+2})$. For $1 \leq i \leq (k/2) - 1$ and $i = k$, $(k/2) + 1 \leq j \leq (k/2) + 3$ and for $2 \leq i \leq (k/2) + 2$, $(k/2) + 2 \leq j \leq k$, these are the edges $c_W(x_{k-1} x_k) = c_W(x_{k-1} u_{k-1})$ and $c_W(u_{k+3} v_{k+4}) = c_W(v_{k+4} y_{k+4})$.
- (vi) If $x_1, u_{2i-1}, v_{2j} \in W$, when $n \equiv 0 \pmod{4}$ and $n \geq 16$, then $c_W(y_k v_k) = c_W(u_{k+1} v_k)$ when $1 \leq i \leq (k/2)$, and $1 \leq j \leq (k/2)$. If $(k/2) + 2 \leq i \leq k$ and $i = 1$, $(k/2) + 1 \leq j \leq k$, then $c_W(y_{k+2} v_{k+2}) = c_W(v_{k+2} u_{k+1})$. When $2 \leq i \leq (k/2) + 1$, $2 \leq j \leq (k/2) + 1$, then $c_W(x_3 u_3) = c_W(u_3 v_2)$. For $(k/2) \leq i \leq k - 1$, $(k/2) - 1 \leq j \leq k - 2$, $c_W(u_{n-3} v_{n-2}) = c_W(x_{n-3} u_{n-3})$ and for $(k/2) + 2 \leq i \leq k$ and $i = 1$, $(k/2) + 2 \leq j \leq k$ and $j = 1$, $c_W(u_3 v_2) = c_W(v_2 y_2)$.
- (vii) If $x_1, u_{2i}, v_{2j-1} \in W$, when $n \equiv 0 \pmod{4}$ and $n \geq 16$, then $c_W(y_{k-1} v_{k-1}) = c_W(u_k v_{k-1})$ for $1 \leq i \leq (k/2) - 1$ and $i = k$, $1 \leq j \leq (k/2)$. If $1 \leq i \leq (k/2) + 1$, $3 \leq j \leq (k/2) + 1$, then $c_W(u_3 v_2) = c_W(v_2 y_2)$. When $(k/2) + 2 \leq i \leq k$ and $i = 1$, $(k/2) + 2 \leq j \leq k$ and $j = 1$, then we have $c_W(u_{k+2} v_{k+3}) = c_W(v_{k+3} y_{k+3})$. For $i = k$ and $1 \leq i \leq (k/2) - 1$, $1 \leq j \leq (k/2)$, $c_W(y_{k-1} v_{k-1}) = c_W(v_{k-1} u_k)$ and when $(k/2) \leq i \leq k - 1$, $(k/2) \leq j \leq k - 1$, then $c_W(x_{n-2} u_{n-2}) = c_W(v_{n-1} u_{n-2})$.

Now, when $n \equiv 1, 3 \pmod{4}$, the remaining cases are as follows:

Claim 4. The set W can contain at most one vertex from either X or Y . On contrary, let $x_1, x_i \in W$, then with out loss of generality, the third vertex of W is either from X or Y or U or V . Thus, we have following possibilities: $c_W(x_{n-1} x_n) = c_W(x_n u_n)$ for $2 \leq i \leq k$, $1 \leq j \leq k$. If $2 \leq i \leq k$, $j = k + 1$ (when $n \equiv 1 \pmod{4}$), then $c_W(x_{k+1} x_{k+2}) = c_W(x_{k+1} u_{k+1})$. If $2 \leq i \leq k$, $j = k + 1$ when $n \equiv 3 \pmod{4}$, then $c_W(x_k x_{k+1}) = c_W(x_k u_k)$. For $i = k + 1$, $j = 1$, $j = k + 1$, then edges with same codes are: $c_W(y_1 y_2) = c_W(y_{n-1} y_n)$. When

$i = k + 1$, $2 \leq j \leq k$, then we have $c_W(u_2 v_1) = c_W(u_{n-1} v_n)$. If $k + 3 \leq i \leq n$, $j = 1$ when $n \equiv 1 \pmod{4}$, then $c_W(x_{k+2} x_{k+3}) = c_W(x_{k+3} u_{k+3})$ and if $k + 2 \leq i \leq n$, $j = 1$ when $n \equiv 3 \pmod{4}$, then $c_W(x_{k+1} x_{k+2}) = c_W(x_{k+2} u_{k+2})$. For $k + 2 \leq i \leq n$, $2 \leq j \leq k + 1$, edges having same codes are: $c_W(x_1 x_2) = c_W(x_1 u_1)$.

- (i) If $u_{2j} \in W$, when $n \equiv 1, 3 \pmod{4}$ and $n \geq 13$, then If $2 \leq i \leq k + 1$, $1 \leq j \leq k$, then edges with same codes are: $c_W(x_n x_1) = c_W(x_1 u_1)$. For $i = k + 2$, $j = 1$, $c_W(y_n y_1) = c_W(y_2 y_3)$. The edges $u_3 v_2$ and $u_n v_1$ have same codes when $i = k + 2$, $2 \leq j \leq k$. For $k + 3 \leq i \leq n$, $j = 1$ when $n \equiv 1 \pmod{4}$, $c_W(x_{k+1} x_{k+2}) = c_W(x_{k+2} u_{k+2})$ and for $k + 3 \leq i \leq n$, $j = 1$ when $n \equiv 3 \pmod{4}$, $c_W(x_{k+2} x_{k+3}) = c_W(x_{k+3} u_{k+3})$. Moreover, if $k + 3 \leq i \leq n$, $2 \leq j \leq k$, the edges having same codes are $x_2 x_3$ and $x_2 u_2$.
- (ii) If $v_{2j-1} \in W$, when $n \equiv 1, 3 \pmod{4}$ and $n \geq 13$, then $c_W(u_{n-2} v_{n-1}) = c_W(v_{n-1} y_{n-1})$ for $2 \leq i \leq k - 1$, $1 \leq j \leq k - 1$. If $2 \leq i \leq k - 1$, $j = k$, then $c_W(x_n x_1) = c_W(x_1 u_1)$. When $2 \leq i \leq k - 2$, $j = k + 1$, then edges having same codes are $v_{n-2} y_{n-2}$ and $y_{n-2} y_{n-1}$. If $k - 1 \leq i \leq k + 1$, $j = k + 1$, then we have $c_W(y_1 v_1) = c_W(y_1 y_2)$. For $k + 2 \leq i \leq n$, $1 \leq j \leq 2$ when $n \equiv 1 \pmod{4}$, then we have following edges with same codes $c_W(x_{k+1} x_{k+2}) = c_W(x_{k+2} u_{k+2})$ and for $k + 2 \leq i \leq n$, $1 \leq j \leq 2$ (when $n \equiv 3 \pmod{4}$), then $u_k v_{k+1}$ and $u_{k+3} v_{k+2}$ are the edges having same codes. If $i = k + 2$, $3 \leq j \leq k$, then $c_W(u_n v_1) = c_W(u_3 v_2)$. For $i = k + 2$, $j = k + 1$ and for $k + 3 \leq i \leq n$, $3 \leq j \leq k + 1$, it can be seen that, $c_W(u_k v_{k+1}) = c_W(u_{k+1} v_k)$ and $c_W(u_3 v_2) = c_W(v_2 y_2)$, respectively.
- (iii) If $v_{2j} \in W$, when $n \equiv 1, 3 \pmod{4}$ and $n \geq 13$, then $c_W(u_{n-1} v_n) = c_W(v_n y_n)$ for $2 \leq i \leq k$, $1 \leq j \leq k - 1$. If $2 \leq i \leq k - 1$ and $i = n$, $j = k$, then we have $c_W(u_{n-2} v_{n-1}) = c_W(y_{n-1} v_{n-1})$. When $2 \leq i \leq k + 1$, $j = k$, then the edges $c_W(x_{k+1} x_{k+2}) = c_W(x_{k+1} u_{k+1})$ have same codes with respect to W . If $i = k + 1$, $2 \leq j \leq k - 1$, $c_W(u_2 v_1) = c_W(u_{n-1} v_n)$. When $i = k + 1$, $j = 1$ and $n \equiv 1 \pmod{4}$, we have $c_W(u_k v_{k+1}) = c_W(u_{k+3} v_{k+2})$. When $i = k + 1$, $j = 1$ and $n \equiv 3 \pmod{4}$, then $c_W(x_{k+1} x_{k+2}) = c_W(x_{k+1} u_{k+1})$. If $k + 2 \leq i \leq n$, $2 \leq j \leq k$, then $c_W(x_1 u_1) = c_W(x_1 x_2)$. If $k + 2 \leq i \leq n - 1$, $1 \leq j \leq k$ and $i = n$, $1 \leq j \leq k - 1$, then $c_W(v_1 y_1) = c_W(y_n y_1)$ and $c_W(x_n u_n) = c_W(x_{n-1} x_n)$.

Claim 5. The set W contains at most one vertex either from U or V . Due to symmetry, it is enough to show that W contains at most one vertex from U . On the contrary, let $u_1, u_j \in W$.

- (i) If $u_1, u_{2i-1}, y_j \in W$ and , when $n \equiv 1, 3 \pmod{4}$ and $n \geq 13$, then $c_W(u_n v_{n-1}) = c_W(v_{n-1} y_{n-1})$ for $2 \leq i \leq k$, $1 \leq j \leq 2$. If $i = k + 1$, $1 \leq j \leq 2$ and when $n \equiv 1 \pmod{4}$, then $c_W(x_{k-1} x_k) = c_W(u_{k+1} v_k)$. For $i = k + 1$, $1 \leq j \leq 2$ and when $n \equiv 3 \pmod{4}$, then we have $c_W(x_{k-1} x_k) = c_W(u_k v_{k+1})$. If $2 \leq i \leq k +$

$1, 3 \leq j \leq k+1$, then $c_W(u_2v_1) = c_W(v_1y_1)$. When $2 \leq i \leq k+1, k+1 \leq j \leq n-2$, then edges having same codes are: $c_W(u_{n-1}v_n) = c_W(v_ny_n)$. For $2 \leq i \leq k-1, n-1 \leq j \leq n$, we have $c_W(u_{n-2}v_{n-3}) = c_W(v_{n-3}y_{n-3})$. If $k \leq i \leq k+1, n-1 \leq j \leq n$ when $n \equiv 1 \pmod{4}$ and if $k \leq i \leq k+1, n-1 \leq j \leq n$ when $n \equiv 3 \pmod{4}$, then we have $c_W(y_ky_{k+1}) = c_W(u_{k+2}v_{k+1})$ and $c_W(y_ky_{k+1}) = c_W(u_{k+1}v_{k+2})$, respectively.

(ii) If $u_1, u_{2i}, y_j \in W$ and, when $n \equiv 1, 3 \pmod{4}$ and $n \geq 13$, then For $1 \leq i \leq k, 4 \leq j \leq k+1$, we have $c_W(u_3v_2) = c_W(v_2y_2)$. If $1 \leq i \leq k, k+2 \leq j \leq n-1$, then $c_W(u_nv_1) = c_W(y_1v_1)$. When $2 \leq i \leq k, j = n$, then $c_W(x_1u_1) = c_W(u_1v_2)$. If $2 \leq i \leq k, j = 1$, $c_W(u_2v_3) = c_W(y_3v_3)$. For $i = 1, 1 \leq j \leq 2$ and $j = n$ when $n \equiv 1 \pmod{4}$, then we have $c_W(x_{k+3}x_{k+4}) = c_W(u_{k+2}v_{k+3})$. If $i = 1, 1 \leq j \leq 2$ and $j = n$ when $n \equiv 3 \pmod{4}$, then $c_W(x_{k+3}x_{k+4}) = c_W(u_{k+3}v_{k+2})$. When $1 \leq i \leq k-4, 2 \leq j \leq 3$ when $n \equiv 1 \pmod{4}$, then $c_W(u_{k+1}v_{k+2}) = c_W(y_{k+2}y_{k+3})$. For $1 \leq i \leq k-4, 2 \leq j \leq 3$ when $n \equiv 3 \pmod{4}$, then $c_W(u_{k+2}v_{k+1}) = c_W(y_{k+2}y_{k+3})$. Moreover, if $k-3 \leq i \leq k, 2 \leq j \leq 3$, then $c_W(u_4v_5) = c_W(v_5y_5)$.

(iii) If $u_1, u_{2i-1}, x_j \in W$ and, when $n \equiv 1, 3 \pmod{4}$ and $n \geq 13$, then for $2 \leq i \leq k, 1 \leq j \leq k$ and $j = n$, the edges having same codes are: $c_W(x_nu_n) = c_W(x_{n-1}x_n)$. If $2 \leq i \leq k, k+1 \leq j \leq n-1$, then $c_W(x_{n-1}x_n) = c_W(x_{n-1}u_{n-1})$. If $i = k+1, 1 \leq j \leq k$, then $c_W(v_ny_n) = c_W(u_{n-1}v_n)$. When $i = k+1, k+2 \leq j \leq n$ and $i = k+1, j = k+1$, the edges having same codes are: $c_W(v_1y_1) = c_W(u_2v_1)$ and $c_W(x_2u_2) = c_W(x_{n-1}u_{n-1})$, respectively.

(iv) If $u_1, u_{2i}, x_j \in W$, when $n \equiv 1, 3 \pmod{4}$ and $n \geq 13$, then $c_W(u_nv_1) = c_W(v_1y_1)$ when $i = 1, 2 \leq j \leq k+1$. If $i = 1, j = k+2$, then $c_W(x_nu_n) = c_W(x_3u_3)$. For $i = 1, k+3 \leq j \leq n$ and $j = 1$, then $c_W(u_3v_2) = c_W(v_2y_2)$. If $2 \leq i \leq k, 3 \leq j \leq k+2$ and $2 \leq i \leq k, 1 \leq j \leq 2$ and $k+3 \leq j \leq n$, then we have $c_W(x_2x_3) = c_W(x_3u_3)$ and $c_W(x_2x_3) = c_W(x_2u_2)$.

Claim 6. If $x_1, u_{2i-1}, y_j \in W$, when $n \equiv 1, 3 \pmod{4}$ and $n \geq 13$, then $c_W(x_{n-1}x_n) = c_W(x_nu_n)$ for $1 \leq i \leq k, k+1 \leq j \leq n-2$. When $k-1 \leq i \leq k+1, k+1 \leq j \leq n$ when $n \equiv 1 \pmod{4}$, then $c_W(y_ky_{k+1}) = c_W(y_{k+1}v_{k+1})$. If $k-2 \leq i \leq k+1, k \leq j \leq n-1$ when $n \equiv 3 \pmod{4}$, then $c_W(y_{k-1}y_k) = c_W(y_kv_k)$. For $2 \leq i \leq k, 1 \leq j \leq k+1$, we have $c_W(v_1y_1) = c_W(y_ny_1)$. If $i = 1, 3 \leq j \leq k+1$ when $n \equiv 1 \pmod{4}$, then $c_W(x_{k+2}x_{k+3}) = c_W(u_{k+3}v_{k+4})$ and when $i = 1, 3 \leq j \leq k+1$ when $n \equiv 3 \pmod{4}$, then $c_W(x_{k+2}x_{k+3}) = c_W(u_{k+4}v_{k+3})$. When $n \equiv 1 \pmod{4}$ and $1 \leq i \leq k-3, n-1 \leq j \leq n$, the edges are $c_W(x_{k+1}x_{k+2}) = c_W(u_kv_{k+1})$. When $n \equiv 3 \pmod{4}$ and $1 \leq i \leq k-3, n-1 \leq j \leq n$, the edges with same codes are: $c_W(y_{k+1}v_{k+1}) = c_W(u_{k+2}v_{k+1})$. If $n \equiv 1 \pmod{4}$ and $i = k-2, n-1 \leq j \leq n$, then $c_W(x_{k+1}u_{k+1}) = c_W(u_{k+1}v_k)$. When $n \equiv 3 \pmod{4}$ and $k-2 \leq i \leq k+1, n-1 \leq j \leq n$, then $c_W(u_kv_{k+1}) = c_W(x_{k+1}x_{k+2})$. For

$i = 1, 1 \leq j \leq 2$ and $i = 1, j = 3$, $c_W(u_nv_1) = c_W(u_2v_1)$ and $c_W(x_{k+2}x_{k+3}) = c_W(u_{k+3}v_{k+4})$.

(i) If $x_1, u_{2i}, y_j \in W$, when $n \equiv 1, 3 \pmod{4}$ and $n \geq 13$, then if $1 \leq i \leq k, k+2 \leq j \leq n-1$, then $c_W(x_nx_1) = c_W(x_1u_1)$. When $1 \leq i \leq k-1, k \leq j \leq k+1$, then $c_W(v_{n-1}y_{n-1}) = c_W(y_{n-1}y_n)$. For $3 \leq i \leq k, 4 \leq j \leq k+1$, we have $c_W(y_3y_4) = c_W(y_4v_4)$. If $1 \leq i \leq k-2, 2 \leq j \leq k-1$ when $n \equiv 1 \pmod{4}$, then we have $c_W(y_{k+2}v_{k+2}) = c_W(u_{k+1}v_{k+2})$. When $n \equiv 3 \pmod{4}$ and $1 \leq i \leq k-2, 2 \leq j \leq k-1$, then $c_W(y_{k+3}v_{k+3}) = c_W(u_{k+2}v_{k+3})$. If $k-1 \leq i \leq k, 3 \leq j \leq k-1$, then $c_W(u_{k+2}v_{k+3}) = c_W(y_{k+3}v_{k+3})$. For $2 \leq i \leq k, j = 1$ and $j = n$, $c_W(y_1v_1) = c_W(y_1y_2)$. When $2 \leq i \leq k, j = 2$, then $c_W(x_2u_2) = c_W(x_2x_3)$. For $i = 1, j = n$ when $n \equiv 1 \pmod{4}$ and $i = 1, j = n$ when $n \equiv 3 \pmod{4}$, $c_W(y_{k+1}v_{k+1}) = c_W(u_{k+2}v_{k+1})$ and $c_W(u_kv_{k+1}) = c_W(x_{k+1}x_{k+2})$.

(ii) If $u_1, v_{2i-1}, y_j \in W$, when $n \equiv 1, 3 \pmod{4}$ and $n \geq 13$, then If $1 \leq i \leq k+1, k+2 \leq j \leq n$, then $c_W(x_1u_1) = c_W(u_1v_2)$. If $3 \leq i \leq k+1, 4 \leq j \leq k+1$, then $c_W(u_3v_2) = c_W(v_2y_2)$. For $3 \leq i \leq k+1, 1 \leq j \leq 3$, we have $c_W(v_3y_3) = c_W(y_3y_4)$. When $n \equiv 1 \pmod{4}$ and $1 \leq i \leq 2, 1 \leq j \leq k$, then $c_W(x_{k+1}x_{k+2}) = c_W(x_{k+2}u_{k+2})$ and when $1 \leq i \leq 3, 1 \leq j \leq k-1$ and $n \equiv 3 \pmod{4}$, then $c_W(u_{k+1}v_{k+2}) = c_W(x_kx_{k+1})$. If $i = 1, k \leq j \leq k+1$ and $n \equiv 3 \pmod{4}$, then the edges with same codes are: $c_W(x_1u_1) = c_W(u_1v_n)$ and if $i = 2, k \leq j \leq k+1$ and $n \equiv 3 \pmod{4}$, then $c_W(x_{k+2}x_{k+3}) = c_W(u_{k+4}v_{k+3})$. For $n \equiv 1 \pmod{4}$ and $i = 1, j = k-2$ and when $n \equiv 1 \pmod{4}$ and $i = 2, j = k+1$, the edges having same codes are: $c_W(x_1u_1) = c_W(u_1v_n)$ and $c_W(x_{k+2}x_{k+3}) = c_W(u_{k+3}v_{k+4})$.

(iii) If $u_1, v_{2i}, y_j \in W$, when $n \equiv 1, 3 \pmod{4}$ and $n \geq 13$, then for $1 \leq i \leq k, 2 \leq j \leq k+1$, $c_W(x_1u_1) = c_W(u_1v_n)$. If $1 \leq i \leq k-1, k+2 \leq j \leq n-2$, then $c_W(u_{n-1}v_n) = c_W(v_ny_n)$. When $i = k, k+2 \leq j \leq n-1$, then $c_W(u_kv_{k-1}) = c_W(x_kx_{k+1})$. For $1 \leq i \leq k-1, j = 1$ and $n-1 \leq j \leq n$, the edges with same codes are: $c_W(v_{n-1}y_{n-1}) = c_W(y_{n-2}y_{n-1})$. If $i = k, j = 1, n$, then $c_W(x_{n-1}u_{n-1}) = c_W(u_{n-1}v_{n-2})$.

(iv) If $x_1, u_{2i-1}, v_{2j} \in W$, when $n \equiv 1, 3 \pmod{4}$ and $n \geq 13$, then $c_W(u_3v_2) = c_W(v_2y_2)$ if $1 \leq i \leq k, 3 \leq j \leq k+1$. For $i = 1, j = k$, $c_W(x_{n-2}x_{n-1}) = c_W(v_1u_2)$. For $2 \leq i \leq k+1, j = k$, $c_W(x_1u_1) = c_W(x_1x_2)$.

(v) If $x_1, u_{2i}, v_{2j-1} \in W$, when $n \equiv 1, 3 \pmod{4}$ and $n \geq 13$, then If $1 \leq i \leq k, 3 \leq j \leq k+1$, then we have $c_W(u_3v_2) = c_W(v_2y_2)$. For $1 \leq i \leq k, 1 \leq j \leq 2$, $c_W(u_{n-2}v_{n-1}) = c_W(v_{n-1}y_{n-1})$.

(vi) If $x_1, u_{2i-1}, v_{2j-1} \in W$, when $n \equiv 1, 3 \pmod{4}$ and $n \geq 13$, then $c_W(v_{n-4}y_{n-4}) = c_W(u_{n-5}v_{n-4})$ for $1 \leq i \leq k-1, k-1 \leq j \leq k+1$. if $n \equiv 1 \pmod{4}$ and $k-2 \leq i \leq k+1, 1 \leq j \leq k-2$, then $c_W(v_{k+1}y_{k+1}) = c_W(v_{k+1}u_{k+2})$. When $n \equiv 3 \pmod{4}$ and $k-2 \leq i \leq k+1, 1 \leq j \leq k-3$, then $c_W(v_kv_k) = c_W(v_ku_{k+1})$. When $n \equiv 1 \pmod{4}$ and $i = k+1, k-1 \leq i \leq k+1$, then $c_W(x_{k+1}x_{k+2}) = c_W(u_kv_{k+1})$. If $n \equiv 3 \pmod{4}$

and $i = k + 1, k - 1 \leq i \leq k + 1$, then $c_W(x_{k+1}x_{k+2}) = c_W(u_{k+1}v_k)$.

(vii) If $x_1, u_{2i}, v_{2j} \in W$ and $n \equiv 1, 3 \pmod{4}$ with $n \geq 13$: for $n \equiv 1 \pmod{4}$ and $1 \leq i \leq k - 2, k - 2 \leq j \leq k$, we have $c_W(v_{k+3}y_{k+3}) = c_W(v_{k+3}u_{k+2})$. Whenever $1 \leq i \leq k - 2, k - 2 \leq j \leq k$, and $c_W(v_{k+1}y_{k+1}) = c_W(v_{k+1}u_{k+2})$. Whenever $k - 3 \leq i \leq k, j \leq k - 3$. For $n \equiv 1, 3 \pmod{4}$ and $i = k, k - 2 \leq j \leq k$, we have $c_W(x_kx_{k+1}) = c_W(u_{k-1}v_k)$ $c_W(x_kx_{k+1}) = c_W(u_kv_{k-1})$, $c_W(v_{k+3}y_{k+3}) = c_W(v_{k+3}u_{k+2})$. If $k - 3 \leq i \leq k, 1 \leq j \leq k - 3$, then $c_W(v_{k+1}y_{k+1}) = c_W(v_{k+1}u_{k+2})$.

For $n \equiv 1 \pmod{4}$ and $i = k, k - 2 \leq i \leq k$ and for $n \equiv 3 \pmod{4}$ and $i = k, k - 2 \leq i$, $c_W(x_kx_{k+1}) = c_W(u_{k-1}v_k)$ $c_W(x_kx_{k+1}) = c_W(u_kv_{k-1})$.

From all these claims, it yields that there is no such edge resolving set W for $DGP(n, 1)$. Therefore $\beta_e(DGP(n, 1)) \geq 4$.

From Lemmas 1–6, we have the following main result:

Theorem 1. For $n \geq 13$, we have

$$\beta_e(DGP(n, 1)) = \begin{cases} 3, & \text{when } n \equiv 2 \pmod{4}, \\ 4, & \text{otherwise.} \end{cases} \quad (2)$$

5. Conclusion

In this study, a family of double generalized Petersen graph $DGP(n, 1)$ has been considered in the context of edge resolvability. It has been investigated that minimum 4 vertices perform the edge resolvability in $DGP(n, 1)$ when $n \equiv 0, 1, 2 \pmod{4}$ and minimum 3 vertices perform the edge resolvability in $DGP(n, 1)$ when $n \equiv 2 \pmod{4}$.

Data Availability

All the required data are available within the article.

Conflicts of Interest

The authors declare that there are no conflicts of interests regarding the publication of this paper.

References

- [1] P. J. Slater, "Leaves of trees, proceeding of the 6th south-eastern conference on combinatorics, graph theory, and computing," *Congressus Numerantium*, vol. 14, pp. 549–559, 1975.
- [2] F. Harary and R. A. Melter, "On the metric dimension of a graph," *Ars Combinatoria*, vol. 2, pp. 191–195, 1976.
- [3] F. E. Alsaadi, M. Salman, F. Ali et al., "An algorithmic approach to compute the metric index of chordal ring networks," *IEEE Access*, vol. 8, pp. 80427–80436, 2020.
- [4] I. Khalid, F. Ali, and M. Salman, "On the metric index of circulant networks-an algorithmic approach," *IEEE Access*, vol. 7, pp. 58595–58601, 2019.
- [5] S. Khuller, B. Raghavachari, and A. Rosenfeld, "Landmarks in graphs," *Discrete Applied Mathematics*, vol. 70, no. 3, pp. 217–229, 1996.
- [6] G. Chartrand, L. Eroh, M. A. Johnson, and O. R. Oellermann, "Resolvability in graphs and the metric dimension of a graph," *Discrete Applied Mathematics*, vol. 105, no. 1–3, pp. 99–113, 2000.
- [7] G. Chartrand, C. Poisson, and P. Zhang, "Resolvability and the upper dimension of graphs," *Computers & Mathematics with Applications*, vol. 39, no. 12, pp. 19–28, 2000.
- [8] M. Johnson, "Structure-activity maps for visualizing the graph variables arising in drug design," *Journal of Biopharmaceutical Statistics*, vol. 3, no. 2, pp. 203–236, 1993.
- [9] J. Cáceres, C. Hernando, M. Mora et al., "On the metric dimension of Cartesian product of graphs," *SIAM Journal on Discrete Mathematics*, vol. 21, no. 2, pp. 423–441, 2007.
- [10] A. Kelenc, N. Tratnik, and I. G. Yero, "Uniquely identifying the edges of a graph: the edge metric dimension," *Discrete Applied Mathematics*, vol. 251, pp. 204–220, 2018.
- [11] A. Kelenc, D. Kuziak, A. Taranenko, and I. G. Yero, "Mixed metric dimension of graphs," *Applied Mathematics and Computation*, vol. 314, pp. 429–438, 2017.
- [12] I. G. Yero, "Vertices, edges, distances and metric dimension in graphs," *Electronic Notes in Discrete Mathematics*, vol. 55, pp. 191–194, 2016.
- [13] I. Peterin and I. G. Yero, "Edge metric dimension of some graph operations," *Bulletin of the Malaysian Mathematical Sciences Society*, vol. 43, 2019.
- [14] N. Zubrilina, "On the edge dimension of a graph," *Discrete Mathematics*, vol. 341, no. 7, pp. 2083–2088, 2018.
- [15] M. Azeem and M. F. Nadeem, "Metric-based resolvability of polycyclic aromatic hydrocarbons," *The European Physical Journal Plus*, vol. 136, 2021.
- [16] B. Deng, M. F. Nadeem, and M. Azeem, "On the edge metric dimension of different families of möbius networks," *Mathematical Problems in Engineering*, vol. 2021, Article ID 6623208, 9 pages, 2021.
- [17] M. Knor, S. Majstorovic, A. T. M. Toshi, R. Škrekovski, and I. G. Yero, "Graphs with the edge metric dimension smaller than the metric dimension," *Applied Mathematics and Computation*, vol. 401, 2021.
- [18] A. N. A. Koam, A. Ahmad, M. Ibrahim, and M. Azeem, "Edge metric and fault-tolerant edge metric dimension of hollow coronoid," *Mathematics*, vol. 9, 2021.
- [19] M. F. Nadeem, M. Hassan, M. Azeem et al., "Application of resolvability technique to investigate the different polyphenyl structures for polymer industry," *Journal of Chemistry*, vol. 2021, 2021.
- [20] Z. Shao, H. Jiang, Z. Li, and J. Zerovnik, "Discharging approach for double roman domination in graphs," *IEEE Access*, vol. 6, 2018.
- [21] V. Filipović, A. Kartelj, and J. Kratica, "Edge metric dimension of some generalized Petersen graphs," *Results in Mathematics*, vol. 74, no. 182, 2019.
- [22] R. C. Brigham, G. Chartrand, R. D. Dutton, and P. Zhang, "Resolving domination in graphs," *Mathematica Bohemica*, vol. 128, no. 1, pp. 25–36, 2003.
- [23] R. F. Bailey and P. J. Cameron, "Base size, metric dimension and other invariants of groups and graphs," *Bulletin of the London Mathematical Society*, vol. 43, no. 2, pp. 209–242, 2011.

- [24] G. Chartrand, V. Saenpholphat, and P. Zhang, "The independent resolving number of a graph," *Mathematica Bohemica*, vol. 128, no. 4, pp. 379–393, 2003.
- [25] G. Chartrand, E. Salehi, and P. Zhang, "The partition dimension of a graph," *Aequationes Mathematicae*, vol. 59, no. 1-2, pp. 45–54, 2000.
- [26] R. A. Melter and I. Tomescu, "Metric bases in digital geometry," *Computer Vision, Graphics, and Image Processing*, vol. 25, no. 1, pp. 113–121, 1984.
- [27] R. Nasir, Z. Zahid, and S. Zafar, "Edge metric dimension of graphs," *Ars Combinatoria*, vol. 147, 2018.
- [28] F. Okamoto, B. Phinezy, and P. Zhang, "The local metric dimension of a graph," *Mathematica Bohemica*, vol. 135, no. 3, pp. 239–255, 2010.
- [29] O. R. Oellermann and J. Peters-Fransen, "The strong metric dimension of graphs and digraphs," *Discrete Applied Mathematics*, vol. 155, no. 3, pp. 356–364, 2007.

Research Article

Comparative Study of Generalized Sum Graphs via Degree-Based Topological Indices

Muhammad Javaid ¹, Saira Javed,¹ and Ebenezer Bonyah ²

¹Department of Mathematics, School of Science, University of Management and Technology, Lahore 54 770, Pakistan

²Department of Mathematics Education, Akenten Appiah-Menka University of Skills Training and Entrepreneurial Development, Kumasi 00233, Ghana

Correspondence should be addressed to Ebenezer Bonyah; ebbonya@gmail.com

Received 17 September 2021; Accepted 3 January 2022; Published 14 February 2022

Academic Editor: Muhammad Imran

Copyright © 2022 Muhammad Javaid et al. This is an open access article distributed under the Creative Commons Attribution License, which permits unrestricted use, distribution, and reproduction in any medium, provided the original work is properly cited.

In theoretical chemistry, topological indices (TIs) have important role to predict various physical and structural properties of the study under molecular graphs. Among all topological indices, Zagreb-type indices have been used more effectively in the chemical literature. In this paper, we have computed first Zagreb, second Zagreb, forgotten, and hyper Zagreb indices of the generalized Q-sum graph $(H_{1(Q_\alpha)}[H_2])$ in the form of different TIs of its basic graphs, where $\alpha \geq 1$ is a positive integer. This family of graphs is obtained by the lexicographic product of the graph $Q_\alpha(H_1)$ and H_2 , where $Q_\alpha(H_1)$ is constructed with the help of the generalized line superposition operation Q_α on H_1 . As a conclusion, we also checked the correlation between predefined graph $H_1[H_2]$ under the operation of lexicographic product H_1 and H_2 with newly defined generalized Q-sum graphs $(H_{1(Q_\alpha)}[H_2])$ using linear regression models of various degree-based TIs.

1. Introduction and Preliminaries

In the computing analysis of chemical compounds, the chemical structural formulas are usually represented by graphs. Mathematically, for a graph H , the vertex and edge sets are denoted by $V(H)$ and $E(H) \subseteq V(H) \times V(H)$, respectively. The degree of the vertex $z \in V(H)$ (denoted by $d(z)$) is the number of incident edges on it. The distance between any two vertices z and y in $V(H)$ is denoted by $d(z, y)$ and defined as the number of edges in a shortest path existing between the vertices z and y . Thoroughly, the graph H is considered as a finite and simple graph.

The subject of chemical graph theory has many applications in chemistry. In a chemical graph, a vertex and an edge correspond to an atom and a chemical bond between them, respectively. A topological index is a function which presents a chemical graph in the form of a numerical number that is used to model the chemical and physical properties of molecules in quantitative structure property and activity relationships.

For a molecular graph H , the first Zagreb index $M_1(H)$ and second Zagreb index $M_2(H)$ are firstly considered by Gutman and Trinajstić [1] in 1972 to study the total π electron energy of the molecular graph H which are defined as follows:

$$\begin{aligned} M_1(H) &= \sum_{z \in V(H)} d^2(z) = \sum_{zy \in E(H)} [d(z) + d(y)], \\ M_2(H) &= \sum_{zy \in E(H)} [d(z) \times d(y)]. \end{aligned} \quad (1)$$

In 2015, forgotten index (F index) is defined as follows [2]:

$$F(H) = \sum_{z \in V(H)} d^3(z) = \sum_{zy \in E(H)} [d^2(z) + d^2(y)]. \quad (2)$$

In 2005, the first general Zagreb index is defined as follows [3]:

$$M_1^{\beta+1}(H) = \sum_{z \in V(H)} d^{\beta+1}(z) = \sum_{zy \in E(H)} [d^\beta(z) + d^\beta(y)]. \quad (3)$$

The concept of the general randic index (GRI) is defined by Bollobas and Erdos as

$$R_\beta(H) = \sum_{zy \in E(H)} [d(z) \times d(y)]^\beta. \quad (4)$$

In 2013, hyper Zagreb index is defined by Shirdel et al. as follows [4]:

$$HM(H) = \sum_{zy \in E(H)} [d(z) + d(y)]^2. \quad (5)$$

For more studies, we refer to [5]. In particular, we can find the results of TIs for various families of graphs such as nanosheets & nanostars dendrimers [6, 7], hex-derived networks [8], benzene networks [9, 10], and cellulose networks [11]. In addition, for the studies of the complex graphs, operations on graphs play a key role, where the original graphs are called the factors of the newly constructed graph under operations [12].

Yan et al. [13] defined the line superposition operation Q_1 related to the subdivision of H and computed the Wiener index of this derived graph $Q_1(H)$, where $Q_1(H)$ is obtained by inserting one new vertex in every edge of H and joining those pairs of new vertices by edges which have common adjacent (original) vertices (see Figure 1). Liu et al. extended this operation for any integral value of $\alpha \geq 1$ and obtained the generalized line superposition graph $Q_\alpha(H)$ from the graph H by inserting α vertices in each edge and joining those pairs of new vertices by edges which have common adjacent (original) vertices [14] (see Figures 2 and 3).

Taeri et al. [15] constructed the Q_1 -sum graph by Cartesian product of $Q_1(H_1)$ and H_2 , where $Q_1(H_1)$ is a line superposition graph, and H_1 and H_2 are assumed to be two connected graphs. Also, they computed the Wiener index of Q_1 -sum graph. Whereas, Chu et al. [16], Deng et al. [17], Akhter et al. [18], and Liu et al. [14] calculated the different indices of Q_1 -sum graph $(H_{1(Q_1)} + H_2)$ based on the Cartesian product. Recently, Liu et al. [19] extended this operation for any integral value of k and obtained the generalized line superposition graph $Q_k(H_1)$ of the graph H_1 . Moreover, they constructed the generalized Q -sum graph $(H_{1(Q_k)} + H_2)$ and computed their Zagreb indices. Javaid et al. [20] constructed the generalized Q -sum graph based on strong product and computed its first and second Zagreb indices.

The composition or lexicographic product of two connected graphs H_1 and H_2 , which is denoted by $H_1[H_2]$, is a graph such that the set of vertices is $V(H_1) \times V(H_2)$, and two vertices (z_1, y_1) and (z_2, y_2) will be adjacent in $H_1[H_2]$ if $[z_1 = z_2, \text{ and } y_1 \text{ is adjacent to } y_2]$ or $[z_1 \text{ is adjacent to } z_2, \text{ and } y_1 \text{ is adjacent to } y_2]$.

Sarala et al. [21], De [22], Pattabiraman [23], Pattabiraman and Santhakumar [24], and Suresh and Devi [25] have computed different degree-related Zagreb indices for the graphs based on line superposition operation and lexicographic product.

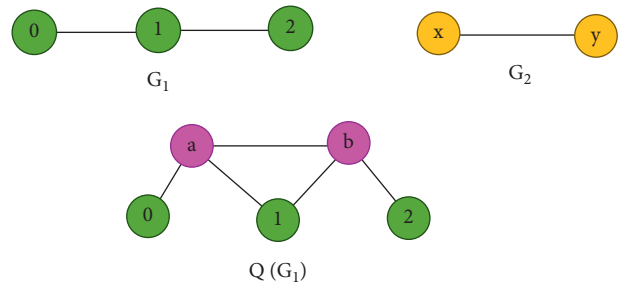


FIGURE 1: Line superposition operation for P_3 denoted by $Q_1(P_3)$.

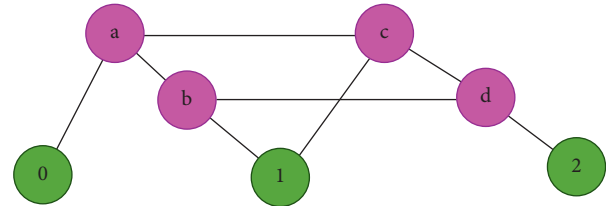


FIGURE 2: Generalized line superposition operation for P_3 and $\alpha = 2$ denoted by $Q_2(P_3)$.

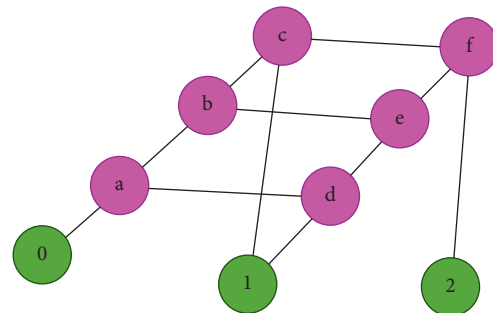


FIGURE 3: Generalized line superposition operation for P_3 for $\alpha = 3$ denoted by $Q_3(P_3)$.

(1) Q_α -sum: let H_1 and H_2 be two graphs; first, we apply generalized line superposition operation on H_1 to get $Q_\alpha(H_1)$ graph. Then, we take lexicographic product between $Q_\alpha(H_1)$ and H_2 to get Q_α -Sum graph denoted by $H_{1(Q_\alpha)}[H_2]$. Q_α -sum graph having vertex-set

$$\begin{aligned} V(H_{1(Q_\alpha)}[H_2]) &= V(Q_\alpha(H_1)) \times V(H_2) \\ &= (V(H_1) \cup \alpha(E(H_1))) \times V(H_2), \end{aligned} \quad (6)$$

such that two vertices (z_1, y_1) and (z_2, y_2) of $V(H_{1(Q_\alpha)}[H_2])$ are adjacent if $[z_1 = z_2 \text{ in } V(H_1), \text{ and } y_1 \text{ is adjacent to } y_2 \text{ in } E(H_2)]$ or $[z_1 \text{ is adjacent to } z_2 \text{ in } E(Q_\alpha(H_1)), \text{ and } y_1 \text{ is adjacent to } y_2 \text{ in } E(H_2)]$, where $\alpha \geq 1$ is a positive integer (see Figure 4).

To check the correlation between the predefined lexicographic product of two simple graphs $(H_1[H_2])$ and newly defined Q_α -sum graphs $(H_{1(Q_\alpha)}[H_2])$, one may use the linear regression when having a linear relationship between the dependent variable $(X = H_1[H_2])$ and the independent variable $(Y = H_{1(Q_\alpha)}[H_2])$. For further studies related to operations and graph products, the readers are referred to

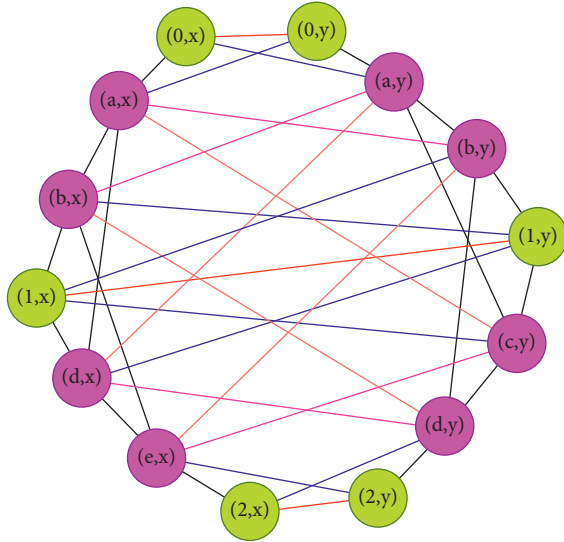


FIGURE 4: Generalized Q_α -sum graph $H_{1(Q_\alpha)}[H_2]$ for $P_{3(Q_3)}[P_2]$.

[26–29]. In this paper, we have used the generalized line superposition operation to construct a new generalized line

superposition graph $Q_\alpha(H_1)$ from the graph actual graph H_1 . Then, we have constructed a Q_α -sum graph based on the lexicographic product of $Q_\alpha(H_1)$ and H_2 , denoted by $H_{1(Q_\alpha)}[H_2]$. Moreover, we have computed the first Zagreb, second Zagreb, forgotten, and hyper Zagreb indices of $H_{1(Q_\alpha)}[H_2]$ in terms of its factor graphs H_1 and H_2 . We have extended this work by constructing linear regression models between $(H_1[H_2])$ and Q_α -sum graphs $(H_{1(Q_\alpha)}[H_2])$ via foresaid degree-based TIs.

2. Main Results

This section covers the main results.

Theorem 1. Let H_1 and H_2 be two connected graphs such that $|V(H_1)|, |V(H_2)| \geq 4$. For $\alpha \geq 1$,

$$M_1(H_{1(Q_\alpha)}[H_2]) = 8|V(H_2)||E(H_1)||E(H_2)| + 3|V(H_2)|^3 M_1(H_1) + |V(H_1)|M_1(H_2) + 2(\alpha - 1)|V(H_2)|^2 M_1(H_1) + (\alpha)|V(H_2)|^3 [M_3(H_1) + 2M_2(H_1) - 2M_1(H_1)]. \tag{7}$$

Proof.

$$\begin{aligned} M_1(H_{1(Q_\alpha)}[H_2]) &= \sum_{(z_1, y_1)(z_2, y_2) \in E(H_{1(Q_\alpha)}[H_2])} [d(z_1, y_1) + d(z_2, y_2)] \\ &= \sum_{z \in V(H_1)} \sum_{y_1, y_2 \in E(H_2)} [d(z, y_1) + d(z, y_2)] + \sum_{y_1 \in V(H_2)} \sum_{y_2 \in V(H_2)} \sum_{z_1, z_2 \in E(Q_\alpha(H_2))} [d(z_1, y_1) + d(z_2, y_2)] \\ &= \sum_A + \sum_B. \end{aligned} \tag{8}$$

Now,

$$\begin{aligned} \sum_A &= \sum_{z \in V(H_1)} \sum_{y_1, y_2 \in E(H_2)} [d(z, y_1) + d(z, y_2)] = \sum_{z \in V(H_1)} \sum_{y_1, y_2 \in E(H_2)} [2|V(H_2)|d_{H_1}(z) + d_{H_2}(y_1) + d_{H_2}(y_2)] \\ &= 4|V(H_2)||E(H_1)||E(H_2)| + |V(H_1)|M_1(H_2), \\ \sum_B &= \sum_{y_1 \in V(H_2)} \sum_{y_2 \in V(H_2)} \sum_{z_1, z_2 \in E(Q_\alpha(H_1))} [d(z_1, y_1) + d(z_2, y_2)] \end{aligned}$$

$$\begin{aligned}
&= \sum_{y_1 \in V(H_2)} \sum_{y_2 \in V(H_2)} \sum_{\substack{z_1 z_2 \in E(Q_\alpha(H_1)) \\ z_1 \in V(H_1) \\ z_2 \in V(Q_\alpha(H_1)) - V(H_1)}} [d(z_1, y_1) + d(z_2, y_2)] + \sum_{y \in V(H_2)} \sum_{\substack{z_1 z_2 \in E(Q_\alpha(H_1)) \\ z_1 z_2 \in V(Q_\alpha(H_1)) - V(H_1)}} [d(z_1, y) + d(z_2, y)] \\
&+ \sum_{y_1 \in V(H_2)} \sum_{y_2 \in V(H_2)} \sum_{\substack{z_1 z_2 \in E(Q_\alpha(H_1)) \\ z_1 z_2 \in V(Q_\alpha(H_1)) - V(H_1)}} [d(z_1, y_1) + d(z_2, y_1)] = \sum_{B_1} + \sum_{B_2} + \sum_{B_3}, \\
\sum_{B_1} &= \sum_{y_1 \in V(H_2)} \sum_{y_2 \in V(H_2)} \sum_{\substack{z_1 z_2 \in E(Q_\alpha(H_1)) \\ z_1 \in V(H_1) \\ z_2 \in V(Q_\alpha(H_1)) - V(H_1)}} [d(z_1, y_1) + d(z_2, y_2)] \\
&= \sum_{y_1 \in V(H_2)} \sum_{y_2 \in V(H_2)} \sum_{\substack{z_1 z_2 \in E(Q_\alpha(H_2)) \\ z_1 \in V(H_1) \\ z_2 \in V(Q_\alpha(H_1)) - V(H_1)}} \left[|V(H_2)| d_{Q_\alpha(H_1)}(z_1) + d_{H_2}(y_1) + |V(H_2)| d_{Q_\alpha(H_1)}(z_2) \right] \\
&= \sum_{y_1 \in V(H_2)} \sum_{y_2 \in V(H_2)} \sum_{\substack{z_1 z_2 \in E(Q_\alpha(H_2)) \\ z_1 \in V(H_1) \\ z_2 \in V(Q_\alpha(H_1)) - V(H_1)}} \left[|V(H_2)| d_{H_1}(z_1) + d_{H_2}(y_1) \right] \\
&+ \sum_{y_1 \in V(H_2)} \sum_{y_2 \in V(H_2)} \sum_{\substack{z_1 z_2 \in E(Q_\alpha(H_2)) \\ z_1 \in V(H_1) \\ z_2 \in V(Q_\alpha(H_1)) - V(H_1)}} \left[|V(H_2)| d_{Q_\alpha(H_1)}(z_2) \right] \\
&= 4|V(H_2)| |E(H_1)| |E(H_2)| + |V(H_2)|^3 M_1(H_1) \\
&+ \sum_{y_1 \in V(H_2)} \sum_{y_2 \in V(H_2)} \sum_{\substack{z_1 z_2 \in E(Q_\alpha(H_1)) \\ z_1 \in V(H_1) \\ z_2 \in V(Q_\alpha(H_1)) - V(H_1)}} \left[|V(H_2)| d_{Q_\alpha(H_1)}(z_2) \right]. \tag{9}
\end{aligned}$$

For $z_2 \in V(Q_\alpha(H_1)) - V(H_1)$ which is inserted into the edge uv of (H_1) , we have $d_{Q_\alpha(H_1)}(z_2) = d_{H_1}(u) + d_{H_1}(v)$. This gives

$$\begin{aligned}
\sum_{\substack{z_1 z_2 \in E(Q_\alpha(H_1)) \\ z_1 \in V(H_1) \\ z_2 \in V(Q_\alpha(H_1)) - V(H_1)}} \left[d_{Q_\alpha(H_1)}(z_2) \right] &= 2 \sum_{uv \in E(H_1)} [d_{H_1}(u) + d_{H_1}(v)] = 2M_1(H_1) \\
\sum_{H_2} \sum_{\substack{z_1 z_2 \in E(Q_\alpha(H_1)) \\ z_1 \in V(H_1) \\ z_2 \in V(Q_\alpha(H_1)) - V(H_1)}} \left[d_{Q_\alpha(H_1)}(z_2) \right] &= 2|V(H_2)| M_1(H_1). \tag{10}
\end{aligned}$$

So, we have

$$\sum_{B_1} = 4|V(H_2)| |E(H_1)| |E(H_2)| + 3|V(H_2)|^3 M_1(H_1). \tag{11}$$

Now, we take

$$\sum_{B_2} = \sum_{y \in V(H_2)} \sum_{\substack{z_1 z_2 \in E(Q_\alpha(H_1)) \\ z_1 z_2 \in V(Q_\alpha(H_1)) - V(H_1)}} [d(z_1, y) + d(z_2, y)]$$

$$\begin{aligned}
 &= \sum_{y \in V(H_2)} \sum_{\substack{z_1 z_2 \in E(Q_\alpha(H_1)) \\ z_1 z_2 \in V(Q_\alpha(H_1)) - V(H_1)}} \left[|V(H_2)| d_{Q_\alpha(H_1)}(z_1) + |V(H_2)| d_{Q_\alpha(H_1)}(z_2) \right] \\
 &= 2(\alpha - 1) |V(H_2)|^2 \sum_{uv \in E(H_1)} [d_{H_1}(u) + d_{H_1}(v)] = 2(\alpha - 1) |V(H_2)|^2 M_1(H_1), \\
 \sum_{B_3} &= \sum_{y_1 \in V(H_2)} \sum_{y_2 \in V(H_2)} \sum_{\substack{z_1 z_2 \in E(Q_\alpha(H_1)) \\ z_1 z_2 \in V(Q_\alpha(H_1)) - V(H_1)}} \left[|V(H_2)| d_{Q_\alpha(H_1)}(z_1) + |V(H_2)| d_{Q_\alpha(H_1)}(z_2) \right] \\
 &= |V(H_2)|^3 (\alpha) \sum_{\substack{uv \in E(H_1) \\ vw \in E(H_2)}} [d_{H_1}(u) + d_{H_1}(v) + d_{H_1}(v) + d_{H_1}(w)], \tag{12}
 \end{aligned}$$

where z_1 and z_2 are the vertices that are inserted into the edges uv of H_1 and vw of H_1 , respectively.

$$\begin{aligned}
 &= (\alpha) |V(H_2)|^3 \left[\sum_{v \in V(H_1)} d_{H_1}^3(v) - d_{H_1}^2(v) + \sum_{v \in V(H_1)} (d_{H_1}(v) - 1) \sum_{\substack{u \in V(H_1) \\ uv \in E(H_1)}} d_{H_1}(u) \right] \tag{13} \\
 &= (\alpha) |V(H_2)|^3 [M_3(H_1) + 2M_2(H_1) - 2M_1(H_1)].
 \end{aligned}$$

Consequently, we have obtained our required result. \square

Theorem 2. Let H_1 and H_2 be two connected graphs such that $|V(H_1)|, |V(H_2)| \geq 4$. For $\alpha \geq 1$,

$$\begin{aligned}
 M_2(H_{1(Q_\alpha)}[H_2]) &= 5|E(H_2)||V(H_2)|^2 M_1(H_1) + 2|E(H_1)||V(H_2)| M_1(H_2) + |V(H_1)| M_2(H_2) \\
 &\quad + |V(H_2)|^4 [M_3(H_1) + 2M_2(H_1)] + (\alpha) |V(H_2)|^4 \\
 &\quad \left[\frac{1}{2} M_4(H_1) - \frac{1}{2} M_3(H_1) + \sum_{uv \in V(H_1)} r d(u) d(v) \right] \tag{14} \\
 &\quad + \sum_{v \in V(H_1)} d^2(v) \sum_{\substack{u \in V(H_1) \\ uv \in E(H_1)}} d(u) - 2M_2(H_1) + (\alpha - 1) |V(H_2)|^3 [2M_2(H_1) + M_3(H_1)],
 \end{aligned}$$

where r is the number of neighbours which are common between u and v in H_1 . Proof.

$$\begin{aligned}
 M_2(H_{1(Q_\alpha)}[H_2]) &= \sum_{(z_1, y_1)(z_2, y_2) \in E(H_{1(Q_\alpha)}[H_2])} [d(z_1, y_1)d(z_2, y_2)] \\
 &= \sum_{z \in V(H_1)} \sum_{y_1, y_2 \in E(H_2)} [d(z, y_1)d(z, y_2)] + \sum_{y_1 \in V(H_2)} \sum_{y_2 \in V(H_2)} \sum_{y_2 \in V(H_2)} \sum_{z_1, z_2 \in E(Q_\alpha(H_1))} [d(z_1, y_1)d(z_2, y_2)] \\
 &= \sum_A + \sum_B.
 \end{aligned} \tag{15}$$

Now, we take

$$\begin{aligned}
 \sum_A &= \sum_{z \in V(H_1)} \sum_{y_1, y_2 \in E(H_2)} [d(z, y_1)d(z, y_2)] \\
 &= \sum_{z \in V(H_1)} \sum_{y_1, y_2 \in E(H_2)} [|V(H_2)|d_{H_1}(z) + d_{H_2}(y_1)][|V(H_2)|d_{H_1}(z) + d_{H_2}(y_2)] \\
 &= |E(H_2)||V(H_2)|^2 M_1(H_1) + 2|E(H_1)||V(H_2)|M_1(H_2) + |V(H_1)|M_2(H_2), \\
 \sum_B &= \sum_{y_1 \in V(H_2)} \sum_{y_2 \in V(H_2)} \sum_{z_1, z_2 \in E(Q_\alpha(H_1))} [d(z_1, y_1)d(z_2, y_2)] \\
 &= \sum_{y_1 \in V(H_2)} \sum_{y_2 \in V(H_2)} \sum_{\substack{z_1, z_2 \in E(Q_\alpha(H_1)) \\ z_1 \in V(H_1) \\ z_2 \in V(Q_\alpha(H_1)) - V(H_2)}} [d(z_1, y_1)d(z_2, y_2)] \sum_{y \in V(H_2)} \sum_{\substack{z_1, z_2 \in E(Q_\alpha(H_1)) \\ z_1, z_2 \in V(Q_\alpha(H_1)) - V(H_1)}} [d(z_1, y)d(z_2, y)] \\
 &+ \sum_{y_1 \in V(H_2)} \sum_{y_2 \in V(H_2)} \sum_{\substack{z_1, z_2 \in E(Q_\alpha(H_1)) \\ z_1, z_2 \in V(Q_\alpha(H_1)) - V(H_1)}} [d(z_1, y_1)d(z_2, y_2)] = \sum_{B_1} + \sum_{B_2} + \sum_{B_3}.
 \end{aligned} \tag{16}$$

So,

$$\begin{aligned}
 \sum_{B_1} &= \sum_{y_1 \in V(H_2)} \sum_{y_2 \in V(H_2)} \sum_{\substack{z_1, z_2 \in E(Q_\alpha(H_1)) \\ z_1 \in V(H_1) \\ z_2 \in V(Q_\alpha(H_1)) - V(H_1)}} [d(z_1, y_1)d(z_2, y_2)] \\
 &= \sum_{y_1 \in V(H_2)} \sum_{y_2 \in V(H_2)} \sum_{\substack{z_1, z_2 \in E(Q_\alpha(H_1)) \\ z_1 \in V(H_1) \\ z_2 \in V(Q_\alpha(H_1)) - V(H_1)}} [||V(H_2)||d_{H_1}(z_1) + d_{H_2}(y_1)][|V(H_2)|d_{Q_\alpha(H_1)}(z_2)] \\
 &= \sum_{y_1 \in V(H_2)} \sum_{y_2 \in V(H_2)} \sum_{\substack{z_1, z_2 \in E(Q_\alpha(H_1)) \\ z_1 \in V(H_1) \\ z_2 \in V(Q_\alpha(H_1)) - V(H_1)}} [|V(H_2)|d_{Q_\alpha(H_1)}(z_2)d_{H_2}(y_1) + |V(H_2)|^2 d_{H_1}(z_1)d_{Q_\alpha(H_1)}(z_2)]
 \end{aligned}$$

$$\begin{aligned}
 &= |V(H_2)|^4 \sum_{\substack{z_1 z_2 \in E(Q(H_1)) \\ \in V(H_1) z_2 \in V(Q(H_1)) - V(H_1)}}^{z_1} d_{Q_\alpha(H_1)}(z_1) d_{Q_\alpha(H_1)}(z_2) + 2|E(H_2)| |V(H_2)|^2 \sum_{\substack{z_1 z_2 \in E(Q(H_1)) \\ \in V(H_1) \\ z_2 \in V(Q(H_1)) - V(H_1)}}^{z_1} d_{Q_\alpha(H_1)}(z_2) \\
 &= |V(H_2)|^4 \sum_{\substack{z_1 z_2 \in E(Q(H_1)) \\ (H_1) z_2 \in V(Q(H_1)) - V(H_1)}}^{z_1} d_{Q_\alpha(H_1)}(z_1) d_{Q_\alpha(H_1)}(z_2) + 4|E(H_2)| |V(H_2)|^2 M_1(H_1), \tag{17}
 \end{aligned}$$

where z_2 is the vertex inserted into the edge $z_1 w_1$ of H_1

$$\begin{aligned}
 &= |V(H_2)|^4 \sum_{z_1 \in V(H_1)} \sum_{w_1 \in V(N_{H_1}(z_1))} d_{Q_\alpha(H_1)}(z_1) [d_{Q_\alpha(H_1)}(z_1) + d_{Q_\alpha(H_1)}(w_1)] \\
 &\quad + 4|E(H_2)| |V(H_2)|^2 M_1(H_1), \tag{18}
 \end{aligned}$$

where $N_{H_1}(z_1)$ is the set of neighbor vertices of z_1 in H_1

$$\begin{aligned}
 &= |V(H_2)|^4 [M_3(H_1) + 2M_2(H_1)] + 4|E(H_2)| |V(H_2)|^2 M_1(H_1), \\
 \sum_{B_2} &= \sum_{y \in V(H_2)} \sum_{\substack{z_1 z_2 \in E(Q_\alpha(H_1)) \\ z_1 z_2 \in V(Q_\alpha(H_1)) - V(H_1)}} [d(z_1, y) d(z_2, y)] \\
 \sum_{B_2} &= \sum_{y \in V(H_2)} \sum_{\substack{z_1 z_2 \in E(Q_\alpha(H_1)) \\ z_1 z_2 \in V(Q_\alpha(H_1)) - V(H_1)}} [|V(H_2)| d_{Q_\alpha(H_1)}(z_1)] [|V(H_2)| d_{Q_\alpha(H_1)}(z_2)] \\
 &= (\alpha - 1) |V(H_2)|^3 [2M_2(H_1) + M_3(H_1)], \tag{19} \\
 \sum_{B_3} &= \sum_{y_1 \in V(H_2)} \sum_{y_2 \in V(H_2)} \sum_{\substack{z_1 z_2 \in E(Q_\alpha(H_1)) \\ z_1 z_2 \in V(Q_\alpha(H_1)) - V(H_1)}} [|V(H_2)| d_{Q_\alpha(H_1)}(z_1)] [|V(H_2)| d_{Q_\alpha(H_1)}(z_2)] \\
 &= |V(H_2)|^2 (\alpha) \sum_{y_1 \in V(H_2)} \sum_{y_2 \in V(H_2)} \sum_{\substack{uv \in E(H_1) \\ vw \in E(H_2)}} [d_{H_1}(u) + d_{H_1}(v)] [d_{H_1}(v) + d_{H_1}(w)],
 \end{aligned}$$

where z_1 is the added vertex in the edge uv , and z_2 is the added vertex in the edges vw of H_1

$$\begin{aligned}
 &= (\alpha)|V(H_2)|^4 \left[\frac{1}{2} \sum_{v \in V(H_1)} (d_{H_1}^4(v) - d_{H_1}^3(v)) + \sum_{uv \in V(H_1)} rd_{H_1}(u)d_{H_1}(v) + \sum_{v \in V(H_1)} d_{H_1}^2(v) \right. \\
 &\quad \left. \times \sum_{\substack{u \in V(H_1) \\ uv \in E(H_1)}} d_{H_1}(u) - 2M_2(H_1) \right] \\
 &= (\alpha)|V(H_2)|^4 \left[\frac{1}{2}M_4(H_1) - \frac{1}{2}M_3(H_1) + \sum_{uv \in V(H_1)} rd_{H_1}(u)d_{H_1}(v) \right. \\
 &\quad \left. + \sum_{v \in V(H_1)} d_{H_1}^2(v) \sum_{\substack{u \in V(H_1) \\ uv \in E(H_1)}} d_{H_1}(u) - 2M_2(H_1) \right].
 \end{aligned} \tag{20}$$

where r is the number of neighbors which are common vertices of u and v in (H_1) . Consequently, we have obtained our required result. \square

Theorem 3. Let H_1 and H_2 be two connected graphs such that $|V(H_1)|, |V(H_2)| \geq 4$. For $\alpha \geq 1$,

$$\begin{aligned}
 F(H_{1(Q_\alpha)}[H_2]) &= 3|V(H_2)|^4 F(H_1) + |V(H_1)|F(H_2) + 6|V(H_2)|^2|E(H_2)|M_1(H_1) + 6|V(H_2)| \\
 &\quad \times |E(H_1)|M_1(H_2) + 4|V(H_2)|^4 M_2(H_1) + (\alpha)|V(H_2)|^4 [M_4(H_1) - F(H_1) - 4M_2(H_1) \\
 &\quad + \sum_{u \in V(H_1)} \left(\sum_{v \in N_{H_1}(u)} d_{H_1}(u)(d_{H_1}(v) - 1) \right) + \sum_{uv \in E(H_1)} d_{H_1}(u)d_{H_1}(v)(d_{H_1}(u) \\
 &\quad + d_{H_1}(v))] + 2(\alpha - 1)|V(H_2)|^3 F(H_1).
 \end{aligned} \tag{21}$$

Proof.

Consider

$$\begin{aligned}
 F(H_{1(Q_\alpha)}[H_2]) &= \sum_{(z_1, y_1), (z_2, y_2) \in E(H_{1(Q_\alpha)}[H_2])} [d(z_1, y_1)^2 + d(z_2, y_2)^2] \\
 &= \sum_{z \in V(H_1)} \sum_{y_1, y_2 \in E(H_2)} [d(z, y_1)^2 + d(z, y_2)^2] + \sum_{y \in V(H_2)} \sum_{z_1, z_2 \in E(Q_\alpha(H_2))} [d(z_1, y)^2 + d(z_2, y)^2] \\
 &= \sum_A + \sum_B.
 \end{aligned} \tag{22}$$

Now,

$$\begin{aligned}
 \sum_A &= \sum_{z \in V(H_1)} \sum_{y_1, y_2 \in E(H_2)} [(d_{H_1}(z) + d_{H_2}(y_1))^2 + (d_{H_1}(z) + d_{H_2}(y_2))^2] \\
 &= \sum_{z \in V(H_1)} \sum_{y_1, y_2 \in E(H_2)} [2|V(H_2)|^2 d_{H_1}(z)^2 + (d_{H_2}(y_1)^2 + d_{H_2}(y_2)^2) + 2d_{H_1}(z)|V(H_1)|(d_{H_2}(y_1) + d_{H_2}(y_2))] \\
 &= \sum_{z \in V(H_1)} [|E(H_2)||V(H_2)||^2 \times 2d_{H_1}(z)^2 + F(H_2) + 2|V(H_2)|M_1(H_2)d_{H_1}(z)]
 \end{aligned}$$

$$\begin{aligned}
 &= 2|E(H_2)|V(H_2)^2M_1(H_1) + |V(H_1)|F(H_2) + 4|V(H_2)||E(H_1)|M_1(H_2), \\
 \sum_B &= \sum_{y_1 \in V(H_2)} \sum_{y_2 \in V(H_2)} \sum_{z_1, z_2 \in E(Q_\alpha(H_1))} [d(z_1, y_1)^2 + d(z_2, y_2)^2] \\
 &= \sum_{y_1 \in V(H_2)} \sum_{y_2 \in V(H_2)} \sum_{\substack{z_1, z_2 \in E(Q_\alpha(H_1)) \\ z_1 \in V(H_1), z_2 \in V(Q_\alpha(H_1)) - V(H_1)}} [d(z_1, y_1)^2 + d(z_2, y_2)^2] \\
 &+ \sum_{y \in V(H_2)} \sum_{\substack{z_1, z_2 \in E(Q_\alpha(H_1)) \\ z_1, z_2 \in V(Q_\alpha(H_1)) - V(H_1)}} [d(z_1, y)^2 + d(z_2, y)^2] \\
 &+ \sum_{y_1 \in V(H_2)} \sum_{y_2 \in V(H_2)} \sum_{\substack{z_1, z_2 \in E(Q_\alpha(H_1)) \\ z_1, z_2 \in V(Q_\alpha(H_1)) - V(H_1)}} [d(z_1, y_1)^2 + d(z_2, y_2)^2] = \sum_{B_1} + \sum_{B_2} + \sum_{B_3}. \tag{23}
 \end{aligned}$$

Now, we take

$$\begin{aligned}
 \sum_{B_1} &= \sum_{y_1 \in V(H_2)} \sum_{y_2 \in V(H_2)} \sum_{\substack{z_1, z_2 \in E(Q_\alpha(H_1)) \\ z_1 \in V(H_1), z_2 \in V(Q_\alpha(H_1)) - V(H_1)}} \left[\left(|V(H_2)|d_{Q_\alpha(H_1)}(z_1) + d_{H_2}(y_1) \right)^2 + |V(H_2)|^2 d_{Q_\alpha(H_1)}(z_2)^2 \right] \\
 &= \sum_{y_1 \in V(H_2)} \sum_{y_2 \in V(H_2)} \sum_{\substack{z_1, z_2 \in E(Q_\alpha(H_1)) \\ z_1 \in V(H_1), z_2 \in V(Q_\alpha(H_1)) - V(H_1)}} \left[|V(H_2)|^2 d_{Q_\alpha(H_1)}(z_1)^2 + d_{H_2}(y_1)^2 + 2|V(H_2)|d_{Q_\alpha(H_1)}(z_1)d_{H_2}(y_1) \right. \\
 &\quad \left. + |V(H_2)|^2 d_{Q_\alpha(H_1)}(z_2)^2 \right] \\
 &= \sum_{y_1 \in V(H_2)} \sum_{y_2 \in V(H_2)} \sum_{z_1 \in V(H_1)} \left[|V(H_2)|^2 d_{Q_\alpha(H_1)}(z_1)^2 + d_{H_2}(y_1)^2 + 2|V(H_2)|d_{Q_\alpha(H_1)}(z_1)d_{H_2}(y_1) \right] \\
 &+ \sum_{y_1 \in V(H_2)} \sum_{y_2 \in V(H_2)} \sum_{\substack{z_1, z_2 \in E(Q_\alpha(H_1)) \\ z_1 \in V(H_1), z_2 \in V(Q_\alpha(H_1)) - V(H_1)}} \left[|V(H_2)|^2 d_{Q_\alpha(H_1)}(z_2)^2 \right] \\
 &= |V(H_2)|F(H_1) + 2|E(H_1)|M_1(H_2) + 4|E(H_2)|M_1(H_1) + |V(H_2)|^2 \sum_{y \in V(H_2)} \\
 &\quad \times \sum_{\substack{z_1, z_2 \in E(Q_\alpha(H_1)) \\ z_1 \in V(H_1), z_2 \in V(Q_\alpha(H_1)) - V(H_1)}} \left[d_{Q_\alpha(H_1)}(z_2)^2 \right]. \tag{24}
 \end{aligned}$$

For $z_2 \in V(Q_\alpha(H_1)) - V(H_1)$ that is introduced into the edges uv of (H_1) , we have $d_{Q_\alpha(H_1)}(z_2) = d_{H_1}(u) + d_{H_1}(v)$. This gives

$$\sum_{\substack{z_1, z_2 \in E(Q_\alpha(H_1)) \\ z_1 \in V(H_1), z_2 \in V(Q_\alpha(H_1)) - V(H_1)}} \left[d_{Q_\alpha(H_1)}(z_2)^2 \right] = 2 \sum_{uv \in E(H_1)} \left[d_{H_1}(u) + d_{H_1}(v) \right]^2 = 2HM(H_1). \tag{25}$$

So,

$$\begin{aligned}
 \sum_{B_1} &= |V(H_2)|^4 [2HM(H_1) + F(H_1)] + 2|V(H_2)||E(H_1)|M_1(H_2) + 4|V(H_2)|^2|E(H_2)|M_1(H_1), \\
 \sum_{B_2} &= \sum_{y \in V(H_2)} \sum_{\substack{z_1, z_2 \in E(Q_\alpha(H_1)) \\ z_1, z_2 \in V(Q_\alpha(H_1)) - V(H_1)}} [|V(H_2)|^2 d(z_1, y)^2 + |V(H_2)|^2 d(z_2, y)^2] \\
 &= \sum_{y \in V(H_2)} \sum_{\substack{z_1, z_2 \in E(Q_\alpha(H_1)) \\ z_1, z_2 \in V(Q_\alpha(H_1)) - V(H_1)}} [|V(H_2)|^2 d_{Q_\alpha(H_1)}(z_1)^2 + |V(H_2)|^2 d_{Q_\alpha(H_1)}(z_2)^2] \\
 &= 2(\alpha - 1)|V(H_2)|^2 \sum_{y \in V(H_2)} \sum_{uv \in E(H_1)} [d_{H_1}(u)^2 + d_{H_1}(v)^2] = 2(\alpha - 1)|V(H_2)|^3 F(H_1), \tag{26} \\
 \sum_{B_3} &= \sum_{y_1 \in V(H_2)} \sum_{y_2 \in V(H_2)} \sum_{\substack{z_1, z_2 \in E(Q_\alpha(H_1)) \\ z_1, z_2 \in V(Q_\alpha(H_1)) - V(H_1)}} [|V(H_2)|^2 d_{Q_\alpha(H_1)}(z_1)^2 + |V(H_2)|^2 d_{Q_\alpha(H_1)}(z_2)^2] \\
 &= (\alpha)|V(H_2)|^4 \sum_{\substack{uv \in E(H_1) \\ vw \in E(H_2)}} [(d_{H_1}(u) + d_{H_1}(v))^2 + (d_{H_1}(v) + d_{H_1}(w))^2],
 \end{aligned}$$

where z_1 and z_2 are the nodes that are introduced into the edge set of uv and vw of H_1

$$\begin{aligned}
 &= (\alpha)|V(H_2)|^4 \left[\sum_{u \in V(H_1)} d_{H_1}(v)^4 - d_{H_1}(v)^3 + \sum_{v \in V(H_1)} (d_{H_1}(v) - 1) \sum_{\substack{u \in V(H_1) \\ uv \in E(H_1)}} d_{H_1}(u)^2 \right. \\
 &\quad \left. + 2 \sum_{v \in V(H_1)} d_{H_1}(v)(d_{H_1}(v) - 1) \sum_{\substack{u \in V(H_1) \\ uv \in E(H_1)}} d_{H_1}(u) \right] \tag{27} \\
 &= (\alpha)|V(H_2)|^4 [M_4(H_1) - F(H_1) - 4M_2(H_1) + \sum_{u \in V(H_1)} \left(\sum_{v \in N_{H_1}(u)} d_{H_1}(u)(d_{H_1}(v) - 1) \right) \\
 &\quad \left. + \sum_{uv \in E(H_1)} d_{H_1}(u)d_{H_1}(v)(d_{H_1}(u) + d_{H_1}(v)) \right],
 \end{aligned}$$

Consequently, we have obtained our required result. \square

Theorem 4. Let H_1 and H_2 be two connected graphs such that $|V(H_1)|, |V(H_2)| \geq 4$. For $\alpha \geq 1$,

$$\begin{aligned}
 HZ(H_{1(Q_\alpha)}[H_2]) &= \alpha|V(H_2)|^4 [HZ(L(H_1)) + 8M_1(L(H_1)) + 8M_1(H_1) - 16|E(H_1)|] \\
 &\quad + 4(\alpha - 1)|V(H_2)|^3 HZ(H_1) + 12|V(H_2)|^2|E(H_2)|M_1(H_1) + |V(H_1)|HZ(H_2) \tag{28} \\
 &\quad + 10|V(H_2)||E(H_1)|M_1(H_2) + |V(H_2)|^4 [2HZ(H_1) + 3F(H_1) + 4M_2(H_1)].
 \end{aligned}$$

Proof.

$$\begin{aligned}
 HZ\left(H_{1(Q_\alpha)}[H_2]\right) &= \sum_{(z_1, y_1)(z_2, y_2) \in E\left(H_{1(Q_\alpha)}[H_2]\right)} [d(z_1, y_1) + d(z_2, y_2)]^2 \\
 &= \sum_{z \in V(H_1)} \sum_{y_1, y_2 \in E(H_2)} [d(z, y_1) + d(z, y_2)]^2 + \sum_{y_1 \in V(H_2)} \sum_{y_2 \in V(H_2)} \sum_{z_1, z_2 \in E(Q_\alpha(H_1))} [d(z_1, y_1) + d(z_2, y_2)]^2 \\
 &= \sum_A + \sum_B.
 \end{aligned} \tag{29}$$

Now,

$$\begin{aligned}
 \sum_A &= \sum_{z \in V(H_1)} \sum_{y_1, y_2 \in E(H_2)} [d(z, y_1) + d(z, y_2)]^2 \\
 &= \sum_{z \in V(H_1)} \sum_{y_1, y_2 \in E(H_2)} \left[\left(|V(H_2)| d_{Q_\alpha(H_1)}(z) + d_{H_2}(y_1) \right) + \left(|V(H_2)| d_{Q_\alpha(H_1)}(z) + d_{H_2}(y_2) \right) \right]^2 \\
 &= \sum_{z \in V(H_1)} \sum_{y_1, y_2 \in E(H_2)} \left[2|V(H_2)| d_{Q_\alpha(H_1)}(z) + d_{H_2}(y_1) + d_{H_2}(y_2) \right]^2 \\
 &= \sum_{z \in V(H_1)} \sum_{y_1, y_2 \in E(H_2)} \left[4|V(H_2)|^2 \left(d_{Q_\alpha(H_1)}(z) \right)^2 + \left(d_{H_2}(y_1) \right)^2 + \left(d_{H_2}(y_2) \right)^2 + 4|V(H_2)| d_{Q_\alpha(H_1)}(z) d_{H_2}(y_1) \right. \\
 &\quad \left. + 4|V(H_2)| d_{Q_\alpha(H_1)}(z) d_{H_2}(y_2) + 2d_{H_2}(y_1) d_{H_2}(y_2) \right] \\
 &= 4|E(H_2)| |V(H_2)|^2 M_1(H_1) + |V(H_1)| HZ(H_2) + \sum_{z \in V(H_1)} \sum_{y_1, y_2 \in E(H_2)} 4d_{H_1}(z) [d_{H_2}(y_1) + d_{H_2}(y_2)] \\
 &= 4|E(H_2)| |V(H_2)|^2 M_1(H_1) + |V(H_1)| HZ(H_2) + 8|E(H_1)| |V(H_2)| M_1(H_2), \\
 \sum_B &= \sum_{y_1 \in V(H_2)} \sum_{y_2 \in V(H_2)} \sum_{z_1, z_2 \in E(Q_\alpha(H_1))} [d(z_1, y) + d(z_2, y)]^2 \\
 &= \sum_{y_1 \in V(H_2)} \sum_{y_2 \in V(H_2)} \sum_{\substack{z_1, z_2 \in E(Q_\alpha(H_1)) \\ z_1, z_2 \in V(Q_\alpha(H_1)) - V(H_1)}} [d(z_1, y_1) + d(z_2, y_2)]^2 \\
 &\quad + \sum_{y \in V(H_2)} \sum_{\substack{z_1, z_2 \in E(Q_\alpha(H_1)) \\ z_1, z_2 \in V(Q_\alpha(H_1)) - V(H_1)}} [d(z_1, y) + d(z_2, y)]^2 \\
 &\quad + \sum_{y_1 \in V(H_2)} \sum_{y_2 \in V(H_2)} \sum_{\substack{z_1, z_2 \in E(Q_\alpha(H_1)) \\ z_1, z_2 \in V(Q_\alpha(H_1)) - V(H_1)}} [d(z_1, y_1) + d(z_2, y_2)]^2 = \sum_{B_1} + \sum_{B_2} + \sum_{B_3}.
 \end{aligned} \tag{30}$$

Now, we take

$$\begin{aligned}
\sum_{B_1} &= \sum_{y_1 \in V(H_2)} \sum_{y_2 \in V(H_2)} \sum_{\substack{z_1, z_2 \in E(Q_\alpha(H_1)) \\ z_1 \in V(H_1), z_2 \in V(Q_\alpha(H_1)) - V(H_1)}} [d(z_1, y_1) + d(z_2, y_2)]^2 \\
&= \sum_{y_1 \in V(H_2)} \sum_{y_2 \in V(H_2)} \sum_{\substack{z_1, z_2 \in E(Q_\alpha(H_1)) \\ z_1 \in V(H_1), z_2 \in V(Q_\alpha(H_1)) - V(H_1)}} \left[|V(H_2)| d_{Q_\alpha(H_1)}(z_1) + d_{H_2}(y_1) + |V(H_2)| d_{Q_\alpha(H_1)}(z_2) \right]^2 \\
&= \sum_{y_1 \in V(H_2)} \sum_{y_2 \in V(H_2)} \sum_{\substack{z_1, z_2 \in E(Q_\alpha(H_1)) \\ z_1 \in V(H_1), z_2 \in V(Q_\alpha(H_1)) - V(H_1)}} \left[|V(H_2)|^2 d_{Q_\alpha(H_1)}(z_1)^2 + d_{H_2}(y_1)^2 + |V(H_2)|^2 d_{Q_\alpha(H_1)}(z_2)^2 \right. \\
&\quad \left. + 2|V(H_2)| d_{Q_\alpha(H_1)}(z_1) d_{H_2}(y_1) + 2|V(H_2)| d_{H_2}(y_1) d_{Q_\alpha(H_1)}(z_2) + 2|V(H_2)|^2 d_{Q_\alpha(H_1)}(z_1) d_{Q_\alpha(H_1)}(z_2) \right] \\
&= |V(H_2)|^4 F(H_1) + 2|V(H_2)| \|E(H_1)\| M_1(H_2) + 4|V(H_2)|^2 |E(H_2)| M_1(H_1) + \sum_{y_1 \in V(H_2)} \sum_{y_2 \in V(H_2)} \\
&\quad \times \sum_{\substack{z_1, z_2 \in E(Q_\alpha(H_1)), z_1 \in V(H_1) \\ z_2 \in V(Q_\alpha(H_1)) - V(H_1)}} \left[|V(H_2)|^2 d_{Q_\alpha(H_1)}(z_2)^2 + \left(2|V(H_2)|^2 d_{H_1}(z_1) + 2|V(H_2)|^2 d_{Q_\alpha(H_1)}(z_1) \right) d_{Q_\alpha(H_1)}(z_2) \right].
\end{aligned} \tag{31}$$

One can see that for a vertex $z_2 \in V(Q_\alpha(H_1)) - V(H_1)$, $d_{Q_\alpha(H_1)}(z_2) = d_{H_1}(z) + d_{H_1}(w)$, where $z_2 = xw \in E(H_1)$. Thus,

$$\begin{aligned}
&= |V(H_2)|^4 F(H_1) + 2|V(H_2)| \|E(H_1)\| M_1(H_2) + 4|V(H_2)|^2 |E(H_2)| M_1(H_1) + \sum_{y_1 \in V(H_2)} \sum_{y_2 \in V(H_2)} \\
&\quad \times \sum_{\substack{z_1, z_2 \in E(Q_\alpha(H_1)), z_1 \\ \in V(H_1), z_2 \in V(Q_\alpha(H_1)) - V(H_1)}} \left[|V(H_2)|^2 (d_{H_1}(z) + d_{H_1}(w))^2 + 2|V(H_2)|^2 (d_{H_1}(z_1) + d_{Q_\alpha(H_1)}(z_1)) (d_{H_1}(z) + d_{H_1}(w)) \right] \\
&= |V(H_2)|^4 F(H_1) + 2|V(H_2)| \|E(H_1)\| M_1(H_2) + 4|V(H_2)|^2 |E(H_2)| M_1(H_1) \\
&\quad + 2|V(H_2)|^4 HZ(H_1) + 2|V(H_2)|^4 (F(H_1) + 2M_2(H_1)) + 8|V(H_2)|^2 |E(H_1)| M_1(H_2) \\
&= 2|V(H_2)|^4 HZ(H_1) + 3|V(H_2)|^4 F(H_1) + 12|V(H_2)|^2 |E(H_2)| M_1(H_1) \\
&\quad + 2|V(H_2)| \|E(H_1)\| M_1(H_2) + 4|V(H_2)|^4 M_2(H_1), \\
\sum_{B_2} &= \sum_{y \in V(H_2)} \sum_{\substack{z_1, z_2 \in E(Q_\alpha(H_1)) \\ z_1, z_2 \in V(Q_\alpha(H_1)) - V(H_1)}} \left[|V(H_2)| d_{Q_\alpha(H_1)}(z_1) + |V(H_2)| d_{Q_\alpha(H_1)}(z_2) \right]^2 \\
&= 4(\alpha - 1) |V(H_2)|^2 \sum_{y \in V(H_2)} \sum_{uv \in E(H_1)} [d_{H_1}(u) + d_{H_1}(v)]^2 = 4(\alpha - 1) |V(H_2)|^3 HM(H_1), \\
\sum_{B_3} &= \sum_{y_1 \in V(H_2)} \sum_{y_2 \in V(H_2)} \sum_{\substack{z_1, z_2 \in E(Q_\alpha(H_1)) \\ z_1, z_2 \in V(Q_\alpha(H_1)) - V(H_1)}} \left[|V(H_2)| d_{Q_\alpha(H_1)}(z_1) + |V(H_2)| d_{Q_\alpha(H_1)}(z_2) \right]^2 \\
&= \alpha |V(H_2)|^4 \sum_{\substack{uv \in E(H_1) \\ vw \in E(H_2)}} [d_{H_1}(u) + d_{H_1}(v) + d_{H_1}(v) + d_{H_1}(w)]^2.
\end{aligned} \tag{32}$$

TABLE 1: $P_n[P_m]$.

$[m, n]$	V	E	M_1	M_2	$F(H)$	$H(H)$
(3,3)	9	24	276	764	1704	3232
(4,4)	16	60	968	3868	8280	16 016
(5,5)	25	120	2460	12 576	26 460	51 612
(6,6)	36	210	5196	32 132	66 948	131 212
(7,7)	49	336	9716	70 276	145 488	286 040

TABLE 2: $P_{n(q_a)}[P_m]$.

$[m, n, k]$	V	E	M_1	M_2	$F(H)$	$H(H)$
(3,3,3)	27	189	6366	53 701	114 786	222 188
(4,4,4)	64	944	69 024	1256 160	2745 760	5258 080
(5,5,5)	125	3175	392 030	$1.219 569 2 \times 10^7$	$2.581 541 \times 10^7$	$5.020 679 4 \times 10^7$
(6,6,6)	216	8424	1561 992	$7.308 936 4 \times 10^7$	$1.522 399 68 \times 10^8$	$2.984 186 96 \times 10^8$
(7,7,7)	343	19 061	4939 998	$3.229 925 64 \times 10^8$	$6.663 437 62 \times 10^8$	$1.312 328 89 \times 10^9$

TABLE 3: Correlation coefficient between $P_{n(q_a)}[P_m]$ and $P_n[P_m]$.

TI's	Value of R	Relationship between X and Y
First Zagreb index	0.9756	Very strong direct relationship
Second Zagreb index	0.953	Very strong direct relationship
Forgotten Zagreb index	0.9123	Very strong direct relationship
Hyper Zagreb index	0.9736	Very strong direct relationship

TABLE 4: Square of correlation coefficient between $P_{n(q_a)}[P_m]$ and $P_n[P_m]$.

TI's	Value of R^2	Variability of Y is explained by X
First Zagreb index	0.9518	95.1 percent
Second Zagreb index	0.9080	90.8 percent
Forgotten Zagreb index	0.8323	83.23 percent
Hyper Zagreb index	0.9478	94.78 percent

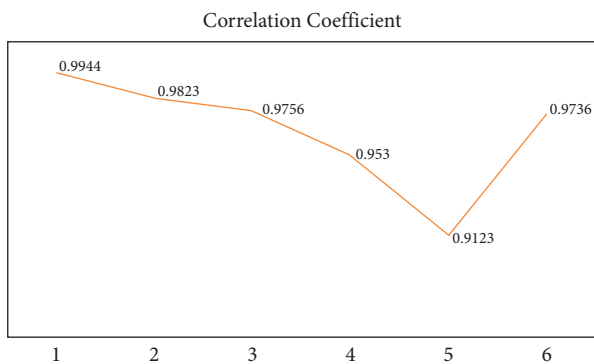


FIGURE 5: Value of R for number of vertices, edges, first, second, forgotten, and hyper Zagreb indices.

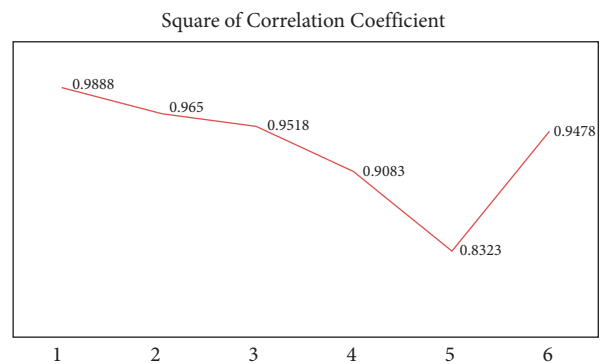


FIGURE 6: Value of R^2 for number of vertices, edges, first, second, forgotten, and hyper Zagreb indices.

W and X are the nodes of $L(H_1)$, so we have

$$\begin{aligned}
 &= \alpha |V(H_2)|^4 \sum_{WX \in E(L(H_1))} \left[d_{L(H_1)}(W)^2 + d_{L(H_1)}(X)^2 \right. \\
 &\quad \left. + 16 + 2d_{L(H_1)}(W)d_{L(H_1)}(X) + 8d_{L(H_1)}(W) + 8d_{L(H_1)}(X) \right] \\
 &= \alpha |V(H_2)|^4 \left[HZ(L(H_1)) + 8M_1(L(H_1)) + 16\left(\frac{1}{2}M_1(H_1) - E(H_1)\right) \right], \\
 \sum_{B_3} &= \alpha |V(H_2)|^4 [HZ(L(H_1)) + 8M_1(L(H_1)) + 8M_1(H_1) - 16E(H_1)].
 \end{aligned} \tag{33}$$

Consequently, the result is over. \square

3. Applications and Conclusion

For any two simple path graphs P_n and P_m with $n, m > 3$, we construct their lexicographic product graphs $P_n[P_m]$ and compute various degree-related TIs, as shown in Table 1 with certain values of m and n . Furthermore, we construct $Q_\alpha(P_n)$ by applying generalized line superposition operation on P_n and then construct Q_α -sum graph $(P_{n(Q_\alpha)}[P_m])$ based on lexicographic product of $Q_\alpha(P_n)$ and P_m . Finally, we compute certain degree-related TIs using Theorem 1–Theorem 4, as given in Table 2. We note that by the addition of vertices $\alpha \geq 1$, the values of obtained TIs are increasing for the newly constructed graphs comparatively to the graphs obtained by the ordinary lexicographic product of graphs.

3.1. Linear Regression Model. To check the correlation between the predefined lexicographic product of two simple graphs $(P_n[P_m])$ and newly defined Q_α -sum graphs $(P_{n(Q_\alpha)}[P_m])$, we have made the linear regression model for all the obtained indices as follows:

3.2. First Zagreb Index.

$$M_1(P_n[P_m]) = b_0 + b_1 \left[M_1(P_{n(Q_\alpha)}[P_m]) \right], \tag{34}$$

where $Y = M_1(P_n[P_m])$ index values, b_0 is the constant, b_1 is the regression coefficient, and $X = M_1(P_{n(Q_\alpha)}[P_m])$ index values (see Tables 1 and 2).

$$Y = 1207.7339 + 0.001805X. \tag{35}$$

3.3. Second Zagreb Index.

$$M_2(P_n[P_m]) = b_0 + b_1 \left[M_2(P_{n(Q_\alpha)}[P_m]) \right], \tag{36}$$

where $Y = M_2(P_n[P_m])$ index values, b_0 is the constant, b_1 is the regression coefficient, and $X = M_2(P_{n(Q_\alpha)}[P_m])$ index values (see Tables 1 and 2).

$$Y = 1548.9242 + 0.00002654X. \tag{37}$$

3.4. Forgotten Topological Index.

$$F(P_n[P_m]) = b_0 + b_1 \left[F(P_{n(Q_\alpha)}[P_m]) \right], \tag{38}$$

where $Y = F(P_n[P_m])$ index values, b_0 is the constant, b_1 is the regression coefficient, and $X = F(P_{n(Q_\alpha)}[P_m])$ index values (see Tables 1 and 2).

$$Y = 11263.1338 + 0.00008912X. \tag{39}$$

3.5. Hyper Zagreb Index.

$$HM(P_n[P_m]) = b_0 + b_1 \left[HM(P_{n(Q_\alpha)}[P_m]) \right], \tag{40}$$

where $Y = HM(P_n[P_m])$ index values, b_0 is the constant, b_1 is the regression coefficient, and $X = HM(P_{n(Q_\alpha)}[P_m])$ index values (see Tables 1 and 2).

$$Y = 30210.7664 + 0.0002023X. \tag{41}$$

Now, we represent a tabular representation of the correlation and square of correlation coefficient values related to the TIs of certain type of graphs $P_{n(Q_\alpha)}[P_m]$ and $P_n[P_m]$ (see Tables 3 and 4). The highest value of R and R^2 are indicated in bold.

For more explanation, see the graphical representation of correlation and square of correlation coefficient in Figures 5 and 6.

Data Availability

All the data are included within this paper. However, the reader may contact the corresponding author for more details of the data.

Conflicts of Interest

The authors have no conflicts of interest.

References

- [1] I. Gutman and N. Trinajstić, "Graph theory and molecular orbitals. Total φ -electron energy of alternant hydrocarbons," *Chemical Physics Letters*, vol. 17, no. 4, pp. 535–538, 1972.
- [2] X. Li and J. Zheng, "A unified approach to the extremal trees for different indices," *MATCH Communications in Mathematical and in Computer Chemistry*, vol. 54, pp. 195–208, 2005.
- [3] B. Furtula and I. Gutman, "A forgotten topological index," *Journal of Mathematical Chemistry*, vol. 53, no. 4, pp. 1184–1190, 2015.
- [4] G. H. Shirdel, H. Rezapour, and A. M. Sayadi, "Hyper-Zagreb index of graph operations," *Iranian Journal of Mathematical Chemistry*, vol. 4, pp. 213–220, 2013.
- [5] I. Gutman and O. Polansky, *Mathematical Concepts in Organic Chemistry*, Springer-Verlag, Berlin, Germany, 1986.
- [6] M. R. F. M. Rezaei, W. Gao, and M. K. Siddiqui, "Computing hyper zagreb index and m-polynomials of titania nanotubes $ti_2[m,n]$," *Sigma Journal of Engineering and Natural Sciences*, vol. 35, no. 4, pp. 707–714, 2016.
- [7] M. K. Siddiqui, M. Imran, and A. Ahmad, "On Zagreb indices, Zagreb polynomials of some nanostar dendrimers," *Applied Mathematics and Computation*, vol. 280, pp. 132–139, 2016.
- [8] A. N. A. Koam, A. Ahmad, and A. A. Ahamdini, "Computation of vertex-edge degree based topological descriptors for hex-derived networks," *IEEE Access*, vol. 9, pp. 82989–83001, 2021.
- [9] A. Iqbal, G. Ali, J. Khan, M. N. G. Rahmat, and A. Kausar, "On topological indices of dual graphs of Benzene ring embedded in P-type surface in 2D-Network," *International Journal of Advanced Trends in Computer Science and Engineering*, vol. 10, no. 3, pp. 1936–1941, 2021.
- [10] U. Ahmad and S. Hameed, "Study of topological indices in a class of benzenoid graphs," *Computational Journal of Combinatorial Mathematics*, vol. 1, pp. 19–30, 2020.
- [11] M. Asif and M. Hussain, "Topological characterization of cellulose network," *Computational Journal of Combinatorial Mathematics*, vol. 2, pp. 21–30, 2020.
- [12] R. Todeschini, V. Consonni, R. Mannhold, H. Kubinyi, and H. Timmerman, *Handbook of Molecular Descriptors*, Wiley VCH, Weinheim, Germany, 2002.
- [13] W. Yan, B.-Y. Yang, and Y.-N. Yeh, "The behavior of Wiener indices and polynomials of graphs under five graph decorations," *Applied Mathematics Letters*, vol. 20, no. 3, pp. 290–295, 2007.
- [14] J.-B. Liu, S. Javed, M. Javaid, and K. Shabbir, "Computing first general zagreb index of operations on graphs," *IEEE Access*, vol. 7, pp. 47494–47502, 2019.
- [15] M. Eliaasi and B. Taeri, "Four new sums of graphs and their Wiener indices," *Discrete Applied Mathematics*, vol. 157, no. 4, pp. 794–803, 2009.
- [16] Y.-M. Chu, S. Javed, M. Javaid, and M. Kamran Siddiqui, "On bounds for topological descriptors of φ -sum graphs," *Journal of Taibah University for Science*, vol. 14, no. 1, pp. 1288–1301, 2020.
- [17] H. Deng, D. Sarala, S. K. Ayyaswamy, and S. Balachandran, "The Zagreb indices of four operations on graphs," *Applied Mathematics and Computation*, vol. 275, pp. 422–431, 2016.
- [18] S. Akhter and M. Imran, "Computing the forgotten topological index of four operations on graphs," *AKCE International Journal of Graphs and Combinatorics*, vol. 14, no. 1, pp. 70–79, 2017.
- [19] J.-B. Liu, M. Javaid, and H. M. Awais, "Computing zagreb indices of the subdivision-related generalized operations of graphs," *IEEE Access*, vol. 7, pp. 105479–105488, 2019.
- [20] M. Javaid, S. Javed, A. M. Alanazi, and M. R. Alotaibi, "Computing analysis of Zagreb indices for generalized sum graphs under strong product," *Journal of Chemistry*, vol. 2021, Article ID 6663624, 20 pages, 2021.
- [21] D. Sarala, H. Deng, S. K. Ayyaswamy, and S. Balachandran, "The Zagreb indices of graphs based on four new operations related to the lexicographic product," *Applied Mathematics and Computation*, vol. 309, pp. 156–169, 2017.
- [22] N. De, "F-index of graphs based on four operations related to the lexicographic product," 2017, <https://arxiv.org/abs/1706.00464>.
- [23] K. Pattabiraman, "Four new operations related to composition and their hyper-zagreb index," *Southeast Asian Bulletin of Mathematics*, vol. 43, no. 6, 2019.
- [24] K. Pattabiraman and A. Santhakumar, "Four new operations related to composition and their reformulated Zagreb index," *Indonesian Journal of Combinatorics*, vol. 2, no. 1, pp. 35–49, 2018.
- [25] M. Suresh and G. S. Devi, "Some operations in hyper Zagreb indices," *AIP Conference Proceedings*, vol. 2277, no. 1, Article ID 140003, 2020.
- [26] M. Javaid, S. Javed, S. Q. Memon, and A. M. Alanazi, "Forgotten index of generalized operations on graphs," *Journal of Chemistry*, vol. 2021, Article ID 9971277, 14 pages, 2021.
- [27] D. A. Alrowaili, S. Javed, and M. Javaid, "On the exact values of HZ-index for the graphs under operations," *Journal of Mathematics*, vol. 2021, Article ID 3304939, 17 pages, 2021.
- [28] M. Javaid, S. Javed, Y. F. Alanazi, and A. M. Alanazi, "Computing correlation among the graphs under lexicographic product via zagreb indices," *Journal of Chemistry*, vol. 2021, Article ID 7465171, 17 pages, 2021.
- [29] Z. B. Peng, S. Javed, M. Javaid, and J. B. Liu, "Computing FGZ index of sum graphs under strong product," *Journal of Mathematics*, vol. 2021, Article ID 6654228, 16 pages, 2021.

Research Article

On the Graphs of Minimum Degree At Least 3 Having Minimum Sum-Connectivity Index

Wael W. Mohammed,^{1,2} Shahzad Ahmed,³ Zahid Raza,⁴ Jia-Bao Liu ,⁵ Farooq Ahmad,^{1,6} and Elsayed M. Elsayed ⁷

¹Department of Mathematics, Faculty of Science, University of Ha'il, Ha'il, Saudi Arabia

²Department of Mathematics, Faculty of Science, Mansoura University, Mansoura 35516, Egypt

³Knowledge Unit of Science, University of Management and Technology, Sialkot, Pakistan

⁴Department of Mathematics, College of Sciences, University of Sharjah, Sharjah, UAE

⁵School of Mathematics and Physics, Anhui Jianzhu University, Hefei 230601, China

⁶School of Mechanical and Aerospace Engineering, NANYANG Technological University, Singapore

⁷Department of Mathematics, Faculty of Science, King Abdulaziz University, Jeddah 21589, Saudi Arabia

Correspondence should be addressed to Jia-Bao Liu; liujiabao@163.com

Received 2 August 2021; Accepted 22 December 2021; Published 4 February 2022

Academic Editor: Tomas Vertik

Copyright © 2022 Wael W. Mohammed et al. This is an open access article distributed under the Creative Commons Attribution License, which permits unrestricted use, distribution, and reproduction in any medium, provided the original work is properly cited.

For a graph G , its sum-connectivity index is denoted by $\chi(G)$ and is defined as the sum of the numbers $(d(u) + d(v))^{-1/2}$ over all edges uv of G , where $d(w)$ denotes the degree of a vertex $w \in V(G)$. In this study, we find a sharp lower bound on the sum-connectivity index of graphs having minimum degree of at least 3 under certain constraints and characterize the corresponding extremal graphs.

1. Introduction

In chemical graph theory, graph invariants are usually known as topological indices. Such indices play an important role in the study of quantitative structure property relationship (QSPR) and quantitative structure activity relationship (QSAR). Information about several good studied topological indices can be found in [1–7] and related references listed therein.

The well-known Randić-connectivity index (also known as the product-connectivity index), proposed by Randić [8] in 1975, is the most used topological index in QSPR and QSAR, which is defined as [8]

$$R(G) = \sum_{uv \in E(G)} (d(u)d(v))^{-1/2}. \quad (1)$$

The sum-connectivity index, a variant of the product-connectivity index, of a graph G is defined as [9]

$$\chi(G) = \sum_{uv \in E(G)} (d(u) + d(v))^{-1/2}. \quad (2)$$

In the previous studies [10–12], the sum-connectivity index of several graphs of molecules was calculated. In [13], relation between the sum-connectivity index and average distance was established. Extremal results concerning minimum sum-connectivity index and matching number were obtained in [14] for trees and connected unicyclic graphs, in [15] for connected bicyclic graphs, and in [16] for cacti. Results on trees with given matching number and maximum sum-connectivity index were found in [17]. Some mathematical aspects of χ index were studied in [9], particularly for the family of trees, which contains molecular

trees representing acyclic hydrocarbons. More detail about the χ index can be found in the recent survey [18] and recent articles [19, 20]. In the present study, we obtained the minimum general sum-connectivity index from the family of all n -vertex (where $n \geq 23$) graphs having minimum degree of at least 3 under certain constraints.

2. Main Results

Theorem 1. For $n \geq 23$, let G be an n -vertex graph with minimum degree of at least 3, such that G satisfies the following two conditions:

- (i) If G has a pair of adjacent vertices of degree 3, then this pair of adjacent vertices has at most one common neighbor
- (ii) If G contains no pair of adjacent vertices of degree 3, then G has a vertex of degree 3 whose all neighbors form a triangle

Then, it holds that

$$\chi(G) \geq \frac{3(n-3)}{\sqrt{n+2}} + \frac{3}{\sqrt{2(n-1)}}, \tag{3}$$

with the equality sign if and only if $G \cong K_3 + \overline{K}_{n-3}$.

3. Some Preliminaries Lemmas

In this section, some lemmas are given, which play a vital role in proving the main result.

Lemma 1 (See [21]). If $e \in E(G)$ is of maximal weight, then $\chi(G) > \chi(G - e)$.

Lemma 2. If $x, y, z, w \geq 3$, then the function f defined by

$$f(x, y, z, w) = \frac{1}{\sqrt{x+3}} + \frac{1}{\sqrt{y+3}} + \frac{1}{\sqrt{z+3}} + \frac{1}{\sqrt{w+3}} - \frac{1}{\sqrt{x+4}} - \frac{1}{\sqrt{y+4}} - \frac{1}{\sqrt{z+4}} - \frac{1}{\sqrt{w+4}}, \tag{4}$$

is strictly decreasing in all x, y, z , and w on the interval $[3, \infty)$.

Proof.

$$\frac{\partial f}{\partial x} = \frac{-1}{2\sqrt{(x+3)^3}} + \frac{1}{2\sqrt{(x+4)^3}} < 0, \tag{5}$$

shows that the function f is strictly decreasing in x . Because of the symmetry, we also conclude that f is strictly decreasing in y, z , and w . \square

Lemma 3. If n is an integer greater than 16, then the function f defined by

$$f(n) = \frac{3n-8}{\sqrt{n+1}} - \frac{3(n-3)}{\sqrt{n+2}} + \frac{3}{\sqrt{2(n-2)}} - \frac{3}{\sqrt{2(n-1)}} + \frac{1}{\sqrt{6}}, \tag{6}$$

is positive valued.

Proof. Clearly,

$$\frac{3n-5}{\sqrt{n+1}} - \frac{3n-5}{\sqrt{n+2}} > 0. \tag{7}$$

Also,

$$\frac{3}{\sqrt{2n-4}} - \frac{3}{\sqrt{2n-2}} > 0. \tag{8}$$

So,

$$\frac{-3}{\sqrt{n+1}} + \frac{1}{\sqrt{6}} > 0, \tag{9}$$

for all $n > 53$.

From the above inequalities, we get that $f(n) > 0$ for all $n > 53$.

If $17 \leq n \leq 53$, then $f(n) > 0$ by using Mathematica. Hence, $f(n) > 0$ for all $n \geq 17$.

This completes the proof of the lemma. \square

Lemma 4. If n is an integer greater than 22, then the function f defined by

$$f(x) = \frac{1}{\sqrt{x+3}} - \frac{2}{\sqrt{x+4}} + \frac{x-1}{\sqrt{x+n-4}} - \frac{x-1}{\sqrt{x+n-3}}, \text{ where } x \geq 3, \tag{10}$$

is strictly increasing on the interval $[3, \infty)$.

Proof.

$$\frac{df}{dx} = \frac{-1}{2\sqrt{(x+3)^3}} + \frac{1}{\sqrt{(x+4)^3}} + \frac{x+2n-7}{2\sqrt{(x+n-4)^3}} - \frac{x+2n-5}{2\sqrt{(x+n-3)^3}}. \tag{11}$$

For $x \geq 3$, it holds that

$$\left(\frac{7}{6}\right)^{3/2} < (\sqrt{2})^2, \tag{12}$$

which together with inequality $1 + (1/x + 3) \leq 7/6$ imply that

$$\left(1 + \frac{1}{x+3}\right)^{3/2} \leq \left(\frac{7}{6}\right)^{3/2} < 2, \tag{13}$$

which further implies that

$$\frac{2}{(x+4)^{3/2}} - \frac{1}{(x+3)^{3/2}} > 0$$

$$\text{or } \frac{1}{(x+4)^{3/2}} - \frac{1}{2(x+3)^{3/2}} > 0.$$
(14)

Let

$$g(n) = \frac{x+2n-7}{2\sqrt{(x+n-4)^3}}$$
(15)

then,

$$\frac{dg}{dn} = \frac{-2n+x+5}{4\sqrt{(x+n-4)^5}} < 0,$$
(16)

this shows that the function g is decreasing in n .

So,

$$\frac{x+2n-7}{2\sqrt{(x+n-4)^3}} - \frac{x+2n-5}{2\sqrt{(x+n-3)^3}} > 0.$$
(17)

Using these inequalities in the above equation, we get

$$\frac{df}{dx} > 0.$$
(18)

Hence, the function f is strictly increasing in x . \square

Lemma 5. *Let*

$$f(n) = \frac{3(n-4)}{\sqrt{n+1}} - \frac{3(n-3)}{\sqrt{n+2}} + \frac{3}{\sqrt{2(n-2)}} - \frac{3}{\sqrt{2(n-1)}} + \frac{2}{\sqrt{n-1}}$$

$$- \frac{2}{\sqrt{n}} + \frac{3}{\sqrt{6}} - \frac{2}{\sqrt{7}}.$$
(19)

If n is an integer greater than 13, then $f(n) > 0$.

Proof. Given,

$$f(n) = \frac{3(n-4)}{\sqrt{n+1}} - \frac{3(n-3)}{\sqrt{n+2}} + \frac{3}{\sqrt{2(n-2)}} - \frac{3}{\sqrt{2(n-1)}} + \frac{2}{\sqrt{n-1}}$$

$$- \frac{2}{\sqrt{n}} + \frac{3}{\sqrt{6}} - \frac{2}{\sqrt{7}}$$

$$> \frac{3(n-4)}{\sqrt{n+1}} - \frac{3(n-3)}{\sqrt{n+2}} + \frac{3}{\sqrt{2(n-2)}} - \frac{3}{\sqrt{2(n-1)}}$$

$$+ \frac{2}{\sqrt{n-1}} - \frac{2}{\sqrt{n}} + \frac{1}{\sqrt{6}}.$$
(20)

As

$$\frac{3(n-3)}{\sqrt{n+1}} - \frac{3(n-3)}{\sqrt{n+2}} > 0,$$

$$\frac{3}{\sqrt{2(n-2)}} - \frac{3}{\sqrt{2(n-1)}} > 0,$$
(21)

also

$$\frac{2}{\sqrt{n-1}} - \frac{2}{\sqrt{n}} > 0,$$
(22)

the expression is

$$\frac{-3}{\sqrt{n+1}} + \frac{1}{\sqrt{6}} > 0,$$
(23)

for all $n > 53$.

From the above inequalities, we get that $f(n) > 0$ for all $n > 53$.

If $14 \leq n \leq 53$, then $f(n) > 0$ by using Mathematica. Hence, $f(n) > 0$ for all $n \geq 14$. \square

Lemma 6. *If n is an integer greater than 22, then the function f defined by*

$$f(x) = \frac{1}{\sqrt{x+3}} - \frac{2}{\sqrt{x+4}} + \frac{x-1}{\sqrt{x+n-3}}$$

$$- \frac{x-1}{\sqrt{x+n-2}}, \text{ where } x \geq 3,$$
(24)

is strictly increasing on the interval $[3, \infty)$.

Proof.

$$\frac{df}{dx} = \frac{-1}{2\sqrt{(x+3)^3}} + \frac{1}{\sqrt{(x+4)^3}} + \frac{x+2n-5}{2\sqrt{(x+n-3)^3}}$$

$$- \frac{x+2n-3}{2\sqrt{(x+n-2)^3}}.$$
(25)

For $x \geq 3$, it holds that

$$\left(\frac{7}{6}\right)^{3/2} < (\sqrt{2})^2,$$
(26)

which together with inequality $1 + (1/x+3) \leq 7/6$ imply that

$$\left(1 + \frac{1}{x+3}\right)^{3/2} \leq \left(\frac{7}{6}\right)^{3/2} < 2,$$
(27)

which further implies that

$$\frac{2}{(x+4)^{3/2}} - \frac{1}{(x+3)^{3/2}} > 0$$
(28)

$$\text{or } \frac{1}{(x+4)^{3/2}} - \frac{1}{2(x+3)^{3/2}} > 0.$$

Let

$$g(n) = \frac{x + 2n - 5}{2\sqrt{(x + n - 3)^3}} \quad (29)$$

Then,

$$\frac{dg}{dn} = \frac{x - 2n + 3}{4\sqrt{(x + n - 3)^5}} < 0. \quad (30)$$

So,

$$\frac{x + 2n - 5}{2\sqrt{(x + n - 3)^3}} - \frac{x + 2n - 3}{2\sqrt{(x + n - 2)^3}} > 0. \quad (31)$$

Using these inequalities in the above equation, we get

$$\frac{df}{dx} > 0. \quad (32)$$

Hence, the function f is strictly increasing in x . \square

Lemma 7. The function f defined is by

$$f(n) = \frac{3n - 14}{\sqrt{n+1}} - \frac{3(n-3)}{\sqrt{n+2}} + \frac{3}{\sqrt{2(n-2)}} - \frac{3}{\sqrt{2(n-1)}} + \frac{2}{\sqrt{n}} + \frac{3}{\sqrt{6}} - \frac{2}{\sqrt{7}}. \quad (33)$$

If n is an integer greater than 13, then $f(n)$ is positive valued.

Proof. Given,

$$\begin{aligned} f(n) &= \frac{3n - 14}{\sqrt{n+1}} - \frac{3(n-3)}{\sqrt{n+2}} + \frac{3}{\sqrt{2(n-2)}} - \frac{3}{\sqrt{2(n-1)}} \\ &\quad + \frac{2}{\sqrt{n}} + \frac{3}{\sqrt{6}} - \frac{2}{\sqrt{7}} \\ &> \frac{3n - 14}{\sqrt{n+1}} - \frac{3(n-3)}{\sqrt{n+2}} + \frac{3}{\sqrt{2(n-2)}} - \frac{3}{\sqrt{2(n-1)}} \\ &\quad + \frac{2}{\sqrt{n}} + \frac{1}{\sqrt{6}}. \end{aligned} \quad (34)$$

As

$$\begin{aligned} \frac{3(n-3)}{\sqrt{n+1}} - \frac{3(n-3)}{\sqrt{n+2}} &> 0, \\ \frac{3}{\sqrt{2(n-2)}} - \frac{3}{\sqrt{2(n-1)}} &> 0, \end{aligned} \quad (35)$$

also

$$\frac{2}{\sqrt{n}} - \frac{2}{\sqrt{n+1}} > 0, \quad (36)$$

so,

$$\frac{-3}{\sqrt{n+1}} + \frac{1}{\sqrt{6}} > 0, \quad (37)$$

for all $n > 53$.

From the above inequalities, we get that $f(n) > 0$ for all $n > 53$.

If $14 \leq n \leq 53$, then $f(n) > 0$ by using Mathematica. Hence, $f(n) > 0$ for all $n \geq 14$. \square

Lemma 8. If $x \geq 3, y \geq 4$, then the function f defined by

$$f(x, y) = \frac{1}{\sqrt{x+y}} - \frac{1}{\sqrt{x+y-1}} + \frac{y-1}{\sqrt{y+3}} - \frac{y-2}{\sqrt{y+2}}, \quad (38)$$

is strictly increasing in x and strictly decreasing in y .

Proof.

$$\frac{\partial f}{\partial x} = \frac{-1}{2\sqrt{(x+y)^3}} + \frac{1}{2\sqrt{(x+y-1)^3}} > 0. \quad (39)$$

Now,

$$\begin{aligned} \frac{\partial f}{\partial y} &= \frac{y+7}{2\sqrt{(y+3)^3}} - \frac{y+6}{2\sqrt{(y+2)^3}} + \frac{1}{\sqrt{(x+y-1)^3}} \\ &\quad - \frac{1}{2\sqrt{(x+y)^3}}, \end{aligned} \quad (40)$$

$$\frac{\partial^2 f}{\partial x \partial y} = \frac{-3}{4\sqrt{(x+y-1)^5}} + \frac{3}{4\sqrt{(x+y)^5}} < 0.$$

So, we have

$$\frac{\partial f}{\partial y} \leq \frac{\partial f(3, y)}{\partial y} = \frac{y+6}{2\sqrt{(y+3)^3}} - \frac{y+5}{2\sqrt{(y+2)^3}}. \quad (41)$$

Let

$$g(y) = \frac{y+6}{2\sqrt{(y+3)^3}}. \quad (42)$$

Then,

$$\frac{dg}{dy} = \frac{-y-12}{4\sqrt{(y+3)^5}} < 0, \quad (43)$$

which shows that g is strictly decreasing in y .

So,

$$\frac{y+6}{2\sqrt{(y+3)^3}} - \frac{y+5}{2\sqrt{(y+2)^3}} < 0. \quad (44)$$

By using this inequality in the above expression, we get

$$\frac{\partial f}{\partial y} < 0. \tag{45}$$

Hence, the function f is strictly decreasing in y . \square

Lemma 9. *Let*

$$f(n) = \frac{2(n-5)}{\sqrt{n+1}} - \frac{2(n-4)}{\sqrt{n+2}} + \frac{3}{\sqrt{2(n-2)}} - \frac{3}{\sqrt{2(n-1)}} + \frac{1}{\sqrt{6}} \tag{46}$$

If n is an integer greater than 9, then $f(n) > 0$.

Proof. As

$$\frac{2(n-4)}{\sqrt{n+1}} - \frac{2(n-4)}{\sqrt{n+2}} > 0, \tag{47}$$

$$\frac{3}{\sqrt{2(n-2)}} - \frac{3}{\sqrt{2(n-1)}} > 0,$$

so,

$$\frac{-2}{\sqrt{n+1}} + \frac{1}{\sqrt{6}} > 0, \tag{48}$$

for all $n > 23$.

From the above inequalities, we get that $f(n) > 0$ for all $n > 23$.

If $10 \leq n \leq 23$, then $f(n) > 0$ by using Mathematica.

Hence, $f(n) > 0$ for all $n \geq 10$. \square

Lemma 10. *If $x \geq 4$, then the function f defined by*

$$f(x) = \frac{x}{\sqrt{x+3}} - \frac{x-1}{\sqrt{x+2}}, \tag{49}$$

is strictly decreasing on the interval $[4, \infty)$.

Proof.

$$\frac{df}{dx} = \frac{x+6}{2\sqrt{(x+3)^3}} - \frac{x+5}{2\sqrt{(x+2)^3}} \tag{50}$$

Let

$$g(x) = \frac{x+6}{2\sqrt{(x+3)^3}}. \tag{51}$$

Then,

$$g'(x) = \frac{-x-12}{4\sqrt{(x+3)^5}} < 0. \tag{52}$$

So,

$$\frac{x+6}{2\sqrt{(x+3)^3}} - \frac{x+5}{2\sqrt{(x+2)^3}} < 0. \tag{53}$$

Using this in the above equation, we get

$$\frac{df}{dx} < 0. \tag{54}$$

Hence, the function f is strictly decreasing in x . \square

Lemma 11. *If n is an integer greater than 9, then the function f defined by*

$$f(n) = \frac{4n-14}{\sqrt{n+1}} - \frac{3(n-3)}{\sqrt{n+2}} + \frac{3}{\sqrt{2(n-2)}} - \frac{3}{\sqrt{2(n-1)}} - \frac{n-3}{\sqrt{n}} + \frac{1}{\sqrt{6}} \tag{55}$$

is positive valued.

Proof. As

$$\frac{3(n-3)}{\sqrt{n+1}} - \frac{3(n-3)}{\sqrt{n+2}} > 0, \tag{56}$$

$$\frac{3}{\sqrt{2(n-2)}} - \frac{3}{\sqrt{2(n-1)}} > 0,$$

the expression is

$$\frac{n-2}{\sqrt{n+1}} - \frac{n-3}{\sqrt{n}} > 0, \tag{57}$$

$$= \sqrt{n+1} - \sqrt{n} + \frac{3}{\sqrt{n}} - \frac{3}{\sqrt{n+1}} > 0.$$

So,

$$\frac{-3}{\sqrt{n+1}} + \frac{1}{\sqrt{6}} > 0, \tag{58}$$

for all $n > 53$.

From the above inequalities, we get that $f(n) > 0$ for all $n > 53$.

If $10 \leq n \leq 53$, then $f(n) > 0$ by using Mathematica.

Hence, $f(n) > 0$ for all $n \geq 10$. \square

Lemma 12. *If $x, y, z \geq 4$, then the function f defined by*

$$f(x, y, z) = \frac{x-2}{\sqrt{x+3}} - \frac{x-3}{\sqrt{x+2}} + \frac{1}{\sqrt{x+y}} - \frac{1}{\sqrt{x+y-2}} + \frac{y-2}{\sqrt{y+3}} - \frac{y-3}{\sqrt{y+2}} + \frac{1}{\sqrt{y+z}} - \frac{1}{\sqrt{y+z-2}} + \frac{z-2}{\sqrt{z+3}} - \frac{z-3}{\sqrt{z+2}} + \frac{1}{\sqrt{x+z}} - \frac{1}{\sqrt{x+z-2}}, \tag{59}$$

is decreasing in all x, y and z .

Proof.

$$\begin{aligned} \frac{\partial f}{\partial x} &= \frac{x+8}{2\sqrt{(x+3)^3}} - \frac{x+7}{2\sqrt{(x+2)^3}} - \frac{1}{2\sqrt{(x+y)^3}} - \frac{1}{2\sqrt{(x+z)^3}} \\ &\quad + \frac{1}{2\sqrt{(x+y-2)^3}} + \frac{1}{2\sqrt{(x+z-2)^3}}, \end{aligned} \quad (60)$$

which implies

$$\begin{aligned} \frac{\partial^2 f}{\partial x \partial y} &= \frac{3}{4\sqrt{(x+y)^5}} - \frac{3}{4\sqrt{(x+y-2)^5}} < 0, \\ \frac{\partial^2 f}{\partial x \partial z} &= \frac{3}{4\sqrt{(x+z)^5}} - \frac{3}{4\sqrt{(x+z-2)^5}} < 0. \end{aligned} \quad (61)$$

Since $\partial^2 f / \partial x \partial y < 0$ and $\partial^2 f / \partial x \partial z < 0$, it holds that

$$\begin{aligned} \frac{\partial f}{\partial x} &\leq \frac{\partial f(x, 4, 4)}{\partial x} \\ &= \frac{x+8}{2\sqrt{(x+3)^5}} - \frac{x+5}{2\sqrt{(x+2)^5}} - \frac{1}{\sqrt{(x+4)^3}}. \end{aligned} \quad (62)$$

Let

$$F(x) = \frac{x+8}{2\sqrt{(x+3)^3}} - \frac{x+5}{2\sqrt{(x+2)^3}} - \frac{1}{\sqrt{(x+4)^3}}, \quad (63)$$

where $x \geq 4$. We note that

$$F(x) = h(x+1) - h(x) + g(x) - g(x+1), \quad (64)$$

where

$$\begin{aligned} h(x) &= \frac{x+5}{2\sqrt{(x+2)^3}}, \\ g(x) &= \frac{1}{\sqrt{(x+3)^3}}. \end{aligned} \quad (65)$$

The functions h and g are continuous as well as differentiable on the closed interval $[x_0, x_0 + 1]$ for every fixed number $x_0 \geq 4$.

By virtue of Cauchy's mean value theorem, we observe that for every x_0 , there exists a number $c_{x_0} \in (x_0, x_0 + 1)$, such that

$$\begin{aligned} \frac{h(x_0+1) - h(x_0)}{g(x_0+1) - g(x_0)} &= \frac{h'(c_{x_0})}{g'(c_{x_0})} \\ &= \left(\frac{c_{x_0} + 3}{c_{x_0} + 2} \right)^{5/2} \left(\frac{c_{x_0} + 11}{6} \right), \end{aligned} \quad (66)$$

which is greater than one, and hence,

$$F(x_0) = h(x_0+1) - h(x_0) + g(x_0) - g(x_0+1) < 0, \quad (67)$$

because the function g is decreasing.

Therefore, for all $x \geq 4$, the function $F(x)$ is negative valued. Using $F(x) < 0$ in the above equation, we get

$$\frac{\partial f}{\partial x} < 0. \quad (68)$$

This shows that the function f is decreasing in x .

By symmetry, it follows that

$$\frac{\partial f}{\partial y} < 0, \quad (69)$$

$$\frac{\partial f}{\partial z} < 0,$$

which means that the function f is decreasing in y and z . Hence, the function f is decreasing in x, y , and z . \square

4. Proof of Theorem 1

Proof. We will prove the result by induction on n . For $n = 23$, by using the AutoGraphiX system [22], we find that $K_3 + \overline{K}_{n-3}$ has the maximum χ value among all n -vertex graphs having a minimum degree of at least 3, which implies that the result is true for $n = 23$. Now, we suppose that the theorem holds for all those k -vertex graphs which satisfy all the constraints of the theorem, where $23 \leq k \leq n - 1$.

If minimum degree of G is at least 4, then we take $v_1 v_2 \in E(G)$, such that $d(v_1) + d(v_2) \leq d(u) + d(v)$ for all $uv \in E(G)$. Clearly, the graph $G - v_1 v_2$ has minimum degree of at least 3, and from Lemma 1, it follows that $\chi(G) > \chi(G - v_1 v_2)$. Hence, it is sufficient to assume that the minimum degree of G is 3. Next, we consider all possible cases.

Case 1:

G contains at least one pair of adjacent vertices having degree 3 without common neighbors

Let $u_1, u_2 \in V(G)$ be two adjacent vertices having degree 3 without any common neighbor. Let v_1 and v_2 be the neighbors of u_1 different from u_2 , and w_1, w_2 be the

neighbors of u_2 different from u_1 . In this case, the vertex degrees $d(v_1), d(v_2), d(w_1)$, and $d(w_2)$ satisfy the inequality $3 \leq d(v_1), d(v_2), d(w_1), d(w_2) \leq n - 2$. By

setting $G_1 \cong G - \{u_1\} + \{u_2v_1, u_2v_2\}$ and then by using Lemma 2, the inductive hypothesis, and Lemma 3, we have

$$\begin{aligned}
 \chi(G) &= \chi(G_1) + \frac{1}{\sqrt{d(u_1) + d(u_2)}} + \frac{1}{\sqrt{d(u_1) + d(v_1)}} + \frac{1}{\sqrt{d(u_1) + d(v_2)}} \\
 &\quad + \frac{1}{\sqrt{d(u_2) + d(w_1)}} - \frac{1}{\sqrt{d(u_2) + 1 + d(w_1)}} + \frac{1}{\sqrt{d(u_2) + d(w_2)}} \\
 &\quad - \frac{1}{\sqrt{d(u_2) + 1 + d(w_2)}} - \frac{1}{\sqrt{d(u_2) + 1 + d(v_1)}} - \frac{1}{\sqrt{d(u_2) + 1 + d(v_2)}} \\
 &= \chi(G_1) + \frac{1}{\sqrt{6}} + \frac{1}{\sqrt{3 + d(v_1)}} + \frac{1}{\sqrt{3 + d(v_2)}} \\
 &\quad + \frac{1}{\sqrt{3 + d(w_1)}} - \frac{1}{\sqrt{4 + d(w_1)}} + \frac{1}{\sqrt{3 + d(w_2)}} \\
 &\quad - \frac{1}{\sqrt{4 + d(w_2)}} - \frac{1}{\sqrt{4 + d(v_1)}} - \frac{1}{\sqrt{4 + d(v_2)}} \\
 &\geq \frac{3(n-4)}{\sqrt{n+1}} + \frac{3}{\sqrt{2(n-2)}} + \frac{4}{\sqrt{n+1}} - \frac{4}{\sqrt{n+2}} + \frac{1}{\sqrt{6}} \\
 &> \frac{3(n-3)}{\sqrt{n+2}} + \frac{3}{\sqrt{2(n-1)}}.
 \end{aligned} \tag{70}$$

Case 2:

G contains at least one pair of adjacent vertices of degree 3 with a common neighbor

Let $u_1, u_2 \in V(G)$ be two adjacent vertices of degree 3 having a common neighbor v . Let v_1 be the neighbor of u_1 different from u_2 , and v and w_1 be the neighbors of u_2 different from u_1, v .

Subcase i:

Let $d(v) = 3$, and there is an edge between v_1 and v . Clearly, it holds that $3 \leq d(v_1) \leq n - 2$ and $3 \leq d(w_1) \leq n - 3$. If we take $G_2 \cong G - \{u_1\} + \{u_2v_1, w_1v\}$, then by using Lemma 4, the inductive hypothesis, and Lemma 5, we get

$$\begin{aligned}
 \chi(G) &= \chi(G_2) + \frac{1}{\sqrt{d(u_1) + d(u_2)}} + \frac{1}{\sqrt{d(u_1) + d(v)}} + \frac{1}{\sqrt{d(u_1) + d(v_1)}} \\
 &\quad - \frac{1}{\sqrt{d(u_2) + d(v_1)}} - \frac{1}{\sqrt{d(v) + d(w_1) + 1}} \\
 &\quad + \frac{1}{\sqrt{d(u_2) + d(w_1)}} - \frac{1}{\sqrt{d(u_2) + d(w_1) + 1}}
 \end{aligned}$$

$$\begin{aligned}
& + \sum_{z \in N(w_1) \setminus \{u_2\}} \left(\frac{1}{\sqrt{d(z) + d(w_1)}} - \frac{1}{\sqrt{d(z) + d(w_1) + 1}} \right) \\
\geq & \chi(G_2) + \frac{2}{\sqrt{6}} - \frac{1}{\sqrt{3 + d(w_1) + 1}} + \frac{1}{\sqrt{3 + d(w_1)}} \\
& - \frac{1}{\sqrt{3 + d(w_1) + 1}} + \frac{d(w_1) - 1}{\sqrt{n - 4 + d(w_1)}} - \frac{d(w_1) - 1}{\sqrt{n - 4 + d(w_1) + 1}} \\
\geq & \chi(G_2) + \frac{2}{\sqrt{n-1}} - \frac{2}{\sqrt{n}} + \frac{3}{\sqrt{6}} - \frac{2}{\sqrt{7}} \\
\geq & \frac{3(n-4)}{\sqrt{n+1}} + \frac{3}{\sqrt{2(n-2)}} + \frac{2}{\sqrt{n-1}} - \frac{2}{\sqrt{n}} + \frac{3}{\sqrt{6}} - \frac{2}{\sqrt{7}} \\
> & \frac{3(n-3)}{\sqrt{n+2}} + \frac{3}{\sqrt{2(n-1)}}.
\end{aligned} \tag{71}$$

Subcase ii:
Let $d(v) = 3$, and there is no edge between v_1 and v .
Clearly, it holds that $3 \leq d(v_1) \leq n - 3$. If $G_3 \cong G -$

$\{u_1\} + \{u_2, v_1, v_1 v\}$, then by using Lemma 6, the induction hypothesis, and Lemma 7, we obtained

$$\begin{aligned}
\chi(G) & = \chi(G_3) + \frac{1}{\sqrt{d(u_1) + d(u_2)}} + \frac{1}{\sqrt{d(u_1) + d(v)}} + \frac{1}{\sqrt{d(u_1) + d(v_1)}} \\
& - \frac{1}{\sqrt{d(u_2) + d(v_1) + 1}} - \frac{1}{\sqrt{d(v) + d(v_1) + 1}} \\
& + \sum_{z \in N(v_1) \setminus \{u_1\}} \left(\frac{1}{\sqrt{d(z) + d(v_1)}} - \frac{1}{\sqrt{d(z) + d(v_1) + 1}} \right) \\
\geq & \chi(G_3) + \frac{2}{\sqrt{6}} + \frac{1}{\sqrt{3 + d(v_1)}} - \frac{1}{\sqrt{3 + d(v_1) + 1}} \\
& - \frac{1}{\sqrt{3 + d(v_1) + 1}} + \frac{d(v_1) - 1}{\sqrt{n - 3 + d(v_1)}} - \frac{d(v_1) - 1}{\sqrt{n - 3 + d(v_1) + 1}} \\
\geq & \chi(G_3) + \frac{2}{\sqrt{n}} - \frac{2}{\sqrt{n+1}} + \frac{3}{\sqrt{6}} - \frac{2}{\sqrt{7}} \\
\geq & \frac{3(n-4)}{\sqrt{n+1}} + \frac{3}{\sqrt{2(n-2)}} + \frac{2}{\sqrt{n}} - \frac{2}{\sqrt{n+1}} + \frac{3}{\sqrt{6}} - \frac{2}{\sqrt{7}} \\
> & \frac{3(n-3)}{\sqrt{n+2}} + \frac{3}{\sqrt{2(n-1)}}.
\end{aligned} \tag{72}$$

Subcase iii:

Let $d(v) \geq 4$, and there is an edge between v_1 and v . Clearly, it holds that $3 \leq d(v_1) \leq n - 2$. If we take

$G_4 \cong G - u_1 + u_2v_1$, then by using Lemma 8, the inductive hypothesis, and Lemma 9, we have

$$\begin{aligned}
 \chi(G) &= \chi(G_4) + \frac{1}{\sqrt{d(u_1) + d(u_2)}} + \frac{1}{\sqrt{d(u_1) + d(v)}} + \frac{1}{\sqrt{d(u_1) + d(v_1)}} - \frac{1}{\sqrt{d(u_2) + d(v_1)}} \\
 &\quad + \frac{1}{\sqrt{d(u_2) + d(v)}} - \frac{1}{\sqrt{d(u_2) + d(v) - 1}} + \frac{1}{\sqrt{d(v_1) + d(v)}} - \frac{1}{\sqrt{d(v_1) + d(v) - 1}} \\
 &\quad + \sum_{z \in N(v) \setminus \{u_1, v_1, v_2\}} \left(\frac{1}{\sqrt{d(v) + d(z)}} - \frac{1}{\sqrt{d(v) - 1 + d(z)}} \right) \\
 &\geq \chi(G_4) + \frac{1}{\sqrt{6}} + \frac{2}{\sqrt{3 + d(v)}} - \frac{1}{\sqrt{3 + d(v) - 1}} + \frac{1}{\sqrt{d(v_1) + d(v)}} - \frac{1}{\sqrt{d(v_1) + d(v) - 1}} \\
 &\quad + \frac{d(v) - 3}{\sqrt{d(v) + d(z)}} + \frac{d(v) - 3}{\sqrt{d(v) - 1 + d(z)}} \\
 &\geq \chi(G_4) + \frac{n - 1}{\sqrt{n + 2}} - \frac{n - 2}{\sqrt{n + 1}} + \frac{1}{\sqrt{6}} \\
 &\geq \frac{3(n - 4)}{\sqrt{n + 1}} + \frac{3}{\sqrt{2(n - 2)}} + \frac{n - 1}{\sqrt{n + 2}} - \frac{n - 2}{\sqrt{n + 1}} + \frac{1}{\sqrt{6}} \\
 &> \frac{3(n - 3)}{\sqrt{n + 2}} + \frac{3}{\sqrt{2(n - 1)}}.
 \end{aligned} \tag{73}$$

Subcase iv:
Let $d(v) \geq 4$, and there is no edge between v_1 and v . Clearly, it holds that $3 \leq d(v_1) \leq n - 3$. If we take

$G_5 \cong G - u_1 + u_2v_1$, then by using Lemma 10, the inductive hypothesis, and Lemma 11, we get

$$\begin{aligned}
 \chi(G) &= \chi(G_5) + \frac{1}{\sqrt{d(u_1) + d(u_2)}} + \frac{1}{\sqrt{d(u_1) + d(v_1)}} + \frac{1}{\sqrt{d(u_1) + d(v)}} - \frac{1}{\sqrt{d(u_2) + d(v_1)}} + \frac{1}{\sqrt{d(u_2) + d(v)}} - \frac{1}{\sqrt{d(u_2) + d(v) - 1}} \\
 &\quad + \sum_{z \in N(v) \setminus \{u_1, u_2\}} \left(\frac{1}{\sqrt{d(v) + d(z)}} - \frac{1}{\sqrt{d(v) - 1 + d(z)}} \right) \\
 &\geq \chi(G_5) + \frac{1}{\sqrt{6}} + \frac{2}{\sqrt{3 + d(v)}} - \frac{1}{\sqrt{3 + d(v) - 1}} + \frac{d(v) - 2}{\sqrt{d(v) + d(z)}} - \frac{d(v) - 2}{\sqrt{d(v) - 1 + d(z)}} \\
 &\geq \chi(G_5) + \frac{n - 2}{\sqrt{n + 1}} - \frac{n - 3}{\sqrt{n}} + \frac{1}{\sqrt{6}} \geq \frac{3(n - 4)}{\sqrt{n + 1}} + \frac{3}{\sqrt{2(n - 2)}} + \frac{n - 2}{\sqrt{n + 1}} - \frac{n - 3}{\sqrt{n}} + \frac{1}{\sqrt{6}} \\
 &> \frac{3(n - 3)}{\sqrt{n + 2}} + \frac{3}{\sqrt{2(n - 1)}}.
 \end{aligned} \tag{74}$$

Case 3:

G does not contain any pair of adjacent vertices of degree 3

Let $u \in V(G)$ be a vertex of degree 3 having neighbors $u_1, u_2,$ and $u_3,$ such that $u_1u_2, u_1u_3, u_2u_3 \in E(G)$; then clearly, $d(u_1), d(u_2), d(u_3) \geq 4$. If we take $G_6 \cong G - \{u\}$,

then by induction hypothesis and by using Lemma 12, we have

$$\begin{aligned}
 \chi(G) &= \chi(G_6) + \frac{1}{\sqrt{d(u) + d(u_1)}} + \frac{1}{\sqrt{d(u) + d(u_2)}} + \frac{1}{\sqrt{d(u) + d(u_3)}} \\
 &\quad + \frac{1}{\sqrt{d(u_1) + d(u_2)}} - \frac{1}{\sqrt{d(u_1) + d(u_2) - 2}} + \frac{1}{\sqrt{d(u_1) + d(u_3)}} \\
 &\quad - \frac{1}{\sqrt{d(u_1) + d(u_3) - 2}} + \frac{1}{\sqrt{d(u_2) + d(u_3)}} - \frac{1}{\sqrt{d(u_2) + d(u_3) - 2}} \\
 &\quad + \sum_{z \in N(u_1) \setminus \{u, u_2, u_3\}} \left(\frac{1}{\sqrt{d(u_1) + d(z)}} - \frac{1}{\sqrt{d(u_1) - 1 + d(z)}} \right) \\
 &\quad + \sum_{z \in N(u_2) \setminus \{u, u_1, u_3\}} \left(\frac{1}{\sqrt{d(u_2) + d(z)}} - \frac{1}{\sqrt{d(u_2) - 1 + d(z)}} \right) \\
 &\quad + \sum_{z \in N(u_3) \setminus \{u, u_1, u_2\}} \left(\frac{1}{\sqrt{d(u_3) + d(z)}} - \frac{1}{\sqrt{d(u_3) - 1 + d(z)}} \right) \\
 &\geq \chi(G_6) + \frac{1}{\sqrt{3 + d(u_1)}} + \frac{1}{\sqrt{3 + d(u_2)}} + \frac{1}{\sqrt{3 + d(u_3)}} \\
 &\quad + \frac{1}{\sqrt{d(u_1) + d(u_2)}} - \frac{1}{\sqrt{d(u_1) + d(u_2) - 2}} + \frac{1}{\sqrt{d(u_1) + d(u_3)}} \\
 &\quad - \frac{1}{\sqrt{d(u_1) + d(u_3) - 2}} + \frac{1}{\sqrt{d(u_2) + d(u_3)}} - \frac{1}{\sqrt{d(u_2) + d(u_3) - 2}} \\
 &\quad + \frac{d(u_1) - 3}{\sqrt{d(u_1) + 3}} - \frac{d(u_1) - 3}{\sqrt{d(u_1) + 3 - 1}} + \frac{d(u_2) - 3}{\sqrt{d(u_2) + 3}} \\
 &\quad - \frac{d(u_2) - 3}{\sqrt{d(u_2) + 3 - 1}} + \frac{d(u_3) - 3}{\sqrt{d(u_3) + 3}} - \frac{d(u_3) - 3}{\sqrt{d(u_3) + 3 - 1}} \\
 &\geq \chi(G_6) + \frac{3(n-3)}{\sqrt{n+2}} - \frac{3(n-4)}{\sqrt{n+1}} + \frac{3}{\sqrt{2(n-1)}} - \frac{3}{\sqrt{2(n-2)}} \\
 &\geq \frac{3(n-4)}{\sqrt{n+1}} + \frac{3}{\sqrt{2(n-2)}} + \frac{3(n-3)}{\sqrt{n+2}} - \frac{3(n-4)}{\sqrt{n+1}} + \frac{3}{\sqrt{2(n-1)}} - \frac{3}{\sqrt{2(n-2)}} \\
 &= \frac{3(n-3)}{\sqrt{n+2}} + \frac{3}{\sqrt{2(n-1)}}.
 \end{aligned} \tag{75}$$

We observe that the equation

$$\chi(G) = \frac{3(n-3)}{\sqrt{n+2}} + \frac{3}{\sqrt{2(n-1)}} \tag{76}$$

holds if and only if

$$d(u_1) = d(u_2) = d(u_3) = n - 1. \quad (77)$$

This completes the proof of Theorem 1. \square

5. Concluding Remarks

We have characterized the minimum sum-connectivity index from the family of all n -vertex graphs having minimum degree at least 3, under certain constraints. More precisely, we have been able to show that $K_3 + \overline{K}_{n-3}$ is the only graph having minimal sum-connectivity index in the family of all those n -vertex (where $n \geq 23$) graphs which have a minimum degree of at least 3 and satisfy the following two conditions:

- (i) If G has a pair of adjacent vertices of degree 3, then this pair of adjacent vertices has at most one common neighbor
- (ii) If G contains no pair of adjacent vertices of degree 3, then G has a vertex of degree 3 whose all neighbors form a triangle.

Data Availability

The data used to support the findings of this study are included within the article.

Conflicts of Interest

The authors declare that they have no conflicts of interest.

Acknowledgments

This research was funded by Scientific Research Deanship at University of Ha'il, Saudi Arabia, through project number RG-20 050.

References

- [1] A. Ali and Z. Du, "On the difference between atom-bond connectivity index and Randić index of binary and chemical trees," *International Journal of Quantum Chemistry*, vol. 117, no. 23, Article ID e25446, 2017.
- [2] A. Ali, S. Elumalai, and T. Mansour, "On the symmetric division deg index of molecular graphs," *MATCH Communications in Mathematical and in Computer Chemistry*, vol. 83, no. 1, pp. 193–208, 2020.
- [3] A. Emanuel, T. Doslić, and A. Ali, "Two upper bounds on the weighted Harary indices," *Discrete Mathematics Letters*, vol. 1, pp. 21–25, 2019.
- [4] Y. Ma, S. Cao, Y. Shi, I. Gutman, M. Dehmer, and B. Furtula, "From the connectivity index to various Randić-type descriptors," *MATCH Communications in Mathematical and in Computer Chemistry*, vol. 80, no. 1, pp. 85–106, 2018.
- [5] I. Milovanović, M. Matejić, and E. Milovanović, "A note on the general zeroth-order Randić coindex of graphs," *Contributions to Mathematics*, vol. 1, pp. 17–21, 2020.
- [6] K. Xu, M. Liu, K. C. Das, I. Gutman, and B. Furtula, "A survey on graphs extremal with respect to distance-based topological indices," *MATCH Communications in Mathematical and in Computer Chemistry*, vol. 71, no. 3, pp. 461–508, 2014.
- [7] L. Zhong and Q. Qian, "The minimum general sum-connectivity index of trees with given matching number," *Bulletin of the Malaysian Mathematical Sciences Society*, vol. 43, no. 2, pp. 1527–1544, 2020.
- [8] M. Randić, "Characterization of molecular branching," *Journal of the American Chemical Society*, vol. 97, no. 23, pp. 6609–6615, 1975.
- [9] B. Zhou and N. Trinajstić, "On a novel connectivity index," *Journal of Mathematical Chemistry*, vol. 46, no. 4, pp. 1252–1270, 2009.
- [10] M. Cancan, S. Ediz, S. Ediz, and M. R. Farahani, "On vertex-degree atom-bond connectivity, sum-connectivity, geometric-arithmetic and harmonic indices of copper oxide," *Eurasian Chemical Communications*, vol. 2, no. 5, pp. 641–645, 2020.
- [11] M. R. Farahani, "On the Randić and sum-connectivity index of nanotubes," *Analele Universitatii de Vest, Timisoara Seria Matematica Informatica*, vol. 2, pp. 39–46, 2013.
- [12] W. Gao, M. R. Farahani, and M. Imran, "About the Randić connectivity, modify Randić connectivity and sum-connectivity indices of titania nanotubes $\text{TiO}_2(m, n)$," *Acta Chimica Slovenica*, vol. 64, no. 1, pp. 256–260, 2017.
- [13] V. Lokesha, B. S. Shetty, P. Raju, and P. S. Ranjini, "Relation between sum-connectivity index and average distance of trees," *International journal of Mathematical Combinatorics*, vol. 4, pp. 92–98, 2015.
- [14] Z. Du, B. Zhou, and N. Trinajstić, "Minimum general sum-connectivity index of unicyclic graphs," *Journal of Mathematical Chemistry*, vol. 48, no. 3, pp. 697–703, 2010.
- [15] Z. Du and B. Zhou, "On sum-connectivity index of bicyclic graphs," *The Bulletin of the Malaysian Mathematical Society Series 2*, vol. 35, no. 1, pp. 101–117, 2012.
- [16] F. Ma and H. Deng, "On the sum-connectivity index of cacti," *Mathematical and Computer Modelling*, vol. 54, no. 1–2, pp. 497–507, 2011.
- [17] Z. Zhu and W. Zhang, "Trees with a given order and matching number that have maximum general sum-connectivity index," *ARS Combinatoria*, vol. 128, pp. 439–446, 2016.
- [18] A. Ali, L. Zhong, and I. Gutman, "Harmonic index and its generalizations: extremal results and bounds," *MATCH Communications in Mathematical and in Computer Chemistry*, vol. 81, pp. 249–311, 2019.
- [19] S. Ahmed, "On the maximum general sum-connectivity index of trees with a fixed order and maximum degree," *Discrete Mathematics Algorithms and Applications*, vol. 13, no. 4, Article ID 2150042, 2021.
- [20] A. Ali, S. Ahmed, Z. Du, W. Gao, and M. A. Malik, "On the minimal general sum-connectivity index of connected graphs without pendant vertices," *IEEE Access*, vol. 7, pp. 136743–136751, 2019.
- [21] S. Wang, Z. Bo, and N. Trinajstić, "On the sum-connectivity index," *Filomat*, vol. 25, no. 3, pp. 29–42, 2011.
- [22] G. Caporossi and P. Hansen, "Variable neighborhood search for extremal graphs: 1 the AutoGraphiX system," *Discrete Mathematics*, vol. 212, no. 1–2, pp. 29–44, 2000.

Research Article

On Edge H -Irregularity Strength of Hexagonal and Octagonal Grid Graphs

Muhammad Ibrahim ¹, Ana Gulzar,¹ Muhammad Fazil ²,
and Muhammad Naeem Azhar ¹

¹Centre for Advanced Studies in Pure and Applied Mathematics, Bahauddin Zakariya University, Multan, Pakistan

²Department of Basic Sciences and Humanities, Faculty of Engineering, Bahauddin Zakariya University, Multan, Pakistan

Correspondence should be addressed to Muhammad Fazil; mfazil@bzu.edu.pk

Received 31 August 2021; Accepted 5 January 2022; Published 31 January 2022

Academic Editor: Firdous A. Shah

Copyright © 2022 Muhammad Ibrahim et al. This is an open access article distributed under the Creative Commons Attribution License, which permits unrestricted use, distribution, and reproduction in any medium, provided the original work is properly cited.

The edge H -irregularity strength, $ehs(\Gamma, H)$, of a graph Γ is the smallest integer k , such that Γ has an H -irregular edge k -labeling. In this study, we compute the exact value of edge H -irregularity strength of hexagonal and octagonal grid graphs.

1. Introduction

Let Γ be a connected graph. A mapping that assigns numbers to graph elements (vertices and edges) is called labeling. A graph labeling is called vertex labeling or edge labeling if its domain set is the vertex set or the edge set of the graph, respectively. The concept of graph labeling plays an important role to construct models for a wide range of engineering applications such as coding theory, X-rays crystallography, astronomy, radar, circuit design, wired communication, and wireless communications. For further detail related to graph labeling, refer to [1].

For an edge k -labeling $\zeta: E(\Gamma) \rightarrow \{1, 2, \dots, k\}$, $k \in \mathbb{Z}^+$, the corresponding weight of $u \in V(\Gamma)$ is $wt_{\zeta}(u) = \sum_{uv \in E(\Gamma)} \zeta(uv)$. The edge k -labeling ζ is called irregular if $wt_{\zeta}(u) \neq wt_{\zeta}(v)$, $\forall u \neq v \in V(\Gamma)$. The irregularity strength of Γ , $s(\Gamma)$, is the minimum $k \in \mathbb{Z}^+$, such that there exists an edge irregular k -labeling of Γ . The concept of the irregularity strength of a graph was introduced by Chartrand et al. [2]. There has been a flurry of research work on the irregularity strength in the last few years [3–12].

A vertex k -labeling $\zeta^*: V(\Gamma) \rightarrow \{1, 2, \dots, k\}$ of Γ is called an edge irregular k -labeling if for every two distinct edges uv and $u'v'$, $wt_{\zeta^*}(uv) \neq wt_{\zeta^*}(u'v')$, where $wt_{\zeta^*}(uv) = \zeta^*(u) + \zeta^*(v)$.

The edge irregularity strength of Γ , $es(\Gamma)$, is the minimum k , such that the graph Γ has an edge irregular k -labeling. The concept of the edge irregularity strength was given by Ahmad et al. [13]. Ashraf et al. [14] have introduced two new graph parameters, i.e., vertex (edge) H -irregularity strength of a graph. These parameters are considered as extensions of the irregularity strength and the edge irregularity strength of Γ .

A family $\mathcal{H} = \{H_i, 1 \leq i \leq t\}$ of subgraphs of a graph Γ , such that each edge of Γ belonging to at least one member of \mathcal{H} is called an edge-covering of Γ . If every member of \mathcal{H} is isomorphic to a graph H , then Γ admits an H -covering. An edge k -labeling ζ is called an H -irregular edge k -labeling of the graph Γ that admits H -covering if for every two distinct subgraphs H_1 and H_2 , which are isomorphic to H , $wt_{\zeta}(H_1) \neq wt_{\zeta}(H_2)$. The edge H -irregularity strength of a graph Γ , $ehs(\Gamma, H)$, is the smallest integer k , such that Γ has an H -irregular edge k -labeling.

In proving lower bound concerning a graph Γ admitting H -covering, the following result is useful.

Theorem 1 (see [14]). *Let Γ be a graph admitting H -covering given by t subgraphs isomorphic to H . Then, $ehs(\Gamma, H) \geq \lceil 1 + (t - 1/|E(H)|) \rceil$.*

In this study, we compute the exact values of the edge H -irregularity strength of the hexagonal grid graph and octagonal grid graph.

2. Motivation and Applications of H -Covering of Graph

The topic of H -covering of the graph is newly addressed by Ashraf et al. in [14] and found the H -covering for different graphs. Still now, the problem of H -covering was addressed on grids by any author. As the topic is related to the networking and communication system, it is needed to work on some networks. So, we choose these two graphs as these graphs are related to network. The H -covering has a wide range of applications in X-rays, circuit design, and especially in communication and networks. The graphs studied in the present study are hexagonal and octagonal grids. These graphs consist of 6 and 8 vertices in each face of the graph, and each face made a cycle consisting of 6 and 8 vertices and edges as well. These graphs and their faces could be served as models for surveillance or security systems, electrical switchboards, circuit design, and communication networks. These networks can be extended in both horizontal and vertical directions, so that the extension in the graphs and networks can be handled and made easy. Moreover, these networks are used especially in communication networks, and the efficiency of the networks may be improved as the weights of the each face have distinct numbers.

3. Hexagonal Grid Graph

For finite $r, s \geq 3$, the hexagonal grid graph (honeycomb), H_r^s , is a graph with s rows and r columns of hexagons [15]. The vertex and the edge sets of this graph are defined as $V(H_r^s) = \{v_j^i, u_j^i; 1 \leq i \leq s, 1 \leq j \leq r\}; E(H_r^s) = \{v_j^i u_j^i, v_j^{i+1} u_j^{i+1}; 1 \leq i \leq s-1, 1 \leq j \leq r\} \cup \{v_j^i u_{j+1}^i, u_j^{i+1} v_{j+1}^{i+1}; 1 \leq i \leq s-1, 1 \leq j \leq r-1\} \cup \{u_j^i v_j^{i+1}; 1 \leq i \leq s-1, 1 \leq j \leq r\}$. The face set of $F(H_r^s)$ consists of $|F(H_r^s)| - 1$ 6-sided faces and one external face which is infinite. Also, $|V(H_r^s)| = 2rs - 2$ and $|E(H_r^s)| = |V(H_r^s)| + s(r - 1)$, while $|F(H_r^s)| = 4(r + s) - 9$. For $r, s \geq 3$, the hexagonal grid graph is shown in Figure 1.

In the following theorem, we determine the edge H -irregularity strength of H_r^s , where $r, s \geq 3$ are finite.

Theorem 2. For hexagonal grid graph $H_r^s, r, s \geq 3$ admitting an H -covering given by $(r - 1)(s - 1)$ subgraphs isomorphic to C_6 , $ehs(H_r^s, C_6) = \lceil 1 + ((r - 1)(s - 1) - 1/6) \rceil$.

Proof. The graph $H_r^s, r, s \geq 3$ obviously admits a C_6 -covering with exactly $(r - 1)(s - 1)$ subcovers of C_6 . Set $k = \lceil 1 + ((r - 1)(s - 1) - 1/6) \rceil$; then, k is the lower bound of $ehs(H_r^s, C_6)$ by Theorem 1. Now, to prove the converse inequality, we have to describe a C_6 -irregular edge k -labeling $\zeta: E(C_6) \rightarrow \{1, 2, \dots, k\}$ as follows:

Case 1: when s is odd,

$$\zeta(v_j^i u_j^i) = \zeta(v_j^{i+1} u_j^{i+1}) = \begin{cases} 1, & \text{for } i = 1; 1 \leq j \leq r, \\ \lceil \frac{j}{2} \rceil, & \text{for } i = 2; 1 \leq j \leq 2 \lceil \frac{i(r-1)+5}{6} \rceil, \\ \lceil \frac{i(r-1)+5}{6} \rceil, & \text{for } i = 2; 2 \lceil \frac{i(r-1)+5}{6} \rceil + 1 \leq j \leq r, \\ \lceil \frac{(i-1)(r-1)+5}{6} \rceil, & \text{for } 3 \leq i \leq s-1; (i \text{ is odd}), 1 \leq j \leq r, \\ \lceil \frac{i(r-1)+5}{6} \rceil, & \text{for } 4 \leq i \leq s-1; (i \text{ is even}), 1 \leq j \leq r, \end{cases} \quad (1)$$

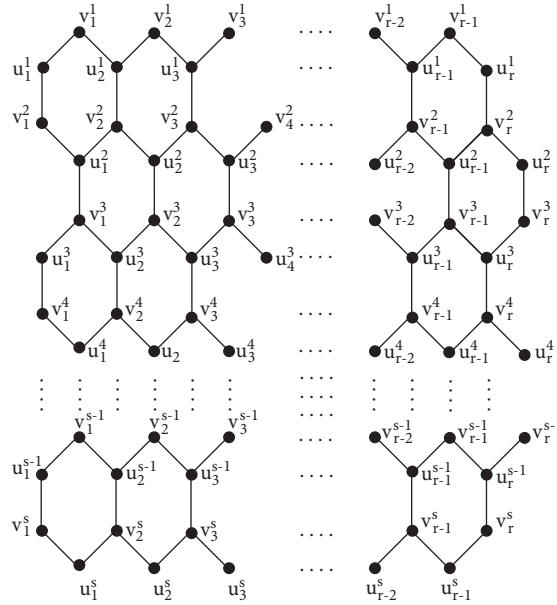


FIGURE 1: Hexagonal grid graph H_r^s .

$$\zeta(v_j^i u_{j+1}^i) = \zeta(u_j^{i+1} v_{j+1}^{i+1}) = \begin{cases} 1, & \text{for } i = 1; 1 \leq j \leq r-1, (j \text{ is odd}), \\ 2, & \text{for } i = 1; 2 \leq j \leq r-1, (j \text{ is even}), \\ \left\lceil \frac{j}{2} \right\rceil, & \text{for } i = 1; 1 \leq j \leq 2 \left\lceil \frac{i(r-1)+5}{6} \right\rceil, \\ \left\lceil \frac{(i+1)(r-1)+5}{6} \right\rceil, & \text{for } i = 2; 2 \left\lceil \frac{i(r-1)+5}{6} \right\rceil + 1 \leq j \leq r-1, \\ \left\lceil \frac{(i-1)(r-1)+5}{6} \right\rceil, & \text{for } 3 \leq i \leq s-1; (i \text{ is odd}), 1 \leq j \leq r-1, \\ j, & \text{for } i = 4; 1 \leq j \leq \left\lceil \frac{i(r-1)+5}{6} \right\rceil, \\ \left\lceil \frac{i(r-1)+5}{6} \right\rceil, & \text{for } i = 4; \left\lceil \frac{i(r-1)+5}{6} \right\rceil + 1 \leq j \leq r-1, \\ \left\lceil \frac{i(r-1)+5}{6} \right\rceil, & \text{for } 6 \leq i \leq s-1; (i \text{ is even}), 1 \leq j \leq r-1, \end{cases} \quad (2)$$

$$\zeta(u_j^i v_j^{i+1}) = \begin{cases} 1, & \text{for } i = 1; 1 \leq j \leq r, \\ \left\lfloor \frac{r+3-2\lceil \frac{i(r-1)+5}{6} \rceil}{2} \right\rfloor, & \text{for } i = 2; \text{for } 1 \leq j \leq 2\left\lceil \frac{i(r-1)+5}{6} \right\rceil + (j \text{ is odd}), \\ \left\lceil \frac{r+3-2\lceil \frac{i(r-1)+5}{6} \rceil}{2} \right\rceil, & \text{for } i = 2; \text{for } 2 \leq j \leq 2\left\lceil \frac{i(r-1)+5}{6} \right\rceil + (j \text{ is even}), \\ \left\lceil \frac{j-2\lceil \frac{i(r-1)+5}{6} \rceil}{2} \right\rceil + \left\lceil \frac{r+3-2\lceil \frac{i(r-1)+5}{6} \rceil}{2} \right\rceil, & \text{for } i = 2; \text{for } 2\left\lceil \frac{i(r-1)+5}{6} \right\rceil + 1 \leq j \leq r, (j \text{ is odd}), \\ \left\lceil r+3-2\left\lceil \frac{i(r-1)+5}{6} \right\rceil \right\rceil - \left\lceil \frac{j-2\lceil \frac{i(r-1)+5}{6} \rceil}{2} \right\rceil, & \text{for } i = 2; \text{for } 2\left\lceil \frac{i(r-1)+5}{6} \right\rceil + 1 \leq j \leq r, (j \text{ is even}), \\ \left\lfloor \frac{(i-1)(r-1)+5-2\lceil \frac{(i-1)(r-1)+5}{6} \rceil - \lceil \frac{(i+1)(r-1)+5}{6} \rceil}{2} \right\rfloor, & \text{for } i = 3; \text{for } 1 \leq j \leq \left\lceil \frac{(i+1)(r-1)+5}{6} \right\rceil + 1, (j \text{ is odd}), \\ \left\lceil \frac{j-1-\lceil \frac{(i+1)(r-1)+5}{6} \rceil}{2} \right\rceil + \left\lceil \frac{2(r-1)+6-2\lceil \frac{(i-1)(r-1)+5}{6} \rceil - \lceil \frac{(i+1)(r-1)+5}{6} \rceil}{2} \right\rceil, & \text{for } i = 3; \left\lceil \frac{(i+1)(r-1)+5}{6} \right\rceil + 2 \leq j \leq r, \\ \left\lceil \frac{2(r-1)+5-2\lceil \frac{(i-1)(r-1)+5}{6} \rceil - \lceil \frac{(i+1)(r-1)+5}{6} \rceil}{2} \right\rceil, & \text{for } i = 3; \text{for } 2 \leq j \leq \left\lceil \frac{(i+1)(r-1)+5}{6} \right\rceil + 1, (j \text{ is even}), \end{cases} \quad (3)$$

$$\zeta(u_j^i v_j^{i+1}) = \begin{cases} \lceil \frac{j-1 - \lceil (i+1)(r-1) + 5/6 \rceil}{2} \rceil + \lceil \frac{2(r-1) + 5 - 2 \lceil (i-1)(r-1) + 5/6 \rceil - \lceil (i+1)(r-1) + 5/6 \rceil}{2} \rceil, & \text{for } i = 3; \lceil \frac{(i+1)(r-1) + 5}{6} \rceil + 2 \leq j \leq r, \\ \lfloor \frac{3(r-1) + 5 - 3 \lceil i(r-1) + 5/6 \rceil}{2} \rfloor, & \text{for } i = 4; 1 \leq j \leq \lceil \frac{i(r-1) + 5}{6} \rceil + 1, (j \text{ is odd}), \\ \lfloor \frac{3(r-1) + 5 - 3 \lceil i(r-1) + 5/6 \rceil}{2} \rfloor + \lceil \frac{j-1 - \lceil i(r-1) + 5/6 \rceil}{2} \rceil, & \text{for } i = 4; \lceil \frac{i(r-1) + 5}{6} \rceil + 2 \leq j \leq r, \\ \lfloor \frac{3(r-1) + 5 - 3 \lceil i(r-1) + 5/6 \rceil}{2} \rfloor, & \text{for } i = 4; 2 \leq j \leq \lceil \frac{i(r-1) + 5}{6} \rceil + 1, (j \text{ is even}), \\ \lceil \frac{3(r-1) + 5 - 3 \lceil i(r-1) + 5/6 \rceil}{2} \rceil + \lceil \frac{j-1 - \lceil i(r-1) + 5/6 \rceil}{2} \rceil, & \text{for } i = 4; \lceil \frac{i(r-1) + 5}{6} \rceil + 2 \leq j \leq r, \\ \lfloor \frac{(i-1)(r-1) + 6 - 2 \lceil (i-1)(r-1) + 5/6 \rceil - 2 \lceil (i+1)(r-1) + 5/6 \rceil}{2} \rfloor + \lceil \frac{j}{2} \rceil - 1, & \text{for } 5 \leq i \leq s-1; (i \text{ is odd}), 1 \leq j \leq r, (j \text{ is odd}), \\ \lfloor \frac{(i-1)(r-1) + 6 - 2 \lceil (i-1)(r-1) + 5/6 \rceil - 2 \lceil (i+1)(r-1) + 5/6 \rceil}{2} \rfloor + \lceil \frac{j}{2} \rceil - 1, & \text{for } 5 \leq i \leq s-1; (i \text{ is odd}), 2 \leq j \leq r, (j \text{ is even}), \\ \lfloor \frac{(i-1)(r-1) + 6 - 4 \lceil i(r-1) + 5/6 \rceil}{2} \rfloor + \lceil \frac{j}{2} \rceil - 1, & \text{for } 6 \leq i \leq s-1; (i \text{ is even}), 1 \leq j \leq r, (j \text{ is odd}), \\ \lfloor \frac{(i-1)(r-1) + 6 - 4 \lceil i(r-1) + 5/6 \rceil}{2} \rfloor + \lceil \frac{j}{2} \rceil - 1, & \text{for } 6 \leq i \leq s-1; (i \text{ is even}), 1 \leq j \leq r, (j \text{ is even}). \end{cases} \quad (4)$$

Case 2: when s is even,

$$\zeta(v_j^i u_j^i) = \zeta(v_j^{i+1} u_j^{i+1}) = \begin{cases} \lceil \frac{j}{3} \rceil, & \text{for } i = 1; 1 \leq j \leq 3, \\ \lceil \frac{j+3}{6} \rceil, & \text{for } i = 1; 4 \leq j \leq r, \\ \lceil \frac{j}{6} \rceil, & \text{for } i = 2; 1 \leq j \leq r, \\ \lceil \frac{i(r-1) + 5}{6} \rceil - 1, & \text{for } r = 3, i = 3; j = 1, \\ \lceil \frac{i(r-1) + 5}{6} \rceil - 2, & \text{for } r > 3, i = 3; j = 1, \\ \lceil \frac{i(r-1) + 5}{6} \rceil - 1, & \text{for } i = 3; j = 2, \\ \lceil \frac{i(r-1) + 5}{6} \rceil, & \text{for } i = 3; 3 \leq j \leq r, \\ \lceil \frac{(i-1)(r-1) + 5}{6} \rceil, & \text{for } 4 \leq i \leq s-1, (i \text{ is even}); 1 \leq j \leq r, \\ \lceil \frac{i(r-1) + 5}{6} \rceil - 2, & \text{for } i = 5; j = 1, \\ \lceil \frac{i(r-1) + 5}{6} \rceil - 1, & \text{for } i = 5; j = 2, \\ \lceil \frac{i(r-1) + 5}{6} \rceil, & \text{for } i = 5; 3 \leq j \leq r, \\ \lceil \frac{i(r-1) + 5}{6} \rceil - 1, & \text{for } 7 \leq i \leq s-1, (i \text{ is odd}); 1 \leq j \leq r, \end{cases}$$

$$\zeta(v_j^i u_{j+1}^i) = \zeta(u_j^{i+1} v_{j+1}^{i+1}) = \begin{cases} \lceil \frac{j}{5} \rceil, & \text{for } i = 1; 1 \leq j \leq 5, \\ \lceil \frac{j+1}{6} \rceil, & \text{for } i = 1; 6 \leq j \leq r-1, \\ \lceil \frac{j}{4} \rceil, & \text{for } i = 2; 1 \leq j \leq 4, \\ \lceil \frac{j+2}{6} \rceil, & \text{for } i = 2; 5 \leq j \leq r-1, \\ \lceil \frac{(i)(r-1)+5}{6} \rceil, & \text{for } 3 \leq i \leq s-1; (i \text{ is odd}), 1 \leq j \leq r-1, \\ \lceil \frac{(i-1)(r-1)+5}{6} \rceil, & \text{for } 4 \leq i \leq s-1; (i \text{ is even}), 1 \leq j \leq r-1, \end{cases} \quad (5)$$

$$\zeta(u_j^i v_j^{i+1}) = \begin{cases} \lceil \frac{j}{2} \rceil, & \text{for } i = 1; 1 \leq j \leq 2, \\ \lceil \frac{j+4}{6} \rceil, & \text{for } i = 1; 3 \leq j \leq r, \\ \lceil \frac{(i-1)(r-1)+4-2\lceil (i+1)(r-1)+5/6 \rceil + \lceil r/13 \rceil}{2} \rceil, & \text{for } i = 2; j = 1, 3, \\ \lceil \frac{(i-1)(r-1)+4-2\lceil (i+1)(r-1)+5/6 \rceil + \lceil r/14 \rceil}{2} \rceil, & \text{for } i = 2; j = 2, \\ \lfloor (i-1)(r-1)+4-2\lceil \frac{(i+1)(r-1)+5}{6} \rceil \rfloor + \lceil \frac{j-1}{3} \rceil, & \text{for } (r \text{ is even}), i = 2; \text{for } 4 \leq j \leq r, (j \text{ is even}), \\ \lfloor (i-1)(r-1)+4-2\lceil \frac{(i+1)(r-1)+5}{6} \rceil + \lceil \frac{r}{14} \rceil \rfloor + \lceil \frac{j-1}{3} \rceil, & \text{for } (r \text{ is even}), i = 2; \text{for } 5 \leq j \leq r, (j \text{ is odd}), \\ \lfloor (i-1)(r-1)+2-2\lceil \frac{(i+1)(r-1)+5}{6} \rceil + \lceil \frac{r}{14} \rceil \rfloor + \lceil \frac{j-1}{3} \rceil, & \text{for } (r \text{ is odd}), i = 2; \text{for } 4 \leq j \leq r, (j \text{ is even}), \\ \lceil \frac{(i-1)(r-1)+4-2\lceil (i+1)(r-1)+5/6 \rceil + \lceil r/13 \rceil}{2} \rceil + \lceil \frac{j-2}{3} \rceil, & \text{for } (r \text{ is odd}), i = 2; \text{for } 5 \leq j \leq r, (j \text{ is odd}), \\ \frac{(i-1)(r-1)+6-4\lceil i(r-1)+5/6 \rceil + 2\lceil r/13 \rceil}{2}, & \text{for } i = 3; 1 \leq j \leq 4, \\ \frac{(i-1)(r-1)+6-4\lceil i(r-1)+5/6 \rceil + 2\lceil r/13 \rceil}{2} + \lceil \frac{j-4}{2} \rceil, & \text{for } i = 3; 5 \leq j \leq r, \\ \lceil \frac{i(r-1)+6-3\lceil (i+1)(r-1)+5/6 \rceil - 2\lceil (i-1)(r-1)+5/6 \rceil + \lceil r/14 \rceil}{2} \rceil, & \text{for } (r \text{ is odd}), i = 2; j = 1, 3, \\ \lceil \frac{i(r-1)+4-3\lceil (i+1)(r-1)+5/6 \rceil - 2\lceil (i-1)(r-1)+5/6 \rceil - \lfloor r/12 \rfloor + 3\lceil r/13 \rceil}{2} \rceil, & \text{for } (r \text{ is even}), i = 4; j = 1, 3, \\ \lfloor \frac{i(r-1)+9-3\lceil (i+1)(r-1)+5/6 \rceil - 2\lceil (i-1)(r-1)+5/6 \rceil}{2} \rfloor, & \text{for } (r = 3, 5), i = 4; j = 2, \\ \lfloor \frac{i(r-1)+4-3\lceil (i+1)(r-1)+5/6 \rceil - 2\lceil (i-1)(r-1)+5/6 \rceil + 3\lceil r/14 \rceil}{2} \rfloor, & \text{for } (r \text{ is odd}); r > 5, i = 4; j = 2, \\ \lceil \frac{i(r-1)+5-3\lceil (i+1)(r-1)+5/6 \rceil - 2\lceil (i-1)(r-1)+5/6 \rceil + 2\lceil r/13 \rceil - \lfloor r/12 \rfloor}{2} \rceil, & \text{for } (r \text{ is even}), i = 4; j = 2, \\ \lfloor \frac{i(r-1)+9-3\lceil (i+1)(r-1)+5/6 \rceil - 2\lceil (i-1)(r-1)+5/6 \rceil}{2} \rfloor + \lceil \frac{j-3}{2} \rceil, & \text{for } (r = 5), i = 4; 4 \leq j \leq r, \\ \lfloor \frac{i(r-1)+4-3\lceil (i+1)(r-1)+5/6 \rceil - 2\lceil (i-1)(r-1)+5/6 \rceil + 3\lceil r/14 \rceil}{2} \rfloor + \lceil \frac{j-3}{2} \rceil, & \text{for } (r \text{ is odd}); r \neq 5, i = 4; \text{for } 4 \leq j \leq r, \\ \lceil \frac{i(r-1)+6-3\lceil (i+1)(r-1)+5/6 \rceil - 2\lceil (i-1)(r-1)+5/6 \rceil + \lceil r/13 \rceil - \lfloor r/12 \rfloor + \lceil \frac{j-3}{2} \rceil}{2} \rceil, & \text{for } (r \text{ is even}), i = 4; \text{for } 4 \leq j \leq r, (j \text{ is even}), \\ \lceil \frac{i(r-1)+4-3\lceil (i+1)(r-1)+5/6 \rceil - 2\lceil (i-1)(r-1)+5/6 \rceil + 3\lceil r/13 \rceil}{2} \rceil + \lceil \frac{j-3}{2} \rceil, & \text{for } (r \text{ is odd}), i = 4; \text{for } 5 \leq j \leq r, (j \text{ is odd}), \\ \frac{(i-1)(r-1)+4-4\lceil i(r-1)+5/6 \rceil + 4\lceil r/13 \rceil}{2}, & \text{for } i = 5; 1 \leq j \leq 4, \\ \frac{(i-1)(r-1)+4-4\lceil i(r-1)+5/6 \rceil + 4\lceil r/13 \rceil + \lceil \frac{j-4/2}{5} \rceil}{2}, & \text{for } i = 5; 5 \leq j \leq r, \end{cases} \quad (6)$$

$$\zeta(u_j^i v_j^{i+1}) = \begin{cases} \lceil \frac{(i-1)(r-1) + 6 - 2\lceil (i-1)(r-1) + 5/6 \rceil - 2\lceil (i+1)(r-1) + 5/6 \rceil + 5\lceil r/13 \rceil}{2} \rceil + \lceil \frac{j}{2} \rceil - 1, & \text{for } 6 \leq i \leq s-1; (i \text{ is even}); \text{for } 1 \leq j \leq r, (j \text{ is odd}), \\ \lceil \frac{(i-1)(r-1) + 6 - 2\lceil (i-1)(r-1) + 5/6 \rceil - 2\lceil (i+1)(r-1) + 5/6 \rceil + 5\lceil r/13 \rceil}{2} \rceil + \lceil \frac{j}{2} \rceil - 1, & \text{for } 6 \leq i \leq s-1; (i \text{ is even}); \text{for } 1 \leq j \leq r, (j \text{ is even}), \\ \frac{(i-1)(r-1) - 2\lceil (i-1)(r-1) + 5/6 \rceil - 2\lceil (i+1)(r-1) + 5/6 \rceil + 4\lceil r/13 \rceil}{2} + \lceil \frac{j}{2} \rceil - 1, & \text{for } r=3; 1 \leq j \leq r; \text{for } 7 \leq i \leq s-1, (i \text{ is odd}), \\ \frac{(i-1)(r-1) + 6 - 2\lceil (i-1)(r-1) + 5/6 \rceil - 2\lceil (i+1)(r-1) + 5/6 \rceil}{2} + \lceil \frac{j}{2} \rceil - 1, & \text{for } (r \text{ is odd}), 3 < r \leq 13; 1 \leq j \leq r; \text{for } 7 \leq i \leq s-1, (i \text{ is odd}), \\ \frac{(i-1)(r-1) + 6 - 2\lceil (i-1)(r-1) + 5/6 \rceil - 2\lceil (i+1)(r-1) + 5/6 \rceil + 4\lceil r/14 \rceil}{2} + \lceil \frac{j}{2} \rceil - 1, & \text{for } r=15+6k, k \geq 0; 1 \leq j \leq r; \text{for } 7 \leq i \leq s-1, (i \text{ is odd}), \\ \frac{(i-1)(r-1) + 8 - 2\lceil (i-1)(r-1) + 5/6 \rceil - 2\lceil (i+1)(r-1) + 5/6 \rceil + 4\lceil r/14 \rceil}{2} + \lceil \frac{j}{2} \rceil - 1, & \text{for } (r \text{ is odd}), r \geq 17; 1 \leq j \leq r; \text{for } 7 \leq i \leq s-1, (i \text{ is odd}), \\ \frac{(i-1)(r-1) + 2 - 2\lceil (i-1)(r-1) + 5/6 \rceil - 2\lceil (i+1)(r-1) + 5/6 \rceil + 4\lceil r/14 \rceil}{2} + \lceil \frac{j}{2} \rceil - 1, & \text{for } r = \text{even} (0 \pmod 6); 1 \leq j \leq r; \text{for } 7 \leq i \leq s-1, (i \text{ is odd}), \\ \frac{(i-1)(r-1) + 4 - 2\lceil (i-1)(r-1) + 5/6 \rceil - 2\lceil (i+1)(r-1) + 5/6 \rceil + 4\lceil r/13 \rceil}{2} + \lceil \frac{j}{2} \rceil - 1, & \text{for } r = \text{even} (2 \pmod 6); 1 \leq j \leq r; \text{for } 7 \leq i \leq s-1, (i \text{ is odd}), \\ \frac{(i-1)(r-1) - 2\lceil (i-1)(r-1) + 5/6 \rceil - 2\lceil (i+1)(r-1) + 5/6 \rceil + 4\lceil r/15 \rceil}{2} + \lceil \frac{j}{2} \rceil - 1, & \text{for } r = \text{even} (4 \pmod 6); 1 \leq j \leq r; \text{for } 7 \leq i \leq s-1, (i \text{ is odd}). \end{cases} \tag{7}$$

Figure 2 shows the weights of the edge C_6 -covering of the hexagonal grid graph, and the formula for the weights of the edge C_6 -covering is given as follows: $w\zeta(C_6^{(v_j^i u_j^i)(v_j^{i+1} u_j^{i+1})(v_j^i u_{j+1}^i)(u_j^{i+1} v_{j+1}^{i+1})(u_j^i v_j^{i+1})}) = 5 + (i-1)(r-1) + j$, $1 \leq i \leq s$; $1 \leq j \leq r$. Observe that all the weights of subcovers of C_6 are distinct. Hence, $\text{ehs}(H_r^s, C_6) = \lceil 1 + ((r-1)(s-1) - 1/6) \rceil$, which completes the proof of this theorem. \square

4. Octagonal Grid Graph

For finite $r, s \geq 3$, the octagonal grid graph, \mathcal{O}_r^s , is a graph with s rows and r columns of octagons [16]. The vertex and the edge sets of this graph are defined as $V(\mathcal{O}_r^s) = \{v_j^i, x_j^i; \text{ for } 1 \leq i \leq s, 1 \leq j \leq r\} \cup \{u_j^i, x_j^i; 1 \leq i \leq s-1, 1 \leq j \leq r\}$; $E(\mathcal{O}_r^s) = \{v_j^i u_j^i, x_j^i u_{j+1}^i, w_{j+1}^{i+1} v_j^{i+1}, x_j^{i+1} w_{j+1}^i; 1 \leq i \leq s-1, 1 \leq j \leq r-1\} \cup \{u_j^i w_j^i; 1 \leq i \leq s-1, 1 \leq j \leq r\} \cup \{v_j^i x_j^i; \text{ for } 1 \leq i \leq s, 1 \leq j \leq r-1\}$. The face set of $F(\mathcal{O}_r^s)$ consists of $|F(\mathcal{O}_r^s)| - 1$ faces as 8-sided faces and one external face which is infinite.

Also, $|V(\mathcal{O}_r^s)| = 4rs - 2(r+s)$ and $|E(\mathcal{O}_r^s)| = |V(\mathcal{O}_r^s)| + r(2s-1) - 3s + 2$, while $|F(\mathcal{O}_r^s)| = (2r-1)(2s-1)$.

For $r, s \geq 3$, the octagonal grid graph is shown in Figure 3. The following result establishes the edge H -irregularity strength of \mathcal{O}_r^s for $3 \leq r \neq 12, 14 \leq 15$ and $s \geq 3$.

Theorem 3. *Let \mathcal{O}_r^s be an octagonal grid graph admitting C_8 -covering given by $(r-1)(s-1)$ subgraphs isomorphic to H ; then, $\text{ehs}(\mathcal{O}_r^s) = \lceil 1 + ((r-1)(s-1) - 1/8) \rceil$.*

Proof. It is clear that the graph \mathcal{O}_r^s for $3 \leq r \leq 15$ and $s \geq 3$ and $r \neq 12, 14$ admits C_8 -covering with exactly $(r-1)(s-1)$ subcovers of C_8 . Set $k = \lceil 1 + ((r-1)(s-1) - 1/8) \rceil$; then, k is the lower bound of $\text{ehs}(\mathcal{O}_r^s, C_8)$ by Theorem 1. Now, to prove the converse inequality, we have to describe a C_8 -irregular edge k -labeling $\zeta: E(C_8) \rightarrow \{1, 2, \dots, k\}$ given as follows:

Case 1: when $3 \leq r \leq 7$ and $s \geq 3$, $1 \leq i \leq s-1$; $1 \leq j \leq r-1$,

$$\begin{aligned} \zeta(v_j^i u_j^i) &= \lceil \frac{(r-1)(i-1) + j}{8} \rceil, \\ \zeta(x_j^i u_{j+1}^i) &= \lceil \frac{(r-1)i - \lceil r-2/2 \rceil + j}{8} \rceil, \\ \zeta(x_j^{i+1} w_{j+1}^i) &= \lceil \frac{(r-1)i \lceil 5-r/2 \rceil + j}{8} \rceil, \\ \zeta(w_j^i v_j^{i+1}) &= \begin{cases} \lceil \frac{(r-1)(i-1) + 1 + j}{8} \rceil, & \text{for } (r=4, 5, 6), 1 \leq i \leq s-1; 1 \leq j \leq r-1, \\ \lceil \frac{(r-1)(i-1) + 2 + j}{8} \rceil, & \text{for } (r=3, 7), 1 \leq i \leq s-1; 1 \leq j \leq r-1, \end{cases} \end{aligned} \tag{8}$$

$$\tag{9}$$

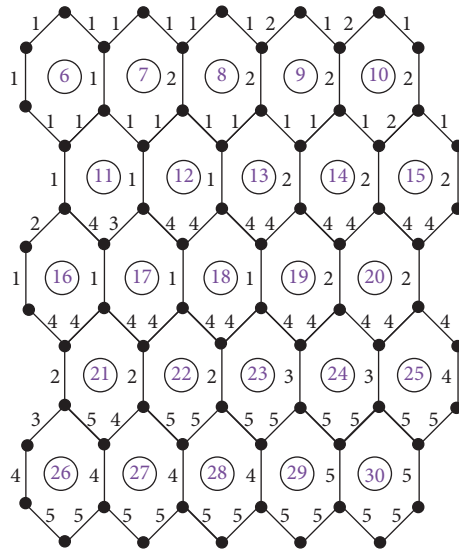


FIGURE 2: Labeling and weights of hexagonal grid graph H_6^6 .

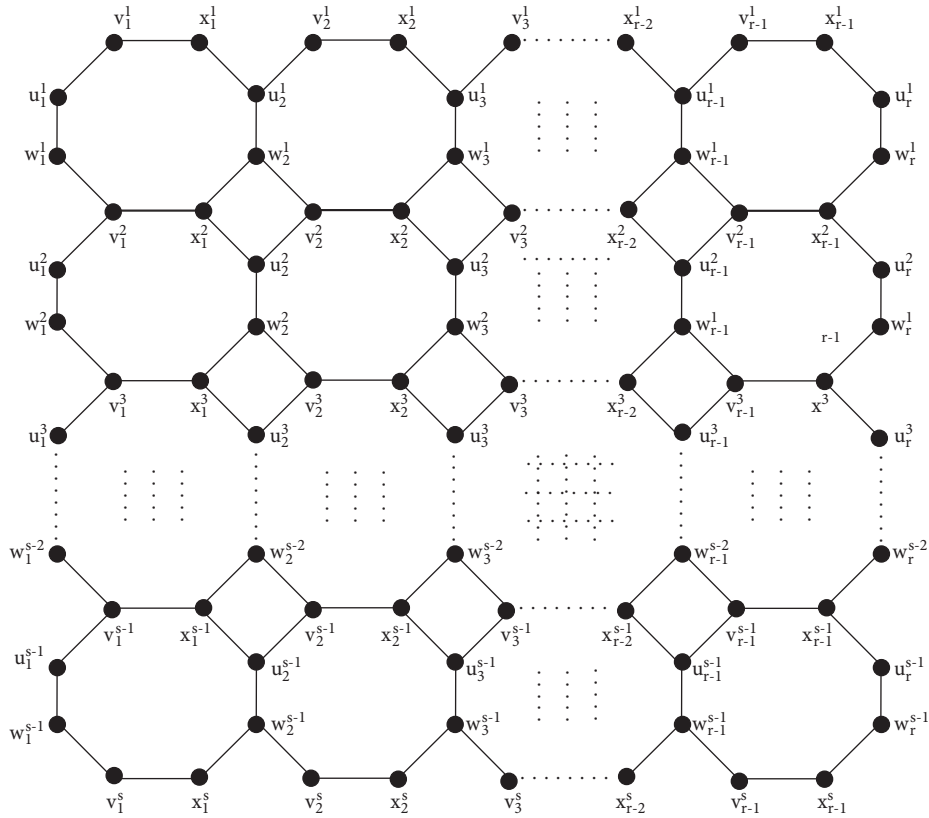


FIGURE 3: Octagonal grid graph \mathcal{O}_r^s .

$$\zeta(u_j^i w_j^i) = \begin{cases} \lceil \frac{(r-1)(i-1) + 5 + j}{8} \rceil, & \text{for } (r = 4, 5, 6, 7), 1 \leq i \leq s-1; 1 \leq j \leq r, \\ \lceil \frac{(r-1)i + 4}{8} \rceil, & \text{for } (r = 3), 1 \leq i \leq s-1; 1 \leq j \leq r, \end{cases} \quad (10)$$

$$\zeta(v_j^i x_j^i) = \left\lceil \frac{(r-1)(i-2) + 7 + j}{8} \right\rceil, \quad \text{for } 1 \leq i \leq s; 1 \leq j \leq r-1. \quad (11)$$

Case 2: when $8 \leq r \leq 13$, $r \neq 12, 14$ and $s \geq 3$, $1 \leq i \leq s-1$;
 $1 \leq j \leq r-1$,

$$\begin{aligned} \zeta(x_j^i u_{j+1}^i) &= \left\lceil \frac{(r-1)(i-1) + 3 + j}{8} \right\rceil, \\ \zeta(w_j^i v_{j+1}^{i+1}) &= \left\lceil \frac{(r-1)(i-1) + 2 + j}{8} \right\rceil, \end{aligned} \quad (12)$$

$$\begin{aligned} \zeta(x_j^{i+1} w_{j+1}^i) &= \left\lceil \frac{(r-1)(i-1) + 4 + j}{8} \right\rceil, \\ \zeta(v_j^i u_j^i) &= \begin{cases} \left\lceil \frac{(r-1)(i-1) + 1 + j}{8} \right\rceil, & \text{for } (r = 8, 9, 10, 11), 1 \leq i \leq s-1; 1 \leq j \leq r-1, \\ \left\lceil \frac{(r-1)(i-1) + 2 + j}{8} \right\rceil, & \text{for } (r = 13), 1 \leq i \leq s-1; 1 \leq j \leq r-1, \end{cases} \end{aligned} \quad (13)$$

$$\zeta(u_j^i w_j^{i+1}) = \left\lceil \frac{(r-1)(i-1) + 5 + j}{8} \right\rceil, \quad \text{for } 1 \leq i \leq s-1; 1 \leq j \leq r, \quad (14)$$

$$\zeta(v_j^i x_j^{i+1}) = \begin{cases} \left\lceil \frac{(r-1)(i-1) + j}{8} \right\rceil, & \text{for } (r = 8), 1 \leq i \leq s; 1 \leq j \leq r-1, \\ \left\lceil \frac{(r-1)i - r + j}{8} \right\rceil + 1, & \text{for } (r = 9), 1 \leq i \leq s, (i \text{ is odd}); j = 1, \\ \left\lceil \frac{(r-1)i - r + j}{8} \right\rceil, & \text{for } (r = 9), 1 \leq i \leq s, (i \text{ is odd}); 2 \leq j \leq r-1, \\ \left\lceil \frac{(r-1)i - r + j}{8} \right\rceil, & \text{for } (r = 9), 1 \leq i \leq s, (i \text{ is even}); 1 \leq j \leq r-1, \\ \left\lceil \frac{(r-1)i - r + j}{8} \right\rceil - (-1)^i, & \text{for } (r = 10, 11), 1 \leq i \leq s; j = 1, \\ \left\lceil \frac{(r-1)i - r + j}{8} \right\rceil, & \text{for } (r = 10, 11), 1 \leq i \leq s; 1 \leq j \leq r-1, \\ \left\lceil \frac{(r-1)i - r + j}{8} \right\rceil - (-1)^i, & \text{for } (r = 13), 1 \leq i \leq s; 1 \leq j \leq 4, \\ \left\lceil \frac{(r-1)i - r + j}{8} \right\rceil, & \text{for } (r = 13), 1 \leq i \leq s; 5 \leq j \leq r-1. \end{cases} \quad (15)$$

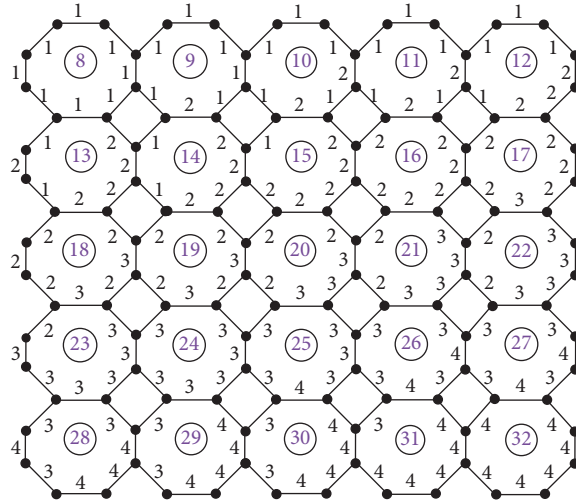


FIGURE 4: Labeling and weights of octagonal grid graph \mathcal{O}_5^5 .

Case 3: when $r = 15$ and $s \geq 3, 1 \leq i \leq s - 1; 1 \leq j \leq r - 1$,

$$\zeta(v_j^i u_j^i) = \lceil \frac{(r-1)(i-1) + 1 + j}{8} \rceil,$$

$$\zeta(x_j^i u_{j+1}^i) = \lceil \frac{(r-1)(i-1) + 3 + j}{8} \rceil, \tag{16}$$

$$\zeta(w_j^i v_j^{i+1}) = \lceil \frac{(r-1)(i-1) + 4 + j}{8} \rceil,$$

$$\zeta(x_j^{i+1} w_{j+1}^i) = \lceil \frac{(r-1)(i-1) + 5 + j}{8} \rceil, \tag{17}$$

$$\zeta(u_j^i w_j^i) = \left\{ \lceil \frac{(r-1)(i-1) + 6 + j}{8} \rceil, \text{ for } 1 \leq i \leq s; 1 \leq j \leq r, \right. \tag{18}$$

$$\zeta(v_j^i x_j^i) = \begin{cases} \lceil \frac{(r-1)(i-1) - 4 + j}{8} \rceil - (-1)^i, & \text{for } 1 \leq i \leq s - 1; 1 \leq j \leq 6, \\ \lceil \frac{(r-1)(i-1) - 4 + j}{8} \rceil, & \text{for } 1 \leq i \leq s; 1 \leq j \leq r - 1. \end{cases} \tag{19}$$

Figure 4 shows the weights of the edge C_8 -covering of the octagonal grid graph, and the formula for the weights of the edge C_8 -covering is given as follows:

$$wt_{\zeta} \left(c_8 \left(v_j^i u_j^i \right) \left(x_j^i u_{j+1}^i \right) \left(w_j^i v_j^{i+1} \right) \left(x_j^{i+1} w_{j+1}^i \right) \left(u_j^i w_j^i \right) \left(v_j^i x_j^i \right) \right) \tag{20}$$

$$= 7 + (i - 1)(r - 1) + j, 1 \leq i \leq s; 1 \leq j \leq r - 1.$$

Observe that all the weights of subcovers of C_8 are distinct. Hence, $ehs(\mathcal{O}_r^s, C_8) = \lceil 1 + ((r - 1)(s - 1) - 1/8) \rceil$, which completes the proof of this theorem. \square

5. Conclusion

In this study, we have determined the edge H -irregularity strength for the hexagonal grid graphs H_r^s for $r, s \geq 3$ and the octagonal grid graphs \mathcal{O}_r^s for $r, s \geq 3$. We have tried to find the edge H -irregularity strength of octagonal grid graph \mathcal{O}_r^s for $r \geq 12$ (r is even) and $s \geq 17$ (s is odd), but so far without success. Hence, we conclude the study with the following open problems.

Open Problem 1. Let \mathcal{O}_r^s be an octagonal grid graph admitting C_8 -covering. Then, $ehs(\mathcal{O}_r^s, C_8) = \lceil 1 + ((r - 1)(s - 1) - 1/8) \rceil$ for $r > 12$ (r is even) and for $r \geq 17$ (r is odd).

Open Problem 2. Let \mathcal{O}_r^s be an octagonal grid graph admitting C_8 -covering. Then, $\text{ehs}(\mathcal{O}_r^s, C_8) = \lceil 1 + ((r-1)(s-1) - 1/8) \rceil$ for $r \geq 3, s \geq 3$ for any choice of r and s .

Data Availability

The data used to support the findings of this study are included within the article.

Conflicts of Interest

The authors declare that they have no conflicts of interest.

References

- [1] J. A. Gallian, "A dynamic survey of graph labeling," *Electronic Journal of Combinatorics*, vol. 17, 2014.
- [2] G. Chartrand, M. S. Jacobson, J. Lehel, O. R. Oellermann, S. Ruiz, and F. Saba, "Irregular networks," *Congressus Numerantium*, vol. 64, pp. 187–192, 1988.
- [3] M. Aigner and E. Triesch, "Irregular assignments of trees and forests," *SIAM Journal on Discrete Mathematics*, vol. 3, no. 4, pp. 439–449, 1990.
- [4] D. Amar and O. Togni, "Irregularity strength of trees," *Discrete Mathematics*, vol. 190, no. 1–3, pp. 15–38, 1998.
- [5] M. Anholcer and C. Palmer, "Irregular labelings of circulant graphs," *Discrete Mathematics*, vol. 312, no. 23, pp. 3461–3466, 2012.
- [6] T. Bohman and D. Kravitz, "On the irregularity strength of trees," *Journal of Graph Theory*, vol. 45, no. 4, pp. 241–254, 2004.
- [7] R. J. Faudree and J. Lehel, "Bound on the irregularity strength of regular graphs," *Colloquia János Bolyai Mathematical Society*, vol. 52, pp. 247–256, 1987.
- [8] A. Frieze, R. J. Gould, M. Karoński, and F. Pfender, "On graph irregularity strength," *Journal of Graph Theory*, vol. 41, no. 2, pp. 120–137, 2002.
- [9] M. Kalkowski, M. Karoński, and F. Pfender, "A new upper bound for the irregularity strength of graphs," *SIAM Journal on Discrete Mathematics*, vol. 25, no. 3, pp. 1319–1321, 2011.
- [10] P. Majerski and J. Przybyło, "On the irregularity strength of dense graphs," *SIAM Journal on Discrete Mathematics*, vol. 28, no. 1, pp. 197–205, 2014.
- [11] T. Nierhoff, "A tight bound on the irregularity strength of graphs," *SIAM Journal on Discrete Mathematics*, vol. 13, no. 3, pp. 313–323, 2000.
- [12] J. Przybyło, "Irregularity strength of regular graphs," *Electronic Journal of Combinatorics*, vol. 15, p. R82, 2008.
- [13] A. Ahmad, O. B. S. Al-Mushayt, and M. Bača, "On edge irregularity strength of graphs," *Applied Mathematics and Computation*, vol. 243, pp. 607–610, 2014.
- [14] F. Ashraf, M. Bača, Z. Kimáková, and A. Semaničová-Feňovčíková, "On vertex and edge H -irregularity strengths of graphs," *Discrete Mathematics, Algorithms and Applications*, vol. 8, no. 4, pp. 1650070–1650082, 2016.
- [15] O. Al-Mushayt, A. Ahmad, and M. K. Siddiqui, "On the total edge irregularity strength of hexagonal grid graphs," *Australasian Journal of Combinatorics*, vol. 53, pp. 263–271, 2012.
- [16] M. K. Siddiqui, M. Miller, and J. Ryan, "Total edge irregularity strength of octagonal grid graph," *Utilitas Mathematica*, vol. 103, pp. 277–287, 2017.

Research Article

Some Resolving Parameters in a Class of Cayley Graphs

Jia-Bao Liu ¹ and Ali Zafari ²

¹School of Mathematics and Physics, Anhui Jianzhu University, Hefei 230601, China

²Department of Mathematics, Faculty of Science, Payame Noor University, P.O. Box 19395-4697, Tehran, Iran

Correspondence should be addressed to Ali Zafari; zafari.math.pu@gmail.com

Received 7 July 2021; Revised 3 December 2021; Accepted 10 December 2021; Published 17 January 2022

Academic Editor: Ali Ahmad

Copyright © 2022 Jia-Bao Liu and Ali Zafari. This is an open access article distributed under the Creative Commons Attribution License, which permits unrestricted use, distribution, and reproduction in any medium, provided the original work is properly cited.

Resolving parameters are a fundamental area of combinatorics with applications not only to many branches of combinatorics but also to other sciences. In this study, we construct a class of Toeplitz graphs and will be denoted by $T_{2n}(W)$ so that they are Cayley graphs. First, we review some of the features of this class of graphs. In fact, this class of graphs is vertex transitive, and by calculating the spectrum of the adjacency matrix related with them, we show that this class of graphs cannot be edge transitive. Moreover, we show that this class of graphs cannot be distance regular, and because of the difficulty of the computing resolving parameters of a class of graphs which are not distance regular, we regard this as justification for our focus on some resolving parameters. In particular, we determine the minimal resolving set, doubly resolving set, and strong metric dimension for this class of graphs.

1. Introduction

The graphs in this paper are simple, undirected, and connected. An automorphism of a graph Γ is a permutation φ of the vertex set of Γ with the property that, for any vertices x and y , we have x is adjacent to y in Γ if and only if $\varphi(x)$ is adjacent to $\varphi(y)$ in Γ . The set of all automorphisms of a graph Γ , with the operation of composition of permutations, is a permutation group on $V(\Gamma)$ and a subgroup of the symmetric group on $V(\Gamma)$. This is the automorphism group of Γ , denoted by $Aut(\Gamma)$. Suppose Γ_1 and Γ_2 are two graphs. If there is a bijection, say φ , from $V(\Gamma_1)$ to $V(\Gamma_2)$ so that x is adjacent to y in Γ_1 if and only if $\varphi(x)$ is adjacent to $\varphi(y)$ in Γ_2 , then we say that Γ_1 is isomorphic to Γ_2 . If we consider a graph Γ as a network, then the network stability is very important to us, and especially, if graph Γ is vertex transitive, that is, $Aut(\Gamma)$ acts transitively on $V(\Gamma)$, then the cost of studying the network will be very low, and hence, the network will be more stable. Consider a finite group G , and suppose Q is a subset of G so that it is closed under taking inverses and does not contain the identity; then, the Cayley graph $\Gamma = Cay(G, Q)$ has vertex set G and edge set $E(\Gamma) = \{\{x, y\} | x^{-1}y \in Q\}$. Thus, the studying of Cayley

graphs is very useful because every Cayley graph is vertex transitive [1]. The distance between any pair $u, v \in V(\Gamma)$ of vertices of Γ is the length of geodesic between u and v , denoted by $d_\Gamma(u, v)$ or simply $d(u, v)$. A vertex $x \in V(\Gamma)$ is said to resolve a pair $u, v \in V(\Gamma)$ if $d(u, x) \neq d(v, x)$. Resolving parameters are a fundamental area of combinatorics with applications not only to many branches of combinatorics but also to other sciences. For an arranged subset $R = \{r_1, r_2, \dots, r_m\}$ of vertices in a connected graph Γ , the metric representation of a vertex v in Γ is the m -vector $r(v|R) = (d(v, r_1), d(v, r_2), \dots, d(v, r_m))$ relative to R . Also, the subset R is considered as the resolving set for Γ if any pair of vertices of Γ is distinguished by some vertices of R . A resolving set with least number of vertices is referred as metric basis for Γ and the cardinality of such resolving set is known as metric dimension denoted by $\beta(\Gamma)$. The metric dimension of a graph Γ is the least number of vertices in a set with the property that the list of distances from any vertex to those in the set uniquely identifies that vertex. The concept of the metric dimension in algebraic graph theory dates back to the 1970s. It was defined independently by Harary and Melter [2] and by Slater [3]. In recent years, a considerable literature has developed [4]. This concept has different applications in

the areas of network discovery and verification [5]. For more details, see [6–9]. An $(n \times n)$ matrix $T = (t_{ij})$ is called a Toeplitz matrix if $t_{ij} = t_{i+1,j+1}$ for each $i, j = 1, \dots, n - 1$, see [10]. In fact, a Toeplitz matrix is a square matrix so that entries in every diagonal parallel to the main diagonal are equal, and hence, a Toeplitz matrix is determined by its first row and column. A simple undirected graph Γ with vertex set $\{1, \dots, n\}$ and its adjacency matrix $T = (t_{ij})$ is called a Toeplitz graph if T is the Toeplitz matrix. In this paper, we consider a class of Toeplitz graphs will be denoted by $T_{2n}(W)$ so that they are Cayley graphs as follows.

Let n be a fixed even integer is greater than or equal 4; also, let $[2n] = \{1, 2, \dots, 2n\}$ and $[x_{2n}] = \{x_1, x_2, \dots, x_{2n}\}$ be corresponding sets so that $x_i = i$. Hence, we say that $x_i < x_j$ if $i < j$. Now, let $W_1 = \{x_1, x_3, \dots, x_{2n-1}\}$ and $W_2 = \{x_n\}$ be subsets of the set $[x_{2n}]$, and let $W = W_1 \cup W_2 = \{x_1, x_3, \dots, x_n, \dots, x_{2n-1}\}$ be a refinement of union of the two sets W_1 and W_2 so that $1 = x_1 < x_3 < \dots < x_n < \dots < x_{2n-1}$. We can see that a graph with $2n$ vertices so that the vertices are labelled by the set $\{1, 2, \dots, 2n\}$ and the edge set:

$$\{ij \mid i, j \in [2n], |j - i| = x_t \text{ for some } x_t \in W\}, \quad (1)$$

which is Toeplitz graph $T_{2n}(W)$. For more result of the Toeplitz graphs, see [11, 12]. Figure 1 shows the Toeplitz graph $T_8(1, 3, 4, 5, 7)$.

In particular, we can verify that the Toeplitz graph $T_{2n}(W)$ which is defined already is isomorphic to the Cayley graph $\Lambda = \text{Cay}(\mathbb{D}_{2n}, \Psi)$, where

$$\mathbb{D}_{2n} = \langle a, b \mid a^n = b^2 = 1, ba = a^{n-1}b \rangle \quad (2)$$

is the dihedral group of order $2n$, and $\Psi = \{ab, a^2b, \dots, a^{n-1}b, b\} \cup \{a^{n/2}\}$ is an inverse closed subset of $\mathbb{D}_{2n} - \{1\}$. Thus, the Toeplitz graph $T_{2n}(W)$ is a vertex transitive. Also, for convenience, we can use the symbols in the Cayley graph $\Lambda = \text{Cay}(\mathbb{D}_{2n}, \Psi)$, instead of the symbols in the Toeplitz graph $T_{2n}(W)$. Some metrics for a class of distance regular graphs is computed in [13, 14]. On the contrary, because of the difficulty of the computing resolving parameters of a class of graphs which are not distance regular, we regard this as justification for our focus on some resolving parameters in the Cayley graph $\Lambda = \text{Cay}(\mathbb{D}_{2n}, \Psi)$. The important results of this study are presented in Sections 3.1 and 3.2. In Section 3.1, first, we will be determining the automorphism group of the Cayley graph $\Lambda = \text{Cay}(\mathbb{D}_{2n}, \Psi)$; also, we will show that the Cayley graph $\Lambda = \text{Cay}(\mathbb{D}_{2n}, \Psi)$ cannot be distance regular. In particular, we will prove that the Cayley graph $\Lambda = \text{Cay}(\mathbb{D}_{2n}, \Psi)$ cannot be edge transitive. Moreover, in Section 3.2, we will be computing some resolving parameters for this class of Cayley graphs.

2. Definitions and Preliminaries

Definition 1 (see [15]). A graph Γ is edge transitive if its automorphism group acts transitively on $E(\Gamma)$.

Definition 2 (see [15]). A graph Γ is 1-transitive or symmetric if its automorphism group acts transitively on the set of paths of length 1 or 1-arcs.

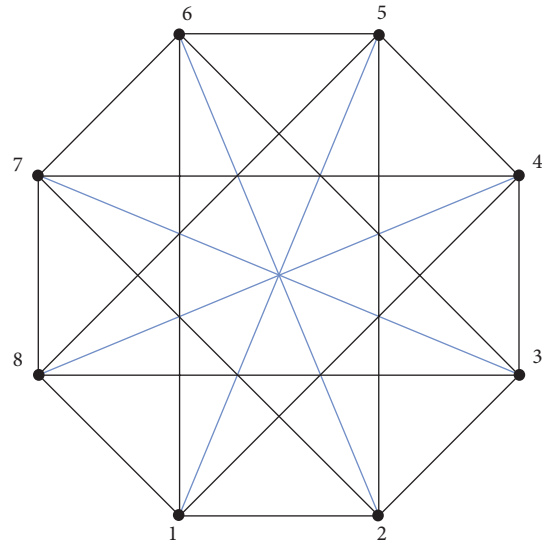


FIGURE 1: The Toeplitz graph $T_8(1, 3, 4, 5, 7)$.

Proposition 1 (see [15]). Let Γ be a symmetric graph of valency k , and let λ be a simple eigenvalue of Γ ; then, $\lambda = \pm k$.

Definition 3 (see [16]). Suppose that Γ is a regular graph of valency k and for any two vertices u and v in Γ ; if $d(u, v) = r$, then we have $|\Gamma_{r+1}(v) \cap \Gamma_1(u)| = b_r$, and $|\Gamma_{r-1}(v) \cap \Gamma_1(u)| = c_r$ ($0 \leq r \leq d$). Then, we say that Γ is a distance regular graph.

Proposition 2 (see [16]). If Γ is a distance regular graph with diameter d , then Γ has exactly $d + 1$ distinct eigenvalues.

Definition 4 (see [17]). Suppose Γ is a graph of order at least 2; vertices $x, y \in V(\Gamma)$ are said to doubly resolve vertices $u, v \in V(\Gamma)$ if $d(u, x) - d(u, y) \neq d(v, x) - d(v, y)$. A set $S = \{s_1, s_2, \dots, s_l\}$ of vertices of Γ is a doubly resolving set of Γ if every two distinct vertices of Γ are doubly resolved by some two vertices of S . A doubly resolving set with minimum cardinality is called the minimal doubly resolving set. This minimum cardinality is denoted by $\psi(\Gamma)$.

Definition 5 (see [18]). Let Γ be a graph. A vertex w of Γ strongly resolves two vertices u and v of Γ if u belongs to a shortest $v - w$ path or v belongs to a shortest $u - w$ path. A set $S = \{s_1, s_2, \dots, s_m\}$ of vertices of Γ is a strong resolving set of Γ if every two distinct vertices of Γ are strongly resolved by some vertex of S . The strong metric dimension of a graph Γ is the cardinality of smallest strong resolving set of Γ and denoted by $sdim(\Gamma)$.

3. Main Results

3.1. Some of the Features of the Cayley Graph $\text{Cay}(\mathbb{D}_{2n}, \Psi)$. In this section, we review some of the features of the Cayley graph $\text{Cay}(\mathbb{D}_{2n}, \Psi)$. It is well known that the spectrum of a graph is the spectrum of the adjacency matrix related with it, that is, its set of eigenvalues together with their multiplicities. If all the eigenvalues of the adjacency matrix of a graph are

integers, in this case, the graph related with it is called an integral graph, see [19]. As we shall see, the theory of integral graphs has connections to some parts of graph theory, edge transitivity, and symmetric graph. In the next theorem, we obtain the automorphism group of the Cayley graph $Cay(\mathbb{D}_{2n}, \Psi)$ by applications of wreath product in graph theory; for more details of the wreath product, see [20].

Proposition 3. *Let n be an even integer greater than or equal 4, and $\Lambda = Cay(\mathbb{D}_{2n}, \Psi)$ be a Cayley graph on the dihedral group \mathbb{D}_{2n} , where Ψ is defined already. If $k = n/2 - 1$, then $Aut(\Lambda) \cong \mathbb{Z}_2 wr_1 Sym(k+1) wr_J Sym(2)$, where $I = \{1, \dots, k+1\}$ and $J = \{1, 2\}$.*

Proof. We can see that the complement of Λ , denoted by $\bar{\Lambda}$, is isomorphic to the disjoint union of 2 copies of cocktail party graph $CP(n/2)$, and we can show that $CP(n/2)$ is isomorphic to the $Cay(\mathbb{Z}_n, S_k)$, where \mathbb{Z}_n is the cyclic group of order n and $S_k = \{1, n-1, 2, n-2, \dots, k, n-k\}$, see Proposition 3.2 of [21]. Hence, given by the above discussion and the theorem in [22], we have $Aut(\bar{\Lambda}) \cong Aut(CP(n/2)) wr_1 Sym(2) = \mathbb{Z}_2 wr_1 Sym(k+1) wr_J Sym(2)$. In particular, we have $Aut(\bar{\Lambda}) = Aut(\Lambda)$ because a simple undirected graph and its complement have the same automorphism group. \square

Proposition 4. *Let n be an even integer greater than or equal 4, and $\Lambda = Cay(\mathbb{D}_{2n}, \Psi)$ be a Cayley graph on the dihedral group \mathbb{D}_{2n} , where Ψ is defined already; then, Λ cannot be a distance regular graph.*

Proof. It is not hard to see that the diameter of Λ is 2 and Λ is not a bipartite graph, because $a^{n/2} \in \Psi$. Now, by a similar way, which is done in proof of Proposition 11 in [23], we can show that the adjacency matrix spectrum of Λ is $n+1, 1-n, 1^{(n-2)}, -1^{(n)}$, where the superscripts give the multiplicities of eigenvalues with multiplicity greater than one. Hence, Λ has exactly four distinct eigenvalues. Moreover, based on Proposition 2, we know that if Λ is a distance regular graph with diameter d , then Λ has exactly $d+1$ distinct eigenvalues. Thus, Λ cannot be a distance regular graph. \square

Proposition 5. *Let n be an even integer greater than or equal 4 and $\Lambda = Cay(\mathbb{D}_{2n}, \Psi)$ be a Cayley graph on the dihedral group \mathbb{D}_{2n} , where Ψ is defined already; then, Λ cannot be an edge transitive graph.*

Proof. By contradiction, suppose Λ is an edge transitive graph. It is well known that a connected graph that is edge transitive and vertex transitive need not be 1-transitive. In particular, in p.59, 7.53 of [24], Tutte proved that if a connected graph, regular of odd valency, is both vertex and edge transitive, then it is 1-transitive. Thus, if Λ is a edge transitive graph, then it must be Λ is a 1-transitive graph because it is vertex transitive of odd valency $n+1$. On the contrary, based on Proposition 1, if λ is a simple eigenvalue of a 1-transitive graph Λ , then $\lambda = \pm(n+1)$, which is not

the case, see Proposition 4. This contradiction shows that Λ cannot be an edge transitive graph. \square

3.2. Metric Dimension, Minimal Doubly Resolving set, and Strong Resolving Set of the Cayley Graph $Cay(\mathbb{D}_{2n}, \Psi)$

Theorem 1. *If n is an even integer greater than or equal 4 and $\Lambda = Cay(\mathbb{D}_{2n}, \Psi)$ is a Cayley graph on the dihedral group \mathbb{D}_{2n} , where Ψ is defined already, then the metric dimension of Λ is n .*

Proof. Let $V(\Lambda) = V_1 \cup V_2$, where $V_1 = \{a, a^2, \dots, a^n\}$ and $V_2 = \{ab, a^2b, \dots, a^nb\}$. For every pair of distinct vertices $x, y \in V(\Lambda)$, the length of a shortest path from x to y is $d(x, y) = 1$ or 2 because the diameter of Λ is 2. In particular, if R is an arranged subset of V_1 or V_2 in graph Λ such that $|R| \leq n$, then we can show that R is not a resolving set of Λ . Let $R = R_1 \cup R_2$ be an arranged subset of vertices in graph Λ such that R_1 is a subset of V_1 , R_2 is a subset of V_2 , and $|R_1 \cup R_2| = n$. In the following cases, we can be concluded that the metric dimension of Λ is n .

Case 1: if $|R_1| \neq |R_2|$, then we can assume that $|R_1| < |R_2|$. Hence, there is a pair of distinct vertices $u_1, u_2 \in V(\Lambda) - R$, such that $u_1, u_2 \in V_1 - R_1$, and a shortest path from u_1 to u_2 is $d(u_1, u_2) = 1$. Therefore, the metric representation of the vertices $u_1, u_2 \in V(\Lambda) - R$ is the same as n -vector, relative to R . Thus, R is not a resolving set of Λ .

Case 2: if $|R_1| = |R_2|$ and there are vertices $x, y \in R_1$, such that x is adjacent to y in Λ , then there are vertices $u, v \in V_1 - R_1$ such that u is adjacent to v in Λ . Therefore, the metric representation of the vertices $u, v \in V(\Lambda) - R$ is the same as n -vector, relative to R . Thus, R is not a resolving set of Λ .

Case 3: now, let $|R_1| = |R_2|$, and suppose that, for all the vertices x, y in R_1 , we have x is not adjacent to y in Λ , that is, $d(x, y) = 2$. Also, for all the vertices u, v in R_2 , we have u is not adjacent to v in Λ , that is, $d(u, v) = 2$. We may assume that $R_1 = \{a, a^2, \dots, a^{n/2}\}$ and $R_2 = \{ab, a^2b, \dots, a^{n/2}b\}$. So, we can assume that an arranged subset R of vertices in graph Λ is $R = \{a, a^2, \dots, a^{n/2}; ab, a^2b, \dots, a^{n/2}b\}$. Hence, $V(\Lambda) - R = \{a^{(n+2i)/2}, \dots, a^n; a^{n+2i/2}b, \dots, a^nb\}$, for $1 \leq i \leq n/2$.

Therefore, the metric representations of the vertices $a^{(n+2)/2}, a^{(n+4)/2}, \dots, a^n; a^{(n+2)/2}b, a^{(n+4)/2}b, \dots, a^nb \in V(\Lambda) - R$ relative to R are the n -vectors:

$$\begin{aligned} r(a^{(n+2)/2}|R) &= (1, 2, 2, \dots, 2; 1, \dots, 1), r(a^{(n+4)/2}|R) \\ &= (2, 1, 2, \dots, 2; 1, \dots, 1), \dots, r(a^n|R) \\ &= (2, 2, \dots, 1; 1, 1, \dots, 1) \end{aligned} \tag{3}$$

and $r(a^{(n+2)/2}b|R) = (1, \dots, 1; 1, 2, 2, \dots, 2), r(a^{(n+4)/2}b|R) = (1, \dots, 1; 2, 1, 2, \dots, 2), \dots, r(a^nb|R) = (1, 1, \dots, 1; 2, 2, \dots, 1)$. Thus, all the vertices in $V(\Lambda) - R$ have different representations relative to R . This implies that R is a resolving set of Λ . \square

Theorem 2. *If n is an even integer greater than or equal 4 and $\Lambda = \text{Cay}(\mathbb{D}_{2n}, \Psi)$ is a Cayley graph on the dihedral group \mathbb{D}_{2n} , where Ψ is defined already, then the cardinality of minimum doubly resolving set of Λ is n .*

Proof. By the previous theorem, we know that the arranged subset $R = \{a, a^2, \dots, ab, a^2b, \dots, a^{n/2}b\}$ of vertices in the graph Λ is a resolving set for Λ . We show that the subset R is a doubly resolving set of Λ . It is sufficient to show that, for two vertices u and v in graph Λ , there are vertices $x, y \in R$ such that $d(u, x) - d(u, y) \neq d(v, x) - d(v, y)$. Consider two vertices u and v of Λ . By the following cases, we can be concluded that the minimum cardinality of a doubly resolving set of Λ is n .

Case 1: consider a pair of distinct vertices $u, v \in \Lambda$ such that $u, v \in R$. Then, the length of a shortest path from u to v is $d(u, v) = 1$ or 2 . Let u and v be two vertices in R such that a shortest path from u to v in graph Λ is $d(u, v) = 1$. We may assume that $u = a$ and $v = ab$. Hence, by taking $x = a \in R$ and $y = a^{n/2} \in R$, we have $-2 = 0 - 2 = d(u, x) - d(u, y) \neq d(v, x) - d(v, y) = 1 - 1 = 0$. Therefore, the vertices x and y of R doubly resolve u, v . Now, let u, v be two vertices in R such that a shortest path from u to v in graph Λ is $d(u, v) = 2$. We may assume that $u = a$ and $v = a^{n/2}$. Hence, by taking $x = a \in R$ and $y = ab \in R$, we have $-1 = 0 - 1 = d(u, x) - d(u, y) \neq d(v, x) - d(v, y) = 2 - 1 = 1$. Therefore, the vertices x and y of R doubly resolve u, v .

Case 2: consider a pair of distinct vertices $u, v \in \Lambda$ such that $u \in R$ and $v \notin R$. Then, the length of a shortest path from u to v is $d(u, v) = 1$ or 2 . Suppose a pair of distinct vertices $u \in R$ and $v \notin R$ are adjacent in graph Λ , that is, $d(u, v) = 1$. We may assume that $u = a$ and $v = a^{n+2/2}$. Hence, by taking $x = a \in R$ and $y = ab \in R$, we have $-1 = 0 - 1 = d(u, x) - d(u, y) \neq d(v, x) - d(v, y) = 1 - 1 = 0$. Therefore, the vertices x and y of R doubly resolve u, v . Now, suppose a pair of distinct vertices $u \in R$ and $v \notin R$ are not adjacent in graph Λ , that is, $d(u, v) = 2$. We may assume that $u = a$ and $v = a^n$. Hence, by taking $x = a \in R$ and $y = ab \in R$, we have $-1 = 0 - 1 = d(u, x) - d(u, y) \neq d(v, x) - d(v, y) = 2 - 1 = 1$. Therefore, the vertices x and y of R doubly resolve u, v .

Case 3: consider a pair of distinct vertices $u, v \in \Lambda$ such that $u \notin R$ and $v \notin R$. Then, the length of a shortest path from u to v is $d(u, v) = 1$ or 2 . We can show that the subset R of vertices in graph Λ is a doubly resolving set of Λ . Because by Theorem 1, we can be concluded that $V(\Lambda) - R$ is also a resolving set of Λ . \square

Lemma 1. *If n is an even integer greater than or equal 4 and $\Lambda = \text{Cay}(\mathbb{D}_{2n}, \Psi)$ is a Cayley graph on the dihedral group \mathbb{D}_{2n} , where Ψ is defined already, then the subset $R = \{a, a^2, \dots, a^{n/2}; ab, a^2b, \dots, a^{n/2}b\}$ of vertices in graph Λ is not a strong resolving set of Λ .*

Proof. We know that the arranged subset $R = \{a, a^2, \dots, a^{n/2}; ab, a^2b, \dots, a^{n/2}b\}$ of vertices in graph Λ is a resolving set for Λ of size n . Now, let $V(\Lambda) = V_1 \cup V_2$, where $V_1 = \{a, a^2, \dots, a^n\}$, $V_2 = \{ab, a^2b, \dots, a^{n/2}b\}$, and $R = R_1 \cup R_2$, where $R_1 = \{a, a^2, \dots, a^{n/2}\}$ is a subset of V_1 and $R_2 = \{ab, a^2b, \dots, a^{n/2}b\}$ is a subset of V_2 . Consider two vertices u, v in Λ such that $u, v \in V_1 - R_1$ and u is not adjacent to v in Λ , that is, $d(u, v) = 2$. In the following cases, we show that there is not $w \in R$ such that w is strongly resolve vertices u and v . For every vertex $w \in R$, we have $w \in R_1$ or $w \in R_2$.

Case 1: if $w \in R_1$, then the length of a shortest path from u to w is $d(u, w) = 1$ or 2 and length of a shortest path from v to w is $d(v, w) = 1$ or 2 . Note that, if $d(u, w) = 1$, then $d(v, w) = 2$. Therefore, w is not strongly resolve vertices u and v . In particular, if $d(u, w) = 2$, then $d(v, w) = 1$ or 2 , and hence, w is not strongly resolve vertices u and v because $d(u, v) = 2$.

Case 2: if $w \in R_2$, then the length of a shortest path from u to w is $d(u, w) = 1$ and length of a shortest path from v to w is $d(v, w) = 1$. Therefore, w is not strongly resolve vertices u and v . \square

Theorem 3. *If n is an even integer greater than or equal 4 and $\Lambda = \text{Cay}(\mathbb{D}_{2n}, \Psi)$ is a Cayley graph on the dihedral group \mathbb{D}_{2n} , where Ψ is defined already, then the strong metric dimension of Λ is $2n - 2$.*

Proof. Let $V(\Lambda) = V_1 \cup V_2$, where $V_1 = \{a, a^2, \dots, a^n\}$ and $V_2 = \{ab, a^2b, \dots, a^{n/2}b\}$. It is not hard to see that if $n \geq 4$, then the size of largest clique in the graph Λ is 4. Moreover, we know that the subset $N = \{a^n, a^{n/2}; a^{n/2}b, a^{n/2}b\}$ of vertices in Λ is a clique in the graph Λ . Now, let the subset S of vertices in Λ be $S = V(\Lambda) - N$. In the following cases, we show that the subset S of vertices in Λ is not a strong resolving set of Λ .

Case 1: let $u = a^n$ and $v = a^{n/2}$. We know that $d(u, v) = 1$ and $u, v \in V_1$, and hence, for every $w \in S$ such that $w \in V_2$, we have $d(u, w) = 1$ and $d(v, w) = 1$. Thus, w is not strongly resolve vertices u and v .

Case 2: now, let $u = a^n$ and $v = a^{n/2}$. We know that $d(u, v) = 1$ and $u, v \in V_1$, and hence, for every $w \in S$ such that $w \in V_1$, we have $d(u, w) = 2$ and $d(v, w) = 2$. Thus, w is not strongly resolve vertices u and v .

Therefore, the subset S of the vertices in graph Λ is not a strong resolving set of Λ . From the above cases, we can be concluded that the minimum cardinality of a strong resolving set for Λ must be $2n - 2$. \square

4. Conclusion

Computing resolving parameters of a graph is an NP-hard problem. In this study, we considered a class of Toeplitz graphs and we denoted by $T_{2n}(W)$ so that they are isomorphic to the Cayley graph $\Lambda = \text{Cay}(\mathbb{D}_{2n}, \Psi)$, which is defined already. In fact, this class of graphs is vertex transitive, and by calculating the spectrum of the adjacency

matrix related with them, we showed that this class of graphs cannot be edge transitive. Also, we proved that this class of graphs cannot be distance regular, and because of the difficulty of the computing resolving parameters of a class of graphs which are not distance regular, we regarded this as justification for our focus on some resolving parameters. In particular, we determined the minimal resolving set, doubly resolving set, and strong metric dimension for this class of graphs.

Data Availability

No data were used to support this study.

Conflicts of Interest

The authors declare that there are no conflicts of interest regarding the publication of this paper.

Acknowledgments

This work was supported in part by Natural Science Fund of Education Department of Anhui Province, under Grant KJ2020A0478.

References

- [1] C. Godsil and G. Royle, *Algebraic Graph Theory*, Springer, New York, NY, USA, 2001.
- [2] F. Harary and R. A. Melter, "On the metric dimension of a graph," *Combinatoria*, vol. 2, pp. 191–195, 1976.
- [3] P. J. Slater, "Leaves of trees," in *Proceedings of the 6th Southeastern Conference on Combinatorics, Graph Theory and Computing*, Boca Raton, FL, USA, 1975.
- [4] R. F. Bailey and P. J. Cameron, "Base size, metric dimension and other invariants of groups and graphs," *Bulletin of the London Mathematical Society*, vol. 43, no. 2, pp. 209–242, 2011.
- [5] Z. Beerliova, F. Eberhard, T. Erlebach et al., "Network discovery and verification," *IEEE Journal on Selected Areas in Communications*, vol. 24, no. 12, pp. 2168–2181, 2006.
- [6] M. Imran, M. K. Siddiqui, and R. Naeem, "On the metric dimension of generalized Petersen multigraphs," *IEEE Access*, vol. 6, pp. 74328–74338, 2018.
- [7] S. Khuller, B. Raghavachari, and A. Rosenfeld, *Localization in Graphs*, University of Maryland, College Park, MD, USA, 1994.
- [8] J.-B. Liu and A. Zafari, "Computing minimal doubly resolving sets and the strong metric dimension of the layer Sun graph and the Line Graph of the Layer Sun Graph," *Complexity*, vol. 2020, Article ID 6267072, 8 pages, 2020.
- [9] T. Vetrík and A. Ahmad, "Computing the metric dimension of the categorical product of some graphs," *International Journal of Computer Mathematics*, vol. 94, no. 2, pp. 363–371, 2015.
- [10] P. Halmos, *A Hilbert Space Problem Book*, American Book Company, Knoxville, TN, USA, 1967.
- [11] J.-B. Liu, M. F. Nadeem, H. M. A. Siddiqui, and W. Nazir, "Computing metric dimension of certain families of Toeplitz graphs," *IEEE Access*, vol. 7, pp. 126734–126741, 2019.
- [12] R. van Dal, G. Tijssen, Z. Tuza, J. A. A. van der Veen, C. Zamfirescu, and T. Zamfirescu, "Hamiltonian properties of Toeplitz graphs," *Discrete Mathematics*, vol. 159, no. 1–3, pp. 69–81, 1996.
- [13] R. F. Bailey, "The metric dimension of small distance-regular and strongly regular graphs," *Australas. J. Combin.*, vol. 62, no. 1, pp. 18–34, 2015.
- [14] J.-B. Liu, A. Zafari, and H. Zarei, "Metric dimension, minimal doubly resolving sets, and the strong metric dimension for jellyfish graph and cocktail party graph," *Complexity*, vol. 2020, pp. 1–7, Article ID 9407456, 2020.
- [15] N. L. Biggs, *Algebraic Graph Theory*, Cambridge University Press, New York, NY, USA, 1993.
- [16] A. E. Brower, A. M. Cohen, and A. Neumaier, *Distance Regular Graphs*, Springer, Berlin, Germany, 1989.
- [17] J. Cáceres, C. Hernando, M. Mora et al., "On the metric dimension of Cartesian products of graphs," *SIAM Journal on Discrete Mathematics*, vol. 21, no. 2, pp. 423–441, 2007.
- [18] A. Sebö and E. Tannier, "On metric generators of graphs," *Mathematics of Operations Research*, vol. 29, no. 2, pp. 383–393, 2004.
- [19] F. Harary and A. J. Schwenk, "Which graphs have integral spectra?" *Lecture Notes in Mathematics*, vol. 406, pp. 45–51, 1974.
- [20] L. W. Beineke and R. J. Wilson, *Topics in Algebraic Graph Theory*, Cambridge University Press, Cambridge, UK, 2004.
- [21] S. M. Mirafzal and A. Zafari, "On the spectrum of a class of distance-transitive graphs," *Electronic Journal of Graph Theory and Applications*, vol. 5, no. 1, pp. 63–69, 2017.
- [22] R. Frucht, "On the groups of repeated graphs," *Bulletin of the American Mathematical Society*, vol. 55, pp. 418–420, 1949.
- [23] S. M. Mirafzal and A. Zafari, "An interesting property of a class of circulant graphs," *Journal of Mathematics*, vol. 2017, 4 pages, 2017.
- [24] W. T. Tutte, *Connectivity in Graphs*, University of Toronto Press, Toronto, Canada, 1966.

Research Article

Some Upper Bounds on the First General Zagreb Index

Muhammad Kamran Jamil ¹, Aisha Javed,² Ebenezer Bonyah ³, and Iqra Zaman¹

¹Department of Mathematics, Riphah Institute of Computing and Applied Sciences, Riphah International University, Lahore, Pakistan

²Abdus Salam School of Mathematical Sciences, Government College University, Lahore, Pakistan

³Department of Mathematics Education, Akenten Appiah Menka University of Skills Training and Entrepreneurial Development, Kumasi, Ghana

Correspondence should be addressed to Ebenezer Bonyah; ebbonya@gmail.com

Received 5 August 2021; Accepted 22 December 2021; Published 12 January 2022

Academic Editor: Ali Ahmad

Copyright © 2022 Muhammad Kamran Jamil et al. This is an open access article distributed under the Creative Commons Attribution License, which permits unrestricted use, distribution, and reproduction in any medium, provided the original work is properly cited.

The first general Zagreb index $M^\gamma(G)$ or zeroth-order general Randić index of a graph G is defined as $M^\gamma(G) = \sum_{v \in V} d(v)^\gamma$ where γ is any nonzero real number, $d(v)$ is the degree of the vertex v and $\gamma = 2$ gives the classical first Zagreb index. The researchers investigated some sharp upper and lower bounds on zeroth-order general Randić index (for $\gamma < 0$) in terms of connectivity, minimum degree, and independent number. In this paper, we put sharp upper bounds on the first general Zagreb index in terms of independent number, minimum degree, and connectivity for γ . Furthermore, extremal graphs are also investigated which attained the upper bounds.

1. Introduction

Let G be a connected, simple, and finite graph with vertex set $V(G)$ and edge set $E(G)$. The total number of elements in $V(G)$ is the order of the graph, and the number of edges which are connected with vertex v is said to be the degree $d(v)$ of the vertex v . A vertex v is isolated if it has zero degree. For nonadjacent vertices v and w , a vw -vertex cut is a subset $R \subseteq V(G) \setminus \{v, w\}$ where v and w are from different components of $G - R$ and the smallest cardinality set of vertices which separates v and w is minimal vertex cut. A subset $H \subseteq V(G)$ of nonadjacent vertices is called an independent set, and the largest cardinality set among all independent sets of G is the independent number. A set $X \subseteq V$ is called clique if all the vertices in X are adjacent. If a smallest set of vertices V_0 exists in a connected graph G whose deletion makes it disconnect, then $|V_0|$ is said to be the vertex connectivity or simple connectivity of G .

For a subset $C \subseteq V(G)$, $G[C]$ is an induced subgraph of G whose vertices are from C and edges are with both ends in C . A graph G is bipartite with $Y_1, Y_2 \subset V(G)$ such that $Y_1 \cap Y_2 = \Phi$, $Y_1 \cup Y_2 = V(G)$, and every edge connects a

vertex from Y_1 to a vertex in Y_2 . A bipartite graph in which each vertex of Y_1 is connected with each vertex of Y_2 by an edge is called a complete bipartite graph. Let F_1 and F_2 be two vertex disjoint graphs; then, $F_1 + F_2$ is a graph with the vertex set $V(F_1) \cup V(F_2)$ and the edge set $E(F_1) \cup E(F_2) \cup \{xy: x \in V(F_1), y \in V(F_2)\}$.

A topological index is a number corresponding to a molecule obtained from the molecular structure of the molecule. This number helps to predict the chemical or physical properties of that molecule. Due to strong applications in chemistry and pharmacy, hundreds of degree-based topological indices have been introduced.

The first Zagreb index of a graph G , $M_1(G)$, is defined as [2]

$$M_1(G) = \sum_{v \in V(G)} d(v)^2. \quad (1)$$

This old and useful topological index helped in obtaining properties of the structure of molecules such as branching, ZE-isomerism, complexity, heterosystems, π -electron energy, and many more [3, 4]. The concept of the first general Zagreb index was introduced by Li and Zheng in [5], and it is defined as

$$M^\gamma(G) = \sum_{v \in V(G)} d(v)^\gamma, \tag{2}$$

where γ is any nonzero real number. The first general Zagreb index has grabbed attention of many chemists and mathematicians. Liu and Liu discussed some properties of $M^\gamma(G)$ in [6] related to different operations on graph such as edge moving, edge separating, and edge switching. In [7], the authors presented some inequalities involving different graph parameters. In [8], the authors calculated the first general Zagreb index of generalized F -sums graphs. We refer the readers to [1, 9–14] for further study about this topological index.

First, we present an auxiliary lemma which is a direct consequence of the definition of the first general Zagreb index [15].

Lemma 1. *Let x and y be two nonadjacent vertices of G ; then, for $\gamma > 0$, we have*

$$M^\gamma(G) < M^\gamma(G + xy). \tag{3}$$

2. Graphs with Given Connectivity and Minimum Degree

In this section, we provide an upper bound on the first general Zagreb index in terms of order, vertex connectivity, and minimum degree. Let $\Theta(n, t, \delta)$ be the set of all graphs on n vertices, t vertex connectivity, and δ minimum degree, where $1 \leq t \leq \delta \leq n$ and $\delta \geq 2$.

Theorem 2. *Let $G \in \Theta(n, t, \delta)$ and $t \leq \delta \leq n - 1$, and for $\gamma > 1$, we have*

$$M^\gamma(G) \leq t(n-1)^\gamma + (\delta-t+1)(\delta)^\gamma + (n-\delta-1)(n+t-\delta-2)^\gamma, \tag{4}$$

and the equality holds if and only if $G = K_t + (K_{\delta-t+1} \cup K_{n-\delta-1})$.

Proof. For $n = t + 1$, we have $t = \delta = n - 1$; in other words, $\Theta(n, t, \delta) = \{K_{t+1}\}$. Suppose that $n \geq t + 2$ and let K be the graph in $\Theta(n, t, \delta)$ with the maximum first general Zagreb index for $\gamma > 1$. Let $C \subset V(K)$ be the vertex cut with cardinality t . We will prove our result by proving the following claims.

Claim I. $K - C$ consists of exactly two components. \square

Proof. On the contrary, suppose that $K - C$ consists of at least three components. S_1 and S_2 are two components of $K - C$; then, there will be $x \in V(S_1)$ and $y \in V(S_2)$ such that $K + xy \in \Theta(n, t, \delta)$ which is against the assumption of K because of Lemma 1. This completes the proof of Claim I.

Now assume that $|V(S_1)| = n_1$ and $|V(S_2)| = n_2$. Clearly, $\delta \leq d(x) \leq n_1 + t - 1$ and $\delta \leq d(y) \leq n_2 + t - 1$ where $n_1, n_2 \geq \delta - t + 1$.

Claim II. $K[C \cup V(S_1)]$ and $K[C \cup V(S_2)]$ are cliques. \square

Proof. On the contrary, suppose that $K[C \cup V(S_1)]$ is not a clique. Then, we have two cases. \square

Case 1. There are nonadjacent vertices $u, v \in C \cup V(S_1)$ such that $K + uv \in \Theta(n, t, \delta)$, which contradicts the assumption of K because of Lemma 1, and we have $M^\gamma(K) < M^\gamma(K + uv)$.

Case 2. Otherwise, joining nonadjacent vertices in K will increase the minimum degree of G . Then, from the proof of Claim III, we have

$$M^\gamma(K) < M^\gamma(K_\delta) + (K_{n_1} \cup K_{n_2}) \leq M^\gamma(K_t + (K_{\delta-t+1} \cup K_{n-t-1})), \tag{5}$$

which again contradicts that K has the maximal first general Zagreb index because $K_t + (K_{\delta-t+1} \cup K_{n-t-1}) \in \Theta(n, t, \delta)$. This completes the proof of Claim II.

From Claim II, for $n_1, n_2 \geq 1$ and $n_1 + n_2$, we suppose that $K = K_t + (K_{n_1} \cup K_{n_2})$.

Let $\phi(x) = x(x+t)^\gamma - (x+1)(x+t+1)^\gamma$; then, $\phi'(x) = (x+t)^{\gamma-1}(x+x\gamma+t) - (x+t+1)^{\gamma-1}(x\gamma+x+\gamma+t+1) < 0$ for $\gamma > 1$. This implies that $\phi(x)$ is a decreasing function.

Claim III. We have $n_1 = \delta - t + 1$ or $n_2 = \delta - t + 1$.

Proof. On the contrary, suppose that $n_1 \geq n_2 > \delta - t + 1$; then, we have $M^\gamma(K_t + (K_{n_1} \cup K_{n_2})) - M^\gamma(K_t + (K_{n_1+1} \cup K_{n_2-1})) = n_1(n_1+t)^\gamma + n_2(n_2+t)^\gamma - (n_1+1)(n_1+t+1)^\gamma - (n_2-1)(n_2+t-1)^\gamma < 0$. The last inequality is due to the fact that $\phi(x)$ is a decreasing function for $\gamma > 1$ and $n_1 > n_2 - 1$. This implies that $M^\gamma(K_t + (K_{n_1} \cup K_{n_2})) < M^\gamma(K_t + (K_{\delta-t+1} \cup K_{n-\delta-1}))$ if $n_1, n_2 > \min\{\delta - t + 1, n - t - 1\}$. This completes the proof of Claim III.

From Claims I, II, and III, we deduce that $K = K_t + (K_{\delta-t+1} \cup K_{n-\delta-1})$, which proves the theorem. \square

3. Bipartite Graphs with Given Connectivity

Let $Y(n, t)$ denote the set of bipartite graphs of order n and vertex connectivity t . Now we introduce a graph K_n^x obtained from the graph $K_{x, n-x-1}$ by joining a new vertex u to t vertices of degree x of $K_{x, n-x-1}$.

Theorem 3. *Let $G \in Y(n, t)$ and $1 \leq t \leq n - 1$. Then, for $\gamma > 1$,*

$$M^\gamma(G) \leq \max\{\varphi(a), \varphi(b)\} \tag{6}$$

and the equality holds if and only if either $G = K_n^a$ or $G = K_n^b$, where

$$\begin{aligned} \varphi(x) &= t^\gamma + t(x+1)^\gamma + (n-x-1-t)x^\gamma + x(n-x-1)^\gamma, \\ a &= \left\lfloor \frac{(n-1)^2 - 2(t+1)}{2n} \right\rfloor, \\ b &= \left\lfloor \frac{(n-1)^2 - 2(t+1)}{2n} \right\rfloor. \end{aligned} \tag{7}$$

Proof. Note that $Y(n, 1) = \{K_{1, n-1}\}$, so we consider $1 < t \leq n/2$. Let $K \in Y(n, t)$ be the graph with the maximum first general Zagreb index having a t -vertex cut set C . Let $X, Y \subset V(K)$ such that $X \cup Y = V(K)$. Furthermore, we have $C_X = C \cap X$ and $C_Y = C \cap Y$. The required result is obtained by proving the following claims.

Claim I. $K[C]$ and $K[C \cup C_1]$ are complete bipartite graphs, where C_1 is one of the components in $K - C$. \square

Proof. Suppose on the contrary that $K[C]$ or $K[C \cup C_1]$ is not a complete bipartite graph. Then, there are two non-adjacent vertices x, y in K and $K + xy \in Y(n, t)$. From Lemma 1, we know that $M^\gamma(K) < M^\gamma(K + xy)$ which is against the maximality of K . Hence, $K[C]$ and $K[C \cup C_1]$ are complete bipartite graphs.

Claim II. If C_X and C_Y are nonempty subsets of K , then $K - C$ has exactly two components. \square

Proof. $K - C$ has at least three components and C_2 and C_3 are two of these components. Then, there are two vertices $x \in V(C_2) \cap X, y \in V(C_3) \cap Y$ such that $K + xy \in Y(n, t)$ with C being a t -vertex cut of $K + xy$. By Lemma 1, we have a contradiction that K has the maximum first general Zagreb index.

Claim III. Either C_X is empty or C_Y is empty. \square

Proof. On the contrary, suppose that S_X and S_Y are non-empty sets; then, by Claim II, $K - C$ has exactly two components named C_2 and C_3 . Let $x \in V(C_2) \cap X$ and $y \in V(C_3) \cap X$. Assume that $a = d(x) \geq d(y) = b > 0$ and $|N_{C_3}(y)| = c > 0$.

(i) Now we construct a new graph G^* from K as $G^* = K - \{zy: z \in N_{C_2}(y)\} + \{zx: z \in N_{C_2}(y)\}$. By the definition of the first general Zagreb index, we have $M^\gamma(G^*) - M^\gamma(K) = (a + c)^\gamma + (b - x)^\gamma - a^\gamma - b^\gamma > 0$, and the last inequality can be seen by considering the function $\phi(x) = (x + c)^\gamma - x^\gamma$. $\phi(x)$ is an increasing function for $x > 0$ and $\gamma > 1$, and we have $a > b - c$; this implies that $\phi(a) > \phi(b - c)$.

(ii) Let $|C_Y| = t$ and consider arbitrary vertices $z_1, z_2, \dots, z_{t-1} \in Y - C$. Now we construct a new graph G^{**} from G_1 by adding more edges between the vertices of $X - y$ and Y and adding further edges $yz_1, yz_2, \dots, yz_{t-1}$. Clearly, $N_{G_2}(y)$ is the vertex cut with cardinality t ; in other words, $G^{**} \in Y(n, t)$. From Lemma 1 and (i) of Claim III, we have $M^\gamma(G^{**}) > M^\gamma(K)$, which is a contradiction.

From above claim, we deduce that $C \subset X$ is the t -vertex cut of K .

Claim IV. $K - C$ consists of an isolated vertex. \square

Proof. On the contrary, suppose that the components C_2, C_3 of $K - C$ are complete bipartite graphs. Also, suppose that $V(C_1) = X_1 \cup Y_1$ and $V(C_2) = X_2 \cup Y_2$, where $X_i \subset X, Y_i \subset Y$ for $i = 1, 2$.

Without loss of generality, suppose that $C \subset X$ and $y \in Y_1$. Construct a new graph H from K as

$H = K - \{yz: z \in X_1\} + \{xz: x \in X - C, z \in B - y, xz \notin E(K)\}$. This implies that C is also a t -vertex cut of H and $H \in Y(n, t)$. Similar to Claim III (i), we have $M^\gamma(H) - M^\gamma(K) > 0$, which is against the maximality of the first general Zagreb index of K .

By definition of the first general Zagreb index, we have

$$M^\gamma(K_n^a) = t^\gamma + t(a + 1)^\gamma + (n - a - 1 - t)a^\gamma + a(n - a - 1)^\gamma. \tag{8}$$

\square

4. Graphs with Given Connectivity and Independent Number

Let $\lambda(n, t, a)$ be the set of graphs of order n , vertex connectivity t , and independent number a . In this section, we investigate the graph which gives the maximum general first Zagreb index from $\lambda(n, t, a)$.

Theorem 4. Let $G \in \lambda(n, t, a)$ with $a \geq 1$ and $1 \leq t \leq n - 1$. Then, for $\gamma \geq 1$, we have

$$M^\gamma(G) \leq (n - t - a)(n - 2)^\gamma + (a - 1)(n - a)^\gamma + t(n - 1)^\gamma + t^\gamma \tag{9}$$

and the equality holds if and only if $G = K_t + (K_1 \cup (K_{n-t-a} + (a - 1)K_1))$.

Proof. For $a = 2$, this result has been discussed in [16]. So, we assume that $2 < a \leq n - 1$, and let K be the graph with the maximum first general Zagreb index in $\lambda(n, t, a)$ and C, D be the t -vertex cut and maximum independent sets of K , respectively. The following claims will prove our main result.

Claim I. Let C_1 be one component of $K - C, |V(C_1)| = p, |V(C_1) - D| = q$ and $|C - D| = r$; then, we have $K[C_1] = K_q + (r - p)K_1, K[C] = K_r + (t - r)K_1$ and $K[C \cup V(C_1)] = K_{q+r} \cup (t + p - q - r)K_1$. \square

Proof. As K has the maximum first general Zagreb index and by Lemma 1, we have $K = K[C] + K[V(G) - C]$. On the contrary, suppose that $K[C_1] \neq K_q + (r - q)K_1$; this implies that we have vertices $x, y \in V(C_1) - D$ and $z \in V(C_1) \cap D$ such that $xy \notin E(K)$ or $xz \notin E(K)$. Furthermore, one can notice that $K + xy, K + xz \in \lambda(n, t, a)$. By Lemma 1, we have a contradiction of the choice of K , which proves the claim.

Claim II. $K - C$ contains exactly two components. \square

Proof. On the contrary, suppose that $K - C$ contains at least three components, and two of them are named as C_2 and C_3 . Let $x \in V(C_1) - D, y \in V(C_2) - D$. Then, $K + xy \in \lambda(n, t, r)$, and we have a contradiction on the maximality of K by Lemma 1.

Claim III. If $|V(C_2)| \geq |V(C_3)|$, then $|V(C_3)| = 1$. \square

Proof. of Claim III. On the contrary, we suppose $|V(C_3)| \geq 2$. Furthermore, if $V(C_3) - D = \phi$, then $|V(C_3)| = 1$ as C_3 is a connected component. Suppose that $V(C_3) - D \neq \phi$; then, $V(C_3) - D \neq \phi$. Otherwise,

$V(C_3) \cap D = \emptyset$, and choosing $x \in V(C_3)$, we have that $D \cup \{x\}$ is an independent set which is a contradiction to the definition of D .

Let $w \in V(C_3) \cap D$, and we construct a new graph H as $H = K - \{xw: x \in V(C_2) - D\} + \{xy: x \in V(C_2) - \{w\}, y \in V(C_2)\}$. Clearly, D is the maximal independent set, and C is the minimal vertex cut set of K ; $H \in \lambda(n, t, a)$.

Let $x \in V(K) - C - \{w\}$ and $w \in V(C_2) - D$; then we have $d_K(x) < d_H(x)$. By applying the definition of M^γ on K and H , we obtain $M^\gamma(K) - M^\gamma(H) < d_H(w)^\gamma + d_H(v)^\gamma - d_K(w)^\gamma - d_K(v)^\gamma < 0$ which is against the choice of K .

From Claims I, II, and III, we have $K \in \{G^*: G^* = (K_{n-a} + (a-1)K_1) \cup \{w\} \cup \{z - iw: z_i \in C, i = 1, 2, \dots, t\}\}$, where w is an isolated vertex of $K - C$. Let $|C \cap D| = p$; then,

$$\begin{aligned} M^\gamma(G^*) &= p(n-a+1)^\gamma + (a-p-1)(n-a)^\gamma + (t-p)(n-1)^\gamma + (n-a-t+p)(n-2)^\gamma + t^\gamma, \\ &= (a-1)(n-a)^\gamma + (n-a)(n-2)^\gamma + t^\gamma + t[(n-1)^\gamma - (n-2)^\gamma] + p[(n-a+1)^\gamma - (n-a)^\gamma - (n-1)^\gamma + (n-2)^\gamma]. \end{aligned} \quad (10)$$

Let $A = [(n-a+1)^\gamma - (n-a)^\gamma - (n-1)^\gamma + (n-2)^\gamma]$. Consider the function $g(x) = (n-x+1)^\gamma - (n-x)^\gamma$ for $x \geq 1$. As $g'(x) < 0$, $g(x)$ is a decreasing function for $\gamma > 1$. This implies that $A \leq n^\gamma - 2(n-1)^\gamma + (n-2)^\gamma < 0$, and the last inequality is due to Jensen's inequality. Hence, (1) attains its maximum value for $p = 0$; in other words, for $K = K_t + (K_1 \cup (K_{n-t-1} + (a-1)K_1))$, the first general Zagreb index attains its maximum value for $\gamma > 1$. \square

Data Availability

The data used to support the findings of this study are included within the article.

Conflicts of Interest

The authors declare that they have no conflicts of interest.

References

- [1] M. K. Jamil, I. Tomescu, M. Imran, and A. Javed, "Some bounds on zeroth-order general Randić index," *Mathematics*, vol. 8, no. 1, p. 98, 2020.
- [2] I. Gutman and N. Trinajstić, "Graph theory and molecular orbitals. Total φ -electron energy of alternant hydrocarbons," *Chemical Physics Letters*, vol. 17, no. 4, pp. 535–538, 1972.
- [3] M. V. Diudea, *QSPR/QSAR Studies by Molecular Descriptors*, Nova Science Publishers, New York, NY, USA, 2001.
- [4] A. T. Balaban and James Devillers, Eds., *Topological Indices and Related Descriptors in QSAR and QSPAR*, CRC Press, Florida, FL, USA, 2014.
- [5] X. Li and J. Zheng, "A unified approach to the extremal trees for different indices," *Mathematical Computational Chemistry*, vol. 54, no. 1, pp. 195–208, 2005.
- [6] M. Liu and B. Liu, "Some properties of the first general Zagreb index," *Australasian Journal of Combinatorics*, vol. 47, p. 285, 2010.
- [7] J. M. Rodríguez, J. L. Sánchez, and J. M. Sigarreta, "CMMSE on the first general Zagreb index," *Journal of Mathematical Chemistry*, vol. 56, no. 7, pp. 1849–1864, 2018.
- [8] H. M. Awais, M. Javaid, and A. Ali, "First general Zagreb index of generalized F -sum graphs," *Discrete Dynamics in Nature and Society*, vol. 2020, Article ID 2954975, 16 pages, 2020.
- [9] X.-F. Pan, H. Liu, and M. Liu, "Sharp bounds on the zeroth-order general Randić index of unicyclic graphs with given

- diameter," *Applied Mathematics Letters*, vol. 24, no. 5, pp. 687–691, 2011.
- [10] L. Volkmann, "Sufficient conditions on the zeroth-order general Randić index for maximally edge-connected digraphs," *Communications in Combinatorics and Optimization*, vol. 1, pp. 1–13, 2016.
- [11] M. K. Jamil and I. Tomescu, "Zeroth-order general Randić index of k -generalized quasi trees," 2018, <https://arxiv.org/abs/1801.03885>.
- [12] M. Azari and A. Iranmanesh, "GENERALIZED ZAGREB INDEX OF GRAPHS. *Studia universitatis babes-bolyai, Chemia*, vol. 56, no. 3, 2011.
- [13] J.-B. Liu, S. Javed, M. Javaid, and K. Shabbir, "Computing first general Zagreb index of operations on graphs," *IEEE access*, vol. 7, pp. 47494–47502, 2019.
- [14] L. Bedratyuk and O. Savenko, "The star sequence and the general first Zagreb index," 2017, <https://arxiv.org/abs/1706.00829>.
- [15] J. A. Bondy and U. S. R. Murty, *Graph Theory*, Graduate texts in Mathematics, vol. 244, , p. 81, 2008.
- [16] I. Tomescu, M. Arshad, and M. K. Jamil, "Extremal topological indices for graphs of given connectivity," *Filomat*, vol. 29, no. 7, pp. 1639–1643, 2020.

Research Article

A Novel Mathematical Model for Radio Mean Square Labeling Problem

Elsayed Badr ¹, Shokry Nada,² Mohammed M. Ali Al-Shamiri ^{3,4}, Atef Abdel-Hay ²,
and Ashraf ELrokh²

¹Scientific Computing Department, Benha University, Benha, Egypt

²Mathematics and Computer Science Department, Menoufia University, Shibin Al Kawm, Egypt

³Department of Mathematics, Faculty of Science and Arts, King Khalid University, Muhayil Assir, Saudi Arabia

⁴Department of Mathematics and Computer, Faculty of Science, Ibb University, Ibb, Yemen

Correspondence should be addressed to Elsayed Badr; badrgraph@gmail.com

Received 27 August 2021; Accepted 27 December 2021; Published 12 January 2022

Academic Editor: Ali Ahmad

Copyright © 2022 Elsayed Badr et al. This is an open access article distributed under the Creative Commons Attribution License, which permits unrestricted use, distribution, and reproduction in any medium, provided the original work is properly cited.

A radio mean square labeling of a connected graph is motivated by the channel assignment problem for radio transmitters to avoid interference of signals sent by transmitters. It is an injective map h from the set of vertices of the graph G to the set of positive integers \mathbb{N} , such that for any two distinct vertices x, y , the inequality $d(x, y) + \lceil (h(x))^2 + (h(y))^2/2 \rceil \geq \dim(G) + 1$ holds. For a particular radio mean square labeling h , the maximum number of $h(v)$ taken over all vertices of G is called its spam, denoted by $\text{rmsn}(h)$, and the minimum value of $\text{rmsn}(h)$ taking over all radio mean square labeling h of G is called the radio mean square number of G , denoted by $\text{rmsn}(G)$. In this study, we investigate the radio mean square numbers $\text{rmsn}(P_n)$ and $\text{rmsn}(C_n)$ for path and cycle, respectively. Then, we present an approximate algorithm to determine $\text{rmsn}(G)$ for graph G . Finally, a new mathematical model to find the upper bound of $\text{rmsn}(G)$ for graph G is introduced. A comparison between the proposed approximate algorithm and the proposed mathematical model is given. We also show that the computational results and their analysis prove that the proposed approximate algorithm overcomes the integer linear programming model (ILPM) according to the radio mean square number. On the other hand, the proposed ILPM outperforms the proposed approximate algorithm according to the running time.

1. Introduction

In wireless networks, each radio station assigns a number called frequency. When different transmitters of district stations send signals, the receiver might get unnecessarily interference of the signals sent by transmitters in particular with close frequencies. This is the channel assignment problem introduced by Hale [1] in 1980 to minimize such interference. In 2001, Chartrand et al. [2] proposed converting this problem to graph theoretical problem using vertex labeling. Many researchers involved with this problem [3–16] and produced different methods to minimize the interference of signals [7]. Recently, Ramesh et al. [8] proposed a new method called radio mean square labeling, which is defined as follows. A radio mean square labeling of a

connected graph G is an injective function h from its vertex set V to the set of natural numbers \mathbb{N} , such that for any two distinct vertices x and y , $\lceil (h(x))^2 + (h(y))^2/2 \rceil \geq \text{diam } G + 1 - d(x, y)$ holds, where $d(x, y)$ denotes the distance between the two vertices, and $\text{diam } G$ represents the diameter of the graph [8]. For a radio mean square labeling h , the maximum number of $h(v)$ taken over all vertices of G is called its spam, denoted by $\text{rsmn}(h)$, and the minimum value of $\text{rsmn}(h)$ taking over all radio mean square labeling h of G is called the radio mean square number of G , denoted as $\text{rsmn}(G)$. The radio mean square number of h , denoted by $\text{rsmn}(h)$ is the maximum number assigned to any vertex of G . Ramesh et al. [8] determined the radio mean square number for some graphs such as in the centric subdivision of spoke wheel graph and biwheel graph.

Due to most of nontrivial coloring models, graph coloring is an NP-hard problem. Therefore, we take into consideration a graph coloring algorithm [9–11]. The judgment of the performance of the used algorithm does include its effectiveness and accuracy for a large number of vertices and the level of complexity regarding suboptimal solutions [12, 13]. Here, we introduce an approximate algorithm that leads to an upper bound of the radio mean square for a large number of vertices. Finally, we turn our attention to reformulate the radio square labeling as a linear programming model and then minimize the suggested linear function. We use of transforming the non-linear constraint to become a linear constraint by using of some large integers dependably on the coefficient range of the given problem under path calculating conditions. Some illustrated examples and comparison between the techniques will be given.

It should be noted that all the considered graphs in this study are finite, simple, connected, and undirected.

The organization of the study goes as follows: in Section 2, the radio mean square number of cycles and paths are given. Section 3 is devoted to present an approximate algorithm that finds the upper bound of the radio mean square number of a given graph and an illustrative example is included. Section 4 deals with a new mathematical model for finding the upper bound of the radio mean square number of the given graph. Section 5 provides the experimental results. Analysis and statistical tests between the mathematical model and the proposed approximate algorithm are provided. The last section is considered for conclusion.

2. Results

The following theorem is about the rmsgn for the path P_n , and next, we will get the rmsgn for cycle C_n .

Theorem 1. For the path P_n , $n \geq 1$, and the radio mean square number is

$$\text{rmsgn}(P_n) = n + k ; \left\{ \begin{array}{l} 1 \leq n \leq 15 \text{ and } k = 0, \\ 16 \leq n \leq 22 \text{ and } k = 1, \\ 23 \leq n \leq 32 \text{ and } k = 2, \\ 33 \leq n \leq 44 \text{ and } k = 3, \\ 45 \leq n \leq 58 \text{ and } k = 4, \\ 59 \leq n \leq 73 \text{ and } k = 5, \\ 74 \leq n \leq 92 \text{ and } k = 6, \\ \vdots \\ k^2 + 5k + 9 \leq n \leq k^2 + 7k + 14, k \geq 7. \end{array} \right. \quad (1)$$

Proof. Clearly, $\text{diam}(P_n) = n - 1$. Then, one can define $h: V(P_n) \rightarrow \mathbb{N}$ as follows: \square

Case a. For

$$\begin{aligned} 1 \leq n \leq 15, & \quad k = 0, \\ 16 \leq n \leq 22, & \quad k = 1, \\ 23 \leq n \leq 32, & \quad k = 2, \\ 33 \leq n \leq 44, & \quad k = 3, \\ 45 \leq n \leq 58, & \quad k = 4, \\ 59 \leq n \leq 73, & \quad k = 5, \\ 74 \leq n \leq 92, & \quad k = 6. \end{aligned} \quad (2)$$

One may label the vertices of P_n as follows:

Subcase a.1: n is even:

$$\begin{aligned} h(x_1) &= 1, h(x_n) = k + 2, \\ h(x_{2+i}) &= n + k - 2i, 0 \leq i < \frac{n}{2} - 1, \end{aligned} \quad (3)$$

$$h(x_{n-1-i}) = n + k - 1 - 2j, 0 \leq j < \frac{n}{2} - 1.$$

Subcase a.1: n is odd:

$$\begin{aligned} h(x_1) &= 1, h(x_n) = k + 2, \\ h(x_{2+i}) &= n + k - 2i, 0 \leq i < \frac{n-1}{2}, \end{aligned} \quad (4)$$

$$h(x_{n-1-i}) = n + k - 1 - 2j, 0 \leq j < \frac{n-1}{2} - 1.$$

Case 2. bFor $n \geq 93$ and $k^2 + 5k + 9 \leq n \leq k^2 + 7k + 14, k \geq 7$, one may label the vertices of P_n as the following subcases:

Subcase b.1: n is even:

$$\begin{aligned} h(x_1) &= 1, h(x_n) = k + 2, \\ h(x_{2+i}) &= n + k - 2i, 0 \leq i < \frac{n}{2} - 1, \end{aligned} \quad (5)$$

$$h(x_{n-1-i}) = n + k - 1 - 2j, 0 \leq j < \frac{n}{2} - 1.$$

Subcase b.1: n is odd:

$$\begin{aligned} h(x_1) &= 1, h(x_n) = k + 2, \\ h(x_{2+i}) &= n + k - 2i, 0 \leq i < \frac{n-1}{2}, \end{aligned} \quad (6)$$

$$h(x_{n-1-i}) = n + k - 1 - 2j, 0 \leq j < \frac{n-1}{2} - 1.$$

Therefore, for any pair $(x_i, x_j), i \neq j, 0 \leq i, j \leq n$, we have $d(x_i, x_j) + \lceil \frac{h(x_i)^2 + h(x_j)^2}{2} \rceil \geq 1 + n - 1 = 1 + \text{diam}(P_n)$.

Hence, h is a valid radio mean square labeling for P_n , and therefore, $\text{rmsn}(P_n) \leq \text{rmsn}(h) = n + k$. Since h is injective, $\text{rmsn}(P_n) = n + k, n \geq 1$ for all radio mean square labeling h , and hence, $\text{rmsn}(P_n) = n + k, n \geq 1$. Therefore, the labeling h defined above satisfies the radio mean square condition.

Example 1. The radio mean square numbers of P_9, P_{10}, P_{96} , and P_{115} are shown in Figure 1. It is clear that $k = 0$ for P_9 and P_{10} , but $k = 7$ for P_{96} , and P_{115} .

Theorem 2. *The radio mean square numbers of the cycles $C_n, n \geq 3$, are given by*

$$\text{rmsn}(C_n) = \begin{cases} n + k; & \begin{cases} n: & 3 \leq n \leq 7, \\ & \begin{cases} 8 \leq n \leq 15 \text{ and } k = 0, \\ 16 \leq n \leq 27 \text{ and } k = 1, \\ 28 \leq n \leq 43 \text{ and } k = 2, \\ \vdots \\ k^2 + 5k + 9 \leq n \leq k^2 + 7k + 14, k \geq 3. \end{cases} \end{cases} \end{cases} \quad (7)$$

Proof. It is clear that the dimension of $C_n = x_1, x_2, \dots, x_n$ is $\lfloor n/2 \rfloor$ since its length is n . Then, one can define $h: V(C_n) \rightarrow \mathbb{N}$ as follows: \square

*Case 3. a*For $3 \leq n \leq 7$, we may label the vertices of C_n by

$$h(x_i) = i; 1 \leq i \leq n. \quad (8)$$

*Case 4. b*For $n \geq 8, 2k^2 + 2k + 4 \leq n \leq 2k^2 + 6k + 7, k \geq 0$. We may label the vertices of C_n by one of the following subcases:

Subcase b.1: n is even:

$$\begin{aligned} h(x_{n/2}) &= k + 1, \\ h(x_{i+1}) &= k + 3 + 2i, 0 \leq i < \frac{n}{2} - 1, \\ h(x_{n-j}) &= k + 2 + 2j, 0 \leq j < \frac{n}{2}. \end{aligned} \quad (9)$$

Therefore, for any pair $(x_i, x_j), i \neq j, 1 \leq i, j \leq n$, we have $d(x_i, x_j) + \lceil \frac{h(x_i)^2 + h(x_j)^2}{2} \rceil \geq 1 + \lfloor n/2 \rfloor = 1 + \dim(C_n)$.

Subcase b.2: n is odd:

$$\begin{aligned} h(x_{(n+1)/2}) &= k + 1, \\ h(x_{i+1}) &= k + 2 + 2i, 0 \leq i < \frac{n+1}{2} - 1, \\ h(x_{n-j}) &= k + 3 + 2j, 0 \leq j < \frac{n+1}{2} - 1. \end{aligned} \quad (10)$$

So, for any pair $(x_i, x_j), i \neq j, 1 \leq i, j \leq n$, the following inequality holds $d(x_i, x_j) + \lceil \frac{h(x_i)^2 + h(x_j)^2}{2} \rceil \geq 1 + \lfloor n/2 \rfloor = 1 + \dim(C_n)$.

Hence, h is a valid radio mean square labeling for C_n , and therefore,

$$\text{rmsn}(C_n) \leq \text{rmsn}(h) = \begin{cases} n, & \text{if } 3 \leq n \leq 7, \\ n + k, & \text{if } n \geq 8 \text{ and } \begin{cases} 2k^2 + 2k + 4 \leq n \leq 2k^2 + 6k + 7, \\ k \geq 0. \end{cases} \end{cases} \quad (11)$$

Since h is injective,

$$\text{rmsn}(C_n) \geq \begin{cases} n, & \text{if } 3 \leq n \leq 7, \\ n + k, & \text{if } n \geq 8, \text{ and } \begin{cases} 2k^2 + 2k + 4 \leq n \leq 2k^2 + 6k + 7, \\ k \geq 0. \end{cases} \end{cases} \quad (12)$$

For all radio mean square labeling h ,

$$\text{rmsn}(C_n) = \begin{cases} n, & \text{if } 3 \leq n \leq 7, \\ n + k, & \text{if } n \geq 8, \text{ and } \begin{cases} 2k^2 + 2k + 4 \leq n \leq 2k^2 + 6k + 7, \\ k \geq 0. \end{cases} \end{cases} \quad (13)$$

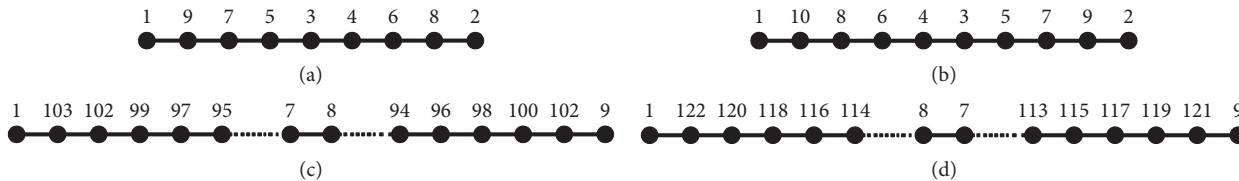


FIGURE 1: The radio mean square number of P_9, P_{10}, P_{96} , and P_{115} . (a) $\text{rmsn}(P_9) = 9$. (b) $\text{rmsn}(P_{10}) = 10$. (c) $\text{rmsn}(P_{96}) = 103$. (d) $\text{rmsn}(P_{115}) = 122$.

Therefore, the labeling h defined above satisfies the radio mean square condition.

Example 2. The radio mean square numbers of cycles C_8, C_9, C_{16} , and C_{17} are shown in Figure 2. It is clear that $k = 1$ for C_{16} and C_{17} , but $k = 7$ for C_{95} and C_{112} .

3. A Novel Graph Radio Mean Square Algorithm

Here, we introduce an approximated algorithm. This algorithm finds an upper bound of the radio mean square for arbitrary graph G . The main idea is to labeling some vertices (initial vertices) by $\text{floor}(\sqrt{\text{diam}})$. On the other hand, the algorithm chooses a different vertex as an initial vertex in each iteration.

The time complexity of an algorithm is defined as the number of instructions of this algorithm multiplied by the running time of each instruction. The time complexity is considered as a good metric to evaluate the given algorithm. Thus, Algorithm 1 has nine steps, and both Step 1 and Step 2 have the same instruction. Step 3 has a nested loop that has $O(n^2)$ time complexity. On the other hand, Step 4, Step 5, and Step 6 have $O(n)$ time complexity. Step 7 has one instruction, while Step 8 and Step 9 have $O(n^3)$ and $O(n^4)$, respectively. Therefore, Algorithm 1 has the time complexity $O(n^4)$.

In the coming example, we show and explain how to compute the radio mean square labeling problem for P_5 .

Example 3. Suppose that x_i is the label of the vertex v_i , $1 \leq i \leq 5$. Therefore, 1 explores an upper bound of the radio mean square labeling problem as follows:

It is known that $\text{diam}(P_5) = 4$. We select a vertex x_1 and $\text{col}(x_1) = 2$. Let $S = \{x_1\}$, and for all $v \in V(G) - S$, compute

$$\begin{aligned} \text{temp}(x_2) &= \max_{x_1} \left\{ 2 + \text{ceil} \left(\frac{\max\{(\sqrt{4+1-1}, 1)\}}{4} \right) \right\} = 3, \\ \text{temp}(x_3) &= \max_{x_1} \left\{ 2 + \text{ceil} \left(\frac{\max\{(\sqrt{4+1-2}, 1)\}}{4} \right) \right\} = 3, \\ \text{temp}(x_4) &= \max_{x_1} \left\{ 2 + \text{ceil} \left(\frac{\max\{(\sqrt{4+1-3}, 1)\}}{4} \right) \right\} = 3, \\ \text{temp}(x_5) &= \max_{x_1} \left\{ 2 + \text{ceil} \left(\frac{\max\{(\sqrt{4+1-4}, 1)\}}{4} \right) \right\} = 3. \end{aligned} \tag{14}$$

Let $\min = \min_{v \in V(G)-S} \{\text{temp}(v)\} = 3$; we choose a vertex $x_2 \in V(G) - S$, such that $\text{temp}(x_2) = 3$. Give $\text{col}(x_2) = 3$ and $S = \{x_1, x_2\}$.

$$\begin{aligned} \text{temp}(x_3) &= \max_{\{x_1, x_2\}} \left\{ \begin{array}{l} 2 + \text{ceil} \left(\frac{\max\{(\sqrt{4+1-2}, 1)\}}{4} \right) \\ 3 + \text{ceil} \left(\frac{\max\{(\sqrt{4+1-1}, 1)\}}{4} \right) \end{array} \right\} = 4, \\ \text{temp}(x_4) &= \max_{\{x_1, x_2\}} \left\{ \begin{array}{l} 2 + \text{ceil} \left(\frac{\max\{(\sqrt{4+1-3}, 1)\}}{4} \right) \\ 3 + \text{ceil} \left(\frac{\max\{(\sqrt{4+1-2}, 1)\}}{4} \right) \end{array} \right\} = 4, \\ \text{temp}(x_5) &= \max_{\{x_1, x_2\}} \left\{ \begin{array}{l} 2 + \text{ceil} \left(\frac{\max\{(\sqrt{4+1-4}, 1)\}}{4} \right) \\ 3 + \text{ceil} \left(\frac{\max\{(\sqrt{4+1-3}, 1)\}}{4} \right) \end{array} \right\} = 4. \end{aligned} \tag{15}$$

Let $\min = \min_{v \in V(G)-S} \{\text{temp}(v)\} = 4$; we choose a vertex $x_3 \in V(G) - S$, where $\text{temp}(x_3) = 4$. Give $\text{col}(x_3) = 4$ and $S = \{x_1, x_2, x_3\}$.

$$\begin{aligned} \text{temp}(x_4) &= \max_{\{x_1, x_2, x_3\}} \left\{ \begin{array}{l} 2 + \text{ceil} \left(\frac{\max\{(\sqrt{4+1-3}, 1)\}}{4} \right) \\ 3 + \text{ceil} \left(\frac{\max\{(\sqrt{4+1-2}, 1)\}}{4} \right) \\ 4 + \text{ceil} \left(\frac{\max\{(\sqrt{4+1-1}, 1)\}}{4} \right) \end{array} \right\} = 5, \\ \text{temp}(x_5) &= \max_{\{x_1, x_2, x_3\}} \left\{ \begin{array}{l} 2 + \text{ceil} \left(\frac{\max\{(\sqrt{4+1-4}, 1)\}}{4} \right) \\ 3 + \text{ceil} \left(\frac{\max\{(\sqrt{4+1-3}, 1)\}}{4} \right) \\ 4 + \text{ceil} \left(\frac{\max\{(\sqrt{4+1-2}, 1)\}}{4} \right) \end{array} \right\} = 5. \end{aligned} \tag{16}$$

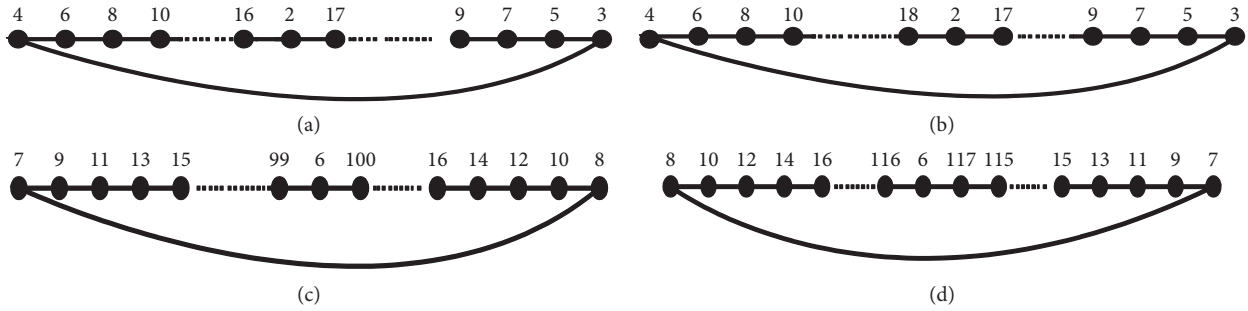


FIGURE 2: The radio mean square number of cycles C_8, C_9, C_{16} , and C_{17} . (a) $\text{rmsn}(C_{16}) = 17$. (b) $\text{rmsn}(C_{17}) = 18$. (c) $\text{rmsn}(C_{95}) = 100$. (d) $\text{rmsn}(C_{112}) = 117$.

Let $\min = \min_{v \in V(G)-S} \{\text{temp}(v)\} = 5$; we choose a vertex $x_4 \in V(G) - S$, where $\text{temp}(x_4) = 5$. Give $\text{col}(x_4) = 5$ and $S = \{x_1, x_2, x_3, x_4\}$.

$$\text{temp}(x_5) = \max_{x_1} \left\{ \begin{array}{l} 2 + \text{ceil}\left(\frac{\max\{\sqrt{4+1-4}, 1\}}{4}\right) \\ 3 + \text{ceil}\left(\frac{\max\{\sqrt{4+1-3}, 1\}}{4}\right) \\ 4 + \text{ceil}\left(\frac{\max\{\sqrt{4+1-2}, 1\}}{4}\right) \\ 5 + \text{ceil}\left(\frac{\max\{\sqrt{4+1-1}, 1\}}{4}\right) \end{array} \right\} = 6 \quad (17)$$

Let $\min = \min_{v \in V(G)-S} \{\text{temp}(v)\} = 6$; we select a vertex $x_5 \in V(G) - S$, where $\text{temp}(x_5) = 6$. Give $\text{col}(x_5) = 6$ and $S = \{x_1, x_2, x_3, x_4, x_5\}$. Plainly, all vertices are labelled and $\text{rmsn}(P_5) = 6$.

4. Formulation of the Radio Mean Square Labeling as a Mathematical Model

In this section, we present the integer linear programming model (ILPM) for the radio mean square labeling problem.

Let G be a connected graph of order n with $V(G) = \{v_1, v_2, \dots, v_n\}$ and let $D = [d_{ij}]$ be the distance matrix of G , that is, $d_{ij} = d(v_i, v_j)$ for $1 \leq i, j \leq n$. Suppose that x_i is the label of the vertex v_i , $1 \leq i \leq n$. Now, we can propose the mathematical model for the radio mean square labeling problem as the ILPM. Let us suppose the function F is $F = x_1 + x_2 + \dots + x_n$.

4.1. *Formulation 1.* Minimize F subject to the $\binom{n}{2}$ constraints $\lceil (x_i)^2 + (x_j)^2 / 2 \rceil \geq \text{diam} + 1 - d(v_i, v_j)$ for $1 \leq i \leq n - 1, 2 \leq j \leq n$, and $i < j$, and as mentioned before, the following steps will transform nonlinear constraints to become linear which is easy to deal with.

4.2. *Formulation 2.* Since $\lceil (x_i)^2 + (x_j)^2 / 2 \rceil \leq \lceil (x_i) + (x_j) / 2 \rceil^2$, we have the following inequalities:

$$\begin{aligned} \left\lceil \frac{(x_i) + (x_j)}{2} \right\rceil^2 &\geq \text{diam} + 1 - d(v_i - v_j), \\ \left\lceil \frac{(x_i) + (x_j)}{2} \right\rceil &\geq \sqrt{\text{diam} + 1 - d(v_i - v_j)}, \\ \frac{(x_i) + (x_j)}{2} &\geq \sqrt{\text{diam} + 1 - d(v_i - v_j)}, \\ \frac{(x_i) + (x_j)}{2} + 1 &\geq \sqrt{\text{diam} + 1 - d(v_i - v_j)}, \\ M \left| (x_i - x_j) \right| &\geq \frac{(x_i) + (x_j)}{2} + 1 \geq \sqrt{\text{diam} + 1 - d(v_i - v_j)}. \end{aligned} \quad (18)$$

M is a large integer number which depends on the coefficients range of the problem.

The absolute value notation is used to get distinct values for x_i , where $i = 1, 2, \dots, n$.

Now, we can reformulate the radio mean square problem as follows:

$$\begin{aligned} \min F &= x_1 + x_2 + \dots + x_n, & (19) \\ \text{Subject to } M \left| (x_i - x_j) \right| &\geq \left\lceil \sqrt{\text{diam} + 1 - d(v_i - v_j)} \right\rceil, \\ &1 \leq i \leq n - 1 \\ &2 \leq j \leq n \text{ and } i < j. & (20) \end{aligned}$$

Here, the floor function is used because the values of $x_i, 1 \leq i \leq n$, are integers.

Example 4. The details of the ILPM to compute the radio mean square labeling for P_3 . Assume that x_i is the label of the vertex v_i , such that $1 \leq i \leq 3$. Thus, the mathematical model for the radio mean square labeling problem as the ILPM is prepared as follows:

$$\min f = x_1 + x_2 + x_3. \quad (21)$$

Subject to

Input: G be an n -vertex graph, simple connected graph, and the diameter of (diam)
Output: an upper bound of radio mean square number of G
 Begin
Step 1: choose a vertex u and $\text{col}(u) = \text{floor}(\sqrt{\text{diam}})$
Step 2: $S = \{u\}$
Step 3: for all $v \in V(G) - S$, compute
 $\text{temp}(v) = \max\{\text{col}(t) + \text{ceil}(\max\{\sqrt{(D+1-d(u,v), 1})/\text{diam}\})\}$
Step 4: let $\min_{v \in V(G)-S} = \min\{\text{temp}(v)\}$
Step 5: choose a vertex $v \in V(G) - S$, such that $\text{temp}(v) = \min$
Step 6: give $\text{col}(v) = \min$
Step 7: $S = S \cup \{v\}$
Step 8: repeat **Step 3–Step 6** until all vertices are labelled
Step 9: repeat **Step 1–Step 7** for every vertex $x \in V(G)$
 End

ALGORITHM 1: Finding an upper bound of the radio mean square number of a graph G .

TABLE 1: Description of the computing environment.

CPU	Intel (R) Core (TM) i5-2430 CPU at 2.40 GHz
RAM size	4 GB RAM
MATLAB version	R2019a (9.6.0.1072779)

TABLE 2: Comparison between standard radio mean square number, algorithm, and integer linear programming for the upper bound of radio mean square number for the path graph.

N	Standard RMS	Path graph			
		Proposed algorithm		Integer linear programming	
		rmsn (P_n)	CPU time	rmsn (P_n)	CPU time
1	1	—	—	—	—
2	2	2	0.0001565	2	0.0135961
3	3	3	0.0007495	3	0.0137607
4	4	4	0.0009242	4	0.0142838
5	5	6	0.0009259	9	0.0148360
6	6	7	0.0011930	11	0.0149701
7	7	8	0.0028154	13	0.0151607
8	8	9	0.0031659	15	0.0153437
9	9	10	0.0086583	17	0.0153530
10	10	12	0.0092995	28	0.0153602
11	11	13	0.0178153	31	0.0154630
12	12	14	0.0179739	34	0.0158122
13	13	15	0.0195242	37	0.0159264
14	14	16	0.0214671	40	0.0160664
15	15	17	0.0323685	43	0.0165312
16	17	18	0.0397062	46	0.0165756
17	18	20	0.0488390	65	0.0166756
18	19	21	0.0521773	69	0.0168593
19	20	22	0.0635412	73	0.0168673
20	21	23	0.0773853	77	0.0173017
21	22	24	0.0926470	81	0.0173982
22	23	25	0.1082337	85	0.0174649
23	25	26	0.1321028	89	0.0176519
24	26	27	0.1680530	93	0.0178209
25	27	28	0.1819503	97	0.0178319
26	28	30	0.2174177	126	0.0178408
27	29	31	0.2423215	131	0.0178502
28	30	32	0.2838989	135	0.0179323
29	31	33	0.3306090	142	0.0181244
30	32	34	0.3907487	146	0.0182150
50	54	56	3.3044964	344	0.0295531

TABLE 3: Comparison between standard radio mean square number, algorithm, and integer linear programming for the upper bound of radio mean square number for the cycle graph.

N	Standard RMS	Cycle graph			
		Proposed algorithm		Integer linear programming	
		rmsn (C_n)	CPU time	rmsn (C_n)	CPU time
1	—	—	—	—	—
2	—	—	—	—	—
3	3	3	0.0002946	3	0.0121703
4	4	4	0.0006198	4	0.0128697
5	5	5	0.0013164	5	0.0130696
6	6	6	0.0017746	6	0.0134300
7	7	7	0.0023419	7	0.0137379
8	8	9	0.0037564	15	0.0137439
9	10	10	0.0050932	17	0.0140673
10	10	11	0.0060342	19	0.0143174
11	11	12	0.0088211	21	0.0143427
12	12	13	0.0148844	23	0.0147269
13	13	14	0.0172248	25	0.0147985
14	14	15	0.0203240	27	0.0149231
15	15	16	0.0251720	29	0.0151018
16	17	17	0.0323380	31	0.0151929
17	18	18	0.0397318	33	0.0155649
18	19	20	0.0492787	52	0.0156036
19	20	21	0.0612156	55	0.0156856
20	21	22	0.0765414	58	0.0157774
21	22	23	0.0898619	61	0.0160212
22	23	24	0.1191102	64	0.0162420
23	24	25	0.1328831	67	0.0163022
24	25	26	0.1583415	70	0.0165312
25	26	27	0.1758159	73	0.0165648
26	27	28	0.2122978	76	0.0165116
27	28	29	0.2491384	79	0.0166234
28	30	30	0.2822584	82	0.0167352
29	31	31	0.3290932	85	0.0168470
30	32	32	0.3655289	88	0.0171844
50	53	54	3.0468593	246	0.0250638

$$\begin{aligned}
 |x_1 - x_2| &\geq \left\lceil \sqrt{\text{diam} + 1 - d(v_1, v_2)} \right\rceil, \\
 |x_1 - x_3| &\geq \left\lceil \sqrt{\text{diam} + 1 - d(v_1, v_3)} \right\rceil, \\
 |x_2 - x_3| &\geq \left\lceil \sqrt{\text{diam} + 1 - d(v_2, v_3)} \right\rceil, \\
 x_1, x_2, x_3 &\geq 0.
 \end{aligned}
 \tag{22}$$

Since $\text{diam} = n - 1$ and $\text{diam} = 2$ for $P_3, M = 1$, the distance matrix of P_3 is

$$D = \begin{bmatrix} 0 & 1 & 2 \\ 1 & 0 & 1 \\ 2 & 1 & 0 \end{bmatrix}.
 \tag{23}$$

Therefore, the above mathematical model can be written as follows:

$$\min f = x_1 + x_2 + x_3.
 \tag{24}$$

Subject to

$$|x_1 - x_2| \geq 1; |x_1 - x_3| \geq 1; |x_2 - x_3| \geq 1; x_1, x_2, x_3 \geq 0.
 \tag{25}$$

The solution of the above model equals to 3.

5. Computational Study

In this article, we propose the analysis of the computational results that show the superiority of Algorithm 1 on the ILPM according to the radio mean square number. On the other hand, the proposed ILPM outperforms Algorithm 1 according to CPU time.

Paths and cycles are used to evaluate the proposed models. The computation environment is given in Table 1. MATLAB solver is used to solve the ILPM. In Tables 2 and 3, the following symbols standard RMS, rmsn, and CPU times are used to indicate the exact radio mean square number, the calculated mean square number, and the running time for path and cycles, respectively. The convergence between the calculated and exact upper bounds of the radio mean square number of paths is given in Table 2. Figures 3 and 4 show that the superiority of the proposed Algorithm 1 on the ILPM according to the radio mean square number. For example, the standard radio mean square number for P_{50} is 54, but it is 56 and 344 by Algorithm 1 and the ILPM, respectively. Figures 5 and show the superiority of the

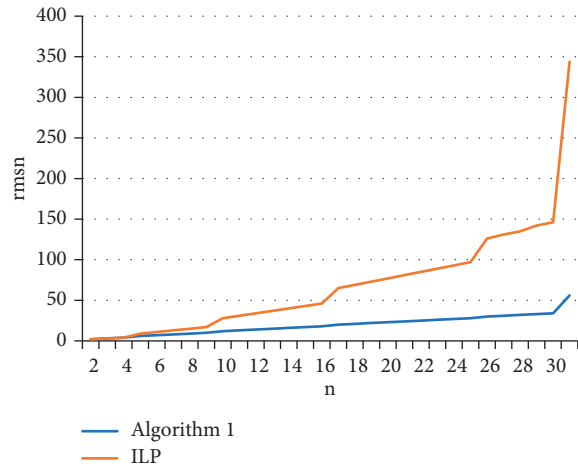


FIGURE 3: Comparison between standard radio mean square number, algorithm, and integer linear programming for the upper bound of radio mean square number for the path graph.

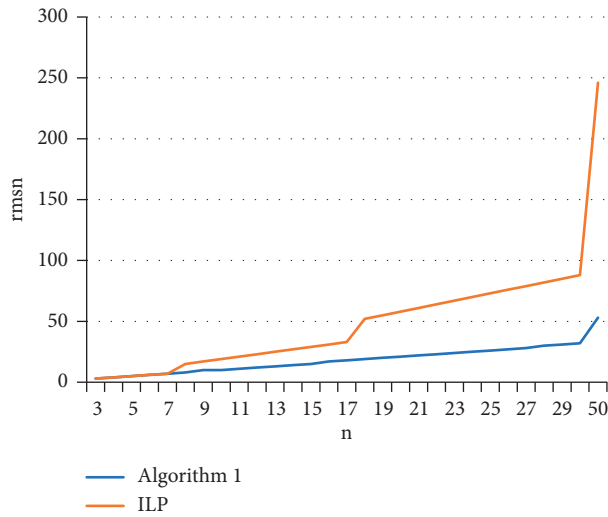


FIGURE 4: Comparison between standard radio mean square number, algorithm, and integer linear programming for the upper bound of radio mean square number for the cycle graph.

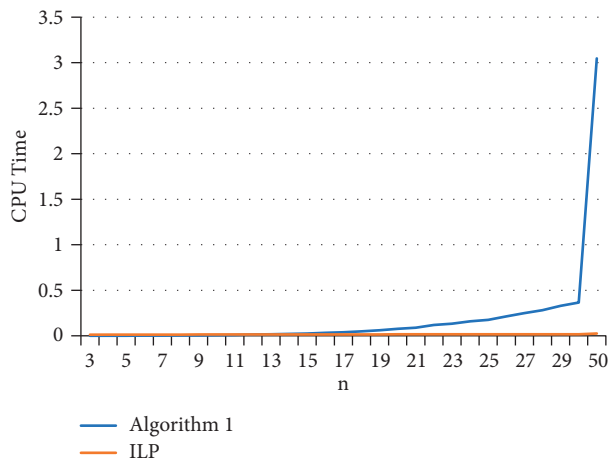


FIGURE 5: Comparison between standard radio mean square number, algorithm, and integer linear programming for the upper bound of radio mean square number for the path graph according to CPU time.

proposed Algorithm 1 on the ILPM according to CPU time. Table 3 provides that the gap between the ILPM and the proposed Algorithm 1 is large according to the radio mean square number. It is clear that 1 is better than the ILPM according to the radio mean square number. According to the CPU time, Tables 2 and 3 explain the superiority of the proposed ILPM on Algorithm 1.

6. Conclusions

In this work, we determined the radio mean square numbers $rmsn(P_n)$ and $rmsn(C_n)$ for paths and cycles. Then, the proposed approximate algorithm is introduced to obtain $rmsn(G)$ for graph G . In addition, a new mathematical model is proposed in order to find the upper bound of $rmsn(G)$ for graph G , and a comparison between the proposed approximate algorithm and the proposed mathematical model is introduced. Finally, the computational results and their analysis have proved that the proposed approximate algorithm overcomes the ILPM according to the radio mean square number.

Data Availability

The data used to support the findings of this study are available from the corresponding author upon request.

Conflicts of Interest

The authors declare that they have no conflicts of interest.

Acknowledgments

The authors extend their appreciation to the Deanship of Scientific Research at King Khalid University for funding this work through General Research Project (R.G.P.1/208/41).

References

- [1] W. K. Hale, "Frequency assignment: theory and applications," *Proceedings of the IEEE*, vol. 68, no. 12, pp. 1497–1514, 1980.
- [2] G. Chartrand, D. Erwin, P. Zhang, and F. Harary, "Radio labelings of graphs," *Bulletin of the Institute of Combinatorics and its Applications*, vol. 33, pp. 77–85, 2001.
- [3] R. Ponraja and S. Sathish Narayanan, "On radio mean number of some graphs," *International Journal of Mathematical Combinatorics*, vol. 3, pp. 41–48, 2014.
- [4] E. Badr, S. Almotairi, A. Eirokh, A. Abdel-Hay, and B. Almutairi, "An integer linear programming model for solving radio mean labeling problem," *IEEE Access*, vol. 8, pp. 162343–162349, 2020.
- [5] K. Sunitha, Dr. C. David Raj, and Dr. A. Subramanian, "Radio mean labeling of Path and Cycle related graphs," *Global Journal of Mathematical Sciences: Theory and Practical*, vol. 9, no. 3, pp. 337–345, 2017.
- [6] R. Ponraja, S. Sathish Narayanan, and R. Kalab, "Radio mean labeling of a graph," *AKCE International Journal of Graphs and Combinatorics*, vol. 12, no. 2-3, pp. 224–228, 2015.
- [7] M. I. Moussa and E. M. Badr, "A data hiding algorithm based on DNA and elliptic curve cryptosystems," *Journal of Information Hiding and Multimedia Signal Processing*, vol. 10, no. 3, 2019.
- [8] D. S. T. Ramesh, A. Subramanian, and K. Sunitha, "Radio mean square labeling of some graphs," *International Journal of Mathematics Trends and Technology (IJMTT) – Volume*, vol. 38, no. 2, pp. 99–105, 2016.
- [9] E. M. Badr and M. I. Moussa, "An upper bound of radio k-coloring problem and its integer linear programming model," *Wireless Networks*, vol. 26, no. 7, pp. 4955–4964, 2020, p.
- [10] L. Saha and P. Panigrahi, "A graph radio k-coloring algorithm," in *Combinatorial Algorithms. IWOCMA*, S. Arumugam and W. F. Smyth, Eds., vol. 7643, Berlin, Heidelberg, Springer, 2012 Lecture Notes in Computer Science.
- [11] L. Saha and P. Panigrahi, "A new graph radio k-coloring algorithm," *Discrete Mathematics, Algorithms and Applications*, vol. 11, no. 1, pp. 1–10, 2019.
- [12] E. S. Badr, K. Paparrizos, N. Samaras, and Sifaleras, "On the basis inverse of the exterior point simplex algorithm," in *Proceedings of the 17th National Conference of Hellenic Operational Research Society (HELORS)*, p. 6, Rio, Greece, June 2005.
- [13] E. S. Badr, K. Paparrizos, B. Thanasis, and G. Varkas, "Some computational results on the efficiency of an exterior point algorithm," in *Proceedings of the 18th National Conference of Hellenic Operational Research Society (HELORS)*, pp. 1103–1115, Rio, Greece, June 2006.
- [14] M. S. Bazaraa, J. J. Jarvis, and H. D. Sherali, *Linear Programming and Network Flows*, Wiley, New York, NY, USA, 3rd edition, 2004.
- [15] P. Zhang, "Radio labelings of cycles," *Ars Combinatoria*, vol. 65, pp. 21–32, 2002.
- [16] R. Balakrishnan and K. Renganathan, *A Text Book of Graph Theory*, Springer, Berlin, Germany, 2000.

Research Article

On the Sum of Degree-Based Topological Indices of Rhombus-Type Silicate and Oxide Structures

Rong Qi,¹ Haidar Ali ,² Usman Babar,³ Jia-Bao Liu ,⁴ and Parvez Ali⁵

¹School of Computer and Data Engineering, Bengbu College of Technology and Business, Bengbu 233000, China

²Department of Mathematics, Riphah International University, Faisalabad Campus, Faisalabad, Pakistan

³Department of Mathematics, Government College University, Lahore, Pakistan

⁴School of Mathematics and Physics, Anhui Jianzhu University, Hefei 230601, China

⁵Department of Mechanical Engineering, College of Engineering, Qassim University, Unaizah, Saudi Arabia

Correspondence should be addressed to Haidar Ali; haidar3830@gmail.com

Received 17 July 2021; Accepted 8 December 2021; Published 29 December 2021

Academic Editor: Giuseppe Gaetano Luciano

Copyright © 2021 Rong Qi et al. This is an open access article distributed under the Creative Commons Attribution License, which permits unrestricted use, distribution, and reproduction in any medium, provided the original work is properly cited.

1. Introduction and Preliminary Results

The representation of a graph is expressed by numbers, polynomials, and matrices. Graphs have their own characteristics that may be calculated by topological indices, and under graph automorphism, the topology of graphs remains unchanged. Degree-based topological indices are exceptionally important in different classes of indices and take on a vital role in graphic theory and in particular in science.

Silicate is a chemical compound and has many commercial uses. It is used for the manufacture of different glass and ceramics organic compounds in large scale due to its cheapness and availability everywhere in the world. Silicates can be obtained from the Earth's crust. In general, solid silicates are well-characterized and stable. Silicates like sodium orthosilicate and metasilicate, which have alkali cations and tiny or chain-like anions, are water soluble. When crystallised from a solution, they generate multiple solid hydrates. Water glass, which is made up of soluble sodium silicates and combinations, is a significant industrial and home chemical. For the construction of networks rhombus oxide and silicate, we refer the readers to 10. Rhombus silicate network $RHSL(t)$ and rhombus oxide network $RHOX(t)$ are shown in Figures 1 and 2, respectively.

In this article, \mathcal{G} is considered a network with a $V(\mathcal{G})$ vertex set and an edge set of $E(\mathcal{G})$ and d_r is the degree of

vertex $r \in V(\mathcal{G})$. Let $S_{\mathcal{G}}(r)$ denote the sum of the degrees of all vertices adjacent to a vertex r . Graovac et al. defined fifth M-Zagreb indices as polynomials for a molecular graph [1], and these are characterized as follows.

Let \mathcal{G} be a graph. Then,

$$M_1 G_5(\mathcal{G}) = \sum_{rs \in E(\mathcal{G})} (S_G(r) + S_G(s)), \quad (1)$$

$$M_2 G_5(\mathcal{G}) = \sum_{rs \in E(\mathcal{G})} (S_G(r) + S_G(s)). \quad (2)$$

V. R. Kulli [2], motivated by the above indices, described some new topological indices, and he named them as the fifth M-Zagreb indices of first and second type and fifth hyper-M-Zagreb indices of first and second type of a graph \mathcal{G} . They are defined as

$$M_1^a G_5(\mathcal{G}) = \sum_{rs \in E(\mathcal{G})} (S_G(r) + S_G(s))^a, \quad (3)$$

$$M_2^a G_5(\mathcal{G}) = \sum_{rs \in E(\mathcal{G})} (S_G(r) + S_G(s))^a, \quad (4)$$

$$HM_1 G_5(\mathcal{G}) = \sum_{rs \in E(\mathcal{G})} (S_G(r) + S_G(s))^2, \quad (5)$$

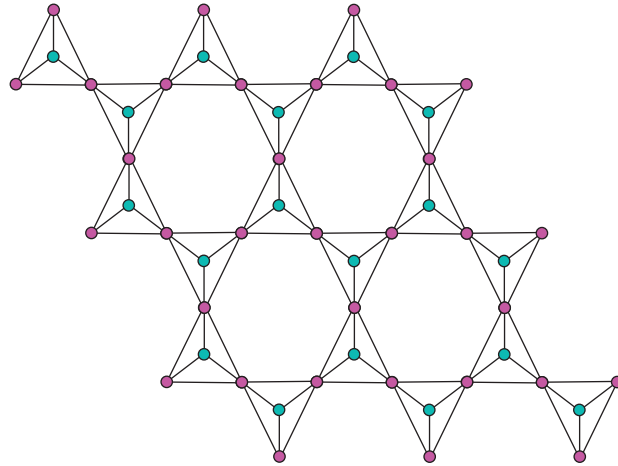


FIGURE 1: Graph of rhombus silicate network (RHSL(t)).

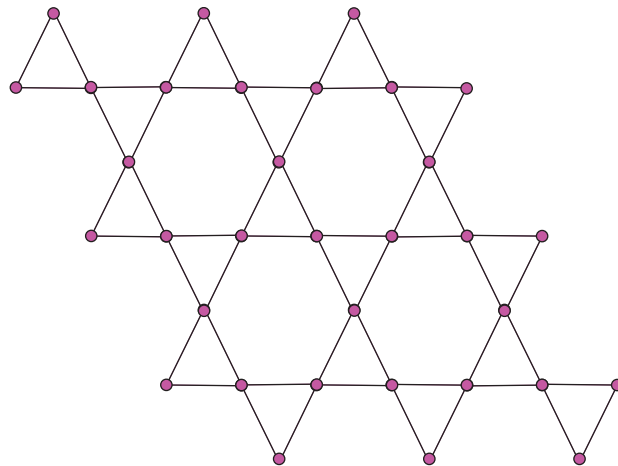


FIGURE 2: Graph of rhombus oxide network (RHOX(t)).

$$HM_2G_5(\mathcal{G}) = \sum_{rs \in E(\mathcal{G})} (S_G(r) + S_G(s))^2. \quad (6)$$

The fifth M_1 - and M_2 - Zagreb polynomials of a graph are defined as

They also define a new version of Zagreb index which is called as the third Zagreb index or fifth M_3 -Zagreb [3].

$$M_1G_5(\mathcal{G}, x) = \prod_{rs \in E(\mathcal{G})} x^{(S_G(r)+S_G(s))}, \quad (10)$$

$$M_3G_5(\mathcal{G}) = \sum_{rs \in E(\mathcal{G})} |S_G(r) - S_G(s)|. \quad (7)$$

$$M_2G_5(\mathcal{G}, x) = \prod_{rs \in E(\mathcal{G})} x^{(S_G(r)+S_G(s))}. \quad (11)$$

Corresponding to the above indices, he defined the general fifth M_1 -Zagreb polynomial and the general fifth M_2 -Zagreb polynomial of a molecular graph \mathcal{G} as

The fifth HM_1 and HM_2 Zagreb polynomials of the graph are defined as

$$M_1^aG_5(\mathcal{G}, x) = \prod_{rs \in E(\mathcal{G})} x^{(S_G(r)+S_G(s))^a}, \quad (8)$$

$$HM_1G_5(\mathcal{G}, x) = \prod_{rs \in E(\mathcal{G})} x^{(S_G(r)+S_G(s))^2}, \quad (12)$$

$$M_2^aG_5(\mathcal{G}, x) = \prod_{rs \in E(\mathcal{G})} x^{(S_G(r)+S_G(s))^a}. \quad (9)$$

$$HM_2G_5(\mathcal{G}, x) = \prod_{rs \in E(\mathcal{G})} x^{(S_G(r)+S_G(s))^2}. \quad (13)$$

2. Main Results

We have studied the topological indices introduced by Kulli [2, 4] named as fifth M-Zagreb indices, fifth M-Zagreb polynomials, and M_3 -Zagreb index and computed exact formulae of these indices for rhombus-type silicate and oxide networks. Ali et al. studied degree-based topological indices for various networks [5–8]. For the basic notations and definitions, see [9–11].

2.1. Results for the Rhombus Type of Silicate Networks. In this section, we calculate degree-based topological indices of the dimension t for rhombus-type silicate networks. In the

following theorems, we compute M -Zagreb indices and polynomials.

Theorem 2.1.1. *Let $\mathcal{G}_1 \cong RHSL(t)$ be the rhombus-type silicate network; then, the first and second fifth M-Zagreb indices are equal to*

$$\begin{aligned} M_1G_5(\mathcal{G}_1) &= 36(1 - 10t + 18t^2), \\ M_2G_5(\mathcal{G}_1) &= 18(119 - 490t + 480t^2). \end{aligned} \tag{14}$$

Proof. The outcome can be obtained by using the edge partition in Table 1.

By using equation [5],

$$M_1G_5(\mathcal{G}_1) = \sum_{rs \in E(\mathcal{G}_1)} (S_G(r) + S_G(s)),$$

$$\begin{aligned} M_1G_5(\mathcal{G}_1) &= (12 + 12)|E_1(\mathcal{G}_1(t))| + (12 + 24)|E_2(\mathcal{G}_1(t))| + (15 + 15)|E_3(\mathcal{G}_1(t))| + (15 + 24)|E_4(\mathcal{G}_1(t))| \\ &\quad + (15 + 27)|E_5(\mathcal{G}_1(t))| + (18 + 24)|E_6(\mathcal{G}_1(t))| + (18 + 27)|E_7(\mathcal{G}_1(t))| \\ &\quad + (18 + 30)|E_8(\mathcal{G}_1(t))| + (24 + 27)|E_9(\mathcal{G}_1(t))| + (27 + 27)|E_{10}(\mathcal{G}_1(t))| + (27 + 30)|E_{11}(\mathcal{G}_1(t))| \\ &\quad + (30 + 30)|E_{12}(\mathcal{G}_1(t))|, \\ &= (12 + 12)(6) + (12 + 24)(6) + (15 + 15)(4t - 4) + (15 + 24)(8) + (15 + 27)(16t - 24) \\ &\quad + (18 + 24)(2) + (18 + 27)(8t - 12) + (18 + 30)(6t^2 - 20t + 16) + (24 + 27)(8) \\ &\quad + (27 + 27)(8t - 14) + (27 + 30)(8t - 16) + (30 + 30)(6t^2 - 24t + 24). \end{aligned} \tag{15}$$

By doing some calculations, we obtain

$$M_1G_5(\mathcal{G}_1) = 36(1 - 10t + 18t^2). \tag{16}$$

Thus, from [6],

$$M_2G_5(\mathcal{G}) = \sum_{rs \in E(\mathcal{G}_1)} (S_G(r) + S_G(s)),$$

$$\begin{aligned} M_2G_5(\mathcal{G}_1) &= (12 \times 12)|E_1(\mathcal{G}_1(t))| + (12 \times 24)|E_2(\mathcal{G}_1(t))| + (15 \times 15)|E_3(\mathcal{G}_1(t))| + (15 \times 24)|E_4(\mathcal{G}_1(t))| \\ &\quad + (15 \times 27)|E_5(\mathcal{G}_1(t))| + (18 \times 24)|E_6(\mathcal{G}_1(t))| + (18 \times 27)|E_7(\mathcal{G}_1(t))| \\ &\quad + (18 \times 30)|E_8(\mathcal{G}_1(t))| + (24 \times 27)|E_9(\mathcal{G}_1(t))| + (27 \times 27)|E_{10}(\mathcal{G}_1(t))| + (27 \times 30)|E_{11}(\mathcal{G}_1(t))| \\ &\quad + (30 \times 30)|E_{12}(\mathcal{G}_1(t))|, \\ &= (12 \times 12)(6) + (12 \times 24)(6) + (15 \times 15)(4t - 4) + (15 \times 24)(8) + (15 \times 27)(16t - 24) \\ &\quad + (18 \times 24)(2) + (18 \times 27)(8t - 12) + (18 \times 30)(6t^2 - 20t + 16) + (24 \times 27)(8) \\ &\quad + (27 \times 27)(8t - 14) + (27 \times 30)(8t - 16) + (30 \times 30)(6t^2 - 24t + 24). \end{aligned} \tag{17}$$

By doing some calculations, we obtain

$$M_2G_5(\mathcal{G}_1) = 18(119 - 490t + 480t^2). \tag{18}$$

Theorem 2.1.2. *Consider the rhombus-type silicate network $\mathcal{G}_1 \cong RHSL(t)$ for $t \in \mathbb{N}$. Then, the first and second general fifth M-Zagreb indices are equal to*

TABLE 1: Edge partition of rhombus-type silicate network ($RHSL(t)$) based on sum of degrees of end vertices of each edge.

(S_r, S_s)	Number of edges
<i>Where $rs \in E(\mathcal{G}_1)$</i>	
(12, 12)	6
(12, 24)	6
(15, 15)	$4t - 4$
(15, 24)	8
(15, 27)	$16t - 24$
(18, 24)	2
<i>Where $rs \in E(\mathcal{G}_2)$</i>	
(18, 27)	$8t - 2$
(18, 30)	$6t^2 - 20t + 16$
(24, 27)	8
(27, 27)	$8t - 14$
(27, 30)	$8t - 16$
(30, 30)	$6t^2 - 24t + 24$

$$\begin{aligned}
 M_1^a G_5(\mathcal{G}_1) &= \left[\left(2^{1+3a} 3^{1+a} + 2^{3+2a} 3^{1+a} 5^a - 4 \times 3^{1+2a} 5^a + 6^{1+2a} - 2^{3+a} 3^{1+a} 7^a - 2^{2+a} 15^a + 3^a 16^{1+a} + 2^{1+a} 21^a \right. \right. \\
 &\quad \left. \left. - 7 \times 2^{1+a} 27^a + 8 \times 39^a + 8 \times 51^a - 16 \times 57^a \right) + t \left(-5 \times 3^a 4^{1+2a} - 2^{3+2a} 3^{1+a} 5^a + 2^{2+a} 15^a + 2^{4+a} 21^a \right. \right. \\
 &\quad \left. \left. + 2^{3+a} 27^a + 8 \times 45^a + 8 \times 57^a \right) + t^2 \left(2^{1+4a} 3 + 2^{1+2a} 3^{1+a} 5^a \right) \right], \\
 M_2^a G_5(\mathcal{G}_1) &= \left[\left(\left(2^{1+4a} 3^{1+2a} + 2^{1+5a} 3^{1+2a} - 2^{2+a} 3^{1+5a} - 8 \times 3^{1+4a} 5^a + 2^{3+2a} 3^{1+2a} 25^a + 2^{1+4a} 27^a + 8^{1+a} 45^a + 8^{1+a} 81^a \right. \right. \right. \\
 &\quad \left. \left. + 4^{2+a} 135^a - 4 \times 225^a - 2^{4+a} 405^a - 14 \times 729^a \right) + t \left(-2^{3+2a} 3^{1+2a} 25^a - 20^{1+a} 27^a + 4 \times 225^a + 2^{3+a} 243^a \right. \right. \\
 &\quad \left. \left. + 16 \times 405^a + 2^{3+a} 405^a + 8 \times 729^a \right) + t^2 \left(2^{1+2a} 3^{1+3a} 5^a + 6^{1+2a} 25^a \right) \right].
 \end{aligned} \tag{19}$$

Proof. Let \mathcal{G}_1 be the rhombus-type silicate network. Table 1 shows such an edge partition of $RHSL(t)$. Thus, from [9], it follows that

$$M_1^a G_5(\mathcal{G}) = \sum_{rs \in E(\mathcal{G})} (S_G(r) + S_G(s))^a. \tag{20}$$

By using edge partitions in Table 1, we obtain

$$\begin{aligned}
 M_1^a G_5(\mathcal{G}_1) &= (12 + 12)^a |E_1(\mathcal{G}_1(t))| + (12 + 24)^a |E_2(\mathcal{G}_1(t))| + (15 + 15)^a |E_3(\mathcal{G}_1(t))| \\
 &\quad + (15 + 24)^a |E_4(\mathcal{G}_1(t))| + (15 + 27)^a |E_5(\mathcal{G}_1(t))| + (18 + 24)^a |E_6(\mathcal{G}_1(t))| + (18 + 27)^a |E_7(\mathcal{G}_1(t))| \\
 &\quad + (18 + 30)^a |E_8(\mathcal{G}_1(t))| + (24 + 27)^a |E_9(\mathcal{G}_1(t))| + (27 + 27)^a |E_{10}(\mathcal{G}_1(t))| \\
 &\quad + (27 + 30)^a |E_{11}(\mathcal{G}_1(t))| + (30 + 30)^a |E_{12}(\mathcal{G}_1(t))|, \\
 &= (12 + 12)^a (6) + (12 + 24)^a (6) + (15 + 15)^a (4t - 4) + (15 + 24)^a (8) + (15 + 24)^a (16t - 24) \\
 &\quad + (18 + 24)^a (2) + (18 + 27)^a (8t - 12) + (18 + 30)^a (6t^2 - 20t + 16) + (24 + 27)^a (8) \\
 &\quad + (27 + 27)^a (8t - 14) + (27 + 30)^a (8t - 16) + (30 + 30)^a (6t^2 - 24t + 24).
 \end{aligned} \tag{21}$$

By doing some calculations, we have

$$\begin{aligned}
 M_1^a G_5(\mathcal{G}_1) &= \left[\left(2^{1+3a} 3^{1+a} + 2^{3+2a} 3^{1+a} 5^a - 4 \times 3^{1+2a} 5^a + 6^{1+2a} - 2^{3+a} 3^{1+a} 7^a - 2^{2+a} 15^a + 3^a 16^{1+a} + 2^{1+a} 21^a \right. \right. \\
 &\quad \left. \left. - 7 \times 2^{1+a} 27^a + 8 \times 39^a + 8 \times 51^a - 16 \times 57^a + t \left(-5 \times 3^a 4^{1+2a} - 2^{3+2a} 3^{1+a} 5^a + 2^{2+a} 15^a \right. \right. \right. \\
 &\quad \left. \left. + 2^{4+a} 21^a + 2^{3+a} 27^a + 8 \times 45^a + 8 \times 57^a \right) + t^2 \left(2^{1+4a} 3^{1+a} + 2^{1+2a} 3^{1+a} 5^a \right) \right].
 \end{aligned} \tag{22}$$

From [12], we have

$$M_2^a G_5(\mathcal{G}) = \sum_{rs \in E(\mathcal{G})} (S_G(r) + S_G(s))^a. \quad (23)$$

By using edge partitions in Table 1, we obtain

$$\begin{aligned} M_2^a G_5(\mathcal{G}_1) &= (12 \times 12)^a |E_1(\mathcal{G}_1(t))| + (12 \times 24)^a |E_2(\mathcal{G}_1(t))| + (15 \times 15)^a |E_3(\mathcal{G}_1(t))| + (15 \times 24)^a |E_4(\mathcal{G}_1(t))| \\ &\quad + (15 \times 27)^a |E_5(\mathcal{G}_1(t))| + (18 \times 24)^a |E_6(\mathcal{G}_1(t))| + (18 \times 27)^a |E_7(\mathcal{G}_1(t))| \\ &\quad + (18 \times 30)^a |E_8(\mathcal{G}_1(t))| + (24 \times 27)^a |E_9(\mathcal{G}_1(t))| + (27 \times 27)^a |E_{10}(\mathcal{G}_1(t))| + (27 \times 30)^a |E_{11}(\mathcal{G}_1(t))| \\ &\quad + (30 \times 30)^a |E_{12}(\mathcal{G}_1(t))|, \\ &= (12 \times 12)^a (6) + (12 \times 24)^a (6) + (15 \times 15)^a (4t - 4) + (15 \times 24)^a (8) + (15 \times 24)^a (16t - 24) \\ &\quad + (18 \times 24)^a (2) + (18 \times 27)^a (8t - 12) + (18 \times 30)^a (6t^2 - 20t + 16) + (24 \times 27)^a \\ &\quad (8) + (27 \times 27)^a (8t - 14) + (27 \times 30)^a (8t - 16) + (30 \times 30)^a (6t^2 - 24t + 24). \end{aligned} \quad (24)$$

By doing some calculations, we have

$$\begin{aligned} M_2^a G_5(\mathcal{G}_1) &= \left[(2^{1+4a} 3^{1+2a} + 2^{1+5a} 3^{1+2a} - 2^{2+a} 3^{1+5a} - 8 \times 3^{1+4a} 5^a + 2^{3+2a} 3^{1+2a} 25^a + 2^{1+4a} 27^a + 8^{1+a} 45^a + 8^{1+a} 81^a \right. \\ &\quad + 4^{2+a} 135^a - 4 \times 225^a - 2^{4+a} 405^a - 14 \times 729^a + t(-2^{3+2a} 3^{1+2a} 25^a - 20^{1+a} 27^a + 4 \times 225^a + 2^{3+a} 243^a \\ &\quad \left. + 16 \times 405^a + 2^{3+a} 405^a + 8 \times 729^a) + t^2(2^{1+2a} 3^{1+3a} 5^a + 6^{1+2a} 25^a) \right]. \end{aligned} \quad (25)$$

Theorem 2.1.3. Consider the rhombus-type silicate network $\mathcal{G}_1 \cong RHSL(t)$ for $t \in \mathbb{N}$. Then, the first and second hyper-fifth M-Zagreb indices are equal to

$$\begin{aligned} HM_1 G_5(\mathcal{G}_1) &= 36(221 - 976t + 984t^2), \\ HM_2 G_5(\mathcal{G}_1) &= 162(28307 - 68242t + 40800t^2). \end{aligned} \quad (26)$$

Proof. Let \mathcal{G}_1 be the rhombus type of silicate network. Table 1 shows such an edge partition of $RHSL(t)$. Thus, from [13], it follows that

$$HM_1 G_5(\mathcal{G}) = \sum_{rs \in E(\mathcal{G})} (S_G(r) + S_G(s))^2. \quad (27)$$

By using edge partitions in Table 1, we obtain

$$\begin{aligned} HM_1 G_5(\mathcal{G}_1) &= (12 \times 12)^2 |E_1(\mathcal{G}_1(t))| + (12 \times 24)^2 |E_2(\mathcal{G}_1(t))| + (15 \times 15)^2 |E_3(\mathcal{G}_1(t))| + (15 \times 24)^2 |E_4(\mathcal{G}_1(t))| \\ &\quad + (15 \times 27)^2 |E_5(\mathcal{G}_1(t))| + (18 \times 24)^2 |E_6(\mathcal{G}_1(t))| + (18 \times 27)^2 |E_7(\mathcal{G}_1(t))| \\ &\quad + (18 \times 30)^2 |E_8(\mathcal{G}_1(t))| + (24 \times 27)^2 |E_9(\mathcal{G}_1(t))| + (27 \times 27)^2 |E_{10}(\mathcal{G}_1(t))| + (27 \times 30)^2 |E_{11}(\mathcal{G}_1(t))| \\ &\quad + (30 \times 30)^2 |E_{12}(\mathcal{G}_1(t))|, \\ &= (12 \times 12)^2 (6) + (12 \times 24)^2 (6) + (15 \times 15)^2 (4t - 4) + (15 \times 24)^2 (8) + (15 \times 24)^2 (16t - 24) \\ &\quad + (18 \times 24)^2 (2) + (18 \times 27)^2 (8t - 12) + (18 \times 30)^2 (6t^2 - 20t + 16) + (24 \times 27)^2 \\ &\quad (8) + (27 \times 27)^2 (8t - 14) + (27 \times 30)^2 (8t - 16) + (30 \times 30)^2 (6t^2 - 24t + 24). \end{aligned} \quad (28)$$

By doing some calculations, we have

$$HM_1 G_5(\mathcal{G}_1) = 36(221 - 976t + 984t^2). \quad (29)$$

From [14], we have

$$HM_2^2 G_5(\mathcal{G}) = \sum_{rs \in E(\mathcal{G})} (S_G(r) + S_G(s))^2. \quad (30)$$

By using edge partitions in Table 1, we obtain

$$\begin{aligned}
 HM_2G_5(\mathcal{G}_1) &= (12 \times 12)^2|E_1(\mathcal{G}_1(t))| + (12 \times 24)^2|E_2(\mathcal{G}_1(t))| + (15 \times 15)^2|E_3(\mathcal{G}_1(t))| \\
 &\quad + (15 \times 24)^2|E_4(\mathcal{G}_1(t))| + (15 \times 27)^2|E_5(\mathcal{G}_1(t))| + (18 \times 24)^2|E_6(\mathcal{G}_1(t))| \\
 &\quad + (18 \times 27)^2|E_7(\mathcal{G}_1(t))| + (18 \times 30)^2|E_8(\mathcal{G}_1(t))| + (24 \times 27)^2|E_9(\mathcal{G}_1(t))| \\
 &\quad + (27 \times 27)^2|E_{10}(\mathcal{G}_1(t))| + (27 \times 30)^2|E_{11}(\mathcal{G}_1(t))| + (30 \times 30)^2|E_{12}(\mathcal{G}_1(t))|, \\
 &= (12 \times 12)^2(6) + (12 \times 24)^2(6) + (15 \times 15)^2(4t - 4) + (15 \times 24)^2(8) \\
 &\quad + (15 \times 24)^2(16t - 24) + (18 \times 24)^2(2) + (18 \times 27)^2(8t - 12) + (18 \times 30)^2(6t^2 - 20t + 16) \\
 &\quad + (24 \times 27)^2(8) + (27 \times 27)^2(8t - 14) + (27 \times 30)^2(8t - 16) + (30 \times 30)^2(6t^2 - 24t + 24).
 \end{aligned} \tag{31}$$

By doing some calculations, we have

$$HM_2^aG_5(\mathcal{G}_1) = 162(28307 - 68242t + 40800t^2). \tag{32}$$

Theorem 2.1.4. Consider the rhombus-type silicate network $\mathcal{G}_1 \cong RHSL(t)$ for $t \in \mathbb{N}$. Then, the third M-Zagreb index is equal to

$$M_3G_5(\mathcal{G}_1) = (-232 + 248t + 12t^2). \tag{33}$$

Proof. Let \mathcal{G}_1 be the rhombus silicate network. Table 1 shows such an edge partition of $RHSL(t)$. Thus, from [15], it follows that

$$M_3G_5(\mathcal{G}) = \sum_{rs \in E(\mathcal{G})} |S_G(r) + S_G(s)|. \tag{34}$$

By using edge partitions in Table 1, we obtain

$$\begin{aligned}
 M_3G_5(\mathcal{G}_1) &= |12 - 12||E_1(\mathcal{G}_1(t))| + |12 - 24||E_2(\mathcal{G}_1(t))| + |15 - 15||E_3(\mathcal{G}_1(t))| + |15 - 24||E_4(\mathcal{G}_1(t))| \\
 &\quad + |15 - 27||E_5(\mathcal{G}_1(t))| + |18 - 24||E_6(\mathcal{G}_1(t))| + |18 - 27||E_7(\mathcal{G}_1(t))| + |18 - 30||E_8(\mathcal{G}_1(t))| \\
 &\quad + |24 - 27||E_9(\mathcal{G}_1(t))| + |27 - 27||E_{10}(\mathcal{G}_1(t))| + |27 - 30||E_{11}(\mathcal{G}_1(t))| + |30 - 30||E_{12}(\mathcal{G}_1(t))|, \\
 &= |12 - 12|(6) + |12 - 24|(6) + |15 - 15|(4t - 4) + |15 - 24|(8) + |15 - 27|(16t - 24) + |18 \\
 &\quad - 24|(2) + |18 - 27|(8t - 12) + |18 - 30|(6t^2 - 20t + 16) + |24 - 27|(8) + |27 - 27|(8t - 14) \\
 &\quad + |27 - 30|(8t - 16) + |30 - 30|(6t^2 - 24t + 24).
 \end{aligned} \tag{35}$$

By doing some calculations, we have

$$M_3G_5(\mathcal{G}_1) = (-232 + 248t + 12t^2). \tag{36}$$

Theorem 2.1.5. Let $\mathcal{G}_1 \cong RHSL(t)$ be the first type of rhombus-type silicate network; then, general fifth M-Zagreb polynomials of first and second type are equal to

Corresponding to the above indices, we are going to compute general fifth M-Zagreb polynomials for rhombus-type silicate network $RHSL(t)$.

$$\begin{aligned}
 M_1^aG_5(\mathcal{G}_1, x) &= 6x^{24^a} + (4t - 4)x^{30^a} + 6x^{36^a} + 8x^{39^a} + (16t - 22)x^{42^a} + (8t - 12)x^{45^a} \\
 &\quad + (6t^2 - 20t + 16)x^{48^a} + 8x^{51^a} + (8t - 14)x^{54^a} + (8t - 16)x^{57^a} + (6t^2 - 24t + 24)x^{60^a}, \\
 M_2^aG_5(\mathcal{G}_1, x) &= 6x^{144^a} + (4t - 4)x^{225^a} + 6x^{288^a} + 8x^{360^a} + 8(2t - 3)x^{405^a} + 2x^{432^a} + 4(2t - 3)x^{486^a} \\
 &\quad + 2(t - 2)(3t - 4)x^{540^a} + 8x^{648^a} + 2(4t - 7)x^{729^a} + 8(t - 2)x^{810^a} + 6(t - 2)^2x^{900^a}.
 \end{aligned} \tag{37}$$

Proof. We obtain the outcome with the edge partition in Table 1. It follows from [1] that

$$M_1^a G_5(\mathcal{G}_1, x) = \sum_{rs \in E(\mathcal{G}_1)} x^{(S_G(r)+S_G(s))^a},$$

$$M_1^a G_5(\mathcal{G}_1, x) = x^{(12+12)^a} |E_1(\mathcal{G}_1(t))| + x^{(12+24)^a} |E_2(\mathcal{G}_1(t))| + x^{(15+15)^a} |E_3(\mathcal{G}_1(t))| + x^{(15+24)^a} |E_4(\mathcal{G}_1(t))|$$

$$+ x^{(15+27)^a} |E_5(\mathcal{G}_1(t))| + x^{(18+24)^a} |E_6(\mathcal{G}_1(t))| + x^{(18+27)^a} |E_7(\mathcal{G}_1(t))| + x^{(18+30)^a} |E_8(\mathcal{G}_1(t))|$$

$$+ x^{(24+27)^a} |E_9(\mathcal{G}_1(t))| + x^{(27+27)^a} |E_{10}(\mathcal{G}_1(t))| + x^{(27+30)^a} |E_{11}(\mathcal{G}_1(t))| + x^{(30+30)^a} |E_{12}(\mathcal{G}_1(t))|, \tag{38}$$

$$M_1^a G_5(\mathcal{G}_1, x) = x^{(12+12)^a} (6) + x^{(12+24)^a} (6) + x^{(15+15)^a} (4t - 4) + x^{(15+24)^a} (8)$$

$$+ x^{(15+27)^a} (16t - 24) + x^{(18+24)^a} (2) + x^{(18+27)^a} (8t - 12) + x^{(18+30)^a} (6t^2 - 20t + 16)$$

$$+ x^{(24+27)^a} (8) + x^{(27+27)^a} (8t - 14) + x^{(27+30)^a} (8t - 16) + x^{(30+30)^a} (6t^2 - 24t + 24).$$

By doing some calculations, we obtain

$$M_1^a G_5(\mathcal{G}_1, x) = 6x^{24^a} + (4t - 4)x^{30^a} + 6x^{36^a} + 8x^{39^a} + (16t - 22)x^{42^a} + (8t - 12)x^{45^a}$$

$$+ (6t^2 - 20t + 16)x^{48^a} + 8x^{51^a} + (8t - 14)x^{54^a} + (8t - 16)x^{57^a} + (6t^2 - 24t + 24)x^{60^a}. \tag{39}$$

Also, from [3],

$$M_2^a G_5(\mathcal{G}_1, x) = \sum_{rs \in E(\mathcal{G}_1)} x^{(S_G(r)+S_G(s))^a},$$

$$M_2^a G_5(\mathcal{G}_1, x) = x^{(12+12)^a} |E_1(\mathcal{G}_1(t))| + x^{(12+24)^a} |E_2(\mathcal{G}_1(t))| + x^{(15+15)^a} |E_3(\mathcal{G}_1(t))| + x^{(15+24)^a} |E_4(\mathcal{G}_1(t))|$$

$$+ x^{(15+27)^a} |E_5(\mathcal{G}_1(t))| + x^{(18+24)^a} |E_6(\mathcal{G}_1(t))| + x^{(18+27)^a} |E_7(\mathcal{G}_1(t))| + x^{(18+30)^a} |E_8(\mathcal{G}_1(t))|$$

$$+ x^{(24+27)^a} |E_9(\mathcal{G}_1(t))| + x^{(27+27)^a} |E_{10}(\mathcal{G}_1(t))| + x^{(27+30)^a} |E_{11}(\mathcal{G}_1(t))| + x^{(30+30)^a} |E_{12}(\mathcal{G}_1(t))|, \tag{40}$$

$$M_2^a G_5(\mathcal{G}_1, x) = x^{(12+12)^a} (6) + x^{(12+24)^a} (6) + x^{(15+15)^a} (4t - 4) + x^{(15+24)^a} (8)$$

$$+ x^{(15+27)^a} (16t - 24) + x^{(18+24)^a} (2) + x^{(18+27)^a} (8t - 12) + x^{(18+30)^a} (6t^2 - 20t + 16)$$

$$+ x^{(24+27)^a} (8) + x^{(27+27)^a} (8t - 14) + x^{(27+30)^a} (8t - 16) + x^{(30+30)^a} (6t^2 - 24t + 24).$$

By making some calculations, we obtain

$$M_2^a G_5(\mathcal{G}_1, x) = 6x^{144^a} + (4t - 4)x^{225^a} + 6x^{288^a} + 8x^{360^a} + 8(2t - 3)x^{405^a} + 2x^{432^a} + 4(2t - 3)$$

$$x^{486^a} + 2(t - 2)(3t - 4)x^{540^a} + 8x^{648^a} + 2(4t - 7)x^{729^a} + 8(t - 2)x^{810^a} + 6(t - 2)^2 x^{900^a}. \tag{41}$$

Corresponding to the above indices, we are going to compute fifth *M*-Zagreb polynomials for rhombus-type silicate network *RHSL*(*t*).

Theorem 2.1.6. *Let $\mathcal{G}_1 \cong RHSL(t)$ be the rhombus type of silicate network; then, fifth *M*-Zagreb polynomials of first and second type are equal to*

$$\begin{aligned}
M_1G_5(\mathcal{G}_1, x) &= 6x^{24} + (4t - 4)x^{30} + 6x^{36} + 8x^{39} + (16t - 22)x^{42} + (8t - 12)x^{45} \\
&\quad + (6t^2 - 20t + 16)x^{48} + 8x^{51} + (8t - 14)x^{54} + (8t - 16)x^{57} + (6t^2 - 24t + 24)x^{60}, \\
M_2G_5(\mathcal{G}_1, x) &= 6x^{144} + (4t - 4)x^{225} + 6x^{288} + 8x^{360} + 8(2t - 3)x^{405} + 2x^{432} + 4(2t - 3)x^{486} \\
&\quad + 2(t - 2)(3t - 4)x^{540} + 8x^{648} + 2(4t - 7)x^{729} + 8(t - 2)x^{810} + 6(t - 2)^2x^{900}.
\end{aligned} \tag{42}$$

Proof. We obtain the outcome with the edge partition in Table 1. It follows from [16] that

$$\begin{aligned}
M_1G_5(\mathcal{G}_1, x) &= \sum_{rs \in E(\mathcal{G}_1)} x^{(S_G(r) + S_G(s))}, \\
M_1G_5(\mathcal{G}_1, x) &= x^{(12+12)}|E_1(\mathcal{G}_1(t))| + x^{(12+24)}|E_2(\mathcal{G}_1(t))| + x^{(15+15)}|E_3(\mathcal{G}_1(t))| + x^{(15+24)}|E_4(\mathcal{G}_1(t))| \\
&\quad + x^{(15+27)}|E_5(\mathcal{G}_1(t))| + x^{(18+24)}|E_6(\mathcal{G}_1(t))| + x^{(18+27)}|E_7(\mathcal{G}_1(t))| + x^{(18+30)}|E_8(\mathcal{G}_1(t))| \\
&\quad + x^{(24+27)}|E_9(\mathcal{G}_1(t))| + x^{(27+27)}|E_{10}(\mathcal{G}_1(t))| + x^{(27+30)}|E_{11}(\mathcal{G}_1(t))| + x^{(30+30)}|E_{12}(\mathcal{G}_1(t))|, \\
&= x^{(12+12)}(6) + x^{(12+24)}(6) + x^{(15+15)}(4t - 4) + x^{(15+24)}(8) \\
&\quad + x^{(15+27)}(16t - 24) + x^{(18+24)}(2) + x^{(18+27)}(8t - 12) + x^{(18+30)}(6t^2 - 20t + 16) \\
&\quad + x^{(24+27)}(8) + x^{(27+27)}(8t - 14) + x^{(27+30)}(8t - 16) + x^{(30+30)}(6t^2 - 24t + 24).
\end{aligned} \tag{43}$$

By doing some calculations, we obtain

$$\begin{aligned}
M_1G_5(\mathcal{G}_1, x) &= 6x^{24} + (4t - 4)x^{30} + 6x^{36} + 8x^{39} + (16t - 22)x^{42} + (8t - 12)x^{45} \\
&\quad + (6t^2 - 20t + 16)x^{48} + 8x^{51} + (8t - 14)x^{54} + (8t - 16)x^{57} + (6t^2 - 24t + 24)x^{60}.
\end{aligned} \tag{44}$$

Also, from [4],

$$\begin{aligned}
M_2G_5(\mathcal{G}_1, x) &= \sum_{rs \in E(\mathcal{G}_1)} x^{(S_G(r) + S_G(s))}, \\
M_2G_5(\mathcal{G}_1, x) &= x^{(6 \times 6)}|E_1(\mathcal{G}_1(t))| + x^{(6 \times 11)}|E_2(\mathcal{G}_1(t))| + x^{(6 \times 12)}|E_3(\mathcal{G}_1(t))| + x^{(6 \times 14)}|E_4(\mathcal{G}_1(t))| \\
&\quad + x^{(7 \times 9)}|E_5(\mathcal{G}_1(t))| + x^{(7 \times 12)}|E_6(\mathcal{G}_1(t))| + x^{(8 \times 11)}|E_7(\mathcal{G}_1(t))| + x^{(8 \times 13)}|E_8(\mathcal{G}_1(t))| \\
&\quad + x^{(9 \times 9)}|E_9(\mathcal{G}_1(t))| + x^{(9 \times 14)}|E_{10}(\mathcal{G}_1(t))| + x^{(11 \times 11)}|E_{11}(\mathcal{G}_1(t))| + x^{(11 \times 12)}|E_{12}(\mathcal{G}_1(t))| \\
&\quad + x^{(11 \times 13)}|E_{13}(\mathcal{G}_1(t))| + x^{(11 \times 14)}|E_{14}(\mathcal{G}_1(t))| + x^{(11 \times 16)}|E_{15}(\mathcal{G}_1(t))| \\
&\quad + x^{(12 \times 14)}|E_{16}(\mathcal{G}_1(t))| + x^{(13 \times 14)}|E_{17}(\mathcal{G}_1(t))| + x^{(13 \times 16)}|E_{18}(\mathcal{G}_1(t))| \\
&\quad + x^{(14 \times 14)}|E_{19}(\mathcal{G}_1(t))| + x^{(14 \times 16)}|E_{20}(\mathcal{G}_1(t))|, \\
&= x^{(6 \times 6)}(4t) + x^{(6 \times 11)}(4t) + x^{(6 \times 12)}(4) + x^{(6 \times 14)}(4t - 4) + x^{(7 \times 9)}(4t - 4) + x^{(7 \times 12)}(4t - 4) \\
&\quad + x^{(8 \times 11)}(12t - 8) + x^{(8 \times 13)}(4t - 4) + x^{(9 \times 9)}(2t - 2) + x^{(9 \times 14)}(4t - 4) \\
&\quad + x^{(11 \times 11)}(9t^2 - 7t + 3) + x^{(11 \times 12)}(4) + x^{(11 \times 13)}(4t - 4) + x^{(11 \times 14)}(36t^2 - 68t + 32) \\
&\quad + x^{(11 \times 16)}(4t - 4) + x^{(12 \times 14)}(4t - 4) + x^{(13 \times 14)}(4t - 4) + x^{(13 \times 16)}(4t - 4) \\
&\quad + x^{(14 \times 14)}(4t - 4) + x^{(14 \times 16)}(36t^2 - 76t + 40).
\end{aligned} \tag{45}$$

By making some calculations, we obtain

$$M_2G_5(\mathcal{G}_1, x) = 6x^{144} + (4t - 4)x^{225} + 6x^{288} + 8x^{360} + 8(2t - 3)x^{405} + 2x^{432} + 4(2t - 3)x^{486} + 2(t - 2)(3t - 4)x^{540} + 8x^{648} + 2(4t - 7)x^{729} + 8(t - 2)x^{810} + 6(t - 2)^2x^{900}. \tag{46}$$

Theorem 2.1.7. Let $\mathcal{G}_1 \cong RHSL(t)$ be the rhombus-type silicate network; then, hyper-fifth M-Zagreb polynomials of first and second type are equal to

$$HM_1G_5(\mathcal{G}_1, x) = 6x^{576} + (4t - 4)x^{900} + 6x^{1296} + 8x^{1521} + (16t - 22)x^{1764} + (8t - 12)x^{2025} + (6t^2 - 20t + 16)x^{2304} + 8x^{2601} + (8t - 14)x^{2916} + (8t - 16)x^{3249} + (6t^2 - 24t + 24)x^{3600},$$

$$HM_2G_5(\mathcal{G}_1, x) = 6x^{20736} + (4t - 4)x^{50625} + 6x^{82944} + 8x^{129600} + (16t - 24)x^{164025} + 2x^{186624} + (8t - 12)x^{236196} + (6t^2 - 20t + 16)x^{291600} + 8x^{419904} + (8t - 14)x^{531441} + (8t - 16)x^{656100} + (6t^2 - 24t + 24)x^{810000}. \tag{47}$$

Proof. We obtain the outcome with the edge partition in Table 1. It follows from [2] that

$$HM_1G_5(\mathcal{G}_1, x) = \sum_{rs \in E(\mathcal{G}_1)} x^{(S_G(r) + S_G(s))^2},$$

$$HM_1G_5(\mathcal{G}_1, x) = x^{(12+12)^2} |E_1(\mathcal{G}_1(t))| + x^{(12+24)^2} |E_2(\mathcal{G}_1(t))| + x^{(15+15)^2} |E_3(\mathcal{G}_1(t))| + x^{(15+24)^2} |E_4(\mathcal{G}_1(t))| + x^{(15+27)^2} |E_5(\mathcal{G}_1(t))| + x^{(18+24)^2} |E_6(\mathcal{G}_1(t))| + x^{(18+27)^2} |E_7(\mathcal{G}_1(t))| + x^{(18+30)^2} |E_8(\mathcal{G}_1(t))| + x^{(24+27)^2} |E_9(\mathcal{G}_1(t))| + x^{(27+27)^2} |E_{10}(\mathcal{G}_1(t))| + x^{(27+30)^2} |E_{11}(\mathcal{G}_1(t))| + x^{(30+30)^2} |E_{12}(\mathcal{G}_1(t))|, \tag{48}$$

$$= x^{(12+12)^2} (6) + x^{(12+24)^2} (6) + x^{(15+15)^2} (4t - 4) + x^{(15+24)^2} (8) + x^{(15+27)^2} (16t - 24) + x^{(18+24)^2} (2) + x^{(18+27)^2} (8t - 12) + x^{(18+30)^2} (6t^2 - 20t + 16) + x^{(24+27)^2} (8) + x^{(27+27)^2} (8t - 14) + x^{(27+30)^2} (8t - 16) + x^{(30+30)^2} (6t^2 - 24t + 24).$$

By doing some calculations, we obtain

$$HM_1G_5(\mathcal{G}_1, x) = 6x^{576} + (4t - 4)x^{900} + 6x^{1296} + 8x^{1521} + (16t - 22)x^{1764} + (8t - 12)x^{2025} + (6t^2 - 20t + 16)x^{2304} + 8x^{2601} + (8t - 14)x^{2916} + (8t - 16)x^{3249} + (6t^2 - 24t + 24)x^{3600}. \tag{49}$$

Also, from [10],

$$\begin{aligned}
 HM_2^a G_5(\mathcal{G}_1, x) &= \sum_{rs \in E(\mathcal{G}_1)} x^{(S_G(r) \times S_G(s))^2}, \\
 HM_2^a G_5(\mathcal{G}_1, x) &= x^{(12 \times 12)^2} |E_1(\mathcal{G}_1(t))| + x^{(12 \times 24)^2} |E_2(\mathcal{G}_1(t))| + x^{(15 \times 15)^2} |E_3(\mathcal{G}_1(t))| \\
 &\quad + x^{(15 \times 24)^2} |E_4(\mathcal{G}_1(t))| + x^{(15 \times 27)^2} |E_5(\mathcal{G}_1(t))| + x^{(18 \times 24)^2} |E_6(\mathcal{G}_1(t))| \\
 &\quad + x^{(18 \times 27)^2} |E_7(\mathcal{G}_1(t))| + x^{(18 \times 30)^2} |E_8(\mathcal{G}_1(t))| + x^{(24 \times 27)^2} |E_9(\mathcal{G}_1(t))| \\
 &\quad + x^{(27 \times 27)^2} |E_{10}(\mathcal{G}_1(t))| + x^{(27 \times 30)^2} |E_{11}(\mathcal{G}_1(t))| + x^{(30 \times 30)^2} |E_{12}(\mathcal{G}_1(t))|, \\
 &= x^{(12 \times 12)^2} (6) + x^{(12 \times 24)^2} (6) + x^{(15 \times 15)^2} (4t - 4) + x^{(15 \times 24)^2} (8) + x^{(15 \times 27)^2} (16t - 24) \\
 &\quad + x^{(18 \times 24)^2} (2) + x^{(18 \times 27)^2} (8t - 12) + x^{(18 \times 30)^2} (6t^2 - 20t + 16) + x^{(24 \times 27)^2} (8) \\
 &\quad + x^{(27 \times 27)^2} (8t - 14) + x^{(27 \times 30)^2} (8t - 16) + x^{(30 \times 30)^2} (6t^2 - 24t + 24).
 \end{aligned} \tag{50}$$

By making some calculations, we obtain

$$\begin{aligned}
 HM_2 G_5(\mathcal{G}_1, x) &= 6x^{20736} + (4t - 4)x^{50625} + 6x^{82944} + 8x^{129600} + (16t - 24)x^{164025} + 2x^{186624} \\
 &\quad + (8t - 12)x^{236196} + (6t^2 - 20t + 16)x^{291600} + 8x^{419904} + (8t - 14)x^{531441} \\
 &\quad + (8t - 16)x^{656100} + (6t^2 - 24t + 24)x^{810000}.
 \end{aligned} \tag{51}$$

2.2. Results for the Rhombus Type of Oxide Networks. Now, we are calculating fifth M-Zagreb topological indices of the rhombus-type oxide network $\mathcal{G}_2 \cong RHOX(t)$, where $t \in \mathbb{N}$.

Theorem 2.2.1. Let $\mathcal{G}_2 \cong RHOX(t)$ be the rhombus-type silicate network; then, the first and second fifth M-Zagreb indices are equal to

$$\begin{aligned}
 M_1 G_5(\mathcal{G}_2) &= 16(1 - 8t + 12t^2), \\
 M_2 G_5(\mathcal{G}_2) &= 16(2t - 1)(48t - 35).
 \end{aligned} \tag{52}$$

Proof. The outcome can be obtained by using the edge partition in Table 2. By using equation [5],

$$\begin{aligned}
 M_1 G_5(\mathcal{G}_2) &= \sum_{rs \in E(\mathcal{G}_2)} (S_G(r) + S_G(s)), \\
 M_1 G_5(\mathcal{G}_2) &= (6 + 6)|E_1(\mathcal{G}_2(t))| + (6 + 12)|E_2(\mathcal{G}_2(t))| + (8 + 12)|E_3(\mathcal{G}_2(t))| + (8 + 14)|E_4(\mathcal{G}_2(t))| \\
 &\quad + (12 + 14)|E_5(\mathcal{G}_2(t))| + (14 + 14)|E_6(\mathcal{G}_2(t))| + (14 + 16)|E_7(\mathcal{G}_2(t))| + (16 + 16)|E_8(\mathcal{G}_2(t))|, \\
 &= (6 + 6)(2) + (6 + 12)(4) + (8 + 12)(4) + (8 + 14)(8t - 12) + (12 + 14)(8) + (14 + 14) \\
 &\quad (8t - 14) + (14 + 16)(8t - 16) + (16 + 16)(6(t - 2)^2).
 \end{aligned} \tag{53}$$

TABLE 2: Edge partition of rhombus-type oxide network ($RHOX(t)$) based on sum of degrees of end vertices of each edge.

(S_r, S_s)	Number of edges
<i>Where $rs \in E(\mathcal{G}_2)$</i>	
(6, 6)	2
(6, 12)	4
(8, 12)	4
(8, 14)	$4(2t - 3)$
<i>Where $rs \in E(\mathcal{G}_2)$</i>	
(12, 14)	8
(14, 14)	$2(4t - 7)$
(14, 16)	$8(t - 2)$
(16, 16)	$6(t - 2)^2$

By doing some calculations, we obtain

$$M_1G_5(\mathcal{G}_2) = 16(1 - 8t + 12t^2). \tag{54}$$

Thus, from [6],

$$\begin{aligned} M_2G_5(\mathcal{G}) &= \sum_{rs \in E(\mathcal{G})} (S_G(r) + S_G(s)), \\ M_2G_5(\mathcal{G}_2) &= (6 + 6)|E_1(\mathcal{G}_2(t))| + (6 + 12)|E_2(\mathcal{G}_2(t))| + (8 + 12)|E_3(\mathcal{G}_2(t))| + (8 + 14)|E_4(\mathcal{G}_2(t))| \\ &\quad + (12 + 14)|E_5(\mathcal{G}_2(t))| + (14 + 14)|E_6(\mathcal{G}_2(t))| + (14 + 16)|E_7(\mathcal{G}_2(t))| + (16 + 16)|E_8(\mathcal{G}_2(t))|, \\ &= (6 + 6)(2) + (6 + 12)(4) + (8 + 12)(4) + (8 + 14)(8t - 12) + (12 + 14)(8) + (14 + 14) \\ &\quad (8t - 14) + (14 + 16)(8t - 16) + (16 + 16)(6(t - 2)^2), \end{aligned} \tag{55}$$

By doing some calculations, we obtain

$$M_2G_5(\mathcal{G}_2) = 16(2t - 1)(48t - 35). \tag{56}$$

Theorem 2.2.2. Consider the rhombus-type oxide network $\mathcal{G}_2 \cong RHOX(t)$ for $t \in \mathbb{N}$. Then, the first and second general fifth M-Zagreb indices are equal to

$$\begin{aligned} M_1^aG_5(\mathcal{G}_2) &= \left[2^a(3 \times 2^{3+4a} + 2^{1+a}3^a + 2^{2+a}5^a + 4 \times 9^a - 12 \times 11^a + 8 \times 13^a - 14^{1+a} - 16 \times 15^a) + \right. \\ &\quad \left. 2^a t(-3 \times 2^{3+4a} + 2^{3+a}7^a + 8 \times 11^a + 8 \times 15^a) + 3 \times 2^{1+5a}t^2 \right], \\ M_2^aG_5(\mathcal{G}_2) &= \left[(3 \times 2^{3+8a} + 2^{2+5a}3^a - 2^{4+5a}7^a - 3 \times 4^{1+2a}7^a + 2^{1+2a}9^a + 2^{2+3a}9^a - 14^{1+2a} + 8^{1+a}21^a) \right. \\ &\quad \left. + t(-3 \times 2^{3+8a} + 2^{3+4a}7^a + 2^{3+5a}7^a + 2^{3+2a}49^a) + 3 \times 2^{1+8a}t^2 \right]. \end{aligned} \tag{57}$$

Proof. Let \mathcal{G}_2 be the rhombus-type oxide network. Table 2 shows such an edge partition of $RHOX(t)$. Thus, from [9], it follows that

$$M_1^aG_5(\mathcal{G}) = \sum_{rs \in E(\mathcal{G})} (S_G(r) + S_G(s))^a. \tag{58}$$

By using edge partitions in Table 2, we obtain

$$\begin{aligned} M_1^aG_5(\mathcal{G}_2) &= (6 + 6)^a|E_1(\mathcal{G}_2(t))| + (6 + 12)^a|E_2(\mathcal{G}_2(t))| + (8 + 12)^a|E_3(\mathcal{G}_2(t))| + (8 + 14)^a|E_4(\mathcal{G}_2(t))| \\ &\quad + (12 + 14)^a|E_5(\mathcal{G}_2(t))| + (14 + 14)^a|E_6(\mathcal{G}_2(t))| + (14 + 16)^a|E_7(\mathcal{G}_2(t))| + (16 + 16)^a|E_8(\mathcal{G}_2(t))|, \\ &= (6 + 6)^a(2) + (6 + 12)^a(4) + (8 + 12)^a(4) + (8 + 14)^a(8t - 12) + (12 + 14)^a(8) + (14 + 14)^a \\ &\quad (8t - 14) + (14 + 16)^a(8t - 16) + (16 + 16)^a(6(t - 2)^2). \end{aligned} \tag{59}$$

By doing some calculations, we have

$$M_1^a G_5(\mathcal{G}_2) = \left[\begin{array}{l} 2^a(3 \times 2^{3+4a} + 2^{1+a}3^a + 2^{2+a}5^a + 4 \times 9^a - 12 \times 11^a + 8 \times 13^a - 14^{1+a} - 16 \times 15^a) + \\ 2^a t(-3 \times 2^{3+4a} + 2^{3+a}7^a + 8 \times 11^a + 8 \times 15^a) + 3 \times 2^{1+5a}t^2 \end{array} \right]. \quad (60)$$

From [12], we have

$$M_2^a G_5(\mathcal{G}) = \sum_{r,s \in E(\mathcal{G})} (S_G(r) + S_G(s))^a. \quad (61)$$

By using edge partitions in Table 2, we obtain

$$\begin{aligned} M_2^a G_5(\mathcal{G}_2) &= (6+6)^a |E_1(\mathcal{G}_2(t))| + (6+12)^a |E_2(\mathcal{G}_2(t))| + (8+12)^a |E_3(\mathcal{G}_2(t))| + (8+14)^a |E_4(\mathcal{G}_2(t))| \\ &\quad + (12+14)^a |E_5(\mathcal{G}_2(t))| + (14+14)^a |E_6(\mathcal{G}_2(t))| + (14+16)^a |E_7(\mathcal{G}_2(t))| + (16+16)^a |E_8(\mathcal{G}_2(t))|, \\ &= (6+6)^a (2) + (6+12)^a (4) + (8+12)^a (4) + (8+14)^a (8t-12) + (12+14)^a (8) + (14+14)^a \\ &\quad (8t-14) + (14+16)^a (8t-16) + (16+16)^a (6(t-2)^2). \end{aligned} \quad (62)$$

By doing some calculations, we have

$$M_2^a G_5(\mathcal{G}_2) = \left[\begin{array}{l} 3 \times 2^{3+8a} + 2^{2+5a}3^a - 2^{4+5a}7^a - 3 \times 4^{1+2a}7^a + 2^{1+2a}9^a + 2^{2+3a}9^a - 14^{1+2a} + 8^{1+a}21^a \\ + t(-3 \times 2^{3+8a} + 2^{3+4a}7^a + 2^{3+5a}7^a + 2^{3+2a}49^a + 3 \times 2^{1+8a}t^2) \end{array} \right]. \quad (63)$$

Theorem 2.2.3. Consider the rhombus-type oxide network $\mathcal{G}_2 \cong RHOX(t)$ for $t \in \mathbb{N}$. Then, the first and second hyper fifth M-Zagreb indices are equal to

$$\begin{aligned} HM_1^a G_5(\mathcal{G}_2) &= 64(31 - 113t + 96t^2), \\ HM_2^a G_5(\mathcal{G}_2) &= 192(1915 - 3978t + 2048t^2). \end{aligned} \quad (64)$$

Proof. Let \mathcal{G}_2 be the rhombus-type oxide network. Table 2 shows such an edge partition of $RHOX(t)$. Thus, from [13], it follows that

$$HM_1 G_5(\mathcal{G}) = \sum_{r,s \in E(\mathcal{G})} (S_G(r) + S_G(s))^2. \quad (65)$$

By using edge partitions in Table 2, we obtain

$$\begin{aligned} HM_1 G_5(\mathcal{G}_2) &= (6+6)^2 |E_1(\mathcal{G}_2(t))| + (6+12)^2 |E_2(\mathcal{G}_2(t))| + (8+12)^2 |E_3(\mathcal{G}_2(t))| + (8+14)^2 |E_4(\mathcal{G}_2(t))| \\ &\quad + (12+14)^2 |E_5(\mathcal{G}_2(t))| + (14+14)^2 |E_6(\mathcal{G}_2(t))| + (14+16)^2 |E_7(\mathcal{G}_2(t))| + (16+16)^2 |E_8(\mathcal{G}_2(t))|, \\ &= (6+6)^2 (2) + (6+12)^2 (4) + (8+12)^2 (4) + (8+14)^2 (8t-12) + (12+14)^2 (8) + (14+14)^2 \\ &\quad (8t-14) + (14+16)^2 (8t-16) + (16+16)^2 (6(t-2)^2). \end{aligned} \quad (66)$$

By doing some calculations, we have

$$HM_1 G_5(\mathcal{G}_2) = 64(31 - 113t + 96t^2). \quad (67)$$

$$HM_2 G_5(\mathcal{G}) = \sum_{r,s \in E(\mathcal{G})} (S_G(r) + S_G(s))^2. \quad (68)$$

By using edge partitions in Table 2, we obtain

From [14], we have

$$\begin{aligned} HM_2 G_5(\mathcal{G}_2) &= (6+6)^2 |E_1(\mathcal{G}_2(t))| + (6+12)^2 |E_2(\mathcal{G}_2(t))| + (8+12)^2 |E_3(\mathcal{G}_2(t))| + (8+14)^2 |E_4(\mathcal{G}_2(t))| \\ &\quad + (12+14)^2 |E_5(\mathcal{G}_2(t))| + (14+14)^2 |E_6(\mathcal{G}_2(t))| + (14+16)^2 |E_7(\mathcal{G}_2(t))| + (16+16)^2 |E_8(\mathcal{G}_2(t))|, \\ &= (6+6)^2 (2) + (6+12)^2 (4) + (8+12)^2 (4) + (8+14)^2 (8t-12) + (12+14)^2 (8) + (14+14)^2 \\ &\quad (8t-14) + (14+16)^2 (8t-16) + (16+16)^2 (6(t-2)^2). \end{aligned} \quad (69)$$

By doing some calculations, we have

$$HM_2G_5(\mathcal{G}_2) = 192(1915 - 3978t + 2048t^2). \tag{70}$$

Theorem 2.2.4. Consider the rhombus-type silicate network $\mathcal{G}_2 \cong RHOX(t)$ for $t \in \mathbb{N}$. Then, the third M-Zagreb index is equal to

$$M_3G_5(\mathcal{G}_2) = (-48 + 64t). \tag{71}$$

Proof. Let \mathcal{G}_2 be the rhombus-type oxide network. Table 2 shows such an edge partition of $RHOX(t)$. Thus, from [15], it follows that

$$M_3G_5(\mathcal{G}) = \sum_{rs \in E(\mathcal{G})} |S_G(r) - S_G(s)|. \tag{72}$$

By using edge partitions in Table 2, we obtain

$$\begin{aligned} M_3G_5(\mathcal{G}_2) &= |6 - 6||E_1(\mathcal{G}_2(t))| + |6 - 12||E_2(\mathcal{G}_2(t))| + |8 - 12||E_3(\mathcal{G}_2(t))| + |8 - 14||E_4(\mathcal{G}_2(t))| + \\ &\quad |12 - 14||E_5(\mathcal{G}_2(t))| + |14 - 14||E_6(\mathcal{G}_2(t))| + |14 - 16||E_7(\mathcal{G}_2(t))| + |16 - 16||E_8(\mathcal{G}_2(t))|, \\ &= |6 - 6|(2) + |6 - 12|(4) + |8 - 12|(4) + |8 - 14|(8t - 12) + |12 - 14|(8) + |14 - 14| \\ &\quad (8t - 14) + |14 - 16|(8t - 16) + |16 - 16|(6(t - 2)^2). \end{aligned} \tag{73}$$

By doing some calculations, we have

$$M_3G_5(\mathcal{G}_2) = (-48 + 64t). \tag{74}$$

Theorem 2.2.5. Let $\mathcal{G}_2 \cong RHOX(t)$ be the rhombus-type oxide network; then, general fifth M-Zagreb polynomials of first and second type are equal to

Corresponding to the above indices, we are going to compute general fifth M-Zagreb polynomials for rhombus type of oxide network $RHOX(t)$.

$$\begin{aligned} M_1^a G_5(\mathcal{G}_2, x) &= 2x^{12^a} + 4x^{18^a} + 4x^{20^a} + 4(2t - 3)x^{22^a} + 8x^{26^a} + 2(4t - 7)x^{28^a} + 8(t - 2)x^{30^a} + 6(t - 2)^2 x^{32^a}, \\ M_2^a G_5(\mathcal{G}_2, x) &= 2x^{36^a} + 4x^{72^a} + 4x^{96^a} + 4(2t - 3)x^{112^a} + 8x^{168^a} + 2(4t - 7)x^{196^a} + 8(t - 2)x^{224^a} \\ &\quad + 6(t - 2)^2 x^{256^a}. \end{aligned} \tag{75}$$

Proof. We obtain the outcome with the edge partition in Table 1. It follows from [1] that

$$\begin{aligned} M_1^a G_5(\mathcal{G}_2, x) &= \sum_{rs \in E(\mathcal{G}_2)} x^{(S_G(r) + S_G(s))^a}, \\ M_1^a G_5(\mathcal{G}_2, x) &= x^{(6+6)^a} |E_1(\mathcal{G}_2(t))| + x^{(6+12)^a} |E_2(\mathcal{G}_2(t))| + x^{(8+12)^a} |E_3(\mathcal{G}_2(t))| + x^{(8+14)^a} |E_4(\mathcal{G}_2(t))| \\ &\quad + x^{(12+14)^a} |E_5(\mathcal{G}_2(t))| + x^{(14+14)^a} |E_6(\mathcal{G}_2(t))| + x^{(14+16)^a} |E_7(\mathcal{G}_2(t))| + x^{(16+16)^a} |E_8(\mathcal{G}_2(t))|, \\ &= x^{(6+6)^a} (2) + x^{(6+12)^a} (4) + x^{(8+12)^a} (4) + x^{(8+14)^a} (8t - 12) + x^{(12+14)^a} (8) + x^{(14+14)^a} \\ &\quad (8t - 14) + x^{(14+16)^a} (8t - 16) + x^{(16+16)^a} (6(t - 2)^2). \end{aligned} \tag{76}$$

By doing some calculations, we obtain

$$M_1^a G_5(\mathcal{G}_2, x) = 2x^{12^a} + 4x^{18^a} + 4x^{20^a} + 4(2t - 3)x^{22^a} + 8x^{26^a} + 2(4t - 7)x^{28^a} + 8(t - 2)x^{30^a} + 6(t - 2)^2 x^{32^a}. \tag{77}$$

Also, from [3],

$$\begin{aligned}
 M_2^a G_5(\mathcal{G}_2, x) &= \sum_{rs \in E(\mathcal{G}_2)} x^{(S_G(r)+S_G(s))^a}, \\
 M_2^a \bar{G}_5(\mathcal{G}_2, x) &= x^{(6+6)^a} |E_1(\mathcal{G}_2(t))| + x^{(6+12)^a} |E_2(\mathcal{G}_2(t))| + x^{(8+12)^a} |E_3(\mathcal{G}_2(t))| + x^{(8+14)^a} |E_4(\mathcal{G}_2(t))| \\
 &\quad + x^{(12+14)^a} |E_5(\mathcal{G}_2(t))| + x^{(14+14)^a} |E_6(\mathcal{G}_2(t))| + x^{(14+16)^a} |E_7(\mathcal{G}_2(t))| + x^{(16+16)^a} |E_8(\mathcal{G}_2(t))|, \\
 &= x^{(6+6)^a} (2) + x^{(6+12)^a} (4) + x^{(8+12)^a} (4) + x^{(8+14)^a} (8t - 12) + x^{(12+14)^a} (8) + x^{(14+14)^a} \\
 &\quad (8t - 14) + x^{(14+16)^a} (8t - 16) + x^{(16+16)^a} (6(t - 2)^2).
 \end{aligned} \tag{78}$$

By making some calculations, we obtain

$$\begin{aligned}
 M_2^a \bar{G}_5(\mathcal{G}_2, x) &= 2x^{36^a} + 4x^{72^a} + 4x^{96^a} + 4(2t - 3)x^{112^a} + 8x^{168^a} + 2(4t - 7)x^{196^a} + 8(t - 2)x^{224^a} \\
 &\quad + 6(t - 2)^2 x^{256^a}.
 \end{aligned} \tag{79}$$

Corresponding to the above indices, we are going to compute fifth M -Zagreb polynomials for rhombus-type oxide network $RHOX(t)$.

Theorem 2.2.6. *Let $\mathcal{G}_2 \cong RHOX(t)$ be the rhombus-type oxide network; then, fifth M -Zagreb polynomials of first and second type are equal to*

$$\begin{aligned}
 M_1^a G_5(\mathcal{G}_2, x) &= 2x^{12} + 4x^{18} + 4x^{20} + 4(2t - 3)x^{22} + 8x^{26} + 2(4t - 7)x^{28} + 8(t - 2)x^{30} + 6(t - 2)^2 x^{32}, \\
 M_2 G_5(\mathcal{G}_2, x) &= 2x^{36} + 4x^{72} + 4x^{96} + 4(2t - 3)x^{112} + 8x^{168} + 2(4t - 7)x^{196} + 8(t - 2)x^{224} + 6 \\
 &\quad (t - 2)^2 x^{256}.
 \end{aligned} \tag{80}$$

Proof. We obtain the outcome with the edge partition in Table 2. It follows from [16] that

$$\begin{aligned}
 M_1 G_5(\mathcal{G}_2, x) &= \sum_{rs \in E(\mathcal{G}_2)} x^{(S_G(r)+S_G(s))}, \\
 M_1 G_5(\mathcal{G}_2, x) &= x^{(6+6)} |E_1(\mathcal{G}_2(t))| + x^{(6+12)} |E_2(\mathcal{G}_2(t))| + x^{(8+12)} |E_3(\mathcal{G}_2(t))| + x^{(8+14)} |E_4(\mathcal{G}_2(t))| \\
 &\quad + x^{(12+14)} |E_5(\mathcal{G}_2(t))| + x^{(14+14)} |E_6(\mathcal{G}_2(t))| + x^{(14+16)} |E_7(\mathcal{G}_2(t))| + x^{(16+16)} |E_8(\mathcal{G}_2(t))|, \\
 &= x^{(6+6)} (2) + x^{(6+12)} (4) + x^{(8+12)} (4) + x^{(8+14)} (8t - 12) + x^{(12+14)} (8) + x^{(14+14)} \\
 &\quad (8t - 14) + x^{(14+16)} (8t - 16) + x^{(16+16)} (6(t - 2)^2).
 \end{aligned} \tag{81}$$

By doing some calculations, we obtain

$$M_1^a G_5(\mathcal{G}_2, x) = 2x^{12} + 4x^{18} + 4x^{20} + 4(2t - 3)x^{22} + 8x^{26} + 2(4t - 7)x^{28} + 8(t - 2)x^{30} + 6(t - 2)^2 x^{32}. \tag{82}$$

Also, from [4],

$$\begin{aligned}
 M_2G_5(\mathcal{G}_2, x) &= \sum_{rs \in E(\mathcal{G}_2)} x^{(S_G(r)+S_G(s))}, \\
 M_2G_5(\mathcal{G}_2, x) &= x^{(6 \times 6)}|E_1(\mathcal{G}_2(t))| + x^{(6 \times 12)}|E_2(\mathcal{G}_2(t))| + x^{(8 \times 12)}|E_3(\mathcal{G}_2(t))| + x^{(8 \times 14)}|E_4(\mathcal{G}_2(t))| + \\
 &\quad x^{(12 \times 14)}|E_5(\mathcal{G}_2(t))| + x^{(14 \times 14)}|E_6(\mathcal{G}_2(t))| + x^{(14 \times 16)}|E_7(\mathcal{G}_2(t))| + x^{(16 \times 16)}|E_8(\mathcal{G}_2(t))|, \\
 &= x^{(6 \times 6)}(2) + x^{(6 \times 12)}(4) + x^{(8 \times 12)}(4) + x^{(8 \times 14)}(8t - 12) + x^{(12 \times 14)}(4) + x^{(14 \times 14)}(8t - 14) \\
 &\quad + x^{(14 \times 16)}(8t - 16) + x^{(16 \times 16)}(6(t - 2)^2).
 \end{aligned} \tag{83}$$

By making some calculations, we obtain

$$\begin{aligned}
 M_2G_5(\mathcal{G}_2, x) &= 2x^{36} + 4x^{72} + 4x^{96} + 4(2t - 3)x^{112} + 8x^{168} + 2(4t - 7)x^{196} + 8(t - 2)x^{224} \\
 &\quad + 6(t - 2)^2x^{256}.
 \end{aligned} \tag{84}$$

Theorem 2.2.7. *Let $\mathcal{G}_2 \cong RHOX(t)$ be the rhombus-type oxide network; then, hyper-fifth M-Zagreb polynomials of first and second type are equal to*

$$\begin{aligned}
 HM_1G_5(\mathcal{G}_2, x) &= 2x^{144} + 4x^{324} + 4x^{400} + 4(2t - 3)x^{484} + 8x^{676} \\
 &\quad + 2(4t - 7)x^{784} + 8(t - 2)x^{900} + 6(t - 2)^2x^{1024}, HM_2G_5(\mathcal{G}_2, x) \\
 &= 2x^{1296} + 4x^{5184} + 4x^{9216} + 4(2t - 3)x^{12544} + 8x^{28224} \\
 &\quad + 2(4t - 7)x^{38416} + 8(t - 2)x^{50176} + 6(t - 2)^2x^{65536}.
 \end{aligned} \tag{85}$$

Proof. We obtain the outcome with the edge partition in Table 2. It follows from [2] that

$$\begin{aligned}
 HM_1G_5(\mathcal{G}_2, x) &= \sum_{rs \in E(\mathcal{G}_2)} x^{(S_G(r)+S_G(s))^2}, \\
 HM_1G_5(\mathcal{G}_2, x) &= x^{(6+6)^2}|E_1(\mathcal{G}_2(t))| + x^{(6+12)^2}|E_2(\mathcal{G}_2(t))| + x^{(8+12)^2}|E_3(\mathcal{G}_2(t))| + x^{(8+14)^2}|E_4(\mathcal{G}_2(t))| \\
 &\quad + x^{(12+14)^2}|E_5(\mathcal{G}_2(t))| + x^{(14+14)^2}|E_6(\mathcal{G}_2(t))| + x^{(14+16)^2}|E_7(\mathcal{G}_2(t))| + x^{(16+16)^2}|E_8(\mathcal{G}_2(t))| \\
 &= x^{(6+6)^2}(2) + x^{(6+12)^2}(4) + x^{(8+12)^2}(4) + x^{(8+14)^2}(8t - 12) + x^{(12+14)^2}(8) \\
 &\quad + x^{(14+14)^2}(8t - 14) + x^{(14+16)^2}(8t - 16) + x^{(16+16)^2}(6(t - 2)^2).
 \end{aligned} \tag{86}$$

By doing some calculations, we obtain

$$\begin{aligned}
 HM_1G_5(\mathcal{G}_2, x) &= 2x^{144} + 4x^{324} + 4x^{400} + 4(2t - 3)x^{484} + 8x^{676} \\
 &\quad + 2(4t - 7)x^{784} + 8(t - 2)x^{900} + 6(t - 2)^2x^{1024}.
 \end{aligned} \tag{87}$$

Also, from [10],

$$\begin{aligned}
HM_2^a G_5(\mathcal{G}_2, x) &= \sum_{rs \in E(\mathcal{G}_2)} x^{(S_G(r) + S_G(s))}, \\
HM_2 G_5(\mathcal{G}_2, x) &= x^{(6 \times 6)^2} |E_1(\mathcal{G}_2(t))| + x^{(6 \times 12)^2} |E_2(\mathcal{G}_2(t))| + x^{(8 \times 12)^2} |E_3(\mathcal{G}_2(t))| + x^{(8 \times 14)^2} |E_4(\mathcal{G}_2(t))| + \\
&\quad x^{(12 \times 14)^2} |E_5(\mathcal{G}_2(t))| + x^{(14 \times 14)^2} |E_6(\mathcal{G}_2(t))| + x^{(14 \times 16)^2} |E_7(\mathcal{G}_2(t))| + x^{(16 \times 16)^2} |E_8(\mathcal{G}_2(t))|, \\
&= x^{(6 \times 6)^2} (2) + x^{(6 \times 12)^2} (4) + x^{(8 \times 12)^2} (4) + x^{(8 \times 14)^2} (8t - 12) + x^{(12 \times 14)^2} (4) + x^{(14 \times 14)^2} (8t - 14) \\
&\quad + x^{(14 \times 16)^2} (8t - 16) + x^{(16 \times 16)^2} (6(t - 2)^2).
\end{aligned} \tag{88}$$

By making some calculations, we obtain

$$\begin{aligned}
HM_2 G_5(\mathcal{G}_2, x) &= 2x^{1296} + 4x^{5184} + 4x^{9216} + 4(2t - 3)x^{12544} + 8x^{28224} \\
&\quad + 2(4t - 7)x^{38416} + 8(t - 2)x^{50176} + 6(t - 2)^2 x^{65536}.
\end{aligned} \tag{89}$$

3. Conclusion

In this study, we computed sum of degree-based indices for $RHSL(t)$ and $RHOX(t)$ graphs of rhombus oxide and silicate structures. We also computed certain sum of degree-based polynomials such as fifth M-Zagreb, fifth hyper M-Zagreb, and generalized fifth M-Zagreb indices for $RHSL(t)$ and $RHOX(t)$ graphs of rhombus oxide and silicate structures. These facts may be useful for people working in computer science and chemistry fields who encounter chemical networks. These results can also play a vital role in the determination of the significance of silicate and oxide networks. Like certain other topological indices, determining the representations of derived graphs like these is an open question.

Data Availability

No data were used to support this study.

Conflicts of Interest

The authors declare no conflicts of interest.

Acknowledgments

This work was supported in part by the Natural Science Fund of Education Department of Anhui Province under Grant KJ2020A0478.

References

- [1] A. Graovac, M. Ghorbani, and M. A. Hosseinzadeh, "Computing degree based topological properties of third type of hex-derived networks," *Journal of Mathematical Nanoscience*, vol. 1, pp. 33–42, 2011.
- [2] V. R. Kulli, "General fifth M-zagreb indices and fifth M-zagreb polynomials of PAMAM dendrimers," *International Journal of Fuzzy Mathematical Archive*, vol. 22, pp. 99–103, 2017.
- [3] M. Husin, R. Hasni, N. Arif, and M. Imran, "On topological indices of certain families of nanostar dendrimers," *Molecules*, vol. 21, no. 7, p. 821, 2016.
- [4] V. R. Kulli, "Multiplicative hyper-Zagreb indices and coincides of graphs: computing these indices of some nanostructures," *International Research Journal of Pure Algebra*, vol. 6, no. 7, pp. 342–347, 2016.
- [5] H. Ali, U. Babar, S. H. Arshad, and A. Sajjad, "On some neighbourhood degree-based indices of graphs derived from honeycomb structure," *Konuralp Journal of Mathematics (KJM)*, vol. 9, no. 1, pp. 164–175, 2020.
- [6] H. Ali, M. A. Binyamin, M. K. Shafiq, and W. Gao, "On the degree-based topological indices of some derived networks," *Mathematics*, vol. 7, no. 7, p. 612, 2019.
- [7] W. Zhen, P. Ali, H. Ali, G. Dustigeer, and J. B. Liu, "On computation degree-based topological descriptors for planar octahedron networks," *Journal of Mathematics*, 2021.
- [8] U. Babar, H. Ali, H. Ali, S. Hussain Arshad, and U. Sheikh, "Multiplicative topological properties of graphs derived from honeycomb structure," *AIMS Mathematics*, vol. 5, no. 2, pp. 1562–1587, 2020.
- [9] M. V. Diudea, I. Gutman, and J. Lorentz, *Molecular Topology*, Nova Science Publishers, Huntington, NY, USA, 2001.
- [10] A. Nayak and I. Stojmenovic, *Hand Book of Applied Algorithms: Solving Scientific, Engineering, and Practical Problems*, p. 560p, John Wiley & Sons, Hoboken, NJ, USA, 2007.
- [11] H. Wiener, "Structural determination of paraffin boiling points," *Journal of the American Chemical Society*, vol. 69, no. 1, pp. 17–20, 1947.
- [12] M. Deza, P. W. Fowler, A. Rassat, and K. M. Rogers, "Fullerenes as tilings of surfaces," *Journal of Chemical Information and Computer Sciences*, vol. 40, no. 3, pp. 550–558, 2000.
- [13] W. Gao, M. K. Siddiqui, M. Naeem, and M. Imran, "Computing multiple ABC index and multiple GA index of some grid graphs," *Open Physics*, vol. 16, no. 1, pp. 588–598, 2018.
- [14] I. Gutman and S. J. Cyvin, *Introduction to the Theory of Benzenoid Hydrocarbons*, Springer, Berlin, Germany, 1989.
- [15] I. Gutman, B. Rusi, and N. Trinajsti, "Graph theory and molecular orbitals. XII. Acyclic polyenes," *The Journal of Chemical Physics*, vol. 62, no. 9, pp. 3399–3405, 1975.
- [16] M. Javaid, M. U. Rehman, and J. Cao, "Topological indices of rhombus type silicate and oxide networks," *Canadian Journal of Chemistry*, vol. 95, no. 2, pp. 134–143, 2017.

Research Article

Modular Irregular Labeling on Double-Star and Friendship Graphs

K. A. Sugeng ¹, Z. Z. Barack,¹ N. Hinding ² and R. Simanjuntak ³

¹Department of Mathematics, Faculty of Mathematics and Natural Sciences, Universitas Indonesia, Depok, Indonesia

²Department of Mathematics, Faculty of Mathematics and Natural Sciences, University of Hasanuddin, Makassar, Indonesia

³Combinatorial Mathematics Research Group, Faculty of Mathematics and Natural, Sciences, Institute Technology Bandung, Bandung, Indonesia

Correspondence should be addressed to K. A. Sugeng; kiki@sci.ui.ac.id

Received 17 September 2021; Revised 8 October 2021; Accepted 23 November 2021; Published 28 December 2021

Academic Editor: Ali Jaballah

Copyright © 2021 K. A. Sugeng et al. This is an open access article distributed under the Creative Commons Attribution License, which permits unrestricted use, distribution, and reproduction in any medium, provided the original work is properly cited.

A modular irregular graph is a graph that admits a modular irregular labeling. A modular irregular labeling of a graph G of order n is a mapping of the set of edges of the graph to $\{1, 2, \dots, k\}$ such that the weights of all vertices are different. The vertex weight is the sum of its incident edge labels, and all vertex weights are calculated with the sum modulo n . The modular irregularity strength is the minimum largest edge label such that a modular irregular labeling can be done. In this paper, we construct a modular irregular labeling of two classes of graphs that are biregular; in this case, the regular double-star graph and friendship graph classes are chosen. Since the modular irregularity strength of the friendship graph also holds the minimal irregularity strength, then the labeling is also an irregular labeling with the same strength as the modular case.

1. Introduction

Graph labeling is a mapping of a set of numbers, called the labels, to the graph elements, usually vertices or edges [1]. Generally, the label is a positive integer. There are several labelings that have been developed; among them are irregular labeling and modular irregular labeling. The reader can check the dynamic survey of graph labeling by Gallian to obtain more information on various labeling [1]. In 1988, irregular labeling was first introduced by Chartrand et al. [2]. To date, there have been studies on the irregular labelings of certain graphs. The terminology not included in this paper can be found in [3].

An irregular labeling is defined as a labeling $f: E \rightarrow \{1, 2, \dots, k\}$ with k as a positive integer, such that $wt_{f(x)} = \sum_{(y \in N(x))} f(xy)$ is different for all vertices, where $N(x)$ is a neighbour of vertex x . The irregularity strength $s(G)$ of a graph G is the minimum value of k for which G has irregular labeling with labels at most k . The irregularity strength $s(G)$ of a graph G is defined only for graphs containing at most one isolated vertex and no connected

component of order 2. The lower bound of the irregularity strength of a graph G is $s(G) \geq \max_{1 \leq i \leq \Delta} \{n_i + i - 1/i\}$, where n_i vertices with degree i , as stated in Theorem 1. For a regular graph G , Przyboylo [4] has proved an upper bound of an irregularity strength is $s(G) < 16n/d + 6$. For tree graphs, Aigner and Triesch [5] proved that the irregularity strength of any tree with no vertices of degree two is equal to the number of its leaves. Ferrara et al. [6] later proved that if the tree T has every two vertices of degree not equal to two at a distance of at least eight with number of leaves at least three, then $s(T) = n_1 + n_2/2$, where n_1 is the number of leaves and n_2 is the number of vertices of degree two. The survey of irregular labeling has been done by Bača et al. [7]. After this survey paper, there are still many results which have been found. See Gallian's survey, for the update [1].

Modular irregular labeling of a graph is a mapping $\varphi: E(G) \rightarrow \{1, 2, \dots, k\}$ so that a bijective function $wt_{\varphi(x)} = \sum_{(y \in N(x))} \varphi(xy)$ can be defined and has different values. The set of the weights of the vertices is a group of integers modulo n . The minimum k such that this kind of labeling exists is called the modular irregularity strength of G

and denoted by $ms(G)$. Bača et al. [8] determined the modular irregularity strength of path, star, triangular graph, cycle, and gear graphs. Muthugurupackiam et al. [9] proved the modular irregularity of the tadpole graph and double-cycle graph. Later, Bača et al. [10] proved the modular irregularity strength of the fan graph. In this paper, we construct the modular irregular labeling and determine its modular irregularity strength of regular double-star graph and friendship graph.

2. Known Results

There are some known results that we will use to prove the modular irregularity strength of the star and friendship graphs that we gave in this section. A lower bound on the irregularity strength is already known by Chartrand et al. as stated in the following theorem.

Theorem 1 (see [2]). *Let G be a connected graph with an order more than 2, which has n_i vertices with degree i . Then,*

$$s(G) \geq \max_{1 \leq i \leq \Delta(G)} \left\{ \frac{n_i - 1}{i} + 1 \right\}. \quad (1)$$

The relation between the irregularity strength and modular irregularity strength has been known and presented in the following theorem.

Theorem 2 (see [8]). *Let G be a graph without a component of order ≤ 2 . Then,*

$$s(G) \leq ms(G), \quad (2)$$

Not all graphs can have modular irregular labeling. In the following theorem, Bača et al. give a requirement of a graph that cannot have a modular irregular labeling, denoted by $ms(G) = \infty$.

Theorem 3 (see [8]). *If G is a graph of order n , $n \equiv 2 \pmod{4}$, then G has no modular irregular k -labeling, i.e., $ms(G) = \infty$.*

3. New Results

This section gives two results on a modular irregular labeling on a regular double-star graph and a friendship graph. Aman and Togni [5] and Ferrara et al. [6] proved the irregularity strength of trees family. The modular irregularity strength of the family of trees which is already known is path and star [8]. Since we consider biregular graphs in this paper, then the regular trees family that we choose is regular double-stars.

A regular double-star graph $S_{k,k}$ is a graph built from two copies of a star graph S_k , and then, we connect the two center vertices of the star. Note that a star S_k has $k + 1$ vertices. Thus, $S_{k,k}$ has $2k + 2$ vertices and $2k + 1$ edges.

Theorem 4. *Let $S_{k,k}$, $k \geq 1$ be a regular double-star graph. Then,*

$$ms(S_{k,k}) = \begin{cases} 2k, & k \text{ is odd.} \\ \infty, & k \text{ is even.} \end{cases} \quad (3)$$

Proof. Let x and y be the two centers of the double-star graph. Let $x_i, i = 1, \dots, k$, be the leaves of the center vertex x and $y_i, i = 1, \dots, k$, be the leaves of the center vertex y .

For k even, $|V(S_{k,k})| = 2k + 2 \equiv 2 \pmod{4}$. Then, following Theorem 3, the graph does not have a modular irregular labeling.

For k odd, label the edges as follows.

For $1 \leq i \leq k$,

$$\varphi(xx_i) = \begin{cases} 2i - 1, & i \text{ odd,} \\ 2i, & i \text{ even,} \end{cases} \quad (4)$$

$$\varphi(yy_i) = \begin{cases} 2i, & i \text{ odd,} \\ 2i - 1, & i \text{ even,} \end{cases}$$

$$\varphi(xy) = \frac{3k + 1}{2} < 2k. \quad (5)$$

The pendant leaves should have the different labels; then, the minimal number of labels is $2k$. The maximal label is at $\varphi(yy_k) = 2k$. Thus, φ is a $2k$ -labeling. Its leaves weight will be elements of $\{1, 2, \dots, 2k\}$, $wt_\varphi(x) \equiv 2k + 1 \pmod{2k + 2}$ and $wt_\varphi(y) \equiv 0 \pmod{2k + 2}$. All vertex weights are different. Thus, $ms(S_{k,k}) = 2k$ for k odd.

A friendship graph F_n is a graph with the vertex set $\{m, x_1, \dots, x_n, y_1, \dots, y_n\}$ and the edge set is $\{mx_1, \dots, mx_n, my_1, \dots, my_n, x_1y_1, \dots, x_ny_n\}$. Thus, the graph F_n has $2n + 1$ vertices and $3n$ edges. Since the graph has $|V(G)| \not\equiv 2 \pmod{4}$, then based on Theorem 3, we have a possibility to find the modular irregularity strength of F_n . In the following lemma, we have a lower bound of $ms(F_n)$. \square

Lemma 1. *Let F_n be a friendship graph with $n \geq 2$. Then,*

$$ms(F_n) \geq n + 1. \quad (6)$$

Proof. A friendship graph F_n has $2n$ vertices with degree two and one vertex with degree $2n$. Based on Theorem 1, we have

$$s(F_n) \geq \max_{1 \leq i \leq 2n} \left\{ \frac{2n - 1}{2} + 1, \frac{1 - 1}{2n} + 1 \right\},$$

$$s(F_n) \geq n + \frac{1}{2}, \quad (7)$$

$$s(F_n) \geq n + 1 \text{ (since } s(F_n) \text{ is an integer).}$$

Then, based on Theorem 2, we obtain

$$\begin{aligned} ms(F_n) &\geq s(F_n) \geq n + 1. \\ ms(F_n) &\geq n + 1. \end{aligned} \quad (8)$$

A modular irregular labeling can be constructed and $ms(F_n)$ can be determined, and the conclusion is written in the following theorem. \square

Theorem 5. Let F_n be a friendship graph with $n \geq 2$. Then, $ms(F_n) = n + 1$.

Proof. We divide the proof in 4 cases. In each case, we define the edge labeling $\varphi: E(G) \rightarrow \{1, 2, \dots, 3n\}$ and show that φ is an $(n + 1)$ -labeling. Then, in the second step, we show that the vertex weights are all different. \square

3.1. Case $n \equiv 0 \pmod{4}$

Label the edges as follows.

$$\begin{aligned} \varphi(x_i y_i) &= \begin{cases} 2, & i = 1, \\ i + 2, & i = 2, 3, \dots, \frac{n}{2} \text{ and } i > \frac{n}{2}, i \text{ odd}, \\ i + 1, & i > \frac{n}{2}, i \text{ even}, \end{cases} \\ \varphi(x_i m) &= \begin{cases} 1, & i = 1, \\ i - 1, & i = 2, 3, \dots, \frac{n}{2} \text{ and } i > \frac{n}{2}, i \text{ odd}, \\ i, & i > \frac{n}{2}, i \text{ even}, \end{cases} \\ \varphi(y_i m) &= \begin{cases} 2, & i = 1, \\ i, & i = 2, 3, \dots, \frac{n}{2} \text{ and } i > \frac{n}{2}, i \text{ odd}, \\ i + 1, & i > \frac{n}{2}, i \text{ even}. \end{cases} \end{aligned} \tag{9}$$

(a) Let φ be an edge labeling of the friendship graph F_n that is defined above; we can obtain $\max\{\varphi(x_i y_i), \varphi(x_i m), \varphi(y_i m) : 1 \leq i \leq n\} = n + 1$.

Then, it is proved that the edge labeling φ is an $(n + 1)$ -labeling.

(b) The edges adjacent to x_1 are $x_1 y_1$ and $x_1 m$ so that for $i = 1$

$$wt_\varphi(x_1) = \varphi(x_1 y_1) + \varphi(x_1 m) = 2 + 1 = 3, \tag{10}$$

for $i = 2, 3, \dots, n/2$ and $i > n/2, i$ odd,

$$wt_\varphi(x_i) = \varphi(x_i y_i) + \varphi(x_i m) = 2i + 1, \tag{11}$$

for $i > n/2, i$ even,

$$wt_\varphi(x_i) = \varphi(x_i y_i) + \varphi(x_i m) = 2i + 1. \tag{12}$$

Thus, we have the vertex weight, $wt_\varphi(x_i) = 2i + 1, i = 1, 2, \dots, n$.

(c) The edges adjacent to y_1 is $x_1 y_1$ and $y_1 m$ so that for $i = 1$,

$$wt_\varphi(y_1) = \varphi(x_1 y_1) + \varphi(y_1 m) = 2 + 2 = 4. \tag{13}$$

For $i = 2, 3, \dots, n/2$ and $i > n/2, i$ odd,

$$\begin{aligned} wt_\varphi(y_i) &= \varphi(x_i y_i) + \varphi(y_i m) \\ &= i + 2 + i = 2i + 2. \end{aligned} \tag{14}$$

For $i > n/2, i$ even,

$$\begin{aligned} wt_\varphi(y_i) &= \varphi(x_i y_i) + \varphi(y_i m) \\ &= i + 1 + i + 1 = 2i + 2. \end{aligned} \tag{15}$$

Thus, we have the vertex weight, $wt_\varphi(y_i) = 2i + 2, i = 1, 2, \dots, n$.

(d) The edges adjacent to m are $x_i m$ and $y_i m$ so that

$$\begin{aligned} wt_\varphi(m) &= \sum_{i=1}^n (\varphi(x_i m) + \varphi(y_i m)) \\ &= 1 + \sum_{i=2}^{\frac{n}{2}} (i - 1) + \sum_{i=1}^{\frac{n}{4}} \left(\frac{n}{2} + (2i - 1) - 1\right) + \sum_{i=1}^{\frac{n}{4}} \left(\frac{n}{2} + 2i\right) \\ &\quad + 2 + \sum_{i=2}^{\frac{n}{2}} i + \sum_{i=1}^{\frac{n}{4}} \left(\frac{n}{2} + (2i - 1)\right) + \sum_{i=1}^{\frac{n}{4}} \left(\frac{n}{2} + 2i + 1\right) \\ &= n^2 + \frac{n}{2} + 2 = (2n + 1)\frac{n}{2} + 2 \equiv 2 \pmod{(2n + 1)}. \end{aligned} \tag{16}$$

3.2. Case $n \equiv 1 \pmod{4}, n > 1$

Label the edges as follows.

$$\begin{aligned} \varphi(x_i y_i) &= \begin{cases} i + 1, & i = 1, 2, \dots, \frac{n+3}{2} \text{ and } i > \frac{n+3}{2}, i \text{ odd}, \\ i + 2, & i > \frac{n+3}{2}, i \text{ even}. \end{cases} \\ \varphi(x_i m) &= \begin{cases} i, & i = 1, 2, \dots, \frac{n+3}{2} \text{ and } i > \frac{n+3}{2}, i \text{ odd}, \\ i - 1, & i > \frac{n+3}{2}, i \text{ even}. \end{cases} \\ \varphi(y_i m) &= \begin{cases} i + 1, & i = 1, 2, \dots, \frac{n+3}{2} \text{ and } i > \frac{n+3}{2}, i \text{ odd}, \\ i, & i > \frac{n+3}{2}, i \text{ even}. \end{cases} \end{aligned} \tag{17}$$

(a) Let φ be an edge labeling of the friendship graph F_n that is defined above; we can have $\max\{\varphi(x_i y_i), \varphi(x_i m), \varphi(y_i m) : 1 \leq i \leq n\} = n + 1$.

Then, it is proved that the edge labeling φ is an $(n+1)$ -labeling for the graph F_n .

- (b) The edges adjacent to x_i is $x_i y_i$ and $x_i m$ so that, for $i = 1, 2, \dots, n+3/2$ and $i > n+3/2$, i odd,

$$\begin{aligned} wt_{\varphi}(x_i) &= \varphi(x_i y_i) + \varphi(x_i m) \\ &= i + 1 + i = 2i + 1. \end{aligned} \quad (18)$$

For $i > n+3/2$, i even,

$$\begin{aligned} wt_{\varphi}(x_i) &= \varphi(x_i y_i) + \varphi(x_i m) \\ &= i + 2 + i - 1 = 2i + 1. \end{aligned} \quad (19)$$

Then, we have the vertex weight, $wt_{\varphi}(x_i) = 2i + 1$, $i = 1, 2, \dots, n$.

- (c) The edges adjacent to y_i are $x_i y_i$ and $y_i m$ so that, for $i = 1, 2, \dots, n+3/2$ and $i > n+3/2$, i odd,

$$\begin{aligned} wt_{\varphi}(y_i) &= \varphi(x_i y_i) + \varphi(y_i m) \\ &= i + 1 + i + 1 = 2i + 2. \end{aligned} \quad (20)$$

For $i > n+3/2$, i even,

$$\begin{aligned} wt_{\varphi}(y_i) &= \varphi(x_i y_i) + \varphi(y_i m) \\ &= i + 2 + i = 2i + 2. \end{aligned} \quad (21)$$

Then, we obtain the vertex weight $wt_{\varphi}(y_i) = 2i + 2$, $i = 1, 2, \dots, n$.

- (d) The edges adjacent to m are $x_i m$ and $y_i m$ so that

$$\begin{aligned} wt_{\varphi}(m) &= \sum_{i=1}^n (\varphi(x_i m) + \varphi(y_i m)) \\ &= \sum_{i=1}^{\frac{n+3}{2}} i + \sum_{i=1}^{\frac{n-1}{2}} \left(\frac{n+3}{2} + (2i-1) \right) \\ &\quad + \sum_{i=1}^{\frac{n-5}{2}} \left(\frac{n+3}{2} + 2i-1 \right) \\ &\quad + \sum_{i=1}^{\frac{n+3}{2}} (i+1) + \sum_{i=1}^{\frac{n-1}{2}} \left(\frac{n+3}{2} + (2i-1) + 1 \right) \\ &\quad + \sum_{i=1}^{\frac{n-5}{2}} \left(\frac{n+3}{2} + 2i \right) \\ &= (2n+1) \frac{n+1}{2} + 2 \equiv 2 \pmod{(2n+1)}. \end{aligned} \quad (22)$$

3.3. Case $n \equiv 2 \pmod{4}$

Label the edges as follows:

$$\varphi(x_i y_i) = \begin{cases} i, & i = 1, 2, \dots, \frac{n}{2}, \\ i+1 & i > \frac{n}{2}, i \text{ even}, \\ i+2 & i > \frac{n}{2}, i \text{ odd}, \end{cases} \quad (23)$$

$$\varphi(x_i m) = \begin{cases} i, & i = 1, 2, \dots, \frac{n}{2}, \\ i-1 & i > \frac{n}{2}, i \text{ even}, \\ i-2 & i > \frac{n}{2}, i \text{ odd}. \end{cases}$$

- (a) Let φ be an edge labeling of the friendship graph F_n that is defined above; we have $\max\{\varphi(x_i y_i), \varphi(x_i m), \varphi(y_i m)\} : 1 \leq i \leq n+1$.

Then, it is proved that the edge labeling φ is an $(n+1)$ -labeling for the graph F_n .

- (b) The edges adjacent to x_i are $x_i y_i$ and $x_i m$ so that, for $i = 1, 2, \dots, n/2$,

$$\begin{aligned} wt_{\varphi}(x_i) &= \varphi(x_i y_i) + \varphi(x_i m) \\ &= i + i = 2i. \end{aligned} \quad (24)$$

For $i > n/2$, i even,

$$\begin{aligned} wt_{\varphi}(x_i) &= \varphi(x_i y_i) + \varphi(x_i m) \\ &= i + 1 + i - 1 = 2i. \end{aligned} \quad (25)$$

For $i > n/2$, i odd,

$$\begin{aligned} wt_{\varphi}(x_i) &= \varphi(x_i y_i) + \varphi(x_i m) \\ &= i + 2 + i - 2 = 2i. \end{aligned} \quad (26)$$

Then, we obtain the vertex weight $wt_{\varphi}(x_i) = 2i$, $i = 1, 2, \dots, n$.

- (c) The edges adjacent to y_i are $x_i y_i$ and $y_i m$ so that, for $i = 1, 2, \dots, n/2$,

$$\begin{aligned} wt_{\varphi}(y_i) &= \varphi(x_i y_i) + \varphi(y_i m) \\ &= i + i + 1 = 2i + 1. \end{aligned} \quad (27)$$

For $i > n/2$, i even,

$$\begin{aligned} wt_{\varphi}(y_i) &= \varphi(x_i y_i) + \varphi(y_i m) \\ &= i + 1 + i = 2i + 1. \end{aligned} \quad (28)$$

For $i > n/2$, i odd,

$$wt_\varphi(y_i) = \varphi(x_i y_i) + \varphi(y_i m) = i + 2 + i - 1 = 2i + 1. \tag{29}$$

Then, we conclude that the vertex weight $wt_\varphi(y_i) = 2i + 1, i = 1, 2, \dots, n$.

(d) The edges adjacent to m are $x_i m$ and $y_i m$ so that

$$wt_\varphi(m) = \sum_{i=1}^n (\varphi(x_i m) + \varphi(y_i m)) = \sum_{i=1}^{\frac{n}{2}} i + \sum_{i=1}^{\frac{n+2}{4}} \left(\frac{n}{2} + (2i-1) - 1\right) + \sum_{i=1}^{\frac{n-2}{4}} \left(\frac{n}{2} + 2i - 2\right) + \sum_{i=1}^{\frac{n}{2}} (i+1) + \sum_{i=1}^{\frac{n+2}{4}} \left(\frac{n}{2} + (2i-1)\right) + \sum_{i=1}^{\frac{n-2}{4}} \left(\frac{n}{2} + 2i - 1\right) wt_\varphi(m) = (2n+1)\frac{n}{2} + 1 \equiv 1 \pmod{(2n+1)}. \tag{30}$$

3.4. Case $n \equiv 3 \pmod{4}, n > 3$

Label the edges as follows:

$$\varphi(x_i y_i) = \begin{cases} i, & i = 1, 2, \dots, \frac{n+3}{2} \text{ and } i > \frac{n+3}{2}, i \text{ even,} \\ i + 1, & i > \frac{n+3}{2}, i \text{ odd,} \end{cases} \varphi(x_i m) = \begin{cases} i, & i = 1, 2, \dots, \frac{n+3}{2} \text{ and } i > \frac{n+3}{2}, i \text{ even,} \\ i - 1, & i > \frac{n+3}{2}, i \text{ odd,} \end{cases} \varphi(y_i m) = \begin{cases} i + 1, & i = 1, 2, \dots, \frac{n+3}{2} \text{ and } i > \frac{n+3}{2}, i \text{ even,} \\ i, & i > \frac{n+3}{2}, i \text{ odd.} \end{cases} \tag{31}$$

(a) Let φ be an edge labeling of the friendship graph F_n that is defined above; we have $\max\{\varphi(x_i y_i), \varphi(x_i m), \varphi(y_i m) : 1 \leq i \leq n + 1\}$.

Then, it is proved that the edge labeling φ is an $(n + 1)$ -labeling for the graph F_n .

(b) The edges adjacent to x_i are $x_i y_i$ and $x_i m$ so that, for $i = 1, 2, \dots, n + 3/2$ and $i > n + 3/2, i$ even,

$$wt_\varphi(x_i) = \varphi(x_i y_i) + \varphi(x_i m) = i + i = 2i. \tag{32}$$

For $i > n + 3/2, i$ odd,

$$wt_\varphi(x_i) = \varphi(x_i y_i) + \varphi(x_i m) = i + 1 + i - 1 = 2i. \tag{33}$$

Then, we have the vertex weight $wt_\varphi(x_i) = 2i, i = 1, 2, \dots, n$.

(c) The edges adjacent to y_i are $x_i y_i$ and $y_i m$ so that, for $i = 1, 2, \dots, n + 3/2$ and $i > n + 3/2, i$ even,

$$wt_\varphi(y_i) = \varphi(x_i y_i) + \varphi(y_i m) = i + i + 1 = 2i + 1. \tag{34}$$

For $i > n + 3/2, i$ odd,

$$wt_\varphi(y_i) = \varphi(x_i y_i) + \varphi(y_i m) = i + 1 + i = 2i + 1. \tag{35}$$

Then, we can conclude that the vertex weight $wt_\varphi(y_i) = 2i + 1, i = 1, 2, \dots, n$.

(d) The edges adjacent to m are $x_i m$ and $y_i m$ so that

$$wt_\varphi(m) = \sum_{i=1}^n (\varphi(x_i m) + \varphi(y_i m)) = \sum_{i=1}^{\frac{n+3}{2}} i + \sum_{i=1}^{\frac{n-3}{4}} \left(\frac{n+3}{2} + (2i-1)\right) + \sum_{i=1}^{\frac{n-3}{4}} \left(\frac{n+3}{2} + 2i - 1\right) + \sum_{i=1}^{\frac{n+3}{2}} (i+1) + \sum_{i=1}^{\frac{n-3}{4}} \left(\frac{n+3}{2} + (2i-1) + 1\right) + \sum_{i=1}^{\frac{n-3}{4}} \left(\frac{n+3}{2} + 2i\right) wt_\varphi(m) = (2n+1)\frac{n+1}{2} + 1 \equiv 1 \pmod{(2k(2n+1))}. \tag{36}$$

In all cases, we proved that the vertex weights are all different and the maximum label is $n + 1$. By combining the results $(ms(F_n) \leq n + 1)$ and Lemma 1 $(ms(F_n) \geq n + 1)$, we conclude that $ms(F_n) = n + 1, \text{ for } n \geq 2$.

From Theorem 5, we have $ms(F_n) = n + 1$ is equal to the lower bound of the irregularity strength from Theorem 1. We can conclude that the friendship graph has irregular labeling with $s(F_n) = n + 1$.

Corollary 1. *The friendship graph F_n has the irregularity strength $s(F_n) = n + 1$ for $n \geq 2$.*

4. Conclusion

In this paper, we prove the modular irregularity strength of two graphs, which are the regular double-star graph $S_{k,k}$, that has $ms(S_{k,k}) = 2k$, for $k \geq 1$ and k is odd and for the friendship graph F_n that has $ms(F_n) = n + 1$ and $s(F_n) = n + 1$, for $n \geq 2$. There are still many families of graphs that can be explored to determine its modular irregularity strength.

Data Availability

No data were used to support this study.

Conflicts of Interest

The authors declare that there are no conflicts of interest.

Authors' Contributions

K.A.S. and Z.Z.B. conceptualized the study; K.A.S. developed the methodology; K.A.S., Z.Z.B, N.H., and R.S. validated the study; K.A.S. and Z.Z.B. wrote and prepared the original draft; K.A.S., Z.Z.B, N.H., and R.S. reviewed and edited the manuscript; K.A.S. helped with funding acquisition. All authors have read and agreed to the published version of the manuscript.

Acknowledgments

This research was funded by PPKI-UI Research (Grant no. NKB-461/UN2.RST/HKP.05.00/2021).



References

- [1] J. A. Gallian, "A dynamic survey of graph labeling," *The Electronic Journal of Combinatorics*, vol. 19, 2020.
- [2] G. Chartrand, M. S. Jacobon, J. Lehel, O. R. Oellermann, S. Ruiz, and F. Saba, "Irregular network," *Congressus Numerantium*, vol. 64, pp. 187–192, 1988.
- [3] D. B. West, *An Introduction to Graph Theory*, Prentice-Hall, Hoboken, NY, USA, 1996.
- [4] J. Przybylo, "Irregularity strength of regular graphs," *Electronic Journal of Combinatorics*, vol. 15, 2008.
- [5] M. Aigner and E. Triesch, "Irregular Assignments of Trees and Forests," *SIAM Journal on Discrete Mathematics*, vol. 3, no. 4, pp. 439–449, 1990.
- [6] M. Ferrara, R. Gould, M. Pfender, and F. Pfender, "An iterative approach to graph irregularity strength," *Discrete Applied Mathematics*, vol. 158, no. 11, pp. 1189–1194, 2010.
- [7] M. Bača, S. Jendrol, K. Kathiresan, K. Muthugurupackiam, and A. Semaničová-Feňovčíková, "A survey of irregularity strength," *Electronic Notes in Discrete Mathematics*, vol. 48, pp. 19–26, 2015.
- [8] M. Baca, K. Muthugurupackiam, K. Kathiresan, and S. Ramya, "Modular irregularity strength of graphs," *Electronic Journal of Graph Theory and Applications*, vol. 8, no. 2, pp. 435–443, 2020.
- [9] K. Muthugurupackiam and S. Ramya, "Modular irregularity strength of two classes of graphs," *Journal of Computer and Mathematical Sciences*, vol. 9, no. 9, pp. 1132–1141, 2018.

- [10] M. Bača, Z. Kimákov, M. Lascsáková, and A. Semaničová-Feňovčíková, "The irregularity and modular irregularity strength of fan graphs," *Symmetry*, vol. 13, no. 4, p. 605, 2021.

Research Article

Research on Energy Efficiency Management of Forklift Based on Improved YOLOv5 Algorithm

Zhenyu Li,¹ Ke Lu,² Yanhui Zhang,³ Zongwei Li ¹ and Jia-Bao Liu ⁴

¹School of Economics and Management, Shanghai Institute of Technology, Shanghai 200030, China

²School of Management Science and Engineering, Anhui University of Technology, Maanshan 243032, China

³Business School, East China University of Science and Technology, Shanghai 200030, China

⁴School of Mathematics and Physics, Anhui Jianzhu University, Hefei 230601, China

Correspondence should be addressed to Zongwei Li; lzw0118@163.com

Received 6 September 2021; Revised 28 September 2021; Accepted 6 December 2021; Published 21 December 2021

Academic Editor: Clemente Cesarano

Copyright © 2021 Zhenyu Li et al. This is an open access article distributed under the Creative Commons Attribution License, which permits unrestricted use, distribution, and reproduction in any medium, provided the original work is properly cited.

As an important tool for loading, unloading, and distributing palletized goods, forklifts are widely used in different links of industrial production process. However, due to the rapid increase in the types and quantities of goods, item statistics have become a major bottleneck in production. Based on machine vision, the paper proposes a method to count the amount of goods loaded and unloaded within the working time limit to analyze the efficiency of the forklift. The proposed method includes the data preprocessing section and the object detection section. In the data preprocessing section, through operations such as framing and clustering the collected video data and using the improved image hash algorithm to remove similar images, a new dataset of forklift goods was built. In the object detection section, the attention mechanism and the replacement network layer were used to improve the performance of YOLOv5. The experimented results showed that, compared with the original YOLOv5 model, the improved model is lighter in size and faster in detection speed without loss of detection precision, which could also meet the requirements for real-time statistics on the operation efficiency of forklifts.

1. Introduction

With the continuous development of intelligent logistics centered on industrial production, the demand for machine vision is increasing. In the industrial logistics system, forklifts play an important role in transferring and storing goods. However, in most factories, due to the huge number of forklifts and the wide variety of goods, the main impediment to the traditional management methods is the inability to effectively evaluate the efficiency of forklifts.

In recent years, intelligent logistics applying machine vision and deep learning has become a research hotspot. As a basic research direction in intelligent logistics, object detection has a profound impact on energy efficiency management [1]. Himstedt and Maehle [2] proposed a forklift detection solution based on 3D camera and SVM classifier, which could accurately detect the object. However, the distance range and size range of the object needed to be preset, and the generalization ability of the model was poor.

Mohamed et al. [3] combined 2D laser rangefinder and Faster R-CNN model for pallet localisation. Although the accuracy was high, the efficiency was low. Li et al. [4] used TITAN X GPU to detect forklift pallets. The detection speed was fast, but the hardware cost was expensive and the embedding effect was poor. Iinuma et al. [5] used single shot multibox detector (SSD) as a detection model. Although the model had good mobility, the detection accuracy was limited due to the insufficient features. In summary, although a large number of scholars have done extensive research on forklift object detection, in real industrial production, data collection, hardware selection, and model selection have limited the application of deep learning.

To address the above problems, achieve a balance regardless of speed, accuracy, and model size, and adapt to complex and diverse operating environments, this research improves the backbone network structure of YOLOv5 and uses a lighter feature extraction network to reduce the redundancy features. In this process, the introduction of

mechanism module maintains the detection accuracy. The experimental results showed that our model performed well on the self-built complex scene forklift goods dataset. The key contributions of this work are as follows:

- (i) The YOLOv5 model is improved by combining the GhostNet module and squeeze-and-excitation attention mechanism, and then the improved model is used to detect forklifts.
- (ii) The improved image hash algorithm based on PCA is used to remove similar images in image pre-processing section.
- (iii) Compared with the original model, the improved YOLOv5 model reduces the amount of calculation by 2/3 while not reducing the precision.
- (iv) The improved YOLOv5 model is more robust and effective for mobile edge computing devices.

2. Related Work

As one of the core segments in the domain of machine vision, object detection is a technology which digs the object potential category and location information from an image. Since there are many types of objects, the size, position, and posture of a similar object in the image are often different, and the interference caused by different imaging conditions also brings some difficulties, so object detection is full of challenges.

Before the widespread application of deep learning, traditional algorithms for object detection determined the object location and size by traversing the image using sliding windows of different sizes and simultaneously extracted artificially defined robust features, for instance, scale-invariant feature transform (SIFT) [6] and histogram of oriented gradients (HOG) [7]. Therefore, object detection combined with deep learning uses convolutional neural network to extract features to break the limitations of manual feature extraction.

2.1. Faster R-CNN. Faster R-CNN [8], originated from R-CNN [9], is widely utilized in object detection work. In R-CNN, 4 independent steps are used: candidate regions generation by selective search, feature extraction by CNN, SVM classification, and bounding box regression, which consumes a lot of time. Fast R-CNN [10] reduces the time consumed and improves accuracy through operations such as mapping candidate regions to features, ROI pooling, and FC layer. Since Fast R-CNN is not a true end-to-end work, Faster R-CNN unifies the 4 independent steps into one neural network. After that, on the basis of Faster R-CNN, many scholars proposed a variety of object detection algorithms to adapt to different tasks. The method of increasing the center loss function to reduce the intra-class variation of the learned features performed well in face detection [11]. Zhong et al. [12] replaced the bounding box regression module with the LocNet-based positioning module, which improved the positioning precision of natural scene text detection. Although the accuracy of these

models has gradually reached the accuracy limit of machine vision tasks, the scale of the models has also grown exponentially. An excessive model size leads to higher requirements for hardware, which causes great resistance to achieve real-time detection in embedded devices.

2.2. YOLOv5. Compared with the R-CNN series, the most significant advantage of the YOLO (You Only Look Once) series is that they have faster detection speed. Redmon et al. [13] first proposed YOLOv1, which unified object classification and bounding box regression into a regression problem. This frame design makes YOLOv1 extremely fast in image processing, but compared with R-CNN, YOLOv1 has a larger coordinate error. Thus, Redmon and Farhadi [14] proposed YOLOv2, which improved the detection accuracy by improving the network structure and training methods. Later, on the basis of YOLOv2, Redmon and Farhadi [15] further proposed YOLOv3 by expanding the network to Darknet-53, which significantly improved the ability of small object recognition.

As the detection accuracy of YOLOv3 still has a gap with Faster R-CNN, Bochkovski et al. [16] proposed YOLOv4. YOLOv4 combines different detection techniques to achieve the best counterpoise between detection precision and inference speed based on a massive convincing experiments. In the same year, Ultralytics released YOLOv5. YOLOv5 is a classic representative of one-stage object detection algorithm, including four parts: Input, Backbone, Neck, and Prediction. In Input, YOLOv5, like YOLOv4, uses the mosaic method to enhance data, which is very effective for small object detection. Compared with YOLOv4, YOLOv5 not only uses Cross Stage Partial Network (CSPNet) [17] for Backbone but also uses the same for Neck to enhance feature fusion. It is also worth mentioning that YOLOv5 uses Path Aggregation Network (PAN) [18] and Feature Pyramid Network (FPN) [19] operations on Neck. FPN conveys powerful semantic features through upsampling, and PAN is used to convey dense positioning features.

YOLOv5 initially provides four object detection network models: yolov5s, yolov5m, yolov5l, and yolov5x, which contain different network depths and feature map widths. From these models, yolov5s shows its character for the lightest size and the fastest speed. On the contrary, it has the lowest average precision (AP), but it is ideal for detecting large objects. For satisfying the demands for real-time object detection on the basic processor, it is meaningful to further improve the YOLOv5 model.

3. Method

First, a monocular 2D camera is deployed on the top of the forklift cab to photograph the goods on the pallet in front of the forklift. After obtaining the video stream of the actual scene, we intercept the images at the same number of frames to form an image resource library. Then, the images are clustered, and an improved image hash algorithm is used to filter duplicate images to avoid manual filtering of differences in subjective judgments and save a lot of time cost.

The final obtained images are used as the source files of the dataset, and the category and location data are obtained through manual marking. In this paper, YOLOv5 is used as the machine vision detection algorithm, and the network framework is improved to achieve real-time and accurate acquisition of the forklift transportation status. Our object detection method is demonstrated in Figure 1.

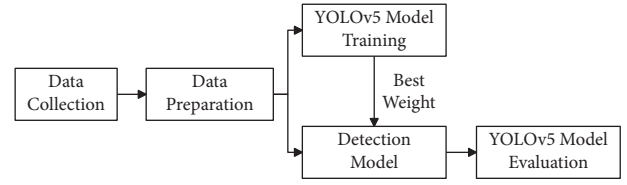


FIGURE 1: Object detection process.

3.1. Data Preprocessing. This paper constructs a forklift dataset to detect the status of goods. Video was obtained by following the driver's driving process in the field workshop. Complex samples of different weather conditions, different time periods, and different locations were collected. Through the operations shown in Figure 2, a dataset containing four different statuses of full tray, half tray, empty, and loading-unloading was constructed. The self-built forklift dataset is close to the complex and changeable industrial reality scene, which poses greater challenges to the network performance of object detection.

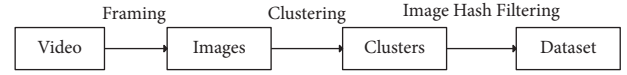


FIGURE 2: Data preprocessing.

Since the amount of data after framing is large and there are many similar images, the workload of direct deletion is too large. Therefore, a clustering algorithm can be used to peel off the semantic information of the images. For balancing the clustering effect and computing time, the number of clusters in this experiment was set to 9. After clustering, it is easy to delete images.

After clustering, the images in the same cluster are relatively similar, and a large-scale comparison is required to eliminate similar images. Hash algorithm [20], as a single mapping function, can compress a fixed-size input into a fixed-length output, which has the advantages of improving storage data utilization and improving data query efficiency. The image hash algorithm [21] takes the human visual system as a reference to extract the perceptual robust features in the image and map images with the same visual perception to the same or similar hash value. For different visual perception images, the hash algorithm generates completely different hash values.

Image hash algorithm based on principal component analysis (PCA) can quickly generate the image hash values [22]. First, the original image with a size of 608×304 is subjected to grayscale processing and a filter is used to eliminate the noise of image. Then, the image is segmented into 32 nonoverlapping image fragments with a size of 76×76 . The pixels of the image fragment are connected in the order of left to right and top to bottom to construct 32 5776-dimensional vectors. Because the vector dimension is too high, the calculation speed will be reduced, so PCA is used to reduce the data dimension to 10 dimensions by the following equation:

$$p^k \times v = v^k, \quad (1)$$

where p^k is the base and v is the high-dimensional vector representing the image. v is mapped to p^k to obtain the reduced dimensionality target v^k .

Finally, a secret key is designed to generate a hash value, and a 32-dimensional feature vector is output to represent

the original image. Figure 3 typically illustrates the circuit of the image hash algorithm.

The correlation coefficient between the hash values of different images is calculated in the same cluster, and a threshold is set to filter similar images to solve the problem of self-built dataset redundancy. The similarity function is given by the following equation:

$$c(h_1, h_2) = \frac{\text{cov}(h_1, h_2)}{\sqrt{\text{var}(h_1)}\sqrt{\text{var}(h_2)}}, \quad (2)$$

where h_1 is the hash value of image 1, h_2 is the hash value of image 2, $\text{var}(h_1)$ is the variance of h_1 , $\text{var}(h_2)$ is the variance of h_2 , and $\text{cov}(h_1, h_2)$ is the covariance between h_1 and h_2 .

3.2. Improved YOLOv5 Model. Although the accuracy of the original YOLOv5 model meets our demand for forklift object detection, the detection speed needs to be improved for embedded devices and mobile terminal operations with limited computing power. Based on the analysis of YOLOv5 network structure, a new lightweight object detection model is rebuilt in this research. The modified model uses GhostBottleneck (GB) module to replace the original network layers and introduces Squeeze-and-Excitation (SE) attention mechanism. While improving the detection speed and making the model more miniature, this model can ensure the accuracy of the detection.

3.2.1. GhostBottleneck Module. Aiming at settling the problem of limited computing power of mobile devices, we adopt the GhostNet [23] structure specially designed for mobile devices. The core of GhostNet is to generate rich feature maps using linear operations. In the convolution module of the original YOLOv5 network, feature extraction produces too many similar redundant feature maps. The GB module used in this paper first uses ordinary convolution to obtain partial feature maps and then performs linear convolution operations to amplify them to the same number of feature maps as the original network. At the same time, because the calculation amount of linear convolution is much smaller than that of ordinary convolution, the calculation amount of the

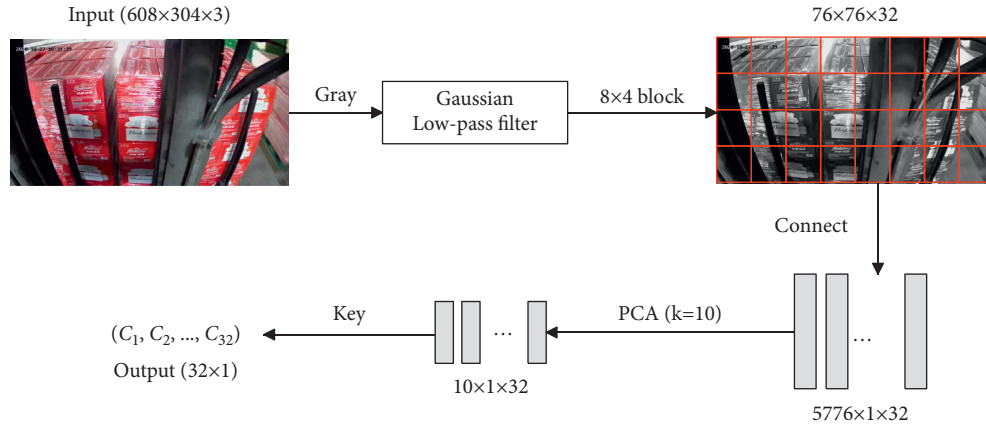


FIGURE 3: Image hash algorithm based on PCA.

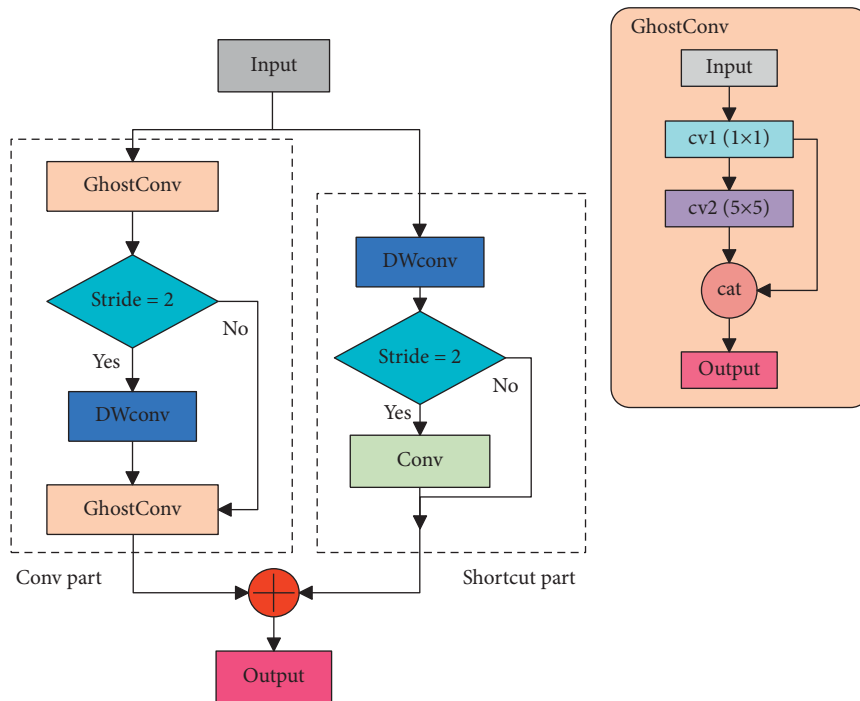


FIGURE 4: GhostBottleneck module.

model is reduced by about half. The GB module is divided into a Conv part and a Shortcut part, with the framework shown in Figure 4.

Figure 4 can be noticed that the feature map is used as the input of GB module. In the Conv part, the first GhostConv layer is used to realize the channel expansion, and then the second GhostConv layer is executed to match the Shortcut part. Due to the divergence of the gradient, simply deepening the network can hardly ensure the improvement of network performance. Actually, Shortcut part and Conv part are added as the output, which adaptively adjusts the quantity of network output channels while ensuring the effect of the model.

GhostConv in the GB module is connected by two different convolutional layers, cv1 and cv2. First, the cv1 layer uses a 1×1 convolution kernel to achieve deeper

feature extraction. Then, the cv2 layer uses a 5×5 convolution kernel to separate multiscale local feature information through linear transformation. Finally, the results of cv1 layer and cv2 layer are connected and output together. The GhostConv network guarantees the convolution effect through grouped convolution while greatly reducing the model complexity.

3.2.2. Squeeze-and-Excitation Module. The forklift pallet occupies a large area in the image, and all channels are of the same importance. There is still room for improvement of detection accuracy in this aspect. SE block was proposed by Hu et al. [24], which adaptively adjusts the feature responses of different channels by paying attention to the relationship between channels.

The SE module includes two parts, Squeeze and Excitation. After the continuous convolution stacking of the GB layer, problems such as model overfitting may occur. In the Squeeze part, the global feature is generated by performing global average pooling operation on the feature map layer. Then, the entire network is regularized to prevent overfitting. The output of $1 \times 1 \times C$ is given by the following equation:

$$z_c = F_{sq}(U_c) = \frac{1}{H \times W} \sum_{i=1}^H \sum_{j=1}^W u_c(i, j), \quad (3)$$

where u_c is the result of the previous layer of convolution and H and W denote the height and width of the feature map, separately.

Subsequently, the Excitation part obtains the connection between the channels by connecting the FC layer. The equation is as follows:

$$F_{ex}(z, W) = \sigma(g(z, W)) = \sigma(W_2 \text{ReLU}(W_1 z)), \quad (4)$$

where W_1 is the parameter of dimensionality reduction layer and W_2 is the parameter of dimensionality enhancement layer. Such an operation balances performance and calculation. To guarantee that the weight of the output is between 0 and 1, the sigmoid activation function is chosen.

Finally, in the scale layer, the normalized weights are multiplied with the original features for output. On our self-built dataset, the SE layer is used to extract more directional features. Although SE block inevitably increases some parameters and calculations, the improved network structure shows better performance.

The improved YOLOv5 model framework in this paper is mainly composed of Input, Backbone, Neck, and Prediction. First, Backbone is utilized to refine fine-grained features of different input images to obtain rich semantic information and location information. Then, the design of FPN + PAN occupies Neck. The FPN of path combination uses upsampling to fuse the features extracted by Backbone to convey strong semantic features. PAN's feature pyramid structure strengthens the model to convey strong positioning features, which is conducive to the detection of an object at different scales. Finally, the Prediction part predicts the bounding box, category, and other information and maps them to the corresponding image. After replacing the network layer with the GhostBottleneck module and introducing the attention mechanism, we cut the quantity of parameters sharply and lower the complexity of the model effectively, while maintaining the precision compared with the original model. The overall improved YOLOv5 model is shown in Figure 5, and the computational complexity is 5.6 GFLOPS.

4. Experiment and Discussion

4.1. Experimental Environment. In this research, two different configurations were used for model training and testing. Table 1 lists the specific configuration of the training environment.

After obtaining the weights after training, the model was deployed on the mobile edge computing device Jetson Nano

for performance testing. The specific information of the device is shown in Table 2. The experimental environment was close to the actual application scenario.

4.2. Training Result Analysis. For objective evaluation, we compared the improved yolov5s model with the original YOLOv5 v3.0 yolov5s model and the YOLOv5 v4.0 yolov5s model on the self-built dataset. The only difference was that YOLOv5 v3.0 used the BottleneckCSP module, and YOLOv5 v4.0 used the C3 module, so we called them the former yolov5s_CSP, the latter yolov5s_C3, and our model yolov5s_GS. Table 3 gathers and compares layers, parameters, and GFLOPS of the three different models.

According to Table 3, our model network was built in a deeper manner through the improvement of the backbone network, while the model parameters were reduced by about 2/3, thereby reaching the goal of model complexity reduction effectively.

4.2.1. Indexes and Training Details. The most commonly used indexes for quantitatively evaluating the effectiveness of object detection algorithms are precision and recall, which are expressed by equations (5) and (6):

$$\text{precision} = \frac{TP}{TP + FP}, \quad (5)$$

$$\text{recall} = \frac{TP}{TP + FN}, \quad (6)$$

where TP refers to the quantity of objects that we judged correctly, FP refers to the quantity of objects that we judged incorrectly, and FN refers to the quantity of objects that we should have judged correctly but missed.

This paper uses mAP@0.5 and mAP@0.5:0.95, which are related to both precision and recall, as indexes to quantitatively judge whether the object detection methods meet accuracy and speed requirements [25].

The training process was monitored, and in each iteration, mAP@0.5 and mAP@0.5:0.95 were calculated. After spending 0.732 h to train yolov5s_C3, 0.758 h to train yolov5s_CSP, and 0.849 h to train our model yolov5s_GS, we obtained two line graphs of the three models of mAP, as shown in Figure 6. The figure reveals that our model had less fluctuation and faster convergence, compared with the original YOLOv5 model.

At the same time, the cls_loss (class loss) and obj_loss (object loss) [26] of each iteration in the training process are shown in Figure 7, indicating the good convergence of our model.

4.3. Performance Test on Mobile Devices. As a small computer, Jetson Nano has good computing power that can complete object detection tasks, and its small size can also meet the needs of embedded development and mobile terminal operation. The model was deployed on Jetson Nano to simulate the object detection reasoning process in real industrial scenarios. In Table 4, the performance indexes of different models are displayed.

On mAP@0.5:0.95, it can be found from Table 4 that our model yolov5s_GS is only about 1.2% lower than the best

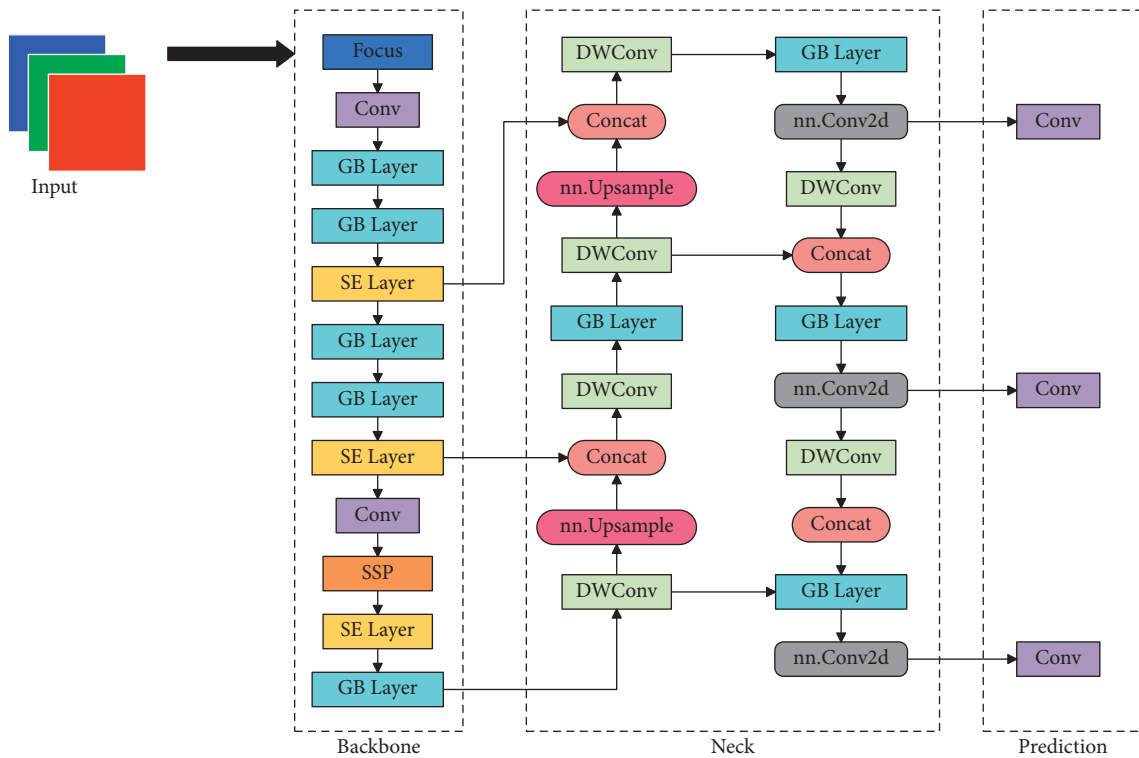


FIGURE 5: Improved YOLOv5 network.

TABLE 1: Configuration of training environment.

Item	Item value
Operation system	Ubuntu18.04
CPU	Intel Core i9-10980XE @ 3.00 GHz
GPU	GeForce RTX 3070
Hardware acceleration	CUDA10.1

TABLE 2: Configuration of inferencing environment.

Item	Items value
Operation system	Ubuntu18.04
CPU	4-core ARM A57 @1.43 GHz
GPU	128-core Maxwell
Hardware acceleration	CUDA10.1

TABLE 3: Models compared.

Model	Layers	Parameters	GFLOPS
yolov5s_C3	283	7071633	16.4
yolov5s_CSP	283	7263185	16.8
yolov5s_GS	419	2551101	5.6

performing model yolov5s_C3, while yolov5s_GS is about 0.85% higher than yolov5s_C3 on mAP@0.5%. In terms of weight, it can be seen that the size of our model after training was only 5.4 MB. From the perspective of detection time, the detection time of our model was reduced to 0.118 s/frame compared with the original network. At the same time, larger frames per second (FPS) also mean that our model could detect more images per second.

Combined with actual application scenarios, our model realized embedded development and met the requirements of real-time detection. Compared with the original YOLOv5 model, the size of our model is reduced to 1/3, and the detection speed is significantly expedited without reducing the detection precision. It can be found from Figure 8 that in complex industrial scenarios, our improved model was more robust.

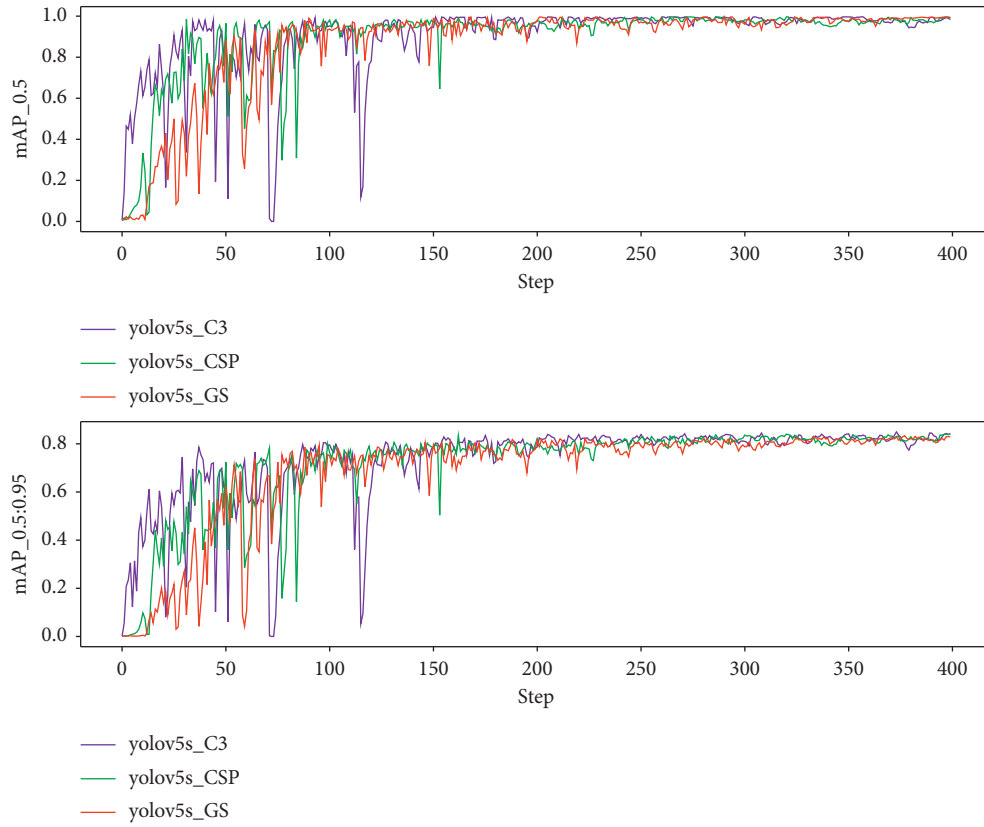


FIGURE 6: mAP of different models.

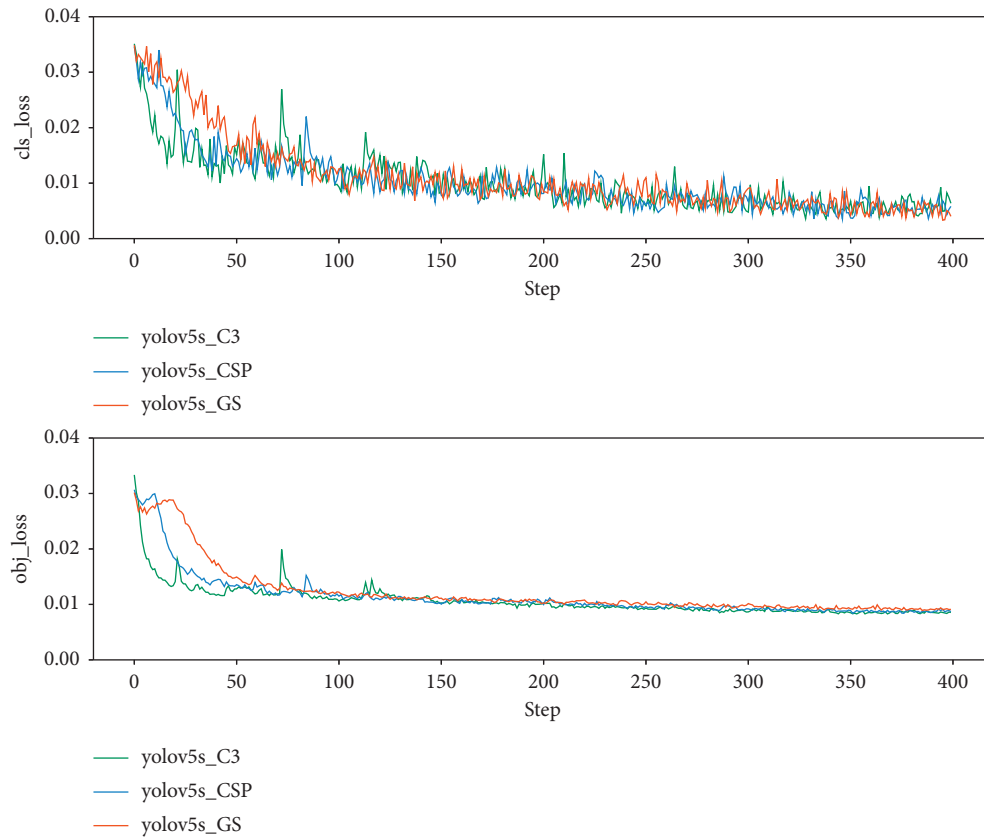


FIGURE 7: Loss of different models.

TABLE 4: Performance indexes of different models.

Model	mAP0.5	mAP0.5:0.95	Model size (MB)	Time (s)	FPS
yolov5s_C3	0.98321	0.84177	14.4	0.146	6.85
yolov5s_CSP	0.99371	0.84001	14.8	0.155	6.45
yolov5s_GS	0.99172	0.82959	5.4	0.118	8.47

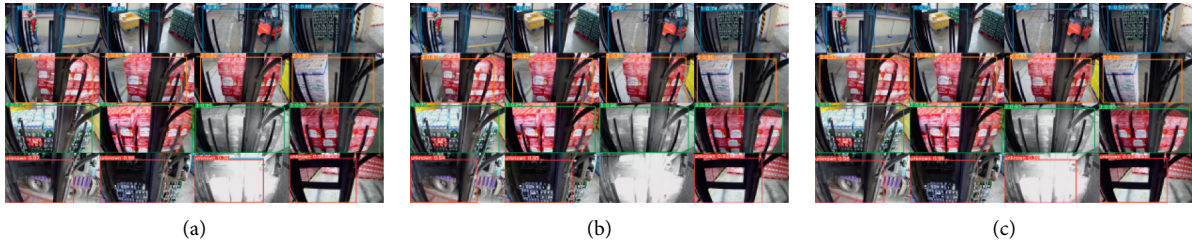


FIGURE 8: Real scene forklift detection images of yolov5s_C3 (a), yolov5s_CSP (b), and yolov5s_GS (c).

5. Conclusions

We present an improved object detection method in this paper which can be applied to forklifts. First, a complex scene forklift goods dataset is constructed. The reason why YOLOv5 is chosen as the object detection algorithm is that compared with Faster R-CNN, YOLOv5 has faster detection speed, smaller model, and lower hardware requirements, which is suitable for mobile device operation and embedded development. Then, in the object detection section, specific modifications are made to the YOLOv5 model, which further enhance the detection speed of YOLOv5 and reduce the model size compared to the original model while maintaining the detection accuracy. Finally, our proposed method performs well on forklift object detection tasks. Due to being lightweight and having extremely fast speed, our method is also fit for other scenarios restricted by hardware resources and applications that have high requirements for real-time detection, such as mobile device QR code positioning, natural scene text detection, and autonomous driving. In the future, we will also consider migrating this method to other fields to orient diverse and complex object detection tasks.

Data Availability

The experimental data used to support the findings of this study are available from the corresponding author upon request.

Conflicts of Interest

The authors declare that they have no conflicts of interest.

Acknowledgments

This study was supported by the National Natural Science Foundation of China (71974130), the National Social Science Fund of China (18BGL093), and the Shanghai Pujiang Program (2019PJ096). The authors are thankful for the support.

References

- [1] A. Al-Shaebi, N. Khader, H. Daoud, J. Weiss, and S. W. Yoon, "The effect of forklift driver behavior on energy consumption and productivity," *Procedia Manufacturing*, vol. 11, pp. 778–786, 2017.
- [2] M. Himstedt and E. Maehle, "Camera-based obstacle classification for automated reach trucks using deep learning," in *Proceedings of the ISR 2016: 47th International Symposium on Robotics*, pp. 1–6, Munich, Germany, June 2016.
- [3] I. S. Mohamed, A. Capitanelli, F. Mastrogiovanni, S. Rovetta, and R. Zaccaria, "Detection, localisation and tracking of pallets using machine learning techniques and 2D range data," *Neural Computing & Applications*, vol. 32, no. 13, pp. 8811–8828, 2019.
- [4] T. Li, B. Huang, C. Li, and M. Huang, "Application of convolution neural network object detection algorithm in logistics warehouse," *Journal of Engineering*, vol. 2019, no. 23, pp. 9053–9058, 2019.
- [5] R. Iinuma, Y. Kojima, H. Onoyama, T. Fukao, S. Hattori, and Y. Nonogaki, "Pallet handling system with an autonomous forklift for outdoor fields," *Journal of Robotics and Mechatronics*, vol. 32, no. 5, pp. 1071–1079, 2020.
- [6] T. Lindeberg, "Scale invariant feature transform," *Scholarpedia*, vol. 7, no. 5, Article ID 10491, 2012.
- [7] P. E. Rybski, D. Huber, D. D. Morris, and R. Hoffman, "Visual classification of coarse vehicle orientation using histogram of oriented gradients features," in *Proceedings of the 2010 IEEE Intelligent Vehicles Symposium*, pp. 921–928, La Jolla, CA, USA, June 2010.
- [8] S. Ren, K. He, R. Girshick, and J. Sun, "Faster R-CNN: towards real-time object detection with region proposal networks," *IEEE Transactions on Pattern Analysis and Machine Intelligence*, vol. 39, no. 6, pp. 1137–1149, 2017.
- [9] R. Girshick, J. Donahue, T. Darrell, and J. Malik, "Rich feature hierarchies for accurate object detection and semantic segmentation," in *Proceedings of the IEEE conference on computer vision and pattern recognition*, pp. 580–587, Columbus, OH, USA, June 2014.
- [10] R. Girshick, "Fast R-CNN," in *Proceedings of the IEEE international conference on computer vision*, pp. 1440–1448, Santiago, Chile, December 2015.
- [11] H. Wang, Z. Li, X. Ji, and Y. Wang, "Face R-CNN," 2017, <https://arxiv.org/abs/1706.01061>.

- [12] Z. Zhong, L. Sun, and Q. Huo, "Improved localization accuracy by LocNet for Faster R-CNN based text detection in natural scene images," *Pattern Recognition*, vol. 96, Article ID 106986, 2017.
- [13] J. Redmon, S. Divvala, R. Girshick, and A. Farhadi, "You only look once: unified, real-time object detection," in *Proceedings of the IEEE conference on computer vision and pattern recognition*, pp. 779–788, Las Vegas, NV, USA, June 2016.
- [14] J. Redmon and A. Farhadi, "YOLO9000: better, faster, stronger," in *Proceedings of the IEEE conference on computer vision and pattern recognition*, pp. 7263–7271, Honolulu, HI, USA, July 2017.
- [15] J. Redmon and A. Farhadi, "Yolov3: an incremental improvement," 2018, <https://arxiv.org/abs/1804.02767>.
- [16] A. Bochkovskiy, C.-Y. Wang, and H.-Y. M. Liao, "Yolov4: optimal speed and accuracy of object detection," 2020, <https://arxiv.org/abs/2004.10934>.
- [17] C.-Y. Wang, H.-Y. M. Liao, Y.-H. Wu, P.-Y. Chen, J.-W. Hsieh, and I.-H. Yeh, "CSPNet: a new backbone that can enhance learning capability of CNN," in *Proceedings of the IEEE/CVF conference on computer vision and pattern recognition workshops*, pp. 390–391, Seattle, WA, USA, June 2020.
- [18] S. Liu, L. Qi, H. Qin, J. Shi, and J. Jia, "Path aggregation network for instance segmentation," in *Proceedings of the IEEE conference on computer vision and pattern recognition*, pp. 8759–8768, Salt Lake City, UT, USA, June 2018.
- [19] T.-Y. Lin, P. Dollár, R. Girshick, K. He, B. Hariharan, and S. Belongie, "Feature pyramid networks for object detection," in *Proceedings of the IEEE conference on computer vision and pattern recognition*, pp. 2117–2125, Honolulu, HI, USA, July 2017.
- [20] D. Eastlake and P. Jones, "US secure hash algorithm 1 (SHA1)," *IETF Request for Comments*, vol. 3174, 2001.
- [21] R. Venkatesan, S.-M. Koon, M. H. Jakubowski, and P. Moulin, "Robust image hashing," in *Proceedings of the 2000 International Conference on Image Processing*, pp. 664–666, Vancouver, BC, Canada, September 2000.
- [22] X. Liang, Z. Tang, X. Xie, J. Wu, and X. Zhang, "Robust and fast image hashing with two-dimensional PCA," *Multimedia Systems*, vol. 27, no. 3, pp. 389–401, 2021.
- [23] K. Han, Y. Wang, Q. Tian, J. Guo, C. Xu, and C. Xu, "GhostNet: more features from cheap operations," in *Proceedings of the IEEE/CVF Conference on Computer Vision and Pattern Recognition*, pp. 1580–1589, Seattle, WA, USA, June 2020.
- [24] J. Hu, L. Shen, and G. Sun, "Squeeze-and-excitation networks," in *Proceedings of the IEEE conference on computer vision and pattern recognition*, pp. 7132–7141, Salt Lake City, UT, USA, June 2018.
- [25] F. Borisyuk, A. Gordo, and V. Sivakumar, "Rosetta: large scale system for text detection and recognition in images," in *Proceedings of the 24th ACM SIGKDD International Conference on Knowledge Discovery & Data Mining*, pp. 71–79, New York, NY, USA, July 2018.
- [26] S. Hoory, T. Shapira, A. Shabtai, and Y. Elovici, "Dynamic adversarial patch for evading object detection models," 2020, <https://arxiv.org/abs/2010.13070>.

Research Article

Radio Labelings of Lexicographic Product of Some Graphs

Muhammad Shahbaz Aasi , Muhammad Asif , Tanveer Iqbal ,
and Muhammad Ibrahim 

Centre for Advanced Studies in Pure and Applied Mathematics, Bahauddin Zakariya University, Multan, Pakistan

Correspondence should be addressed to Muhammad Shahbaz Aasi; mshahbazasi@gmail.com

Received 13 September 2021; Accepted 2 November 2021; Published 7 December 2021

Academic Editor: Antonio Di Crescenzo

Copyright © 2021 Muhammad Shahbaz Aasi et al. This is an open access article distributed under the Creative Commons Attribution License, which permits unrestricted use, distribution, and reproduction in any medium, provided the original work is properly cited.

Labeling of graphs has defined many variations in the literature, e.g., graceful, harmonious, and radio labeling. Secrecy of data in data sciences and in information technology is very necessary as well as the accuracy of data transmission and different channel assignments is maintained. It enhances the graph terminologies for the computer programs. In this paper, we will discuss multidistance radio labeling used for channel assignment problems over wireless communication. A radio labeling is a one-to-one mapping $\wp: V(G) \rightarrow \mathbb{Z}^+$ satisfying the condition $|\wp(\mu) - \wp(\mu')| \geq \text{diam}(G) + 1 - d(\mu, \mu')$: $\mu, \mu' \in V(G)$ for any pair of vertices μ, μ' in G . The span of labeling \wp is the largest number that \wp assigns to a vertex of a graph. Radio number of G , denoted by $rn(G)$, is the minimum span taken over all radio labelings of G . In this article, we will find relations for radio number and radio mean number of a lexicographic product for certain families of graphs.

1. Introduction

The notion of graph labeling was first introduced in 1966 by Rosa in [1], and since then, many different graph labelings have been defined and studied. In the 19th century, for studying the channel assignment problem, the term graph labeling was used where the transmitters are used as the vertices of the graph. Two vertices (transmitters) are said to be adjacent if they are sufficiently close to each other. A model of the channel assignment problem was provided by Hale [2] in 1980. Basic notions and definitions can be found in [3].

Let $G = (V(G), E(G))$ be a connected graph with vertex set $V(G)$ and edge set $E(G)$. For any $\mu, \mu' \in V(G)$, let $d(\mu, \mu')$ be the shortest length of the path between the vertices μ and μ' . A distance-two labeling is a function $\wp: V(G) \rightarrow \{1, 2, 3, \dots, k\}$ with span k having the maximum value k such that for any $\mu, \mu' \in V(G), \mu \neq \mu'$, the following relations are satisfied:

$$|\wp(\mu) - \wp(\mu')| \geq \begin{cases} 2, & \text{if } d(\mu, \mu') = 1 \\ 1, & \text{if } d(\mu, \mu') = 2 \end{cases}. \quad (1)$$

In 1992, Griggs and Yeh [4] extensively studied about distance-two labeling.

An assignment of positive integers to the vertices of G by \wp of G is said to be a radio k -labeling if $|\wp(\mu) - \wp(\mu')| \geq k + 1 - d(\mu, \mu')$, where k is an integer, $k \geq 1$. The span of labeling \wp , denoted by $sp(\wp)$, is the max $\{|\wp(\mu) - \wp(\mu')|: \mu, \mu' \in V(G)\}$. Radio number of G , denoted by $rn(G)$, is the minimum span taken over all radio labelings of G . The radio k -labeling number of G is the minimum span among all radio k -labelings of G .

The study of radio k -labelings was motivated by Chartrand et al. [5] where they found the radio k -labeling number for paths. In [5], the lower and upper bounds were given for the radio k -labeling number for paths which have been improved lately by Kchikech et al. [6]. The radio k -labeling becomes a radio labeling, when $k = \text{diam}(G)$. A radio labeling is a mapping from the vertices of the graph to some subsets of positive integers. The task of radio labeling is to assign to each station a positive smallest integer such that the interference in the nearest channel should be minimized. In 2001, multilevel distance labeling problem was introduced by Chartrand et al. [7].

A radio labeling is a one-to-one mapping $\wp: V(G) \rightarrow \mathbb{Z}^+$ satisfying the condition

$$\{|\wp(\mu) - \wp(\mu')| \geq \text{diam}(G) + 1 - d(\mu, \mu') : \mu, \mu' \in V(G)\}. \tag{2}$$

In [8], multilevel distance (or radio) labeling for paths and cycles are determined by Liu and Zhu. Rahim et al. in [9] discussed and determined the radio number of Helm graphs. In [8], Liu et al. calculated the radio number of path graph. The radio numbers of hypercube graphs and square cycles have been computed by Khennoufa [10] and Liu et al. [11], respectively. In [12], Naseem et al. gave a lower bound for the radio number of edge-joint graphs. Adefokun and Ajayi [13] proved that for $p \geq 4$ and q even $rn(S_p \times P_q) = pq^2/2 + q - 1$ and that for q even $rn(S_3 \times P_q) = 3q^2/2 + q$. Kim et al. [14] determined the radio numbers of P_q with $q \geq 4$ and K_p with $p \geq 3$. Lower bound has been improved by Bantva [15] for the radio number of graphs which was earlier given by Das et al. in [16]. For more results, we have [17–21].

In [22], Ali et al. proposed a formula for finding a lower bound for $rn(G)$, for graphs with small diameter. It is sometimes very useful to determine how many pairs $(\mu_s, \mu_{(s+1)})$ with $\wp(\mu_{(s+1)}) - \wp(\mu_s) = 1$ we can have. If there can be atmost ‘ y ’ such pairs in a graph G , then

$$rn(G) \geq y + 2(q - 1 - y) + 1. \tag{3}$$

In this paper, firstly, we determine the radio number and then radio mean number for the lexicographic product of path with path, path with cycle, and cycle with cycle. Finally, we present computer programs for finding such radio labelings of these families of graphs.

2. Applications

Labeling of graphs is one of the most popular parameters due to its diverse applications in real life. Radio labeling process proved as an efficient way of determining the time of communication for sensor networks. For giving valuable mathematical models, it has a wide scope of applications such as coding theory, electrical switchboards, circuit design, communication network addressing, channel assignment process, social networks, astronomy, demand and supply scenario, radar, database management, X-ray crystallography, and data security.

3. Lexicographic Product of Graphs

The lexicographic product was first studied by Hausdorff in 1914 [23]. The lexicographic product of two graphs G_1 and G_2 is denoted by $G_1[G_2]$ which is a graph with (Figure 1)

- (1) The vertex set of the Cartesian product $V(G_1) \times V(G_2)$, and
- (2) Distinct vertices (μ, μ') and (μ_0, μ'_0) are adjacent in $G_1[G_2]$ iff
 - (a) $\mu\mu_0 \in E(G_1)$, or
 - (b) $\mu = \mu_0$ and $\mu'\mu'_0 \in E(G_2)$.

4. Main Results

In this section, we discuss the radio labelings and compute the radio number for the lexicographic product of path with path $P_p[P_q]$ and path with cycle $P_p[C_q]$ for $p = 2, 3$. Moreover, we also presented a computer program for computing the radio number of these families of graphs.

4.1. Results of Radio Labeling. Let P_q be the path with q vertices. The lexicographic product of P_1 with P_q is isomorphic to graph P_q . The radio number of paths is investigated by Liu et al. in [8] as stated in the following result.

Theorem 4.1 (see [8]). *For any $q \geq 3$,*

$$rn(P_1[P_q]) = rn(P_q) = \begin{cases} 2k(k-1) + 1, & \text{if } q = 2k, \\ 2k^2 + 2, & \text{if } q = 2k + 1, \end{cases} \tag{4}$$

$$rn(P_2[P_q]) = \begin{cases} 2q, & \text{if } q = 1, 2, \\ 2q + 2, & \text{if } q = 3, \\ 2q + 1, & \text{if } q \geq 4, \end{cases} \tag{5}$$

$$rn(P_2[C_q]) = \begin{cases} 2q, & \text{if } q = 3, \\ 2q + 3, & \text{if } q = 4, \\ 2q + 1, & \text{if } q \geq 5. \end{cases}$$

We have a result for lower bound of $rn(P_p[P_q])$ for $p = 2, 3$ and $q \geq 4$.

Theorem 4.2. *For all $q \geq 4$, $rn(P_p[P_q]) \geq pq + 1$.*

Proof. In order to prove that the value stated above is a lower bound for the radio number, we will use the idea of distance-two labeling, i.e., expression 1.

The order of the graph $P_p[P_q]$ is pq for $p = 2, 3$ and there exists $pq - 2$, such pairs with labeling difference equals to 1. So, 3 implies that

$$\begin{aligned} rn(P_p[P_q]) &\geq (pq - 2) + 2[(pq) - 1 - (pq - 2)] \\ &= pq - 2 + 2[pq - 1 - pq + 2] + 1 \\ &= pq - 2 + 2pq - 2 - 2pq + 4 + 1 \\ &= pq + 1, \end{aligned} \tag{6}$$

$$rn(P_p[P_q]) \geq pq + 1. \quad \square$$

Theorem 4.3. *For all $q \geq 4$, $rn(P_2[P_q]) \leq 2q + 1$.*

Proof. The vertex set is partitioned in two disjoint sets V_l and V_r . Each partition is given as $V_l = V_l^1 \cup V_l^2$ and $V_r = V_r^1 \cup V_r^2$. For $t = l, r$, $V_t^1 = \{v_t^1, v_t^2, v_t^3, \dots, v_t^{\lceil q/2 \rceil}\}$ and $V_t^2 = \{v_t^{\lceil q/2 \rceil + 1}, v_t^{\lceil q/2 \rceil + 2}, v_t^{\lceil q/2 \rceil + 3}, \dots, v_t^q\}$. Define a mapping $\wp: V(P_2[P_q]) \rightarrow \mathbb{N}$ as follows:

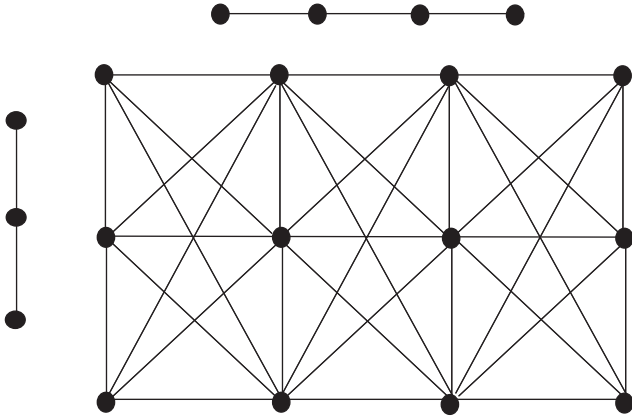


FIGURE 1: $P_4[P_3]$.

$$\begin{aligned} \wp\left(v_l^{\left\lfloor \frac{q}{2} \right\rfloor - s + 1}\right) &= q + 2s \text{ for } s = 1, 2, 3, \dots, \left\lfloor \frac{q}{2} \right\rfloor \\ \wp\left(v_l^{q-s+1}\right) &= q + 1 + 2s \text{ for } s = 1, 2, 3, \dots, q - \left\lfloor \frac{q}{2} \right\rfloor. \\ \wp\left(v_c^{\left\lfloor \frac{q}{2} \right\rfloor - s + 1}\right) &= 2s - 1 \text{ for } s = 1, 2, 3, \dots, \left\lfloor \frac{q}{2} \right\rfloor \\ \wp\left(v_c^{q-s+1}\right) &= 2s \text{ for } s = 1, 2, 3, \dots, q - \left\lfloor \frac{q}{2} \right\rfloor. \\ \wp\left(v_r^{\left\lfloor \frac{q}{2} \right\rfloor - s + 1}\right) &= 2(q + s) \text{ for } s = 1, 2, 3, \dots, \left\lfloor \frac{q}{2} \right\rfloor \\ \wp\left(v_r^{q-s+1}\right) &= 2(q + s) + 1 \text{ for } s = 1, 2, 3, \dots, q - \left\lfloor \frac{q}{2} \right\rfloor. \end{aligned} \tag{7}$$

Claim: the mapping \wp is a valid radio labeling. We must show that condition 2 for radio labeling holds for all pair of vertices $\mu, \eta \in V(P_2[P_q])$.

Case 1: suppose μ and η are any two vertices in V_l , then two subcases can be obtained.

Case 1.1: let μ and η be any two distinct vertices in V_l^1 , then $\mu = v_k$ and $\eta = v_l$, $1 \leq k \neq l \leq \lfloor q/2 \rfloor$; therefore, $\wp(\mu) = q + 2k$ and $\wp(\eta) = q + 2l$. Also, we note that $d(\mu, \eta) \geq 1$; hence, $d(\mu, \eta) + |\wp(\mu) - \wp(\eta)| \geq 1 + 2 = 3$ $d(\mu, \eta) + |2(k - l)| \geq 3$.

Case 1.2: let μ and η be any two distinct vertices in V_l^2 , then $\mu = v_k$ and $\eta = v_l$, $1 \leq k \neq l \leq q - \lfloor q/2 \rfloor$; therefore, $\wp(\mu) = q + 1 + 2k$ and $\wp(\eta) = q + 1 + 2l$. Also, we note that $d(\mu, \eta) \geq 1$; hence, $d(\mu, \eta) + |\wp(\mu) - \wp(\eta)| \geq 1 + 2 = 3$ $d(\mu, \eta) + |2(k - l)| \geq 3$.

Case 2: suppose μ and η are any two vertices in V_c , then two subcases can be obtained.

Case 2.1: let μ and η be any two distinct vertices in V_c^1 , then $\mu = v_k$ and $\eta = v_l$, $1 \leq k \neq l \leq \lfloor q/2 \rfloor$; therefore, $\wp(\mu) = 2k - 1$ and $\wp(\eta) = 2l - 1$. Also, we note that $d(\mu, \eta) \geq 1$; hence, $d(\mu, \eta) + |\wp(\mu) - \wp(\eta)| \geq 1 + 2 = 3$ $d(\mu, \eta) + |2(k - l)| \geq 3$.

Case 2.2: let μ and η be any two distinct vertices in V_c^2 , then $\mu = v_k$ and $\eta = v_l$, $1 \leq k \neq l \leq q - \lfloor q/2 \rfloor$; therefore, $\wp(\mu) = 2k$ and $\wp(\eta) = 2l$. Also, we note that $d(\mu, \eta) \geq 1$; hence, $d(\mu, \eta) + |\wp(\mu) - \wp(\eta)| \geq 1 + 2 = 3$ $d(\mu, \eta) + |2(k - l)| \geq 3$.

Case 3: suppose μ and η are any two vertices in V_r , then two subcases can be obtained.

Case 3.1: let μ and η be any two distinct vertices in V_r^1 , then $\mu = v_k$ and $\eta = v_l$, $1 \leq k \neq l \leq \lfloor q/2 \rfloor$. therefore, $\wp(\mu) = 2(q + k)$ and $\wp(\eta) = 2(q + l)$. Also, we note that $d(\mu, \eta) \geq 1$; hence, $d(\mu, \eta) + |\wp(\mu) - \wp(\eta)| \geq 1 + 2 = 3$ $d(\mu, \eta) + |2(k - l)| \geq 3$.

Case 3.2: let μ and η be any two distinct vertices in V_r^2 , then $\mu = v_k$ and $\eta = v_l$, $1 \leq k \neq l \leq q - \lfloor q/2 \rfloor$; therefore, $\wp(\mu) = 2(q + k) + 1$ and $\wp(\eta) = 2(q + l) + 1$. Also, we note that $d(\mu, \eta) \geq 1$; hence, $d(\mu, \eta) + |\wp(\mu) - \wp(\eta)| \geq 1 + 2 = 3$ $d(\mu, \eta) + |2(k - l)| \geq 3$. \square

Theorem 4.4

$$rn(P_3[P_q]) = \begin{cases} 4, & \text{if } q = 1, \\ 3q + 2, & \text{if } q = 2, 3, \\ 3q + 1, & \text{if } q \geq 4, \end{cases} \tag{8}$$

$$rn(P_3[C_q]) = \begin{cases} 3(q + 1), & \text{if } q = 3, \\ 3q + 2, & \text{if } q = 4, \\ 3q + 1, & \text{if } q \geq 5, \end{cases} \tag{9}$$

Theorem 4.5. For all $q \geq 4$, $rn(P_3[P_q]) \leq 3q + 1$.

Proof. The vertex set is partitioned in three disjoint sets V_l, V_c , and V_r . Each partition is further partitioned in two disjoint sets, i.e., $V_l = V_l^1 \cup V_l^2$, $V_c = V_c^1 \cup V_c^2$ and $V_r = V_r^1 \cup V_r^2$. For $t = l, c, r$, $V_t^1 = \{v_t^1, v_t^2, v_t^3, \dots, v_t^{\lfloor q/2 \rfloor}\}$ and $V_t^2 = \{v_t^{\lfloor q/2 \rfloor + 1}, v_t^{\lfloor q/2 \rfloor + 2}, v_t^{\lfloor q/2 \rfloor + 3}, \dots, v_t^q\}$. Define a mapping $\wp: V(P_3[P_q]) \rightarrow \mathbb{N}$ as follows:

$$\begin{aligned} \wp\left(v_l^{\lfloor q/2 \rfloor - s + 1}\right) &= q + 2s \text{ for } s = 1, 2, 3, \dots, \lfloor q/2 \rfloor \\ \wp\left(v_l^{q-s+1}\right) &= q + 1 + 2s \text{ for } s = 1, 2, 3, \dots, q - \left\lfloor \frac{q}{2} \right\rfloor. \\ \wp\left(v_c^{\left\lfloor \frac{q}{2} \right\rfloor - s + 1}\right) &= 2s - 1 \text{ for } s = 1, 2, 3, \dots, \left\lfloor \frac{q}{2} \right\rfloor \\ \wp\left(v_c^{q-s+1}\right) &= 2s \text{ for } s = 1, 2, 3, \dots, q - \left\lfloor \frac{q}{2} \right\rfloor. \\ \wp\left(v_r^{\lfloor q/2 \rfloor - s + 1}\right) &= 2(q + s) \text{ for } s = 1, 2, 3, \dots, \left\lfloor \frac{q}{2} \right\rfloor \\ \wp\left(v_r^{q-s+1}\right) &= 2(q + s) + 1 \text{ for } s = 1, 2, 3, \dots, q - \left\lfloor \frac{q}{2} \right\rfloor. \end{aligned} \tag{10}$$

Claim: the mapping \wp is a valid radio labeling. We must show that condition 2 for radio labeling holds for all pair of vertices $\mu, \eta \in V(P_3[P_q])$.

Case 1: suppose μ and η are any two vertices in V_l , then two subcases can be obtained.

Case 1.1: let μ and η be any two distinct vertices in V_l^1 , then $\mu = v_k$ and $\eta = v_l$, $1 \leq k \neq l \leq \lfloor q/2 \rfloor$; therefore, $\wp(\mu) = q + 2k$ and $\wp(\eta) = q + 2l$. Also, we note that $d(\mu, \eta) \geq 1$; hence, $d(\mu, \eta) + |\wp(\mu) - \wp(\eta)| \geq 1 + 2 = 3$
 $d(\mu, \eta) + |2(k - l)| \geq 3$.

Case 1.2: let μ and η be any two distinct vertices in V_l^2 , then $\mu = v_k$ and $\eta = v_l$, $1 \leq k \neq l \leq q - \lfloor q/2 \rfloor$; therefore, $\wp(\mu) = q + 1 + 2k$ and $\wp(\eta) = q + 1 + 2l$. Also, we note that $d(\mu, \eta) \geq 1$; hence, $d(\mu, \eta) + |\wp(\mu) - \wp(\eta)| \geq 1 + 2 = 3$
 $d(\mu, \eta) + |2(k - l)| \geq 3$.

Case 2: suppose μ and η are any two vertices in V_c , then two subcases can be obtained.

Case 2.1: let μ and η be any two distinct vertices in V_c^1 , then $\mu = v_k$ and $\eta = v_l$, $1 \leq k \neq l \leq \lfloor q/2 \rfloor$; therefore, $\wp(\mu) = 2k - 1$ and $\wp(\eta) = 2l - 1$. Also, we note that $d(\mu, \eta) \geq 1$; hence, $d(\mu, \eta) + |\wp(\mu) - \wp(\eta)| \geq 1 + 2 = 3$
 $d(\mu, \eta) + |2(k - l)| \geq 3$.

Case 2.2: let μ and η be any two distinct vertices in V_c^2 , then $\mu = v_k$ and $\eta = v_l$, $1 \leq k \neq l \leq q - \lfloor q/2 \rfloor$; therefore, $\wp(\mu) = 2k$ and $\wp(\eta) = 2l$. Also, we note that $d(\mu, \eta) \geq 1$; hence, $d(\mu, \eta) + |\wp(\mu) - \wp(\eta)| \geq 1 + 2 = 3$
 $d(\mu, \eta) + |2(k - l)| \geq 3$.

Case 3: suppose μ and η are any two vertices in V_r , then two subcases can be obtained.

Case 3.1: let μ and η be any two distinct vertices in V_r^1 , then $\mu = v_k$ and $\eta = v_l$, $1 \leq k \neq l \leq \lfloor q/2 \rfloor$; therefore, $\wp(\mu) = 2(q + k)$ and $\wp(\eta) = 2(q + l)$. Also, we note that $d(\mu, \eta) \geq 1$; hence, $d(\mu, \eta) + |\wp(\mu) - \wp(\eta)| \geq 1 + 2 = 3$
 $d(\mu, \eta) + |2(k - l)| \geq 3$.

Case 3.2: let μ and η be any two distinct vertices in V_r^2 , then $\mu = v_k$ and $\eta = v_l$, $1 \leq k \neq l \leq q - \lfloor q/2 \rfloor$; therefore, $\wp(\mu) = 2(q + k) + 1$ and $\wp(\eta) = 2(q + l) + 1$. Also, we note that $d(\mu, \eta) \geq 1$; hence, $d(\mu, \eta) + |\wp(\mu) - \wp(\eta)| \geq 1 + 2 = 3$
 $d(\mu, \eta) + |2(k - l)| \geq 3$. \square

4.2. Computing Radio Number of Lexicographic Product of Graphs by Using Computer Language. This computer code has been composed by using Python language.

```
import numpy as np
import math as mt
def main():
    m = int(input('m = Enter the number of vertices (either 2 or 3) = '))
    n = int(input('n = Enter the number of vertices (n >= 5) = '))
    name3 = input('Type rnPP for lexico of two path graphs, Type rnPC for radio number of path and cycles, Type exist to quit the program: ')
    while name3 != 'exit':
        if name3 == 'rnPP':
            print('Executing rnPP')
            rnpp(n, m)
        elif name3 == 'rnPC':
            print('Executing rnPC')
            rnpc(n, m)
        else:
            print('Input error: Enter the correct input value.')
            name3 = input('Enter rnPP for lexico of two path graphs, rnPC for radio number of path and cycles, or exist to quit the program: ')
    def rnpp(n, m):
        if m == 2:
            q1 = mt.ceil(n/2)
            l = np.zeros(n, dtype = int)
            r = np.zeros(n, dtype = int)
            for i in range(0, q1, 1):
                l[q1-1-i] = 2*i
                r[q1-1-i] = (n+1) + 2*i
            for j in range(1, n-q1+1, 1):
                l[n-j] = 2*j-1
                r[n-j] = n+2*j
            for lc, rc in zip(l, r):
                print(lc, rc)
        elif m == 3:
            q2 = mt.ceil(n/2)
            l = np.zeros(n, dtype = int)
            r = np.zeros(n, dtype = int)
            c = np.zeros(n, dtype = int)
            for i in range(0, q2, 1):
                l[q2-1-i] = (n+1) + 2*i
                r[q2-1-i] = 2*(n+i) + 1
                c[q2-1-i] = 2*i
            for j in range(1, n-q2+1, 1):
                l[n-j] = n + 2*j
                r[n-j] = 2 * (n+j)
                c[n-j] = 2 * j-1
            for lc, cc, rc in zip(l, c, r):
                print(lc, cc, rc)
        else:
            print("Try again! Enter either 2 or 3 for the value of m.")
            exit()
    def rnpc(n, m):
        if m == 2:
            q1 = mt.ceil(n/2)
            l = np.zeros(n, dtype = int)
```

```
            while name3 != 'exit':
                if name3 == 'rnPP':
                    print('Executing rnPP')
                    rnpp(n, m)
                elif name3 == 'rnPC':
                    print('Executing rnPC')
                    rnpc(n, m)
                else:
                    print('Input error: Enter the correct input value.')
                    name3 = input('Enter rnPP for lexico of two path graphs, rnPC for radio number of path and cycles, or exist to quit the program: ')
            def rnpc(n, m):
                if m == 2:
                    q1 = mt.ceil(n/2)
                    l = np.zeros(n, dtype = int)
                    r = np.zeros(n, dtype = int)
                    for i in range(0, q1, 1):
                        l[q1-1-i] = 2*i
                        r[q1-1-i] = (n+1) + 2*i
                    for j in range(1, n-q1+1, 1):
                        l[n-j] = 2*j-1
                        r[n-j] = n+2*j
                    for lc, rc in zip(l, r):
                        print(lc, rc)
                elif m == 3:
                    q2 = mt.ceil(n/2)
                    l = np.zeros(n, dtype = int)
                    r = np.zeros(n, dtype = int)
                    c = np.zeros(n, dtype = int)
                    for i in range(0, q2, 1):
                        l[q2-1-i] = (n+1) + 2*i
                        r[q2-1-i] = 2*(n+i) + 1
                        c[q2-1-i] = 2*i
                    for j in range(1, n-q2+1, 1):
                        l[n-j] = n + 2*j
                        r[n-j] = 2 * (n+j)
                        c[n-j] = 2 * j-1
                    for lc, cc, rc in zip(l, c, r):
                        print(lc, cc, rc)
                else:
                    print("Try again! Enter either 2 or 3 for the value of m.")
                    exit()
            def rnpp(n, m):
                if m == 2:
                    q1 = mt.ceil(n/2)
                    l = np.zeros(n, dtype = int)
```

```

r = np.zeros(n, dtype = int)
for i in range(0, q1, 1):
l[q1-1-i] = 2*i + 1
r[q1-1-i] = (n+2) + 2*i
for j in range(1, n-q1+1, 1):
l[n-j] = 2*j
r[n-j] = (n+1) + 2*j
for lc, rc in zip(l, r):
print(lc, rc)
elif m == 3:
q2 = mt.ceil(n/2)
l = np.zeros(n, dtype = int)
r = np.zeros(n, dtype = int)
c = np.zeros(n, dtype = int)
for i in range(0, q2, 1):
l[q2-1-i] = (n+2) + 2*i
r[q2-1-i] = 2*(n+i+1)
c[q2-1-i] = 2*i+1
for j in range(1, n-q2+1, 1):
l[n-j] = n + 2*j+1
r[n-j] = 2 * (n+j) + 1
c[n-j] = 2 * j
for lc, cc, rc in zip(l, c, r):
print(lc, cc, rc)
else:
print("Try again! Enter either 2 or 3 for the value of m.")
exit()
main()

```

5. Results of Radio Mean Labeling

Ponraj et al. [24] discussed the radio mean labeling. In this section, we discuss the radio mean labeling and compute the radio mean number for the lexicographic product of path with path $P_p[P_q]$ and path with cycle $P_p[C_q]$ for $p = 2, 3$. Moreover, we also presented a computer program for computing the radio number of these families of graphs.

Definition 5.1. Radio mean labeling of a connected graph G is a one-to-one map \wp from the vertex set $V(G)$ to the set of natural numbers \mathbb{N} such that for two distinct vertices μ and μ' of G ,

$$d(\mu, \mu') + \left\lceil \frac{\wp(\mu) + \wp(\mu')}{2} \right\rceil \geq 1 + \text{diam}(G). \quad (11)$$

The radio mean number of \wp , denoted by $\text{rmn}(\wp)$, is the maximum number assigned to any vertex of G . The radio mean number of G , $\text{rmn}(G)$ is the minimum value of $\text{rmn}(\wp)$ taken over all radio mean labeling \wp of G .

Theorem 5.2. For $p = 2, 3$ and $q \geq 1$, $\text{rmn}(P_p[P_q]) = pq$.

Proof. Let $V(P_p[P_q]) = \cup_{t=1}^p V_t^s$ for $p = 2, 3$ and $1 \leq s \leq q$ and $E(P_p[P_q]) = \{v_t^s v_{t+1}^{s+1} : 1 \leq t \leq p; 1 \leq s \leq q\} \cup \{v_t^s v_{t+1}^{s'} : 1 \leq s, s' \leq q\}$. It is clear that $\text{diam}(P_p[P_q]) = 2$. We define a vertex labeling $\wp: V(P_p[P_q]) \rightarrow \mathbb{N}$ as follows: $\wp(v_t^s) = ps - p + t$ for $1 \leq t \leq p$ and $1 \leq s \leq q$. Now, we check the radio mean condition.

$$d(\mu, \mu') + \left\lceil \frac{\wp(\mu) + \wp(\mu')}{2} \right\rceil \geq 1 + \text{diam}(P_p[P_q]), \quad (12)$$

for all $\mu, \mu' \in V(P_p[P_q])$.

Case 1: the vertex labeling for the pair (v_t^s, v_t^{s+1}) for a fixed t , $1 \leq t \leq p$ and $1 \leq s \leq q-1$, is given as $\wp(v_t^s) = ps - p + t$ and $\wp(v_t^{s+1}) = p(s+1) - p + t = ps + t$. Here, $d(v_t^s, v_t^{s+1}) = 1$. So, $d(v_t^s, v_t^{s+1}) + \lceil \frac{ps - p + t + ps + t}{2} \rceil = 1 + \lceil \frac{2ps - p + 2t}{2} \rceil \geq 1 + 2 \geq 3$.

Case 2: check the pair $(v_t^s, v_{t+1}^{s'})$ for a fixed t , $1 \leq t \leq p-1$ and $1 \leq s, s' \leq q$. $\wp(v_t^s) = ps - p + t$, $\wp(v_{t+1}^{s'}) = ps' - p + t + 1$, and $d(v_t^s, v_{t+1}^{s'}) = 1$. So, $d(v_t^s, v_{t+1}^{s'}) + \lceil \frac{(ps - p + t) + (ps' - p + t + 1)}{2} \rceil = 1 + \lceil \frac{p(s + s' - 2) + 2t + 1}{2} \rceil \geq 1 + 2 \geq 3$.

Case 3: check the pair $(v_t^s, v_t^{s'})$ for a fixed t , $1 \leq t \leq p$ and $s' = s + 2$, for $1 \leq s \leq q-2$. $\wp(v_t^s) = ps - p + t$, $\wp(v_t^{s'}) = ps' - p + t$, and $d(v_t^s, v_t^{s'}) = 2$. So, $d(v_t^s, v_t^{s'}) + \lceil \frac{(ps - p + t) + (ps' - p + t)}{2} \rceil = 1 + \lceil \frac{p(s + s') - 2(p - t)}{2} \rceil \geq 1 + 2 \geq 3$. \square

5.1. Computing Radio Mean Number of Lexicographic Product of Graphs by Using Computer Language. This computer code has been composed by using Python language.

```

import numpy as np
print('Program to calculate the Radio Mean Labelling')
m = int(input('m = Enter the number of vertices (either 2 or 3) = '))
n = int(input('n = Enter the number of vertices (n > = 1) = '))
if m == 2:
lt = np.zeros(n, dtype = int)
rt = np.zeros(n, dtype = int)
for j in range(1, m+1, 1):
if j == 1:
for i in range(1, n+1, 1):
lt[i-1] = m*i - m + j.
else:
for i in range(1, n+1, 1):
rt[i-1] = m*i - m + j.
for lc, rc in zip(lt, rt):
print(lc, rc)

```

```

elif m == 3:
lt = np.zeros(n, dtype = int)
rt = np.zeros(n, dtype = int)
ct = np.zeros(n, dtype = int)
for j in range(1, m+1, 1):
if j == 1:
for i in range(1, n+1, 1):
lt[i-1] = m*i - m + j
elif j == 2:
for i in range(1, n+1, 1):
ct[i-1] = m*i - m + j
else:
for i in range(1, n+1, 1):
rt[i-1] = m*i - m + j
for lc, cc, rc in zip(lt, ct, rt):
print(lc, cc, rc)
else:
print('Error! The input value of m is either 2 or 3. Try
again.')
```

6. Conclusion

In this paper, we have discussed the radio number and radio mean number of lexicographic product of graphs, namely, $P_2[P_q]$, $P_3[P_q]$, $P_2[C_q]$, and $P_3[C_q]$ for $q \geq 5$. We also computed the exact value of radio number and radio mean number of these families. Moreover, in this paper, we have presented their computer codes and also two open problems for future work have been given.

7. Open Problems

- (1) Determining the radio number of $P_p[P_q]$ for $p \geq 4$.
- (2) Determining the radio mean number of $P_p[P_q]$ for $p \geq 4$.

Data Availability

To support this study, no data were used.

Conflicts of Interest

The authors declare that they have no conflicts of interest.

References

- [1] A. Rosa, *On Certain Valuations of the Vertices of a Graph*. 1967 *Theory Of Graphs*, pp. 349–355, International Symposium, Rome, Italy, 1966.
- [2] W. K. Hale, "Frequency assignment: theory and applications," *Proceedings of the IEEE*, vol. 68, pp. 1497–1514, 1980.
- [3] B. Andrásfai, *Introductory Graph Theory*, The Institute of Physics, London, UK, 1978.
- [4] J. R. Griggs and R. K. Yeh, "Labeling graphs with a condition at distance 2," *SIAM Journal on Discrete Mathematics*, vol. 5, pp. 586–595, 1992.
- [5] G. Chartrand, L. Nebeský, and P. Zhang, "Radio k -colorings of paths," *Discussiones Mathematicae Graph Theory*, vol. 24, pp. 5–21, 2004.
- [6] M. Kchikech, R. Khenoufa, and O. Togni, "Radio k -labelings for cartesian products of graphs," *Discussiones Mathematicae Graph Theory*, vol. 28, pp. 165–178, 2008.
- [7] G. Chartrand, D. Erwin, P. Zhang, and F. Harary, "Radio labelings of graphs," *Bulletin of the Institute of Combinatorics and its Applications*, vol. 33, pp. 77–85, 2001.
- [8] D. D. F. Liu and X. Zhu, "Multilevel distance labelings for paths and cycles," *SIAM Journal on Discrete Mathematics*, vol. 19, pp. 610–621, 2005.
- [9] M. T. Rahim and I. Tomescu, "Multi-level distance labelings for Helm graphs," *Ars Combinatoria*, vol. 104, pp. 513–523, 2012.
- [10] R. Khenoufa and O. Togni, "The radio antipodal and radio numbers of the hypercube," *Ars Combinatoria*, vol. 102, pp. 447–461, 2011.
- [11] D. D. F. Liu and M. Xie, "Radio number for square cycles," *Congressus Numerantium*, vol. 169, pp. 105–125, 2004.
- [12] A. Naseem, K. Shabbir, and H. Shaker, "The radio number of edge-joint graphs," *Ars Combinatoria*, vol. 139, pp. 337–315, 2018.
- [13] T. C. Adefokun and D. O. Ajayi, "On radio number of stacked-book graphs," pp. 1–9, 2019, <https://arxiv.org/abs/1901.00355>.
- [14] B. M. Kim, W. Hwang, and B. C. Song, "Radio number for the product of a path and a complete graph," *Journal of Combinatorial Optimization*, vol. 30, no. 1, pp. 139–149, 2015.
- [15] D. Bantva, "A lower bound for the radio number of graphs, Algorithms and Discrete Applied Mathematics," vol. 11394, Springer, Lecture Notes in Computer Science, , pp. 161–173, 2019.
- [16] S. Das, S. Ghosh, S. Nandi, and S. Sen, "A lower bound technique for radio k -coloring," *Discrete Mathematics*, vol. 340, pp. 855–861, 2017.
- [17] C. Y. Jung, W. Nazeer, S. Nazeer, A. Rafiq, and S. M. Kang, "Radio number for cross product $P_n(P_2)$," *International Journal of Pure and Applied Mathematics*, vol. 97, pp. 515–525, 2014.
- [18] I. Kousar, S. Nazeer, and W. Nazeer, "Multilevel distance labelings for generalized Petersen graph $P(n, 3)$," *Science International*, vol. 27, pp. 1767–1777, 2015.
- [19] S. Nazeer, I. Kousar, and W. Nazeer, "Multilevel distance labeling for the graphs having diameter equal to diameter of cycle," *Science International*, vol. 26, pp. 519–525, 2014.
- [20] S. Nazeer, I. Kousar, and W. Nazeer, "Radio number for prism related graphs D_n^* ," *Science International*, vol. 26, pp. 551–555, 2014.
- [21] S. Nazeer, I. Kousar, and W. Nazeer, "Radio and radio antipodal labelings for circulant graphs $G(4k + 2; 1; 2)$," *Journal of Applied Mathematics and Informatics*, vol. 33, pp. 173–183, 2015.
- [22] A. Ahmad and R. M. Ghemici, "Radio labeling of some ladder related graphs," *Mathematical Reports*, vol. 19, no. 9, pp. 107–119, 2017.
- [23] F. Hausdorff, *Grundzge der Mengenlehre*, Leipzig, Germany, 1914.
- [24] R. Ponraj, S. S. Narayanan, and R. Kala, "Radio mean labeling of graphs," *AKCE International Journal of Graphs and Combinatorics*, vol. 12, pp. 224–228, 2015.

Research Article

3-Total Edge Product Cordial Labeling for Stellation of Square Grid Graph

Rizwan Ullah,¹ Gul Rahmat,¹ Muhammad Numan,² Kraidi Anoh Yannick ,³
and Adnan Aslam ⁴

¹Department of Mathematics, Islamia College, Peshawar, Pakistan

²Department of Mathematics, COMSATS University Islamabad, Attock, Pakistan

³UFR of Mathematics and Computer Science, University Felix Houphouët Boigny of Coclody, Abidjan, Côte d'Ivoire

⁴Department of Natural Sciences and Humanities, University of Engineering and Technology, Lahore, Pakistan

Correspondence should be addressed to Kraidi Anoh Yannick; kayanoh2000@yahoo.fr

Received 6 September 2021; Accepted 10 November 2021; Published 6 December 2021

Academic Editor: Elena Guardo

Copyright © 2021 Rizwan Ullah et al. This is an open access article distributed under the Creative Commons Attribution License, which permits unrestricted use, distribution, and reproduction in any medium, provided the original work is properly cited.

Let G be a simple graph with vertex set $V(G)$ and edge set $E(G)$. An edge labeling $\delta: E(G) \rightarrow \{0, 1, \dots, p-1\}$, where p is an integer, $1 \leq p \leq |E(G)|$, induces a vertex labeling $\delta^*: V(G) \rightarrow \{0, 1, \dots, p-1\}$ defined by $\delta^*(v) = \delta(e_1)\delta(e_2) \cdot \delta(e_n) \pmod{p}$, where e_1, e_2, \dots, e_n are edges incident to v . The labeling δ is said to be p -total edge product cordial (TEPC) labeling of G if $|e_\delta(i) + v_{\delta^*}(i) - (e_\delta(j) + v_{\delta^*}(j))| \leq 1$ for every i, j , $0 \leq i \leq j \leq p-1$, where $e_\delta(i)$ and $v_{\delta^*}(i)$ are numbers of edges and vertices labeled with integer i , respectively. In this paper, we have proved that the stellation of square grid graph admits a 3-total edge product cordial labeling.

1. Introduction and Definitions

Let G be a simple, finite, and connected graph with the vertex set $V(G)$ and edge set $E(G)$. For basic notions related to graph theory, we refer the reader to the book by West [1]. A graph labeling δ is a map that sends one of the graph element (vertex set or edge set or both) to set of numbers. If the domain is the vertex set (edge set), then δ is called vertex (edge) labeling. If the domain is $V(G) \cup E(G)$, then δ is called total labeling. Graph labeling has a wide range of applications such as X-ray crystallography, coding theory, radar, astronomy, circuit design, network, and communication design.

Let $\delta: V(H) \rightarrow \{0, 1\}$ be a vertex labeling which induces edge labeling $\delta^*: E(H) \rightarrow \{0, 1\}$ defined by $\delta^*(xy) = |\delta(x) - \delta(y)|$. δ . The labeling δ is said to be cordial if $|v_\delta(0) - v_\delta(1)| \leq 1$ and $|e_{\delta^*}(0) - e_{\delta^*}(1)| \leq 1$, where $v_\delta(i)$ and $e_{\delta^*}(i)$ denote the number of vertices and number of edges labeled with integer i , respectively. The concept of cordial labeling was first introduced by Cahit [2]. A

considerable amount of work have been done on cordial labeling. For latest results, see [3–10]. A vertex labeling $\delta: V(G) \rightarrow \{0, 1\}$ induces an edge labeling $\delta^*: E(G) \rightarrow \{0, 1\}$ defined by $\delta^*(xy) = \delta(x)\delta(y)$ which is called product cordial labeling if $|v_\delta(0) - v_\delta(1)| \leq 1$ and $|e_{\delta^*}(0) - e_{\delta^*}(1)| \leq 1$, where $v_\delta(0)$ and $v_\delta(1)$ represent the number of vertices that are labeled 0 and 1, respectively. While $e_{\delta^*}(0)$ and $e_{\delta^*}(1)$ represent the number of edges labeled with 0 and 1, respectively. The concept named product cordial labeling was first presented by Sundaram et al. [11]. A variation in the cordial theme, namely, edge product cordial labeling and a TEPC labeling was introduced by Vaidya and Barasara [12, 13].

Let $2 \leq p \leq |E(G)|$ be an integer. An edge labeling $\delta: E(G) \rightarrow \{0, 1, \dots, p-1\}$ induces a vertex labeling $\delta^*: V(H) \rightarrow \{0, 1, \dots, p-1\}$ defined by $\delta^*(v) = \delta(e_1)\delta(e_2) \cdot \delta(e_n) \pmod{p}$, where e_1, e_2, \dots, e_n are edges incident to v . The labeling δ is said to be p -TEPC labeling of G if $|e_\delta(i) + v_{\delta^*}(i) - (e_\delta(j) + v_{\delta^*}(j))| \leq 1$ for every i, j , $0 \leq i \leq j \leq p-1$, where $e_\delta(i)$ and $v_{\delta^*}(i)$ are numbers of edges

and vertices labeled with integer i , respectively. Azaizeh et al. [14] introduced the concept of p -TEPC labeling. A graph G that admits a p -TEPC labeling is called a p -TEPC graph. Baca et al. [15] investigated the 3-TEPC labeling of carbon nanotube networks. Ahmad et al. [16] showed that the grid graph $P_m \square P_n$ admits a 3-TEPC labeling. Ahmad et al. [3] proved that the hexagonal grid H_m^n admits 3-TEPC labeling. Javed and Jamil [17] proved that the Rhombic grid R_m^n is 3-TEPC for $m, n \geq 1$.

Let P_n denote a path graph on n vertices. A rectangular grid is an $m \times n$ lattice graph and is obtained by taking the Cartesian product of P_m with P_n . The graph of rectangular product of P_m with P_n . The graph of rectangular grid is denoted by $L(m, n)$ and has n and m squares in each row and column respectively. It is easy to observe that rectangular grid $L(m, n)$ has mn vertices and $mn - m - n + 1$ edges. The stellation of $L(m, n)$ is obtained by adding a vertex in each face of $L(m, n)$ and then joining this vertex to each vertex of the respective face. We denote the stellation of $L(m, n)$ by G_n^m , as shown in Figure 1. In this paper, we show that the graph G_n^m admits 3-TEPC labeling.

2. Main Results

Let $m, n \geq 1$ and G_n^m be stellation of rectangular grid containing m rows and n columns. Observe that G_n^m has $2mn + m + n + 1$ vertices and $6mn + m + n$ edges. We use the notations $G_1 \oplus_v G_2$ for gluing the graph G_1 with G_2 vertically. Similarly, $G_1 \oplus_h G_2$ represent gluing G_1 with G_2 horizontally. If we have a labeled segment or labeled graph H and we rotate it by 90 degree in clockwise direction, then we will denote it by \vec{H} .

Theorem 1. For $m \geq 1$, the graph G_1^m is 3-TEPC.

Proof. The 3-TEPC labeling of G_1^1 and G_1^2 is shown in Figure 2. Similarly, the 3-TEPC labeling of G_1^3 and the labeled segment S_1^3 are shown in Figure 3. The segment S_1^3 has the property that open edges are assigned labeled 1. Hence, if we glue the segment S_1^3 with itself vertically, then it will not change the vertex labels in $S_1^3 \oplus_v S_1^3 = 2S_1^3$. Observe that the labels 0, 1, and 2 are used 10 times in the segment S_1^3 . Table 1 shows the multiplicity of numbers 0, 1, and 2, respectively, used in the labeled graph G_1^m for $m = 1, 2, 3$.

Case (i). $m = 3r, r \geq 1$.

To construct labeled graph G_1^m , we will use the labeled segments S_1^3 . First, glue $r - 1$ copies of labeled segment S_1^3 vertically that is $S_1^3 \oplus_v S_1^3 \oplus_v \dots \oplus_v S_1^3 = (r - 1)S_1^3$. Finally, glue vertically the label segment G_1^3 to the open edges of $(r - 1)S_1^3$ to get labeled graph G_1^m , that is,

$$G_1^m = \begin{bmatrix} (r - 1)S_1^3 \\ \oplus_v \\ G_1^3 \end{bmatrix}. \tag{1}$$

In the labeled graph G_1^m , the multiplicity of 0, 1, and 2 is $10r + 1$ exactly.

Case (ii): $m = 3r + 1, r \geq 1$.

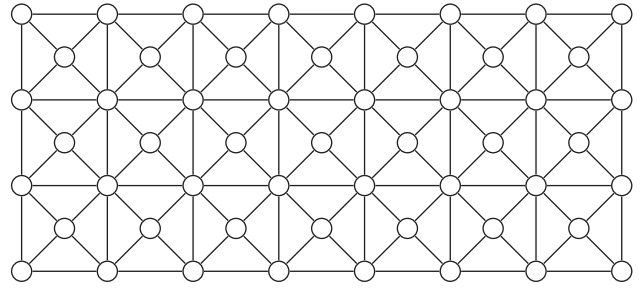


FIGURE 1: Stellation of square grid graph G_7^3 .

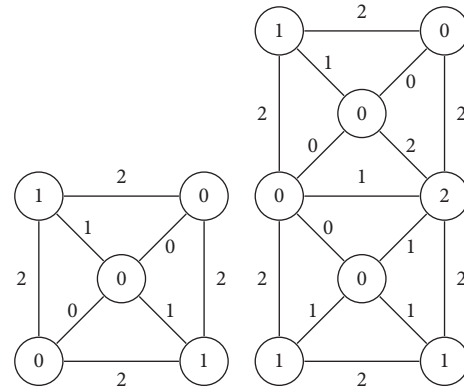


FIGURE 2: 3-TEPC labeling G_1^1 and G_1^2 .

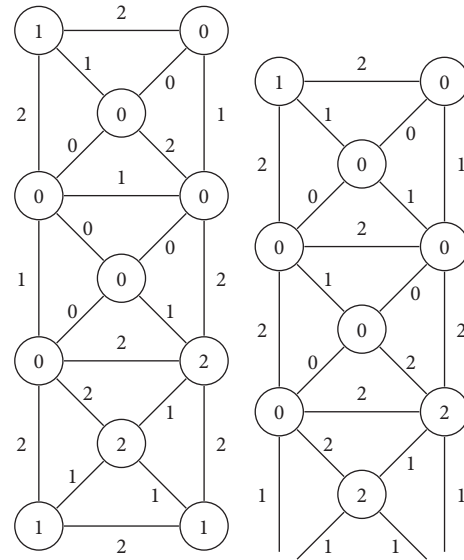


FIGURE 3: 3-TEPC labeling G_1^3 and label segment S_1^3 .

TABLE 1: The multiplicity of 0, 1, and 2 used in G_1^m , for $m = 1, 2, 3$.

G_1^m	$e_\delta(0) + v_{\delta^*}(0)$	$e_\delta(1) + v_{\delta^*}(1)$	$e_\delta(2) + v_{\delta^*}(2)$
$m = 1$	5	4	4
$m = 2$	7	8	8
$m = 3$	11	11	11

To construct the labeled graph G_1^m , we glue r copies of the labeled segment S_1^3 and then finally glue G_1^1 vertically. That is,

$$G_1^m = \begin{bmatrix} rS_1^3 \\ \oplus_v \\ G_1^1 \end{bmatrix}. \quad (2)$$

In the labeled graph G_1^m , the multiplicity of 0 is $10r + 5$, whereas the multiplicity of 1 and 2 is $10r + 4$.

Case (iii): $m = 3r + 2, r \geq 1$.

We obtain the labeled graph G_1^m by gluing r times the labeled segment S_1^3 and finally gluing G_1^2 in vertical direction. That is,

$$G_1^m = \begin{bmatrix} rS_1^3 \\ \oplus_v \\ G_1^2 \end{bmatrix}. \quad (3)$$

In the labeled graph G_1^m , the multiplicity of 0 is $10r + 7$, whereas the multiplicity of 1 and 2 is $10r + 8$. \square

Theorem 2. For $m \geq 1$, the graph G_2^m is 3-total edge product cordial.

Proof. Observe that the graphs G_1^2 and G_2^1 are isomorphic and the 3-total edge cordial labeling of G_1^2 is given in Figure 2. Therefore, G_2^1 is 3-TEPC. The 3-total edge product cordial labeling of the graphs G_2^2 and G_2^3 is given in Figures 4 and 5, respectively. Table 2 shows the multiplicity of numbers 0, 1, and 2 used in G_2^2 and G_2^3 .

Figure 6 depicts the labeled segment S_2^3 , which has the property that open edges are assigned labeled 1 and each number 0, 1, and 2 is used 18 times.

Case (i): $m = 3r, r \geq 1$.

To construct labeled graph G_2^m , we will use the labeled segments S_2^3 . First, we glue $r - 1$ copies of labeled segment S_2^3 vertically, that is, $S_2^3 \oplus_v S_2^3 \oplus_v \dots \oplus_v S_2^3 := (r - 1)S_2^3$. Since the open edges of S_2^3 are labeled with 1, therefore, this gluing process does not change the label of other vertices of $(r - 1)S_2^3$. Finally, we glue vertically the label segment G_2^3 to the open edges of $(r - 1)S_2^3$ to get labeled graph G_2^m . That is,

$$G_2^m = \begin{bmatrix} (r - 1)S_2^3 \\ \oplus_v \\ G_2^3 \end{bmatrix}. \quad (4)$$

In the labeled graph G_2^m , the multiplicity of 0 is $18r + 1$, whereas the multiplicity of 1 and 2 is $18r + 2$.

Case (ii): $m = 3r + 1, r \geq 1$.

To construct the labeled graph G_2^m , we glue r copies of the labeled segment S_2^3 and then finally glue G_2^1 vertically. That is,

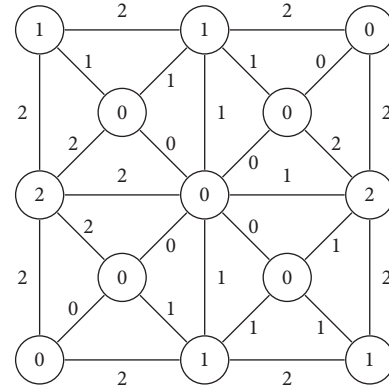


FIGURE 4: 3-TEPC labeling of G_2^2 .

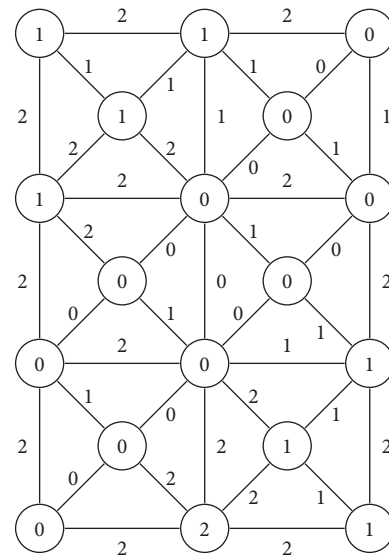


FIGURE 5: 3-TEPC labeling of G_2^3 .

TABLE 2: The multiplicity of 0, 1, and 2 in G_2^m , for $m = 2, 3$.

G_2^m	$e_\delta(0) + v_{\delta^*}(0)$	$e_\delta(1) + v_{\delta^*}(1)$	$e_\delta(2) + v_{\delta^*}(2)$
$m = 2$	13	14	14
$m = 3$	19	20	20

$$G_2^m = \begin{bmatrix} rS_2^3 \\ \oplus_v \\ G_2^1 \end{bmatrix}. \quad (5)$$

In the labeled graph G_2^m , the multiplicity of 0 is $18r + 7$ whereas the multiplicity of 1 and 2 is $18r + 8$.

Case (iii): $m = 3r + 2, r \geq 1$.

The labeled graph G_2^m can be obtained by gluing r times the labeled segment S_2^3 and then gluing G_2^2 in vertical direction. That is,

$$G_2^m = \begin{bmatrix} rS_2^3 \\ \oplus_v \\ G_2^2 \end{bmatrix}. \quad (6)$$

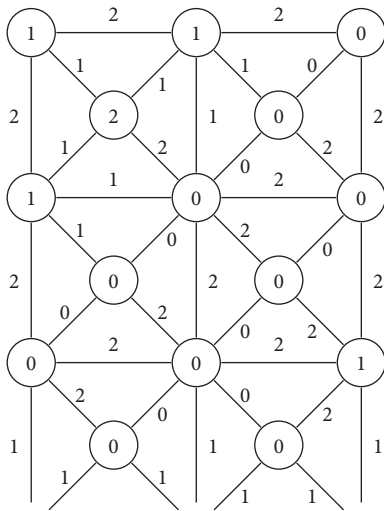


FIGURE 6: Label segment S_2^3 .

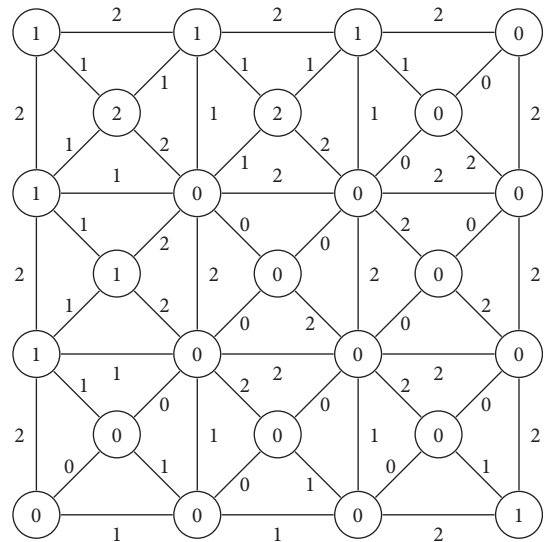


FIGURE 7: 3-TEPC labeling of G_3^3 .

In the labeled graph G_2^m , the multiplicity of 0 is $18r + 13$, whereas the multiplicity of 1 and 2 is $18r + 14$. \square

Theorem 3. *The graph G_3^m is 3-TEPC for $m \geq 1$.*

Proof. Observe that the graphs G_1^3 and G_3^1 are isomorphic. Similarly, the graphs G_2^3 and G_3^2 are also isomorphic. The 3-TEPC labeling of G_1^3 and G_2^3 are given in Figures 3 and 5, respectively. The 3-TEPC labeling of G_3^3 is shown in Figure 7. In the labeled graph G_3^3 , the multiplicity of 0 is 29, whereas the multiplicity of 1 and 2 is 28.

Figure 8 shows the labeled segment S_3^3 which has the property that open edges are assigned with label 1 and each number 0, 1, and 2 appears 26 times.

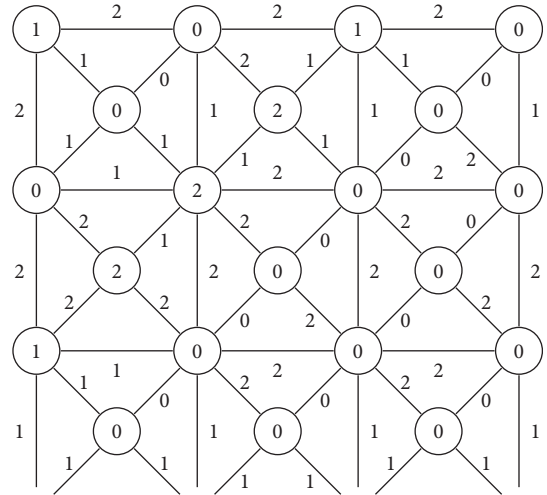


FIGURE 8: Label segment S_3^3 .

Case (i): $m = 3r, r \geq 1$.

To construct labeled graph G_3^m , we use the labeled segment S_3^3 . First, glue $r - 1$ copies of labeled segment S_3^3 vertically, that is, $S_3^3 \oplus_\nu S_3^3 \oplus_\nu \dots \oplus_\nu S_3^3 = (r - 1)S_3^3$. Since the open edges of S_3^3 are labeled with 1, therefore, this gluing process does not change the label of other vertices of $(r - 1)S_3^3$. Finally, glue vertically the label segment S_3^3 to the open edges of $(r - 1)S_3^3$ to get labeled graph G_3^m . That is,

$$G_3^m = \begin{bmatrix} (r - 1)S_3^3 \\ \oplus_\nu \\ G_3^3 \end{bmatrix}. \tag{7}$$

In the labeled graph G_3^m , the multiplicity of 0 is $26r + 3$, whereas the multiplicity of 1 and 2 is $26r + 2$.

Case (ii): $m = 3r + 1, r \geq 1$.

To construct the labeled graph G_3^m , we glue r copies of the labeled segment S_3^3 vertically and then finally glue G_3^1 vertically. That is,

$$G_3^m = \begin{bmatrix} rS_3^3 \\ \oplus_\nu \\ G_3^1 \end{bmatrix}. \tag{8}$$

In the labeled graph G_3^m , the multiplicity of 0, 1, and 2 is $26r + 11$.

Case (iii): $m = 3r + 2, r \geq 1$.

We obtain the labeled graph G_3^m by gluing r times the labeled segment S_3^3 vertically and then finally glue G_3^2 in vertical direction. That is,

$$G_3^m = \begin{bmatrix} rS_3^3 \\ \oplus_\nu \\ G_3^2 \end{bmatrix}. \tag{9}$$

In the labeled graph G_3^m , the multiplicity of 0 is $26r + 19$, whereas the multiplicity of 1 and 2 is $26r + 20$. \square

Theorem 4. *The graph G_n^m is 3-TEPC for $m, n \geq 1$.*

Proof. To construct the labeled graph of G_n^m and to examine its 3-TEPC labeling, we introduced a new segment R_3^3 . This segment has 17 open edges which are labeled with the number 1 and multiplicity of 0, 1, and 2 is 24. The labeled segment R_3^3 is shown in Figure 9.

Case 1: $m = 3r, r \geq 1$.

First, we glue the segment R_3^3 vertically $r - 1$ times, that is, $R_3^3 \oplus_\nu R_3^3 \oplus_\nu \dots \oplus_\nu R_3^3 = (r - 1)R_3^3$. Since the open edges in the segment are labeled with number 1, it follows that gluing these segments do not change the vertex labels in the segment $(r - 1)R_3^3$. Finally, we glue the segment S_3^3 in the vertical direction. This gives a new segment X and is defined as

$$X = \begin{bmatrix} (r - 1)R_3^3 \\ \oplus_\nu \\ \vec{S}_3^3 \end{bmatrix}. \quad (10)$$

Note that the labels of open edges of X are 1 and multiplicity of each number 0, 1, and 2 is $24r + 2$.

Subcase 1: $n = 3s, s \geq 1$.

First, we glue $s - 1$ times the segment X horizontally and finally glue the labeled segment G_3^m horizontally to obtain the labeled graph G_n^m . That is,

$$G_n^m = [(s - 1)X \oplus_h G_3^m]. \quad (11)$$

Subcase 2: $n = 3s + 1, s \geq 1$.

First, we glue s times the segment X horizontally and finally glue the labeled segment G_1^m horizontally with sX to obtain the labeled graph G_n^m . That is,

$$G_n^m = [sX \oplus_h G_1^m]. \quad (12)$$

Subcase 3: $n = 3s + 2, s \geq 1$.

First, we glue s times the segment X horizontally and finally glue the labeled segment G_2^m horizontally with sX to obtain the labeled graph G_n^m . That is,

$$G_n^m = [sX \oplus_h G_2^m]. \quad (13)$$

Case 2: when $m = 3r + 1, r \geq 1$.

First, we glue the segment R_3^3 vertically r times, that is, $R_3^3 \oplus_\nu R_3^3 \oplus_\nu \dots \oplus_\nu R_3^3 = rR_3^3$. Then, we glue the segment S_1^3 in the vertical direction. This gives us a new segment Y defined as

$$Y = \begin{bmatrix} rR_3^3 \\ \oplus_\nu \\ \vec{S}_1^3 \end{bmatrix}. \quad (14)$$

Note that the labels of open edges of Y are 1 and multiplicity of each number 0, 1, and 2 is $24r + 10$.

Subcase 1: $n = 3s, s \geq 1$.

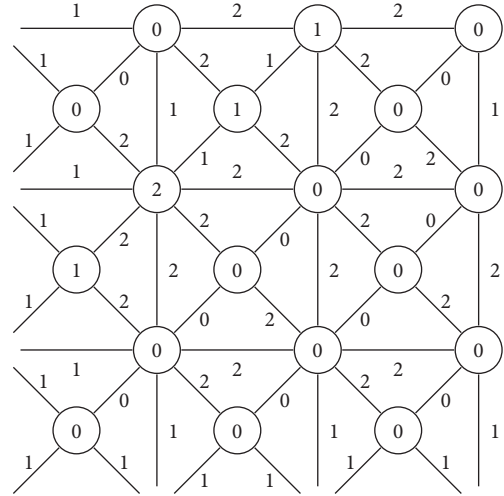


FIGURE 9: Label segment R_3^3 .

First, we glue $s - 1$ times the segment Y horizontally and finally glue the labeled segment G_3^m horizontally with $(s - 1)Y$ to obtain the labeled graph G_n^m . That is,

$$G_n^m = [(s - 1)Y \oplus_h G_3^m]. \quad (15)$$

Subcase 2: $n = 3s + 1, s \geq 1$.

First, we glue s times the segment Y horizontally and finally glue the labeled segment G_1^m horizontally with sY to obtain the labeled graph G_n^m . That is,

$$G_n^m = [sY \oplus_h G_1^m]. \quad (16)$$

Subcase 3: $n = 3s + 2, s \geq 1$.

First, we glue s times the segment Y horizontally and finally glue the labeled segment G_2^m horizontally with sY to obtain the labeled graph G_n^m . That is,

$$G_n^m = [sY \oplus_h G_2^m]. \quad (17)$$

Case 3: $m = 3r + 2, r \geq 1$.

First, we glue the segment R_3^3 vertically r times, that is, $R_3^3 \oplus_\nu R_3^3 \oplus_\nu \dots \oplus_\nu R_3^3 = rR_3^3$. Then, we glue in the vertical direction of the segment S_2^3 . This gives us a new segment Z defined as

$$Z = \begin{bmatrix} rR_3^3 \\ \oplus_\nu \\ \vec{S}_2^3 \end{bmatrix}. \quad (18)$$

Note that the labels of open edges of Z are 1 and multiplicity of each number 0, 1, and 2 is $24r + 18$.

Subcase 1: $n = 3s, s \geq 1$.

First, we glue $s - 1$ times the segment Z horizontally and finally glue the labeled segment G_3^m horizontally with $(s - 1)Z$ to obtain the labeled graph G_n^m . That is,

TABLE 3: The multiplicity of 0, 1, and 2 in G_n^m , for $m, n \geq 1$.

G_n^m	$e_\delta(0) + v_{\delta^*}(0)$	$e_\delta(1) + v_{\delta^*}(1)$	$e_\delta(2) + v_{\delta^*}(2)$
$m = 3r, n = 3s$	$24rs + 2s + 2r + 1$	$24rs + 2s + 2r$	$24rs + 2s + 2r$
$m = 3r, n = 3s + 1$	$24rs + 2s + 10r + 1$	$24rs + 2s + 10r + 1$	$24rs + 2s + 10r + 1$
$m = 3r, n = 3s + 2$	$24rs + 2s + 18r + 1$	$24rs + 2s + 18r + 2$	$24rs + 2s + 18r + 2$
$m = 3r + 1, n = 3s$	$24rs + 10s + 2r + 1$	$24rs + 10s + 2r + 1$	$24rs + 10s + 2r + 1$
$m = 3r + 1, n = 3s + 1$	$24rs + 10s + 10r + 5$	$24rs + 10s + 10r + 4$	$24rs + 10s + 10r + 4$
$m = 3r + 1, n = 3s + 2$	$24rs + 10s + 18r + 7$	$24rs + 10s + 18r + 8$	$24rs + 10s + 18r + 8$
$m = 3r + 2, n = 3s$	$24rs + 18s + 2r + 1$	$24rs + 18s + 2r + 2$	$24rs + 18s + 2r + 2$
$m = 3r + 2, n = 3s + 1$	$24rs + 18s + 10r + 8$	$24rs + 18s + 10r + 8$	$24rs + 18s + 10r + 8$
$m = 3r + 2, n = 3s + 2$	$24rs + 18s + 18r + 13$	$24rs + 18s + 18r + 14$	$24rs + 18s + 18r + 14$

$$G_n^m = [(s-1)Z \oplus_h G_3^m]. \quad (19)$$

Subcase 2: $n = 3s + 1, s \geq 1$.

First, we glue s times the segment Y horizontally and finally glue the labeled segment G_1^m horizontally with sZ to obtain the labeled graph G_n^m . That is,

$$G_n^m = [sZ \oplus_h G_1^m]. \quad (20)$$

Subcase 3: $n = 3s + 2, s \geq 1$.

First, we glue s times the segment Z horizontally and finally glue the labeled segment G_2^m horizontally with sZ to obtain the labeled graph G_n^m . That is,

$$G_n^m = [sZ \oplus_h G_2^m]. \quad (21)$$

The multiplicity of the numbers 0, 1, and 2 in the graph G_n^m for $m, n \geq 1$ is shown in Table 3. \square

3. Conclusion

In this paper, we constructed 3-TEPC labeling for the stellation of square grid graph G_n^m . For every $m \geq 1$ and every $n \geq 1$, we proved that G_n^m is 3-TEPC.

Data Availability

No data were used to support the findings of the study.

Conflicts of Interest

The authors declare that they have no conflicts of interest.

References

- [1] D. B. West, *Introduction to Graph Theory*, Prentice-Hall, Hoboken, NJ, USA, 2nd edition, 2003.
- [2] I. Cahit, "Cordial graphs: a weaker version of graceful and harmonious graphs," *Ars Combinatoria*, vol. 23, pp. 201–207, 1987.
- [3] A. Ahmad, M. Bača, M. Naseem, and A. Semaničová-Feňovčíková, "On 3-TEPC labeling of honeycomb," *AKCE International Journal of Graphs and Combinatorics*, vol. 14, no. 2, pp. 149–157, 2017.
- [4] I. Cahit, "On cordial and 3-equitable labelings of graphs," *Utilitas Mathematica*, vol. 37, pp. 189–198, 1990.
- [5] M. Hovey, "A-cordial graphs," *Discrete Mathematics*, vol. 93, no. 2-3, pp. 183–194, 1991.
- [6] Y. S. Ho, S. M. Lee, and S. C. Shee, "Cordial labelings of the Cartesian product and composition of graphs," *Ars Combinatoria*, vol. 29, pp. 169–180, 1990.
- [7] Y. S. Ho and S. C. Shee, "The cordiality of one-point union of n copies of a graph," *Discrete Mathematics*, vol. 117, pp. 225–243, 1993.
- [8] W. W. Kirchherr, "On the cordiality of some specific graphs," *Ars Combinatoria*, vol. 31, pp. 127–137, 1991.
- [9] D. Kuo, G. J. Chang, and Y. H. H. Kwong, "Cordial labeling of mK_n ," *Discrete Mathematics*, vol. 169, no. 1–3, pp. 121–131, 1997.
- [10] S. M. Lee and A. Liu, "A construction of cordial graphs from smaller cordial graphs," *Ars Combinatoria*, vol. 32, pp. 209–214, 1991.
- [11] M. Sundaram, R. Ponraj, and S. Somasundaram, "Product cordial labeling of graphs," *Bulletin of Pure and Applied Sciences Section-E-Mathematics & Statistics*, vol. 23, pp. 155–163, 2004.
- [12] S. K. Vaidya and C. M. Barasara, "Edge product cordial labeling of graphs," *Journal of Mathematics and Computer Science*, vol. 2, no. 5, pp. 1436–1450, 2012.
- [13] S. K. Vaidya and C. M. Barasara, "TEPC labeling of graphs," *Malaya Journal of Matematik*, vol. 3, no. 1, pp. 55–63, 2013.
- [14] A. Azaizeh, R. Hasni, A. Ahmad, and G.-C. Lau, "3-TEPC labeling of graphs," *Far East Journal of Mathematical Sciences*, vol. 96, no. 2, pp. 193–209, 2015.
- [15] M. Baca, M. Irfan, and A. Semanícová-Fenovčíková, "On 3-TEPC labeling of a carbon nanotube network," *AKCE International Journal of Graphs and Combinatorics*, vol. 16, pp. 310–318, 2019.
- [16] A. Ahmad, R. Hasni, M. Irfan, M. Naseem, and M. K. Siddiqui, "On 3-TEPC labeling of grid," *Asian-European Journal of Mathematics*, vol. 14, no. 6, Article ID 2150096, 2021.
- [17] A. Javed and M. K. Jamil, "3-TEPC labeling of rhombic grid," *AKCE International Journal of Graphs and Combinatorics*, vol. 16, no. 2, pp. 213–221, 2019.

Research Article

On the Exact Values of HZ-Index for the Graphs under Operations

Dalal Awadh Alrowaili ¹, Saira Javed ², and Muhammad Javaid ²

¹Department of Mathematics, College of Science, Jouf University, Sakaka 2014, Saudi Arabia

²Department of Mathematics, School of Science, University of Management and Technology, Lahore, Pakistan

Correspondence should be addressed to Muhammad Javaid; javaidmath@gmail.com

Received 4 August 2021; Accepted 25 October 2021; Published 20 November 2021

Academic Editor: Ali Ahmad

Copyright © 2021 Dalal Awadh Alrowaili et al. This is an open access article distributed under the Creative Commons Attribution License, which permits unrestricted use, distribution, and reproduction in any medium, provided the original work is properly cited.

Topological index (TI) is a function from the set of graphs to the set of real numbers that associates a unique real number to each graph, and two graphs necessarily have the same value of the TI if these are structurally isomorphic. In this note, we compute the HZ – index of the four generalized sum graphs in the form of the various Zagreb indices of their factor graphs. These graphs are obtained by the strong product of the graphs G and $D_k(G)$, where $D_k \in \{S_k, R_k, Q_k, T_k\}$ represents the four generalized subdivision-related operations for the integral value of $k \geq 1$ and $D_k(G)$ is a graph that is obtained by applying D_k on G . At the end, as an illustration, we compute the HZ – index of the generalized sum graphs for exactly $k = 1$ and compare the obtained results.

1. Introduction

A structural formula of a chemical compound is represented by a molecular graph, where atoms and bonds between atoms are represented by the vertices and edges of the molecular graphs, respectively. A topological index (TI) is a mathematical tool which associates a real number to a graph under certain conditions. For two graphs, a TI remains constant if the graphs are isomorphic (see [1–3]). These are used to study different physical attributes, biological activities, and chemical reactivities such as viscosity, critical temperatures (boiling, freezing, melting, and flash points) [4, 5], vapor pressure, surface tension, stability, weight, density, solubility, and connectivity [6–8] in the field of chemical engineering, pharmaceutical industries, and drugs discoveries. TIs are also used in the subject of cheminformatics to study the quantitative structural activity and property relationships (see [9–11]).

In 1947, the very first TI is introduced by Winer to check the critical temperature of paraffin [12]. Trinajstić and Gutman (1972) [13] defined the first and second Zagreb indices that are used to compute the different structure base characteristics of the molecular graphs. After that, many degree, distance, and polynomials based TIs came into existence but the degree-based indices got more attention of the researchers (see [14–16]). For various results on TIs of

different graphs, see [17–20]. In 2008, Zhou and Trinajstić defined the general sum connectivity (GSC) index and discussed its various properties [21]. Shirdel et al. [22] studied the concept of hyper-Zagreb index (HZ – index) as a particular case of the GSC index. In addition, the results for the index HZ under the operation of Cartesian, composition, join, and disjunction of graphs can be found in [23–25].

On the other hand, for the studies of the complex graphs, operations for graphs play a key role. Yan et al. (2007) defined four types of operations related to the subdivision of G and computed the Wiener indices of the derived graphs $D_1(G)$, where $D_1 \in \{S_1, R_1, Q_1, T_1\}$ [26]. Taeri et al. (2009) gave the construction of the D_1 -sum graphs $G_{D_1} + H$ (Cartesian product of $F_1(G)$ and H) and computed their Wiener indices, where H and G are assumed to be two connected graphs [27]. Furthermore, Deng et al. [28], Akhter and Imran [29], Chu et al. [30], and Liu et al. [31] computed the various indices of these graphs with the help of the Cartesian product.

Liu et al. (2019) [32] extended these operations for any integral value of k and obtained the generalized derived graphs $D_k(G)$ of the graph G , where $D_k \in \{S_k, R_k, Q_k, T_k\}$. Moreover, using the concept of Cartesian product of graphs, they constructed the generalized sum graphs or D_k -sum graphs (denoted by $G_{D_k} + H$) and computed their first and second Zagreb indices.

Javaid et al. (2021) [33] redefined these graphs using strong product and computed their Zagreb indices (first and second). In this development, we compute hyper-Zagreb indices (HZ – index) for these graphs in terms of various degree-based TIs of their factor graphs, where these generalized sum graphs are obtained with the help of strong product. The remaining paper is settled as follows. Section 2 contains the notations and key concepts which are utilized in methodology, Section 3 deals main results, and Section 4 covers examples and conclusion.

2. Preliminaries

This section explains the basic definitions and terminologies.

Definition 1. Let $G = (V(G), E(G))$ be a (molecular) graph with $V(G)$ and $E(G)$ as sets of vertices and edges, respectively. The degree of a vertex $v \in V(G)$ is the number of edges which are incident on v and denoted by $d(v)$.

Definition 2 (see [13, 34]). For a graph G , the first, second, and forgotten Zagreb indices are defined as follows: $M_1(G) = \sum_{z \in V(G)} d^2(z) = \sum_{zt \in E(G)} [d(z) + d(t)]$, $M_2(G) = \sum_{zt \in E(G)} [d(z) \times d(t)]$, and $F(G) = \sum_{z \in V(G)} d^3(z) = \sum_{zt \in E(G)} [d^2(z) + d^2(t)]$.

These indices have been used to find the various properties of molecular graphs such as entropy, π -electron energy, and heat capacity. These are also used in the studies of the molecular structural relationships such as QSPR and QSAR [13, 35–37]. However, the hyper-Zagreb index of a graph (G) (given below) is studied by Shirdel et al. in 2013 [22]:

$$HZ(G) = \sum_{yz \in E(G)} [d(y) + d(z)]^2. \tag{1}$$

Definition 3 (see [32]). For some integral value of $k \geq 1$, the graphs obtained by the generalized subdivision-related operations are defined as follows:

- (i) $S_k(G)$ is a graph that is obtained by inserting k vertices in each edge of G
- (ii) $R_k(G)$ is a graph obtained from $S_k(G)$ by joining the vertices which are adjacent in G
- (iii) $Q_k(G)$ is a graph obtained from $S_k(G)$ by joining the new vertices which are on the incident edges in G for each of its vertex
- (iv) $T_k(G)$ is obtained from $S_k(G)$ after using both R_k and Q_k , respectively

For $k = 3$, see Figure 1.

Definition 4 (see [33]). Let G_1 and G_2 be two graphs, $D_k \in \{S_k, R_k, Q_k, T_k\}$ be generalized subdivision-related operations, and $D_k(G_1)$ be a graph obtained using D_k on G_1 having edge-set $E(D_k(G_1))$ and vertex-set $V(D_k(G_1))$. The generalized sum graph $G_1 \boxtimes_{D_k} G_2$ under the operation of strong product is a graph having vertex-set $V(G_1 \boxtimes_{D_k} G_2) = V(D_k(G_1)) \times V(G_2) = (V(G_1) \cup k(E(G_1))) \times V(G_2)$ such that two vertices (r_1, s_1) and (r_2, s_2) of $V(G_1 \boxtimes_{D_k} G_2)$ are adjacent iff $[r_1 = r_2$ in $V(G_1)$ and s_1 is adjacent to s_2 in $E(G_2)]$ or $[s_1 = s_2$ in $V(G_2)$ and s_1 is adjacent to s_2 in $E(G_1)]$ or $[r_1$ is adjacent to r_2 in $E(D_k(G_1))$ and s_1 is adjacent to s_2 in $E(G_2)]$, where $k \geq 1$ is a positive integer. For more explanation, see Figures 2 and 3.

3. Main Results

The main developments are covered by this section.

Theorem 1. For $k \geq 1$, the HZ-index of $G_1 \boxtimes_{S_k} G_2$ is

$$\begin{aligned} HZ(G_1 \boxtimes_{S_k} G_2) &= 8e_{G_1} M_1(G_2) + n_{G_1} HZ(G_2) + 4e_{G_2} M_1(G_1) + 4e_{G_1} HZ(G_2) + M_1(G_1) HZ(G_2) + 4M_1(G_1) M_1(G_2) \\ &\quad + n_{G_2} HZ S_1(G_1) + 4e_{G_2} M_1 S_1(G_1) + 2e_{G_1} M_1(G_2) + 4e_{G_2} HZ S_1(G_2) + 2M_1(G_2) M_1 S_1(G_1) \\ &\quad + M_1(G_2) HZ S_1(G_1) + 16(k-1)e_{G_1} [n_{G_2} + M_1(G_2) + 4e_{G_2}] + HZ_1 G_1 F(G_2) + 2M_1(G_2) HZ S_1(G_1) \\ &\quad + 2M_1(G_2) M_1(S(G_1)) + 2F(G_2) M_1(S(G_1)) + 16e_{G_1} e_{G_2} + 4e_{G_1} F(G_2) + 2e_{G_2} M_1(G_1) \\ &\quad + 4(k-1)e_{G_1} [8e_{G_2} + 2HZ(G_2) + 8M_1(G_2)]. \end{aligned} \tag{2}$$

Proof. Let the degree of a vertex $(r, s) \in G_1 \boxtimes_{S_k} G_2$ be denoted by $d(r, s)$:

$$\begin{aligned} HZ(G_1 \boxtimes_{S_k} G_2) &= \sum_{(r_1, s_1)(r_2, s_2) \in E(G_1 \boxtimes_{S_k} G_2)} [d(r_1, s_1) + d(r_2, s_2)]^2 \\ &= \sum_{r \in V(G_1)} \sum_{s_1, s_2 \in E(G_2)} [d(r, s_1) + d(r, s_2)]^2 + \sum_{r_1, r_2 \in E(S_k(G_1))} \sum_{s \in V(G_2)} [d(r_1, s) + d(r_2, s)]^2 \\ &\quad + \sum_{r_1, r_2 \in E(S_k(G_1))} \sum_{s_1, s_2 \in V(G_2)} [d(r_1, s_1) + d(r_2, s_2)]^2 = \sum_A + \sum_B + \sum_C. \end{aligned} \tag{3}$$

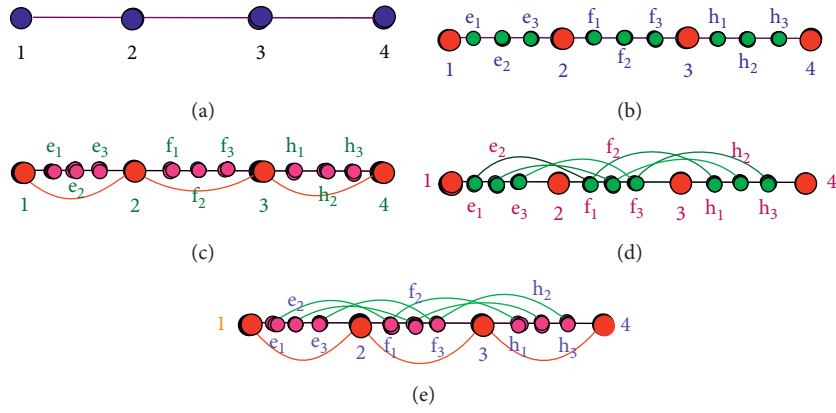


FIGURE 1: (a) $G_1 \cong P_4$, (b) $S_3(P_4)$, (c) $R_3(P_4)$, (d) $Q_3(P_4)$ and (e) $T_3(P_4)$.

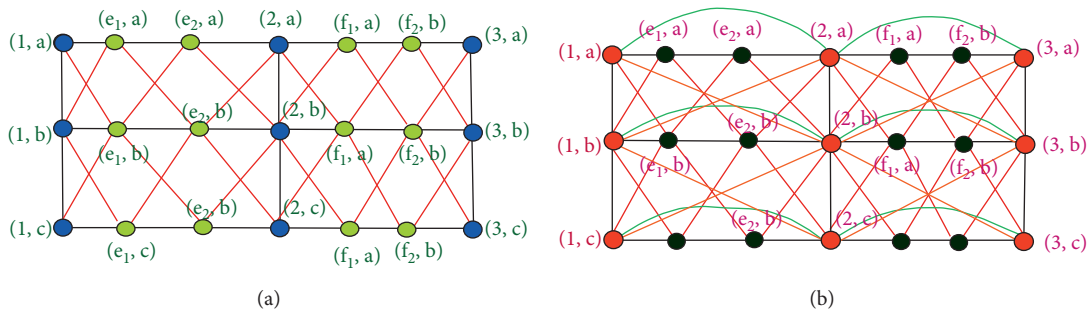


FIGURE 2: (a) $P_3 \boxtimes_{S_2} P_3$ and (b) $P_3 \boxtimes_{R_2} P_3$.

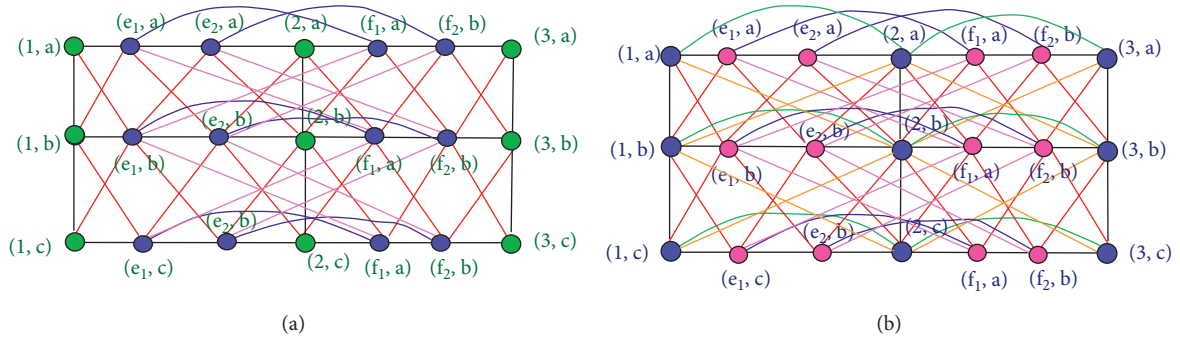


FIGURE 3: (a) $P_3 \boxtimes_{Q_2} P_3$ and (b) $P_3 \boxtimes_{T_2} P_3$.

Consider

$$\begin{aligned}
& \sum_A = \sum_{r \in V(G_1)} \sum_{s_1, s_2 \in E(G_2)} [d(r, s_1) + d(r, s_2)]^2 \\
& = \sum_{r \in V(G_1)} \sum_{s_1, s_2 \in E(G_2)} [2d(r) + d(s_1) + d(s_2) + d(r)(d(s_1) + d(s_2))]^2 \\
& = \sum_{r \in V(G_1)} \sum_{s_1, s_2 \in E(G_2)} [4d(r)(d(s_1) + d(s_2)) + (d^2(s_1) + d(s_2) + 2d(s_1)d(s_2)) + 4d^2(r) + 2d(r)(d^2(s_1) + d^2(s_2) \\
& \quad + 2d(s_1)d(s_2)) + d^2(r)(d^2(s_1) + d^2(s_2) + 2d(s_1)d(s_2)) + 4d^2(r)(d(s_1) + d(s_2))] \\
& = 8e_{G_1}M_1(G_2) + n_{G_1}HZ(G_2) + 4e_{G_2}M_1(G_1) + 4e_{G_1}HZ(G_2) + M_1(G_1)HZ(G_2) + 4M_1(G_1)M_1(G_2), \\
& \sum_B = \sum_{r_1, r_2 \in E(S_k(G_1))} \sum_{s \in V(G_2)} [d(r_1, s) + d(r_2, s)]^2 = \sum_{\substack{r_1 \in V(G_1), \\ r_2 \in V(S_k(G_1) - G_1)}} \sum_{s \in V(G_2)} [d(r_1, s) + d(r_2, s)]^2 \\
& \quad + \sum_{\substack{r_1, r_2 \in \\ V(S_k(G_1) - G_1)}} \sum_{s \in V(G_2)} [d(r_1, s) + d(r_2, s)]^2 = \sum_{B_1} + \sum_{B_2}, \\
& \sum_{B_1} = \sum_{\substack{r_1, r_2 \in E(S_k(G_1)) \\ r_1 \in V(G_1), r_2 \in V(S_k(G_1) - V(G_1))}} \sum_{s \in V(G_2)} [d(r_1, s) + d(r_2, s)]^2 \\
& = \sum_{\substack{r_1, r_2 \in E(S_k(G_1)) \\ r_1 \in V(G_1), r_2 \in V(S_k(G_1) - V(G_1))}} \sum_{s \in V(G_2)} [(d(r_1) + d(r_2)) + d(s) + (d(r_1) + d(r_2))d(s)]^2 \tag{4} \\
& = \sum_{\substack{r_1, r_2 \in E(S_k(G_1)) \\ r_1 \in V(G_1), r_2 \in V(S_k(G_1) - V(G_1))}} \sum_{s \in V(G_2)} [(d^2(r_1) + d^2(r_2) + 2d(r_1)d(r_2)) + 2d(s)(d(r_1) + d(r_2)) + d^2(s) \\
& \quad + 2d(s)(d^2(r_1) + d^2(r_2) + 2d(r_1)d(r_2)) + 2d^2(s)(d(r_1) + d(r_2)) + d^2(s)(d^2(r_1) + d^2(r_2))] \\
& = n_{G_2}HZS_1(G_1) + 4e_{G_2}M_1S_1(G_1) + 2e_{G_1}M_1(G_2) + 4e_{G_2}HZS_1(G_1) + 2M_1(G_2)M_1S_1(G_1) \\
& \quad + M_1(G_2)HZS_1(G_1), \\
& \sum_{B_2} = \sum_{\substack{r_1, r_2 \in E(S_k(G_1)) \\ r_1, s_2 \in V(S_k(G_1) - V(G_1))}} \sum_{s \in V(G_2)} [d(r_1, s) + d(r_2, s)]^2 \\
& = \sum_{\substack{r_1, r_2 \in E(S_k(G_1)) \\ r_1, r_2 \in V(S_k(G_1) - V(G_1))}} \sum_{s \in V(G_2)} [d(r_1) + d(r_1)d(s) + d(r_2) + d(r_2)d(s)]^2 \\
& = \sum_{\substack{r_1, r_2 \in E(S_k(G_1)) \\ r_1, r_2 \in V(S_k(G_1) - V(G_1))}} \sum_{s \in V(G_2)} [4 + 4d(s)]^2 = \sum_{\substack{r_1, r_2 \in E(S_k(G_1)) \\ r_1, r_2 \in V(S_k(G_1) - V(G_1))}} \sum_{s \in V(G_2)} [16 + 16d^2(s) + 32d(s)].
\end{aligned}$$

Since in this case $|E(S_k(G_1))| = (k - 1)|E(G_1)|$, we have

$$\begin{aligned}
 &= \sum_{s \in V(G_2)} 16(k - 1)e_{G_1} [1 + d^2(s) + 2d(s)] \\
 \sum_C &= \sum_{r_1 r_2 \in E(S_k(G_1))} [d(r_1, s_1) + d(r_2, s_2)]^2 = \sum_{\substack{r_1 r_2 \in E(S_k(G_1)) \\ r_1 \in V(G_1), r_2 \in ((S_k(G_1)) - V(G_1))}} \sum_{s_1 s_2 \in V(G_2)} [d(r_1, s_1) + d(r_2, s_2)]^2 \\
 &+ \sum_{\substack{r_1 r_2 \in E(S_k(G_1)) \\ r_1, r_2 \in V((S_k(G_1)) - V(G_1))}} \sum_{s_1 s_2 \in V(G_2)} [d(r_1, s_1) + d(r_2, s_2)]^2 = \sum_{C_1} + \sum_{C_2}, \\
 \sum_{C_1} &= \sum_{\substack{r_1 r_2 \in E(S_k(G_1)) \\ r_1 \in V(G_1), r_2 \in ((S_k(G_1)) - V(G_1))}} \sum_{s_1 s_2 \in V(G_2)} [d(r_1, z_1) + d(r_2, s_2)]^2 \\
 &= \sum_{\substack{r_1 \in V(G_1), \\ r_2 \in V((S_k(G_1)) - V(G_1))}} \sum_{s_1 s_2 \in V(G_2)} [(d(r_1) + d(r_2)) + d(s_1) + d(r_1)d(s_1) + d(r_2)d(s_2)]^2 \\
 &= \text{HZ } G_1 F(G_2) + 2M_1(G_2)\text{HZ } S_1(G_1) + 2M_1(G_2)M_1(S(G_1)) \\
 &+ 2F(G_2)M_1(S(G_1)) + 16e_{G_1}e_{G_2} + 4e_{G_1}F(G_2) + 2e_{G_2}M_1(G_1), \\
 \sum_{C_2} &= \sum_{\substack{r_1 r_2 \in E(S_k(G_1)) \\ r_1, r_2 \in V((S_k(G_1)) - V(G_1))}} \sum_{s_1 s_2 \in V(G_2)} [d(r_1, s_1) + d(r_2, s_2)]^2 \\
 &= \sum_{\substack{r_1 r_2 \in E(S_k(G_1)) \\ r_1, r_2 \in V((S_k(G_1)) - V(G_1))}} \sum_{s_1 s_2 \in V(G_2)} [4 + 2(d(s_1) + d(s_2))]^2 \\
 &= \sum_{\substack{r_1 r_2 \in E(S_k(G_1)) \\ r_1, r_2 \in V((S_k(G_1)) - V(G_1))}} \sum_{s_1 s_2 \in V(G_2)} [16 + 4(d(z_1) + d(z_2))^2 + 16(d(z_1) + d(z_2))] \\
 &= 4(k - 1)e_{G_1} [8e_{G_2} + 2\text{HZ}(G_2) + 8M_1(G_2)].
 \end{aligned} \tag{5}$$

Hence, we obtained our required result. \square

Theorem 2. For $k \geq 1$, the HZ-index of $G_1 \boxtimes_{R_k} G_2$ is

$$\begin{aligned}
 \text{HZ}(G_1 \boxtimes_{R_k} G_2) &= 8[n_{G_2} + 6e_{G_2}]F(G_1) + [n_{G_1} + 20e_{G_1}]F(G_2) + 8F(G_1)F(G_2) + 24e_{G_2}M_1(G_1) + 36e_{G_1}M_1(G_2) \\
 &+ 24M_1(G_1)M_1(G_2) + 24F(G_1)M_1(G_2) + 8n_{G_2}e_{G_1} + 8(k - 1)e_{G_1}[n_{G_2} + F(G_2) + 4e_{G_2} + 3M_1(G_2)] \\
 &+ 48e_{G_1}e_{G_2} + 12F(G_2)M_1(G_1) + 2[M_2(G_2)[4e_{G_1} + n_{G_1}] + k[n_{G_2} + 6e_{G_2} + 3M_1(G_2) + 2M_2(G_2)]] \\
 &\times \left[\frac{1}{2} \sum_{v \in V(G_1)} (d_{G_1}^4(v) - d_{G_1}^3(v)) + \sum_{v \in V(G_1)} r d_{G_1}(u) d_{G_1}(v) + \sum_{v \in V(G_1)} d_{G_1}^2(v) \sum_{\substack{u \in V(G_1) \\ uv \in E(G_1)}} d_{G_1}(u) - 2M_2(G_1) \right] \\
 &+ M_1(G_1)[5e_2 + 5M_1(G_2) + 5M_2(G_2)] + k[M_3(G_1) + 2M_2(G_1)][6e_{G_2} + 3M_1(G_2) + 2M_2(G_2) + n_{G_2}] \\
 &+ 2e_{G_1}M_1(G_2).
 \end{aligned} \tag{6}$$

Proof. Let the degree of a vertex $(r, s) \in G_1 \boxtimes_{R_k} G_2$ be denoted by $d(r, s)$:

$$\begin{aligned}
\text{HZ}(G_1 \boxtimes_{R_k} G_2) &= \sum_{(r_1, s_1)(r_2, s_2) \in E(G_1 \boxtimes_{R_k} G_2)} [d(r_1, s_1) + d(r_2, s_2)]^2 \\
&\cdot \sum_{r \in V(G_1)} \sum_{s_1, s_2 \in E(G_2)} [d(r, s_1) + d(r, s_2)]^2 + \sum_{s \in V(G_2)} \sum_{r_1, r_2 \in E(R_k(G_1))} [d(r_1, s) + d(r_2, s)]^2 \\
&+ \sum_{r_1, r_2 \in E(R_k(G_1))} \sum_{s_1, s_2 \in V(G_2)} [d(r_1, s_1) + d(r_2, s_2)]^2 = \sum_A + \sum_B + \sum_C, \\
\sum_A &= \sum_{r \in V(G_1)} \sum_{s_1, s_2 \in E(G_2)} [d(r, s_1) + d(r, s_2)]^2 \\
&= \sum_{r \in V(G_1)} \sum_{s_1, s_2 \in E(G_2)} [2d(r) + d(s_1) + 2d(r)d(s_1) + 2d(r) + d(s_2) + 2d(r)d(s_2)]^2 \\
&= \sum_{r \in V(G_1)} \sum_{s_1, s_2 \in E(G_2)} [4d(r) + d(s_1) + d(s_2) + 2d(r)(d(s_1) + d(s_2))]^2 \\
&= \sum_{r \in V(G_1)} \sum_{s_1, s_2 \in E(G_2)} [(4d^2(r) + 1 + 4d(r))(d^2(s_1) + d^2(s_2) + 2d(s_1)d(s_2)) + (8d(r) + 16d^2(r)) \\
&\quad \times (d(s_1) + d(s_2)) + 16d^2(r)] \\
&= \text{HZ}G_2 [4M_1(G_1) + n_{G_1} + 8e_{G_1}] + 16M_1(G_2) [e_{G_1} + M_1(G_1)] + 16M_1(G_1)e_{G_2}
\end{aligned}$$

OR

$$\begin{aligned}
&= 8e_{G_2}M_1(G_1) + n_{G_1}F(G_2) + 4M_1(G_1)F(G_2) + 8e_{G_1}M_1(G_2) + 8M_1(G_1)M_1(G_2) + 8e_{G_1}F(G_2) \\
&\quad + 2[4M_1(G_1)[e_{G_2} + M_1(G_2) + M_2(G_2)] + 4e_{G_1}[M_1(G_2) + 2M_2(G_2)] + M_2(G_2)n_{G_1}], \\
\sum_B &= \sum_{r_1, r_2 \in E(R_k(G_1))} \sum_{s \in V(G_2)} [d(r_1, s) + d(r_2, s)]^2 = \sum_{\substack{r_1, r_2 \in E(R_k(G_1)) \\ r_1, r_2 \in V(G_1)}} \sum_{s \in V(G_2)} [d(r_1, s) + d(r_2, s)]^2 \\
&\quad + \sum_{\substack{r_1, r_2 \in E(R_k(G_1)) \\ r_2 \in V(R_k(G_1)) - V(G_1)}} \sum_{s \in V(G_2)} [d(r_1, s) + d(r_2, s)]^2 + \sum_{\substack{r_1, r_2 \in E(R_k(G_1)) \\ r_1, r_2 \in V(R_k(G_1)) - V(G_1)}} \sum_{s \in V(G_2)} [d(r_1, s) + d(r_2, s)]^2 \\
&= \sum_{B_1} + \sum_{B_2} + \sum_{B_3}, \\
\sum_{B_1} &= \sum_{\substack{r_1, r_2 \in E(R_k(G_1)) \\ r_1, r_2 \in V(G_1)}} \sum_{s \in V(G_2)} [d(r_1, s) + d(r_2, s)]^2 \\
&= \sum_{\substack{r_1, r_2 \in E(R_k(G_1)) \\ r_1, r_2 \in V(G_1)}} \sum_{s \in V(G_2)} [d(r_1) + d(s) + d(r_1)d(s) + d(r_2) + d(s) + d(r_2)d(s)]^2 \\
&= \sum_{\substack{r_1, r_2 \in E(R_k(G_1)) \\ r_1, r_2 \in V(G_1)}} \sum_{s \in V(G_2)} [d(r_1) + d(r_2) + 2d(s) + d(s)(d(r_1) + d(r_2))]^2 \\
&= \sum_{\substack{r_1, r_2 \in E(R_k(G_1)) \\ r_1, r_2 \in V(G_1)}} \sum_{s \in V(G_2)} [4d^2(r_1) + 4d^2(s) + 4d(4d^2(r_2) + 8d(r_1)d(s) + 8d(r_1)d(r_2) + 8d(s)d(r_2)) \\
&\quad + 4d^2(s)(d^2(r_1) + d^2(r_2) + 2d(s)d^2(r_1)) + 8d(s_1)(d^2(r_1) + d^2(r_2) + 2d(s)d^2(r_1)) + 8d^2(s_1)(d(r_1) + d(r_2))] \\
&= 4e_{G_1}M_1(G_2) + [4n_{G_2} + 4M_1(G_2) + 16e_{G_2}]\text{HZ}(G_1) + 16e_{G_2}M_1(G_1) + 8M_1(G_1)M_1(G_2).
\end{aligned}$$

OR

$$\begin{aligned}
&= 4n_{G_2}F(G_1) + 2e_{G_1}M_1(G_2) + 4M_1(G_2)F(G_1) + 8e_{G_2}M_1(G_1) + 4M_1(G_1)M_1(G_2) + 16e_{G_2}F(G_1) \\
&\quad + 2[4M_2(G_1)[n_{G_2} + 4e_{G_2} + M_1(G_2)] + 2M_1(G_1)[M_1(G_2) + 2e_{G_2}] + e_{G_1}M_1(G_2)],
\end{aligned}$$

$$\begin{aligned}
 \sum_{B_2} &= \sum_{\substack{r_1 r_2 \in E(R_k(G_1)) \\ r_1 \in V(G_1), r_2 \in V(R_k(G_1)) - V(G_1)}} \sum_{seV(G_2)} [d(r_1, s) + d(r_2, s)]^2 \\
 &= \sum_{\substack{r_1 r_2 \in E(R_k(G_1)) \\ r_1 \in V(G_1), r_2 \in V(R_k(G_1)) - V(G_1)}} \sum_{seV(G_2)} [d(r_1) + d(r_2) + d(s) + (d(r_1) + d(r_2))d(s)]^2 \\
 &= \sum_{\substack{r_1 r_2 \in E(R_k(G_1)) \\ r_1 \in V(G_1), r_2 \in V(R_k(G_1)) - V(G_1)}} \sum_{seV(G_2)} [2d(r_1) + 3d(s) + 2d(r_1)d(s) + 2]^2 \\
 &= 4n_{G_2}F(G_1) + 18e_{G_1}M_1(G_2) + 8e_{G_1}n_{G_2} + 40e_{G_2}M_1(G_1) + 48e_{G_1}e_{G_2} + 8n_{G_2}M_1(G_1) \\
 &\quad + 4F(G_1)M_1(G_2) + 12M_1(G_1)M_1(G_2) + 16e_{G_2}F(G_1), \\
 \sum_{B_3} &= \sum_{\substack{r_1 r_2 \in E(R_k(G_1)) \\ r_1, r_2 \in V(R_k(G_1)) - V(G_1)}} \sum_{seV(G_2)} [d(r_1, s) + d(r_2, s)]^2 \\
 &= \sum_{\substack{r_1 r_2 \in E(R_k(G_1)) \\ r_1, r_2 \in V(R_k(G_1)) - V(G_1)}} \sum_{seV(G_2)} [d(r_1) + d(r_1)d(s) + d(r_2) + d(r_2)d(s)]^2 \\
 &= \sum_{\substack{r_1 r_2 \in E(R_k(G_1)) \\ r_1, r_2 \in V(R_k(G_1)) - V(G_1)}} \sum_{seV(G_2)} [4 + 4d(s)]^2 = \sum_{\substack{r_1 r_2 \in E(R_k(G_1)) \\ r_1, r_2 \in V(R_k(G_1)) - V(G_1)}} \sum_{seV(G_2)} [16 + 16d^2(s) + 32d(s)] \\
 &= \sum_{seV(G_2)} 16(k-1)e_{G_1}[1 + d^2(s) + 2d(s)] = 16(k-1)e_{G_1}[n_{G_2} + M_1(G_2) + 4e_{G_2}], \\
 \sum_C &= \sum_{r_1 r_2 \in E(R_k(G_1))} \sum_{s_1 s_2 \in V(G_2)} [d(r_1, s_1) + d(r_2, s_2)]^2 = \sum_{\substack{r_1 r_2 \in E(R_k(G_1)) \\ r_1, r_2 \in V(G_1)}} \sum_{s_1 s_2 \in V(G_2)} [d(r_1, s_1) + d(r_2, s_2)]^2 \\
 &\quad + \sum_{\substack{r_1 r_2 \in E(R_k(G_1)) \\ r_1 \in V(G_1), r_2 \in V(R_k(G_1)) - V(G_1)}} \sum_{s_1 s_2 \in V(G_2)} [d(r_1, s_1) + d(r_2, s_2)]^2 \\
 &\quad + \sum_{\substack{r_1 r_2 \in E(R_k(G_1)) \\ r_1, r_2 \in V(R_k(G_1)) - V(G_1)}} \sum_{s_1 s_2 \in V(G_2)} [d(r_1, s_1) + d(r_2, s_2)]^2 = \sum_{C_1} + \sum_{C_2} + \sum_{C_3}, \\
 \sum_{C_1} &= \sum_{\substack{r_1 r_2 \in E(R_k(G_1)) \\ r_1, r_2 \in V(G_1)}} \sum_{s_1 s_2 \in V(G_2)} [d(r_1, s_1) + d(r_2, s_2)]^2 \\
 &= \sum_{\substack{r_1 r_2 \in E(R_k(G_1)) \\ r_1, r_2 \in V(G_1)}} \sum_{s_1 s_2 \in V(G_2)} [d(r_1) + d(s_1) + d(r_1)d(s_1) + d(r_2) + d(s_2) + d(r_2)d(s_2)]^2 \\
 &= \sum_{\substack{r_1 r_2 \in E(R_k(G_1)) \\ r_1, r_2 \in V(G_1)}} \sum_{s_1 s_2 \in V(G_2)} [(d(r_1) + d(s_1) + d(r_1)d(s_1))^2 + (d(r_1) + d(s_2) + d(r_2)d(s_2))^2] \\
 &\quad + 2[4d(r_1)d(r_2) + 2[d(r_1)d(s_2) + d(r_2)d(s_1)] + d(s_1)d(s_2)] \\
 &\quad + 4d(r_1)d(r_2)d(s_1)d(s_2) + 4d(r_1)d(r_2)[d(s_1) + d(s_2)] + 2[d(r_1) + d(r_2)]d(s_1)d(s_2) \\
 &= 8e_{G_2}F(G_1) + 2e_{G_1}F(G_2) + 4F(G_1)F(G_2) + 4M_1(G_1)M_1(G_2) + 4M_1(G_1)F(G_2) + 8M_1(G_2)F(G_1) \\
 &\quad + 2[8M_2(G_1)e_{G_2} + 2M_1(G_1)M_1(G_2) + 2M_2(G_2)e_{G_1} + 8M_2(G_1)[M_2(G_2) + M_1(G_2)] + 4M_1(G_1)M_2(G_2)],
 \end{aligned}$$

$$\begin{aligned}
\sum_{C_2} &= \sum_{\substack{r_1, r_2 \in E(R_k(G_1)) \\ r_1 \in V(G_1), r_2 \in V((R_k(G_1))^{-V}(G_1))}} \sum_{s_1, s_2 \in V(G_2)} [d(r_1, s_1) + d(r_2, s_2)]^2 \\
&= \sum_{\substack{r_1, r_2 \in E(R_k(G_1)) \\ r_1 \in V(G_1), r_2 \in V((R_k(G_1))^{-V}(G_1))}} \sum_{s_1, s_2 \in V(G_2)} [d(r_1) + d(s_1) + d(r_1)d(s_1) + d(r_2) + d(r_2)d(s_2)]^2 \\
&= \sum_{\substack{r_1, r_2 \in E(R_k(G_1)) \\ r_1 \in V(G_1), r_2 \in V((R_k(G_1))^{-V}(G_1))}} \sum_{s_1, s_2 \in V(G_2)} [(d(r_1) + d(s_1) + d(r_1)d(s_1))^2 + (d(r_2) + d(r_2)d(s_2))^2] \\
&\quad + 2[(d(r_1) + d(s_1) + d(r_1)d(s_1))(d(r_2) + d(r_2)d(s_2))] \\
&= 8e_{G_2}F(G_1) + 32e_{G_1}e_{G_2} + 4F(G_1)F(G_2) + 4M_1(G_1)M_1(G_2) + 8F(G_1)M_1(G_2) \\
&\quad + 2e_{G_1}F(G_2) + 4M_1(G_1)F(G_2) + 8e_{G_1}F(G_2) + 16e_{G_1}M_1(G_2) + 8e_{G_1}[M_1(G_2) + M_2(G_2)] \\
&\quad + 2[M_2(R_1(G_1)) - 4M_2(G_1)][2e_{G_2} + 2M_1(G_2) + 2M_2(G_2)], \\
\sum_{C_3} &= \sum_{\substack{r_1, r_2 \in E((R_k(G_1))) \\ r_1, r_2 \in V((R_k(G_1))^{-V}(G_1))}} \sum_{s_1, s_2 \in V(G_2)} [d(r_1, s_1) + d(r_2, s_2)]^2 \\
&= \sum_{\substack{r_1, r_2 \in E((R_k(G_1))) \\ r_1, r_2 \in V((R_k(G_1))^{-V}(G_1))}} \sum_{s_1, s_2 \in V(G_2)} [d(r_1) + d(r_2) + d(r_1)d(s_1) + d(r_2)d(s_2)]^2 \\
&= [(2 + 2d(s_1))^2 + (2 + 2d(s_2))^2 + 2[2 + 2d(s_1)](2 + 2d(s_2))] \\
&= 8(k-1)e_{G_1}[2e_{G_2} + F(G_2) + 2M_1(G_2)] + 16(k-1)e_{G_1}[e_{G_2} + M_1(G_2) + M_2(G_2)].
\end{aligned} \tag{7}$$

Hence, we reached at our required result. \square

Theorem 3. For $k \geq 1$, the HZ-index of $G_1 \boxtimes_{Q_k} G_2$ is

$$\begin{aligned}
\text{HZ}(G_1 \boxtimes_{R_k} G_2) &= 2(k-1)[F(G_1) + 2M_2(G_1)][3n_{G_2} + 5M_1(G_1) + 14e_{G_2} + F(G_2)] \\
&\quad + k[n_{G_2} + 6e_{G_2} + 3M_1(G_2) + F(G_2)] \\
&\quad \left[M_4(G_1) - 2F(G_1) + 2M_2(G_1) - 4M_2(G_1) + \sum_{u \in V(G_1)} d^2(u) \sum_{v \in N(u)} d(v) \right] + 6e_{G_2}M_1(G_1) \\
&\quad + 10e_{G_2}F(G_2) + 3F(G_1)F(G_2) + 6M_1(G_1)M_1(G_2) + F(G_2)[n_{G_1} + 3M_1(G_1) + 6e_{G_2} + 4M_2(G_1)] \\
&\quad + F(G_1)[n_{G_2} + 7M_1(G_2)] + 6e_{G_2}M_2(G_1) + 8M_2(G_1)[e_{G_2} + M_1(G_2)] + 2[k[n_{G_2} + 6e_{G_2} + 3M_1(G_2) \\
&\quad + 2M_2(G_2)]] \frac{1}{2} \sum_{u \in V(G_1)} d_{G_1}^4(v) - d_{G_1}^3(v) + \sum_{u \in V(G_1)} td_{G_1}(u)d_{G_1}(v) + \sum_{u \in V(G_1)} d_{G_1}^2(v) \sum_{\substack{u \in V(G_1) \\ uv \in E(G_1)}} d_{G_1}(u) \\
&\quad - 2M_2(G_1)] + M_2(G_2)[4e_{G_1} + n_{G_1}] + 2e_{G_1}M_1(G_2) + M_1(G_1)[5e_2 + 5M_1(G_2) + 5M_2(G_2)] \\
&\quad + k[M_3(G_1) + 2M_2(G_1)][6e_{G_2} + 3M_1(G_2) + 2M_2(G_2) + n_{G_2}]].
\end{aligned} \tag{8}$$

Proof. Let the degree of a vertex $(r, s) \in G_1 \boxtimes_{Q_k} G_2$ be denoted by $d(r, s)$:

$$\begin{aligned} \text{HZ}(G_1 \boxtimes_{Q_k} G_2) &= \sum_{(r_1, s_1)(r_2, s_2) \in E(G_1 \boxtimes_{Q_k} G_2)} [d(r_1, s_1) + d(r_2, s_2)]^2 \\ &= \sum_{r \in V(G_1)} \sum_{s_1, s_2 \in E(G_2)} [d(r, s_1) + d(r, s_2)]^2 + \sum_{s \in V(G_2)} \sum_{r_1, r_2 \in E(Q_k(G_1))} [d(r_1, s) + d(r_2, s)]^2 \\ &\quad + \sum_{r_1, r_2 \in E(Q_k(G_1))} \sum_{s_1, s_2 \in V(G_2)} [d(r_1, s_1) + d(r_2, s_2)]^2 = \sum_A + \sum_B + \sum_C, \\ \sum_A &= \sum_{r \in V(G_1)} \sum_{s_1, s_2 \in E(G_2)} [d(r, s_1) + d(r, s_2)]^2 \\ &= 8e_1 M_1(G_2) + n_1 \text{HZ}(G_2) + 4e_2 M_1(G_1) + 4e_1 \text{HZ}(G_2) + M_1(G_1) \text{HZ}(G_2) + 4M_1(G_1) M_1(G_2) \end{aligned}$$

OR

$$\begin{aligned} &= 2|E(H_2)|M_1(H_1) + |V(H_1)|F(H_2) + M_1(H_1)F(H_2) \\ &\quad + 4|E(H_1)|M_1(H_2) + 2M_1(H_1)M_1(H_2) + 4|E(H_1)|F(H_2) \\ &\quad + 2[M_1(G_1)e_{G_2} + M_1(G_1)[M_1(G_2) + M_2(G_2)] + 2e_{G_1}[M_1(G_2) + 2M_2(G_2)] + M_2(G_2)n_{G_1}], \quad (9) \\ \sum_B &= \sum_{s \in V(G_2)} \sum_{r_1, r_2 \in E(Q_k(G_1))} [d(r_1, s) + d(r_2, s)]^2 \\ &\quad + \sum_{s \in V(G_2)} \sum_{\substack{r_1, r_2 \in E(Q_k(G_1)) \\ r_1, r_2 \in V(Q_k(G_1)) - V(G_1)}} [d(r_1, s) + d(r_2, s)]^2 \\ \sum_{B_1} &= \sum_{s \in V(G_2)} \sum_{\substack{r_1, r_2 \in E(Q_k(G_1)) \\ r_1 \in V(G_1), r_2 \in V(Q_k(G_1)) - V(G_1)}} [d(r_1, s) + d(r_2, s)]^2 \\ &= \sum_{s \in V(G_2)} \sum_{\substack{r_1, r_2 \in E(Q_k(G_1)) \\ r_1 \in V(G_1), r_2 \in V(Q_k(G_1)) - V(G_1)}} [d(r_1) + d(s) + d(r_1)d(r) + d(r_2) + d(r_2)d(s)]^2 \\ &= \sum_{\substack{r_1, r_2 \in E(Q_k(G_1)) \\ s_1 \in V(H_1), s_2 \in V(Q_k(H_1)) - H_1}} \sum_{s \in V(G_2)} [(d(r_1) + d(s) + d(r_1)d(s))^2 (d(r_2) + d(r_2)d(s))^2 \\ &\quad + 2[d(r_1) + d(s) + d(r_1)d(s)][d(r_2) + d(s) + d(r_2)d(s)]]. \end{aligned}$$

Consider $r_1 \in V(G_1)$ and $d^2(r_1)$ occurs $d(r_1)$ times. Thus,

$$D_1 = \sum_{\substack{r_1, r_2 \in E(Q(G_1)), \\ r_1 \in V(G_1), r_2 \in V(Q(G_1)) - V(G_1)}} d^3(r_1) = F(G_1). \quad (10)$$

Let

$$D_2 = \sum_{\substack{r_1, r_2 \in E(Q(G_1)), \\ r_1 \in V(G_1), r_2 \in V(Q(G_1)) - V(G_1)}} d^2(s_2), \quad (11)$$

as $s_2 = uv \in E(G_1)$ and $d^2(s_2)$ occurs two times. Therefore,

$$\begin{aligned}
 D_2 &= 2 \sum_{s_2=uv \in E(G_1)-V(G_1)} [d(u) + d(v)]^2 = 2 \sum_{uv \in E(G_1)} [d^2(u) + d^2(v) + 2d(u)d(v)] = 2[F(G_1) + 2M_2(G_1)], \\
 \sum_{B_1} &= n_{G_2}F(G_1) + 2e_{G_1}M_1(G_2) + M_1(G_2)F(G_1) + 4e_{G_2}[M_1(G_1) + F(G_1)] + 2M_1(G_1)M_1(G_2) \\
 &\quad + 2n_{G_2}[F(G_1) + 2M_2(G_1)] + 2M_1(G_2)[F(G_1) + 2M_2(G_1)] + 8e_{G_2}[F(G_1) + 2M_2(G_1)] \\
 &\quad + 2[[M_3(G_1) + 2M_2(G_1)][n_{G_2} + 4e_{G_2} + M_1(G_2)] + 2M_1(G_1)[2e_{G_2} + M_1(G_2)]], \\
 \sum_{B_2} &= \sum_{\substack{r_1 r_2 \in E(Q_k(G_1)) \\ r_1 r_2 \in V(Q_k(G_1))-V(G_1)}} \sum_{s \in V(G_2)} [d(r_1, s) + d(r_2, s)]^2.
 \end{aligned} \tag{12}$$

Now, assume $\Sigma_{B_2} = \Sigma_{B_3} + \Sigma_{B_4}$ as follows:

$$\begin{aligned}
 \sum_{B_3} &= \sum_{\substack{r_1 r_2 \in E(Q_k(G_1)) \\ r_1 r_2 \in V(Q_k(G_1))-V(G_1)}} \sum_{s \in V(G_2)} [(d(r_1) + d(r_1)d(s))^2 + (d(r_2) + d(r_2)d(s))^2 \\
 &\quad + 2[(d(r_1) + d(r_1)d(s))(d(r_2) + d(r_2)d(s))]] \\
 &= 2(k-1)[(F(G_1) + 2M_2(G_1))(n_{G_2} + M_1(G_2) + 4e_{G_2}) + (M_3(G_1) + 2M_2(G_1))(n_{G_2} + 4e_{G_2} + M_1(G_2))], \\
 \sum_{B_4} &= \sum_{\substack{r_1 r_2 \in E(Q_k(G_1)) \\ r_1 r_2 \in V(Q_k(G_1))-V(G_1)}} \sum_{s \in V(G_2)} [d(r, s_1) + d(r, s_2)]^2 \\
 &= \sum_{\substack{r_1 r_2 \in E(Q_k(G_1)) \\ r_1 r_2 \in V(Q_k(G_1))-V(G_1)}} \sum_{s \in V(G_2)} [d(r_1) + d(r_1)d(s) + d(r_2) + d(r_2)d(s)]^2 \\
 &= \sum_{\substack{r_1 r_2 \in E(Q_k(G_1)) \\ r_1 r_2 \in V(Q_k(G_1))-V(G_1)}} \sum_{s \in V(G_2)} [d(r_1)^2 + d(r_2)^2 + d(s)^2(d(r_1)^2 + d(r_2)^2) + 2d(s)(d(r_1)^2 + d(r_2)^2)] \\
 &\quad + 2[(d(r_1) + d(r_1)d(s))(d(r_2) + d(r_2)d(s))], \\
 D_3 &= \sum_{\substack{r_1 r_2 \in E(Q(G_1)) \\ r_1 r_2 \in V(Q(G_1))-V(G_1)}} [d^2(r_1) + d^2(r_2)].
 \end{aligned} \tag{13}$$

In D_3 , coefficient of

$$d^2(u) = 2 \binom{2}{d_{G_1}(u)} + \sum_{v \in N(u)} d(v) - d(u) = d^2(u) - 2d(u) + \sum_{v \in N(u)} d(v). \tag{14}$$

Therefore,

$$\sum_{u \in V(G_1)} d^2(u) = M_4(G_1) - 2F(G_1) + \sum_{u \in V(G_1)} d^2(u) \sum_{v \in N(u)} d(v). \tag{15}$$

For coefficient of $d(u)d(v)$, let $r_1r_2 \in E(Q(G_1))$ with $r_1 = uv$ and $r_2 = wz$. As $r_1r_2 \in E(Q(G_1))$, we have either $v = w$ or $z = u = w$ or z . So, uv is adjacent to all those vertices in G_1

which are adjacent to u and v . Consequently, the number of such $d(u)d(v)$ is $(d(u) + d(v) - 2)$. Therefore,

$$\begin{aligned} 2 \sum_{uv \in E(G_1)} d(u)d(v) &= 2 \sum_{uv \in E(G_1)} (d(u) + d(v) - 2)dudv \\ &= 2 \sum_{uv \in E(G_1)} (d(u) + d(v))d(u)d(v) - 4 \sum_{uv \in E(G_1)} d(u)d(v) = 2M_2(G_1) - 4M_2(G_1), \end{aligned} \tag{16}$$

so

$$\begin{aligned} D_3 &= M_4(G_1) - 2F(G_1) + \sum_{u \in V(G_1)} d^2(u) \sum_{v \in N(u)} d(v) + 2M_2(G_1) - 4M_2(G_1), \\ \sum_{B_4} &= (k)[n_{G_2} + 4e_{G_2} + M_1(G_2)] \left[M_4(G_1) - 2F(G_1) + 2M_2(G_1) - 4M_2(G_1) + \sum_{u \in V(H_1)} d^2(u) \sum_{v \in N(u)} d(v) \right] \\ &+ 2 \left[(k)[n_{G_2} + 4e_{G_2} + M_1(G_2)] \left[\frac{1}{2} \sum_{v \in V(G_1)} (d_{G_1}^4(v) - d_{G_1}^3(v)) + \sum_{uv \in V(G_1)} td_{G_1}(u)d_{G_1}(v) \right] \right. \\ &\left. + \sum_{v \in V(G_1)} d_{G_1}^2(v) \sum_{\substack{v \in V(G_1) \\ uv \in E(G_1)}} d_{G_1}(u) - 2M_2(G_1) \right] \end{aligned} \tag{17}$$

where t is the number of neighbors which are common vertices of u and v in (G_1) .

$$\begin{aligned} \sum_C &= \sum_{r_1r_2 \in E(Q_k(G_1))} \sum_{s_1s_2 \in V(G_2)} [d(r_1, s_1) + d(r_2, s_2)]^2 = \sum_{\substack{r_1r_2 \in E(Q_k(G_1)) \\ r_1 \in V(G_1), r_2 \in V(Q_k(G_1)) - V(G_1)}} \sum_{s_1s_2 \in V(G_2)} [d(r_1, s_1) + d(r_2, s_2)]^2 \\ &+ \sum_{\substack{r_1r_2 \in E(Q_k(G_1)) \\ r_1 \in V(G_1), r_2 \in V(Q_k(G_1)) - V(G_1)}} \sum_{s_1s_2 \in V(G_2)} [d(r_1, s_1) + d(r_2, s_2)]^2 = \sum_{C_1} + \sum_{C_2}, \\ \sum_{C_1} &= \sum_{\substack{r_1r_2 \in E(Q_k(G_1)) \\ r_1 \in V(G_1), r_2 \in V(Q_k(G_1)) - V(G_1)}} \sum_{s_1s_2 \in V(G_2)} [d(r_1, s_1) + d(r_2, s_2)]^2 \\ &= \sum_{\substack{r_1r_2 \in E(Q_k(G_1)) \\ r_1 \in V(G_1), r_2 \in V(Q_k(G_1)) - V(G_1)}} \sum_{s_1s_2 \in V(G_2)} [d(r_1) + d(s_1) + d(r_1)d(s_1) + d(r_2) + d(s_2) + d(r_2s_2)]^2 \\ &= \sum_{\substack{r_1r_2 \in E(Q_k(G_1)) \\ r_1 \in V(G_1), r_2 \in V(Q_k(G_1)) - V(G_1)}} \sum_{s_1s_2 \in V(G_2)} [(d(r_1) + d(s_1) + d(r_1)d(s_1))^2 + (d(r_2) + d(r_2)d(s_2))^2] \end{aligned}$$

$$\begin{aligned}
& + 2[d(r_1, s_1)d(r_2, s_2)]) \\
= & 6[e_{G_2} + M_1(G_2)]F(G_1) + 3F(G_1)F(G_2) + 2M_1(G_1)M_1(G_2) + 2[e_{G_1} + M_1(G_1) + 2M_2(G_1)]F(G_2) + 8M_2(G_1) \quad (18) \\
& \times [e_{G_2} + M_1(G_2)] + 2[[M_3(G_1) + 2M_2(G_1)][2e_{G_2} + 2M_1(G_2) + 2M_2(G_2)] + 2M_1(G_1)[2M_2(G_2) + M_1(G_2)]].
\end{aligned}$$

Now, assume $\Sigma_{C_2} = \Sigma_{C_3} + \Sigma_{C_4}$ as follows:

$$\begin{aligned}
\Sigma_{C_3} &= \sum_{s_1 s_2 \in V(G_2)} \sum_{\substack{r_1 r_2 \in E(Q_k(G_1)) \\ r_1 \in V(G_1), r_2 \in V(Q_k(G_1)) - V(G_1)}} [d(r_1, s_1) + d(r_2, s_2)]^2 \\
&= \sum_{s_1 s_2 \in V(G_2)} \sum_{\substack{r_1 r_2 \in E(Q_k(G_1)) \\ r_1 \in V(G_1), r_2 \in V(Q_k(G_1)) - V(G_1)}} [d(r_1) + d(r_1)d(s_1) + d(r_2) + d(r_2)d(s_2)]^2 \\
&= \sum_{t_1 t_2 \in E(H_2)} \sum_{\substack{s_1 s_2 \in E(Q_k(H_1)) \\ s_1, s_2 \in V(Q_k(H_1)) - H_1}} [(d(s_1) + d(s_1)d(t_1))^2 + (d(s_2) + d(s_2)d(t_2))^2] \\
&\quad + 2[(d(r_1) + d(r_1)d(s_1))(d(r_2) + d(r_2)d(s_2))] \\
&= 2(k-1)[(F(G_1) + 2M_2(G_1))][2e_{G_2} + F(G_2) + 2M_1(G_2)] + 2(k-1)[2e_{G_2} + 2M_1(G_2) + 2M_2(G_2)][M_3(G_1) + 2M_2(G_1)], \\
\Sigma_{C_4} &= \sum_{s_1 s_2 \in V(G_2)} \sum_{\substack{r_1 r_2 \in E(Q_k(G_1)) \\ r_1, r_2 \in V(Q_k(G_1)) - V(G_1)}} [d(r_1, s_1) + d(r_2, s_2)]^2 \\
&= \sum_{s_1 s_2 \in V(G_2)} \sum_{\substack{r_1 r_2 \in E(Q_k(G_1)) \\ r_1, r_2 \in V(Q_k(G_1)) - V(G_1)}} [d(r_1) + d(r_2) + d(r_1)d(s_1) + d(r_2)d(s_2)]^2 \\
&= \sum_{s_1 s_2 \in V(G_2)} \sum_{\substack{r_1 r_2 \in E(Q_k(G_1)) \\ r_1, r_2 \in V(Q_k(G_1)) - V(G_1)}} [(d(r_1) + d(r_1)d(s_1))^2 + (d(r_2) + d(r_2)d(s_2))^2] \\
&\quad + 2[(d(r_1) + d(r_1)d(s_1))(d(r_2) + d(r_2)d(s_2))] \\
&= (k)[2e_{G_2} + F(G_2) + 2M_1(G_2)] \left[M_4(G_1) - 2F(G_1) + 2M_2(G_1) - 4M_2(G_1) + \sum_{u \in V(G_1)} d^2(u) \sum_{v \in N(u)} d(v) \right] \\
&\quad + (2k)[2e_{G_2} + 2M_1(G_2) + 2M_2(G_2)] \left[\frac{1}{2} \sum_{v \in V(G_1)} (d_{G_1}^4(v) - d_{G_1}^3(v)) + \sum_{uv \in E(G_1)} td_{G_1}(u)d_{G_1}(v) \right. \\
&\quad \left. + \sum_{u \in V(G_1)} d_{G_1}^2(v) \sum_{\substack{u \in V(G_1) \\ uv \in E(G_1)}} d_{G_1}(u) - 2M_2(G_1) \right],
\end{aligned} \tag{19}$$

where t is the number of neighbors which are common vertices of u and v in (G_1) .

Thus, we arrive at our desired result. □

Theorem 4. For $k \geq 1$, the HZ-index of $G_1 \boxtimes_{T_k} G_2$ is

$$\begin{aligned}
 \text{HZ}(G_1 \boxtimes_{T_k} G_2) &= 2(k-1)[F(G_1) + 2M_2(G_1)][n_{G_2} + 3M_1(G_2) + 6e_{G_2} + F(G_2)] + k[n_{G_2} \\
 &+ 6e_{G_2} + 3M_1(G_2) + F(G_2)][M_4(G_1) - 2F(G_1) + 2M_2(G_1) - 4M_2(G_1) \\
 &+ \sum_{u \in V(G_1)} d^2(u) \sum_{v \in N(u)} dv] + [F(G_1) + 2M_2(G_1)][2n_{G_2} + 6M_1(G_2) + 12e_{G_2} + 2F(G_2)] \\
 &+ 4F(G_1)[2n_{G_2} + 6M_1(G_2) + 12e_{G_2} + 2F(G_2)] + F(G_2)[n_{G_1} + 12M_1(G_1) \\
 &+ 12e_{G_2}] + 12e_{G_1}M_1(G_2) + 16e_{G_2}M_1(G_1) + 20M_1(G_1)M_1(G_2)] \\
 &+ 2 \left[k[n_{G_2} + 6e_{G_2} + 3M_1(G_2)2M_2(G_2)] \left[\frac{1}{2} \sum_{v \in V(G_1)} (d_{G_1}^4(v) - d_{G_1}^3(v)) + \sum_{uv \in E(G_1)} d_{G_1}(u)d_{G_1}(v) \right. \right. \\
 &\left. \left. + \sum_{v \in V(G_1)} d_{G_1}^2(v) \sum_{\substack{u \in V(G_1) \\ uv \in E(G_1)}} d_{G_1}(u) - 2M_2(G_1) \right] + M_2(G_1)[4n_{G_2} + 24e_{G_2} + 8M_2(G_2) + 12M_1(G_2)] \right] \\
 &+ k[M_3(G_1) + 2M_2(G_1)][6e_{G_2} + n_{G_2} + 3M_1(G_2) + 2M_2(G_2)] + 5M_1(G_2)e_{G_1} \\
 &+ M_2(G_2)[10e_{G_1} + n_{G_1}] + M_1(G_1)[10e_{G_2} + 11M_1(G_2) + 10M_2(G_2)].
 \end{aligned} \tag{20}$$

4. Applications and Discussion

(i) S_1 -sum:

Using $k = 1$, in Theorems 1–4, the results are obtained for the generalized D_1 -sum graphs as follows:

$$\begin{aligned}
 \text{HZ}(G_1 \boxtimes_{S_1} G_2) &= [n_{G_2} + 3M_1(G_2) + 6e_{G_2}]F(G_1) + [n_{G_1} + 3M_1(G_1) + 14e_{G_1}]F(G_2) + 6e_{G_2}M_1(G_1) + 30e_{G_1}M_1(G_2) \\
 &+ 6M_1(G_1)M_1(G_2) + 48e_{G_1}e_{G_2} + F(G_1)F(G_2) + 8n_{G_2}e_{G_1} + 2[[M_2(G_1) + 4e_{G_1}][5e_{G_2} + 3M_1(G_2) \\
 &+ 2M_2(G_2) + n_{G_2}] + 14e_{G_1}M_1(G_2) + M_2(G_2)][12e_{G_1} + n_{G_1}] + M_1(G_1)[e_{G_2} + M_1(G_2) + M_2(G_2)] \\
 &+ 8e_{G_1}e_{G_2}].
 \end{aligned} \tag{21}$$

TABLE 1: Hyper-Zagreb index of F_1 -sum path graphs.

$[n_1, n_2]$	$\text{HZ}(P_{n_1} \boxtimes_{S_1} P_{n_2})$	$\text{HZ}(P_{n_1} \boxtimes_{R_1} P_{n_2})$	$\text{HZ}(P_{n_1} \boxtimes_{Q_1} P_{n_2})$	$\text{HZ}(P_{n_1} \boxtimes_{T_1} P_{n_2})$
(3, 3)	4144	11870	8834	16168
(4, 4)	11040	30260	24500	47180
(5, 5)	21232	62122	46516	89230
(6, 6)	33696	99344	75416	145204
(7, 7)	51384	147638	110384	212318

(ii) R_1 -sum:

$$\begin{aligned}
 \text{HZ}(G_1 \boxtimes_{R_1} G_2) &= 8[n_{G_2} + 6e_{G_2}]F(G_1) + [n_{G_1} + 20e_{G_1}]F(G_2) + 8F(G_1)F(G_2) + 24e_{G_2}M_1(G_1) + 36e_{G_1}M_1(G_2) \\
 &\quad + 24M_1(G_1)M_1(G_2) + 24F(G_1)M_1(G_2) + 8n_{G_2}e_{G_1} + 48e_{G_1}e_{G_2} + 12F(G_2)M_1(G_1) \\
 &\quad + 2[2M_1(G_1)[4e_{G_2} + 6M_1(G_2) + 2M_2(G_2)] + 4e_{G_1}[3M_1(G_2) + 3M_2(G_2) + 4e_{G_2}] \tag{22} \\
 &\quad + [M_2(R_1(G_1)) - 4M_2G_1][6e_{G_2} + 3M_1(G_2) + 2M_2(G_2) + n_{G_2}] + e_{G_1}M_1(G_2) \\
 &\quad + 4M_2(G_1)[n_{G_2} + 6e_{G_2} + 3M_1(G_2)] + M_2(G_2)[n_{G_1} + 2e_{G_1}].
 \end{aligned}$$

(iii) Q_1 -sum:

$$\begin{aligned}
 \text{HZ}(G_1 \boxtimes_{Q_1} G_2) &= 2 \left[[n_{G_2} + 6e_{G_2} + 3M_1(G_2) + 2M_2(G_2)] \left[\frac{1}{2} \sum_{v \in V(G_1)} (d_{G_1}^4(v) - d_{G_1}^3(v)) + \sum_{uv \in E(G_1)} td_{G_1}(u)d_{G_1}(v) \right. \right. \\
 &\quad \left. \left. + \sum_{v \in V(G_1)} d_{G_1}^2(v) \sum_{\substack{ue \in V(G_1) \\ uve \in E(G_1)}} d_{G_1}(u) - 2M_2(G_1) \right] + M_2(G_2)[4e_{G_1} + n_{G_1}] + 2e_{G_1}M_1(G_2) + M_1(G_1) \right] \\
 &\quad \times [5e_2 + 5M_1(G_2) + 5M_2(G_2)] + [M_3(G_1) + 2M_2(G_1)][6e_{G_2} + 3M_1(G_2) + 2M_2(G_2) + n_{G_2}] \\
 &\quad + [n_{G_2} + e_{G_2} + 3M_1(G_2) + F(G_2)] \left[M_4(G_1) - 2F(G_1) + 2M_2(G_1) - 4M_2(G_1) + \sum_{u \in V(G_1)} d^2(u) \right. \\
 &\quad \left. \times \sum_{v \in N(u)} d(v) \right] + 6e_{G_2}M_1(G_1) + 10e_{G_2}F(G_2) + 3F(G_1)F(G_2) + 6M_1(G_1)M_1(G_2) + F(G_2)[n_{G_1} \\
 &\quad + 3M_1(G_1) + 6e_{G_2} + 4M_2(G_1)] + F(G_1)[n_{G_2} + 7M_1(G_2)] + 6e_{G_2}M_2(G_1) + 8M_2(G_1)[e_{G_2} + M_1(G_2)]. \tag{23}
 \end{aligned}$$

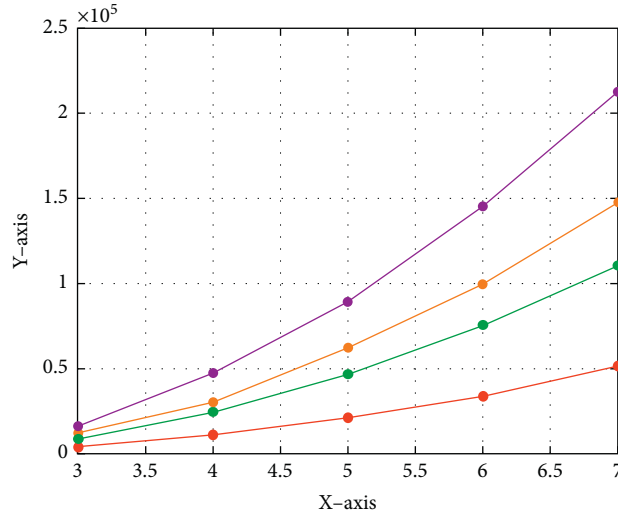


FIGURE 4: Graphical representation of $HZ(P_{n_1} \boxtimes_{S_1} P_m)$, $HZ(P_{n_1} \boxtimes_{R_1} P_m)$, $HZ(P_{n_1} \boxtimes_{Q_1} P_m)$, and $HZ(P_{n_1} \boxtimes_{T_1} P_m)$ in red, green, orange, and purple colour, respectively.

(iv) T_1 -sum:

$$\begin{aligned}
 HZ(G_1 \boxtimes_{T_1} G_2) &= [n_{G_2} + 6e_{G_2} + 3M_1(G_2) + F(G_2)] \left[M_4(G_1) - 2F(G_1) + 2M_2(G_1) - 4M_2(G_1) + \sum_{u \in V(G_1)} d^2(u) \right. \\
 &\quad \left. \times \sum_{v \in N(u)} d(v) \right] + [F(G_1) + 2M_2(G_1)] [2n(G_2) + 6M_1(G_2) + 12e_{G_2} + 2F(G_2)] + 4F(G_1) [2n_{G_2} \\
 &\quad + 6M_1(G_2) + 12e_{G_2} + 2F(G_2)] + F(G_2) [n_{G_1} + 12M_1(G_1) + 12e_{G_2}] + 12e_{G_1} M_1(G_2) + 16e_{G_2} M_1(G_1) \\
 &\quad + 20M_1(G_1) M_1(G_2) + 2 \left[[n_{G_2} + 6e_{G_2} + 3M_1(G_2) + 2M_2(G_2)] \left[\frac{1}{2} \sum_{v \in V(G_1)} (d_{G_1}^4(v) - d_{G_1}^3(v)) \right. \right. \\
 &\quad \left. \left. + \sum_{uv \in E(G_1)} td_{G_1}(u)d_{G_1}(v) + \sum_{v \in V(G_1)} d_{G_1}^2(v) \sum_{\substack{u \in V(G_1) \\ uv \in E(G_1)}} d_{G_1}(u) - 2M_2(G_1) \right] + [M_3(G_1) + 2M_2(G_1)] \right. \\
 &\quad \left. \times [6e_{G_2} + n_{G_2} + 3M_1(G_2) + 2M_2(G_2)] + 5M_1(G_2)e_{G_1} + M_1(G_1) [10e_{G_2} + 11M_1(G_2) + 10M_2(G_2)] \right. \\
 &\quad \left. + M_2(G_2) [10e_{G_1} + n_{G_1}] + M_2(G_1) [4n_{G_2} + 24e_{G_2} + 8M_2(G_2) + 12M_1(G_2)] \right]. \tag{24}
 \end{aligned}$$

Now, we present tabular form in Table 1 and graphical representation in Figure 4 of path graphs for $k = 1$.

Finally, we close this section with the comment that the problem is still open for other topological indices and product of graphs, in particular the general randic index of F_k -sum graphs under corona product.

Data Availability

The data are included within this paper and are available from the corresponding author upon request.

Conflicts of Interest

The authors declare that they have no conflicts of interest.

Acknowledgments

The authors extend their appreciation to the Deanship of Scientific Research at Jouf University for funding this work through research grant no. DSR-2021-03-0222.

References

- [1] I. Gutman and O. Polansky, *Mathematical Concepts in Organic Chemistry*, Springer-Verlag, Berlin, Germany, 1986.
- [2] R. Todeschini, V. Consonni, R. Mannhold, H. Kubinyi, and H. Timmerman, *Handbook of Molecular Descriptors*, Wiley-VCH, Weinheim, Germany, 2002.
- [3] D. M. Cvetkovic, M. Doob, and H. Sachs, *Spectra of Graphs: Theory and Application*, Academic Press, New York, NY, USA, 1980.
- [4] G. Rücker and C. Rucker, "On topological indices, boiling points, and cycloalkanes," *Journal of Chemical Information and Computer Sciences*, vol. 39, no. 5, pp. 788–802, 1999.
- [5] M. Randic, "Characterization of molecular branching," *Journal of the American Chemical Society*, vol. 97, no. 23, pp. 6609–6615, 1975.
- [6] A. R. Matamala and E. Estrada, "Generalised topological indices: optimisation methodology and physico-chemical interpretation," *Chemical Physics Letters*, vol. 410, no. 4–6, pp. 343–347, 2005.
- [7] F. Yan, Q. Shang, S. Xia, Q. Wang, and P. Ma, "Application of topological index in predicting ionic liquids densities by the quantitative structure property relationship method," *Journal of Chemical & Engineering Data*, vol. 60, no. 3, pp. 734–739, 2015.
- [8] L. H. Hall and L. B. Kier, *Molecular Connectivity in Chemistry and Drug Research*, Academic Press, Boston, MA, USA, 1976.
- [9] H. Gonzalez-Diaz, S. Vilar, L. Santana, and E. Uriarte, "Medicinal chemistry and bioinformatics-current trends in drugs discovery with networks topological indices," *Current Topics in Medicinal Chemistry*, vol. 7, no. 10, pp. 1015–1029, 2007.
- [10] M. V. Diudea, *QSPR/QSAR Studies by Molecular Descriptors*, NOVA, New York, NY, USA, 2001.
- [11] J. Devillers and A. T. Balaban, *Topological Indices and Related Descriptors in QSAR and QSPR*, Gordon Breach, Amsterdam, Netherlands, 1999.
- [12] H. Wiener, "Structural determination of paraffin boiling points," *Journal of the American Chemical Society*, vol. 69, no. 1, pp. 17–20, 1947.
- [13] I. Gutman and N. Trinajstić, "Graph theory and molecular orbitals. Total ϕ -electron energy of alternant hydrocarbons," *Chemical Physics Letters*, vol. 17, no. 4, pp. 535–538, 1972.
- [14] I. Gutman, "Degree-based topological indices," *Croatica Chemica Acta*, vol. 86, no. 4, pp. 351–361, 2013.
- [15] Z. Ahmad, M. Naseem, M. Naseem, M. K. Jamil, M. F. Nadeem, and S. Wang, "Eccentric connectivity indices of titania nanotubes TiO_2 [m;n]," *Eurasian Chemical Communications*, vol. 2, no. 6, pp. 712–721, 2020.
- [16] S. Imran, M. Siddiqui, M. Imran, and M. Nadeem, "Computing topological indices and polynomials for line graphs," *Mathematics*, vol. 6, no. 8, p. 137, 2018.
- [17] A. Aslam, Y. Bashir, S. Ahmad, and W. Gao, "On topological indices of certain dendrimer structures," *Zeitschrift für Naturforschung A*, vol. 72, no. 6, pp. 559–566, 2017.
- [18] A. Ahmad, R. Hasni, K. Elahi, and M. A. Asim, "Polynomials of degree-based indices for swapped networks modeled by optical transpose interconnection system," *IEEE Access*, vol. 8, pp. 214293–214299, 2020.
- [19] A. Ahmad, "Comparative study of ve-degree and ev-degree topological descriptors for benzene ring embedded in p-type-surface in 2D network," *Polycyclic Aromatic Compounds*, pp. 1–10, 2020.
- [20] H. M. A. Siddiqui, "Computation of Zagreb indices and Zagreb polynomials of sierpinski graphs," *Haceteppe Journal of Mathematics and Statistics*, vol. 49, no. 2, pp. 754–765, 2020.
- [21] B. Zhou and N. Trinajstić, "On general sum-connectivity index," *Journal of Mathematical Chemistry*, vol. 47, no. 1, pp. 210–218, 2010.
- [22] G. H. Shirdel, H. Rezapour, and A. M. Sayadi, "Hyper-Zagreb index of graph operations," *Iranian Journal of Mathematical Chemistry*, vol. 4, pp. 213–220, 2013.
- [23] V. Anandkumar and R. R. Iyer, "On the hyper-Zagreb index of some operations on graphs," *Indian Journal of Pure and Applied Mathematics*, vol. 112, pp. 239–252, 2017.
- [24] B. Basavanagoud and S. Patil, "A note on hyper-Zagreb index of graph operations," *Journal of Applied Mathematical Chemistry*, vol. 7, pp. 89–92, 2016.
- [25] W. Gao, M. K. Jamil, and M. R. Farahani, "The Hyper-Zagreb index and some graph operations," *Journal of Applied Mathematics and Computer Science*, vol. 54, pp. 263–275, 2016.
- [26] W. Yan, B.-Y. Yang, and Y.-N. Yeh, "The behavior of Wiener indices and polynomials of graphs under five graph decorations," *Applied Mathematics Letters*, vol. 20, no. 3, pp. 290–295, 2007.
- [27] M. Eliasi and B. Taeri, "Four new sums of graphs and their Wiener indices," *Discrete Applied Mathematics*, vol. 157, no. 4, pp. 794–803, 2009.
- [28] H. Deng, D. Sarala, S. K. Ayyaswamy, and S. Balachandran, "The Zagreb indices of four operations on graphs," *Applied Mathematics and Computation*, vol. 275, pp. 422–431, 2016.
- [29] S. Akhter and M. Imran, "Computing the forgotten topological index of four operations on graphs," *AKCE International Journal of Graphs and Combinatorics*, vol. 14, no. 1, pp. 70–79, 2017.
- [30] Y.-M. Chu, S. Javed, M. Javaid, and M. Kamran Siddiqui, "On bounds for topological descriptors of ϕ -sum graphs," *Journal of Taibah University for Science*, vol. 14, no. 1, pp. 1288–1301, 2020.
- [31] J.-B. Liu, S. Javed, M. Javaid, and K. Shabbir, "Computing first general Zagreb index of operations on graphs," *IEEE Access*, vol. 7, pp. 47494–47502, 2019.

- [32] J.-B. Liu, M. Javaid, and H. M. Awais, "Computing Zagreb indices of the subdivision-related generalized operations of graphs," *IEEE Access*, vol. 7, pp. 105479–105488, 2019.
- [33] M. Javaid, S. Javed, A. M. Alanazi, and M. R. Alotaibi, "Computing analysis of Zagreb indices for generalized sum graphs under strong product," *Journal of Chemistry*, vol. 2021, Article ID 6663624, 20 pages, 2021.
- [34] B. Furtula and I. Gutman, "A forgotten topological index," *Journal of Mathematical Chemistry*, vol. 53, no. 4, pp. 1184–1190, 2015.
- [35] M. Alsharafi, M. Shubatah, and A. Alameri, "The hyper-Zagreb index of some complement graphs," *Advances in Mathematics: Scientific Journal*, vol. 9, no. 6, pp. 3631–3642, 2020.
- [36] I. Gutman, B. Ruscic, N. Trinajstic, and C. F. Wilcox, "Graph theory and molecular orbitals. XII. Acyclic polyenes," *The Journal of Chemical Physics*, vol. 62, no. 9, pp. 3399–3405, 1975.
- [37] I. Gutman and N. Trinajstic, "Graph theory and molecular orbitals," in *New Concept*, vol. 2, pp. 49–93, Springer, Berlin, Heidelberg, 1973.

Research Article

An Application of Sombor Index over a Special Class of Semigroup Graph

Seda Oğuz Ünal 

Department of Secondary School Science and Mathematics Education, Education Faculty, Cumhuriyet University, Sivas 58140, Turkey

Correspondence should be addressed to Seda Oğuz Ünal; sdaoguz@gmail.com

Received 18 August 2021; Revised 18 October 2021; Accepted 25 October 2021; Published 15 November 2021

Academic Editor: R. Vadivel

Copyright © 2021 Seda Oğuz Ünal. This is an open access article distributed under the Creative Commons Attribution License, which permits unrestricted use, distribution, and reproduction in any medium, provided the original work is properly cited.

Recently, Gutman introduced a class of novel topological invariants named Sombor index which is defined as $SO(G) = \sum_{uv \in E(G)} \sqrt{(d_u)^2 + (d_v)^2}$. In this study, the Sombor index of monogenic semigroup graphs, which is an important class of algebraic structures, is calculated.

1. Introduction and Preliminaries

The monogenic semigroup graph is inspired by zero divisor graphs. Therefore, before moving on to the main topic, we will focus on the studies on zero divisor graphs (see [1–4]). In relation to the study of zero divisor graphs that has many authors researching commutative and noncommutative rings and how it has advanced, DeMeyer et al. [5, 6] have developed research on commutative and noncommutative semigroups related to zero divisor graphs. The authors in [7] utilised the adjacent rule of vertices while still keeping the original idea. The authors determined a finite multiplicative monogenic semigroup with 0 as follows:

$$S_M = \{0, x, x^2, x^3, \dots, x^n\}. \quad (1)$$

By utilizing the idea defined in [5, 6], the authors obtained a new graph related to monogenic semigroups in [7]. The vertices of this graph are all nonzero elements in S_M and for any two different vertices x^i and x^j where $(1 \leq i, j \leq n)$ are linked to each other, if and only if $i + j > n$. There are many studies concerning monogenic semigroup graphs which were published by Akgüneş et al. (see for example [8–10]).

In chemistry, topological indices have been around for more than half a century [11]. In newer times, they are being extensively investigated also by mathematicians. These

indices are used to model structural properties of molecules and provide information of value for physical chemistry, material science, pharmacology, environmental sciences, and biology [12]. Recently, a new such graph-based topological index, called Sombor index, was put forward by Gutman [13]. Initially, the index was applied in chemistry [14–18] and soon attracted the interest of mathematicians [19–22]. Eventually, however, the Sombor index found applications also in network science and was used for modeling dynamical effects in biology, social, and technological complex systems [23]. It seems that this index became interesting also for military purposes [24]. All this happened within less than one year since the publication of the paper [13]. In view of this wide research activity on Sombor index, it may be of interest to seek for its deeper algebraic connections. In this paper, we report some results relating the Sombor index with an important class of algebraic structures, namely, with monogenic semigroups.

For a graph G , its edge set and vertex set are denoted by $E(G)$ and $V(G)$, respectively.

Sombor index discovered by; Gutman [13] is one of the vertex-degree-based topological indices defined by

$$SO(G) = \sum_{uv \in E(G)} \sqrt{(d_u)^2 + (d_v)^2}, \quad (2)$$

because the function $F(x, y) = \sqrt{x^2 + y^2}$ was not utilised.

Also, as a reminder, for a real number r , we identify by $\lfloor r \rfloor$ the greatest integer $\leq r$, and by $\lceil r \rceil$, the least integer $\geq r$. It is clear that $r - 1 < \lfloor r \rfloor \leq r$ and $r \leq \lceil r \rceil < r + 1$. However, for a natural number n , we have

$$\lfloor \frac{n}{2} \rfloor = \begin{cases} \frac{n}{2}, & \text{if } n \text{ is even,} \\ \frac{n-1}{2}, & \text{if } n \text{ is odd.} \end{cases} \tag{3}$$

In this paper, we focus on determining the explicit formula of Sombor index of the monogenic semigroup graph.

2. An Algorithm

The authors in [8] to simplify their research gave the algorithm concerning the neighborhood of vertices by utilizing the initial statement of monogenic semigroup graph. We will use this algorithm in our main theorem in the next section.

I_n : the vertex x^n is adjoining to every vertex x^{i_1} ($1 \leq i_1 \leq n - 1$) except itself.

I_{n-1} : the vertex x^{n-1} is adjoining to every vertex x^{i_2} ($2 \leq i_2 \leq n - 2$) except itself and the vertex x^n .

I_{n-2} : the vertex x^{n-2} is adjoining to every vertex x^{i_3} ($3 \leq i_3 \leq n - 3$) except itself and the vertices x^n and x^{n-1} .

Carrying on the algorithm this way, we get the following result, depending on whether the number n is odd or even.

If n is even,

$I_{(n/2)+2}$: the vertex $x^{(n/2)+2}$ is adjoining not only to the vertices $x^{(n/2)-1}$, $x^{(n/2)}$, and $x^{(n/2)+1}$ but also to the vertices $x^n, x^{n-1}, x^{n-2}, \dots, x^{(n/2)+3}$.

$I_{(n/2)+1}$: the vertex $x^{(n/2)+1}$ is adjoining not only to the single vertex $x^{(n/2)}$ but also to the vertices $x^n, x^{n-1}, x^{n-2}, \dots, x^{(n/2)+2}$.

If n is odd,

$I_{(n+1)/2}$: the vertex $x^{(n+1)/2}$ is adjoining not only to the vertices $x^{(n+1/2)-2}, x^{(n+1/2)-1}, x^{(n+1/2)}$, and $x^{(n+1/2)+1}$ also adjoining to the vertices $x^n, x^{n-1}, x^{n-2}, \dots, x^{(n+1/2)+3}$.

$I_{(n+1)/2+1}$: the vertex $x^{(n+1)/2+1}$ is adjoining not only to the vertices $x^{(n+1/2)-1}$ and $x^{(n+1/2)}$ also adjoining to the vertices $x^{n-1}, x^{n-2}, \dots, x^{(n+1)/2+2}$.

In the lemma given below, the degrees of vertices $x^1, x^2, \dots, x^n \in \Gamma(S_M)$ are denoted by d_1, d_2, \dots, d_n . There are many studies on the degree series. Regarding this, you can refer to [7, 25] and references cited in these studies. In fact, in the lemma below, it is mentioned that there is an ordering between the degrees d_1, d_2, \dots, d_n . You can reach the proof of this lemma from [7], as well as from the algorithm given above (see [8]).

Lemma 1.

$$d_1 = 1, d_2 = 2, \dots, d_{\lfloor n/2 \rfloor} = \lfloor \frac{n}{2} \rfloor, d_{\lfloor n/2 \rfloor + 1} = \lfloor \frac{n}{2} \rfloor + 1, \dots, d_n = n - 1. \tag{4}$$

Remark 1. Paying attention to Lemma 1, the repeated terms are given in the following:

$$d_{\lfloor n/2 \rfloor} = \lfloor \frac{n}{2} \rfloor = d_{\lfloor n/2 \rfloor + 1}. \tag{5}$$

Therefore, the degree of d_n is denoted by $n - 1$, although the number of vertices is n .

3. Calculating Sombor Index of $\Gamma(S_M)$

In this section, we will obtain an exact formula of Sombor index over monogenic semigroup graph.

Theorem 1. For any monogenic semigroup S_M as given in (1), the Sombor index of the graph $\Gamma(S_M)$ is

$$SO(\Gamma(S_M)) = \begin{cases} \sum_{k=1}^{(n/2)-1} \sum_{i=k}^{n-k-1} \sqrt{(n-k)^2 + i^2} + \sum_{k=1}^{n/2} \sqrt{(n-k)^2 + \left(\frac{n}{2}\right)^2}, & \text{if } n \text{ is even,} \\ \sum_{k=1}^{(n-1)/2} \sum_{i=k}^{n-k-1} \sqrt{(n-k)^2 + i^2} + \sum_{k=1}^{(n-1)/2} \sqrt{(n-k)^2 + \left(\frac{n}{2}\right)^2}, & \text{if } n \text{ is odd.} \end{cases} \tag{6}$$

Proof. Since our aim is to formulate $SO(\Gamma(S_M))$ in terms of the total number of degrees, we need to treat the sum as the

sum of different blocks and then calculate each separately. During our calculations, we will use the algorithm given in

Section 2 here, as it offers a very systematic way of calculating the degrees of vertices. We will also make use of equations (3) and (4) and Remark 1

If n is odd,

$$\begin{aligned}
 [SO]\left(\Gamma(S_M) = \sqrt{d_n^2 + d_1^2} + \sqrt{d_n^2 + d_2^2} + \sqrt{d_n^2 + d_3^2} + \dots + \sqrt{d_n^2 + d_{n-2}^2} + \sqrt{d_n^2 + d_{n-1}^2} + \dots + \sqrt{d_{n-1}^2 + d_2^2} + \sqrt{d_{n-1}^2 + d_3^2} \right. \\
 \left. + \dots + \sqrt{d_{n-1}^2 + d_{n-2}^2} + \dots + \sqrt{d_{(n+1/2)+2}^2 + d_{(n+1/2)-2}^2} + \sqrt{d_{(n+1/2)+2}^2 + d_{(n+1/2)-1}^2} + \sqrt{d_{(n+1/2)+2}^2 + d_{(n+1/2)}^2} \right. \\
 \left. + \sqrt{d_{(n+1/2)+2}^2 + d_{(n+1/2)+1}^2} + \sqrt{d_{(n+1/2)+1}^2 + d_{(n+1/2)-1}^2} + \sqrt{d_{(n+1/2)+1}^2 + d_{(n+1/2)}^2} \right)
 \end{aligned} \tag{7}$$

As a result, the Sombor index of $\Gamma(S_M)$ is written as the sum below:

$$[SO]\left(\Gamma(S_M) = \sum_{ij \in E(G)} \sqrt{d_i^2 + d_j^2} = [SO]_n + [SO]_{n-1} + \dots + [SO]_{(n+1/2)+2} + [SO]_{(n+1/2)+1} \right) \tag{8}$$

When calculating the Sombor index sum, we will write the smallest degree at the end of the line, so we will get a second total and this will provide us with ease of operation.

By the way, while making these calculations, we use the equation $\lfloor n/2 \rfloor = ((n-1)/(2))$ given in (2) for the case where n is odd.

$$\begin{aligned}
 [SO]_n &= \sqrt{(n-1)^2 + 1^2} + \sqrt{(n-1)^2 + 2^2} + \sqrt{(n-1)^2 + 3^2} + \dots + \sqrt{(n-1)^2 + \lfloor \frac{n}{2} \rfloor^2} + \dots + \\
 &\quad + \sqrt{(n-1)^2 + (n-2)^2} + \sqrt{(n-1)^2 + \lfloor \frac{n}{2} \rfloor^2} \\
 &= \sum_{i=1}^{n-2} \sqrt{(n-i)^2 + i^2} + \sqrt{\left(n-1\right)^2 + \left(\frac{n-1}{2}\right)^2}.
 \end{aligned} \tag{9}$$

If similar operations applied in $[SO]_n$ are applied in $[SO]_{n-1}$, we obtain

$$\begin{aligned}
 [SO]_{n-1} &= \sum_{i=2}^{n-3} \sqrt{(n-i)^2 + i^2} + \sqrt{(n-2)^2 + \left(\frac{n-1}{2}\right)^2}, \\
 [SO]_{(n+1)/2+2} &= \sqrt{\left(\frac{n+3}{2}\right)^2 + \left(\frac{n-3}{2}\right)^2} + \sqrt{\left(\frac{n+3}{2}\right)^2 + \left(\frac{n-1}{2}\right)^2} + \sqrt{\left(\frac{n+3}{2}\right)^2 + \left(\frac{n-1}{2}\right)^2} + \sqrt{\left(\frac{n+3}{2}\right)^2 + \left(\frac{n+1}{2}\right)^2},
 \end{aligned} \tag{10}$$

and finally,

$$[SO]_{(n+1)/2+1} = \sqrt{\left(\frac{n+1}{2}\right)^2 + \left(\frac{n-1}{2}\right)^2} + \sqrt{\left(\frac{n+1}{2}\right)^2 + \left(\frac{n-1}{2}\right)^2} \tag{11}$$

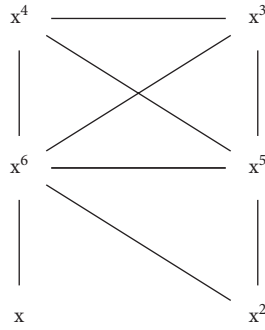


FIGURE 1: S_M^6 monogenic semigroup graph.

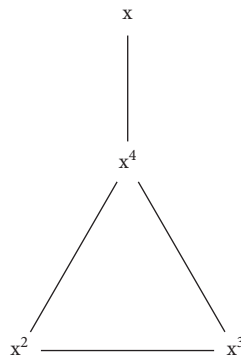


FIGURE 2: S_M^4 monogenic semigroup graph (corresponding hydrogen-suppressed molecular graph).

Hence,

$$[SO]_n + [SO]_{n-1} + \dots + [SO]_{(n+1)/2+2} + [SO]_{(n+1)/2+1} = \sum_{k=1}^{(n-1)/2} \sum_{i=k}^{n-k-1} \sqrt{(n-k)^2 + i^2} + \sum_{k=1}^{(n-1)/2} \sqrt{(n-k)^2 + \left(\frac{n}{2}\right)^2}. \quad (12)$$

If we follow similar steps as if n is odd, we will get the following sum if n is even:

$$[SO]_n + [SO]_{n-1} + \dots + [SO]_{(n/2)+2} + [SO]_{(n/2)+1} = \sum_{k=1}^{(n/2)-1} \sum_{i=k}^{n-k-1} \sqrt{(n-k)^2 + i^2} + \sum_{k=1}^{(n/2)} \sqrt{(n-k)^2 + \left(\frac{n}{2}\right)^2}. \quad (13)$$

Corollary 1. In [26, 27], the authors exhibited that the Sombor index can be an integer in several graph structures. In monogenic semigroup graphs, it is seen that it is not possible for the Sombor index to take an integer value according to the formula given in Theorem 1.

We will give the following examples to reinforce Theorem 1.

Example 1. Consider the monogenic semigroup S_M^6 given below and calculate the Sombor index of $\Gamma(S_M^6)$ graph by applying the rule given in Theorem 1:

$$S_M^6 = \{x, x^2, x^3, x^4, x^5, x^6\} \cup \{0\}. \quad (14)$$

Monogenic semigroup graphs, which are defined with inspiration from zero divisor graphs, also contain the 0

element. Because the vertices of x^i and x^j , which are taken arbitrarily in the monogenic semigroup, can be connected with each other, that is, the necessary and sufficient

condition for the condition of $x^i x^j = 0$ is to be $i + j > n$. In line with this information, the S_M^6 graph is given in Figure 1.

$$\begin{aligned} \text{SO}(\Gamma(S_M^6)) &= \sum_{k=1}^2 \sum_{i=k}^{5-k} \sqrt{(6-k)^2 + i^2} + \sum_{k=1}^3 \sqrt{(6-k)^2 + (3)^2} \\ &= \sqrt{5^2 + 1^2} + \sqrt{5^2 + 2^2} + \sqrt{5^2 + 3^2} + \sqrt{5^2 + 4^2} + \sqrt{4^2 + 2^2} \\ &\quad + \sqrt{4^2 + 3^2} + \sqrt{5^2 + 3^2} + \sqrt{4^2 + 3^2} + \sqrt{3^2 + 3^2}. \end{aligned} \quad (15)$$

In the example below, the Sombor index of the corresponding hydrogen-suppressed molecular graph, which is equivalent to $\Gamma(S_M^4)$ monogenic semigroup graph, is calculated.

Example 2. The Sombor index of the monogenic semigroup S_M^4 given below is calculated by applying Theorem 1.

$$S_M^4 = \{x, x^2, x^3, x^4\} \cup \{0\}. \quad (16)$$

The S_M^4 graph is given in Figure 2.

$$\begin{aligned} \text{SO}(\Gamma(S_M^4)) &= \sum_{k=1}^2 \sum_{i=1}^2 \sqrt{(4-k)^2 + i^2} + \sum_{k=1}^2 \sqrt{(4-k)^2 + (2)^2} \\ &= \sqrt{3^2 + 1^2} + \sqrt{3^2 + 2^2} + \sqrt{3^2 + 2^2} + \sqrt{2^2 + 2^2}. \end{aligned} \quad (17)$$

As can be seen, the Sombor index of a monogenic semigroup graph can be calculated very easily with the given formula in Theorem 1.

Data Availability

No data were used to support this study.

Conflicts of Interest

The author declares no conflicts of interest.

Acknowledgments

The author wishes to express his appreciation to Professor Dr. Ivan Gutman for his invaluable support and expertise during the research phase of this paper.

References

- [1] D. D. Anderson and M. Naseer, "Beck's coloring of a commutative ring," *Journal of Algebra*, vol. 159, pp. 500–514, 1991.
- [2] D. F. Anderson and P. S. Livingston, "The zero-divisor graph of a commutative ring," *Journal of Algebra*, vol. 217, no. 2, pp. 434–447, 1999.
- [3] D. F. Anderson and A. Badawi, "On the zero-divisor graph of a ring," *Communications in Algebra*, vol. 36, no. 8, pp. 3073–3092, 2008.
- [4] I. Beck, "Coloring of commutative rings," *Journal of Algebra*, vol. 116, no. 1, pp. 208–226, 1988.
- [5] F. DeMeyer and L. DeMeyer, "Zero divisor graphs of semigroups," *Journal of Algebra*, vol. 283, no. 1, pp. 190–198, 2005.
- [6] F. R. DeMeyer, T. McKenzie, and K. Schneider, "The zero-divisor graph of a commutative semigroup," *Semigroup Forum*, vol. 65, no. 2, pp. 206–214, 2002.
- [7] K. C. Das, N. Akgüneş, and A. S. Çevik, "On a graph of monogenic semigroup," *Journal of Inequalities and Applications*, vol. 44, 2013.
- [8] N. Akgüneş, K. C. Das, and A. S. Çevik, "Topological indices on a graph of monogenic semigroups in topics in chemical graph theory," in *Mathematical Chemistry Monographs*, I. Gutman, Ed., University of Kragujevac and Faculty of Science Kragujevac, Kragujevac, Serbia, 2014.
- [9] N. Akgüneş and B. Çağan, "On the dot product of graphs over monogenic semigroups," *Applied Mathematics and Computation*, vol. 322, pp. 1–5, 2018.
- [10] N. Akgüneş, "A further note on the graph of monogenic semigroups," *Konuralp Journal of Mathematics*, vol. 6, no. 1, pp. 49–53, 2018.
- [11] R. Todeschini and V. Consonni, *Molecular Descriptors for Chemoinformatics*, Wiley VCH, Weinheim, Germany, 2009.
- [12] J. Devillers and A. T. Balaban, *Topological Indices and Related Descriptors in QSAR and QSPR*, Gordon & Breach, Amsterdam, Netherlands, 1999.
- [13] I. Gutman, "Geometric approach to degree-based topological indices: sombor indices," *MATCH Commun. Math. Comput. Chem.* vol. 86, pp. 11–16, 2021.
- [14] S. Alikhani and N. Ghanbari, "Sombor index of polymers," *MATCH Communications in Mathematical and in Computer Chemistry*, vol. 86, pp. 715–728, 2021.
- [15] S. Amin, A. U. Rehman Virk, M. A. Rehman, and N. A. Shah, "Analysis of dendrimer generation by Sombor indices,"

- Hindawi Journal of Chemistry*, vol. 2021, Article ID 9930645, 11 pages, 2021.
- [16] R. Cruz, I. Gutman, and J. Rada, "Sombor index of chemical graphs," *Applied Mathematics and Computation*, vol. 399, Article ID 126018, 2021.
- [17] H. Liu, L. You, and Y. Huang, "Ordering chemical graphs by Sombor indices and its applications," *MATCH Communications in Mathematical and in Computer Chemistry*, vol. 87, 2022 In press.
- [18] I. Redzepovic, "Chemical applicability of Sombor indices," *Journal of the Serbian Chemical Society*, vol. 86, no. 5, pp. 445–457, 2021.
- [19] K. C. Das, A. S. Çevik, I. N. Cangül, and Y. Shang, "On Sombor index," *Symmetry*, vol. 13, p. 140, 2021.
- [20] B. Horoldagva and C. Xu, "On Sombor index of graphs," *MATCH Communications in Mathematical and in Computer Chemistry*, vol. 86, pp. 793–713, 2021.
- [21] I. Milovanovic, E. Milovanovic, A. Ali, and M. Matejic, "Some results on the Sombor indices of graphs," *Contributions to Mathematics*, vol. 3, pp. 59–67, 2021.
- [22] J. Rada, J. M. Rodríguez, and J. M. Sigarreta, "General properties on Sombor indices," *Discrete Applied Mathematics*, vol. 299, pp. 87–97, 2021.
- [23] Y. Shang, "Sombor index and degree-related properties of simplicial networks," *Applied Mathematics and Computation*, In press.
- [24] I. Gutman, "Spectrum and energy of the Sombor matrix," *Military Technical Courier*, vol. 69, pp. 551–561, 2021.
- [25] N. Akgüneş and A. S. Çevik, "A new bound of radius of irregularity index," *Applied Mathematics and Computation*, vol. 219, pp. 5750–5753, 2013.
- [26] T. Réti, T. Došlic, and A. Ali, "On the Sombor index of graphs," *Contributions to Mathematics*, vol. 3, pp. 11–18, 2021.
- [27] T. Došlic, T. Réti, and A. Ali, "On the structure of graphs with integer Sombor indices," *Discrete Mathematics Letters*, vol. 7, pp. 1–4, 2021.

Research Article

Computing Gutman Connection Index of Thorn Graphs

Muhammad Javaid ¹, Muhammad Khubab Siddique,¹ and Ebenezer Bonyah ²

¹Department of Mathematics, School of Science, University of Management and Technology, Lahore 54770, Pakistan

²Department of Mathematics Education, Akenten Appiah-Menka University of Skills Training and Entrepreneurial Development, Kumasi 00233, Ghana

Correspondence should be addressed to Ebenezer Bonyah; ebbonya@gmail.com

Received 17 September 2021; Accepted 27 October 2021; Published 15 November 2021

Academic Editor: Muhammad Imran

Copyright © 2021 Muhammad Javaid et al. This is an open access article distributed under the Creative Commons Attribution License, which permits unrestricted use, distribution, and reproduction in any medium, provided the original work is properly cited.

Chemical structural formula can be represented by chemical graphs in which atoms are considered as vertices and bonds between them are considered as edges. A topological index is a real value that is numerically obtained from a chemical graph to predict its various physical and chemical properties. Thorn graphs are obtained by attaching pendant vertices to the different vertices of a graph under certain conditions. In this paper, a numerical relation between the Gutman connection (GC) index of a graph and its thorn graph is established. Moreover, the obtained result is also illustrated by computing the GC index for the particular families of the thorn graphs such as thorn paths, thorn rods, thorn stars, and thorn rings.

1. Introduction

Let $\Gamma = (V(\Gamma), E(\Gamma))$ be a simple, finite, and connected graph with vertex set $V(\Gamma)$ and edge set $E(\Gamma) \subseteq V(\Gamma) \times V(\Gamma)$. Let Θ be a collection of such graphs; then, a topological index (TI) is a function from Θ to the set of real numbers defined under certain conditions on the vertices and edges of the graphs. Moreover, for $\Gamma_1, \Gamma_2 \in \Theta$, if $\Gamma_1 \cong \Gamma_2$, then $TI(\Gamma_1) = TI(\Gamma_2)$. The TIs are one of the graph-theoretic techniques which are widely used to study the different properties of the chemical graphs such as boiling point, melting point, flash point, temperature, pressure, tension, heat of evaporation, heat of formation, partition coefficient, retention times in chromatographic, and density [1, 2].

TIs are also used in chemoinformatics which is combination of the three different subjects such as information science, chemistry, and mathematics. In chemoinformatics, on the bases of quantitative structural activity relationship (QSAR) and the qualitative structural property relationship (QSPR), the different chemical properties of a chemical graph are correlated with its structure [3, 4]. Gutman and Trinajstić [5] evaluated the total π -electron energy of the molecular structure by using the sum of square of degree (number of neighborhoods) of vertices of molecular graphs

that is known by first Zagreb index nowadays. In the same paper, another descriptor appeared that is called as second Zagreb index. Furtula and Gutman [6] introduced another TI called third Zagreb index, which is also known as a forgotten index. After that, many TIs based on the degrees of vertices were established, see [7]. In 2018, Ali and Trinajstić [8] established a descriptor known as modified first Zagreb connection index. In the same paper, they also presented two more descriptors with the name first and second Zagreb connection indices. Ali et al. [9] introduced modified second and third Zagreb connection indices and compared Zagreb connection indices and modified Zagreb connection indices for T -sum graphs. Recently, Javaid et al. [10] defined the Gutman connection (GC) index with the help of connection numbers of a graph. For the various computational results, we refer [11–13].

In 1947, Wiener [14] first time applied a distance-based TI to find the boiling point of paraffin. Now, it is called as the Wiener index. Gutman [15] introduced Schultz index of the second kind (Gutman index) as a type of vertex-valency-weighted sum of the distances between all pairs of vertices in a graph. In 1998, Gutman [16] introduced the idea of thorn graph with many applications in chemical graph theory. Bytautas et al. [17] developed an algorithm to find the mean

Wiener terminal numbers for some thorny graphs. In 2005, Zhou [18] worked on modified Wiener indices for thorn trees. In 2011, Li [19] computed the Zagreb polynomials for thorny graphs. The study of thorn graphs provides mathematical results that relate numerical values of TIs of plerograms and kenograms. Plerograms are obtained from a molecule by expressing each atom with a vertex, but if the hydrogen atoms are not considered, then corresponding mathematical representation of a molecule is called as kenogram. The relation between the terminal Wiener indices of plerograms and kenograms was discussed in [20]. For more details about thorn graphs, see [21–23].

In this study, we establish a relationship between the Gutman connection index of a simple connected graph and its thorn graph. It is also applied to evaluate the Gutman connection index of thorn paths, thorn rods, thorn rings, and thorn stars. Rest of the paper is organized as follows. Section 2 contains the definitions and key concepts that are used in the remaining part of the paper. In Section 3, main and some related results are proved, and in Section 4, application of the main result is discussed for some thorn graphs.

2. Preliminaries

Here, Γ is considered as a finite connected graphs without loops and multiples edges, and let $V(\Gamma) = \{v_1, v_2, \dots, v_n\}$ be its vertex set for an n -vertex simple connected graph Γ . Consider $H = (h_1, h_2, \dots, h_n)$ as an n -tuple of nonnegative integers. Since distance between any two vertices of Γ is the same in both Γ and Γ^h , so we denote distance between vertices u and v with respect to both Γ and Γ^h as $d(u, v)$.

2.1. Related Graphs. In this section, we recall the definition of caterpillar, thorn paths, thorn rods, thorn rings, and thorn stars.

Definition 1 (see [24]). For $i = 1, 2, \dots, n$, a thorn graph Γ^h is constructed by attaching h_i pendant vertices to the vertex v_i of graph Γ , where $|V(\Gamma)| = n$. If V_i is the set of h_i thorns of the vertex v_i , then $V(\Gamma^h) = V(\Gamma) \cup \cup_{i=1}^n V_i$. For more explanation, see Figure 1.

Definition 2 (see [24]). A thorn path $P_{n,h,k}$ is a graph formed from a path P_n by attaching k neighbors to its terminal vertices and h neighbors to its nonterminal vertices. For more detail, see Figure 2.

Definition 3 (see [24]). A caterpillar ($T_{m,n}'$) is a thorn path obtained from path P_n such that its thorn vertices (other than pendant) are of the same degree $m > 2$. It is clear that $P_{n,m-2,m-1} = T_{m,n}'$, see Figure 3.

Definition 4 (see [24]). A thorn rod $P_{n,m}$ is a graph that is obtained by adding $m - 1$ pendant vertices to each terminal vertex of P_n . It is clear that $P_{n,2,m} = P_{n,m}$, see Figure 4.

Definition 5 (see [24]). The thorn star S_{n,h_1,h_2,\dots,h_n} is obtained from the star S_n by attaching h_i pendant neighbors to vertex

v_i for $i = 1, 2, \dots, n$. Thorn star S_{n,h_1,h_2,\dots,h_n} defined here is shown in Figure 5.

Definition 6 (see [24]). If for each vertex of a cycle graph C_n and a thorn of length $m - 2$ is attached, then it is called thorn ring (denoted by $C_{n,m}$). For more details, see Figure 6.

2.2. Chemical Applicability of GC Index. This section covers the definition of Gutman connection (GC) index with its applicability.

Definition 7 (see [15]). The Gutman index of a simple connected graph Γ (denoted by $\text{Gut}(\Gamma)$) is defined as

$$\text{Gut}(\Gamma) = \sum_{\{u,v\} \subseteq \Gamma} d_{\Gamma}(u)d_{\Gamma}(v)d(u,v). \quad (1)$$

In the above definition, Javaid et al. [10] replaced the vertex degree with the connection number and defined a new connection-based index known as the Gutman connective (GC) index as follows.

Definition 8. For a simple and connected graph Γ , the Gutman connection index is

$$\text{GC}(\Gamma) = \sum_{\{u,v\} \subseteq \Gamma} \tau\left(\frac{u}{\Gamma}\right)\tau\left(\frac{v}{\Gamma}\right)d(u,v), \quad (2)$$

where $\tau(u/\Gamma)$ and $\tau(v/\Gamma)$ denote the connection number of vertices u and v , respectively, of graph Γ and $d(u, v)$ is the distance between vertices u and v in Γ .

The correlation coefficients between the values of GCI and eleven physicochemical properties of octane isomer boiling point (B. P), heat capacity at constant temperature (C. T), heat capacity at constant pressure (C. P), entropy (S), density (D), mean radius (Rm2), change in heat of vaporization ($-\Delta H_v$), standard heat of formation ($-\Delta H_f$), accentric factor (A. F), enthalpy of vaporization (HVAP), and standard enthalpy of vaporization (DHSVAP) are shown in Table 1. It is clear that absolute value of correlation coefficient of GCI with S, A. F, HVAP, and DHSVAP is above 0.9. Also, the value of its correlation coefficient with ΔH_f is 0.8386. Consequently, the GC index may be a very useful index in the studies of QSPR and QSAR.

Now, before presenting the most frequent used lemma, we define some important notations as $M_{21}(\Gamma) = \sum_{i=1}^n \tau(v_i/\Gamma)$ and $M_{2,j} = \sum_{i=1}^n \tau(v_i/\Gamma)d(v_i, v_j)$, where $j \in \{1, 2, 3, \dots, n\}$.

Lemma 1. Let Γ be a $\{C_3, C_4\}$ -free simple and connected graph with vertex set $V(\Gamma) = \{v_1, v_2, \dots, v_n\}$ and edge set $E(\Gamma)$. Then, $M_{21}(\Gamma) = M_1(\Gamma) - |E(\Gamma)|$, where $M_1(\Gamma)$ is the first Zagreb index.

Proof. As $M_{21}(\Gamma) = \sum_{i=1}^n \tau(v_i/\Gamma) = \sum_{i=1}^n \sum_{u \in N_{\Gamma}(v_i)} (d(u) - 1)$, where $N_{\Gamma}(v_i)$ denotes the neighborhood of v_i , where $|N_{\Gamma}(v_i)| = d(v_i)$, for all $v_i \in V(\Gamma)$. Now, if $u \in N_{\Gamma}(v_i)$, then $v_i \in N_{\Gamma}(u)$. Hence, the number of neighborhoods in which

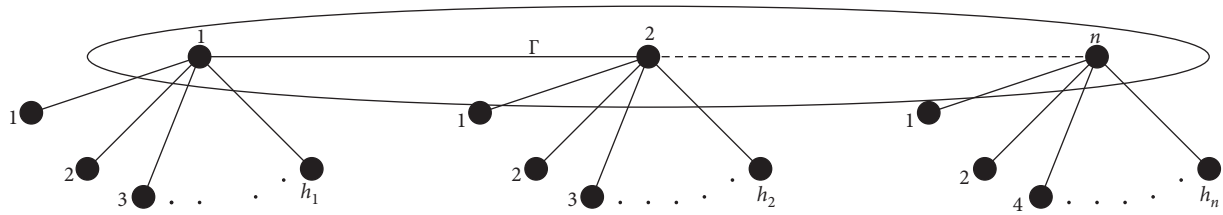


FIGURE 1: Thorn graph Γ^h of the path graph $\Gamma \cong P_n$ with parameter $h = (h_1, h_2, h_3, \dots, h_n)$.

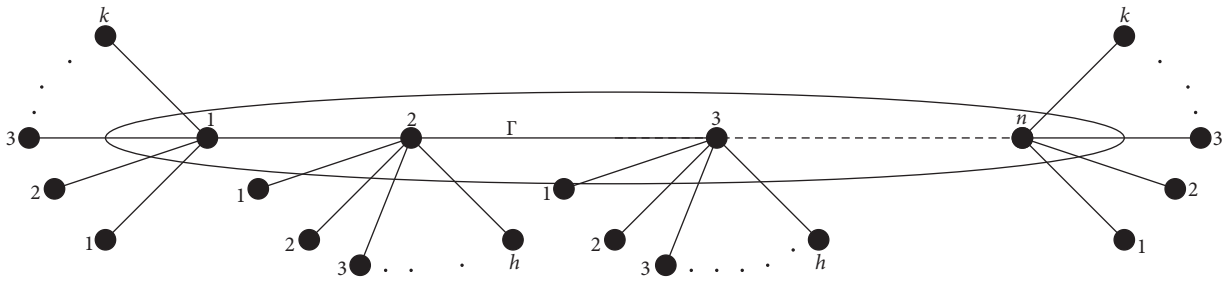


FIGURE 2: Thorn path, $P_{n,h,k}$.

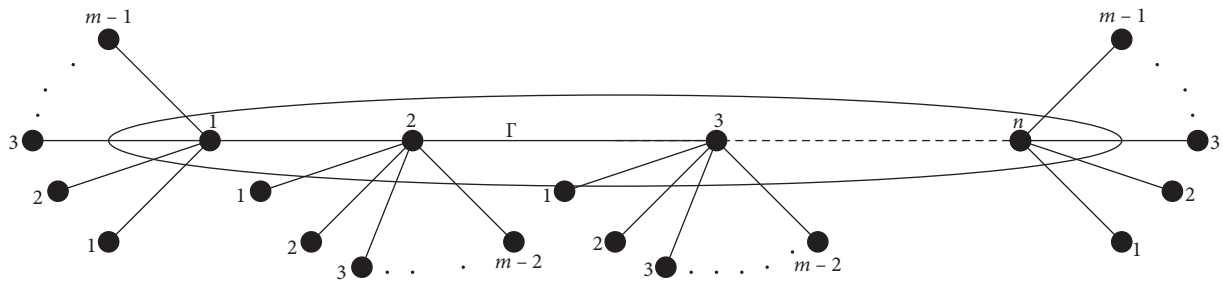


FIGURE 3: Caterpillar, $T_{m,n}'$.

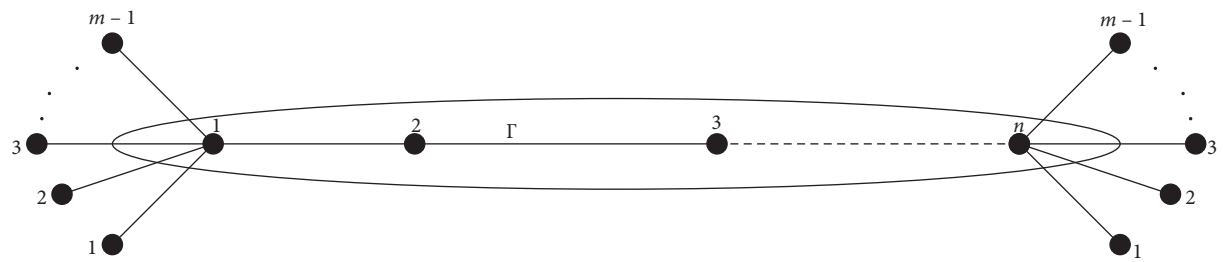


FIGURE 4: Thorn rod, $P_{n,m}$.

v_i lies is equal to the $|N_\Gamma(v_i)| = d(v_i)$, and then, the component of v_i which contribute to $\tau(u)$ will be $d(v_i) - 1$, for any $u \in N_\Gamma(v_i)$. Consequently, $M_{21}(\Gamma) = \sum_{i=1}^n d(v_i) (d(v_i) - 1) = \sum_{i=1}^n d(v_i)^2 - \sum_{i=1}^n d(v_i) = M_1(\Gamma) - |E(\Gamma)|$.

3. Main Development

This section covers the main results of the Gutman connection (GC) index of the thorn graphs in its general form.

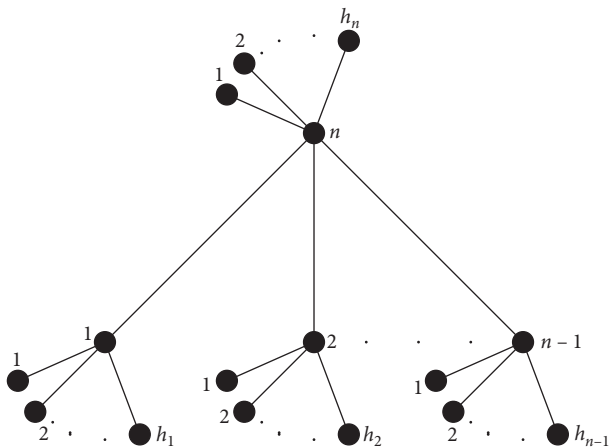


FIGURE 5: Thorn star.

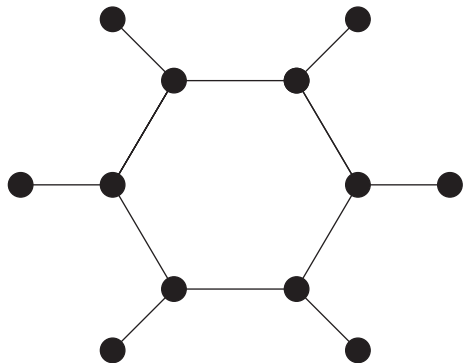


FIGURE 6: Thorn ring, $C_{5,3}$.

TABLE 1: Comparison of correlation coefficients between TIs and physicochemical properties of octane isomers.

	GCI	ZC ₁ [*]	M ₁	M ₂	ZC ₁	ZC ₂
B. P	-0.789	-0.352	-0.718	-0.498	-0.770	-0.168
C. T	-0.513	0.0822	-0.340	-0.072	-0.389	0.165
C. P	0.090	0.581	0.294	-0.492	0.267	0.524
S	-0.910	-0.891	-0.954	-0.942	-0.920	-0.836
D	0.616	0.748	0.640	-0.730	0.564	0.838
Rm2	-0.723	-0.790	-0.789	-0.814	-0.759	0.659
$-\Delta H_f$	0.839	0.392	0.760	0.541	0.784	0.259
$-\Delta H_v$	-0.171	-0.071	-0.222	-0.129	-0.294	0.145
A. F	-0.901	-0.949	-0.973	-0.986	-0.951	-0.862
HVAP	-0.910	-0.606	-0.886	-0.728	-0.914	-0.433
DHVAP	-0.941	-0.705	-0.936	-0.812	-0.955	-0.551

Theorem 1. Let Γ^h be a thorn graph of the graph Γ , where $|V(\Gamma)| = n$; then,

$$\begin{aligned}
 GC(\Gamma^h) &= GC\left(\frac{\Gamma}{\Gamma^h}\right) + \sum_{i=1}^n \left(d\left(\frac{v_i}{\Gamma}\right) + h_i - 1\right)^2 h_i (h_i - 1) \\
 &+ \sum_{j=1}^n \left(d\left(\frac{v_j}{\Gamma}\right) + h_j - 1\right) h_j (M_{2,j}(\Gamma) + M_{21}(\Gamma) \\
 &+ \sum_{i=1}^n \sum_{p \in N(v_i)} h_p (d(v_i, v_j) + 1)) \\
 &+ \sum_{1 \leq i < j \leq n} \left(d\left(\frac{v_i}{\Gamma}\right) + h_i - 1\right) \left(d\left(\frac{v_j}{\Gamma}\right) + h_j - 1\right) \\
 &\cdot (d(v_i, v_j) + 2) h_i h_j.
 \end{aligned} \tag{3}$$

Proof. Assume that $\tau(u/\Gamma^h)$ represents the connection numbers of u in graph Γ^h and $\tau(u/\Gamma)$ represents the connection number of u in graph Γ . By the definition of the Gutman connection index, we have

$$GC(\Gamma^h) = \sum_{\{u,v\} \subseteq V(\Gamma^h)} \tau\left(\frac{u}{\Gamma^h}\right) \tau\left(\frac{v}{\Gamma^h}\right) d(u, v). \tag{4}$$

By the definition of $V(\Gamma^h)$, the sum in equation (5) can be partitioned into four sums as

$$\sum_{\{u,v\} \subseteq V(\Gamma^h)} \tau\left(\frac{u}{\Gamma^h}\right) \tau\left(\frac{v}{\Gamma^h}\right) d(u, v) = S_1 + S_2 + S_3 + S_4, \tag{5}$$

where S_1 consists of contributions to $GC(\Gamma^h)$ of pair of vertices from Γ , S_2 consists of pair of vertices from V_i for all $1 \leq i \leq n$, S_3 is the contribution of pair of vertices one from $u \in V(\Gamma)$ and the other one v is in V_i , for all $1 \leq i \leq n$, and S_4 is taken from all the pair of vertices such that one of them u is from V_i and other vertex v from V_j .

Now,

$$S_1 = \sum_{\{u,v\} \subseteq V(\Gamma)} \tau\left(\frac{u}{\Gamma^h}\right) \tau\left(\frac{v}{\Gamma^h}\right) d(u, v) = GC\left(\frac{\Gamma}{\Gamma^h}\right) \tag{6}$$

and

$$\begin{aligned}
 S_2 &= \sum_{i=1}^n \sum_{\{u,v\} \subseteq V_i} \tau\left(\frac{u}{\Gamma^h}\right) \tau\left(\frac{v}{\Gamma^h}\right) d(u, v) \\
 &= \sum_{i=1}^n \sum_{\{u,v\} \subseteq V_i} \left(d\left(\frac{v_i}{\Gamma}\right) + h_i - 1\right) \left(d\left(\frac{v_i}{\Gamma}\right) + h_i - 1\right) \cdot 2 \\
 &= \sum_{i=1}^n \left(d\left(\frac{v_i}{\Gamma}\right) + h_i - 1\right)^2 \cdot h_i (h_i - 1).
 \end{aligned} \tag{7}$$

Similarly,

$$\begin{aligned}
 S_3 &= \sum_{i=1}^n \sum_{j=1}^n \sum_{u=v_i} \sum_{v \in V_j} \tau\left(\frac{u}{\Gamma^h}\right) \tau\left(\frac{v}{\Gamma^h}\right) d(u, v) \\
 &= \sum_{i=1}^n \sum_{j=1}^n \sum_{u=v_i} \sum_{v \in V_j} \tau\left(\frac{u}{\Gamma^h}\right) \left(d\left(\frac{v}{\Gamma}\right) + h_j - 1\right) (d(v_i, v_j) + 1) \\
 &= \sum_{i=1}^n \tau\left(\frac{v_i}{\Gamma^h}\right) \sum_{j=1}^n \left(d\left(\frac{v_j}{\Gamma}\right) + h_j - 1\right) h_j (d(v_i, v_j) + 1) \\
 &= \sum_{j=1}^n \left(d\left(\frac{v_j}{\Gamma}\right) + h_j - 1\right) h_j \sum_{i=1}^n \tau\left(\frac{v_i}{\Gamma^h}\right) (d(v_i, v_j) + 1) \\
 &= \sum_{j=1}^n \left(d\left(\frac{v_j}{\Gamma}\right) + h_j - 1\right) h_j \sum_{i=1}^n \\
 &\quad \left(\tau\left(\frac{v_i}{\Gamma}\right) + \sum_{k \in N(v_i)} h_k \right) (d(v_i, v_j) + 1) \\
 &= \sum_{j=1}^n \left(d\left(\frac{v_j}{\Gamma}\right) + h_j - 1\right) h_j \\
 &\quad \cdot \left(M_{2,j}(\Gamma) + M_{21}(\Gamma) + \sum_{i=1}^n \sum_{p \in N(v_i)} h_p (d(v_i, v_j) + 1) \right), \tag{8}
 \end{aligned}$$

$$\begin{aligned}
 S_4 &= \sum_{1 \leq i < j \leq n} \sum_{u \in V_i} \sum_{v \in V_j} \tau\left(\frac{u}{\Gamma^h}\right) \tau\left(\frac{v}{\Gamma^h}\right) d(u, v) \\
 &= \sum_{1 \leq i < j \leq n} \sum_{u \in V_i} \sum_{v \in V_j} \left(d\left(\frac{v_i}{\Gamma}\right) + h_i - 1\right) \\
 &\quad \cdot \left(d\left(\frac{v_j}{\Gamma}\right) + h_j - 1\right) (d(v_i, v_j) + 2) \\
 &= \sum_{1 \leq i < j \leq n} \left(d\left(\frac{v_i}{\Gamma}\right) + h_i - 1\right) \left(d\left(\frac{v_j}{\Gamma}\right) + h_j - 1\right) \\
 &\quad \cdot (d(v_i, v_j) + 2) \left(\sum_{u \in V_i} 1\right) \left(\sum_{v \in V_j} 1\right) \\
 &= \sum_{1 \leq i < j \leq n} \left(d\left(\frac{v_i}{\Gamma}\right) + h_i - 1\right) \left(d\left(\frac{v_j}{\Gamma}\right) + h_j - 1\right) (d(v_i, v_j) + 2) h_i h_j. \tag{9}
 \end{aligned}$$

By substituting the values of $S_1, S_2, S_3,$ and S_4 in equation (5), the required result is obtained.

Now, using Lemma 1 and the result of Theorem 1, we obtain Corollary 1 under the condition on Γ that it is free from cycles of length three and four. Moreover, Corollary 2 is obtained by attaching the same number of pendant vertices to each vertex of Γ .

Corollary 1. *If Γ is a graph free from cycles of length three and four, then*

$$\begin{aligned}
 GC(\Gamma^h) &= GC\left(\frac{\Gamma}{\Gamma^h}\right) + \sum_{i=1}^n \left(d\left(\frac{v_i}{\Gamma}\right) + h_i - 1\right)^2 \cdot h_i (h_i - 1) + \sum_{j=1}^n \left(d\left(\frac{v_j}{\Gamma}\right) + h_j - 1\right) h_j \\
 &\quad \cdot \left(M_{2,j}(\Gamma) + M_1(\Gamma) - |E(\Gamma)| + \sum_{i=1}^n \sum_{p \in N(v_i)} h_p (d(v_i, v_j) + 1) \right) \\
 &\quad + \sum_{1 \leq i < j \leq n} \left(d\left(\frac{v_i}{\Gamma}\right) + h_i - 1\right) \left(d\left(\frac{v_j}{\Gamma}\right) + h_j - 1\right) (d(v_i, v_j) + 2) h_i h_j. \tag{10}
 \end{aligned}$$

Corollary 2. *Let Γ^h be thorn graph of Γ with parameters $h_1 = h_2 = \dots = h_n = h;$ then,*

$$\begin{aligned}
 GC(\Gamma^h) &= GC\left(\frac{\Gamma}{\Gamma^h}\right) + h(h-1)(M_1(\Gamma) + (h-1)^2 \cdot (n-1) + 2(h-1)|E(\Gamma)|) \\
 &\quad \cdot \sum_{j=1}^n \left(d\left(\frac{v_j}{\Gamma}\right) + h - 1\right) h (M_{2,j}(\Gamma) + M_1(\Gamma) - |E(\Gamma)|) + h \sum_{i=1}^n \sum_{p \in N(v_i)} (d(v_i, v_j) + 1) \\
 &\quad + \sum_{1 \leq i < j \leq n} \left(d\left(\frac{v_j}{\Gamma}\right) + h - 1\right) \left(d\left(\frac{v_i}{\Gamma}\right) + h - 1\right) (d(v_i, v_j) + 2) h^2. \tag{11}
 \end{aligned}$$

4. Applications

In this section, we find the GC index of the thorn path, thorn rod, and thorn ring graphs with the help of the main developed result (Theorem 1).

Theorem 2. Let $n \geq 2$ and h and k be nonnegative integers and $P_{n,h,k}$ be a thorn graph of P_n ; then,

$$\begin{aligned} \text{GC}(P_{n,h,k}) &= \frac{1}{6}h^4n^3 - \frac{13}{6}h^4n + 3h^4 + h^3n^3 - 2h^3n^2 - 4h^3n + 8h^3 + h^2k^2n^2 + h^2k^2n - 6h^2k^2 + h^2kn^2 \\ &\quad - 3h^2kn + 2h^2k + \frac{13}{6}h^2n^3 - 8h^2n^2 + \frac{59}{6}h^2n - 7h^2 + 3hk^2n^2 - hk^2n - 10hk^2 + 3hkn^2 - 13hk + 16kn + 18hk + 2hn^3 \\ &\quad - 10hn^2 + 23hn - 26h + k^4n + 3k^4 + 2k^3n + 2k^2n^2 - k^2n - 7k^2 + 2kn^2 - 10kn + \frac{2}{3}n^3 - 4n^2 + \frac{34}{3}n - 14. \end{aligned} \tag{12}$$

Proof. Here, $h_1 = h_n = k$ and $h_i = h$, for $2 \leq i \leq n-1$. Now, we find S_1, S_2, S_3 , and S_4 as derived in Theorem 1.

$$\begin{aligned} S_1 &= \text{GC}(\Gamma) = \sum_{\{u,v\} \subseteq \Gamma} \tau\left(\frac{u}{\Gamma^h}\right) \tau\left(\frac{v}{\Gamma^h}\right) d(u, v) \\ &= \tau\left(\frac{v_1}{\Gamma^h}\right) \sum_{j=3}^{n-2} \tau\left(\frac{v_j}{\Gamma^h}\right) d(v_1, v_j) + \tau\left(\frac{v_2}{\Gamma^h}\right) \sum_{j=3}^{n-2} \tau\left(\frac{v_j}{\Gamma^h}\right) d(v_2, v_j) + \tau\left(\frac{v_{n-1}}{\Gamma^h}\right) \sum_{j=2}^{n-2} \tau\left(\frac{v_n}{\Gamma^h}\right) d(v_{n-1}, v_j) \\ &\quad + \tau\left(\frac{v_n}{\Gamma^h}\right) \sum_{j=3}^{n-2} \tau\left(\frac{v_n}{\Gamma^h}\right) d(v_n, v_j) + \tau\left(\frac{v_1}{\Gamma^h}\right) \tau\left(\frac{v_2}{\Gamma^h}\right) d(v_1, v_2) + \tau\left(\frac{v_1}{\Gamma^h}\right) \tau\left(\frac{v_{n-1}}{\Gamma^h}\right) d(v_1, v_{n-1}) \\ &\quad + \tau\left(\frac{v_1}{\Gamma^h}\right) \tau\left(\frac{v_n}{\Gamma^h}\right) d(v_1, v_n) + \tau\left(\frac{v_2}{\Gamma^h}\right) \tau\left(\frac{v_{n-1}}{\Gamma^h}\right) d(v_2, v_{n-1}) + \tau\left(\frac{v_2}{\Gamma^h}\right) \tau\left(\frac{v_n}{\Gamma^h}\right) d(v_2, v_n) \\ &\quad + \tau\left(\frac{v_{n-1}}{\Gamma^h}\right) \tau\left(\frac{v_n}{\Gamma^h}\right) d(v_{n-1}, v_n) + \sum_{\{u,v\} \subseteq V(\Gamma/\{v_1, v_2, v_{n-1}, v_n\})} \tau\left(\frac{u}{\Gamma^h}\right) \tau\left(\frac{v}{\Gamma^h}\right) d(u, v) \\ &= (h+1) \sum_{j=3}^{n-2} (2h+2)(j-1) + (h+k+1) \sum_{j=3}^{n-2} (2h+2)(j-2) + (h+k+1) \sum_{j=3}^{n-2} (2h+2)(n-1-j) \\ &\quad + (h+1) \sum_{j=3}^{n-2} (2h+2)(n-j) + (h+1)(h+k+1) + (h+1)(h+k+1)(n-2) + (h+1)^2(n-1) + (h+k+1)^2(n-3) \\ &\quad + (h+1)(h+k+1)(n-2) + (h+1)(h+k+1) + \sum_{\{u,v\} \subseteq V(\Gamma/\{v_1, v_2, v_{n-1}, v_n\})} (2h+2) \cdot (2h+2) d(u, v) \\ &= \sum_{j=3}^{n-2} (2(h+1)^2(n-1) + 2(h+1)(h+k+1)(n-3)) + 2(h+1)(h+k+1)(n-1) + (h+1)^2(n-1) \\ &\quad + (h+k+1)^2(n-3) + 4(h+1)^2 \sum_{\{u,v\} \subseteq V(\Gamma/\{v_1, v_2, v_{n-1}, v_n\})} d(u, v) = (2(h+1)^2(n-1) + 2(h+1)(h+k+1)(n-3)) \sum_{j=3}^{n-2} 1 \\ &\quad + 2(h+1)(h+k+1)(n-1) + (h+1)^2(n-1) + (h+k+1)^2(n-3) + 4(h+1)^2 \sum_{j=1}^{n-5} \frac{j(j+1)}{2} \\ &= \frac{2}{3}h^2n^3 - 4h^2n^2 + \frac{34}{3}h^2n - 14h^2 + 2hkn^2 - 10hkn + 16hk + \frac{4}{3}hn^3 - 8hn^2 + \frac{68}{3}hn - 28h + k^2n - 3k^2 \\ &\quad + 2kn^2 - 10kn + 16k + \frac{2}{3}n^3 - 4n^2 + \frac{34}{3}n - 14s. \end{aligned} \tag{13}$$

and

$$\begin{aligned}
S_2 &= \sum_{i=1}^n \left(d\left(\frac{v_i}{\Gamma}\right) + h_i - 1 \right)^2 h_i (h_i - 1) \\
&= \left(d\left(\frac{v_1}{\Gamma}\right) + h_1 - 1 \right)^2 h_1 (h_1 - 1) + \sum_{i=2}^{n-1} \left(d\left(\frac{v_i}{\Gamma}\right) + h_i - 1 \right)^2 h_i (h_i - 1) + \left(d\left(\frac{v_n}{\Gamma}\right) + h_n - 1 \right)^2 h_n (h_n - 1) \\
&= (1 + k - 1)^2 k (k - 1) + \sum_{i=2}^{n-1} (2 + h - 1)^2 h (h - 1) + (1 + k - 1)^2 k (k - 1) \\
&= 2k^3 (k - 1) + h(h + 1)^2 (h - 1)(n - 2).
\end{aligned} \tag{14}$$

Now, to find S_3 , M_{21} and $M_{2,j}$, $j = 1, 2, \dots, n$, are required:

$$M_{21}(\Gamma) = \sum_{i=1}^n \tau(v_i) = 1 + 1 + \sum_{i=3}^{n-2} 2 + 1 + 1 = 2 + 2(n - 4) + 2 = 2(n - 2) = 2n - 4, \tag{15}$$

$$\begin{aligned}
M_{2,1} &= \sum_{i=1}^n \tau\left(\frac{v_i}{\Gamma}\right) d(v_i, v_1) \\
&= \sum_{i=3}^{n-2} \tau\left(\frac{v_i}{\Gamma}\right) d(v_i, v_1) + \tau\left(\frac{v_2}{\Gamma}\right) d(v_2, v_1) + \tau\left(\frac{v_{n-1}}{\Gamma}\right) d(v_{n-1}, v_1) + \tau\left(\frac{v_n}{\Gamma}\right) d(v_n, v_1) \\
&= 2 \sum_{i=3}^{n-2} d(v_i, v_1) + 1 + (n - 2) + n - 1 = (n - 2)(n - 1) = n^2 - 3n + 2,
\end{aligned} \tag{16}$$

$$\begin{aligned}
M_{2,2} &= \sum_{i=1}^n \tau\left(\frac{v_i}{\Gamma}\right) d(v_i, v_2) \\
&= \sum_{i=3}^{n-2} \tau\left(\frac{v_i}{\Gamma}\right) d(v_i, v_2) + \tau\left(\frac{v_1}{\Gamma}\right) d(v_1, v_2) + \tau\left(\frac{v_{n-1}}{\Gamma}\right) d(v_{n-1}, v_2) + \tau\left(\frac{v_n}{\Gamma}\right) d(v_n, v_2) \\
&= 2 \sum_{i=3}^{n-2} d(v_i, v_2) + 1 + (n - 3) + (n - 2) = (n - 3)(n - 4) + 2(n - 2) = n^2 - 5n + 8,
\end{aligned} \tag{17}$$

and

$$\begin{aligned}
M_{2,(n-1)} &= \sum_{i=1}^n \tau\left(\frac{v_i}{\Gamma}\right) d(v_i, v_{n-1}) \\
&= \sum_{i=3}^{n-2} \tau\left(\frac{v_i}{\Gamma}\right) d(v_i, v_{n-1}) + \tau\left(\frac{v_1}{\Gamma}\right) d(v_1, v_{n-1}) + \tau\left(\frac{v_2}{\Gamma}\right) d(v_2, v_{n-1}) + \tau\left(\frac{v_n}{\Gamma}\right) d(v_n, v_{n-1}) \\
&= 2 \sum_{i=3}^{n-2} d(v_i, v_{n-1}) + (n - 2) + (n - 3) + 1 = (n - 3)(n - 4) + 2(n - 2) = n^2 - 5n + 8.
\end{aligned} \tag{18}$$

Also,

$$\begin{aligned}
 M_{2,n} &= \sum_{i=1}^n \tau\left(\frac{v_i}{\Gamma}\right) d(v_i, v_n) \\
 &= \sum_{i=3}^{n-2} \tau\left(\frac{v_i}{\Gamma}\right) d(v_i, v_n) + \tau\left(\frac{v_1}{\Gamma}\right) d(v_1, v_n) + \tau\left(\frac{v_2}{\Gamma}\right) d(v_2, v_n) + \tau\left(\frac{v_{n-1}}{\Gamma}\right) d(v_{n-1}, v_n) \\
 &= 2 \sum_{i=3}^{n-2} d(v_i, v_n) + (n-1) + (n-2) + 1 = (n-4)(n-1) + 2(n-1) = (n-1)(n-2).
 \end{aligned} \tag{19}$$

For the next result, we will assume $3 \leq j \leq n-2$:

$$\begin{aligned}
 M_{2,j} &= \sum_{i=1}^n \tau\left(\frac{v_i}{\Gamma}\right) d(v_i, v_j) \\
 &= \tau\left(\frac{v_1}{\Gamma}\right) d(v_1, v_j) + \tau\left(\frac{v_2}{\Gamma}\right) d(v_2, v_j) + \tau\left(\frac{v_{n-1}}{\Gamma}\right) d(v_{n-1}, v_j) + \tau\left(\frac{v_n}{\Gamma}\right) d(v_n, v_j) + \sum_{i=3}^{n-2} \tau\left(\frac{v_i}{\Gamma}\right) d(v_i, v_j) \\
 &= (j-1) + (j-2) + (n-1-j) + (n-j) + 2 \left(\sum_{i=3}^{j-1} (j-i) + \sum_{i=j+1}^{n-2} (i-j) \right) = 2j^2 - 2jn - 2j + n^2 - n + 4.
 \end{aligned} \tag{20}$$

Now, we take $B_j = \sum_{i=1}^n \sum_{p \in N(v_i)} h_p(d(v_i, v_j) + 1)$, for $j = 1, 2, \dots, n$. We will find out B_1 , B_2 , and B_{n-1} and a general expression for B_j for $j = 3, 4, \dots, n-2$. So,

$$\begin{aligned}
 B_1 &= \sum_{i=1}^n \sum_{p \in N(v_i)} h_p(d(v_i, v_1) + 1) \\
 &= \sum_{p \in N(v_1)} h_p(d(v_1, v_1) + 1) + \sum_{p \in N(v_2)} h_p(d(v_2, v_1) + 1) + \sum_{p \in N(v_{n-1})} h_p(d(v_{n-1}, v_1) + 1) \\
 &\quad + \sum_{p \in N(v_n)} h_p(d(v_n, v_1) + 1) + \sum_{i=3}^{n-2} \sum_{p \in N(v_i)} h_p(d(v_i, v_1) + 1) \\
 &= h(1) + (h+k)(2) + (h+k)(n-1) + h(n) + 2h \sum_{i=3}^{n-2} (j-1+1) \\
 &= (n+1)(2h+k) + h(n-4)(n+1) = (n+1)(2h+k+h(n-4)) = (n+1)(k+(n-2)h),
 \end{aligned} \tag{21}$$

$$\begin{aligned}
 B_2 &= \sum_{i=1}^n \sum_{p \in N(v_i)} h_p(d(v_i, v_2) + 1) \\
 &= \sum_{p \in N(v_1)} h_p(d(v_1, v_2) + 1) + \sum_{p \in N(v_2)} h_p(d(v_2, v_2) + 1) + \sum_{p \in N(v_{n-1})} h_p(d(v_{n-1}, v_2) + 1) + \sum_{p \in N(v_n)} h_p(d(v_n, v_2) + 1) \\
 &\quad + \sum_{i=3}^{n-2} \sum_{p \in N(v_i)} h_p(d(v_i, v_2) + 1) = h(2) + (h+k)(1) + (h+k)(n-2) + h(n-1) + 2h \sum_{i=3}^{n-2} (i-2+1) \\
 &= 2nh + k(n-1) + h(n-4)(n-1).
 \end{aligned} \tag{22}$$

$B_{n-1} = (n+1)(2h+k) + h(n-4)(n+1)$ and $B_n = 2nh + k(n-1) + h(n-4)(n-1)$ For $3 \leq j \leq n-2$,

$$\begin{aligned}
 B_j &= \sum_{i=1}^n \sum_{p \in N(v_i)} h_p(d(v_i, v_j) + 1) \\
 &= \sum_{p \in N(v_1)} h_p(d(v_1, v_j) + 1) + \sum_{p \in N(v_2)} h_p(d(v_2, v_j) + 1) + \sum_{p \in N(v_{n-1})} h_p(d(v_{n-1}, v_j) + 1) \\
 &\quad + \sum_{p \in N(v_n)} h_p(d(v_i, v_j) + 1) + \sum_{i=3}^{n-2} \sum_{p \in N(v_i)} h_p(d(v_i, v_j) + 1) \\
 &= h(j-1+1) + (h+k)(j-2+1) + (h+k)(n-1-j+1) + h(n-j+1) + \sum_{i=3}^{n-2} (h+h)(d(v_i, v_j) + 1) \\
 &= 2nh + k(n-1) + 2h \left(\sum_{i=3}^j (d(v_i, v_j) + 1) + \sum_{i=j+1}^{n-2} (d(v_i, v_j) + 1) \right) \\
 &= 2nh + k(n-1) + 2h \left(\sum_{i=3}^j (j-i+1) + \sum_{i=j+1}^{n-2} (i-j+1) \right) \\
 &= 2nh + k(n-1) + h((j-1)(j-2) + (n-j-2)(n-j+1)).
 \end{aligned} \tag{23}$$

So,

$$\begin{aligned}
 S_3 &= \sum_{j=1}^n \left(d\left(\frac{v_j}{\Gamma}\right) h_j - 1 \right) h_j (M_{2,j}(\Gamma) + M_{21}(\Gamma) + B_j) \\
 &= \left(d\left(\frac{v_1}{\Gamma}\right) h_1 - 1 \right) h_1 (M_{2,1}(\Gamma) + M_{21}(\Gamma) + B_1) + \left(d(v_2\Gamma) + h_2 - 1 \right) h_2 (M_{2,2}(\Gamma) + M_{21}(\Gamma) + B_2) \\
 &\quad + \left(d\left(\frac{v_{n-1}}{\Gamma}\right) h_{n-1} - 1 \right) h_{n-1} (M_{2,(n-1)}(\Gamma) + M_{21}(\Gamma) + B_{n-1}) + \left(d\left(\frac{v_n}{\Gamma}\right) h_n - 1 \right) h_n (M_{2,n}(\Gamma) + M_{21}(\Gamma) + B_n) \\
 &\quad + \sum_{j=3}^{n-2} \left(d\left(\frac{v_j}{\Gamma}\right) h_j - 1 \right) h_j (M_{2,j}(\Gamma) + M_{21}(\Gamma) + B_j) \\
 &= (1+k-1)k(n^2 - 3n + 2 + 2n - 4 + (n+1)(k + (n-2)h) + (2+h-1)h
 \end{aligned}$$

$$\begin{aligned}
& (n^2 - 5n + 8 + 2n - 4 + 2nh + k(n - 1) + h(n - 4)(n - 1)) + (2 + h - 1)h(n^2 - 5n + 8 + 2n - 4) \\
& + h(n - 4)(n - 1) + (1 + k - 1)k(n^2 - 3n + 2 + 2n - 4 + (n + 1)(k + (n - 2)h)) \\
& + \sum_{j=3}^{n-2} (2 + h - 1)h(M_{2,j}(\Gamma) + 2n - 4 + 2nh + k(n - 1)) + h((j - 1)(j - 2) + (n - j - 2)(n - j + 1)) \\
= & 2k^2(n^2 - n - 2 + (n + 1)(k + (n - 2)h)) + 2h(h + 1)(n^2 - 3n + 4 + 2nh + k(n - 1) + h(n - 4)(n - 1)) \\
& + h(h + 1) \sum_{j=3}^{n-2} 2j^2 - 2jn - 2j + n^2 - n + 4 + 2n - 4 + 2nh + k(n - 1) + h((j - 1)(j - 2) + (n - j - 2)(n - j + 1)) \\
= & 2k^2(n^2 - n - 2 + (n + 1)(k + (n - 2)h)) + 2h(h + 1)(n^2 - 3n + 4 + 2nh + k(n - 1) + h(n - 4)(n - 1)) \\
& + h(h + 1) \left(4k - 8h + \frac{22}{3}n - 4hn^2 + \frac{2}{3}hn^3 + kn^2 + \frac{22}{3}hn - 5kn - 4n^2 + \frac{2}{3}n^3 - 8 \right). \tag{24}
\end{aligned}$$

Also,

$$\begin{aligned}
S_4 &= \sum_{1 \leq i < j \leq n} \left(d\left(\frac{v_i}{\Gamma}\right) + h_i - 1 \right) \left(d\left(\frac{v_j}{\Gamma}\right) + h_j - 1 \right) (d(v_i, v_j) + 2) h_i h_j \\
&= \left(d\left(\frac{v_1}{\Gamma}\right) + h_1 - 1 \right) \left(d\left(\frac{v_n}{\Gamma}\right) + h_n - 1 \right) (d(v_1, v_n) + 2) h_1 h_n + \sum_{j=2}^{n-1} \left(d\left(\frac{v_1}{\Gamma}\right) + h_1 - 1 \right) \left(d\left(\frac{v_j}{\Gamma}\right) + h_j - 1 \right) \\
&\quad \cdot (d(v_1, v_j) + 2) h_1 h_j + \sum_{j=2}^{n-1} \left(d\left(\frac{v_n}{\Gamma}\right) + h_n - 1 \right) \left(d\left(\frac{v_j}{\Gamma}\right) + h_j - 1 \right) (d(v_n, v_j) + 2) h_n h_j \\
&\quad + \sum_{2 \leq i < j \leq n-1} \left(d\left(\frac{v_i}{\Gamma}\right) + h_i - 1 \right) \left(d\left(\frac{v_j}{\Gamma}\right) + h_j - 1 \right) (d(v_i, v_j) + 2) h_i h_j \\
&= (1 + k - 1)(1 + k - 1)(n + 1)k \cdot k + \sum_{j=2}^{n-1} (1 + k - 1)(2 + h - 1)(j - 1 + 2)kh \\
&\quad + \sum_{j=2}^{n-1} (1 + k - 1)(2 + h - 1)(n - j + 2)kh + \sum_{2 \leq i < j \leq n-1} (2 + h - 1)(2 + h - 1)(j - i + 2)hh \\
&= k^4(n + 1) + k^2h(h + 1) \sum_{j=2}^{n-1} (j + 1) + k^2h(h + 1) \sum_{j=2}^{n-1} (n - j + 2) + h^2(h + 1)^2 \sum_{2 \leq i < j \leq n-1} (j - i + 2) \\
&= k^4(n + 1) + k^2h(h + 1)(n - 2)(n + 3) + \frac{h^2(h + 1)^2(n - 3)(n - 2)(n + 5)}{6}.
\end{aligned} \tag{25}$$

By substituting the values in $S_1, S_2, S_3,$ and S_4 in equation (5), we will get the required result.

For $k = m - 2$ and $h = m - 1$, thorn path $P_{n,h,k}$ represents a caterpillar $T_{m,m}'$. Similarly, a thorn path $P_{n,h,k}$ will be thorn rod $P_{n,m}$ if $h = 0$ and $k = m - 1$, i.e., $P_{n,m} = P_{n,0,m-1}$. Thus, the GI index of the thorn path and thorn rod is defined in the following corollaries.

Corollary 3. For $n, m \geq 2$, the GC index of caterpillar is

$$\begin{aligned}
GC(T'm, n) &= \frac{1}{6} m^4 n^3 + m^4 n^2 - \frac{1}{6} m^4 n + \frac{1}{3} m^3 n^3 - 4m^3 n^2 \\
&\quad - \frac{34}{3} m^3 n + \frac{1}{6} m^2 n^3 \\
&\quad - 3m^2 n^2 + \frac{221}{6} m^2 n + 34m^2 + 2mn^2 - 10mn \\
&\quad - 104m + 4n + 36.
\end{aligned} \tag{26}$$

Corollary 4. For $n, m \geq 2$, the GC index of thorn rod is

$$\begin{aligned} GC(P_{n,m}) &= m^4n + 3m^4 - 2m^3n - 12m^3 \\ &+ 2m^2n^2 - m^2n + 11m^2 \\ &- 2mn^2 - 6mn + 18m + \frac{2}{3}n^3 - 4n^2 + \frac{58}{3}n - 34. \end{aligned} \tag{27}$$

Now, we present the GC index for the thorn star. Suppose that L is the number of all pendant vertices other than the pendant vertices attached to n th vertex, i.e., $L = \sum_{p=1}^{n-1} h_p$.

Theorem 3. Let S_{n,h_1,h_2,\dots,h_n} be a thorn star graph; then,

$$\begin{aligned} GC(S_{n,h_1,h_2,\dots,h_n}) &= (n-1)(n-2+h_n)(L+(n-2)(n-2+h_n)) + \sum_{i=1}^{n-1} h_i^3(h_i-1) \\ &+ (n+h_n-2)^2h_n(h_n-1) + (n+h_n-2)h_n(2(n-1)(n-2+h_n)+L) \\ &+ ((3n-5)(n+h_n-2)+2L) \sum_{j=1}^{n-1} h_j^2 + 3(h_n+n-2)h_n \sum_{j=1}^{n-1} h_j^2 + 4 \sum_{1 \leq i < j \leq n-1} h_i^2 h_j^2. \end{aligned} \tag{28}$$

Proof. The proof is followed by Theorem 1. Some special cases of Theorem 3 are discussed in the following corollaries.

Corollary 5. If thorn of length h is attached with all the vertices other than the root vertex $h_i = h$, for $i \leq n-1$, then $L = (hn(n-1))/2$ and

$$\begin{aligned} GC(\Gamma^h) &= (n-1)(n-2+h_n)(L+(n-2)(n-2+h_n)) + h^3(h-1)(n-1) + (n+h_n-2)^2h_n(h_n-1) \\ &+ (n+h_n-2)h_n(2(n-1)(n-2+h_n)+L) + ((3n-5)(n+h_n-2)+hn(n-1)) \\ &\cdot \frac{hn(n-1)}{2} + 3(h_n+n-2)h_n \frac{hn(n-1)}{2} + 2h^4(n-1)(n-2), \end{aligned} \tag{29}$$

where $\Gamma^h = S_{n,h,\dots,h,h_n}$.

Corollary 6. If no thorn is attached with root vertex of thorn star, then

$$GC(\Gamma^h) = (n-1)(n-2)(L+(n-2)^2) + \sum_{i=1}^{n-1} h_i^3(h_i-1) + ((3n-5)(n-2)+2L) \sum_{j=1}^{n-1} h_j^2 + 4 \sum_{1 \leq i < j \leq n-1} h_i^2 h_j^2, \tag{30}$$

where $\Gamma^h = S_{n,h_1,h_2,\dots,h_{n-1},0}$.

Corollary 7. If no thorn is attached with root vertex and with other vertices a thorn of length h is attached, then

$$\begin{aligned} GC(\Gamma^h) &= (n-1)(n-2)(h(n-1)+(n-2)^2) + h^3(h-1)(n-1) \\ &+ ((3n-5)(n-2)+2h(n-1))h^2(n-1) + 2h^4(n-1)(n-2), \end{aligned} \tag{31}$$

where $\Gamma^h = S_{n,h,\dots,h,0}$.

Now, we will discuss the GC index for the thorn ring graph.

$$\text{GC}(C_{m,n}) = \begin{cases} \frac{(m-1)^2 n(n^2-1)}{2} + (m-1)^2 (m-2)(m-3)n \\ + (m-1)(m-2)n \left(\frac{n^2-1}{2} + 2n + \frac{(m-2)(n^2+4n-1)}{2} \right) \\ + \frac{(m-1)^2 (m-2)^2 n(n-1)(n+9)}{8}, & \text{if } n \text{ is odd,} \\ \frac{(m-1)^2 n^3}{2} + (m-1)^2 (m-2)(m-3)n \\ + (m-1)(m-2)n \left(\frac{n^2}{2} + 2n + \frac{(m-2)n(n+4)}{2} \right) \\ + \frac{(m-1)^2 (m-2)^2 n(n^2+8n-8)}{8}, & \text{if } n \text{ is even.} \end{cases} \quad (32)$$

Proof. The proof is followed by Theorem 1.

5. Conclusion

In this section, we conclude our study as follows:

- (i) Chemical applicability of GCI for several octane isomers is discussed, and it is found that it has high correlations with entropy, accentric factor, enthalpy of vaporization, standard enthalpy of vaporization, and standard heat of formation
- (ii) The GC index of thorn graphs is obtained in its general form
- (iii) The GC index of thorn paths, caterpillars, thorn rods, thorn stars, and thorn rings are also computed
- (iv) A descriptor M_{21} (sum of connection numbers of vertices of a graph) is provided in Lemma 1 that is called as connection degree sum

Now, we close this discussion that the various investigations are still needed for different (molecular) graphs or networks with the help of newly defined GC index.

Data Availability

The data used to support the findings of this study are cited at relevant places within article as references.

Theorem 4. Let $C_{m,n}$ be a thorn graph of cycle graph C_n with $n \geq 5$; then,

Conflicts of Interest

The authors declare that there are no conflicts of interest regarding this publication.

References

- [1] F. M. Brückler, T. Došlić, A. Graovac, and I. Gutman, "On a class of distance-based molecular structure descriptors," *Chemical Physics Letters*, vol. 503, no. 4-6, pp. 336-338, 2011.
- [2] H. Gonzalez-Diaz, S. Vilar, L. Santana, and E. Uriarte, "Medicinal chemistry and bioinformatics-current trends in drugs discovery with networks topological indices," *Current Topics in Medicinal Chemistry*, vol. 7, no. 10, pp. 1015-1029, 2007.
- [3] R. Todeschini and V. Consonni, *Molecular Descriptors for Chemoinformatics*, Wiley-VCH Verlag GmbH, vol. 2, p. 1252, Weinheim, Germany, 2009.
- [4] F. Yan, Q. Shang, S. Xia, Q. Wang, and P. Ma, "Application of topological index in predicting ionic liquids densities by the quantitative structure property relationship method," *Journal of Chemical & Engineering Data*, vol. 60, no. 3, pp. 734-739, 2015.
- [5] I. Gutman and N. Trinajstić, "Graph theory and molecular orbitals. Total ϕ -electron energy of alternant hydrocarbons," *Chemical Physics Letters*, vol. 17, no. 4, pp. 535-538, 1972.
- [6] B. Furtula and I. Gutman, "A forgotten topological index," *Journal of Mathematical Chemistry*, vol. 53, no. 4, pp. 1184-1190, 2015.

- [7] S. Klavzar and I. Gutman, "Selected properties of the Schultz molecular topological index," *The Journal for Chemical Information and Computer Scientists*, vol. 36, pp. 1001–1003, 1996.
- [8] A. Ali and N. Trinajstić, "A novel/old modification of the first Zagreb index," *Molecular Informatics*, vol. 37, no. 6-7, Article ID 1800008, 2018.
- [9] U. Ali, M. Javaid, and A. Kashif, "Modified Zagreb connection indices of the T -sum graphs," *Main Group Metal Chemistry*, vol. 43, no. 1, pp. 43–55, 2020.
- [10] M. Javaid, U. Ali, and M. K. Siddique, "Novel connection based Zagreb indices of several wheel-related graphs," *Computational Journal of Combinatorial Mathematics*, vol. 2, pp. 31–58, 2020.
- [11] A. Ahmad, M. F. Nadeem, K. Elahi, and R. Hasni, "Computing topological indices of chemical structures of the conductive 2D MOFs," *Journal of Information and Optimization Sciences*, vol. 42, no. 3, pp. 563–578, 2021.
- [12] A. Ahmad, M. A. Asim, and M. F. Nadeem, "Polynomials of degree-based indices of metal-organic networks," *Combinatorial Chemistry and High Throughput Screening*, vol. 24, pp. 1–9, 2020.
- [13] M. Siddique, Y. Chu, M. Nasir, M. Nadeem, and M. Hanif, "On topological descriptors of ceria oxide and their applications," *Main Group Metal Chemistry*, vol. 44, no. 1, pp. 103–116, 2021.
- [14] H. Wiener, "Structural determination of paraffin boiling points," *Journal of the American Chemical Society*, vol. 69, no. 1, pp. 17–20, 1947.
- [15] I. Gutman, "Selected properties of the Schultz molecular topological index," *Journal of Chemical Information and Computer Sciences*, vol. 34, no. 5, pp. 1087–1089, 1994.
- [16] I. Gutman, "Distance in thorny graph," *Publications de l'Institut Mathématique (Beograd)*, vol. 63, pp. 31–36, 1998.
- [17] L. Bytautas, D. Bonchev, and D. J. Klein, "On the generation of mean Wiener numbers of thorny graphs," *MATCH Communications in Mathematical and in Computer Chemistry*, vol. 44, pp. 31–40, 2001.
- [18] B. Zhou, "On modified Wiener indices of thorn trees," *Kragujevac Journal of Mathematics*, vol. 27, pp. 5–9, 2005.
- [19] S. Li, "Zagreb polynomials of thorn graphs," *Kragujevac Journal of Science*, vol. 33, pp. 33–38, 2011.
- [20] I. Gutman, B. Furtula, J. Tovsic, E. Mohamed, and M. El marraki, "On terminal Wiener indices of kenograms and plerograms," *Iranian Journal of Mathematical Chemistry*, vol. 4, no. 1, pp. 77–89, 2013.
- [21] Y. Alizadeh, A. Iranmanesh, T. Došlić, and M. Azari, "The edge wiener index of suspensions, bottlenecks, and thorny graphs," *Glasnik Matematički*, vol. 49, no. 1, pp. 1–12, 2014.
- [22] M. Azari and A. Iranmanesh, "Dendrimer graphs as thorn graphs and their topological edge properties," *National Academy Science Letters*, vol. 39, no. 6, pp. 455–460, 2016.
- [23] D. Bonchev and D. J. Klein, "On the Wiener number of thorn trees, stars, rings and rods," *Croatica Chemica Acta*, vol. 75, no. 2, pp. 613–620, 2002.
- [24] M. Azari, "On the Gutman index of Thorn graphs," *Kragujevac Journal of Science*, vol. 40, no. 40, pp. 33–48, 2018.

Research Article

Edge Weight-Based Entropy of Magnesium Iodide Graph

Maryam Salem Alatawi ¹, Ali Ahmad ², Ali N. A. Koam ³, Sadia Husain ²,
and Muhammad Azeem ⁴

¹Department of Mathematics, Faculty of Sciences, University of Tabuk, Tabuk 71491, Saudi Arabia

²College of Computer Science & Information Technology, Jazan University, Jazan, Saudi Arabia

³Department of Mathematics, College of Science, Jazan University, New Campus, Jazan 2097, Saudi Arabia

⁴Department of Mathematics, Riphah Institute of Computing and Applied Sciences, Riphah International University, Lahore, Pakistan

Correspondence should be addressed to Ali Ahmad; ahmadms@gmail.com

Received 15 September 2021; Accepted 27 October 2021; Published 15 November 2021

Academic Editor: Ji Gao

Copyright © 2021 Maryam Salem Alatawi et al. This is an open access article distributed under the Creative Commons Attribution License, which permits unrestricted use, distribution, and reproduction in any medium, provided the original work is properly cited.

Among the inorganic compounds, there are many influential crystalline structures, and magnesium iodide is the most selective. In the making of medicine and its development, magnesium iodide is considered a multipurpose and rich compound. Chemical structures and networks can be studied by given tools of molecular graph theory. Given tools of molecular graph theory can be studied for chemical structures and networks, which are considered economical with simple methodology. Edge weight-based entropy is a recent advent tool of molecular graph theory to study chemical networks and structures. It provides the structural information of chemical networks or their related build-up graphs and highlights the molecular properties in the form of a polynomial function. In this work, we provide the edge weight-based entropy of magnesium iodide structure and compute different entropies, such as Zagreb and atom bond connectivity entropies.

1. Introduction

Magnesium iodide is a chemical compound and known for its chemical formula MgI_2 . Magnesium iodide is an inorganic compound that is used for synthesis in various organic substances, as well as it has other commercial uses. The major availability measures of MgI_2 are having their high impurity and volumes as a submicron and nanopowder. Magnesium iodide is obtained by the combined chemical mixture of hydro-iodic acid and magnesium carbonate and also the major chemical compounds magnesium oxide and magnesium hydroxide can be found. In the major applications of magnesium iodide, it is a highly valuable asset in internal medicine. By a unique pattern of C_4 -graph, the molecular graph of magnesium iodide can be constructed. Having each C_4 -graph inside, multiple heptagons are connected to each other [1]. For the easy readability and better understanding of the molecular graph of magnesium iodide, we labeled the parameters as p is the number of C_4 's of upper

sides in a row and q denoted for the count of lower side C_4 in heptagons. For all values of $q \in \mathbb{Z}$ with $q \geq 1$, magnesium iodide graph is needed to maintain for even and odd values of p separately with the relation of $p = 2(q + 1)$ and $p = 2q + 1$, respectively.

“The entropy of a probability distribution known as a measure of the unpredictability of information content or a measure of the uncertainty of a system.” This quotation was the foundation, described in [2], as a seminal theory for the idea of entropy. Due to this concept is strongly based on statistical methodology, it became well-known for chemical structures and their corresponding graphs. This parameter provides a piece of extensive information about graphs, structures, and chemical topologies. In 1955, the notion and its idea were used first time for graphs. In sociology, ecology, biology, chemistry, and in a variety of other technical fields, graph-based entropy or simply entropy has applications [3, 4]. Taking into consideration distinct graph elements associated with probability distributions, two types of

entropy measurements are determined which are intrinsic and extrinsic entropies. The idea named degree-powers is a mathematical application of applied graph theory towards network theory to investigate networks as information functionals [5, 6]. The physical sound of a network associated with the idea of entropy came forward from the authors in [7].

The major concern of this study is to determine some edge weight-based entropies of magnesium iodide structure for both cases of p . The methodology of this study of edge weight-based entropy is defined in Definitions 1–6, with their other fundamentals.

Definition 1. The first and second Zagreb index is introduced in 1972 by [8, 9] as

$$M_1(F) = \sum_{\mathbf{uv} \in E(F)} (\lambda_{\mathbf{u}} + \lambda_{\mathbf{v}}), \quad (1)$$

$$M_2(F) = \sum_{\mathbf{uv} \in E(F)} (\lambda_{\mathbf{u}} \times \lambda_{\mathbf{v}}). \quad (2)$$

Definition 2. The researcher in [10] introduced the atom bond connectivity index as

$$ABC(F) = \sum_{\mathbf{uv} \in E(F)} \sqrt{\frac{\lambda_{\mathbf{u}} + \lambda_{\mathbf{v}} - 2}{\lambda_{\mathbf{u}} \times \lambda_{\mathbf{v}}}}. \quad (3)$$

Definition 3. The geometric arithmetic index of a graph is introduced by [11] as

$$GA(F) = \sum_{\mathbf{uv} \in E(F)} \frac{2\sqrt{\lambda_{\mathbf{u}} \times \lambda_{\mathbf{v}}}}{\lambda_{\mathbf{u}} + \lambda_{\mathbf{v}}}. \quad (4)$$

Definition 4. In 2014, entropy for an edge weighted graph F is introduced in [12]:

$$\Omega_{\psi}(F) = - \sum_{\mathbf{u}'\mathbf{v}' \in E(F)} \frac{\psi(\mathbf{u}'\mathbf{v}')}{\sum_{\mathbf{uv} \in E(F)} \psi(\mathbf{uv})} \log \left[\frac{\psi(\mathbf{u}'\mathbf{v}')}{\sum_{\mathbf{uv} \in E(F)} \psi(\mathbf{uv})} \right], \quad (5)$$

where $\psi(\mathbf{uv})$ is a weight for an edge \mathbf{uv} .

By letting the edge of weight equal to the main part of the topological index, Manzoor et al. [13, 14] introduced the following entropies for an edge weighted-based graph. The following are some important formulas for this research work and all these are based on equation (5).

Definition 5. The first and second Zagreb entropies are defined as follows [14, 15]:

$$\Omega_{M_1}(F) = -\frac{1}{M_1(F)} \log \left[\prod_{\mathbf{uv} \in E(F)} [\lambda_{\mathbf{u}} + \lambda_{\mathbf{v}}]^{[\lambda_{\mathbf{u}} + \lambda_{\mathbf{v}}]} \right] + \log(M_1(F)), \quad (6)$$

$$\Omega_{M_2}(F) = -\frac{1}{M_2(F)} \log \left[\prod_{\mathbf{uv} \in E(F)} [\lambda_{\mathbf{u}}\lambda_{\mathbf{v}}]^{[\lambda_{\mathbf{u}}\lambda_{\mathbf{v}}]} \right] + \log(M_2(F)). \quad (7)$$

Definition 6. The atom bond connectivity and geometric arithmetic entropies are defined as follows [13]:

$$\Omega_{ABC}(F) = -\frac{1}{ABC(F)} \log \left[\prod_{\mathbf{uv} \in E(F)} \left[\sqrt{\frac{\lambda_{\mathbf{u}} + \lambda_{\mathbf{v}} - 2}{\lambda_{\mathbf{u}}\lambda_{\mathbf{v}}}} \right]^{[\sqrt{\lambda_{\mathbf{u}} + \lambda_{\mathbf{v}} - 2/\lambda_{\mathbf{u}}\lambda_{\mathbf{v}}}]}} \right] + \log(ABC(F)), \quad (8)$$

$$\Omega_{GA}(F) = -\frac{1}{GA(F)} \log \left[\prod_{\mathbf{uv} \in E(F)} \left[\frac{2\sqrt{\lambda_{\mathbf{u}}\lambda_{\mathbf{v}}}}{\lambda_{\mathbf{u}} + \lambda_{\mathbf{v}}} \right]^{[2\sqrt{\lambda_{\mathbf{u}}\lambda_{\mathbf{v}}}/\lambda_{\mathbf{u}} + \lambda_{\mathbf{v}}]} \right] + \log(GA(F)). \quad (9)$$

The topic of discussion of this study is closely related to the numerical descriptors or topological indices, so read the fundamentals and basics; we refer to see the recent cluster [16–23]. In the recent decade, this concept has been studied intensively and numerous literatures are available. We will

discuss only limited recent most articles on this concept and few are left for the interest of readers [24–28].

To investigate and gain the contents of a network, the entropy formulas as put forward by [2], along with this, it helps to know about the structural information of networks

and chemical structures [29]. The concept of edge weight-based entropy of a graph developed the applications and exploration in biological systems. For example, by creating a graph of chemical or any biological system, it has been used to investigate live organisms in the systems. For the biological and chemical applications of this study, see [30, 31]. In computer science, in structural chemistry, and in even biology, the entropy can be found by [32]. This entropy, which is also explored in this study document, can be found in [29, 33] in-network heterogeneity work. In more recent literature about edge weight-based entropy, one can find [34, 35].

The edge weight-based entropies of the first and second Zagreb index, atom bond connectivity index, and geometric arithmetic index are figured out for the magnesium iodide or Mgl_2 structure, for both even and odd cases of parameter p . The topological index of the magnesium iodide or Mgl_2 structure, for both even and odd cases of parameter p , are computed in [1]. We will use the results of theorems from

[1], which are summarized in Tables 1 and 2. Moreover, due to long expressions of theorems, we reduced the calculations up to four decimal digits.

2. Results on the Edge Weight-Based Entropy of Magnesium Iodide

Given in this section are some important results of this research work. The idea is totally dependent on the structural values of Mgl_2 or magnesium iodide graph, which is defined in Table 3 (for $p = \text{odd}$ and Table 4 (for $p = \text{even}$, and the structure is shown in Figure 1.

Case 1. For the odd values of p with given $q \geq 1$, let $p = 2q + 1$ and $q \in \mathbb{Z}$.

Theorem 1. Let Ω_{M_1} be the edge weight-based first Zagreb entropy for the $MG_{p,q}$ magnesium graph, with $p = 2q + 1$, $q \geq 1$, then $\Omega_{M_1}(MG_{p,q})$ is

$$\Omega_{M_1}(MG_{p,q}) = \frac{1}{284q + 172} \log [2304 \cdot 4^4 \cdot (25)^5 \cdot (36)^6 \cdot (343)^7 \cdot (64)^8 \cdot 9^9 \times q(q + 4)(q + 5)(27q - 13)]. \quad (10)$$

Proof. The edge partition of $MG_{p,q}$ magnesium graph for the parameters $p = 2q + 1$ and $q \geq 1$, given in Table 3, which are used to determine the topological indices of $MG_{p,q}$, is summarized in Table 1. Using the value of first Zagreb

topological index from Table 1, along with the edge types from Table 3, in the formula defined in equation (6), after simplification, the entropy of first Zagreb resulted in

$$\Omega_{M_1}(F) = \frac{1}{284q + 172} \log [2304 \cdot 4^4 \cdot (25)^5 \cdot (36)^6 \cdot (343)^7 \cdot (64)^8 \cdot 9^9 \times q(q + 4)(q + 5)(27q - 13)]. \quad (11)$$

Theorem 2. Let Ω_{M_2} be the edge weight-based second Zagreb entropy for the $MG_{p,q}$ magnesium graph, with $p = 2q + 1$, $q \geq 1$, then $\Omega_{M_2}(MG_{p,q})$ is

$$\Omega_{M_2}(MG_{p,q}) = \frac{1}{543q + 190} \log [2304 \cdot 3^3 \cdot 4^4 \cdot (36)^6 \cdot 8^8 \cdot 9^9 \cdot (10)^{10} \cdot (144)^{12} \cdot (15)^{15} \cdot (18)^{18} \times q(q + 4)(q + 5)(27q - 13)]. \quad (12)$$

Proof. Using the value of second Zagreb topological index from Table 1, along with the edge types from Table 3, in the

formula defined in equation (7), after simplification, the entropy of second Zagreb resulted in

$$\Omega_{M_2}(MG_{p,q}) = \frac{1}{543q + 190} \log [2304 \cdot 3^3 \cdot 4^4 \cdot (36)^6 \cdot 8^8 \cdot 9^9 \cdot (10)^{10} \cdot (144)^{12} \cdot (15)^{15} \cdot (18)^{18} \times q(q + 4)(q + 5)(27q - 13)]. \quad (13)$$

□

TABLE 1: Topological indices of $MG_{p,q}$.

I	$I(MG_{p,q})$
M_1	$284q + 172$
M_2	$543q + 190$
ABC	$21.1645q + 22.8602$
GA	$30.8878q + 23.5189$
For	$p = 2q + 1, q \geq 1.$

TABLE 2: Topological indices of $MG_{p,q}$.

I	$I(MG_{p,q})$
M_1	$284q + 258$
M_2	$543q + 375$
ABC	$21.1645q + 22.8602$
GA	$30.8878q + 23.5189$
For	$p = 2(q + 1), q \geq 1.$

TABLE 3: Edge partition of $MG_{p,q}$ for $p = 2q + 1, q \geq 1.$

(λ_u, λ_v)	Frequency	Set of edges
(1, 3)	1	E_1
(1, 4)	1	E_2
(1, 6)	$q + 5$	E_3
(2, 3)	2	E_4
(2, 4)	2	E_5
(2, 5)	8	E_6
(2, 6)	$2q + 8$	E_7
(3, 3)	$3q$	E_8
(3, 4)	1	E_9
(3, 5)	12	E_{10}
(3, 6)	$27q - 13$	E_{11}

TABLE 4: Edge partition of $MG_{p,q}$ for $p = 2(q + 1), q \geq 1.$

(λ_u, λ_v)	Frequency	Set of edges
(1, 3)	1	E_1
(1, 5)	1	E_2
(1, 6)	$q + 5$	E_3
(2, 2)	2	E_4
(2, 3)	2	E_5
(2, 5)	8	E_6
(2, 6)	$2q + 8$	E_7
(3, 3)	$3q$	E_8
(3, 5)	1	E_9
(3, 6)	12	E_{10}

Theorem 3. Let Ω_{ABC} be the edge weight-based atom bond connectivity entropy for the $MG_{p,q}$ magnesium graph, with $p = 2q + 1, q \geq 1$, then $\Omega_{ABC}(MG_{p,q})$ is

$$\Omega_{ABC}(MG_{p,q}) = \frac{1}{21.1645q + 22.8602} \log[4778.1804q(q + 4)(q + 5)(27q - 13)]. \tag{14}$$

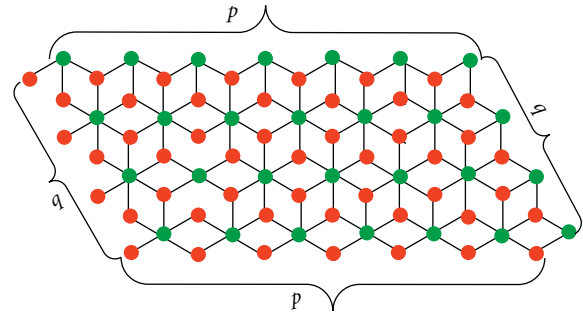


FIGURE 1: Magnesium iodide graph.

Proof. Using the value of atom bond connectivity topological index from Table 1, along with the edge types from Table 3, in the formula defined in equation (8), after simplification, the entropy of atom bond connectivity resulted in

$$\Omega_{ABC}(MG_{p,q}) = \frac{1}{21.1645q + 22.8602} \log[4778.1804q(q + 4)(q + 5)(27q - 13)]. \tag{15}$$

Theorem 4. Let Ω_{GA} be the edge weight-based geometric arithmetic entropy for the $MG_{p,q}$ magnesium graph, with $p = 2q + 1, q \geq 1$, then $\Omega_{GA}(MG_{p,q})$ is

$$\Omega_{GA}(MG_{p,q}) = \frac{1}{30.8878q + 23.5189} \log[949.8757q(q + 4)(q + 5)(27q - 13)]. \tag{16}$$

Proof. Using the value of geometric arithmetic topological index from Table 1, along with the edge types from Table 3, in the formula defined in equation (9), after simplification, the entropy of geometric arithmetic resulted in

$$\Omega_{GA}(MG_{p,q}) = \frac{1}{30.8878q + 23.5189} \log[949.8757q(q + 4)(q + 5)(27q - 13)]. \tag{17}$$

Case 2. For the even values of p with given $q \geq 1$, let $p = 2(q + 1)$ and $q \in \mathbb{Z}$.

Theorem 5. Let Ω_{M_1} be the edge weight-based first Zagreb entropy for the $MG_{p,q}$ magnesium graph, with $p = 2(q + 1), q \geq 1$, then $\Omega_{M_1}(MG_{p,q})$ is

$$\Omega_{M_1}(MG_{p,q}) = -\frac{1}{284q + 258} \log[240 \cdot (16)^4 \cdot 5^5 \cdot 6^6 \cdot (49)^7 \cdot (64)^8 \cdot (81)^9 \times (q + 4)(q + 5)(3q + 1)(27q + 7)]. \quad (18)$$

Proof. The edge partition of $MG_{p,q}$ magnesium graph for the parameters $p = 2(q + 1)$ and $q \geq 1$, given in Table 4, which are used to determine the topological indices of $MG_{p,q}$, is summarized in Table 2. Using the value of first

Zagreb topological index from Table 2, along with the edge types from Table 4, in the formula defined in equation (6), after simplification, the entropy of first Zagreb resulted in

$$\Omega_{M_1}(MG_{p,q}) = -\frac{1}{284q + 258} \log[240 \cdot (16)^4 \cdot 5^5 \cdot 6^6 \cdot (49)^7 \cdot (64)^8 \cdot (81)^9 \times (q + 4)(q + 5)(3q + 1)(27q + 7)]. \quad (19)$$

Theorem 6. Let Ω_{M_2} be the edge weight-based second Zagreb entropy for the $MG_{p,q}$ magnesium graph, with $p = 2(q + 1)$, $q \geq 1$, then $\Omega_{M_2}(MG_{p,q})$ is

$$\Omega_{M_2}(MG_{p,q}) = -\frac{1}{543q + 375} \log[240 \cdot 3^3 \cdot 4^4 \cdot 5^5 \cdot (36)^6 \cdot 9^9 \cdot (10)^{10} \cdot (12)^{12} \cdot (15)^{15} \cdot (18)^{18} \times (q + 4)(q + 5)(3q + 1)(27q + 7)]. \quad (20)$$

Proof. Using the value of second Zagreb topological index from Table 2, along with the edge types from Table 4, in the

formula defined in equation (7), after simplification, the entropy of second Zagreb resulted in

$$\Omega_{M_2}(MG_{p,q}) = -\frac{1}{543q + 375} \log[240 \cdot 3^3 \cdot 4^4 \cdot 5^5 \cdot (36)^6 \cdot 9^9 \cdot (10)^{10} \cdot (12)^{12} \cdot (15)^{15} \cdot (18)^{18} \times (q + 4)(q + 5)(3q + 1)(27q + 7)]. \quad (21)$$

Theorem 7. Let Ω_{ABC} be the edge weight-based atom bond connectivity entropy for the $MG_{p,q}$ magnesium graph, with $p = 2(q + 1)$, $q \geq 1$, then $\Omega_{ABC}(MG_{p,q})$ is

$$\Omega_{ABC}(MG_{p,q}) = -\frac{1}{21.1645q + 22.8602} \log[2165.7809(q + 4)(q + 5)(3q + 1)(27q + 7)]. \quad (22)$$

Proof. Using the value of atom bond connectivity topological index from Table 2, along with the edge types from Table 4, in the formula defined in equation (8), after

simplification, the entropy of atom bond connectivity resulted in

$$\Omega_{ABC}(MG_{p,q}) = -\frac{1}{21.1645q + 22.8602} \log[2165.7809(q + 4)(q + 5)(3q + 1)(27q + 7)]. \quad (23)$$

Theorem 8. Let Ω_{GA} be the edge weight-based geometric arithmetic entropy for the $MG_{p,q}$ magnesium graph, with $p = 2(q + 1)$, $q \geq 1$, then $\Omega_{GA}(MG_{p,q})$ is

$$\Omega_{GA}(MG_{p,q}) = \frac{1}{30.8878q + 23.5189} \log[2895.9383(q + 4)(q + 5)(3q + 1)(27q + 7)]. \quad (24)$$

Proof. Using the value of geometric arithmetic topological index from Table 2, along with the edge types from Table 4,

in the formula defined in equation (9), after simplification, the entropy of geometric arithmetic resulted in

$$\Omega_{GA}(MG_{p,q}) = \frac{1}{30.8878q + 23.5189} \log[2895.9383(q + 4)(q + 5)(3q + 1)(27q + 7)]. \quad (25)$$

3. Conclusion

The edge weight-based entropy of a network or structure provides structural information and detailed content in the form of mathematical equations. To add up some structural information and properties of magnesium iodide or MgI_2 structure, we determined the edge weight-based entropies of the first and second Zagreb index, atom bond connectivity index, and geometric arithmetic index. The results carried information for both even and odd cases of parameter p , of magnesium iodide, or MgI_2 structure.

Data Availability

There are no data associated with this article.

Conflicts of Interest

The authors declare that they have no conflicts of interest.

References

- [1] F. Afzal, F. Asmat, and D. Afzal, "Molecular description for magnesium iodide," *Mathematical Models in Engineering*, vol. 5, no. 4, pp. 175–189, 2019.
- [2] C. E. Shannon, "A mathematical theory of communication," *Bell System Technical Journal*, vol. 27, no. 3, pp. 379–423, 1948.
- [3] M. Dehmer and M. Graber, "The discrimination power of molecular identification numbers revisited," *MATCH Community of Mathematics and Computational Chemistry*, vol. 69, pp. 785–794, 2013.
- [4] R. E. Ulanowicz, "Quantitative methods for ecological network analysis," *Computational Biology and Chemistry*, vol. 28, no. 5–6, pp. 321–339, 2004.
- [5] S. Cao, M. Dehmer, and Y. Shi, "Extremality of degree-based graph entropies," *Information Sciences*, vol. 278, pp. 22–33, 2014.
- [6] S. Cao and M. Dehmer, "Degree-based entropies of networks revisited," *Applied Mathematics and Computation*, vol. 261, pp. 141–147, 2015.
- [7] E. Estrada and N. Hatano, "Statistical-mechanical approach to subgraph centrality in complex networks," *Chemical Physics Letters*, vol. 439, no. 1–3, pp. 247–251, 2007.
- [8] I. Gutman and N. Trinajstić, "Graph theory and molecular orbitals, total π -electron energy of alternant hydrocarbons," *Chemical Physics Letters*, vol. 17, no. 4, pp. 535–538, 1972.
- [9] I. Gutman and K. C. Das, "The first zagreb index 30 years after," *Match Community of Mathematics and Computational Chemistry*, vol. 50, pp. 83–92, 2004.
- [10] E. Estrada, L. Torres, L. Rodríguez, and I. Gutman, "An atom-bond connectivity index modeling the enthalpy of formation of alkanes," *Indian Journal of Chemistry*, vol. 37, pp. 849–855, 1998.
- [11] D. Vukičević and B. Furtula, "Topological index based on the ratios of geometrical and arithmetical means of end-vertex degrees of edges," *Journal of Mathematical Chemistry*, vol. 46, pp. 1369–1376, 2009.
- [12] Z. Chen, M. Dehmer, and Y. Shi, "A note on distance based graph entropies," *Entropy*, vol. 16, no. 10, pp. 5416–5427, 2014.
- [13] S. Manzoor, M. K. Siddiqui, and S. Ahmad, "On entropy measures of molecular graphs using topological indices," *Arabian Journal of Chemistry*, vol. 13, no. 8, pp. 6285–6298, aug 2020.
- [14] S. Manzoor, M. K. Siddiqui, and S. Ahmad, "On entropy measures of polycyclic hydroxychloroquine used for novel coronavirus (covid-19) treatment," *Polycyclic Aromatic Compounds*, 2020.
- [15] X. Zuo, M. F. Nadeem, M. K. Siddiqui, and M. Azeem, "Edge weight based entropy of different topologies of carbon nanotubes," *IEEE Access*, vol. 9, pp. 102019–102029, 2021.
- [16] M. F. Nadeem, M. Imran, H. M. Afzal Siddiqui, M. Azeem, A. Khalil, and Y. Ali, "Topological aspects of metal-organic structure with the help of underlying networks," *Arabian Journal of Chemistry*, vol. 14, no. 6, Article ID 103157, 2021.
- [17] A. Shabbir, M. F. Nadeem, S. Mukhtar, and A. Raza, "On edge version of some degree-based topological indices of HAC5c7 [p,q] and VC5c7[p,q] nanotubes," *Polycyclic Aromatic Compounds*, pp. 1–17, 2020.
- [18] M. F. Nadeem, M. Azeem, and H. M. A. Siddiqui, "Comparative study of zagreb indices for capped, semi-capped, and uncapped carbon nanotubes," *Polycyclic Aromatic Compounds*, pp. 1–18, 2021.
- [19] M. F. Nadeem, M. Azeem, and I. Farman, "Comparative study of topological indices for capped and uncapped carbon nanotubes," *Polycyclic Aromatic Compounds*, pp. 1–18, 2021.
- [20] M. F. Nadeem, S. Zafar, and Z. Zahid, "On topological properties of the line graphs of subdivision graphs of certain

□

- nanostructures,” *Applied Mathematics and Computation*, vol. 273, pp. 125–130, 2016.
- [21] A. Ahmad and S. C. López, “Distance-based topological polynomials associated with zero-divisor graphs,” *Mathematical Problems in Engineering*, vol. 2021, Article ID 4959559, 8 pages, 2021.
- [22] G. Hong, Z. Gu, M. Javaid, H. M. Awais, and M. K. Siddiqui, “Degree-based topological invariants of metal-organic networks,” *IEEE Access*, vol. 8, pp. 68288–68300, 2020.
- [23] S. Hayat, M. A. Malik, and M. Imran, “Computing topological indices of honeycomb derived networks,” *Romanian Journal of Information Science and Technology*, vol. 18, pp. 144–165, 2015.
- [24] A. Ali, K. C. Das, D. Dimitrov, and B. Furtula, “Atom–bond connectivity index of graphs: a review over extremal results and bounds,” *Discrete Mathematics Letters*, vol. 5, no. 1, pp. 68–93, 2021.
- [25] A. Ali, I. Gutman, E. Milovanovic, and I. Milovanovic, “Sum of powers of the degrees of graphs: extremal results and bounds,” *MATCH Communications in Mathematical and in Computer Chemistry*, vol. 80, pp. 5–84, 2018.
- [26] B. Borovicanin, K. C. Das, B. Furtula, and I. Gutman, “Bounds for zagreb indices,” *MATCH Communications in Mathematical and in Computer Chemistry*, vol. 78, pp. 17–100, 2017.
- [27] K. C. Das, I. Gutman, and B. Furtula, “Survey on geometric–arithmetic indices of graphs,” *MATCH Communications in Mathematical and in Computer Chemistry*, vol. 65, pp. 595–644, 2011.
- [28] A. Portillaa, J. M. Rodriguezb, and J. M. Sigarreta, “Recent lower bounds for geometric-arithmetic index,” *Discrete Mathematics Letters*, vol. 1, pp. 59–82, 2019.
- [29] R. V. Sol and S. I. Valverde, “Information theory of complex networks: on evolution and architectural constraints,” *Complex Network Lectures Notes Physics*, vol. 650, pp. 189–207, 2004.
- [30] N. Rashevsky, “Life, information theory, and topology,” *Bulletin of Mathematical Biophysics*, vol. 17, no. 3, pp. 229–235, 1955.
- [31] E. Trucco, “A note on the information content of graphs,” *Bulletin of Mathematical Biophysics*, vol. 18, no. 2, pp. 129–135, 1956.
- [32] M. Dehmer and A. Mowshowitz, “A history of graph entropy measures,” *Information Sciences*, vol. 181, no. 1, pp. 57–78, 2011.
- [33] Y. J. Tan and J. Wu, “Network structure entropy and its application to scale-free networks,” *System Engineering-Theory & Practice*, vol. 6, pp. 1–3, 2004.
- [34] Y. C. Kwun, H. M. ur Rehman, M. Yousaf, W. Nazeer, and S. M. Kang, “The entropy of weighted graphs with atomic bond connectivity edge weights,” *Discrete Dynamics in Nature and Society*, vol. 2018, Article ID 8407032, 10 pages, 2018.
- [35] S. Sindhu, B. J. Gireesha, and G. Sowmya, “Entropy generation analysis of multi-walled carbon nanotube dispersed nanoliquid in the presence of heat source through a vertical microchannel,” *International Journal of Numerical Methods for Heat & Fluid Flow*, vol. 30, no. 12, pp. 5063–5085, 2020.

Research Article

Topological Indices of Pent-Heptagonal Nanosheets via M-Polynomials

Hafiza Bushra Mumtaz,¹ Muhammad Javaid ,¹ Hafiz Muhammad Awais,¹
and Ebenezer Bonyah ²

¹Department of Mathematics, School of Science, University of Management and Technology (UMT), Lahore, Pakistan

²Department of Mathematics Education, Akenten Appiah-Menka University of Skills Training and Entrepreneurial Development, Kumasi 00233, Ghana

Correspondence should be addressed to Ebenezer Bonyah; ebbonya@gmail.com

Received 16 September 2021; Accepted 20 October 2021; Published 12 November 2021

Academic Editor: Ali Ahmad

Copyright © 2021 Hafiza Bushra Mumtaz et al. This is an open access article distributed under the Creative Commons Attribution License, which permits unrestricted use, distribution, and reproduction in any medium, provided the original work is properly cited.

The combination of mathematical sciences, physical chemistry, and information sciences leads to a modern field known as cheminformatics. It shows a mathematical relationship between a property and structural attributes of different types of chemicals called quantitative-structures' activity and qualitative-structures' property relationships that are utilized to forecast the chemical sciences and biological properties, in the field of engineering and technology. Graph theory has originated a significant usage in the field of physical chemistry and mathematics that is famous as chemical graph theory. The computing of topological indices (TIs) is a new topic of chemical graphs that associates many physiochemical characteristics of the fundamental organic compounds. In this paper, we used the M-polynomial-based TIs such as 1st Zagreb, 2nd Zagreb, modified 2nd Zagreb, symmetric division deg, general Randić, inverse sum, harmonic, and augmented indices to study the chemical structures of pent-heptagonal nanosheets of VC_5C_7 and HC_5C_7 . An estimation among the computed TIs with the help of numerical results is also presented.

1. Introduction

Nanostructures [1, 2] have been studied as new materials with the size of elemental structures that has been engineered at the nanometers' scale. Most of the materials in this size range usually show novel behavior. Therefore, intervention in the characteristics of structures at the nanoscale allows the formation of devices and nanomaterials with completely or enhanced novel functionalities and properties. Understanding the science of nanostructures is curiosity and important driven not only for the interesting nature of the topic but also for novel and overwhelming usage of nanoscale systems in various fields of science and technology. Nanotechnology can be recognized as a technology of design, application, and fabrication of nanomaterials, and nanostructures [3].

The branch of nanotechnology and nanoscience is being perused by chemists, physicists, materials scientists,

engineers, biologists, computer scientists, and mathematicians [4]. So, it is also interdisciplinary. Nanostructures may be divided based on modulation and dimensionality. Most of the distinct nanotubes, zeolites, aerogel, core-shell structure, and nanoporous materials have unique properties. Numerous techniques have been utilized for the synthesis of nanomaterials with no. of degrees of success, and several direct as well as indirect methods are used for their properties [5]. The motivation to develop the nanomaterials is that the characteristics become size based in the nanometer range due to quantum confinement effect and surface effect. The chemical bonds, magnetic properties, geometric structure, electronic properties, ionization potential, mechanical strength, optical properties, and thermal properties are affected due to particle size in nanometers range. Nanostructures show characteristics mostly higher than the conventional coarse-grained material. These contain hardness/increased strength, toughness/improved ductility,

enhanced diffusivity, reduced density, higher electrical resistance, reduced elastic modulus, lower thermal conductivity, increase specific heat, higher thermal expansion coefficient, increased oscillator and strength luminescence, blue shift absorption, and superior soft magnetic characteristics in comparison to the conventional bulk material. Furthermore, these characteristics are being briefly examined to discover new tools. The interesting branch of nanotechnology has a vast range of different types of applications. The use of nanomaterials has manufactured transistors having low speed and laser having low threshold current. These are utilized in satellite receivers having low noise amplification as a source for fiber optics communications and compact disk player systems. Constructive tools of nanostructures contain UV-resistant wood coating and self-cleaning glass. On the other hand, nanoscale tools are being utilized in the field of medicine for the prevention and treatment of diseases, diagnosis, and in magnetic resonance imaging, drug delivery system, radioactive tracers, etc. [6]. The importance of nanomaterials is rising nowadays. Many other types of tools may be possible with the peculiar and novel characteristics of nanomaterials [7, 8].

Therefore, TIs are useful to define molecular nanomaterials. Nanostructures, that have a scale of less than 100 nm, contain nanosheets, nanotubes, and nanoparticles. Nanosheets (two-dimensional nanomaterials) have a sharp edge and large surface area that cause them to play a vital role in various types of tools such as catalysis, energy storage bioelectronics, and optoelectronics [9, 10]. Silicone, borophene, and graphene are specific nanosheets. Due to the rare optical, electrical, mechanical, and structural characteristics, graphene nanosheets received great recognition from industrial and academic researchers [11]. The different properties of the C_5C_7 nanosheet have become the most advanced field in research. A C_5C_7 structure is developed by alternating C_5 and C_7 [7]. In 2009, Graovac et al. studied the GA index of TUC_4C_8 (S) nanotubes. In 2011, Graovac et al. [12] studied the fifth geometric arithmetic index for nanostar dendrimers, and Asadpour et al. calculated, Zagreb, Randi c , and ABC indices of TUC_4C_8 (R) and TUC_4C_8 (S) V-Phenylene nanotorus and nanotubes. In 2014, Al-Fozan et al. solved Szeged index of H-naphthalene nanosheets (2n, 2m) and C_4C_8 (S). Loghman and Ashrafi studied the Padmakar-Ivan (PI) index of TUC_4C_8 (S) nanotubes. For further discussion, see [13–15].

However, the combination of three fields such as mathematics, physical chemistry, and information sciences lead to a modern field known as cheminformatics [16–18]. It develops a mathematical relationship between a property and structural attributes of different types of chemicals called by quantitative-structures' activity and qualitative-structures' property relationship that are utilized to forecast the organic sciences and biological properties in the field of engineering and technology [19, 20]. Graph theory has originated a significant usage in the field of mathematical chemistry that is famous as chemical graph theory.

Polya gave the idea for counting polynomials in the field of chemistry [21], and Wiener introduced the concept of TI related to the paraffin's boiling point [22]. Computing the

TIs is a new field of chemical graphs that associates many physiochemical characteristics of the fundamental chemical compounds [23–27].

2. Preliminaries

A molecular structure $\Gamma = (V(\Gamma), E(\Gamma))$; $V(\Gamma) = \{s_1, s_2, s_3, \dots, s_n\}$ and $E(\Gamma)$ are nodes (vertices) and edge set of Γ . $|V(\Gamma)| = v$ and $|E(\Gamma)| = e$ is the order and size of Γ . In a connected and simple molecular graph, a path is represented within two vertices and the distance between the two vertices s and t is mentioned as $\varphi(s, t)$, in a graph Γ , see [28–30]. In this paper, a graph is connected and simple, having no multiple edges or loops.

1st and 2nd Zagreb indices: let Γ be a molecular structure; then, its 1st and 2nd Zagreb indices [31] are

$$M_1(\Gamma) = \sum_{s \in V(\Gamma)} [\varphi(s)]^2 = \sum_{st \in E(\Gamma)} [\varphi(s) + \varphi(t)],$$

$$M_2(\Gamma) = \sum_{st \in E(\Gamma)} [\varphi(s) \times \varphi(t)].$$
(1)

General Randi c index: if R is the real number, $\alpha \in R$, and Γ is a molecular structure, the general Randi c index [32] is

$$R_\alpha(\Gamma) = \sum_{st \in E(\Gamma)} [\varphi(s)\varphi(t)]^\alpha.$$
(2)

Symmetric division deg index: for a molecular structure Γ , the symmetric division deg index [33] is

$$SDD(\Gamma) = \sum_{st \in E(\Gamma)} \left[\frac{\min(\varphi(s), \varphi(t))}{\max(\varphi(s), \varphi(t))} + \frac{\max(\varphi(s), \varphi(t))}{\min(\varphi(s), \varphi(t))} \right].$$
(3)

Harmonic index: for a molecular structure Γ , the harmonic index [34] is

$$H(\Gamma) = \sum_{st \in E(\Gamma)} \frac{2}{\varphi(s) + \varphi(t)}.$$
(4)

Inverse sum index: for a molecular structure Γ , the inverse sum index [35] is

$$IS(\Gamma) = \sum_{st \in E(\Gamma)} \frac{\varphi(s)\varphi(t)}{\varphi(s) + \varphi(t)}.$$
(5)

Augmented Zagreb index: for a molecular structure Γ , the augmented Zagreb index [13] is

$$AZI(\Gamma) = \sum_{st \in E(\Gamma)} \left[\frac{\varphi(s) \times \varphi(t)}{\varphi(s) + \varphi(t) - 2} \right]^3.$$
(6)

A graph polynomial is a graph invariant whose values are polynomials. So, all these invariants are discussed in algebraic graph theory [36]. Among such types of algebraic polynomials, the M-polynomial, defined in 2015, shows the same role in finding the much closed form of various degree-based TIs that correlate different types of chemical properties of the various materials under

investigation. In 2019, Yang et al. [37] find out the M-polynomial and topological indices of benzene ring embedded in P-type surface network. In 2020, Khalaf et al. [38] computed the M-polynomial and topological indices of book graph and Raza and Sakaiti [2] solved the M-polynomial and degree-based topological indices of some nanostructures. In 2021, Mondal et al. [39] find out the neighborhood M-polynomial of titanium compounds and Irfan et al. [1] computed the M-polynomials and topological indices for line graphs of chain silicate network and H-naphthalene nanotubes.

M-Polynomial: let Γ be a molecular structure and $m_{i,j} \Gamma, i, j \geq 1$, be the number of edges $e = st$ of Γ in such a way that $\{\varphi(s)\varphi(t)\} = \{i, j\}$. The M-polynomial of Γ is

$$M(\Gamma, \mu, \nu) = \sum_{i \leq j(\Gamma)} (m_{i,j} \Gamma \mu^i \nu^j). \quad (7)$$

Now, we discussed the relationship between the M-polynomial and some important TIs in the form of Tables 1 and 2.

3. Pent-Heptagonal Nanosheet

Firstly, we discuss the structure of pent-heptagonal nanosheet VC_5C_7 . For nanosheet of $VC_5C_7(a, b)$, we represent the number of pentagons in the first row by b , and the first four rows of nodes as well as edges are repeated. Therefore, we represent the number of repetitions as a . The nanosheet $VC_5C_7(2, 4)$ has $16ab + 2a + 5b$ nodes or vertices and $24ab + 4b$ edges. Additionally, it has $6a + 7b$ nodes having degree 2 and $16ab - 4a - 2b$ nodes having degree 3. The degree-based edge partition of nanosheet $a = 2$ and $b = 4$ is shown in Table 3.

From Figure 1, we note that 2 distinct types of vertices in VC_5C_7 are 2 and 3. So,

$$\begin{aligned} V_1 &= \{s \in V(\Gamma_1) | \varphi(s) = 2\} \\ V_2 &= \{s \in V(\Gamma_1) | \varphi(s) = 3\}. \end{aligned} \quad (8)$$

We have 3 different types of edges that is based on the degree of end nodes in (Γ_1) that are

$$\begin{aligned} E_{2,2} &= \{st \in (\Gamma_1) | \varphi(s) = 2, \varphi(t) = 2\} \\ E_{2,3} &= \{st \in (\Gamma_1) | \varphi(s) = 2, \varphi(t) = 3\} \\ E_{3,3} &= \{st \in (\Gamma_1) | \varphi(s) = 3, \varphi(t) = 3\}, \end{aligned} \quad (9)$$

where $|E_1| = (2a + 2b + 4)$, $|E_2| = (8a + 10b - 8)$, $|E_3| = (24ab - 10a - 8b + 4)$, and $a = 2$ and $b = 4$. Then,

$$|E(\Gamma_1)| = |E_1| + |E_2| + |E_3| = 16 + 48 + 144 = 208. \quad (10)$$

Now, we discuss the structure of pent-heptagonal nanosheet HC_5C_7 . For the nanosheet $HC_5C_7(a, b)$, we represent the number of pentagons in the first row by b , and the 1st four rows of nodes and edges are repeated. So, we represent the number of repetitions as a . The nanosheets $HC_5C_7(2, 4)$ have $16ab + 2a + 4b$ vertices and $24ab + 3b$ edges. Moreover, it has $6a + 6b$ vertices with degree 2 and $16ab - 4a - 2b$ vertices with degree 3. The degree-based edge

TABLE 1: Derivation of TIs from M-polynomial.

Indices	$f(\mu, \nu)$	Derivation from $M(\Gamma, \mu, \nu)$
M_1	$\mu + \nu$	$(D_\mu + D_\nu)(M(\Gamma, \mu, \nu)) _{\mu=1=\nu}$
M_2	$\mu\nu$	$(D_\mu D_\nu)(M(\Gamma, \mu, \nu)) _{\mu=1=\nu}$
MM_2	$1/\mu\nu$	$(S_\mu^1 S_\nu^1)(M(\Gamma, \mu, \nu)) _{\mu=1=\nu}$
R_α	$(\mu\nu)^\alpha, \alpha \in N$	$(D_\mu^\alpha D_\nu^\alpha)(M(\Gamma, \mu, \nu)) _{\mu=1=\nu}$
$R_\alpha R_\alpha$	$1/(\mu\nu)^\alpha, \alpha \in N$	$(S_\mu^\alpha S_\nu^\alpha)(M(\Gamma, \mu, \nu)) _{\mu=1=\nu}$
SDD	$\mu^2 + \nu^2/\mu\nu$	$(D_\mu S_\nu + D_\nu S_\mu)(M(\Gamma, \mu, \nu)) _{\mu=1=\nu}$

TABLE 2: Other TIs from M-polynomial.

Indices	$f(\mu, \nu)$	Derivation from $M(\Gamma, \mu, \nu)$
H	$2/\mu + \nu$	$2S_\mu J(M(\Gamma, \mu, \nu)) _{\mu=1=\nu}$
IS	$\mu\nu/\mu + \nu$	$S_\mu Q_2 J D_\mu D_\nu(M(\Gamma, \mu, \nu)) _{\mu=1=\nu}$
AZI	$(\mu\nu/\mu + \nu - 2)^3$	$S_\mu^3 J D_\mu^3 D_\nu^3(M(\Gamma, \mu, \nu)) _{\mu=1=\nu}$

TABLE 3: Partition of edge set, VC_5C_7 .

Edges partitions	$E_1 = E_{2,2}$	$E_2 = E_{2,3}$	$E_3 = E_{3,3}$
Cardinality	$2a + 2b + 4$	$8a + 10b - 8$	$24ab - 10a - 8b + 4$

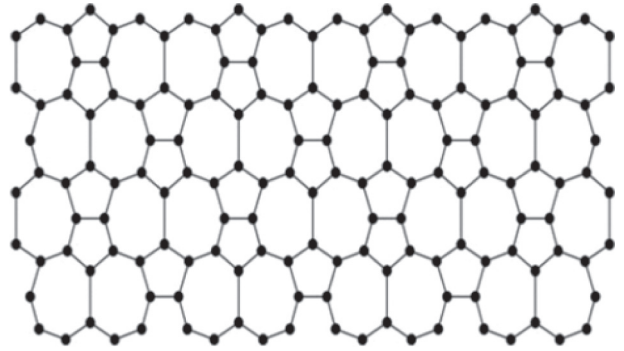


FIGURE 1: Pent-heptagonal nanosheet VC_5C_7 .

partition of nanosheets for $a = 2$ and $b = 4$ is shown in Table 4.

From Figure 2, we note that 2 distinct types of vertices in HC_5C_7 are 2 and 3. So,

$$\begin{aligned} V_1 &= \{s \in V(\Gamma_2) | \varphi(u) = 2\}, \\ V_2 &= \{s \in V(\Gamma_2) | \varphi(u) = 3\}. \end{aligned} \quad (11)$$

We have 3 different types of edges that is based on the degree of end nodes in (Γ_1) :

$$\begin{aligned} E_{2,2} &= \{st \in (\Gamma_2) | \varphi(s) = 2, \varphi(t) = 2\}, \\ E_{2,3} &= \{st \in (\Gamma_2) | \varphi(s) = 2, \varphi(t) = 3\}, \\ E_{3,3} &= \{st \in (\Gamma_2) | \varphi(s) = 3, \varphi(t) = 3\}. \end{aligned} \quad (12)$$

4. Main Results

This section deals with the main results consisting of polynomials and TIs of the nanosheets.

TABLE 4: Partition of edge set of HC_5C_7 .

Edges' partitions	$E_1 = E_{2,2}$	$E_2 = E_{2,3}$	$E_3 = E_{3,3}$
Cardinality	$2a + 3b + 2$	$8a + 6b - 4$	$24ab - 10a - 6b + 10$

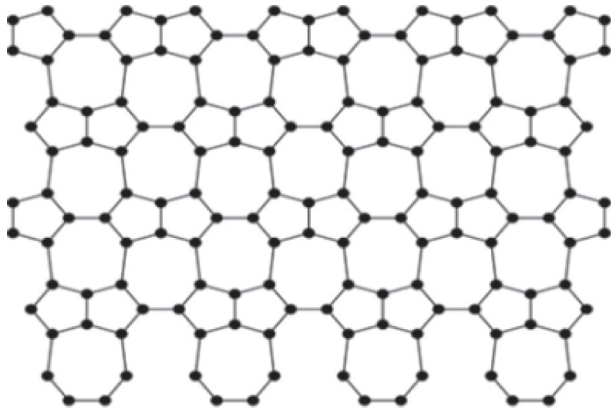


FIGURE 2: Pent-heptagonal nanosheet HC_5C_7 .

Theorem 1. Let $\Gamma_1 = VC_5C_7$ be the pent-heptagonal nanosheet. Then, the M-polynomial of Γ is

$$M(\Gamma_1, \mu, \nu) = (2a + 2b + 4)\mu^2\nu^2 + (8a + 10b - 8)\mu^2\nu^3 + (24ab - 10a - 8b + 4)\mu^3\nu^3. \tag{13}$$

Proof. Now, by using definition of M-polynomial of (Γ_1) , we obtain

$$\begin{aligned} M(\Gamma_1, \mu, \nu) &= \sum_{s \leq t} [E_{s,t}(\Gamma_1)\mu^s\nu^t] \\ &= \sum_{2 \leq 2} [E_{2,2}(\Gamma_1)\mu^2\nu^2] + \sum_{2 \leq 3} [E_{2,3}(\Gamma_1)\mu^2\nu^3] \\ &\quad + \sum_{3 \leq 3} [E_{3,3}(\Gamma_1)\mu^3\nu^3] \\ &= |E_1|\mu^2\nu^2 + |E_2|\mu^2\nu^3 + |E_3|\mu^3\nu^3 \\ &= (2a + 2b + 4)\mu^2\nu^2 + (8a + 10b - 8)\mu^2\nu^3 \\ &\quad + (24ab - 10a - 8b + 4)\mu^3\nu^3. \end{aligned} \tag{14}$$

The M-polynomial of (Γ_1) is

$$M(\Gamma_1, \mu, \nu) = (2a + 2b + 4)\mu^2\nu^2 + (8a + 10b - 8)\mu^2\nu^3 + (24ab - 10a - 8b + 4)\mu^3\nu^3. \tag{15}$$

□

Theorem 2. Let $\Gamma = VC_5C_7$ be the pent-heptagonal nanosheet. Then, the M-polynomial of Γ is

$$M(\Gamma_1, \mu, \nu) = (2a + 2b + 4)\mu^2\nu^2 + (8a + 10b - 8)\mu^2\nu^3 + (24ab - 10a - 8b + 4)\mu^3\nu^3. \tag{16}$$

So, the 1st Zagreb index $(M_1(\Gamma_1))$, 2nd Zagreb index $(M_2(\Gamma_1))$, 2nd modified Zagreb $(MM_2(\Gamma_1))$, general Randic $(R_\gamma(\Gamma_1))$, reciprocal general Randic $RR_\gamma(\Gamma_1)$, where $\gamma \in \alpha$, and the symmetric division deg index $(SDD(\Gamma_1))$ obtained from M-polynomial are as follows:

- (a) $M_1(\Gamma_1) = 144ab - 12a + 10b$
- (b) $M_2(\Gamma_1) = 216ab - 34a - 4b + 4$
- (c) $MM_2(\Gamma_1) = 8/3ab + 13/18a + 23/18b + 1/9$
- (d) $R_\gamma(\Gamma_1) = (4)^\gamma(2a + 2b + 4) + (6)^\gamma(8a + 10b - 8) + (9)^\gamma(24ab - 10a - 8b + 4)$
- (e) $RR_\gamma(\Gamma_1) = 2a + 2b + 4/(4)^\gamma + 8a + 10b - 8/(6)^\gamma + 24ab - 10a - 8b + 4/(9)^\gamma$
- (f) $SSD(\Gamma_1) = 48ab + 4/3a + 29/3b - 4/3$

Proof. Let $f(\mu, \nu) = M(\Gamma_1, \mu, \nu)$ be the M-polynomial of the pent-heptagonal nanosheet VC_5C_7 ; then,

$$f(\mu, \nu) = (2a + 2b + 4)\mu^2\nu^2 + (8a + 10b - 8)\mu^2\nu^3 + (24ab - 10a - 8b + 4)\mu^3\nu^3. \tag{17}$$

Firstly, we find out the required partial derivatives and integrals as

$$\begin{aligned} D_\mu f(\mu, \nu) &= 2(2a + 2b + 4)\mu\nu^2 + 2(8a + 10b - 8)\mu\nu^3 + 3(24ab - 10a - 8b + 4)\mu^2\nu^3 \\ D_\nu f(\mu, \nu) &= 2(2a + 2b + 4)\mu^2\nu + 3(8a + 10b - 8)\mu^2\nu^2 + 3(24ab - 10a - 8b + 4)\mu^3\nu^2 \\ D_\mu(D_\nu f(\mu, \nu)) &= 4(2a + 2b + 4)\mu\nu + 6(8a + 10b - 8)\mu\nu^2 + 9(24ab - 10a - 8b + 4)\mu^2\nu^2 \\ T_\mu(f(\mu, \nu)) &= (a + b + c)\mu^2\nu^2 + (4a + 5b - 4)\mu^2\nu^3 + (8ab - 10/3a - 8/3b + 4/3)\mu^3\nu^3 \\ T_\nu(f(\mu, \nu)) &= (a + b + c)\mu^2\nu^2 + (8a + 10b - 8)/3\mu^2\nu^3 + (8ab - 10/3a - 8/3b + 4/3)\mu^3\nu^3 \\ T_\mu T_\nu(f(\mu, \nu)) &= T_\mu(T_\nu(f(\mu, \nu))) = (a + b + 2)/2\mu^2\nu^2 + (8a + 10b - 8)/6\mu^2\nu^3 + (4ab - 5/3a - 4/3b + 2/3)\mu^3\nu^3 \\ D_\nu T_\mu(f(\mu, \nu)) &= D_\nu(T_\mu(f(\mu, \nu))) = 2(a + b + c)\mu^2\nu + 3(4a + 5b - 4)\mu^2\nu^2 + 3(8ab - 10/3a - 8/3b + 4/3)\mu^3\nu^2 \\ D_\mu T_\nu(f(\mu, \nu)) &= D_\mu(T_\nu(f(\mu, \nu))) = 2(a + b + c)\mu\nu^2 + 2/3(8a + 10b - 8)\mu\nu^3 + (24ab - 10a - 8b + 4)\mu^2\nu^3 \\ D_\mu^\gamma D_\nu^\gamma &= (4)^\gamma(2a + 2b + 4)\mu\nu + (6)^\gamma(8a + 10b - 8)\mu\nu^2 + (9)^\gamma(24ab - 10a - 8b + 4)\mu^2\nu^2 \\ T_\mu^\gamma T_\nu^\gamma &= (2a + 2b + 4)/(4)^\gamma\mu^2\nu^2 + (8a + 10b - 8)/(6)^\gamma\mu^2\nu^3 + (24ab - 10a - 8b + 4)/(9)^\gamma\mu^3\nu^3 \end{aligned}$$

Now, we obtain $\mu = \nu = 1$:

$$\begin{aligned} D_\mu f(\mu, \nu)|_{\mu=\nu=1} &= 72ab - 10a + 4 \\ D_\nu f(\mu, \nu)|_{\mu=\nu=1} &= 72ab - 2a + 10b - 4 \\ D_\mu(D_\nu f(\mu, \nu))|_{\mu=\nu=1} &= 216ab - 34a - 4b + 4 \\ T_\mu(f(\mu, \nu))|_{\mu=\nu=1} &= 8ab + 5/3a + 10/3b - 8/3 \\ T_\nu(f(\mu, \nu))|_{\mu=\nu=1} &= 8ab + 1/3a + 5/3b - 4/3 \end{aligned}$$

$$\begin{aligned}
 T_\mu(T_\nu(f(\mu, \nu)))|_{\mu=\nu=1} &= 8/3ab + 13/18a + 23/18b - 8/9 \\
 D_\nu(T_\mu(f(\mu, \nu)))|_{\mu=\nu=1} &= 24ab + 4a + 9b - 4 \\
 D_\mu(T_\nu(f(\mu, \nu)))|_{\mu=\nu=1} &= 24ab - 8/3a + 2/3b + 8/3 \\
 D_\mu^y(D_\nu^y(f(\mu, \nu)))|_{\mu=\nu=1} &= (4)^y(2a + 2b + 4) + (6)(8a + 10b - 8) + (9)^y(24ab - 10a - 8b + 4) \\
 T_\mu^y(T_\nu^y(f(\mu, \nu)))|_{\mu=\nu=1} &= (2a + 2b + 4)/(4)^y + (8a + 10b - 8)/(6)^y + (24ab - 10a - 8b + 4)/(9)^y
 \end{aligned}$$

Consequently,

- (i) First Zagreb index: $M_1(\Gamma_1) = (D_\mu + D_\nu)(f(\mu, \nu))|_{\mu=\nu=1} = D_\mu(f(\mu, \nu))|_{\mu=\nu=1} + D_\nu(f(\mu, \nu))|_{\mu=\nu=1} = (72ab - 10a + 4) + (72ab - 2a + 10b - 4) = 144ab - 12a + 10b$
- (ii) Second Zagreb index: $M_2(\Gamma_1) = (D_\mu D_\nu)(f(\mu, \nu))|_{\mu=\nu=1} = D_\mu(D_\nu(f(\mu, \nu)))|_{\mu=\nu=1} = 216ab - 34a - 4b + 4$
- (iii) Second modified Zagreb index: $MM_2(\Gamma_1) = (T_\mu T_\nu)(f(\mu, \nu))|_{\mu=\nu=1} = T_\mu(T_\nu(f(\mu, \nu)))|_{\mu=\nu=1} = 8/3ab + 13/18a + 23/18b + 1/9$
- (iv) General Randic index: $R_y(\Gamma_1) = (D_\mu^y D_\nu^y)(f(\mu, \nu))|_{\mu=\nu=1} = (4)^y(2a + 2b + 4) + (6)^y(8a + 10b - 8) + (9)^y(24ab - 10a - 8b + 4)$
- (v) Reciprocal general Randic index: $RR_y(\Gamma_1) = (2a + 2b + 4)/(4)^y \mu^2 \nu^2 + (8a + 10b - 8)/(6)^y \mu^2 \nu^3 + (24ab - 10a - 8b + 4)/(9)^y$
- (vi) Symmetric division deg index: $SDD(\Gamma_1) = (D_\mu T_\nu + D_\nu T_\mu)(f(\mu, \nu))|_{\mu=\nu=1} = D_\mu T_\nu(f(\mu, \nu))|_{\mu=\nu=1} + D_\nu T_\mu(f(\mu, \nu))|_{\mu=\nu=1} = (24ab - 8/3 + 2/3b + 8/3) + (24ab + 4a + 9b - 4) = 48ab + 4/3a + 29/3b - 4/3$ \square

Theorem 3. Let $\Gamma_1 = VC_5C_7$ be the pent-heptagonal nanosheets. Then, the M-polynomial of Γ_1 is

$$\begin{aligned}
 M(\Gamma, \mu, \nu) &= (2a + 2b + 4)\mu^2\nu^2 + (8a + 10b - 8)\mu^2\nu^3 \\
 &+ (24ab - 10a - 8b + 4)\mu^3\nu^3.
 \end{aligned} \tag{18}$$

Then, harmonic index ($H(\Gamma_1)$), inverse index ($IS(\Gamma_1)$) and augmented Zagreb index ($AZI(\Gamma_1)$) obtained from M-polynomial are as follows:

- (a) $H(\Gamma_1) = 13/15a + 7/3b + 8ab + 2/15$
- (b) $IS(\Gamma_1) = 36ab - 17/5a - 44b + 2/5$
- (c) $AZI(\Gamma_1) = 273.375ab - 33.90625a + 4.875b + 13.5625$

Proof. Let $f(\mu, \nu) = M(\Gamma_1, \mu, \nu)$ be the M-polynomial of the pent-heptagonal nanosheets VC_5C_7 ; then,

$$\begin{aligned}
 f(\mu, \nu) &= (2a + 2b + 4)\mu^2\nu^2 + (8a + 10b - 8)\mu^2\nu^3 \\
 &+ (24ab - 10a - 8b + 4)\mu^3\nu^3.
 \end{aligned} \tag{19}$$

Firstly, we find out the required partial derivatives and integrals are as follows:

$$\begin{aligned}
 J(f(\mu, \nu)) &= (2a + 2b + 4)\mu^4 + (8a + 10b - 8)\mu^5 + (24ab - 10a - 8b + 4)\mu^6 \\
 T_\mu(J(f(\mu, \nu))) &= (a/2 + b/2 + 1)\mu^4 + (8/5a + 2b - 8/5)\mu^5 + (4ab - 5/3a - 4/3b + 2/3)\mu^6 \\
 J(D_\mu(D_\nu(f(\mu, \nu)))) &= (8a + 8b + 16)\mu^2 + (48a + 60b - 48)\mu^3 + (216ab - 90a - 72b + 36)\mu^4 \\
 Q_2(J(D_\mu(D_\nu(f(\mu, \nu)))))) &= (8a + 8b + 16)\mu^4 + (48a + 60b - 48)\mu^5 + (216ab - 90a - 72b + 36)\mu^6 \\
 T_\mu(Q_2(J(D_\mu(D_\nu(f(\mu, \nu)))))) &= (2a + 2b + 4)\mu^4 + 1/5(48a + 60b - 48)\mu^5 + (36ab - 15a - 12b + 6)\mu^6 \\
 D_\mu^3(D_\nu^3(f(\mu, \nu))) &= (4)^3(2a + 2b + 4)\mu\nu + (6)^3(8a + 10b - 8)\mu\nu^2 + (9)^3(24ab - 10a - 8b + 4)\mu^2\nu^2 \\
 J(D_\mu^3D_\nu^3(f(\mu, \nu))) &= (4)^3(2a + 2b + 4)\mu^2 + (6)^3(8a + 10b - 8)\mu^3 + (9)^3(24ab - 10a - 8b + 4)\mu^4 \\
 T_\mu^3(J(D_\mu^3D_\nu^3(f(\mu, \nu)))) &= (4)^3(2a + 2b + 4)/2\mu^2 + (6)^3(8a + 10b - 8)/3\mu^3 + (9)^3(24ab - 10a - 8b + 4)/4\mu^4
 \end{aligned}$$

Now, we obtain $\mu = \nu = 1$:

$$\begin{aligned}
 T_\mu(J(f(\mu, \nu)))|_{\mu=\nu=1} &= \frac{13}{30}a + \frac{7}{6}b + 4ab + \frac{1}{15} \\
 T_\mu(Q_2(J(D_\mu(D_\nu(f(\mu, \nu))))))|_{\mu=\nu=1} &= 36ab - \frac{17}{5}a + 2b + \frac{2}{5} \\
 T_\mu^3(J(D_\mu^3D_\nu^3(f(\mu, \nu))))|_{\mu=\nu=1} &= 8(2a + 2b + 4) + 8(8a + 10b - 8) \\
 &+ \left(\frac{729}{64}\right)(24ab - 10a - 8b + 4) \\
 &= 273.375ab - 33.90625a + 4.875b + 13.5625.
 \end{aligned} \tag{20}$$

Consequently,

- (i) Harmonic index:

$$\begin{aligned}
H(\Gamma_1) &= 2T_\mu(J(f(\mu, \nu)))|_{\mu=\nu=1} \\
&= 2\left(\frac{13}{30}a + \frac{7}{6}b + 4ab + \frac{1}{15}\right) \\
&= \frac{13}{15}a + \frac{7}{3}b + 8ab + \frac{2}{15}.
\end{aligned} \tag{21}$$

(ii) Inverse index:

$$\begin{aligned}
IS(\Gamma_1) &= T_\mu(Q_2(J(D_\mu(D_\nu(f(\mu, \nu))))))|_{\mu=\nu=1} \\
&= (2a + 2b + 4) + \frac{1}{5}(48a + 60b - 48) \\
&\quad + (36ab - 15a - 12b + 6) \\
&= 36ab - \frac{17}{5}a + 2b + \frac{2}{5}.
\end{aligned} \tag{22}$$

(iii) Augmented Zagreb index:

$$\begin{aligned}
AZI(\Gamma_1) &= T_\mu^3(J(D_\mu^3 D_\nu^3(f(\mu, \nu))))|_{\mu=\nu=1} \\
&= \left(\frac{4}{2}\right)^3 (2a + 2b + 4) + \left(\frac{6}{3}\right)^3 (8a + 10b - 8) \\
&\quad + \left(\frac{9}{4}\right)^3 (24ab - 10a - 8b + 4) \\
&= 273.375ab - 33.90625a + 4.875b + 13.5625.
\end{aligned} \tag{23}$$

Theorem 4. Let $\Gamma_2 = HC_5C_7$ be the second pent-heptagonal nanosheets; the M-polynomial of (Γ_2) is

$$\begin{aligned}
M(\Gamma_2, \mu, \nu) &= (2a + 3b + 2)\mu^2\nu^2 + (8a + 6b - 4) \\
&\quad \mu^2\nu^3 + (24ab - 10a - 6b + 10)\mu^3\nu^3.
\end{aligned} \tag{24}$$

Proof. Now, by using definition of M-polynomial for (Γ_2) ,

$$\begin{aligned}
M(\Gamma_2, \mu, \nu) &= \sum_{s \leq t} [E_{s,t}(\Gamma)\mu^s\nu^t] \\
&= \sum_{2 \leq 2} [E_{2,2}(\Gamma_2)\mu^2\nu^2] + \sum_{2 \leq 3} [E_{2,3}(\Gamma_2)\mu^2\nu^3] \\
&\quad + \sum_{3 \leq 3} [E_{3,3}(\Gamma_2)\mu^3\nu^3] \\
&= |E_1|\mu^2\nu^2 + |E_2|\mu^2\nu^3 + |E_3|\mu^3\nu^3 \\
&= (2a + 3b + 2)\mu^2\nu^2 + (8a + 6b - 4)\mu^2\nu^3 \\
&\quad + (24ab - 10a - 6b + 10)\mu^3\nu^3.
\end{aligned} \tag{25}$$

The M-polynomial of (Γ_2) is

$$\begin{aligned}
M(\Gamma_2, \mu, \nu) &= (2a + 3b + 2)\mu^2\nu^2 + (8a + 6b - 4)\mu^2\nu^3 \\
&\quad + (24ab - 10a - 6b + 10)\mu^3\nu^3.
\end{aligned} \tag{26}$$

□

Theorem 5. Let $\Gamma_2 = HC_5C_7$ be the pent-heptagonal nanosheets. Then, the M-polynomial of Γ_2 is

$$\begin{aligned}
M(\Gamma_2, \mu, \nu) &= (2a + 2b + 4)\mu^2\nu^2 + (8a + 10b - 8)\mu^2\nu^3 \\
&\quad + (24ab - 10a - 8b + 4)\mu^3\nu^3.
\end{aligned} \tag{27}$$

So, the 1st Zagreb index ($M_1(\Gamma_2)$), 2nd modified Zagreb ($MM_2(\Gamma_2)$), general Randic ($R_\gamma(\Gamma_2)$) where $\gamma \in \alpha$, reciprocal general Randic ($RR_\gamma(\Gamma_2)$), where $\gamma \in \alpha$, and the symmetric division deg index ($SDD(\Gamma_2)$) obtained from M-polynomial are as follows:

- (a) $M_1(\Gamma_2) = 144ab - 12a + 6b + 48$
- (b) $M_2(\Gamma_2) = 216ab - 34a - 6b + 74$
- (c) $MM_2(\Gamma_2) = 8/3ab + 13/18a + 13/12b + 17/18$
- (d) $R_\gamma(\Gamma_2) = (4)^\gamma(2a + 3b + 2) + (6)^\gamma(8a + 6b - 4) + (9)^\gamma(24ab - 10a - 6b + 10)$
- (e) $RR_\gamma(\Gamma_2) = 2a + 3b + 2/(4)^\gamma + 8a + 6b - 4/(6)^\gamma + 24ab - 10a - 6b + 10/(9)^\gamma$
- (f) $SSD(\Gamma_2) = 48ab + 4/3a + 7b + 46/3$

Proof. Let $f(\mu, \nu) = M(\Gamma_2, \mu, \nu)$ be the M-polynomial of the pent-heptagonal nanosheets HC_5C_7 ; then,

$$\begin{aligned}
f(\mu, \nu) &= (2a + 3b + 2)\mu^2\nu^2 + (8a + 6b - 4)\mu^2\nu^3 \\
&\quad + (24ab - 10a - 6b + 10)\mu^3\nu^3.
\end{aligned} \tag{28}$$

Firstly, we find out the required partial derivatives and integrals as follows:

$$\begin{aligned}
D_\mu f(\mu, \nu) &= 2(2a + 3b + 2)\mu\nu^2 + 2(8a + 6b - 4)\mu\nu^3 + 3(24ab - 10a - 6b + 10)\mu^2\nu^3 \\
D_\nu f(\mu, \nu) &= 2(2a + 3b + 2)\mu^2\nu + 3(8a + 6b - 4)\mu^2\nu^2 + 3(24ab - 10a - 6b + 10)\mu^3\nu^2 \\
D_\mu(D_\nu f(\mu, \nu)) &= 4(2a + 3b + 2)\mu\nu + 6(8a + 6b - 4)\mu\nu^2 + 9(24ab - 10a - 6b + 10)\mu^2\nu^2 \\
T_\mu(f(\mu, \nu)) &= (a + (3/2)b + 1)\mu^2\nu^2 + (4a + 3b - 2)\mu^2\nu^3 + (8ab - (10/3)a - 2b + (10/3))\mu^3\nu^3 \\
T_\nu(f(\mu, \nu)) &= (a + (3/2)b + 1)\mu^2\nu^2 + ((8/3)a + 2b - (4/3))\mu^2\nu^3 + (8ab - (10/3)a - 2b + (10/3))\mu^3\nu^3 \\
T_\mu T_\nu(f(\mu, \nu)) &= T_\mu(T_\nu(f(\mu, \nu))) = 1/4(2a + 3b + 2)2\mu^2\nu^2 + 1/6(8a + 6b - 4)\mu^2\nu^3 + 1/9(24ab - 10a - 6b + 10)\mu^3\nu^3 \\
D_\nu T_\mu(f(\mu, \nu)) &= D_\nu(T_\mu(f(\mu, \nu))) = (2a + 3b + 2)\mu^2\nu + 3(4a + 3b - 2)\mu^2\nu^2 + 3(8ab - 10/3a - 2b + 10/3)\mu^3\nu^2 \\
D_\mu T_\nu(f(\mu, \nu)) &= D_\mu(T_\nu(f(\mu, \nu))) = (2a + 3b + 2)\mu\nu^2 + 2(8/3a + 2b - 4/3)\mu\nu^3 + (24ab - 10a - 6b + 10)\mu^2\nu^3
\end{aligned}$$

$$D_\mu^\gamma D_\nu^\gamma = (4)^\gamma (2a + 3b + 2)\mu\nu + (6)^\gamma (8a + 6b - 4)\mu\nu^2 + (9)^\gamma (24ab - 10a - 6b + 10)\mu^2\nu^2$$

$$T_\mu^\gamma T_\nu^\gamma = (2a + 3b + 2)/(4)^\gamma \mu^2\nu^2 + (8a + 6b - 4)/(6)^\gamma \mu^2\nu^3 + (24ab - 10a - 6b + 10)/(9)^\gamma \mu^3\nu^3$$

Now, we obtain $\mu = \nu = 1$:

$$D_\mu f(\mu, \nu)|_{\mu=\nu=1} = 72ab - 10a + 26$$

$$D_\nu f(\mu, \nu)|_{\mu=\nu=1} = 72ab - 2a + 6b + 22$$

$$D_\mu(D_\nu f(\mu, \nu))|_{\mu=\nu=1} = 216ab - 34a - 6b + 74$$

$$T_\mu(f(\mu, \nu))|_{\mu=\nu=1} = 8ab + 5/3a + 5/2b + 7/3$$

$$T_\nu(f(\mu, \nu))|_{\mu=\nu=1} = 8ab + 1/3a + 3/2b + 3$$

$$T_\mu(T_\nu(f(\mu, \nu)))|_{\mu=\nu=1} = 8/3ab + 13/18a + 13/12b + 17/18$$

$$D_\nu(T_\mu(f(\mu, \nu)))|_{\mu=\nu=1} = 24ab + 4a + 6b + 6$$

$$D_\mu(T_\nu(f(\mu, \nu)))|_{\mu=\nu=1} = 24ab - 8/3a + b + 28/3$$

$$D_\mu^\gamma(D_\nu^\gamma(f(\mu, \nu)))|_{\mu=\nu=1} = (4)^\gamma (2a + 3b + 2) + (6)^\gamma (8a + 6b - 4) + (9)^\gamma (24ab - 10a - 6b + 10)$$

$$T_\mu^\gamma(T_\nu^\gamma(f(\mu, \nu)))|_{\mu=\nu=1} = (2a + 3b + 2)/(4)^\gamma + (8a + 6b - 4)/(6)^\gamma + (24ab - 10a - 6b + 10)/(9)^\gamma$$

Consequently,

- (i) First Zagreb index: $M_1(\Gamma_2) = (D_\mu + D_\nu)(f(\mu, \nu))|_{\mu=\nu=1} = D_\mu(f(\mu, \nu))|_{\mu=\nu=1} + D_\nu(f(\mu, \nu))|_{\mu=\nu=1} = 144ab - 12a + 6b + 48$
- (ii) Second Zagreb index: $M_2(\Gamma_2) = (D_\mu D_\nu)(f(\mu, \nu))|_{\mu=\nu=1} = D_\mu(D_\nu(f(\mu, \nu)))|_{\mu=\nu=1} = 216ab - 34a - 6b + 74$
- (iii) Second modified Zagreb index: $MM_2(\Gamma_2) = (T_\mu T_\nu)(f(\mu, \nu))|_{\mu=\nu=1} = T_\mu(T_\nu(f(\mu, \nu)))|_{\mu=\nu=1} = 8/3ab + 13/18a + 13/12b + 17/18$
- (iv) General Randic index: $R_\gamma(\Gamma_2) = (D_\mu^\gamma D_\nu^\gamma)(f(\mu, \nu))|_{\mu=\nu=1} = (4)^\gamma (2a + 3b + 2) + (6)^\gamma (8a + 6b - 4) + (9)^\gamma (24ab - 10a - 6b + 10)$
- (v) Reciprocal general Randic index: $RR_\gamma(\Gamma_2) = (T_\mu^\gamma T_\nu^\gamma)(f(\mu, \nu))|_{\mu=\nu=1} = (2a + 3b + 2)/(4)^\gamma + (8a + 6b - 4)/(6)^\gamma + (24ab - 10a - 6b + 10)/(9)^\gamma$
- (vi) Symmetric division deg index: $SDD(\Gamma_2) = (D_\mu T_\nu + D_\nu T_\mu)(f(\mu, \nu))|_{\mu=\nu=1} = D_\mu T_\nu(f(\mu, \nu))|_{\mu=\nu=1} + D_\nu T_\mu(f(\mu, \nu))|_{\mu=\nu=1} = (24ab - 8/3a + b + 28/3) + (24ab + 4a + 6b + 6) = 48ab + 4/3a + 7b + 46/3 \quad \square$

Theorem 6. Let $\Gamma_2 = HC_5C_7$ be the pent-heptagonal nanosheets. Then, the M-polynomial of Γ_2 is

$$M(\Gamma_2, \mu, \nu) = (2a + 3b + 2)\mu^2\nu^2 + (8a + 6b - 4)\mu^2\nu^3 + (24ab - 10a - 6b + 10)\mu^3\nu^3. \tag{29}$$

Then, harmonic index ($H(\Gamma_2)$), inverse index ($IS(\Gamma_2)$), and augmented Zagreb index ($AZI(\Gamma_2)$) obtained from M-polynomial are as follows:

- (a) $H(\Gamma_2) = 13/15a + 19/10b + 8ab - 11/3$
- (b) $IS(\Gamma_2) = 36ab - 17/5a - 9/5b + 61/5$
- (c) $AZI(\Gamma_2) = 273.3744ab - 33.90625a + 3.6564b + 97.906$

Proof. Let $f(\mu, \nu) = M(\Gamma_2, \mu, \nu)$ be the M-polynomial of the pent-heptagonal nanosheet HC_5C_7 ; then,

$$f(\mu, \nu) = (2a + 3b + 2)\mu^2\nu^2 + (8a + 6b - 4)\mu^2\nu^3 + (24ab - 10a - 6b + 10)\mu^3\nu^3. \tag{30}$$

First, we find out the required partial derivatives and integrals as

$$J(f(\mu, \nu)) = (2a + 3b + 2)\mu^4 + (8a + 6b - 4)\mu^5 + (24ab - 10a - 6b + 10)\mu^6$$

$$T_\mu(J(f(\mu, \nu))) = 2a + 3b + 2/4\mu^4 + 8a + 6b - 4/5\mu^5 + 24ab - 10a - 6b + 10/6\mu^6$$

$$J(D_\mu(D_\nu(f(\mu, \nu)))) = (8a + 12b + 8)\mu^2 + (48a + 36b - 24)\mu^3 + (216ab - 90a - 54b + 90)\mu^4$$

$$Q_2(J(D_\mu(D_\nu(f(\mu, \nu)))))) = (8a + 12b + 8)\mu^4 + (48a + 36b - 24)\mu^5 + (216ab - 90a - 54b + 90)\mu^6$$

$$T_\mu(Q_2(J(D_\mu(D_\nu(f(\mu, \nu)))))) = (2a + 3b + 2)\mu^4 + 1/5(48a + 36b - 24)\mu^5 + (36ab - 15a - 9b + 15)\mu^6$$

$$D_\mu^3(D_\nu^3(f(\mu, \nu))) = (4)^3(2a + 3b + 2)\mu\nu + (6)^3(8a + 6b - 4)\mu\nu^2 + (9)^3(24ab - 10a - 6b + 10)\mu^2\nu^2$$

$$J(D_\mu^3 D_\nu^3(f(\mu, \nu))) = (4)^3(2a + 3b + 2)\mu^2 + (6)^3(8a + 6b - 4)\mu^3 + (9)^3(24ab - 10a - 6b + 10)\mu^4$$

$$T_\mu^3(J(D_\mu^3 D_\nu^3(f(\mu, \nu)))) = 8(2a + 3b + 2)\mu^2 + 8(8a + 6b - 4)\mu^3 + (9/4)^3(24ab - 10a - 6b + 10/4)\mu^4$$

Now, we obtain $\mu = \nu = 1$:

$$T_\mu(J(f(\mu, \nu)))|_{\mu=\nu=1} = \frac{1}{4}(2a + 3b + 2) + \frac{1}{5}(8a + 6b - 4) + \frac{1}{6}(24ab - 10a - 6b + 10)$$

$$= \frac{13}{30}a + \frac{19}{20}b + 4ab + \frac{41}{30}$$

$$T_\mu(Q_2(J(D_\mu(D_\nu(f(\mu, \nu))))))|_{\mu=\nu=1} = \frac{1}{4}(8a + 12b + 8) + \frac{1}{5}(48a + 36b - 24) + \frac{1}{6}(216ab - 90a - 54b + 90)$$

$$= \frac{1}{5}(180ab - 17a - 6b + 36),$$

TABLE 5: Comparison between $M_1(\Gamma_1)$, $M_2(\Gamma_1)$, $MM_1(\Gamma_1)$, and $SDD(\Gamma_1)$ of VC_5C_7 .

a, b	$M_1(\Gamma_1)$	$M_2(\Gamma_1)$	$MM_1(\Gamma_1)$	$SDD(\Gamma_1)$
$a = 2, b = 4$	1168	1648	28.016	423.91
$a = 4, b = 6$	3468	5028	74.68	1214
$a = 6, b = 8$	6920	10134	142.69	2390.68
$a = 8, b = 10$	11524	16972	232.02	3945.99
$a = 10, b = 12$	17280	25536	343.086	5887.99
$a = 12, b = 14$	24188	35828	475.248	8214
$a = 14, b = 16$	32248	47848	628.77	10924.14
$a = 16, b = 18$	41460	61596	803.652	14018.16
$a = 18, b = 20$	51824	77072	999.894	17496.18
$a = 20, b = 22$	63340	94276	1217.496	21358.2

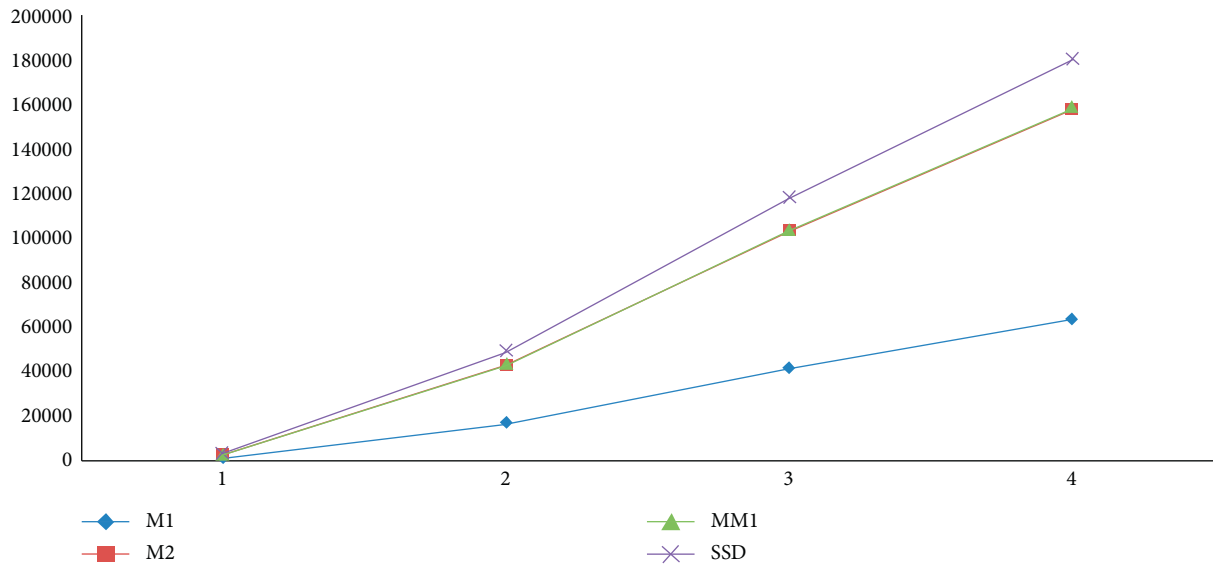


FIGURE 3: Graphical comparison between $M_1(\Gamma_1)$, $M_2(\Gamma_1)$, $MM_1(\Gamma_1)$, and $SDD(\Gamma_1)$ of VC_5C_7 and comparison between $M_1(\Gamma_2)$, $M_2(\Gamma_2)$, $MM_1(\Gamma_2)$, and $SDD(\Gamma_2)$ of HC_5C_7 .

TABLE 6: Comparison between $M_1(\Gamma_2)$, $M_2(\Gamma_2)$, $MM_1(\Gamma_2)$, and $SDD(\Gamma_2)$ of HC_5C_7 .

a, b	$M_1(\Gamma_2)$	$M_2(\Gamma_2)$	$MM_1(\Gamma_2)$	$SDD(\Gamma_2)$
$a = 2, b = 4$	1200	1710	28.07	429.97
$a = 4, b = 6$	3492	5086	74.33	1214.66
$a = 6, b = 8$	6936	10190	141.94	2383.33
$a = 8, b = 10$	11532	17022	231.105	3936.06
$a = 10, b = 12$	17280	25582	341.505	5872.74
$a = 12, b = 14$	24180	35870	473.265	8193.42
$a = 14, b = 16$	32232	47886	626.385	10898.1
$a = 16, b = 18$	41436	61630	800.865	13986.78
$a = 18, b = 20$	51792	77102	996.705	17459.46
$a = 20, b = 22$	63300	94302	1211.745	21316.14

$$\begin{aligned}
 T_\mu^3(J(D_\mu^3 D_\nu^3(f(\mu, \nu))))|_{\mu=\nu=1} &= 8(2a + 3b + 2) + 8(8a + 6b - 4) + \left(\frac{9}{4}\right)^3 (24ab - 10a - 6b + 10) \\
 &= 8(2a + 3b + 2) + 8(8a + 6b - 4) + (11.3906)(24ab - 10a - 6b + 10) \tag{31} \\
 &= 273.3744ab - 33.90625a + 3.6564b + 97.906.
 \end{aligned}$$

Consequently,

(i) Harmonic index:

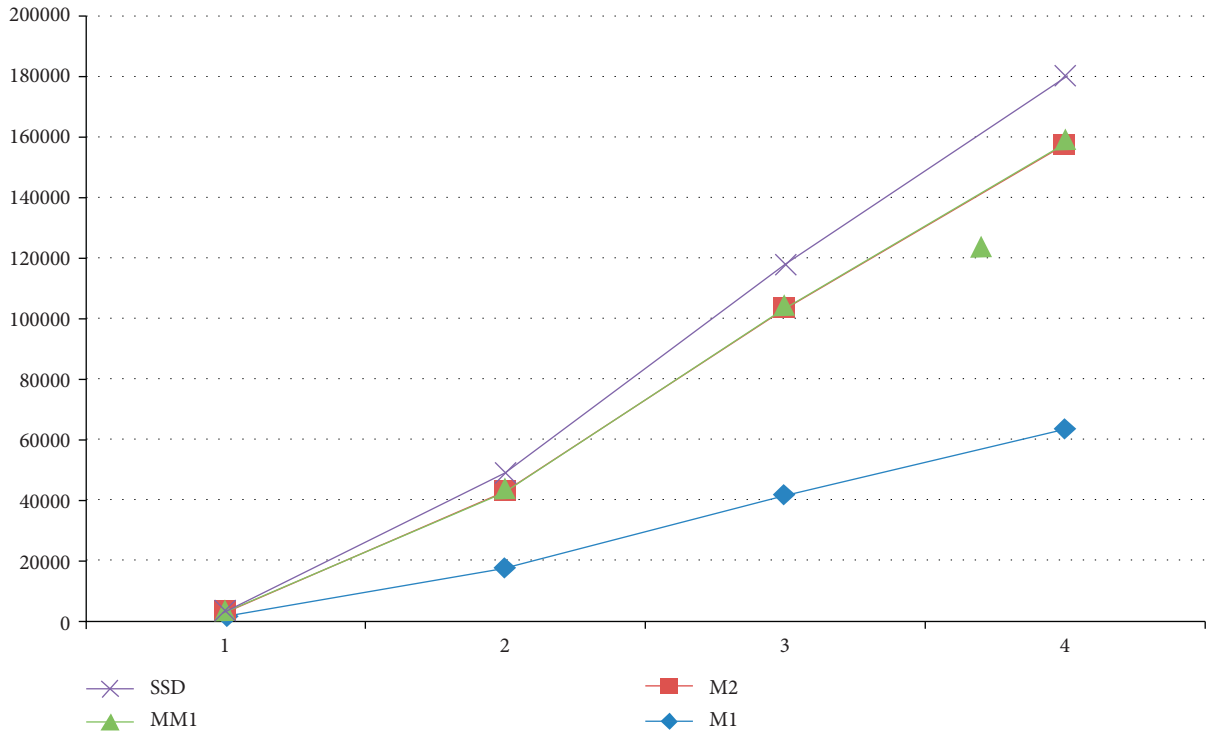


FIGURE 4: Graphical comparison between $M_1(\Gamma_2)$, $M_2(\Gamma_2)$, $MM_1(\Gamma_2)$, and $SDD(\Gamma_2)$ of HC_5C_7 and comparison between $H(\Gamma_1)$, $IS(\Gamma_1)$, and $AZI(\Gamma_1)$ of VC_5C_7 .

TABLE 7: Comparison between $H(\Gamma_1)$, $IS(\Gamma_1)$, and $AZI(\Gamma_1)$ of VC_5C_7 .

a, b	$H(\Gamma_1)$	$IS(\Gamma_1)$	$AZI(\Gamma_1)$
$a = 2, b = 4$	75.208	105.6	2152.25
$a = 4, b = 6$	209.68	586	6468.18
$a = 6, b = 8$	408	1354	12971.12
$a = 8, b = 10$	670.454	2413.2	21661.1125
$a = 10, b = 12$	996.864	3758.4	32538.0625
$a = 12, b = 14$	1387.274	5391.6	45602.0125
$a = 14, b = 16$	1841.684	7312.8	60852.9625
$a = 16, b = 18$	2360.094	9522	78290.9125
$a = 18, b = 20$	2942.504	12019.2	97915.8625
$a = 20, b = 22$	3588.914	14804.4	119727.8125

$$\begin{aligned}
 H(\Gamma_2) &= 2T_\mu(J(f(\mu, \nu)))|_{\mu=\nu=1} \\
 &= 2\left[\frac{1}{4}(2a + 3b + 2) + \frac{1}{5}(8a + 6b - 4) + \frac{1}{6}(24ab - 10a - 6b + 10)\right] \\
 &= 8ab + \frac{13}{15}a + \frac{19}{10}b - \frac{11}{3}.
 \end{aligned}
 \tag{32}$$

(ii) Inverse index:

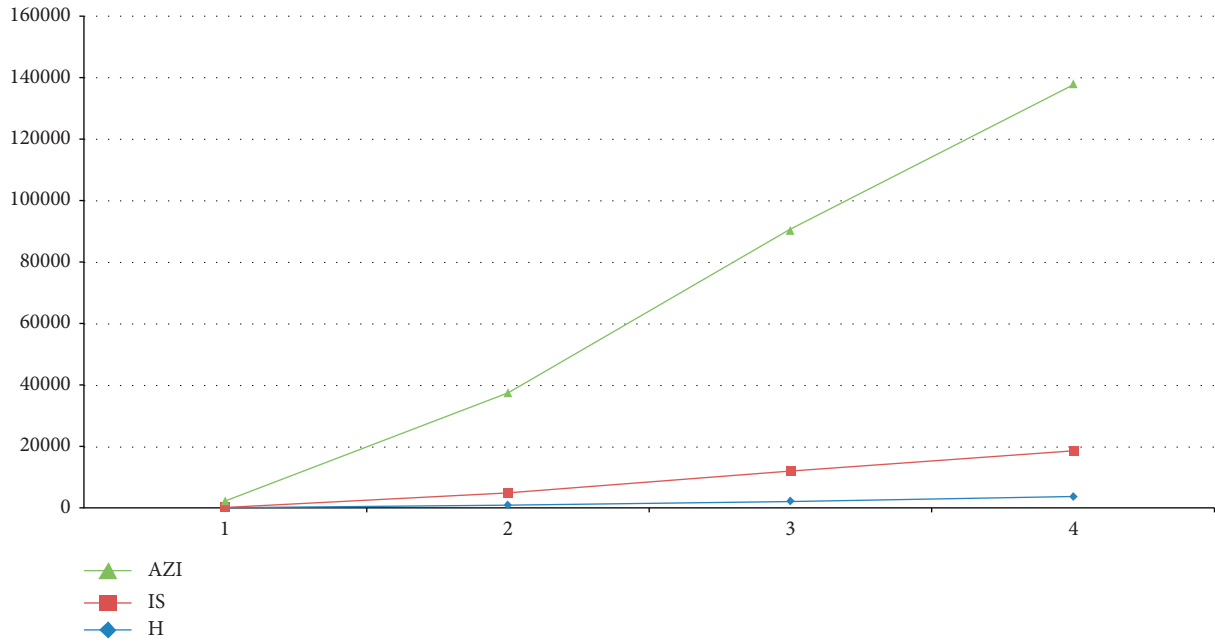


FIGURE 5: Graphical comparison between $H(\Gamma_1)$, $IS(\Gamma_1)$, and $AZI(\Gamma_1)$ of VC_5C_7 and comparison between $H(\Gamma_2)$, $IS(\Gamma_2)$, and $AZI(\Gamma_2)$ of HC_5C_7 .

TABLE 8: Comparison between $H(\Gamma_2)$, $IS(\Gamma_2)$, and $AZI(\Gamma_2)$ of HC_5C_7 .

a, b	$H(\Gamma_2)$	$IS(\Gamma_2)$	$AZI(\Gamma_2)$
$a = 2, b = 4$	69.66	236.2	2231.7143
$a = 4, b = 6$	203.20	851.80	6545.22
$a = 6, b = 8$	400.73	1705.40	13045.69
$a = 8, b = 10$	662.266	2847	21732.8
$a = 10, b = 12$	987.8	4276.6	32607.1
$a = 12, b = 14$	1377.34	599.2	45668.36
$a = 14, b = 16$	1830.86	8000	60916.58
$a = 16, b = 18$	2348.402	10293.4	78351.76
$a = 18, b = 20$	2929.936	12875	97974.1
$a = 20, b = 22$	3575.47	15744.6	119782.2

$$\begin{aligned}
 IS(\Gamma_2) &= T_\mu(Q_2(J(D_\mu(D_\nu(f(\mu, \nu))))))|_{\mu=\nu=1} \\
 &= \frac{1}{4}(8a + 12b + 8) + \frac{1}{5}(48a + 36b - 24) + \frac{1}{6}(216ab - 90a - 54b + 90) \\
 &= 36ab - \frac{17}{5}a - \frac{9}{5}b + \frac{61}{5}.
 \end{aligned}
 \tag{33}$$

(iii) Augmented Zagreb index:

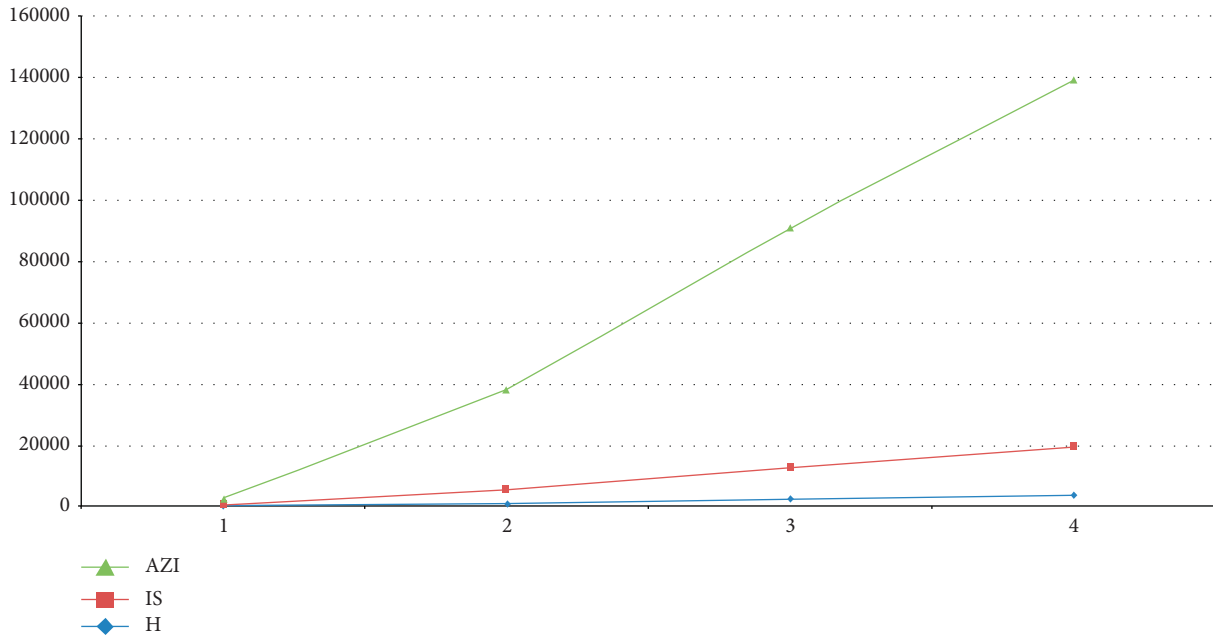


FIGURE 6: Graphical comparison between $H(\Gamma_2)$, $IS(\Gamma_2)$, and $AZI(\Gamma_2)$ of HC_5C_7 .

$$\begin{aligned}
 AZI(\Gamma_2) &= T_\mu^3(J(D_\mu^3 D_\nu^3(f(\mu, \nu))))|_{\mu=\nu=1} \\
 &= (2a + 3b + 2) + 8(8a + 6b - 4) + \left(\frac{9}{4}\right)^3 (24ab - 10a - 6b + 10) \\
 &= 8(2a + 3b + 2) + 8(8a + 6b - 4) + (11.3906)(24ab - 10a - 6b + 10) \\
 &= 273.3744ab - 33.90625a + 3.6564b + 97.906
 \end{aligned}
 \tag{34}$$

5. Conclusion

In this section, we used the various degree-based TIs and show the comparison in the form of tables and figures. Comparison between $M_1(\Gamma_1)$, $M_2(\Gamma_1)$, $MM_1(\Gamma_1)$, and $SDD(\Gamma_1)$ of VC_5C_7

The comparison of 1st Zagreb, 2nd Zagreb, 2nd modified Zagreb, and symmetric division deg indices of pent-heptagonal nanosheets (Γ_1) is computationally computed by using these M-polynomials. We calculated these indices for different values of a and b in Table 5, and we noted that when we increase the values of a and b , then all of the TIs of VC_5C_7 are increasing with the same order, as shown in Figure 3.

The comparison of 1st Zagreb, 2nd Zagreb, 2nd modified Zagreb, and symmetric division deg indices of pent-heptagonal nanosheets (Γ_2) is computationally computed by using these M-polynomials. We calculated these indices for different values of a and b in Table 6, and we noted that when we increase the values of a and b , then all of the TIs of HC_5C_7 are increasing with the same order, as shown in Figure 4.

The comparison of the harmonic index, the inverse sum index, and the augmented Zagreb index of pent-heptagonal nanosheets (Γ_1) is computationally computed by these

□

M-polynomials. We calculated these indices for different values of a and b in Table 7, and we noted that when we increase the values of a and b , then all of the TIs of VC_5C_7 are increasing with the same order, as shown in Figure 5.

The comparison of the harmonic index, the inverse sum index, and the augmented Zagreb index of pent-heptagonal nanosheets (Γ_2) is computationally computed by these M-polynomials. We calculated these indices for different values of a and b in Table 8, and we noted that when we increase the values of a and b , then all of the TIs of HC_5C_7 are increasing with the same order, as shown in Figure 6.

In this paper, the calculated M-polynomials and enumerated TIs assist us to recognize the physical characteristic, chemical sensitivity, and biological animation of the pent-heptagonal nanosheets (Γ_1) and (Γ_2). These consequences give us remarkable ascertainment in the field of pharmaceutical production.

However, the problem is still open to compute the different TIs (degree and distance based) for various nanosheets:

- (i) To compute the nanosheet for other topological indices
- (ii) To compute the various nanosheets for different topological indices

Data Availability

No data were used to support this study.

Conflicts of Interest

The authors declare that there are no conflicts of interest regarding this publication.

References

- [1] M. Irfan, H. U. Rehman, H. Almusawa, S. Rasheed, and I. A. Baloch, "M-polynomials and topological indices for line graphs of chain silicate network and h-naphthalenic nanotubes," *Journal of Mathematics*, vol. 2021, Article ID 5551825, 11 pages, 2021.
- [2] Z. Raza and E. K. Sukaiti, "M-polynomial and degree based topological indices of some nanostructures," *Symmetry*, vol. 12, no. 5, p. 831, 2020.
- [3] K. Culik, *Applications of Graph Theory to Mathematical Logic and Linguistics. Theory of Graphs and its Applications*, Czech Academy of Sciences, Prague, Czechia, 1963.
- [4] M. Baca, J. Horvthov, M. Mokriov, A. Semanicov-Fenovckov, and A. Suhnyiov, "On topological indices of a carbon nanotube network," *Canadian Journal of Chemistry*, vol. 93, no. 10, pp. 1157–1160, 2015.
- [5] O. M. Yaghi, M. O'Keeffe, N. W. Ockwig, H. K. Chae, M. Eddaoudi, and J. Kim, "A route to high surface area, porosity and inclusion of large molecules in crystals," *Nature*, vol. 423, no. 6941, pp. 705–714, 2003.
- [6] H. Gonzalez-Diaz, S. Vilar, L. Santana, and E. Uriarte, "Medicinal chemistry and bioinformatics-current trends in drugs discovery with networks topological indices," *Current Topics in Medicinal Chemistry*, vol. 7, no. 10, pp. 1015–1029, 2007.
- [7] M. R. Farahani, "Connectivity indices of pent-heptagonal nanotubes," *Advance in Materials and Corrosion*, vol. 2, pp. 33–35, 2013.
- [8] S. Hayat and M. Imran, "Computation of certain topological indices of nanotubes covered by C 5 and C 7," *Journal of Computational and Theoretical Nanoscience*, vol. 12, no. 4, pp. 533–541, 2015.
- [9] S. Klavar and I. Gutman, "A comparison of the schultz molecular topological index with the wiener index," *Journal of Chemical Information and Computer Sciences*, vol. 36, no. 5, pp. 1001–1003, 1996.
- [10] X. Li and J. Zheng, "Extremal chemical trees with minimum or maximum general randic index," *MATCH Communications in Mathematical and in Computer Chemistry*, vol. 55, no. 2, pp. 381–390, 2006.
- [11] A. W. Bharati Rajan, C. Grigorious, and S. Stephen, "On certain topological indices of silicate, honeycomb and hexagonal networks," *Journal of Computer and Mathematical Sciences*, vol. 3, no. 5, pp. 498–556, 2012.
- [12] A. Graovac, M. Ghorbani, and M. A. Hosseinzadeh, "Computing fifth geometric-arithmetic index for nanostar dendrimers," *Journal of Mathematical Nanoscience*, vol. 1, no. 1–2, pp. 33–42, 2011.
- [13] B. Furtula, A. Graovac, and D. Vukičević, "Augmented zagreb index," *Journal of Mathematical Chemistry*, vol. 48, no. 2, pp. 370–380, 2010.
- [14] K. C. Das and N. Trinajstić, "Relationship between the eccentric connectivity index and zagreb indices," *Computers & Mathematics with Applications*, vol. 62, no. 4, pp. 1758–1764, 2011.
- [15] C. K. Gupta, V. Lokesh, S. B. Shwetha, and P. S. Ranjini, "On the symmetric division deg index of graph," *Southeast Asian Bulletin of Mathematics*, vol. 40, no. 1, 2016.
- [16] A. R. Matamala and E. Estrada, "Generalised topological indices: optimisation methodology and physico-chemical interpretation," *Chemical Physics Letters*, vol. 410, no. 4–6, pp. 343–347, 2005.
- [17] A. Rani and U. Ali, "Degree-Based topological indices of polysaccharides: amylose and blue starch-iodine complex," *Journal of Chemistry*, vol. 2021, Article ID 6652014, 10 pages, 2021.
- [18] G. Abbas, A. Rani, M. Salman, T. Noreen, and U. Ali, "Hosoya properties of the commuting graph associated with the group of symmetries," *Main Group Metal Chemistry*, vol. 44, no. 1, pp. 173–184, 2021.
- [19] J. Devillers, D. Domine, C. Guillon, S. Bintein, and W. Karcher, "Prediction of partition coefficients (log p oct) using autocorrelation descriptors," *SAR and QSAR in Environmental Research*, vol. 7, no. 1–4, pp. 151–172, 1997.
- [20] I. Gutman and O. E. Polansky, *Mathematical Concepts in Organic Chemistry*, Springer Science & Business Media, Berlin, Germany, 2012.
- [21] G. Plya, "Algebraische berechnung der anzahl der isomeren einiger organischer verbindungen," *Zeitschrift fr Kristallographie-Crystalline Materials*, vol. 93, no. 1, pp. 415–443, 1936.
- [22] H. Wiener, "Structural determination of paraffin boiling points," *Journal of the American Chemical Society*, vol. 69, pp. 17–20, 1947.
- [23] S. Akhter and M. Imran, "On molecular topological properties of benzenoid structures," *Canadian Journal of Chemistry*, vol. 94, no. 8, pp. 687–698, 2016.
- [24] M. Baca, J. Horvthov, M. Mokriov, and A. Suhnyiov, "On topological indices of fullerenes," *Applied Mathematics and Computation*, vol. 251, pp. 154–161, 2015.
- [25] F. M. Brckler, T. Dolic, A. Graovac, and I. Gutman, "On a class of distance-based molecular structure descriptors," *Chemical Physics Letters*, vol. 503, no. 4–6, pp. 336–338, 2011.
- [26] B. Furtula and I. Gutman, "A forgotten topological index," *Journal of Mathematical Chemistry*, vol. 53, no. 4, pp. 1184–1190, 2015.
- [27] M. Javaid, M. U. Rehman, and J. Cao, "Topological indices of rhombus type silicate and oxide networks," *Canadian Journal of Chemistry*, vol. 95, no. 2, pp. 134–143, 2017.
- [28] A. Vasilyev, "Upper and lower bounds of symmetric division deg index," *Iranian Journal of Mathematical Chemistry*, vol. 5, no. 2, pp. 91–98, 2014.
- [29] M. Javaid, J. B. Liu, M. A. Rehman, and S. Wang, "On the certain topological indices of titania nanotube TiO₂ [m, n]," *Zeitschrift für Naturforschung A*, vol. 72, no. 7, pp. 647–654, 2017.
- [30] H. M. Awais, M. Jamal, and M. Javaid, "Topological properties of metal-organic frameworks," *Main Group Metal Chemistry*, vol. 43, no. 1, pp. 67–76, 2020.
- [31] I. Gutman and N. Trinajstić, "Graph theory and molecular orbitals. total f-electron energy of alternant hydrocarbons," *Chemical Physics Letters*, vol. 17, no. 4, pp. 535–538, 1972.
- [32] D. Amic, D. Belo, B. Lucic, S. Nikolic, and N. Trinajstić, "The vertex-connectivity index revisited," *Journal of Chemical Information and Computer Sciences*, vol. 38, no. 5, pp. 819–822, 1998.

- [33] V. Loksha and T. Deepika, "Symmetric division deg index of tricyclic and tetracyclic graphs," *International journal of Science and Engineering Research*, vol. 7, pp. 53–55, 2016.
- [34] L. Zhong, "The harmonic index for graphs," *Applied Mathematics Letters*, vol. 25, no. 3, pp. 561–566, 2012.
- [35] K. Pattabiraman, "Inverse sum indeg index of graphs," *AKCE International Journal of Graphs and Combinatorics*, vol. 15, no. 2, pp. 155–167, 2018.
- [36] Y. Shi, M. Dehmer, X. Li, and I. Gutman, *Graph Polynomials*, CRC Press, Boca Raton, FL. USA, 2016.
- [37] H. Yang, A. Q. Baig, W. Khalid, M. R. Farahani, and X. Zhang, "M-polynomial and topological indices of benzene ring embedded in P-type surface network," *Journal of Chemistry*, vol. 2019, Article ID 7297253, 9 pages, 2019.
- [38] A. J. M. Khalaf, S. Hussain, D. Afzal, F. Afzal, and A. Maqbool, "M-polynomial and topological indices of book graph," *Journal of Discrete Mathematical Sciences and Cryptography*, vol. 23, no. 6, pp. 1217–1237, 2020.
- [39] S. Mondal, M. Imran, N. De, and A. Pal, "Neighborhood M-polynomial of titanium compounds," *Arabian Journal of Chemistry*, vol. 14, no. 8, Article ID 103244, 2021.

Research Article

Bicyclic Graphs with the Second-Maximum and Third-Maximum Degree Resistance Distance

Wenjie Ning ¹, Kun Wang ², and Hassan Raza ³

¹College of Science, China University of Petroleum (East China), Qingdao 266580, China

²College of Mathematics and Systems Science, Shandong University of Science and Technology, Qingdao 266590, China

³Business School, University of Shanghai for Science and Technology, Shanghai 200093, China

Correspondence should be addressed to Kun Wang; wangkun26@163.com

Received 7 August 2021; Accepted 14 September 2021; Published 10 November 2021

Academic Editor: Francisco Balibrea

Copyright © 2021 Wenjie Ning et al. This is an open access article distributed under the Creative Commons Attribution License, which permits unrestricted use, distribution, and reproduction in any medium, provided the original work is properly cited.

Let $G = (V, E)$ be a connected graph. The resistance distance between two vertices u and v in G , denoted by $R_G(u, v)$, is the effective resistance between them if each edge of G is assumed to be a unit resistor. The degree resistance distance of G is defined as $D_R(G) = \sum_{\{u,v\} \subseteq V(G)} (d_G(u) + d_G(v))R_G(u, v)$, where $d_G(u)$ is the degree of a vertex u in G and $R_G(u, v)$ is the resistance distance between u and v in G . A bicyclic graph is a connected graph $G = (V, E)$ with $|E| = |V| + 1$. This paper completely characterizes the graphs with the second-maximum and third-maximum degree resistance distance among all bicyclic graphs with $n \geq 6$ vertices.

1. Introduction

All graphs considered in this paper are simple and undirected. Let $G = (V, E)$ be a graph with n vertices and m edges. Let $N_G(v)$ be the set of vertices adjacent to v in G . The degree of v in G , denoted by $d_G(v)$, is equal to $|N_G(v)|$. Denote the minimum degree of vertices in G by $\delta(G)$. A vertex of degree one is called a *pendant vertex*, and the edge incident with a pendant vertex is called a *pendant edge*. The distance between two vertices u and v of G , denoted by $d_G(u, v)$ or $d(u, v)$, is the length of a shortest path connecting u and v in G . For a subset S of V , denote by $G[S]$, the subgraph induced by S and $G - S$ the graph $G[V(G) \setminus S]$. We use $G - v$ instead of $G - \{v\}$ if $S = \{v\}$ for simplicity. Let P_n and C_n be the path and the cycle graphs on n vertices, respectively.

A topological index or a graph-theoretic index is a real number related to a graph. Topological indices of molecular graphs are one of the oldest and most widely used descriptors in quantitative structure-activity relationships [1, 2]. One of the most exhaustively studied [3, 4] topological indices is the *Wiener index*. The Wiener index was introduced in 1947 [5] and defined as $W(G) = \sum_{\{u,v\} \subseteq V(G)} d_G(u, v)$. It is well

correlated with many physical and chemical properties of organic molecules and chemical compounds.

Based on the electrical network theory, Klein and Randić [6] proposed a novel distance function called *resistance distance* in 1993. They treated a graph G as an electric network by considering each edge of G as a unit resistor. Then, the resistance distance between two vertices u and v in G , denoted by $R_G(u, v)$, is defined as the effective resistance between them. Klein and Randić [6] also proved that $R_G(u, v) \leq d_G(u, v)$, with equality if and only if there is a unique path connecting u and v in G . In recent years, this new type of distance between vertices in a graph has attracted prominent attention in mathematics and chemistry [6–11].

Similar to the Wiener index, the *Kirchhoff index* of a graph G is defined as

$$Kf(G) = \sum_{\{u,v\} \subseteq V(G)} R_G(u, v). \quad (1)$$

This invariant has wide applications in electric circuit, physical interpretations, chemistry, and graph theory [12–16].

In 2012, Gutman et al. [17] introduced the concept of the degree resistance distance defined as

$$D_R(G) = \sum_{\{u,v\} \in V(G)} (d_G(u) + d_G(v))R_G(u, v). \quad (2)$$

Palacios called it as *additive degree-Kirchhoff index* in [18]. In [17], Gutman et al. [17] presented some properties of $D_R(G)$ and characterized the unicyclic graphs with the minimum and second-minimum $D_R(G)$. Later, the unicyclic graphs with the maximum and second-maximum D_R -value were considered in [19, 20]. In [21, 22], the cactus graphs with the minimum, the second-minimum, and the third-minimum D_R -values were also completely characterized. Recently, the bicyclic graphs with maximum and minimum D_R -values were determined in [23, 24], respectively.

A bicyclic graph $G = (V, E)$ is a connected graph such that $|E| = |V| + 1$. The kernel of G , denoted by G , is the unique bicyclic subgraph of G with no pendant vertices. Any bicyclic graph G is obtained from its kernel G by attaching trees to some vertices in G . Given a family of graphs \mathcal{G} , the graphs with the maximum and second maximum values of topological indices among \mathcal{G} are examined widely, see in [25–29]. Motivated by this, in this paper, we determine the graphs with the second-maximum and third-maximum degree resistance distance among all bicyclic graphs with $n \geq 6$ vertices.

2. Preliminaries

Let \mathcal{B}_n be the set of bicyclic graphs of order n , \mathcal{B}_n^∞ be the set of bicyclic graphs of order n with exactly two cycles, and $\mathcal{B}_n^\theta = \mathcal{B}_n \setminus \mathcal{B}_n^\infty$. Let $B(p, q)$ be obtained from two vertex-disjoint cycles C_p and C_q by identifying a vertex $u \in V(C_p)$ and a vertex $v \in V(C_q)$, $B(p, l, q)$ be obtained from two vertex-disjoint cycles C_p and C_q by connecting a vertex $u \in V(C_p)$ and a vertex $v \in V(C_q)$ by a path $uv_1v_2 \dots v_{l-1}v$ of length l ($l \geq 1$), and $B(P_r, P_s, P_t)$ be the union of three internally disjoint paths P_r , P_s , and P_t , respectively, with common end vertices, where $r, s, t \geq 2$ and at most one of them is 2.

Let G be a graph and v be a vertex in G . Define $Kf_v(G) = \sum_{u \in V(G)} R_G(u, v)$ and $D_v(G) = \sum_{u \in V(G)} d_G(u)R_G(u, v)$.

We present a few lemmas which will be employed later to establish our main results.

Lemma 1 (see [13]). *Let G be a connected graph with a pendant vertex v with its unique neighbor w . Then, $Kf_v(G) = Kf_w(G - v) + n - 1$.*

Lemma 2 (see [13]). *Let G be a bicyclic graph of order n and $v \in V(G)$. Then, $Kf_v(G) \leq n^2/2 - n/2 - 15/4$. Moreover, if $d_G(v) \geq 2$, then $Kf_v(G) \leq n^2/2 - 3n/2 + 1/3$.*

The following remark can be obtained from the proof of Lemma 2.

Remark 1. *Let G be a graph in \mathcal{B}_n^∞ and $v \in V(G)$. Then, $Kf_v(G) \leq n^2/2 - n/2 - 6$.*

Lemma 3 (see [17]). *Let G be a connected graph with a cut vertex v such that G_1 and G_2 are two connected subgraphs of G having v as the only common vertex and $V(G_1) \cup V(G_2) = V(G)$. Let $n_1 = |V(G_1)|$, $n_2 = |V(G_2)|$, $m_1 = |E(G_1)|$, and $m_2 = |E(G_2)|$. Then, $D_R(G) = D_R(G_1) + D_R(G_2) + 2m_2Kf_v(G_1) + 2m_1Kf_v(G_2) + (n_2 - 1)D_v(G_1) + (n_1 - 1)D_v(G_2)$.*

Lemma 4 (see [17]). *Let C_k be a cycle with length k and $v \in C_k$. Then, $Kf_v(C_k) = (k^3 - k)/12$, $D_R(C_k) = (k^3 - k)/3$, $Kf_v(C_k) = (k^2 - 1)/6$, and $D_v(C_k) = (k^2 - 1)/3$.*

Lemma 5 (see [23]). *Let H be a connected graph of order $h > 2$ and C_k be a cycle of order $k \geq 4$. Let F be the graph of order $k - 3$ to one vertex of C_3 . Further suppose G_1 is the graph obtained from H and C_k by identifying one vertex in H and one vertex in C_k ; G_2 is the graph obtained from H and F by identifying one vertex in H and the pendant vertex in F . Then, we have $D_R(G_1) < D_R(G_2)$.*

By an argument similar to that of Lemma 5, we easily get the following result.

Lemma 6. *Let G be a connected graph of order $n > 2$ and C_k be a cycle of order $k \geq 5$. Let F be obtained by identifying a pendant vertex of P_{k-3} with any vertex of C_4 . Suppose G_1 is the graph obtained from G and C_k by identifying one vertex in G and one vertex in C_k ; G_2 is obtained from G and F by identifying one vertex in G and the pendant vertex in F . Then, $D_R(G_1) < D_R(G_2)$.*

In [23], Du and Tu characterized the unique bicyclic graph with maximum degree resistance distance. They also presented two significant lemmas in [23].

Theorem 1 (see [23]). *Let G be a bicyclic graph of order $n \geq 6$; then, $D_R(G) \leq 2n^3/3 + n^2 - 19n + 88/3$, with equality if and only if $G \cong B(3, n - 5, 3)$.*

Lemma 7 (see [23]). *Let G be a bicyclic graph of order n and $v \in V(G)$. Then, $D_v(G) \leq n^2 + 2n - 73/4$.*

Lemma 8 (see [23]). *Let G be a bicyclic graph of order n , v be a pendant vertex of G , and w be its neighbor. Then, $D_R(G) = D_R(G - v) + D_w(G - v) + 2Kf_w(G - v) + 3n$.*

3. Bicyclic Graphs with the Second-Maximum Degree Resistance Distance

In this section, we will determine the bicyclic graphs with the second-maximum degree resistance distance.

Suppose $n \geq 6$. Let $B(3, n - 5, 3)$ be obtained from two 3-cycles $v_1v_2v_3v_1$ and $v_{n-2}v_{n-1}v_nv_{n-2}$ by connecting v_3 and v_{n-2} by a path $v_3v_4 \dots v_{n-3}v_{n-2}$. Define $G_n^1 = B(3, n - 5, 3) - v_{n-1}v_n + v_{n-1}v_{n-3}$ and $G_n^{2,i} = G_n^1 - v_{n-2}v_n + v_iv_n$, where $3 \leq i \leq n - 3$. Let $G_n^3(G_n^5)$ be obtained from a 4-cycle $C_4 = v_1v_2v_3v_4v_1$ and a path $P = v_5 \dots v_n$ by adding the edges v_1v_3 (v_2v_4 , resp.) and v_4v_5 . Let $G_n^4 \cong B(4, n - 6, 3)$ be obtained

from a 4-cycle $v_1v_2v_3v_4v_1$ and a 3-cycle $v_{n-2}v_{n-1}v_nv_{n-2}$ by connecting v_4 and v_{n-2} by a path $v_4v_5 \dots v_{n-3}v_{n-2}$ (see Figure 1). Then, we have the following lemma.

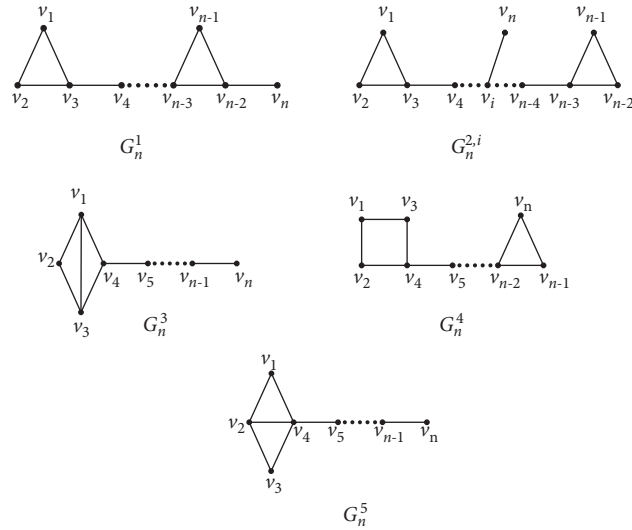
Lemma 9. Let $G_n^1, G_n^{2,i}, G_n^3, G_n^4,$ and G_n^5 be defined as above. Then, $D_R(G_n^1) = 2/3n^3 + n^2 - 79/3n + 56, D_R(G_n^{2,i})$

$$= 2/3n^3 + n^2 - 17n + 4i^2 - 4ni + 88/3, \quad D_R(G_n^3) = 2/3n^3 + n^2 - 293/12n + 117/2, \quad D_R(G_n^4) = 2/3n^3 + n^2 - 82/3n + 167/3, \text{ and } D_R(G_n^5) = 2/3n^3 + n^2 - 163/6n + 139/2.$$

Proof. By Lemma 8 and Theorem 1, we easily obtain

$$\begin{aligned} D_R(G_n^1) &= D_R(G_n^1 - v_n) + D_{v_{n-2}}(G_n^1 - v_n) + 2Kf_{v_{n-2}}(G_n^1 - v_n) + 3n \\ &= \left[\frac{2}{3}(n-1)^3 + (n-1)^2 - 19(n-1) + \frac{88}{3} \right] \\ &\quad + \left[2 \cdot \frac{2}{3} + 3 \cdot \frac{2}{3} + 2 \cdot \left(\frac{2}{3} + 1 \right) + 2 \cdot \left(\frac{2}{3} + 2 \right) + \dots + 2 \cdot \left(\frac{2}{3} + n - 7 \right) + 3 \cdot \left(\frac{2}{3} + n - 6 \right) \right. \\ &\quad \left. + 2 \cdot \left(\frac{4}{3} + n - 6 \right) + 2 \cdot \left(\frac{4}{3} + n - 6 \right) \right] + 2 \cdot \left[\frac{2}{3} + \frac{2}{3} + \left(\frac{2}{3} + 1 \right) \right. \\ &\quad \left. + \left(\frac{2}{3} + 2 \right) + \dots + \left(\frac{2}{3} + n - 6 \right) + 2 \left(\frac{4}{3} + n - 6 \right) \right] + 3n \\ &= \left[\frac{2}{3}(n-1)^3 + (n-1)^2 - 19(n-1) + \frac{88}{3} \right] \\ &\quad + \left(n^2 - \frac{14}{3}n + \frac{4}{3} \right) + 2 \cdot \left(\frac{n^2}{2} - \frac{17}{6}n + 3 \right) + 3n \\ &= \frac{2}{3}n^3 + n^2 - \frac{79}{3}n + 56, \\ D_R(G_n^{2,i}) &= D_R(G_n^{2,i} - v_n) + D_{v_i}(G_n^{2,i} - v_n) + 2Kf_{v_i}(G_n^{2,i} - v_n) + 3n \tag{3} \\ &= \left[\frac{2}{3}(n-1)^3 + (n-1)^2 - 19(n-1) + \frac{88}{3} \right] + [2 \cdot 1 + 2 \cdot 2 \\ &\quad + \dots + 2 \cdot (i-4) + 3 \cdot (i-3) + 4 \cdot \left(i-3 + \frac{2}{3} \right) + 2 \cdot 1 + 2 \cdot 2 \\ &\quad + \dots + 2 \cdot (n-4-i) + 3 \cdot (n-3-i) + 4 \cdot \left(n-3-i + \frac{2}{3} \right)] \\ &\quad + 2 \cdot [1 + 2 + \dots + (i-3) + 2 \cdot \left(i-3 + \frac{2}{3} \right) + 1 + 2 + \dots \\ &\quad + (n-3-i) + 2 \cdot \left(n-3-i + \frac{2}{3} \right)] + 3n \\ &= \left(\frac{2}{3}n^3 - n^2 - 19n + \frac{146}{3} \right) + \left(n^2 + 2i^2 - 2ni - \frac{38}{3} \right) \\ &\quad + 2 \cdot \frac{3n^2 - 3n + 6i^2 - 6ni - 20}{6} + 3n \\ &= \frac{2}{3}n^3 + n^2 - 17n + 4i^2 - 4ni + \frac{88}{3}. \end{aligned}$$

Let $H = G_n^3[\{v_1, v_2, v_3, v_4\}]$. By Lemma 3,

FIGURE 1: Graphs $G_n^1, G_n^{2,i}, G_n^3, G_n^4,$ and G_n^5 .

$$\begin{aligned}
 D_R(G_n^3) &= D_R(H) + D_R(P_{n-3}) + 2(n-4)Kf_{v_4}(H) + 10Kf_{v_4}(P_{n-3}) \\
 &\quad + (n-4)D_{v_4}(H) + 3D_{v_4}(P_{n-3}) \\
 &= \frac{39}{2} + \left[\frac{2}{3}(n-3)^3 - (n-3)^2 + \frac{1}{3}(n-3) \right] + 2 \cdot (n-4) \cdot \frac{9}{4} \\
 &\quad + 10 \cdot \frac{(n-3)(n-4)}{2} + (n-4) \cdot \frac{23}{4} + 3 \cdot (n-4)^2 \\
 &= \frac{2}{3}n^3 + n^2 - \frac{293}{12}n + \frac{117}{2}.
 \end{aligned} \tag{4}$$

Let $F = G_n^4 - \{v_{n-1}, v_n\}$. By Lemmas 3 and 6,

$$\begin{aligned}
 D_R(G_n^4) &= D_R(C_3) + D_R(F) + 2(n-2)Kf_{v_{n-2}}(C_3) + 6Kf_{v_{n-2}}(F) \\
 &\quad + (n-3)D_{v_{n-2}}(C_3) + 2D_{v_{n-2}}(F) \\
 &= 8 + \left[\frac{2}{3}(n-2)^3 - \frac{53}{3}(n-2) + 48 \right] + \frac{8}{3}(n-2) + 6 \left[\frac{(n-2)^2}{2} \right. \\
 &\quad \left. - \frac{n-2}{2} - \frac{7}{2} \right] + \frac{8}{3}(n-3) + 2[(n-2)^2 - 11] \\
 &= \frac{2}{3}n^3 + n^2 - \frac{82}{3}n + \frac{167}{3}.
 \end{aligned} \tag{5}$$

Let $S = G_n^5[\{v_1, v_2, v_3, v_4\}]$. By Lemma 3,

$$\begin{aligned}
 D_R(G_n^5) &= D_R(S) + D_R(P_{n-3}) + 2(n-4)Kf_{v_4}(S) + 10Kf_{v_4}(P_{n-3}) \\
 &\quad + (n-4)D_{v_4}(S) + 3D_{v_4}(P_{n-3}) \\
 &= \frac{39}{2} + \left[\frac{2}{3}(n-4)^3 + (n-4)^2 + \frac{1}{3}(n-4) \right] + 2(n-4) \cdot \frac{7}{4} \\
 &\quad + 10 \cdot \frac{(n-3)(n-4)}{2} + 4(n-4) + 3(n-4)^2 \\
 &= \frac{2}{3}n^3 + n^2 - \frac{163}{6}n + \frac{139}{2}.
 \end{aligned} \tag{6}$$

Theorem 2. Suppose G is a graph in \mathcal{B}_n^∞ with $G \neq B(3, n-5, 3)$ and $n \geq 6$. Then, $D_R(G) \leq 2/3n^3 + n^2 - 79/3n + 56$, with equality if and only if $G \cong G_n^1$, where G_n^1 is defined as in Lemma 9.

Proof. It is easy to verify that, for any graph G in \mathcal{B}_6^∞ with $G \neq B(3, 1, 3)$, $D_R(G) \leq 78 = 2/3 \cdot 6^3 + 6^2 - 79/3 \cdot 6 + 56$, with equality if and only if $G \cong G_6^1$.

Now, we assume $n \geq 7$ and consider the following two cases.

Case 1 $\delta(G) = 1$: let v be a pendant vertex in G . If $G - v \cong B(3, n-6, 3)$, then either $G \cong G_n^1$, or $G \cong G_n^{2,i}$, where G_n^1 and $G \cong G_n^{2,i}$ are defined as in Lemma 9. By Lemma 9,

$$\begin{aligned}
 D_R(G_n^{2,i}) &= \frac{2}{3}n^3 + n^2 - 17n + 4i^2 - 4ni + \frac{88}{3} \\
 &\leq \frac{2}{3}n^3 + n^2 - 17n + 4 \cdot 3^2 - 4n \cdot 3 + \frac{88}{3} \tag{7} \\
 &< \frac{2}{3}n^3 + n^2 - \frac{79}{3}n + 56.
 \end{aligned}$$

If $G - v \not\cong B(3, n-6, 3)$, we prove it by induction on n . Let w be the neighbor of v . By the inductive hypothesis, Remark 1, and Lemmas 7-9

$$\begin{aligned}
 D_R(G) &= D_R(G-v) + D_w(G-v) + 2Kf_w(G-v) + 3n \\
 &\leq \frac{2}{3}(n-1)^3 + (n-1)^2 - \frac{79}{3}(n-1) \\
 &\quad + 56 + \left[(n-1)^2 + 2(n-1) \right. \\
 &\quad \left. - \frac{73}{4} \right] + 2 \left(\frac{(n-1)^2}{2} - \frac{n-1}{2} - 6 \right) + 3n \\
 &= \frac{2}{3}n^3 + n^2 - \frac{79}{3}n + \frac{641}{12} \\
 &< \frac{2}{3}n^3 + n^2 - \frac{79}{3}n + 56.
 \end{aligned} \tag{8}$$

Case 2 ($\delta(G) \geq 2$): in this case, G is of the form $B(p, q)$ or $B(p, l, q)$. By Lemmas 5 and 6, we have $D_R(G) \leq D_R(G_n^4)$, with equality if and only if $G \cong G_n^4$.

Note that $D_R(G_n^4) < D_R(G_n^1)$ by Lemma 9. Therefore, the proof is complete. \square

Theorem 3. Suppose G is a graph of order $n \geq 4$ in \mathcal{B}_n^θ . Then, $D_R(G) \leq 2/3n^3 + n^2 - 293/12n + 117/2$, with equality if and only if $G \cong G_n^3$, where G_n^3 is defined in Lemma 9.

Proof. It is easy to verify that the only graph in \mathcal{B}_4^θ is G_4^3 and $D_R(G_4^3) = 2/3 \cdot 4^3 + 4^2 - 293/12 \cdot 4 + 117/2$. We assume $n \geq 5$ next, and consider the following two cases.

Case 1 ($\delta(G) = 1$): let v be a pendant vertex in G and w be the neighbor of v . We prove it by induction on n . By the inductive hypothesis, Lemma 2, and Lemmas 7-9,

$$\begin{aligned}
 D_R(G) &= D_R(G-v) + D_w(G-v) + 2Kf_w(G-v) + 3n \\
 &\leq \frac{2}{3}(n-1)^3 + (n-1)^2 - \frac{293}{12}(n-1) \\
 &\quad + \frac{117}{2} + \left[(n-1)^2 + 2(n-1) \right. \\
 &\quad \left. - \frac{73}{4} \right] + 2 \cdot \left(\frac{(n-1)^2}{2} - \frac{n-1}{2} - \frac{15}{4} \right) + 3n \\
 &= \frac{2}{3}n^3 + n^2 - \frac{293}{12}n + \frac{117}{2}.
 \end{aligned} \tag{9}$$

The equality $D_R(G-v) = 2/3n^3 + n^2 - 293/12n + 117/2$ holds if and only if $D_R(G-v) = 2/3(n-1)^3 + (n-1)^2 - 293/12(n-1) + 117/2$, $D_w(G-v) = (n-1)^2 + 2 \cdot (n-1) - 73/4$, and $Kf_w(G-v) = (n-1)^2/2 - (n-1)/2 - 15/4 = n^2/2 - 3/2n - 11/4$. By the inductive hypothesis, $G-v \cong G_{n-1}^3$, which is obtained from a 4-cycle $C_4 = v_1v_2v_3v_4v_1$ and a path $P = v_5 \dots v_{n-1}$ by adding the edges v_1v_3 and v_4v_5 . We show that $w = v_{n-1}$, i.e., $G \cong G_n^3$. By direct calculation, we have $Kf_{v_{n-1}}(G_{n-1}^3) = n^2/2 - 3/2n - 11/4$, $Kf_{v_1}(G_{n-1}^3) = Kf_{v_3}(G_{n-1}^3) = n^2/2 - 31/8n + 69/8 < n^2/2 - 3/2n - 11/4$, and $Kf_{v_2}(G_{n-1}^3) = n^2/2 - 7/2n + 29/4 < n^2/2 - 3/2n - 11/4$. Obviously, $Kf_u(G_{n-1}^3) < Kf_{v_{n-1}}(G_{n-1}^3)$ if $u \in V(G_{n-1}^3) \setminus \{v_1, v_2, v_3, v_{n-1}\}$. Therefore, $w = v_{n-1}$, i.e., $G \cong G_n^3$.

Case 2 ($\delta(G) \geq 2$): then, G is of the form $B(P_k, P_l, P_m)$. Suppose x and y are the only two vertices of degree 3. Since $Kf(G) \leq 1/8n^3$ (see [13]), we have

$$\begin{aligned} D_R(G) &= \sum_{\{u,v\} \in V(G)} (d(u) + d(v))R(u, v) \\ &= 4Kf(G) + Kf_x(G) + Kf_y(G) \\ &\leq 4 \cdot \frac{1}{8}n^3 + 2 \cdot \left(\frac{1}{2}n^2 - \frac{3}{2}n + \frac{1}{3}\right) \text{ (by Lemma 2)} \\ &= \frac{1}{2}n^3 + n^2 - 3n + \frac{2}{3}. \end{aligned} \tag{10}$$

If $n \geq 10$, then $1/2n^3 + n^2 - 3n + 2/3 < 2/3n^3 + n^2 - 293/12n + 117/2$. For any graph $G \cong B(P_k, P_l, P_m)$ when $n = 5, 6, 7, 8, 9$, we have calculated $D_R(G)$ and found that $D_R(G) < 2/3n^3 + n^2 - 293/12n + 117/2$.

Combining Theorems 1–3, we can obtain the first main result of our paper. \square

Theorem 4. Suppose G is a bicyclic graph of order $n \geq 6$ with $G \neq B(3, n - 5, 3)$. Then, $D_R(G) \leq 2/3n^3 + n^2 - 293/12n + 117/2$, with equality if and only if $G \cong G_n^3$, where G_n^3 is defined as in Lemma 9.

4. Bicyclic Graphs with the Third-Maximum Degree Resistance Distance

In this section, we will determine the bicyclic graphs with the third-maximum degree resistance distance.

Lemma 10. Let $G_n^{3,i}$ be obtained from a 4-cycle $C_4 = v_1v_2v_3v_4v_1$, a path $P = v_5 \dots v_{n-1}$ and an isolated vertex v_n by adding the edges v_1v_3, v_4v_5 , and v_iv_n , where $1 \leq i \leq n - 2$ and $n \geq 6$. Then, $D_R(G_n^{3,1}) = D_R(G_n^{3,3}) = 2/3n^3 + n^2 - 455/12n + 493/4$, $D_R(G_n^{3,2}) = 2/3n^3 + n^2 - 437/12n + 237/2$, $D_R(G_n^{3,4}) = 2/3n^3 + n^2 - 485/12n + 277/2$, and $D_R(G_n^{3,i}) = 2/3n^3 + n^2 - 293/12n - 4ni + 4i^2 + 4i + 117/2$, for $5 \leq i \leq n - 2$.

Proof. By Lemmas 8 and 9, we easily obtain

$$\begin{aligned} D_R(G_n^{3,1}) &= D_R(G_n^{3,3}) = D_R(G_{n-1}^3) + D_{v_1}(G_{n-1}^3) + 2Kf_{v_1}(G_{n-1}^3) + 3n \\ &= \left[\frac{2}{3}(n-1)^3 + (n-1)^2 - \frac{293}{12}(n-1) + \frac{117}{2} \right] \\ &\quad + 2 \cdot \frac{5}{8} + 3 \cdot \frac{5}{8} + 3 \cdot \frac{1}{2} + 2 \cdot \left(\frac{5}{8} + 1 \right) + \dots + 2 \cdot \left(\frac{5}{8} + n - 6 \right) + \left(n - 5 + \frac{5}{8} \right) \\ &\quad + 2 \cdot \left[\frac{5}{8} + \frac{5}{8} + \frac{1}{2} + \left(\frac{5}{8} + 1 \right) + \dots + \left(\frac{5}{8} + n - 5 \right) \right] + 3n \\ &= \left[\frac{2}{3}(n-1)^3 + (n-1)^2 - \frac{293}{12}(n-1) + \frac{117}{2} \right] + \left(n^2 - \frac{35}{4}n + \frac{91}{4} \right) \\ &\quad + \left(n^2 - \frac{31}{4}n + \frac{69}{4} \right) + 3n = \frac{2}{3}n^3 + n^2 - \frac{455}{12}n + \frac{493}{4}, \end{aligned}$$

$$\begin{aligned} D_R(G_n^{3,2}) &= D_R(G_{n-1}^3) + D_{v_2}(G_{n-1}^3) + 2Kf_{v_2}(G_{n-1}^3) + 3n \\ &= \left[\frac{2}{3}(n-1)^3 + (n-1)^2 - \frac{293}{12}(n-1) + \frac{117}{2} \right] \\ &\quad + 3 \cdot \frac{5}{8} + 3 \cdot \frac{5}{8} + 3 \cdot 1 + 2 \cdot 2 + \dots + 2 \cdot (n-5) + (n-4) + 2 \cdot \left(\frac{5}{8} + \frac{5}{8} + 1 \right) \\ &\quad + \dots + (n-4) + 3n \end{aligned}$$

$$\begin{aligned}
 &= \left[\frac{2}{3}(n-1)^3 + (n-1)^2 - \frac{293}{12}(n-1) + \frac{117}{2} \right] \\
 &\quad + \left(n^2 - 8n + \frac{83}{4} \right) \\
 &\quad + \left(n^2 - 7n + \frac{29}{2} \right) + 3 \\
 &= \left[\frac{2}{3}n^3 + n^2 - \frac{437}{12}n + \frac{237}{2}, \right. \\
 &\quad \left. D_R(G_n^{3,4}) = D_R(G_{n-1}^3) + D_{v_4}(G_{n-1}^3) + 2Kf_{v_4}(G_{n-1}^3) + 3n \right. \tag{11} \\
 &= \left[\frac{2}{3}(n-1)^3 + (n-1)^2 - \frac{293}{12}(n-1) + \frac{117}{2} \right] \\
 &\quad \left[+ 2 \cdot 3 \cdot \frac{5}{8} + 2 \cdot 1 + 2 \cdot 1 + 2 \cdot 2 + \dots + 2 \cdot (n-6) + (n-5) \right] + 2 \cdot \left(2 \cdot \frac{5}{8} + 1 + 1 \right. \\
 &\quad \left. + \dots + n - 5 + 3n = \left[\frac{2}{3}(n-1)^3 + (n-1)^2 - \frac{293}{12}(n-1) + \frac{117}{2} \right] + \left(n^2 - 10n + \frac{123}{4} \right) \right. \\
 &\quad \left. + \left(n^2 - 9n + \frac{49}{2} \right) + 3n = \frac{2}{3}n^3 + n^2 - \frac{485}{12}n + \frac{277}{2}, \right.
 \end{aligned}$$

and for $5 \leq i \leq n-2$,

$$\begin{aligned}
 D_R(G_n^{3,i}) &= D_R(G_{n-1}^3) + D_{v_i}(G_{n-1}^3) + 2Kf_{v_i}(G_{n-1}^3) + 3n \\
 &= \left[\frac{2}{3}(n-1)^3 + (n-1)^2 - \frac{293}{12}(n-1) + \frac{117}{2} \right] \\
 &\quad + 2 \cdot 1 + 2 \cdot 2 + \dots \\
 &\quad + 2 \cdot (n-2-i) + (n-1-i) + 2 \cdot \left[1 + 2 \cdot 2 + \dots + 2 \cdot (i-5) \right. \\
 &\quad \left. + 3 \cdot (i-4) + 2 \cdot 3 \cdot \left(i-4 + \frac{5}{8} \right) + 2 \cdot (i-3) + 2 \cdot 1 + 2 + \dots \right. \tag{12} \\
 &\quad \left. + (n-1-i) + 1 + 2 + \dots + i-3 + 2 \cdot \left(i-4 + \frac{5}{8} \right) \right] + 3n \\
 &= \left[\frac{2}{3}(n-1)^3 + (n-1)^2 - \frac{293}{12}(n-1) + \frac{117}{2} \right] \\
 &\quad + \left(n^2 - 2ni - 2n + 2i^2 + 4i - \frac{69}{4} + n^2 - 2ni - n + 2i^2 - \frac{15}{2} \right) + 3n \\
 &= \frac{2}{3}n^3 + n^2 - \frac{293}{12}n - 4ni + 4i^2 + 4i + \frac{117}{2}.
 \end{aligned}$$

Proposition 1. Suppose $G \neq G_n^3$ is a bicyclic graph of order $n \geq 5$ and $v \in V(G)$, where G_n^3 is defined as in Lemma 9. Then, $Kf_v(G) \leq n^2/2 - n/2 - 17/4$.

Proof. It is not hard to verify that, for any bicyclic graph $G \neq G_n^3$ of order $n \geq 5$ and $v \in V(G)$, $Kf_v(G) \leq 5^2/2 - 5/2 - 17/4$. Thus, we assume $n \geq 6$ in the following cases.

Case 1 ($d(v) = 1$): let w be the neighbor of v .

Suppose $G - v \cong G_{n-1}^3$, where G_{n-1}^3 is obtained from a 4-cycle $C_4 = v_1v_2v_3v_4v_1$ and a path $P = v_5 \dots v_{n-1}$ by adding the edges v_1v_3 and v_4v_5 . Then, $w \neq v_{n-1}$ since $G \not\cong G_n^3$. By Lemma 1,

$$\begin{aligned} Kf_v(G) &= Kf_w(G - v) + n - 1 \\ &\leq \max\{Kf_{v_{n-2}}(G_{n-1}^3), Kf_{v_2}(G_{n-1}^3)\} + n - 1 \\ &= \max\left\{\frac{n^2}{2} - \frac{5}{2}n + \frac{1}{4}, \frac{n^2}{2} - \frac{7}{2}n + \frac{29}{4}\right\} + n - 1 \\ &= \max\left\{\frac{n^2}{2} - \frac{3}{2}n - \frac{3}{4}, \frac{n^2}{2} - \frac{5}{2}n + \frac{25}{4}\right\} \\ &< \frac{n^2}{2} - \frac{n}{2} - \frac{17}{4}. \end{aligned} \tag{13}$$

If $G - v \not\cong G_{n-1}^3$, we shall prove it by induction on n . By the inductive hypothesis, $Kf_v(G) = Kf_w(G - v) + n - 1 \leq (n - 1)^2/2 - (n - 1)/2 - 17/4 + n - 1 = n^2/2 - n/2 - 17/4$.

Case 2: $d(v) \geq 2$.

By Lemma 2, $Kf_v(G) \leq n^2/2 - 3n/2 + 1/3 < n^2/2 - n/2 - 17/4$. \square

Lemma 11 (see [23]). *Let G be a bicyclic graph of order n , v be a pendant vertex of G , and w be its neighbor. Then, $D_v(G) = D_w(G - v) + 2n + 1$.*

Proposition 2. *Let $G \not\cong G_n^3$ be a graph in \mathcal{B}_n^θ of order $n \geq 5$ and $v \in V(G)$, where G_n^3 is defined as in Lemma 9. Then, $D_v(G) \leq n^2 + 2n - 20$.*

Proof. It is easy to verify that for any graph $G \in \mathcal{B}_5^\theta$ with $G \not\cong G_5^3$ and $v \in V(G)$, $D_v(G) \leq 15 = 5^2 + 2 \cdot 5 - 20$. Thus, we assume $n \geq 6$ in the following cases.

Case 1 ($d_G(v) = 1$): let w be the neighbor of v .

Suppose $G - v \cong G_{n-1}^3$, where G_{n-1}^3 is obtained from a 4-cycle $C_4 = v_1v_2v_3v_4v_1$ and a path $P = v_5 \dots v_{n-1}$ by adding the edges v_1v_3 and v_4v_5 . Then, $w \neq v_{n-1}$ since $G \not\cong G_n^3$. Moreover, $D_v(G) = D_w(G_{n-1}^3) + 2n + 1$ by Lemma 11. By direct calculation, we get $D_{v_1}(G_{n-1}^3) = D_{v_3}(G_{n-1}^3) = n^2 - 35/4n + 91/4$, $D_{v_2}(G_{n-1}^3) = n^2 - 8n + 83/4$, $D_{v_4}(G_{n-1}^3) = n^2 - 10n + 123/4$, and

$$\begin{aligned} D_{v_i}(G_{n-1}^3) &= n^2 - 2n + 2i^2 + (4 - 2n)i - \frac{69}{4} \\ &\leq n^2 - 2n + 2(n - 2)^2 + (4 - 2n)(n - 2) - \frac{69}{4} \\ &= n^2 - 2n - \frac{69}{4} (= D_{v_{n-2}}(G_{n-1}^3)), \end{aligned} \tag{14}$$

if $5 \leq i \leq n - 2$. Thus, $D_w(G_{n-1}^3) \leq D_{v_{n-2}}(G_{n-1}^3)$ and $D_v(G) \leq D_{v_{n-2}}(G_{n-1}^3) + 2n + 1 = n^2 - 65/4 < n^2 + 2n - 20$. If $G - v \not\cong G_{n-1}^3$, we prove it by induction on n . By the inductive hypothesis, $D_v(G) = D_w(G) + 2n + 1 \leq (n - 1)^2 + 2(n - 1) - 20 + 2n + 1 = n^2 + 2n - 20$.

Case 2: $d_G(v) \geq 2$.

Subcase 1: v is not contained by any cycle of G .

By the same argument as that of Case 2 of Lemma 2.6 in [23], we can construct a series of bicyclic graphs G_1, G_2, \dots, G_{k-1} in \mathcal{B}_n^θ such that $D_v(G) < D_v(G_1) < \dots < D_v(G_{k-1})$ and v is a pendant vertex in G_{k-1} , where $k = d_G(v) \geq 2$.

Suppose $G_{k-1} \cong G_n^3$. Then, G_{k-1} is obtained from a 4-cycle $C_4 = v_1v_2v_3v_4v_1$ and a path $P = v_5 \dots v_{n-1}v$ by adding the edges v_1v_3 and v_4v_5 . By the transformation from G_{k-2} to G_{k-1} , we can conclude that $G_{k-2} = G_{k-1} - v_{n-2}v_{n-1} + v_{n-2}v$, i.e., $G_{k-2} \cong G_{k-1}$. Note that $D_v(G_{k-2}) = n^2 - 73/4$. We have $D_v(G) \leq D_v(G_{k-2}) < n^2 + 2n - 20$.

If $G_{k-1} \not\cong G_n^3$, then, by Case 1, $D_v(G) < D_v(G_{k-1}) \leq n^2 + 2n - 20$.

Subcase 2: v is in a cycle of G .

Let \hat{G} be the kernel of G . By Claims 1 and 2 of Lemma 2.6 in [23], we can construct a graph G'' in \mathcal{B}_n^θ having G as its kernel and $D_v(G) \leq D_v(G'')$. Moreover, G'' is obtained from G by attaching a pendant path to the vertex u , where u is a vertex of G such that $R_G(u, v) = \max_{u \in V(G)} R_G(u, v)$.

Suppose G'' has only two vertices of degree three, say w_1 and w_2 . Without loss of generality, we assume that $v \neq w_1$, and $v \neq w_2$. Then, by Lemma 2,

$$\begin{aligned} D_v(G'') &= 3(R_{G''}(w_1, v) + R_{G''}(w_2, v)) + \sum_{w \neq w_1, w_2} 2R_{G''}(w, v) \\ &= R_{G''}(w_1, v) + R_{G''}(w_2, v) + 2Kf_v(G'') \\ &< d_{G''}(w_1, v) + d_{G''}(w_2, v) + 2Kf_v(G'') \\ &\leq n + 2\left(\frac{n^2}{2} - \frac{3}{2}n + \frac{1}{3}\right) \\ &< n^2 + 2n - 20. \end{aligned} \tag{15}$$

Suppose G'' has exactly three vertices of degree three, say w_1, w_2 , and w_3 . Let w_4 be the pendant vertex of G'' . Without loss of generality, we assume that $v \neq w_1, w_2, w_3$. Then, by Lemma 2,

$$\begin{aligned} D_v(G'') &= 3(R_{G''}(w_1, v) + R_{G''}(w_2, v) + R_{G''}(w_3, v)) + R_{G''}(w_4, v) \\ &\quad + \sum_{w \neq w_1, w_2, w_3, w_4} 2R_{G''}(w, v) \\ &< R_{G''}(w_1, v) + R_{G''}(w_2, v) + R_{G''}(w_3, v) + 2Kf_v(G'') \\ &< d_{G''}(w_1, v) + d_{G''}(w_2, v) + d_{G''}(w_3, v) + 2Kf_v(G'') \end{aligned}$$

$$\begin{aligned} &\leq \frac{3(n-1)}{2} + 2 \cdot \left(\frac{n^2}{2} - \frac{3}{2}n + \frac{1}{3} \right) \\ &\leq n^2 + 2n - 20. \end{aligned} \tag{16}$$

Suppose G'' has a vertex of degree four, say w_1 , and a vertex of degree three, say w_2 . Let w_3 be the pendant vertex of G'' . Without loss of generality, we assume that $v \neq w_1, w_2$. Then, by Lemma 2,

$$\begin{aligned} D_v(G'') &= 4R_{G''}(w_1, v) + 3R_{G''}(w_2, v) \\ &\quad + R_{G''}(w_3, v) + \sum_{w \neq w_1, w_2, w_3} 2R_{G''}(w, v) \\ &< 2R_{G''}(w_1, v) + R_{G''}(w_2, v) + 2Kf_v(G'') \\ &< 2d_{G''}(w_1, v) + d_{G''}(w_2, v) + 2Kf_v(G'') \\ &\leq \frac{3(n-1)}{2} + 2 \cdot \left(\frac{n^2}{2} - \frac{3}{2}n + \frac{1}{3} \right) \\ &\leq n^2 + 2n - 20, \end{aligned} \tag{17}$$

which completes the proof. \square

Theorem 5. *Suppose G is a graph of order $n \geq 5$ in $\mathcal{B}_n^\theta \setminus \{G_n^3\}$. Then, $D_R(G) \leq 2/3n^3 + n^2 - 163/6n + 139/2$, with equality if and only if $G \cong G_n^5$, where G_n^3 and G_n^5 are defined as in Lemma 9.*

Proof. It is not hard to verify that, for any graph G in $\mathcal{B}_5^\theta \setminus \{G_5^3\}$, $D_R(G) \leq 42 = 2/3 \cdot 5^3 + 5^2 - 163/6 \cdot 5 + 139/2$, with equality if and only if $G \cong G_5^5$.

We assume that $n \geq 6$, and consider the following two cases.

Case 1: $\delta(G) = 1$.

Let v_n be a pendant vertex of G . Suppose $G - v_n \cong G_{n-1}^3$, where G_{n-1}^3 is obtained from a 4-cycle $C_4 = v_1v_2v_3v_4v_1$, and a path $P = v_5 \cdots v_{n-1}$ by adding the edges v_1v_3 and v_4v_5 . Then, $G \cong G_n^{3,i}$, where $1 \leq i \leq n-2$, and $G_n^{3,i}$ is defined in the Lemmas 10. By Lemma 10,

$$\begin{aligned} D_R(G_n^{3,1}) &= D_R(G_n^{3,3}) = \frac{2}{3}n^3 + n^2 - \frac{455}{12}n + \frac{493}{4} < \frac{2}{3}n^3 + n^2 - \frac{163}{6}n + \frac{139}{2}, \\ D_R(G_n^{3,2}) &= \frac{2}{3}n^3 + n^2 - \frac{437}{12}n + \frac{237}{2} < \frac{2}{3}n^3 + n^2 - \frac{163}{6}n + \frac{139}{2}, \\ D_R(G_n^{3,4}) &= \frac{2}{3}n^3 + n^2 - \frac{485}{12}n + \frac{277}{2} < \frac{2}{3}n^3 + n^2 - \frac{163}{6}n + \frac{139}{2}, \\ D_R(G_n^{3,i}) &= \frac{2}{3}n^3 + n^2 - \frac{293}{12}n - 4ni + 4i^2 + 4i + \frac{117}{2} \\ &\leq \frac{2}{3}n^3 + n^2 - \frac{293}{12}n - 4n(n-2) + 4(n-2)^2 + 4(n-2) + \frac{117}{2} \\ &= \frac{2}{3}n^3 + n^2 - \frac{341}{12}n + \frac{133}{2} \\ &< \frac{2}{3}n^3 + n^2 - \frac{163}{6}n + \frac{139}{2}, \end{aligned} \tag{18}$$

for $5 \leq i \leq n-2$.

If $G - v_n \not\cong G_{n-1}^3$, we prove it by induction on n . Let w be the neighbor of v_n . By the inductive hypothesis, Lemma 8, and Propositions 1 and 2,

$$\begin{aligned}
D_R(G) &= D_R(G - v_n) + D_w(G - v_n) + 2Kf_w(G - v_n) + 3n \\
&\leq \left[\frac{2}{3}(n-1)^3 + (n-1)^2 - \frac{163}{6}(n-1) \right. \\
&\quad \left. + \frac{139}{2} \right] + (n-1)^2 + 2(n-1) \\
&\quad - 20 + 2 \cdot \left(\frac{(n-1)^2}{2} - \frac{n-1}{2} - \frac{17}{4} \right) + 3n \\
&= \frac{2}{3}n^3 + n^2 - \frac{163}{6}n + \frac{139}{2}.
\end{aligned} \tag{19}$$

The equality $D_R(G) = 2/3n^3 + n^2 - 163/6n + 139/2$ holds if and only if $D_R(G - v_n) = 2/3(n-1)^3 + (n-1)^2 - 163/6(n-1) + 139/2$, $D_w(G - v_n) = (n-1)^2 + 2(n-1) - 20$, and $Kf_w(G - v_n) = (n-1)^2/2 - (n-1)/2 - 17/4 = n^2/2 - 3/2n - 13/4$. By the inductive hypothesis, $G - v_n \cong G_{n-1}^5$, where G_{n-1}^5 is obtained from a 4-cycle $C_4 = v_1v_2v_3v_4v_1$ and a path $P = v_5 \dots v_{n-1}$ by adding the edges v_2v_4 and v_4v_5 . We show that $w = v_{n-1}$, i.e., $G \cong G_n^5$.

By direct calculation, we have $Kf_{v_{n-1}}(G_{n-1}^5) = n^2/2 - 3/2n - 13/4$, $Kf_{v_2}(G_{n-1}^5) = n^2/2 - 4n + 37/4 < n^2/2 - 3/2n - 13/4$, and $Kf_{v_1}(G_{n-1}^5) = Kf_{v_3}(G_{n-1}^5) = n^2/2 - 31/8n + 73/8 < n^2/2 - 3/2n - 13/4$. Obviously, $Kf_v(G_{n-1}^5) < Kf_{v_{n-1}}(G_{n-1}^5)$ if $v \in V(G_{n-1}^5) \setminus \{v_1, v_2, v_3, v_{n-1}\}$. Therefore, $w = v_{n-1}$, i.e., $G \cong G_n^5$.

Case 2: $\delta(G) \geq 2$.

By a similar argument to that of Case 2 in Theorem 3, we obtain

$$D_R(G) \leq \frac{1}{2}n^3 + n^2 - 3n + \frac{2}{3}. \tag{20}$$

If $n \geq 11$, then $1/2n^3 + n^2 - 3n + 2/3 < 2/3n^3 + n^2 - 163/6n + 139/2$. For any graph of the form $B(P_k, P_l, P_m)$ when $n = 6, 7, 8, 9, 10$, we have calculated $D_R(G)$ and found that $D_R(G) \leq 2/3n^3 + n^2 - 163/6n + 139/2$.

From Theorems 2 and 4, we obtain the following result. \square

Theorem 6. Let G_n^1 and G_n^5 be defined as in Lemma 9. Then, among all bicyclic graphs of order n ,

- (i) If $6 \leq n \leq 16$, the graph G_n^5 is the unique graph with the third-maximum degree resistance distance of value $2/3n^3 + n^2 - 163/6n + 139/2$
- (ii) If $n \geq 17$, the graph G_n^1 is the unique graph with the third-maximum degree resistance distance of value $2/3n^3 + n^2 - 79/3n + 56$

5. Conclusion

As a molecular structure descriptor, the Wiener index is one of the widely employed topological indices, as it is well correlated with many physical and chemical properties of a variety of classes of chemical compounds. A weighted

version of the Wiener index is the degree resistance distance. In this paper, we characterize the graphs with the second-maximum and third-maximum degree resistance distance among all bicyclic graphs with fixed order. Furthermore, we present an open problem.

Problem 1. Characterize the tricyclic graphs of order n with the maximum and second-maximum degree resistance distance.

Data Availability

All the proofs and exemplary data of this study are included within the article.

Conflicts of Interest

The authors declare that they have no conflicts of interest.

Acknowledgments

The research of the first author was supported by National Natural Science Foundation of China (no. 11801568).

References

- [1] R. Gozalbes, J. Doucet, and F. Derouin, "Application of topological descriptors in QSAR and drug design: history and new trends," *Current Drug Targets-Infectious Disorders*, vol. 2, pp. 93–102, 2002.
- [2] O. Ivanciuc, "QSAR comparative study of Wiener descriptor for weighted molecular graphs," *Journal of Chemical Information and Computer Sciences*, vol. 40, pp. 1412–1422, 2000.
- [3] K. C. Das, I. Gutman, and M. J. Nadjafi-Arani, "Relations between distance-based and degree-based topological indices," *Applied Mathematics and Computation*, vol. 270, pp. 142–147, 2015.
- [4] K. Xu, M. Liu, K. C. Das, I. Gutman, and B. Furtula, "A survey on graphs extremal with respect to distance-based topological indices," *MATCH Communications in Mathematical and in Computer Chemistry*, vol. 71, pp. 461–508, 2014.
- [5] H. Wiener, "Structural determination of paraffin boiling points," *Journal of the American Chemical Society*, vol. 69, pp. 17–20, 1947.
- [6] D. J. Klein and M. Randić, "Resistance distance," *Journal of Mathematical Chemistry*, vol. 12, pp. 81–95, 1993.
- [7] D. Babić, D. J. Klein, I. Lukovits, S. Nikolić, and N. Trinajstić, "Resistance-distance matrix: a computational algorithm and its application," *International Journal of Quantum Chemistry*, vol. 90, pp. 166–176, 2002.
- [8] R. B. Bapat, I. Gutman, and W. Xiao, "A simple method for computing resistance distance," *Zeitschrift für Naturforschung*, vol. 58a, pp. 494–498, 2003.
- [9] X. Gao, Y. Luo, and W. Liu, "Resistance distances and the Kirchhoff index in Cayley graphs," *Discrete Applied Mathematics*, vol. 159, pp. 2050–2057, 2011.
- [10] Y. Yang and D. J. Klein, "A recursion formula for resistance distances and its applications," *Discrete Applied Mathematics*, vol. 161, pp. 2702–2715, 2013.
- [11] Y. Yang and H. Zhang, "Some rules on resistance distance with applications," *Journal of Physics A: Mathematical and Theoretical*, vol. 41, Article ID 445203, 2008.

- [12] C. Arauz, "The Kirchhoff indexes of some composite networks," *Discrete Applied Mathematics*, vol. 160, pp. 1429–1440, 2012.
- [13] L. Feng, G. Yu, K. Xu, and Z. Jiang, "A note on the Kirchhoff index of bicyclic graphs," *Ars Combinatoria*, vol. 114, pp. 33–40, 2014.
- [14] J. L. Palacios and J. M. Renom, "Another look at the degree-Kirchhoff index," *International Journal of Quantum Chemistry*, vol. 111, pp. 3453–3455, 2011.
- [15] B. Zhou and N. Trinajstić, "Mathematical properties of molecular descriptors based on distances," *Croatica Chemica Acta*, vol. 83, pp. 227–242, 2010.
- [16] A. D. Maden, A. S. Cevik, I. N. Cangul, and K. C. Das, "On the Kirchhoff matrix, a new Kirchhoff index and the Kirchhoff energy," *Journal of Inequalities and Applications*, vol. 337, 2013.
- [17] I. Gutman, L. Feng, and G. Yu, "Degree resistance distance of unicyclic graphs," *Trans. Comb.* vol. 1, no. 2, pp. 27–40, 2012.
- [18] J. L. Palacios, "Upper and lower bounds for the additive degree-Kirchhoff index," *MATCH Communications in Mathematical and in Computer Chemistry*, vol. 70, pp. 651–655, 2013.
- [19] S. Chen, Q. Chen, X. Cai, and Z. Guo, "Maximal degree resistance distance of unicyclic graphs," *MATCH Communications in Mathematical and in Computer Chemistry*, vol. 75, pp. 157–168, 2016.
- [20] J. Tu, J. Du, and G. Su, "The unicyclic graphs with maximum degree resistance distance," *Applied Mathematics and Computation*, vol. 268, pp. 859–864, 2015.
- [21] J. Du, G. Su, J. Tu, and I. Gutman, "The degree resistance distance of cacti," *Discrete Applied Mathematics*, vol. 188, pp. 16–24, 2015.
- [22] J. Liu, W. Wang, Y. Zhang, and X. Pan, "On degree resistance distance of cacti," *Discrete Applied Mathematics*, vol. 203, pp. 217–225, 2016.
- [23] J. Du and J. Tu, "Bicyclic graphs with maximum degree resistance distance," *Filomat*, vol. 30, pp. 1625–1632, 2016.
- [24] J. Liu, S. Zhang, X. Pan, S. Wang, and S. Hayat, "Bicyclic graphs with extremal degree resistance distance," arXiv: 1606.01281v1, 2016.
- [25] Z. Du and B. Zhou, "On sum-connectivity index of bicyclic graphs," *Bulletin of the Malaysian Mathematical Sciences Society*, vol. 35, pp. 101–117, 2012.
- [26] R. Xing, B. Zhou, and F. Dong, "On atom-bond connectivity index of connected graphs," *Discrete Applied Mathematics*, vol. 159, pp. 1617–1630, 2011.
- [27] J. Li and J. Zhang, "On the second Zagreb eccentricity indices of graphs," *Applied Mathematics and Computation*, vol. 352, pp. 180–187, 2019.
- [28] J. Fei and J. Tu, "Complete characterization of bicyclic graphs with the maximum and second-maximum degree Kirchhoff index," *Applied Mathematics and Computation*, vol. 330, pp. 118–124, 2018.
- [29] L. Zhong and Q. Cui, "The harmonic index for unicyclic graphs with given girth," *Filomat*, vol. 29, pp. 673–686, 2015.

Research Article

On Some Properties of Multiplicative Topological Indices in Silicon-Carbon

Abid Mahboob ¹, Sajid Mahboob,² Mohammed M. M. Jaradat ³, Nigait Nigar,² and Imran Siddique ⁴

¹Department of Mathematics, Division of Science and Technology, University of Education, Lahore, Pakistan

²Department of Mathematics, Minhaj University, Lahore, Pakistan

³Mathematics Program, Department of Mathematics, Statistics and Physics, College of Arts and Sciences, Doha 2713, Qatar

⁴Department of Mathematics, University of Management and Technology, Lahore 54770, Pakistan

Correspondence should be addressed to Mohammed M. M. Jaradat; mmjst4@qu.edu.qa

Received 13 September 2021; Accepted 7 October 2021; Published 8 November 2021

Academic Editor: Ali Ahmad

Copyright © 2021 Abid Mahboob et al. This is an open access article distributed under the Creative Commons Attribution License, which permits unrestricted use, distribution, and reproduction in any medium, provided the original work is properly cited.

The use of graph theory can be visualized in nanochemistry, computer networks, Google maps, and molecular graph which are common areas to elaborate application of this subject. In nanochemistry, a numeric number (topological index) is used to estimate the biological, physical, and structural properties of chemical compounds that are associated with the chemical graph. In this paper, we compute the first and second multiplicative Zagreb indices ($M_1(G)$ and $(M_1(G))$), generalized multiplicative geometric arithmetic index ($GA^{aII}(G)$), and multiplicative sum connectivity and multiplicative product connectivity indices ($SCII(G)$ and $PCII(G)$) of $SiC_4 - I[m, n]$ and $SiC_4 - II[m, n]$.

1. Introduction

Chemical graph theory is the branch in which mathematical chemistry is concerned with nontrivial graphs and its applications in molecular issues. The major purpose of chemical graph theory is to employ algebraic invariants to reduce a molecule's topological structure to a single number which characterizes to the molecule's energy, orbitals, molecular branching, structural fragments, and electronic structures, among others. The topological index is a numerical value associated with chemical constitutions that suggest a link between chemical structures and a variety of physical qualities which measure chemical reactivity or biological activity. Topological indices are also called molecular descriptor. They are used to investigate certain physical features of a molecule by analyzing mathematical values. As a result, it is an effective way to eliminate costly and time-consuming laboratory trials. Molecular descriptors play an important role in mathematical chemistry, especially in quantitative structure

relationships (QSAR) and quantitative structure activity relationship (QSAR) investigation.

There are some other valueable structure problems existing in real life which can be addressed by graphical representation such as optimal frequency assignments in Radio (see [1, 2]). The topological indices are beneficial to justify the characteristics of chemical compounds such as melting, boiling, and flash points; other properties such as heat of formation, heat of vaporization, density, and pressure can also be estimated by these graph invariants. Due to great significance, it attracts the interest of many researchers. The first topological index was Wiener index given by Harnold Wiener in 1947 [2]. Some Zagreb indices are very close to the wiener index [3], Gutman [4] worked on the multiplicative degree-based TIs for tree graphs, Kwunet et al. studied the multiplicative degree-based TIs for the silicon carbides [5], Hayat et al. [6] worked on many degree-based molecular descriptors for silicates, oxides, hexagonal, and honeycombs, Darafsheh [7] introduced various suitable ways and techniques to estimate the Wiener index, Padmaker-Ivan index,

and Szeged index, Kulli [8] wrote on F-indices on chemical networks, M. Saddiqui defined Zagreb indices for symmetrical nanotubes [9], Geo et al. worked for the Zagreb indices for the nanotubes [10], and Idrees et al. apply molecular descriptors to the benzenoid system [11]. Ayachye and Alameri [12] defined the topological indices such as Wiener index, hyper-Wiener index, Zagreb index, Schultz index, and modified Schultz index for mk graphs. Geo et al. [13] defined the eccentricity-based TIs for the class of cycloalkanes. For more studies about the TIs for chemical and other graphs, see [14–17].

2. Preliminaries

Let $G = (V, E)$ be a graph with $V(G)$ as vertex set and $E(G)$ as edges' set. The degree of vertex V is denoted by $d(v)$ as the number of edges incident to a vertex V . In this paper, we will discuss simple (with no loops or multiple edges), undirected (graph has no distinction between two vertices associated with each edge), and connected graph is said to be connected if there is a path between every pair vertex. In [18], Kulli et al. defined the first and second generalized multiplicative Zagreb indices:

$$\begin{aligned} M_1(G) &= \prod_{uv \in E(G)} (d(u) + d(v))^\alpha, \\ M_2(G) &= \prod_{uv \in E(G)} (d(u) \times d(v))^\alpha. \end{aligned} \quad (1)$$

For the properties of multiplicative Zagreb indices, see [19–22].

Multiplicative sum connectivity and multiplicative product connectivity indices are defined as

$$\begin{aligned} \text{SCII}(G) &= \prod_{uv \in E(G)} \frac{1}{\sqrt{d(u) + d(v)}}, \\ \text{PCII}(G) &= \prod_{uv \in E(G)} \frac{1}{\sqrt{d(u) \times d(v)}}. \end{aligned} \quad (2)$$

For more information, see [23].

In [24], multiplicative atomic bond connectivity index is defined as

$$\text{ABCII}(G) = \prod_{uv \in E(G)} \sqrt{\frac{d(u) + d(v) - 2}{d(u) \times d(v)}}. \quad (3)$$

Multiplicative geometric arithmetic index [25] and generalized multiplicative geometric arithmetic index [26] are defined as

$$\begin{aligned} \text{GAII}(G) &= \prod_{uv \in E(G)} \frac{2\sqrt{d(u) \times d(v)}}{d(u) + d(v)}, \\ \text{GA}^\alpha\text{II}(G) &= \prod_{uv \in E(G)} \left(\frac{2\sqrt{d(u) \times d(v)}}{d(u) + d(v)} \right)^\alpha. \end{aligned} \quad (4)$$

Note: if we put

- (i) For $\alpha = 1$, first and second generalized multiplicative Zagreb indices become first and second multiplicative Zagreb indices
- (ii) For $\alpha = 2$, first and second generalized multiplicative Zagreb indices become first and second hypermultiplicative Zagreb indices
- (iii) For $\alpha = (-1/2)$, first and second generalized multiplicative Zagreb indices become multiplicative sum connectivity and multiplicative product connectivity indices.
- (iv) For $\alpha = (-1/2)$, first and second generalized multiplicative Zagreb indices become multiplicative sum connectivity and multiplicative product connectivity indices

3. 2D Structure of Silicon Carbide for $\text{SiC}_4 - I[m, n]$

The construction of 2D structure of silicon carbide for $\text{SiC}_4 - I[m, n]$ is shown in Figure 1, where one unit of $\text{SiC}_4 - I[m, n]$ is displayed in (a). In this molecular graph, m denotes the number of cells attached in a single row and n denotes the number of total rows in which each row contains m cells. Figures 1(b)–1(d) indicate how unit cells are connected in one row and then one row to another row and so on. Furthermore, it is discussed how unit cell connect each other to get more columns and rows which enhance physical development of the structure $\text{SiC}_4 - I[m, n]$ with different orders.

The simple methodology of constructing chemical structure above by considering increment in number to connect the unit cells in m direction increases the length of row, while increase in unit cell in n style means the number of row is increasing. Consequently, the total numbers of vertices, edges, and faces in $\text{SiC}_4 - I[m, n]$ are

$$\begin{aligned} |V(\text{SiC}_4 - I[m, n])| &= 10mn, \\ |E(\text{SiC}_4 - I[m, n])| &= 12mn - m - n, \\ |F(\text{SiC}_4 - I[m, n])| &= 2mn - m - n + 2. \end{aligned} \quad (5)$$

Later on, by changing rows and columns, we discuss the different properties of carbon and silicon structure.

3.1. Methodology of Silicon Carbide $\text{SiC}_4 - I[m, n]$ Formulas. We will make different order structures of $\text{SiC}_4 - I[m, n]$ by connecting the unit cells in different sequences, in horizontal way, and then in vertical way to form new structures. It is a very easy method to calculate the melting and boiling points and other properties of chemical structures without costly experiments.

3.2. Edge Partition for $\text{SiC}_4 - I[m, n]$. According to the end point, degrees of edges $\text{SiC}_4 - I[m, n]$ are divided into five categories.

By Table 1, the general form of edges partition with the frequency is given in Table 2, where $m, n \geq 1$ and edge parcel uv contains 2 edges when $d(u) = 2$ and $d(v) = 1$; other four parcels are also shown. In graph G of $\text{SiC}_4 - I[m, n]$, it is

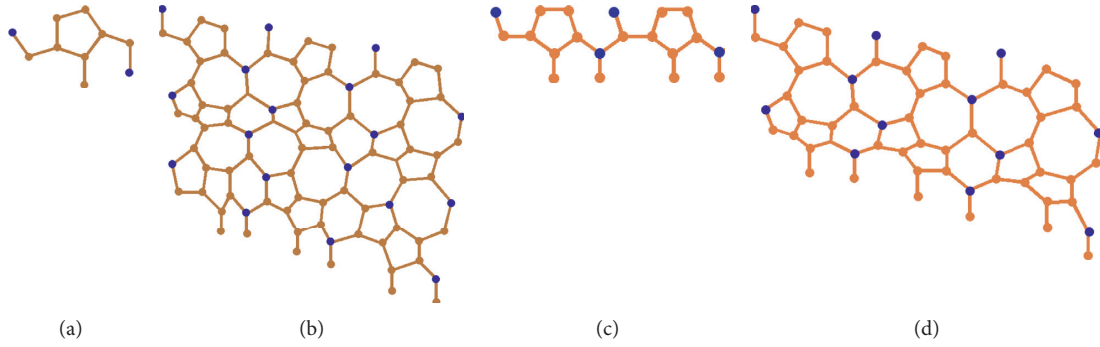


FIGURE 1: Two-dimensional structure of $\text{SiC}_4I[m, n]$: chemical unit cell of (a) $\text{SiC}_4 - I[m, n]$, (b) $\text{SiC}_4 - I[3, 3]$, (c) $\text{SiC}_4 - I[3, 1]$, and (d) $\text{SiC}_4 - I[3, 2]$, where carbon atoms C are brown and silicon atoms Si are blue.

TABLE 1: Edge partition of $\text{SiC}_4 - I[m, n]$.

$[m, n]$	[1, 1]	[2, 1]	[3, 1]	[1, 2]	[2, 2]	[3, 2]	[1, 3]	[2, 3]	[3, 3]
E_{12}	2	2	2	2	2	2	2	2	2
E_{13}	1	4	7	1	4	7	1	4	7
E_{22}	1	2	3	3	4	5	5	6	7
E_{23}	4	6	8	8	10	12	12	14	16
E_{33}	2	7	12	9	29	49	16	51	86

TABLE 2: Edges' partition of $\text{SiC}_4 - I[m, n]$, for $m, n \geq 2$.

Edges	$(d(u), d(v))$	Frequency
E_1	(2,1)	2
E_2	(3,1)	$3m-2$
E_3	(2,2)	$m+2n-2$
E_4	(2,3)	$2m+4n-2$
E_5	(3,3)	$15mn-10m-8n+5$

calculated that the total number of vertices and edges are $10mn$ and $12mn - m - n$, respectively. Thus, the edge set of $\text{SiC}_4 - I[m, n]$ with $m, n \geq 1$ has 5 partitions.

4. Computational Results for Silicon Carbide $\text{SiC}_4 - I[m, n]$

In this partition, we compute ev -degree- and ve -degree-based topological indices such as the ev -degree Zagreb index, first ve -

degree Zagreb beta index, the second ve -degree Zagreb index, ev -degree Randic index, ve -degree atom bond connectivity index, ve -degree geometric index, and ve -degree sun connectivity index of silicon carbide $\text{SiC}_4 - I[m, n]$.

Theorem 1. Let $\text{SiC}_4 - I[m, n]$ be the silicon carbide. Then,

$$\begin{aligned}
 MZ_1^\alpha(\text{SiC}_4 - I[m, n]) &= (2)^{\alpha(15mn - 2m - 4n - 3)} \times (3)^{\alpha(15mn - 10m - 8n + 7)} \times (5)^{\alpha(2m + 4n - 2)}, \\
 MZ_2^\alpha(\text{SiC}_4 - I[m, n]) &= (2)^{4\alpha(m + 2n - 1)} \times (3)^{3\alpha(10mn - 5m - 4n + 2)}, \\
 GA^\alpha\Pi(\text{SiC}_4 - I[m, n]) &= (\sqrt{2})^{\alpha(12n - 4)} \times (\sqrt{3})^{\alpha(5m + 4n - 8)} \times (5)^{\alpha(-2m - 4n + 2)}.
 \end{aligned}
 \tag{6}$$

Proof

$$\begin{aligned}
 MZ_1^\alpha(\text{SiC}_4 - I[m, n]) &= \prod_{uv \in E(\text{SiC}_4 - I[m, n])} (d(u) + d(v))^\alpha \\
 &= (2 + 1)^{2\alpha} \times (2)^{\alpha(6m - 4)} \times (2)^{\alpha(2m + 4n - 4)} \times (5)^{\alpha(2m + 4n - 2)} \times (2)^{\alpha(15mn - 10m - 8n + 5)} \times (3)^{\alpha(15mn - 10m - 8n + 5)} \\
 &= (2)^{\alpha(15mn - 2m - 4n - 3)} \times (3)^{\alpha(15mn - 10m - 8n + 7)} \times (5)^{\alpha(2m + 4n - 2)},
 \end{aligned}$$

$$\begin{aligned}
MZ_2^\alpha(\text{SiC}_4 - I[m, n]) &= \prod_{uv \in E(\text{SiC}_4 - I[m, n])} (d(u) \times d(v))^\alpha \\
&= (2)^{2\alpha} \times (3)^{\alpha(3m-2)} \times (2)^{\alpha(2m+4n-4)} \times (2)^{\alpha(2m+4n-2)} \times (3)^{\alpha(2m+4n-2)} \times (3)^{\alpha(30mn-20m-16n+10)} \\
&= (2)^{4\alpha(m+2n-1)} \times (3)^{3\alpha(10mn-5m-4n+2)}, \\
\text{GA}^\alpha \text{II}(\text{SiC}_4 - I[m, n]) &= \prod_{uv \in E(\text{SiC}_4 - I[m, n])} \left(2 \frac{\sqrt{d(u) \times d(v)}}{d(u) + d(v)} \right)^\alpha \\
&= \left(\frac{2\sqrt{2}}{3} \right)^{2\alpha} \times \left(\frac{2\sqrt{3}}{4} \right)^{\alpha(3m-2)} \times \left(\frac{2(2)}{4} \right)^{\alpha(m+2n-2)} \times \left(\frac{2\sqrt{6}}{5} \right)^{\alpha(2m+4n-2)} \times \left(\frac{2(3)}{3+3} \right)^{\alpha(15mn-10m-8n+5)} \\
&= (\sqrt{2})^{\alpha(12n+4)} \times (\sqrt{3})^{\alpha(5m+4n-8)} \times (5)^{\alpha(-2m-4n+2)}.
\end{aligned} \tag{7}$$

□

Theorem 2. Let $(\text{SiC}_4 - I[m, n])$ be the silicon carbide. Then,

$$\begin{aligned}
MZ_1(\text{SiC}_4 - I[m, n]) &= (2)^{(15mn-2m-4n-3)} \times (3)^{(15mn-10m-8n+7)} \times (5)^{(2m+4n-2)}, \\
MZ_2(\text{SiC}_4 - I[m, n]) &= (2)^{4(m+2n-1)} \times (3)^{3(10mn-5m-4n+2)}, \\
\text{GAII}(\text{SiC}_4 - I[m, n]) &= (\sqrt{2})^{(12n-4)} \times (\sqrt{3})^{(5m+4n-8)} \times (5)^{(-2m-4n+2)}.
\end{aligned} \tag{8}$$

Proof. Taking $\alpha = 1$ in Theorem 1, we get results. □

Theorem 3. Let $\text{SiC}_4 - I[m, n]$ be the silicon carbide. Then,

$$\begin{aligned}
\text{HII}_1(\text{SiC}_4 - I[m, n]) &= (2)^{2(15mn-2m-4n-3)} \times (3)^{2(15mn-10m-8n+7)} \times (5)^{2(2m+4n-2)}, \\
\text{HII}_2(\text{SiC}_4 - I[m, n]) &= (2)^{8(m+2n-1)} \times (3)^{6(10mn-5m-4n+2)}.
\end{aligned} \tag{9}$$

Proof. Taking $\alpha = 2$ in Theorem 1, we get results. □

Theorem 4. Let $(\text{SiC}_4 - I[m, n])$ be the silicon carbide. Then,

$$\begin{aligned}
\text{SCII}(\text{SiC}_4 - I[m, n]) &= \left(\frac{1}{\sqrt{2}} \right)^{(15mn-2m-4n-3)} \times \left(\frac{1}{\sqrt{3}} \right)^{(15mn-10m-8n+7)} \times \left(\frac{1}{\sqrt{5}} \right)^{(2m+4n-2)}, \\
\text{PCII}(\text{SiC}_4 - I[m, n]) &= \left(\frac{1}{\sqrt{2}} \right)^{4(m+2n-1)} \times \left(\frac{1}{\sqrt{3}} \right)^{3(10mn-5m-4n+2)}.
\end{aligned} \tag{10}$$

Proof. Taking $\alpha = (-1/2)$ in Theorem 1,

$$\begin{aligned} \text{SCII}(\text{SiC}_4 - I[m, n]) &= (2)^{(-1/2)(15mn-2m-4n-3)} \times (3)^{(-1/2)(15mn-10m-8n+7)} \times (5)^{(-1/2)(2m+4n-2)} \\ &= \left(\frac{1}{\sqrt{2}}\right)^{(15mn-2m-4n-3)} \times \left(\frac{1}{\sqrt{3}}\right)^{(15mn-10m-8n+7)} \times \left(\frac{1}{\sqrt{5}}\right)^{(2m+4n-2)}, \\ \text{PCII}(\text{SiC}_4 - I[m, n]) &= (2)^{4(-1/2)(m+2n-1)} \times (3)^{3(-1/2)(10mn-5m-4n+2)} \\ &= \left(\frac{1}{\sqrt{2}}\right)^{4(m+2n-1)} \times \left(\frac{1}{\sqrt{3}}\right)^{3(10mn-5m-4n+2)}. \end{aligned} \quad (11)$$

Theorem 5. Let $\text{SiC}_4 - I[m, n]$ be a graph of silicon carbide. Then,

$$\text{ABCII}(\text{SiC}_4 - I[m, n]) = \left(\frac{1}{\sqrt{2}}\right)^{(3m+6n-2)} \times \left(\frac{2}{3}\right)^{(3/2)(15mn-7m-8n+3)}. \quad (12)$$

Proof.

$$\begin{aligned} \text{ABCII}(\text{SiC}_4 - I[m, n]) &= \prod_{uv \in \text{ESiC}_4 - I[m, n]} \sqrt{\frac{d(u) + d(v) - 2}{d(u) \times d(v)}} \\ &= \left(\sqrt{\frac{1}{2}}\right)^2 \times \left(\sqrt{\frac{2}{3}}\right)^{(3m-2)} \times \left(\sqrt{\frac{2}{4}}\right)^{(m+2n-2)} \times \left(\sqrt{\frac{3}{6}}\right)^{(2m+4n-2)} \times \left(\sqrt{\frac{4}{9}}\right)^{(15mn-10m-8n+5)} \\ &= \left(\frac{1}{\sqrt{2}}\right)^{(3m+6n-2)} \times \left(\frac{2}{3}\right)^{(3/2)(15mn-7m-8n+3)}. \end{aligned} \quad (13)$$

4.1. Discussion and Graphical Representations. In this section, we discuss graphs related to multiplicative degree-based topological indices which notify the variation in the characteristics of $\text{SiC}_4 - I[m, n]$.

Figure 2 graphs are panned drawing formed by lines and points used to express the specific sequence in data and information. As graphs have different dimensions, accordingly, the used parameter such as in Figure 2 all graphs of silicon carbide are three dimensional. We have seven graphs in Figure 2 (say 2(a), 2(b), 2(c), 2(d), 2(e), 2(f), and 2(g)) representing first multiplicative Zagreb index (MZ_1), second multiplicative Zagreb index (MZ_2), multiplicative geometric arithmetic index ($\text{GA}^\alpha \text{II}(G)$), first and second hyper-Zagreb index, sum connectivity, and product connectivity index ($\text{SCII}(G)$ and $\text{PCII}(G)$), respectively. Our parameters have ranged from zero to one in which most of the changes in our graphs (including in Figure 2) occur in constant behavior. For instant, in Figure 2(a), multiplicative first Zagreb index (MZ_1) shows mode straight from 0 to 1 and then increasing uniformly. All the graphs except Figure 2(c) are derived from generalized Zagreb index.

Zagreb index (ZI) is very useful, old, and effective graph parameter. It is used in network theory, molecular chemistry, and many branches of mathematics, drugs and organic chemistry. It is also used for the measurement of Skelton of branching of carbon atoms and π -electron energy in the organic compounds in chemistry. These graphs first decrease and then increase quickly which means the values of ZI are changes with respect to our parameters m and n . In graph in Figure 2(c), by increasing the values of m and n , multiplicative geometric arithmetic ($\text{GAII}(\text{SiC}_4 - I[m, n])$) index also increases. The GA index is beneficial to find Kovats constants and boiling points of molecules.

5. 2D Structure of Silicon Carbide $\text{SiC}_4 - \text{II}[m, n]$

The 2D molecular structure of $\text{SiC}_4 - \text{II}[m, n]$ is given in Figures 3 and 4, respectively. As the unit cell is the basic of any structure which provides building blocks of the chemical structures, if we connect the unit cells in m direction, then it increases the length of row, while if it increases unit cell in n style, then it enhances the number of rows.

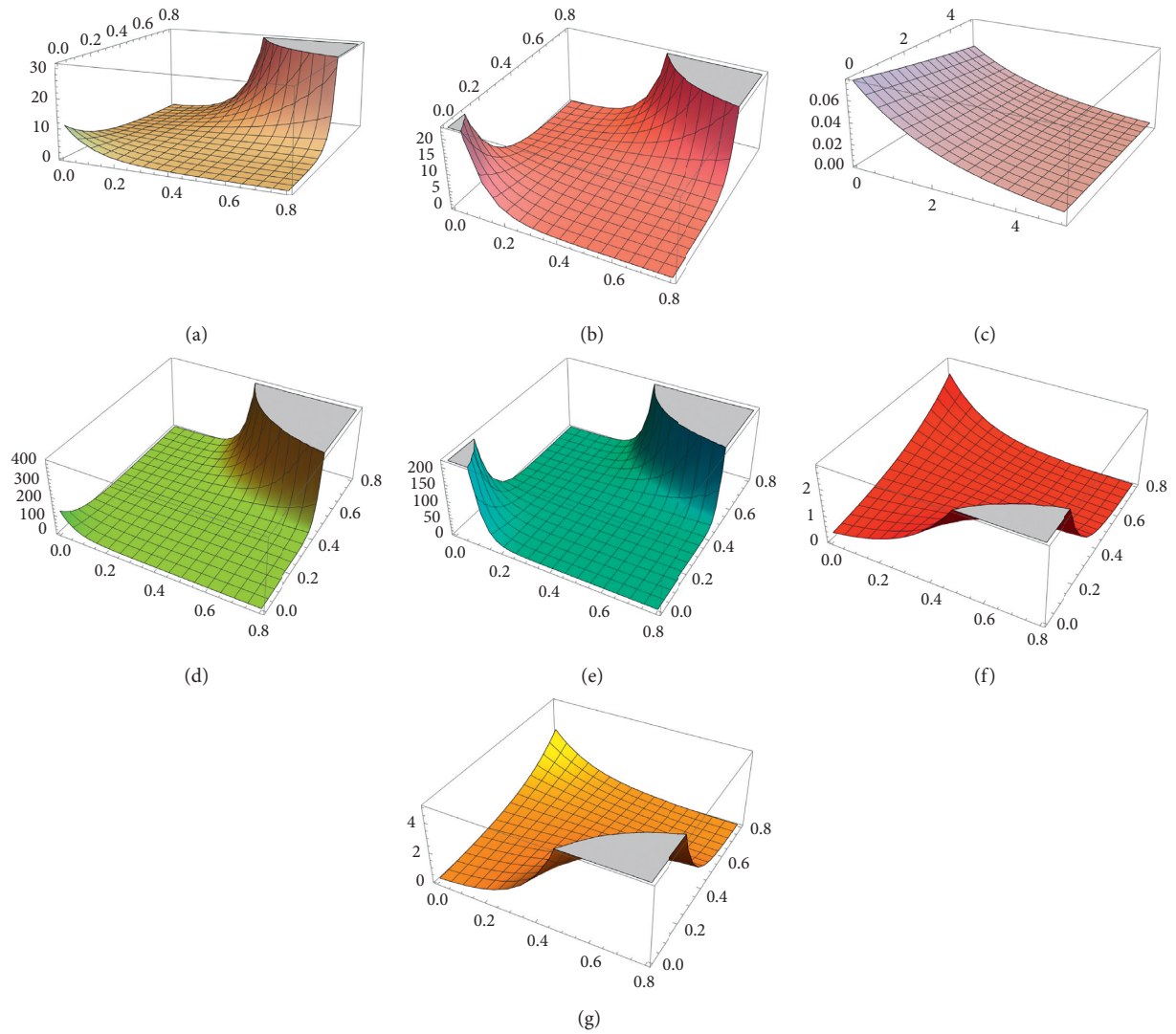


FIGURE 2: The graph of seven multiplicative degree-based topological indices for the silicon carbide $SiC_4 - I[m, n]$ described for $0 \leq m$ and $n \leq 0.8$. (a) MZ_1 for $SiC_4 - I[m, n]$. (b) MZ_2 for $SiC_4 - I[m, n]$. (c) GAI for $SiC_4 - I[m, n]$. (d) HII_1 for $SiC_4 - I[m, n]$. (e) HII_2 for $SiC_4 - I[m, n]$. (f) $SCII$ for $SiC_4 - I[m, n]$. (g) $PCII$ for $SiC_4 - I[m, n]$.

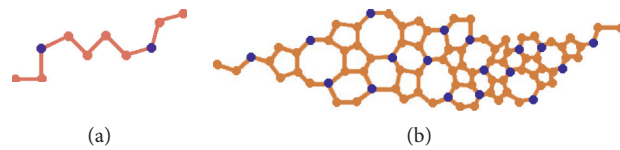


FIGURE 3: Two-dimensional structure of $SiC_4 - II[m, n]$. (a) A unit cell of $SiC_4 - II[m, n]$. (b) $SiC_4 - II[m, n]$ for $m=3$ and $n=3$.

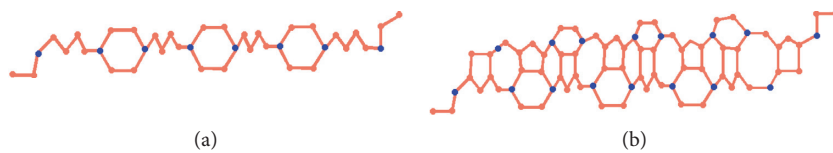


FIGURE 4: $SiC_4 - II[m, n]$, two rows connected each other by edges, where $m=4$ and $n=1$. (a) $SiC_4 - II[m, n]$, one row with $m=4$ and $n=1$. (b) $SiC_4 - II[m, n]$ for $m=3$ and $n=3$.

The quantity of vertices and edges in $\text{SiC}_4 - \text{II}[m, n]$ are represented as

$$\begin{aligned} |V(\text{SiC}_4 - \text{II}[m, n])| &= 10mn, \\ |E(\text{SiC}_4 - \text{II}[m, n])| &= 15mn - 4m - 2n. \end{aligned} \quad (14)$$

5.1. Methodology of Silicon Carbide $\text{SiC}_4 - \text{II}[m, n]$ and Formula. For the derivation of the formulae, firstly, use unit cell and then combine it to make different order structures of $\text{SiC}_4 - \text{II}[m, n]$. If we connect the unit cells in the horizontal way up to m unit cells, then we connect these unit cells in a vertical way up to n , and we obtained various form of chemical graph of $\text{SiC}_4 - \text{II}[m, n]$, as shown previously in Figures 3 and 4. For this, MATLAB is basically used for the generalizing of formulas, where the generalized formula can be found by the calculations.

5.2. Edge Partition of $\text{SiC}_4 - \text{II}[m, n]$. In order to find the other topological indices, we make partition of the edges of $\text{SiC}_4 - \text{II}[m, n]$. By using combinatorial counting and standard edge partition, one can find the generalizing formulae of the edge partition for $\text{SiC}_4 - \text{II}[m, n]$. There are total four different edge parcels in the case of $\text{SiC}_4 - \text{II}[m, n]$.

The first parcel contains only 2 edges uv , where $d(u) = 1$ and $d(v) = 2$, while in second parcel, there are $2m + 2$ edges uv , where $d(u) = 2$ and $d(v) = 2$. Furthermore, third parcel contains $12m + 8n - 14$ edges uv , where $d(u) = 2$ and $d(v) = 3$, and in the final parcel, the number of edges uv are $15mn - 10n - 18m + 10$ with both degrees of 3 as given in Table 3. Consider G as the graph of $\text{SiC}_4 - \text{II}[m, n]$ (see Figures 3 and 4) and note that the total number of vertices, edges, and faces are $10mn$, $15mn - 4m - 2n$, and $5mn - 4m - 2n + 2$, respectively. Thus, the edge set of $\text{SiC}_4 - \text{II}[m, n]$ with $m, n \geq 1$ has 4 partitions.

6. Computational Results for Silicon Carbide $\text{SiC}_4 - \text{II}[m, n]$

In this partition, we compute ev -degree- and ve -degree-based topological indices such as the ev -degree Zagreb index, first ve -degree Zagreb beta index, the second ve -degree Zagreb index, ev -degree Randić index, ve -degree atom bond connectivity index, ve -degree geometric index, and ve -degree sum connectivity index for silicon carbide $\text{SiC}_4 - \text{II}[m, n]$.

Theorem 6. Let $\text{SiC}_4 - \text{II}[m, n]$ be the silicon carbide. Then,

$$\begin{aligned} MZ_1^\alpha(\text{SiC}_4 - \text{II}[m, n]) &= (2)^{\alpha(15mn - 14m - 10n + 14)} \times (3)^{\alpha(15mn - 18m - 10n + 12)} \times (5)^{2\alpha(6m + 4n - 7)}, \\ MZ_2^\alpha(\text{SiC}_4 - \text{II}[m, n]) &= (2)^{8\alpha(2m + n - 1)} \times (3)^{6\alpha(5mn - 4m - 2n + 4)}, \\ GA^\alpha \text{II}(\text{SiC}_4 - \text{II}[m, n]) &= (2)^{\alpha(18n + 12n - 18)} \times (3)^{\alpha(6m + 4n - 9)} \times (5)^{\alpha(-12m - 8n + 14)}. \end{aligned} \quad (15)$$

Proof.

$$\begin{aligned} MZ_1^\alpha(\text{SiC}_4 - \text{II}[m, n]) &= \prod_{uv \in E(\text{SiC}_4 - \text{II}[m, n])} (d(u) + d(v))^\alpha \\ &= (3)^{2\alpha} \times (2)^{2\alpha(2m + 2)} \times (5)^{\alpha(12m + 8n - 14)} \times (2)^{\alpha(15mn - 10n - 18m + 10)} \times (3)^{\alpha(15mn - 10n - 18m + 10)} \\ &= (2)^{\alpha(15mn - 14m - 10n + 14)} \times (3)^{\alpha(15mn - 18m - 10n + 12)} \times (5)^{2\alpha(6m + 4n - 7)}, \\ MZ_2^\alpha(\text{SiC}_4 - \text{II}[m, n]) &= \prod_{uv \in E(\text{SiC}_4 - \text{II}[m, n])} (d(u) \times d(v))^\alpha \\ &= (2)^{2\alpha} \times (2)^{2\alpha(2m + 2)} \times (2)^{\alpha(12m + 8n - 14)} \times (3)^{\alpha(12m + 8n - 14)} \times (3)^{2\alpha(15mn - 10n - 18m + 10)} \\ &= (2)^{8\alpha(2m + n - 1)} \times (3)^{6\alpha(5mn - 4m - 2n + 4)}, \\ GA^\alpha \text{II}(\text{SiC}_4 - \text{II}[m, n]) &= \prod_{uv \in E(\text{SiC}_4 - \text{II}[m, n])} \left(2 \frac{\sqrt{d(u) \times d(v)}}{d(u) + d(v)} \right)^\alpha \\ &= \left(\frac{2\sqrt{2}}{3} \right)^{2\alpha} \times \left(\frac{2(2)}{4} \right)^{\alpha(2m + 2)} \times \left(\frac{2\sqrt{2} \sqrt{3}}{5} \right)^{\alpha(12m + 8n - 14)} \times \left(\frac{2(3)}{6} \right)^{\alpha(15mn - 10n - 18m + 10)} \\ &= (2)^{\alpha(18m + 12n - 18)} \times (3)^{\alpha(6m + 4n - 9)} \times (5)^{\alpha(-12m - 8n + 14)}. \end{aligned} \quad (16)$$

□

TABLE 3: Edges' partition of $\text{SiC}_4 - \text{II}[m, n]$.

Edges	$(d(u), d(v))$	Frequency
E_1	(1, 2)	2
E_2	(2, 2)	$2m + 2$
E_3	(2, 3)	$12m + 8n - 14$
E_4	(3, 3)	$15mn - 10n - 18m + 10$

Theorem 7. Let $(\text{SiC}_4 - \text{II}[m, n])$ be the silicon carbide. Then,

$$\begin{aligned} MZ_1(\text{SiC}_4 - \text{II}[m, n]) &= (2)^{(15mn - 14m - 10n + 14)} \times (3)^{(15mn - 18m - 10n + 12)} \times (5)^{2(6m + 4n - 7)}, \\ MZ_2(\text{SiC}_4 - \text{II}[m, n]) &= (2)^{8(2m + n - 1)} \times (3)^{6(5mn - 4m - 2n + 4)}, \\ \text{GAII}(\text{SiC}_4 - \text{II}[m, n]) &= (2)^{\alpha(18m + 12n - 18)} \times (3)^{\alpha(6m + 4n - 9)} \times (5)^{\alpha(-12m - 8n + 14)}. \end{aligned} \quad (17)$$

Proof. Taking $\alpha = 1$ in Theorem 6, we get results. \square

Theorem 8. Let $\text{SiC}_4 - \text{II}[m, n]$ be the silicon carbide. Then,

$$\begin{aligned} \text{HII}_1(\text{SiC}_4 - \text{II}[m, n]) &= (2)^{2(15mn - 14m - 10n + 14)} \times (3)^{2(15mn - 18m - 10n + 12)} \times (5)^{4(6m + 4n - 7)}, \\ \text{HII}_2(\text{SiC}_4 - \text{II}[m, n]) &= (2)^{16(2m + n - 1)} \times (3)^{12(5mn - 4m - 2n + 4)}. \end{aligned} \quad (18)$$

Proof. Taking $\alpha = 2$ in Theorem 4.6, we get results. \square

Theorem 9. Let $\text{SiC}_4 - \text{II}[m, n]$ be the silicon carbide. Then,

$$\begin{aligned} \text{SCH}(\text{SiC}_4 - \text{II}[m, n]) &= \left(\frac{1}{\sqrt{2}}\right)^{(15mn - 14m - 10n + 14)} \times \left(\frac{1}{\sqrt{3}}\right)^{(15mn - 18m - 10n + 12)} \times \left(\frac{1}{\sqrt{5}}\right)^{2(6m + 4n - 7)}, \\ \text{PCII}(\text{SiC}_4 - \text{II}[m, n]) &= \left(\frac{1}{\sqrt{2}}\right)^{8(2m + n - 1)} \times \left(\frac{1}{\sqrt{3}}\right)^{6(5mn - 4m - 2n + 4)}. \end{aligned} \quad (19)$$

Proof. Using $\alpha = (-1/2)$ in Theorem 4.6, we obtain

$$\begin{aligned} \text{SCH}(\text{SiC}_4 - \text{II}[m, n]) &= (2)^{(-1/2)(15mn - 14m - 10n + 14)} \times (3)^{(-1/2)(15mn - 18m - 10n + 12)} \times (5)^{2(-1/2)(6m + 4n - 7)} \\ &= \left(\frac{1}{\sqrt{2}}\right)^{(15mn - 14m - 10n + 14)} \times \left(\frac{1}{\sqrt{3}}\right)^{(15mn - 18m - 10n + 12)} \times \left(\frac{1}{\sqrt{5}}\right)^{2(6m + 4n - 7)}, \\ \text{PCII}(\text{SiC}_4 - \text{II}[m, n]) &= (2)^{8(-1/2)(2m + n - 1)} \times (3)^{6(-1/2)(5mn - 4m - 2n + 4)} \\ &= \left(\frac{1}{\sqrt{2}}\right)^{8(2m + n - 1)} \times \left(\frac{1}{\sqrt{3}}\right)^{6(5mn - 4m - 2n + 4)}. \end{aligned} \quad (20)$$

Theorem 10. Let $\text{SiC}_4 - \text{II}[m, n]$ be the silicon carbide. Then,

$$\text{ABCII}(\text{SiC}_4 - \text{II}[m, n]) = \left(\frac{1}{\sqrt{2}}\right)^{(-30mn + 50m + 28n - 30)} \times \left(\frac{1}{\sqrt{3}}\right)^{(30mn - 36m - 20n + 20)}. \quad (21)$$

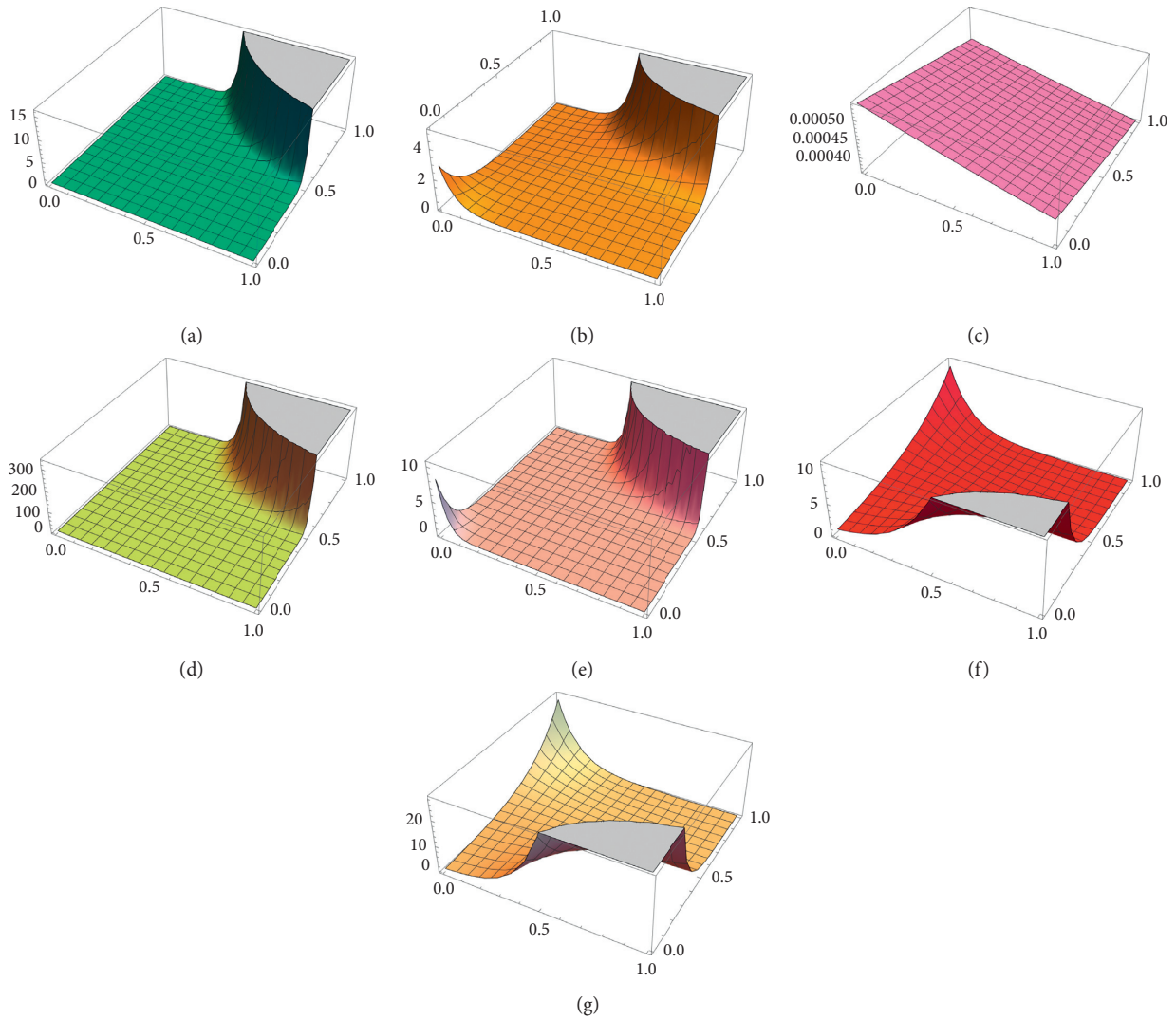


FIGURE 5: The graph of seven multiplicative degree-based topological indices for the silicon carbide $\text{SiC}_4 - \text{II}[m, n]$ are described above for $0 \leq m, n \leq 0.8$. (a) MZ_1 for $\text{SiC}_4 - \text{II}[m, n]$. (b) MZ_2 for $\text{SiC}_4 - \text{II}[m, n]$. (c) GAI for $\text{SiC}_4 - \text{II}[m, n]$. (d) HII_1 for $\text{SiC}_4 - \text{II}[m, n]$. (e) HII_2 for $\text{SiC}_4 - \text{II}[m, n]$. (f) $SCII$ for $\text{SiC}_4 - \text{II}[m, n]$. (g) $PCII$ for $\text{SiC}_4 - \text{II}[m, n]$.

Proof.

$$\begin{aligned}
 ABCII(\text{SiC}_4 - \text{II}[m, n]) &= \prod_{uv \in E(\text{SiC}_4 - \text{II}[m, n])} \sqrt{\frac{d(u) + d(v) - 2}{d(u) \times d(v)}} \\
 &= \left(\frac{1}{\sqrt{2}}\right)^2 \times \left(\frac{1}{\sqrt{2}}\right)^{(2m+2)} \times \left(\frac{1}{\sqrt{2}}\right)^{(12m+8n-14)} \times \left(\frac{2}{3}\right)^{(15mn-18m-10n+10)} \\
 &= \left(\frac{1}{\sqrt{2}}\right)^{(-30mn+50m+28n-30)} \times \left(\frac{1}{\sqrt{3}}\right)^{(30mn-36m-20n+20)}.
 \end{aligned}
 \tag{22}$$

□

6.1. Discussion and Graphical Representations. The graphs given in Figure 5 tell us about the behavior of different multiplicative degree-based topological indices of silicon carbide $\text{SiC}_4 - \text{II}[m, n]$. Silicon carbide is a semiconductor

with many isomers used in almost all electronic gadgets. The range of our parameters is from zero to one. Most of the changes that occur in this range than graphs show constant behavior. In Figure 5(a), multiplicative first Zagreb index is

discussed, where graph from 0 to 1 is straight and constantly uniform and then it eventually increases. The GA index is the extended form of the Randic index which gives faster and better information about the physical and chemical properties of compounds. By increasing the values of m and n , the graph also increase which means the values of boiling points of $\text{SiC}_4 - \text{II}[m, n]$ also increase. Other graphs describe the variation in the values of Zagreb indices by increasing m and n .

7. Conclusion

The graph is an easy way to describe chemistry of relationship in data. Graph is used to present numerous or complicated data in a picture form in less space and has lots of application in almost every field of science. We have discussed many graphical invariants (topological indices) above which considered fixed numbers related to the graphs of chemical structures. We have studied the behavior of different multiplicative versions of degree-based topological indices such as first (MZ_1) and (MZ_2) second Zagreb indices, first and second hyper-Zagreb indices, geometric arithmetic index (GAI), atom bond connectivity index (HII_1) and (HII_2), and sum (SCII) and product connectivity (PCII) index of silicon carbide $\text{SiC}_4 - \text{II}[m, n]$.

Data Availability

No data were used to support the findings of the study.

Conflicts of Interest

The authors declare that they have no conflicts of interest.

References

- [1] K. Yenoke, K. M. Kaabar, M. M. Ali Al-Shamiri, and R. C. Thiviyarathi, "Radial Radio number of hexagonal and its derived networks," *International Journal of Mathematics and Mathematical Sciences*, vol. 2021, Article ID 5101021, 8 pages, 2021.
- [2] K. Yenoke and K. M. Kaabar, "The bounds for the distance two labelling and radio labelling of nanostar tree dendrimer," *Journal of the American Chemical Society*, vol. 69, pp. 17–20, 2021.
- [3] I. Gutman, Ruscic, B. Trinajstić, and N. Wilcox, "Graph theory and molecular orbitals. XII. Acyclic polyenes," *The Journal of Chemical Physics*, vol. 62, no. 9, pp. 3399–4340, 1975.
- [4] I. Gutman, "Multiplicative Zagreb indices of trees," *Bulletin of International Mathematical Virtual Institute*, vol. 18, pp. 17–23, 2011.
- [5] Y. Kwun, A. Virk, W. Nazeer, M. Rehman, and S. Kang, "On the multiplicative degree-based topological indices of silicon-carbon $\text{Si}_2\text{C}_3\text{-I}[p, q]$ and $\text{Si}_2\text{C}_3\text{-II}[p, q]$," *Symmetry*, vol. 10, no. 8, p. 320, 2018.
- [6] S. Hayat and M. Imran, "Computation of topological indices of certain networks," *Applied Mathematics and Computation*, vol. 240, pp. 213–228, 2014.
- [7] M. R. Darafsheh, "Computation of topological indices of some graphs," *Acta Applicandae Mathematicae*, vol. 110, no. 3, pp. 1225–1235, 2010.
- [8] V. R. Kulli, "F-indices of chemical networks," *International Journal of Mathematical Archive*, vol. 10, pp. 21–30, 2019.
- [9] Z. Shao, M. Siddiqui, and M. Muhammad, "Computing Zagreb indices and Zagreb polynomials for symmetrical nanotubes," *Symmetry*, vol. 10, no. 7, pp. 244–254, 2018.
- [10] W. Gao, M. R. Farahani, M. K. Jamil, and M. K. Siddiqui, "The redefined first, second and third Zagreb indices of titania nanotubes $\text{TiO}_2[m, n]$," *The Open Biotechnology Journal*, vol. 10, no. 1, pp. 272–277, 2016.
- [11] N. Idrees, M. N. Naeem, F. Hussain, A. Sadiq, and M. K. Siddiqui, "Molecular descriptors of benzenoid system," *Quimica Nova*, vol. 40, pp. 143–145, 2017.
- [12] A. Ayache and A. Alameri, "Topological indices of the -graph," *Journal of the Association of Arab Universities for Basic and Applied Sciences*, vol. 24, no. 1, pp. 283–291, 2017.
- [13] W. Gao, Y. Chen, and W. Wang, "The topological variable computation for a special type of cycloalkanes," *Journal of Chemistry*, vol. 2017, Article ID 6534758, 8 pages, 2017.
- [14] M. Perc, J. Gmez-Gardes, A. Szolnoki, L. M. Flora, and Y. Moreno, "Evolutionary dynamics of group interactions on structured populations, a review," *Journal of The Royal Society Interface*, vol. 10, 2013.
- [15] Z. Wang, A. Szolnoki, and M. Perc, "If players are sparse social dilemmas are too: importance of percolation forevolution of cooperation," *Scientific Reports*, vol. 2, 2012.
- [16] M. Bacca, J. Horvthov, M. Mokriov, and A. Suhnyiov, "On topological indices of fullerenes," *Applied Mathematics and Computation*, vol. 251, pp. 154–161, 2015.
- [17] S. M. Kamran, S. Manzoor, S. Ahmad, and K. M. Kaabar, "On computation and analysis of entropy measures for crystal structures," *Mathematical Problems in Engineering*, vol. 2021, Article ID 9936949, 16 pages, 2021.
- [18] V. R. Kulli, B. Stone, S. Wang, and B. Wei, "Generalised multiplicative indices of polycyclic aromatic hydrocarbons and benzenoid systems," *Zeitschrift für Naturforschung A*, vol. 72, no. 6, pp. 573–576, 2017.
- [19] C. D. Kinker, Y. Aysun, and N. C. Ismail, "The multiplicative Zagreb indices of graph operations," *Journal of Inequalities and Applications*, vol. 90, pp. 1–8, 2013.
- [20] I. Gutman, "Multiplicative Zagreb indices of trees," *Bulletin of the International Mathematical Virtual Institute*, vol. 18, pp. 17–23, 2011.
- [21] M. Eliasi, A. Iranmanes, and S. Gutmans, "Multiplicative version of first Zagreb index, MATCH common," *MATCH Communications in Mathematical and in Computer Chemistry*, vol. 68, pp. 217–230, 2012.
- [22] S. Wang and B. Wei, "Multiplicative Zagreb indices of k-trees," *Discrete Applied Mathematics*, vol. 180, pp. 168–175, 2015.
- [23] V. R. Kulli, "Multiplicative connectivity indices of $\text{TUC}_4\text{C}_8[m, n]$ and $\text{TUC}_4[m, n]$ nanotubes," *Journal of Mathematical and Computational Science*, vol. 7, pp. 599–605, 2016.
- [24] V. R. Kulli, "New connectivity topological indices," *Annals of pure and applied mathematics*, vol. 20, no. 1, pp. 1–2, 2019.
- [25] I. Gutman, A. Merve, and I. N. Cangul, "Multiplicative geometric arithmetic index," *International Journal of Applied graph theory*, vol. 2, no. 2, pp. 16–28, 2018.
- [26] V. R. Kulli, "Some new multiplicative geometric-arithmetic indices," *Journal of Ultra Scientist of Physical Sciences Section A*, vol. 29, no. 2, pp. 52–57, 2017.

Research Article

On Computation of Edge Degree-Based Banhatti Indices of a Certain Molecular Network

Jiang-Hua Tang,¹ Muhammad Abid,² Kashif Ali,² Asfand Fahad ,³
Muhammad Anwar Chaudhry,⁴ Muhammad Imran Qureshi ,³ and Jia-Bao Liu ,⁵

¹Department of General Education, Anhui Xinhua University, Hefei 230088, China

²Department of Mathematics, COMSATS University Islamabad, Lahore Campus, Lahore, Pakistan

³Department of Mathematics, COMSATS University Islamabad, Vehari Campus, Vehari 61100, Pakistan

⁴Department of Mathematics and Statistics, Institute of Southern Punjab, Multan, Pakistan

⁵School of Mathematics and Physics, Anhui Jianzhu University, Hefei, China

Correspondence should be addressed to Muhammad Imran Qureshi; imranqureshi18@gmail.com

Received 19 August 2021; Accepted 16 October 2021; Published 5 November 2021

Academic Editor: Xiangfeng Yang

Copyright © 2021 Jiang-Hua Tang et al. This is an open access article distributed under the Creative Commons Attribution License, which permits unrestricted use, distribution, and reproduction in any medium, provided the original work is properly cited.

Chemical graph theory deals with the basic properties of a molecular graph. In graph theory, we correlate molecular descriptors to the properties of molecular structures. Here, we compute some Banhatti molecular descriptors for water-soluble dendritic unimolecular polyether micelle. Our results prove to be very significant to understand the behaviour of water-soluble dendritic unimolecular polyether micelle as a drug-delivery agent.

1. Introduction

Topological indices are graph invariants associated with numbers that describe the properties of the graph. In chemical graph theory, topological indices play a vital role to explore the structures of different graphs. In 1947, Harold Wiener gave the idea of topological indices [1]. After that, he published a series of papers describe the relation between wiener index and physicochemical properties of carbon-based compounds [2, 3] in 1947 and [4, 5] in 1948. The analysis of topological indices has great importance in nanotechnology and theoretical chemistry. The irregularity of graph was discussed [6] in 1997. In the last decade of the 20th century, a large number of topological indices were introduced that were related to the Wiener index. In the second decade of the 21st century, irregularity topological indices were computed for different chemical structures. In [7], it was shown that Randic and modified Zagreb indices are in one-to-one correspondence for all acyclic molecules which consist of no more than 100 atoms. In [8], the new notion of total irregularity was introduced, and the authors determined the

graphs with maximum total irregularity. In [9–11], the total irregularity of graphs was discussed under the graph operations. In [12], the total irregularity of graphs was discussed to study QSPR. An Indian mathematician Kulli in 2016 [13] introduced some new Banhatti indices such as K Banhatti indices, modified Banhatti indices and, hyper K Banhatti indices. In the last decade, irregular, distance- and degree-based topological indices became hot topics for research in chemical graph theory. Many researchers computed these indices for different chemical graphs to study their biochemical properties. In [14], Zheng et al. computed some eccentricity-based topological indices and polynomials of Poly(EThylene Amido Amine) (PETAA) dendrimers. In [15], Ye et al. worked on the Zagreb connection number index of nanotubes and regular hexagonal lattice. In [16], Fahad et al. studied the topological descriptors of Poly Propyl Ether Imine (PETIM) dendrimers. In [17], Qureshi studied the Zagreb connection index of drug-related chemical structures. In [18], Zhang et al. worked on a newly defined topological index named face index for silicon carbides. In [19], Luo et al. computed lower bounds on the entire Zagreb indices

of trees. In [20], Chu et al. studied the irregular indices for metal organic frameworks and certain 2D lattices. The Zagreb connection index is computed for silicate, hexagonal, honeycomb, and oxide networks in [21] in 2021. In [22], Rao et al. studied some degree-based topological indices of a caboxy-terminated dendritic macromolecule. In [23], the authors computed the face index for Boron triangular nanotubes and for quadrilateral sections cut from a regular hexagonal lattice. In [24], Hussain et al. computed topological indices for new classes of Benes network.

Let $G(V, E)$ be a graph where V is a set of vertices and E is a set of edges. A cardinality of edges associated with a vertex is called the degree of the vertex. Here, we use a special term of $e = st$ as an edge of G where the vertex s and vertex t are linked together by edge e . Let $d_G(e)$ denote the degree of an edge e in G , which is defined by $d_G(e) = d_G(s) + d_G(t) - 2$ with $e = st$. For more details, refer the work of Kulli [25].

The first and second K Banhatti indices were introduced by Kulli in [13] as

$$\begin{aligned} B_1(G) &= \sum_{e=st \in E(G)} [d_G(s) + d_G(e)], \\ B_2(G) &= \sum_{e=st \in E(G)} [d_G(s) * d_G(e)]. \end{aligned} \quad (1)$$

The first and second K hyper Banhatti index of G were introduced by Kulli in [26] defined as

$$\begin{aligned} HB_1(G) &= \sum_{e=st \in E(G)} [d_G(s) + d_G(e)]^2, \\ HB_2(G) &= \sum_{e=st \in E(G)} [d_G(s) * d_G(e)]^2. \end{aligned} \quad (2)$$

The first and second modified Banhatti indices of G were introduced by Kulli in [27] as

$$\begin{aligned} mB_1(G) &= \sum_{e=st \in E(G)} \left[\frac{1}{(d_G(s) + d_G(e)) + (d_G(t) + d_G(e))} \right], \\ mB_2(G) &= \sum_{e=st \in E(G)} \left[\frac{2}{(d_G(s) + d_G(e)) + (d_G(t) + d_G(e))} \right]. \end{aligned} \quad (3)$$

The harmonic K -Banhatti index of a graph G was introduced by Kulli in [27] as

$$H_b(G) = \sum_{e=st \in E(G)} \left[\frac{2}{(d_G(s) + d_G(e)) + (d_G(t) + d_G(e))} \right]. \quad (4)$$

Let G be a graph of water-soluble dendritic unimolecular polyether micelle. It has $38(2^n) - 4$ number of vertices and $42(2^n) - 5$ number of edges where n is the number of growth of the graph. The graph has $4(2^n)$ number of vertices having degree 1, $22(2^n) - 2$ vertices having degree 2 and $12(2^n) - 2$ vertices having degree 3. The graph has $4(2^n)$ number of edges having degree (1, 3), $8(2^n) + 2$ edges having degree (2, 2), $28(2^n) - 8$ edges having degree (2, 3), and $(2, 3)$ number of edges having degree (3, 3). In Figure 1, the graph G is given for $n = 4$. Dendritic unimolecular micelles play an important role in drug delivery systems. Unimolecular micelles have a unique property of uniform size and high stability. Also, they have attracted increasing attention due to their high functionality in various applications.

In the next section, we will compute the Banhatti indices for the water-soluble dendritic unimolecular polyether micelle.

2. Main Results

Table 1 shows the partition of the edge set for the molecular graph G of water-soluble dendritic unimolecular polyether micelle.

Theorem 1. *Let G be the molecular graph of water-soluble dendritic unimolecular polyether micelle; then, the first K Banhatti index of G is*

$$B_1(G) = 432(2^n) - 58. \quad (5)$$

Proof. By using Table 1 and the definition of the first K Banhatti index, we have

$$\begin{aligned} B_1(G) &= \sum_{e=st \in E(G)} [d_G(s) + d_G(e)], \\ &= 4(2^n)[(1 + 2) + (3 + 2)] + (8(2^n) + 2)[(2 + 2) + (2 + 2)] \\ &\quad + (28(2^n) - 8)[(2 + 3) + (3 + 3)] + (2(2^n) + 1)[(3 + 4) + (3 + 4)], \\ &= 32(2^n) + 64(2^n) + 16 + 308(2^n) - 88 + 28(2^n) + 14, \\ &= 432(2^n) - 58. \end{aligned} \quad (6)$$

□

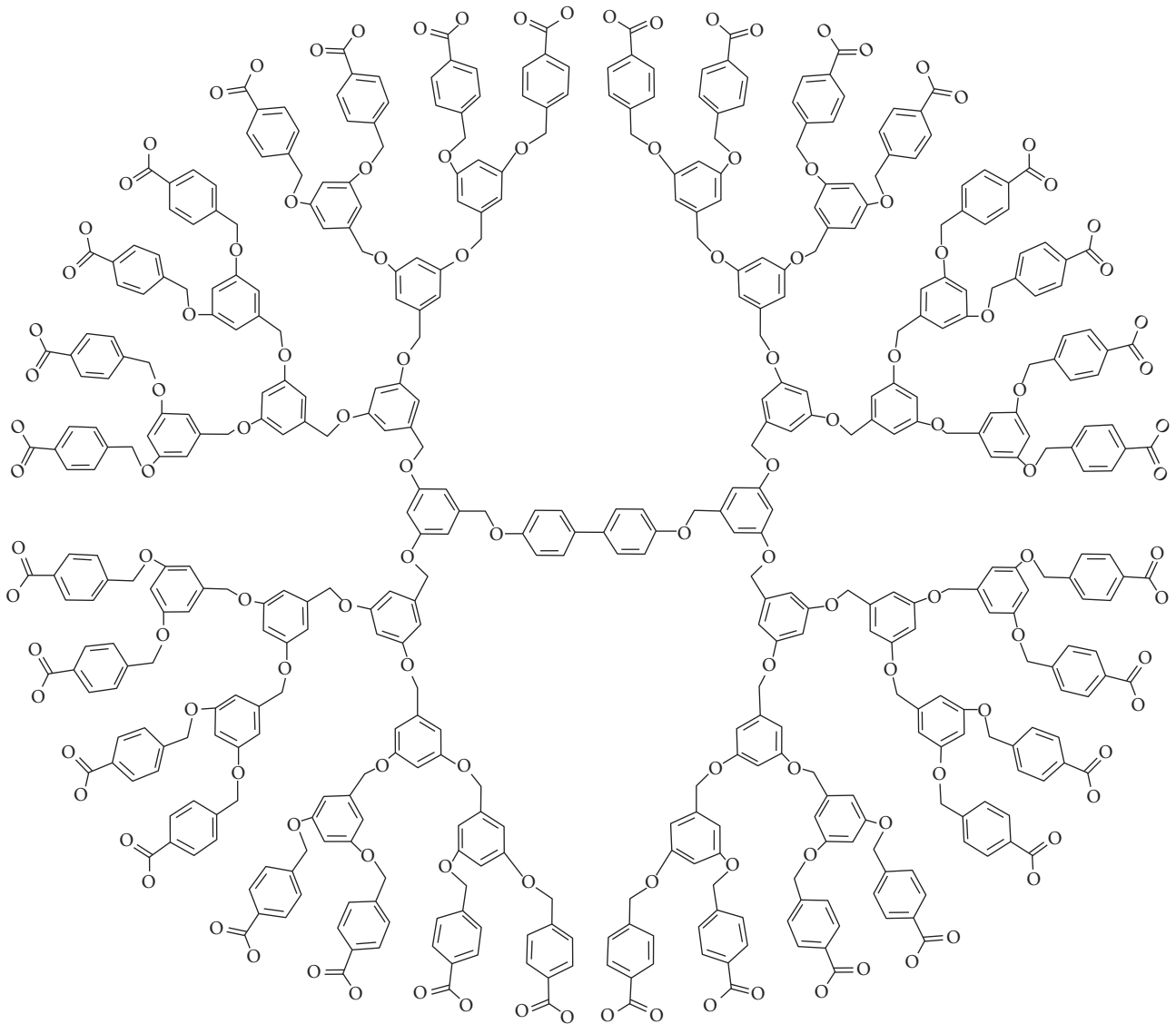


FIGURE 1: Graph of water-soluble unimolecular polyether micelle for growth four.

TABLE 1: Edge partition of water-soluble dendritic unimolecular polyether micelle.

$(d_G(s), d_G(t))$, where $st \in E(G)$	$d_G(e)$	Number of edges
(1, 3)	2	$4(2^n)$
(2, 2)	2	$8(2^n) + 2$
(2, 3)	3	$28(2^n) - 8$
(3, 3)	4	$2(2^n) + 1$

Theorem 2. Let G be the molecular graph of water-soluble dendritic unimolecular polyether micelle; then, the second K Banhatti index of G is

$$B_2(G) = 564(2^n) - 80. \quad (7)$$

Proof. To compute the second K Banhatti index, we will use Table 1.

$$\begin{aligned} B_2(G) &= \sum_{e=steE(G)} [d_G(s) * d_G(e)], \\ &= 4(2^n)[(1 * 2) + (3 * 2)] + (8(2^n) + 2)[(2 * 2) + (2 * 2)] \\ &\quad + (28(2^n) - 8)[(2 * 3) + (3 * 3)] + (2(2^n) + 1)[(3 * 4) + (3 * 4)], \\ &= 32(2^n) + 64(2^n) + 16 + 420(2^n) - 120 + 48(2^n) + 24, \\ &= 564(2^n) - 80. \end{aligned} \quad (8)$$

□

Theorem 3. Let G be the molecular graph of water-soluble dendritic unimolecular polyether micelle; then, the first K hyper Banhatti index of G is

$$HB_1(G) = 2296(2^n) - 326. \quad (9)$$

Proof. The edge partition given in Table 1 and the definition of the first K hyper Banhatti index give

$$\begin{aligned} HB_1(G) &= \sum_{e=steE(G)} [d_G(s) + d_G(e)]^2, \\ &= 4(2^n)[(1 + 2)^2 + (3 + 2)^2] + (8(2^n) + 2)[(2 + 2)^2 + (2 + 2)^2] \\ &\quad + (28(2^n) - 8)[(2 + 3)^2 + (3 + 3)^2] + (2(2^n) + 1)[(3 + 4)^2 + (3 + 4)^2], \\ &= 136(2^n) + 256(2^n) + 64 + 1708(2^n) - 488 + 196(2^n) + 98, \\ &= 2296(2^n) - 326. \end{aligned} \quad (10)$$

□

Theorem 4. Let G be the molecular graph of water-soluble dendritic unimolecular polyether micelle; then, the second K hyper Banhatti index of G is

$$HB_2(G) = 4268(2^n) - 584. \quad (11)$$

Proof. The result follows by using the values from Table 1 and the definition of the second K hyper Banhatti index.

$$\begin{aligned} HB_2(G) &= \sum_{e=steE(G)} [d_G(s) * d_G(e)]^2, \\ &= 4(2^n)[(1 * 2)^2 + (3 * 2)^2] + (8(2^n) + 2)[(2 * 2)^2 + (2 * 2)^2] \\ &\quad + (28(2^n) - 8)[(2 * 3)^2 + (3 * 3)^2] + (2(2^n) + 1)[(3 * 4)^2 + (3 * 4)^2], \\ &= 160(2^n) + 256(2^n) + 64 + 3276(2^n) - 936 + 576(2^n) + 288, \\ &= 4268(2^n) - 584. \end{aligned} \quad (12)$$

□

TABLE 2: Banhatti indices of water-soluble dendritic unimolecular polyether micelle.

Banhatti indices	$n = 1$	$n = 2$	$n = 3$	$n = 4$	$n = 5$
$B_1(G)$	806	1670	3398	6854	13766
$B_2(G)$	1048	2176	4432	8944	17968
$HB_1(G)$	4266	8858	18042	36410	73146
$HB_2(G)$	7952	16488	33560	67704	135992
$mB_1(G)$	7.9709	16.3477	33.1013	66.6085	133.6229
$mB_2(G)$	6.6584	13.5584	27.3584	54.9584	110.1584
$H_b(G)$	15.9416	32.6948	66.2012	133.214	267.2396

Theorem 5. Let G be the molecular graph of water-soluble dendritic unimolecular polyether micelle; then, the first modified Banhatti index of G is

$$mB_1(G) = 4.1884(2^n) - 0.4059. \tag{13}$$

Proof. By using the definition of the first modified Banhatti index and Table 1, we have

$$\begin{aligned} mB_1(G) &= \sum_{e=st \in E(G)} \left[\frac{1}{(d_G(s) + d_G(e)) + (d_G(t) + d_G(e))} \right], \\ &= 4(2^n) \left[\frac{1}{(1+2) + (3+2)} \right] + (8(2^n) + 2) \left[\frac{1}{(2+2) + (2+2)} \right] + \\ &\quad (28(2^n) - 8) \left[\frac{1}{(2+3) + (3+3)} \right] + (2(2^n) + 1) \left[\frac{1}{(3+4) + (3+4)} \right], \\ &= \frac{2^n}{2} + 2^n + \frac{1}{4} + \frac{28(2^n)}{11} - \frac{8}{11} + \frac{2^n}{7} + \frac{1}{14}, \\ &= 4.1884(2^n) - 0.4059. \end{aligned} \tag{14}$$

Theorem 6. Let G be the molecular graph of water-soluble dendritic unimolecular polyether micelle; then, the second modified Banhatti index of G is

$$mB_2(G) = 3.45(2^n) - 0.2416. \tag{15}$$

Proof. The second modified Banhatti index can be computed by using Table 1 as

$$\begin{aligned} mB_2(G) &= \sum_{e=st \in E(G)} \left[\frac{2}{(d_G(s) + d_G(e)) + (d_G(t) + d_G(e))} \right], \\ &= 4(2^n) \left[\frac{1}{(1 \times 2) + (3 \times 2)} \right] + (8(2^n) + 2) \left[\frac{2}{(2 \times 2) + (2 \times 2)} \right] + \\ &\quad (28(2^n) - 8) \left[\frac{2}{(2 \times 3) + (3 \times 3)} \right] + (2(2^n) + 1) \left[\frac{2}{(3 \times 4) + (3 \times 4)} \right], \\ &= \frac{2^n}{2} + 2^n + \frac{1}{4} + \frac{28(2^n)}{15} - \frac{8}{15} + \frac{2^n}{12} + \frac{1}{24}, \\ &= 3.45(2^n) - 0.2416. \end{aligned} \tag{16}$$

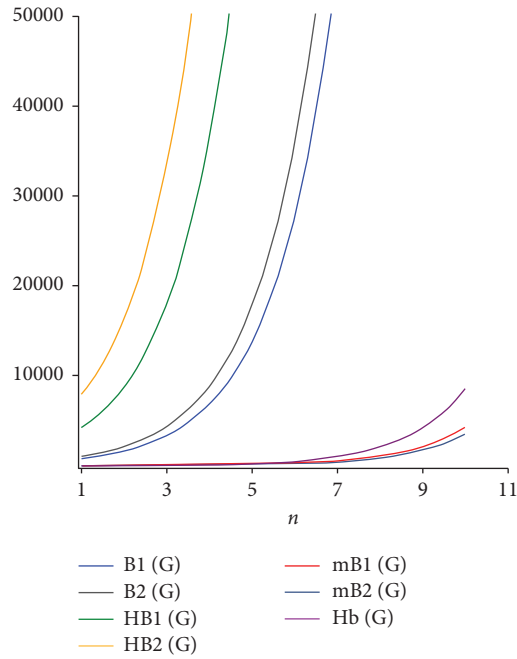


FIGURE 2: Comparison graph of Bhatti indices of water-soluble unimolecular polyether micelle for growth four.

Theorem 7. Let G be the molecular graph of water-soluble dendritic unimolecular polyether micelle; then, the harmonic Bhatti index of G is

$$H_b(G) = 8.3766(2^n) - 0.8116. \tag{17}$$

Proof. The result can be obtained as follows by using Table 1 and the definition of the harmonic Bhatti index:

$$\begin{aligned}
 H_b(G) &= \sum_{e=st \in E(G)} \left[\frac{2}{(d_G(s) + d_G(e)) + (d_G(t) + d_G(e))} \right], \\
 &= 4(2^n) \left[\frac{2}{(1+2) + (3+2)} \right] + (8(2^n) + 2) \left[\frac{2}{(2+2) + (2+2)} \right] + \\
 &\quad (28(2^n) - 8) \left[\frac{2}{(2+3) + (3+3)} \right] + (2(2^n) + 1) \left[\frac{2}{(3+4) + (3+4)} \right], \\
 &= 2^n + 2(2^n) + \frac{1}{2} + \frac{56(2^n)}{11} - \frac{16}{11} + \frac{2(2^n)}{7} + \frac{2}{14}, \\
 &= 8.3766(2^n) - 0.8116.
 \end{aligned} \tag{18}$$

□

3. Graphical Analysis and Conclusions

This section actually provides the summary of this article. Table 2 gives the comparison for the said topological indices of the graph. We can see that $mB_2(G)$ gives the least values for different growths of the graph whereas $HB_2(G)$ gives largest values. In Table 2, we can check the values for some test values of parameter n . Also, the graphical comparison is presented in Figure 2.

Data Availability

No data were used to support for this research.

Conflicts of Interest

The authors declare no conflicts of interest.

Authors' Contributions

All authors contributed equally to the writing of this article.

Acknowledgments

This work was supported in part by the General Project of Anhui 2021 University excellent talent support plan under Grant gxyq2021235.

References

- [1] H. Wiener, "Structural determination of Paraffin boiling points," *Journal of the American Chemical Society*, vol. 69, pp. 17–20, 1947.
- [2] H. Wiener, "Correlation of heats of isomerization, and differences in heats of vaporization of isomers, among the paraffin hydrocarbons," *Journal of the American Chemical Society*, vol. 69, no. 11, pp. 2636–2638, 1947.
- [3] H. Wiener, "Influence of interatomic forces on paraffin properties," *The Journal of Chemical Physics*, vol. 15, no. 10, p. 766, 1947.
- [4] H. Wiener, "The prediction of thermal pressure," *Journal of Physical Chemistry*, vol. 52, no. 6, pp. 1082–1089, 1948.
- [5] H. Wiener, "Vapour pressure-temperature relationships among the branched paraffin hydrocarbons," *Journal of Physical Chemistry*, vol. 52, pp. 425–430, 1948.
- [6] M. Albertson, "The irregularity of a graph," *Ars Combinatoria*, vol. 46, pp. 219–225, 1997.
- [7] D. Vukicevic and A. Groavac, "Valence connectivities verses Randic, Zagreb and modified Zagreb index: a linear algorithm to check discriminative properties of indices in acyclic molecular graphs," *Croatica Chemica Acta*, vol. 77, no. 3, pp. 501–508, 2004.
- [8] H. Abdo, S. Brandit, and D. Dimitrov, "The total irregularity of a graph," *Discrete Mathematics & Theoretical Computer Science*, vol. 16, pp. 201–206, 2014.
- [9] H. Abdo and D. Dimitrov, "The total irregularity of graphs under graph operations," *Miskolc Mathematical Notes*, vol. 15, pp. 3–17, 2014.
- [10] H. Abdo and D. Dimitrov, "The irregularity of graphs under graph operations," *Discussiones Mathematicae Graph Theory*, vol. 34, no. 2, pp. 263–278, 2014.
- [11] I. Gutman, "Topological indices and irregularity measures," *Jewish Bulletin*, vol. 8, pp. 469–475, 2018.
- [12] T. Reti, R. Sharfdini, A. Dregelyi-kiss, and H. Hagobin, "Graph Irregularity indices used as molecular descriptors on QSPR studies," *MATCH Communications in Mathematical and in Computer Chemistry*, vol. 79, no. 2, pp. 509–524, 2018.
- [13] V. R. Kulli, "On K banhatti indices of graphs," *Journal of Computer and Mathematical Sciences*, vol. 7, pp. 213–218, 2016.
- [14] J. Zheng, Z. Iqbal, A. Fahad et al., "Some eccentricity-based topological indices and Polynomials of poly(-EThyleneAmidoAmine) (PETAA) dendrimers," *Processes*, vol. 7, no. 7, p. 433, 2019.
- [15] A. Ye, M. I. Qureshi, A. Fahad et al., "Zagreb Connection number index of Nanotubes and regular hexagonal lattice," *Open Chemistry*, vol. 17, no. 1, pp. 75–80, 2019.
- [16] A. Fahad, M. I. Qureshi, S. Noureen, Z. Iqbal, A. Zafar, and M. Ishaq, "Topological descriptors of poly propyl ether imine (PETIM) dendrimers," *Biointerface Research in Applied Chemistry*, vol. 11, pp. 10968–10978, 2021.
- [17] M. I. Qureshi, A. Fahad, M. K. Jamil, and S. Ahmad, "Zagreb connection index of drugs related chemical structures," *Biointerface Research in Applied Chemistry*, vol. 11, pp. 11920–11930, 2021.
- [18] X. Zhang, A. Raza, A. Fahad, M. K. Jameel, M. A. Chaudhry, and Z. Iqbal, "On face index of Silicon carbides," *Discrete Dynamics in Nature and Society*, vol. 8, 2020.
- [19] L. Luo, N. Dehgard, and A. Fahad, "Lower bounds on the entire zagreb indices of trees," *Discrete Dynamics in Nature and Society*, vol. 8, 2020.
- [20] Y.-M. Chu, M. Abid, M. I. Qureshi, A. Fahad, and A. Aslam, "Irregular topological indices of certain metal organic frameworks," *Main Group Metal Chemistry*, vol. 44, no. 1, pp. 73–81, 2021.
- [21] A. Fahad, A. Aslam, M. I. Qureshi, M. K. Jamil, and A. Jaleel, "Zagreb connection indices of some classes of networks," *Biointerface Research in Applied Chemistry*, vol. 11, no. 3, pp. 10074–10081, 2021.
- [22] Y. Rao, A. Kanwal, R. Abbas, S. Noureen, A. Fahad, and M. I. Qureshi, "Some degree-based topological indices of caboxy-terminated dendritic macromolecule," *Main Group Metal Chemistry*, vol. 44, no. 1, pp. 165–172, 2021.
- [23] S. Ding, M. I. Qureshi, S. F. Shah, A. Fahad, M. K. Jamil, and J. B. Liu, "Face index of nanotubes and regular hexagonal lattices," *International Journal of Quantum Chemistry*, vol. 1-11, 2021.
- [24] A. Hussain, M. Numan, N. Naz, S. I. butt, A. Aslam, and A. Fahad, "On topological indices for new classes of Benes network," *Jurnal Matematika*, vol. 7, 2021.
- [25] V. R. Kulli, *College Graph Theory*, Vishwa International Publications, Gulbarga, India, 2012.
- [26] V. R. Kulli, "On K hyper Banhatti indices and coindices of graphs," *International Research Journal of Pure Algebra*, vol. 6, no. 5, pp. 300–304, 2016.
- [27] V. R. Kulli, "New K -banhatti topological indices," *International Journal of Fuzzy Mathematical Archive*, vol. 12, no. 1, pp. 29–37, 2017.

Research Article

New Results on the Forgotten Topological Index and Coindex

Akbar Jahanbani ¹, Maryam Atapour ², and Rana Khoelilar¹

¹Department of Mathematics, Azarbaijan Shahid Madani University Tabriz, Tabriz, Iran

²Department of Mathematics and Computer Science, Basic Science Faculty, University of Bonab, P.O. Box 55513-95133, Bonab, Iran

Correspondence should be addressed to Akbar Jahanbani; akbar.jahanbani92@gmail.com and Maryam Atapour; maryam.atapour@gmail.com

Received 7 September 2021; Accepted 22 October 2021; Published 2 November 2021

Academic Editor: Ali Ahmad

Copyright © 2021 Akbar Jahanbani et al. This is an open access article distributed under the Creative Commons Attribution License, which permits unrestricted use, distribution, and reproduction in any medium, provided the original work is properly cited.

The \mathcal{F} -coindex (forgotten topological coindex) for a simple connected graph \mathcal{G} is defined as the sum of the terms $\zeta_{\mathcal{G}}^2(y) + \zeta_{\mathcal{G}}^2(x)$ over all nonadjacent vertex pairs (x, y) of \mathcal{G} , where $\zeta_{\mathcal{G}}(y)$ and $\zeta_{\mathcal{G}}(x)$ are the degrees of the vertices y and x in \mathcal{G} , respectively. The \mathcal{F} -index of a graph is defined as the sum of cubes of the vertex degrees of the graph. This was introduced in 1972 in the same paper where the first and second Zagreb indices were introduced to study the structure dependency of total π -electron energy. Therefore, considering the importance of the \mathcal{F} -index and \mathcal{F} -coindex, in this paper, we study these indices, and we present new bounds for the \mathcal{F} -index and \mathcal{F} -coindex.

1. Introduction

Suppose \mathcal{G} be a simple graph with vertex set $V = V(\mathcal{G})$ and edge set $E(\mathcal{G})$. The integers $\aleph = \aleph(\mathcal{G}) = |V(\mathcal{G})|$ and $\epsilon = \epsilon(\mathcal{G}) = |E(\mathcal{G})|$ are the order and the size of the graph \mathcal{G} , respectively; we say \mathcal{G} is a (\aleph, ϵ) -graph. The open neighborhood of vertex v is $N_{\mathcal{G}}(x) = N(x) = \{y \in V(\mathcal{G}) \mid xy \in E(\mathcal{G})\}$, and the degree of v is $\zeta_{\mathcal{G}}(x) = |N(x)|$. We write Θ and δ for the maximum and minimum degrees of \mathcal{G} , respectively. A graph \mathcal{G} is said to be t -regular if all of its vertices have degree t . An (r, s) -semiregular graph is a graph whose each vertex is of degree s or r , and a (k, s, t) -triangular graph is a graph whose each vertex is of degree k, s , or t . The complement $\overline{\mathcal{G}}$ of a graph \mathcal{G} is a graph that has the same vertices as \mathcal{G} and in which two vertices are adjacent if and only if they are not adjacent in \mathcal{G} . The number of vertex pairs (x_i, x_j) in \mathcal{G} such that $x_i x_j \notin E(\mathcal{G})$ is $\overline{\epsilon} = \aleph(\aleph - 1) / 2 - \epsilon(\mathcal{G})$. A pendant vertex is a vertex of degree one. The number of pendant vertices in \mathcal{G} is denoted by $r = r(\mathcal{G})$. We denote by π_1 the minimal nonpendant vertex degree.

In [1, 2], the first and second Zagreb indices are defined as the following:

$$M_1 = M_1(\mathcal{G}) = \sum_{x \in V(\mathcal{G})} \zeta_{\mathcal{G}}^2(x) = \sum_{xy \in E(\mathcal{G})} (\zeta_{\mathcal{G}}(y) + \zeta_{\mathcal{G}}(x)),$$

$$M_2 = M_2(\mathcal{G}) = \sum_{xy \in E(\mathcal{G})} \zeta_{\mathcal{G}}(y)\zeta_{\mathcal{G}}(x),$$
(1)

respectively. The first and second Zagreb coindices are defined in [3, 4] as

$$\overline{M}_1(\mathcal{G}) = \sum_{xy \notin E(\mathcal{G})} (\zeta_{\mathcal{G}}(y) + \zeta_{\mathcal{G}}(x)),$$

$$\overline{M}_2(\mathcal{G}) = \sum_{xy \notin E(\mathcal{G})} \zeta_{\mathcal{G}}(y)\zeta_{\mathcal{G}}(x).$$
(2)

Furtula and Gutman [5] defined the forgotten topological index (\mathcal{F} -index) as the following:

$$\mathcal{F} = \mathcal{F}(\mathcal{G}) = \sum_{x \in V(\mathcal{G})} \zeta_{\mathcal{G}}^3(x) = \sum_{xy \in E(\mathcal{G})} (\zeta_{\mathcal{G}}^2(y) + \zeta_{\mathcal{G}}^2(x)).$$
(3)

For more information on the \mathcal{F} -index, see [6–8]. The \mathcal{F} -coindex introduced in [9] is as follows:

$$\overline{\mathcal{F}}(\mathcal{G}) = \sum_{xy \notin E(\mathcal{G})} (\zeta_{\mathcal{G}}^2(y) + \zeta_{\mathcal{G}}^2(x)). \quad (4)$$

Gutman in [10] introduced the hyper-Zagreb coindex as follows:

$$\overline{\text{HM}}(\mathcal{G}) = \sum_{xy \notin E(\mathcal{G})} (\zeta_{\mathcal{G}}(y) + \zeta_{\mathcal{G}}(x))^2. \quad (5)$$

Usha et al. [11] introduced the redefined first Zagreb indices as the following:

$$\text{ReZG}_1(\mathcal{G}) = \sum_{xy \in E(\mathcal{G})} \frac{\zeta_{\mathcal{G}}(y) + \zeta_{\mathcal{G}}(x)}{\zeta_{\mathcal{G}}(y)\zeta_{\mathcal{G}}(x)}. \quad (6)$$

Here, we introduce the redefined first Zagreb coindex as the following:

$$\overline{\text{ReZG}}_1(\mathcal{G}) = \sum_{xy \notin E(\mathcal{G})} \frac{\zeta_{\mathcal{G}}(y) + \zeta_{\mathcal{G}}(x)}{\zeta_{\mathcal{G}}(y)\zeta_{\mathcal{G}}(x)}. \quad (7)$$

The authors introduced the first general Zagreb coindex in [12], and it is defined as follows:

$$\overline{M}_1^{\alpha}(\mathcal{G}) = \sum_{xy \notin E(\mathcal{G})} (\zeta_{\mathcal{G}}^{\alpha-1}(y) + \zeta_{\mathcal{G}}^{\alpha-1}(x)), \quad (8)$$

where $\alpha \in R$. The second general Zagreb coindex was introduced in [13] and defined as follows:

$$\overline{M}_2^{\alpha}(\mathcal{G}) = \sum_{xy \notin E(\mathcal{G})} (\zeta_{\mathcal{G}}(y)\zeta_{\mathcal{G}}(x))^{\alpha}. \quad (9)$$

Topological indices are numerical quantity derived from a molecular graph which correlate the physico-chemical properties of the molecular graph. Recently, topological indices have been studied by many researchers due to their applications in various sciences such as chemistry, physics, and electricity; see [14–16]. Among the topological indices, the first Zagreb index is one of the oldest and most applied topological indices, and for this reason, it is of great importance and has been considered by many researchers today. Furtula and Gutman in [5] recently investigated this index and named this index as “forgotten topological index” or “ F -index” and showed that the predictive ability of this index is almost similar to that of the first Zagreb index and for the entropy and acetic factor; both of them yield correlation coefficients greater than 0.95. Therefore, due to the importance of the F -index in this paper, we have decided to study this index.

In [17, 18], some of bounds for the general Zagreb coindices were obtained. Ranjini et al. [19] presented some of the bounds for Zagreb indices and the Zagreb coindices. In [20], some bounds were presented for the \mathcal{F} -index and \mathcal{F} -coindex. For more other bounds, see [21–23].

Given the importance of the forgotten topological index and the fact that it has recently attracted the attention of researchers and the interest of many readers, in this paper, we intend to discuss new bounds for this index.

2. Preliminaries

Here, we recall several published results that we will need for proof.

The following result obtained the relationship between the first Zagreb index and the maximum and minimum degrees.

Theorem 1 (see [24]). *Let \mathcal{G} be an (\aleph, ϵ) -connected graph and $\aleph \geq 2$. Then,*

$$M_1 \geq \frac{4\epsilon^2}{\aleph} + \frac{1}{2}(\Theta - \delta)^2, \quad (10)$$

with equality if and only if \mathcal{G} is isomorphic with a regular graph.

The following result comes from [18].

Theorem 2. *Suppose \mathcal{G} be a (\aleph, ϵ) -graph and $\aleph \geq 2$. Then,*

$$M_1 \leq \frac{4\epsilon^2}{\aleph} + \frac{\aleph}{4}(\Theta - \delta)^2, \quad (11)$$

with equality if and only if \mathcal{G} is isomorphic with the t -regular graph, $1 \leq t \leq \aleph - 1$.

In [19], the authors gave the relation of the second Zagreb coindex, the maximum degree, and the first Zagreb index as follows.

Theorem 3. *Let \mathcal{G} be an (\aleph, ϵ) -graph and maximal degree be Θ . Then,*

$$\overline{M}_2(\mathcal{G}) \leq 2\Theta\epsilon(\aleph - 1) - \Theta M_1(\mathcal{G}). \quad (12)$$

Zhou and Trinajstić [25] proved the following result.

Theorem 4. *Suppose \mathcal{G} be a (\aleph, ϵ) -graph. Then,*

$$\mathcal{F}(\mathcal{G}) \geq \frac{16\epsilon^3}{\aleph^2} - 2M_2(\mathcal{G}), \quad (13)$$

with equality if and only if \mathcal{G} is regular.

Furtula and Gutman [5] showed the following.

Theorem 5. *Suppose \mathcal{G} be a graph of size ϵ . Then,*

$$\mathcal{F}(\mathcal{G}) \geq \frac{M_1(\mathcal{G})^2}{2\epsilon}, \quad (14)$$

with equality if and only if \mathcal{G} is regular.

In [26], Elumalai et al. obtained the following two results.

Theorem 6. *Suppose \mathcal{G} be a simple graph of order $\aleph \geq 2$. Then,*

$$\mathcal{F}(\mathcal{G}) \geq \Theta^3 + \Theta^2 + \Phi, \quad (15)$$

with equality if and only if \mathcal{G} is regular, where

$$\Phi = \frac{(M_1(\mathcal{G}) - \Theta^2 + \Theta_2^2)^2 + (\aleph - 2)(M_1(\mathcal{G}) - \Theta^2 + \Theta_2^2)}{(2\epsilon - \Theta + \Theta_2)} - (2\epsilon - \Theta + \Theta_2). \tag{16}$$

Theorem 7. Suppose \mathcal{G} be a simple graph of order $\aleph \geq 2$. Then,

$$\mathcal{F}(\mathcal{G}) \geq \Theta^3 + \Theta_2^3 + Y, \tag{17}$$

with equality if and only if \mathcal{G} is regular, where

$$Y = \frac{(M_1(\mathcal{G}) - \Theta^2 - \delta^2)^2 + (2\epsilon - \Theta - \delta)(ID(\mathcal{G}) - 1/\Theta - 1/\delta) - (\aleph - 2)^2}{(2\epsilon - \Theta - \delta)}. \tag{18}$$

In [5], Furtula and Gutman mentioned the following result.

Theorem 8. Suppose \mathcal{G} be a connected (\aleph, ϵ) -graph and second Zagreb index $M_2(\mathcal{G})$. Then,

$$\mathcal{F}(\mathcal{G}) \leq 2M_2(\mathcal{G}) + \epsilon(\aleph - 2), \tag{19}$$

with equality if and only if \mathcal{G} is the star graph.

The following result was first proved in [27].

Theorem 9. Suppose \mathcal{G} be a simple graph of order \aleph . Then,

$$\overline{\mathcal{F}}(\mathcal{G}) + \mathcal{F}(\mathcal{G}) = (\aleph - 1)M_1(\mathcal{G}). \tag{20}$$

3. New Bounds for the \mathcal{F} -Coindex

In this section, we will obtain some bounds for the \mathcal{F} -coindex in terms of the maximal degree, minimum degree, order, size, pendant vertex, and the first and the second Zagreb indices.

Theorem 10. Suppose \mathcal{G} be a (\aleph, ϵ) -graph. Then,

$$\mathcal{F}(\overline{\mathcal{G}}) + \mathcal{F}(\mathcal{G}) = 2(\aleph - 1)^2(\overline{\epsilon} - 2\epsilon) + 3(\aleph - 1)M_1(\mathcal{G}). \tag{21}$$

Proof. By applying the definition of the \mathcal{F} -index for complement graphs, we have

$$\begin{aligned} \mathcal{F}(\overline{\mathcal{G}}) &= \sum_{x \in V(\mathcal{G})} \zeta_{\overline{\mathcal{G}}}^3(x) = \sum_{x \in V(\mathcal{G})} (\aleph - 1 - \zeta_{\mathcal{G}}(x))^3, \\ &= \sum_{x \in V(\mathcal{G})} ((\aleph - 1)^3 - \zeta_{\mathcal{G}}^3(x) - 3(\aleph - 1)\zeta_{\mathcal{G}}^2(x) + 3(\aleph - 1)^2\zeta_{\mathcal{G}}(x)), \\ &= \sum_{x \in V(\mathcal{G})} (\aleph - 1)^3 - \sum_{x \in V(\mathcal{G})} \zeta_{\mathcal{G}}^3(x) + 3(\aleph - 1) \sum_{x \in V(\mathcal{G})} \zeta_{\mathcal{G}}^2(x) - 3 \sum_{x \in V(\mathcal{G})} (\aleph - 1)^2\zeta_{\mathcal{G}}(x), \\ &= \aleph(\aleph - 1)^3 - \mathcal{F}(\mathcal{G}) + 3(\aleph - 1)M_1(\mathcal{G}) - 6\epsilon(\aleph - 1)^2, \\ &= 2(\aleph - 1)^2(\overline{\epsilon} - 2\epsilon) - \mathcal{F}(\mathcal{G}) + 3(\aleph - 1)M_1(\mathcal{G}). \end{aligned} \tag{22}$$

Theorem 11. Suppose \mathcal{G} be a (\aleph, ϵ) -graph. Then,

$$\overline{\mathcal{F}}(\overline{\mathcal{G}}) = 2\epsilon(\aleph - 1)^2 - 2(\aleph - 1)M_1(\mathcal{G}) + \mathcal{F}(\mathcal{G}). \tag{23}$$

Proof. For any vertex $y \in V(\mathcal{G})$, we have $\zeta_{\overline{\mathcal{G}}}(y) = \aleph - 1 - \zeta_{\mathcal{G}}(y)$, and by applying the definition of the \mathcal{F} -coindex, we have

$$\begin{aligned} \overline{\mathcal{F}}(\overline{\mathcal{G}}) &= \sum_{xy \notin E(\mathcal{G})} (\zeta_{\overline{\mathcal{G}}}^2(y) + \zeta_{\overline{\mathcal{G}}}^2(x)), \\ &= \sum_{xy \in E(\mathcal{G})} ((\aleph - 1 - \zeta_{\mathcal{G}}(x))^2 + (\aleph - 1 - \zeta_{\mathcal{G}}(y))^2), \\ &= \sum_{xy \in E(\mathcal{G})} ((\aleph - 1)^2 + \zeta_{\mathcal{G}}^2(x) - 2(\aleph - 1)\zeta_{\mathcal{G}}(x) + (\aleph - 1)^2 + \zeta_{\mathcal{G}}^2(y) - 2(\aleph - 1)\zeta_{\mathcal{G}}(y)), \end{aligned}$$

$$\begin{aligned}
 &= \sum_{xy \in E(\mathcal{G})} (2(\aleph - 1)^2 - 2(\aleph - 1)(\zeta_{\mathcal{G}}(x) + \zeta_{\mathcal{G}}(y)) + (\zeta_{\mathcal{G}}^2(x) + \zeta_{\mathcal{G}}^2(y))), \\
 &= 2(\aleph - 1)^2\epsilon - 2(\aleph - 1)M_1(\mathcal{G}) + \mathcal{F}(\mathcal{G}).
 \end{aligned} \tag{24}$$

Now, we give a lower bound for the \mathcal{F} -coindex in terms of pendant vertices. \square

Theorem 12. *Suppose \mathcal{G} be a connected graph of order \aleph and r pendant vertices. Then,*

$$\overline{\mathcal{F}}(\mathcal{G}) \geq 6\aleph r - 4r^2 - 7r. \tag{25}$$

Proof. It is easy to see that our result holds for $r = 0$. Now, we assume that $r \geq 1$. Here, we let that \mathcal{G} has exactly one pendant vertex, called x , and y is the unique neighbor of x . Hence,

$$\begin{aligned}
 \overline{\mathcal{F}}(\mathcal{G}) &\geq \sum_{z \in V(\mathcal{G}) \setminus \{y, x\}} (\zeta_{\mathcal{G}}^2(z) + 1) \geq \sum_{w \in V(\mathcal{G}) \setminus \{y, x\}} 5, \\
 &= 5(\aleph - 2).
 \end{aligned} \tag{26}$$

Here, we can let that $r \geq 2$. Each pair of pendant vertices contributes 2 to $\overline{\mathcal{F}}(\mathcal{G})$. The total contribution of pendant vertex pairs to $\overline{\mathcal{F}}(\mathcal{G})$ is $2\binom{r}{2}$. Assume that x is a pendant vertex in \mathcal{G} and y is its unique neighbor. Then, for any nonpendant vertex z such that $w \in V(\mathcal{G}) \setminus \{y, x\}$, the contribution of vertex pairs $\{x, z\}$ to $\overline{\mathcal{F}}(\mathcal{G})$ is $1 + \zeta_{\mathcal{G}}^2(z)$. The total contribution of such vertex pairs $\{x, z\}$ to $\overline{\mathcal{F}}(\mathcal{G})$ is $(\aleph - r - 1)\binom{r}{1}(1 + \zeta_{\mathcal{G}}^2(z))$. Note that $\zeta_{\mathcal{G}}(z) \geq 2$ for any nonpendant vertex z in \mathcal{G} ; therefore, we get $\overline{\mathcal{F}}(\mathcal{G}) \geq \binom{r}{2}(1 + 1) + (\aleph - r - 1)\binom{r}{2}(1 + 5) = 6\aleph r - 4r^2 - 7r$, as desired. $\square \quad \square$

Theorem 13. *If \mathcal{G} is a t -regular graph of order \aleph , then*

$$\begin{aligned}
 \mathcal{F}(\overline{\mathcal{G}}) &= (\aleph - 1)^2(\aleph(\aleph - 1) - 3t\aleph) - \aleph t^3 + 3\aleph(\aleph - 1)t^2, \\
 \overline{\mathcal{F}}(\overline{\mathcal{G}}) &= \aleph t^2(\aleph - t - 1), \\
 \overline{\mathcal{F}}(\mathcal{G}) &= \aleph t((\aleph - 1)^2 - 2t(\aleph - 1) + t^2).
 \end{aligned} \tag{27}$$

Proof. We know that any t -regular graph of order \aleph has $\aleph t/2$ edges.

(1) By applying Theorem 10, we have

$$\begin{aligned}
 \mathcal{F}(\overline{\mathcal{G}}) &= 2(\aleph - 1)^2(\overline{\epsilon} - 2\epsilon) + 3(\aleph - 1)M_1(\mathcal{G}) - \mathcal{F}(\mathcal{G}), \\
 &= 2(\aleph - 1)^2\left(\frac{\aleph(\aleph - 1)}{2} - \frac{3\aleph t}{2}\right) + 3(\aleph - 1)\aleph t^2 - \aleph t^3, \\
 &= (\aleph - 1)^2(\aleph(\aleph - 1) - 3t\aleph) - \aleph t^3 + 3\aleph(\aleph - 1)t^2.
 \end{aligned} \tag{28}$$

(2) By applying Theorem 9, we can write

$$\mathcal{F}(\overline{\mathcal{G}}) = (\aleph - 1)M_1(\mathcal{G}) - \mathcal{F}(\mathcal{G}) = \aleph(\aleph - 1)t^2 - \aleph t^3. \tag{29}$$

(3) Similarly, by applying Theorem 11, we obtain

$$\begin{aligned}
 \overline{\mathcal{F}}(\overline{\mathcal{G}}) &= 2(\aleph - 1)^2\epsilon - 2(\aleph - 1)M_1(\mathcal{G}) + \mathcal{F}(\mathcal{G}), \\
 &= 2(\aleph - 1)^2\frac{\aleph t}{2} - 2\aleph t^2(\aleph - 1) + \aleph t^3, \\
 &= \aleph t((\aleph - 1)^2 - 2t(\aleph - 1) + t^2).
 \end{aligned} \tag{30}$$

Now, we give lower and upper bounds for the \mathcal{F} -coindex. \square

Theorem 14. *Suppose \mathcal{G} be a connected (\aleph, ϵ) -graph, maximum degree be Θ , and nonpendant minimum degree be π_1 and with s leaves. Then,*

$$\begin{aligned}
 \overline{\mathcal{F}}(\mathcal{G}) &\leq \left(s(\aleph - s - 1)\left(\Theta + \frac{1}{\Theta}\right) + \left(\frac{\Theta}{\pi_1} + \frac{\pi_1}{\Theta}\right)\left(\left(\frac{\aleph^2}{2} + \frac{s^2}{2} + \frac{3s}{2} - \frac{\aleph}{2} - \epsilon\right) + s(s - 1) - \aleph s\right) \right) (\aleph - 2)^2, \\
 \overline{\mathcal{F}}(\mathcal{G}) &\geq \left(s(\aleph - s - 1)\left(\pi_1 + \frac{1}{\pi_1}\right) + \left(\frac{\pi_1}{\Theta} + \frac{\Theta}{\pi_1}\right)\left(\left(\frac{\aleph^2}{2} + \frac{s^2}{2} + \frac{3s}{2} - \frac{\aleph}{2} - \epsilon\right) + s(s - 1) - \aleph s\right) \right).
 \end{aligned} \tag{31}$$

Proof. It can be easily seen that the number of vertices pairs (x_i, x_j) is as follows:

$$\begin{aligned}
 X_1 &= \{(x_i, x_j) | x_i x_j \notin E(\mathcal{G})\}, |X_1| = \frac{\aleph(\aleph - 1)}{2} - \epsilon, \\
 X_2 &= \{(x_i, x_j) | x_i x_j \notin E(\mathcal{G}) \text{ and } \zeta_{\mathcal{G}}(x_i) = \zeta_{\mathcal{G}}(x_j) = 1\}, |X_2| = \frac{s(s - 1)}{2}, \\
 X_3 &= \{(x_i, x_j) | x_i x_j \notin E(\mathcal{G}) \zeta_{\mathcal{G}}(x_i) = 1 \text{ or } \zeta_{\mathcal{G}}(x_j) = 1\}, |X_3| = s(\aleph - s - 1), \\
 X_4 &= \{(x_i, x_j) | x_i x_j \notin E(\mathcal{G}) \zeta_{\mathcal{G}}(x_i) > 1, \text{ and } \zeta_{\mathcal{G}}(x_j) > 1\}, |X_4| = \frac{\aleph(\aleph - 1)}{2} - \epsilon - \frac{s(s - 1)}{2} - s(\aleph - s - 1).
 \end{aligned} \tag{32}$$

For any vertex x_i , we have $\pi_1 \leq \zeta_{\mathcal{G}}(x_i) \leq \Theta$ and $\pi_1^2 \leq \zeta_{\mathcal{G}}(x_i)\zeta_{\mathcal{G}}(x_j) \leq \Theta^2$ for nonpendant vertices. Therefore, $x_i x_j \notin E(\mathcal{G})$.

We continue the proof with the following four cases.
 Let $x_i x_j \notin E(\mathcal{G})$. □

Case 1. If $\zeta_{\mathcal{G}}(x_i) > 1$ and $\zeta_{\mathcal{G}}(x_j) > 1$, we have

$$\frac{\zeta_{\mathcal{G}}(x_i)}{\zeta_{\mathcal{G}}(x_j)} + \frac{\zeta_{\mathcal{G}}(x_j)}{\zeta_{\mathcal{G}}(x_i)} \leq \left(\frac{\Theta}{\pi_1} + \frac{\pi_1}{\Theta} \right). \tag{33}$$

Case 2. If $\zeta_{\mathcal{G}}(x_i) > 1$ and $\zeta_{\mathcal{G}}(x_j) = 1$, hence, we get

$$\frac{\zeta_{\mathcal{G}}(x_i)}{\zeta_{\mathcal{G}}(x_j)} + \frac{\zeta_{\mathcal{G}}(x_j)}{\zeta_{\mathcal{G}}(x_i)} \leq \left(\Theta + \frac{1}{\Theta} \right). \tag{34}$$

It is clear that, for each $x_i x_j \notin E(\mathcal{G})$, $\zeta_{\mathcal{G}}(x_i), \zeta_{\mathcal{G}}(x_j) \leq \aleph - 2$. Hence, by applying the definition of the \mathcal{F} -coindex and above facts, we can write

$$\begin{aligned}
 \frac{\overline{\mathcal{F}}}{|\mathcal{G}|} (\aleph - 2)^2 &= \frac{\sum_{x_i x_j \notin E(\mathcal{G})} (\zeta_{\mathcal{G}}^2(x_i) + \zeta_{\mathcal{G}}^2(x_j))}{(n - 2)^2} \leq \sum_{x_i x_j \notin E(\mathcal{G})} \frac{\zeta_{\mathcal{G}}^2(x_i) + \zeta_{\mathcal{G}}^2(x_j)}{\zeta_{\mathcal{G}}(x_i)\zeta_{\mathcal{G}}(x_j)}, \\
 &= \sum_{x_i x_j \notin E(\mathcal{G})} \left(\frac{\zeta_{\mathcal{G}}(x_i)}{\zeta_{\mathcal{G}}(x_j)} + \frac{\zeta_{\mathcal{G}}(x_j)}{\zeta_{\mathcal{G}}(x_i)} \right), \\
 &= \sum_{\substack{x_i x_j \notin E(\mathcal{G}), \\ \zeta_{\mathcal{G}}(x_i)=1, \\ \zeta_{\mathcal{G}}(x_j)=1}} \left(\frac{\zeta_{\mathcal{G}}(x_i)}{\zeta_{\mathcal{G}}(x_j)} + \frac{\zeta_{\mathcal{G}}(x_j)}{\zeta_{\mathcal{G}}(x_i)} \right) + \sum_{\substack{x_i x_j \notin E(\mathcal{G}), \\ \zeta_{\mathcal{G}}(x_i)>1, \\ \zeta_{\mathcal{G}}(x_j)=1}} \left(\frac{\zeta_{\mathcal{G}}(x_i)}{\zeta_{\mathcal{G}}(x_j)} + \frac{\zeta_{\mathcal{G}}(x_j)}{\zeta_{\mathcal{G}}(x_i)} \right) + \sum_{\substack{x_i x_j \notin E(\mathcal{G}), \\ \zeta_{\mathcal{G}}(x_i)>1, \\ \zeta_{\mathcal{G}}(x_j)>1}} \left(\frac{\zeta_{\mathcal{G}}(x_i)}{\zeta_{\mathcal{G}}(x_j)} + \frac{\zeta_{\mathcal{G}}(x_j)}{\zeta_{\mathcal{G}}(x_i)} \right) \\
 &\leq \sum_{\substack{x_i x_j \notin E(\mathcal{G}), \\ \zeta_{\mathcal{G}}(x_i)=1, \\ \zeta_{\mathcal{G}}(x_j)=1}} 2 + \sum_{\substack{x_i x_j \notin E(\mathcal{G}), \\ \zeta_{\mathcal{G}}(x_i)>1, \\ \zeta_{\mathcal{G}}(x_j)=1}} \left(\Theta + \frac{1}{\Theta} \right) + \sum_{\substack{x_i x_j \notin E(\mathcal{G}), \\ \zeta_{\mathcal{G}}(x_i)>1, \\ \zeta_{\mathcal{G}}(x_j)>1}} \left(\frac{\Theta}{\pi_1} + \frac{\pi_1}{\Theta} \right), \\
 &= s(s - 1) + \left(\Theta + \frac{1}{\Theta} \right) s(\aleph - s - 1) + \left(\frac{\Theta}{\pi_1} + \frac{\pi_1}{\Theta} \right) \left(\frac{\aleph(\aleph - 1)}{2} - \epsilon - \frac{s(s - 1)}{2} - s(\aleph - s - 1) \right), \\
 &= s(\aleph - s - 1) \left(\Theta + \frac{1}{\Theta} \right) + \left(\frac{\Theta}{\pi_1} + \frac{\pi_1}{\Theta} \right) \left(\left(\frac{\aleph^2}{2} + \frac{s^2}{2} + \frac{3s}{2} - \frac{n}{2} - \epsilon \right) + s(s - 1) - \aleph s \right),
 \end{aligned} \tag{35}$$

as desired.

Case 3. If $\zeta_{\mathcal{G}}(x_i) > 1$ and $\zeta_{\mathcal{G}}(x_j) > 1$, we get

$$\frac{\zeta_{\mathcal{G}}(x_i)}{\zeta_{\mathcal{G}}(x_j)} + \frac{\zeta_{\mathcal{G}}(x_j)}{\zeta_{\mathcal{G}}(x_i)} \geq \left(\frac{\pi_1}{\Theta} + \frac{\Theta}{\pi_1} \right). \tag{36}$$

Case 4. If $\zeta_{\mathcal{G}}(x_i) > 1$ and $\zeta_{\mathcal{G}}(x_j) = 1$, we get that

$$\frac{\zeta_{\mathcal{G}}(x_i)}{\zeta_{\mathcal{G}}(x_j)} + \frac{\zeta_{\mathcal{G}}(x_j)}{\zeta_{\mathcal{G}}(x_i)} \geq \left(\pi_1 + \frac{1}{\pi_1} \right). \tag{37}$$

Thus,

$$\begin{aligned} \overline{\mathcal{F}}(\mathcal{G}) &= \sum_{x_i, x_j \notin E(\mathcal{G})} \zeta_{\mathcal{G}}^2(x_i) + \zeta_{\mathcal{G}}^2(x_j) \geq \sum_{x_i, x_j \notin E(\mathcal{G})} \frac{\zeta_{\mathcal{G}}^2(x_i) + \zeta_{\mathcal{G}}^2(x_j)}{\zeta_{\mathcal{G}}(x_i)\zeta_{\mathcal{G}}(x_j)}, \\ &= \sum_{x_i, x_j \notin E(\mathcal{G})} \left(\frac{\zeta_{\mathcal{G}}(x_i)}{\zeta_{\mathcal{G}}(x_j)} + \frac{\zeta_{\mathcal{G}}(x_j)}{\zeta_{\mathcal{G}}(x_i)} \right), \\ &= \sum_{\substack{x_i, x_j \notin E(\mathcal{G}), \\ \zeta_{\mathcal{G}}(x_i)=1, \\ \zeta_{\mathcal{G}}(x_j)=1}} \left(\frac{\zeta_{\mathcal{G}}(x_i)}{\zeta_{\mathcal{G}}(x_j)} + \frac{\zeta_{\mathcal{G}}(x_j)}{\zeta_{\mathcal{G}}(x_i)} \right) + \sum_{\substack{x_i, x_j \notin E(\mathcal{G}), \\ \zeta_{\mathcal{G}}(x_i) > 1, \\ \zeta_{\mathcal{G}}(x_j)=1}} \left(\frac{\zeta_{\mathcal{G}}(x_i)}{\zeta_{\mathcal{G}}(x_j)} + \frac{\zeta_{\mathcal{G}}(x_j)}{\zeta_{\mathcal{G}}(x_i)} \right) + \sum_{\substack{x_i, x_j \notin E(\mathcal{G}), \\ \zeta_{\mathcal{G}}(x_i) > 1, \\ \zeta_{\mathcal{G}}(x_j) > 1}} \left(\frac{\zeta_{\mathcal{G}}(x_i)}{\zeta_{\mathcal{G}}(x_j)} + \frac{\zeta_{\mathcal{G}}(x_j)}{\zeta_{\mathcal{G}}(x_i)} \right) \\ &\geq \sum_{\substack{x_i, x_j \notin E(\mathcal{G}), \\ \zeta_{\mathcal{G}}(x_i)=1, \\ \zeta_{\mathcal{G}}(x_j)=1}} 2 + \sum_{\substack{x_i, x_j \notin E(\mathcal{G}), \\ \zeta_{\mathcal{G}}(x_i) > 1, \\ \zeta_{\mathcal{G}}(x_j)=1}} \left(\pi_1 + \frac{1}{\pi_1} \right) + \sum_{\substack{x_i, x_j \notin E(\mathcal{G}), \\ \zeta_{\mathcal{G}}(x_i) > 1, \\ \zeta_{\mathcal{G}}(x_j) > 1}} \left(\frac{\pi_1}{\Theta} + \frac{\Theta}{\pi_1} \right), \\ &= s(s-1) + \left(\pi_1 + \frac{1}{\pi_1} \right) s(\aleph - s - 1) + \left(\frac{\pi_1}{\Theta} + \frac{\Theta}{\pi_1} \right) \left(\frac{\aleph(\aleph-1)}{2} - \epsilon - \frac{s(s-1)}{2} - s(\aleph - s - 1) \right), \\ &= s(\aleph - s - 1) \left(\pi_1 + \frac{1}{\pi_1} \right) + \left(\frac{\pi_1}{\Theta} + \frac{\Theta}{\pi_1} \right) \left(\left(\frac{\aleph^2}{2} + \frac{s^2}{2} + \frac{3s}{2} - \frac{\aleph}{2} - \epsilon \right) + s(s-1) - \aleph s \right), \end{aligned} \tag{38}$$

and the proof is completed.

By setting $s = 0$ in Theorem 14, we can obtain the following results.

Corollary 1. Suppose \mathcal{G} be a connected (\aleph, ϵ) -graph, maximum degree be Θ , and nonpendant minimum degree be π_1 . Then,

$$\overline{\mathcal{F}}(\mathcal{G}) \leq \left(\frac{\Theta}{\pi_1} + \frac{\pi_1}{\Theta} \right) \left(\frac{\aleph^2}{2} - \frac{\aleph}{2} - \epsilon \right) (\aleph - 2)^2, \tag{39}$$

$$\overline{\mathcal{F}}(\mathcal{G}) \geq \left(\frac{\pi_1}{\Theta} + \frac{\Theta}{\pi_1} \right) \left(\frac{\aleph^2}{2} - \frac{\aleph}{2} - \epsilon \right).$$

Here, we give a lower bound for the \mathcal{F} -coindex.

Proposition 1. Suppose \mathcal{G} be a connected graph of order \aleph and size ϵ . Then,

$$\overline{\mathcal{F}}(\mathcal{G}) \geq \aleph^2 - 2\epsilon - \aleph. \tag{40}$$

Proof. By applying the definition of the \mathcal{F} -coindex, we have

$$\overline{\mathcal{F}}(\mathcal{G}) = \sum_{x_i, x_j \notin E(\mathcal{G})} (\zeta_{\mathcal{G}}^2(x_i) + \zeta_{\mathcal{G}}^2(x_j)) \geq \sum_{x_i, x_j \notin E(\mathcal{G})} 2 = 2 \left(\frac{\aleph(\aleph-1)}{2} - \epsilon \right) = \aleph^2 - 2\epsilon - \aleph. \tag{41}$$

In the following result, we obtain the lower bound for the \mathcal{F} -coindex. \square

Proof. Clearly, for each $x_i, x_j \notin E(\mathcal{G})$, we have $\max\{\zeta_{\mathcal{G}}(x_i), \zeta_{\mathcal{G}}(x_j)\} \leq \aleph - 2$. It follows that

Theorem 15. Suppose \mathcal{G} be a connected (\aleph, ϵ) -graph and $\aleph \geq 2$. Then,

$$\overline{\mathcal{F}}(\mathcal{G}) \geq \frac{\overline{M}_1^5(\mathcal{G}) + 2\overline{M}_2^2(\mathcal{G})}{2(\aleph - 2)^2}. \tag{42}$$

$$\begin{aligned} 2(n-2)^2 \overline{\mathcal{F}}(\mathcal{G}) &= 2(\aleph - 2)^2 \sum_{x_i, x_j \notin E(\mathcal{G})} (\zeta_{\mathcal{G}}^2(x_i) + \zeta_{\mathcal{G}}^2(x_j)) \geq \sum_{x_i, x_j \notin E(\mathcal{G})} (\zeta_{\mathcal{G}}^2(x_i) + \zeta_{\mathcal{G}}^2(x_j))^2, \\ &= \sum_{x_i, x_j \notin E(\mathcal{G})} (\zeta_{\mathcal{G}}^4(x_i) + \zeta_{\mathcal{G}}^4(x_j) + 2\zeta_{\mathcal{G}}^2(x_i)\zeta_{\mathcal{G}}^2(x_j)), \\ &= \sum_{x_i, x_j \notin E(\mathcal{G})} (\zeta_{\mathcal{G}}^4(x_i) + \zeta_{\mathcal{G}}^4(x_j)) + 2 \sum_{x_i, x_j \notin E(\mathcal{G})} (\zeta_{\mathcal{G}}(x_i)\zeta_{\mathcal{G}}(x_j))^2, \\ &= \overline{M}_1^5(\mathcal{G}) + 2\overline{M}_2^2(\mathcal{G}), \end{aligned} \tag{43}$$

and the proof is completed.

Now, we give an upper bound for the \mathcal{F} -coindex in terms of the second Zagreb coindex and the redefined first Zagreb coindex. \square

$$\overline{\mathcal{F}}(\mathcal{G}) \leq 2(\aleph - 2)^3 \overline{\text{ReZG}}_1(\mathcal{G}) - 2(\aleph - 2)^2 \overline{M}_2(\mathcal{G}). \tag{44}$$

Proof. By applying the definition of the \mathcal{F} -coindex, we have

Theorem 16. Suppose \mathcal{G} be a graph of order \aleph . Then,

$$\begin{aligned} \frac{\overline{\mathcal{F}}(\mathcal{G})}{(n-2)^2} &= \frac{\sum_{x_i, x_j \notin E(\mathcal{G})} (\zeta_{\mathcal{G}}^2(x_i) + \zeta_{\mathcal{G}}^2(x_j))}{(n-2)^2} \leq \sum_{v_i, v_j \notin E(\mathcal{G})} \left(\frac{\zeta_{\mathcal{G}}(x_i)}{\zeta_{\mathcal{G}}(x_j)} + \frac{\zeta_{\mathcal{G}}(x_j)}{\zeta_{\mathcal{G}}(x_i)} \right), \\ &= \sum_{x_i, x_j \notin E(\mathcal{G})} \left(\left(\frac{1}{\zeta_{\mathcal{G}}(x_i)} + \frac{1}{\zeta_{\mathcal{G}}(x_j)} \right) (\zeta_{\mathcal{G}}(x_j) + \zeta_{\mathcal{G}}(x_i)) - 2\zeta_{\mathcal{G}}(x_i)\zeta_{\mathcal{G}}(x_j) \right), \\ &= \sum_{x_i, x_j \notin E(\mathcal{G})} \left(\left(\frac{1}{\zeta_{\mathcal{G}}(x_i)} + \frac{1}{\zeta_{\mathcal{G}}(x_j)} \right) (\zeta_{\mathcal{G}}(x_j) + \zeta_{\mathcal{G}}(x_i)) \right) - 2 \sum_{x_i, x_j \notin E(\mathcal{G})} \zeta_{\mathcal{G}}(x_i)\zeta_{\mathcal{G}}(x_j) \\ &\leq 2(n-2) \sum_{x_i, x_j \notin E(\mathcal{G})} \left(\frac{1}{\zeta_{\mathcal{G}}(x_i)} + \frac{1}{\zeta_{\mathcal{G}}(x_j)} \right) - 2 \sum_{x_i, x_j \notin E(\mathcal{G})} \zeta_{\mathcal{G}}(x_i)\zeta_{\mathcal{G}}(x_j), \\ &= 2(n-2) \sum_{x_i, x_j \notin E(\mathcal{G})} \left(\frac{\zeta_{\mathcal{G}}(x_i) + \zeta_{\mathcal{G}}(x_j)}{\zeta_{\mathcal{G}}(x_i)\zeta_{\mathcal{G}}(x_j)} \right) - 2\overline{M}_2(\mathcal{G}), \\ &= 2(\aleph - 2)\overline{\text{ReZG}}_1(\mathcal{G}) - 2\overline{M}_2(\mathcal{G}), \end{aligned} \tag{45}$$

which leads to the result.

In the following results, we obtain upper bounds for the \mathcal{F} -coindex in terms of the first and second Zagreb indices and hyper-Zagreb coindex. \square

Theorem 17. *Suppose \mathcal{G} be a (\aleph, ϵ) -graph. Then,*

$$\overline{\mathcal{F}}(\mathcal{G}) + \overline{M}_2(\mathcal{G}) \leq 3\overline{\epsilon}(\aleph - 2)^2, \tag{46}$$

$$\overline{\mathcal{F}}(\mathcal{G}) + \overline{M}_1(\mathcal{G}) \leq 2\overline{\epsilon}(\aleph^2 - 3\aleph + 2), \tag{47}$$

$$\overline{\mathcal{F}}(\mathcal{G}) + \overline{HM}(\mathcal{G}) \leq 6\overline{\epsilon}(\aleph - 2)^2. \tag{48}$$

The equalities hold if and only if $\mathcal{G} \cong K_\aleph$ or \mathcal{G} is $(\aleph - 2)$ -regular or $(\aleph - 2, \aleph - 1)$ -semiregular.

Proof. By applying the definitions of the \mathcal{F} -coindex and second Zagreb coindex, we can write

$$\begin{aligned} \overline{\mathcal{F}}(\mathcal{G}) + \overline{M}_2(\mathcal{G}) &= \sum_{x_i, x_j \notin E(\mathcal{G})} (\zeta_{\mathcal{G}}^2(x_i) + \zeta_{\mathcal{G}}^2(x_j) + \zeta_{\mathcal{G}}(x_i)\zeta_{\mathcal{G}}(x_j)) \leq \sum_{x_i, x_j \notin E(\mathcal{G})} ((\aleph - 2)^2 + (\aleph - 2)^2 + (\aleph - 2)^2), \\ &= 3\overline{\epsilon}(\aleph - 2)^2. \end{aligned} \tag{49}$$

Likewise, we have

$$\begin{aligned} \overline{\mathcal{F}}(\mathcal{G}) + \overline{M}_1(\mathcal{G}) &= \sum_{x_i, x_j \notin E(\mathcal{G})} (\zeta_{\mathcal{G}}^2(x_i) + \zeta_{\mathcal{G}}^2(x_j) + \zeta_{\mathcal{G}}(x_i) + \zeta_{\mathcal{G}}(x_j)) \leq \sum_{x_i, x_j \notin E(\mathcal{G})} ((\aleph - 2)^2 + (\aleph - 2)^2 + 2(\aleph - 2)), \\ &= 2\overline{\epsilon}(\aleph^2 - 3\aleph + 2), \end{aligned} \tag{50}$$

and

$$\begin{aligned} \overline{\mathcal{F}}(\mathcal{G}) + \overline{HM}(\mathcal{G}) &= \sum_{x_i, x_j \notin E(\mathcal{G})} (\zeta_{\mathcal{G}}^2(x_i) + \zeta_{\mathcal{G}}^2(x_j) + (\zeta_{\mathcal{G}}(x_i) + \zeta_{\mathcal{G}}(x_j))^2), \\ &= \sum_{x_i, x_j \notin E(\mathcal{G})} (\zeta_{\mathcal{G}}^2(x_i) + \zeta_{\mathcal{G}}^2(x_j) + \zeta_{\mathcal{G}}^2(x_i) + \zeta_{\mathcal{G}}^2(x_j) + 2\zeta_{\mathcal{G}}(x_i)\zeta_{\mathcal{G}}(x_j)), \\ &= \sum_{x_i, x_j \notin E(\mathcal{G})} (2\zeta_{\mathcal{G}}^2(x_i) + 2\zeta_{\mathcal{G}}^2(x_j) + 2\zeta_{\mathcal{G}}(x_i)\zeta_{\mathcal{G}}(x_j)) \leq \sum_{x_i, x_j \notin E(\mathcal{G})} (4(\aleph - 2)^2 + 2(\aleph - 2)^2), \\ &= 6\overline{\epsilon}(\aleph - 2)^2. \end{aligned} \tag{51}$$

The equalities hold in (46)–(48) if and only if $\zeta_{\mathcal{G}}(x_i) = \zeta_{\mathcal{G}}(x_j) = \aleph - 2$, for each $x_i, x_j \notin E(\mathcal{G})$. This implies that each vertex of \mathcal{G} has degree $\aleph - 1$ or $\aleph - 2$; that is, $\mathcal{G} \cong K_\aleph$ or \mathcal{G} is $(\aleph - 2)$ -regular or $(\aleph - 2, \aleph - 1)$ -semiregular.

By using Theorems 1, 8, 10, and 9, we get the following result. \square

Theorem 18. *Suppose \mathcal{G} be a (\aleph, ϵ) -graph. Then,*

$$\begin{aligned} \mathcal{F}(\overline{\mathcal{G}}) &\geq 2(\aleph - 1)^2(\overline{\epsilon} - 2\epsilon) + 3(\aleph - 1)\left(\frac{4\epsilon^2}{\aleph} + \frac{1}{2}(\Theta - \delta)^2\right) - (2M_2(\mathcal{G}) + \epsilon(\aleph - 2)), \\ \overline{\mathcal{F}}(\mathcal{G}) &\geq (\aleph - 1)\left(\frac{4\epsilon^2}{\aleph} + \frac{1}{2}(\Theta - \delta)^2\right) - (2M_2(\mathcal{G}) + \epsilon(\aleph - 2)). \end{aligned} \tag{52}$$

The following results were obtained by combining Theorems 1, 4, 5, 6, and 11.

Theorem 19. Suppose \mathcal{G} be a (N, ϵ) -graph. Then,

$$\begin{aligned} \overline{\mathcal{F}}(\overline{\mathcal{G}}) &\geq 2\epsilon(N-1)^2 - 2(N-1)\left(\left(\frac{4\epsilon^2}{N} + \frac{1}{2}(\Theta - \delta)^2\right)\right) + \left(\frac{16\epsilon^3}{N^2} - 2M_2(\mathcal{G})\right), \\ \overline{\mathcal{F}}(\overline{\mathcal{G}}) &\geq 2\epsilon(N-1)^2 - 2(N-1)\left(\left(\frac{4\epsilon^2}{N} + \frac{1}{2}(\Theta - \delta)^2\right)\right) + \left(\frac{M_1(\mathcal{G})^2}{2\epsilon}\right), \\ \overline{\mathcal{F}}(\overline{\mathcal{G}}) &\geq 2\epsilon(N-1)^2 - 2(N-1)\left(\left(\frac{4\epsilon^2}{N} + \frac{1}{2}(\Theta - \delta)^2\right)\right) + (\Theta^3 + \Theta_2^3 + \Phi). \end{aligned} \tag{53}$$

The following results were obtained by combining Theorems 2, 4, 10, and 9.

Theorem 20. Suppose \mathcal{G} be a (N, ϵ) -graph. Then,

$$\begin{aligned} \mathcal{F}(\overline{\mathcal{G}}) &\leq 2(N-1)^2(\overline{\epsilon} - 2\epsilon) + 3(N-1)\left(\frac{4\epsilon^2}{N} + \frac{N}{4}(\Theta - \delta)^2\right) - \left(\frac{16\epsilon^3}{N^2} - 2M_2(\mathcal{G})\right), \\ \overline{\mathcal{F}}(\mathcal{G}) &\leq (N-1)\left(\frac{4\epsilon^2}{N} + \frac{N}{4}(\Theta - \delta)^2\right) - \left(\frac{16\epsilon^3}{N^2} - 2M_2(\mathcal{G})\right). \end{aligned} \tag{54}$$

By applying Theorems 2, 8, and 11, we can obtain the following theorem.

The following results were obtained by Theorems 2, 5, 10, and 9.

Theorem 21. Suppose \mathcal{G} be a (N, ϵ) -graph. Then,

Theorem 22. Suppose \mathcal{G} be a (N, ϵ) -graph. Then,

$$\begin{aligned} \overline{\mathcal{F}}(\overline{\mathcal{G}}) &\leq 2\epsilon(N-1)^2 - 2(N-1)\left(\left(\frac{4\epsilon^2}{N} + \frac{N}{4}(\Theta - \delta)^2\right)\right) \\ &\quad + (2M_2(\mathcal{G}) + \epsilon(N-2)). \end{aligned} \tag{55}$$

$$\begin{aligned} \mathcal{F}(\overline{\mathcal{G}}) &\leq 2(N-1)^2(\overline{\epsilon} - 2\epsilon) + 3(N-1)\left(\frac{4\epsilon^2}{N} + \frac{N}{4}(\Theta - \delta)^2\right) - \left(\frac{M_1(\mathcal{G})^2}{2\epsilon}\right), \\ \overline{\mathcal{F}}(\mathcal{G}) &\leq (N-1)\left(\frac{4\epsilon^2}{N} + \frac{N}{4}(\Theta - \delta)^2\right) - \left(\frac{M_1(\mathcal{G})^2}{2\epsilon}\right). \end{aligned} \tag{56}$$

The following results were obtained by combining Theorems 7, 10, and 9.

$$\begin{aligned}\mathcal{F}(\overline{\mathcal{G}}) &\leq 2(\aleph - 1)^2(\overline{\epsilon} - 2\epsilon) + 3(\aleph - 1)\left(\frac{4\epsilon^2}{\aleph} + \frac{\aleph}{4}(\Theta - \delta)^2\right) - (\Theta^3 + \Theta_2^3 + Y), \\ \overline{\mathcal{F}}(\mathcal{G}) &\leq (\aleph - 1)\left(\frac{4\epsilon^2}{\aleph} + \frac{\aleph}{4}(\Theta - \delta)^2\right) - (\Theta^3 + \Theta_2^3 + Y).\end{aligned}\tag{57}$$

4. Conclusion

In this paper, we investigate the relationship between the \mathcal{F} -coindex and the other topological coindices, such as the first and second Zagreb coindices, the hyper-Zagreb coindex, and the redefined first Zagreb coindex. However, there are still open and challenging problems for researchers, for example, the problem on the relationship among the \mathcal{F} -coindex and GA-coindex, harmonic coindex, Randić coindex, etc.

Data Availability

The data involved in the examples of our manuscript are included within the article.

Disclosure

The authors would like to declare that the work described was original research that has not been published previously [28].

Conflicts of Interest

The authors declare that they have no conflicts of interest.

References

- [1] A. T. Balaban, I. Motoc, D. Bonchev, and O. Mekenyan, "Topological indices for structure-activity correlations," *Steric effects in drug design*, vol. 114, pp. 21-55, 1983.
- [2] I. Gutman, B. Ruščić, N. Trinajstić, and C. F. Wilcox, "Graph theory and molecular orbitals. XII. Acyclic polyenes," *The Journal of Chemical Physics*, vol. 62, no. 9, pp. 3399-3405, 1975.
- [3] P. S. Ranjini and V. Lokesh, "The smarandache-zagreb indices on the three graph operators," *International Journal of Mathematical Combinatorics*, vol. 3, pp. 1-10, 2010.
- [4] P. S. Ranjini, V. Lokesh, and I. N. Cangül, "On the Zagreb indices of the line graphs of the subdivision graphs," *Applied Mathematics and Computation*, vol. 218, no. 3, pp. 699-702, 2011.
- [5] B. Furtula and I. Gutman, "A forgotten topological index," *Journal of Mathematical Chemistry*, vol. 53, no. 4, pp. 1184-1190, 2015.
- [6] Z. Du, A. Jahanbai, and S. M. Sheikholeslami, "Relationships between Randić index and other topological indices," *Communications in Combinatorics and Optimization*, vol. 6, pp. 137-154, 2021.

Theorem 23. Suppose \mathcal{G} be a (\aleph, ϵ) -graph. Then,

- [7] I. Gutman and N. Trinajstić, "Graph theory and molecular orbitals. Total ϕ -electron energy of alternant hydrocarbons," *Chemical Physics Letters*, vol. 17, no. 4, pp. 535-538, 1972.
- [8] J. Varghese Kureethara, A. Asok, and I. Naci Cangul, "Inverse problem for the forgotten and the hyper Zagreb indices of trees," *Communications in Combinatorics and Optimization*, vol. 7, 2021.
- [9] N. De, S. M. A. Nayeem, and A. Pal, *The \mathcal{F} -Co-Index of Some Graph Operations*, Springer, vol. 5 New York, NY, USA, , 2016.
- [10] I. Gutman, "On hyper-Zagreb index and co-index," *Bulletin (Académie serbe des sciences et des arts. Classe des sciences mathématiques et naturelles. Sciences mathématiques)*, vol. 150, pp. 1-8, 2017.
- [11] A. Usha, P. S. Ranjini, and V. Lokesh, "Zagreb coindices, augmented Zagreb index, redefined Zagreb indices and their polynomials for phenylene and hexagonal squeeze," in *Proceedings of the International Congress in Honour of Dr. Ravi P. Agarwal*, Uludag University, Bursa, Turkey, June 2014.
- [12] M. Berhe Belay and C. Wang, "The first general Zagreb coindex of graph operations," *Applied Mathematics and Nonlinear Sciences*, vol. 5, no. 2, pp. 109-120, 2020.
- [13] H. Aram and N. Dehgardi, "Reformulated F-index of graph operations," *Communications in Combinatorics and Optimization*, vol. 2, pp. 87-98, 2017.
- [14] M. F. Nadeem, M. Imran, H. M. Afzal Siddiqui, M. Azeem, A. Khalil, and Y. Ali, "Topological aspects of metal-organic structure with the help of underlying networks," *Arabian Journal of Chemistry*, vol. 14, no. 6, Article ID 103157, 2021.
- [15] H. M. A. Siddiqui, S. Baby, M. F. Nadeem, and M. K. Shafiq, "Bounds of some degree based indices of lexicographic product of some connected graphs," *Polycyclic Aromatic Compounds*, vol. 2020, Article ID 1852266, 13 pages, 2020.
- [16] T. Vetrik and S. Balachandran, "General multiplicative Zagreb indices of graphs with given clique number," *Opuscula Mathematica*, vol. 39, no. 3, pp. 433-446, 2019.
- [17] M. Matejić, E. Milovanović, I. Milovanović, and R. Khoelir, "A note on the first Zagreb index and co-index of graphs," *Communications in Combinatorics and Optimization*, vol. 6, pp. 41-51, 2021.
- [18] E. Milovanovic and I. Milovanovic, "Sharp bounds for the first Zagreb index and first Zagreb coindex," *Miskolc Mathematical Notes*, vol. 16, no. 2, pp. 1017-1024, 2015.
- [19] P. S. Ranjini, V. Lokesh, A. R. Bindusree, and M. Phani Raju, "New bounds on Zagreb indices and the Zagreb co-indices," *Boletim da Sociedade Paranaense de Matemática*, vol. 31, pp. 51-55, 2013.
- [20] J. B. Liu, M. M. Matejić, E. I. Milovanović, and I. Z. Milovanović, "Some new inequalities for the forgotten topological index and co-index of graphs, MATCH Commun," *MATCH Communications in Mathematical and in Computer*, vol. 84, pp. 719-738, 2020.

- [21] R. Amin and S. M. A. Nayeem, "Extremal F-index of a graph with k cut edges," *Matematički Vesnik*, vol. 72, pp. 146–153, 2020.
- [22] D. Maji and G. Ghorai, "Computing F-index, coindex and Zagreb polynomials of the k th generalized transformation graphs," *Heliyon*, vol. 6, no. 12, Article ID e05781, 2020.
- [23] D. Sarala, H. Deng, C. Natarajan, and S. K. Ayyaswamy, "F index of graphs based on four new operations related to the strong product," *AKCE International Journal of Graphs and Combinatorics*, vol. 17, no. 1, pp. 25–37, 2020.
- [24] C. S. Edwards, "The largest vertex degree sum for a triangle in a graph," *Bulletin of the London Mathematical Society*, vol. 9, no. 2, pp. 203–208, 1977.
- [25] B. Zhou and N. Trinajstić, "On general sum-connectivity index," *Journal of Mathematical Chemistry*, vol. 47, no. 1, pp. 210–218, 2010.
- [26] S. Elumalai, T. Mansour, and M. A. Rostami, "On the bounds of the forgotten topological index," *Turkish Journal of Mathematics*, vol. 41, pp. 1687–1702, 2017.
- [27] N. De, "F-index and co-index of some derived graphs," 2016, <https://arxiv.org/abs/1610.02175>.
- [28] T. Došlić, T. Réti, and D. Vukičević, "On the vertex degree indices of connected graphs," *Chemical Physics Letters*, vol. 512, pp. 283–286, 2011.

Research Article

On the Number of Conjugate Classes of Derangements

Wen-Wei Li ^{1,2}, Zhong-Lin Cheng,¹ and Jia-Bao Liu ³

¹School of Information and Mathematics, Anhui International Studies University, Hefei 231201, China

²School of Mathematical Science, University of Science and Technology of China, Hefei 230026, China

³School of Mathematics and Physics, Anhui Jianzhu University, Hefei 230601, China

Correspondence should be addressed to Wen-Wei Li; liwenwei@ustc.edu

Received 14 June 2021; Accepted 27 August 2021; Published 28 October 2021

Academic Editor: Gaetano Luciano

Copyright © 2021 Wen-Wei Li et al. This is an open access article distributed under the Creative Commons Attribution License, which permits unrestricted use, distribution, and reproduction in any medium, provided the original work is properly cited.

The number of conjugate classes of derangements of order n is the same as the number $h(n)$ of the restricted partitions with every portion greater than 1. It is also equal to the number of isotopy classes of $2 \times n$ Latin rectangles. Sometimes the exact value is necessary, while sometimes we need the approximation value. In this paper, a recursion formula of $h(n)$ will be obtained and also will some elementary approximation formulae with high accuracy for $h(n)$ be presented. Although we may obtain the value of $h(n)$ in some computer algebra system, it is still meaningful to find an efficient way to calculate the approximate value, especially in engineering, since most people are familiar with neither programming nor CAS software. This paper is mainly for the readers who need a simple and practical formula to obtain the approximate value (without writing a program) with more accuracy, such as to compute the value in a pocket science calculator without programming function. Some methods used here can also be applied to find the fitting functions for some types of data obtained in experiments.

1. Introduction

Below n is a positive integer greater than 1.

On some occasions, it is necessary to know the number of conjugate classes of derangements.

When generating the representatives of all the isotopy classes of Latin rectangles of order n by some method, we need to know the number of the isotopy classes of $2 \times n$ Latin rectangles for verification. In some cases, we need the approximate value in a simple and efficient method. (When writing a C program to generate the representatives of all the isotopy classes of Latin rectangles of order n , we need to prepare some space in the memory module (RAM) to store the cycle structures of derangements so as to make the program more efficient; otherwise, we have to allocate memory dynamically, which will cost more time in memory addressing when writing and reading data frequently in the particular position in the memory module. So, we need to know the number of the isotopy classes of $2 \times n$ Latin rectangles for verification.)

Let S_n be the symmetry group of the set $X = \{1, 2, \dots, n\}$, i.e., the set (together with the operation of combination) of

the bijections from X to itself. An element σ in the symmetry group S_n is also called a permutation (of order n). If $\sigma \in S_n$, $\sigma(i) \neq i$ ($\forall i \in X$), σ will be called a derangement of order n . If a permutation σ transforms any element in X to a distinct element, then the sequence $[\sigma(1), \sigma(2), \dots, \sigma(n)]$ will also be called a derangement. The number of derangements of order n is denoted by D_n (or $!n$ in some literatures). It is mentioned in nearly every combinatorics textbook that

$$\begin{aligned} D_n &= (n-1)(D_{n-1} + D_{n-2}) \\ &= n! \sum_{i=0}^n \frac{(-1)^i}{i!} \doteq \left\lfloor \frac{n!}{e} + \frac{1}{2} \right\rfloor, \quad n \geq 1, \end{aligned} \quad (1)$$

where $\lfloor x \rfloor$ is the floor function, which stands for the maximum integer that is less than or equal to the real x .

For $x, y \in S_n$, if $\exists z \in S_n$, s.t. $x = zyz^{-1}$, then x and y will be called conjugate and y is called the conjugation of x . Of course the conjugacy relation is an equivalence relation. So, the set of derangements of order n can be divided into some conjugate classes. This paper is mainly concerned on the number of conjugate classes of

derangements of order n . The main method is similar to that described in reference [1].

A matrix of size $k \times n$ ($1 \leq k \leq n - 1$) with every row being a reordering of a fixed set of n elements and every column being a part of a reordering of the same set of n elements is called a Latin rectangle. Usually, the set of the n elements is assumed to be $\{1, 2, 3, \dots, n\}$. (In some literatures, the members in a Latin rectangle is assumed in the set $\{0, 1, 2, \dots, n - 1\}$.)

A $2 \times n$ Latin rectangle with the first row in increasing order could be considered as a derangement. An isotopy class of $2 \times n$ Latin rectangles will correspond to a unique conjugate class of derangements. So, the number of isotopy classes of $2 \times n$ Latin rectangles is the same as the number of conjugate classes of derangements of order n .

All the members in a conjugate class of derangements in S_n share the same cycle structure. Here, we define the cycle structure of a derangement as the sequence in nondecreasing order of the lengths (with duplicate entries) of all the cycles in the cycle decomposition of the derangement. A cycle structure of a derangement of order n could be considered as an integer solution of the equation as follows:

$$s_1 + s_2 + \dots + s_q = n, \quad (2 \leq s_1 \leq s_2 \leq \dots \leq s_q), \quad (2)$$

where s_1, s_2, \dots, s_q are unknowns.

For a fixed q , designate the number of integer solutions of equation (2) as $H_q(n)$ where q is less than $\lfloor n/2 \rfloor + 1$ (otherwise, $H_q(n)$ is defined by 0), and denote $h(n)$ the number of all the integer solutions of equation (1) for all possible q , i.e.,

$$h(n) = \sum_{q=1}^{\lfloor n/2 \rfloor} H_q(n). \quad (3)$$

So, the number of conjugate classes of derangements of order n is $h(n)$. Since $h(n)$ is the number of a type of restricted partitions, it is tightly connected with the partition number $p(n)$.

Following the notation of [2], denote by $P_q(n)$ the number of integer solutions of equation

$$s_1 + s_2 + \dots + s_q = n, \quad (1 \leq s_1 \leq s_2 \leq \dots \leq s_q), \quad (4)$$

for a fixed q , where $1 \leq q \leq n$, and by $p(n)$ the number of all the (unrestricted) partitions of n . It is clear that (in a lot of articles, $p(n, q)$ is used instead of $P_q(n)$, but in some other literatures, $p(n, q)$ stands for some other number.)

$$p(n) = \sum_{q=1}^n P_q(n). \quad (5)$$

There is a brief introduction of the important results on the partition number (or partition function) $p(n)$ and $P_q(n)$ in reference [2], such as the recursion formula of $p(n)$ and $P_q(n)$. More information about the partition number $p(n)$ may be found in reference [3]. There is a list of some important papers and book chapters on the partition number in [4] (including the "LINKS" and "REFERENCES") and [5]. Reference [1] presented some estimation formulae with high

accuracy for $p(n)$, which are revised from Hardy-Ramanujan's asymptotic formula.

There are also a lot of literatures on the number of some types of restricted partitions of n (such as [6-13]) or on the congruence properties of (restricted) partition function (such as [14-21]).

In [22], we can find many cases of restricted partitions (some of them are introduced in [23, 24] or [25]). One class is concerned on the restriction of the sizes of portions, such as portions restricted to Fibonacci numbers, powers (of 2 or 3), unit, primes, nonprimes, composites, or noncomposites; another class is related to the restriction of the number of portions, such as the cases that the number of parts will not exceed k ; the third class is about the restrictions for both, for example, the cases that the number of parts is restricted while the parts restricted to powers or primes. However, the author has not found too much information on the number $h(n)$, especially on the approximate calculation, although we can find a lot of information on other restricted partition numbers.

The basic method of function fitting (curve fitting) could be found in any textbook of numerical analysis, such as [26, 27]. Some tricks used here may be found in some books of data analysis such as [28]. They may be helpful for understanding the methods described in Section 3.

Section 2 will deduce the recursion formula for $h(n)$ and will show the relation of $h(n)$ and $p(n)$. Subsection 3.1 will deduce the asymptotic formula of $h(n)$ from Hardy-Ramanujan's asymptotic formula of $p(n)$ (mentioned in [1]). This new asymptotic formula $I_g(n)$ coincides with Ingham's result (refer [29, 30]). By bringing in two parameters $C_1(n)$ and $C_2(n)$ in the new asymptotic formula $I_g(n)$, we have reached several estimation formulae for $h(n)$ with high accuracy in Subsection 3.3, using the same ideas described in [1]. By fitting $h(n) - I_g(n)$, we have another two estimation formulae for $h(n)$ in Subsection 3.4. When $n < 100$, we have a more accurate estimation formula for $h(n)$ in Subsection 3.5. The relative errors of these estimation formulae will be presented to shown the accuracy.

2. Some Formulae for $h(n)$

In this section, we will derive a recursive formula from the method mentioned in reference ([2], p. 5355).

By definition, $h(k) = 0$ when $k < 2$, but here we assume that $h(k) = 0$ when $k < 0$, $h(0) = 1$, and $h(1) = 0$, for convenience.

It is mentioned in reference ([2], p. 52) that in 1942, Auluck gave an estimation of $P_q(n)$ by $P_q(n) \approx (1/q!) \binom{n-1}{q-1}$ when n is large enough.

By the same method shown in reference ([2], p. 53, 57), we can obtain the generation function of $h(n)$:

$$\begin{aligned} G(x) &= \sum_{n=0}^{\infty} h(n)x^n = \prod_{i=2}^{\infty} (1 - x^i)^{-1} \\ &= \frac{1}{(1-x^2)} \frac{1}{(1-x^3)} \frac{1}{(1-x^4)} \dots \frac{1}{(1-x^i)} \dots, \end{aligned} \quad (6)$$

and a formula

$$h(n) = \frac{1}{2\pi i} \oint_C \frac{G(x)}{x^{n+1}} dx, \tag{7}$$

where $h(0) = 1$, $h(1) = 0$, and C is a contour around the original point.

It is difficult to get a simple formula to count the solutions of equation (2) in general. However, for a fixed integer q , the number $H_q(n)$ of solutions is 0 (when $q > \lfloor n/2 \rfloor$) or

$$\begin{aligned} & \sum_{s_1=2}^{\lfloor n/q \rfloor} \sum_{s_2=s_1}^{\lfloor n-s_1/q-1 \rfloor} \cdots \sum_{s_{q-1}=s_{q-2}}^{\lfloor (n-s_1-s_2-\cdots-s_{q-2})/2 \rfloor} 1 \\ &= \sum_{s_1=2}^{\lfloor n/q \rfloor} \sum_{s_2=s_1}^{\lfloor n-s_1/q-1 \rfloor} \cdots \sum_{s_{q-2}=s_{q-3}}^{\lfloor (n-s_1-s_2-\cdots-s_{q-3})/3 \rfloor} \\ & \left(\frac{n-s_1-s_2-\cdots-s_{q-2}}{2} - s_{q-2} + 1 \right) \\ &= P_q(n-q) \left(\text{when } \left\lfloor q \leq \left\lfloor \frac{n}{2} \right\rfloor \right\right). \end{aligned} \tag{8}$$

It is not difficult to find out that

$$h(n) = \sum_{q=1}^{\lfloor n/2 \rfloor} H_q(n) = \sum_{q=1}^{\lfloor n/2 \rfloor} P_q(n-q). \tag{9}$$

and there is a recursion for $P_q(n)$ in reference ([2], p. 51) as follows:

$$P_q(n) = \sum_{j=1}^t P_j(n-q), \tag{10}$$

where $t = \min\{q, n-q\}$, so there is no difficulty to obtain the values of $P_q(n)$ and $h(n)$ when n is small.

For the value of $p(n)$, there is a recursion as follows:

$$\begin{aligned} p(n) &= p(n-1) + p(n-2) - p(n-5) \\ & \quad - p(n-7) + \cdots + (-1)^{k-1} p\left(n - \frac{3k^2 \pm k}{2}\right) + \cdots, \\ &= \sum_{k=1}^{k_1} (-1)^{k-1} p\left(n - \frac{3k^2 + k}{2}\right) \\ & \quad + \sum_{k=1}^{k_2} (-1)^{k-1} p\left(n - \frac{3k^2 - k}{2}\right), \end{aligned} \tag{11}$$

where

$$k_1 = \left\lfloor \frac{\sqrt{24n+1} - 1}{6} \right\rfloor, k_2 = \left\lfloor \frac{\sqrt{24n+1} + 1}{6} \right\rfloor, \tag{12}$$

and assume that $p(0) = 1$ (refer [2], p. 55). Here, we assume that $p(x) = 0$ when $x < 0$.

We can obtain the same recursion for $h(n)$ as follows:

$$\begin{aligned} h(n) &= h(n-1) + h(n-2) - h(n-5) - h(n-7) \\ & \quad + \cdots + (-1)^{k-1} h\left(n - \frac{3k^2 \pm k}{2}\right) + \cdots \\ &= \sum_{k=1}^{k_1} (-1)^{k-1} h\left(n - \frac{3k^2 + k}{2}\right) \\ & \quad + \sum_{k=1}^{k_2} (-1)^{k-1} h\left(n - \frac{3k^2 - k}{2}\right), \end{aligned} \tag{13}$$

where k_1 and k_2 are determined by equation (12), and assume that $h(0) = 1$ and $h(k) = 0$ when $k < 0$.

The proof of equation (13) is easy to understand.

By equation (6), we have

$$\left(\sum_{n=0}^{\infty} h(n)x^n \right) \left(\prod_{i=2}^{\infty} (1-x^i) \right) = 1. \tag{14}$$

Since $F(x) = \sum_{n=0}^{\infty} p(n)x^n = \prod_{i=1}^{\infty} (1-x^i)^{-1}$ (where $p(0) = 1$), $(\sum_{n=0}^{\infty} p(n)x^n) (\prod_{i=1}^{\infty} (1-x^i)) = 1$ or

$$\left(\sum_{n=0}^{\infty} p(n)x^n \right) (1-x) \left(\prod_{i=2}^{\infty} (1-x^i) \right) = 1. \tag{15}$$

Comparing equations (14) and (15), we have

$$\begin{aligned} \sum_{n=0}^{\infty} h(n)x^n &= \left(\sum_{n=0}^{\infty} p(n)x^n \right) (1-x) \\ &= \sum_{n=0}^{\infty} (p(n) - p(n-1))x^n, \end{aligned} \tag{16}$$

by assumption $h(k) = p(k) = 0$ when $k < 0$. Hence,

$$h(n) = p(n) - p(n-1), \quad (n = 0, 1, 2, \dots). \tag{17}$$

By equation (17),

$$\begin{aligned} h(n) &= h(n-1) + h(n-2) - h(n-5) - h(n-7) \\ & \quad + \cdots + (-1)^{k-1} h\left(n - \frac{3k^2 \pm k}{2}\right) + \cdots \\ &= \sum_{k=1}^{k_1} (-1)^{k-1} h\left(n - \frac{3k^2 + k}{2}\right) \\ & \quad + \sum_{k=1}^{k_2} (-1)^{k-1} h\left(n - \frac{3k^2 - k}{2}\right). \end{aligned} \tag{18}$$

We can easily obtain the solutions of equation (2) by hand when $n < 13$. By equation (13), we can obtain the number $h(n)$ of solutions of equation (2) by writing a small program in some Computer Algebra System (CAS) software such as “maple,” “maxima,” and “axiom” or some other software likewise (be aware of that 0 is not a valid index value in some software such like maple).

The value of $h(n)$ when $n < 250$ is shown in Table 1 (on page 5) and Table 2 (on page 5). Some values of $H_q(n)$ are shown on Table 3 (on page 5).

Obviously, $h(n) < p(n)$ holds by definition (when $n > 1$). As $p(n)$ grows much more slowly than exponential functions, i.e., for any $r > 1$, $p(n) < r^n$ will hold when n is large enough, which means we cannot estimate $p(n)$ and $h(n)$ by an exponential function. As $p(n)$ grows faster than any power of n , it means we cannot estimate $p(n)$ by a polynomial function (refer [2], p. 53). So, $h(n)$ cannot be estimated by a polynomial function, either.

3. The Estimation of $h(n)$

The recursion formula equation (13) for $h(n)$ is not convenient in practical for a lot of people who do not want to write programs. Sometimes we need the approximation value, such as the cases mentioned in [1], so an estimation formula is necessary.

The graph of data $(n, \ln(h(n)))$ ($n = 60 + 20k, k = 1, 2, \dots, 397$) is shown in Figure 1 on page 5. Here, the data points are displayed by small hollow circles, and the circles are very crowded that we may believe that the circles themselves be a very thick curve if we notice only the right-hand part. In this figure, the data points in the lower left part are sparse (compared with the points in the upper right part), and we may find some hollow circles easily. If there is a curve passes through these hollow circles, we will notice it (as shown in Figure 2 on page 14). However, later in Figure 3, the circles distribute uniformly on a curve, it will be difficult to distinguish the circles, and the curve passes through the centers of them.

The author has not found a practical estimation formula with high accuracy of the number $h(n)$ before.

Actually, it is very difficult to find directly a simple function to fit the data on Figure 1 with high accuracy. The main reason is that the fitting functions obtained by the methods used frequently could not reach satisfying accuracy.

We have several accurate estimation formula of $p(n)$ (refer [1]), such as

$$R'_{h_2}(n) = \left[\frac{\exp(\sqrt{2/3} \pi \sqrt{n})}{4\sqrt{3} (n + a_2 \sqrt{n} + c_2 + b_2)} + \frac{1}{2} \right], (n \geq 80), \quad (19)$$

and

TABLE 1: The value of $h(n)$ when $1 \leq n \leq 100$.

n	$h(n)$	n	$h(n)$	n	$h(n)$	n	$h(n)$	n	$h(n)$
1	0	21	165	41	7245	61	155038	81	2207851
2	1	22	210	42	8591	62	178651	82	2501928
3	1	23	253	43	10087	63	205343	83	2832214
4	2	24	320	44	11914	64	236131	84	3205191
5	2	25	383	45	13959	65	270928	85	3623697
6	4	26	478	46	16424	66	310962	86	4095605
7	4	27	574	47	19196	67	356169	87	4624711
8	7	28	708	48	22519	68	408046	88	5220436
9	8	29	847	49	26252	69	466610	89	5887816
10	12	30	1039	50	30701	70	533623	90	6638248
11	14	31	1238	51	35717	71	609237	91	7478186
12	21	32	1507	52	41646	72	695578	92	8421448
13	24	33	1794	53	48342	73	792906	93	9476370
14	34	34	2167	54	56224	74	903811	94	10659543
15	41	35	2573	55	65121	75	1028764	95	11981699
16	55	36	3094	56	75547	76	1170827	96	13462885
17	66	37	3660	57	87331	77	1330772	97	15116626
18	88	38	4378	58	101066	78	1512301	98	16967206
19	105	39	5170	59	116600	79	1716486	99	19031739
20	137	40	6153	60	134647	80	1947826	100	21339417

$$R'_{h_0}(n) = \left[\frac{\exp(\sqrt{2/3} \pi \sqrt{n})}{4\sqrt{3} (n + C'_2(n))} + \frac{1}{2} \right], \quad 1 \leq n \leq 100, \quad (20)$$

where $a_2 = 0.4432884566$, $b_2 = 0.1325096085$, $c_2 = 0.274078$, and

$$C'_2(n) = \begin{cases} 0.4527092482 \times \sqrt{n + 4.35278} - \\ 0.05498719946, & n = 3, 5, 7, \dots, 99; \\ 0.4412187317 \times \sqrt{n - 2.01699} + \\ 0.2102618735, & n = 4, 6, 8 \dots, 100. \end{cases} \quad (21)$$

By (17), we can obtain $h(n)$ by

$$h_1(n) = \begin{cases} R'_{h_0}(n) - R'_{h_0}(n-1), & 2 \leq n \leq 80, \\ R'_{h_2}(n) - R'_{h_2}(n-1), & n > 80. \end{cases} \quad (22)$$

and the error of this formula will not exceed twice of the error of $R'_{h_2}(n)$ or $R'_{h_0}(n)$. Of course, this formula is not as simple as we want, but the accuracy is very good.

3.1. Asymptotic Formula. As $h(n) = p(n) - p(n-1)$, by Hardy–Ramanujan’s asymptotic formula,

$$p(n) \sim \frac{1}{4n\sqrt{3}} \exp\left(\sqrt{\frac{2}{3}} \pi \sqrt{n}\right), \quad (23)$$

(refer [1, 3, 31–35]), we assume that, when $n \gg 1$, $h(n) \sim \exp(\sqrt{2/3} \pi \sqrt{n})/4\sqrt{3}n - \exp(\sqrt{2/3} \pi \sqrt{n-1})/4\sqrt{3}(n-1)$. So,

TABLE 2: The value of $h(n)$ when $101 \leq n \leq 250$.

n	$h(n)$	n	$h(n)$	n	$h(n)$	n	$h(n)$
101	23911834	116	124763797	131	593224104	146	2608194590
102	26784253	117	138801828	132	656291385	147	2871619379
103	29983571	118	154364067	133	725798623	148	3160747519
104	33552415	119	171594522	134	802411183	149	3477935703
105	37524344	120	190680895	135	886795381	150	3825880113
106	41950627	121	211798491	136	979745604	160	9775430911
107	46873053	122	235172861	137	1082063336	170	24329692015
108	52353455	123	261017329	138	1194696815	180	59110637816
109	58443396	124	289602259	139	1318608064	190	140453804468
110	65217506	125	321186852	140	1454928240	200	326926597263
111	72739457	126	356095340	141	1604811073	210	746521272980
112	81098953	127	394641603	142	1769604112	220	1674422848222
113	90374472	128	437214305	143	1950689437	230	3693304861665
114	100674037	129	484193270	144	2149671688	240	8019313019148
115	112093786	130	536043530	145	2368203564	250	17156634544056

TABLE 3: The number of solutions of equation (1) for different q .

n	$h(n)$	$H_1(n)$	$H_2(n)$	$H_3(n)$	$H_4(n)$	$H_5(n)$	$H_6(n)$	$H_7(n)$
4	2	1	1					
5	2	1	1					
6	4	1	2	1				
7	4	1	2	1				
8	7	1	3	2	1			
9	8	1	3	3	1			
10	12	1	4	4	2	1		
11	14	1	4	5	3	1		
12	21	1	5	7	5	2	1	
13	24	1	5	8	6	3	1	
14	34	1	6	10	9	5	2	1
15	41	1	6	12	11	7	3	1

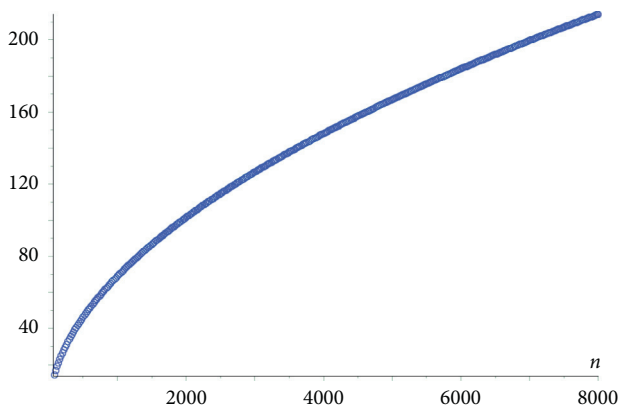


FIGURE 1: The graph of the data $(n, \ln h(n))$.

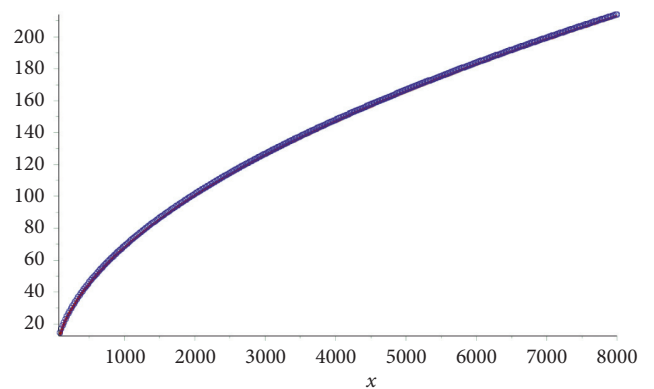


FIGURE 2: The graph of the data $(n, \ln h(n))$ and the fitting curve $\ln(I_{g1}(n))$.

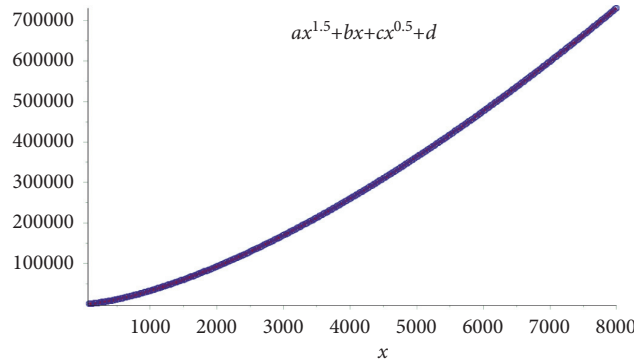


FIGURE 3: The graph of the data $(n, \pi \exp(\pi\sqrt{2/3} \sqrt{n})/12\sqrt{2h(n)})$ and the fitting curve.

$$\begin{aligned}
 h(n) &\sim \frac{\exp(\sqrt{2/3} \pi \sqrt{n-1})}{4\sqrt{3}} \left(\frac{\exp(\pi\sqrt{2/3} (\sqrt{n} - \sqrt{n-1}))}{n} - \frac{1}{n-1} \right) \\
 &= \frac{\exp(\sqrt{2/3} \pi \sqrt{n-1})}{4\sqrt{3}} \left(\frac{\exp(\pi\sqrt{2/3} / \sqrt{n} + \sqrt{n-1})}{n} - \frac{1}{n-1} \right) \\
 &\sim \frac{\exp(\sqrt{2/3} \pi \sqrt{n})}{4\sqrt{3}} \left(\frac{\exp(\pi\sqrt{2/3} / 2\sqrt{n})}{n} - \frac{1}{n-1} \right) \sim \frac{\exp(\sqrt{2/3} \pi \sqrt{n})}{4\sqrt{3}} \left(\frac{1 + \pi/\sqrt{6n}}{n} - \frac{1}{n-1} \right) \\
 &\sim \frac{\exp(\sqrt{2/3} \pi \sqrt{n})}{4\sqrt{3}} \left(\frac{\pi}{\sqrt{6n^3}} \right) = \frac{\pi \exp(\sqrt{2/3} \pi \sqrt{n})}{12\sqrt{2n^3}}.
 \end{aligned} \tag{24}$$

So,

$$h(n) \sim \frac{\pi}{12\sqrt{2n^3}} \exp(\sqrt{2/3} \pi \sqrt{n}). \tag{25}$$

In coincidence, half a year after the main results were obtained in this paper, the author found an asymptotic formula as follows:

$$P_{a,b}(n) \sim \Gamma(b/a) \pi^{b/a-1} 2^{-(3/2)-(b/2a)} 3^{-(b/2a)} a^{-(1/2)+(b/2a)} n^{-a+b/2a} e^{\pi\sqrt{2n/3a}}, \tag{26}$$

in [30]. When $a = 1$ and $b = 2$, we will have

$$P_{1,2}(n) \sim \frac{\pi}{12\sqrt{2n^3}} \exp(\pi\sqrt{2/3}n), \tag{27}$$

which coincides with the asymptotic formula obtained here.

Formula (25) will be called the Ingham–Meinardus asymptotic formula in this paper since Daniel mentioned in [30] that this general asymptotic formula (26) was first given by A. E. Ingham in [29] and the proof was refined by G. Meinardus later in another two papers written in German.

Later in this paper, $(\pi/12\sqrt{2n^3}) \exp(\sqrt{2/3} \pi \sqrt{n})$ will be denoted by $I_g(n)$ for short.

It is not satisfying to estimate $h(n)$ by $I_g(n)$ when n is small. The relative error of $I_g(n)$ to $h(n)$ is greater than

6% as shown in Table 4 (on page 6). The round approximation

$$I'_g(n) = \left\lfloor I_g(n) + \frac{1}{2} \right\rfloor, \tag{28}$$

will not change the accuracy distinctly, as shown in Table 5 (on page 6). So, it is necessary to modify the asymptotic formula for better accuracy.

3.2. Method A: Modifying the Exponent. In this subsection, we consider fitting $h(n)$ by $I_{ga} = (\pi/12\sqrt{2n^3}) \exp(\sqrt{2/3} \pi \sqrt{n + C_1(n)})$ or fitting $(n, (3/2\pi^2) (\ln(12\sqrt{2n^3} h(n)/\pi))^2 - n)$ ($n = 60 + 20k, k = 1, 2, \dots, 397$) by a function

$$f_1(x) \doteq \frac{a_1}{(x + c_1)^{e_1}} + b_1. \tag{29}$$

Let $C_1(n) = (3/2\pi^2) (\ln(12\sqrt{2n^3} h(n)/\pi))^2 - n$. The reason that we fit $C_1(x)$ by the function in the form displayed in (29) is the same as that described in Section 3 of [1] (although the data differ distinctly). Many other types of functions have been tested, but they cannot fit these data very well.

However, here it is not valid to obtain the constants in $f_1(n)$ by the iteration method described in reference [1].

The graph of the data $(n, (3/2\pi^2) (\ln(12\sqrt{2n^3} h(n)/\pi))^2 - n)$ ($n = 60 + 20k, k = 1, 2, \dots, 397$) is shown in Figure 4 on page 7.

TABLE 4: The relative error of $I_g(n)$ to $h(n)$ when $n \leq 1000$.

n	Rel-Err (%)	n	Rel-Err (%)	n	Rel-Err (%)	n	Rel-Err (%)	n	Rel-Err (%)
1		16	50.30	40	32.10	220	13.10	520	8.39
2	146.24	17	56.82	50	28.60	240	12.50	540	8.23
3	202.89	18	46.69	60	25.90	260	12.00	560	8.08
4	95.59	19	52.75	70	23.90	280	11.50	580	7.93
5	156.43	20	44.94	80	22.30	300	11.10	600	7.79
6	68.62	21	48.48	90	20.90	320	10.80	640	7.54
7	121.38	22	43.47	100	19.80	340	10.40	680	7.31
8	65.43	23	46.00	110	18.80	360	10.10	720	7.10
9	88.38	24	41.09	120	18.00	380	9.86	760	6.91
10	62.58	25	43.68	130	17.20	400	9.60	800	6.73
11	79.47	26	39.93	140	16.60	420	9.36	840	6.56
12	53.29	27	41.27	150	16.00	440	9.14	880	6.41
13	70.98	28	38.50	160	15.40	460	8.93	920	6.27
14	53.12	29	39.70	180	14.50	480	8.74	960	6.13
15	60.35	30	37.00	200	13.70	500	8.56	1000	6.01

TABLE 5: The relative error of $[I_g(n) + 1/2]$ to $h(n)$ when $n \leq 30$.

n	Rel-Err	n	Rel-Err	n	Rel-Err	n	Rel-Err	n	Rel-Err
1	—	7	125%	13	70.83%	19	52.38%	25	43.60%
2	100%	8	71.43%	14	52.94%	20	45.26%	26	39.96%
3	200%	9	87.50%	15	60.98%	21	48.48%	27	41.29%
4	100%	10	66.67%	16	50.91%	22	43.33%	28	38.56%
5	150%	11	78.57%	17	57.58%	23	45.85%	29	39.67%
6	75%	12	52.38%	18	46.59%	24	40.94%	30	37.05%

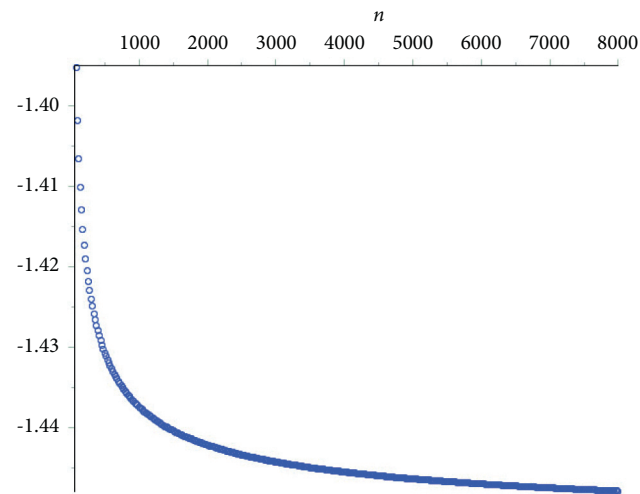


FIGURE 4: The graph of the data $(n, (3/2\pi^2)(\ln(12\sqrt{2n^3}h(n)/\pi))^2 - n)$.

First, we try to fit $(n, (3/2\pi^2)(\ln(12\sqrt{2n^3}h(n)/\pi))^2 - n)$ ($n = 60 + 20k, k = 1, 2, \dots, 397$) by a function in the form as follows:

$$f_1(x) \doteq \frac{a_1}{\sqrt{x+c_1}} + b_1. \tag{30}$$

That means we have assumed that $e_1 = 1/2$, temporarily. We will explain the reason in Subsection 3.2.3.

The average error of $f_1(x)$ is

$$\begin{aligned} E_1 &= \sqrt{\frac{1}{K_1} \sum_n (C_1(n) - f_1(n))^2} \\ &= \sqrt{\frac{1}{K_1} \sum_n \left(C_1(n) - \frac{a_1}{\sqrt{n+c_1}} - b_1 \right)^2} \\ E_1 &= \sqrt{\frac{1}{K_1} \sum_{k=1}^{K_1} \left(C_1(60+20k) - \frac{a_1}{\sqrt{60+20k+c_1}} - b_1 \right)^2}, \end{aligned} \tag{31}$$

where $K_1 = 397$ and n ranges from 80 to 8000, by step 20. Here, only a_1, b_1 , and c_1 are unknown, so we can consider E_1 as a function of the variables (a_1, b_1, c_1) .

We want to find a triple (a_1, b_1, c_1) such that E_1 reaches its minimum or to make E_1 as small as possible.

Since a lot of functions have several local minimum points, it is necessary to find out whether $E_1 = E_1(a_1, b_1, c_1)$ has more than one local minimum before we start to calculate the minimum point by the numeral method. However, $E_1 = E_1(a_1, b_1, c_1)$ is too complicate, and it is very difficult to know all the critical points in the range we are considering.

3.2.1. Preparation Work. For a given pair (a_1, c_1) , by the property of the arithmetic mean (for some given data $x_i (i=1, 2, \dots, k; x_i \in \mathbb{R})$, the function $s(t) = \sqrt{(1/k) \sum_{i=1}^k (x_i - t)^2}$ reaches its minimum at $t = (1/k) \sum_{i=1}^k x_i$), it is clear that E_1 reaches its minimum when

$$\begin{aligned} b_1 &= \frac{1}{K_1} \sum_n \left(C_1(n) - \frac{a_1}{\sqrt{n+c_1}} \right), \\ &= \overline{C_1} - \frac{1}{K_1} \sum_{n'} \frac{a_1}{\sqrt{n'+c_1}}, \end{aligned} \tag{32}$$

where $\overline{C_1} = (1/K_1) \sum_{n'} C_1(n')$.

Let $E_1 = \sqrt{(1/K_1)\sum_n(C_1(n) - a_1/\sqrt{n+c_1} - \bar{C}_1 + (1/K_1)\sum_n a_1/\sqrt{n'+c_1})^2}$ be the average error of the fitting function $f_1(x) \doteq a_1/\sqrt{x+c_1} + \bar{C}_1 - (1/K_1)\sum_n a_1/\sqrt{n'+c_1}$. (Here, a_1 and b_1 are undetermined coefficients.)

Let $G_1 = E_1^2 = (1/K_1)\sum_n(C_1(n) - a_1/\sqrt{n+c_1} - \bar{C}_1 + (1/K_1)\sum_n a_1/\sqrt{n'+c_1})^2$. Here, only a_1 and b_1 are unknowns. G_1 could be considered as a function of (a_1, c_1) . In order to find the minimum point of G_1 , we can draw the figure of the function $G_1 = G_1(a_1, c_1)$ (in a cube coordinate system with axis a_1, c_1 , and G_1) as shown in Figures 5–7. Figures 8 and 9 are the projection of the graph of (a_1, c_1, G_1) (when $-100 \leq a_1 \leq 100$ and $-50 \leq c_1 \leq 100$, which is a part of a surface) on the $a_1 - G_1$ plane (spanned by the axis a_1 and G_1) and $c_1 - G_1$ plane, respectively.

From these figures, we can find out that the influence of c_1 to G_1 is much less than that of a_1 . In Figure 10, we find that when G_1 reaches its minimum, a_1 is between 0.50 and 0.53, but there is not a definite range for c_1 .

It is possible that for different range of c_1 , the range of a_1 when G_1 reaches its minimum will be different. However, considering that $a_1/\sqrt{n+c_1} + b_1$ is a real, c_1 should be greater than -1 in theory. (For the fitting data used here, c_1 should be greater than -80 .) From Figure 8, we can see that G_1 touches its bottom when $-15 \leq a_1 \leq 15$. Although we cannot see clearly the exact value of a_1 in the minimum points, we can draw another figure of (a_1, c_1, G_1) when $-15 \leq a_1 \leq 15$ and $-1 \leq c_1 \leq 100$ to observe more details (the figure is not presented here), and then we will find that the more detailed range of a_1 for the minimum points is $[-3, 3]$ in the new figure (not presented), and next we will draw the figures of (a_1, c_1, G_1) when $-3 \leq a_1 \leq 3$, $0 \leq a_1 \leq 1$, $0.2 \leq a_1 \leq 0.8$, or $0.45 \leq a_1 \leq 0.6$, respectively, while $-1 \leq c_1 \leq 100$, we will find the range of a_1 of the minimum points of G_1 is about $[0.50, 0.53]$. The projections of Figure 7 of (a_1, c_1, G_1) when $0.45 \leq a_1 \leq 0.6$ and $-1 \leq c_1 \leq 100$ are shown in Figures 11 and 10.

In Figure 9, for the curves on the bottom, G_1 decreases with c_1 at first then increases with c_1 , but it is difficult to find the critical point in the figure since different curves have different critical points.

Although we cannot find a satisfying value of a_1 or c_1 from the figures to construct a fitting function f_1 , these pictures show that the figure of $G_1 = (a_1, c_1, G_1)$ has only one bottom in the domain we are considering, unlike the figure of another function shown in Figure 12, so the existence of the minimum point is almost confirmed; therefore, we are confident to find the value of a_1 or c_1 in the minimum point by the numerical method. This guarantees the validity of the numerical calculation by loop in the next step.

3.2.2. Find c_1 . On the other hand, by the least square method, to fit the data (x_k, y_k) ($k=1, 2, \dots, K_1$) by a linear function $y = a \times x + b$, the result is that

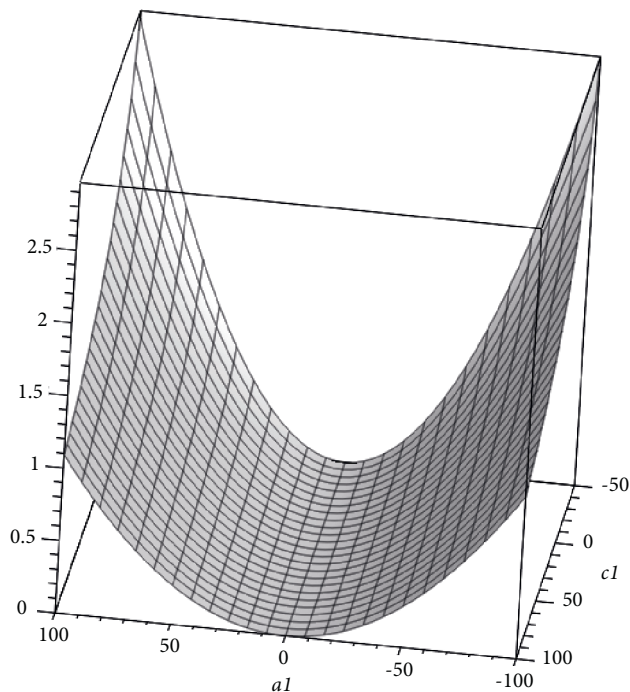


FIGURE 5: The graph of the data (a_1, c_1, G_1) when $-100 \leq a_1 \leq 100$ and $-50 \leq c_1 \leq 100$.

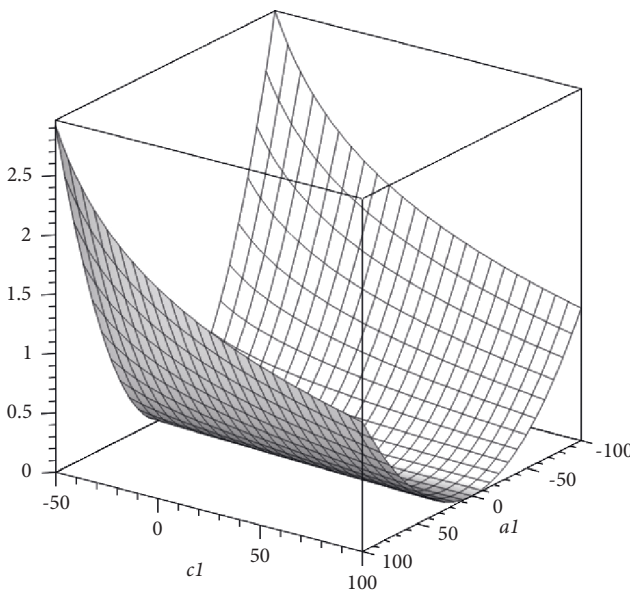


FIGURE 6: The graph of the data (a_1, c_1, G_1) when $-100 \leq a_1 \leq 100$ and $-50 \leq c_1 \leq 100$ version 2.

$$a = \frac{\overline{x_n \cdot y_n} - \overline{x_n} \cdot \overline{y_n}}{\overline{x_n^2} - (\overline{x_n})^2}, \tag{33}$$

$$b = \frac{\overline{x_n \cdot x_n \cdot y_n} - \overline{x_n^2} \cdot \overline{y_n}}{(\overline{x_n})^2 - \overline{x_n^2}} = \overline{y_n} - \overline{x_n} \cdot a, \tag{34}$$

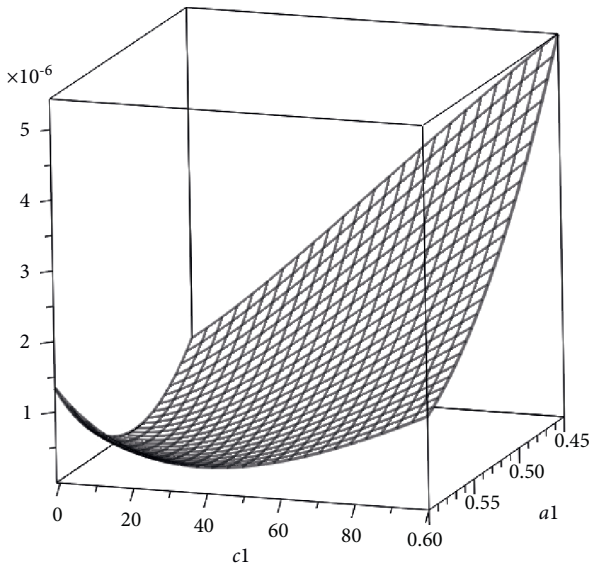


FIGURE 7: The graph of the data (a_1, c_1, G_1) when $0.45 \leq a_1 \leq 0.60$ and $-1 \leq c_1 \leq 100$.

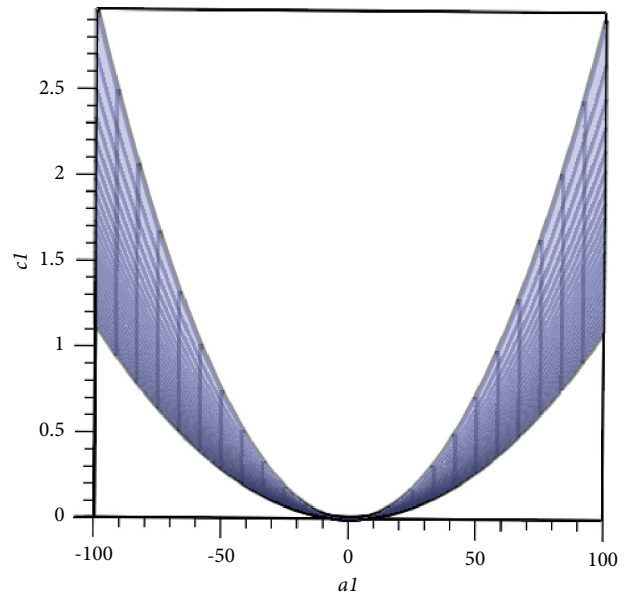


FIGURE 9: The projection of the graph of the data (a_1, c_1, G_1) on the $c_1 - G_1$ plane when $-100 \leq a_1 \leq 100$ and $-50 \leq c_1 \leq 100$.

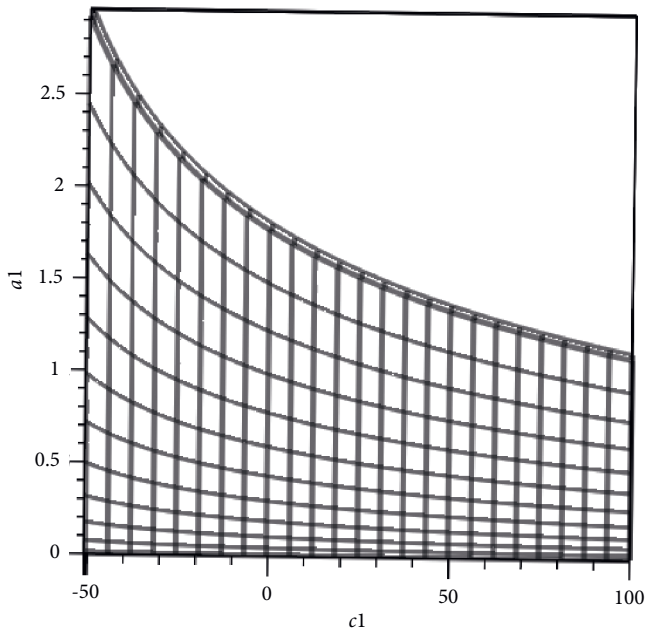


FIGURE 8: The projection of the graph of the data (a_1, c_1, G_1) on the $a_1 - G_1$ plane when $-100 \leq a_1 \leq 100$ and $-50 \leq c_1 \leq 100$.

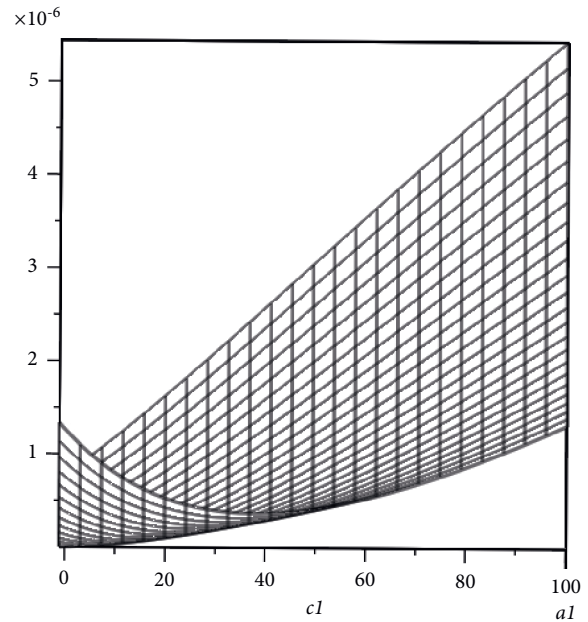


FIGURE 10: The projection of the graph of the data (a_1, c_1, G_1) on the $c_1 - G_1$ plane when $0.45 \leq a_1 \leq 0.60$ and $-1 \leq c_1 \leq 100$.

where $\bar{x}_n = (1/K_1) \sum_{i=1}^{K_1} x_i$ is the average value of x_i , $\bar{y}_n = (1/K_1) \sum_{i=1}^{K_1} y_i$, $\bar{x}_i^2 = (1/K_1) \sum_{i=1}^{K_1} x_i^2$, and $\bar{x}_n \cdot \bar{y}_n = (1/K_1) \sum_{i=1}^{K_1} x_i \cdot y_i$. By definition, $(\bar{x}_n)^2 = ((1/K_1) \sum_{i=1}^{K_1} x_i)^2$ is the square of

the average value of x_n . So, by the least square method, a and b are uniquely determined by the given data (x_k, y_k) ($k=1, 2, \dots, K_1$).

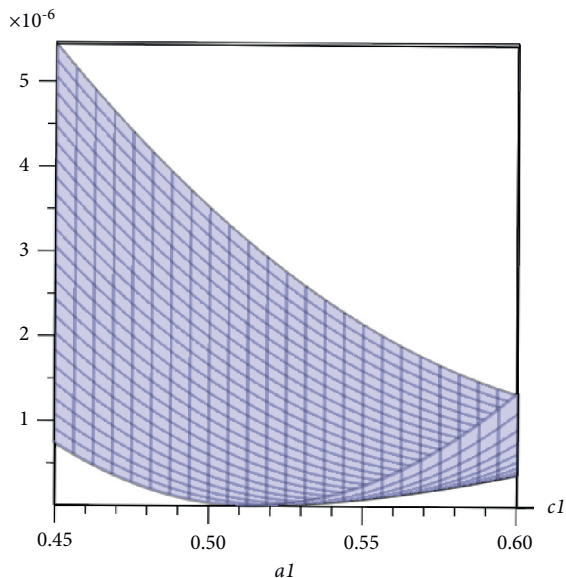


FIGURE 11: The projection of the graph of the data (a_1, c_1, G_1) on the $a_1 - G_1$ plane when $0.45 \leq a_1 \leq 0.60$ and $-1 \leq c_1 \leq 100$.

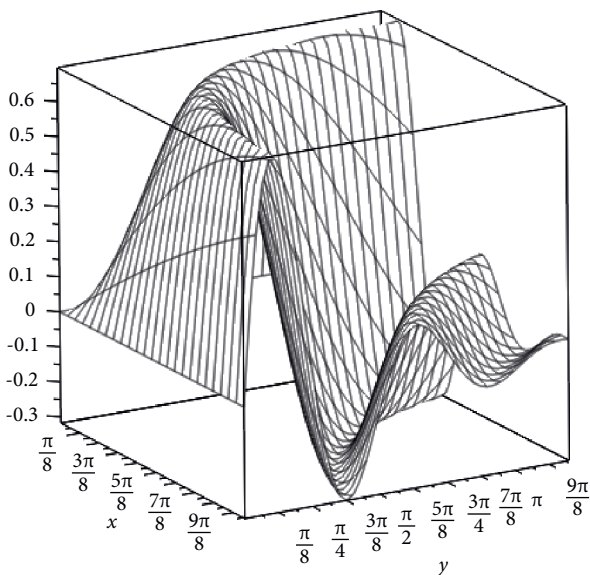


FIGURE 12: Example of a surface with more than one bottom.

For every given value of c_1 (greater than -80), we can fit $(n, C_1(n))$ ($n = 60 + 20k, k = 1, 2, \dots, 397$) by a function $f_1(x) \doteq a_1/\sqrt{x+c_1} + b_1$ by the least square method if we consider $1/\sqrt{60+20k+c_1}$ and $C_1(60+20k)$ as x_k and y_k , respectively. Then,

$$\begin{aligned} \overline{x_n} &= \frac{1}{K_1} \sum_{k=1}^{K_1} x_k = \frac{1}{K_1} \sum_{k=1}^{K_1} \frac{1}{\sqrt{60+20k+c_1}}, \\ \overline{y_n} &= \frac{1}{K_1} \sum_{k=1}^{K_1} y_k = \frac{1}{K_1} \sum_{k=1}^{K_1} C_1(60+20k), \\ \overline{x_n^2} &= \frac{1}{K_1} \sum_{k=1}^{K_1} x_k^2 = \frac{1}{K_1} \sum_{k=1}^{K_1} \frac{1}{60+20k+c_1}, \\ \overline{x_n \cdot y_n} &= \frac{1}{K_1} \sum_{k=1}^{K_1} x_k \cdot y_k = \frac{1}{K_1} \sum_{k=1}^{K_1} \frac{C_1(60+20k)}{\sqrt{60+20k+c_1}}, \\ a_1 &= \frac{\overline{x_n \cdot y_n} - \overline{x_n} \cdot \overline{y_n}}{\overline{x_n^2} - (\overline{x_n})^2}, \\ b_1 &= \overline{y_n} - \overline{x_n} \cdot a_1. \end{aligned} \tag{35}$$

So, a_1 and b_1 could both be considered as functions of c_1 , denoted by $a_1 = a_1(c_1)$ and $b_1 = b_1(c_1)$, since they are uniquely determined by c_1 with the given data.

Then, $G_2 = E_1^2 = (1/K_1) \sum_{k=1}^{K_1} (C_1(60+20k) - a_1(c_1)/\sqrt{60+20k+c_1} - b_1(c_1))^2$ is a function of c_1 .

It will cost some time to plot the figure of the function $G_2 = G_2(c_1)$ in a CAS software.

If we plot the figure of the function $G_2 = G_2(c_1)$ on the coordinates (as shown in Figures 13–15), we will find that G_2 reaches its minimum when $c_1 \approx -3.2594807$. In Figure 15, we find that the curve of $G_2 = G_2(c_1)$ is not so smooth. The reason is that we hold up 18 significant digits in the process. If we compute more significant digits in the process, the curve on Figure 15 will be more smooth, at the cost of much more time. By writing a small program (since the default function to find the minimum provided by the software Maple 18 is unable to deal with such a complicated function $G_2 = G_2(c_1)$ involving so much data), we can obtain a more accurate value of the critical point as follows:

$$c_1 = -3.259480684. \tag{36}$$

When the value of c_1 is obtained, we can find the value of a_1 and b_1 by the least square method without difficulty, i.e.,

$$\begin{aligned} a_1 &= 0.5097429624, \\ b_1 &= -1.453552800. \end{aligned} \tag{37}$$

However, here c_1 is less than -1 , so the estimation formula for $h(n)$ constructed from these coefficients is invalid when $n < 4$.

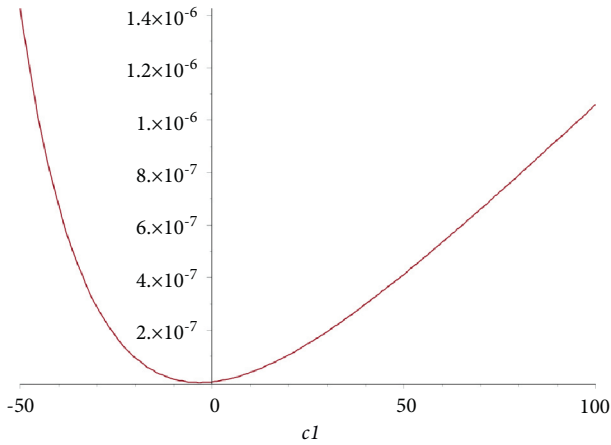


FIGURE 13: The graph of the function $G_2 = G_2(c_1)$ when $-50 \leq c_1 \leq 100$.

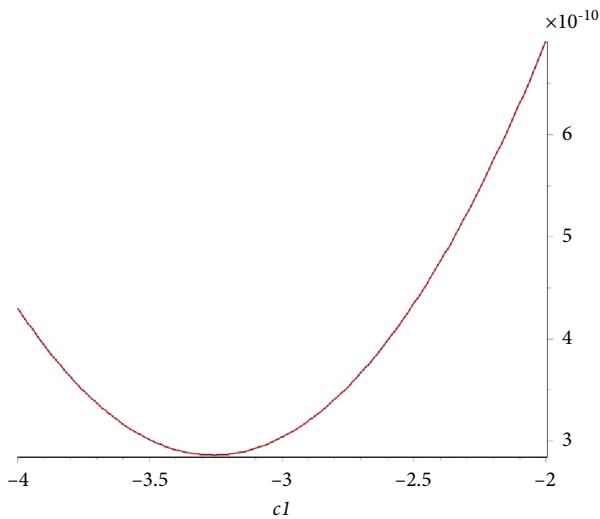


FIGURE 14: The graph of the function $G_2 = G_2(c_1)$ when $-4 \leq c_1 \leq -2$.

3.2.3. *Confirm e_1 .* In [1], we fit $C_1(n) = 3/2 \cdot (\ln(4n\sqrt{3} p(n)))^2 / \pi^2 - n$ by a function $f_1(x) \doteq a_1 / (n + c_1)^{e_1} + b_1$ when estimating $p(n)$ and found that $e_1 \approx 0.50$ by iteration. Here, the iteration method does not work well, so we fit $C_1(n) = (3/2\pi^2)(\ln(12\sqrt{2n^3} h(n)/\pi))^2 - n$ by a function $f_1(x) \doteq a_1 / \sqrt{n + c_1} + b_1$ directly, which means that we have assumed that $e_1 = 1/2$. Here, we may doubt that whether $e_1 = 0.5$ is the best option for us?

Here, we use the same idea described in Subsection 3.2.1.

For every pair (e_1, c_1) , we can obtain corresponding a_1 and b_1 by the least square method, just like (33) and (34), except that here $x_k = 1/(60 + 20k + c_1)^{e_1}$.

So, the square of the average error

$$G_3 = E_1^2 = \frac{1}{K_1} \sum_n \left(C_1(n) - \frac{a_1(e_1, c_1)}{(n + c_1)^{e_1}} - b_1(e_1, c_1) \right)^2, \quad (38)$$

could be considered as a function of e_1 and c_1 as both $a_1 = a_1(e_1, c_1)$ and $b_1 = b_1(e_1, c_1)$ could be expressed by certain elementary functions of e_1 and c_1 .

If we draw the figure of the function $G_3 = G_3(e_1, c_1)$, we will find that the surface has only one bottom when $0.1 \leq e_1 \leq 0.9$ and $-50 \leq c_1 \leq 100$, as shown in Figure 16. However, the process to draw the figure is time-consuming. It costs more than 5 hours on a notebook (ThinkPad E40 Edge, with 6 GB RAM and AMD P360 Dual-Core Processor 2.30 GHz) by Maple 18 in Ubuntu 14.04.1 system.

After that, by writing another program, we can obtain the approximate value of (e_1, c_1) where G_3 touches the bottom, i.e., $e_1 \approx 0.494$ and $c_1 \approx -4.85$, when 18 significant digits are involved in the process, which still costs tens of minutes. Considering that we have used only a small part of data, we cannot afford the time for computing more significant digits in process, and the computing is so complicated; hence, error accumulation effect is considerable, so we choose $e_1 = 0.50$ while it differs very little with 0.494. Another reason is that we prefer simple exponent, as the time spent on computing a square root is much less than that to compute a power with exponent 0.494 in general. Here, the value of $c_1 \approx -4.85$ is obviously different from the value obtained at the end of Subsection 3.2.2 because of the little difference on e_1 . Therefore, it will be fine to use the result in Subsection 3.2.2).

In this figure, the points are shown as small circles which are very close to each other. These crowded circles seem like a thick curve. A fitting curve passes through the center of these circles. The fitting curve might not be found in reduce printing. That means the curve fits the points (displayed as circles) very well.

3.2.4. *The Result.* By the value $a_1 = 0.5097429624$, $b_1 = -1.453552800$, and $c_1 = -3.259480684$ obtained in Subsection 3.2.2, we will have a fitting function $f_1(x) \doteq a_1 / \sqrt{x + c_1} + b_1$.

The graph of $f_1(x)$ (when $-80 \leq x \leq 8000$) and the graph of the data $(n, (3/2\pi^2)(\ln(12\sqrt{2n^3} h(n)/\pi))^2 - n)$ ($n = 60 + 20k, k = 1, 2, \dots, 397$) are shown in Figure 17. It shows that $f_1(n)$ fits $(3/2\pi^2)(\ln(12\sqrt{2n^3} h(n)/\pi))^2 - n$ very well.

Then, we could fit $h(n)$ by

$$I_{ga}(n) = \frac{\pi \exp(\sqrt{2/3} \pi \sqrt{n + a_1 / \sqrt{x + c_1} + b_1})}{12\sqrt{2n^3}}, \quad n \geq 4. \quad (39)$$

The graph of the function $\ln(I_{ga}(x))$ and the graph of the data $(n, \ln(h(n)))$ ($n = 60 + 20k, k = 1, 2, \dots, 397$) is shown in Figure 18. It seems that $I_{ga}(n)$ fits $h(n)$ very well.

The relative error of I_{ga} is shown in Table 6 (when $n \leq 1000$) and Figure 19 (when $1000 < n \leq 10000$).

When $n < 20$, the relative error of I_{ga} is still greater than 2%. Although it is much better than the error of I_g , it is not as good as expected when $n < 40$. If we take the round approximation by

$$I'_{ga}(n) = \left[\frac{\pi \exp(\sqrt{2/3} \pi \sqrt{n + a_1 / \sqrt{x + c_1} + b_1})}{12\sqrt{2n^3}} + \frac{1}{2} \right], \quad n \geq 4, \quad (40)$$

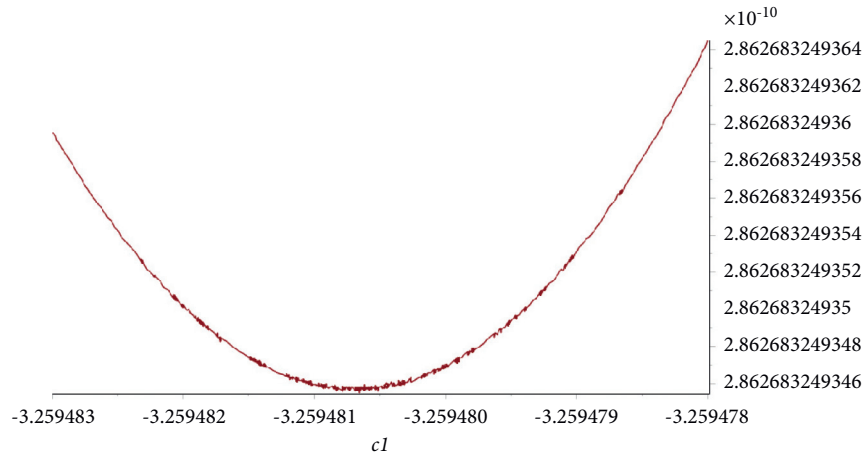


FIGURE 15: The graph of the function $G_2 = G_2(c_1)$ when $-3.259483 \leq c_1 \leq -3.259478$.

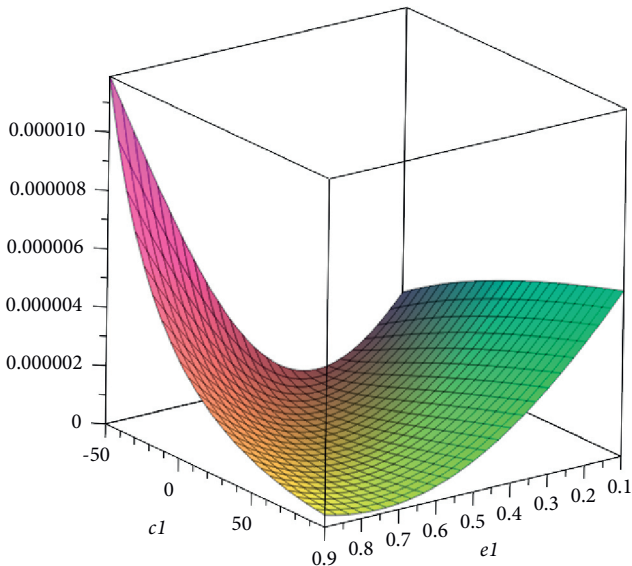


FIGURE 16: The graph of the function $G_3 = G_3(e_1, c_1)$ when $0.1 \leq e_1 \leq 0.9$ and $-50 \leq c_1 \leq 100$.

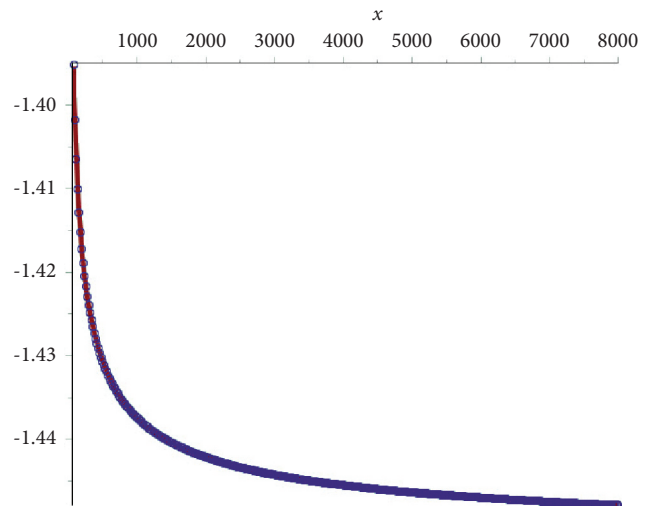


FIGURE 17: The graph of the data $(n, (3/2\pi^2)(\ln(12\sqrt{2n^3} h(n)/\pi))^2 - n)$ and the fitting curve.

the relative error will be obviously smaller with a few exceptions, as shown in Table 7.

Later, we will find out that it is obviously greater than the relative error of I_{g_1} and I_{g_2} obtained in the next subsection by modifying the denominator part; when $4000 < n < 10000$, the relative error of I_{ga} is about 1000 times of that of I_{g_2} .

When $30 < n \leq 1000$, the relative error of $[I_{ga}(n) + 1/2]$ is close to that of $I_{ga}(n)$.

3.3. Method B: Modifying the Denominator. Since $h(n) \sim (\pi/12\sqrt{2n^3})\exp(\sqrt{2/3}\pi\sqrt{n})$, we consider estimating $h(n)$ by $(\pi/12\sqrt{2C_3(n)})\exp(\sqrt{2/3}\pi\sqrt{n})$ (i.e., fit $\pi^2 \exp(2\pi\sqrt{2/3}\sqrt{n})/288h^2(n)$ by a function $C_3(n)$), where $C_3(x)$ is a cubic function or a function like

$$ax^3 + bx^{2.5} + cx^2 + dx^{1.5} + ex + fx^{0.5} + g. \quad (41)$$

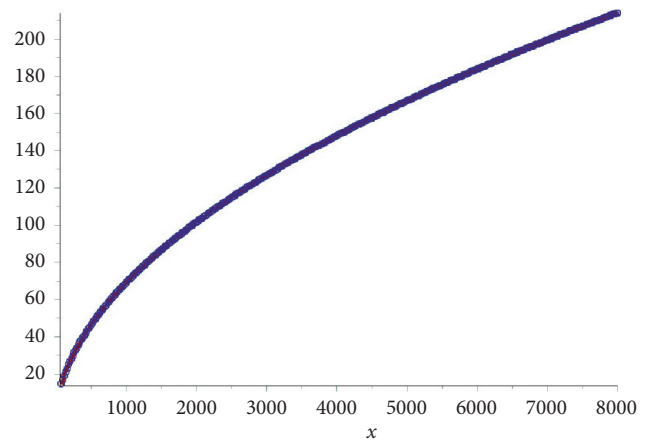


FIGURE 18: The graph of the data $(n, \ln(h(n)))$ and the fitting curve.

TABLE 6: The relative error of $I_{ga}(n)$ to $h(n)$ when $n \leq 1000$.

n	Rel-Err	n	Rel-Err	n	Rel-Err	n	Rel-Err	n	Rel-Err
1	—	16	-2.16%	40	-0.18%	220	2.62E-06	520	-8.93E-07
2	—	17	3.29%	50	-7.12E-04	240	1.60E-06	540	-9.04E-07
3	—	18	-2.34%	60	-3.12E-04	260	8.76E-07	560	-8.75E-07
4	8.89%	19	2.71%	70	-1.01E-04	280	3.54E-07	580	-8.50E-07
5	34.03%	20	-1.64%	80	-3.21E-05	300	3.00E-09	600	-8.46E-07
6	-10.34%	21	1.64%	90	-2.28E-06	320	-2.87E-07	640	-8.04E-07
7	21.05%	22	-1.00%	100	1.16E-05	340	-4.83E-07	680	-7.54E-07
8	-6.99%	23	1.51%	110	1.51E-05	360	-6.16E-07	720	-7.43E-07
9	8.67%	24	-1.20%	120	1.51E-05	380	-7.26E-07	760	-6.98E-07
10	-4.02%	25	1.29%	130	1.40E-05	400	-8.05E-07	800	-6.69E-07
11	8.17%	26	-0.72%	140	1.22E-05	420	-8.47E-07	840	-6.06E-07
12	-5.88%	27	0.83%	150	1.04E-05	440	-8.98E-07	880	-5.64E-07
13	6.76%	28	-0.58%	160	8.81E-06	460	-8.97E-07	920	-5.65E-07
14	-2.93%	29	0.80%	180	6.04E-06	480	-8.94E-07	960	-5.17E-07
15	3.07%	30	-0.59%	200	4.02E-06	500	-9.00E-07	1000	-4.75E-07

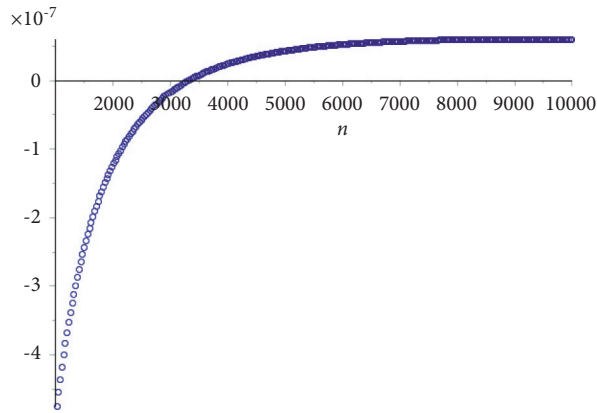


FIGURE 19: The relative error of $I_{ga}(n)$ when $1000 \leq n \leq 10000$, step 300.

TABLE 7: The relative error of $[I_{ga}(n) + 1/2]$ to $h(n)$ when $n \leq 30$.

n	Rel-Err	n	Rel-Err	n	Rel-Err	n	Rel-Err	n	Rel-Err
1	—	7	25%	13	8.33%	19	2.86%	25	1.31%
2	—	8	0	14	-2.94%	20	-1.46%	26	-0.63%
3	—	9	12.5%	15	2.44%	21	1.82%	27	0.87%
4	0	10	0	16	-1.82%	22	-0.95%	28	-0.56%
5	50%	11	7.14%	17	3.03%	23	1.58%	29	0.83%
6	0	12	-4.76%	18	-2.27%	24	-1.25%	30	-0.58%

However, the results are worse as the relative errors are obviously much greater than the relative error of $I_g(n)$ when $n < 350$.

Then, we consider estimating $h(n)$ by $(\pi/12\sqrt{2} C_4(n) \exp(\sqrt{2/3} \pi \sqrt{n})$ or fit $\pi \exp(\pi\sqrt{2/3} \sqrt{n})/12\sqrt{2}h(n)$ by a function as follows:

$$C_4(n) = a_4 n^{1.5} + b_4 n + c_4 n^{0.5} + d_4. \tag{42}$$

The result is very good. The graph of the data $(n, \pi \exp(\pi\sqrt{2/3} \sqrt{n})/12\sqrt{2}h(n))$ and the fitting curve $C_4(n)$ is shown in Figure 3. Here, the fitting curve is displayed by a thick continuous curve, which lies in the middle of the area the circles occupied. Since the circles are

too crowded, the circles themselves look like a very thick curve.

The values of the coefficients in the expression of $C_4(n)$ are as follows:

$$\begin{aligned} a_4 &= 1.000010809, \\ b_4 &= 1.862505234, \\ c_4 &= 1.169930087, \\ d_4 &= -0.7005460222. \end{aligned} \tag{43}$$

The value of a_4 is very close to 1, which means that this fitting function coincides with the Ingham–Meinardus asymptotic formula very well.

So, we have an estimation formula as follows:

$$h(n) \sim I_{g_1}(n) = \frac{\pi}{12\sqrt{2}C_4(n)} \exp\left(\sqrt{\frac{2}{3}}\pi\sqrt{n}\right). \quad (44)$$

We may call it the Ingham–Meinardus revised estimation formula (1). The graph of $\ln(I_{g_1}(n))$ is shown in Figure 2, together with the data points of $(n, \ln h(n))$. This revised estimation formula is much more accurate than the asymptotic formula. The relative error is less than 1×10^{-6} when $n > 2000$ (as shown in Figure 20 on page 14) and less than 3 when $n \geq 30$ (as shown in Table 8 on page 14). The relative error of the round approximation $I_{g_1}'(n) = \lfloor I_{g_1}(n) + 1/2 \rfloor$ is shown in Table 9 on page 13.

However, equation (44) is not so satisfying when $n < 30$, especially when $n < 15$ as the relative error is not negligible for some value of n .

As we already know that $h(n) \sim (\pi/12\sqrt{2}n^3)\exp(\sqrt{2/3}\pi\sqrt{n})$, or $n^{3/2} \sim (\pi/12\sqrt{2}h(n))\exp(\sqrt{2/3}\pi\sqrt{n})$, which means that when fitting $\pi \exp(\pi\sqrt{2/3}\sqrt{n})/12\sqrt{2}h(n)$ by a function $C_4(n)$ shown in equation (42), the coefficient a_4 should be exactly 1; hence, we should fit $\pi \exp(\pi\sqrt{2/3}\sqrt{n})/12\sqrt{2}h(n)$ by a function $C_4'(n) = n^{3/2} + b_5n + c_5n^{1/2} + d_5$ or fit $\pi \exp(\pi\sqrt{2/3}\sqrt{n})/12\sqrt{2}h(n) - n^{3/2}$ by a function

$$C_5(n) = b_5n + c_5n^{1/2} + d_5. \quad (45)$$

The graph of the data $(n, \pi \exp(\pi\sqrt{2/3}\sqrt{n})/12\sqrt{2}h(n) - n^{3/2})$ is shown in Figure 21 on page 14 (together with the figure of the fitting function $C_5(n)$ generated by the least square method).

The values of the coefficients in equation (45) are as follows:

$$\begin{aligned} b_5 &= 1.864260743, \\ c_5 &= 1.084436400, \\ d_5 &= 0.4754177757. \end{aligned} \quad (46)$$

So, we have another estimation formula for $h(n)$ as follows:

$$h(n) \sim I_{g_2}(n) = \frac{\pi \exp(\sqrt{2/3}\pi\sqrt{n})}{12\sqrt{2}(n^{3/2} + C_5(n))}. \quad (47)$$

We may call it the Ingham–Meinardus revised estimation formula (2). The graph of $\ln(I_{g_2}(n))$ is nearly the same as that of $\ln(I_{g_1}(n))$ shown in Figure 2. The second revised estimation formula is much more accurate than the first one. The relative error is less than 2×10^{-9} when $n > 3000$ (as shown in Figure 22 on page 14), about 1/500 of the relative error of $I_{g_1}(n)$. When $n < 10$, the relative error is also distinctly less than that of $I_{g_1}(n)$ (as shown in Table 10 on page 15). The relative error of the round approximation $I_{g_2}'(n) = \lfloor I_{g_2}(n) + 1/2 \rfloor$ is shown in Table 11 (on page 15).

It should be mentioned that in Figure 21 on page 14, the graph of the data points lies in a line, so we might be willing to fit this line by a first-order equation. The result is

$$C_5'(n) = 1.873818457 \times n + 27.08318017. \quad (48)$$

If we use this fitting function instead of $C_5(n)$ generated before, the relative error to fit $h(n)$ will be about 10000 times more, that is, about 20 times more than that of $I_{g_1}(n)$. So, we did not use linear function to fit the data $(n, \pi \exp(\pi\sqrt{2/3}\sqrt{n})/12\sqrt{2}h(n) - n^{3/2})$ before.

3.4. Method C: Fitting $I_g(n) - h(n)$. We wonder whether we can fit $I_g(n) - h(n)$ by a function $r(n)$ and then estimate $h(n)$ by $I_g(n) - r(n)$ which may be believed more accurate than $I_{g_2}(n)$ at the price of being more complicated.

By the same tricks used at the beginning of this subsection, we will have

$$I_g(n) - I_g(n-t) \sim \frac{t\pi^2}{24\sqrt{3}n^2} \exp\left(\sqrt{\frac{2}{3}}\pi\sqrt{n}\right). \quad (t \ll n), \quad (49)$$

So, we may fit $I_g(n) - h(n)$ by $(\pi^2/24\sqrt{3}C_6(n))\exp(\sqrt{2/3}\pi\sqrt{n})$ where $C_6(n)$ is a quadratic function or a function like

$$an^2 + bn^{1.5} + cn + dn^{0.5} + e. \quad (50)$$

That means, we can fit $\pi^2 \exp(\sqrt{2/3}\pi\sqrt{n})/24\sqrt{3}(I_g(n) - h(n))$ by a function $C_6(n)$. However, the result is useless. Although $C_6(n)$ will fit the data $\pi^2 \exp(\sqrt{2/3}\pi\sqrt{n})/24\sqrt{3}(I_g(n) - h(n))$ very well, the relative error of $I_g(n) - (\pi^2/24\sqrt{3}C_6(n))\exp(\sqrt{2/3}\pi\sqrt{n})$ to $h(n)$ is much greater than that of $I_{g_1}(n)$ or $I_{g_2}(n)$, and the relative error differs very little with that of $I_g(n)$ when n is small. Besides, the formula $I_g(n) - (\pi^2/24\sqrt{3}C_6(n))\exp(\sqrt{2/3}\pi\sqrt{n})$ is much more complicated than $I_{g_1}(n)$ and $I_{g_2}(n)$.

If we fit $I_g(n) - h(n)$ by $(\pi^2/24\sqrt{3}(n^2 + E_6(n)))\exp(\sqrt{2/3}\pi\sqrt{n})$ with the trick described in subsection 3.3, where $E_6(n)$ is a function in the form as follows:

$$bn^{1.5} + cn + dn^{0.5} + e, \quad (51)$$

as we already know the coefficient of n^2 should be 1 in theory. The result will be a little better, but useless too. The accuracy is not as good as that of $I_{g_0}(n)$.

Then, we consider fitting $\pi^2 \exp(\sqrt{2/3}\pi\sqrt{n})/24\sqrt{3}n^2(I_g(n) - h(n))$ by a function $C_7(n)$. If $C_7(n)$ is in the form $a/n + b$ or $a/n + b/n^2 + c$, the result is useless, too. If $C_7(n)$ is in the form $a/n^{0.5} + b$, it will be barely satisfactory. If $C_7(n)$ is in the form $a/n^{0.5} + b/n + c/n^{1.5} + d/n^2 + e$ or $a/n^{0.5} + b/n + c/n^{1.5} + e$, the result will be much better than the previous forms, but the accuracy (when estimating $h(n)$) is not as good as that of $I_{g_1}(n)$ and $I_{g_2}(n)$.

The result of $C_7(n)$ is

$$C_{7a}(n) = \frac{0.8782296151}{n^{0.5}} + \frac{0.2567016063}{n} - \frac{3.580442785}{n^{1.5}} + \frac{21.28305831}{n^2} + 0.6879945549, \quad (52)$$

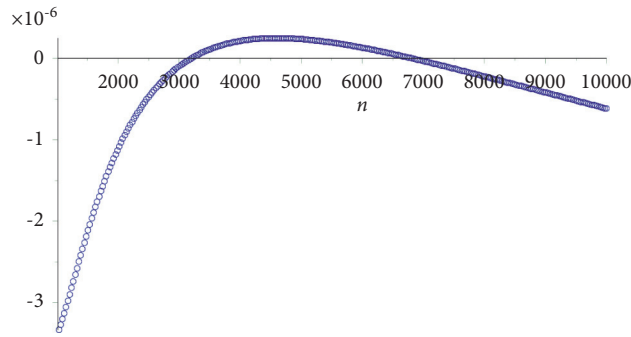


FIGURE 20: The relative error of $I_{g_1}(n)$ when $1000 \leq n \leq 10000$, step 300.

TABLE 8: The relative error of $I_{g_1}(n)$ to $h(n)$ when $n \leq 1000$.

n	Rel-Err (%)	n	Rel-Err (%)	n	Rel-Err	n	Rel-Err	n	Rel-Err
1	—	16	-1.63	40	-2.21E-05	220	7.23E-05	520	1.04E-06
2	-7.23	17	3.82	50	5.35E-04	240	5.74E-05	540	3.01E-07
3	29.97	18	-1.87	60	6.16E-04	260	4.59E-05	560	-3.53E-07
4	-8.44	19	3.18	70	6.15E-04	280	3.68E-05	580	-8.95E-07
5	27.94	20	-1.21	80	5.35E-04	300	2.97E-05	600	-1.37E-06
6	-11.61	21	2.06	90	4.56E-04	320	2.40E-05	640	-2.10E-06
7	20.76	22	-0.61	100	3.89E-04	340	1.93E-05	680	-2.64E-06
8	-6.74	23	1.89	110	3.30E-04	360	1.55E-05	720	-2.97E-06
9	9.21	24	-0.85	120	2.80E-04	380	1.24E-05	760	-3.20E-06
10	-3.44	25	1.63	130	2.40E-04	400	9.79E-06	800	-3.36E-06
11	8.85	26	-0.40	140	2.06E-04	420	7.63E-06	840	-3.43E-06
12	-5.28	27	1.14	150	1.78E-04	440	5.82E-06	880	-3.51E-06
13	7.42	28	-0.29	160	1.55E-04	460	4.32E-06	920	-3.49E-06
14	-2.35	29	1.08	180	1.18E-04	480	3.04E-06	960	-3.43E-06
15	3.66	30	-0.32	200	9.20E-05	500	1.97E-06	1000	-3.37E-06

TABLE 9: The relative error of $[I_{g_1}(n) + 1/2]$ to $h(n)$ when $n \leq 30$.

n	Rel-Err	n	Rel-Err	n	Rel-Err	n	Rel-Err	n	Rel-Err
1	—	7	25%	13	8.33%	19	2.86%	25	1.57%
2	0	8	0	14	-2.94%	20	-1.46%	26	-0.42%
3	0	9	12.5%	15	4.88%	21	1.82%	27	1.22%
4	0	10	0	16	-1.82%	22	-0.48%	28	-0.28%
5	50%	11	7.14%	17	4.55%	23	1.98%	29	1.06%
6	0	12	-4.76%	18	-2.27%	24	-0.94%	30	-0.29%

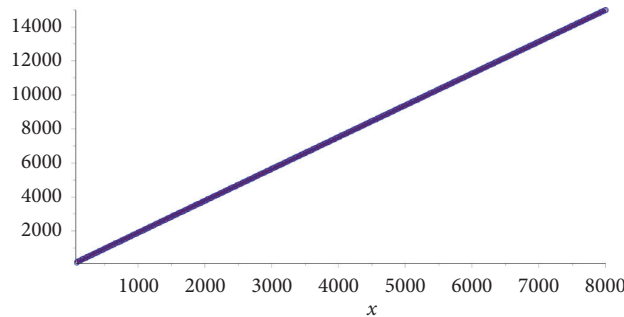


FIGURE 21: The graph of the data $(n, \pi \exp(\pi\sqrt{2/3} \sqrt{n})/12\sqrt{2} h(n) - n^{3/2})$ and the fitting curve $C_5(n)$.

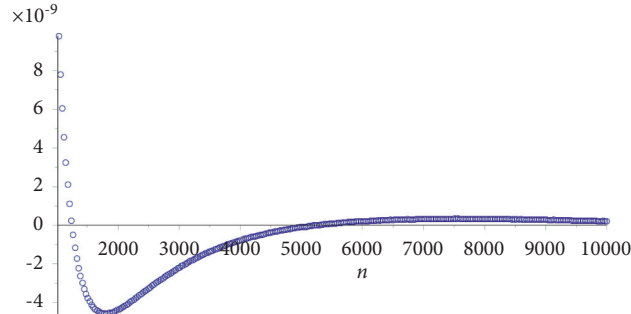


FIGURE 22: The relative error of $I_{g_2}(n)$ when $1000 \leq n \leq 10000$, step 300.

TABLE 10: The relative error of $I_{g_2}(n)$ to $h(n)$ when $n \leq 1000$.

N	Rel-Err (%)	n	Rel-Err (%)	n	Rel-Err	n	Rel-Err	n	Rel-Err
1		16	-2.49	40	-0.21%	220	2.15E-06	520	1.78E-07
2	-18.69	17	2.99	50	-9.06E-04	240	1.76E-06	540	1.83E-07
3	19.75	18	-2.59	60	-4.33E-04	260	1.46E-06	560	1.59E-07
4	-13.56	19	2.48	70	-1.80E-04	280	1.20E-06	580	1.51E-07
5	22.51	20	-1.83	80	-8.70E-05	300	9.94E-07	600	1.32E-07
6	-14.58	21	1.46	90	-4.13E-05	320	8.51E-07	640	1.03E-07
7	17.43	22	-1.15	100	-1.68E-05	340	7.18E-07	680	5.80E-08
8	-8.89	23	1.37	110	-5.98E-06	360	6.14E-07	720	6.80E-08
9	7.06	24	-1.32	120	-7.10E-07	380	5.23E-07	760	6.70E-08
10	-5.09	25	1.18	130	2.07E-06	400	4.61E-07	800	5.10E-08
11	7.23	26	-0.82	140	3.17E-06	420	3.90E-07	840	5.40E-08
12	-6.53	27	0.74	150	3.54E-06	440	3.34E-07	880	-4.30E-09
13	6.16	28	-0.66	160	3.59E-06	460	2.96E-07	920	7.00E-09
14	-3.38	29	0.72	180	3.16E-06	480	2.50E-07	960	2.80E-08
15	2.67	30	-0.66	200	2.64E-06	500	2.22E-07	1000	3.30E-08

or

$$C_{7b}(n) = \frac{0.8861039149}{n^{0.5}} - \frac{0.05719053203}{n} + \frac{0.9843423289}{n^{1.5}} + 0.6879343652. \tag{53}$$

The relative errors of

$$F_{7a}(n) = I_g(n) - \frac{\pi^2 \exp(\sqrt{2/3} \pi \sqrt{n})}{24\sqrt{3}n^2 C_{7a}(n)}, \tag{54}$$

and

$$F_{7b}(n) = I_g(n) - \frac{\pi^2 \exp(\sqrt{2/3} \pi \sqrt{n})}{24\sqrt{3}n^2 C_{7b}(n)}. \tag{55}$$

to $h(n)$ when $1000 \leq n \leq 10000$ are shown in Figures 23 and 24 (page 16), respectively. In this interval (1000, 10000), $F_{7a}(n)$ is obviously more accurate than $F_{7b}(n)$. When $n \leq 1000$, the relative error of $[F_{7a}(n) + 1/2]$ and $[F_{7b}(n) + 1/2]$

is shown in Table 12 (page 15) and Table 13 (page 15). In this case, $F_{7b}(n)$ is better than $F_{7a}(n)$. However, neither of them is as good as $I_{g_1}(n)$ or $I_{g_2}(n)$ although they are more complicated than $I_{g_1}(n)$ and $I_{g_2}(n)$.

3.5. Estimate $h(n)$ When $n \leq 100$. All the estimation functions for $h(n)$ found now are with very good accuracy when n is greater than 1000, but they are not so accurate when $n < 50$, especially when $n < 25$. Although $I_{g_1}'(n)$ and $I_{g_2}'(n)$ are better than others, the relative error is still greater than 1 when $n < 40$.

When $n < 40$, it is too difficult to fit $\pi \exp(\pi\sqrt{2/3} \sqrt{n})/12\sqrt{2}h(n) - n^{3/2}$ by a simple smooth function with high accuracy, as shown in Figure 25 (on page 16). The points $(n, \pi \exp(\pi\sqrt{2/3} \sqrt{n})/12\sqrt{2} h(n) - n^{3/2})$ ($n = 3, 4, \dots, 100$) are not so complicated (as shown in Figure 25). It seems that we can fit them by a simple piecewise function with 2 pieces, as the even points (where n is even) lie roughly on a smooth curve, so do the odd points. If we try to fit them, respectively, we will have the fitting function as follows:

TABLE 11: The relative error of $[I_{g^2}(n) + 1/2]$ to $h(n)$ when $n \leq 30$.

n	Rel-Err (%)	n	Rel-Err (%)	n	Rel-Err (%)	n	Rel-Err (%)	n	Rel-Err (%)
1		16	50.30	40	32.10	220	13.10	520	8.39
2	146.24	17	56.82	50	28.60	240	12.50	540	8.23
3	202.89	18	46.69	60	25.90	260	12.00	560	8.08
4	95.59	19	52.75	70	23.90	280	11.50	580	7.93
5	156.43	20	44.94	80	22.30	300	11.10	600	7.79
6	68.62	21	48.48	90	20.90	320	10.80	640	7.54
7	121.38	22	43.47	100	19.80	340	10.40	680	7.31
8	65.43	23	46.00	110	18.80	360	10.10	720	7.10
9	88.38	24	41.09	120	18.00	380	9.86	760	6.91
10	62.58	25	43.68	130	17.20	400	9.60	800	6.73
11	79.47	26	39.93	140	16.60	420	9.36	840	6.56
12	53.29	27	41.27	150	16.00	440	9.14	880	6.41
13	70.98	28	38.50	160	15.40	460	8.93	920	6.27
14	53.12	29	39.70	180	14.50	480	8.74	960	6.13
15	60.35	30	37.00	200	13.70	500	8.56	1000	6.01

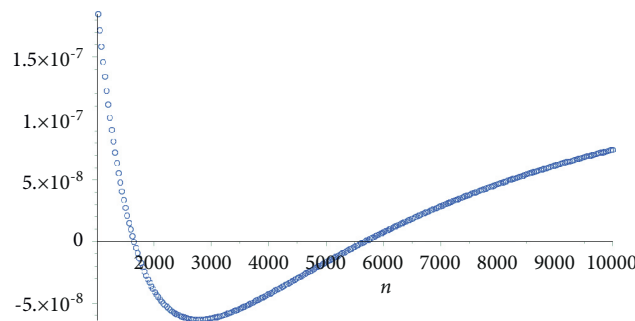


FIGURE 23: The relative error of $F_{7a}(n)$ when $1000 \leq n \leq 10000$, step 300.

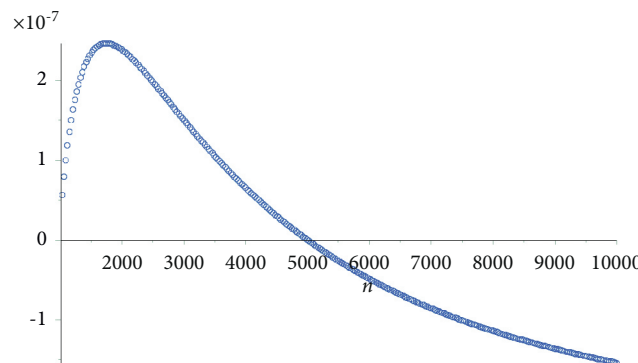


FIGURE 24: The relative error of $F_{7b}(n)$ when $1000 \leq n \leq 10000$, step 300.

$$C_8(x) = \begin{cases} 1.942141112 \times x - 0.4796781366 \times \sqrt{x} + 8.291226268, & n = 3, 5, 7, \dots, 99; \\ 1.803056782 \times x + 2.356539877 \times \sqrt{x} - 6.043824511, & n = 4, 6, 8, \dots, 100. \end{cases} \quad (56)$$

Hence, we can calculate $h(n)$ ($3 \leq n \leq 100$) by

$$h(n) \sim I_{g^0}(n) = \frac{\pi \exp(\sqrt{2/3} \pi \sqrt{n})}{12\sqrt{2}(n^{3/2} + C_8(n))}, \quad 3 \leq n \leq 100. \quad (57)$$

Considering that $h(n)$ is an integer, we can take the round approximation of equation (57):

$$I'_{g^0}(n) = \left\lfloor \frac{\pi \exp(\sqrt{2/3} \pi \sqrt{n})}{12\sqrt{2}(n^{3/2} + C_8(n))} + \frac{1}{2} \right\rfloor, \quad 3 \leq n \leq 100. \quad (58)$$

TABLE 12: The relative error of $[F_{7a}(n) + 1/2]$ to $h(n)$ when $n \leq 1000$.

n	Rel-Err	n	Rel-Err	n	Rel-Err	n	Rel-Err	n	Rel-Err
1	—	16	0	40	$-8.13E-04$	220	$-1.74E-06$	520	$3.10E-07$
2	100%	17	4.55%	50	$-3.26E-04$	240	$-1.51E-06$	540	$3.29E-07$
3	100%	18	-1.14%	60	$-1.49E-04$	260	$-1.25E-06$	560	$3.42E-07$
4	50%	19	3.81%	70	$-2.81E-05$	280	$-9.91E-07$	580	$3.51E-07$
5	50%	20	-0.73%	80	$-4.62E-06$	300	$-7.56E-07$	600	$3.56E-07$
6	0	21	2.42%	90	$3.46E-06$	320	$-5.49E-07$	640	$3.57E-07$
7	50%	22	-0.48%	100	$6.70E-06$	340	$-3.72E-07$	680	$3.49E-07$
8	0	23	1.98%	110	$5.27E-06$	360	$-2.23E-07$	720	$3.36E-07$
9	12.5%	24	-0.63%	120	$3.37E-06$	380	$-9.87E-08$	760	$3.19E-07$
10	0	25	1.83%	130	$1.93E-06$	400	$3.54E-09$	800	$3.00E-07$
11	14.29%	26	-0.21%	140	$5.77E-07$	420	$8.70E-08$	840	$2.80E-07$
12	0	27	1.22%	150	$-4.01E-07$	440	$1.55E-07$	880	$2.59E-07$
13	8.33%	28	-0.28%	160	$-1.04E-06$	460	$2.09E-07$	920	$2.39E-07$
14	0	29	1.06%	180	$-1.72E-06$	480	$2.51E-07$	960	$2.19E-07$
15	4.88%	30	-0.29%	200	$-1.86E-06$	500	$2.85E-07$	1000	$1.99E-07$

TABLE 13: The relative error of $[F_{7b}(n) + (1/2)]$ to $h(n)$ when $n \leq 1000$.

n	Rel-Err	n	Rel-Err (%)	n	Rel-Err	n	Rel-Err	n	Rel-Err
1	—	16	-1.82	40	-0.16%	220	$-1.21E-06$	520	$-1.11E-06$
2	0	17	3.03	50	$-6.19E-04$	240	$-1.77E-06$	540	$-1.01E-06$
3	0	18	-2.27	60	$-2.60E-04$	260	$-2.08E-06$	560	$-9.24E-07$
4	0	19	2.86	70	$-7.50E-05$	280	$-2.21E-06$	580	$-8.41E-07$
5	50%	20	-1.46	80	$-1.85E-05$	300	$-2.24E-06$	600	$-7.64E-07$
6	0	21	1.82	90	$3.62E-06$	320	$-2.20E-06$	640	$-6.25E-07$
7	25%	22	-0.95	100	$1.30E-05$	340	$-2.12E-06$	680	$-5.05E-07$
8	0	23	1.58	110	$1.37E-05$	360	$-2.02E-06$	720	$-4.00E-07$
9	12.5%	24	-1.25	120	$1.21E-05$	380	$-1.90E-06$	760	$-3.10E-07$
10	0	25	1.31	130	$1.01E-05$	400	$-1.78E-06$	800	$-2.31E-07$
11	7.14%	26	-0.63	140	$7.74E-06$	420	$-1.66E-06$	840	$-1.63E-07$
12	-4.76%	27	0.87	150	$5.68E-06$	440	$-1.54E-06$	880	$-1.04E-07$
13	8.33%	28	-0.56	160	$3.97E-06$	460	$-1.42E-06$	920	$-5.24E-08$
14	-2.94%	29	0.83	180	$1.40E-06$	480	$-1.31E-06$	960	$-7.83E-09$
15	2.44%	30	-0.58	200	$-2.22E-07$	500	$-1.21E-06$	1000	$3.08E-08$

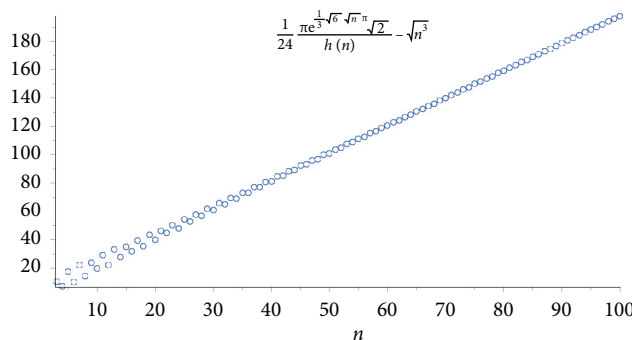


FIGURE 25: The graph of the data $(n, C_8(n))$.

Here, n begins from 3, not 1 or 2, because $(I'_{g_0}(1) - h(1))/h(1)$ is meaningless since $h(1) = 0$, and $I'_{g_0}(2)$ differs from $h(2)$ a lot. Besides, the value of $h(1)$ and $h(2)$ is clear by definition, so there is no need to use a complicated formula to estimate them.

The relative error of $I_{g_0}(n)$ (or $I'_{g_0}(n)$) to $h(n)$ is shown in Table 14 (or Table 15) on page 17. Compared them with Table 11 on page 15, we will find that when $n \geq 80$, $I'_{g_2}(n)$ is more accurate than $I'_{g_0}(n)$; when $n < 80$, $I'_{g_0}(n)$ is better.

TABLE 14: The relative error of $I_{g_0}(n)$ to $h(n)$ when $n \leq 100$.

n	Rel-Err (%)	n	Rel-Err	n	Rel-Err	n	Rel-Err	n	Rel-Err
1	—	21	-0.16%	41	-5.72E-04	61	-1.04E-04	81	7.19E-05
2	—	22	0.12%	42	3.75E-04	62	1.43E-04	82	-5.18E-05
3	-14.85	23	0.05%	43	-4.68E-04	63	-1.04E-04	83	8.12E-05
4	12.72	24	-0.28%	44	4.91E-04	64	1.18E-04	84	-6.50E-05
5	1.99	25	8.37E-04	45	-6.29E-04	65	-5.63E-05	85	8.69E-05
6	-1.83	26	4.75E-04	46	5.45E-04	66	7.10E-05	86	-6.90E-05
7	4.76	27	-0.17%	47	-4.45E-04	67	-2.40E-05	87	8.65E-05
8	-0.64	28	6.69E-04	48	3.17E-04	68	5.74E-05	88	-7.40E-05
9	-0.92	29	-3.78E-04	49	-3.42E-04	69	-1.67E-05	89	9.01E-05
10	0.69	30	-4.43E-04	50	3.79E-04	70	4.05E-05	90	-8.07E-05
11	1.44	31	-1.98E-04	51	-3.98E-04	71	1.30E-05	91	9.09E-05
12	-2.46	32	4.21E-04	52	3.55E-04	72	6.81E-06	92	-8.24E-05
13	1.86	33	-0.12%	53	-2.81E-04	73	3.41E-05	93	8.80E-05
14	-0.24	34	9.27E-04	54	2.47E-04	74	-1.74E-06	94	-8.37E-05
15	-0.54	35	-7.86E-04	55	-2.21E-04	75	3.84E-05	95	8.70E-05
16	-0.04	36	1.82E-04	56	2.44E-04	76	-1.56E-05	96	-8.65E-05
17	0.46	37	-4.80E-04	57	-2.25E-04	77	5.70E-05	97	8.44E-05
18	-0.67	38	6.53E-04	58	2.29E-04	78	-3.58E-05	98	-8.56E-05
19	0.47	39	-9.11E-04	59	-1.55E-04	79	6.90E-05	99	7.92E-05
20	-0.28	40	6.34E-04	60	1.44E-04	80	-4.41E-05	100	-8.48E-05

TABLE 15: The relative error of $I'_{g_0}(n)$ to $h(n)$ when $n \leq 100$.

n	Rel-Err	n	Rel-Err	n	Rel-Err	n	Rel-Err	n	Rel-Err
1	—	9	0	17	0	25	0	33	-0.11%
2	—	10	0	18	-1.14%	26	0	34	9.23E-04
3	0	11	0	19	0	27	-0.17%	35	-7.77E-04
4	0	12	-4.76%	20	0	28	0	36	3.23E-04
5	0	13	0	21	0	29	0	37	-5.46E-04
6	0	14	0	22	0	30	0	38	6.85E-04
7	0	15	0	23	0	31	0	39	-9.67E-04
8	0	16	0	24	-0.31%	32	0.07%	40	6.50E-04

4. Conclusion

We have presented a recursion formula and several practical estimation formulae with high accuracy to calculate the number $h(n)$ of conjugate classes of derangements of order n or the number of isotopy classes of $2 \times n$ Latin rectangles.

If we want to obtain the accurate value of $h(n)$, we can use the recursion formula (13) and write a program based on it, while sometimes we need to know the estimation value in a program for technique reason especially when we use a general programming language.

If we want to obtain the approximation value of $h(n)$ with high accuracy, we can use formulae (29), (31), (36), and so on.

When $2 \leq n \leq 80$, we can use $I'_{g_0}(n)$ (equation (58)), with a relative error less than 0.11% (while $32 \leq n \leq 80$) or mainly 0 with very few exceptions (while $2 \leq n \leq 31$); when $n > 80$, we can use $I'_{g_2}(n)$ (equation (47)).

When $n \geq 100$, formulae $I'_{ga}(n)$ (equation (40)), $I'_{g1}(n)$ (equation (44)), $F_{7a}(n)$ (equation (54)), and $F_{7b}(n)$ (equation (55)) are also very accurate although they are not as good as equation (47).

With the asymptotic formula (26) described in [30], we can obtain some estimation formulae with high accuracy for some other types of restricted partition numbers by the

methods mentioned in this paper or in [1]. The updated version of this paper is shown on <https://arxiv.org/abs/1612.08186>.

Data Availability

The figures and tables used to support this study are included within the article. The other data used to support this study are obtained from a program made by the first author.

Conflicts of Interest

The authors declare that there are no conflicts of interest regarding the publication of this paper.

Acknowledgments

This work was supported in part by the Fund of Research Team of Anhui International Studies University, No. awktyd1909.

References

- [1] W.-W. Li, "Estimation of the partition number: after hardy and ramanujan," 2016, <https://arxiv.org/abs/1612.05526>.
- [2] M. Hall Jr., "A survey of combinatorial analysis," in *Some Aspects of Analysis and Probability, Volume IV of Surveys in*

- Applied Mathematics*, I. Kaplansky, Ed., pp. 35–104, John Wiley & Sons, New York, NY, USA, 1958.
- [3] E. W. Weisstein: "Partition function P." from MathWorld—a wolfram web resource," 2015, Internet: <http://mathworld.wolfram.com/PartitionFunctionP.html>.
 - [4] N. J. A. Sloane: A000041, number of partitions of n (the partition numbers). (Formerly M0663 N0244) , in "The On-Line Encyclopedia of Integer Sequences (OEIS \circledR)".2015.
 - [5] Anonymous, "Bibliography on Partitions" in "Mathematical BBS", 2007, <http://felix.unife.it/Root/d-Mathematics/d-Number-theory/b-Partitions>.
 - [6] M. Newman, "Weighted restricted partitions," *Acta Arithmetica*, vol. 5, no. 4, pp. 371 – 380, 1959.
 - [7] D. B. Lahiri, "Some restricted partition functions: congruences modulo 3," *Pacific Journal of Mathematics*, vol. 28, no. 3, pp. 575 – 581, Article ID 05602, 1969.
 - [8] D. B. Lahiri, "Some restricted partition functions: congruences modulo 5," *Journal of the Australian Mathematical Society*, vol. 9, pp. 424 – 432, 1969.
 - [9] D. B. Lahiri, "Some restricted partition functions: congruences modulo 7," *Transactions of the American Mathematical Society*, vol. 140, pp. 475 – 484, Article ID 0242784, 1969.
 - [10] R. Jakimczuk, "Restricted partitions: elementary methods," *International Journal of Contemporary Mathematical Sciences*, vol. 4, no. 2, pp. 93–103, 2009.
 - [11] B. Kronholm, "A result on ramanujan-like congruence properties of the restricted partition function $P(n, m)$ across both variables," *INTEGERS: The Electronic Journal of Combinatorial Number Theory*, vol. 12, p. A63, 2012.
 - [12] A. Folsom, Z. A. Kent, and K. Ono, " ℓ -adic properties of the partition function," *Advances in Mathematics*, vol. 229, pp. 1586 – 1609, 2012.
 - [13] E. Belmont, H. Lee, A. Musat, and S. Trebat-Leder, " ℓ -adic properties of the partition function," *Monatshefte für Mathematik*, vol. 173, pp. 1–34, 2014.
 - [14] K. Thanigasalam, "Congruence properties of certain restricted partitions," *Mathematics Magazine*, vol. 47, pp. 154 – 156, 1974.
 - [15] D. R. Hickerson, "A note on congruence properties of certain restricted partitions," *Mathematics Magazine*, vol. 48, no. 2, p. 102, 1975.
 - [16] M. Culek and A. Knecht: Congruences of restricted partition functions.", 2002, <http://citeseerx.ist.psu.edu/viewdoc/download?doi=10.1.1.509.2649&rep=rep1&type=pdf>.
 - [17] B. Kronholm, "On congruence properties of $p(n, m)$," *Proceedings of the American Mathematical Society*, vol. 133, pp. 2891–2895, 2005.
 - [18] B. Kronholm, "On congruence properties of consecutive values of $p(n, m)$," *INTEGERS: The Electronic Journal of Combinatorial Number Theory*, vol. 7, 2007.
 - [19] B. C. Berndt, "Ramanujan's congruences for the partition function, modulo 5, 7, and 11," *International Journal of Number Theory*, vol. 3, pp. 349 – 354, 2007.
 - [20] G. E. Andrews and B. C. Berndt, "Ramanujan's unpublished manuscript on the partition and tau functions," in *Ramanujan's Lost Notebook: Part III*, pp. 89–180, Springer Science+Business Media, New York, NY, USA, 2012.
 - [21] B. Kronholm, "Generalized congruence properties of the restricted partition function $p(n, m)$," *The Ramanujan Journal*, vol. 30, pp. 425 – 436, 2013.
 - [22] N. J. A. Sloane: "Restricted partitions," in OEIS wiki, 2011, http://oeis.org/wiki/Restricted_partitions.
 - [23] D. M. Bressoud, "Integer partitions: restricted number and part size," in *NIST Digital Library of Mathematical Functions (DLMF)*, F. W. J. Olver, D. W. Lozier, and R. F. Boisvert, Eds., NIST, Gaithersburg, MD, USA, 2015.
 - [24] F. W. J. Olver, D. W. Lozier, and R. F. Boisvert, "Integer partitions: other restrictions," in *NIST Digital Library of Mathematical Functions (DLMF)*, F. W. J. Olver, D. W. Lozier, and R. F. Boisvert, Eds., National Institute of Standards and Technology (NIST), Gaithersburg, MD, USA, 2015.
 - [25] F. W. J. Olver, D. W. Lozier, and R. F. Boisvert, *NIST Handbook of Mathematical Functions*, Cambridge University Press, New York, NY, USA, 2010.
 - [26] A. Greenbaum and T. P. Chartier, *Numerical Methods: Design, Analysis, and Computer Implementation of Algorithms*, Princeton University Press, New Jersey, NJ, USA, 2012.
 - [27] D. Kincaid and W. Cheney, *Numerical Analysis: Mathematics of Scientific Computing, 3rd Edition, vol. 2 of Pure and Applied Undergraduate Texts*, American Mathematical Society, Providence, Rhode Island, USA, 2002.
 - [28] W. Lichten, *Data and Error Analysis*, Prentice Hall, Hoboken, NJ, USA, Oct 1998.
 - [29] A. E. Ingham, "A tauberian Theorem for partitions," *Annals of Mathematics*, vol. 42, no. 5, pp. 1075 – 1090, 1941.
 - [30] D. M. Kane, "An elementary derivation of the asymptotics of partition functions," *The Ramanujan Journal*, vol. 11, pp. 49 – 66, 2006.
 - [31] G. H. Hardy and S. R. Ramanujan, "Asymptotic formulae in combinatory analysis," *Proceedings of the London Mathematical Society*, vol. s2–17, no. 1, pp. 75–115, 1918.
 - [32] P. Erdős, "The evaluation of the constant in the formula for the number of partitions of n ," *Annals of Mathematics. Second Series*, vol. 43, pp. 437 – 450, 1942.
 - [33] D. J. Newman, "The evaluation of the constant in the formula for the number of partitions of n ," *American Journal of Mathematics*, vol. 73, pp. 599 – 601, 1951.
 - [34] D. J. Newman, "A simplified proof of the partition formula," *The Michigan Mathematical Journal*, vol. 9, pp. 283 – 287, 1962.
 - [35] T. M. Apostol, "Functions of number theory, additive number theory: unrestricted partitions," in *NIST Digital Library of Mathematical Functions (DLMF)*, F. W. J. Olver, D. W. Lozier, and R. F. Boisvert, Eds., NIST, Gaithersburg, MD, USA, 2015.

Research Article

Characterization of the Congestion Lemma on Layout Computation

Jia-Bao Liu ¹, Arul Jeya Shalini ², Micheal Arockiaraj,³ and J. Nancy Delaila³

¹School of Mathematics and Physics, Anhui Jianzhu University, Hefei 230601, China

²Department of Mathematics, Women's Christian College, Chennai 600006, India

³Department of Mathematics, Loyola College, Chennai 600034, India

Correspondence should be addressed to Arul Jeya Shalini; aruljeyashalini@gmail.com

Received 8 June 2021; Accepted 15 October 2021; Published 27 October 2021

Academic Editor: Firdous Shah

Copyright © 2021 Jia-Bao Liu et al. This is an open access article distributed under the Creative Commons Attribution License, which permits unrestricted use, distribution, and reproduction in any medium, provided the original work is properly cited.

An embedding of a guest network GN into a host network HN is to find a suitable bijective function between the vertices of the guest and the host such that each link of GN is stretched to a path in HN . The layout measure is attained by counting the length of paths in HN corresponding to the links in GN and with a complexity of finding the best possible function overall graph embedding. This measure can be computed by summing the minimum congestions on each link of HN , called the congestion lemma. In the current study, we discuss and characterize the congestion lemma by considering the regularity and optimality of the guest network. The exact values of the layout are generally hard to find and were known for very restricted combinations of guest and host networks. In this series, we derive the correct layout measures of circulant networks by embedding them into the path- and cycle-of-complete graphs.

1. Introduction

Nowadays, there is an emerging demand for high-performance concurrent functional in different fields which can be successfully achieved through parallel processing techniques. The core of a parallel processing system is the interconnected network by which the system processors are connected. One of the important challenges in parallel processing techniques is how to allocate the subprocesses to the processors within the system in such a way that the total communication cost is minimized. This issue in parallel processing can be reduced to a graph embedding problem [1, 2]. For this purpose, the network topology is formulated as a simple graph, in which the vertex set denotes the system processors and the edge set denotes the links connecting them.

In this paper, the collection of vertices and edges of a simple graph network GN are, respectively, represented by $V(GN)$ and $E(GN)$. A graph embedding of a guest network GN into a host network HN is a kind of vertex and edge labeling denoted by a 1-1 and onto mapping $\mu: V(GN) \rightarrow V(HN)$ together with 1-1 mapping $R: E(GN) \rightarrow \mathcal{R}(HN)$ such that $R(e)$ is

a $\mu(x)$ to $\mu(y)$ path in HN , where $e = (x, y)$ and $\mathcal{R}(HN)$ contains the collection of routes or paths in HN [2, 3]. The congestion of an edge s of HN is measured by counting the routes in $\{R(e)\}_{e \in E(GN)}$ such that s is in the route $R(e)$ and denoted by $EC_\mu(s)$. In other words, $EC_\mu(s) = |\{e \in E(GN) : s \in E(R(e))\}|$. The layout/wire length [4, 5] of GN by embedding μ in HN is defined as

$$L_\mu(GN, HN) = \sum_{e \in E(GN)} |E(R(e))| = \sum_{s \in E(HN)} EC_\mu(s). \quad (1)$$

Let D be any subset of $E(HN)$. If we represent $EC_\mu(D) = \sum_{e \in D} EC_\mu(e)$, then $L_\mu(GN, HN) = \sum_{i=1}^p EC_f(F_i)$, where $E(HN) = \{F_1, F_2, \dots, F_p\}$ is a partition. For $\lambda \geq 1$, construct a set based on the edges of HN such that each edge in HN is duplicated λ -times. Such a set is denoted by $E^\lambda(HN)$. Then,

$$L_\mu(GN, HN) = \frac{1}{\lambda} \sum_{s \in E(HN)} EC_\mu(s). \quad (2)$$

Furthermore, if $E^\lambda(HN) = \{D_1, D_2, \dots, D_m\}$, then $L_\mu(GN, HN) = (1/\lambda) \sum_{i=1}^m EC_\mu(D_i)$. The correct layout of GN by embedding in HN is measured by

$$L(GN, HN) = \min_{\mu} L_{\mu}(GN, HN). \quad (3)$$

The main objective of parallel computing is to execute embeddings with the correct layout, and we certainly fix the accompanying function R such that each edge e of GN is to a shortest $R(e)$ path under μ , see Figure 1. Apart from that, the important topological descriptor, Wiener index [6], which is used in the characterization of chemical compounds can be obtained through $L(K_q, MS)$, where K_q is the complete graph and MS is the considered molecular structure.

The minimum layout problem plays an important role in finding an optimal solution for very large-scale integration (VLSI) chips physical layout [2], minimizing time delay of simulations in parallel computer systems, computer aided designs, structural engineering, cloning and visual stimuli models, and parallel architecture [7, 8]. The computation of layout measure has been already studied in a variety of papers, see [9, 10] and the references cited therein, for more details. The present study continues the layout computation of circulant graphs into path- and cycle-of-complete graphs.

2. Congestion Lemma

The combinatorial isoperimetric problems have emerged with important applications in the fields of communication systems and computer and physical sciences related disciplines. Harper [11, 12] has discovered the primary significance of edge isoperimetric problem (EIP), and it has been categorized into two types as follows [13].

Definition 1 (EIP(1)). For a graph network GN , if $F \subseteq V(GN)$, then $\Theta_{GN}(F) = \{(v, w) \in E(GN) : v \in F \& w \notin F\}$. Given a positive integer k , $\Theta_{GN}(k) = \min_{F \subseteq V(GN), |F|=k} |\Theta_{GN}(F)|$. Then, EIP(1) finds $F \subseteq V(GN)$ and $|F| = k$ such that $\Theta_{GN}(k) = |\Theta_{GN}(F)|$.

Definition 2 (EIP(2)). For a graph network GN , if $F \subseteq V(GN)$, then $I_{GN}(F) = \{(v, w) \in E(GN) : v, w \in F\}$. Given a positive integer k , $I_{GN}(k) = \max_{F \subseteq V(GN), |F|=k} |I_{GN}(F)|$. Then, EIP(2) finds $F \subseteq V(GN)$ and $|F| = k$ such that $I_{GN}(k) = |I_{GN}(F)|$.

In such a case, F is identified as optimal set corresponding to the EIP.

Lemma 1 (see [11]). (i) For a graph network GN , $\Theta_{GN}(V(GN) - F) = \Theta_{GN}(F)$ for all $F \subseteq V(GN)$. (ii) If GN is an r -regular graph, $|\Theta_{GN}(F)| + 2|I_{GN}(F)| = r|F|$ and, for any positive integer k , $\Theta_{GN}(k) = rk - 2I_{GN}(k)$.

The minimum layout of the hypercube network by embedding in a grid structure is derived using congestion lemma [14]. The generalized version of the congestion lemma appeared in [15] and the modified version in [16]. Here, we present a more general result that exemplifies the regularity and the optimality on the guest network.

In what follows, let GN and HN be two given networks and $F \subseteq E(HN)$. Suppose the removal of F from HN splits the network into m components, namely, HN_1, HN_2, \dots, HN_m . A graph embedding μ of GN into HN is F -repulsive if, when we let $GN_j = GN[\mu^{-1}(HN_j)]$, $1 \leq j \leq m$, the following conditions hold:

- (i) If $e \in E(GN_j)$, $1 \leq j \leq m$, then $|E(R(e)) \cap F| = 0$
- (ii) If $e = (v, w)$, such that $v \in V(GN_j)$ and $w \in V(GN_k)$, for $j < k$, then $|E(R(e)) \cap F| = 1$

Lemma 2. Let $F \subseteq E(HN)$ and μ be an F -repulsive graph embedding of GN into HN . We have $EC_{\mu}(F) = |E(GN)| - \sum_{j=1}^m |E(GN_j)|$. Moreover, among all the graph embeddings of GN into HN , $EC_{\mu}(F)$ is minimum if and only if the value $\sum_{j=1}^m |E(GN_j)|$ is maximum among all partitions of $V(GN) = \cup_{j=1}^m W_j$ with $|W_j| = |V(GN_j)|$, $j = 1, 2, \dots, m$.

Proof. Let $X = \{(x, y) \in E(GN) : x \in V(GN_j), y \in V(GN_k) \text{ for } j < k\}$. Since any edge (x, y) in GN either belongs to one of GN_j or x in GN_j and y in GN_k for some j and k , we obtain

$$|E(GN)| = \sum_{j=1}^m |E(GN_j)| + |X|. \quad (4)$$

We now easily compute $EC_{\mu}(F)$ bearing the conditions of the F -repulsive embedding. By assumption (i), the contribution to $EC_{\mu}(F)$ from the edges of GN_j , $1 \leq j \leq m$, is zero. By assumption (ii), every edge (x, y) of X increases $EC_{\mu}(F)$ by 1. Thus, $EC_{\mu}(F) = |X| = |E(GN)| - \sum_{j=1}^m |E(GN_j)|$.

Assume that $EC_{\mu}(F)$ is minimum. Suppose we had a partition giving a larger value than $\sum_{j=1}^m |E(GN_j)|$, and we could define an embedding β using this partition such that $EC_{\beta}(F) < EC_{\mu}(F)$, a contradiction. Conversely, let $EC_{\mu}(F)$ be not minimum. Suppose there exists a graph embedding γ such that $EC_{\gamma}(F) < EC_{\mu}(F)$, and consequently, we can find a partition with a larger value than $\sum_{j=1}^m |E(GN_j)|$, which is not possible because of the F -repulsive embedding under μ . \square

Lemma 3. Let $F \subseteq E(HN)$ and μ be an F -repulsive graph embedding of GN into HN . Among all the graph embeddings of GN into HN , (a) $EC_{\mu}(F)$ is minimum if GN_j s are optimal with respect to EIP(1) and $EC_{\mu}(F) = (1/2) \sum_{j=1}^m \Theta_{GN}(m_j)$, $m_j = |V(GN_j)|$, and (b) when GN is an r -regular network, $EC_{\mu}(F)$ is minimum if GN_j s are optimal with respect to EIP(2) and $EC_{\mu}(F) = (r/2)|V(GN)| - \sum_{j=1}^m |E(GN_j)|$.

Proof. We assume that GN_j s are optimal sets with respect to EIP(1). Such a case results in $\sum_{j=1}^m \Theta_{GN}(m_j)$ is minimum. Hence, $EC_{\mu}(F) = (1/2) \sum_{j=1}^m \Theta_{GN}(m_j)$ is minimum [15]. By extending the idea to EIP(2), we can easily derive the case of r -regular network by applying the simple fact $2|E(GN)| = r|V(GN)|$. \square

It is interesting as well as crucial to note that all GN_j s are not optimal, yet imply that $EC_{\mu}(F)$ is minimum. Furthermore, when $m = 2$, the above lemma is reduced to the

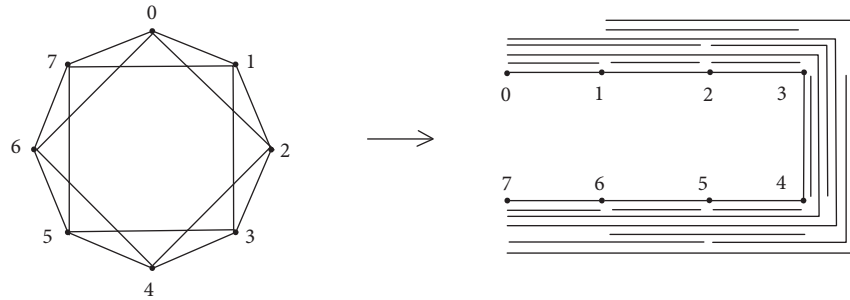


FIGURE 1: The correct layout of the embedding circulant network into path by $\mu(x) = x$.

modified congestion lemma [16], as in Case (a), and the congestion lemma [14], as in Case (b).

3. Layout Computation

The purpose of the section is to derive the layout of circulant networks into a few graph structures generated from the path and the cycle. We begin with the basic results on circulant networks [2, 17, 18].

Definition 3 (see [2]). A circulant network, denoted by $CN(q; \pm D)$, $D \subseteq \{1, 2, \dots, \lfloor q/2 \rfloor\}$, $q \geq 3$, is constructed from $V(CN) = \{0, 1, \dots, q - 1\}$ such that $E(CN) = \{(i, j) : |j - i| \equiv d \pmod{q}, d \in \pm D\}$.

With the optimum fault tolerance and best routing functionality, the circulant network is considered an excellent network over the years on account of its applications in the areas of computer binary code designs and

telecommunication network systems. Particularly, circulant network is a natural generalized form of the double loop network, and in addition, a matrix representation generates the circulant if all its rows are periodic rotations of the first one. From the construction of circulant networks, one can easily see that $CN(q; \pm 1)$ and $CN(q; \pm \{1, 2, \dots, \lfloor q/2 \rfloor\})$ are, respectively, the cycle C_q and the complete graph K_q . In our study, we denote the cycle $CN(q; \pm 1)$ as a peripheral cycle. From the symmetry of circulant network, we have that $CN(q; \pm \{1, 2, \dots, l\})$, $1 \leq l < \lfloor q/2 \rfloor$, is a regular network of degree $2l$.

Lemma 4 (see [19]). *A set of m consecutive vertices of $CN(q; \pm 1)$, $1 \leq m \leq q$, is an optimal set with respect to $EIP(2)$ in $G(q; \pm D)$, $D = \{1, 2, \dots, l\}$, $1 \leq l < \lfloor q/2 \rfloor$.*

Lemma 5 (see [19]). *For a circulant network $CN(q; \pm D)$, $D = \{1, 2, \dots, l\}$ and $1 \leq l < \lfloor q/2 \rfloor$, $1 \leq m \leq q$, we have*

$$I_{CN}(m) = \begin{cases} m \frac{(m-1)}{2}; & m \leq l+1 \\ ml - \frac{l(l+1)}{2}; & l+1 < m \leq q-l \\ \frac{1}{2} \{(q-m)^2 + (4l+1)m - (2l+1)q\}; & q-l < m \leq q \end{cases} \quad (5)$$

Definition 4. A path-of-complete graph is obtained by unifying a bone path v_1, v_2, \dots, v_m and $m-1$ complete graphs $K_{q_1}, K_{q_2}, \dots, K_{q_{m-1}}$ such that the edge (v_i, v_{i+1}) , $1 \leq i \leq m-1$, of the bone path shares an edge of the complete graph K_{q_i} . We denote it by $PC(m; q_1, q_2, \dots, q_{m-1})$. In an analogous way, we can define a cycle-of-complete graph by combining a bone cycle of length m and $K_{q_1}, K_{q_2}, \dots, K_{q_m}$ complete graphs. This graph is denoted by $CC(m; q_1, q_2, \dots, q_m)$.

Clearly, the number of vertices in $PC(m; q_1, q_2, \dots, q_{m-1})$ and $CC(m; q_1, q_2, \dots, q_m)$ are $q_1 + q_2 + \dots + q_{m-1} - (m-2)$

and $q_1 + q_2 + \dots + q_m - m$, respectively. The different cases of path- and cycle-of-complete graphs are shown in Figure 2. In the literature, these structures are sometimes called necklace graphs and also sharing between graphs by vertices, see [20, 21].

In what follows, $q_0 = 0$ and $q_\alpha = q_{\alpha-m}$, $\alpha > m$.

Theorem 1. *The minimum layout of circulant network $GN = CN(q; \pm \{1, 2, \dots, l\})$, $1 \leq l < \lfloor q/2 \rfloor$, into path-of-complete graph $HN = PC(m; q_1, q_2, \dots, q_{m-1})$ such that $q = q_1 + q_2 + \dots + q_{m-1} - (m-2)$ is given by $L(GN, HN) = m|E(G)| - \sum_{i=1}^m [I_G(q_1 + q_2 + \dots + q_{i-1} - i + 2) + I_G(q - (q_1 + q_2 + \dots + q_i - i))]$.*

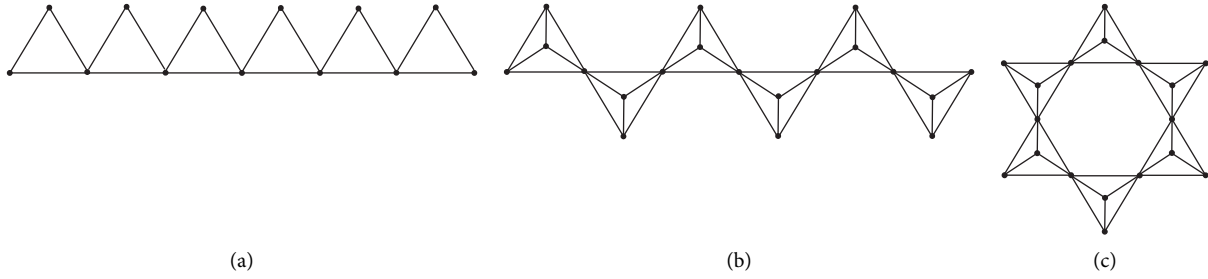


FIGURE 2: Path-of-complete graphs. (a) $PC(7; 3(6 - \text{times}))$. (b) $PC(7; 4(6 - \text{times}))$. (c) Cycle-of-complete graph $CC(6; 4(6 - \text{times}))$.

Proof. We begin with the embedding method of GN and HN . Label the peripheral cycle vertices of GN as $0, 1, \dots, q-1$ and the bone path vertices $v_i, 1 \leq i \leq m$, of HN as $q_1 + q_2 + \dots + q_{i-1} - i + 1$ in such a way that label the vertices (except on the path) of i^{th} complete graph $K_{q_i}, 1 \leq i \leq m-1$, from $q_1 + q_2 + \dots + q_{i-1} - i + 2$ to $q_1 + q_2 + \dots + q_i - i - 1$. We prove that the graph embedding μ of GN into HN defined by $\mu(w) = w$ yields the minimum layout. For $1 \leq i \leq m-1$, let S_i be the set of edges in the complete graph K_{q_i} . Then, $HN - S_i$ reduced to q_i components $HN_1, HN_2, \dots, HN_{q_i}$ with $V(HN_1) = \{0, 1, \dots, q_1 + q_2 + \dots + q_{i-1} - i + 1\}$, $2 \leq j \leq q_i - 1$, $V(HN_j) = \{q_1 + q_2 + \dots + q_{i-1} - i + j\}$, and $V(HN_{q_i}) = \{q_1 + q_2 + \dots + q_i - i, q_1 +$

$q_2 + \dots + q_i - i + 1, \dots, q - 1\}$. By Lemma 4, the induced subgraph by $\{\mu^{-1}(v) : v \in V(HN_i)\}$ on GN is an optimal set. We now conclude that μ is S_i -repulsive embedding of GN into HN . By Lemma 3, $EC_\mu(S_i)$ is minimum and $EC_\mu(S_i) = |E(GN)| - [I_{GN}(q_1 + q_2 + \dots + q_{i-1} - i + 2) + I_{GN}(q - (q_1 + q_2 + \dots + q_i - i))]$. Therefore, $L(GN, HN) = \sum_{i=1}^m EC_\mu(S_i) = m|E(GN)| - \sum_{i=1}^m [I_{GN}(q_1 + q_2 + \dots + q_{i-1} - i + 2) + I_{GN}(q - (q_1 + q_2 + \dots + q_i - i))]$. \square

Theorem 2. The minimum layout of circulant network $GN = CN(q; \pm \{1, 2, \dots, l\})$, $1 \leq l < \lfloor q/2 \rfloor$, into cycle-of-complete graph $HN = CC(m; q_1, q_2, \dots, q_m)$ such that $q = q_1 + q_2 + \dots + q_{m-1} - (m-1)$ is given by

$$L(GN, HN) = \frac{m}{2} |E(GN)| - \begin{cases} \sum_{i=1}^{m/2} [I_{GN}(q_{i+1} + \dots + q_{m/2+i-1} - m/2 + 1) \\ + I_{GN}(q_{m/2+i+1} + \dots + q_{i-1} - m/2 + 1)] & : m \text{ even} \\ \frac{1}{2} \sum_{i=1}^m [I_{GN}(q_{i+1} + \dots + q_{(m-1)/2+i-1} - (m-3)/2 + 1) \\ + I_{GN}(q_{(m-1)/2+i+1} + \dots + q_{i-1} - (m-1)/2 + 1)] & : m \text{ odd} \end{cases} \quad (6)$$

Proof. We first give the labeling of GN into HN and followed by embedding algorithm. Label the peripheral cycle vertices of GN as $0, 1, \dots, q-1$ and the bone cycle vertices $v_i, 1 \leq i \leq m$, of HN as $q_1 + q_2 + \dots + q_{i-1} - i + 1$ along the vertices (except on the cycle) of i^{th} complete graph $K_{q_i}, 1 \leq i \leq m$, from $q_1 + q_2 + \dots + q_{i-1} - i + 2$ to $q_1 + q_2 + \dots + q_i - i - 1$. Let μ be an embedding from GN into HN defined by $\mu(w) = w$.

Case 1 (m even): for $1 \leq i \leq m/2$, let S_i be the set of edges in the complete graphs K_{q_i} and $K_{q_{m/2+i}}$. Then, $HN - S_i$ reduced to $q_i + q_{m/2+i} - 2$ number of components HN_i s in which $q_i + q_{m/2+i} - 4$ components have cardinalities one each and the remaining components with $q_{i+1} + \dots + q_{m/2+i-1} - m/2 + 1$ and $q_{m/2+i+1} + \dots + q_{i-1} - m/2 + 1$ vertices. By Lemma 4, the induced subgraph by $\{\mu^{-1}(v) : v \in V(HN_j)\}$ on GN is an optimal set. Therefore, μ is S_i -repulsive embedding of GN into HN .

By Lemma 3, $EC_\mu(S_i)$ is minimum and $EC_\mu(S_i) = |E(GN)| - [I_{GN}(q_{i+1} + \dots + q_{m/2+i} - i - 1 - m/2 + 1) + I_{GN}(q_{m/2+i+1} + \dots + q_{i-1} - m/2 + 1)]$. By the construction of the edge cuts, we infer that $\{S_i : 1 \leq i \leq m/2\}$ is a partition of $E(HN)$, and hence, $L(GN, HN) = \sum_{i=1}^{m/2} EC_\mu(S_i) = (m/2)|E(GN)| - \sum_{i=1}^{m/2} [I_{GN}(q_{i+1} + \dots + q_{m/2+i-1} - m/2 + 1) + I_{GN}(q_{m/2+i+1} + \dots + q_{i-1} - m/2 + 1)]$.

Case 2 (m odd): for $1 \leq i \leq m$, let S_i be the set of edges in the complete graphs K_{q_i} and $K_{q_{(m-1)/2+i}}$. Then, $HN - S_i$ reduced to $q_i + q_{(m-1)/2+i} - 2$ number of components HN_j s in which $q_i + q_{(m-1)/2+i} - 4$ components have cardinalities one each and the remaining components with $q_{i+1} + \dots + q_{(m-1)/2+i-1} - (m-3)/2 + 1$ and $q_{(m-1)/2+i+1} + \dots + q_{i-1} - (m-1)/2 + 1$ vertices. By Lemma 4, the induced subgraph by $\{\mu^{-1}(v) : v \in V(HN_j)\}$ is an optimal set. Therefore, μ is

S_i -repulsive embedding of GN into HN . By Lemma 3, $EC_\mu(S_i)$ is minimum and $EC_\mu(S_i) = |E(GN)| - [I_{GN}(q_{i+1} + \dots + q_{(m-1)/2+i-1} - (m-3)/2 + 1) + I_{GN}(q_{(m-1)/2+i+1} + \dots + q_{i-1} - (m-1)/2 + 1)]$. We note that $\{S_i; 1 \leq i \leq m\}$ is a partition of $E^2(HN)$, and hence, $L(GN, HN) = (1/2) \sum_{i=1}^m EC_\mu(S_i) = (m/2)|E(GN)| - (1/2) \sum_{i=1}^m [I_{GN}(q_{i+1} + \dots + q_{(m-1)/2+i-1} - (m-3)/2 + 1) + I_{GN}(q_{(m-1)/2+i+1} + \dots + q_{i-1} - (m-1)/2 + 1)]$. \square

4. Conclusion

In analyzing the structural properties of a connected network, the measure such as graph embedding is of greater interest. As we know that the path, cycle, complete, and circulant graphs are important interconnection networks due to their simplicity, in this article, we successfully embedded circulant graphs into path- and cycle-of-complete graphs with minimum layout by the way of characterizing the congestion lemma with respect to regularity and optimality on the guest network.

Data Availability

No data were used to support this study.

Conflicts of Interest

The authors declare that they have no conflict of interest.

Authors' Contributions

M. A. and A. J. S. conceptualized the study; J. B. L. and J. N. D. investigated the study; M. A. wrote and prepared the original draft; A. J. S. and J. N. D. reviewed and edited the manuscript; J. B. L. supervised the study

References

- [1] A. L. Rosenberg, "Graph embeddings 1988: recent breakthroughs, new directions, VLSI algorithms and architectures (Corfu, 1988)," *Lecture Notes in Computer Science*, vol. 319, pp. 160–169, Springer, New York, NY, USA, 1988.
- [2] J.-M. Xu, *Topological Structure and Analysis of Interconnection Networks*, Kluwer Academic Publishers, New York, NY, USA, 2001.
- [3] J. Opatrny and D. Sotteau, "Embeddings of complete binary trees into grids and extended grids with total vertex-congestion 1," *Discrete Applied Mathematics*, vol. 98, no. 3, pp. 237–254, 2000.
- [4] J. Díaz, J. Petit, and M. Serna, "A survey of graph layout problems," *ACM Computing Surveys*, vol. 34, no. 3, pp. 313–356, 2002.
- [5] D. Muradian, *On Three Graph Layout Problems*, Lap Lambert Academic Publishing, Sunnysvale, CA, USA, 2018.
- [6] M. Arockiaraj, J. Clement, D. Paul, and K. Balasubramanian, "Quantitative structural descriptors of sodalite materials," *Journal of Molecular Structure*, vol. 1223, Article ID 128766, 2021.
- [7] S. N. Bhatt and F. Thomson Leighton, "A framework for solving VLSI graph layout problems," *Journal of Computer and System Sciences*, vol. 28, no. 2, pp. 300–343, 1984.
- [8] Y.-L. Lai and K. Williams, "A survey of solved problems and applications on bandwidth, edgesum, and profile of graphs," *Journal of Graph Theory*, vol. 31, no. 2, pp. 75–94, 1999.
- [9] M. Arockiaraj, J. N. Delaila, and J. Abraham, "Optimal wirelength of balanced complete multipartite graphs onto cartesian product of {path, cycle} and trees," *Fundamenta Informaticae*, vol. 178, no. 3, pp. 187–202, 2021.
- [10] W.-B. Fan, J.-X. Fan, C.-K. Lin, Y. Wang, Y.-J. Han, and R.-C. Wang, "Optimally embedding 3-ary n-cubes into grids," *Journal of Computer Science and Technology*, vol. 34, no. 2, pp. 372–387, 2019.
- [11] L. H. Harper, *Global Methods for Combinatorial Isoperimetric Problems*, Cambridge University Press, Cambridge, MA, USA, 2004.
- [12] L. H. Harper, "Optimal assignments of numbers to vertices," *Journal of the Society for Industrial and Applied Mathematics*, vol. 12, no. 1, pp. 131–135, 1964.
- [13] S. L. Bezrukov, S. K. Das, and R. Elsässer, "An edge-isoperimetric problem for powers of the Petersen graph," *Annals of Combinatorics*, vol. 4, no. 2, pp. 153–169, 2000.
- [14] P. Manuel, I. Rajasingh, B. Rajan, and H. Mercy, "Exact wirelength of hypercubes on a grid," *Discrete Applied Mathematics*, vol. 157, no. 7, pp. 1486–1495, 2009.
- [15] M. Arockiaraj, J. Quadras, I. Rajasingh, and A. J. Shalini, "Embedding of hypercubes into sibling trees," *Discrete Applied Mathematics*, vol. 169, pp. 9–14, 2014.
- [16] M. Miller, R. S. Rajan, N. Parthiban, and I. Rajasingh, "Minimum linear arrangement of incomplete hypercubes," *The Computer Journal*, vol. 58, no. 2, pp. 331–337, 2015.
- [17] J. C. Bermond, F. Comellas, and D. F. Hsu, "Distributed loop computer-networks: a survey," *Journal of Parallel and Distributed Computing*, vol. 24, no. 1, pp. 2–10, 1995.
- [18] G. K. Wong and D. A. Coppersmith, "A combinatorial problem related to multimodule memory organization," *Journal of the ACM*, vol. 21, no. 3, pp. 392–401, 1994.
- [19] I. Rajasingh, P. Manuel, M. Arockiaraj, and B. Rajan, "Embeddings of circulant networks," *Journal of Combinatorial Optimization*, vol. 26, no. 1, pp. 135–151, 2013.
- [20] I. Rajasingh, B. Rajan, and R. S. Rajan, "Embedding of hypercubes into necklace, windmill and snake graphs," *Information Processing Letters*, vol. 112, no. 12, pp. 509–515, 2012.
- [21] I. Rajasingh and R. S. Rajan, "Exact wirelength of embedding circulant networks into necklace and windmill graphs," *Ars Combinatoria*, vol. 130, pp. 215–237, 2017.

Research Article

On the Connected Safe Number of Some Classes of Graphs

Rakib Iqbal,¹ Muhammad Shoaib Sardar ,² Dalal Alrowaili ,³ Sohail Zafar,¹
and Imran Siddique ¹

¹Department of Mathematics, University of Management and Technology, Lahore 54770, Pakistan

²School of Mathematics, Minhaj University, Lahore, Pakistan

³Mathematics Department, College of Science, Jouf University, P.O. Box: 2014, Sakaka, Saudi Arabia

Correspondence should be addressed to Imran Siddique; imransmsrazi@gmail.com

Received 9 September 2021; Accepted 7 October 2021; Published 23 October 2021

Academic Editor: Muhammad Kamran Siddiqui

Copyright © 2021 Rakib Iqbal et al. This is an open access article distributed under the Creative Commons Attribution License, which permits unrestricted use, distribution, and reproduction in any medium, provided the original work is properly cited.

For a connected simple graph \mathcal{G} , a nonempty subset \mathcal{S} of $V(\mathcal{G})$ is a connected safe set if the induced subgraph $\mathcal{G}[\mathcal{S}]$ is connected and the inequality $|\mathcal{S}| \geq |\mathcal{D}|$ satisfies for each connected component \mathcal{D} of $\mathcal{G} \setminus \mathcal{S}$ whenever an edge of \mathcal{G} exists between \mathcal{S} and \mathcal{D} . A connected safe set of a connected graph \mathcal{G} with minimum cardinality is called the minimum connected safe set and that minimum cardinality is called the connected safe numbers. We study connected safe sets with minimal cardinality of the ladder, sunlet, and wheel graphs.

1. Introduction

A facility location problem (FLP) means to place and manage a certain facility in such a way as to get or achieve the maximum objective with minimizing cost. For further study of FLPs, we refer to the literature of combinatorial optimization [1]. Fujita et al. [2] studied the FLP and proposed a notion of a safe set of graphs.

We refer to [3] for terminology and notation not explained here. Throughout the paper, we will consider only simple and connected graphs. Let \mathcal{G} be a graph with $V(\mathcal{G})$ and $E(\mathcal{G})$ as its vertex and edge set, respectively. The number of vertices in a graph \mathcal{G} is the order of \mathcal{G} . For $v \in V(\mathcal{G})$, $N(v) = \{u \in V(\mathcal{G}) : u \text{ is adjacent to } v\}$ and $N[v] = N(v) \cup \{v\}$ is called open and closed neighborhood of v in \mathcal{G} , respectively. For $v \in V(\mathcal{G})$, the degree of vertex v is defined as $\deg(v) = |N(v)|$. For subset $\mathcal{S} \subset V(\mathcal{G})$, $\mathcal{G}[\mathcal{S}]$ denotes the subgraph induced by \mathcal{S} . For subset $X \subset V(\mathcal{G})$, if $\mathcal{G} \setminus X$ is disconnected, then X is known as vertex cut. The vertex connectivity denoted by $\kappa(\mathcal{G})$ is defined as $\min\{|X| : X \text{ is vertex cut}\}$. Let $C(\mathcal{G})$ denote the set of all connected components of \mathcal{G} .

Suppose A and B are disjoint subgraphs of \mathcal{G} ; then, the set of edges of $E(\mathcal{G})$ that joins some vertices of A and B is

denoted by $E(A, B)$. A nonempty subset \mathcal{S} of $V(\mathcal{G})$ is a safe set if, for each $X \in C(\mathcal{G} \setminus \mathcal{S})$ and each $Y \in C(\mathcal{G}[\mathcal{S}])$, the inequality $|Y| \geq |X|$ holds whenever $E(X, Y) \neq \emptyset$. If $\mathcal{G}[\mathcal{S}]$ is connected, then \mathcal{S} is known as a connected safe set. For any graph \mathcal{G} , $s(\mathcal{G}) = \min\{|\mathcal{S}| : \mathcal{S} \text{ is a safe set of } \mathcal{G}\}$ and $cs(\mathcal{G}) = \min\{|\mathcal{S}| : \mathcal{S} \text{ is a connected safe set of } \mathcal{G}\}$ are known as the safe number and connected safe number, respectively. It is clear from the definition that $s(P_n) = cs(P_n) = \lceil n/3 \rceil$ and $s(C_n) = cs(C_n) = \lceil n/2 \rceil$, where P_n and C_n are the path and cycle of order n , respectively. Fujita et al. [2] proved that for any graph \mathcal{G} , $s(\mathcal{G}) \leq cs(\mathcal{G}) \leq 2s(\mathcal{G}) - 1$.

In general, there is no algorithm available to compute a safe number and a connected safe number of a graph \mathcal{G} . It was shown in [2] that the computation of safe number and connected safe number is an NP-complete problem. But, on the contrary, Fujita et al. [2] show that $cs(\mathcal{G})$ can be computed in linear time in case of trees. Also, Árueda et al. [4] show that $s(\mathcal{G})$ can be computed in $O(n^5)$ time on trees. Any tree T with one vertex of degree not more than 3 holds that $s(T) = cs(T)$. Motivated by this equality, for the Cartesian product of two complete graphs, say \mathcal{G} , Kang et al. [5] proved that the safe number $s(\mathcal{G})$ and connected safe number $cs(\mathcal{G})$ are also the same.

For a vertex-weighted graph, Bapat et al. [6] presented the weighted safe set problem by considering the graph as a community network. For further study about the weighted safe set, we refer to [7–9]. Furthermore, the study on safe set and weighted safe set was conducted by several authors. The parameterized complexity of safe set problems was investigated by Belmonte et al. [10]. Macambiraa et al. [11] presented a mixed integer linear programming formulation and an algorithm for both the weighted safe set and the safe set problems. Fujita and Furuya [12] investigated the comparison between integrity and the safe number of graphs.

In this paper, we describe the connected safe set and compute the connected safe number of ladder, wheel, and sunlet graphs, respectively. The paper is concluded in Section 5.

2. Safe Set of the Ladder Graph

For convenience, we consider the ladder graph \mathcal{G} of order $n \geq 4$ with vertex set $V(\mathcal{G}) = \{v_1, v_2, \dots, v_n\}$ labeled as shown in Figure 1 [13].

Theorem 1. *Let \mathcal{G} be a ladder graph; then, the connected safe set is*

$$\mathcal{S} = \begin{cases} \{v_{\lfloor n/8 \rfloor + 2}, v_{\lfloor n/8 \rfloor + 3}, \dots, v_{\lfloor n/8 \rfloor + \lfloor n/4 \rfloor + 1}, v_{n - \lfloor n/8 \rfloor - \lfloor n/4 \rfloor}, v_{n - \lfloor n/8 \rfloor - 1}\}, & \text{if } n \equiv 0, 2, 6 \pmod{8}, \\ \{v_{\lfloor n/8 \rfloor + 2}, v_{\lfloor n/8 \rfloor + 3}, \dots, v_{\lfloor n/8 \rfloor + \lfloor n/4 \rfloor}, v_{n - \lfloor n/8 \rfloor - \lfloor n/4 \rfloor + 1}, v_{n - \lfloor n/8 \rfloor - 1}\}, & \text{otherwise.} \end{cases} \quad (1)$$

Proof 1. The proof is divided into two cases:

Case 1: assume that $n \equiv 0, 2, 6 \pmod{8}$. Let $\mathcal{S} = \{v_{\lfloor n/8 \rfloor + 2}, v_{\lfloor n/8 \rfloor + 3}, \dots, v_{\lfloor n/8 \rfloor + \lfloor n/4 \rfloor + 1}, v_{n - \lfloor n/8 \rfloor - \lfloor n/4 \rfloor}, v_{n - \lfloor n/8 \rfloor - 1}\}$ be a subset of $V(\mathcal{G})$. Clearly, $v_1 v_n, v_2 v_{n-1}, \dots, v_{n/2} v_{(n/2)-1} \in E(\mathcal{G})$. Hence, $v_{\lfloor n/8 \rfloor + 2}$ and $v_{n - \lfloor n/8 \rfloor - 1}$ as well as $v_{\lfloor n/8 \rfloor + \lfloor n/4 \rfloor + 1}$ and $v_{n - \lfloor n/8 \rfloor - \lfloor n/4 \rfloor}$ are adjacent. Therefore, $\mathcal{G}[\mathcal{S}]$ is connected. Now, $C(\mathcal{G} \setminus \mathcal{S}) = \{\mathcal{D}_1, \mathcal{D}_2, \mathcal{D}_3\}$, where $\mathcal{D}_1 = \{v_{n - \lfloor n/8 \rfloor - \lfloor n/4 \rfloor + 1}, v_{n - \lfloor n/8 \rfloor - \lfloor n/4 \rfloor + 2}, \dots, v_{n - \lfloor n/8 \rfloor - 2}\}$, $\mathcal{D}_2 = \{v_{\lfloor n/8 \rfloor + \lfloor n/4 \rfloor + 2}, v_{\lfloor n/8 \rfloor + \lfloor n/4 \rfloor + 3}, \dots, v_{n - \lfloor n/8 \rfloor - \lfloor n/4 \rfloor - 1}\}$, and $\mathcal{D}_3 = \{v_1, v_2, \dots, v_{\lfloor n/8 \rfloor + 1}, v_{n - \lfloor n/8 \rfloor}, \dots, v_{n-1}, v_n\}$. It is easy to see that $|\mathcal{S}| = \lfloor n/4 \rfloor + 2$, $|\mathcal{D}_1| = \lfloor n/4 \rfloor - 2$, $|\mathcal{D}_2| = n - 2\lfloor n/8 \rfloor - 2\lfloor n/4 \rfloor - 2$, and $|\mathcal{D}_3| = 2\lfloor n/8 \rfloor + 2$. This implies $|\mathcal{D}_i| \leq |\mathcal{S}|$ and $E(\mathcal{D}_i, \mathcal{S}) \neq \emptyset$ for $1 \leq i \leq 3$. Hence, both the conditions of connected safe set are satisfied.

Case 2: the similar arguments might work for the other case. \square

Theorem 2. *For a ladder graph \mathcal{G} of order n , the following holds:*

$$cs(\mathcal{G}) = \begin{cases} \lfloor \frac{n}{3} \rfloor, & \text{if } 4 \leq n \leq 8, \\ \lfloor \frac{n}{4} \rfloor + 2, & \text{if } n \geq 10 \text{ and } n \equiv 0, 2, 6 \pmod{8}, \\ \lfloor \frac{n}{4} \rfloor + 1, & \text{otherwise.} \end{cases} \quad (2)$$

Proof 2. Assume that \mathcal{S} is a connected safe set of cardinality $cs(\mathcal{G})$ and $C(\mathcal{G} \setminus \mathcal{S}) = \{\mathcal{D}_1, \mathcal{D}_2, \dots, \mathcal{D}_t\}$, ordered so that $|\mathcal{D}_1| \leq |\mathcal{D}_2| \leq \dots \leq |\mathcal{D}_t|$.

If $t = 1$, then either $v_1, v_n \in \mathcal{S}$ or $v_{n/2}, v_{n/2+1} \in \mathcal{S}$. We assume that $v_1, v_n \in \mathcal{S}$. Let $u \in \mathcal{D}_1$ such that $E(\{u\}, \mathcal{S}) \neq \emptyset$. Then, by removing vertex v_1 from \mathcal{S} and adding vertex u in

\mathcal{S} , we get a connected safe set \mathcal{S}^* and for \mathcal{S}^* , $|\mathcal{D}_1| < \max\{|\mathcal{D}| \mid \mathcal{D} \in C(\mathcal{G} \setminus \mathcal{S}^*)\}$, which is a contradiction. Hence, $t \geq 2$.

Consider that $n \geq 10$ and $n \equiv 0, 2, 6 \pmod{8}$.

We want to show that $|\mathcal{S}| = \lfloor n/4 \rfloor + 2$. Suppose on the contrary $|\mathcal{S}| = \lfloor n/4 \rfloor + 1$ since $\kappa(\mathcal{G}) = 2$.

Let $\mathcal{X} = \{\{v_i, v_j\} \mid v_i, v_j \in V(\mathcal{G}) \text{ and } i + j = n + 1\}$ be the vertex cut sets, where $1 < i < n/2$ and $n/2 < j < n$ and clearly $|\mathcal{X}| = n/2 - 2$. We assume that \mathcal{S} contains X_l , where $l \geq 2$. Suppose, for contradictions $l = 1$, clearly $t = 2$. Let w be a vertex of \mathcal{D}_2 such that $E(X_1, \{w\}) = \emptyset$ and $E(\mathcal{S}, \{w\}) \neq \emptyset$. Then, there exists a vertex x of \mathcal{S} such that we have the following:

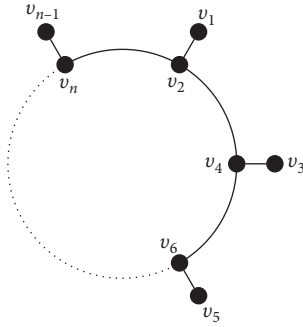
- (i) $\mathcal{S} - \{x\}$ is connected
- (ii) $X_1 \cap \{x\} = \emptyset$
- (iii) $E(\{w\}, \{x\}) = \emptyset$

Then, by removing vertex x from \mathcal{S} and adding vertex w in \mathcal{S} , we get a connected safe set \mathcal{S}^* and for \mathcal{S}^* , we have $|\mathcal{D}_1| < \max\{|\mathcal{D}| \mid \mathcal{D} \in C(\mathcal{G} \setminus \mathcal{S}^*)\}$, which is a contradiction. Hence, $l \geq 2$. It is sufficient to show for X_1 and X_2 that $|\mathcal{S}| = cs(\mathcal{G})$. Note that if $E(X_1, X_2) \neq \emptyset$, then $t = 2$. Hence, we assume that $E(X_1, X_2) = \emptyset$. Suppose that $v_{i_1}, v_{i_2} \in \mathcal{S}$ such that $E(\{v_{i_1}\}, X_1) \neq \emptyset$ and $E(\{v_{i_2}\}, X_2) \neq \emptyset$ since \mathcal{S} is connected. Therefore, half vertices between X_1 and X_2 belong to \mathcal{S} and the other half belongs to a component of $\mathcal{G} \setminus \mathcal{S}$ (say \mathcal{D}_1). This implies $|\mathcal{D}_1| \leq |\mathcal{S}| - 4 = \lfloor n/4 \rfloor - 3$. Note that $|\mathcal{D}_2| \leq |\mathcal{D}_3|$. Thus, $|\mathcal{D}_3| \geq (n - |\mathcal{S}| - |\mathcal{D}_1|)/2 = (n - 2\lfloor n/4 \rfloor + 2)/2 \geq |\mathcal{S}|$, a contradiction. Hence, $|\mathcal{S}| = \lfloor n/4 \rfloor + 2$.

The similar arguments might work for other cases. \square

3. Safe Set of the Wheel Graph

For convenience, we consider the wheel graph \mathcal{G} of order $n \geq 4$ with vertex set $V(\mathcal{G}) = \{v_1, v_2, \dots, v_n\}$ labeled as shown in Figure 2 [14].

FIGURE 3: The sunlet graph \mathcal{G} .

$$cs(\mathcal{G}) = \lfloor \frac{n}{3} \rfloor. \quad (7)$$

Proof 6. Assume that \mathcal{S} is a connected safe set of cardinality $cs(\mathcal{G})$; then, $C(\mathcal{G} \setminus \mathcal{S}) = \{\mathcal{D}_1, \mathcal{D}_2, \dots, \mathcal{D}_t\}$, ordered such that $|\mathcal{D}_1| \leq |\mathcal{D}_2| \leq \dots \leq |\mathcal{D}_t|$.

If $t = 1$, then $\mathcal{S} = X \cup Y$, where $X = \{v \mid v \in \mathcal{S} \text{ and } \deg(v) = 3\}$ and $Y = \{u \mid u \in \mathcal{S} \text{ and } \deg(v) = 1\}$. Note that $\mathcal{S} - \{v\}$ is disconnected for all $v \in X$. Let $u \in Y$ and $w \in \mathcal{D}_1$ such that $E(\{w\}, \mathcal{S}) \neq \emptyset$; then, $\mathcal{S}^* = (\mathcal{S} - \{u\}) \cup \{w\}$ is a connected safe set and for \mathcal{S}^* , $|\mathcal{D}_1| < \max\{|\mathcal{D}| \mid \mathcal{D} \in C(\mathcal{G} \setminus \mathcal{S}^*)\}$, a contradiction. Thus, $t \geq 2$.

Let $Z \subset V(\mathcal{G})$ such that $Z \cap \mathcal{S} = \emptyset$, $E(\mathcal{S}, Z) \neq \emptyset$, and $\mathcal{G}[Z]$ is a path. Note that $\mathcal{S}' = (\mathcal{S} - Y) \cup Z$ is a connected safe set; then, obviously $\mathcal{G}[\mathcal{S}']$ is the path, and for that choice of the connected safe set, we have $|C(\mathcal{G} \setminus \mathcal{S}')| = \text{Max}\{|C(\mathcal{G} \setminus \mathcal{S})| \mid \mathcal{S} \text{ is a connected safe set}\}$. As a result, $2 \leq t \leq |\mathcal{S}'| + 1$.

Suppose on the contrary that $cs(\mathcal{G}) = \lfloor n/3 \rfloor - 1$. Since $2 \leq t \leq |\mathcal{S}'| + 1$, $d = \sum_{i=1}^{k-1} |\mathcal{D}_i| \leq |\mathcal{S}'|$ and $n - 2\lfloor n/3 \rfloor + 2 \geq |V(\mathcal{G}) - \mathcal{S}' - d| = |\mathcal{D}_k| > |\mathcal{S}'|$, a contradiction. Hence, $cs(\mathcal{G}) = \lfloor n/3 \rfloor$. \square

5. Conclusion

In this article, the connected safe set and connected safe number of ladder, wheel, and sunlet graphs are studied. The computation of connected safe number is an NP-complete problem and is known for few classes of graphs. A nontrivial graph of order n whose degree set consists of $n - 1$ elements is called an antiregular graph. Hence, in the future, it is interesting to study the safe set number for some other standard classes of graphs such as regular graphs, antiregular graphs, and well-known computer networks.

Data Availability

No data were used to support this study.

Conflicts of Interest

The authors declare that they have no conflicts of interest.

References

- [1] B. Korte and J. Vygen, *Combinatorial Optimization*, Springer-Verlag, Berlin, Heidelberg, 5th edition, 2011.
- [2] S. Fujita, G. MacGillivray, and T. Sakuma, "Safe set problem on graphs," *Discrete Applied Mathematics*, vol. 215, pp. 106–111, 2016.
- [3] G. Chartrand, L. Lesniak, and P. Zhang, *Graphs and Digraphs*, Chapman & Hall, London, UK, 5th edition, 2011.
- [4] R. Águeda, N. Cohen, S. Fujita et al., "Safe sets in graphs: graph classes and structural parameters," *Journal of Combinatorial Optimization*, vol. 36, no. 4, pp. 1221–1242, 2018.
- [5] B. Kang, S. Kim, and B. Park, "On safe sets of the cartesian product of two complete graphs," *Ars Combinatoria*, vol. 141, pp. 243–257, 2018.
- [6] R. B. Bapat, S. Fujita, S. Legay et al., "Safe sets, network majority on weighted trees," *Networks*, vol. 71, no. 1, pp. 81–92, 2018.
- [7] S. Ehard and D. Rautenbach, "Approximating connected safe sets in weighted trees," *Discrete Applied Mathematics*, vol. 281, pp. 216–223, 2020.
- [8] S. Fujita, T. Jensen, B. Park, and T. Sakuma, "On the weighted safe set problem on paths and cycles," *Journal of Combinatorial Optimization*, vol. 37, no. 2, pp. 685–701, 2019.
- [9] S. Fujita, B. Park, and T. Sakuma, "Stable structure on safe set problems in vertex-weighted graphs," *European Journal of Combinatorics*, vol. 91, Article ID 103211, 2021.
- [10] R. Belmonte, T. Hanaka, I. Katsikarelis, M. Lampis, H. Ono, and Y. Otachi, "Parameterized complexity of safe set," in *Proceedings of the International Conference on Algorithms and Complexity*, Springer, Larnaca, Cyprus, May 2019.
- [11] A. F. U. Macambira, L. Simonetti, H. Barbalho, P. H. Gonzalez, and N. Maculan, "A new formulation for the safe set problem on graphs," *Computers and Operations Research*, vol. 111, pp. 346–356, 2019.
- [12] S. Fujita and M. Furuya, "Safe number and integrity of graphs," *Discrete Applied Mathematics*, vol. 247, pp. 398–406, 2018.
- [13] S. N. Daoud and A. Elsonbaty, "Complexity of some graphs generated by ladder graph," *International Journal of Applied Mathematics and Statistics*, vol. 36, no. 6, pp. 87–94, 2013.
- [14] X. Yu, L. Zhou, and X. Li, "A novel hybrid localization scheme for deep mine based on wheel graph and chicken swarm optimization," *Computer Networks*, vol. 154, pp. 73–78, 2019.
- [15] T. N. Saibavani and N. Parvathi, "Power domination number of sunlet graph and other graphs," *Journal of Discrete Mathematical Sciences and Cryptography*, vol. 22, no. 6, pp. 1121–1127, 2019.

Research Article

Computation of Edge Resolvability of Benzenoid Tripod Structure

Ali Ahmad ¹, Sadia Husain,¹ Muhammad Azeem ², Kashif Elahi,³ and M. K. Siddiqui ⁴

¹College of Computer Science & Information Technology, Jazan University, Jazan, Saudi Arabia

²Department of Mathematics, Riphah Institute of Computing and Applied Sciences, Riphah International University, Lahore, Pakistan

³Deanship of E-Learning and Information Technology, Jazan University, Jazan, Saudi Arabia

⁴Department of Mathematics, COMSATS University Islamabad, Lahore Campus, Lahore 54000, Pakistan

Correspondence should be addressed to Ali Ahmad; ahmadsms@gmail.com

Received 14 August 2021; Accepted 9 October 2021; Published 21 October 2021

Academic Editor: Gaetano Luciano

Copyright © 2021 Ali Ahmad et al. This is an open access article distributed under the Creative Commons Attribution License, which permits unrestricted use, distribution, and reproduction in any medium, provided the original work is properly cited.

In chemistry, graphs are commonly used to show the structure of chemical compounds, with nodes and edges representing the atom and bond types, respectively. Edge resolving set λ_e is an ordered subset of nodes of a graph C , in which each edge of C is distinctively determined by its distance vector to the nodes in λ . The cardinality of a minimum edge resolving set is called the edge metric dimension of C . An edge resolving set $L_{e,f}$ of C is fault-tolerant if $\lambda_{e,f} \setminus b$ is also an edge resolving set, for every b in $\lambda_{e,f}$. Resolving set allows obtaining a unique representation for chemical structures. In particular, they were used in pharmaceutical research for discovering patterns common to a variety of drugs. In this paper, we determine the exact edge metric and fault-tolerant edge metric dimension of benzenoid tripod structure and proved that both parameters are constant.

1. Introduction

Mathematical chemistry has recently presented a wide range of approaches to understanding the chemical structures that underpin existing chemical theories and developing and exploring new mathematical models of chemical phenomena and applying mathematical concepts and processes to chemistry. Only a few scientists have been convinced to exploit linkages between mathematics and chemistry and the possibility of using arithmetic to deduce known and anticipate new chemical characteristics, throughout the history of science. In many areas of physical chemistry, such as thermodynamics and compound energy, extensive use of mathematical approaches is commonplace. After physicists revealed in the first few years of the twentieth century that the key features of chemical compounds can be predicted using quantum theory approaches, a significant need for mathematics in chemistry arose. The main driving force that drove the mathematics and its concepts into chemistry laboratories was the realization that chemistry cannot be comprehended without knowledge of quantum physics, including its complicated mathematical instruments. For the

different study of mathematical chemistry in terms of graph theory, we suggest some literature here [1].

Chemical graph theory is a branch of mathematical science that is used to characterise the structural properties of molecules, processes, crystals, polymers, clusters, and other objects. The vertex of a chemical graph theory might be an electron, an atom, a molecule, a collection of atoms, intermediates, orbitals, and many other things. Intermolecular bonding, bonded and nonbonded connections, basic reactions, and other forces such as van der Waals forces, Keesom forces, and Debye forces can all be used to illustrate the relationships between vertices of a structure.

The general convex polytope structures are discussed in [2, 3], in which authors consider the problem of edge metric resolvability. In the reply to aroused question from seminal work of edge resolvability, Raza and Bataineh [4] answered some questions and provided interesting results as well as analysis between vertex and edge resolvability. The detailed discussion of identifying edges and vertices of general graph is studied in [5]. Necklace graph's edge resolvability is discussed in [6]. Polycyclic aromatic hydrocarbons in terms of edge and fault-tolerant edge resolvability are deeply

investigated in [7]. The generalized version of edge resolvability is introduced in [8]. Few efficient techniques of finding edge resolving set are found in [9]. The graph having larger edge resolvability rather than vertex resolvability is generally studied in [10]. The generalized Peterson graph's edge resolvability is found in [11]. The k-multiwheel graph point of discussion with its edge resolvability is found in [12].

Slater [13] presented the idea of resolving sets, which was later discussed by Harary and Melter [14]. Metric generators, as detailed in [15, 16], allow for alternative representations of chemical substances. Precisely, they were used in pharmaceutical research for determining patterns similar to a variety of drugs [17]. Metric dimension has various other applications, such as robot navigation [18], weighing problems [19], computer networks [20], combinatorial optimization [21], image processing, facility location problems, and sonar and coastguard loran [13]; for further detail, see [22, 23]. Due to its variety of applications, the concept of metric dimension is widely used to solve many difficult problems. Hussain et al. [24], Krishnan et al. [25], and Siddiqui et al. [26] have computed the resolvability parameter for alpha-boron nanotube, certain crystal structures, and certain nanotube lattices, respectively. For the NP-harness of these topics, for example, and for the metric dimension [27, 28] and application along with its NP-hardness, see [29]. Rather than separating two unique vertices of a graph based on a subset of vertices, two edges might be distinguished based on the same subset of vertices. Kelenc et al. [30] created a new parameter called the edge metric dimension to represent this idea. They employed graph metric to identify each pair of edges based on the graph's distance from a selection of vertices.

The following are basic preliminaries for the concepts studied here.

Definition 1 (see [31]). Assume that C is an associated graph of chemical structure/network, whose vertex/node set are denoted by symbol $N(C)$ or simply N , while $B(C)$ or B is the edge/bond set, and the shortest distance between two bonds $b_1, b_2 \in N(C)$ is denoted by S_{b_1, b_2} and calculated by counting the number of bonds while moving through the $b_1 - b_2$ path.

Definition 2 (see [32]). The distance between an edge $e = b_1 b_2 \in B(C)$ and a node $b \in N(C)$ is counted by the relation $Se, b = \min\{Sb_1, b, Sb_2, b\}$. Assuming a subset of selected nodes λ_e , if the position $\mathfrak{p}(e|\lambda_e)$ of each edge e is unique of a graph, then λ_e is called as edge metric resolving set and $\dim_e(C)$ is the minimum count of members of λ_e , called as edge metric dimension.

Definition 3. Assuming that any of the member of edge metric resolving set λ_e is not working or any of the node from κ members is spoiled, then one cannot get the unique position of the entire edge set. To tackle this issue, the definition is known as fault-tolerant edge resolving set which is dealt with by eliminating any of the member from λ_e and still obtains the unique position of the entire edge set of a graph, symbolized as $\lambda_{e, f}$, and the minimum members in the set denoted as $\dim_{e, f}(C)$ and named as fault-tolerant edge metric dimension.

Theorem 1 (see [30]). *If $\dim_e(C)$ is the edge metric dimension, then $\dim_e(C) = 1$, iff C is a path P_n .*

2. Construction of Tripod Structure

Because it is significant in theoretical chemistry, benzenoid systems are natural graph representations of benzenoid hydrocarbons. It is a well-known fact that hydrocarbons generated from benzenoids are important and beneficial in the chemical, food, and environmental industries, according to [33]. The authors in [34] describe the benzenoid system we mentioned above in our work. Polynomial types were discussed in relation to various catacondensed and pericondensed benzenoid structures. This is a pericondensed benzenoid tripod construction. It has $4(\delta_1 + \delta_2 + \delta_3) - 8$ nodes and $5(\delta_1 + \delta_2 + \delta_3) - 11$ bonds, with all the running parameters $\delta_1, \delta_2, \delta_3 \geq 2$. Furthermore, Jamil et al. [35] provide a comprehensive topological investigation of benzenoid structures, and metric-based study of benzenoid networks is available in [36]. The node and bond or vertex and edge set for the benzenoid structure $T(\delta_1, \delta_2, \delta_3)$ is shown as follows. In our primary results, we apply the labelling of nodes and edges specified in Figure 1.

$$\begin{aligned}
 N(T(\delta_1, \delta_2, \delta_3)) &= \{a_\kappa: 1 \leq \kappa \leq 2\delta_3\} \cup \{b_\kappa: 1 \leq \kappa \leq 2\delta_1\} \cup \{c_\kappa, c'_\kappa: 1 \leq \kappa \leq 2\delta_2 - 1\} \\
 &\quad \cup \{a'_\kappa: 1 \leq \kappa \leq 2\delta_3 - 3\} \cup \{b'_\kappa: 1 \leq \kappa \leq 2\delta_1 - 3\}, \\
 B(T(\delta_1, \delta_2, \delta_3)) &= \{a_\kappa a_{\kappa+1}: 1 \leq \kappa \leq 2\delta_3 - 1\} \cup \{b_\kappa b_{\kappa+1}: 1 \leq \kappa \leq 2\delta_1 - 1\} \\
 &\quad \cup \{c_\kappa c_{\kappa+1}, c'_\kappa c'_{\kappa+1}: 1 \leq \kappa \leq 2\delta_2 - 2\} \cup \{a'_\kappa a'_{\kappa+1}: 1 \leq \kappa \leq 2\delta_3 - 4\} \\
 &\quad \cup \{b'_\kappa b'_{\kappa+1}: 1 \leq \kappa \leq 2\delta_1 - 4\} \cup \{a_\kappa a'_\kappa: 1 \leq \kappa(\text{odd}) \leq 2\delta_3 - 3\} \\
 &\quad \cup \{b_{\kappa+3} b'_\kappa: 1 \leq \kappa(\text{odd}) \leq 2\delta_1 - 3\} \cup \{c_\kappa c'_\kappa: 1 \leq \kappa(\text{odd}) \leq 2\delta_2 - 1\} \\
 &\quad \cup \{a_{2\delta_3} b_1, a_{2\delta_3-1} c'_1, b_2 c_1, a_{2\delta_3-3} c'_2, b'_1 c_2\}.
 \end{aligned} \tag{1}$$

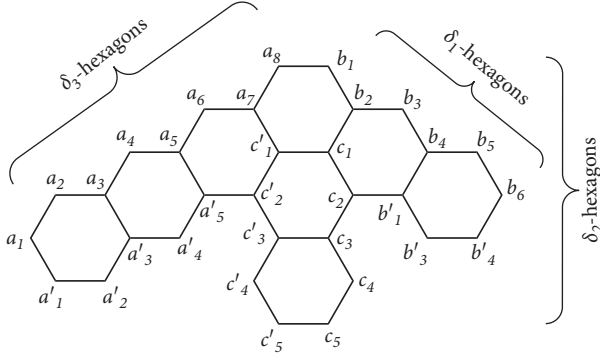


FIGURE 1: Benzenoid tripod with $\{\delta_1, \delta_2, \delta_3\} = \{3, 3, 4\}$.

Lemma 1. *If $T(\delta_1, \delta_2, \delta_3)$ is a graph of benzenoid tripod with $\delta_1, \delta_2, \delta_3 \geq 2$, then the minimum members in its edge resolving set are two.*

Proof. The total number of nodes in the corresponding graph of benzenoid tripod with $\delta_1, \delta_2, \delta_3 \geq 2$ is $4(\delta_1 + \delta_2 + \delta_3) - 8$ and to check the possibilities of edge resolving set with cardinality two is $C(4(\delta_1 + \delta_2 + \delta_3) - 8, 2) = ((4(\delta_1 + \delta_2 + \delta_3) - 8)! / (2 \times (4(\delta_1 + \delta_2 + \delta_3) - 10)!))$. Here, we are checking with cardinality two because by Theorem 1, the edge resolving set with cardinality one is reserved for path graph only. Now due to the NP-hardness of choosing edge resolving set, we cannot find the exact number of edge resolving sets for a graph, but from $((4(\delta_1 + \delta_2 + \delta_3) - 8)! / (2 \times (4(\delta_1 + \delta_2 + \delta_3) - 10)!))$ -possibilities, we choose a subset λ_e and defined as $\lambda_e = \{a_1, b_1\}$. Now to prove this claim that λ_e is actually one of the candidates for the edge resolving set of benzenoid tripod graph or $T(\delta_1, \delta_2, \delta_3)$, we will follow Definition 2. To fulfill the requirements of definition, we will check the unique positions or locations of each edge and the methodology is defined above in Definition 2.

Positions $\mathfrak{p}(a_\kappa a_{\kappa+1} | \lambda_e)$ with respect to λ_e , for the edges $a_\kappa a_{\kappa+1}$ with $\kappa = 1, 2, \dots, 2\delta_3 - 1$, are given as

$$\mathfrak{p}(a_\kappa a_{\kappa+1} | \lambda_e) = (\kappa - 1, 2\delta_3 - \kappa). \quad (2)$$

Positions $\mathfrak{p}(b_\kappa b_{\kappa+1} | \lambda_e)$ with respect to λ_e , for the edges $b_\kappa b_{\kappa+1}$ with $\kappa = 1, 2, \dots, 2\delta_1 - 1$, are given as

$$\mathfrak{p}(b_\kappa b_{\kappa+1} | \lambda_e) = (2\delta_3 + \kappa - 1, \kappa - 1). \quad (3)$$

Positions $\mathfrak{p}(c_\kappa c_{\kappa+1} | \lambda_e)$ with respect to λ_e , for the edges $c_\kappa c_{\kappa+1}$ with $\kappa = 1, 2, \dots, 2\delta_2 - 2$, are given as

$$\mathfrak{p}(c_\kappa c_{\kappa+1} | \lambda_e) = \begin{cases} (2\delta_3, \kappa + 1), & \text{if } \kappa = 1, 2, \\ (2\delta_3 + \kappa - 3, \kappa + 1), & \text{if } \kappa = 3, 4, \dots, 2\delta_2 - 1. \end{cases} \quad (4)$$

Positions $\mathfrak{p}(a'_\kappa a'_{\kappa+1} | \lambda_e)$ with respect to λ_e , for the edges $a'_\kappa a'_{\kappa+1}$ with $\kappa = 1, 2, \dots, 2\delta_3 - 4$, are given as

$$\mathfrak{p}(a'_\kappa a'_{\kappa+1} | \lambda_e) = (\kappa, 2\delta_3 + 1 - \kappa). \quad (5)$$

Positions $\mathfrak{p}(b'_\kappa b'_{\kappa+1} | \lambda_e)$ with respect to λ_e , for the edges $b'_\kappa b'_{\kappa+1}$ with $\kappa = 1, 2, \dots, 2\delta_1 - 4$, are given as

$$\mathfrak{p}(b'_\kappa b'_{\kappa+1} | \lambda_e) = (2\delta_3 + \kappa + 1, \kappa + 3). \quad (6)$$

Positions $\mathfrak{p}(c'_\kappa c'_{\kappa+1} | \lambda_e)$ with respect to λ_e , for the edges $c'_\kappa c'_{\kappa+1}$ with $\kappa = 1, 2, \dots, 2\delta_2 - 2$, are given as

$$\mathfrak{p}(c'_\kappa c'_{\kappa+1} | \lambda_e) = \begin{cases} (2(\delta_3 - 1), \kappa + 2), & \text{if } \kappa = 1, \\ (2(\delta_3 - 2) + \kappa, \kappa + 2), & \text{if } \kappa = 2, 3, \dots, 2\delta_2 - 1. \end{cases} \quad (7)$$

Positions $\mathfrak{p}(a_\kappa a'_\kappa | \lambda_e)$ with respect to λ_e , for the edges $a_\kappa a'_\kappa$ with $\kappa = 1, 3, \dots, 2\delta_3 - 3$, are given as

$$\mathfrak{p}(a_\kappa a'_\kappa | \lambda_e) = (\kappa - 1, 2\delta_3 - \kappa + 1). \quad (8)$$

Positions $\mathfrak{p}(b_{\kappa+3} b'_\kappa | \lambda_e)$ with respect to λ_e , for the edges $b_{\kappa+3} b'_\kappa$ with $\kappa = 1, 3, \dots, 2\delta_1 - 3$, are given as

$$\mathfrak{p}(b_{\kappa+3} b'_\kappa | \lambda_e) = (2\delta_3 + \kappa + 1, \kappa + 2). \quad (9)$$

Positions $\mathfrak{p}(c_\kappa c'_\kappa | \lambda_e)$ with respect to λ_e , for the edges $c_\kappa c'_\kappa$ with $\kappa = 1, 3, \dots, 2\delta_2 - 3$, are given as

$$\mathfrak{p}(c_\kappa c'_\kappa | \lambda_e) = \begin{cases} (2\delta_3 - 1, \kappa + 1), & \text{if } \kappa = 1, \\ (2(\delta_3 - 2) + \kappa, \kappa + 1), & \text{if } \kappa = 2, 3, \dots, 2\delta_2 - 1. \end{cases} \quad (10)$$

Positions of the joint edges are given as

$$\begin{aligned} \mathfrak{p}(a_{2\delta_3} b_1 | \lambda_e) &= (2\delta_3 - 1, 0), \\ \mathfrak{p}(a_{2\delta_3} c'_1 | \lambda_e) &= (2\delta_3 - 2, 2), \\ \mathfrak{p}(b_2 c_1 | \lambda_e) &= (2\delta_3, 1), \\ \mathfrak{p}(a_{2\delta_3-3} c'_2 | \lambda_e) &= (2\delta_3 - 3, 4), \\ \mathfrak{p}(b'_1 c_2 | \lambda_e) &= (2\delta_3 + 1, 3). \end{aligned} \quad (11)$$

The given positions $\mathfrak{p}(\cdot | \lambda_e)$ of all $5(\delta_1 + \delta_2 + \delta_3) - 11$ -bonds of $T(\delta_1, \delta_2, \delta_3)$ graph of benzenoid tripod with $\delta_1, \delta_2, \delta_3 \geq 2$, with respect to λ_e , are unique and no two bonds have the same position \mathfrak{p} . So we can conclude that we resolve the bonds of $T(\delta_1, \delta_2, \delta_3)$ with two nodes. It is implied that the minimum members in the edge resolving set of $T(\delta_1, \delta_2, \delta_3)$ are two. \square

Remark 1. If $T(\delta_1, \delta_2, \delta_3)$ is a graph of benzenoid tripod with $\delta_1, \delta_2, \delta_3 \geq 2$, then

$$\dim_e(T(\delta_1, \delta_2, \delta_3)) = 2. \quad (12)$$

Proof. From the definition of edge metric dimension, the concept is solemnly based on the selected subset (λ_e) chosen in such a way that the entire edge set has unique position with respect to the selected nodes or subset. In Lemma 1, we already discussed the possibility of selected subset (edge resolving set) and, according to the definition, its minimum possible cardinality. In that lemma, we choose $\lambda_e = \{a_1, b_1\}$ as an edge resolving set for the graph of benzenoid tripod or $T(\delta_1, \delta_2, \delta_3)$ for all the possible combinatorial values of $\delta_1, \delta_2, \delta_3 \geq 2$. We also proved in such lemma that $|\lambda_e| = 2$ is the least possible cardinality of edge resolving set for the

benzenoid tripod $T(\delta_1, \delta_2, \delta_3)$. It is enough for the proof of what we claim in the statement that edge metric dimension of benzenoid tripod is two, which completes the proof. \square

Lemma 2. *If $T(\delta_1, \delta_2, \delta_3)$ is a graph of benzenoid tripod with $\delta_1, \delta_2, \delta_3 \geq 2$, then the minimum members in its fault-tolerant edge resolving set are four.*

Proof. The total number of nodes in the corresponding graph of benzenoid tripod with $\delta_1, \delta_2, \delta_3 \geq 2$, are $4(\delta_1 + \delta_2 + \delta_3) - 8$ and to check the possibilities of fault-tolerant edge resolving set with cardinality four are $C(4(\delta_1 + \delta_2 + \delta_3) - 8, 4) = ((4(\delta_1 + \delta_2 + \delta_3) - 8)! / (2 \times (4(\delta_1 + \delta_2 + \delta_3) - 12)!))$. Here we are checking with cardinality four, and later, we will

also check cardinality three. Now due to the NP-hardness of choosing fault-tolerant edge resolving set, we cannot find the exact number of fault-tolerant edge resolving sets for a graph, but from $((4(\delta_1 + \delta_2 + \delta_3) - 8)! / (2 \times (4(\delta_1 + \delta_2 + \delta_3) - 12)!))$ -possibilities, we choose a subset $\lambda_{e,f}$ and defined as $\lambda_{e,f} = \{a_1, b_1, a_{2\delta_3}, b_{2\delta_3}\}$. Now to prove this claim that $\lambda_{e,f}$ is actually one of the candidates for the fault-tolerant edge resolving set of benzenoid tripod graph or $T(\delta_1, \delta_2, \delta_3)$, we will follow Definition 3. To fulfill the requirements of definition, we will check the unique positions or locations of each node and the methodology is defined above in Definition 3.

Positions $\mathfrak{p}(a_\kappa a_{\kappa+1} | \lambda_{e,f})$ with respect to $\lambda_{e,f}$, for the edges $a_\kappa a_{\kappa+1}$ with $\kappa = 1, 2, \dots, 2\delta_3 - 1$, are given as

$$\mathfrak{p}(a_\kappa a_{\kappa+1} | \lambda_{e,f}) = \begin{cases} (\kappa - 1, 2\delta_3 - \kappa, 2\delta_3 - 1 - \kappa, 2(\delta_3 + \delta_1) - 1 - \kappa), & \text{if } \kappa = 1, 2, \dots, 2\delta_3 - 2, \\ (\kappa - 1, 2\delta_3 - \kappa, 2\delta_3 - 1 - \kappa, 2\delta_3), & \text{if } \kappa = 2\delta_3 - 1. \end{cases} \quad (13)$$

Positions $\mathfrak{p}(b_\kappa b_{\kappa+1} | \lambda_{e,f})$ with respect to $\lambda_{e,f}$, for the edges $b_\kappa b_{\kappa+1}$ with $\kappa = 1, 2, \dots, 2\delta_1 - 1$, are given as

$$\mathfrak{p}(b_\kappa b_{\kappa+1} | \lambda_{e,f}) = (2\delta_3 + \kappa - 1, \kappa - 1, \kappa, 2\delta_1 - 1 - \kappa). \quad (14)$$

Positions $\mathfrak{p}(c_\kappa c_{\kappa+1} | \lambda_{e,f})$ with respect to $\lambda_{e,f}$, for the edges $c_\kappa c_{\kappa+1}$ with $\kappa = 1, 2, \dots, 2\delta_2 - 2$, are given as

$$\mathfrak{p}(c_\kappa c_{\kappa+1} | \lambda_{e,f}) = \begin{cases} (2\delta_3, \kappa + 1, \kappa + 2, 2\delta_1 - 2), & \text{if } \kappa = 1, \\ (2\delta_3, \kappa + 1, \kappa + 2, 2(\delta_1 - 2) + \kappa), & \text{if } \kappa = 2, \\ (2\delta_3 + \kappa - 3, \kappa + 1, \kappa + 2, 2(\delta_1 - 2) + \kappa), & \text{if } \kappa = 3, 4, \dots, 2\delta_2 - 1. \end{cases} \quad (15)$$

Positions $\mathfrak{p}(a'_\kappa a'_{\kappa+1} | \lambda_{e,f})$ with respect to $\lambda_{e,f}$, for the edges $a'_\kappa a'_{\kappa+1}$ with $\kappa = 1, 2, \dots, 2\delta_3 - 4$, are given as

$$\mathfrak{p}(a'_\kappa a'_{\kappa+1} | \lambda_{e,f}) = (\kappa, 2\delta_3 + 1 - \kappa, 2\delta_3 - \kappa, 2(\delta_3 + \delta_1 - 1) - \kappa). \quad (16)$$

Positions $\mathfrak{p}(b'_\kappa b'_{\kappa+1} | \lambda_{e,f})$ with respect to $\lambda_{e,f}$, for the edges $b'_\kappa b'_{\kappa+1}$ with $\kappa = 1, 2, \dots, 2\delta_1 - 4$, are given as

$$\mathfrak{p}(b'_\kappa b'_{\kappa+1} | \lambda_{e,f}) = (2\delta_3 + \kappa + 1, \kappa + 3, \kappa + 4, 2\delta_1 - 3 - \kappa). \quad (17)$$

Positions $\mathfrak{p}(c'_\kappa c'_{\kappa+1} | \lambda_{e,f})$ with respect to $\lambda_{e,f}$, for the edges $c'_\kappa c'_{\kappa+1}$ with $\kappa = 1, 2, \dots, 2\delta_2 - 2$, are given as

$$\mathfrak{p}(c'_\kappa c'_{\kappa+1} | \lambda_{e,f}) = \begin{cases} (2(\delta_3 - 1), \kappa + 2, \kappa + 1, 2\delta_1), & \text{if } \kappa = 1, \\ (2(\delta_3 - 1), \kappa + 2, \kappa + 1, 2\delta_1), & \text{if } \kappa = 2, \\ (2(\delta_3 - 2) + \kappa, \kappa + 2, \kappa + 1, 2\delta_1 - 3 + \kappa), & \text{if } \kappa = 3, 4, \dots, 2\delta_2 - 1. \end{cases} \quad (18)$$

Positions $\mathfrak{p}(a_\kappa a'_\kappa | \lambda_{e,f})$ with respect to $\lambda_{e,f}$, for the edges $a_\kappa a'_\kappa$ with $\kappa = 1, 3, \dots, 2\delta_3 - 3$, are given as:

$$\mathfrak{p}(a_\kappa a'_\kappa | \lambda_{e,f}) = (\kappa - 1, 2\delta_3 - \kappa + 1, 2\delta_3 - \kappa, 2(\delta_3 + \delta_1) - 1 - \kappa). \quad (19)$$

Positions $\mathfrak{p}(b_{\kappa+3} b'_\kappa | \lambda_{e,f})$ with respect to $\lambda_{e,f}$, for the edges $b_{\kappa+3} b'_\kappa$ with $\kappa = 1, 3, \dots, 2\delta_1 - 3$, are given as

$$\mathfrak{p}(b_{\kappa+3} b'_\kappa | \lambda_{e,f}) = (2\delta_3 + \kappa + 1, \kappa + 2, \kappa + 3, 2\delta_1 - 3 - \kappa). \quad (20)$$

Positions $\mathfrak{p}(c_\kappa a'_\kappa | \lambda_{e,f})$ with respect to $\lambda_{e,f}$, for the edges $c_\kappa c'_\kappa$ with $\kappa = 1, 3, \dots, 2ml - 3$, are given as

$$\mathfrak{p}(c_\kappa c'_\kappa | \lambda_{e,f}) = \begin{cases} (2\delta_3 - 1, \kappa + 1, \kappa + 1, 2\delta_1 - 1), & \text{if } \kappa = 1, \\ (2(\delta_3 - 2) + \kappa, \kappa + 1, \kappa + 1, 2(\delta_1 - 2) + \kappa), & \text{if } \kappa = 2, 3, \dots, 2\delta_2 - 1. \end{cases} \quad (21)$$

Positions of the joint edges with respect to $\lambda_{e,f}$ are given as

$$\begin{aligned} \mathfrak{p}(a_{2\delta_3} b_1 | \lambda_{e,f}) &= (2\delta_3 - 1, 0, 0, 2\delta_1 - 1), \\ \mathfrak{p}(a_{2\delta_3} c'_1 | \lambda_{e,f}) &= (2\delta_3 - 2, 2, 1, 2\delta_1), \\ \mathfrak{p}(b_2 c_1 | \lambda_{e,f}) &= (2\delta_3, 1, 2, 2\delta_1 - 2), \\ \mathfrak{p}(a_{2\delta_3-3} c'_2 | \lambda_{e,f}) &= (2\delta_3 - 3, 4, 3, 2\delta_1 + 1), \\ \mathfrak{p}(b'_1 c_2 | \lambda_{e,f}) &= (2\delta_3 + 1, 3, 4, 2\delta_1 - 3). \end{aligned} \quad (22)$$

On the behalf of given fact for the fulfillment of definition of fault-tolerant edge resolving set, we can say that $\lambda_{e,f}$ with cardinality four is possible, but when it comes to optimized value of $|\lambda_{e,f}|$, we still need to investigate about the minimum value of $|\lambda_{e,f}|$. Following are some possible cases to check that whether $|\lambda_{e,f}| = 3$ is possible or not. However, we find the fault-tolerant edge resolving set with the help of algorithm satisfying that $|\lambda_{e,f}| \neq 3$, but for the proving purpose we build some general cases and try to conclude that only $|\lambda_{e,f}| > 3$ is possible.

Case 1: assume that $\lambda_{e,f} \subset \{a_\kappa: \kappa = 1, 2, \dots, 2\delta_3\}$, with a condition according to our requirement of theorem that $|\lambda_{e,f}| = 3$, and removal of any vertex from $\lambda_{e,f}$ to fulfill the definition. The result is implied in the same edge's position and contradicts our assumption with the fact that $p(a_r a_{r+1} | \lambda_{e,f}) = p(a_s a'_s | \lambda_{e,f})$, where $1 \leq r \leq 2\delta_3 - 1$ and $1 \leq s \text{ (odd)} \leq 2\delta_3 - 3$.

Case 2: assume that $\lambda_{e,f} \subset \{b_\kappa: \kappa = 1, 2, \dots, 2\delta_1\}$, with a condition according to our requirement of theorem that $|\lambda_{e,f}| = 3$, and removal of any vertex from $\lambda_{e,f}$ to fulfill the definition. The result is implied in the same edge's position and contradicts our assumption with the fact that $p(a_r a_{r+1} | \lambda_{e,f}) = p(a'_s a_{s+1} | \lambda_{e,f})$, where $1 \leq r \leq 2\delta_3 - 1$ and $1 \leq s \leq 2\delta_3 - 4$.

Case 3: assume that $\lambda_{e,f} \subset \{c_\kappa: \kappa = 1, 2, \dots, 2\delta_2 - 1\}$, with a condition according to our requirement of theorem that $|\lambda_{e,f}| = 3$, and removal of any vertex from $\lambda_{e,f}$ to fulfill the definition. The result is implied in the same edge's position and contradicts our assumption with the fact that $p(b_{r+3} b'_r | \lambda_{e,f}) = p(a_s a_{s+1} | \lambda_{e,f})$, where $1 \leq r \text{ (odd)} \leq 2\delta_1 - 3$ and $1 \leq s \leq 2\delta_3 - 1$.

Case 4: assume that $\lambda_{e,f} \subset \{a_\kappa: \kappa = 1, 2, \dots, 2\delta_3 - 3\}$, with a condition according to our requirement of theorem that $|\lambda_{e,f}| = 3$, and removal of any vertex from $\lambda_{e,f}$ to fulfill the definition. The result is implied in the same edge's position and contradicts our assumption with the fact that $p(a_r a_{r+1} | \lambda_{e,f}) = p(c_s c'_s | \lambda_{e,f})$, where $1 \leq r \leq 2\delta_3 - 1$ and $1 \leq s \text{ (odd)} \leq 2\delta_2 - 1$.

Case 5: assume that $\lambda_{e,f} \subset \{b_\kappa: \kappa = 1, 2, \dots, 2\delta_1 - 3\}$, with a condition according to our requirement of theorem that $|\lambda_{e,f}| = 3$, and removal of any vertex from $\lambda_{e,f}$ to fulfill the definition. The result is implied in the same edge's position and contradicts our assumption with the fact that $p(a_r a_{r+1} | \lambda'_{e,f}) = p(a'_s a'_{s+1} | \lambda'_{e,f})$, where $1 \leq r \leq 2\delta_3 - 1$ and $1 \leq s \leq 2\delta_3 - 4$.

Case 6: assume that $\lambda_{e,f} \subset \{c_\kappa: \kappa = 1, 2, \dots, 2\delta_2 - 1\}$, with a condition according to our requirement of theorem that $|\lambda_{e,f}| = 3$, and removal of any vertex from $\lambda_{e,f}$ to fulfill the definition. The result is implied in the same edge's position and contradicts our assumption with the fact that $p(a_r a_{r+1} | \lambda'_{e,f}) = p(a_s a_{s+1} | \lambda'_{e,f})$, where $1 \leq r, s \leq 2\delta_3 - 1$.

Case 7: assume that $\lambda'_{e,f} \subset \{a_\kappa, b_j: \kappa = 1, 2, \dots, 2\delta_3, j = 1, 2, \dots, 2\delta_1\}$, with a condition according to our requirement of theorem that $|\lambda_{e,f}| = 3$, and removal of any vertex from $\lambda'_{e,f}$ to fulfill the definition. The result is implied in the same edge's position and contradicts our assumption with the fact that $p(b_r b_{r+1} | \lambda'_{e,f}) = p(b'_s b'_{s+1} | \lambda'_{e,f})$, where $1 \leq r \leq 2\delta_1 - 1$ and $1 \leq s \leq 2\delta_1 - 4$.

Case 8: assume that $\lambda_{e,f} \subset \{a_\kappa, c_j: \kappa = 1, 2, \dots, 2\delta_3, j = 1, 2, \dots, 2\delta_2 - 1\}$, with a condition according to our requirement of theorem that $|\lambda_{e,f}| = 3$, and removal of any vertex from $\lambda_{e,f}$ to fulfill the definition. The result is implied in the same edge's position and contradicts our assumption with the fact that $p(b_{r+3} b'_r | \lambda_{e,f}) = p(b'_s b'_{s+1} | \lambda_{e,f})$, where $1 \leq r \text{ (odd)} \leq 2\delta_1 - 3$ and $1 \leq s \leq 2\delta_1 - 4$.

Case 9: assume that $\lambda_{e,f} \subset \{a_\kappa, a'_j: \kappa = 1, 2, \dots, 2\delta_3, j = 1, 2, \dots, 2\delta_3 - 3\}$, with a condition according to our requirement of theorem that $|\lambda_{e,f}| = 3$, and removal of any vertex from $\lambda_{e,f}$ to fulfill the definition. The result is implied in the same edge's position and contradicts our assumption with the fact that $p(b_r b_{r+1} | \lambda_{e,f}) = p(b_{s+3} b'_r | \lambda_{e,f})$, where $1 \leq r \leq 2\delta_1 - 1$ and $1 \leq s \text{ (odd)} \leq 2\delta_1 - 3$.

Case 10: assume that $\lambda_{e,f} \subset \{a_\kappa, b'_j: \kappa = 1, 2, \dots, 2\delta_3, j = 1, 2, \dots, 2\delta_1 - 3\}$, with a condition according to our requirement of theorem that $|\lambda_{e,f}| = 3$, and removal of any vertex from $\lambda_{e,f}$ to fulfill the definition. The result is implied in the same edge's position and contradicts our assumption with the fact that $p(a_r a_{r+1} | \lambda_{e,f}) = p(a_s a'_s | \lambda_{e,f})$, where $1 \leq r \leq 2\delta_3 - 1$ and $1 \leq s \text{ (odd)} \leq 2\delta_3 - 3$.

Case 11: assume that $\lambda_{e,f} \subset \{a_\kappa, c'_j: \kappa = 1, 2, \dots, 2\delta_3, j = 1, 2, \dots, 2\delta_2 - 1\}$, with a condition

according to our requirement of theorem that $|\lambda_{e,f}'| = 3$, and removal of any vertex from $\lambda_{e,f}'$ to fulfill the definition. The result is implied in the same edge's position and contradicts our assumption with the fact that $p(b_r b_{r+1} | \lambda_{e,f}') = p(b'_s b'_{s+1} | \lambda_{e,f}')$, where $1 \leq r \leq 2\delta_1 - 1$ and $1 \leq s \leq 2\delta_1 - 4$.

Case 12: assume that $\lambda_{e,f}' \subset \{b_\kappa, c_j; \kappa = 1, 2, \dots, 2\delta_1, j = 1, 2, \dots, 2\delta_2 - 1\}$, with a condition according to our requirement of theorem that $|\lambda_{e,f}'| = 3$, and removal of any vertex from $\lambda_{e,f}'$ to fulfill the definition. The result is implied in the same edge's position and contradicts our assumption with the fact that $p(a_r a_{r+1} | \lambda_{e,f}') = p(a'_s a'_s | \lambda_{e,f}')$, where $1 \leq r \leq 2\delta_3 - 1$ and $1 \leq s(\text{odd}) \leq 2\delta_3 - 3$.

Case 13: assume that $\lambda_{e,f}' \subset \{b_\kappa, a'_j; \kappa = 1, 2, \dots, 2\delta_1, j = 1, 2, \dots, 2\delta_3 - 3\}$, with a condition according to our requirement of theorem that $|\lambda_{e,f}'| = 3$, and removal of any vertex from $\lambda_{e,f}'$ to fulfill the definition. The result is implied in the same edge's position and contradicts our assumption with the fact that $p(a_r a_{r+1} | \lambda_{e,f}') = p(a'_s a'_s | \lambda_{e,f}')$, where $1 \leq r \leq 2\delta_3 - 1$ and $1 \leq s(\text{odd}) \leq 2\delta_3 - 3$.

Case 14: assume that $\lambda_{e,f}' \subset \{b_\kappa, b'_j; \kappa = 1, 2, \dots, 2\delta_1, j = 1, 2, \dots, 2\delta_3 - 3\}$, with a condition according to our requirement of theorem that $|\lambda_{e,f}'| = 3$, and removal of any vertex from $\lambda_{e,f}'$ to fulfill the definition. The result is implied in the same edge's position and contradicts our assumption with the fact that $p(a_r a_{r+1} | \lambda_{e,f}') = p(a'_s a'_s | \lambda_{e,f}')$, where $1 \leq r \leq 2\delta_3 - 1$ and $1 \leq s(\text{odd}) \leq 2\delta_3 - 3$.

Case 15: assume that $\lambda_{e,f}' \subset \{b_\kappa, c'_j; \kappa = 1, 2, \dots, 2\delta_1, j = 1, 2, \dots, 2\delta_2 - 1\}$, with a condition according to our requirement of theorem that $|\lambda_{e,f}'| = 3$, and removal of any vertex from $\lambda_{e,f}'$ to fulfill the definition. The result is implied in the same edge's position and contradicts our assumption with the fact that $p(a_r a_{r+1} | \lambda_{e,f}') = p(a'_s a'_{s+1} | \lambda_{e,f}')$, where $1 \leq r \leq 2\delta_3 - 1$ and $1 \leq s \leq 2\delta_3 - 4$.

Case 16: assume that $\lambda_{e,f}' \subset \{c_\kappa, a'_j; \kappa = 1, 2, \dots, 2\delta_2 - 1, j = 1, 2, \dots, 2\delta_3 - 3\}$, with a condition according to our requirement of theorem that $|\lambda_{e,f}'| = 3$, and removal of any vertex from $\lambda_{e,f}'$ to fulfill the definition. The result is implied in the same edge's position and contradicts our assumption with the fact that $p(b_r b_{r+1} | \lambda_{e,f}') = p(b'_s b'_{s+1} | \lambda_{e,f}')$, where $1 \leq r \leq 2\delta_1 - 1$ and $1 \leq s \leq 2\delta_1 - 4$.

Case 17: assume that $\lambda_{e,f}' \subset \{c_\kappa, b'_j; \kappa = 1, 2, \dots, 2\delta_2 - 1, j = 1, 2, \dots, 2\delta_1 - 3\}$, with a condition according to our requirement of theorem that $|\lambda_{e,f}'| = 3$, and removal of any vertex from $\lambda_{e,f}'$ to fulfill the definition. The result is implied in the same edge's position and contradicts our assumption with the fact that $p(a_r a_{r+1} | \lambda_{e,f}') = p(a'_s a'_{s+1} | \lambda_{e,f}')$, where $1 \leq r \leq 2\delta_3 - 1$ and $1 \leq s \leq 2\delta_3 - 4$.

Case 18: assume that $\lambda_{e,f}' \subset \{c_\kappa, c'_j; \kappa, j = 1, 2, \dots, 2\delta_2 - 1\}$, with a condition according to our requirement of theorem that $|\lambda_{e,f}'| = 3$,

and removal of any vertex from $\lambda_{e,f}'$ to fulfill the definition. The result is implied in the same edge's position and contradicts our assumption with the fact that $p(b_r b_{r+1} | \lambda_{e,f}') = p(b'_s b'_{s+1} | \lambda_{e,f}')$, where $1 \leq r, s \leq 2\delta_1 - 1$.

Case 19: assume that $\lambda_{e,f}' \subset \{a'_\kappa, b'_j; \kappa = 1, 2, \dots, 2\delta_3 - 3, j = 1, 2, \dots, 2\delta_1 - 3\}$, with a condition according to our requirement of theorem that $|\lambda_{e,f}'| = 3$, and removal of any vertex from $\lambda_{e,f}'$ to fulfill the definition. The result is implied in the same edge's position and contradicts our assumption with the fact that $p(b_r b_{r+1} | \lambda_{e,f}') = p(b'_s b'_{s+1} | \lambda_{e,f}')$, where $1 \leq r \leq 2\delta_1 - 1, 1 \leq s \leq 2\delta_1 - 4$.

Case 20: assume that $\lambda_{e,f}' \subset \{a'_\kappa, c'_j; \kappa = 1, 2, \dots, 2\delta_3 - 3, j = 1, 2, \dots, 2\delta_2 - 1\}$, with a condition according to our requirement of theorem that $|\lambda_{e,f}'| = 3$, and removal of any vertex from $\lambda_{e,f}'$ to fulfill the definition. The result is implied in the same edge's position and contradicts our assumption with the fact that $p(b_r b_{r+1} | \lambda_{e,f}') = p(b'_s b'_{s+1} | \lambda_{e,f}')$, where $1 \leq r \leq 2\delta_1 - 1, 1 \leq s \leq 2\delta_1 - 4$.

Case 21: assume that $\lambda_{e,f}' \subset \{b'_\kappa, c'_j; \kappa = 1, 2, \dots, 2\delta_1 - 3, j = 1, 2, \dots, 2\delta_2 - 1\}$, with a condition according to our requirement of theorem that $|\lambda_{e,f}'| = 3$, and removal of any vertex from $\lambda_{e,f}'$ to fulfill the definition. The result is implied in the same edge's position and contradicts our assumption with the fact that $p(a_r a_{r+1} | \lambda_{e,f}') = p(a'_s a'_{s+1} | \lambda_{e,f}')$, where $1 \leq r, s \leq 2\delta_1$.

The given positions $\mathfrak{p}(\cdot | \lambda_{e,f}')$ of all $5(\delta_1 + \delta_2 + \delta_3) - 11$ -bonds of $T(\delta_1, \delta_2, \delta_3)$ graph of benzenoid tripod with $\delta_1, \delta_2, \delta_3 \geq 2$, with respect to $\lambda_{e,f}'$, having $|\lambda_{e,f}'| = 4$, are unique and no two bonds have the same position \mathfrak{p} . It can also be accessed that eliminating any of arbitrary nodes from $\lambda_{e,f}'$ will not affect the definition of edge resolving set. We also checked that the fault-tolerant edge resolving set $\lambda_{e,f}'$ with $|\lambda_{e,f}'| = 3$ resulted in two edges having the same position \mathfrak{p} . So we can conclude that we resolve the bonds of $T(\delta_1, \delta_2, \delta_3)$ with four nodes. It is implied that the minimum members in the fault-tolerant edge resolving set of $T(\delta_1, \delta_2, \delta_3)$ are four. \square

Remark 2. If $T(\delta_1, \delta_2, \delta_3)$ is a graph of benzenoid tripod with $\delta_1, \delta_2, \delta_3 \geq 2$, then

$$\dim_{e,f}(T(\delta_1, \delta_2, \delta_3)) = 4. \quad (23)$$

Proof. From the definition of fault-tolerant edge metric dimension (same as in parent concept), the concept is solemnly based on the selected subset $(\lambda_{e,f}')$ chosen in such a way that the entire edge set has unique position with respect to the selected nodes or subset. Addition or removal of any arbitrary single member of $\lambda_{e,f}'$ does not affect the resolvability of edges or position of the entire edge set of graph remains unique. In Lemma 2, we already discussed the possibility of selected subset (fault-tolerant edge resolving set) and, according to the definition, its minimum possible

cardinality. In that lemma, we choose $\lambda_{e,f} = \{a_1, b_1, a_{2\delta_3}, b_{2\delta_3}\}$ as a fault-tolerant edge resolving set for the graph of benzenoid tripod or $T(\delta_1, \delta_2, \delta_3)$ for all the possible combinatorial values of $\delta_1, \delta_2, \delta_3 \geq 2$. We also proved in such lemma that $|\lambda_{e,f}| = 4$ is the least possible cardinality of fault-tolerant edge resolving set for the benzenoid tripod $T(\delta_1, \delta_2, \delta_3)$. It is enough for the proof of what we claim in the statement that fault-tolerant edge metric dimension of benzenoid tripod is four, which completes the proof. \square

3. Conclusion

Mathematical chemistry, particularly graphical chemistry, has made it simpler to examine complicated networks and chemical structures in their simplest forms. Similarly, resolvability is a parameter in which the complete node or edge set, and occasionally both, reconfigure themselves into unique outfits in order to call or access them. Edge metric dimension is also a parameter with this property to gain each edge into a unique form. In this work, we consider benzenoid tripod structure to achieve its resolvability and found its minimum edge-resolving set. We concluded that edge metric and fault-tolerant edge metric resolving set are with constant and exact number of members for this structure.

Data Availability

There are no data associated with this manuscript.

Conflicts of Interest

The authors declare that they have no conflicts of interest.

References

- [1] B. Yang, M. Rafiullah, H. M. A. Siddiqui, and S. Ahmad, "On resolvability parameters of some wheel-related graphs," *Journal of Chemistry*, vol. 2019, Article ID 9259032, 9 pages, 2019.
- [2] Y. Zhang and S. Gao, "On the edge metric dimension of convex polytopes and its related graphs," *Journal of Combinatorial Optimization*, vol. 39, no. 2, pp. 334–350, 2020.
- [3] M. Ahsan, Z. Zahid, S. Zafar, A. Rafiq, M. S. Sindhu, and M. Umar, "Computing the edge metric dimension of convex polytopes related graphs," *The Journal of Mathematics and Computer Science*, vol. 22, no. 2, pp. 174–188, 2020.
- [4] Z. Raza and M. S. Bataineh, "The comparative analysis of metric and edge metric dimension of some subdivisions of the wheel graph," *Asian-European Journal of Mathematics*, vol. 14, no. 4, Article ID 2150062, 2020.
- [5] I. G. Yero, "Vertices, edges, distances and metric dimension in graphs," *Electronic Notes in Discrete Mathematics*, vol. 55, pp. 191–194, 2016.
- [6] J. B. Liu, Z. Zahid, R. Nasir, and W. Nazeer, "Edge version of metric dimension and doubly resolving sets of the necklace graph," *Mathematics*, vol. 6, no. 43, 2018.
- [7] M. Azeem and M. F. Nadeem, "Metric-based resolvability of polycyclic aromatic hydrocarbons," *European Physical Journal Plus*, vol. 136, no. 395, 2021.
- [8] M. N. A. T. Iqbal and S. A. H. Bokhary, "The k-size edge metric dimension of graphs," *Journal of Mathematics*, vol. 2020, Article ID 1023175, 7 pages, 2020.
- [9] M. Wei, J. Yue, J. Yue, and X. Zhu, "On the edge metric dimension of graphs," *AIMS Mathematics*, vol. 5, no. 5, pp. 4459–4465, 2020.
- [10] M. Knor, S. Majstorović, A. T. Masa Toshi, R. Škrekovski, and I. G. Yero, "Graphs with the edge metric dimension smaller than the metric dimension," *Applied Mathematics and Computation*, vol. 401, Article ID 126076, 2021.
- [11] V. Filipovic, A. Kartelj, and J. Kratica, "Edge metric dimension of some generalized peterson graphs," *Results in Mathematics*, vol. 74182 pages, 2019.
- [12] M. S. Bataineh, N. Siddiqui, and Z. Raza, "Edge metric dimension of k multiwheel graph," *Rocky Mountain Journal of Mathematics*, vol. 50, no. 4, pp. 1175–1180, 2020.
- [13] P. Slater, "Leaves of trees," proceeding of the 6th southeastern conference on combinatorics, graph theory, and computing," *Congressus Numerantium*, vol. 14, pp. 549–559, 1975.
- [14] F. Harary and R. A. Melter, "On the metric dimension of a graph," *Ars Combinatoria*, vol. 2, pp. 191–195, 1976.
- [15] G. Chartrand, E. Salehi, and P. Zhang, "The partition dimension of a graph," *Aequationes Mathematicae*, vol. 59, no. 1, pp. 45–54, 2000.
- [16] G. Chartrand, L. Eroh, M. A. Johnson, and O. R. Oellermann, "Resolvability in graphs and the metric dimension of a graph," *Discrete Applied Mathematics*, vol. 105, no. 1-3, pp. 99–113, 2000.
- [17] M. Johnson, "Structure-activity maps for visualizing the graph variables arising in drug design," *Journal of Biopharmaceutical Statistics*, vol. 3, no. 2, pp. 203–236, 1993.
- [18] S. Khuller, B. Raghavachari, and A. Rosenfeld, "Landmarks in graphs," *Discrete Applied Mathematics*, vol. 70, no. 3, pp. 217–229, 1996.
- [19] S. Söderberg and H. S. Shapiro, "A combinatory detection problem," *The American Mathematical Monthly*, vol. 70, no. 10, pp. 1066–1070, 1963.
- [20] P. Manuel, R. Bharati, I. Rajasingh, and C. Monica M, "On minimum metric dimension of honeycomb networks," *Journal of Discrete Algorithms*, vol. 6, no. 1, pp. 20–27, 2008.
- [21] A. Sebö and E. Tannier, "On metric generators of graphs," *Mathematics and Operational Research*, vol. 29, pp. 383–393, 2004.
- [22] M. Perc, J. Gómez-Gardeñes, A. Szolnoki, L. M. Floría, and Y. Moreno, "Evolutionary dynamics of group interactions on structured populations: a review," *Journal of The Royal Society Interface*, vol. 10, no. 80, Article ID 20120997, 2013.
- [23] M. Perc and A. Szolnoki, "Coevolutionary games—a mini review," *Biosystems*, vol. 99, no. 2, pp. 109–125, 2010.
- [24] Z. Hussain, M. Munir, M. Choudhary, and S. M. Kang, "Computing metric dimension and metric basis of 2d lattice of alpha-boron nanotubes," *Symmetry*, vol. 10, 2018.
- [25] S. Krishnan and B. Rajan, "Fault-tolerant resolvability of certain crystal structures," *Applied Mathematics*, vol. 7, no. 7, pp. 599–604, 2016.
- [26] H. M. A. Siddiqui and M. Imran, "Computing metric and partition dimension of 2-dimensional lattices of certain nanotubes," *Journal of Computational and Theoretical Nanoscience*, vol. 11, no. 12, pp. 2419–2423, 2014.
- [27] M. Hauptmann, R. Schmied, and C. Viehmann, "Approximation complexity of metric dimension problem," *Journal of Discrete Algorithms*, vol. 14, pp. 214–222, 2012.
- [28] H. R. Lewis, M. Garey, and D. Johnson, "Michael R. Garey and David S. Johnson. Computers and intractability. A guide

- to the theory of NP-completeness. W. H. Freeman and Company, San Francisco 1979, x + 338 pp,” *The Journal of Symbolic Logic*, vol. 48, no. 2, pp. 498–500, 1983.
- [29] M. A. Johnson, “Browsable structure-activity datasets,” *Advances in Molecular Similarity*, pp. 153–170, JAI Press Connecticut, Stamford, CT, USA, 1998.
- [30] A. Kelenc, N. Tratnik, and I. G. Yero, “Uniquely identifying the edges of a graph: the edge metric dimension,” *Discrete Applied Mathematics*, vol. 251, pp. 204–220, 2018.
- [31] M. F. Nadeem, M. Azeem, and A. Khalil, “The locating number of hexagonal möbius ladder network,” *Journal of Applied Mathematics and Computing*, vol. 66, no. 1-2, pp. 149–165, 2020.
- [32] B. Deng, M. F. Nadeem, and M. Azeem, “On the edge metric dimension of different families of möbius networks,” *Mathematical Problems in Engineering*, vol. 20219 pages, Article ID 6623208, 2021.
- [33] A. Ali, W. Nazeer, M. Munir, and S. M. Kang, “M-polynomials and topological indices of zigzag and rhombic benzenoid systems,” *Open Chemistry*, vol. 16, no. 73–78, pp. 122–135, 2018.
- [34] C. P. Chou, Y. Li, and H. A. Witek, “Zhang–zhang polynomials of various classes of benzenoid systems,” *MATCH Communications in Mathematical and Computer Chemistry*, vol. 68, pp. 31–64, 2012.
- [35] M. K. Jamil, M. Imran, and K. A. Sattar, “Novel face index for benzenoid hydrocarbons,” *Mathematics*, vol. 8, no. 312, 2020.
- [36] A. N. A. Koam, A. Ahmad, M. E. Abdelhag, and M. Azeem, “Metric and fault-tolerant metric dimension of hollow coronoid,” *IEEE Access*, vol. 9, pp. 81527–81534, 2021.

Research Article

Some Vertex/Edge-Degree-Based Topological Indices of r -Apex Trees

Akbar Ali ¹, Waqas Iqbal,² Zahid Raza,³ Ekram E. Ali,^{1,4} Jia-Bao Liu ⁵, Farooq Ahmad,^{1,6} and Qasim Ali Chaudhry^{1,7}

¹Department of Mathematics, Faculty of Science, University of Ha'il, Ha'il, Saudi Arabia

²Knowledge Unit of Science, University of Management and Technology, Sialkot, Pakistan

³Department of Mathematics, College of Sciences, University of Sharjah, Sharjah, UAE

⁴Department of Mathematics and Computer Science, Faculty of Science, Port Said University, Port Said 42521, Egypt

⁵School of Mathematics and Physics, Anhui Jianzhu University, Hefei 230601, China

⁶School of Mechanical and Aerospace Engineering, NANYANG technological University, Singapore

⁷Department of Mathematics, University of Engineering and Technology, Lahore 54890, Pakistan

Correspondence should be addressed to Jia-Bao Liu; liujiabaoad@163.com

Received 11 August 2021; Accepted 16 September 2021; Published 21 October 2021

Academic Editor: Muhammad Kamran Siddiqui

Copyright © 2021 Akbar Ali et al. This is an open access article distributed under the Creative Commons Attribution License, which permits unrestricted use, distribution, and reproduction in any medium, provided the original work is properly cited.

In chemical graph theory, graph invariants are usually referred to as topological indices. For a graph G , its vertex-degree-based topological indices of the form $BID(G) = \sum_{uv \in E(G)} \beta(d_u, d_v)$ are known as bond incident degree indices, where $E(G)$ is the edge set of G , d_w denotes degree of an arbitrary vertex w of G , and β is a real-valued-symmetric function. Those BID indices for which β can be rewritten as a function of $d_u + d_v - 2$ (that is degree of the edge uv) are known as edge-degree-based BID indices. A connected graph G is said to be r -apex tree if r is the smallest nonnegative integer for which there is a subset R of $V(G)$ such that $|R| = r$ and $G - R$ is a tree. In this paper, we address the problem of determining graphs attaining the maximum or minimum value of an arbitrary BID index from the class of all r -apex trees of order n , where r and n are fixed integers satisfying the inequalities $n - r \geq 2$ and $r \geq 1$.

1. Introduction

All the graphs discussed in the present paper are finite. The vertex set and edge set of a graph G are denoted by $V(G)$ and $E(G)$, respectively. Denote by $d_u(G)$ (or simply by d_u if there is no confusion about the graph under consideration) the degree of a vertex $u \in V(G)$. Those graph-theoretical notation and terminology that are used in this paper without defining here can be found in some standard graph-theoretical books, such as [1, 2].

For a graph G , its graph invariant I is a numerical quantity calculated from G by using any rule in such a way that the equation $I(G) = I(G')$ holds for every graph G' isomorphic to G . In chemical graph theory, graph invariants are usually referred to as topological indices [3–10]. A topological index of a graph G that depends on the degrees of the vertices of G is known as a vertex-degree-based topological index; similarly, edge-degree-based topological

indices are defined. To the best of the present authors' knowledge, the Platt index [11, 12] is the oldest vertex-degree-based topological index; for a graph G , its Platt index is defined as

$$Pl(G) = \sum_{uv \in E(G)} (d_u + d_v - 2). \quad (1)$$

Since $d_u + d_v - 2$ is degree of the edge uv , the Platt index is also an edge-degree-based topological index.

In the present paper, we are concerned with the following type of vertex-degree-based topological indices:

$$BID(G) = \sum_{uv \in E(G)} \beta(d_u, d_v), \quad (2)$$

which are known as bond incident degree (BID) indices (see, for example, [13]), where β is a real-valued-symmetric function. Those BID indices for which β can be rewritten as a function of $d_u + d_v - 2$ are known as edge-degree-based BID

indices. Note that the Platt index defined in equation (1) is a vertex/edge-degree-based BID index. Other examples of BID indices include the first Zagreb index [14], second Zagreb index [15], general Randić index [16, 17], general zeroth-order Randić index [17, 18], general sum-connectivity index [19], natural logarithm of the multiplicative second Zagreb index [20], variable sum exdeg index [21], sum lordeg index [21], augmented Zagreb index [22], general Platt index [23], and Sombor index [24]. The choices of the function β that correspond to the aforementioned BID indices are specified in Table 1.

In order to solve an extremal problem concerning the topological index R_1 (which is same as the second Zagreb index, see Table 1), Bollobás et al. [25] considered following generalization of the general Randić index of a graph G :

$$\sum_{uv \in E(G)} [(d_u + l)(d_v + l)]^\alpha, \quad (3)$$

by taking α as any real number and l as any nonnegative integer. We note that the graph invariant (3)

- (i) Remains well-defined if l is any real number greater than -1
- (ii) Gives the reduced second Zagreb index [11] when one takes $\alpha = 1$ and $l = -1$
- (iii) Coincides with the variable connectivity index [26–28] if $\alpha = -1/2$ and l is any nonnegative real number

Thus, in what follows, we assume that $(l, \alpha) \in (A \times \mathbb{R}) \cup (B \times \mathbb{R}^+)$ and call the graph invariant (3) as the Bollobás—Erdős—Sarkar index and denote it by $BES_{(l, \alpha)}$, where A is the set of all real numbers greater than -1 , \mathbb{R} is the set of all real numbers, \mathbb{R}^+ is the set of all positive real numbers, and $B = \{-1\}$. Thus, the Bollobás—Erdős—Sarkar index of a graph G is defined as

$$BES_{(l, \alpha)}(G) = \sum_{uv \in E(G)} [(d_u + l)(d_v + l)]^\alpha, \quad (4)$$

with $(l, \alpha) \in (A \times \mathbb{R}) \cup (B \times \mathbb{R}^+)$. Certainly, the Bollobás—Erdős—Sarkar index is a BID index (here, it needs to be mentioned that the graph invariant $BES_{(l, 1)}$ was defined in [29] for any real number l).

A connected graph G is said to be r -apex tree if r is the smallest nonnegative integer for which there is a subset R of $V(G)$ such that $|R| = r$ and $G - R$ is a tree. (Unfortunately, the terminology of apex trees and r -apex trees, being used by many researchers particularly in chemical graph theory, may arise confusion with the terminology of apex graphs and r -apex graphs, respectively. According to Mohar [30], a graph G is an apex graph if it contains a vertex w such that $G - w$ is planar. Also, according to Thilikos and Bodlaender [31], a graph is an r -apex graph if it can be made planar by removing at most r vertices.) The set R is known as r -apex set and its members are known as apex vertices. Every tree is a 0-apex tree. (Throughout this paper, whenever we consider a class of graphs of the same order, we assume that all the graphs of the considered class are pairwise nonisomorphic.) In this paper, we address the problem of determining graphs

attaining the maximum or minimum value of an arbitrary BID index from the class of all r -apex trees of order n , where r and n are fixed integers satisfying the inequalities $n - r \geq 2$ and $r \geq 1$.

2. Main Results

The join $G_1 + G_2$ of two graphs G_1 and G_2 is the graph with the vertex set $V(G_1) \cup V(G_2)$ and the edge set $E(G_1) \cup E(G_2) \cup \{uv : u \in V(G_1), v \in V(G_2)\}$. If $e = uv$ is not an edge in a graph G , then $G + e$ denotes the graph formed by adding the edge e in G . The complete graph and the star graph of order n are denoted by K_n and S_n , respectively. To state and prove the first main result, we need the following known result.

Lemma 1 (see [32]). *Let I be a topological index.*

- (i) *If for every connected noncomplete graph G , the inequality $I(G + e) > I(G)$ holds for every $e \notin E(G)$; then, the graph attaining the maximum value of the topological index I among all r -apex trees of order n is isomorphic to the join $K_r + T$, where r and n are fixed integers satisfying the inequalities $r \geq 1$ and $n - r \geq 2$ and T is a tree of order $n - r$.*
- (ii) *If for every connected noncomplete graph G , the inequality $I(G + e) < I(G)$ holds for every $e \notin E(G)$; then, the graph attaining the minimum value of the topological index I among all r -apex trees of order n is isomorphic to the join $K_r + T$, where r and n are fixed integers satisfying the inequalities $r \geq 1$ and $n - r \geq 2$ and T is a tree of order $n - r$.*

For a graph G and a vertex $u \in V(G)$, denote by $N_G(u)$ the set of all those vertices of G that are adjacent to u . Now, we state and prove our first main result.

Theorem 1. *Let \mathbb{R} be the set of all real numbers. Let $\beta: \mathbb{R} \times \mathbb{R} \rightarrow \mathbb{R}$ be a real-valued-symmetric function such that*

- (i) *The inequality $\beta(x + s, y - s) - \beta(x, y) \geq 0$ holds for $x \geq y > s \geq 1$ and $y \geq 3$*
- (ii) *Both β and β_x are increasing in x , where β_x denotes the partial derivative of β with respect to x*
- (iii) *The function β satisfies at least one the following additional conditions: β is strictly increasing; $\beta(x + s, y - s) - \beta(x, y) > 0$*

If $BID(G) = \sum_{uv \in E(G)} \beta(d_u, d_v)$ is a bond incident degree index such that, for every connected noncomplete graph H , the inequality $BID(H + e) > BID(H)$ holds for every $e \notin E(H)$; then, $K_r + S_{n-r}$ uniquely attains the maximum BID index among all r -apex trees of order n , where r and n are fixed integers satisfying the inequalities $r \geq 1$ and $n - r \geq 2$.

Proof. Let G^* be a graph attaining the maximum BID index in the given class of graphs. From Lemma 1, it follows that G^* is the join of the complete graph K_r and a tree T of order $n - r$. It remains to prove that $T \cong S_{n-r}$. Suppose to the

TABLE 1: Some of the existing bond incident degree indices.

Function $\beta(d_u, d_v)$	Equation (2) gives	Notation
$d_u + d_v$	First Zagreb index [14]	M_1
$d_u d_v$	Second Zagreb index [15]	M_2
$(d_u d_v)^\alpha$	General Randić index [16,17]	R_α
$(d_u)^{\alpha-1} + (d_v)^{\alpha-1}$	General zeroth-order Randić index [17,18]	${}^0R_\alpha$
$(d_u + d_v)^\alpha$	General sum-connectivity index [19]	χ_α
$\ln(d_u d_v)$	Natural logarithm of the multiplicative second Zagreb index [20]	$\ln(\Pi_2)$
$a^{d_u} + a^{d_v}$	Variable sum exdeg index [21]	SEI_a
$\sqrt{\ln d_u} + \sqrt{\ln d_v}$	Sum lordeg index [21]	SL
$(d_u d_v / (d_u + d_v - 2))^3$	Augmented Zagreb index [22]	AZI
$(d_u + d_v - 2)^\alpha$	General Platt index [23]	Pl_α
$\sqrt{d_u^2 + d_v^2}$	Sombor index [24]	SO

contrary that $T \neq S_{n-r}$. Let $v \in V(T)$ be a vertex of maximum degree in T . Then, there exist vertices u and $u_1 \in V(T)$ such that vu_1 is a path in T . Take $N_T(u) = \{v, u_1, u_2, \dots, u_t\}$. Let G' be the graph deduced from G^* by deleting the edges u_1u, u_2u, \dots, u_tu and adding the edges u_1v, u_2v, \dots, u_tv . Observe that the graph G' remains an r -apex tree of order n . In the remaining proof, by the vertex degree d_s , we mean degree of the vertex s in the graph G^* . Now, by using the definition of the BID index and the constraints on the function β , we get

$$\begin{aligned}
 \text{BID}(G') - \text{BID}(G^*) &= \sum_{w \in N_T(v), w \neq u} (\beta(d_v + t, d_w) - \beta(d_v, d_w)) \\
 &+ \sum_{z \in V(K_r)} (\beta(d_v + t, d_z) - \beta(d_v, d_z)) \\
 &+ \sum_{z \in V(K_r)} (\beta(d_u - t, d_z) - \beta(d_u, d_z)) \\
 &+ \sum_{i=1}^t (\beta(d_v + t, d_{u_i}) - \beta(d_u, d_{u_i})) \\
 &+ \beta(d_v + t, d_u - t) - \beta(d_v, d_u) \\
 &> r(\beta(d_v + s, n - 1) - \beta(d_v, n - 1)) \\
 &+ r(\beta(d_u - s, n - 1) - \beta(d_u, n - 1)).
 \end{aligned}
 \tag{5}$$

Since β_x is increasing, the right hand side of (5) is nonnegative, which contradicts our assumption that G^* attains the maximum BID index among all r -apex trees of order n .

Since every function $\beta(x, y) \in \{(x + y)^\alpha, (x + y - 2)^\alpha, \sqrt{x^2 + y^2}, a^x + a^y\}$ satisfies all the conditions of Theorem 1, with $\alpha \geq 1$ and $a > 1$, the next result is an immediate consequence of Theorem 1. \square

Corollary 1. *Among all r -apex trees of order n , the join $K_r + S_{n-r}$ uniquely attains the maximum values of the Sombor index, general sum-connectivity index χ_α , general Platt index Pl_α , and variable sum exdeg index SEI_a , where $\alpha \geq 1$, $a > 1$, and r and n are fixed integers satisfying the inequalities $r \geq 1$ and $n - r \geq 2$.*

The extremal result concerning the general sum-connectivity index χ_α mentioned in Corollary 1 was proven by using some other way: in [33], for $\alpha = 1$ and $r = 1$; in [34, 35], for $\alpha = 1$ and $r \geq 1$; in [36], for $\alpha > 1$ and $r \geq 1$. Also, the result

concerning SEI_a mentioned in Corollary 1 was proven in [37] for $r = 1$ by other means. Moreover, the result concerning the topological index Pl_2 mentioned in Corollary 2 was proven by using some other way in [38] for $r \geq 1$.

Since the proof of the next result is fully analogous to that of Theorem 1, we omit it.

Theorem 2. *Let \mathbb{R} be the set of all real numbers. Let $\beta: \mathbb{R} \times \mathbb{R} \rightarrow \mathbb{R}$ be a real-valued-symmetric function such that*

- (i) *The inequality $\beta(x + s, y - s) - \beta(x, y) \leq 0$ holds for $x \geq y > s \geq 1$ and $y \geq 3$*
- (ii) *Both β and β_x are decreasing in x , where β_x denotes the partial derivative of β with respect to x*
- (iii) *The function β satisfies at least one the following additional conditions: β is strictly decreasing; $\beta(x + s, y - s) - \beta(x, y) \leq 0$*

If $\text{BID}(G) = \sum_{uv \in E(G)} \beta(d_u, d_v)$ is a bond incident degree index such that, for every connected noncomplete graph H , the inequality $\text{BID}(H + e) < \text{BID}(H)$ holds for every $e \notin E(H)$; then, $K_r + S_{n-r}$ uniquely attains the minimum BID index among all r -apex trees of order n , where r and n are fixed integers satisfying the inequalities $r \geq 1$ and $n - r \geq 2$.

Theorems 1 and 2 can be improved if one considers the BID indices of the following form:

$$\text{BID}_i(G) = \sum_{uv \in E(G)} \left[\frac{\beta_i(d_u)}{d_u} + \frac{\beta_i(d_v)}{d_v} \right] = \sum_{u \in V(G)} \beta_i(d_u), \tag{6}$$

where $i \in \{1, 2\}$, β_1' is a strictly increasing function, and β_2' is a strictly decreasing function (where β_i' denotes the derivative of β_i).

Theorem 3. *Let \mathbb{R} be the set of all real numbers. For $i = 1$ and 2, let $\beta_i: \mathbb{R} \rightarrow \mathbb{R}$ be a real-valued symmetric function. Also, let β_1' be strictly increasing and β_2' be strictly decreasing, where β_i' denotes the derivative of β_i . Let $\text{BID}_i(G) = \sum_{uv \in E(G)} [\beta_i(d_u)/d_u + \beta_i(d_v)/d_v] = \sum_{v \in V(G)} \beta_i(d_v)$ such that, for every connected noncomplete graph H , the inequality*

- (i) *$\text{BID}_1(H + e) > \text{BID}_1(H)$ holds for every $e \notin E(H)$; then, $K_r + S_{n-r}$ uniquely attains the maximum value*

of the BID_1 index among all r -apex trees of order n , where r and n are fixed integers satisfying the inequalities $r \geq 1$ and $n - r \geq 2$

- (ii) $BID_2(H + e) < BID_2(H)$ holds for every $e \notin E(H)$; then, $K_r + S_{n-r}$ uniquely attains the minimum value of the BID_2 index among all r -apex trees of order n , where r and n are fixed integers satisfying the inequalities $r \geq 1$ and $n - r \geq 2$

Proof. We prove part (i) of the theorem. Part (ii) can be proved in a fully analogous way. Let G^* be a graph attaining the maximum value of the BID_1 index in the given class of r -apex trees. From Lemma 1, it follows that G^* is the join of the complete graph K_r and a tree T of order $n - r$. It remains to prove that $T \cong S_{n-r}$. Suppose to the contrary that $T \not\cong S_{n-r}$. Let $v \in V(T)$ be a vertex of maximum degree in T . Then, there exist vertices u and $u_1 \in V(T)$ such that vuu_1 is a path in T . Take $N_T(u) = \{v, u_1, u_2, \dots, u_t\}$. Let G' be the graph deduced from G^* by deleting the edges u_1u, u_2u, \dots, u_tu and adding the edges u_1v, u_2v, \dots, u_tv . Observe that the graph G' remains an r -apex tree. In the remaining proof, by the vertex degree d_s , we mean degree of the vertex s in the graph G^* . Here, we have

$$\begin{aligned} BID_1(G^*) - BID_1(G') &= \beta_1(d_v) - \beta_1(d_v + t) + \beta_1(d_u) \\ &\quad \&9; \quad -\beta_1(d_u - t). \end{aligned} \quad (7)$$

By Lagrange's mean value theorem, there exist real numbers a_1 and a_2 such that

$$\begin{aligned} a_1 &\in (d_u - t, d_u), \\ a_2 &\in (d_v, d_v + t), \end{aligned} \quad (8)$$

and

$$BID_1(G^*) - BID_1(G') = t[\beta'_1(a_1) - \beta'_1(a_2)]. \quad (9)$$

The inequality $d_u \leq d_v$ gives $a_1 < a_2$, which implies that the right hand side of equation (9) is negative, because β'_1 is strictly increasing. Thus, we have $BID_1(G^*) - BID_1(G') < 0$, which contradicts our assumption that G^* attains the maximum value of the BID_1 index among all r -apex trees of order n .

The next result follows directly from the first part of Theorem 3. \square

Corollary 2. Among all r -apex trees of order n , the join $K_r + S_{n-r}$ uniquely attains the maximum values of the general zeroth-order Randić index ${}^0R_\alpha$ for $\alpha > 1$, multiplicative second Zagreb index Π_2 , and sum lordeg index, where r and n are fixed integers satisfying the inequalities $r \geq 1$ and $n - r \geq 2$.

Proof. It is clear that any graph G has the maximum Π_2 value in a given graph class if and only if G has the maximum $\ln \Pi_2$ value in the considered graph class. Define the functions $\phi_1(x) = x^\alpha$ with $x \geq 1$ and $\alpha > 1$, $\phi_2(x) = x \ln x$ with $x \geq 1$, and $\phi_3(x) = x\sqrt{\ln x}$ with $x \geq 2$ (see [39]). Observe that, for every $i \in \{1, 2, 3\}$, the derivative function ϕ'_i of ϕ_i is

strictly increasing. Hence, the desired result now follows from Theorem 3. \square

Remark 1. The result concerning the general zeroth-order Randić index mentioned in Corollary 3 was proven by using some other way: in [40] for $\alpha > 1$ and $r = 1$; in [41] for $\alpha = 3$ and $r \geq 1$; in [42] for $\alpha > 1$ and $r \geq 1$.

For proving our next result, we need the following known result.

Lemma 2 (see [32]). Let I be a topological index.

- (i) If for every connected noncomplete graph, the inequality $I(G + e) > I(G)$ holds for every $e \notin E(G)$; then, the graph attaining the minimum value of the topological index I among all 1-apex trees of a fixed order is a unicyclic graph, and its unique cycle has a vertex of degree 2.
- (ii) If for every connected noncomplete graph, the inequality $I(G + e) < I(G)$ holds for every $e \notin E(G)$; then, the graph attaining the maximum value of the topological index I among all 1-apex trees of a fixed order is a unicyclic graph, and its unique cycle has a vertex of degree 2.

Note that, for the general zeroth-order Randić index ${}^0R_\alpha$, it holds that, for every connected noncomplete graph G , one has

$${}^0R_\alpha(G + e) \begin{cases} > {}^0R_\alpha(G), & \text{if } \alpha > 0, \\ < {}^0R_\alpha(G), & \text{if } \alpha < 0, \end{cases} \quad (10)$$

for every $e \notin E(G)$. Also, note that the class of all (connected) unicyclic graphs forms a subclass of the class of all 1-apex trees. Moreover, in [43], it was proven that among all unicyclic graphs of a fixed order $n \geq 4$, the graph S_n^+ formed by adding an edge in the star S_n attains the maximum general zeroth-order Randić index ${}^0R_\alpha$ for $\alpha < 0$, S_n^+ attains the minimum general zeroth-order Randić index ${}^0R_\alpha$ for $0 < \alpha < 1$, and the cycle graph C_n attains the minimum general zeroth-order Randić index ${}^0R_\alpha$ for $\alpha > 1$. Thus, keeping in mind these observations and Lemma 5, one gets the next result.

Corollary 3. Among all 1-apex trees of a fixed order $n \geq 4$, the graph S_n^+ formed by adding an edge in the star S_n attains the maximum general zeroth-order Randić index ${}^0R_\alpha$ for $\alpha < 0$, S_n^+ attains the minimum general zeroth-order Randić index ${}^0R_\alpha$ for $0 < \alpha < 1$, and the cycle graph C_n attains the minimum general zeroth-order Randić index ${}^0R_\alpha$ for $\alpha > 1$.

We remark here that Corollary 3 was proven in [40] by using some other way.

Next, we derive a result about the augmented Zagreb index of 1-apex trees. For this, we need the following lemma first.

Lemma 3 (see [44]). For every fixed integer $n \geq 4$, the graph formed by adding an edge in the star S_n uniquely attains the minimum AZI in the class of all unicyclic graphs with n vertices, and the minimum value is

$$\frac{(n-3)(n-1)^3}{(n-2)^3} + 24. \tag{11}$$

Since for every connected noncomplete graph G , it holds that $AZI(G+e) > AZI(G)$ for every $e \in E(G)$ (see [44]), and the next result follows from Lemmas 5 and 7.

Theorem 4. For every fixed integer $n \geq 6$, the graph formed by adding an edge in the star S_n uniquely attains the minimum AZI in the class of all 1-apex trees of order n , and the minimum value is

$$\frac{(n-3)(n-1)^3}{(n-2)^3} + 24. \tag{12}$$

Theorem 4 was proven in [45] by using some other way.

Finally, we determine the unique graph attaining the maximum value of $BES_{(l,1)}$. For this, we need the following two results concerning the Zagreb indices of r -apex trees.

Lemma 4 (see [34, 35]). If G is an r -apex tree of order n , then it holds that

$$M_1(G) \leq (r+1) [(n-1)^2 + (n-r-1)(r+1)], \tag{13}$$

with equality if and only if $G \cong S_{n-r} + K_r$, where $n-r \geq 2$ and $r \geq 1$.

Lemma 5 (see [34, 35]). If G is an r -apex tree of order n , then it holds that

$$M_2(G) \leq \frac{(r+1)(n-1)(3nr+2n-2r^2-5r-2)}{2}, \tag{14}$$

with equality if and only if $G \cong S_{n-r} + K_r$, where $n-r \geq 2$ and $r \geq 1$.

From the following identity,

$$BES_{(l,1)} = M_2(G) + l \cdot M_1(G) + l^2, \tag{15}$$

Lemmas 4 and 5, the next result follows.

Theorem 5. In the class of all r -apex trees of order n , the join $S_{n-r} + K_r$ uniquely attains the maximum $BES_{(l,1)}$ -value, where n and r are fixed integers satisfying the inequalities $n-r \geq 2$ and $r \geq 1$ and l is any nonnegative real number. In other words, if G is an r -apex tree of order n , then it holds that

$$BES_{(l,1)}(G) \leq (r+1) \cdot \left(\frac{r(n-1+l)}{2} + (r+1+l)(n-1+l)(n-r-1) \right), \tag{16}$$

with equality if and only if $G \cong S_{n-r} + K_r$.

Theorem 5 remains true if one replace the condition “ l is any nonnegative real number” with “ l is any real number greater than or equal to -1 .” To prove this modified statement of Theorem 5, we cannot use identity (15) because of the negative values of l . In what follows, we prove the aforementioned statement (Theorem 6) by using some other way. For this, we need some additional lemmas first.

Lemma 6. Let u_1 and u_2 be two nonadjacent vertices of a graph G . The inequality $BES_{(l,1)}(G+u_1u_2) > BES_{(l,1)}(G)$ holds for every real number l greater than -1 . Also, it holds that

$$BES_{(-1,1)}(G+u_1u_2) \begin{cases} = BES_{(-1,1)}(G), & \text{if one of } u_1 \text{ and } u_2 \text{ is isolated and the other has} \\ & \text{either no neighbor or pendent neighbors only,} \\ > BES_{(-1,1)}(G), & \text{otherwise.} \end{cases} \tag{17}$$

Proof. The result immediately follows from the definition of $BES_{(l,1)}$. \square

Lemma 7 (see [46, 47]). If T is a tree of order $n \geq 4$, then it holds that

$$M_1(T) \leq n(n-1), \tag{18}$$

with equality if and only if $T \cong S_n$.

Lemma 8 (see [48]). If T is a tree of order $n \geq 4$, then it holds that

$$M_2(T) \leq (n-1)^2, \tag{19}$$

with equality if and only if $T \cong S_n$.

Now, we are able to state and prove our final result.

Theorem 6. In the class of all r -apex trees of order n , the join $S_{n-r} + K_r$ uniquely attains the maximum $BES_{(l,1)}$ -value, where n and r are fixed integers satisfying the inequalities $n-r \geq 2$ and $r \geq 1$ and l is any real number greater than or equal to -1 . In other words, if G is an r -apex tree of order n , then it holds that

$$BES_{(l,1)}(G) \leq (r+1)(n-1+l) \cdot \left(\frac{r(n-1+l)}{2} + (r+1+l)(n-r-1) \right), \tag{20}$$

with equality if and only if $G \cong S_{n-r} + K_r$.

Proof. Suppose that G^* is a graph attaining the maximum $BES_{(l,1)}$ -value in the given class of graphs. From Lemmas 1 and 6, it follows that the graph G^* is isomorphic to the join $K_r + T$, where T is a tree of order $n - r$. Let $u \in V(G^*)$ be a vertex of degree $n - 1$. Note that the size of the graph $K_r + T$ is

$$\frac{r(r-1)}{2} + r(n-r) + n-r-1 = \frac{r(2n-r-3)}{2} + n-1. \quad (21)$$

Thus, the size of $G^* - u$ is

$$\frac{r(2n-r-3)}{2}. \quad (22)$$

Also, one has

$$\begin{aligned} BES_{(l,1)}(G^*) &= (d_u(G^*) + l) \sum_{x \in V(G^*-u)} (d_x(G^*) + l) + \sum_{yz \in E(G^*-u)} (d_y(G^*) + l)(d_z(G^*) + l) \\ &= (n+l-1) \sum_{x \in V(G^*-u)} (d_x(G^*-u) + l + 1) \\ &\quad + \sum_{yz \in E(G^*-u)} (d_y(G^*-u) + l + 1)(d_z(G^*-u) + l + 1) \\ &= (n+l-1)[r(2n-r-3) + (n-1)(l+1)] \\ &\quad + M_2(G^*-u) + (l+1) \cdot M_1(G^*-u) + \frac{r(2n-r-3)(l+1)^2}{2}. \end{aligned} \quad (23)$$

We note that the vertex u is an apex vertex and the graph $G^* - u$ is an $(r-1)$ -apex tree of order $n-1$. If $r=1$, then one gets the desired result by using Lemmas 7 and 8 in equation (23). If $r \geq 2$, then one gets the desired result by using Lemmas 4 and 5 in equation (23).

The next result about the reduced second Zagreb index RM_2 is a special but notable case of Theorem 6. \square

Corollary 4. *If G is an r -apex tree of order n , then it holds that*

$$RM_2(G) \leq (r+1)(n-2) \left(\frac{r(n-2)}{2} + r(n-r-1) \right), \quad (24)$$

with equality if and only if $G \cong S_{n-r} + K_r$, where $n-r \geq 2$ and $r \geq 1$.

Data Availability

The data used to support the findings of the study are available from the corresponding author upon request.

Conflicts of Interest

The authors declare that they have no conflicts of interest.

Acknowledgments

This research was funded by Scientific Research Deanship at University of Ha'il, Saudi Arabia, through project no. RG-20 050.

References

- [1] J. A. Bondy and U. S. R. Murty, *Graph Theory*, Springer, London, UK, 2008.
- [2] G. Chartrand, L. Lesniak, and P. Zhang, *Graphs & Digraphs*, CRC Press, Boca Raton, FL, USA, 2016.
- [3] S. Akram, M. Javaid, and M. Jamal, "Bounds on F -index of tricyclic graphs with fixed pendant vertices," *Open Mathematics*, vol. 18, pp. 150–161, 2020.
- [4] M. Azari, "Generalized Zagreb index of product graphs," *Transactions on Combinatorics*, vol. 8, no. 4, pp. 35–48, 2019.
- [5] M. Azari and F. Falahati-Nezhad, "Some results on forgotten topological coindex," *Iranian Journal of Mathematical Chemistry*, vol. 10, no. 4, pp. 307–318.
- [6] N. Dehgardi and J. B. Liu, "Lanzhou index of trees with fixed maximum degree," *MATCH Communications in Mathematical and in Computer Chemistry*, vol. 86, pp. 3–10, 2021.
- [7] M. Javaid, S. Javed, S. Q. Memon, and A. M. Alanazi, "Forgotten index of generalized operations on graphs," *Journal of Chemistry*, vol. 2021, Article ID 9971277, 2021.
- [8] J. B. Liu, M. Arockiaraj, M. Arulperumjothi, and S. Prabhu, "Distance based and bond additive topological indices of certain repurposed antiviral drug compounds tested for treating COVID-19," *International Journal of Quantum Chemistry*, vol. 121, no. 10, Article ID e26617, 2021.
- [9] J. B. Liu, M. M. Matejić, E. I. Milovanović, and I. Ž. Milovanović, "Some new inequalities for the forgotten topological index and coindex of graphs," *MATCH Communications in Mathematical and in Computer Chemistry*, vol. 84, pp. 719–738, 2020.
- [10] J. B. Liu and R. M. Singaraj, "Topological analysis of para line graph of Remdesivir used in the prevention of corona virus,"

- International Journal of Quantum Chemistry*, vol. 121, no. 22, Article ID e26778, 2021.
- [11] I. Gutman, B. Furtula, and C. Elphick, "Three new/old vertex-degree-based topological indices," *MATCH Communications in Mathematical and in Computer Chemistry*, vol. 72, no. 3, pp. 617–632, 2014.
- [12] J. R. Platt, "Prediction of isomeric differences in paraffin properties," *Journal of Physical Chemistry A*, vol. 56, pp. 328–336, 1952.
- [13] A. Ali and D. Dimitrov, "On the extremal graphs with respect to bond incident degree indices," *Discrete Applied Mathematics*, vol. 238, pp. 32–40, 2018.
- [14] I. Gutman and N. Trinajstić, "Graph theory and molecular orbitals. Total π -electron energy of alternant hydrocarbons," *Chemical Physics Letters*, vol. 17, pp. 535–538, 1972.
- [15] I. Gutman, B. Rušćić, N. Trinajstić, and C. F. Wilcox, "Graph theory and molecular orbitals. XII. Acyclic polyenes," *The Journal of Chemical Physics*, vol. 62, no. 9, pp. 3399–3405, 1975.
- [16] B. Bollobás and P. Erdős, "Graphs of extremal weights," *Ars Combinatoria*, vol. 50, pp. 225–233, 1998.
- [17] X. Li and Y. Shi, "A survey on the Randić index," *MATCH Communications in Mathematical and in Computer Chemistry*, vol. 59, no. 1, pp. 127–156, 2008.
- [18] X. Li and J. Zheng, "A unified approach to the extremal trees for different indices," *MATCH Communications in Mathematical and in Computer Chemistry*, vol. 54, pp. 195–208, 2005.
- [19] B. Zhou and N. Trinajstić, "On general sum-connectivity index," *Journal of Mathematical Chemistry*, vol. 47, pp. 210–218, 2010.
- [20] I. Gutman, "Multiplicative Zagreb indices of trees," *Bulletin of International Mathematical Virtual Institute*, vol. 1, pp. 13–19, 2011.
- [21] B. Vukičević, "Bond additive modeling 4. QSPR and QSAR studies of the variable Adriatic indices," *Croatica Chemica Acta*, vol. 84, no. 1, pp. 87–91, 2011.
- [22] B. Furtula, A. Graovac, and D. Vukičević, "Augmented Zagreb index," *Journal of Mathematical Chemistry*, vol. 48, pp. 370–380, 2010.
- [23] A. Ali, D. Dimitrov, Z. Du, and F. Ishfaq, "On the extremal graphs for general sum-connectivity index (χ_α) with given cyclomatic number when $\alpha > 1$," *Discrete Applied Mathematics*, vol. 257, pp. 19–30, 2019.
- [24] I. Gutman, "Geometric approach to degree-based topological indices: Sombor indices," *MATCH Communications in Mathematical and in Computer Chemistry*, vol. 86, pp. 11–16, 2021.
- [25] B. Bollobás, P. Erdős, and A. Sarkar, "Extremal graphs for weights," *Discrete Mathematics*, vol. 200, no. 1-3, pp. 5–19, 1999.
- [26] M. Randić, "Novel graph theoretical approach to heteroatoms in quantitative structure-activity relationships," *Chemo-metrics and Intelligent Laboratory Systems*, vol. 10, no. 1-2, pp. 213–227, 1991.
- [27] M. Randić, "On computation of optimal parameters for multivariate analysis of structure-property relationship," *Journal of Computational Chemistry*, vol. 12, no. 8, pp. 970–980, 1992.
- [28] S. Yousaf, A. A. Bhatti, and A. Ali, "Minimum variable connectivity index of trees of a fixed order," *Discrete Dynamics in Nature and Society*, vol. 2020, Article ID 3976274, 2020.
- [29] B. Horoldagva, L. Buyantogtokh, K. C. Das, and S. G. Lee, "On general reduced second Zagreb index of graphs," *Hacettepe Journal of Mathematics and Statistics*, vol. 48, no. 4, pp. 1046–1056, 2019.
- [30] B. Mohar, "Face covers and the genus problem for apex graphs," *Journal of Combinatorial Theory—Series B*, vol. 82, no. 1, pp. 102–117, 2001.
- [31] D. M. Thilikos and H. L. Bodlaender, "Fast partitioning l -apex graphs with applications to approximating maximum induced-subgraph problems," *Information Processing Letters*, vol. 61, no. 5, pp. 227–232, 1997.
- [32] M. Knor, M. Imran, M. K. Jamil, and R. Skrekovski, "Remarks on distance based topological indices for l -apex trees," *Symmetry*, vol. 12, no. 5, p. 802, 2020.
- [33] S. N. Qiao, "On the Zagreb index of quasi-tree graphs," *Applied Mathematics E-Notes*, vol. 10, pp. 147–150, 2010.
- [34] N. Akhter, M. K. Jamil, and I. Tomescu, "Extremal first and second Zagreb indices of apex trees," *UPB Scientific Bulletin, Series A: Applied Mathematics and Physics*, vol. 78, no. 4, pp. 221–230, 2016.
- [35] T. Selenge and B. Horoldagva, "Maximum Zagreb indices in the class of k -apex trees," *Korean Journal of Mathematics*, vol. 23, no. 3, pp. 401–408, 2015.
- [36] M. K. Jamil, I. Tomescu, and M. Imran, "Extremal k -generalized quasi trees for general sum-connectivity index," *UPB Scientific Bulletin, Series A: Applied Mathematics and Physics*, vol. 82, pp. 101–106, 2020.
- [37] X. Sun and J. Du, "On variable sum exdeg indices of quasi-tree graphs and unicyclic graphs," *Discrete Dynamics in Nature and Society*, vol. 2020, Article ID 1317295, 2020.
- [38] N. Akhter, S. Naz, and M. K. Jamil, "Extremal first reformulated Zagreb index of k -apex trees," *International Journal of Applied Graph Theory*, vol. 2, pp. 29–41, 2018.
- [39] I. Tomescu, "Properties of connected (n, m) -graphs extremal relatively to vertex degree function index for convex functions," *MATCH Communications in Mathematical and in Computer Chemistry*, vol. 85, pp. 285–294, 2021.
- [40] S. Qiao, "On zeroth order general Randić index of quasi tree graphs containing cycles," *Discrete Optimization*, vol. 7, no. 3, pp. 93–98, 2010.
- [41] N. De, "Extremal F -index of apex tree," *Advances in Mathematics: Scientific Journal*, vol. 9, no. 9, pp. 7637–7642, 2020.
- [42] M. K. Jamil and I. Tomescu, "Zeroth-order general Randić index of k -generalized quasi trees," arXiv:1801.03885, 2018.
- [43] S. Zhang and H. Zhang, "Unicyclic graphs with the first three smallest and largest first general Zagreb index," *MATCH Communications in Mathematical and in Computer Chemistry*, vol. 55, no. 2, pp. 427–438, 2006.
- [44] Y. Huang, B. Liu, and L. Gan, "Augmented Zagreb index of connected graphs," *MATCH Communications in Mathematical and in Computer Chemistry*, vol. 67, no. 2, pp. 483–494, 2012.
- [45] K. Cheng, M. Liu, and F. Belardo, "The minimal augmented Zagreb index of k -apex trees for $k \in \{1, 2, 3\}$," *Applied Mathematics and Computation*, vol. 402, Article ID 126139, 2021.
- [46] D. De Caen, "An upper bound on the sum of squares of degrees in a graph," *Discrete Mathematics*, vol. 185, no. 1-3, pp. 245–248, 1998.

- [47] K. C. Das, "Sharp bounds for the sum of the squares of the degrees of a graph," *Kragujevac Journal of Mathematics*, vol. 25, pp. 31–49, 2003.
- [48] K. C. Das, K. Das, and I. Gutman, "Some properties of second Zagreb index," *MATCH Communications in Mathematical and in Computer Chemistry*, vol. 52, no. 1, pp. 103–112, 2004.

Research Article

Connectivity of Semicartesian Products

Metrose Metsidik¹ and Helin Gong²

¹College of Mathematical Sciences, Xinjiang Normal University, Urumqi 830054, China

²Department of Mathematics, Shaoxing University, Shaoxing 312000, China

Correspondence should be addressed to Metrose Metsidik; metrose@163.com

Received 11 July 2021; Revised 10 September 2021; Accepted 24 September 2021; Published 20 October 2021

Academic Editor: R. Vadivel

Copyright © 2021 Metrose Metsidik and Helin Gong. This is an open access article distributed under the Creative Commons Attribution License, which permits unrestricted use, distribution, and reproduction in any medium, provided the original work is properly cited.

Semicartesian product is defined on the basis of two special bipartite graphs and labeling of their vertices, and it has a pleasing property that it is composed of hexagonal structures. In this study, we give two formulae to calculate separately the connectivity and edge connectivity of a semicartesian product graph.

1. Introduction

The notion of the graph products is a central topic in the graph theory since many structural models such as physical networks, electrical circuits, roadways, and organic molecules can be viewed as the graph products of two or more graphs. Many properties of such structural models can be obtained by considering the properties of the factors of their corresponding product graphs. This not only facilitates certain combinatorial optimization problems such as ordering and partitioning for parallel computing but also makes it possible to find the topological properties of the models in a much easier manner employing the topological properties of their factors, refer [1, 2] for details and examples.

Hexagonal structures are everywhere, for instance, the honeycomb cells are composed of hexagons, and they are commonly believed as an example of geometric efficiency. The carbon nanotubes are the superfibers with light weight and a perfectly connected hexagonal cylindrical structure; they are also viewed as one of the most valuable objects for nanotechnology, electronics, optics, and other fields of material science and technology. Since the structures of most familiar graph products constructed by the product operation are triangles or quadrangles, it is somewhat difficult to see the hexagonal system as the product of two graphs. For this purpose, a semicartesian product graph was defined in

[3], such that zigzag/armchair polyhex nanotube, polyhex nanotorus, and polyhex lattice are the semicartesian products of cycles and paths.

Since connectivity measures reliability and efficiency of a graph, computing the connectivity is a fundamental problem in combinatorial optimization. The connectivity of product graphs is well studied. The authors consider the connectivity mainly in [4–6] for the Cartesian products, in [7–10] for the direct products, in [11] for the strong products, and in [12] for the lexicographic products. In almost all cases, more explicit formulae expressed in terms of corresponding graph invariants of factors are obtained; the following result is an example about Cartesian products.

Theorem 1 (see [5]). *Let $\kappa(G)$ be the connectivity of a graph G and $G \square H$, the cartesian product of two connected graphs G and H . Then,*

$$\kappa(G \square H) = \min\{\kappa(G)|V(H)|, \kappa(H)|V(G)|, \delta(G) + \delta(H)\}, \quad (1)$$

where $\delta(G)$ denotes the minimum degree of G .

In this study, we obtain two such formulae to determine the connectivity and edge connectivity of a semicartesian product graph separately.

2. Preliminaries

Every graph $G = (V(G), E(G))$ considered in this study is simple and finite. The set $\{G' | G' \cong G\}$ is called the isomorphic class of G . A subgraph S of G is induced if it contains exactly all edges with both ends in $V(S)$. The connectivity $\kappa(G)$ of a connected graph G is the fewest number of vertices whose removal from G results in a disconnected or trivial graph, and the edge connectivity $\lambda(G)$ equals the smallest cardinality of an edge subset whose removal leads to disconnection. The neighborhood of a vertex u in G is the set $N_G(u) = \{x \in V(G) | xu \in E(G)\}$ and the degree $\deg_G(u)$ of u in G equals the cardinality of $N_G(u)$. Then, $\delta(G) = \min\{\deg_G(u) | u \in V(G)\}$ is the minimum degree of G . It is well-known that $\kappa(G) \leq \lambda(G) \leq \delta(G)$ for any graph G .

A bipartite graph (2-colorable graph) is a graph whose vertex set can be partitioned into two sets A and B , such that every edge connects a vertex in A to one in B , and it is symmetric if it has a symmetric drawing with respect to a straight line that passes through the middle point of each

edge, or equivalently, there is a numeration of the vertices of the bipartition sets as $A = \{a_1, \dots, a_n\}$ and $B = \{b_1, \dots, b_n\}$, such that both the two edges $a_i b_j$ and $a_j b_i$ appear simultaneously.

An orientation of a graph G means directing every edge of G from one of its ends to the other; it is connected if there is a directed path (a sequence of vertices in which there is a directed edge pointing from each vertex in the sequence to its successor in the sequence) between any two vertices of G , and it is cycle preserving if any induced cycle of G is a directed cycle (a directed path whose first and last vertices are the same), and reversing the direction of any induced cycle does not change the isomorphic class of the oriented graph G .

Definition 1 (see [3]). Let G and H be two connected bipartite graphs with proper 2-coloring and G symmetric and H connected cycle preserving oriented. Then, the semicartesian product (semisum) of the graphs G and H , denoted by $G \sqcup H$, is defined as the follows:

$$\begin{aligned} V(G \sqcup H) &= V(G) \times V(H), \\ E(G \sqcup H) &= \{(u, v)(u', v') : v = v' \text{ and } uu' \in E(G) \text{ or } u = u' \text{ and } v \longrightarrow v' \text{ and } u, v \text{ colored with same color}\}, \end{aligned} \quad (2)$$

where the symbol $v \longrightarrow v'$ denotes that the edge vv' of H directed from v to v' in the connected cycle preserving orientation of H .

The vertex set and the edge set of the Cartesian product $G \square H$ of two graphs G and H are listed as follows:

$$\begin{aligned} V(G \square H) &= V(G) \times V(H), \\ E(G \square H) &= \{(u, v)(u', v') : v = v' \text{ and } uu' \in E(G) \text{ or } u = u' \text{ and } vv' \in E(H)\}. \end{aligned} \quad (3)$$

Hence, the semicartesian product $G \sqcup H$ is a spanning subgraph of the corresponding Cartesian product $G \square H$, where G is a connected symmetric bipartite graph and H is a connected cycle preserving orientable bipartite graph, and that is why we call the product graph $G \sqcup H$ semicartesian product.

Since G and H are the connected bipartite graphs and G is symmetric, the vertex set of the disjoint union $G \cup H$ has a unique bipartition up to isomorphism. This implies that the semicartesian product of such two graphs is not changed under switching the colors of any factor. It is clear from the following lemma that the semicartesian product $G \sqcup H$ is independent of the choice of a connected cycle preserving orientation of H .

Lemma 1. *If a connected bipartite graph H is a connected cycle preserving orientable, then H has exactly two such orientations up to isomorphism.*

Proof. Any induced even cycle C has a clockwise or an anticlockwise direction in a cycle preserving orientation of

H . By the definition of the cycle preserving orientation, reversing the direction of C does not change the connected cycle preserving orientation of H .

So, it remains to consider the case for the paths not on a cycle. There are only two kinds of such paths in H : a path hanging on a cycle and a bridge path connecting two cycles. Since the orientation of H is connected, H contains at most two hanging paths and some bridge paths, and moreover, if the orientation of one of them is chosen, then the orientation of all others are fixed. \square

A G -layer of a semicartesian product $G \sqcup H$ is the set $G_v = \{(u, v) | u \in V(G)\}$, and analogously, an H -layer is $H_u = \{(u, v) | v \in V(H)\}$, where $v \in V(H)$ and $u \in V(G)$. Notice that a subgraph of $G \sqcup H$ induced by a G -layer is isomorphic to G , but a subgraph induced by an H -layer possibly consists of some stars, independent edges, and isolated vertices. If we contract each edge of the set $\{(u, v_i)(u', v_i) | v_i \in V(H)\}$ in the induced subgraph on $H_u \cup H_{u'}$, then we obtain an isomorphic copy of H , where $uu' \in E(G)$.

By a G -layer G_v or an H -layer H_u , we again denote the subgraph of $G \sqcup H$ induced on G_v or H_u , respectively. An ambiguity could not arise since it is clear in the text whether G_v (or H_u) denotes a vertex set or a graph.

In Figure 1, G is a symmetric bipartite graph with black and white coloring, and H is a connected cycle preserving orientable bipartite graph. Since H has two 2-coloring and two connected cycle preserving orientations, there are four connected cycle preserving orientations together with 2-coloring of H , see graphs H_1, H_2, H_3, H_4 in Figure 1. It is easy to check that $G \sqcup H_1 \cong G \sqcup H_2 \cong G \sqcup H_3 \cong G \sqcup H_4$. Notice that black and white colors in $G \sqcup H_i$ comes from G , nothing but identify H -layers of the product.

3. Connectivity of Semicartesian Products

Let $\lfloor x \rfloor$ be the greatest integer not bigger than x and $\lceil x \rceil$ be the smallest integer not less than x . Then, we observe that $\deg_G(u) + \lfloor \deg_H(v)/2 \rfloor \leq \deg_{G \sqcup H}(u, v) \leq \deg_G(u) + \lceil \deg_H(v)/2 \rceil$ for any $(u, v) \in V(G \sqcup H)$. More precisely, if $\deg_G(u_1) + \lfloor \deg_H(v)/2 \rfloor = \deg_{G \sqcup H}(u_1, v)$, then $\deg_{G \sqcup H}(u_2, v) = \deg_G(u_2) + \lceil \deg_H(v)/2 \rceil$ and vice versa, where u_1 is symmetric to u_2 in G . So we have.

Lemma 2. *Let G be a connected symmetric bipartite graph and H be a connected cycle preserving the orientable bipartite graph. Then,*

$$\delta(G \sqcup H) = \delta(G) + \lfloor \frac{\delta(H)}{2} \rfloor. \quad (4)$$

A k -set is a set consisted of k elements. A cut set, an edge cut set, or a mixed cut set of a graph is a subset of the vertex set, the edge set or the union of the vertex set, and edge set of the graph, respectively, such that its deletion creates at least one more component. A subset S' of a cut set S is replaceable if $(S \setminus S') \cup \{e_v | v \in S'\}$ is a mixed cut set, where e_v is an edge incident with v . A maximal k -replaceable set S^* of a graph is a replaceable set of a k -cut set of the graph, such that $|S^*| = \max\{|S'| | S' \text{ is a replaceable set of a } k\text{-cut set}\}$. Now, we are ready to state a main result of this study.

Theorem 2. *Let G be a connected symmetric bipartite graph and H be a connected cycle preserving the orientable bipartite graph. Then,*

$$\kappa(G \sqcup H) = \min \left\{ \kappa(G)|V(H)|, \kappa(H)|V(G)| - |S^*| \frac{|V(G)|}{2}, \delta(G) + \lfloor \frac{\delta(H)}{2} \rfloor \right\}, \quad (5)$$

where S^* is a maximal $\kappa(H)$ -replaceable set of H .

Proof. Clearly, $\kappa(G \sqcup H) \leq \delta(G \sqcup H) = \delta(G) + \lfloor \delta(H)/2 \rfloor$. Let S_1 be a $\kappa(G)$ -cut set of G . Then, $S_1 \times V(H)$ is a $\kappa(G)|V(H)|$ -cut set of $G \sqcup H$. Let S_2 be a $\kappa(H)$ -cut set of H

with $S^* \subseteq S_2$. Then, $(V(G) \times (S_2 \setminus S^*)) \cup (\cup_{u \in S^*} (\text{either } A \times \{u\} \text{ or } B \times \{u\}))$ is a $(\kappa(H) - |S^*|)|V(G)| + |S^*|(|V(G)|/2)$ -cut set of $G \sqcup H$, where A and B are the bipartitions of $V(G)$. Thus,

$$\kappa(G \sqcup H) \leq \min \left\{ \kappa(G)|V(H)|, \kappa(H)|V(G)| - |S^*| \frac{|V(G)|}{2}, \delta(G) + \lfloor \frac{\delta(H)}{2} \rfloor \right\}. \quad (6)$$

In the following, we show the inverse inequality; specifically, we prove that $|S| \geq \delta(G) + \lfloor \delta(H)/2 \rfloor$ for any cut set S of $G \sqcup H$ with the following property:

$$|S| < \min \left\{ \kappa(G)|V(H)|, \kappa(H)|V(G)| - |S^*| \frac{|V(G)|}{2} \right\}. \quad (7)$$

Notice that $|G_v| = |V(G)| \geq 2\delta(G)$, $|H_u| = |V(H)| \geq 2\delta(H)$, and $|G_v \cap H_u| = 1$. If both a G -layer G_v and an H -layer H_u are contained in S , then $|S| \geq 2(\delta(G) + \delta(H)) - 1$ and the result follows. Hence, if S contains a G -layer, then it contains no H -layer and vice versa .

Case A: there is no G -layer contained in S

Let $G'_v := G_v \setminus S$ and $S^G_v := G_v \cap S$, and similarly, $H'_u := H_u \setminus S$ and $S^H_u := H_u \cap S$, where $v \in V(H)$ and $u \in V(G)$. Then, $G_v = G'_v \cup S^G_v$ and $H_u = H'_u \cup S^H_u$, and $G'_v \neq \emptyset$ for all $v \in V(H)$. Since $|S| < \kappa(G)|V(H)|$, there is $h \in V(H)$, such that G'_h is connected.

Let C_1 denote the component of $(G \sqcup H) - S$, including G'_h and $V := \{v \in V(H) | G'_v \subseteq C_1\}$. Obviously, $V \neq \emptyset$ since $h \in V$. And $V \neq V(H)$; otherwise, $(G \sqcup H) - S = C_1$ contradicts to the choice of S . Since H is connected, there are adjacent vertices $v_1, v_2 \in V(H)$, such that $v_2 \in V(H) \setminus V$ and $v_1 \in V$. Since $v_2 \in V(H) \setminus V$, we have $G'_{v_2} \not\subseteq C_1$. Therefore, there is another component C_2 of $(G \sqcup H) - S$, such that $G^*_{v_2} := C_2 \cap G'_{v_2} \neq \emptyset$, as shown in Figure 2. And what is more, if $(g, v_1)(g, v_2)$ is an edge with $(g, v_2) \in G^*_{v_2}$, then $(g, v_1) \in S^G_{v_1}$. Hence, $X := \{(g, v_1) | (g, v_1)(g, v_2) \in E(G \sqcup H) \text{ and } (g, v_2) \in G^*_{v_2}\} \subseteq S^G_{v_1}$.

There is an edge $(g, v_1)(g, v_2) \in E(G^*_{v_2})$; otherwise, $N_{G_{v_2}}(g, v_2) \subseteq S^G_{v_2}$ for all $(g, v_2) \in G^*_{v_2}$; therefore, $|S^G_{v_2}| \geq \deg_{G_{v_2}}(g, v_2) \geq \delta(G)$, and we have a desired result. Since $G_{v_2} \cong G$ and G is bipartite, we have $N_{G_{v_2}}(g_1, v_2) \cap N_{G_{v_2}}(g_2, v_2) = \emptyset$. Obviously,

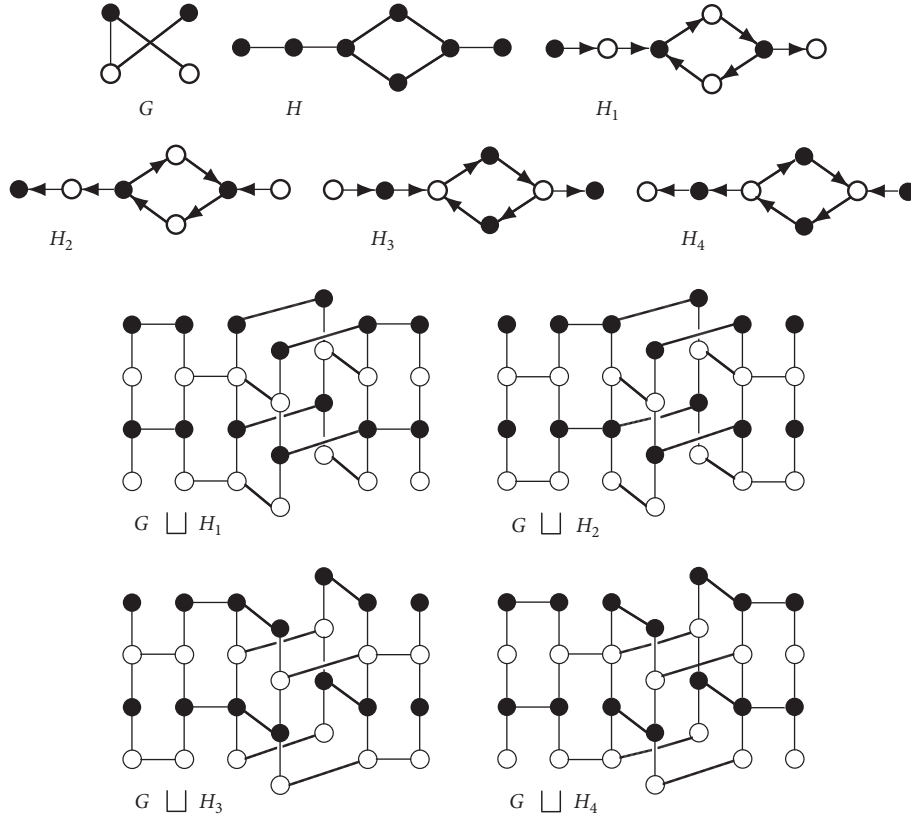


FIGURE 1: An example of a semicartesian product.

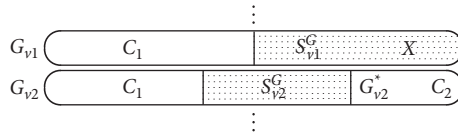


FIGURE 2: Situation from the case that no G -layer is contained in S .

$N_{G_{v_2}}(g_1, v_2) \cup N_{G_{v_2}}(g_2, v_2) \subseteq S_{v_2}^G \cup G_{v_2}^*$. By the definition of the semicartesian product, if $(g'_1, v_1) (g'_1, v_2) \notin E(G \sqcup H)$; then $(g'_2, v_1) (g'_2, v_2) \in E(G \sqcup H)$, where $(g'_i, v_2) \in N_{G_{v_2}^*}(g_i, v_2)$ for $i = 1, 2$. Thus,

$$\begin{aligned} |S_{v_1}^G \cup S_{v_2}^G| &= |S_{v_1}^G| + |S_{v_2}^G| \geq |X| + |S_{v_2}^G| \\ &\geq |N_{G_{v_2}^*}(g_i, v_2)| + |N_{S_{v_2}^G}(g_i, v_2)| \\ &= \deg_{G_{v_2}}(g_i, v_2) \geq \delta(G_{v_2}) = \delta(G), \end{aligned} \tag{8}$$

Where $i = 1$ or $i = 2$.

Suppose that there is a $u \in V(G)$, such that $S_u^H = H_u$. Since $|S_u^H \cap (X \cup S_{v_2}^G)| \leq 1$ and $|S_u^H| \geq 2\delta(H)$, we have $|S| \geq |S_{v_2}^G| + |X| + |S_u^H| - 1 \geq \delta(G) + 2\delta(H) - 1$.

Case B: there is no H -layer contained in S

Although H_u possibly consists of some stars, independent edges, and vertices, we can also proceed analogously to Case A. Let F_1 be a component of $(G \sqcup H) - S$, such that $H'_u \subseteq F_1$ (possibly $F_1 = C_1$) and

let $U = \{u \in V(G) | H'_u \subseteq F_1\}$. Since $|S| < \kappa(H) |V(G)| - |S^*| (|V(G)|/2)$, there are two adjacent vertices u and u' of G with the following property: the induced subgraph $H'_u \cup H'_{u'}$ of $G \sqcup H$ is connected. Thus, $U \neq \emptyset$. Obviously, $U \neq V(G)$, and therefore, there are two adjacent vertices $u_1 \in U$ and $u_2 \in V(G) \setminus U$. By a similar reason as in Case A, we obtain a set $Y := \{(u_1, h) | (u_2, h) \in H_{u_2}^* \subseteq S_{u_1}^H\}$ with $|Y| + |S_{u_2}^H| \geq \lfloor \delta(H)/2 \rfloor + 1$, where $H_{u_2}^* := F_2 \cap H_{u_2}'$ and F_2 is another component of $(G \sqcup H) - S$ with $F_2 \cap H_{u_2}' \neq \emptyset$. If the cut set S contains a G -layer, i.e., $S_v^G = G_v$ for a $v \in V(H)$, then we have again $|S| \geq |S_v^G| + |Y| + |S_{u_2}^H| - 1 \geq 2\delta(G) + \lfloor \delta(H)/2 \rfloor$, since $|S_v^G| \geq 2\delta(G)$ and $|S_v^G \cap (Y \cup S_{u_2}^H)| \leq 1$. Case C: neither a G -layer nor an H -layer is contained in S

Obviously, $|(X \cup S_{v_2}^G) \cap (Y \cup S_{u_2}^H)| \leq 2$. The following three statements cannot be simultaneously true; otherwise, it is easy to drive a contradiction to the choice of S .

$$(1) S = S_{v_1}^G \cup S_{v_2}^G \cup S_{u_1}^H \cup S_{u_2}^H = X \cup S_{v_2}^G \cup Y \cup S_{u_2}^H$$

- (2) $|(X \cup S_{v_2}^G) \cap (Y \cup S_{u_2}^H)| = 2$
- (3) $|X \cup S_{v_2}^G| = \delta(G)$ and $|Y \cup S_{u_2}^H| = \lfloor \delta(H)/2 \rfloor + 1$

Hence, it follows that $|S| \geq |X \cup S_{v_2}^G \cup Y \cup S_{u_2}^H| \geq \delta(G) + \lfloor \delta(H)/2 \rfloor$. \square

4. Edge Connectivity of Semicartesian Products

Let V_1 and V_2 be two disjoint vertex subsets of a graph. We use the symbol $[V_1, V_2]$ for the number of edges whose one end is V_1 and another is V_2 . In this section, we show another main result of this study.

Theorem 3. *Let G be a connected symmetric bipartite graph and H be a connected cycle preserving orientable bipartite graph. Then,*

$$|X| > [V(C), V(G \sqcup H) \setminus V(G_v)] \geq i \times \lfloor \frac{\delta(H)}{2} \rfloor > \delta(G) + \lfloor \frac{\delta(H)}{2} \rfloor, \quad \text{for } \delta(H) \geq 2. \tag{11}$$

Now, we handle the subcase $\delta(H) = 1$. If every vertex of C has a neighbor in other G -layer except for G_v itself, then

$$|X| > [V(C), V(G \sqcup H) \setminus V(G_v)] \geq |V(C)| > \delta(G) + \lfloor \frac{\delta(H)}{2} \rfloor. \tag{12}$$

So, we suppose that there is a vertex $(u, v) \in V(C)$, such that $N_{G \sqcup H}(u, v) \subseteq G_v$. Since H is connected, there is $v' \in V(H)$, such that $vv' \in E(H)$. Then, by the definition of the semicartesian product of graphs, we have $(u', v)(u', v') \in E(G \sqcup H)$ for all $u' \in N_{G_u}(u)$. Thus,

$$|X| \geq [V(C), V(G_v) \setminus V(C)] + [V(C), V(G \sqcup H) \setminus V(G_v)]$$

$$\begin{aligned} &\geq |N_{G_v \setminus C}(u, v)| + |N_C(u, v)| \\ &= \deg_{G_v}(u) \geq \delta(G) = \delta(G) + \lfloor \frac{\delta(H)}{2} \rfloor. \end{aligned} \tag{13}$$

In the following three cases, we set analogous to the proof of Theorem 2 that $C_v^G := V(C) \cap G_v, C_u^H := V(C) \cap H_u$ and $G_v' := G_v \setminus V(C), H_u' := H_u \setminus V(C)$, where $v \in V(H)$ and $u \in V(G)$.

Case 3. An H -layer is contained in C and C contains no G -layer.

Since $[C_v^G, G_v'] \geq \lambda(G)$ for all $v \in V(H)$, we have

$$|X| \geq \sum_{v \in V(H)} [C_v^G, G_v'] \geq \lambda(G)|V(H)|. \tag{14}$$

Case 4. A G -layer is contained in C and C contains no H -layer.

$$\lambda(G \sqcup H) = \min \left\{ \lambda(G)|V(H)|, \lambda(H) \frac{|V(G)|}{2}, \delta(G) + \lfloor \frac{\delta(H)}{2} \rfloor \right\}. \tag{9}$$

Proof. Let X be an arbitrary edge cut of $G \sqcup H$ and C a component of $(G \sqcup H) - X$. Then, $|X| \geq [V(C), V(G \sqcup H) \setminus V(C)]$. If $|V(C)| := i \leq \delta(G) + \lfloor \delta(H)/2 \rfloor$, then $|X| \geq i(\delta(G) + \lfloor \delta(H)/2 \rfloor - (i-1)) \geq \delta(G) + \lfloor \delta(H)/2 \rfloor$. So, in the following, we suppose that $i > \delta(G) + \lfloor \delta(H)/2 \rfloor$.

Case 1. $C \subseteq H_u$.

$$|X| \geq i \times \delta(G) > \delta(G) + \lfloor \frac{\delta(H)}{2} \rfloor. \tag{10}$$

Case 2. $C \subseteq G_v$.

By the definition of the semicartesian product, either $(u, v)(u, v') \in E(G \sqcup H)$ or $(u', v)(u', v') \in E(G \sqcup H)$ for all $vv' \in E(H)$, where u is symmetric to u' in G . And therefore, $[C_u^H, H_u'] + [C_u^H, H_u'] \geq \lambda(H)$. Thus,

$$|X| \geq \sum_{u \in V(G)} [C_u^H, H_u'] \geq \lambda(H) \frac{|V(G)|}{2}. \tag{15}$$

If C contains both an H -layer and a G -layer, then there exists another component of $(G \sqcup H) - X$, such that it contains neither an H -layer nor a G -layer.

Case 5. C contains neither a G -layer nor an H -layer, and also, C is contained neither in a G -layer nor in an H -layer.

Notice that $C_v^G \neq \emptyset, C_u^H \neq \emptyset$, and $G_v' \neq \emptyset, H_u' \neq \emptyset$ for all $(u, v) \in V(C)$. We call a vertex $(u', v) \in N_{G_v}(u, v)$ as a G -layer neighbor of (u, v) and a vertex $(u, v') \in N_{H_u}(u, v)$ as an H -layer neighbor. In the following, we find an H -layer neighbor in $H_{u'}'$ for every $(u', v) \in N_{C_v^G}(u, v)$ and a G -layer neighbor in $G_{v'}'$ for all $(u, v') \in N_{C_u^H}(u, v) \cup \{(u, v)\}$.

If all H -layer neighbors of (u', v) belong to C , then we find a substitute $(u', v^*) \in C_{u'}^H$ for (u', v) , such that an H -layer neighbor of (u', v^*) is in $H_{u'}'$. Indeed, since no H -layer is contained in C and a subgraph of $G \sqcup H$ induced by $H_u \cup H_{u'}$ is connected for $uu' \in E(G)$, if we fail to find a substitute (u', v^*) in $C_{u'}^H$ for (u', v) , then, for each vertex $(u'', v) \in N_{C_v^G}(u', v)$, there exists a substitute $(u'', v^*) \in C_{u''}^H$ of (u'', v) , such that (u'', v^*) has a neighbor in $H_{u''}'$. In this case, we consider the vertex (u', v) instead of (u, v) .

Since the subgraph induced by a G -layer is isomorphic to G and G is connected, (u, v) and each of its neighbors in C_u^H have at least $\delta(G)$ G -layer neighbors. Using analogous argument for (u, v) and its neighbors in C_u^H as the above, we can easily find desired substitutes $(u^o, v) \in C_v^G$ for (u, v) and

$(u^*, v') \in C_v^G$ for (u, v') , such that (u°, v) has a G -layer neighbor in G'_v and (u^*, v') has a G -layer neighbor in G'_v . Note that (u', v^*) has at least one H -layer neighbor and one G -layer neighbor in $V(G \sqcup H) \setminus V(C)$ if $(u', v^*) = (u^*, v')$. Hence,

$$\begin{aligned} |X| &\geq [V(C), V(G \sqcup H) \setminus V(C)] \\ &\geq \deg_{G'_v}(u, v) + \deg_{C_u^G}(u, v) \\ &\quad + \lfloor \frac{\deg_{H'_u}(u, v) + \deg_{C_u^H}(u, v)}{2} \rfloor + 1 \\ &> \delta(G) + \lfloor \frac{\delta(H)}{2} \rfloor, \end{aligned} \quad (16)$$

and then, it follows that

$$\lambda(G \sqcup H) \geq \min \left\{ \lambda(G)|V(H)|, \lambda(H) \frac{|V(G)|}{2}, \delta(G) + \lfloor \frac{\delta(H)}{2} \rfloor \right\}. \quad (17)$$

The proof of the inverse inequality is somewhat obvious. Since each G -layer is isomorphic to G and there are $|V(H)|$ disjoint G -layers in $G \sqcup H$, if we choose same $\lambda(G)$ -edge cut for each G -layer, then we get an edge cut of $G \sqcup H$ with cardinality $\lambda(G)|V(H)|$. Let S be a $\lambda(H)$ -edge cut of H and H_1, H_2 be the two components of $H - S$. Then, $V(G) \times V(H_1)$ and $V(G) \times V(H_2)$ are partitions of $V(G \sqcup H)$ with

$$[V(G) \times V(H_1), V(G) \times V(H_2)] = \lambda(H) \frac{|V(G)|}{2}. \quad (18) \quad \square$$

5. Conclusion

In this study, we have studied the connectivity and edge connectivity of semicartesian product graphs, and we gave two formulae to calculate separately these two parameters of a semicartesian product graph.

Data Availability

The data used to support the findings of this study are included within the article.

Conflicts of Interest

The authors declare that they have no conflicts of interest.

Acknowledgments

The authors thank the referees for their helpful suggestions. This work was supported by the Natural Science Foundation of China (11961070).

References

- [1] M. V. Diudea, I. Gutman, and L. Jantschi, *Molecular Topology*, Huntington, New York, NY, USA, 2001.
- [2] W. Imrich and S. Klavzar, *Product Graphs: Structure and Recognition*, John Wiley & Sons, New York, NY, USA, 2000.
- [3] M. Metsidik, "Semi-cartesian product of graphs," *Journal of Mathematical Chemistry*, vol. 52, no. 3, pp. 856–865, 2014.
- [4] W.-S. Chiue and B.-S. Shieh, "On connectivity of the Cartesian product of two graphs," *Applied Mathematics and Computation*, vol. 102, no. 2-3, pp. 129–137, 1999.
- [5] S. Špacapan, "Connectivity of Cartesian product graphs," *Applied Mathematics Letters*, vol. 21, pp. 682–685, 2008.
- [6] J.-M. Xu and C. Yang, "Connectivity of Cartesian product graphs," *Discrete Mathematics*, vol. 306, no. 1, pp. 159–165, 2006.
- [7] X.-L. Cao, Š. Brglez, S. Špacapan, and E. Vumar, "On edge connectivity of direct products of graphs," *Information Processing Letters*, vol. 111, no. 18, pp. 899–902, 2011.
- [8] R. Guji and E. Vumar, "A note on the connectivity of Kronecker products of graphs," *Applied Mathematics Letters*, vol. 22, no. 9, pp. 1360–1363, 2009.
- [9] S. Špacapan, "A characterization of the edge connectivity of direct products of graphs," *Discrete Mathematics*, vol. 313, pp. 1385–1393, 2013.
- [10] W. Wang and Z. Yan, "Connectivity of Kronecker products with complete multipartite graphs," *Discrete Applied Mathematics*, vol. 161, no. 10-11, pp. 1655–1659, 2013.
- [11] S. Špacapan, "Connectivity of strong products of graphs," *Graphs and Combinatorics*, vol. 26, pp. 457–467, 2010.
- [12] C. Yang and J. M. Xu, "Connectivity of lexicographic product and direct product of graphs," *Ars Combinatoria*, vol. 111, pp. 3–12, 2013.

Research Article

On $\mathbb{L}(\varphi, \varphi - 1, \dots, 1)$ Labelings of Circulant Graphs

K. Mageshwaran,¹ Ali Ahmad ,² Bundit Unyong,³ G. Kalaimurugan ,¹
and S. Gopinath ¹

¹Department of Mathematics, Thiruvalluvar University, Vellore-632115, India

²College of Computer Science & Information Technology, Jazan University, Jazan, Saudi Arabia

³Department of Mathematics, Phuket Rajabhat University, Phuket-83000, Thailand

Correspondence should be addressed to Ali Ahmad; ahmadsms@gmail.com

Received 26 August 2021; Accepted 4 October 2021; Published 19 October 2021

Academic Editor: Niansheng Tang

Copyright © 2021 K. Mageshwaran et al. This is an open access article distributed under the Creative Commons Attribution License, which permits unrestricted use, distribution, and reproduction in any medium, provided the original work is properly cited.

An m - $\mathbb{L}(\varphi, \varphi - 1, \dots, 1)$ labeling of a simple graph \mathcal{G} is a mapping τ from the vertex set $V(\mathcal{G})$ to $\{0, 1, \dots, m\}$ such that $|\tau(u) - \tau(v)| \geq \varphi + 1 - \mathfrak{d}(u, v)$, $\forall u, v \in V(\mathcal{G})$, where length of the shortest route connecting u and v is represented by $\mathfrak{d}(u, v)$. The smallest m for which there exists a m - $\mathbb{L}(\varphi, \varphi - 1, \dots, 1)$ labeling of \mathcal{G} is known as the $\mathbb{L}(\varphi, \varphi - 1, \dots, 1)$ labeling number of \mathcal{G} , and it is described by $\lambda_{\varphi}(\mathcal{G})$. We define m - $\mathbb{L}'(\varphi, \varphi - 1, \dots, 1)$ as the same as the m - $\mathbb{L}(\varphi, \varphi - 1, \dots, 1)$ labeling if τ is one to one. The $\mathbb{L}'(\varphi, \varphi - 1, \dots, 1)$ labeling number of \mathcal{G} represented by $\lambda(\varphi, \varphi - 1, \dots, 1)$, (\mathcal{G}) and is called minimum span. In this paper, we prove that the circulant graphs with specified generating sets admit m - $\mathbb{L}(\varphi, \varphi - 1, \dots, 1)$ and m - $\mathbb{L}'(\varphi, \varphi - 1, \dots, 1)$ labeling and also find $\lambda_{\varphi}(\mathcal{G})$ and $\lambda(\varphi, \varphi - 1, \dots, 1)'(\mathcal{G})$. Moreover, we find the $\mathbb{L}(\varphi, \varphi - 1, \dots, 1)$ labeling number of any simple graph with diameter less than φ .

1. Introduction

Let \mathcal{G} be a simple connected graph with finite whose vertex set $V(\mathcal{G})$ and edge set $\varepsilon(\mathcal{G})$ with $|V(\mathcal{G})| = \alpha$ and $|\varepsilon(\mathcal{G})| = \beta$. The open neighbouring of $v \in V(\mathcal{G})$ is $N(v) = \{u \in V(\mathcal{G}) | \mathfrak{d}(v, u) = 1\}$. Assigning integer values to the vertices or edges or both subject to the certain rules is called *labeling* of the graph \mathcal{G} . For more about graph labeling, refer the survey [1]. Specially, for graph distance labeling, we refer to [2–5], and we follow [6] for graph theoretic terminology. The frequency assignment problem (FAP) is a process to allocate frequencies to the set of transmitters under the condition that there is no interference between the different transmitters. The aim of the problem is to reduce the span (the variation among lower and higher frequencies) of the allocated frequencies. A good number of graph theoretic methods are used for analyzing FAP and majority of them are NP-hard [7]. Especially, FAP can be modeled as mobile communication, satellite communication, and radio/TV broadcasting. In [8, 9], authors studied the results based on (h, k) -distance labeling of the graph. Also, Nandi et al. [10]

originated and explored the idea of m - $\mathbb{L}(\varphi, \varphi - 1, \dots, 1)$ labeling of graphs.

Throughout this paper, let $n, r \in \mathbb{Z}^+$ such that $1 \leq r \leq [n - 1/2]$, $\Lambda = \{1, 2, \dots, r, n - 1, n - 2, \dots, n - r\}$ is the generating set of \mathbb{Z}_n . The circulant graph with vertex set $V(\mathcal{G}) = \{v_0, v_1, \dots, v_{n-1}\}$ and edge set $\varepsilon(\mathcal{G}) = \{v_i v_{i+j} : 0 \leq i \leq n - 1, j \in \Lambda\}$, the indices $i + j$ being taken as modulo n . This graph is represented by $\text{Cir}(n, \Lambda)$.

2. m - $\mathbb{L}(\varphi, \varphi - 1, \dots, 1)$ Labeling of Circulant Graphs

We use the following lemma to obtain the minimum span of a m - $\mathbb{L}(\varphi, \varphi - 1, \dots, 1)$ labeling of a graph. Fact: if τ is m - $\mathbb{L}(\varphi, \varphi - 1, \dots, 1)$ labeling function with $\lambda_{\varphi}(\mathcal{G}) = m$, then at least one vertex v such that $\tau(v) = 0$.

Lemma 1. *Let \mathcal{G} be a simple graph which allows m - $\mathbb{L}(\varphi, \varphi - 1, \dots, 1)$ labeling by the function τ with each vertex $u \in V$; there exists some $v \in V$ such that $\mathfrak{d}(u, v) = t$ and $|\tau(u) - \tau(v)| = \varphi + 1 - t$; then, $\lambda_{\varphi}(\mathcal{G}) = m$.*

Proof. Suppose $\lambda_{\wp}(\mathcal{G}) < m$; then, there exists a m' - $\mathbb{L}(\wp, \wp - 1, \dots, 1)$ labeling function τ' such that $m' < m$. Without lack of generalization, $m' = m - 1$, there exist $u, v \in V$ such that $\tau(u) = m$ and $\tau'(v) = m'$. By the assumption, there exists $u', v' \in V$; we obtain $\mathfrak{d}(u, u') = t$ and $\mathfrak{d}(v, v') = t$ with $|\tau(u) - \tau(u')| = \wp + 1 - t \leq |\tau'(v) - \tau'(v')|$, since, by the definition,

$$\begin{aligned} |\tau(u) - \tau(u')| &\leq |\tau'(v) - \tau'(v')| \\ |m - \tau(u')| &\leq |m' - \tau'(v')| \\ |m - \tau(u')| &\leq |m - (1 + \tau'(v'))|. \end{aligned} \quad (1)$$

Clearly, $\tau'(v') \leq \tau(u') - 1$ if there exist $u'' \neq u$ and $v'' \neq v$ such that $\mathfrak{d}(u', u'') = t$ and $\mathfrak{d}(v', v'') = t$ with $|\tau(u') - \tau(u'')| = \wp + 1 - t \leq |\tau'(v') - \tau'(v'')| \Rightarrow \tau'(v'') \leq \tau(u'') - 1$. Otherwise, we choose $u'' \in V$, such that $\tau(u'') = \max\{\tau(v)/\tau(u), \tau(u')\}$. Continue this process up to the last vertex; this gives the contradiction to the fact that the distance labeling function is τ' . \square

$$|\tau(v_h) - \tau(v_{r((\wp/2)+1)})| = \left| t - \frac{\wp}{2} \right| < \frac{\wp}{2} < \frac{\wp}{2} + 1 \leq \wp + 1 - \mathfrak{d}(v_h, v_{r((\wp/2)+1)}). \quad (3)$$

Case 3: if $t = \wp/2$, since τ is $\mathbb{L}(\wp, \wp - 1, \dots, 2, 1)$ labeling of \mathcal{G} , then the following one of the subcase holds.

Subcase (i): if $\mathfrak{d}(v_0, v_h) = \wp/2 + 1$, then the vertices v_h and $v_{r((\wp/2)+1)}$ are adjacent:

$$|\tau(v_h) - \tau(v_{r((\wp/2)+1)})| = 0 < \wp = \wp + 1 - \mathfrak{d}(v_h, v_{r((\wp/2)+1)}). \quad (4)$$

Subcase (ii): if $\mathfrak{d}(v_{r((\wp/2)+1)}, v_h) = \wp/2 + 1$, then the vertices v_0 and v_h are adjacent:

$$|\tau(v_0) - \tau(v_h)| = \frac{\wp}{2} < \wp = \wp + 1 - \mathfrak{d}(v_0, v_h). \quad (5)$$

This gives the contradiction; clearly, no such v_h exists. This argument leads to any other vertex in H which is labeled with multiple \wp under the minimum required condition of this labeling. Then, we are starting with 0; we get the minimum span $[r((\wp/2) + 1) - 1]\wp$. Hence, $\lambda(H) = [(r((\wp/2) + 1) - 1)]\wp$. \square

Similarly, we can derive the succeeding lemma.

Lemma 3. Let $\wp, n, r \in \mathbb{Z}^+$ such that \wp is odd and $1 \leq r \leq \lfloor (n-1)/2 \rfloor$. Let $\mathcal{G} = \text{Cir}(n, \Lambda)$, $\Lambda = \{1, 2, \dots, r, n-1, n-2, \dots, n-r\}$, and $\vee(\mathcal{G}) = \{v_0, v_1, \dots, v_{n-1}\}$. Let H be the induced subgraph of \mathcal{G} whose vertex set is any set of $r\lfloor \wp/2 \rfloor + \lfloor r/2 \rfloor + 1$, consecutive vertices of $\vee(\mathcal{G})$; if \mathcal{G} admits the m - $\mathbb{L}(\wp, \wp - 1, \dots, 1)$ labeling, then $\lambda(H) = [(r\lfloor \wp/2 \rfloor + \lfloor r/2 \rfloor - 1)]\wp$.

Lemma 2. Let $\wp, n, r \in \mathbb{Z}^+$ such that \wp is even and $1 \leq r \leq \lfloor (n-1)/2 \rfloor$. Let $\mathcal{G} = \text{Cir}(n, \Lambda)$, $\Lambda = \{1, 2, \dots, r, n-1, n-2, \dots, n-r\}$, and $\vee(\mathcal{G}) = \{v_0, v_1, \dots, v_{n-1}\}$. Let H be the induced subgraph of \mathcal{G} whose vertex set is any set of $r(\wp/2 + 1) + 1$ consecutive vertices of $\vee(\mathcal{G})$; if \mathcal{G} admits the m - $\mathbb{L}(\wp, \wp - 1, \dots, 1)$ labeling, then $\lambda(H) = [(r((\wp/2) + 1) - 1)]\wp$.

Proof. Let us assume that $\vee(H) = \{v_0, v_1, \dots, v_{r((\wp/2)+1)}\}$; clearly, at most, the distance between any pair vertices of H is $(\wp/2) + 1$. Let τ be $\mathbb{L}(\wp, \wp - 1, \dots, 2, 1)$ labeling function of \mathcal{G} . In general, we assume that $\tau(v_0) = x$ and $\tau(v_{r((\wp/2)+1)}) = x + \wp/2$ because of the distance between $\mathfrak{d}(v_0, v_{r((\wp/2)+1)}) = (\wp/2) + 1$. Suppose $v_h \in H$ with $\tau(v_h) = x + t \in [x, x + \wp)$.

Case 1: if $t < \wp/2$,

$$|\tau(v_0) - \tau(v_h)| = |t| < \frac{\wp}{2} < \frac{\wp}{2} + 1 \leq \wp + 1 - \mathfrak{d}(v_0, v_h). \quad (2)$$

Case 2: if $t > \wp/2$,

Lemma 4. Let \mathcal{G} be any simple finite graph with n vertices; if $\wp > \text{diam}(\mathcal{G}) = d$, then $\lambda_{\wp}(\mathcal{G}) = (n-1)\wp - \sum_{s=1}^n (\mathfrak{d}(v_{s-1}, v_s) - 1)$, where $v_s = y \in \vee(\mathcal{G})$ such that $\mathfrak{d}(v_{s-1}, y) = \max\{\mathfrak{d}(v_{s-1}, x) : \forall x \neq v_{i < s} \in \vee(\mathcal{G})\}$, $s \in \mathbb{N}$, and v_0 is an any arbitrary vertex of \mathcal{G} .

Proof. Let us describe the condition:

$$\tau(v_i) = i\wp - \sum_{s=1}^n (\mathfrak{d}(v_{s-1}, v_s) - 1). \quad (6)$$

Here, we have to prove that the function is $\mathbb{L}(\wp, \wp - 1, \dots, 2, 1)$ labeling and take any arbitrary vertex v_i and v_j :

$$\begin{aligned} |\tau(v_i) - \tau(v_j)| &\geq \left| i\wp - \sum_{s=1}^i (\mathfrak{d}(v_{s-1}, v_s) - 1) \right. \\ &\quad \left. - \left(j\wp - \sum_{s=1}^j (\mathfrak{d}(v_{s-1}, v_s) - 1) \right) \right| \\ &\geq \left| (i-j)\wp - \sum_{s=j}^i (\mathfrak{d}(v_{s-1}, v_s) - 1) \right| \\ &\geq |(i-j)\wp - (i-j)(d-1)| \\ &\geq |(i-j)(\wp - d) + (i-j)| \\ &\geq \wp - d + 1 \end{aligned} \quad (7)$$

$$|\tau(v_i) - \tau(v_j)| \geq \wp + 1 - \mathfrak{d}(v_i, v_j).$$

This shows that the function τ is $\mathbb{L}(\wp, \wp - 1, \dots, 1)$ labeling. We have to prove that the minimum span of this

function; let us consider the vertices in the order v_0, v_1, \dots, v_n such that

$$|\tau(v_{s-1}, v_s)| = \wp + 1 - \mathfrak{d}(v_{s-1}, v_s). \quad (8)$$

This sequence of the vertices shows the minimum span of $L(\wp, \wp - 1, \dots, 2, 1)$ labeling of the graph \mathcal{G} . Hence, $\lambda_\wp(\mathcal{G}) = (n - 1)\wp - \sum_{s=1}^n (\mathfrak{d}(v_{s-1}, v_s) - 1)$. \square

Theorem 1. Let $\wp, n \in \mathbb{Z}^+$ with n as even and $\mathcal{G} = \text{Cir}(n, \Lambda)$, where $\Lambda = \{1, 2, \dots, n/2 - 1, n - 1, n - 2, \dots, n - ((n/2) - 1)\}$. Then,

$$\lambda_\wp(\mathcal{G}) = (n - 1)\wp - \frac{n}{2}. \quad (9)$$

Proof. Let $\mathcal{G} = \text{Cir}(n, \Lambda)$, with $\Lambda = \{1, 2, \dots, (n/2) - 1, n - 1, n - 2, \dots, n - ((n/2) - 1)\}$. Let $\mathcal{V}(\mathcal{G}) = \{v_0, v_1, v_2, \dots, v_{n-1}\}$ and $\tau: \mathcal{V} \rightarrow [0, \infty]$ be given by

$$\tau(v_i) = \begin{cases} 2i\wp - i, & \text{if } i < \frac{n}{2}, \\ (2\wp - 1)\left(i - \frac{n}{2}\right) + \wp - 1, & \text{if } i \geq \frac{n}{2}. \end{cases} \quad (10)$$

Let $v_i, v_j \in \mathcal{V}(\mathcal{G})$ with $i, j < n/2$; then, $\mathfrak{d}(v_i, v_j) = 1$ and $|\tau(v_i) - \tau(v_j)| = |(2\wp - 1)i - (2\wp - 1)j| \geq 2\wp - 1 \geq \wp \geq \wp + 1 - \mathfrak{d}(v_i, v_j)$.

Let $v_i, v_j \in \mathcal{V}(\mathcal{G})$ with $i, j < n/2$; then, $\mathfrak{d}(v_i, v_j) = 1$ and $|\tau(v_i) - \tau(v_j)| = |(2\wp - 1)(i - j)| \geq 2\wp - 1 \geq \wp \geq \wp + 1 - \mathfrak{d}(v_i, v_j)$.

Let $v_i, v_j \in \mathcal{V}(\mathcal{G})$ with $i < n/2$ and $j \geq n/2$; then, $\mathfrak{d}(v_i, v_j) = 1$ or 2 and $|\tau(v_i) - \tau(v_j)| = |(2\wp - 1)(i - n/2) + \wp - 1 - 2i\wp + i| \geq \wp(1 - n) + n/2 - 1 \geq \wp \geq \wp + 1 - \mathfrak{d}(v_i, v_j)$. Thus, τ is $L(\wp, \wp - 1, \dots, 2, 1)$ labeling function, and Lemma 1 holds the theorem. \square

Example 1. If $\wp = 4$ and $n = 6$, then the circulant graph $\mathcal{G} = \text{Cir}(6, \{1, 2, 4, 5\})$ has $L(\wp, \wp - 1, \dots, 2, 1)$ labeling number $\lambda_4(\mathcal{G}) = 17$. Figure 1 illustrates that the span is sharp.

Theorem 2. Let $\wp, n, r \in \mathbb{Z}^+$ such that \wp is even and $1 \leq r \leq \lfloor (n - 1)/2 \rfloor$. Let $\mathcal{G} = \text{Cir}(n, \Lambda)$ with $\Lambda = \{1, 2, \dots, r, n - 1, n - 2, \dots, n - r\}$. If $2r((\wp/2) + 1)|n$, then

$$\lambda_\wp(\mathcal{G}) = \left[r\left(\frac{\wp}{2} + 1\right) - 1 \right] \wp + \frac{\wp}{2}. \quad (11)$$

Proof. Let $\mathcal{G} = \text{Cir}(n, \Lambda)$, where $\Lambda = \{1, 2, \dots, r, n - 1, n - 2, \dots, n - r\}$. Let $\ell = n/r(\wp/2 + 1)$, $\mathcal{V}(\mathcal{G}) = \{v_0, v_1, v_2, \dots, v_{n-1}\}$, and $\tau: \mathcal{V} \rightarrow [0, \infty]$ by

$$\tau(v_i) = \begin{cases} \left[i \bmod r\left(\frac{\wp}{2} + 1\right) \right] \wp, & \text{if } \lfloor \frac{i}{r((\wp/2) + 1)} \rfloor = 0, 2, \dots, \ell, \\ \left[i \bmod r\left(\frac{\wp}{2} + 1\right) \right] \wp + \frac{\wp}{2}, & \text{if } \lfloor \frac{i}{r((\wp/2) + 1)} \rfloor = 1, 3, \dots, \ell - 1. \end{cases} \quad (12)$$

The distance between arbitrary vertices v_i and v_j in $\mathcal{V}(\mathcal{G})$ is

$$\mathfrak{d}(v_i, v_j) = \begin{cases} \lfloor \frac{|i - j|}{r} \rfloor, & \text{if } |i - j| \leq \frac{n}{2}, \\ \lfloor \frac{n - |i - j|}{r} \rfloor, & \text{if } |i - j| > \frac{n}{2}. \end{cases} \quad (13)$$

Case (i): if $\lfloor i/r((\wp/2) + 1) \rfloor = \lfloor j/r((\wp/2) + 1) \rfloor$,

$$|\tau(v_i) - \tau(v_j)| = \left| \left[(i - j) \bmod r\left(\frac{\wp}{2} + 1\right) \right] \wp \right|. \quad (14)$$

Here, $\lfloor (i - j) \bmod r((\wp/2) + 1) \rfloor \neq 0$ since i and j are distinct, so $0 < i - j < r((\wp/2) + 1)$ because $\lfloor i/r((\wp/2) + 1) \rfloor = \lfloor j/r((\wp/2) + 1) \rfloor$.

$$\begin{aligned} |\tau(v_i) - \tau(v_j)| &= \left| \left[(i - j) \bmod r\left(\frac{\wp}{2} + 1\right) \right] \wp \right| \\ &\geq \wp \geq \wp + 1 - \mathfrak{d}(v_i, v_j). \end{aligned} \quad (15)$$

This satisfied the $L(\wp, \wp - 1, \dots, 2, 1)$ labeling condition.

Case (ii): if $\lfloor i/r((\wp/2) + 1) \rfloor \neq \lfloor j/r((\wp/2) + 1) \rfloor$.

Subcase (a): if $|\tau(v_i) - \tau(v_j)| = \left| \left[(i - j) \bmod r((\wp/2) + 1) \right] \wp - \wp/2 \right|$.

There exist $a, b \in \mathbb{Z}^+$ such that $(i - j) \bmod r((\wp/2) + 1) = a \Rightarrow i - j = b[r((\wp/2) + 1)] + a$ with $1 \leq b < \ell$. Hence,

$$\mathfrak{d}(v_i, v_j) = \left\lfloor \frac{b[r((\wp/2) + 1)] + a}{r} \right\rfloor \geq \frac{\wp}{2} + 1, \text{ or} \quad (16)$$

$$\left\lfloor \frac{\ell[r((\wp/2) + 1)] - \{b[r((\wp/2) + 1)] + a\}}{r} \right\rfloor \geq \frac{\wp}{2} + 1.$$

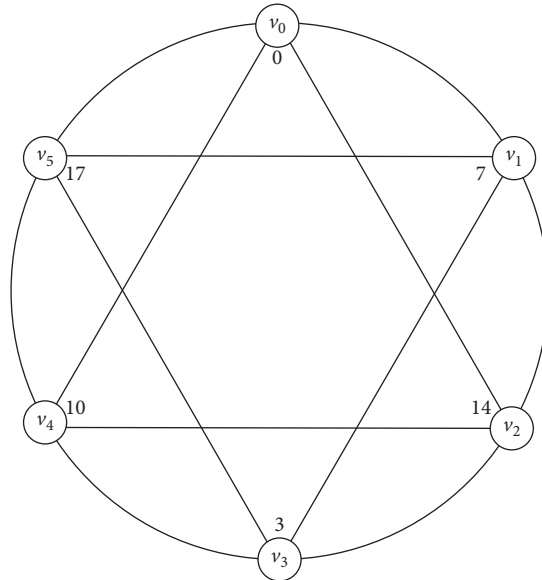


FIGURE 1: $\lambda_4(\mathcal{G}) = 17$.

Therefore, this implies that $\mathfrak{d}(v_i, v_j) \geq \varphi/2 + 1$:

$$|\tau(v_i) - \tau(v_j)| \geq \frac{\varphi}{2} = \varphi - \frac{\varphi}{2} + 1 - 1 \geq \varphi + 1 - \mathfrak{d}(v_i, v_j). \tag{17}$$

Subcase (b): if $|\tau(v_i) - \tau(v_j)| = \lfloor [(i - j) \bmod r ((\varphi/2) + 1)] \rfloor \varphi$.

There exist $a, b \in \mathbb{Z}^+$ such that $(i - j) \bmod r ((\varphi/2) + 1) = a \Rightarrow i - j = b \lfloor ((\varphi/2) + 1) \rfloor + a$ with $2 \leq b < \ell - 1$. Hence, by equation (13),

$$\mathfrak{d}(v_i, v_j) \geq 2 \left(\frac{\varphi}{2} + 1 \right) = \varphi + 2, \text{ or,} \tag{18}$$

$$\left\lfloor \frac{\ell \lfloor r((\varphi/2) + 1) \rfloor - \{b \lfloor r((\varphi/2) + 1) \rfloor + a\}}{r} \right\rfloor \geq \varphi + 2.$$

Therefore, $\mathfrak{d}(v_i, v_j) \geq \varphi + 2$ implies that

$$\left| \left[(i - j) \bmod r \left(\frac{\varphi}{2} + 1 \right) \right] \varphi \right| \geq 0 \geq \varphi - \varphi + 1 - 1 \geq \varphi + 1 - (\varphi + 1) \geq \varphi + 1 - \mathfrak{d}(v_i, v_j). \tag{19}$$

Now, each vertex has some vertex with distance $(\varphi/2) + 1$ and absolute difference between those vertices is $\varphi/2$. Hence, by Lemma 1, τ is minimum span function of \mathcal{G} ; this proves the theorem. \square

Example 2. If $\varphi = 4$ and $r = 2$, then the circulant graph $\mathcal{G} = \text{Cir}(24, \{1, 2, 22, 23\})$ has $\mathbb{L}(\varphi, \varphi - 1, \dots, 2, 1)$ labeling

number $\lambda_4(\mathcal{G}) = 22$. Figure 2 illustrates that the span is sharp.

Theorem 3. Let $\varphi, n, r \in \mathbb{Z}^+$ such that φ is odd and $1 \leq r \leq \lfloor (n - 1)/2 \rfloor$. Let $\mathcal{G} = \text{Cir}(n, \Lambda)$, where $\Lambda = \{1, 2, \dots, r, n - 1, n - 2, \dots, n - r\}$. If $2(r \lfloor \varphi/2 \rfloor + \lfloor r/2 \rfloor) | n$, then

$$\lambda_\varphi(\mathcal{G}) = \left[r \left\lfloor \frac{\varphi}{2} \right\rfloor + \left\lfloor \frac{r}{2} \right\rfloor - 1 \right] \varphi + \left\lfloor \frac{\varphi}{2} \right\rfloor. \tag{20}$$

Proof. Let $\mathcal{G} = \text{Cir}(n, \Lambda)$ with $\Lambda = \{1, 2, \dots, r, n - 1, n - 2, \dots, n - r\}$. Let $\ell = n/r \lfloor \varphi/2 \rfloor + \lfloor r/2 \rfloor$, $\mathcal{V}(\mathcal{G}) = \{v_0, v_1, v_2, \dots, v_{n-1}\}$, and $\tau: \mathcal{V} \rightarrow [0, \infty]$ by

$$\tau(i) = \begin{cases} \left[i \bmod r \left\lfloor \frac{\varphi}{2} \right\rfloor + \left\lfloor \frac{r}{2} \right\rfloor \right] \varphi, & \text{if } \left\lfloor \frac{i}{r \lfloor \varphi/2 \rfloor + \lfloor r/2 \rfloor} \right\rfloor = 0, 2, \dots, \ell, \\ \left[i \bmod r \left\lfloor \frac{\varphi}{2} \right\rfloor + \left\lfloor \frac{r}{2} \right\rfloor \right] \varphi + \left\lfloor \frac{\varphi}{2} \right\rfloor, & \text{if } \left\lfloor \frac{i}{r \lfloor \varphi/2 \rfloor + \lfloor r/2 \rfloor} \right\rfloor = 1, 3, \dots, \ell - 1. \end{cases} \tag{21}$$

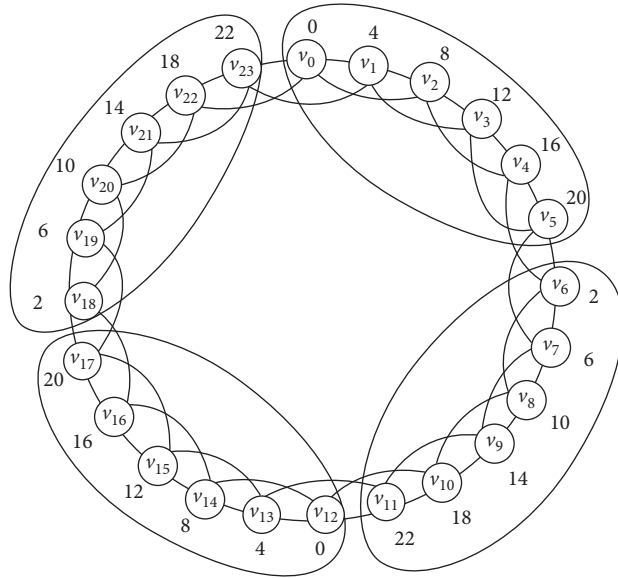


FIGURE 2: $\lambda_4(\mathcal{G}) = 22$.

The distance between arbitrary vertices v_i and v_j in $\mathcal{V}(\mathcal{G})$ is

$$d(v_i, v_j) = \begin{cases} \lfloor \frac{|i-j|}{r} \rfloor, & \text{if } |i-j| \leq \frac{n}{2}, \\ \lfloor \frac{n-|i-j|}{r} \rfloor, & \text{if } |i-j| > \frac{n}{2}. \end{cases} \quad (22)$$

Case (i): if $\lfloor i/r \rfloor + \lfloor r/2 \rfloor = \lfloor j/r \rfloor + \lfloor r/2 \rfloor$,

$$|\tau(v_i) - \tau(v_j)| = \left| \left[(i-j) \bmod r \left\lfloor \frac{\varrho}{2} \right\rfloor + \left\lfloor \frac{r}{2} \right\rfloor \right] \varrho \right|. \quad (23)$$

Here, $(i-j) \bmod (r \lfloor \varrho/2 \rfloor + \lfloor r/2 \rfloor) \neq 0$, since i and j are distinct, so $0 < i-j < r \lfloor \varrho/2 \rfloor + \lfloor r/2 \rfloor$ because $\lfloor i/r \rfloor + \lfloor r/2 \rfloor = \lfloor j/r \rfloor + \lfloor r/2 \rfloor$:

$$d(v_i, v_j) = \lfloor \frac{b[r \lfloor \varrho/2 \rfloor + \lfloor r/2 \rfloor] + a}{r} \rfloor \geq \lfloor \varrho/2 \rfloor + \lfloor r/2 \rfloor, \text{ or,} \quad (25)$$

$$\lfloor \frac{\ell(r \lfloor \varrho/2 \rfloor + \lfloor r/2 \rfloor) - \{b[r \lfloor \varrho/2 \rfloor + \lfloor r/2 \rfloor] + a\}}{r} \rfloor \geq \lfloor \frac{\varrho}{2} \rfloor + \lfloor \frac{r}{2} \rfloor.$$

Therefore, $d(v_i, v_j) \geq \lfloor \varrho/2 \rfloor + \lfloor r/2 \rfloor$:

$$|\tau(v_i) - \tau(v_j)| \geq \lfloor \frac{\varrho}{2} \rfloor \geq \varrho - \lfloor \frac{\varrho}{2} \rfloor \geq \varrho + 1 - d(v_i, v_j). \quad (26)$$

$$|\tau(v_i) - \tau(v_j)| = \left| \left[(i-j) \bmod r \left\lfloor \frac{\varrho}{2} \right\rfloor + \left\lfloor \frac{r}{2} \right\rfloor \right] \varrho \right| \geq \varrho \geq \varrho + 1 - d(v_i, v_j). \quad (24)$$

This satisfied the $L(\varrho, \varrho - 1, \dots, 2, 1)$ labeling condition.

Case (ii): if $\lfloor i/r \rfloor + \lfloor r/2 \rfloor = \lfloor j/r \rfloor + \lfloor r/2 \rfloor$.

Subcase (a): if $|\tau(v_i) - \tau(v_j)| = \left| \left[(i-j) \bmod r \left\lfloor \frac{\varrho}{2} \right\rfloor + \left\lfloor \frac{r}{2} \right\rfloor \right] \varrho - \lfloor \varrho/2 \rfloor \right|$.

There exist $a, b \in \mathbb{Z}^+$ such that $(i-j) \bmod r \lfloor \varrho/2 \rfloor + \lfloor r/2 \rfloor = a \Rightarrow i-j = b[r \lfloor \varrho/2 \rfloor + \lfloor r/2 \rfloor] + a$ with $1 \leq b < \ell$. Hence, by equation (22), we have

Subcase (b): if $|\tau(v_i) - \tau(v_j)| = \left| \left[(i-j) \bmod r \left\lfloor \frac{\varrho}{2} \right\rfloor + \left\lfloor \frac{r}{2} \right\rfloor \right] \varrho \right|$.

Let $(i-j) \bmod r \lfloor \varrho/2 \rfloor + \lfloor r/2 \rfloor = a \Rightarrow i-j = b[r \lfloor \varrho/2 \rfloor + \lfloor r/2 \rfloor] + a$ with $2 \leq b < \ell - 1$. Hence, by equation (22),

$$d(v_i, v_j) = \lfloor \frac{b[r \lfloor \varrho/2 \rfloor + \lfloor r/2 \rfloor] + a}{r} \rfloor \geq 2 \left(\lfloor \frac{\varrho}{2} \rfloor + \lfloor \frac{r}{2} \rfloor \right), \text{ or} \quad (27)$$

$$\lfloor \frac{\ell(r \lfloor \varrho/2 \rfloor + \lfloor r/2 \rfloor) - \{b[r \lfloor \varrho/2 \rfloor + \lfloor r/2 \rfloor] + a\}}{r} \rfloor \geq 2 \left(\lfloor \frac{\varrho}{2} \rfloor + \lfloor \frac{r}{2} \rfloor \right).$$

Therefore, $\mathfrak{d}(v_i, v_j) \geq 2(\lfloor \varphi/2 \rfloor + \lfloor r/2 \rfloor) > \varphi$.

Thus, τ is $\mathbb{L}(\varphi, \varphi - 1, \dots, 2, 1)$ labeling and $\lambda_\varphi(\mathcal{G}) = [r\lfloor \varphi/2 \rfloor + \lfloor r/2 \rfloor - 1]\varphi$. Now, each vertex has some vertex with distance $\lfloor \varphi/2 \rfloor + \lfloor r/2 \rfloor$ and absolute difference between those vertices is $\lfloor \varphi/2 \rfloor$. Hence, by Lemma 1, τ is minimum span function of \mathcal{G} ; this proves the theorem. \square

Example 3. If $k = 3$ and $r = 3$, then the circulant graph $\mathcal{G} = \text{Cir}(14, \{1, 2, 3, 11, 12, 13\})$ has $\mathbb{L}(\varphi, \varphi - 1, \dots, 2, 1)$ labeling number $\lambda_3(\mathcal{G}) = 19$. Figure 3 illustrates that the span is sharp.

3. $\mathbb{L}'(\varphi, \varphi - 1, \dots, 2, 1)$ Labeling of Circulant Graphs

We prove the following theorems for the circulant graph $\text{Cir}(n, \Lambda)$, $\Lambda = \{1, 2, \dots, r, n - 1, n - 2, \dots, n - r\}$, and $1 \leq r < \lfloor n/2 \rfloor$ admits $\mathbb{L}'(\varphi, \varphi - 1, \dots, 2, 1)$ labeling with $\lambda_{(\varphi, \varphi - 1, \dots, 1)}'(\mathcal{G}) = n - 1$.

Theorem 4. Let $n, r \in \mathbb{Z}^+$ with $1 \leq r < \lfloor n/2 \rfloor$. If $n \geq 2(r + 1) + 1$ and $(r + 1) \nmid n$, then the circulant graph $\text{Cir}(n, \Lambda)$, $\Lambda = \{1, 2, \dots, r, n - 1, n - 2, \dots, n - r\}$ admits $\mathbb{L}'(2, 1)$ labeling with $\lambda_{(2, 1)}'(\mathcal{G}) = n - 1$.

Proof. Let $n, \ell \in \mathbb{Z}^+$, $\mathcal{G} = \text{Cir}(n, \Lambda)$ be the circulant graph with $n \geq 2(r + 1) + 1$ where $1 \leq r < \lfloor n/2 \rfloor$ and $\ell = n/(r + 1)$. By the division algorithm, for every vertex $v \in \mathcal{V}(\mathcal{G})$, we can write $v = v_{i(r+1)+j}$, where $0 \leq i \leq \ell - 1, 0 \leq j \leq r$. By using $\tau: \mathcal{V}(\mathcal{G}) \rightarrow \{0, 1, \dots, n - 1\}$,

$$\tau(v_{i(r+1)+j}) = i + \ell j. \tag{28}$$

For $i = 0, 0 \leq j \leq r - 1$, and $1 \leq d \leq \ell/2$ we have

$$\begin{aligned} N^d(v_j) = & \{v_{(d-1)(r+1)+j+1}, v_{(d-1)(r+1)+j+2}, \dots, \\ & \cdot v_{(d-1)(r+1)+j+r}, v_{((\ell-1)+(d-1))(r+1)+j+1}, \\ & \cdot v_{((\ell-1)+(d-1))(r+1)+j+2}, \dots, v_{((\ell-1)+(d-1))(r+1)+j+r}\}. \end{aligned} \tag{29}$$

Also, for $1 \leq i \leq \ell - 1, 0 \leq j \leq r - 1$, and $1 \leq d \leq \ell/2$, we have

$$\begin{aligned} N^d(v_{i(r+1)+j}) = & \{v_{(i+d-1)(r+1)+j+1}, v_{(i+d-1)(r+1)+j+2}, \dots, \\ & \cdot v_{(i+d-1)(r+1)+j+r}, v_{((i-1)+(d-1))(r+1)+j+1}, \\ & \cdot v_{((i-1)+(d-1))(r+1)+j+2}, \dots, \\ & \cdot v_{((i-1)+(d-1))(r+1)+j+r}\}. \end{aligned} \tag{30}$$

The function τ is injective, and the values assigned to $\mathcal{V}(\mathcal{G})$ is from $\{0, 1, 2, \dots, n - 1\}$. So, for every $e = uv \in \mathcal{E}(\mathcal{G})$, the difference of the labels $|\tau(u) - \tau(v)|$ gets one of the values in the set $\{1, 2, \dots, n - 1\}$. By the function τ , for every $u \in \mathcal{V}(\mathcal{G})$ and $v \in N^d(u)$, we get the difference values $|\tau(u) - \tau(v)|$ in the set $\{\ell + d - 1, 2\ell + d - 1, \dots, r\ell + d - 1, \ell - 1 +$

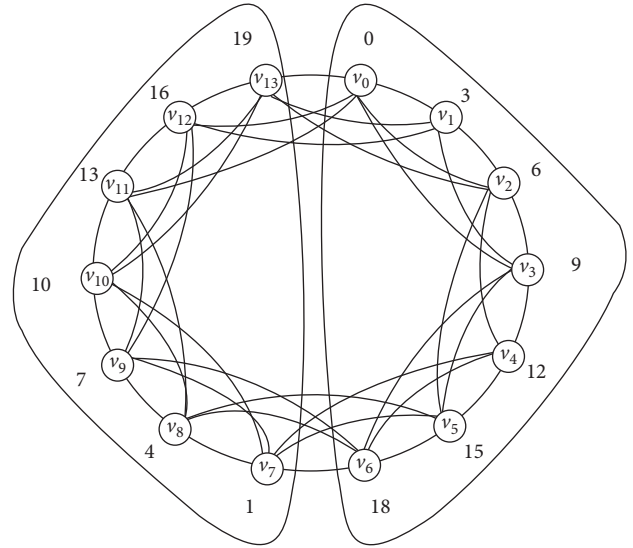


FIGURE 3: $\lambda_3(\mathcal{G}) = 19$.

$r\ell + d - 1, \ell - 1 + (r - 1)\ell + d - 1, \ell - 1 + (r - 2)\ell + d - 1, \dots, \ell - 1 + \ell + d - 1\}$. Since $n \geq 2(r + 1) + 1, n/(r + 1) = \ell$ which implies $\ell \geq 2$. For $\varphi = 1$ and $\varphi = 2$, the difference $|\tau(u) - \tau(v)| \geq \varphi + 1 - \mathfrak{d}(u, v)$, for all $u, v \in \mathcal{V}(\mathcal{G})$. Hence, the function τ is a $\mathbb{L}'(2, 1)$ -labeling with $\lambda_{(2, 1)}'(\mathcal{G}) = n - 1$. \square

Theorem 5. Let $n, r \in \mathbb{Z}^+$ with $1 \leq r < \lfloor n/2 \rfloor$. If $n \geq 2(r + 1) + 1$ and $(r + 1) \nmid n$ with $\text{gcd}(n, r + 1) = 1$, then the circulant graph $\text{Cir}(n, \Lambda)$, $\Lambda = \{1, 2, \dots, r, n - 1, n - 2, \dots, n - r\}$, admits $\mathbb{L}'(2, 1)$ labeling with $\lambda_{(2, 1)}'(\mathcal{G}) = n - 1$.

Proof. Let $n, \ell \in \mathbb{Z}^+$ and $\text{Cir}(n, \Lambda)$ be the circulant graph with $n \geq 2(r + 1) + 1$, where $1 \leq r < \lfloor n/2 \rfloor$ and $\ell = \lfloor n/(r + 1) \rfloor$. By the division algorithm, for every vertex $v \in \mathcal{V}(\mathcal{G})$, we can write $v = v_{i(r+1)\text{mod}n}$, where $0 \leq i \leq \ell - 1, 0 \leq j \leq r$. Let $\tau: \mathcal{V}(\mathcal{G}) \rightarrow \{0, 1, \dots, n - 1\}$ by

$$\tau(v_{i(r+1)\text{mod}n}) = i \text{ for } i = 0, 1, \dots, n - 1. \tag{31}$$

For $0 \leq i \leq n - 1$, we have

$$\begin{aligned} N(v_{i(r+1)\text{mod}n}) = & \{v_{(i(r+1)\text{mod}n)+1}, v_{(i(r+1)\text{mod}n)+2}, \dots, \\ & \cdot v_{(i(r+1)\text{mod}n)+r}, v_{(i(r+1)\text{mod}n)+n-1}, \\ & \cdot v_{(i(r+1)\text{mod}n)+n-2}, \dots, v_{(i(r+1)\text{mod}n)+n-r}\}. \end{aligned} \tag{32}$$

Since $\text{gcd}(n, r + 1) = 1$, then the function τ is injective, and the values assigned to $\mathcal{V}(\mathcal{G})$ is from $\{0, 1, 2, \dots, n - 1\}$. So, for every $e = uv \in \mathcal{E}(\mathcal{G})$, the difference of the labels $|\tau(u) - \tau(v)|$ gets one of the values in the set $\{1, 2, \dots, n - 1\}$. By the function τ , for every $u \in \mathcal{V}(\mathcal{G})$, $v \in N^d(u)$, and $1 \leq d \leq \ell/2$, we get the difference values $|\tau(u) - \tau(v)|$ in the set $\{\ell + d - 1, 2\ell + d - 1, \dots, r\ell + d - 1, \ell - 1 + r\ell + d - 1, \ell - 1 + (r - 1)\ell + d - 1, \ell - 1 + (r - 2)\ell + d - 1, \dots, \ell - 1 + \ell + d - 1\}$. Since $n \geq 2(r + 1) + 1, n/(r + 1) = \ell$ which implies $\ell \geq 2$. For

$\wp = 1$ and $\wp = 2$, the difference $|\tau(u) - \tau(v)| \geq \wp + 1 - \mathfrak{d}(u, v)$ for all $u, v \in V(\mathcal{G})$. Hence, the function τ is a $L(2, 1)$ -labeling with $\lambda(2, 1), (\mathcal{G}) = n - 1$. \square

Theorem 6. Let $n, \wp, r \in \mathbb{Z}^+$ with $1 \leq r < \lfloor n/2 \rfloor$. If $n \geq \wp((\wp - 1)r + 1) - r(\wp - 3)$, for $\wp (\geq 3)$ and $((\wp - 1)r + 1) | n$, then the circulant graph $Cir(n, \Lambda)$, $\Lambda = \{1, 2, \dots, r, n - 1, n - 2, \dots, n - r\}$, admits $L'(\wp, \wp - 1, \dots, 2, 1)$ labeling with $\lambda(\wp, \wp - 1, \dots, 2, 1), (\mathcal{G}) = n - 1$.

Proof. Let $n, \wp, \ell \in \mathbb{Z}^+$ and $\mathcal{G} = Cir(n, \Lambda)$ with $n \geq \wp((\wp - 1)r + 1) - r(\wp - 3)$, where $1 \leq r < \lfloor n/2 \rfloor$. $(\wp - 1)r + 1$ divides n .

Take $\ell = n/(\wp - 1)r + 1$. By the division algorithm, for every vertex $v \in V(\mathcal{G})$, we can write $v = v_{i((\wp - 1)r + 1) + j}$, where $0 \leq i \leq \ell - 1, 0 \leq j \leq r$. Let $\tau: V(\mathcal{G}) \rightarrow \{0, 1, \dots, n - 1\}$ by

$$\tau(v_{i((\wp - 1)r + 1) + j}) = i + \ell j. \tag{33}$$

For $i = 0, 0 \leq j \leq r - 1$, and $1 \leq d \leq \ell/2$, we have

$$\begin{aligned} N^d(v_j) = & \{v_{(d-1)((\wp - 1)r + 1) + j + 1}, v_{(d-1)((\wp - 1)r + 1) + j + 2}, \dots, \\ & \cdot v_{(d-1)((\wp - 1)r + 1) + j + r}, v_{((\ell - 1) + (d - 1))((\wp - 1)r + 1) + j + 1}, \\ & \cdot v_{((\ell - 1) + (d - 1))((\wp - 1)r + 1) + j + 2}, \dots, \\ & \cdot v_{((\ell - 1) + (d - 1))((\wp - 1)r + 1) + j + r}\}. \end{aligned} \tag{34}$$

Also, for $1 \leq i \leq \ell - 1, 0 \leq j \leq r - 1$, and $1 \leq d \leq \ell/2$, we have

$$\begin{aligned} N^d(v_{i((\wp - 1)r + 1) + j}) = & \{v_{(i + d - 1)((\wp - 1)r + 1) + j + 1}, \\ & \cdot v_{(i + d - 1)((\wp - 1)r + 1) + j + 2}, \dots, \\ & \cdot v_{(i + d - 1)((\wp - 1)r + 1) + j + r} \\ & \cdot v_{((i - 1) + (d - 1))((\wp - 1)r + 1) + j + 1}, \\ & \cdot v_{((i - 1) + (d - 1))((\wp - 1)r + 1) + j + 2}, \dots, \\ & \cdot v_{((i - 1) + (d - 1))((\wp - 1)r + 1) + j + r}\}. \end{aligned} \tag{35}$$

The function τ is injective, and the values assigned to $v \in V(\mathcal{G})$ is from $\{0, 1, 2, \dots, n - 1\}$. So, for every $e = uv \in \mathcal{E}(\mathcal{G})$, the difference of the labels $|\tau(u) - \tau(v)|$ gets one of the values in the set $\{1, 2, \dots, n - 1\}$. By the function τ , for every $u \in V(\mathcal{G})$ and $v \in N^d(u)$, we get the difference values $|\tau(u) - \tau(v)|$ in the set $\{\ell + d - 1, 2\ell + d - 1, \dots, r\ell + d - 1, \ell - 1 + r\ell + d - 1, \ell - 1 + (r - 1)\ell + d - 1, \dots, \ell - 1 + (r - 2)\ell + d - 1, \dots, \ell - 1 + \ell + d - 1\}$. Since $n \geq \wp((\wp - 1)r + 1) - r(\wp - 3)$, $n/(\wp - 1)r + 1 = \ell$ which implies $\ell \geq \wp$. For $\wp \geq 3$, the difference $|\tau(u) - \tau(v)| \geq \wp + 1 - \mathfrak{d}(u, v)$, for all $u, v \in V(\mathcal{G})$. Hence, the function τ is a $L'(\wp, \wp - 1, \dots, 1)$ -labeling for $\wp \geq 3$ with $\lambda(\wp, \wp - 1, \dots, 2, 1), (\mathcal{G}) = n - 1$. \square

4. Conclusion

We show in this study that the circulant graphs with specific generating sets are allowed m - $L(\wp, \wp - 1, \dots, 2, 1)$ labeling and $L(\wp, \wp - 1, \dots, 2, 1)$ -labeling. Also, we identified the

minimum span of m - $L(\wp, \wp - 1, \dots, 2, 1)$ labeling. However, a major challenge of the problems m - $L(\wp, \wp - 1, \dots, 2, 1)$ labeling and $L'(\wp, \wp - 1, \dots, 1)$ labeling with minimum span for the arbitrary circulant graphs remains under investigation. Another future work is addressed to find m - $L(\wp, \wp - 1, \dots, 1)$ and $L'(\wp, \wp - 1, \dots, 2, 1)$ labeling with minimum span for the Cayley graphs.

Data Availability

No data were used to support the findings of the study.

Conflicts of Interest

The authors declare that they have no conflicts of interest.

References

- [1] J. A. Gallian, "A dynamic survey of graph labeling," *The Electronic Journal of Combinatorics*, vol. 23, p. DS6, 2019.
- [2] S. K. Amanuthulla and M. Pal, " $L(3, 2, 1)$ - and $L(4, 3, 2, 1)$ -labeling problems on interval graphs," *AKCE International Journal of Graphs and Combinatorics*, vol. 14, no. 3, pp. 205–215, 2017.
- [3] T. Calamoneri and R. Petreschi, " $L(2, 1)$ -labeling of unigraphs," *Discrete Applied Mathematics*, vol. 159, no. 12, pp. 1196–1206, 2011.
- [4] G. J. Chang and D. Kuo, "The $L(2, 1)$ -labeling problem on graphs," *SIAM Journal on Discrete Mathematics*, vol. 9, no. 2, pp. 309–316, 1996.
- [5] J. R. Griggs and R. K. Yeh, "Labeling graphs with a condition at distance two," *SIAM Journal on Discrete Mathematics*, vol. 5, no. 4, pp. 586–595, 1992.
- [6] D. W. West, *Introduction to Graph Theory*, Prentice-Hall Inc., Hoboken, NJ, USA, 2001.
- [7] W. K. Hale, "Frequency assignment: theory and application," *Proceedings of the IEEE*, vol. 68, no. 12, pp. 1497–1514, 1980.
- [8] B. M. Kim, B. C. Song, Y. Rho, and W. Hwang, "New $L(h, k)$ -labelings for direct products of complete graphs," *Taiwanese Journal of Mathematics*, vol. 18, no. 3, pp. 793–807, 2014.
- [9] K. Mageshwaran, G. Kalaimurugan, B. Hammachukiattikul, V. Govindan, and I. N. Cangul, "On $L(h, k)$ -labeling index of inverse graphs associated with finite cyclic groups," *Journal of Mathematics*, vol. 2021, Article ID 5583433, 7 pages, 2021.
- [10] S. Nandi, S. Sen, S. C. Ghosh, and S. Das, "On $L(k, k - 1, \dots, 1)$ labeling of triangular lattice," *Electronic Notes in Discrete Mathematics*, vol. 48, pp. 281–288, 2015.

Research Article

The Normalized Laplacians, Degree-Kirchhoff Index, and the Complexity of Möbius Graph of Linear Octagonal-Quadrilateral Networks

Jia-Bao Liu ¹, Qian Zheng ¹, and Sakander Hayat ²

¹School of Mathematics and Physics, Anhui Jianzhu University, Hefei 230601, China

²Faculty of Engineering Sciences, GIK Institute of Engineering Sciences and Technology, Topi Swabi, Khyber Pakhtunkhwa, Pakistan

Correspondence should be addressed to Jia-Bao Liu; liujiabaoad@163.com and Qian Zheng; zhengqian19960202@163.com

Received 6 July 2021; Accepted 3 September 2021; Published 12 October 2021

Academic Editor: Kenan Yildirim

Copyright © 2021 Jia-Bao Liu et al. This is an open access article distributed under the Creative Commons Attribution License, which permits unrestricted use, distribution, and reproduction in any medium, provided the original work is properly cited.

The normalized Laplacian plays an indispensable role in exploring the structural properties of irregular graphs. Let $L_n^{8,4}$ represent a linear octagonal-quadrilateral network. Then, by identifying the opposite lateral edges of $L_n^{8,4}$, we get the corresponding Möbius graph $MQ_n(8, 4)$. In this paper, starting from the decomposition theorem of polynomials, we infer that the normalized Laplacian spectrum of $MQ_n(8, 4)$ can be determined by the eigenvalues of two symmetric quasi-triangular matrices \mathcal{L}_A and \mathcal{L}_S of order $4n$. Next, owing to the relationship between the two matrix roots and the coefficients mentioned above, we derive the explicit expressions of the degree-Kirchhoff indices and the complexity of $MQ_n(8, 4)$.

1. Introduction

It is well established that networks can be represented by graphs. The graphs we consider in this paper are simple, undirected, and connected. Let us first recall some definitions commonly used in graph theory. Suppose G represents a simple undirected graph with $|V_G| = n$ and $|E_G| = m$. For more notations, the readers are referred to [1].

Note that $D(G) = \text{diag}\{d_1, d_2, \dots, d_n\}$ represents a degree matrix, where d_p is the degree of v_p . $A(G)$ is the adjacency matrix of G . The Laplacian matrix of G is $L(G) = D(G) - A(G)$. The (p, q) -entry of the normalized Laplacian matrix is given by

$$(\mathcal{L}(G))_{pq} = \begin{cases} 1, & p = q, \\ -\frac{1}{\sqrt{d_p d_q}}, & p \neq q \text{ and } v_p \sim v_q, \\ 0, & \text{otherwise.} \end{cases} \quad (1)$$

As a matter of fact, there are many parameters that can be used to describe the structure and properties of molecular graphs in graph networks. One of the parameters based on resistance distance is defined as the Wiener index [2, 3], which is

$$W(G) = \sum_{i < j} d_{ij}, \quad (2)$$

where $d_{ij} = d_G(v_i, v_j)$ represents the length of the shortest path between two vertices v_i and v_j in G . The Wiener index is widely used in chemical and mathematical research. For details, see [4–7].

The parameter of resistance distance was first proposed by Klein and Randić [8] in 1993. It means that if every edge of a graph G is regarded as a unit resistance, then the distance between any two vertices i and j in G is called resistance distance, which is denoted as r_{ij} . Similar to the Wiener index, we give the expression of the Kirchhoff index [9, 10] according to the resistance distance, namely,

$$Kf(G) = \sum_{i < j} r_{ij} = n \sum_{i=2}^n \frac{1}{\mu_i}. \quad (3)$$

In 2007, Chen and Zhang [11] proposed that the eigenvalues and eigenvectors of normalized Laplacian spectrum can be used to describe the resistance distance, and the concept of Kirchhoff index is put forward. However, it is very difficult to calculate the degree-Kirchhoff index from the complexity division of graphs, so it is important to find the explicit expression of degree-Kirchhoff index. In recent years, many scholars have devoted themselves to the study of Kirchhoff index of various graphs. Huang et al. [12, 13] proved the Kirchhoff index of linear hexagonal chains and linear polyomino chains successively. Ma and Bian [14] determined the normalized Laplacians and degree-Kirchhoff index of cylinder phenylene chain. Liu et al. [15] described the normalized Laplacian and degree-Kirchhoff index of linear octagonal-quadrilateral networks. For more excellent results, refer to [16–21]. After learning the excellent works of scholars, in this paper, we use the correlation properties of Laplace matrix to calculate the degree-Kirchhoff index and the complexity of Möbius graph of linear octagonal-quadrilateral networks. The investigation of complex graph and network has gone through a spectacular development in the past decades. Especially in organic chemistry, more and more attention has been paid to the application of polyomino in polycyclic aromatic compounds. Many scholars are interested in the study of linear octagonal networks and related molecular graphs. We all know that linear octagonal network is an octagonal system without branch compression. It is constructed by regularly inserting some new points on the straight line of the linear polyomino network. The research on the structure and properties of this kind of natural graph network lays a solid foundation for the advancement of theoretical chemistry, as well as for the development of applied mathematics.

Let $L_n^{8,4}$ be the linear octagonal-quadrilateral networks, and octagons and quadrilaterals are connected by a common edge, which are depicted in Figure 1. Then, the corresponding Möbius graph $MQ_3(8, 4)$ of octagonal-quadrilateral networks is obtained by the reverse identification of the opposite edge by $L_n^{8,4}$ (see Figure 2). Obviously, we can obtain that $|V_{MQ_n}(8, 4)| = 8n$, $|E_{MQ_n}(8, 4)| = 10n$.

The rest of the paper will be divided into the following sections. In Section 2, we put forward some basic notations and related lemmas. In Section 3, we determine the normalized Laplacian spectrum of $MQ_n(8, 4)$. In Section 4, we present Kemeny's constant, the degree-Kirchhoff index, and the complexity of $MQ_n(8, 4)$.

2. Preliminary

In this section, we introduce some common symbols and related calculation methods [1], which are applied to the rest of the article.

The characteristic polynomial of matrix R of order n is defined as $P_R(x) = \det(xI - R)$. It is not difficult to find that

π is an automorphism of G , and we can write the product of disjoint 1-cycles and transposition, namely,

$$\pi = (\bar{1})(\bar{2}), \dots, (\bar{m})(1, 1')(2, 2'), \dots, (k, k'). \quad (4)$$

Then, one has $|V(G)| = m + 2k$, and let $v_0 = \{\bar{1}, \bar{2}, \dots, \bar{m}\}$, $v_1 = \{1, 2, \dots, k\}$, $v_2 = \{1', 2', \dots, k'\}$. Thus, the Laplacian matrix can be expressed in the form of block matrix, that is,

$$\mathcal{L}(G) = \begin{pmatrix} \mathcal{L}_{V_0V_0} & \mathcal{L}_{V_0V_1} & \mathcal{L}_{V_0V_2} \\ \mathcal{L}_{V_1V_0} & \mathcal{L}_{V_1V_1} & \mathcal{L}_{V_1V_2} \\ \mathcal{L}_{V_2V_0} & \mathcal{L}_{V_2V_1} & \mathcal{L}_{V_2V_2} \end{pmatrix}, \quad (5)$$

where

$$\begin{aligned} \mathcal{L}_{V_0V_1} &= \mathcal{L}_{V_0V_2}, \\ \mathcal{L}_{V_1V_2} &= \mathcal{L}_{V_2V_1}, \\ \mathcal{L}_{V_1V_1} &= \mathcal{L}_{V_2V_2}. \end{aligned} \quad (6)$$

Let

$$P = \begin{pmatrix} I_m & 0 & 0 \\ 0 & \frac{1}{\sqrt{2}}I_k & \frac{1}{\sqrt{2}}I_k \\ 0 & \frac{1}{\sqrt{2}}I_k & -\frac{1}{\sqrt{2}}I_k \end{pmatrix}, \quad (7)$$

and then

$$P' \mathcal{L}(G) P = \begin{pmatrix} \mathcal{L}_A(G) & 0 \\ 0 & \mathcal{L}_S(G) \end{pmatrix}. \quad (8)$$

Note that P' is the transposition of P , where

$$\begin{aligned} \mathcal{L}_A &= \begin{pmatrix} \mathcal{L}_{V_0V_0} & \sqrt{2} \mathcal{L}_{V_0V_1} \\ \sqrt{2} \mathcal{L}_{V_1V_0} & \mathcal{L}_{V_1V_1} + \mathcal{L}_{V_1V_2} \end{pmatrix}, \\ \mathcal{L}_S &= \mathcal{L}_{V_1V_1} - \mathcal{L}_{V_1V_2}. \end{aligned} \quad (9)$$

Lemma 1 (see [12]). *Let $\mathcal{L}(L_n)(G)$, $\mathcal{L}_A(G)$, $\mathcal{L}_S(G)$ be determined as above; then,*

$$P_{\mathcal{L}(L_n)}(G) = P_{\mathcal{L}_A}(G) P_{\mathcal{L}_S}(G). \quad (10)$$

Lemma 2. *Let G be a graph with $|V_G| = n$ and $|E_G| = m$, and $0 = \mu_1 < \mu_2 \leq \dots \leq \mu_n (n \geq 2)$ are the eigenvalues of $\mathcal{L}(G)$. Then, we can quickly confirm that the following formulas hold.*

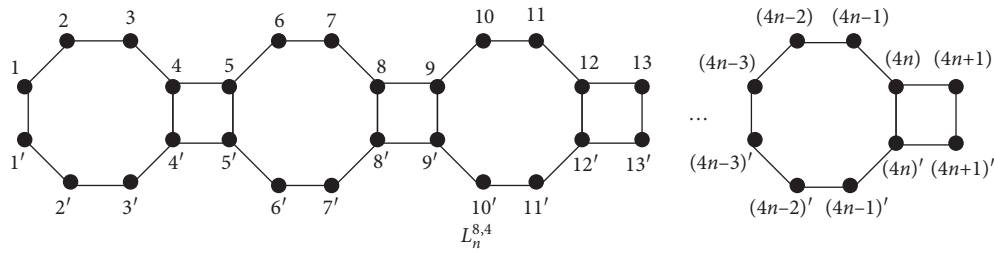


FIGURE 1: Linear octagonal-quadrilateral networks.

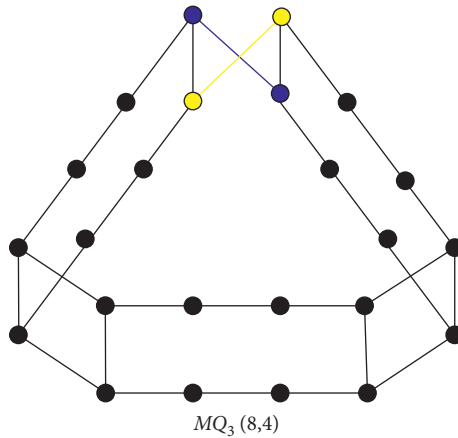


FIGURE 2: Graph $MQ_3(8,4)$.

(a) (see [22]). Kemeny's constant of G can be denoted as

$$K_c(G) = \sum_{i=2}^n \frac{1}{\mu_i} \tag{11}$$

(b) (see [11]). The degree-Kirchhoff index of G is defined as

$$Kf^*(G) = 2m \sum_{k=2}^n \frac{1}{\mu_k} \tag{12}$$

(c) (see [1]). The number of spanning trees of G can also be called the complexity of G . Then, the complexity of G is

$$\prod_{i=1}^n d_i \sum_{k=2}^n \lambda_k = 2m\tau(G). \tag{13}$$

3. The Normalized Laplacian Spectrum of $MQ_n(8,4)$

In this section, we focus on obtaining the normalized Laplacian spectrum of $MQ_n(8,4)$ by Lemma 1.

Given a square matrix T of order n . We will use $T[\{p_1, p_2, \dots, p_k\}]$ to denote the submatrix obtained by deleting the $p_1^{\text{th}}, p_2^{\text{th}}, \dots, p_k^{\text{th}}$ rows and corresponding columns of T . With a suitable labeling, the vertices of $MQ_n(8,4)$ are shown in Figure 2. Apparently, $\pi = (1, 1')(2, 2'), \dots, (4n, (4n)')$ is an automorphism of $MQ_n(8,4)$. Then, $v_0 = \emptyset, v_1 = \{1, 2, 3, \dots, 4n\}$ and $v_2 = \{1', 2', 3', \dots, (4n)'\}$. Besides, we express $\mathcal{L}_A(MQ_n(8,4))$ and $\mathcal{L}_S(MQ_n(8,4))$ as \mathcal{L}_A and \mathcal{L}_S . Then, one can get

$$\begin{aligned} \mathcal{L}_A &= \mathcal{L}_{V_1V_1} + \mathcal{L}_{V_1V_2}, \\ \mathcal{L}_S &= \mathcal{L}_{V_1V_1} - \mathcal{L}_{V_1V_2}. \end{aligned} \tag{14}$$

In view of equation (1), we have

Hence,

$$\mathcal{L}_A = \begin{pmatrix} \frac{2}{3} & \frac{-1}{\sqrt{6}} & & & & & & & \frac{-1}{3} \\ \frac{-1}{\sqrt{6}} & 1 & \frac{-1}{2} & & & & & & \\ & \frac{-1}{2} & 1 & \frac{-1}{\sqrt{6}} & & & & & \\ & & \frac{-1}{\sqrt{6}} & \frac{2}{3} & \frac{-1}{3} & & & & \\ & & & \frac{-1}{3} & \frac{2}{3} & \frac{-1}{\sqrt{6}} & & & \\ & & & & \frac{-1}{\sqrt{6}} & 1 & \frac{-1}{2} & & \\ & & & & & \ddots & & & \\ & & & & & & \frac{-1}{3} & \frac{2}{3} & \frac{-1}{\sqrt{6}} \\ & & & & & & & \frac{-1}{\sqrt{6}} & 1 & \frac{-1}{2} \\ & & & & & & & & & \ddots & \\ & & & & & & & & & & \frac{-1}{3} & \frac{2}{3} & \frac{-1}{\sqrt{6}} \\ & & & & & & & & & & & \frac{-1}{2} & 1 & \frac{-1}{\sqrt{6}} \\ \frac{-1}{3} & & & & & & & & & & & & \frac{-1}{\sqrt{6}} & \frac{2}{3} & \frac{-1}{3} \end{pmatrix}_{(4n) \times (4n)}$$

$$\mathcal{L}_S = \begin{pmatrix} \frac{4}{3} & \frac{-1}{\sqrt{6}} & & & & & & & \frac{-1}{3} \\ \frac{-1}{\sqrt{6}} & 1 & \frac{-1}{2} & & & & & & \\ & \frac{-1}{2} & 1 & \frac{-1}{\sqrt{6}} & & & & & \\ & & \frac{-1}{\sqrt{6}} & \frac{4}{3} & \frac{-1}{3} & & & & \\ & & & \frac{-1}{3} & \frac{4}{3} & \frac{-1}{\sqrt{6}} & & & \\ & & & & \frac{-1}{\sqrt{6}} & 1 & \frac{-1}{2} & & \\ & & & & & \ddots & & & \\ & & & & & & \frac{-1}{3} & \frac{4}{3} & \frac{-1}{\sqrt{6}} \\ & & & & & & & \frac{-1}{\sqrt{6}} & 1 & \frac{-1}{2} \\ & & & & & & & & & \ddots & \\ & & & & & & & & & & \frac{-1}{3} & \frac{4}{3} & \frac{-1}{\sqrt{6}} \\ & & & & & & & & & & & \frac{-1}{2} & 1 & \frac{-1}{\sqrt{6}} \\ \frac{-1}{3} & & & & & & & & & & & & \frac{-1}{\sqrt{6}} & \frac{4}{3} & \frac{-1}{3} \end{pmatrix}_{(4n) \times (4n)}$$

(16)

$$r_p^3 = \frac{2}{3}r_{p-1}^0 - \frac{1}{9}r_{p-2}^1. \tag{25}$$

Proof. of Fact 1. Take $r_p^0 = \det R_p^0$, $r_p^1 = \det R_p^1$, $r_p^2 = \det R_p^2$, and $r_p^3 = \det R_p^3$. By a straightforward calculation, one can get the following values (see Table 1).

For $4 \leq p \leq 4n - 1$, we can get expansion formula of $\det R_p^0$ with respect to its last row:

$$r_p^0 = \begin{cases} \frac{2}{3}r_{p-1}^0 - \frac{1}{6}r_{p-2}^0, & \text{if } p \equiv 0 \pmod{4}, \\ \frac{2}{3}r_{p-1}^0 - \frac{1}{9}r_{p-2}^0, & \text{if } p \equiv 1 \pmod{4}, \\ r_{p-1}^0 - \frac{1}{6}r_{p-2}^0, & \text{if } p \equiv 2 \pmod{4}, \\ r_{p-1}^0 - \frac{1}{4}r_{p-2}^0, & \text{if } p \equiv 3 \pmod{4}. \end{cases} \tag{26}$$

For $1 \leq p \leq n - 1$, let $a_p = r_{4p}^0$; for $0 \leq p \leq n - 1$, let $b_p = r_{4p+1}^0$, $c_p = r_{4p+2}^0$, $d_p = r_{4p+3}^0$. Then, we can get $a_1 = (5/36)$, $b_0 = (2/3)$, $c_0 = (1/2)$, $d_0 = (5/36)$, $b_1 = (3/54)$, $c_1 = (7/216)$, $d_1 = (1/54)$, and for $p \geq 2$, we have

$$\begin{cases} a_p = \frac{2}{3}d_{p-1} - \frac{1}{6}c_{p-1}, \\ b_p = \frac{2}{3}a_p - \frac{1}{9}d_{p-1}, \\ c_p = b_p - \frac{1}{6}a_p, \\ d_p = c_p - \frac{1}{4}b_p. \end{cases} \tag{27}$$

Then, it is not difficult to obtain that

$$\begin{cases} a_p = 18c_p - 24d_p, \\ b_p = 4c_p - 4d_p, \\ c_p = \frac{1}{18}c_{p-1} - \frac{1}{1296}c_{p-2}, \\ d_p = \frac{1}{18}d_{p-1} - \frac{1}{1296}d_{p-2}. \end{cases} \tag{28}$$

According to the equation of d_p in (28), it is evident to see that $x^2 - (1/18)x + (1/1296) = 0$, and its two roots are $(1/36)$ and $(1/36)$. Therefore, $d_p = (x_p + y)(1/36)^p$ is the general solution. Then, we can get

$$\begin{cases} y = \frac{1}{3}, \\ \frac{1}{36}(x + y) = \frac{1}{54}, \\ x = \frac{1}{3}, \\ y = \frac{1}{3}. \end{cases} \tag{29}$$

Thus, we can obtain $d_p = (1/3)(p + 1)(1/36)^p$ ($p \geq 1$). Similarly, we have $c_p = ((2p/3) + (1/2))(1/36)^p$ ($p \geq 1$); $a_p = (4p + 1)(1/36)^p$ ($p \geq 1$); and $b_p = (2/3)(2p + 1)(1/36)^p$ ($p \geq 1$).

The result is obtained as desired. \square

By similar consideration, Fact 2 is available. Then, based on the conclusion of Facts 1 and 2, we quickly get Facts 3 and 4.

Now, we will further calculate $(-1)^{4n-1}a_{4n-1}$ and $(-1)^{4n-2}a_{4n-2}$ in equation (20). For the sake of discussion, it is assumed that $r_0 = 1$.

Claim 1. $(-1)^{4n-1}a_{4n-1} = 40n^2(1/36)^n$.

Proof. of Claim 1. Since $(-1)^{4n-1}a_{4n-1}$ is the total of all the principal minors of order $4n - 1$ of \mathcal{L}_A , we have

$$\begin{aligned} (-1)^{4n-1}a_{4n-1} &= \sum_{p=1}^{4n} \det \mathcal{L}_A[p] = \sum_{p=4, p \equiv 0 \pmod{4}}^{4n} \det \mathcal{L}_A[p] + \sum_{p=1, p \equiv 1 \pmod{4}}^{4n-3} \det \mathcal{L}_A[p] \\ &+ \sum_{p=2, p \equiv 2 \pmod{4}}^{4n-2} \det \mathcal{L}_A[p] + \sum_{p=3, p \equiv 3 \pmod{4}}^{4n-1} \det \mathcal{L}_A[p], \end{aligned} \tag{30}$$

where

TABLE 1: Initial value.

r_p^0	Value	r_p^0	Value	r_p^0	Value	r_p^0	Value
r_1^0	(2/3)	r_2^0	(1/2)	r_3^0	(1/3)	r_4^0	(5/36)
r_5^0	(3/54)	r_6^0	(7/216)	r_7^0	(1/54)	r_8^0	(1/144)

$$\begin{aligned}
 \sum_{p=4, p \equiv 0 \pmod{4}}^{4n} \det \mathcal{L}_A [p] &= \sum_{p=4, p \equiv 0 \pmod{4}}^{4n} \left(r_{p-1}^0 r_{4n-p}^0 - \frac{1}{9} r_{p-2}^1 r_{4n-p-1}^0 \right), \\
 \sum_{p=1, p \equiv 1 \pmod{4}}^{4n-3} \det \mathcal{L}_A [p] &= \sum_{p=1, p \equiv 1 \pmod{4}}^{4n-3} \left(r_{p-1}^0 r_{4n-p}^1 - \frac{1}{9} r_{p-2}^1 r_{4n-p-1}^1 \right), \\
 \sum_{p=2, p \equiv 2 \pmod{4}}^{4n-2} \det \mathcal{L}_A [p] &= \sum_{p=2, p \equiv 2 \pmod{4}}^{4n-2} \left(r_{p-1}^0 r_{4n-p}^2 - \frac{1}{9} r_{p-2}^1 r_{4n-p-1}^2 \right), \\
 \sum_{p=3, p \equiv 3 \pmod{4}}^{4n-1} \det \mathcal{L}_A [p] &= \sum_{p=3, p \equiv 3 \pmod{4}}^{4n-1} \left(r_{p-1}^0 r_{4n-p}^3 - \frac{1}{9} r_{p-2}^1 r_{4n-p-1}^3 \right).
 \end{aligned} \tag{31}$$

By Facts 1 and 2, we have

$$\begin{aligned}
 \sum_{p=4, p \equiv 0 \pmod{4}}^{4n} \left(r_{p-1}^0 r_{4n-p}^0 - \frac{1}{9} r_{p-2}^1 r_{4n-p-1}^0 \right) &= \sum_{p=4, p \equiv 0 \pmod{4}}^{4n} \left[\frac{p}{12} \left(\frac{1}{36} \right)^{\binom{p-4}{4}} (4n-p+1) \frac{1}{12} \left(\frac{1}{36} \right)^{\binom{(4n-p)}{4}} \right. \\
 &\quad \left. - \frac{1}{9} (p-1) \frac{1}{4} \left(\frac{1}{36} \right)^{\binom{p-4}{4}} \frac{1}{12} (4n-p) \left(\frac{1}{36} \right)^{\binom{(4n-p-4)}{4}} \right] \\
 &= \sum_{p=4, p \equiv 0 \pmod{4}}^{4n} 12n \left(\frac{1}{36} \right)^n \\
 &= 12n^2 \left(\frac{1}{36} \right)^n.
 \end{aligned} \tag{32}$$

Similarly, by Facts 1–4, we can get

$$\begin{aligned}
 \sum_{p=1, p \equiv 1 \pmod{4}}^{4n-3} \left(r_{p-1}^0 r_{4n-p}^1 - \frac{1}{9} r_{p-2}^1 r_{4n-p-1}^1 \right) &= 12n^2 \left(\frac{1}{36} \right)^n, \\
 \sum_{p=2, p \equiv 2 \pmod{4}}^{4n-2} \left(r_{p-1}^0 r_{4n-p}^2 - \frac{1}{9} r_{p-2}^1 r_{4n-p-1}^2 \right) &= 8n^2 \left(\frac{1}{36} \right)^n, \\
 \sum_{p=3, p \equiv 3 \pmod{4}}^{4n-1} \left(r_{p-1}^0 r_{4n-p}^3 - \frac{1}{9} r_{p-2}^1 r_{4n-p-1}^3 \right) &= 8n^2 \left(\frac{1}{36} \right)^n.
 \end{aligned} \tag{33}$$

Hence, according to the above results, we have

$$(-1)^{4n-1} a_{4n-1} = \sum_{p=1}^{4n} \det \mathcal{L}_A [p] = 40n^2 \left(\frac{1}{36}\right)^n. \quad (34)$$

The proof of Claim 1 is completed. \square

Claim 2. $(-1)^{4n-2} a_{4n-2} = (2/3)(200n^4 - 11n^2)(1/36)^n$.

Proof. of Claim 2. It is not hard to see that $(-1)^{4n-2} a_{4n-2}$ is the total of those principal minors \mathcal{L}_A , which have $(4n - 2)$ rows and columns. Thus, we have

$$(-1)^{4n-2} a_{4n-2} = \sum_{1 \leq i < j \leq 4n} \det \mathcal{L}_A [p, q]. \quad (35)$$

By equation (35), it can be seen that the change of i and j values will lead to different $\det \mathcal{L}_A [p, q]$ results. Therefore, we will choose different p and q to list the following equations:

$$\begin{aligned} \sum_{1 \leq p < q \leq 4n} \det \mathcal{L}_A [p, q] &= \sum_{p=0 \pmod{4}}^{4n-4} \sum_{q=0 \pmod{4}}^{4n} \det \mathcal{L}_A [p, q] + \sum_{p=0 \pmod{4}}^{4n-4} \sum_{q=1 \pmod{4}}^{4n-3} \det \mathcal{L}_A [p, q] \\ &+ \sum_{p=0 \pmod{4}}^{4n-4} \sum_{q=2 \pmod{4}}^{4n-2} \det \mathcal{L}_A [p, q] + \sum_{p=0 \pmod{4}}^{4n-4} \sum_{q=3 \pmod{4}}^{4n-1} \det \mathcal{L}_A [p, q] \\ &+ \sum_{p=1 \pmod{4}}^{4n-3} \sum_{q=0 \pmod{4}}^{4n} \det \mathcal{L}_A [p, q] + \sum_{p=1 \pmod{4}}^{4n-3} \sum_{q=1 \pmod{4}}^{4n-3} \det \mathcal{L}_A [p, q] \\ &+ \sum_{p=1 \pmod{4}}^{4n-3} \sum_{q=2 \pmod{4}}^{4n-2} \det \mathcal{L}_A [p, q] + \sum_{p=1 \pmod{4}}^{4n-3} \sum_{q=3 \pmod{4}}^{4n-1} \det \mathcal{L}_A [p, q] \\ &+ \sum_{p=2 \pmod{4}}^{4n-2} \sum_{q=0 \pmod{4}}^{4n} \det \mathcal{L}_A [p, q] + \sum_{p=2 \pmod{4}}^{4n-2} \sum_{q=1 \pmod{4}}^{4n-3} \det \mathcal{L}_A [p, q] \\ &+ \sum_{p=2 \pmod{4}}^{4n-2} \sum_{q=2 \pmod{4}}^{4n-2} \det \mathcal{L}_A [p, q] + \sum_{p=2 \pmod{4}}^{4n-2} \sum_{q=3 \pmod{4}}^{4n-1} \det \mathcal{L}_A [p, q] \\ &+ \sum_{p=3 \pmod{4}}^{4n-1} \sum_{q=0 \pmod{4}}^{4n} \det \mathcal{L}_A [p, q] + \sum_{p=3 \pmod{4}}^{4n-2} \sum_{q=1 \pmod{4}}^{4n-3} \det \mathcal{L}_A [p, q] \\ &+ \sum_{p=3 \pmod{4}}^{4n-1} \sum_{q=2 \pmod{4}}^{4n-2} \det \mathcal{L}_A [p, q] + \sum_{p=3 \pmod{4}}^{4n-1} \sum_{q=3 \pmod{4}}^{4n-1} \det \mathcal{L}_A [p, q]. \end{aligned} \quad (36)$$

By Facts 1–4, we can compute the following results.

Case 1.

$$\begin{aligned} \sum_{p=0 \pmod{4}}^{4n-4} \sum_{q=0 \pmod{4}}^{4n} \det \mathcal{L}_A [p, q] &= \sum_{p=0 \pmod{4}}^{4n-4} \sum_{q=0 \pmod{4}}^{4n} \left(r_{p-1}^0 r_{q-p-1}^0 r_{4n-q}^0 - \frac{1}{9} r_{p-2}^1 r_{q-p-1}^0 r_{4n-q-1}^0 \right) \\ &= \sum_{p=0 \pmod{4}}^{4n-4} \sum_{q=0 \pmod{4}}^{4n} 9(q-p)(4n-q+p) \left(\frac{1}{36}\right)^n \\ &= 12(n^4 - n^2) \left(\frac{1}{36}\right)^n. \end{aligned} \quad (37)$$

Case 2.

$$\begin{aligned}
 \sum_{p \equiv 0 \pmod{4}}^{4n-4} \sum_{q \equiv 1 \pmod{4}}^{4n-3} \det \mathcal{L}_A[p, q] &= \sum_{p \equiv 0 \pmod{4}}^{4n-4} \sum_{q \equiv 1 \pmod{4}}^{4n-3} \left(r_{p-1}^0 r_{q-p-1}^0 r_{4n-q}^1 - \frac{1}{9} r_{p-2}^1 r_{q-p-1}^0 r_{4n-q-1}^1 \right) \\
 &= \sum_{p \equiv 0 \pmod{4}}^{4n-4} \sum_{q \equiv 1 \pmod{4}}^{4n-3} 9(q-p)(4n-q+p) \left(\frac{1}{36} \right)^n \\
 &= \frac{3}{2} (8n^4 - 12n^3 + n^2 + 3n) \left(\frac{1}{36} \right)^n.
 \end{aligned} \tag{38}$$

Case 3.

$$\begin{aligned}
 \sum_{p \equiv 0 \pmod{4}}^{4n-4} \sum_{q \equiv 2 \pmod{4}}^{4n-2} \det \mathcal{L}_A[p, q] &= \sum_{p \equiv 0 \pmod{4}}^{4n-4} \sum_{q \equiv 2 \pmod{4}}^{4n-2} \left(r_{p-1}^0 r_{q-p-1}^0 r_{4n-q}^2 - \frac{1}{9} r_{p-2}^1 r_{q-p-1}^0 r_{4n-q-1}^2 \right) \\
 &= \sum_{p \equiv 0 \pmod{4}}^{4n-4} \sum_{q \equiv 2 \pmod{4}}^{4n-2} 6(q-p)(4n-q+p) \left(\frac{1}{36} \right)^n \\
 &= (8n^4 + 8n^3 + 4n^2 + 4n) \left(\frac{1}{36} \right)^n.
 \end{aligned} \tag{39}$$

Case 4.

$$\begin{aligned}
 \sum_{p \equiv 0 \pmod{4}}^{4n-4} \sum_{q \equiv 3 \pmod{4}}^{4n-1} \det \mathcal{L}_A[p, q] &= \sum_{p \equiv 0 \pmod{4}}^{4n-4} \sum_{q \equiv 3 \pmod{4}}^{4n-1} \left(r_{p-1}^0 r_{q-p-1}^0 r_{4n-q}^3 - \frac{1}{9} r_{p-2}^1 r_{q-p-1}^0 r_{4n-q-1}^3 \right) \\
 &= \sum_{p \equiv 0 \pmod{4}}^{4n-4} \sum_{q \equiv 3 \pmod{4}}^{4n-1} 6(q-p)(4n-q+p) \left(\frac{1}{36} \right)^n \\
 &= (8n^4 - 4n^3 + n^2 - 5n) \left(\frac{1}{36} \right)^n.
 \end{aligned} \tag{40}$$

Case 5.

$$\begin{aligned}
 \sum_{p \equiv 1 \pmod{4}}^{4n-3} \sum_{q \equiv 0 \pmod{4}}^{4n} \det \mathcal{L}_A[p, q] &= \sum_{p \equiv 1 \pmod{4}}^{4n-3} \sum_{q \equiv 0 \pmod{4}}^{4n} \left(r_{p-1}^0 r_{q-p-1}^1 r_{4n-q}^0 - \frac{1}{9} r_{p-2}^1 r_{q-p-1}^1 r_{4n-q-1}^0 \right) \\
 &= \sum_{p \equiv 1 \pmod{4}}^{4n-3} \sum_{q \equiv 0 \pmod{4}}^{4n} 9(q-p)(4n-q+p) \left(\frac{1}{36} \right)^n \\
 &= \frac{3}{2} (8n^4 + 12n^3 + n^2 - 3n) \left(\frac{1}{36} \right)^n.
 \end{aligned} \tag{41}$$

Case 6.

$$\begin{aligned}
 \sum_{p \equiv 1 \pmod{4}}^{4n-3} \sum_{q \equiv 1 \pmod{4}}^{4n-3} \det \mathcal{L}_A[p, q] &= \sum_{p \equiv 1 \pmod{4}}^{4n-3} \sum_{q \equiv 1 \pmod{4}}^{4n-3} \left(r_{p-1}^0 r_{q-p-1}^1 r_{4n-q}^1 - \frac{1}{9} r_{p-2}^1 r_{q-p-1}^1 r_{4n-q-1}^1 \right) \\
 &= \sum_{p \equiv 1 \pmod{4}}^{4n-3} \sum_{q \equiv 1 \pmod{4}}^{4n-3} 9(q-p)(4n-q+p) \left(\frac{1}{36} \right)^n \\
 &= 12(n^4 - n^2) \left(\frac{1}{36} \right)^n.
 \end{aligned} \tag{42}$$

Case 7.

$$\begin{aligned}
 \sum_{p \equiv 1 \pmod{4}}^{4n-3} \sum_{q \equiv 2 \pmod{4}}^{4n-2} \det \mathcal{L}_A[p, q] &= \sum_{p \equiv 1 \pmod{4}}^{4n-3} \sum_{q \equiv 2 \pmod{4}}^{4n-2} \left(r_{p-1}^0 r_{q-p-1}^1 r_{4n-q}^2 - \frac{1}{9} r_{p-2}^1 r_{q-p-1}^1 r_{4n-q-1}^2 \right) \\
 &= \sum_{p \equiv 1 \pmod{4}}^{4n-3} \sum_{q \equiv 2 \pmod{4}}^{4n-2} 9(q-p)(4n-q+p) \left(\frac{1}{36} \right)^n \\
 &= (8n^4 + 4n^3 + n^2 + 5n) \left(\frac{1}{36} \right)^n.
 \end{aligned} \tag{43}$$

Case 8.

$$\begin{aligned}
 \sum_{p \equiv 1 \pmod{4}}^{4n-3} \sum_{q \equiv 3 \pmod{4}}^{4n-1} \det \mathcal{L}_A[p, q] &= \sum_{p \equiv 1 \pmod{4}}^{4n-3} \sum_{q \equiv 3 \pmod{4}}^{4n-1} \left(r_{p-1}^0 r_{q-p-1}^1 r_{4n-q}^3 - \frac{1}{9} r_{p-2}^1 r_{q-p-1}^1 r_{4n-q-1}^3 \right) \\
 &= \sum_{p \equiv 1 \pmod{4}}^{4n-3} \sum_{q \equiv 3 \pmod{4}}^{4n-1} 6(q-p)(4n-q+p) \left(\frac{1}{36} \right)^n \\
 &= (8n^4 - 8n^3 + 4n^2 - 4n) \left(\frac{1}{36} \right)^n.
 \end{aligned} \tag{44}$$

Case 9.

$$\begin{aligned}
 \sum_{p \equiv 2 \pmod{4}}^{4n-2} \sum_{q \equiv 0 \pmod{4}}^{4n} \det \mathcal{L}_A[p, q] &= \sum_{p \equiv 2 \pmod{4}}^{4n-2} \sum_{q \equiv 0 \pmod{4}}^{4n} \left(r_{p-1}^0 r_{q-p-1}^2 r_{4n-q}^0 - \frac{1}{9} r_{p-2}^1 r_{q-p-1}^2 r_{4n-q-1}^0 \right) \\
 &= \sum_{p \equiv 2 \pmod{4}}^{4n-2} \sum_{q \equiv 0 \pmod{4}}^{4n} 6(q-p)(4n-q+p) \left(\frac{1}{36} \right)^n \\
 &= (8n^4 + 8n^3 + 4n^2 + 4n) \left(\frac{1}{36} \right)^n.
 \end{aligned} \tag{45}$$

Case 10.

$$\begin{aligned}
 \sum_{p \equiv 2 \pmod{4}}^{4n-2} \sum_{q \equiv 1 \pmod{4}}^{4n-3} \det \mathcal{L}_A[p, q] &= \sum_{p \equiv 2 \pmod{4}}^{4n-2} \sum_{q \equiv 1 \pmod{4}}^{4n-3} \left(r_{p-1}^0 r_{q-p-1}^2 r_{4n-q}^1 - \frac{1}{9} r_{p-2}^1 r_{q-p-1}^2 r_{4n-q-1}^1 \right) \\
 &= \sum_{p \equiv 2 \pmod{4}}^{4n-2} \sum_{q \equiv 1 \pmod{4}}^{4n-3} 6(q-p)(4n-q+p) \left(\frac{1}{36} \right)^n \\
 &= (8n^4 - 4n^3 + n^2 - 5n) \left(\frac{1}{36} \right)^n.
 \end{aligned} \tag{46}$$

Case 11.

$$\begin{aligned}
 \sum_{p \equiv 2 \pmod{4}}^{4n-2} \sum_{q \equiv 2 \pmod{4}}^{4n-2} \det \mathcal{L}_A[p, q] &= \sum_{p \equiv 2 \pmod{4}}^{4n-2} \sum_{q \equiv 2 \pmod{4}}^{4n-2} \left(r_{p-1}^0 r_{q-p-1}^2 r_{4n-q}^2 - \frac{1}{9} r_{p-2}^1 r_{q-p-1}^2 r_{4n-q-1}^2 \right) \\
 &= \sum_{p \equiv 2 \pmod{4}}^{4n-2} \sum_{q \equiv 2 \pmod{4}}^{4n-2} 4(q-p)(4n-q+p) \left(\frac{1}{36} \right)^n \\
 &= \frac{16}{3} (n^4 - n^2) \left(\frac{1}{36} \right)^n.
 \end{aligned} \tag{47}$$

Case 12.

$$\begin{aligned}
 \sum_{p \equiv 2 \pmod{4}}^{4n-2} \sum_{q \equiv 3 \pmod{4}}^{4n-1} \det \mathcal{L}_A[p, q] &= \sum_{p \equiv 2 \pmod{4}}^{4n-2} \sum_{q \equiv 3 \pmod{4}}^{4n-1} \left(r_{p-1}^0 r_{q-p-1}^2 r_{4n-q}^3 - \frac{1}{9} r_{p-2}^1 r_{q-p-1}^2 r_{4n-q-1}^3 \right) \\
 &= \sum_{p \equiv 2 \pmod{4}}^{4n-2} \sum_{q \equiv 3 \pmod{4}}^{4n-1} 4(q-p)(4n-q+p) \left(\frac{1}{36} \right)^n \\
 &= \frac{2}{3} (8n^4 + 4n^3 + n^2 + 5n) \left(\frac{1}{36} \right)^n.
 \end{aligned} \tag{48}$$

Case 13.

$$\begin{aligned}
 \sum_{p \equiv 3 \pmod{4}}^{4n-1} \sum_{q \equiv 0 \pmod{4}}^{4n} \det \mathcal{L}_A[p, q] &= \sum_{p \equiv 3 \pmod{4}}^{4n-1} \sum_{q \equiv 0 \pmod{4}}^{4n} \left(r_{p-1}^0 r_{q-p-1}^3 r_{4n-q}^0 - \frac{1}{9} r_{p-2}^1 r_{q-p-1}^3 r_{4n-q-1}^0 \right) \\
 &= \sum_{p \equiv 3 \pmod{4}}^{4n-1} \sum_{q \equiv 0 \pmod{4}}^{4n} 6(q-p)(4n-q+p) \left(\frac{1}{36} \right)^n \\
 &= (8n^4 + 4n^3 + n^2 + 5n) \left(\frac{1}{36} \right)^n.
 \end{aligned} \tag{49}$$

Case 14.

$$\begin{aligned}
 \sum_{p \equiv 3 \pmod{4}}^{4n-1} \sum_{q \equiv 1 \pmod{4}}^{4n-3} \det \mathcal{L}_A[p, q] &= \sum_{p \equiv 3 \pmod{4}}^{4n-1} \sum_{q \equiv 1 \pmod{4}}^{4n-3} \left(r_{p-1}^0 r_{q-p-1}^3 r_{4n-q}^1 - \frac{1}{9} r_{p-2}^1 r_{q-p-1}^3 r_{4n-q-1}^1 \right) \\
 &= \sum_{p \equiv 3 \pmod{4}}^{4n-1} \sum_{q \equiv 1 \pmod{4}}^{4n-3} 6(q-p)(4n-q+p) \left(\frac{1}{36} \right)^n \\
 &= (8n^4 - 8n^3 + 4n^2 - 4n) \left(\frac{1}{36} \right)^n.
 \end{aligned} \tag{50}$$

Case 15.

$$\begin{aligned}
 \sum_{p \equiv 3 \pmod{4}}^{4n-1} \sum_{q \equiv 2 \pmod{4}}^{4n-2} \det \mathcal{L}_A[p, q] &= \sum_{p \equiv 3 \pmod{4}}^{4n-1} \sum_{q \equiv 2 \pmod{4}}^{4n-2} \left(r_{p-1}^0 r_{q-p-1}^3 r_{4n-q}^2 - \frac{1}{9} r_{p-2}^1 r_{q-p-1}^3 r_{4n-q-1}^2 \right) \\
 &= \sum_{p \equiv 3 \pmod{4}}^{4n-1} \sum_{q \equiv 2 \pmod{4}}^{4n-2} 4(q-p)(4n-q+p) \left(\frac{1}{36} \right)^n \\
 &= \frac{2}{3} (8n^4 - 4n^3 + n^2 - 5n) \left(\frac{1}{36} \right)^n.
 \end{aligned} \tag{51}$$

Case 16.

$$\begin{aligned}
 \sum_{p \equiv 3 \pmod{4}}^{4n-1} \sum_{q \equiv 3 \pmod{4}}^{4n-1} \det \mathcal{L}_A[p, q] &= \sum_{p \equiv 3 \pmod{4}}^{4n-1} \sum_{q \equiv 3 \pmod{4}}^{4n-1} \left(r_{p-1}^0 r_{q-p-1}^3 r_{4n-q}^3 - \frac{1}{9} r_{p-2}^1 r_{q-p-1}^3 r_{4n-q-1}^3 \right) \\
 &= \sum_{p \equiv 3 \pmod{4}}^{4n-1} \sum_{q \equiv 3 \pmod{4}}^{4n-1} 4(q-p)(4n-q+p) \left(\frac{1}{36} \right)^n \\
 &= \frac{16}{3} (n^4 - n^2) \left(\frac{1}{36} \right)^n.
 \end{aligned} \tag{52}$$

Then, according to the value of p , the above sixteen cases can be divided into the following four categories:

$$\begin{aligned}
 F_0 &= \sum_{p \equiv 0 \pmod{4}}^{4n-4} \sum_{q \equiv 0 \pmod{4}}^{4n} \det \mathcal{L}_A[p, q] + \sum_{p \equiv 0 \pmod{4}}^{4n-4} \sum_{q \equiv 1 \pmod{4}}^{4n-3} \det \mathcal{L}_A[p, q] \\
 &\quad + \sum_{p \equiv 0 \pmod{4}}^{4n-4} \sum_{q \equiv 2 \pmod{4}}^{4n-2} \det \mathcal{L}_A[p, q] + \sum_{p \equiv 0 \pmod{4}}^{4n-4} \sum_{q \equiv 3 \pmod{4}}^{4n-1} \det \mathcal{L}_A[p, q] \\
 &= \frac{1}{2} (80n^4 - 28n^3 - 11n^2 + 7n) \left(\frac{1}{36} \right)^n,
 \end{aligned}$$

$$\begin{aligned}
 F_1 &= \sum_{p \equiv 1 \pmod{4}}^{4n-3} \sum_{q \equiv 0 \pmod{4}}^{4n} \det \mathcal{L}_A[p, q] + \sum_{p \equiv 1 \pmod{4}}^{4n-3} \sum_{q \equiv 1 \pmod{4}}^{4n-3} \det \mathcal{L}_A[p, q] \\
 &\quad + \sum_{p \equiv 1 \pmod{4}}^{4n-3} \sum_{q \equiv 2 \pmod{4}}^{4n-2} \det \mathcal{L}_A[p, q] + \sum_{p \equiv 1 \pmod{4}}^{4n-3} \sum_{q \equiv 3 \pmod{4}}^{4n-1} \det \mathcal{L}_A[p, q] \\
 &= \frac{1}{2} (80n^4 + 28n^3 - 11n^2 - 7n) \left(\frac{1}{36}\right)^n. \\
 F_2 &= \sum_{p \equiv 2 \pmod{4}}^{4n-2} \sum_{q \equiv 0 \pmod{4}}^{4n} \det \mathcal{L}_A[p, q] + \sum_{p \equiv 2 \pmod{4}}^{4n-2} \sum_{q \equiv 1 \pmod{4}}^{4n-3} \det \mathcal{L}_A[p, q] \\
 &\quad + \sum_{p \equiv 2 \pmod{4}}^{4n-2} \sum_{q \equiv 2 \pmod{4}}^{4n-2} \det \mathcal{L}_A[p, q] + \sum_{p \equiv 2 \pmod{4}}^{4n-2} \sum_{q \equiv 3 \pmod{4}}^{4n-1} \det \mathcal{L}_A[p, q] \\
 &= \frac{1}{3} (80n^4 + 20n^3 + n^2 + 7n) \left(\frac{1}{36}\right)^n, \\
 F_3 &= \sum_{p \equiv 3 \pmod{4}}^{4n-1} \sum_{q \equiv 0 \pmod{4}}^{4n} \det \mathcal{L}_A[p, q] + \sum_{p \equiv 3 \pmod{4}}^{4n-2} \sum_{q \equiv 1 \pmod{4}}^{4n-3} \det \mathcal{L}_A[p, q] \\
 &\quad + \sum_{p \equiv 3 \pmod{4}}^{4n-1} \sum_{q \equiv 2 \pmod{4}}^{4n-2} \det \mathcal{L}_A[p, q] + \sum_{p \equiv 3 \pmod{4}}^{4n-1} \sum_{q \equiv 3 \pmod{4}}^{4n-1} \det \mathcal{L}_A[p, q] \\
 &= \frac{1}{3} (80n^4 - 20n^3 + 10n^2 - 7n) \left(\frac{1}{36}\right)^n.
 \end{aligned} \tag{53}$$

Substituting $F_0, F_1, F_2,$ and F_3 into equation (35), one has

$$(-1)^{4n-2} a_{4n-2} = F_0 + F_1 + F_2 + F_3 = \frac{2}{3} (200n^4 - 11n^2) \left(\frac{1}{36}\right)^n. \tag{54}$$

This completes the proof. \square

Proof. Let

So, substituting the results of Claims 1 and 2 into equation (20) yields

$$\begin{aligned}
 P_{L_S}(x) &= \det(xI - \mathcal{L}_S) = x^{4n} + b_1 x^{4n-1} + \dots + b_{4n-1} x + b_{4n} \\
 &= x(x^{4n-1} + b_1 x^{4n-2} + \dots + b_{4n-2} x + b_{4n-1}), \quad b_{4n-1} \neq 0.
 \end{aligned} \tag{57}$$

$$\begin{aligned}
 \sum_{p=2}^{4n} \frac{1}{n_p} &= \frac{(-1)^{4n-2} a_{4n-2}}{(-1)^{4n-1} a_{4n-1}} \\
 &= \frac{(2/3)(200n^4 - 11n^2)(1/36)^n}{40n^2 (1/36)^n} \\
 &= \frac{200n^2 - 11}{60}.
 \end{aligned} \tag{55}$$

Then, we can exactly get that $\varphi_1, \varphi_2, \dots, \varphi_{4n}$ are the roots of the following equation:

$$x^{4n-1} + b_1 x^{4n-2} + \dots + b_{4n-2} x + b_{4n-1} = 0. \tag{58}$$

Based on Vieta's theorem of $P_{\mathcal{L}_S}(x)$, one has

$$\sum_{q=1}^{4n} \frac{1}{\varphi_q} = \frac{(-1)^{4n-1} b_{4n-1}}{(-1)^{4n} b_{4n}} = \frac{(-1)^{4n-1} b_{4n-1}}{\det \mathcal{L}_S}. \tag{59}$$

Theorem 2.

Before calculating $(-1)^{4n-1} b_{4n-1}$ and $\det \mathcal{L}_S$, we must determine i th order principal submatrices $S_q^0, S_q^1, S_q^2,$ and S_q^3 , which consist of the first q rows and columns of the matrices $\mathcal{L}_S^0, \mathcal{L}_S^1, \mathcal{L}_S^2,$ and \mathcal{L}_S^3 , respectively, $q = 1, 2, \dots, 4n$. Let

$$\sum_{q=1}^{4n} \frac{1}{\varphi_q} = \frac{41n\sqrt{14}}{28} \left[\frac{((15 + 4\sqrt{14})^n - (15 - 4\sqrt{14})^n)}{((15 + 4\sqrt{14})^n + (15 - 4\sqrt{14})^n) + 2} \right]. \tag{56}$$

n this way, let us start with the following facts.

Fact 5. For $1 \leq q \leq 4n$,

$$s_q^0 = \begin{cases} \left(\frac{4}{8} + \frac{9\sqrt{14}}{56}\right)\left(\frac{5}{12} + \frac{\sqrt{14}}{9}\right)^{(q/4)} + \left(\frac{4}{8} - \frac{9\sqrt{14}}{56}\right)\left(\frac{5}{12} - \frac{\sqrt{14}}{9}\right)^{(q/4)}, & \text{if } q \equiv 0 \pmod{4}, \\ \left(\frac{2}{3} + \frac{31\sqrt{14}}{168}\right)\left(\frac{5}{12} + \frac{\sqrt{14}}{9}\right)^{(q-1/4)} + \left(\frac{2}{3} - \frac{31\sqrt{14}}{168}\right)\left(\frac{5}{12} - \frac{\sqrt{14}}{9}\right)^{(q-1/4)}, & \text{if } q \equiv 1 \pmod{4}, \\ \left(\frac{7}{12} + \frac{53\sqrt{14}}{336}\right)\left(\frac{5}{12} + \frac{\sqrt{14}}{9}\right)^{(q-2/4)} + \left(\frac{7}{12} - \frac{53\sqrt{14}}{336}\right)\left(\frac{5}{12} - \frac{\sqrt{14}}{9}\right)^{(q-2/4)}, & \text{if } q \equiv 1 \pmod{4}, \\ \left(\frac{5}{12} + \frac{25\sqrt{14}}{224}\right)\left(\frac{5}{12} + \frac{\sqrt{14}}{9}\right)^{(q-3/4)} + \left(\frac{5}{12} - \frac{25\sqrt{14}}{224}\right)\left(\frac{5}{12} - \frac{\sqrt{14}}{9}\right)^{(q-3/4)}, & \text{if } q \equiv 3 \pmod{4}. \end{cases} \tag{61}$$

Fact 6. For $1 \leq q \leq 4n$,

$$s_q^1 = \begin{cases} \left(\frac{1}{2} + \frac{11\sqrt{14}}{56}\right)\left(\frac{5}{12} + \frac{\sqrt{14}}{9}\right)^{(q/4)} + \left(\frac{1}{2} - \frac{11\sqrt{14}}{56}\right)\left(\frac{5}{12} - \frac{\sqrt{14}}{9}\right)^{(q/4)}, & \text{if } q \equiv 0 \pmod{4}, \\ \left(\frac{1}{2} + \frac{17\sqrt{14}}{112}\right)\left(\frac{5}{12} + \frac{\sqrt{14}}{9}\right)^{(q-1/4)} + \left(\frac{1}{2} - \frac{17\sqrt{14}}{112}\right)\left(\frac{5}{12} - \frac{\sqrt{14}}{9}\right)^{(q-1/4)}, & \text{if } q \equiv 1 \pmod{4}, \\ \left(\frac{3}{8} + \frac{23\sqrt{14}}{224}\right)\left(\frac{5}{12} + \frac{\sqrt{14}}{9}\right)^{(q-2/4)} + \left(\frac{3}{8} - \frac{23\sqrt{14}}{224}\right)\left(\frac{5}{12} - \frac{\sqrt{14}}{9}\right)^{(q-2/4)}, & \text{if } q \equiv 1 \pmod{4}, \\ \left(\frac{5}{12} + \frac{25\sqrt{14}}{224}\right)\left(\frac{5}{12} + \frac{\sqrt{14}}{9}\right)^{(q-3/4)} + \left(\frac{5}{12} - \frac{25\sqrt{14}}{224}\right)\left(\frac{5}{12} - \frac{\sqrt{14}}{9}\right)^{(q-3/4)}, & \text{if } q \equiv 3 \pmod{4}. \end{cases} \tag{62}$$

Fact 7. For $1 \leq q \leq 4n$,

$$s_q^2 = \frac{7}{6}s_{q-2}^0 - \frac{1}{9}s_{q-3}^1. \tag{63}$$

Fact 8. For $1 \leq q \leq 4n$,

$$s_q^3 = \frac{4}{3}s_{q-1}^0 - \frac{1}{9}s_{q-2}^1. \tag{64}$$

Proof. of Fact 5. Take $s_q^0 = \det S_q^0$, $s_q^1 = \det S_q^1$, $s_q^2 = \det S_q^2$, and $s_q^3 = \det S_q^3$. By direct calculation, it is not difficult to get the following values (see Table 2).

For $4 \leq q \leq 4n$, we have $\det S_q^0$

$$s_q^0 = \begin{cases} \frac{4}{3}s_{q-1}^0 - \frac{1}{6}s_{q-2}^0, & \text{if } q \equiv 0 \pmod{4}, \\ \frac{4}{3}s_{q-1}^0 - \frac{1}{9}s_{q-2}^0, & \text{if } q \equiv 1 \pmod{4}, \\ s_{q-1}^0 - \frac{1}{6}s_{q-2}^0, & \text{if } q \equiv 2 \pmod{4}, \\ s_{q-1}^0 - \frac{1}{4}s_{q-2}^0, & \text{if } q \equiv 3 \pmod{4}. \end{cases} \tag{65}$$

For $1 \leq q \leq n$, let $A_q = s_{4q}$; for $0 \leq q \leq n-1$, let $B_q = s_{4q+1}$, $C_q = s_{4q+2}$, $D_q = s_{4q+3}$. Then, we may obtain that

TABLE 2: Initial value.

s_q^0	Value	s_q^0	Value	s_q^0	Value	s_q^0	Value
s_1^0	(4/3)	s_2^0	(7/6)	s_3^0	(5/6)	s_4^0	(33/36)
s_5^0	(61/54)	s_6^0	(211/216)	s_7^0	(25/36)	s_8^0	(989/1296)

$$\begin{cases} A_q = \frac{4}{3}D_{q-1} - \frac{1}{6}C_{q-1}, \\ B_q = \frac{4}{3}A_q - \frac{1}{9}D_{q-1}, \\ C_q = B_q - \frac{1}{6}A_q, \\ D_q = C_q - \frac{1}{4}B_q. \end{cases} \quad (66)$$

From the first three equations in (66), one can get $A_q = (12/13)C_q + (1/78)C_{q-1}$. Next, substituting A_q into the third equation, one has $B_q = (15/13)C_q + (1/468)C_{q-1}$. Then, substituting B_q into the fourth equation, we have $D_q = (37/52)C_q - (1/1872)C_{q-1}$. Finally, substituting A_q and d_q into the first equation, one has $c_q - 30c_{q-1} + c_{q-2} = 0$. Thus,

$$C_q = k_1 \left(\frac{5}{12} + \frac{\sqrt{14}}{9} \right)^q + k_2 \left(\frac{5}{12} - \frac{\sqrt{14}}{9} \right)^q. \quad (67)$$

In view of $C_0 = (7/6), C_1 = (211/216)$, we have

$$\begin{cases} k_1 + k_2 = \frac{7}{6}, \\ k_1 \left(\frac{5}{12} + \frac{\sqrt{14}}{9} \right) + k_2 \left(\frac{5}{12} - \frac{\sqrt{14}}{9} \right) = \frac{211}{216}, \\ k_1 = \left(\frac{7}{12} + \frac{53\sqrt{14}}{336} \right), \\ k_2 = \left(\frac{7}{12} - \frac{53\sqrt{14}}{336} \right). \end{cases} \quad (68)$$

Thus, it is routine to deduce that

$$\begin{cases} A_q = \left(\frac{4}{8} + \frac{9\sqrt{14}}{56} \right) \left(\frac{5}{12} + \frac{\sqrt{14}}{9} \right)^q + \left(\frac{4}{8} - \frac{9\sqrt{14}}{56} \right) \left(\frac{5}{12} - \frac{\sqrt{14}}{9} \right)^q, & \text{if } q \equiv 0 \pmod{4}, \\ B_q = \left(\frac{2}{3} + \frac{31\sqrt{14}}{168} \right) \left(\frac{5}{12} + \frac{\sqrt{14}}{9} \right)^q + \left(\frac{2}{3} - \frac{31\sqrt{14}}{168} \right) \left(\frac{5}{12} - \frac{\sqrt{14}}{9} \right)^q, & \text{if } q \equiv 1 \pmod{4}, \\ C_q = \left(\frac{7}{12} + \frac{53\sqrt{14}}{336} \right) \left(\frac{5}{12} + \frac{\sqrt{14}}{9} \right)^q + \left(\frac{7}{12} - \frac{53\sqrt{14}}{336} \right) \left(\frac{5}{12} - \frac{\sqrt{14}}{9} \right)^q, & \text{if } q \equiv 1 \pmod{4}, \\ D_q = \left(\frac{5}{12} + \frac{25\sqrt{14}}{224} \right) \left(\frac{5}{12} + \frac{\sqrt{14}}{9} \right)^q + \left(\frac{5}{12} - \frac{25\sqrt{14}}{224} \right) \left(\frac{5}{12} - \frac{\sqrt{14}}{9} \right)^q, & \text{if } q \equiv 3 \pmod{4}. \end{cases} \quad (69)$$

In the same way, we can quickly prove the result of Fact 6.

Then, we expand dets_q^2 and dets_q^3 according to the properties of determinant, and we can get Facts 7 and 8.

Now by exploiting the property of determinant, we can get

$$\begin{aligned}
 \det \mathcal{L}_S &= \begin{vmatrix} \frac{4}{3} & \frac{-1}{\sqrt{6}} & 0 & \dots & 0 & 0 & \frac{1}{3} \\ \frac{-1}{\sqrt{6}} & 1 & \frac{-1}{2} & \dots & 0 & 0 & 0 \\ 0 & \frac{-1}{2} & 1 & \dots & 0 & 0 & 0 \\ \vdots & \vdots & \vdots & \ddots & \vdots & \vdots & \vdots \\ 0 & 0 & 0 & \dots & 1 & \frac{-1}{2} & 0 \\ 0 & 0 & 0 & \dots & 0 & 1 & \frac{-1}{\sqrt{6}} \\ \frac{1}{3} & 0 & 0 & \dots & 0 & \frac{-1}{\sqrt{6}} & \frac{4}{3} \end{vmatrix}_{4n} = \begin{vmatrix} \frac{4}{3} & \frac{-1}{\sqrt{6}} & 0 & \dots & 0 & 0 & 0 \\ \frac{-1}{\sqrt{6}} & 1 & \frac{-1}{2} & \dots & 0 & 0 & 0 \\ 0 & \frac{-1}{2} & 1 & \dots & 0 & 0 & 0 \\ \vdots & \vdots & \vdots & \ddots & \vdots & \vdots & \vdots \\ 0 & 0 & 0 & \dots & 1 & \frac{-1}{2} & 0 \\ 0 & 0 & 0 & \dots & 0 & 1 & \frac{-1}{\sqrt{6}} \\ \frac{1}{3} & 0 & 0 & \dots & 0 & \frac{-1}{\sqrt{6}} & \frac{4}{3} \end{vmatrix}_{4n} \\
 &+ \begin{vmatrix} \frac{4}{3} & \frac{-1}{\sqrt{6}} & 0 & \dots & 0 & 0 & \frac{1}{3} \\ \frac{-1}{\sqrt{6}} & 1 & \frac{-1}{2} & \dots & 0 & 0 & 0 \\ 0 & \frac{-1}{2} & 1 & \dots & 0 & 0 & 0 \\ \vdots & \vdots & \vdots & \ddots & \vdots & \vdots & \vdots \\ 0 & 0 & 0 & \dots & 1 & \frac{-1}{2} & 0 \\ 0 & 0 & 0 & \dots & 0 & 1 & 0 \\ \frac{1}{3} & 0 & 0 & \dots & 0 & \frac{-1}{\sqrt{6}} & 0 \end{vmatrix}_{4n} \\
 &= s_{4n}^0 - \frac{1}{9} s_{4n-2}^1 + 2 \left(\frac{1}{36} \right)^n.
 \end{aligned} \tag{70}$$

With Facts 1 and 2, we can obtain one interesting claim.

Claim 3. $\det \mathcal{L}_S = ((5/12) + (\sqrt{14}/9))^n + ((5/12) - (\sqrt{14}/9))^n + 2(1/36)^n$.

Then, we are going to concentrate on calculating $(-1)^{4n-1} b_{4n-1}$.

Claim 4. $(-1)^{4n} - 1 b_{4n-1} = (41n\sqrt{14}/28) [((15 + 4\sqrt{14})^n - (15 - 4\sqrt{14})^n) / ((15 + 4\sqrt{14})^n + (15 - 4\sqrt{14})^n + 2)]$.

Proof. Since $(-1)^{4n-1} b_{4n-1}$ is the total of all the principal minors of order $4n - 1$ of \mathcal{L}_S , we have

$$\begin{aligned}
 (-1)^{4n-1} b_{4n-1} &= \sum_{q=1}^{4n} \det \mathcal{L}_S[q] = \sum_{q=4, q \equiv 0 \pmod{4}}^{4n} \det \mathcal{L}_S[q] + \sum_{q=1, q \equiv 1 \pmod{4}}^{4n-3} \det \mathcal{L}_S[q] \\
 &+ \sum_{q=2, q \equiv 2 \pmod{4}}^{4n-2} \det \mathcal{L}_S[q] + \sum_{q=3, q \equiv 3 \pmod{4}}^{4n-1} \det \mathcal{L}_S[q],
 \end{aligned} \tag{71}$$

where

$$\det \mathcal{L}_S[q] = \begin{cases} s_{q-1}^0 s_{4n-q}^0 - \frac{1}{9} s_{q-2}^1 s_{4n-q-1}^0, & \text{if } q \equiv 0 \pmod{4}, \\ s_{q-1}^0 s_{4n-q}^1 - \frac{1}{9} s_{q-2}^1 s_{4n-q-1}^1, & \text{if } q \equiv 1 \pmod{4}, \\ s_{q-1}^0 s_{4n-q}^2 - \frac{1}{9} s_{q-2}^1 s_{4n-q-1}^2, & \text{if } q \equiv 2 \pmod{4}, \\ s_{q-1}^0 s_{4n-q}^3 - \frac{1}{9} s_{q-2}^1 s_{4n-q-1}^3, & \text{if } q \equiv 3 \pmod{4}. \end{cases} \tag{72}$$

For $q \equiv 0 \pmod{4}$ and $4 \leq q \leq 4n - 4$, in view of (72) and Facts 5–8, one gets

$$\begin{aligned} \det \mathcal{L}_S[q] &= s_{q-1}^0 s_{4n-q}^0 - \frac{1}{9} s_{q-2}^1 s_{4n-q-1}^0 \\ &= \left(\frac{5}{12} + \frac{25\sqrt{14}}{224} \right) \left(\frac{5}{12} + \frac{\sqrt{14}}{9} \right)^{(j-4/4)} \\ &\quad + \left(\frac{5}{12} - \frac{25\sqrt{14}}{224} \right) \left(\frac{5}{12} - \frac{\sqrt{14}}{9} \right)^{(j-4/4)} \\ &\quad \times \left[\left(\frac{4}{8} + \frac{25\sqrt{14}}{56} \right) \left(\frac{5}{12} + \frac{\sqrt{14}}{9} \right)^{((4n-j)/4)} + \left(\frac{4}{8} - \frac{25\sqrt{14}}{56} \right) \left(\frac{5}{12} - \frac{\sqrt{14}}{9} \right)^{((4n-j)/4)} \right] \\ &\quad - \frac{1}{9} \left[\left(\frac{3}{8} + \frac{23\sqrt{14}}{224} \right) \left(\frac{5}{12} + \frac{\sqrt{14}}{9} \right)^{((j-4)/4)} + \left(\frac{3}{8} - \frac{23\sqrt{14}}{224} \right) \left(\frac{5}{12} - \frac{\sqrt{14}}{9} \right)^{((j-4)/4)} \right] \\ &\quad \times \left[\left(\frac{5}{12} + \frac{25\sqrt{14}}{224} \right) \left(\frac{5}{12} + \frac{\sqrt{14}}{9} \right)^{((4n-j-4)/4)} + \left(\frac{5}{12} - \frac{25\sqrt{14}}{224} \right) \left(\frac{5}{12} - \frac{\sqrt{14}}{9} \right)^{((4n-j-4)/4)} \right] \\ &= \frac{15n\sqrt{14}}{56} \left[\left(\frac{5}{12} + \frac{\sqrt{14}}{9} \right)^n - \left(\frac{5}{12} - \frac{\sqrt{14}}{9} \right)^n \right]. \end{aligned} \tag{73}$$

Similarly, for $q \equiv 1 \pmod{4}$ and $1 \leq q \leq 4n - 3$, we have

$$\begin{aligned} \sum_{q=1, q \equiv 1 \pmod{4}}^{4n-3} \det \mathcal{L}_S[q] &= s_{q-1}^0 s_{4n-q}^1 - \frac{1}{9} s_{q-2}^1 s_{4n-q-1}^1 \\ &= \frac{15n\sqrt{14}}{56} \left[\left(\frac{5}{12} + \frac{\sqrt{14}}{9} \right)^n - \left(\frac{5}{12} - \frac{\sqrt{14}}{9} \right)^n \right]. \end{aligned} \tag{74}$$

For $q \equiv 2 \pmod{4}$ and $2 \leq q \leq 4n - 2$, we have

$$\begin{aligned} \sum_{q=2, q \equiv 2 \pmod{4}}^{4n-2} \det \mathcal{L}_S[q] &= s_{q-1}^0 s_{4n-q}^2 - \frac{1}{9} s_{q-2}^1 s_{4n-q-1}^2 \\ &= \frac{13n\sqrt{14}}{28} \left[\left(\frac{5}{12} + \frac{\sqrt{14}}{9} \right)^n - \left(\frac{5}{12} - \frac{\sqrt{14}}{9} \right)^n \right]. \end{aligned} \tag{75}$$

For $q \equiv 3 \pmod{4}$ and $3 \leq q \leq 4n - 1$, we have

$$\begin{aligned} \sum_{q=3, q \equiv 3 \pmod{4}}^{4n-1} \det \mathcal{L}_S[q] &= s_{q-1}^0 s_{4n-q}^3 - \frac{1}{9} s_{q-2}^1 s_{4n-q-1}^3 \\ &= \frac{13n\sqrt{14}}{28} \left[\left(\frac{5}{12} + \frac{\sqrt{14}}{9} \right)^n - \left(\frac{5}{12} - \frac{\sqrt{14}}{9} \right)^n \right]. \end{aligned} \tag{76}$$

Thus, one has the following equation:

$$(-1)^{4n-1} b_{4n-1} = \frac{41n\sqrt{14}}{28} \left[\left(\frac{5}{12} + \frac{\sqrt{14}}{9} \right)^n - \left(\frac{5}{12} - \frac{\sqrt{14}}{9} \right)^n \right]. \tag{77}$$

Therefore, substituting the results of Claims 3 and 4 into (59) yields

$$\sum_{q=1}^{4n} \frac{1}{\varphi_q} = \frac{41n\sqrt{14}}{28} \left[\frac{((15 + 4\sqrt{14})^n - (15 - 4\sqrt{14})^n)}{((15 + 4\sqrt{14})^n + (15 - 4\sqrt{14})^n) + 2} \right], \tag{78}$$

as desired. \square

Note that $|E_{MQ_n}(8, 4)| = 10n$. Taking the results of Theorems 1 and 2 to (a) and (b) of Lemma 2, we can immediately get the following two theorems.

Theorem 3. *Let $MQ_n(8, 4)$ be a Möbius graph with n octagons and n quadrilaterals. Then,*

$$\begin{aligned} Kc(MQ_n(8, 4)) &= \sum_{p=2}^{4n} \frac{1}{\eta_p} + \sum_{q=1}^{4n} \frac{1}{\varphi_q} \\ &= \frac{200n^2 - 11}{60} + \frac{41n\sqrt{14}}{28} \left[\frac{((15 + 4\sqrt{14})^n - (15 - 4\sqrt{14})^n)}{((15 + 4\sqrt{14})^n + (15 - 4\sqrt{14})^n) + 2} \right]. \end{aligned} \tag{79}$$

Theorem 4. *Let $MQ_n(8, 4)$ be a Möbius graph with n octagons and n quadrilaterals. Then,*

$$\begin{aligned} Kf^*(MQ_n(8, 4)) &= 20n \left(\sum_{p=2}^{4n} \frac{1}{\eta_p} + \sum_{q=1}^{4n} \frac{1}{\varphi_q} \right) \\ &= 20n \left(\frac{200n^2 - 11}{60} + \frac{41n\sqrt{14}}{28} \left[\frac{((15 + 4\sqrt{14})^n - (15 - 4\sqrt{14})^n)}{((15 + 4\sqrt{14})^n + (15 - 4\sqrt{14})^n) + 2} \right] \right) \\ &= \frac{200n^3 - 11n}{3} + 20n\varrho(n), \end{aligned} \tag{80}$$

Table 3 shows the degree-Kirchhoff indices of Möbius graph of linear octagonal-quadrilateral networks.

Finally, we will concentrate on calculating the complexity of $MQ_n(8, 4)$.

Theorem 5. *Let $MQ_n(8, 4)$ denote a Möbius graph of linear octagonal-quadrilateral networks of length $n \geq 2$. Then,*

$$\tau(MQ_n(8, 4)) = 4n((15 + 4\sqrt{14})^n + (15 - \sqrt{14})^n + 2). \tag{81}$$

Proof. By Claim 1, one can get

$$\tau(Q_n(8, 4)) = \frac{1}{10n} \prod_{p=2}^{4n} \eta_p \cdot \prod_{q=1}^{4n} \varphi_q = 4n((15 + 4\sqrt{14})^n + (15 - \sqrt{14})^n + 2). \tag{84}$$

$$\prod_{p=2}^{4n} \eta_p = (-1)^{4n-1} a_{4n-1} = 40n^2 \left(\frac{1}{36} \right)^n. \tag{82}$$

Similarly, according to Claim 3, we have

$$\prod_{q=1}^{4n} \varphi_q = \det \mathcal{L}_S = \left(\frac{5}{12} + \frac{\sqrt{14}}{9} \right)^n + \left(\frac{5}{12} - \frac{\sqrt{14}}{9} \right)^n + 2 \left(\frac{1}{36} \right)^n. \tag{83}$$

Note that $\prod_{i=1}^{8n} d_i(MQ_n) = 2^{4n} 3^{4n}$ and $|E_{MQ_n}(8, 4)| = 10n$. By Lemma 2(c), one gets

TABLE 3: The degree-Kirchhoff indices of $MQ_1(8, 4), MQ_2(8, 4), \dots, MQ_{16}(8, 4)$.

G	$Kf^*(G)$	G	$Kf^*(G)$	G	$Kf^*(G)$	G	$Kf^*(G)$
$MQ_1(8, 4)$	165.50	$MQ_5(8, 4)$	11054.43	$MQ_9(8, 4)$	57442.75	$MQ_{13}(8, 4)$	164937.53
$MQ_2(8, 4)$	963.33	$MQ_6(8, 4)$	18322.78	$MQ_{10}(8, 4)$	77587.71	$MQ_{14}(8, 4)$	204359.11
$MQ_3(8, 4)$	2775.12	$MQ_7(8, 4)$	28210.28	$MQ_{11}(8, 4)$	101951.83	$MQ_{15}(8, 4)$	249599.85
$MQ_4(8, 4)$	6005.23	$MQ_8(8, 4)$	41116.93	$MQ_{12}(8, 4)$	130935.10	$MQ_{16}(8, 4)$	301059.74

TABLE 4: The complexity of Q_1, Q_2, \dots, Q_{10} .

G	$\tau(G)$	G	$\tau(G)$
Q_1	128	Q_5	17379554400
Q_2	7200	Q_7	607607778176
Q_3	322944	Q_8	20809093939328
Q_4	12902464	Q_9	701525710449792
Q_5	483303040	Q_{10}	23358178980900000

This completes the proof. □

Thus, we can get the complexity of $MQ_n(8, 4)$, which is listed in Table 4.

Data Availability

The figures, tables, and other data used to support this study are included within the article.

Conflicts of Interest

The authors declare that there are no conflicts of interest regarding the publication of this paper.

Acknowledgments

This work was supported in part by the Anhui Provincial Natural Science Foundation under grant 2008085J01 and Natural Science Fund of Education Department of Anhui Province under grant KJ2020A0478.

References

[1] F. R. K. Chung, *Spectral Graph Theory*, American Mathematical Society Providence, Providence, RI, USA, 1997.

[2] H. Wiener, "Structural determination of paraffin boiling points," *Journal of the American Chemical Society*, vol. 69, no. 1, pp. 17–20, 1947.

[3] A. Dobrynin, "Branchings in trees and the calculation of the Wiener index of a tree," *Match Communications in Mathematical and in Computer Chemistry*, vol. 41, pp. 119–134, 2000.

[4] A. Dobrynin, R. Entriger, and I. Gutman, "Wiener index of trees: theory and applications," *Acta Applicandae Mathematica*, vol. 66, pp. 211–249, 2002.

[5] A. Dobrynin, I. Gutman, S. Klavžar, and P. Žigert, "Wiener index of hexagonal systems," *Acta Applicandae Mathematica*, vol. 72, pp. 94–247, 2002.

[6] I. Gutman, S. Li, and W. Wei, "Cacti with n -vertices and t cycles having extremal Wiener index n vertices and t cycles having extremal Wiener index," *Discrete Applied Mathematics*, vol. 232, pp. 189–200, 2017.

[7] I. Gutman, S. Klavžar, and B. Mohar, "Match communications in mathematical and in computer chemistry," *Applied Mathematics*, vol. 35, pp. 1–259, 1997.

[8] D. J. Klein and M. Randić, "Resistance distance," *Journal of Mathematical Chemistry*, vol. 12, no. 1, pp. 81–95, 1993.

[9] D. J. Klein, "Resistance-distance sum rules," *Croatica Chemica Acta*, vol. 75, pp. 633–649, 2002.

[10] D. J. Klein and O. Ivanciuc, "Graph cyclicity, excess conductance, and resistance deficit," *Journal of Mathematical Chemistry*, vol. 30, no. 3, pp. 271–287, 2001.

[11] H. Chen and F. Zhang, "Resistance distance and the normalized Laplacian spectrum," *Discrete Applied Mathematics*, vol. 155, no. 5, pp. 654–661, 2007.

[12] J. Huang, S. Li, and L. Sun, "The normalized Laplacians, degree-Kirchhoff index and the spanning trees of linear hexagonal chains," *Discrete Applied Mathematics*, vol. 207, pp. 67–79, 2016.

[13] J. Huang, S. Li, and X. Li, "The normalized Laplacian, degree-Kirchhoff index and spanning trees of the linear polyomino chains," *Applied Mathematics and Computation*, vol. 289, pp. 324–334, 2016.

[14] X. Ma and H. Bian, "The normalized Laplacians, degree-Kirchhoff index and the spanning trees of cylinder phenylene chain," *Polycyclic Aromatic Compounds*, vol. 41, no. 6, pp. 1159–1179, 2019.

[15] J. B. Liu, J. Zhao, and Z. Zhu, "On the number of spanning trees and normalized Laplacian of linear octagonal-quadrilateral networks," *International Journal of Quantum Chemistry*, vol. 119, no. 17, Article ID e25971, 2019.

[16] Y. J. Peng and S. C. Li, "On the Kirchhoff index and the number of spanning trees of linear phenylenes," *MATCH Communications in Mathematical and in Computer Chemistry*, vol. 77, pp. 765–780, 2017.

[17] X. Geng, P. Wang, L. Lei, and S. Wang, "On the Kirchhoff indices and the number of spanning trees of Möbius phenylenes chain and cylinder phenylenes chain," *Polycyclic Aromatic Compounds*, vol. 41, no. 8, pp. 1681–1693, 2019.

[18] J. B. Liu, Z. Y. Shi, Y. H. Pan, J. Cao, M. Abdel-Aty, and U. Al-Juboori, "Computing the Laplacian spectrum of linear octagonal-quadrilateral networks and its applications," *Polycyclic Aromatic Compounds*, vol. 2020, Article ID 1748666, 12 pages, 2020.

[19] J. Huang, S. C. Li, and X. Li, "The normalized Laplacian, degree-Kirchhoff index and spanning trees of the linear polyomino chains," *Applied Mathematics and Computation*, vol. 289, pp. 324–334, 2016.

- [20] Z. X. Zhu and J. B. Liu, "The normalized Laplacian, degree-Kirchhoff index and the spanning tree numbers of generalized phenylenes," *Discrete Applied Mathematics*, vol. 254, pp. 256–267, 2019.
- [21] S. Li, W. Sun, and S. Wang, "Multiplicative degree-Kirchhoff index and number of spanning trees of a zigzag polyhex nanotube TUHC[2n, 2]," *International Journal of Quantum Chemistry*, vol. 119, no. 17, Article ID e25969, 2019.
- [22] S. Butler, "Algebraic aspects of the normalized Laplacian," in *Recent Trends in Combinatorics, Vol. To Appear of the IMA Volumes in Mathematics and its Applications*, A. Beveridge, J. Griggs, L. Hogben, G. Musiker, and P. Tetali, Eds., IMA, 2016.

Research Article

Several Topological Indices of Two Kinds of Tetrahedral Networks

Jia-Bao Liu  and Lu-Lu Fang 

School of Mathematics and Physics, Anhui Jianzhu University, Hefei 230601, China

Correspondence should be addressed to Jia-Bao Liu; liujiabaoad@163.com and Lu-Lu Fang; fangluluajd@163.com

Received 29 July 2021; Accepted 1 September 2021; Published 28 September 2021

Academic Editor: Ljubisa Kocinac

Copyright © 2021 Jia-Bao Liu and Lu-Lu Fang. This is an open access article distributed under the Creative Commons Attribution License, which permits unrestricted use, distribution, and reproduction in any medium, provided the original work is properly cited.

Tetrahedral network is considered as an effective tool to create the finite element network model of simulation, and many research studies have been investigated. The aim of this paper is to calculate several topological indices of the linear and circle tetrahedral networks. Firstly, the resistance distances of the linear tetrahedral network under different classifications have been calculated. Secondly, according to the above results, two kinds of degree-Kirchhoff indices of the linear tetrahedral network have been achieved. Finally, the exact expressions of Kemeny's constant, Randic index, and Zagreb index of the linear tetrahedral network have been deduced. By using the same method, the topological indices of circle tetrahedral network have also been obtained.

1. Introduction

In actual life, many problems can be described using graph models. The graph model as a tool to describe network has been widely studied. Each network can be considered as graph. The problems of the vertices in the graph correspond to the points in the network, and the edges in the graph correspond to the network connection relationship between the points. In this paper, only simple, undirected, and connected graphs are considered. Suppose $G = (V(G), E(G))$ is a graph, and it satisfies $|V(G)| = n$ and $|E(G)| = m$. The degree of vertex p in the graph G is denoted by d_p . Connecting the two vertices $p, q \in V(G)$, the distance $d_G(p, q)$ [1] is defined as the length of the shortest path. And the resistance distance between vertex p and vertex q is delimited as the effective resistance, which is denoted as $r_G(p, q)$ [2]. For more terminologies, one can refer to reference [3].

The sum of the resistance distance between each pair of vertices in the graph G is defined as the Kirchhoff index [2], as follows:

$$Kf(G) = \sum_{p, q \in V(G)} r_G(p, q). \quad (1)$$

Similarly, Chen and Zhang [4] put forward the following definition of the multiplicative degree-Kirchhoff index, that is, as follows:

$$Kf^*(G) = \sum_{p, q \in V(G)} d_p d_q r_G(p, q). \quad (2)$$

Subsequently, Gutman et al. [5] proposed the following definition of the additive degree-Kirchhoff index, that is, as follows:

$$Kf^+(G) = \sum_{p, q \in V(G)} (d_p + d_q) r_G(p, q). \quad (3)$$

For a random walk [6, 7] in a network, the expectation of the average first arrival time [8, 9] from a vertex p to another vertex q selected according to the stable distribution of Markov process [10–13] is called Kemeny's constant of the network. Kemeny's constant is given by

$$K(G) = \frac{1}{4a} \sum_{p, q \in V(G)} d_p d_q r_G(p, q), \quad (4)$$

where a is the number of edges in the graph G .

In previous studies, several topological indices based on vertex-degree have been applied in research. The following

three topological indices (Kemeny’s constant, Randic index, and Zagreb index) are the most widely used:

$$M_1 = M_1(G) = \sum_{p \in V(G)} (d_p)^2, \tag{5}$$

$$M_2 = M_2(G) = \sum_{pq \in E(G)} d_p d_q, \tag{6}$$

$$R = R(G) = \sum_{pq \in E(G)} \frac{1}{\sqrt{d_p d_q}} \tag{7}$$

By the definition of the multiplicative (the additive) degree-Kirchhoff index, the main job is to calculate $r_G(p, q)$. From the perspective of practical application, the resistance distance considers all the paths between any two vertices, not just the short path, so the resistance distance can reflect the relationship between any two vertices better than the distance. This paper applies the expressions of the resistance distance between any two vertices of the linear and circle tetrahedral networks to derive the multiplicative (the additive) degree-Kirchhoff index of them, respectively. This kind of linear tetrahedral network is a one-dimensional infinitely extended network which is linked by a series of tetrahedrons. Its structure is morphologically manifested as elongation in one direction (see Figure 1), and n is the number of the tetrahedron in the network. The structure of this kind of circle tetrahedral network is a combination of tetrahedrons and octahedrons whose form is a two-dimensional wireless extension. And the octahedrons are connected by common edge (see Figure 2).

The structure of this paper is shown as follows: we introduce several fundamental definitions of the electrical network and give two important lemmas in Section 2. We present some proofs of our main results, namely, the multiplicative (the additive) degree-Kirchhoff index, Kemeny’s constant [14–16], Randic index [17–20], and Zagreb index [21, 22] of the linear and circle tetrahedral networks in Section 3. We summarize this article in Section 4.

2. Preliminaries

In the following section, we will give two important lemmas that will make a tremendous effect on our conclusions.

Lemma 1 (see [23]). Suppose the distance between vertex p and vertex q is t and $p, q \in L(n), (n \geq 3)$.

$$r_G(p, q) = \frac{t}{2}. \tag{8}$$

Lemma 2 (see [23]). Suppose the distance between vertex p and vertex q is t and $p, q \in C(n), (n \geq 3)$.

- (1) $r_G(p, q) = (t(n - t)/2n)$ when $d_p = d_q = 6$ and $1 \leq t \leq \lfloor n/2 \rfloor$
- (2) $r_G(p, q) = ((2t - 1)(2n - 2t + 1)/8n) + (1/4)$ when $d_p = 3, d_q = 6,$ and $1 \leq t \leq \lfloor (n + 1)/2 \rfloor$

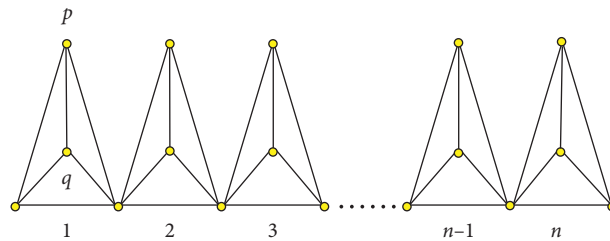


FIGURE 1: A kind of linear tetrahedron $L(n)$.

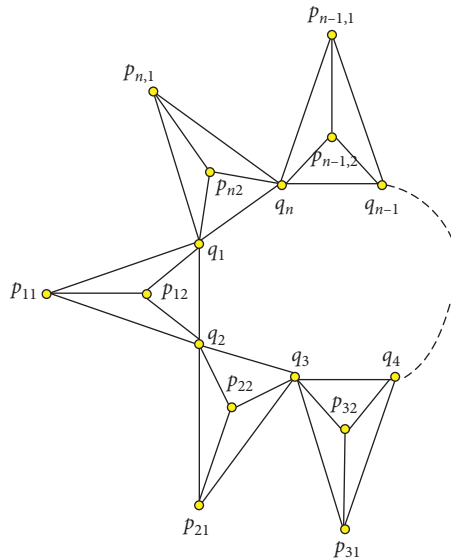


FIGURE 2: A kind of circle tetrahedron $C(n)$.

- (3) $r_G(p, q) = ((t - 1)(n - t + 1)/2n) + (1/2)$ when $d_p = d_q = 3$ and $1 < t \leq \lfloor (n/2) + 1 \rfloor$
- (4) $r_G(p, q) = (1/2)$ when $d_p = d_q = 3$ and $t = 1$

3. Main Results

In this section, the main purpose is to derive the multiplicative (the additive) degree-Kirchhoff index, Kemeny’s constant, Randic index, and Zagreb index of the linear (the circle) network (see Figures 3 and 4).

3.1. The Linear Tetrahedral Network

3.1.1. The Additive Degree-Kirchhoff Index

Theorem 1. Let $L(n), (n \geq 3)$ be a linear tetrahedral network.

$$Kf^+(L(n)) = \frac{12n^3 + 27n^2 - 3n}{2}. \tag{9}$$

Proof. The linear tetrahedral network $L(n)$ is shown in Figure 3. The number of vertices in $L(n)$ is $3n + 1$, and the number of edges in $L(n)$ is $6n$. When the distance between any two vertices is 1, the number of pairs of degree three and

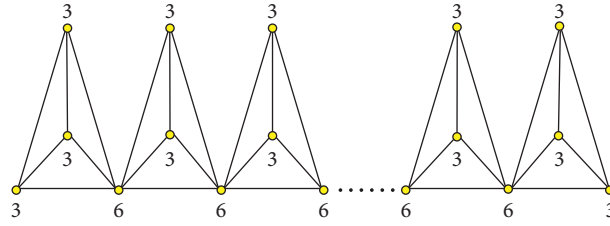


FIGURE 3: The linear tetrahedral network $L(n)$.

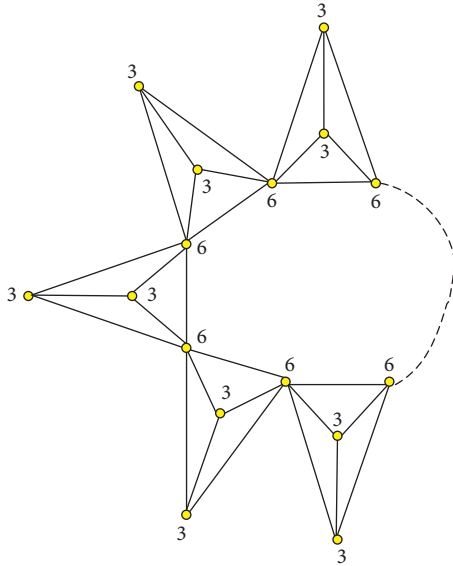


FIGURE 4: The circle tetrahedral network $C(n)$.

and degree six is $n - 2$. Besides, the maximum distance between the vertices of degree three and degree three in $L(n)$ is n . The maximum distance between the vertices of degree three and degree six in $L(n)$ is $n - 1$. The maximum distance between the vertices of degree six and degree six in $L(n)$ is $n - 2$. When the distance between any two vertices is t , there are $4[n - (t + 1)] + 12$ pairs of degree three and degree three and $4[n - (t + 1)] + 6$ pairs of degree three and degree six, where $t = 2, 3, \dots, n - 1$. And when the distance between any two vertices is t , the number of pairs of degree six and degree six is $n - (t + 1)$, where $t = 2, 3, \dots, n - 2$. Specially, when $t = n$, there are 9 pairs of vertices between degree three and degree three. The above contents are shown in Table 1.

By using equation (3) and Lemma 1, we calculate the following result:

degree three is $n + 4$, the number of pairs of degree three and degree six is $4n - 2$, and the number of pairs of degree six

$$\begin{aligned}
 Kf^+(L(n)) &= \left[\frac{(3 + 3)(n + 4) + (3 + 6)(4n - 2) + (6 + 6)(n - 2)}{2} \right] \\
 &+ \left[\sum_{t=2}^{n-2} \frac{[n - (t + 1)]t}{2} \times (6 + 6) + \sum_{t=2}^{n-1} \frac{t[4(n - (t + 1)) + 12]}{2} \times (3 + 3) \right. \\
 &\left. + \frac{9n}{2} \times (3 + 3) + \sum_{t=2}^{n-1} \frac{t[4(n - (t + 1)) + 6]}{2} \times (3 + 6) \right] \\
 &= (54n - 9) + \left[-36 \sum_{t=2}^{n-1} t^2 + (36n + 27) \sum_{t=2}^{n-1} t \right] \\
 &= (54n - 9) + \left[-36 \frac{(n - 1)(n - 1 + 1)[2(n - 1) + 1]}{6} + 36 \right] + (36n + 27) \left[\frac{[2 + (n - 1)](n - 2)}{2} \right] \\
 &= \frac{12n^3 + 27n^2 - 3n}{2}.
 \end{aligned}
 \tag{10}$$

TABLE 1: The classification of edge-pairs of $C(n)$.

(d_p, d_q)	(3, 3)	(6, 6)	(3, 6)
Number of the edges ($d=1$)	$n+4$	$n-2$	$4n-2$
Number of the edges ($d=t$)	$4[n-(t+1)]+12$	$n-(t+1)$	$4[n-(t+1)]+6$

Then, we obtain our desired consequence. \square

$$Kf^*(L(n)) = 12n^3 + 18n^2 - 3n. \tag{11}$$

3.1.2. *The Multiplicative Degree-Kirchhoff Index.* As shown above, we can find the multiplicative degree-Kirchhoff index of the linear network.

Proof. By using equation (2) and Lemma 1, we calculate the following result:

Theorem 2. . Let $L(n)$, ($n \geq 3$) be a linear tetrahedral network.

$$\begin{aligned}
 Kf^*(L(n)) &= \left[\frac{(3+3)(n+4) + (3+6)(4n-2) + (6+6)(n-2)}{2} \right] \\
 &+ \left[\sum_{t=2}^{n-2} \frac{(n-(t+1))t}{2} \times (6 \times 6) + \sum_{t=2}^{n-1} \frac{t[4(n-(t+1))+12]}{2} \times (3 \times 3) \right. \\
 &\left. + \frac{9n}{2} \times (3 \times 3) + \sum_{t=2}^{n-1} \frac{t[4(n-(t+1))+6]}{2} \times (3 \times 6) \right] \\
 &= (99n - 36) + 2 \left[-36 \sum_{t=2}^{n-1} t^2 + (36n + 18) \sum_{t=2}^{n-1} t \right] \\
 &= (99n - 36) + 2 \left[-36 \frac{(n-1)(n-1+1)[2(n-1)+1]}{6} + 36 \right] + 2(36n + 18) \left[\frac{[2+(n-1)](n-2)}{2} \right] \\
 &= 12n^3 + 18n^2 - 3n.
 \end{aligned} \tag{12}$$

\square

3.1.3. *Kemeny’s Constant, Randic Index, and Zagreb Index.* The relationship between vertices and edges of $L(n)$ based on degree is shown in Tables 2 and 3.

By utilizing equations (4)–(7) and Tables 2 and 3, the following three indices can be achieved easily:

TABLE 2: The classification of vertex-pairs of $L(n)$.

Degrees	3	6
Number of vertices	$2n + 2$	$n - 1$

TABLE 3: The classification of edge-pairs of $L(n)$.

(d_p, d_q)	(3, 3)	(6, 6)	(3, 6)
Number of edges	$n + 4$	$n - 2$	$4n - 2$

$$M_1(L(n)) = (2n + 2)3^2 + (n - 1)6^2 = 54n - 17,$$

$$M_2(L(n)) = (n + 4)(3 \times 3) + (n - 2)(6 \times 6) + (4n - 2)(3 \times 6) = 117n - 72,$$

$$R(L(n)) = (n + 4) \frac{1}{\sqrt{3 \times 3}} + (n - 2) \frac{1}{\sqrt{6 \times 6}} + (4n - 2) \frac{1}{\sqrt{3 \times 6}}$$

$$= \frac{(3 + 4\sqrt{2})n + 6 - 2\sqrt{2}}{6},$$

$$K(L(n)) = \frac{1}{4 \times 6n} \left[\frac{(3 + 3)(n + 4) + (3 + 6)(4n - 2) + (6 + 6)(n - 2)}{2} \right. \tag{13}$$

$$+ \sum_{t=2}^{n-2} \frac{[n - (t + 1)]t}{2} \times (6 \times 6) + \sum_{t=2}^{n-1} \frac{t[4(n - (t + 1)) + 12]}{2} \times (3 \times 3)$$

$$\left. + \frac{9n}{2} \times (3 \times 3) + \sum_{t=2}^{n-1} \frac{t[4(n - (t + 1)) + 6]}{2} \times (3 \times 6) \right]$$

$$= \frac{4n^2 + 6n - 1}{8}.$$

3.2. The Circle Tetrahedral Network

3.2.1. The Additive Degree-Kirchhoff Index

Theorem 3. Let $C(n)$, ($n \geq 3$) be a circle tetrahedral network.

$$Kf^+(C(n)) = \frac{12n^3 + 42n^2 - 15n}{4}. \tag{14}$$

Proof. The labels for all vertices are shown in Figure 2. In order to calculate conveniently, allow $p_m = p_n$ if $m \equiv n \pmod{s}$ and $p_{mk} = p_{nk}$ if $m \equiv n \pmod{s}$ ($s = 1, 2$). Set p and q as different vertices in $C(n)$. Results can be divided into the following six cases:

Case 1. $\sum_{\substack{\{p,q\} \subset V(G) \\ d_p = d_q = 3}} r(p, q)$ for even n .

When $t = 1$, the number of vertices of degree three in $L(n)$ is n . For every $p \in \{p_{m1}, p_{m2}\}$ ($m = 1, 2, \dots, n$), if $2 \leq t \leq (n/2)$, then p must be a member of the set $\{p_{m+t-1,1}, p_{m+t-1,2}, p_{m-(t-1),1}, p_{m-(t-1),2}\}$, so when the distance between any two vertices is p , there are $((2 \times 4 \times n)/2) = 4n$ pairs of them. For every $p \in \{p_{m1}, p_{m2}\}$ ($m = 1, 2, \dots, n$), if $t = (n/2) + 1$, then m must be a member of the set $\{p_{m+(n/2),1}, p_{m+(n/2),2}\}$ and thus when distance between any two vertices is $(n/2) + 1$, there are $((2 \times 2 \times n)/2) = 2n$ pairs. Then, through Lemma 2, we gain

$$\sum_{\substack{\{p,q\} \subset V(G) \\ d_p = d_q = 3}} (d_p + d_q)r(p, q) = \frac{3n^2 + 18n}{2} + 12 \sum_{t=2}^{(n/2)} [t(n - t + 2) - 1]$$

$$= \frac{3n^2 + 18n}{2} + 12 \sum_{t=2}^{(n/2)} (nt - t^2 + 2t - 1). \tag{15}$$

Case 2. $\sum_{\substack{\{p,q\} \subset V(G) \\ d_p = d_q = 3}} r(p,q)$ for odd n .

When $t = 1$, the number of vertices of degree three in $L(n)$ is n . For each $p \in \{p_{m1}, p_{m2}\}$ ($m = 1, 2, \dots, n$), if $2 \leq t \leq ((n+1)/2)$, then $n \in \{p_{m+t-1,1}, p_{m+t-1,2}, p_{m-(t-1),1}, p_{m+(t-1),2}\}$, so when $d_{pq} = t$, the number of the pairs of the vertex p and q is $4n$. Through Lemma 2, we gain

$$\sum_{\substack{\{p,q\} \subset V(G) \\ d_p = d_q = 3}} (d_p + d_q)r(p,q) = 3n + 12 \sum_{t=2}^{((n+1)/2)} (nt - t^2 + 2t - 1). \tag{16}$$

Case 3. $\sum_{\substack{\{p,q\} \subset V(G) \\ d_p = d_q = 6}} r(p,q)$ for even n .

For each $p = q_m$ ($m = 1, 2, \dots, n$), if $1 \leq t \leq (n/2)$, then $p \in \{p_{m+t}, p_{m-t}\}$, and thus when $d_{pq} = t$, the number of the pairs of the vertex p and q is n . For every $p = q_m$ ($m = 1, 2, \dots, n$), if $t = (n/2)$, then $p \in \{p_{m+(n/2)}\}$, and thus when $d_{pq} = (n/2)$, there are $(n/2)$ pairs. Then, by using Lemma 2, we infer

$$\begin{aligned} \sum_{\substack{\{p,q\} \subset V(G) \\ d_p = d_q = 6}} (d_p + d_q)r(p,q) &= \frac{3n^2}{4} + 6 \sum_{t=1}^{(n/2)-1} [t(n-t)] \\ &= \frac{3n^2}{4} + 6 \sum_{t=1}^{(n/2)-1} (nt - t^2). \end{aligned} \tag{17}$$

Case 4. $\sum_{\substack{\{p,q\} \subset V(G) \\ d_p = d_q = 6}} r(p,q)$ for odd n .

When $p = q_m$ ($m = 1, 2, \dots, n$), if $1 \leq t \leq (n/2)$, then $p \in \{p_{m+t}, p_{m-t}\}$, and thus when $d_{pq} = t$, there are n pairs. Then, by using Lemma 2, we deduce

$$\sum_{\substack{\{p,q\} \subset V(G) \\ d_p = d_q = 6}} (d_p + d_q)r(p,q) = 6 \sum_{t=1}^{((n-1)/2)} (nt - t^2). \tag{18}$$

Case 5. $\sum_{\substack{\{p,q\} \subset V(G) \\ d_p = 3, d_q = 6}} r(p,q)$ for even n .

For each p_{m1}, p_{m2} ($m = 1, 2, \dots, n$), if $1 \leq t \leq (n/2)$, then $p \in \{p_{m+t}, p_{m+1-t}\}$, and thus when $d_{pq} = t$, there are $4n$ pairs. Then, by using Lemma 2, we gain

$$\begin{aligned} \sum_{\substack{\{p,q\} \subset V(G) \\ d_p = 3, d_q = 6}} (d_p + d_q)r(p,q) &= 9 \sum_{t=1}^{(n/2)} \left[\frac{(2t-1)(2n-2t+1)}{2} + n \right] \\ &= 9 \sum_{t=1}^{(n/2)} \left(2nt - 2t^2 + 2t - \frac{1}{2} \right). \end{aligned} \tag{19}$$

Case 6. $\sum_{\substack{\{p,q\} \subset V(G) \\ d_p = 3, d_q = 6}} r(p,q)$ for odd n .

For every p_{m1}, p_{m2} ($m = 1, 2, \dots, n$), if $1 \leq t \leq ((n-1)/2)$, then $p \in \{p_{m+t}, p_{m+1-t}\}$, so when $d_{pq} = t$, the number of the pairs of the vertex p and q is $4n$. For each p_{m1}, p_{m2} ($m = 1, 2, \dots, n$), if $t = ((n+1)/2)$, then p must be $p_{m+(n+1)/2}$, and thus when $d_{pq} = ((n+1)/2)$, there are $2n$ pairs. Then, by using Lemma 2, we attain

$$\begin{aligned} \sum_{\substack{\{p,q\} \subset V(G) \\ d_p = 3, d_q = 6}} (d_p + d_q)r(p,q) &= \frac{9n^2 + 18n}{4} + 9 \sum_{t=1}^{((n-1)/2)} \\ &\cdot \left(2nt - 2t^2 + 2t - \frac{1}{2} \right). \end{aligned} \tag{20}$$

If n is even, by applying equations (15), (17), and (19) and Lemma 2, then

$$\begin{aligned} Kf^+(C(n)) &= \frac{3n^2 - 12n}{4} + \sum_{t=1}^{(n/2)} \left(36nt - 36t^2 + 42t - \frac{33}{2} \right) \\ &= \frac{3n^2 - 12n}{4} + \left[-36 \sum_{t=1}^{(n/2)} t^2 + 36n \sum_{t=1}^{(n/2)} t + \sum_{t=1}^{(n/2)} \left(42t - \frac{33}{2} \right) \right] \\ &= \frac{3n^2 - 12n}{4} + \left[-36 \frac{(n/2)((n/2)+1)(n+1)}{6} + 36n \frac{(n/2)((n/2)+1)}{2} + \frac{(n/2)(21n+9)}{2} \right] \\ &= \frac{12n^3 + 42n^2 - 15n}{4}. \end{aligned} \tag{21}$$

If n is odd, by applying equations (16), (18), and (20) and Lemma 2, then

$$\begin{aligned}
 Kf^+(C(n)) &= \frac{21n^2 + 30n - 12}{4} + \sum_{t=1}^{((n-1)/2)} \left(36nt - 36t^2 + 42t - \frac{33}{2} \right) \\
 &= \frac{21n^2 + 30n - 12}{4} + \left[-36 \sum_{t=1}^{((n-1)/2)} t^2 + 36n \sum_{t=1}^{((n-1)/2)} t + \sum_{t=1}^{((n-1)/2)} \left(42t - \frac{33}{2} \right) \right] \\
 &= \frac{21n^2 + 30n - 12}{4} + \left[-36 \frac{((n-1)/2)((n-1)/2 + 1)(n-1 + 1)}{6} + 36n \frac{((n-1)/2)((n-1)/2 + 1)}{2} \right. \\
 &\quad \left. + \frac{((n-1)/2)(21n - 12)}{2} \right] \\
 &= \frac{12n^3 + 42n^2 - 15n}{4}.
 \end{aligned} \tag{22}$$

Consequently, the proof is completed. \square

3.2.2. *The Multiplicative Degree-Kirchhoff Index.* As shown above, the multiplicative degree-Kirchhoff index of the circle network can be derived by classification.

Theorem 4. Let $C(n)$, ($n \geq 3$) be a circle tetrahedral network.

$$Kf^*(C(n)) = 6n^3 + 18n^2 - 6n. \tag{23}$$

Proof. The results in six cases are given as follows:

Case 1. $\sum_{\substack{\{p,q\} \subset V \\ d_p = d_q = 3}} r(p, q)$ for even n .

$$\sum_{\substack{\{p,q\} \subset V \\ d_p = d_q = 3}} d_p d_q r(p, q) = \frac{9n^2 + 54n}{4} + 18 \sum_{t=2}^{(n/2)} (nt - t^2 + 2t - 1). \tag{24}$$

Case 2. $\sum_{\substack{\{p,q\} \subset V(G) \\ d_p = d_q = 3}} r(p, q)$ for odd n .

$$\sum_{\substack{\{p,q\} \subset V \\ d_p = d_q = 3}} d_p d_q r(p, q) = \frac{9n}{2} + 18 \sum_{t=2}^{((n+1)/2)} (nt - t^2 + 2t - 1). \tag{25}$$

Case 3. $\sum_{\substack{\{p,q\} \subset V(G) \\ d_p = d_q = 6}} r(p, q)$ for even n .

$$\sum_{\substack{\{p,q\} \subset V \\ d_p = d_q = 6}} d_p d_q r(p, q) = \frac{9n^2}{4} + 18 \sum_{t=1}^{(n/2)-1} (nt - t^2). \tag{26}$$

Case 4. $\sum_{\substack{\{p,q\} \subset V(G) \\ d_p = d_q = 6}} r(p, q)$ for odd n .

$$\sum_{\substack{\{p,q\} \subset V \\ d_p = d_q = 6}} d_p d_q r(p, q) = 18 \sum_{t=1}^{((n-1)/2)} (nt - t^2). \tag{27}$$

Case 5. $\sum_{\substack{\{p,q\} \subset V(G) \\ d_p = 3, d_q = 6}} r(p, q)$ for even n .

$$\sum_{\substack{\{p,q\} \subset V \\ d_p = 3, d_q = 6}} d_p d_q r(p, q) = 18 \sum_{t=1}^{(n/2)} \left(2nt - 2t^2 + 2t - \frac{1}{2} \right). \tag{28}$$

Case 6. $\sum_{\substack{\{p,q\} \subset V(G) \\ d_p = 3, d_q = 6}} r(p, q)$ for odd n .

$$\sum_{\substack{\{p,q\} \subset V \\ d_p = 3, d_q = 6}} d_p d_q r(p, q) = \frac{9n^2 + 18n}{2} + 18 \sum_{t=1}^{((n-1)/2)} \left(2nt - 2t^2 + 2t - \frac{1}{2} \right). \tag{29}$$

If n is even, through equations (24), (26), and (28) and Lemma 2, then

$$\begin{aligned}
 Kf^*(C(n)) &= \frac{9}{2}n + 9 \sum_{t=1}^{(n/2)} (8nt - 8t^2 + 8t - 3) \\
 &= \frac{9}{2}n + 9 \left[-8 \sum_{t=1}^{(n/2)} t^2 + 8n \sum_{t=1}^{(n/2)} t + \sum_{t=1}^{(n/2)} (8t - 3) \right] \\
 &= \frac{9}{2}n + 9 \left[-8 \frac{(n/2)((n/2) + 1)(n + 1)}{6} + 8n \frac{(n/2)((n/2) + 1)}{2} + \frac{(n/2)(4n + 2)}{2} \right] \\
 &= 6n^3 + 18n^2 - 6n.
 \end{aligned} \tag{30}$$

If n is odd, through equations (25), (27), and (29) and Lemma 2, then

$$\begin{aligned}
 Kf^*(C(n)) &= \frac{18n^2 + 27n - 9}{2} + 9 \sum_{t=1}^{((n-1)/2)} (8nt - 8t^2 + 8t - 3) \\
 &= \frac{18n^2 + 27n - 9}{2} + 9 \left[-8 \sum_{t=1}^{((n-1)/2)} t^2 + 8n \sum_{t=1}^{((n-1)/2)} t + \sum_{t=1}^{((n-1)/2)} (8t - 3) \right] \\
 &= \frac{18n^2 + 27n - 9}{2} + 9 \left[-8 \frac{((n-1)/2)((n-1)/2 + 1)(n - 1 + 1)}{6} + 8n \frac{((n-1)/2)((n-1)/2 + 1)}{2} + \frac{((n-1)/2)(4n - 2)}{2} \right] \\
 &= 6n^3 + 18n^2 - 6n.
 \end{aligned} \tag{31}$$

This completes the proof. \square

3.2.3. *Kemeny's Constant, Randic Index, and Zagreb Index.* The relationship between vertices and edges of $C(n)$ based on degree is shown in Tables 4 and 5.

By utilizing equations (4)–(7) and Tables 4 and 5, the following three indices can be obtained easily:

$$M_1(C(n)) = 2n \times 3^2 + n \times 6^2 = 54n,$$

$$M_2(C(n)) = n \times (3 \times 3) + n \times (6 \times 6) + 4n \times (3 \times 6) = 117n,$$

$$\begin{aligned}
 R(C(n)) &= n \times \frac{1}{\sqrt{3 \times 3}} + n \times \frac{1}{\sqrt{6 \times 6}} + 4n \times \frac{1}{\sqrt{3 \times 6}} \\
 &= \frac{(3 + 4\sqrt{2})n}{6}.
 \end{aligned} \tag{32}$$

If n is even, then

$$\begin{aligned}
 K(C(n)) &= \frac{1}{4 \times 6n} \left[\frac{9}{2}n + 9 \sum_{t=1}^{(n/2)} (8nt - 8t^2 + 8t - 3) \right] \\
 &= \frac{n^2 + 3n - 1}{4}.
 \end{aligned} \tag{33}$$

If n is odd, then

$$\begin{aligned}
 K(C(n)) &= \frac{1}{4 \times 6n} \left[\frac{18n^2 + 27n - 9}{2} + 9 \sum_{t=1}^{((n-1)/2)} (8nt - 8t^2 + 8t - 3) \right] \\
 &= \frac{n^2 + 3n - 1}{4}.
 \end{aligned} \tag{34}$$

TABLE 4: The classification of vertex-degree of $C(n)$.

d_p	3	6
Number of vertices	$2n$	n

TABLE 5: The classification of edge-degree of $C(n)$.

(d_p, d_q)	(3, 3)	(6, 6)	(3, 6)
Number of edges	n	n	$4n$

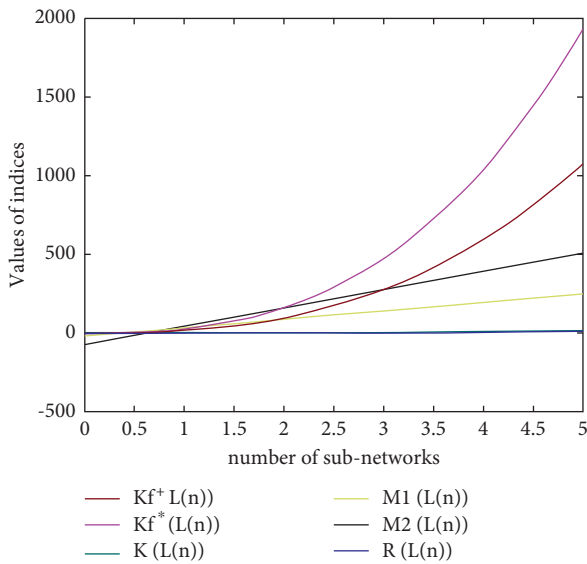


FIGURE 5: Comparisons of the topological indices for the linear tetrahedral network.

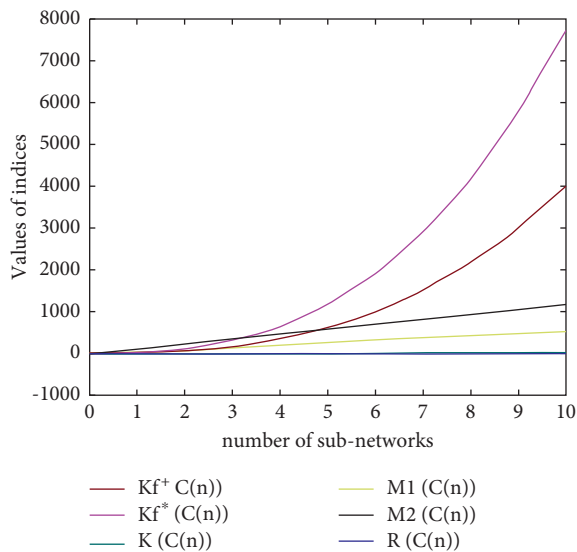


FIGURE 6: Comparisons of the topological indices for the circle tetrahedral network.

And the comparisons of the five topological indices obtained above are shown in Figures 5 and 6.

According to Figures 5 and 6, it is clear that the multiplicative degree-Kirchhoff index of both the linear and circle graph is the fast growing, and the additive degree-Kirchhoff index is the second growing. Other than that, in the circle graph, whenever n is odd or even, the Zagreb index is growing faster than Randic index and Kemeny’s constant. And in the linear graph, the Zagreb index is also growing faster than Kemeny’s constant and Randic index.

4. Conclusion

In this paper, two types of tetrahedral networks have been discussed and the resistance distance in different cases has been computed, respectively. Above all, the multiplicative (the additive) degree-Kirchhoff index of the networks has been calculated. Then, Kemeny’s constant, Randic index, and Zagreb index have also been derived. Furthermore, the comparisons of the topological indices for the linear and circle networks have been studied. In future, we will devote ourselves to research more properties for types of stereochemical networks.

Data Availability

The figures, tables, and other data used to support this study are included within the article.

Conflicts of Interest

The authors declare that there are no conflicts of interest regarding the publication of this paper.

Acknowledgments

This work was supported in part by Anhui Provincial Natural Science Foundation under Grant 2008085J01 and Natural Science Fund of Education Department of Anhui province under Grant KJ2020A0478.

References

- [1] Z. M. Li, Z. Xie, J. P. Li, and Y. G. Pan, “Resistance distance-based graph invariants and spanning trees of graphs derived from the strong prism of a star,” *Applied Mathematics and Computation*, vol. 382, pp. 1–9, 2020.
- [2] D. J. Klein and M. Randić, “Resistance distance,” *Journal of Mathematical Chemistry*, vol. 12, no. 1, pp. 81–95, 1993.
- [3] D. A. Spielman and N. Srivastava, “Graph sparsification by effective resistances,” *SIAM Journal on Computing*, vol. 40, no. 6, pp. 1913–1926, 2011.
- [4] H. Chen and F. Zhang, “Resistance distance and the normalized Laplacian spectrum,” *Discrete Applied Mathematics*, vol. 155, no. 5, pp. 654–661, 2017.
- [5] I. Gutman, L. Fei, and G. Yu, “Degree resistance distance of unicyclic graphs,” *Transactions on Combinatorics*, vol. 1, no. 2, pp. 27–40, 2012.
- [6] R. van der Hofstad, T. Hulshof, and J. Nagel, “Random walk on barely supercritical branching random walk,” *Probability Theory and Related Fields*, vol. 177, no. 1-2, pp. 1–53, 2020.

- [7] J. Engländer and S. Volkov, “Impatient random walk,” *Journal of Theoretical Probability*, vol. 32, no. 4, pp. 2020–2043, 2019.
- [8] Y. Li, Y. Wang, H. Lin, and T. Zhong, “First arrival time picking for microseismic data based on DSW algorithm,” *Journal of Seismology*, vol. 22, no. 4, pp. 833–840, 2018.
- [9] X. Liao, J. Cao, J. Hu, J. You, X. Jiang, and Z. Liu, “First arrival time identification using transfer learning with continuous wavelet transform feature images,” *IEEE Geoscience and Remote Sensing Letters*, vol. 17, no. 11, pp. 2002–2006, 2020.
- [10] A. E. Kyprianou, V. Rivero, and B. Şengül, “Conditioning subordinators embedded in Markov processes,” *Stochastic Processes and their Applications*, vol. 127, no. 4, pp. 1234–1254, 2017.
- [11] A. Schnurr, “On deterministic Markov processes: expandability and related topics,” *Markov Processes and Related Fields*, vol. 19, no. 4, pp. 693–720, 2013.
- [12] Y. Ephraim and W. J. J. Roberts, “An EM algorithm for Markov modulated Markov processes,” *IEEE Transactions on Signal Processing*, vol. 57, no. 2, pp. 463–470, 2009.
- [13] F. Grabski, “Semi-Markov failure rates processes,” *Applied Mathematics and Computation*, vol. 217, no. 24, pp. 9956–9965, 2011.
- [14] R. Pinsky, “Kemeny’s constant for one-dimensional diffusions,” *Electronic Communications in Probability*, vol. 24, pp. 1–5, 2019.
- [15] R. E. Kooij and J. L. A. Dubbeldam, “Kemeny’s constant for several families of graphs and real-world networks,” *Discrete Applied Mathematics*, vol. 285, pp. 96–107, 2020.
- [16] X. Wang, J. L. A. Dubbeldam, and P. Van Mieghem, “Kemeny’s constant and the effective graph resistance,” *Linear Algebra and its Applications*, vol. 535, pp. 231–244, 2017.
- [17] R. Cruz, J. Monsalve, and J. Rada, “Trees with maximum exponential Randić index,” *Discrete Applied Mathematics*, vol. 283, pp. 634–643, 2020.
- [18] Y. Shi, “Note on two generalizations of the Randić index,” *Applied Mathematics and Computation*, vol. 265, pp. 1019–1025, 2015.
- [19] Z. Iqbal, A. Aslam, M. Ishaq, and W. Gao, “The edge versions of degree-based topological descriptors of dendrimers,” *Journal of Cluster Science*, vol. 31, no. 2, pp. 445–452, 2020.
- [20] S. M. Kang, W. Nazeer, M. A. Zahid, A. R. Nizami, A. Aslam, and M. Munir, “M-polynomials and topological indices of hex-derived networks,” *Open Physics*, vol. 16, no. 1, pp. 394–403, 2018.
- [21] J.-B. Liu, C. Wang, S. Wang, and B. Wei, “Zagreb indices and multiplicative Zagreb indices of Eulerian graphs,” *Bulletin of the Malaysian Mathematical Sciences Society*, vol. 42, no. 1, pp. 67–78, 2019.
- [22] B. Furtula, A. Graovac, and D. Vukičević, “Augmented Zagreb index,” *Journal of Mathematical Chemistry*, vol. 48, no. 2, pp. 370–380, 2010.
- [23] M. S. Sardar, X. F. Pan, and S. A. Xu, “Computation of resistance distance and Kirchhoff index of the two classes of silicate networks,” *Applied Mathematics and Computation*, vol. 381, pp. 1–10, 2020.

Research Article

On Locating-Dominating Set of Regular Graphs

Anuwar Kadir Abdul Gafur ¹ and Suhadi Wido Saputro ²

¹Department of Mathematics, Pasific Morotai University, Morotai, Indonesia

²Department of Mathematics, Bandung Institute of Technology, Bandung, Indonesia

Correspondence should be addressed to Suhadi Wido Saputro; suhadi@math.itb.ac.id

Received 16 July 2021; Accepted 28 August 2021; Published 25 September 2021

Academic Editor: Muhammad Kamran Siddiqui

Copyright © 2021 Anuwar Kadir Abdul Gafur and Suhadi Wido Saputro. This is an open access article distributed under the Creative Commons Attribution License, which permits unrestricted use, distribution, and reproduction in any medium, provided the original work is properly cited.

Let G be a simple, connected, and finite graph. For every vertex $v \in V(G)$, we denote by $N_G(v)$ the set of neighbours of v in G . The locating-dominating number of a graph G is defined as the minimum cardinality of $W \subseteq V(G)$ such that every two distinct vertices $u, v \in V(G) \setminus W$ satisfies $\emptyset \neq N_G(u) \cap W \neq N_G(v) \cap W \neq \emptyset$. A graph G is called k -regular graph if every vertex of G is adjacent to k other vertices of G . In this paper, we determine the locating-dominating number of k -regular graph of order n , where $k = n - 2$ or $k = n - 3$.

1. Introduction

Given a simple, connected, and finite graph G . The neighbours of a vertex v of G are defined as the vertex set $N_G(v) = \{u \in V(G) | uv \in E(G)\}$. A set of vertices $W \subseteq V(G)$ is called a locating-dominating set of a graph G if every two distinct vertices $u, v \in V(G) \setminus W$ satisfies $\emptyset \neq N_G(u) \cap W \neq N_G(v) \cap W \neq \emptyset$. The minimum cardinality of locating-dominating sets of G is called the locating-dominating number of G , denoted by $\lambda(G)$. This concept was introduced by Slater [1, 2].

Let us model a building floor as a graph. Locating-dominating set can be used to determine an exact location of a fire alarm which sends a signal when detecting a fire in any of its adjacent vertices. The activated signals will univocally determine the place of the fire.

Charon et al. [3] have proved that determining locating-dominating number of a graph is NP-complete problem which is reduced from 3-SAT. However, some results for certain classes of graphs have been obtained, such as paths [2], cycles [4], stars [5], complete graphs [6], bipartite graphs [7, 8], complete multipartite graphs [5], wheels [7], twin-free graphs [9, 10], and hypergraphs [11]. In [12], Balbuena et al. investigated a locating-dominating set of graphs with girth at least 5. In the other hand, Rajasekar and Nagarajan [13]

studied the locating-dominating number of a graph containing a bridge.

Furthermore, some authors have been characterized all graphs with a given locating-dominating number. Henning and Oellermann [6] have proved that for a connected graph G of order $n \geq 2$, $\lambda(G) = n - 1$ if and only if G is either complete graphs K_n or star graphs $K_{1,n-1}$. They also characterized all graphs G of order $n \geq 4$ with locating-dominating number $n - 2$. Meanwhile, Caceres et al. [7] have proved that there are 16 nonisomorphic graphs G satisfying $\lambda(G) = 2$.

Some authors also have determined the locating-dominating number of graphs obtained from a product graphs. Canoy and Malacas [14] provided the lower and upper bounds for the locating-dominating number of corona product graphs. They also determined an exact value of the locating-dominating number of a composition of graphs between G and H where G is a connected totally point determining graph and H is a nontrivial connected graph. An exact value of the locating-dominating number of comb product of any two connected graphs of order at least two has been determined by Pribadi and Saputro [15]. Murtaza et al. [16] studied the locating-domination number of functigraphs of complete graphs. A study of a locating-dominating set of a graph by adding a universal vertex can be seen in [17].

In this paper, we consider a regular graph. A graph G is called k -regular graph if every vertex in G is adjacent to k other vertices. Since every vertex of G is adjacent to the same number of vertices of G , every vertex of G has the same probability to distinguish some distinct vertices of G . Let $G = (V, E)$ be a model of the multiprocessor system, such that $V(G)$ is the set of processors and $E(G)$ is the set of links between processors. Assume that at most one processor is malfunctioning and we want to test the system and find the faulty processor. Some processors can be chosen and assigned to check their neighbours. In case a selected processor detects a fault, it sends an alarm signal. Since we need an exact location of a faulty processor, we must choose some processors such that the chosen processors can uniquely tell the location of the malfunctioning processor. Then, a locating-dominating set of G can be used to choose those processors.

Bertrand et al. [4] have initiated the study of the locating-dominating number on regular graph. They determined the locating-dominating number of 2-regular connected graphs (cycles). The locating-dominating number of $(n-1)$ -regular graph of order n can be seen in [7]. In this paper, we determine the locating-dominating number of k -regular graph of order n where $k = n-2$ or $k = n-3$.

The purpose of this paper is to further investigate the locating-dominating number of certain family of graphs, namely, to determine the locating-dominating number of certain regular graphs. We obtain two main results, one of them is the following result related with an $(n-2)$ -regular graph.

Theorem 1. For $n \geq 4$, let G be an $(n-2)$ -regular graph. Then, $\lambda(G) = n/2$.

Our second result is related with an $(n-3)$ -regular graph. In preparing the proof for the second result, we are able to obtain the intermediate result as follows.

Theorem 2. For $m \geq 7$, let $H = K_m \setminus E(C_m)$. Then, $\lambda(H) = \lceil (2m-2)/5 \rceil$.

For $n \geq 5$, we consider certain cycles contained in a complete graph K_n . In this paper, we assume that a cycle contains at least three vertices. For $r \in \{1, 2, \dots, \lfloor n/3 \rfloor\}$, let R_1, R_2, \dots, R_r be r disjoint cycles contained in K_n such that $V(R_1) \cup V(R_2) \cup \dots \cup V(R_r) = V(K_n)$. Note that an $(n-3)$ -regular graph is isomorphic to $K_n \setminus (E(R_1) \cup E(R_2) \cup \dots \cup E(R_r))$. In case $r = 1$, the locating-dominating number of an $(n-3)$ -regular graph of order at least 7 has been determined in Theorem 2. In Theorem 3, we provide the locating-dominating number of an $(n-3)$ -regular graph of order $n \geq 5$ with $1 \leq r \leq \lfloor n/3 \rfloor$.

Theorem 3. For $n \geq 5$ and $1 \leq r \leq \lfloor n/3 \rfloor$, let R_1, R_2, \dots, R_r be r disjoint cycles contained in K_n such that $V(R_1) \cup V(R_2) \cup \dots \cup V(R_r) = V(K_n)$. For $i \in \{1, 2, \dots, r\}$, let $G = K_n \setminus (E(R_1) \cup E(R_2) \cup \dots \cup E(R_r))$, $m_i = |V(R_i)|$, and $G_i = K_{m_i} \setminus E(R_i)$. If k is the number of cycles R_i of order $m_i \geq 7$ and $m_i \equiv 1$ or $3 \pmod{5}$, then

$$\lambda(G) = \begin{cases} \sum_{i=1}^r \lambda(G_i), & \text{if } k \leq 1, \\ k-1 + \sum_{i=1}^r \lambda(G_i), & \text{if } k \geq 2. \end{cases} \quad (1)$$

2. $(n-2)$ -Regular Graph and Proof of Theorem 1

Theorem 1 is a direct consequence of Lemmas 1 and 2 in this section.

In this section, we define G as an $(n-2)$ -regular graph of order $n \geq 4$. Note that if we count the sum of degree of all vertices, then every edge will be counted twice. Therefore, we have $2|E(G)| = n(n-2)$. It implies that n must be even.

Now, we can define $V(G) = \{x_i, y_i \mid 1 \leq i \leq (n/2)\}$ and $E(G) = \{uv \mid u, v \in V(G)\} \setminus \{x_i y_i \mid 1 \leq i \leq (n/2)\}$.

Lemma 1. Let W be a locating-dominating set of G . Then, for $1 \leq i \leq (n/2)$, $x_i \in W$ or $y_i \in W$.

Proof. Suppose that there exists $i \in \{1, 2, \dots, (n/2)\}$ such that $x_i, y_i \notin W$. Note that every vertex in $V(G) \setminus \{x_i, y_i\}$ is adjacent to both x_i and y_i . So, we will obtain that $N_G(x_i) \cap W = N_G(y_i) \cap W$, a contradiction. \square

Lemma 2. A vertex set $\{x_i \mid 1 \leq i \leq (n/2)\}$ is a locating-dominating set of G .

Proof. Let $S = \{x_i \mid 1 \leq i \leq (n/2)\}$. Then, $V(G) \setminus S = \{y_i \mid 1 \leq i \leq (n/2)\}$. Let us consider y_i and y_j for $1 \leq i < j \leq (n/2)$. Since $x_i \in N_G(y_j)$ but $x_i \notin N_G(y_i)$, we obtain $\emptyset \neq N_G(y_i) \cap S \neq N_G(y_j) \cap S \neq \emptyset$. Therefore, S is a locating-dominating set of G . \square

3. $(n-3)$ -Regular Graph and Proof of Theorem 2

In this section, we define G as an $(n-3)$ -regular graph of order $n \geq 5$. Note that G contains a subgraph which is isomorphic to $K_m \setminus E(C_m)$ where $m \in \{3, 4, \dots, n\}$. Let $G' \subseteq G$ and $G' = K_m \setminus E(C_m)$ where $m \in \{3, 4, \dots, n\}$. Then, every vertex in G' is adjacent to all vertices of $G \setminus G'$. In Lemma 3, we show that every subgraph is contributed to a locating-dominating set of G , which is a direct consequence of Observation 1 which has been proved by Henning and Oellermann [6].

Observation 1 (see [6]). Let W be a locating-dominating set of a connected graph G . If there exists two distinct vertices $u, v \in V(G)$ such that $d_G(u, z) = d_G(v, z)$ for all $z \in V(G) \setminus \{u, v\}$, then $u \in W$ or $v \in W$.

Lemma 3. For $n \geq 5$, let $G' \subseteq G$ and $G' = K_m \setminus E(C_m)$ where $m \in \{3, 4, \dots, n\}$. If W is a locating-dominating set of G , then $W \cap V(G') \neq \emptyset$.

From Lemma 3, we have Lemma 4.

Lemma 4. For $n \geq 5$, let $G' \subseteq G$ and $G' = K_m \setminus E(C_m)$ where $m \in \{3, 4, \dots, n\}$. Let W be a locating-dominating set of G and $W' = V(G') \cap W$. Then, every two distinct vertices $u, v \in V(G') \setminus W'$ satisfies $N_{G'}(u) \cap W' \neq N_{G'}(v) \cap W'$.

Proof. Suppose that there exists two distinct vertices $u, v \in V(G') \setminus W'$ such that $N_{G'}(u) \cap W' = N_{G'}(v) \cap W'$. Note that $N_{G'}(u) \cap W' = N_G(u) \cap W'$. Let $G^* = G \setminus G'$ and $W^* = W \setminus W'$. Since $N_G(u) \cap V(G^*) = V(G^*) = N_G(v) \cap V(G^*)$, we obtain $N_G(u) \cap W = (N_G(u) \cap W^*) \cup (N_G(u) \cap W') = (N_G(v) \cap W^*) \cup (N_G(v) \cap W') = N_G(v) \cap W$, a contradiction. \square

By Lemma 4, if W is a locating-dominating set of G , then we can say that $V(G') \cap W$ is a locating-dominating set of a subgraph G' of G . Note that, in this case, for $u \in V(G')$, $N_{G'}(u) \cap V(G') \cap W$ can be an empty set. In Lemma 5, we provide a locating-dominating set of a subgraph $G' = K_m \setminus E(C_m)$ of G where $m \in \{3, 4, 5, 6\}$.

Lemma 5. For $n \geq 5$, let $G' \subseteq G$ and $G' = K_m \setminus E(C_m)$ where $m \in \{3, 4, 5, 6\}$. Let W be a locating-dominating set of G . Then,

$$|W \cap V(G')| \geq \begin{cases} 3, & \text{if } m = n = 6, \\ 2, & \text{otherwise.} \end{cases} \quad (2)$$

The lower bounds are sharp.

Proof. Let $V(G') = \{x_1, x_2, \dots, x_m\}$ and $E(C_m) = \{x_1x_2, x_2x_3, \dots, x_{m-1}x_m, x_mx_1\}$ where $m \in \{3, 4, 5, 6\}$. We distinguish two cases.

(1) $|W \cap V(G')| \geq 3$ for $m = n = 6$.

In this case, $G' = G$. Suppose that $|W \cap V(G')| \leq 2$. Let W' be a locating-dominating set of G' . Then, there exists $u, v \in V(G') \setminus W'$ such that either $u \neq v$ and $N_{G'}(u) \cap W' = N_{G'}(v) \cap W'$, or $N_{G'}(u) \cap W' = \emptyset$, a contradiction. Now, we define $S = \{x_1, x_3, x_5\}$. Since $N_{G'}(x_2) \cap S = \{x_5\}$, $N_{G'}(x_4) \cap S = \{x_1\}$, and $N_{G'}(x_6) \cap S = \{x_3\}$, the vertex set S is a locating-dominating set of G' .

(2) $|W \cap V(G')| \geq 2$ for $m \neq 6$ or $n \neq 6$.

Suppose that $|W \cap V(G')| \leq 1$. If $|W \cap V(G')| = 0$, then for two distinct vertices $u, v \in V(G') \setminus W$, $N_G(u) \cap W = W = N_G(v) \cap W$, a contradiction. So, we assume that $|W \cap V(G')| = 1$. Let $W \cap V(G') = \{x_i\}$ with $i \in \{1, 2, \dots, m\}$. Let x_j and x_k be two different vertices in G' such that $x_jx_k, x_kx_i \notin E(G')$. So, $N_{G'}(x_j) \cap W = \emptyset = N_{G'}(x_k) \cap W$. Since every vertex in $G \setminus G'$ is adjacent to both x_j and x_k , we have $N_G(x_j) \cap W = W = N_G(x_k) \cap W$, a contradiction. For the sharpness, we define a vertex set S_m as follows:

$$S_m = \begin{cases} \{x_1, x_2\}, & \text{if } m \in \{3, 4, 5\}, \\ \{x_1, x_3\}, & \text{if } m = 6. \end{cases} \quad (3)$$

We will show that S_m is a locating-dominating set of a subgraph G' of G . Let us consider vertices in $V(G') \setminus S_m$.

- (a) $m = 3$: we obtain that $|V(G') \setminus S_m| = 1$. So, it is clear that S_m is a locating-dominating set of G' .
- (b) $m = 4$: we obtain that $V(G') \setminus S_m = \{x_3, x_4\}$. Note that $N_{G'}(x_3) \cap S_m = \{x_1\} \neq \{x_2\} = N_{G'}(x_4) \cap S_m$. Therefore, S_m is a locating-dominating set of G' .
- (c) $m = 5$: we obtain that $V(G') \setminus S_m = \{x_3, x_4, x_5\}$. It is easy to see that $N_{G'}(x_3) \cap S_m = \{x_1\}$, $N_{G'}(x_4) \cap S_m = \{x_1, x_2\}$, and $N_{G'}(x_5) \cap S_m = \{x_2\}$. Therefore, it is clear that S_m is a locating-dominating set of G' .
- (d) $m = 6$: we obtain that $V(G') \setminus S_m = \{x_2, x_4, x_5, x_6\}$. It is easy to see that $N_{G'}(x_2) \cap S_m = \emptyset$, $N_{G'}(x_4) \cap S_m = \{x_1\}$, $N_{G'}(x_5) \cap S_m = \{x_1, x_3\}$, and $N_{G'}(x_6) \cap S_m = \{x_3\}$. Therefore, it is clear that S_m is a locating-dominating set of G' . \square

Remark 1. We can say that the locating-dominating number of G' in Lemma 5 is given by

$$\lambda(G') = \begin{cases} 2, & \text{if } m \in \{3, 4, 5, 6\} \text{ and } n > m, \\ 3, & \text{if } n = m = 6. \end{cases} \quad (4)$$

Now, let us consider $G' \subseteq G$ and $G' = K_m \setminus E(C_m)$ for $m \geq 7$. Thus, the order of G must be $n \geq 7$. For $n \geq 7$, in order to determine a locating-dominating set of $G' = K_m \setminus E(C_m)$ for $7 \leq m \leq n$, we define some definitions. For $u, v \in V(G)$, let $P(u, v)$ be a shortest (u, v) -path in C_m . So, all edges in $P(u, v)$ are not element of $E(G')$. Let $W \subseteq V(G')$. For $u, v \in W$, let us consider the set of vertices of $P(u, v) \setminus \{u, v\}$. If all vertices of $P(u, v) \setminus \{u, v\}$ are not in W , then the set of vertices in $P(u, v) \setminus \{u, v\}$ is called a gap between u and v . Then, we called vertices u and v as the end points of gap. The two gaps are called neighbouring gaps if they have common end point. These definitions were firstly introduced by Buczkowski et al. [18]. They used this gap technique to determine the metric dimension of wheel graphs. In lemma 6, we provide the necessary and sufficient conditions for a locating-dominating set of G' which is related to gap definition.

Lemma 6. For $n \geq 7$, let $G' = K_m \setminus E(C_m)$ where $m \in \{7, 8, \dots, n\}$. The vertex set $W \subseteq V(G')$ is a locating-dominating set of G' if and only if W satisfies all conditions as follows:

- (1) Every gap with respect to W contains at most 3 vertices
- (2) W contains at most one gap of 3 vertices
- (3) If A is a gap with respect to W , containing 2 or 3 vertices, then any neighbouring gaps of A have at most one vertex

Proof. (\Rightarrow) We will prove all three conditions by contradiction.

- (1) Suppose that there exists a gap with respect to W containing at least 4 vertices.

Let $a_1, a_2, a_3, a_4 \in V(G')$ where $a_i a_{i+1} \in E(C_m)$ with $1 \leq i \leq 3$ and all those vertices are not in W . Then, we have $N_{G'}(a_2) \cap W = W = N_{G'}(a_3) \cap W$, a contradiction.

- (2) Suppose that there exists two gaps containing 3 vertices.

Let $\{a_1, a_2, a_3\}$ and $\{b_1, b_2, b_3\}$ be two different gaps where $a_i a_{i+1}, b_i b_{i+1} \in E(C_m)$ with $1 \leq i \leq 2$. Then, we have $N_{G'}(a_2) \cap W = W = N_{G'}(b_2) \cap W$, a contradiction.

- (3) Suppose that there exists a neighbouring gap of A containing at least 2 vertices.

Let $a_1, a_2, a_3, a_4, a_5 \in V(G')$ where $a_i a_{i+1} \in E(C_m)$ with $1 \leq i \leq 4$ and a_3 is the only element of W among them. Then, we have $N_{G'}(a_2) \cap W = W \setminus \{a_3\} = N_{G'}(a_4) \cap W$, a contradiction.

(\Leftarrow) Let $S \subseteq V(G')$ satisfying all three conditions above. Since $m \geq 7$, we obtain $|S| \geq 3$. Now, we consider a vertex $u \in V(G') \setminus S$.

- (i) u belongs to a gap containing one vertex.

Let a and b be two end points of this gap. So, u is the only vertex which is not adjacent to a and b . Since $|S| \geq 3$ and for every vertex $x \in V(G') \setminus (S \cup \{u\})$, $a \in N_{G'}(x)$ or $b \in N_{G'}(x)$, we obtain $\emptyset \neq N_{G'}(u) \cap S \neq N_{G'}(x) \cap S \neq \emptyset$.

- (ii) u belongs to a gap containing two vertices.

Let a and b be two end points of this gap. Without loss of generality, let $au \in E(C_m)$. So, $N_{G'}(u) \cap S = S \setminus \{a\}$. For $x \in V(G') \setminus (S \cup \{u\})$, if $a \in N_{G'}(x)$, then $\emptyset \neq N_{G'}(u) \cap S \neq N_{G'}(x) \cap S \neq \emptyset$; otherwise, x belongs to a gap containing one vertex. From (i) above, we obtain that $\emptyset \neq N_{G'}(u) \cap S \neq N_{G'}(x) \cap S \neq \emptyset$.

- (iii) u belongs to a gap containing three vertices.

Let c_1, c_2 , and c_3 be a gap of three vertices where $c_i c_{i+1} \in E(C_m)$ with $1 \leq i \leq 2$ and a and b be end points of this gap. Let $ac_1, bc_3 \in E(C_m)$. If $u = c_2$, then $N_{G'}(u) \cap S = S$. Since u is the only vertex having this property, we obtain that for every vertex $x \in V(G') \setminus (S \cup \{u\})$ and $\emptyset \neq N_{G'}(u) \cap S \neq N_{G'}(x) \cap S \neq \emptyset$. If $u = c_1$, then $N_{G'}(u) \cap S = S \setminus \{a\}$. For $x \in V(G') \setminus (S \cup \{u\})$, if $a \in N_{G'}(x)$, then $\emptyset \neq N_{G'}(u) \cap S \neq N_{G'}(x) \cap S \neq \emptyset$; otherwise, x belongs to a gap containing one vertex. From (i) above, we obtain that $\emptyset \neq N_{G'}(u) \cap S \neq N_{G'}(x) \cap S \neq \emptyset$. \square

Now, we are ready to prove Theorem 2.

Proof of Theorem 2.

For $m \geq 7$, let $H = K_m \setminus E(C_m)$ where $V(H) = \{x_1, x_2, \dots, x_m\}$ and $E(C_m) = \{x_1 x_2, x_2 x_3, \dots, x_{m-1} x_m, x_m x_1\}$. We distinguish two cases as follows:

- (1) $\lambda(H) \leq \lceil (2m-2)/5 \rceil$: we distinguish five cases of m as follows:

- (a) $m \equiv 0 \pmod{5}$: let $m = 5k$ for an integer $k \geq 2$. Then, $\lceil (2m-2)/5 \rceil = \lceil (10k-2)/5 \rceil = 2k$. We define $W = \{x_2, x_6\} \cup \{x_{5i+3}, x_{5i+6} \mid 1 \leq i \leq k-2\} \cup \{x_{5k-2}, x_{5k}\}$. Since $|W| = 2k$ and satisfies all conditions in Lemma 6, then W is a locating-dominating set of H .
- (b) $m \equiv 1 \pmod{5}$: let $m = 5k + 1$ for an integer $k \geq 2$. Then, $\lceil (2m-2)/5 \rceil = \lceil 10k/5 \rceil = 2k$. We define $W = \{x_2, x_6\} \cup \{x_{5i+3}, x_{5i+6} \mid 1 \leq i \leq k-2\} \cup \{x_{5k-2}, x_{5k+1}\}$. Since $|W| = 2k$ and satisfies all conditions in Lemma 6, then W is a locating-dominating set of H .
- (c) $m \equiv 2 \pmod{5}$: let $m = 5k + 2$ for an integer $k \geq 1$. Then, $\lceil (2m-2)/5 \rceil = \lceil (10k+2)/5 \rceil = 2k + 1$. We define $W = \{x_2, x_6\} \cup \{x_{5i+3}, x_{5i+6} \mid 1 \leq i \leq k-1\} \cup \{x_{5k+2}\}$. Since $|W| = 2k + 1$ and satisfies all conditions in Lemma 6, then W is a locating-dominating set of H .
- (d) $m \equiv 3 \pmod{5}$: let $m = 5k + 3$ for an integer $k \geq 1$. Then, $\lceil (2m-2)/5 \rceil = \lceil (10k+4)/5 \rceil = 2k + 1$. We define $W = \{x_2, x_6\} \cup \{x_{5i+3}, x_{5i+6} \mid 1 \leq i \leq k-1\} \cup \{x_{5k+3}\}$. Since $|W| = 2k + 1$ and satisfies all conditions in Lemma 6, then W is a locating-dominating set of H .
- (e) $m \equiv 4 \pmod{5}$: let $m = 5k + 4$ for an integer $k \geq 1$. Then, $\lceil (2m-2)/5 \rceil = \lceil (10k+6)/5 \rceil = 2k + 2$. We define $W = \{x_2, x_6\} \cup \{x_{5i+3}, x_{5i+6} \mid 1 \leq i \leq k-1\} \cup \{x_{5k+3}, x_{5k+4}\}$. Since $|W| = 2k + 2$ and satisfies all conditions in Lemma 6, then W is a locating-dominating set of H .

- (2) $\lambda(H) \geq \lceil (2m-2)/5 \rceil$: let S be a locating-dominating set of H with minimum cardinality. We consider two following cases:

- (a) $|S|$ is even.

Let $|S| = 2k$ for a positive integer k . So, the number of gap of H with respect to S is $2k$. Since S must be satisfy all conditions in Lemma 6, the number of gap containing at least 2 vertices is at most k . It follows that the number of vertex which is not in S is at most $3k + 1$. So, we obtain that $k \geq ((m-1)/5)$. Therefore,

$$\lambda(H) = |S| = 2k \geq 2 \cdot \left\lfloor \frac{m-1}{5} \right\rfloor = \left\lfloor \frac{2m-2}{5} \right\rfloor. \quad (5)$$

- (b) $|S|$ is odd.

Let $|S| = 2k + 1$ for a positive integer k . So, the number of gap of H with respect to S is $2k + 1$. Since S must be satisfy all conditions in Lemma 6, the number of gap containing at least 2 vertices is at most k . It follows that the number of vertex which is not in S is at most $3k + 2$. So, we obtain that $k \geq ((m-3)/5)$. Therefore,

$$\begin{aligned} \lambda(H) = |S| = 2k + 1 &\geq 2 \cdot \left\lceil \frac{m-3}{5} \right\rceil + 1 \\ &= \left\lceil \frac{2m-1}{5} \right\rceil \geq \left\lceil \frac{2m-2}{5} \right\rceil. \end{aligned} \tag{6}$$

4. (n - 3)-Regular Graph and Proof of Theorem 3

For $n \geq 5$, we consider certain cycles contained in a complete graph K_n . For $1 \leq r \leq \lfloor n/3 \rfloor$, let R_1, R_2, \dots, R_r be r disjoint cycles contained in K_n such that $V(R_1) \cup V(R_2) \cup \dots \cup V(R_r) = V(K_n)$. Note that an $(n - 3)$ -regular graph is isomorphic to $K_n \setminus (E(R_1) \cup E(R_2) \cup \dots \cup E(R_r))$. In case $r = 1$, the locating-dominating number of an $(n - 3)$ -regular graph of order at least 7 has been determined in Theorem 2. Now, we will determine the locating-dominating number of an $(n - 3)$ -regular graph of order $n \geq 5$ with $1 \leq r \leq \lfloor n/3 \rfloor$.

Let $G = K_n \setminus (E(R_1) \cup E(R_2) \cup \dots \cup E(R_r))$ and $m_i = |V(R_i)|$ where $1 \leq i \leq r$. Let G_i be a subgraph of G where $G_i = K_{m_i} \setminus E(R_i)$. Considering Lemma 4, a locating-dominating set of G consists of a locating-dominating set of G_i with $1 \leq i \leq r$. Therefore, we obtain that

$$\lambda(G) \geq \lambda(G_1) + \lambda(G_2) + \dots + \lambda(G_r). \tag{7}$$

Note that a locating-dominating of G also must satisfy all three conditions in Lemma 6. Let $W = \cup_{i=1}^r W_i$ where W_i is a locating-dominating set of G_i where $|W_i| = \lambda(G_i)$. If there exists distinct $i, j \in \{1, 2, \dots, r\}$ such that both locating-dominating sets G_i and G_j contain a gap of three vertices, then we must add at least one more vertex on W . So, we need to know the gap properties of a locating-dominating set of G_i .

Lemma 7. For $n \geq 5$, let G be an $(n - 3)$ -regular graph. Let $G' \subseteq G$ such that $G' = K_{m_i} \setminus E(C_{m_i})$ with $m \in \{3, 4, \dots, n\}$.

- (1) If $m = 3, n > m = 5$, or $m \equiv 0, 2, 4 \pmod{5}$, then there exists a locating-dominating set of G' where every gap contains at most two vertices.
- (2) If $m = n = 5$ or $m \equiv 1, 3 \pmod{5}$ with $m \neq 3$, then a locating-dominating set of G' has a gap containing three vertices.

Proof. First, let $m = 3, n > m = 5$, or $m \equiv 0, 2, 4 \pmod{5}$. Note that, in this case of m , we have $G' \subset G$. Let $V(G') = \{x_1, x_2, \dots, x_m\}$ and $E(C_m) = \{x_1x_2, x_2x_3, \dots, x_{m-1}x_m, x_mx_1\}$. We distinguish five cases as follows:

- (1) $m = 3$ or $m = 5$: by Remark 1, $\lambda(G') = 2$. We define $W' = \{x_1, x_3\}$.
- (2) $m = 4$: by Remark 1, $\lambda(G') = 2$. We define $W' = \{x_1, x_4\}$.
- (3) $m \equiv 0 \pmod{5}$: let $m = 5k$ for integer $k \geq 2$. By Theorem 2, $\lambda(G') = 2k$. We define $W' = \{x_1, x_4, x_6, x_9\} \cup \{x_{5i+6}, x_{5i+9} \mid 1 \leq i \leq k - 2\}$.
- (4) $m \equiv 2 \pmod{5}$: let $m = 5k + 2$ for integer $k \geq 1$. By Theorem 2, $\lambda(G') = 2k + 1$. We define $W' = \{x_1, x_4, x_6\} \cup \{x_{5i+4}, x_{5i+6} \mid 1 \leq i \leq k - 1\}$.

- (5) $m \neq 4$ and $m \equiv 4 \pmod{5}$: let $m = 5k + 4$ for integer $k \geq 1$. By Theorem 2, $\lambda(G') = 2k + 2$. We define $W' = \{x_1, x_4, x_6, x_9\} \cup \{x_{5i+6}, x_{5i+9} \mid 1 \leq i \leq k - 1\}$.

Note that every gap with respect to W' above contains at most two vertices. Since W' satisfies Lemma 6, then W' is a locating-dominating set of G' .

Now, let $m = n = 5$ or $m \equiv 1, 3 \pmod{5}$ with $m \neq 3$. Suppose that every gap in G' contains at most two vertices. We distinguish three cases as follows:

- (1) $m \equiv 1 \pmod{5}$: let $m = 5k + 1$ for integer $k \geq 1$. By Theorem 2, $\lambda(G') = 2k$. Let W be a locating-dominating set of G' with $2k$ vertices. By Lemma 6, k gaps with respect to W , containing one vertex, and k other gaps with respect to W , containing two vertices. Thus, the total number of vertices of G' which are not element of W is $3k$. It follows that $m = |V(G') \setminus W| + |W| = 3k + 2k = 5k$, a contradiction.
- (2) $m \neq 3$ and $m \equiv 3 \pmod{5}$: let $m = 5k + 3$ for integer $k \geq 1$. By Theorem 2, $\lambda(G') = 2k + 1$. Let W be a locating-dominating set of G' with $2k + 1$ vertices. By Lemma 6, $k + 1$ gaps with respect to W , containing one vertex, and k other gaps with respect to W , containing two vertices. Thus, the total number of vertices of G' which are not element of W is $3k + 1$. It follows that $m = |V(G') \setminus W| + |W| = (3k + 1) + 2k = 5k + 1$, a contradiction.
- (3) $m = n = 5$: thus, $G = G'$. Let $V(G') = \{x_1, x_2, \dots, x_5\}$ and $E(C_5) = \{x_1x_2, x_2x_3, \dots, x_4x_5, x_5x_1\}$. By Remark 1, $\lambda(G') = 2$. Since every gap in G' contains at most two vertices, without loss of generality, let W be a locating-dominating set of G' where $W = \{x_1, x_3\}$. Since $N_G(x_2) = \{x_4, x_5\}$, we obtain that $N_G(x_2) \cap W = \emptyset$, a contradiction. \square

Now, we are ready to prove Theorem 3.

Proof of Theorem 3.

The first case for $\lambda(G)$ is a direct consequence of Theorem 2, Lemmas 6 and 7, and Remark 1.

For the last case, let $H_{m_1}, H_{m_2}, \dots, H_{m_k}$ be disjoint k subgraphs of G such that $H_{m_i} = K_{m_i} \setminus E(C_{m_i})$ where $1 \leq i \leq k$, $m_i \neq 3$, and $m_i \equiv 1$ or $3 \pmod{5}$. Let B_i be a locating-dominating set of H_{m_i} with $\lambda(H_{m_i})$ vertices. By Lemma 7, B_i has a gap containing three vertices, say a_1^i, a_2^i , and a_3^i where $a_j^i a_{j+1}^i \notin E(H_{m_i})$ with $1 \leq j \leq 2$. We define $B_i' = B_i \cup \{a_2^i\}$. It is easy to see that B_i' is a locating-dominating set of H_{m_i} which all the gaps contain at most two vertices. So, by using this property to subgraphs $H_{m_1}, H_{m_2}, \dots, H_{m_{k-1}}$ of G , Theorem 2, Lemmas 6 and 7, and Remark 1, we prove the last case.

Data Availability

This research article is the theoretical study of locating-dominating set in graphs. There is no data supporting used. All results in the manuscript can be obtained by the analytical method.

Conflicts of Interest

The authors declare there are no conflicts of interest.

Authors' Contributions

A.K.A.G and S.W.S conceptualized and wrote the study. S.W.S revised the study. All authors have read and agreed to the published version of the manuscript.

Acknowledgments

This research was partially supported by Riset Unggulan of Bandung Institute of Technology 2021 Indonesia.

References

- [1] P. J. Slater, "Domination and location in acyclic graphs," *Networks*, vol. 17, no. 1, pp. 55–64, 1987.
- [2] P. J. Slater, "Dominating and reference sets in a graph," *Journal of Mathematical and Physical Sciences*, vol. 22, pp. 445–455, 1988.
- [3] I. Charon, O. Hudry, and A. Lobstein, "Minimizing the size of an identifying or locating-dominating code in a graph is NP-hard," *Theoretical Computer Science*, vol. 290, no. 3, pp. 2109–2120, 2003.
- [4] N. Bertrand, I. Charon, O. Hudry, and A. Lobstein, "Identifying and locating-dominating codes on chains and cycles," *European Journal of Combinatorics*, vol. 25, no. 7, pp. 969–987, 2004.
- [5] G. R. Argiroffo, S. M. Bianchi, and A. K. Wagler, "A polyhedral approach to locating-dominating sets in graphs," *Electronic Notes in Discrete Mathematics*, vol. 50, pp. 89–94, 2015.
- [6] M. A. Henning and O. R. Oellermann, "Metric-locating-dominating sets in graphs," *Ars Combinatoria*, vol. 73, pp. 129–141, 2004.
- [7] J. Cáceres, C. Hernando, M. Mora, I. M. Pelayo, and M. L. Puertas, "Locating-dominating codes: bounds and extremal cardinalities," *Applied Mathematics and Computation*, vol. 220, pp. 38–45, 2013.
- [8] C. Hernando, M. Mora, and I. M. Pelayo, "Locating domination in bipartite graphs and their complements," *Discrete Applied Mathematics*, vol. 263, pp. 195–203, 2019.
- [9] F. Foucaud, M. A. Henning, and C. Löwenstein, "Locating-dominating sets in twin-free graphs," *Discrete Applied Mathematics*, vol. 200, pp. 52–58, 2016.
- [10] D. Garijo, A. González, and A. Márquez, "The difference between the metric dimension and the determining number of a graph," *Applied Mathematics and Computation*, vol. 249, pp. 487–501, 2014.
- [11] M. Fazil, I. Javaid, M. Salman, and U. Ali, "Locating-dominating sets in hypergraphs," *Periodica Mathematica Hungarica*, vol. 72, no. 2, pp. 224–234, 2016.
- [12] C. Balbuena, F. Foucaud, and A. Hansberg, "Locating-dominating sets and identifying codes in graphs of girth at least 5," *Electronic Journal of Combinatorics*, vol. 22, no. 2, 2015.
- [13] G. Rajasekar and K. Nagarajan, "Algorithm for finding location domination number of a graph connected by a bridge," *International Journal of Pure and Applied Mathematics*, vol. 118, no. 6, pp. 313–321, 2018.
- [14] S. R. Canoy Jr, G. A. Malacas, and D. Tarepe, "Locating dominating sets in graphs," *Applied Mathematical Sciences*, vol. 8, no. 8, pp. 4381–4388, 2014.
- [15] A. A. Pribadi and S. W. Saputro, "On locating-dominating number of comb product graphs," *Indonesian Journal of Combinatorics*, vol. 4, no. 1, pp. 27–33, 2020.
- [16] M. Murtaza, M. Fazil, and I. Javaid, "Locating-dominating sets of functigraphs," *Theoretical Computer Science*, vol. 799, pp. 115–123, 2019.
- [17] G. Argiroffo, S. Bianchi, Y. Lucarini, and A. Wagler, "The identifying code, the locating-dominating, the open locating-dominating and the locating total-dominating problems under some graph operations," *Electronic Notes in Theoretical Computer Science*, vol. 346, pp. 135–145, 2019.
- [18] P. S. Buczkowski, G. Chartrand, C. Poisson, and P. Zhang, "On k -dimensional graphs and their bases," *Periodica Mathematica Hungarica*, vol. 46, no. 1, pp. 9–15, 2003.

Research Article

(k, l) -Anonymity in Wheel-Related Social Graphs Measured on the Base of k -Metric Antidimension

Jiang-Hua Tang,¹ Tahira Noreen,² Muhammad Salman ,² Masood Ur Rehman ,³ and Jia-Bao Liu ⁴

¹Department of General Education, Anhui Xinhua University, Hefei 230088, China

²Department of Mathematics, The Islamia University of Bahawalpur, Bahawalpur 63100, Pakistan

³Department of Basic Sciences, Balochistan University of Engineering and Technology Khuzdar, Khuzdar 89100, Pakistan

⁴School of Mathematics and Physics, Anhui Jianzhu University, Hefei, Anhui 230601, China

Correspondence should be addressed to Masood Ur Rehman; masoodqau27@gmail.com

Received 22 July 2021; Accepted 28 August 2021; Published 16 September 2021

Academic Editor: Ali Ahmad

Copyright © 2021 Jiang-Hua Tang et al. This is an open access article distributed under the Creative Commons Attribution License, which permits unrestricted use, distribution, and reproduction in any medium, provided the original work is properly cited.

For the study and valuation of social graphs, which affect an extensive range of applications such as community decision-making support and recommender systems, it is highly recommended to sustain the resistance of a social graph G to active attacks. In this regard, a novel privacy measure, called the (k, l) -anonymity, is used since the last few years on the base of k -metric antidimension of G in which l is the maximum number of attacker nodes defining the k -metric antidimension of G for the smallest positive integer k . The k -metric antidimension of G is the smallest number of attacker nodes less than or equal to l such that other k nodes in G cannot be uniquely identified by the attacker nodes. In this paper, we consider four families of wheel-related social graphs, namely, Jahangir graphs, helm graphs, flower graphs, and sunflower graphs. By determining their k -metric antidimension, we prove that each social graph of these families is the maximum degree metric antidimensional, where the degree of a vertex is the number of vertices linked with that vertex.

1. Introduction

Since 2016, a novel privacy measure, “the (k, l) anonymity,” is defined and used, for the sake of a social graph confrontation from various active attacks, in connection with the concept of k -metric antidimension. Trujillo-Rasua and Yero defined, studied in detail, and promoted the idea of k -metric antidimension, which provides a basis for the privacy measure (k, l) -anonymity [7]. They defined this privacy measure as follows:

“The (k, l) -anonymity for a social graph G will be preserved according to active attacks if the k -metric antidimension of G is bounded above by l for the least positive integer k , where l is an upper bound on the expected number of attacker nodes.”

Accordingly, it can be seen that having a k -antimetric generator (a set defining the k -metric antidimension) as the

set of attacker nodes, the probability of unique identification of other nodes by an adversary in a social graph is less than or equal to $(1/k)$.

Besides, providing many significant theoretical properties of the k -metric antidimension of graphs, Trujillo-Rasua and Yero also supplied the k -metric antidimension of complete graphs, paths, cycles, complete bipartite graphs, and trees [7]. This significant work of Trujillo-Rasua and Yero attracted many researchers to work on this idea, and therefore, the literature has been updated with the following remarkable contributions up till now:

- (i) Trujillo-Rasua and Yero further contributed by characterizing 1-metric antidimensional trees and unicyclic graphs [8]
- (ii) Mauw et al. contributed by providing a privacy-preserving graph transformation, which improves

privacy in social network graphs by contracting active attacks [6]

- (iii) Čangalović et al. contributed by considering wheels and grid graphs in the context of the k -metric antidimension [1]
- (iv) DasGupta et al. contributed by analyzing and evaluating privacy-violation properties of eight social network graphs [4]
- (v) Kratica et al. contributed by investigating the k -metric antidimension of two families of generalized Petersen graphs $GP(n, 1)$ (also called prism graphs) and $GP(n, 2)$ [5]
- (vi) Zhang and Gao and, later on, Chatterjee et al. contributed by proving that the problem of finding the k -metric antidimension of a graph is, generally, an NP-complete problem [3, 9]

Inspired by all these contributions and, particularly, motivated by the work done by Čangalović et al. on wheel graphs, we place our contribution by extending the study of (k, l) -anonymity privacy measure based on k -metric antidimension towards four families of wheel-related social graphs.

2. Basic Works

Let $G = (V(G), E(G))$ be a simple and connected graph. We denote two adjacent vertices x and y by $x \sim y$ and non-adjacent by $x \not\sim y$ in G . Two vertices of G are said to be neighbors of each other if there is an edge between them. The (open) neighborhood of a vertex x in G is $N(x) = \{y \in V(G) : y \sim x \in E(G)\}$. The neighborhood $N(x)$ is closed if it includes x and is denoted by $N[x]$. The number of vertices adjacent with a vertex x is called its degree and is denoted by $d(x)$. The maximum degree in G is $\Delta = \max_{x \in V(G)} d(x)$. The metric on G is a mapping $d : V(G) \times V(G) \rightarrow \mathbb{Z}^+ \cup \{0\}$ defined by $d(x, y) = l$, where l is the length of the number of edges in the shortest path between vertices x and y in G . A vertex u of G identifies a pair (x, y) of vertices in G if $d(x, u) \neq d(y, u)$. The sum $G + H$ of two graphs G and H is obtained by joining each vertex of G with every vertex of H . We refer the book in [2] for nonmentioned graphical notations and terminologies used in this paper.

Let $S = \{s_1, s_2, \dots, s_t\} \subseteq V(G)$ be an ordered set. Then, the metric code, or simply code, of a vertex $u \in V(G)$ with respect to S is the t -vector $c_S(u) = (d(u, s_1), d(u, s_2), \dots, d(u, s_t))$. A chosen set S of vertices of G unique identifies each pair (x, y) of vertices in G if $c_S(x) \neq c_S(y)$. The following concepts are defined by Trujillo-Rasua and Yero in [7]:

- (i) A set S of vertices of G is called a k -antimetric generator (k -antiresolving set) for G if k is the largest positive integer such that k vertices of G , other than the vertices in S , are not uniquely

identified by S ; i.e., for every vertex $w \in V(G) - S$, there exist at least $k - 1$ different vertices $u_1, \dots, u_{k-1} \in V(G) - S$ such that $c_S(w) = c_S(u_1) = \dots = c_S(u_{k-1})$

- (ii) The cardinality of the smallest k -antimetric generator for G is called the k -metric antidimension of G , denoted by $adim_k(G)$, and such a smallest generator is known as k -antimetric basis of G
- (iii) If k is the largest positive integer such that G has a k -antimetric generator, then G is said to be k -metric antidimensional graph

If S is a set of vertices of a graph G , then it has been defined as a relation on $V(G) - S$ according to the vertices having equal metric codes with respect to S as follows.

2.1. Equivalence Relation and Classes [5, 7]. Let $S \subset V(G)$ be a set of vertices of a connected graph G and let ρ_S be a relation on $V(G) - S$ defined by

$$\begin{aligned} \text{for all } x, y \in V(G) - S, \\ x \rho_S y \Leftrightarrow c_S(x) = c_S(y). \end{aligned} \quad (1)$$

This relation is an equivalence relation and partitioned $V(G) - S$ into classes, say S_1, \dots, S_m , called the equivalence classes corresponds to the relation ρ_S .

Accordingly, we get the following useful property from [5].

Remark 1 (see [5]). For a fixed integer $k \geq 1$, a set S is a k -antimetric generator for G if and only if $\min_{i=1}^m |S_i| = k$, where each $S_i, 1 \leq i \leq m$, is an equivalence class defined by the relation ρ_S .

3. Wheel-Related Social Graphs

In this section, we consider five wheel-related social graphs. The (k, l) -anonymity of one of them, called a wheel graph, has been measured previously in [1], by investigating its k -metric antidimension. Here, we focus to investigate the k -metric antidimension of other four graphs. For $n \geq 3$, a wheel graph is $W_{1,n} = K_1 + C_n$, where K_1 is the trivial graph having only one vertex v , and C_n is a cycle graph with vertices in $V = V(C_n) = \{v_1, v_2, \dots, v_n\}$. Accordingly, the vertex set of this graph is $V(W_{1,n}) = \{v\} \cup V$ and edge set is $E(W_{1,n}) = \{v \sim v_i, v_i \sim v_{i+1}; 1 \leq i \leq n\}$, where the indices greater than n or less than 1 will be taken modulo n . Each edge $v \sim v_i$ is called a spoke in a wheel graph. One such graph is depicted in Figure 1.

In 2018, Čangalović et al. supplied the following investigations.

Observation 1 (see [1])

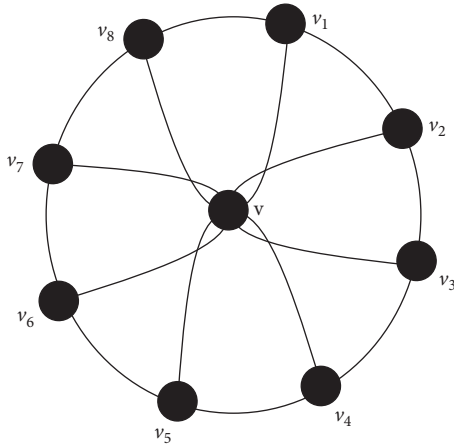


FIGURE 1: One wheel graph $W_{1,8}$.

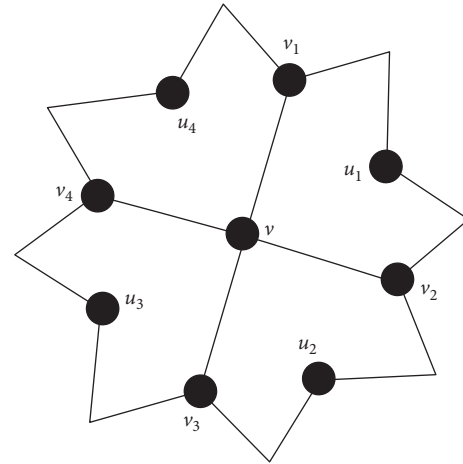


FIGURE 2: One Jahangir graph J_8 .

$$\text{adim}_k(W_{1,3}) = \begin{cases} 1, & \text{for } k = 3, \\ 2, & \text{for } k = 2, \\ 3, & \text{for } k = 1, \end{cases} \quad (2)$$

$$\text{adim}_k(W_{1,4}) = \begin{cases} 1, & \text{for } k = 1, 4, \\ 2, & \text{for } k = 3, \\ 3, & \text{for } k = 2, \end{cases} \quad (3)$$

$$\text{adim}_k(W_{1,5}) = \begin{cases} 1, & \text{for } k = 2, 5, \\ 2, & \text{for } k = 1. \end{cases} \quad (4)$$

Theorem 1 (see [1]). For all $n \geq 6$,

$$\text{adim}_k(W_{1,n}) = \begin{cases} 1, & \text{for } k = 3, n, \\ 2, & \text{for } k = 1, 2. \end{cases} \quad (5)$$

The rest of the section is aimed to investigate the k -metric antidimensions of Jahangir graphs, helm graphs, flower graphs, and sunflower graphs.

3.1. Jahangir Graphs. For $n \geq 2$, a Jahangir (Gear) graph, J_{2n} , is obtained from a wheel graph $W_{1,2n} = K_1 + C_{2n}$ by deleting alternating spokes from the wheel. Let $V(C_{2n}) = V \cup U$, where $V = \{v_1, v_2, \dots, v_n\}$ and $U = \{u_1, u_2, \dots, u_n\}$. Then, the vertex set of a Jahangir graph is $V(J_{2n}) = \{v\} \cup V \cup U$ and its edge set is $E(J_{2n}) = \{v \sim v_i, v_i \sim u_i, v_i \sim u_{i-1}; 1 \leq i \leq n\}$, where the indices greater than n or less than 1 will be taken modulo n . Figure 2 depicts graphical view of one Jahangir graph.

The following observation is easy to verify for $n = 2, 3$, and 4.

Observation 2

$$\text{adim}_k(J_4) = \begin{cases} 1, & \text{for } k = 1, 2, \\ 2, & \text{for } k = 3, \end{cases} \quad (6)$$

$$\text{adim}_k(J_6) = \begin{cases} 1, & \text{for } k = 1, 3, \\ 3, & \text{for } k = 2, \end{cases} \quad (7)$$

and $\text{adim}_k(J_8) = 1$ for each $k \in \{1, 2, 4\}$.

For all values of $n \geq 5$, the following result provides the k -metric antidimension of Jahangir graphs.

Theorem 2. For $n \geq 5$, let J_{2n} be a Jahangir graph. Then,

$$\text{adim}_k(J_{2n}) = \begin{cases} 1, & \text{for } k = 2, 3, n, \\ 2, & \text{for } k = 1. \end{cases} \quad (8)$$

Proof. First of all, it is worthy to note that $N(v) = V(C_{2n})$ and $N(v_i) = \{v, u_i, u_{i-1}\}$, for any $v_i \in V$, and $N(u_i) = \{v_i, v_{i+1}\}$, for any $u_i \in U$. Now, we need to discuss the following seven claims.

Claim 1: the set $S = \{v\}$ is an n -antimetric generator for J_{2n} .

Note that $c_S(x) = (1)$, for all $x \in V$, and $c_S(y) = (2)$, for all $y \in U$. According to the relation ρ_S , there are only two equivalence classes each has cardinality n . So, the result followed by Remark 1.

Claim 2: every singleton subset of V is a 3-antimetric generator for J_{2n} .

Let $S = \{v_i\} \subset V$ for any fixed $1 \leq i \leq n$. Then, $c_S(x) = (1)$, for all $x \in N(v_i)$, $c_S(y) = (2)$, for all $y \in V - \{v_i\}$, and $c_S(z) = (3)$, for all $z \in U - \{u_i, u_{i-1}\}$. Hence, the relation ρ_S supplies three equivalence classes $S_1 = N(v_i)$, $S_2 = V - \{v_i\}$, and $S_3 = U - \{u_i, u_{i-1}\}$. Thus,

$\min_{i=1}^3 |S_i| = 3$, and hence, S is 3-antimetric generator, by Remark 1.

Claim 3: every singleton subset of U is a 2-antimetric generator for J_{2n} .

Let $S = \{u_i\} \subset U$; then, metric codes of the vertices are

$$\begin{aligned} c_S(x) &= (1) \forall x \in N(u_i); c_S(u_{i+1}) \\ &= (2) = c_S(u_{i-1}) = c_S(v), \end{aligned} \quad (9)$$

$$\begin{aligned} c_S(y) &= (3) \forall y \in V - N(u_i); c_S(z) \\ &= (4) \forall z \in U - \{u_{i-1}, u_i, u_{i+1}\}. \end{aligned} \quad (10)$$

Clearly, we receive four equivalence classes according to the relation ρ_S , $S_1 = N(u_i)$, $S_2 = N(v_i)$, $S_3 = V - N(u_i)$, and $S_4 = U - \{u_{i-1}, u_i, u_{i+1}\}$. Hence, $\min_{i=1}^4 |S_i| = 2$, and S is a 2-antimetric generator, by Remark 1.

Claim 4: every 2 element subset of $V(J_{2n})$ is either 1-antimetric generator or 2-antimetric generator for J_{2n} .

Let S be a 2-element subset of $V(J_{2n})$. Then, we have the following two cases to discuss.

Case 1 (S contains v): here, we have two subcases.

Subcase 1.1: let $S = \{v, x\}$ with $x \in V$; then, $c_S(p) = (2, 1) = c_S(q)$, for distinct $p, q \in N(x) - \{v\}$:

$$\begin{aligned} c_S(y) &= (1, 2) \forall y \in V - \{x\}; c_S(z) \\ &= (2, 3) \forall z \in U - N(x). \end{aligned} \quad (11)$$

So, the equivalence classes corresponds to the relation ρ_S are $S_1 = N(x) - \{v\}$, $S_2 = V - \{x\}$, and $S_3 = U - N(x)$. Here, $\min_{i=1}^3 |S_i| = 2$, which implies that S is a 2-antimetric generator, by Remark 1.

Subcase 1.2: let $S = \{v, x\}$ with $x \in U$; then, $c_S(t) = (1, 1)$, for $t \in N(x)$:

$$\begin{aligned} c_S(p) &= (2, 2) = c_S(p') \text{ for } p, p' \in U \text{ such that } d(p, x) \\ &= d(p', x) = 2, \end{aligned} \quad (12)$$

$$\begin{aligned} c_S(y) &= (1, 3) \forall y \in V - N(x); c_S(z) \\ &= (2, 4) \forall z \in U - \{p, x, p'\}. \end{aligned} \quad (13)$$

Due to the above metric coding, it is clear that we find four equivalence classes according to the relation ρ_S , which are $S_1 = N(x)$, $S_2 = \{p, p'\}$, $S_3 = V - N(x)$, and $S_4 = U - \{p, x, p'\}$. Thus, $\min_{i=1}^4 |S_i| = 2$, which implies that S is a 2-antimetric generator, by Remark 1.

Case 2 (S does not contain v): again, we have three subcases to discuss.

Subcase 2.1: let $S \subset V$ and $S = \{v, v'\}$. Then, $d(v, v') = 2$. If $N(v) \cap N(v') = \{x\} \subset U$, then a vertex

$y \in U$, such that $d(y, x) = 2$, has the unique metric code from the set $\{(1, 3), (3, 1)\}$ with respect to S . If no vertex from U is a common neighbor of v and v' , then the vertex v has the unique metric code $(1, 1)$ with respect to S .

Subcase 2.2: let $S \subset U$ and $S = \{u, u'\}$. Then, either $d(u, u') = 2$ or $d(u, u') = 4$. In the former case, a vertex $v \in V$, such that $v \in N(u) \cap N(u')$, has the unique metric code $(1, 1)$. In the later case, we have two possibilities. If there is a vertex $x \in U$ such that $d(x, u) = 2 = d(x, u')$, then a vertex $y \in U$, with $d(y, u) = 2$ and $d(y, u') = 4$, has the unique metric code $(2, 4)$ with respect to S . If there is no such x in U , then the vertex v has the unique metric code $(2, 2)$ with respect to S .

Subcase 2.3: let $S = \{u, v\}$ for $u \in U$ and $v \in V$. Then, either $d(u, v) = 1$ or $d(u, v) = 3$. For the later case, let $N(v) = \{v, x, y\}$, where $x, y \in U$ are distinct vertices. Here, we have two possibilities. If one of the neighbors x and y of v , say x , has the property that $d(x, u) = 2$, then the neighbor y of v has the unique metric code $(4, 1)$ with respect to S . If $d(x, u) = 4 = d(y, u)$, then the vertex v has the unique metric code $(2, 1)$ with respect to S . In the former case, v is a one neighbor of u from V , and the other neighbor of u from V has the unique metric code $(1, 2)$ with respect to S .

In each possibility of these subcases, the relation ρ_S proposes at least one singleton equivalence class, which follows that $\min_i |S_i| = 1$. Hence, S is an 1-antimetric generator, by Remark 1.

Claim 5: for $n \geq 7$, the set $A' = \{v_i, v, x\} \subseteq V(J_{2n})$ is a 2-antimetric generator whenever $x \in (V \cup U) - \{u_{i-2}, v_{i-1}, u_{i-1}, v_i, u_i, v_{i+1}, u_{i+1}\}$. Otherwise, A' is 1-antimetric generator for J_{2n} .

If $x \in (V \cup U) - \{u_{i-2}, v_{i-1}, u_{i-1}, v_i, u_i, v_{i+1}, u_{i+1}\}$, the following two cases are need to be discussed for x .

Case 1: whenever $x \in U - \{u_{i-2}, u_{i-1}, u_i, u_{i+1}\}$, metric codes with respect to A' are

$$\begin{aligned} c_{A'}(t) &= (1, 2, 4) \forall t \in N(v_i) - \{v\}, \\ c_{A'}(p) &= (2, 1, 1) \forall p \in N(x), \end{aligned} \quad (14)$$

$$\begin{aligned} c_{A'}(q) &= (2, 1, 3) \forall q \in V - N(x), \\ c_{A'}(u_{i+1}) &= (3, 2, 2) = c_{A'}(u_{i+3}) \text{ for } 1 \leq i \leq n, \end{aligned} \quad (15)$$

$$\begin{aligned} c_{A'}(y) &= (3, 2, 4) \forall y \in U \\ &\quad - \{u_{i-1}, u_i, x, u_{i+2}, u_{i+3}\}. \end{aligned} \quad (16)$$

So, the equivalence classes corresponds to the relation $\rho_{A'}$ are $S_1 = N(v_i) - \{v\}$, $S_2 = N(x)$, $S_3 = V - N(x)$, $S_4 = \{u_{i+1}, u_{i+3}\}$, and $S_5 = U - \{u_{i-1}, u_i, x, u_{i+1}, u_{i+2}, u_{i+3}\}$. Note that $\min_{i=1}^5 |S_i| = 2$, so Remark 1 yields the required result.

Case 2: whenever $x \in V - \{v_{i-1}, v_i, v_{i+1}\}$, metric codes with respect to A' are

$$\begin{aligned} c_{A'}(f) &= (1, 2, 3) \forall f \in N(v_i) - \{v\}; \\ c_{A'}(g) &= (3, 2, 1) \forall g \in N(x) - \{v\}, \end{aligned} \quad (17)$$

$$\begin{aligned} c_{A'}(h) &= (2, 1, 2) \forall h \in V - \{v_i, x\}; \\ c_{A'}(m) &= (3, 2, 3) \forall m \in U - (N(v_i) \cup N(x)). \end{aligned} \quad (18)$$

Hence, the equivalence classes corresponds to relation $\rho_{A'}$ are $S_1 = N(v_i) - \{v\}$, $S_2 = N(x) - \{v\}$, $S_3 = V - \{v_i, x\}$, and $S_4 = U - (N(v_i) \cup N(x))$. It follows that $\min_{i=1}^4 |S_i| = 2$ because $n \geq 7$. Thus, Remark 1 proves that A' is a 2-antimetric generator.

Now, if $x \in \{u_{i-2}, v_{i-1}, u_{i-1}, u_i, v_{i+1}, u_{i+1}\}$, then again we have two cases.

Case 1: whenever $x \in \{v_{i-1}, v_{i+1}\}$, we have a vertex $t \in N(x) - \{v\}$ such that $c_{A'}(t) \neq c_{A'}(t')$, for all $t' \in V(C_{2n}) - \{t\}$

Case 2: whenever $x \in \{u_{i-2}, u_{i-1}, u_i, u_{i+1}\}$, we have a vertex $t \in U$ with $d(t, x) = 2$ and $c_{A'}(t) \neq c_{A'}(t')$, for all $t' \in V(C_{2n}) - \{t\}$

In both the cases, we get at least one singleton equivalence class $\{t\}$ with respect to the relation $\rho_{A'}$, which implies that $\min_i |S_i| = 1$. Hence, A' is a 1-antimetric generator, by Remark 1.

Claim 6: except $n = 5, 7$, the set $B = \{u_i, v, u\} \subseteq V(J_{2n})$ is a 2-antimetric generator whenever $u \in U - \{u_{i-2}, u_{i-1}, u_i, u_{i+1}, u_{i+2}\}$. Otherwise, B is a 1-antimetric generator for J_{2n} .

Whenever $u \in U - \{u_{i-2}, u_{i-1}, u_i, u_{i+1}, u_{i+2}\}$, then the metric coding with respect to B is

$$\begin{aligned} c_B(p) &= (1, 1, 3) \forall p \in N(u_i), c_B(u_{i-1}) = (2, 2, 4) \\ &= c_S(u_{i+1}), c_B(q) = (3, 1, 1) \forall q \in N(u), \end{aligned} \quad (19)$$

$$\begin{aligned} c_B(x') &= (4, 2, 2) = c_S(y'), \text{ where } x', y' \\ &\in U \text{ such that } d(x', u) = d(y', u) = 2, \end{aligned} \quad (20)$$

$$\begin{aligned} c_B(x) &= (3, 1, 3) \forall x \in V - (N(u_i) \cup N(u)), c_B(z) \\ &= (4, 2, 4) \forall z \in U - \{u_{i-1}, u_i, u_{i+1}, x', u, y'\}. \end{aligned} \quad (21)$$

Hence, we have the equivalence classes $S_1 = N(u_i)$, $S_2 = \{u_{i-1}, u_{i+1}\}$, $S_3 = N(u)$, $S_4 = \{x', y'\}$, $S_5 = V - (N(u_i) \cup N(u))$, and $S_6 = U - \{u_{i-1}, u_i, u_{i+1}, x', u, y'\}$

in accordance with the relation ρ_B . Thus, $\min_{i=1}^6 |S_i| = 2$, o B is a 2-antimetric generator, by Remark 1.

Next, whenever $u \in \{u_{i-2}, u_{i-1}, u_{i+1}, u_{i+2}\}$, then

$$\begin{aligned} c_B(v_i) &= (1, 1, 1) \text{ when } u = u_{i-1}, \\ c_B(v_{i+1}) &= (1, 1, 1) \text{ when } u = u_{i+2}, \end{aligned} \quad (22)$$

$$\begin{aligned} c_B(v_{i-1}) &= (2, 2, 2) \text{ when } u = u_{i-2}, \\ c_B(v_{i+1}) &= (2, 2, 2) \text{ when } u = u_{i+2}. \end{aligned} \quad (23)$$

In each possibility, the given metric code is unique, which provides a singleton equivalence class according to the relation ρ_B . Hence, $\min |S_i| = 1$, and B is a 1-antimetric generator, by Remark 1.

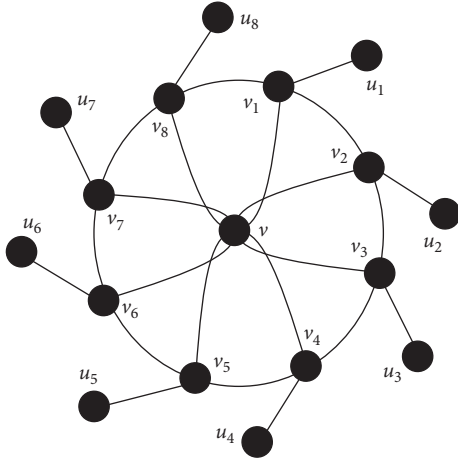
Claim 7: every set $S \subseteq V(J_{2n})$ of cardinality $t \geq 3$ is a 1-antimetric generator for J_{2n} , except the sets A' and B discussed in Claims 5 and 6, respectively.

If S contains the vertex v , then there exists a vertex $g \in U$ (or $g \in V$) such that g is a neighbor of some element in S , and $c_S(g) \neq c_S(g')$, for any $g' \in V(J_{2n}) - \{g\}$. If S does not contain the vertex v , then v has the unique metric code with respect to S . In both the cases, we get a singleton equivalence class according to the relation ρ_S . Hence, $\min |S_i| = 1$, and Remark 1 implies that S is a 1-antimetric generator.

All these claims conclude the proof with the following points:

- (i) For $k \in \{4, 5, \dots, n-1\}$, there does not exist a k -antimetric generator for J_{2n} .
- (ii) Claims 1, 2, and 3 provide that $\text{adim}_1(J_{2n}) \geq 2$. Furthermore, there exist 1-antimetric generators for J_{2n} of cardinality at least 2, by Claims 4 to 7. It follows that $\text{adim}_1(J_{2n}) = 2$.
- (iii) Claim 3 provides the existence of a 2-antimetric generator for J_{2n} of cardinality 1, which yields that $\text{adim}_2(J_{2n}) = 1$.
- (iv) Claim 2 provides the existence of a 3-antimetric generator for J_{2n} of cardinality 1, which implies that $\text{adim}_3(J_{2n}) = 1$.
- (v) An n -antimetric generator for J_{2n} of cardinality 1 exists due to Claim 1, and hence, $\text{adim}_n(J_{2n}) = 1$. \square

3.2. Helm Graphs. For $n \geq 3$, a helm graph, H_n , is obtained from a wheel graph $W_{1,n} = K_1 + C_n$ by attaching one leaf (a vertex of degree one) with each vertex of the cycle C_n . Let $U = \{u_1, u_2, \dots, u_n\}$ be the set of leaves; then, the vertex set of a helm graph is $V(H_n) = V(W_{1,n}) \cup U$, and its edge set is $E(H_n) = E(W_{1,n}) \cup \{v_i \sim u_i; 1 \leq i \leq n\}$, where the indices greater than n or less than 1 will be taken modulo n . One helm graph is shown in Figure 3.

FIGURE 3: One helm graph H_8 .

It is an easy task to verify the following observation.

Observation 3. When $n \in \{3, 5\}$, $\text{adim}_k(H_n) = 1$, for $k = 1, 2, \dots, n$. While

$$\text{adim}_k(H_4) = \begin{cases} 1, & \text{for } k = 1, 4, \\ 5, & \text{for } k = 2, \end{cases} \quad (24)$$

$$\text{adim}_k(H_6) = \begin{cases} 1, & \text{for } k = 1, 3, 6, \\ 3, & \text{for } k = 2. \end{cases} \quad (25)$$

Theorem 3. For $n \geq 7$, let H_n be a helm graph. Then,

$$\text{adim}_k(H_n) = \begin{cases} 1, & \text{for } k = 1, 4, n, \\ 2, & \text{for } k = 3, \\ 3, & \text{for } k = 2. \end{cases} \quad (26)$$

Proof. It is significant to keep in hand the neighborhoods $N(v) = V$ and $N(v_i) = \{v, v_{i+1}, v_{i-1}, u_i\}$, for any $v_i \in V$, and $N(u_i) = \{v_i\}$, for any leaf $u_i \in U$. Now, we have to discuss the following eight claims.

Claim 1: the set $S = \{v\}$ is an n -antimetric generator for H_n .

Note that $c_S(x) = (1)$, for all $x \in V$, and $c_S(y) = (2)$, for all $y \in U$. There are only two equivalence classes $S_1 = V$ and $S_2 = U$, both of cardinality n , according to the relation ρ_S . Hence, $\min_{i=1}^2 |S_i| = n$, which implies that S is an n -antimetric generator, by Remark 1.

Claim 2: every single leaf form a 1-antimetric generator for H_n .

Let $S = \{u_i\}$ be a set of one leaf $u_i \in U$. Then, $c_S(v_i) = (1)$, where $v_i \in N(u_i)$, and no other vertex of H_n has the code similar to v_i . It follows that there exists a singleton equivalence class due to the relation ρ_S . Accordingly, Remark 1 refers that S is an 1-antimetric generator.

Claim 3: every singleton subset of V is a 4-antimetric generator for H_n .

Let $S = \{v_i\} \subset V$, for any fixed $1 \leq i \leq n$; then, $c_S(x) = (1)$, for all $x \in N(v_i)$, $c_S(y) = (2)$, for all $y \in \{u_{i-1}, u_{i+1}\} \cup (V - \{v_{i-1}, v_i, v_{i+1}\})$, and $c_S(z) = (3)$, for all $z \in U - \{u_{i-1}, u_i, u_{i+1}\}$. Thus, the relation ρ_S produces three equivalence classes $S_1 = N(v_i)$, $S_2 = \{u_{i-1}, u_{i+1}\} \cup (V - \{v_{i-1}, v_i, v_{i+1}\})$, and $S_3 = U - \{u_{i-1}, u_i, u_{i+1}\}$. Hence, $\min_{i=1}^3 |S_i| = 4$, and S is a 4-antimetric generator for H_n , by Remark 1.

Claim 4: the set $S' = \{u_i, w\}$ is a 3-antimetric generator for H_n whenever $w \in N(u_i)$. Otherwise, S' is a 1-antimetric generator.

Whenever $w \in N(u_i)$, we have $w = v_i$, and the metric codes with respect to S' are

$$c_{S'}(x) = (2, 1) \forall x \in N(v_i) - \{u_i\}; \quad (27)$$

$$c_{S'}(y) = (4, 3) \forall y \in U - \{u_{i-1}, u_i, u_{i+1}\},$$

$$c_{S'}(z) = (3, 2) \forall z \in \{u_{i-1}, u_{i+1}\} \cup (V - \{v_{i-1}, v_i, v_{i+1}\}). \quad (28)$$

The equivalence classes corresponds to the relation $\rho_{S'}$ are $S_1 = N(v_i) - \{u_i\}$, $S_2 = U - \{u_{i-1}, u_i, u_{i+1}\}$, and $S_3 = \{u_{i-1}, u_{i+1}\} \cup (V - \{v_{i-1}, v_i, v_{i+1}\})$. It follows, by Remark 1, that S' is a 3-antimetric generator since $\min_{i=1}^3 |S_i| = 3$.

When $w \in N(u_i)$, then the vertex $v_i \in N(u_i)$ has the metric code which is not similar to the metric code of any other vertex of H_n . This creates at least one singleton equivalence class $\{v_i\}$ in accordance with the relation $\rho_{S'}$, which implies that S' is a 1-antimetric generator for H_n , by Remark 1.

Claim 5: every 2-element subset of $V(H_n)$, except the set S' of Claim 4, is a 1-antimetric generator for H_n .

Let S be a 2-element subset of $V(H_n)$ and $S \neq S'$. Then, we discuss the following two cases:

Case 1 (S does not contain v): let $S \subset U$. When $S = \{u_i, u_{i+2}\}$, the vertex u_{i+1} has the unique metric code $(3, 3)$ with respect to S . When $S = \{u_i, u_{i-2}\}$, the vertex u_{i-1} has the unique metric code $(3, 3)$ with respect to S . Otherwise, the vertex v has the unique metric code $(2, 2)$ with respect to S . Next, we let $S \subset V$. When $S = \{v_i, v_{i+2}\}$, the vertex v_{i-1} has the unique metric code $(1, 2)$ with respect to S . Otherwise, the vertex v has the unique metric code $(1, 1)$ with respect to S .

Case 2 (S contains v): let $S = \{v_i, v\}$; then, the leaf $u_i \in N(v_i)$ has the unique metric code $(1, 2)$ with respect to S .

Each possibility in both the cases yields at least one singleton equivalence class according to the relation ρ_S , which implies that S is a 1-antimetric generator, by Remark 1.

Claim 6: the set $E = \{u_i, v_i, v\} \subset V(H_n)$ is a 2-antimetric generator for H_n .

Note that $c_E(u_{i-1}) = (3, 2, 2) = c_S(u_{i+1})$, $c_E(v_{i-1}) = (2, 1, 1) = c_S(v_{i+1})$,

$$\begin{aligned} c_E(x) &= (3, 2, 1), \forall x \in V - \{v_{i-1}, v_i, v_{i+1}\}, \\ c_E(y) &= (4, 3, 2) \forall y \in U - \{u_{i-1}, u_i, u_{i+1}\}. \end{aligned} \tag{29}$$

So, there are four equivalence classes $S_1 = \{u_{i-1}, u_{i+1}\}$, $S_2 = \{v_{i-1}, v_{i+1}\}$, $S_3 = V - \{v_{i-1}, v_i, v_{i+1}\}$, and $S_4 = U - \{u_{i-1}, u_i, u_{i+1}\}$ with respect to the relation ρ_E . That is, $\min_{i=1}^4 |S_i| = 2$, and Remark 1 assists that E is a 2-antimetric generator.

Claim 7: for even values of $n \geq 8$, the set $S = \{\nu, v_i, u_i, v_{i+(n/2)}, u_{i+(n/2)}\} \subset V(H_n)$ is a 2-antimetric generator for H_n .

Note the metric coding of the vertices with respect to S is as follows:

$$\begin{aligned} c_S(v_{i-1}) &= (2, 1, 1, 2, 3) = c_S(v_{i+1}), \\ c_S(u_{i-1}) &= (3, 2, 2, 3, 4) = c_S(u_{i+1}), \end{aligned} \tag{30}$$

$$\begin{aligned} c_S(x) &= (3, 2, 1, 2, 3) \forall x \in V \\ &\quad - \{v_{i-1}, v_i, v_{i+1}, v_{i+(n/2)-1}, v_{i+(n/2)+1}\}, \end{aligned} \tag{31}$$

$$\begin{aligned} c_S(y) &= (4, 3, 2, 3, 4) \forall y \in U \\ &\quad - \{u_{i-1}, u_i, u_{i+1}, u_{i+(n/2)-1}, u_{i+(n/2)+1}\}, \end{aligned} \tag{32}$$

$$\begin{aligned} c_S(v_{i+(n/2)-1}) &= (3, 2, 1, 1, 2) = c_S(v_{i+(n/2)+1}), \\ c_S(u_{i+(n/2)-1}) &= (4, 3, 2, 2, 3) = c_S(u_{i+(n/2)+1}). \end{aligned} \tag{33}$$

Hence, the classes according to the relation ρ_S are $S_1 = \{v_{i-1}, v_{i+1}\}$, $S_2 = \{u_{i-1}, u_{i+1}\}$, $S_3 = \{v_{i+(n/2)-1}, v_{i+(n/2)+1}\}$, $S_4 = \{u_{i+(n/2)-1}, u_{i+(n/2)+1}\}$, $S_5 = V - \{v_{i-1}, v_i, v_{i+1}, v_{i+(n/2)-1}, v_{i+(n/2)+1}\}$, and $S_6 = U - \{u_{i-1}, u_i, u_{i+1}, u_{i+(n/2)-1}, u_{i+(n/2)+1}\}$. Here, $\min_{i=1}^6 |S_i| = 2$, which implies that S is a 2-antimetric generator, by Remark 1.

Claim 8: any subset of $V(H_n)$ of cardinality $t \geq 3$ is a 1-antimetric generator for H_n , except the sets E and S considered in Claims 6 and 7, respectively.

Let W be a subset of $V(H_n)$ with $|W| = t \geq 3$ and $W \neq E, S$. Then, note the following two possibilities:

- (1) W contains ν : if $|W| = 3$ and $W = \{u, \nu, v\}$ with $u \in U, v \in V$ but $\nu \in N(u)$ (because this case is already discussed in Claim 6). Then, the vertex $x \in N(u)$ has the unique metric code from the set $\{(1, 1, 1), (1, 1, 2)\}$ with respect to W . If $|W| \geq 4$, then a neighbor of some $w \in W - \{\nu\}$ receives the unique metric code with respect to W .
- (2) W does not contain ν : the vertex ν has the unique metric code with respect to W .

In both the possibilities, we get at least one singleton equivalence class according to the relation ρ_W . Thus, $\min |S_i| = 1$, and Remark 1 provides that S is a 1-antimetric generator.

The proof will reach to its end by discussing the following points on the base of formerly discussed claims:

- (i) For $k \in \{5, 6, \dots, n-1\}$, there does not exist a k -antimetric generator for H_n .
- (ii) We find a 1-antimetric generator for H_n of (1) cardinality 1 due to Claim 2, (2) cardinality 2 due to Claims 4 and 5, and (3) cardinality $t \geq 3$ due to Claim 8. Since a 1-antimetric generator for H_n of cardinality 1 is the smallest one, so $\text{adim}_1(H_n) = 1$.
- (iii) Claim 6 assures the existence of a 2-antimetric generator for H_n of cardinality 3 for all values of n , while Claim 7 assures the existence of a 2-antimetric generator for H_n of cardinality 5 just for even values of n . Moreover, no singleton set or 2-element set of vertices in H_n is a 2-antimetric generator for H_n due to Claims 1 to 5. It follows that $\text{adim}_2(H_n) = 3$.
- (iv) We receive a 3-antimetric generator of cardinality 2 from Claim 4, and no singleton set is a 3-antimetric generator for H_n due to Claims 1 to 3, which implies that $\text{adim}_3(H_n) = 2$.
- (v) Claim 3 assists that $\text{adim}_4(H_n) = 1$ because of the existence of a 4-antimetric generator for H_n of cardinality 1.
- (vi) Finally, $\text{adim}_n(H_n) = 1$ due to an n -antimetric generator for H_n of cardinality 1 exists by Claim 1. \square

3.3. *Flower Graphs.* For $n \geq 3$, a flower graph, F_n , is obtained from a helm graph H_n by joining its each leaf u_i to the vertex ν of K_1 . Accordingly, the vertex set of a flower graph is $V(F_n) = V(H_n)$, and its edge set is $E(F_n) = E(H_n) \cup \{\nu \sim u_i; 1 \leq i \leq n\}$, where the indices greater than n or less than 1 will be taken modulo n . Figure 4 provides graphical appearance of one flower graph.

The following observation is easy to understand for the flower graph F_3 .

Observation 4

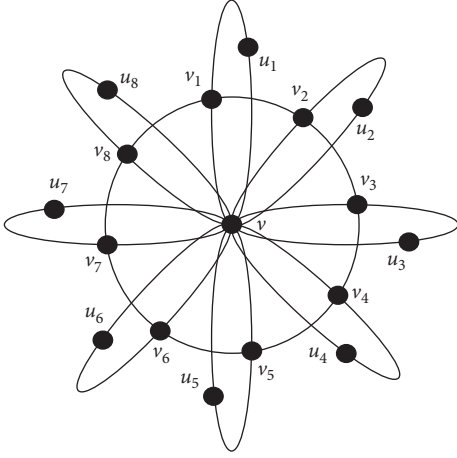
$$\text{adim}_k(F_3) = \begin{cases} 1, & \text{for } k = 2, 6, \\ 2, & \text{for } k = 1. \end{cases} \tag{34}$$

Theorem 4. For all $n \geq 4$, let F_n be a flower graph. Then,

$$\text{adim}_k(F_n) = \begin{cases} 1, & \text{for } k = 2, 4, 2n, \\ 2, & \text{for } k = 1, 3. \end{cases} \tag{35}$$

Proof. The following listed neighborhoods of the vertices of F_n will be used in the proof: $N(\nu) = V \cup U$ and $N(v_i) = \{\nu, v_{i+1}, v_{i-1}, u_i\}$, for any $v_i \in V$, and $N(u_i) = \{\nu, v_i\}$, for any $u_i \in U$. We have to discuss the following nine claims to prove the required result.

Claim 1: the set $S = \{\nu\}$ is a $2n$ -antimetric generator for F_n .

FIGURE 4: One flower graph F_8 .

Note that $c_S(x) = (1)$, for all $x \in V(F_n)$. So, the only one equivalence class of cardinality $2n$ is produced by the relation ρ_S . Hence, S is a $2n$ -antimetric generator.

Claim 2: every singleton subset of U is a 2-antimetric generator for F_n .

Let $S = \{u_i\} \subset U$ for any fixed $1 \leq i \leq n$; then, $c_S(x) = (1)$, for all $x \in N(u_i)$, and $c_S(y) = (2)$, for all $y \in V(F_n) - N[u_i]$. The relation ρ_S creates two equivalence classes $S_1 = N(u_i)$ and $S_2 = V(F_n) - N[u_i]$. It follows that $\min_{i=1}^2 |S_i| = 2$, and Remark 1 proposes that S is a 2-antimetric generator.

Claim 3: every singleton subset of V is a 4-antimetric generator for F_n .

Let $S = \{v_i\} \subset V$ for any fixed $1 \leq i \leq n$; then, $c_S(x) = (1)$, for all $x \in N(v_i)$, and $c_S(y) = (2)$, for all $y \in V(F_n) - N[v_i]$. Thus, we get two equivalence classes $S_1 = N(v_i)$ and $S_2 = V(F_n) - N[v_i]$ by the relation ρ_S with $\min_{i=1}^2 |S_i| = 4$. Hence, S is a 4-antimetric generator, by Remark 1.

Claim 4: the set $W = \{v_i, v\} \subset V(F_n)$ is a 3-antimetric generator for F_n .

Note the metric codes with respect to W is as follows: $c_W(x) = (1, 1)$, for all $x \in N(v_i) - \{v\}$, and $c_W(y) = (2, 1)$, for all $y \in V(F_n) - N[v_i]$. Here, the equivalence classes obtained through the relation ρ_W are $S_1 = N(v_i) - \{v\}$ and $S_2 = V(F_n) - N[v_i]$. Hence, $\min_{i=1}^2 |S_i| = 3$, and Remark 1 implies that W is a 3-antimetric generator.

Claim 5: the set $W' = \{v_i, u\} \subset V(F_n)$ is a 2-antimetric generator for F_n , where $u \in \{u_{i-1}, u_{i+1}\}$.

The metric codes with respect W' are $c_{W'}(x) = (1, 1)$, for all $x \in N(u)$, $c_{W'}(y) = (1, 2)$, for all $y \in N(v_i) - N(u)$, and $c_{W'}(z) = (2, 2)$, for all $z \in V(F_n) - (N[v_i] \cup N[u])$. Accordingly, three equivalence classes $S_1 = N(u)$, $S_2 = N(v_i) - N(u)$, and $S_3 = V(F_n) - (N[v_i] \cup N[u])$ are generated by the relation $\rho_{W'}$ with $\min_{i=1}^3 |S_i| = 2$. Therefore, Remark 1 provides that W' is a 2-antimetric generator.

Claim 6: any 2-element set, $S \subseteq V(F_n)$, is a 1-antimetric generator for F_n , except the sets W and W' discussed in Claims 4 and 5, respectively. We discuss the following two possibilities:

- (1) Either $S \subset V$ or $S \subset U$ or $S = \{v_i, u_j\}$ with $S \neq W'$. Then, $c_S(v) = (1, 1)$ is the unique metric code in F_n .
- (2) If $S = \{u_i, v\}$, then $c_S(v_i) = (1, 1)$ is the unique metric code in F_n .

In both the possibilities, we receive at least one singleton equivalence class, in accordance with the relation ρ_S , which implies that $\min |S_i| = 1$. Hence, Remark 1 yields that S is a 1-antimetric generator.

Claim 7: the set $M = \{u_i, v_i, v\} \subset V(F_n)$ is a 2-antimetric generator for F_n .

The metric coding with respect to M is

$$\begin{aligned} c_M(x) &= (2, 1, 1) \forall x \in N(v_i) - \{u_i, v\}; \\ c_M(y) &= (2, 2, 1) \forall y \in V(F_n) - \{v_{i-1}, v_{i+1}\}. \end{aligned} \quad (36)$$

It follows that $S_1 = N(v_i) - \{u_i, v\}$ and $S_2 = V(F_n) - N[v_i]$ are the equivalence classes produced by the relation ρ_M . Here, $\min_{i=1}^2 |S_i| = 2$, which implies that M is a 2-antimetric generator, by Remark 1.

Claim 8: the set $M' = \{v_i, v, f\} \subset V(F_n)$ is a 3-antimetric generator for F_n whenever $f \in V - \{v_{i-2}, v_{i-1}, v_i, v_{i+1}, v_{i+2}\}$. Otherwise, M' is a 1-antimetric generator for F_n .

$f \in V - \{v_{i-2}, v_{i-1}, v_i, v_{i+1}, v_{i+2}\}$, and we have the metric codes of the vertices with respect to M' as follows:

$$\begin{aligned} c_{M'}(x) &= (1, 1, 2) \forall x \in N(v_i) - \{v\}; \\ c_{M'}(y) &= (2, 1, 1) \forall y \in N(f) - \{v\}, \end{aligned} \quad (37)$$

$$c_{M'}(z) = (2, 1, 2) \forall z \in V(F_n) - (N[v_i] \cup N[f]). \quad (38)$$

Thus, the relation $\rho_{M'}$ partitioned $V(F_n) - M'$ into three equivalence classes $S_1 = N(v_i) - \{v\}$, $S_2 = N(f) - \{v\}$, and $S_3 = V(F_n) - (N[v_i] \cup N[f])$, with $\min_{i=1}^3 |S_i| = 3$. It follows, by Remark 1, that M' is a 3-antimetric generator.

Whenever $f \in \{v_{i-2}, v_{i-1}, v_{i+1}, v_{i+2}\}$, if $f = v_{i+1}$ or v_{i-1} , then a neighbor of f lying in U has the unique metric code $(2, 1, 1)$ with respect to M' . If $f = v_{i+2}$ or v_{i-2} , then v_{i+1} or v_{i-1} , respectively, has the unique metric code $(1, 1, 1)$ with respect to M' . In either cases, we obtain at least one singleton equivalence class according to the relation $\rho_{M'}$, which implies that M' is a 1-antimetric generator, by Remark 1.

Claim 9: any set $S \subseteq V(F_n)$ of cardinality $t \geq 3$ is a 1-antimetric generator for F_n , except the sets M and M' discussed in Claims 7 and 8, respectively.

We discuss the following two cases:

Case 1 (S does not contain v): in this case, the vertex v has the unique metric code with respect to S

Case 2 (S contains v): since $S \neq M, M'$, there exists a vertex $x \in N(s)$ for at least one $s \in S - \{v\}$ such that x has the unique metric code with respect to S

In both the cases, we get at least one singleton equivalence class according to the relation ρ_S , which implies that S is a 1-antimetric generator, by Remark 1.

We conclude the proof by discussing the following points using preceding claims:

- (i) For $k \in \{5, 6, \dots, 2n - 1\}$, there does not exist a k -antimetric generator for F_n .
- (ii) We get an 1-antimetric generator for F_n of (1) cardinality 2 by Claim 6 and (2) cardinality $t \geq 3$ by Claims 8 and 9. Furthermore, no singleton set possesses the property of 1-antimetric generator in F_n , by Claims 1 to 3. It follows that $\text{adim}_1(F_n) = 2$.
- (iii) For F_n , Claim 2 promises the existence of a 2-antimetric generator of cardinality 1, Claim 5 promises the existence of a 2-antimetric generator of cardinality 2, and Claim 7 promises the existence of a 2-antimetric generator of cardinality 3. All these promises conclude that $\text{adim}_2(F_n) = 1$.
- (iv) There exists a 3-antimetric generator for F_n of cardinality 2 due to Claim 4, and a 3-antimetric generator of cardinality 3 due to Claim 8. Thus, Claims 1 to 3 conclude that $\text{adim}_3(F_n) = 2$.
- (v) Claim 3 declares the existence of a 4-antimetric generator for F_n of cardinality 1, which implies that $\text{adim}_4(F_n) = 1$.
- (vi) A $2n$ -antimetric generator for F_n exists due to Claim 1, so $\text{adim}_{2n}(F_n) = 1$. \square

3.4. Sunflower Graphs. For $n \geq 3$, a sunflower graph, SF_n , is obtained from a wheel graph $W_{1,n} = K_1 + C_n$ by attaching one vertex u_i to every two consecutive vertices of the cycle C_n . Let $U = \{u_1, u_2, \dots, u_n\}$; then, the vertex set of a sunflower graph is $V(SF_n) = V(W_{1,n}) \cup U$ and its edge set is $E(SF_n) = E(W_{1,n}) \cup \{u_i \sim v_i, u_i \sim v_{i+1}; 1 \leq i \leq n\}$, where the indices greater than n or less than 1 will be taken modulo n . A graphical preview of this graph is displayed in Figure 5.

The following observation is an easy exercise to understand.

Observation 5. When $n \in \{3, 5, 6\}$, $\text{adim}_k(SF_n) = 1$, for $k = 1, 2, \dots, n$. While

$$\text{adim}_k(SF_4) = \begin{cases} 1, & \text{for } k = 1, 3, 4, \\ 3, & \text{for } k = 2, \end{cases} \quad (39)$$

$$\text{adim}_k(SF_7) = \begin{cases} 1, & \text{for } k = 2, 3, 7, \\ 2, & \text{for } k = 1, \end{cases} \quad (40)$$

$$\text{adim}_k(SF_8) = \begin{cases} 1, & \text{for } k = 2, 4, 8, \\ 2, & \text{for } k = 1. \end{cases} \quad (41)$$

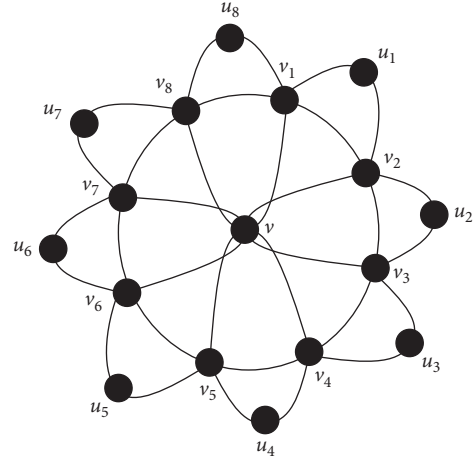


FIGURE 5: One sunflower graph SF_8 .

Theorem 5. For $n \geq 9$, let SF_n be a sunflower graph. Then,

$$\text{adim}_k(SF_n) = \begin{cases} 1, & \text{for } k = 2, 5, n, \\ 2, & \text{for } k = 1. \end{cases} \quad (42)$$

Proof. The neighborhoods, $N(v) = V$ and $N(v_i) = \{v, v_{i+1}, v_{i-1}, u_i, u_{i-1}\}$ for any $v_i \in V$, and $N(u_i) = \{v_i, v_{i+1}\}$, for any $u_i \in U$, of the vertices in SF_n are useful to discuss the following nine claims.

Claim 1: the set $S = \{v\}$ is an n -antimetric generator for SF_n .

Note that $c_S(x) = (1)$, for all $x \in V$, and $c_S(y) = (2)$, for all $y \in U$. Thus, there are two equivalence classes V and U according to the relation ρ_S , and each class has n elements. Hence, Remark 1 yields that S is an n -antimetric generator.

Claim 2: every singleton subset S of V is a 5-antimetric generator for SF_n .

Let $S = \{v_i\} \subset V$ for any fixed $1 \leq i \leq n$. Then, $c_S(x) = (1)$, for all $x \in N(v_i)$:

$$\begin{aligned} c_S(y) &= (3) \forall y \in U - \{u_{i-2}, u_{i-1}, u_i, u_{i+1}\}; \\ c_S(z) &= (2) \forall z \in \{u_{i-2}, u_{i+1}\} \cup (V - \{v_{i-1}, v_i, v_{i+1}\}). \end{aligned} \quad (43)$$

Therefore, the equivalence classes, corresponding to the relation ρ_S , are $S_1 = N(v)$, $S_2 = \{u_{i-2}, u_{i+1}\} \cup (V - \{v_{i-1}, v_i, v_{i+1}\})$, and $S_3 = U - \{u_{i-2}, u_{i-1}, u_i, u_{i+1}\}$. It follows that $\min_{i=1}^3 |S_i| = 5$, and S is a 5-antimetric generator, by Remark 1.

Claim 3: every singleton subset S of U is a 2-antimetric generator for SF_n .

Let $S = \{u_i\} \subset U$, for any fixed $1 \leq i \leq n$. Then,

$$\begin{aligned} c_S(q) &= (1) \forall q \in N(u_i); \\ c_S(x) &= (2) \forall x \in \{v\} \cup \{v_{i-1}, u_{i-1}, u_{i+1}, v_{i+2}\}, \end{aligned} \quad (44)$$

$$c_S(y) = (3) \forall y \in \{u_{i-2}, u_{i+2}\} \cup (V - \{v_{i-1}, v_i, v_{i+1}, v_{i+2}\}), \quad (45)$$

$$c_S(z) = (4), \forall z \in U - \{u_{i-2}, u_{i-1}, u_i, u_{i+1}, u_{i+2}\}. \quad (46)$$

We have four equivalence classes $S_1 = N(u_i)$, $S_2 = \{v\} \cup \{v_{i-1}, u_{i-1}, u_{i+1}, v_{i+2}\}$, $S_3 = \{u_{i-2}, u_{i+2}\} \cup (V - \{v_{i-1}, v_i, v_{i+1}, v_{i+2}\})$, and $S_4 = U - \{u_{i-2}, u_{i-1}, u_i, u_{i+1}, u_{i+2}\}$, in accordance with the relation ρ_S . Thus, $\min_{i=1}^4 |S_i| = 2$, which implies that S is a 2-antimetric generator, by Remark 1.

Claim 4: the set $S = \{v_i, v\} \subset V(SF_n)$ is a 2-antimetric generator for SF_n .

The metric coding with respect to S is listed as follows:

$$\begin{aligned} c_S(u_{i-1}) &= (1, 2) = c_S(u_i); \quad c_S(v_{i-1}) = (1, 1) \\ &= c_S(v_{i+1}); \quad c_S(u_{i-2}) = (2, 2) = c_S(u_{i+1}), \end{aligned} \quad (47)$$

$$\begin{aligned} c_S(x) &= (2, 1) \forall x \in V - \{v_{i-1}, v_i, v_{i+1}\}; \\ c_S(y) &= (3, 2) \forall y \in U - \{u_{i-2}, u_{i-1}, u_i, u_{i+1}\}. \end{aligned} \quad (48)$$

So, the relation ρ_S supplies five equivalence classes $S_1 = \{u_{i-1}, u_i\}$, $S_2 = \{v_{i-1}, v_{i+1}\}$, $S_3 = \{u_{i-2}, u_{i+1}\}$, $S_4 = V - \{v_{i-1}, v_i, v_{i+1}\}$, and $S_5 = U - \{u_{i-2}, u_{i-1}, u_i, u_{i+1}\}$. Hence, $\min_{i=1}^5 |S_i| = 2$, and S is a 2-antimetric generator, by Remark 1.

Claim 5: the set $S = \{u_i, v\} \subset V(SF_n)$ is a 2-antimetric generator for SF_n .

We have the following metric coding with respect to S : $c_S(t) = (1, 1)$, for all $t \in N(u_i)$:

$$\begin{aligned} c_S(u_{i-1}) &= (2, 2) = c_S(u_{i+1}); \quad c_S(v_{i-1}) = (2, 1) \\ &= c_S(v_{i+2}); \quad c_S(u_{i-2}) = (3, 2) = c_S(u_{i+2}), \end{aligned} \quad (49)$$

$c_S(x) = (3, 1)$, for all $x \in V - (N(u_i) \cup \{v_{i-1}, v_{i+2}\})$, and $c_S(y) = (4, 2)$, for all $y \in U - \{u_{i-2}, u_{i-1}, u_i, u_{i+1}, u_{i+2}\}$. So, the equivalence classes, in accordance with the relation ρ_S , are $S_1 = N(u_i)$, $S_2 = \{u_{i-1}, u_{i+1}\}$, $S_3 = \{v_{i-1}, v_{i+2}\}$, $S_4 = \{u_{i-2}, u_{i+2}\}$, $S_5 = V - (N(u_i) \cup \{v_{i-1}, v_{i+2}\})$, and $S_6 = U - \{u_{i-2}, u_{i-1}, u_i, u_{i+1}, u_{i+2}\}$. Here, $\min_{i=1}^6 |S_i| = 2$, which implies that S is a 2-antimetric generator, by Remark 1.

Claim 6: each 2-element set $S \subset V(SF_n) - \{v\}$ is a 1-antimetric generator for SF_n .

We discuss the following three possibilities:

- (1) Let $S = \{u, v\}$ for $u \in U$ and $v \in V$. If either $d(u, v) = 1$ or $d(u, v) = 2$, then there is a vertex p in V such that $p \in N(u) \cap N(v)$, and $c_S(p) = (1, 1) \neq c_S(p')$, for any $p' \in V(SF_n) - \{p\}$. If $d(u, v) = 3$, then there is a neighbor q of v from U such that $c_S(q) = (4, 1) \neq c_S(q')$, for any $q' \in V(SF_n) - \{q\}$. If

$d(u, v) \geq 4$, then the vertex v has the unique metric code $(2, 1)$ with respect to S .

- (2) Let $S \subset V$ and $S = \{v, v'\}$. Then, either $d(v, v') = 1$ or $d(v, v') = 2$. In the former case, a vertex $u \in U$, for which $d(u, v) = 2$ and $d(u, v') = 3$, has the unique metric code $(2, 3)$ with respect to S . In the later case, we have two discussions: If $N(v) \cap N(v') = \{v''\} \subset V$, then a vertex $u \in U$, such that $d(u, v'') = 2$, has the unique metric code from the set $\{(1, 3), (3, 1)\}$ with respect to S . If no vertex in V is a common neighbor of v and v' , then the vertex v has the unique metric code $(1, 1)$ with respect to S .

- (3) Let $S \subset U$; then, $c_S(v) = (2, 2)$ is the unique metric code in SF_n . In all these possibilities, we get at least one singleton equivalence class according to the relation ρ_S , which implies that $\min |S_i| = 1$. Hence, S is a 1-antimetric generator, by Remark 1.

Claim 7: the set $E = \{v_i, v, x\} \subset V(SF_n)$ is a 2-antimetric generator of SF_n whenever $x \in V - \{v_{i-3}, v_{i-2}, v_{i-1}, v_i, v_{i+1}, v_{i+2}, v_{i+3}\}$. Otherwise, E is a 1-antimetric generator.

Whenever $x \in V - \{v_{i-3}, v_{i-2}, v_{i-1}, v_i, v_{i+1}, v_{i+2}, v_{i+3}\}$, note that $c_E(u_{i-2}) = (2, 2, 3) = c_E(u_{i+1})$ and

$$\begin{aligned} c_E(u_{i-1}) &= (1, 2, 3) = c_E(u_i), \text{ where } u_{i-1}, u_i \in N(v_i) \\ &\quad - \{v_{i-1}, v, v_{i+1}\}, \end{aligned} \quad (50)$$

$$\begin{aligned} c_E(v_{i-1}) &= (1, 1, 2) = c_E(v_{i+1}), \text{ where } v_{i-1}, v_{i+1} \in N(v_i) \\ &\quad - \{v, u_{i-1}, u_i\}, \end{aligned} \quad (51)$$

$$\begin{aligned} c_E(h) &= (3, 2, 2) = c_E(h'), \text{ where } h, h' \in U \text{ with } d(h, x) \\ &= d(h', x) = 2, \end{aligned} \quad (52)$$

$$\begin{aligned} c_E(g) &= (2, 1, 1) = c_E(g'), \text{ where } g, g' \in V \text{ with } d(g, x) \\ &= d(g', x) = 1, \end{aligned} \quad (53)$$

$$\begin{aligned} c_E(l) &= (3, 2, 1) = c_E(l'), \text{ where } l, l' \in U \text{ with } d(l, x) \\ &= d(l', x) = 1, \end{aligned} \quad (54)$$

$$c_E(y) = (2, 1, 2) \forall y \in V - \{v_{i-1}, v_i, v_{i+1}, g, x, g'\}, \quad (55)$$

$$c_E(z) = (3, 2, 3) \forall z \in U - \{u_{i-2}, u_{i-1}, u_i, u_{i+1}, h, h', l, l'\}. \quad (56)$$

Hence, we have eight equivalence classes $S_1 = \{u_{i-1}, u_i\}$, $S_2 = \{v_{i-1}, v_{i+1}\}$, $S_3 = \{u_{i-2}, u_{i+1}\}$, $S_4 = \{h, h'\}$, $S_5 = \{l, l'\}$, $S_6 = \{g, g'\}$, $S_7 = V - (S_2 \cup S_6)$, and $S_8 = U - (S_1 \cup S_3 \cup S_4 \cup S_5)$ in accordance with the relation ρ_E . It can be seen that $\min_{i=1}^8 |S_i| = 2$, which yields that E is a 2-antimetric generator, by Remark 1.

Whenever $x \in \{v_{i-3}, v_{i-2}, v_{i-1}, v_{i+1}, v_{i+2}, v_{i+3}\}$, we have a vertex $u \in U$ such that $c_E(u) \neq c_E(u')$ for any $u' \in V(SF_n) - \{u\}$. Hence, we receive at least one singleton equivalence class due to the relation ρ_E , which implies that E is a 1-antimetric generator, by Remark 1.

Claim 8: the set $E' = \{u_i, v, a\} \subset V(SF_n)$ is a 2-antimetric generator for SF_n whenever $a \in U - \{u_{i-4}, u_{i-3}, u_{i-2}, u_{i-1}, u_i, u_{i+1}, u_{i+2}, u_{i+3}, u_{i+4}\}$. Otherwise, E' is a 1-antimetric generator.

Whenever $a \in U - \{u_{i-4}, u_{i-3}, u_{i-2}, u_{i-1}, u_i, u_{i+1}, u_{i+2}, u_{i+3}, u_{i+4}\}$, we have the metric codes with respect to E' as follows:

$$\begin{aligned} c_{E'}(t) &= (1, 1, 3) \forall t \in N(u_i); \\ c_{E'}(u_{i-2}) &= (3, 2, 4) = c_{E'}(u_{i+2}), \end{aligned} \tag{57}$$

$$\begin{aligned} c_{E'}(u_{i-1}) &= (2, 2, 4) = c_{E'}(u_{i+1}); \\ c_{E'}(v_{i-1}) &= (2, 1, 3) = c_{E'}(v_{i+2}), \end{aligned} \tag{58}$$

$$c_{E'}(p) = (3, 1, 1) = c_{E'}(p'), \text{ where } p, p' \in N(a), \tag{59}$$

$$\begin{aligned} c_{E'}(q) &= (4, 2, 2) = c_{E'}(q'), \text{ where } q, q' \in U \\ &\text{such that } d(q, a) = d(q', a) = 2, \end{aligned} \tag{60}$$

$$\begin{aligned} c_{E'}(r) &= (3, 1, 2) = c_{E'}(r'), \text{ where } r, r' \in V \\ &\text{such that } d(r, a) = d(r', a) = 2, \end{aligned} \tag{61}$$

$$\begin{aligned} c_{E'}(x) &= (4, 2, 3) = c_{E'}(x'), \text{ where } x, x' \in U \\ &\text{such that } d(x, a) = d(x', a) = 3, \end{aligned} \tag{62}$$

$$\begin{aligned} c_{E'}(y) &= (3, 1, 3) \forall y \in V \\ &- (N(u_i) \cup N(a) \cup \{v_{i-1}, v_{i+2}, r, r'\}), \end{aligned} \tag{63}$$

$$\begin{aligned} c_{E'}(z) &= (4, 2, 4) \forall z \in U \\ &- \{u_{i-2}, u_{i-1}, u_i, u_{i+1}, u_{i+2}, x, q, l, q', x'\}. \end{aligned} \tag{64}$$

Therefore, we get 10 equivalence classes $S_1 = N(u_i)$, $S_2 = \{u_{i-1}, u_{i+1}\}$, $S_3 = \{v_{i-1}, v_{i+2}\}$, $S_4 = \{u_{i-2}, u_{i+2}\}$, $S_5 = N(a)$, $S_6 = \{q, q'\}$, $S_7 = \{r, r'\}$, $S_8 = \{x, x'\}$, $S_9 = V - (S_1 \cup S_3 \cup S_5 \cup S_7)$, and $S_{10} = U - (S_2 \cup S_4 \cup S_6 \cup S_8)$ in accordance with the relation $\rho_{E'}$. It has been observed that $\min_{i=1}^{10} |S_i| = 2$, so E' is a 2-antimetric generator, by Remark 1.

Whenever $a \in \{u_{i-4}, u_{i-3}, u_{i-2}, u_{i-1}, u_{i+1}, u_{i+2}, u_{i+3}, u_{i+4}\}$, we have a vertex $u \in U$ such that $c_{E'}(u) \neq c_{E'}(u')$, for any $u' \in V(SF_n) - \{u\}$. Hence, we receive at least one singleton equivalence class by the relation $\rho_{E'}$, which implies that $\min_i |S_i| = 1$. Hence, E' is a 1-antimetric generator, by Remark 1.

Claim 9: except the sets $E, E' \subset V(SF_n)$ discussed in Claims 7 and 8, respectively, each set $S \subseteq V(SF_n)$ of cardinality $k \geq 3$ is a 1-antimetric generator for SF_n .

We have to discuss the following two cases:

Case 1 (S contains v): let $|S| \geq 4$ (because the case, when $|S| = 3$, has been discussed in Claims 7 and 8). Then, there a vertex $x \in V$ such that x is a neighbor of some $s \in S$ whenever $S \cap V = \emptyset$, or there a vertex $x \in U$ such that x is a neighbor of some $s \in S$ whenever either $S \cap U = \emptyset$ or $S \cap V \neq \emptyset \neq S \cap U$, and we get the unique metric code of x with respect to S .

Case 2 (S does not contain v): whenever $S \subseteq V$ or $S \subseteq U$, the vertex v has the unique metric code of x with respect to S . Whenever $S \cap U \neq \emptyset \neq S \cap V$, there is a vertex $x \in U$ (or $x \in V$) such that $d(x, s) = 1$ for some element $s \in S$, and $c_S(x) \neq c_S(x')$, for any $x' \in V(SF_n) - \{x\}$.

In both the cases, the relation ρ_S supplies at least one singleton equivalence class, which yields that $\min |S_i| = 1$. Hence, S is a 1-antimetric generator, by Remark 1.

These claims complete the proof with the following deductions:

- (i) There does not exist a k -antimetric generator for SF_n when $k \in \{3, 4, 6, 7, \dots, n-1\}$.
- (ii) Claim 6 supplies a 1-antimetric generator for SF_n of cardinality 2, and Claims 7 to 9 supply a 1-antimetric generator for SF_n of cardinality $t \geq 3$. Claims 1 to 3 provide the guaranty of nonexistence of singleton 1-antimetric generator for SF_n . It follows that $\text{adim}_1(SF_n) = 2$.
- (iii) The existence of a 2-antimetric generator for SF_n of cardinalities 1, 2, and 3 is assured by Claim 3, by Claims 4 and 5, and by Claims 7 and 8, respectively. Accordingly, $\text{adim}_2(SF_n) = 1$.
- (iv) $\text{adim}_5(SF_n) = 1$ because of the existence of a 5-antimetric generator for SF_n of cardinality 1 in Claim 2.
- (v) Claim 1 provides an n -antimetric generator for SF_n of cardinality 1, which yields that $\text{adim}_n(SF_n) = 1$. \square

4. Concluding Remarks

For a connected graph G , the number $\text{rad}(G) = \min\{\text{ecc}(x) = \max_{y \in V(G)} d(x, y); x \in V(G)\}$ is called the radius of G , where $\text{ecc}(x)$ is the eccentricity of x . The center of G is a subgraph $G[X]$ induced by the set $X = \{x \in V(G) : \text{ecc}(x) = \text{rad}(G)\}$. It has been observed the following useful properties about a k -antimetric dimensional graph in [7].

Remarks 2 (see [7])

- (a) If a connected graph is k -metric antidimensional, then $1 \leq k \leq \Delta$
- (b) If the center of a connected graph is trivial, then it is k -metric antidimensional for some $k \geq 2$

It can be easily seen that each wheel-related social graph, considered in this paper, has the trivial center. Remark 2 (a) insures that each of these graphs has k -metric antidimension, for some $k \geq 1$, and it must be k -metric antidimensional for some $k \geq 2$. So, naturally, it raises the following two questions:

Q1. For how many and for which values of $k \geq 1$ a wheel-related social graph admits k -metric antidimension?

Q2. For which maximum value of k , $2 \leq k \leq \Delta$, a wheel-related social graph is k -metric antidimensional?

The results of Čangalović et al., proved in [1] and listed in Observation 1 and Theorem 1, were the pioneers to address the answers of questions Q1 and Q2. These results revealed that (1) when $n = 3, 5$, a wheel graph $W_{1,n}$ admits k -metric antidimension for three values of $k \in \{1, 2, n\}$ and (2) when $n = 4$ and for all $n \geq 6$, $W_{1,n}$ admits k -metric antidimension for four values of $k \in \{1, 2, 3, n\}$. It follows that $W_{1,n}$ is Δ -metric antidimensional.

To extend the study of (k, l) -anonymity based on the k -metric antidimension, we considered four graphs related to wheel graphs in this article. By investigating their k -metric antidimension, we addressed the answers of questions Q1 and Q2 as follows:

(i) For a Jahangir graph J_{2n} , Observation 2 and Theorem 2 revealed that (1) J_4 admits k -metric antidimension for three values of $k \in \{1, 2, 3\}$, (2) when $n = 3, 4$, J_{2n} admits k -metric antidimension for three values of $k \in \{1, 2, n\}$, and (3) for all $n \geq 5$, J_{2n} admits k -metric antidimension for four values of $k \in \{1, 2, 3, n\}$

(ii) For a helm graph H_n , Observation 3 and Theorem 3 revealed that (1) when $n = 3, 4, 5$, H_n admits k -metric antidimension for three values of $k \in \{1, 2, n\}$, (2) H_6 admits k -metric antidimension for four values of $k \in \{1, 2, 3, 6\}$, and (3) for all $n \geq 7$, H_n admits k -metric antidimension for five values of $k \in \{1, 2, 3, 4, n\}$

(iii) For a flower graph F_n , Observation 4 and Theorem 4 revealed that (1) F_3 admits k -metric antidimension for three values of $k \in \{1, 2, 6\}$ and (2) for all $n \geq 4$, F_n admits k -metric antidimension for five values of $k \in \{1, 2, 3, 4, 2n\}$.

(iv) For a sunflower graph SF_n , Observation 5 and Theorem 5 revealed that (1) when $n = 3, 5, 6$, SF_n admits k -metric antidimension for three values of $k \in \{1, 2, n\}$, (2) when $n = 4, 7$, SF_n admits k -metric antidimension for four values of $k \in \{1, 2, 3, n\}$, (3) SF_8 admits k -metric antidimension for four values of $k \in \{1, 2, 4, 8\}$, and (4) for all $n \geq 9$, SF_n admits k -metric antidimension for four values of $k \in \{1, 2, 5, n\}$.

From all these results, it can be concluded that each considered wheel-related social graph is Δ -metric antidimensional.

Furthermore, according to the computed k -metric antidimension of wheel-related social graphs, we investigated that each of them meets the (k, l) -anonymity in the following ways (skipping particular cases which can be observed straightforwardly).

Wheel graph: for $n \geq 6$ and $\Delta = n$ and by Theorem 1, we have

$$\begin{array}{l}
 k \quad \quad \quad \quad \quad \quad \quad \quad : \quad 1 \quad 2 \quad 3 \quad \Delta \\
 k \text{ - metric antidimension} \quad : \quad 2 \quad 2 \quad 1 \quad 1 \quad . \\
 (k, l) \text{ - anonymity} \quad \quad \quad : \quad (1, 2) \quad (2, 2) \quad (3, 1) \quad (\Delta, 1)
 \end{array} \tag{65}$$

Jahangir graph: for $n \geq 5$ and $\Delta = n$ and by Theorem 2, we have

$$\begin{array}{l}
 k \quad \quad \quad \quad \quad \quad \quad \quad : \quad 1 \quad 2 \quad 3 \quad \Delta \\
 k \text{ - metric antidimension} \quad : \quad 2 \quad 1 \quad 1 \quad 1 \quad . \\
 (k, l) \text{ - anonymity} \quad \quad \quad : \quad (1, 2) \quad (2, 1) \quad (3, 1) \quad (\Delta, 1)
 \end{array} \tag{66}$$

Helm graph: for $n \geq 7$ and $\Delta = n$ and by Theorem 3, we have

$$\begin{array}{l}
 k \quad \quad \quad \quad \quad \quad \quad \quad : \quad 1 \quad 2 \quad 3 \quad 4 \quad \Delta \\
 k \text{ - metric antidimension} \quad : \quad 1 \quad 3 \quad 2 \quad 1 \quad 1 \quad . \\
 (k, l) \text{ - anonymity} \quad \quad \quad : \quad (1, 1) \quad (2, 3) \quad (3, 2) \quad (4, 1) \quad (\Delta, 1)
 \end{array} \tag{67}$$

Flower graph: for $n \geq 4$ and $\Delta = 2n$ and by Theorem 4, we have

$$\begin{array}{l}
 k \quad \quad \quad \quad \quad \quad \quad \quad : \quad 1 \quad 2 \quad 3 \quad 4 \quad \Delta \\
 k \text{ - metric antidimension} \quad : \quad 2 \quad 1 \quad 2 \quad 1 \quad 1 \quad . \\
 (k, l) \text{ - anonymity} \quad \quad \quad : \quad (1, 2) \quad (2, 1) \quad (3, 2) \quad (4, 1) \quad (\Delta, 1)
 \end{array} \tag{68}$$

Sunflower graph: for $n \geq 9$ and $\Delta = n$ and by Theorem 5, we have

$$\begin{array}{lcl} k & : & 1 \quad 2 \quad 5 \quad \Delta \\ k - \text{metric antidimension} & : & 2 \quad 1 \quad 1 \quad 1 \quad . \\ (k, l) - \text{anonymity} & : & (1, 2) \quad (2, 1) \quad (3, 1) \quad (\Delta, 1) \end{array} \quad (69)$$

The (k, l) -anonymity, measured on the base of k -metric antidimension for the maximum value of $k = \Delta$, assures that a user can be reidentified with the probability less than or equal $(1/\Delta)$ by a rival controlling only single attacker node v in every considered wheel-related social graph. It is remarkably interesting to leave the following conjecture for the readers.

Conjecture 1. *Each wheel-related social graph and generalizations of wheels are Δ -metric antidimensional and meet $(\Delta, 1)$ -anonymity.*

Data Availability

The figures, tables, and other data used to support this study are included within the article.

Conflicts of Interest

The authors declare that there are no conflicts of interests regarding the publication of this paper.

Acknowledgments




This work was supported in part by general project of Anhui University excellent talent support plan 2021 under Grant Number gxyq2021235.

References

- [1] M. Čangalović, V. Kovačević-Vujčić, and J. Kratica, “ k -metric antidimension of wheels and grid graphs,” in *XIII Balkan Conference on Operational Research Proceedings*, pp. 17–24, Belgrade, Serbia, May 2018.
- [2] G. Chartrand and P. Zhang, *A First Course in Graph Theory*, Dover Publications Inc., New York, NY, USA, 2012.
- [3] T. Chatterjee, B. DasGupta, N. Mobasher, V. Srinivasan, and I. G. Yero, “On the computational complexities of three problems related to a privacy measure for large networks under active attack,” *Theoretical Computer Science*, vol. 775, pp. 53–67, 2019.
- [4] B. DasGupta, N. Mobasher, and I. G. Yero, “On analyzing and evaluating privacy measures for social networks under active attack,” *Information Sciences*, vol. 473, pp. 87–100, 2019.
- [5] J. Kratica, V. Kovacevic-Vujcic, and M. Cangalovic, “ k -metric antidimension of some generalized Petersen graphs,” *Filomat*, vol. 33, no. 13, pp. 4085–4093, 2019.
- [6] S. Mauw, R. Trujillo-Rasua, and B. Xuan, “Counteracting active attacks in social network graphs,” in *IFII Annual Conference on Data and Applications Security and Privacy*, pp. 233–248, Springer, Trento, Italy, July 2016.
- [7] R. Trujillo-Rasua and I. Yero, “ k -metric antidimension: a privacy measure for social graphs,” *Information Sciences*, vol. 328, pp. 403–417, 2016.
- [8] R. Trujillo-Rasua and I. G. Yero, “Characterizing 1-metric antidimensional trees and unicyclic graphs –metric antidimension trees and unicyclic graphs,” *The Computer Journal*, vol. 59, no. 8, pp. 1264–1273, 2016.
- [9] C. Zhang and Y. Gao, “On the complexity of k -metric antidimension problem and the size of k -antiresolving sets in random graphs,” in *International Computing and Combinatorics Conference- COCOON 2017*, pp. 555–567, Springer, Hong Kong, China, August 2017.

Research Article

New Cubic Trigonometric Bézier-Like Functions with Shape Parameter: Curvature and Its Spiral Segment

Abdul Majeed ¹, Muhammad Abbas ², Amna Abdul Sittar,¹ Mohsin Kamran,¹ Saba Tahseen,¹ and Homan Emadifar ³

¹Department of Mathematics, Division of Science and Technology, University of Education, Lahore, Pakistan

²Department of Mathematics, University of Sargodha, Sargodha 40100, Pakistan

³Department of Mathematics, Islamic Azad University, Hamedan Branch, Hamedan, Iran

Correspondence should be addressed to Muhammad Abbas; muhammad.abbas@uos.edu.pk and Homan Emadifar; homan_emadi@yahoo.com

Received 4 July 2021; Revised 25 August 2021; Accepted 2 September 2021; Published 13 September 2021

Academic Editor: Ali Ahmad

Copyright © 2021 Abdul Majeed et al. This is an open access article distributed under the Creative Commons Attribution License, which permits unrestricted use, distribution, and reproduction in any medium, provided the original work is properly cited.

This work presents the new cubic trigonometric Bézier-type functions with shape parameter. Basis functions and the curve satisfy all properties of classical Bézier curve-like partition of unity, symmetric property, linear independent, geometric invariance, and convex hull property and have been proved. The C^3 and G^3 continuity conditions between two curve segments have also been achieved. To check the applicability of proposed functions, different types of open and closed curves have been constructed. The effect of shape parameter and control points has been observed. It is observed that, by decreasing the value of shape parameter, the curve moves toward the control polygon and vice versa. The CT-Bézier curve is closer to the cubic Bézier curve for a fixed value of shape parameter. The proposed CT-Bézier curve can be used to represent ellipse. Using proposed basis functions, we have constructed the spiral segment which is very useful to construct fair curves and desirable to design trajectories of mobile robots, highway, and railway routes' designing.

1. Introduction

Spline curves have been considered a major tool for the geometric modelling in computer aided geometric design. In recent past, trigonometric Bézier-like functions and curves have also attained the attention in computer aided geometric design, computer aided design, and bio-modelling [1, 2]. The concept of trigonometric B-spline (TBS) was introduced by [3], and the scheme of trigonometric B-spline with recurrence relation of the arbitrary order has been presented in [4]. A technique based on cubic Bézier curves (CBC) with the association of a shape parameter is proposed by [5]. This technique is useful for the construction of planer curves and the shape parameter is used to control the curve. Han et al. [6] proposed the trigonometric cubic Bézier curves with two shape parameters. Spiral segments are considered useful to construct fair curves and desirable to design trajectories of mobile robots, highway, and railway routes' designing. The scheme proposed in [7] is suitable for the "S" shaped curves.

Spiral and transition curves have been constructed using CTB with appropriate conditions in [8]. And, this work has been extended to cubic Bézier curve and Bézier-like curves with exponential functions in [9].

A technique, based on quadratic trigonometric Bézier (QTB) basis functions using one shape parameter, has been introduced in [10]. Generalized trigonometric Bézier curves with one shape parameter is introduced in [11]. For corner cutting algorithm, Bosner and Rogina [12] have proposed the cycloidal splines. Wen and Wang [13] have proposed the uniform trigonometric B-spline of order n^{th} with shape parameters. These basis functions are very suitable for designing the circular and elliptic type objects. Class of nonuniform B-spline basis functions with local shape parameter is presented in [14]. Using these nonuniform basis functions, one can attain the C^2 continuity for single knot and C^3 and C^5 continuity can be attained for unique shape parameters. Han [15] demonstrated the trigonometric cubic B-spline with exponential shape parameter. Cubic B-spline

basis functions on uniform knot with one shape parameter are proposed in [16]. Chouby and Ojha [17] proposed the trigonometric spline curve. In this scheme, the shape parameter is a variable which is helpful in adjusting and controlling the curve and surface locally. Denominator trigonometric DT-B-spline basis function i proposed in [18] is similar to trigonometric B-spline functions. These functions have denominator shape parameter. Troll [19] introduced the trigonometric cubic Bézier curve with constrained and two shape parameters. Trigonometric B-spline basis functions of degree 2 and the quadratic NUAT-B-spline curve of many shape parameters are proposed in [20, 21]. Cubic trigonometric B-spline curve has been proposed in [22, 23]. Xie and Li [24] proposed the cubic trigonometric B-spline basis and curve with real shape parameter called alpha-B-spline curve. Hang et al. [25] proposed the cubic B-spline curve with shape parameter and mainly focus on the quasi-uniform B-spline curve. The authors used the proposed the curve for generating the fractal curves. Hu et al. [26] proposed the generalized developable surface shape parameters. The generalized developable H -Bézier surfaces are designed by using control planes with generalized H -Bézier basis functions, and their shapes can be adjusted by altering the values of shape parameters. Kovcs and Vradý [27] introduced P -Bézier and P -B-spline curve. Cubic B-spline collocation method has been used in [28] for the numerical solution of time fractional advection diffusion equation. Crank–Nicolson with cubic B-spline has been used in [29] for the solution parabolic partial differential equation.

In this work, new trigonometric Bézier basis functions with a shape parameter are constructed. The proposed bases are more efficient as the degree of proposed bases is two but it works with four control points. We have also constructed the spiral segment using the proposed bases which is not common in literature, using trigonometric functions. The proposed basis functions and the curve satisfy all basic properties such as partition of unity, linear independency, symmetric property, convex hull property, and geometric invariance. Different curve segments are constructed using proposed basis functions. The C^3 and G^3 continuity conditions are also discussed. The shape of the curve can be rearranged by varying values of the shape parameter. The proposed CT-Bézier curve behaves like cubic Bézier curve for a specific value of the shape parameter. By decreasing the value of the shape parameter, the curve gets closer to the control polygon. The ellipse can be represented exactly using proposed cubic trigonometric Bézier curve. To illustrate the application of proposed cubic Bézier curves, different open and closed curves are designed; the constructed curves are very flexible and easy to handle.

The present work is organized as follows. In Section 2, new proposed cubic trigonometric bases functions and their properties are described. Cubic trigonometric Bézier curves, their properties, effect of shape parameter, and parametric and geometric continuity are part of Section 3. In Section 4, application of the proposed curve is discussed. In Sections 5 and 6, representation of ellipse and approximation of cubic

trigonometric Bézier curve to the ordinary cubic Bézier curve is presented. In Section 7, curvature and spiral curves are discussed, and Section 8 is all about conclusions.

2. Cubic Trigonometric Bézier Functions

For a shape parameter $m \in [0, 1]$, the proposed trigonometric Bézier-like functions $b_i(u)$, $i = 0, \dots, 3$, are defined as

$$\begin{aligned} b_0(u) &= \left(1 - \sin \frac{\pi}{2}u\right) \left[\left(1 - \sin \frac{\pi}{2}u\right) + m \sin \frac{\pi}{2}u \right], \\ b_1(u) &= \sin \frac{\pi}{2}u \left(1 - \sin \frac{\pi}{2}u\right) (2 - m), \\ b_2(u) &= \cos \frac{\pi}{2}u \left(1 - \cos \frac{\pi}{2}u\right) (2 - m), \\ b_3(u) &= \left(1 - \cos \frac{\pi}{2}u\right) \left[\left(1 - \cos \frac{\pi}{2}u\right) + m \cos \frac{\pi}{2}u \right]. \end{aligned} \tag{1}$$

The graphical behavior of proposed basis functions defined in equation (1) can be observed in Figure 1. The effect of shape parameter m can also be observed in this figure.

2.1. Properties of the Basis Functions

Theorem 1. *Proposed trigonometric basis functions defined in equation (1) satisfy the following properties:*

Positivity: all trigonometric functions are positive, i.e., $b_j(u) \geq 0$, for $j = 0, \dots, 3$

Partition of unity: sum of all trigonometric functions is one, mathematically, $\sum_{i=0}^3 b_i = 1$

Symmetry: proposed functions are symmetric means; b_0 becomes b_3 and vice versa by replacing u by $u - 1$; mathematically, $b_i(u; m) = b_{3-i}(1 - u; m)$, for $i = 0, \dots, 3$

Linearly independent: the basic functions are linearly independent, as they cannot be written as a linear combination of each other for any nonzero constant P_0, \dots, P_3

Proof. (a) For $u \in [0, 1]$ and $m \in [0, 1]$, then

$$\begin{aligned} 0 &\leq (1 - \sin(\pi/2)u)^2 \leq 1 \\ 0 &\leq (1 - \sin(\pi/2)u)(m \sin(\pi/2)u) \leq 1 \\ 0 &\leq (1 - \cos(\pi/2)u)^2 \leq 1 \\ 0 &\leq (1 - \cos(\pi/2)u)(m \cos(\pi/2)u) \leq 1 \end{aligned}$$

It is observed that $b_i \geq 0$, $i = 0, 1, 2, 3$.

$$\begin{aligned} \text{(b)} \quad \sum_{i=0}^3 b_i(u) &= (1 - \sin(\pi/2)u) \left[(1 - \sin(\pi/2)u) + m \sin(\pi/2)u \right] \\ &+ (\sin(\pi/2)u) (1 - \sin(\pi/2)u) (2 - m) + (\cos(\pi/2)u) (1 - \cos(\pi/2)u) (2 - m) \\ &+ (1 - \cos(\pi/2)u) \left[(1 - \cos(\pi/2)u) + m \cos(\pi/2)u \right] = 1. \end{aligned}$$

The remaining cases follow obviously. \square

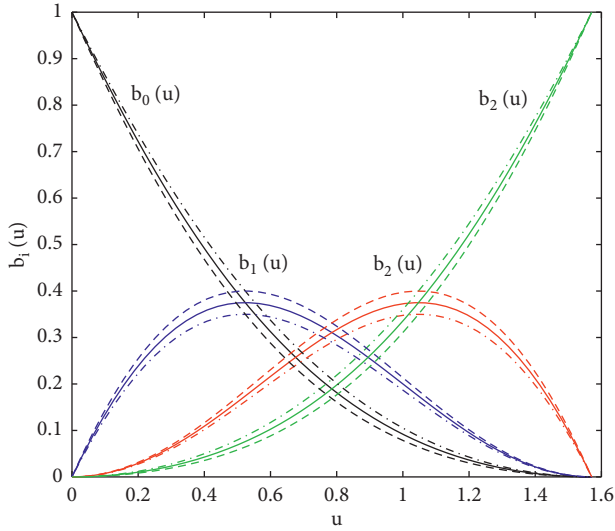


FIGURE 1: Cubic trigonometric functions with different shape parameters.

3. Trigonometric Cubic Bézier Curve

For given control points p_i ($i = 0, 1, 2, 3$) in R^2 or R^3 , the cubic trigonometric Bézier curve with a shape parameter m is defined as

$$r(u) = \sum_{i=0}^3 b_i p_i, \quad u \in [0, 1], m \in [0, 1]. \quad (2)$$

3.1. Properties of CT-Bézier Curve

Theorem 2. The CT-Bézier curve defined in equation (2) satisfies the following properties:

Endpoint interpolation:

Cubic trigonometric curve always passes through the first and last control point:

$$\begin{aligned} r(0) &= p_0, \\ r(1) &= p_3. \end{aligned} \quad (3)$$

Geometric invariance:

The shape of a cubic trigonometric Bézier curve is independent of the choice of coordinates; i.e., equation (2) satisfies the following two equations:

$$\begin{aligned} r(u; m; p_0 + q, p_1 + q, p_2 + q, p_3 + q) &= r(u; m; p_0, p_1, p_2, p_3) + q, \\ r(u; m; p_0 + T, p_1 + T, p_2 + T, p_3 + T) &= r(u; m; p_0, p_1, p_2, p_3) + T, \end{aligned} \quad t \in [0, 1], m \in [0, 1], \quad (4)$$

where q is arbitrary vector in R^2 or R^3 and T is an arbitrary $d \times d$ matrix, $d = 2$ or 3 .

Convex hull property:

The cubic curve always lies within the convex hull of control polygon.

Coordinate system independence:

The proposed curve is independent of the coordinate system means by changing the coordinated curve remains unchanged.

3.2. Continuity Conditions between Two Curve Segments. In this section, we will derive the different parametric and geometric continuity conditions between two curve segments.

3.2.1. Parametric Continuity. (i) C^0 Continuity ($p_3 = q_0$). It is obvious, which means C_0 continuity holds.

(ii) C^1 Continuity.

$$\begin{aligned} r'(1) &= \frac{\pi}{2} (2 - m)(p_3 - p_2), \\ r'_1(1) &= \frac{\pi}{2} (2 - m)(q_1 - q_0), \end{aligned} \quad (5)$$

as $p_3 = q_0$ and $r'(1) = r'_1(0)$, so C_1 continuity holds.

(iii) C^2 Continuity.

$$r''(1) = \left(\frac{\pi}{2}\right)^2 [mp_0 + (2 - m)p_1 - 2(2 - m)p_2 + (2 - 2m)p_3], \quad (6)$$

$$r''_1(1) = \left(\frac{\pi}{2}\right)^2 [(2 - 2m)q_0 + 2(2 - m)q_1 + (2 - m)q_2 + mq_3],$$

as $p_3 = q_0$, $r'(1) = r'_1(0)$, and $r''(1) = r''_1(0)$, so C_2 continuity holds.

(iv) C^3 Continuity.

$r'''(1) = (\pi/2)^3 (2 - m)(p_2 - p_3)$ and $r'''_1(0) = (\pi/2)^3 (2 - m)(p_0 - p_1)$ as $r'(1) = r'_1(0)$, $r''(1) = r''_1(0)$, and $r'''(1) = r'''_1(0)$, so C_3 continuity holds.

3.2.2. Geometric Continuity. (i) G^0 Continuity ($p_3 = q_0$). It is obvious, which means G_0 continuity holds.

(ii) G^1 Continuity.

$$r'(1) = \frac{\pi}{2} (2 - m)(p_3 - p_2),$$

$$r'_1(1) = \frac{\pi}{2} (2 - m)(q_1 - q_0),$$

$$\frac{\pi}{2} (2 - m)(q_1 - q_0) = \lambda \left(\frac{\pi}{2} (2 - m)(p_3 - p_2) \right), \text{ i.e.,}$$

$$r'_1(0) = \lambda r'(1).$$

All conditions are satisfied. So, G_1 continuity holds.

(iii) G^2 Continuity.

$$r''(1) = \left(\frac{\pi}{2}\right)^2 [mp_0 + (2-m)p_1 - 2(2-m)p_2 + (2-2m)p_3],$$

$$r_1''(1) = \left(\frac{\pi}{2}\right)^2 [(2-2m)q_0 + 2(2-m)q_1 + (2-m)q_2 + mq_3], \quad (8)$$

$p_3 = q_0$, and $r_1'(0) = \lambda r'(1)$; also,

$$\begin{aligned} \left(\frac{\pi}{2}\right)^2 [(2-2m)q_0 + 2(2-m)q_1 + (2-m)q_2 + mq_3] &= \lambda^2 \left(\frac{\pi}{2}\right)^2 [mp_0 + (2-m)p_1 - 2(2-m)p_2 + (2-2m)p_3] \\ &+ \gamma \frac{\pi}{2} (2-m)(p_3 - p_2), \end{aligned} \quad (9)$$

i.e., $r_1''(0) = \lambda^2 r''(1) + \gamma r'(1)$. So, G_2 continuity holds.

(iv) G^3 Continuity. $r'''(1) = (\pi/2)^3 (2-m)(p_2 - p_3)$, and $r_1'''(0) = (\pi/2)^3 (2-m)(p_0 - p_1)$ as $r'(1) = r_1'(0)$, $p_3 = q_0$, and $r_1''(0) = \lambda^2 r''(1) + \gamma r'(1)$; also,

$$\begin{aligned} \left(\frac{\pi}{2}\right)^3 (2-m)(p_0 - p_1) &= \lambda^3 \left(\frac{\pi}{2}\right)^3 (2-m)(p_2 - p_3) + \gamma^2 \left(\frac{\pi}{2}\right)^2 [mp_0 + (2-m)p_1 - 2(2-m)p_2 + (2-2m)p_3] \\ &+ \beta \left(\frac{\pi}{2}\right) (2-m)(p_3 - p_2), \text{ i.e.,} \end{aligned} \quad (10)$$

$$r_1'''(0) = \lambda^3 r'''(1) + \gamma^2 r''(1) + \beta r'(1).$$

All conditions are satisfied. So, G_3 continuity holds.

4. Application of Proposed Curves

In this section, different open and closed curves have been constructed using proposed functions. The effect of shape parameter m and control points will also be observed in detail as in Figure 2; the open curve has been constructed using different values of m as $m = 0.1$ (green dashed dotted), $m = 0.3$ (blue dotted), and $m = 0.5$ (red solid), $m = 0.7$ (black dotted), and $m = 0.9$ (magenta dash dotted).

The effect of control point can be observed in Figures 3 and 4. In Figure 3, we constructed the two segment curve using seven control points. The effect of first and last control point is observed in this figure. The curve follows the direction of control point as the control point moves toward outside curve move in the same direction, as shown in Figure 3(b). Similarly, in Figure 3(d), the curve moves toward inside. Figure 4 represents the effect of second and second-last control point.

Another way to control the curve is the shape parameter. In this case, there is no need to change the control points, as shown in Figure 5. In this figure, the four-segment curve has been constructed using different values of m such as $m = 0.1$ (green dashed), $m = 0.3$ (black dash dotted), $m = 0.5$ (red solid), $m = 0.7$ (blue dash dotted), and $m = 0.9$ (magenta dashed). For $m = 0$, the curve becomes a straight line.

In Figure 6, different values of m are $m = 0.1$ (magenta dotted), $m = 0.3$ (black dash dotted), $m = 0.5$ (red solid), $m = 0.7$ (blue dash dotted), and $m = 1$ (red dotted). The

curves become the straight line when $m = 0$. It is observed that, by increasing the value of m , the curve moves toward the control polygon, and by decreasing, it moves away from the control polygon.

To check the applicability of the proposed scheme, different closed curves using different shape parameters have also been designed in this paper, as shown in Figures 7 and 8. In Figure 7, $m = 0.1$ (magenta dashed), $m = 0.3$ (red dash dotted), $m = 0.5$ (black solid), $m = 0.7$ (blue dashed), and $m = 0.8$ (magenta dash dotted), and in Figure 8, $m = 0.1$ (green dashed), $m = 0.3$ (black dash dotted), $m = 0.5$ (red solid), $m = 0.7$ (blue dash dotted), and $m = 0.9$ (magenta dashed) have been used for designing.

5. Representation of Ellipse

Theorem 3. Let p_i be control points for ellipse with semiaxes " k " and " n ," for suitable coordinates, coordinates of ellipse can be written in the following form:

$$\begin{aligned} p_0 &= \begin{pmatrix} 2k \\ 0 \end{pmatrix}, \\ p_1 &= \begin{pmatrix} 2k \\ n \end{pmatrix}, \\ p_2 &= \begin{pmatrix} k \\ 2n \end{pmatrix}, \\ p_3 &= \begin{pmatrix} 0 \\ 2n \end{pmatrix}. \end{aligned} \quad (11)$$

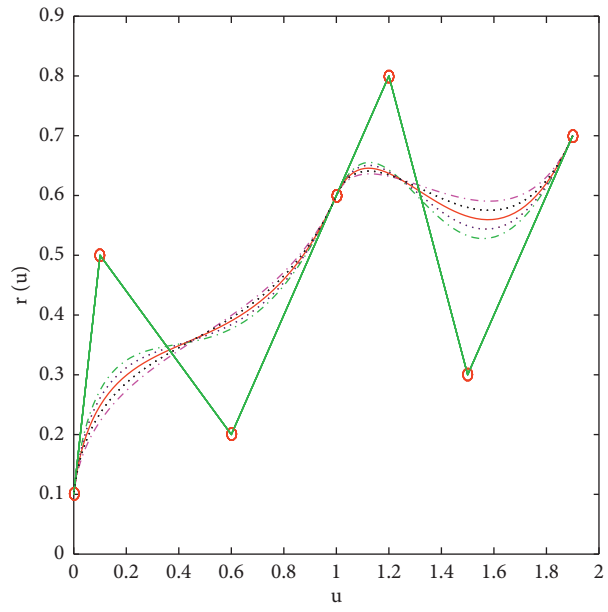


FIGURE 2: Open curve using CT-Bézier basis functions.

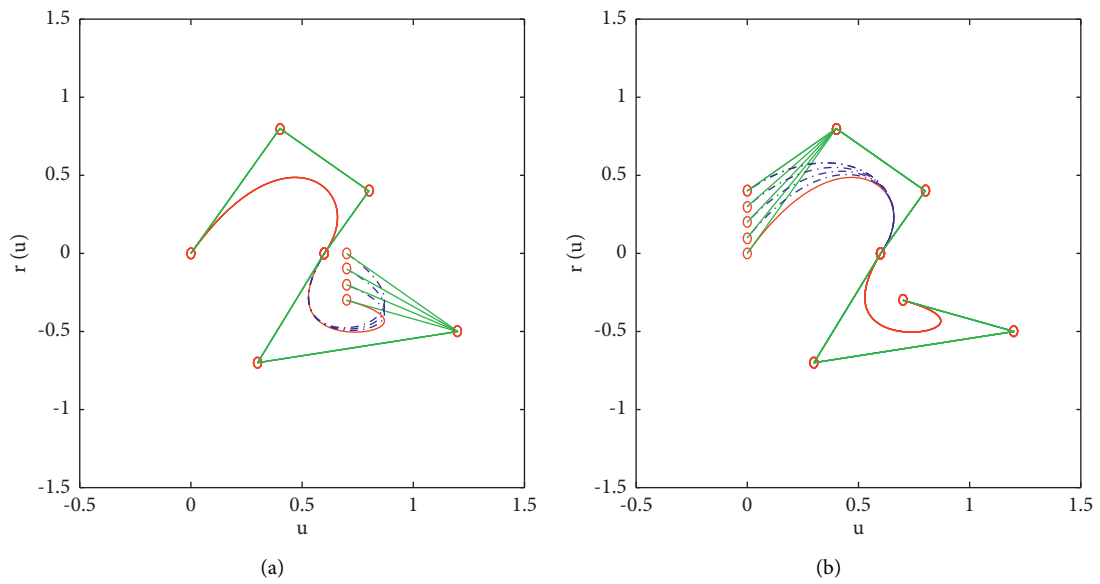


FIGURE 3: Continued.

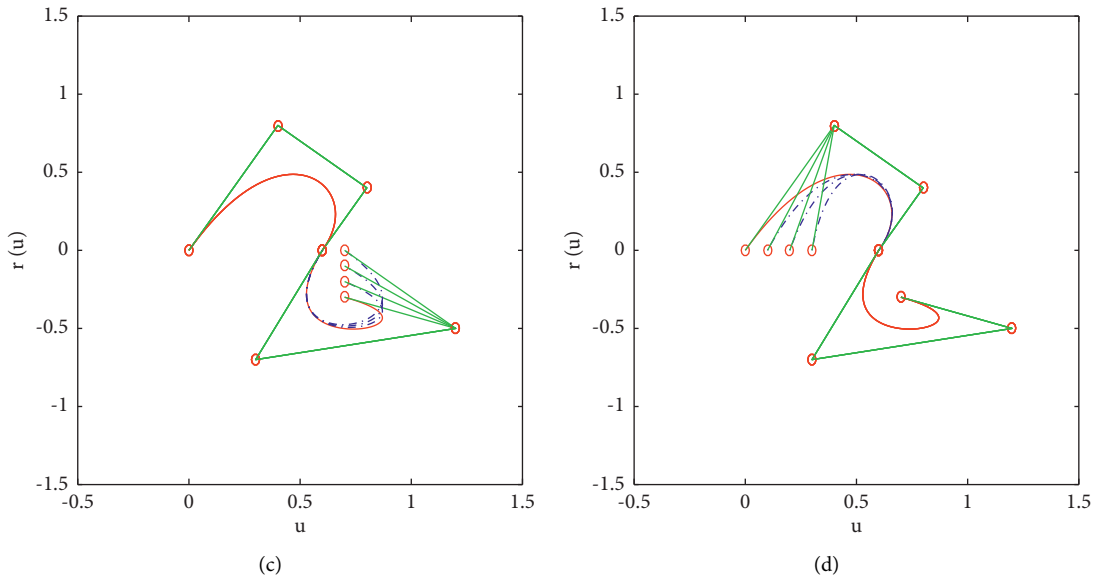


FIGURE 3: Effect of control points on open curve (a-d).

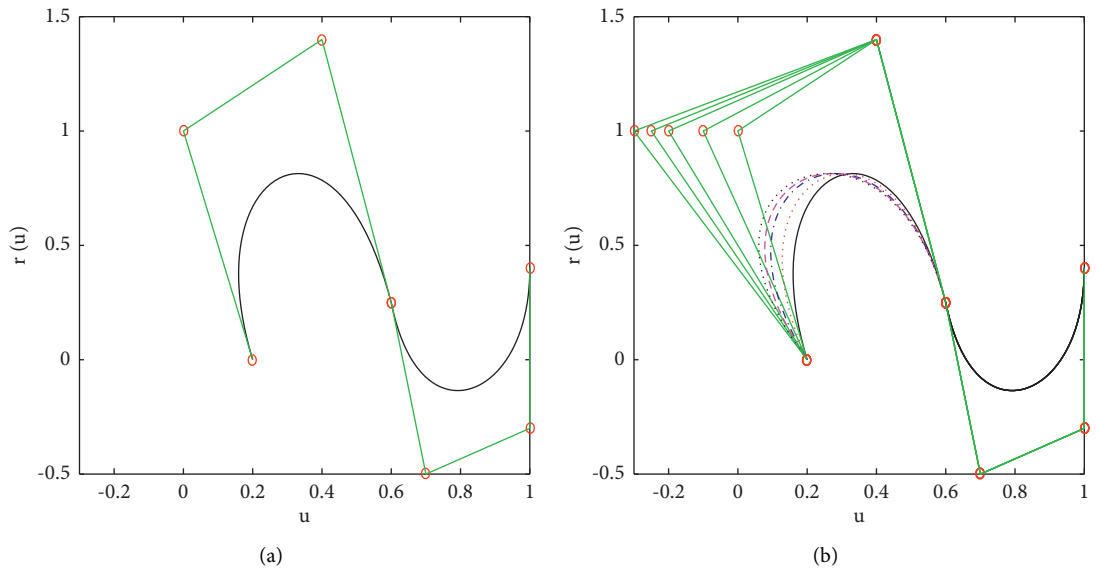


FIGURE 4: Continued.

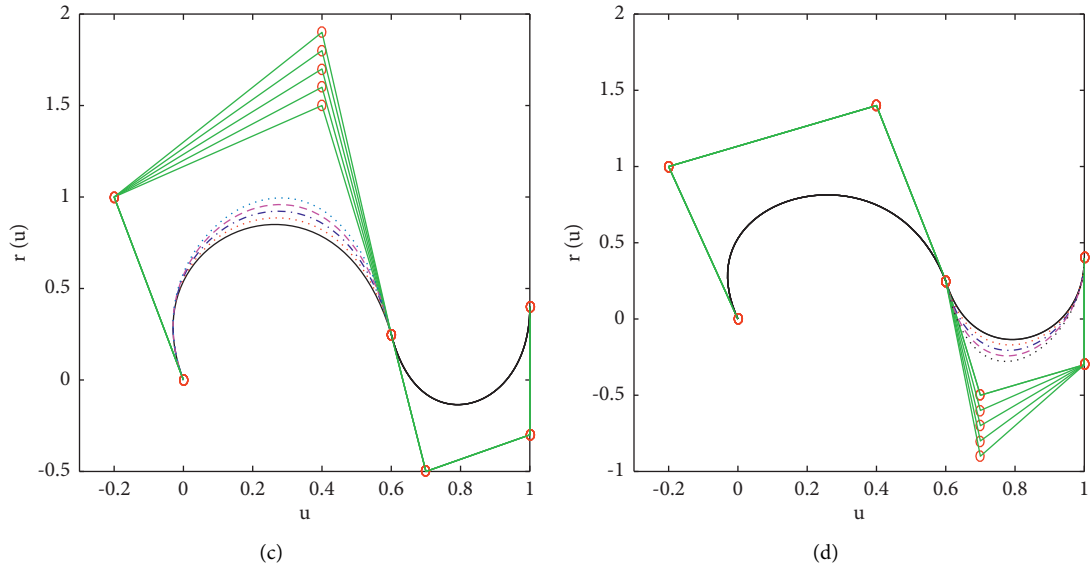


FIGURE 4: Effect of control points (a–d).

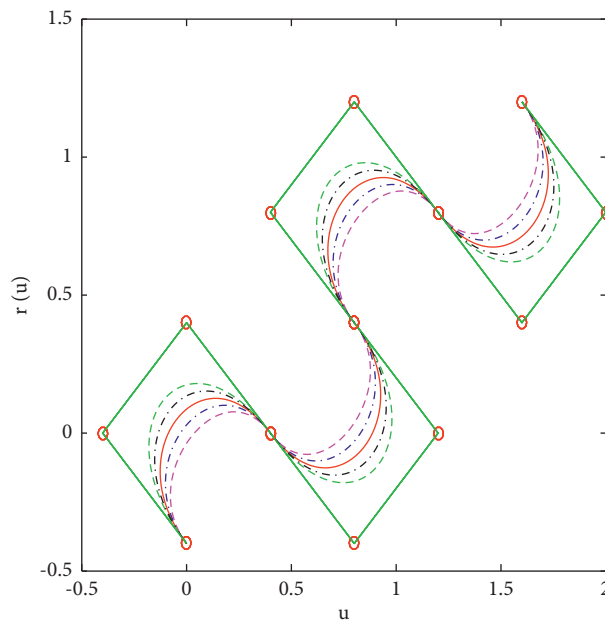


FIGURE 5: The effect of the shape parameter.

Then, the corresponding CT-Bézier curve with shape parameter $m = 0$ and local domain $u \in [0, 1]$ represents an arc of an ellipse with

$$\begin{aligned} r_x(u) &= 2k \cos \frac{\pi}{2}u, \\ r_y(u) &= 2n \sin \frac{\pi}{2}u. \end{aligned} \tag{12}$$

$$\begin{cases} x(u) = 2k \cos \frac{\pi}{2}u, \\ y(u) = 2n \sin \frac{\pi}{2}u. \end{cases} \tag{13}$$

This gives the intrinsic equation:

$$\left(\frac{x}{2k}\right)^2 + \left(\frac{y}{2n}\right)^2 = 1. \tag{14}$$

Proof. If we put the given points in equation (2), coordinates of CT-Bézier curve becomes

It is equation of ellipse, and Figure 9 represents the graphical behavior of ellipse. \square

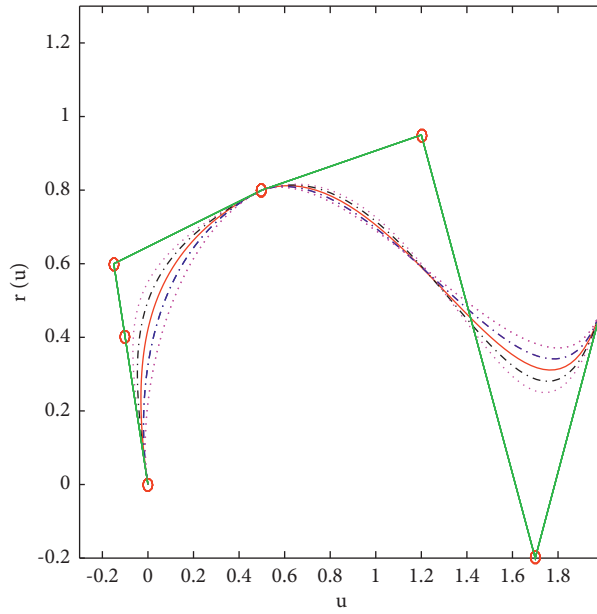


FIGURE 6: The effect of different values of m .

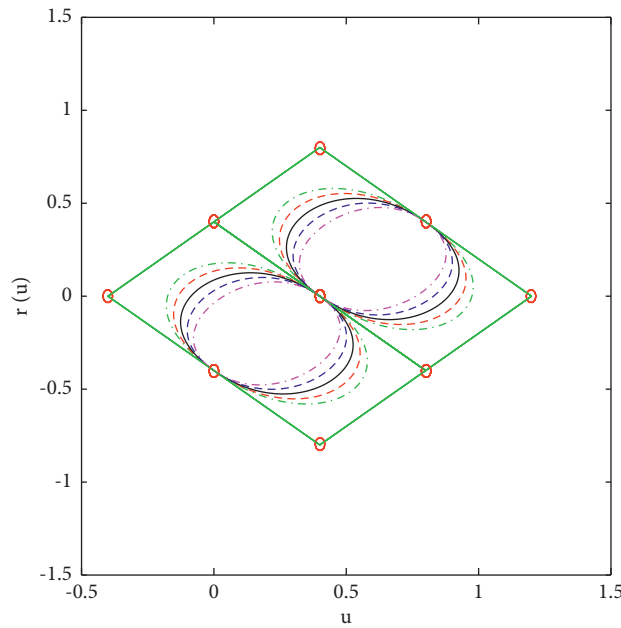


FIGURE 7: Closed curve using CT-Bézier.

6. Approximability

For curve construction, the control polygon plays a vital role. In this section, we will develop the relation between the classic and trigonometric Bézier curve corresponding to their control polygons by adjusting the control point and shape parameter.

Theorem 4. For noncollinear control points $p_0, p_1, p_2,$ and $p_3,$ the relation between classical and trigonometric Bézier

curve $B(u) = \sum_{i=0}^3 p_i \binom{3}{i} (1-u)^{3-i} u^i, u \in [0, 1],$ with control points $p_i (i = 0, \dots, 3)$ are as follows:

$$\begin{cases} r(0) = B(0), \\ r(1) = B(1), \end{cases} \tag{15}$$

$$r\left(\frac{1}{2}\right) - P' = 4(\sqrt{2} - 1)(\sqrt{2} - 1 + m)\left(B\left(\frac{1}{2}\right) - P'\right),$$

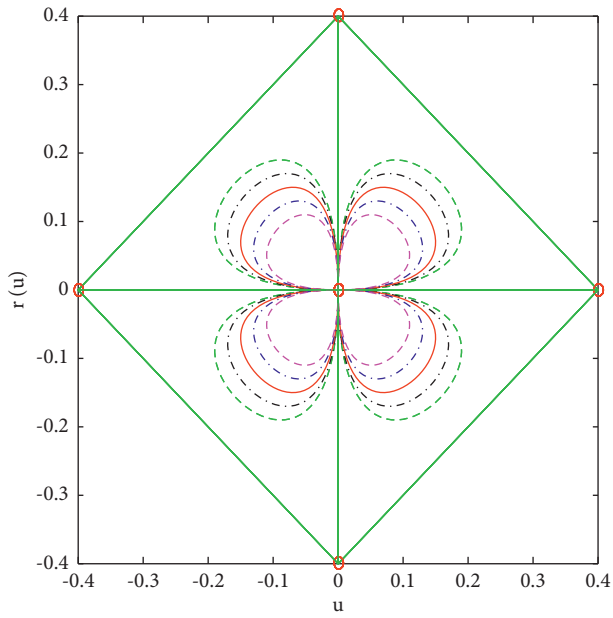


FIGURE 8: Flower designing using CT-Bézier basis functions.

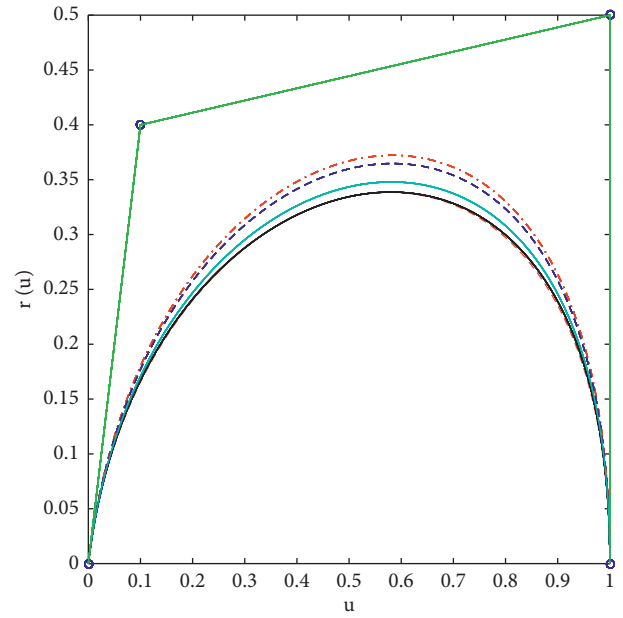


FIGURE 10: Classic vs. trigonometric Bézier Curves.

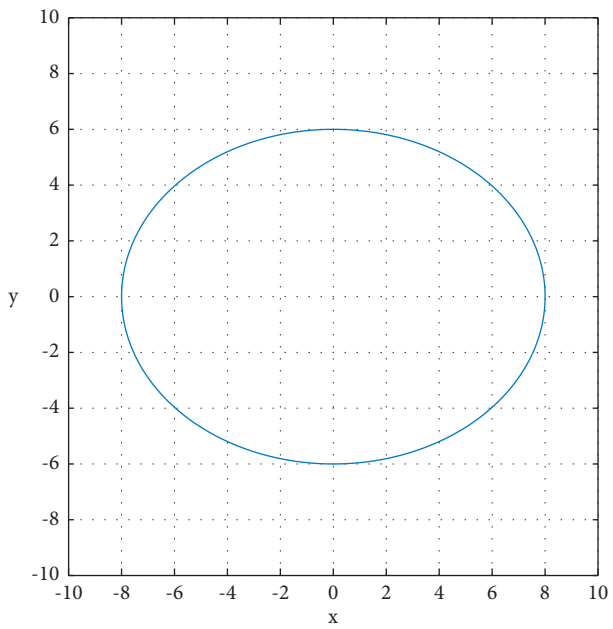


FIGURE 9: Representation of ellipse using the CT-Bézier curve.

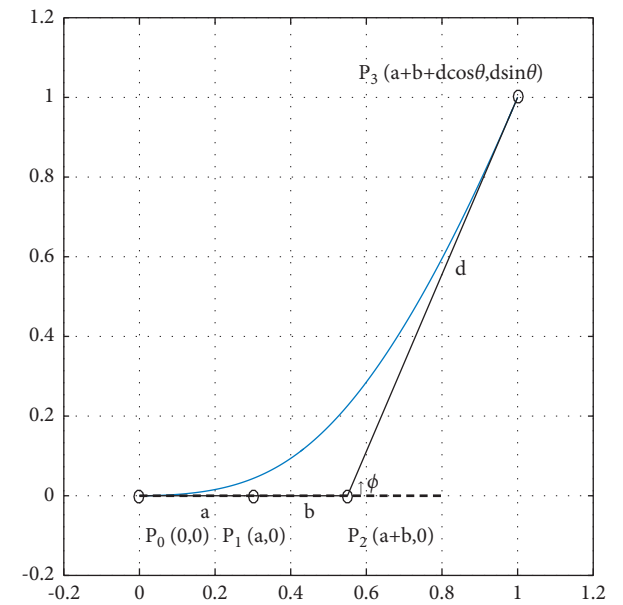


FIGURE 11: Planer CT-Bézier spiral curve and its control points.

where $P' = (1/2)(P_1 + P_2)$.

Proof. After some computation, $r(0) = P_0 = B(0)$ and $r(1) = P_3 = B(1)$.

Since

$$B(u) = (1-u)^3 P_0 + 3(1-u)^2 u P_1 + 3(1-u)u^2 P_2 + u^3 P_3, \tag{16}$$

so

$$\begin{aligned} B\left(\frac{1}{2}\right) - P' &= \frac{1}{8} (P_0 - P_1 - P_2 + P_3) \\ r\left(\frac{1}{2}\right) - P' &= \frac{1}{4} ((\sqrt{2}-1)(\sqrt{2}-1+m)(P_0 + P_3) - (\sqrt{2}-1)(\sqrt{2}-1+m)(P_1 + P_3)) \\ &= \frac{1}{2} (\sqrt{2}-1)(\sqrt{2}-1+m)(P_0 - P_1 - P_2 + P_3) \\ &= 4(\sqrt{2}-1)(\sqrt{2}-1+m)\left(B\left(\frac{1}{2}\right) - P'\right). \end{aligned} \tag{17}$$

Hence, it is proved. \square

Corollary 1. The CT-Bézier curve approaches to control polygon more than the Bézier curve for

$$0 \leq m \leq \frac{(5-3\sqrt{2})}{4}. \tag{18}$$

Corollary 2. CT-Bézier curve will be closer to classical Bézier curve when $m = (5-3\sqrt{2})/4$, i.e., $r(1/2) = B(1/2)$.

The relation between the classic and trigonometric Bézier curve is given in Figure 10.

7. Curvature and Spiral Curve

A planer curve is defined by the set of points $r(u) = (Y(u), X(u))$ for real u . The tangent vector of $r(u)$ is given by $r'(u) = (Y'(u), X'(u))$. If $r'(u) \neq 0 = (0, 0)$, then the signed curvature of $r(t)$ is defined as [11]

$$k(t) = \frac{\overrightarrow{r'(u)} \times \overrightarrow{r''(u)}}{\|\overrightarrow{r'(u)}\|^3}, \tag{19}$$

where $\overrightarrow{r'(u)} \times \overrightarrow{r''(u)} = r'_x r''_y - r''_x r'_y$.
Differentiate equation (19):

$$k'(t) = \frac{E(u)}{\|\overrightarrow{r'(u)}\|^5}, \tag{20}$$

where $E(u) = \left\{ \overrightarrow{r'(u)} \cdot \overrightarrow{r''(u)} \right\} \left\{ \overrightarrow{r'(u)} \times \overrightarrow{r''(u)} \right\} - 3 \left\{ \overrightarrow{r'(u)} \times \overrightarrow{r''(u)} \right\} \overrightarrow{r'(u)} \cdot \overrightarrow{r''(u)}$.

7.1. Planer Cubic Trigonometric Bézier Spiral Segment.
Given a starting point p_0 at origin, i.e., $p_0 = (0, 0)$, the other points are

$$\begin{aligned} p_1 &= p_0 + at_0, \\ p_2 &= p_1 + bt_0, \\ p_3 &= p_2 + d \cos \theta t_0 + d \sin \theta n_0, \end{aligned} \tag{21}$$

where $|p_1 - p_0| = a$, $|p_2 - p_1| = b$, and $|p_3 - p_2| = d$. Here, θ is a positive angle from $|p_2 - p_1|$ to $|p_3 - p_2|$. The tangent unit vectors and the unit normal vector at the beginning points of the Bézier curve, see Figure 11, from [4] are

$$\begin{aligned} r(u) &= \left(1 - \sin \frac{\pi}{2} u\right) \left[\left(1 - \sin \frac{\pi}{2} u\right) + m \sin \frac{\pi}{2} u \right] p_0 + \sin \frac{\pi}{2} u \left(1 - \sin \frac{\pi}{2} u\right) (2-m) p_1 \\ &\quad + \cos \frac{\pi}{2} u \left(1 - \cos \frac{\pi}{2} u\right) (2-m) p_2 + \left(1 - \cos \frac{\pi}{2} u\right) \left[\left(1 - \cos \frac{\pi}{2} u\right) + m \cos \frac{\pi}{2} u \right] p_3. \end{aligned} \tag{22}$$

Now, equation (22) can be written as

where

$$r(t) = (X(t), Y(t)), \tag{23}$$

$$\begin{aligned} X(u) &= \sin \frac{\pi}{2}u \left(1 - \sin \frac{\pi}{2}u\right) (2-m)a + \cos \frac{\pi}{2}u \left(1 - \cos \frac{\pi}{2}u\right) (2-m)(a+b) \\ &\quad + \left(1 - \cos \frac{\pi}{2}u\right) \left[\left(1 - \cos \frac{\pi}{2}u\right) + m \cos \frac{\pi}{2}u\right] (a+b+d \cos \theta), \\ Y(t) &= \left(1 - \cos \frac{\pi}{2}u\right) \left[\left(1 - \cos \frac{\pi}{2}u\right) + m \cos \frac{\pi}{2}u\right] (d \sin \theta). \end{aligned} \tag{24}$$

The more general form for spiral segment is now obtained by taking the derivatives of the curvature of (12). The first three derivatives of equations (23) and (24) are

$$\begin{aligned} X'(u) &= \left(\frac{\pi}{2}\right) \left[(2-m)a \left[\cos \frac{\pi}{2}u - 2 \cos \frac{\pi}{2}u \sin \frac{\pi}{2}u \right] + (2-m)(a+b) \left[2 \cos \frac{\pi}{2}u \sin \frac{\pi}{2}u - \sin \frac{\pi}{2}u \right] \right. \\ &\quad \left. + \left(\sin \frac{\pi}{2}u \right) \left(2-m-2 \cos \frac{\pi}{2}u(1-m) \right) \right] (a+b+d \cos \theta), \end{aligned} \tag{25}$$

$$\begin{aligned} X''(u) &= \left(\frac{\pi}{2}\right)^2 \left[(2-m) \left(\cos \frac{\pi}{2}u \left(2b \cos \frac{\pi}{2}u - a - b \right) - \sin \frac{\pi}{2}u \left(a + 2b \sin \frac{\pi}{2}u \right) \right) \right. \\ &\quad \left. + \left[\left(\cos \frac{\pi}{2}u \right) \left(2-m-2 \cos \frac{\pi}{2}u(1-m) \right) + \left(\sin^2 \frac{\pi}{2}u \right) (2-2m) \right] (a+b+d \cos \theta), \end{aligned} \tag{26}$$

$$\begin{aligned} X'''(u) &= \left(\frac{\pi}{2}\right)^3 \left[(2-m) \left(\sin \frac{\pi}{2}u \left(a + b - 8b \cos \frac{\pi}{2}u \right) - a \cos \frac{\pi}{2}u \right) \right. \\ &\quad \left. + \left[5 \sin \frac{\pi}{2}u \cos \frac{\pi}{2}u(1-m) + \left(\sin \frac{\pi}{2}u + \cos \frac{\pi}{2}u \right) (m-1) + 1 \right] (a+b+d \cos \theta), \end{aligned} \tag{27}$$

$$Y'(u) = \left(\frac{\pi}{2}\right) \left(\sin \frac{\pi}{2}u \right) \left(2-m-2 \cos \frac{\pi}{2}u(1-m) \right) (d \sin \theta), \tag{28}$$

$$Y''(u) = \left(\frac{\pi}{2}\right)^2 \left[\cos \frac{\pi}{2}u \left(2-m-2 \cos \frac{\pi}{2}u(1-m) \right) + \left(\sin^2 \frac{\pi}{2}u \right) (2-2m) \right] (d \sin \theta), \tag{29}$$

$$Y'''(u) = \left(\frac{\pi}{2}\right)^3 \left[5 \sin \frac{\pi}{2}u \cos \frac{\pi}{2}u(1-m) + \left(\sin \frac{\pi}{2}u + \cos \frac{\pi}{2}u \right) (m-1) + 1 \right] (d \sin \theta). \tag{30}$$

It follows from equations (19), (25), (26), (28), and (29) that the curvature of equation (23) at $u = 0$ and $u = 1$ are, respectively,

$$k(0) = \frac{m d \sin \theta}{((2-m)a)^2}, \tag{31}$$

$$k(1) = \frac{\sin \theta [(2-2m)d \cos \theta - ((2-2m)(a+b+d \cos \theta - (2-m)(a+2b)))]}{((2-m)d)^2}, \tag{32}$$

and by using equation (20), we obtain

$$k'(0) = \frac{-3md^2 \sin^2 \theta}{((2-m)a)^3}, \quad (33)$$

$$k(1) = \frac{-3 \sin^2 \theta \left[((2-2m)d \cos \theta)^2 - ((2-2m)(a+b+d \cos \theta - (2-m)(a+2b)))^2 \right]}{((2-m)d)^3}. \quad (34)$$

From equations (32) and (33), we conclude that the curve given in equation (22) is not a Bloss curve because it does not satisfy the conditions. However, if we put $\theta = 0$, then curvature and its derivative values drop to zero; $r(u)$ is not a curve, it is a line. Thus, a cubic trigonometric Bézier Bloss curve is nothing but just a straight line.

8. Conclusions

New trigonometric cubic Bézier-like functions have been proposed in this work. Proposed bases' functions and curves satisfy the basic properties and have been proved. Open and closed curves with different control points and shape parameters have been constructed using proposed basis to check its applicability and flexibility. Furthermore, cubic trigonometric Bézier curve behave like a classical Bézier curve and have been proved. In the end, trigonometric spiral curve segment has also been constructed using cubic trigonometric functions, which indicate that proposed basis functions can be used in CAD/CAM modelling especially road and railway track designing.

8.1. Limitations and Future Work. The proposed bases' functions work well for all type of curves such as open and closed and are a good addition in literature; however, functions can be improved by increasing the interval of the free-shape parameter. In our future work, we will use the proposed work for the construction of craniofacial fracture and will develop the surface.

Data Availability

No data were used to support this study.

Conflicts of Interest

The authors declare that they have no conflicts of interest or personal relationships that could have appeared to influence the work reported in this paper.

Authors' Contributions

All authors equally contributed to this work. All authors read and approved the final manuscript.

References

- [1] A. Majeed, A. R. Mt Piah, and Z. Ridzuan Yahya, "Surface reconstruction from parallel curves with application to parietal bone fracture reconstruction," *PLoS one*, vol. 11, no. 3, Article ID e0149921, 2016.
- [2] A. Majeed, A. R. Mt Piah, R. U. Gobithaasan, and Z. R. Yahya, "Craniofacial reconstruction using rational cubic ball curves," *PLoS one*, vol. 10, no. 4, Article ID e0122854, 2015.
- [3] I. Schoenberg, "On trigonometric spline interpolation," *Indiana University Mathematics Journal*, vol. 13, no. 5, pp. 795–825, 1964.
- [4] T. Lyche and R. Winther, "A stable recurrence relation for trigonometric B-splines," *Journal of Approximation Theory*, vol. 25, no. 3, pp. 266–279, 1979.
- [5] R. Sharma, "Cubic trigonometric bezier curve with shape parameter," *International Journal of Innovative Research in Computer and Communication Engineering*, vol. 4, no. 4, pp. 7718–7723, 2016.
- [6] X.-A. Han, Y. Ma, and X. Huang, "The cubic trigonometric Bézier curve with two shape parameters," *Applied Mathematics Letters*, vol. 22, no. 2, pp. 226–231, 2009.
- [7] D. J. Walton and D. S. Meek, "A further generalisation of the planar cubic Bézier spiral," *Journal of Computational and Applied Mathematics*, vol. 236, no. 11, pp. 2869–2882, 2012.
- [8] A. Ayar and B. Sahin, "Trigonometric Bézier-like curves and transition curves," *Applicationes Mathematicae*, pp. 1–29, 2021.
- [9] Y. Zhu and X. Han, "Curves and surfaces construction based on new basis with exponential functions," *Acta applicandae mathematicae*, vol. 129, no. 1, pp. 183–203, 2014.
- [10] B. Uzma, M. Abbas, M. N. H. Awang, and J. M. Ali, "The quadratic trigonometric Bzier curve with single shape parameter," *Journal of basic and applied scientific research*, vol. 2, no. 3, pp. 2541–2546, 2012.
- [11] S. Maqsood, M. Abbas, G. Hu, A. L. A. Ramli, and K. T. Miura, "A novel generalization of trigonometric bezier curve and surface with shape parameters and its applications," *Mathematical Problems in Engineering*, vol. 2020, no. 1, 25 pages, Article ID 4036434, 2020.
- [12] T. Bosner and M. Rogina, "Numerically stable algorithm for cycloidal splines," *Annali dell'Universita di Ferrara*, vol. 53, no. 2, pp. 189–197, 2007.
- [13] T. Wen, G.-Z. Wang, "Trigonometric polynomial uniform B-spline with shape parameter," *Chinese Journal of computers. Chinese edition*, vol. 28, no. 7, p. 1192, 2005.
- [14] L. Y. Lan, "Cubic Trigonometric non uniform spline curves and surfaces," *Mathematical Problems in Engineering*, vol. 2016, Article ID 7067408, 9 pages, 2016.

- [15] Y. Z. A. X. Han, "New Trigonometric basis possessing exponential shape parameters," *Journal of Computational Mathematics*, vol. 33, no. 6, pp. 642–684, 2015.
- [16] U. Mishra, "A $\lambda\mu - B$ - spline curve with shape parameter," *Journal of Innovative research in computer and communication engineering*, no. 8, pp. 2320–9801, 2016.
- [17] N. Chouby and A. Ojha, "Trigonometric splines with variable shape parameter," *Journal of Mathematics*, vol. 38, 2008.
- [18] K. Wang and G. Zhang, "New trigonometric basis possessing denominator shape parameter," *Mathematics problems in Engineering*, vol. 2018, Article ID 9569834, 25 pages, 2018.
- [19] E. Troll, "Constrained modification of the Cubic trigonometric Bézier curve with two shape parameters," *Annals Mathematics et Informaticae*, vol. 43, pp. 145–156, 2014.
- [20] X. Han, "Cubic Trigonometric polynomial curves with a shape parameter," *Computer Aided Geometric Design*, vol. 21, no. 6, pp. 535–548, 2004.
- [21] M. Dube and R. Sharma, "Quadratic NUAT-B-spline curves with multiple shape parameters," *International Journal of Machine Intelligence*, vol. 3, no. 1, pp. 18–24, 2011.
- [22] X. Han, "Quadratic trigonometric polynomial curves with a shape parameter," *Computer Aided Geometric Design*, vol. 19, no. 7, pp. 503–512, 2002.
- [23] X. Han, "Piecewise quadratic trigonometric polynomial curves," *Mathematics of Computation*, vol. 72, no. 243, pp. 1369–1378, 2003.
- [24] W. Xie and J. Li, "C3 cubic trigonometric B-spline curves with a real parameter," *Journal of the National Science Foundation of Sri Lanka*, vol. 46, no. 1, 2018.
- [25] H. Hang, X. Yao, Q. Li, and M. Artiles, "Cubic B-Spline curves with shape parameter and their applications," *Mathematical Problems in Engineering*, vol. 2017, Article ID 3962617, 7 pages, 2017.
- [26] G. Hu, J. Wu, and X. Qin, "A new approach in designing of local controlled developable H-Bézier surfaces," *Advances in Engineering Software*, vol. 121, pp. 26–38, 2018.
- [27] I. Kovcs and T. Vradý, "P-Bzier and P-Bspline curves new representations with proximity control," *Computer Aided Geometric Design*, vol. 62, pp. 117–132, 2018.
- [28] M. Shafiq, M. Abbas, K. M. Abualnaja, M. J. Huntul, A. Majeed, and T. Nazir, "An efficient technique based on cubic B-spline functions for solving time-fractional advection diffusion equation involving Atangana-Baleanu derivative," *Engineering with Computers*, pp. 1–17, 2021.
- [29] M. J. Huntul, M. Tamsir, A. A. H. Ahmadini, and S. R. Thottoli, "A novel collocation technique for parabolic partial differential equations," *Ain Shams Engineering Journal*, 2021.

Research Article

Distance-Based Polynomials and Topological Indices for Hierarchical Hypercube Networks

Tingmei Gao¹ and Iftikhar Ahmed²

¹School of Mathematical and Computer Science, Shaanxi University of Technology, Hanzhong 723000, China

²Department of Mathematics, Riphah International University, Lahore Campus, Lahore 54000, Pakistan

Correspondence should be addressed to Tingmei Gao; dghnn021@163.com

Received 19 July 2021; Revised 2 August 2021; Accepted 16 August 2021; Published 11 September 2021

Academic Editor: Muhammad Kamran Siddiqui

Copyright © 2021 Tingmei Gao and Iftikhar Ahmed. This is an open access article distributed under the Creative Commons Attribution License, which permits unrestricted use, distribution, and reproduction in any medium, provided the original work is properly cited.

Topological indices are the numbers associated with the graphs of chemical compounds/networks that help us to understand their properties. The aim of this paper is to compute topological indices for the hierarchical hypercube networks. We computed Hosoya polynomials, Harary polynomials, Wiener index, modified Wiener index, hyper-Wiener index, Harary index, generalized Harary index, and multiplicative Wiener index for hierarchical hypercube networks. Our results can help to understand topology of hierarchical hypercube networks and are useful to enhance the ability of these networks. Our results can also be used to solve integral equations.

1. Introduction

The field of mathematics which deals with the problems of chemistry mathematically is mathematical chemistry. The topology of chemical structures, for example, topological labels or indices, is investigated in chemical graph theory. Actually, topological indices are real numbers associated with graph of chemical compounds and are useful in quantitative structure-property relationships and quantitative structure-activity relationships. Topological indices predict some important properties of chemical structures even without using lab, for example, boiling point, viscosity, radius of gyration, and so on [1–3] can be obtained from the indices.

Just like topological indices, polynomials also have significant applications in chemistry, for example, Hosoya polynomial [4] plays a vital role in calculation of distance-based topological indices. Like Hosoya polynomial, M-polynomial [5] plays the same role in calculation of many degree-based TIs [6–12].

Wiener defined the first topological index when he was examining boiling point of paraffins [13]. Consequently, Wiener set up the skeleton of topological indices [14–18].

This paper concerns with the topological indices of hierarchical hypercube networks. Interconnection networks have a pivotal role in the execution of parallel systems. This paper studies the interconnection topology that is called the hierarchical hypercube (HHC) [19]. This topology is suitable for extensively parallel systems with many number of processors. An appealing property of this network is the low number of connections per processor, which enhances the VLSI design and fabrication of the system [20, 21]. Other alluring features include symmetry and logarithmic diameter, which imply easy and fast algorithms for communication [22]. Moreover, the HHC is scalable, that is, it can embed HHCs of lower dimensions. Malluhi and Bayoumi [21] introduced the hierarchical hypercube network of order n (n -HHC). The structure of an n -HHC consists of three levels of hierarchy. At the lowest level of hierarchy, there is a pool of $2n$ nodes. These nodes are grouped into clusters of $2m$ nodes each, and the nodes in each cluster are interconnected to form an m -cube called the Son-cube or the S-cube. The set of the S-cubes constitutes the second level of hierarchy [23].

Being a hierarchical structure, the HHC bears the advantages usually gained by hierarchy [24]. In general,

hierarchy is a useful means for modular design. In addition, hierarchical structures are capable of exploiting the locality of reference (communication), and they are fault tolerant [25]. Other attractive properties of the HHC structure are logarithmic diameter and a topology inherited from, and closely related to, the hypercube topology. The former property implies fast communication, and the latter implies easy mapping of operations from HC to HHC. The HHC can emulate the hypercube for a large class of problems (divide and conquer), without a significant increase in processing time. The HHC can embed rings and HHCs of lower dimension. In addition, the HHC embeds the cube connected cycle (CCC) [26–28]. As a result, the performance of HHC is in the worst case equivalent to the performance of the CCC [29–34]. The number of vertices and edges in $(\text{HHC} - 1)$ is $16a + 16$ and $24a + 20$, respectively, where a is a natural number. The number of vertices and edges in $(\text{HHC} - 2)$ is $16a + 16$ and $32a + 28$, respectively. $(\text{HHC} - 1)$ and $(\text{HHC} - 2)$ are shown in Figures 1 and 2, respectively.

In this paper, we computed Hosoya polynomials, Harary polynomials, Wiener index, modified Wiener index, hyper-Wiener index, Harary index, generalized Harary index, and multiplicative Wiener index for hierarchical hypercube networks.

2. Preliminaries

In this section, we give the definitions and known results that are used in proving main results of this paper. A graph G is simple if it has no loop or multiple edges and is connected if there is a path between every two vertices of it. The distance between any two vertices u and v is denoted by $d(u, v)$ and is the length of the shortest path between u and v . The diameter of a graph is the maximum distance between any two vertices of G . The notions that are used in this paper but not defined can be found in [35, 36].

Definition 1 (Hosoya polynomial [16]).

For a simple connected graph G , the Hosoya polynomial is defined as

$$H(G, x) = \frac{1}{2} \sum_{y \in V(G)} \sum_{z \in V(G)} x^{d(y,z)}, \quad (1)$$

where $d(y, z)$ represents the distance between the vertices y and z .

Definition 2 (Wiener index [37]). The Wiener index for a simple connected graph G is denoted by $W(G)$ and is defined as the sum of distances between all pairs of vertices in G , i.e.,

$$W(G) = \frac{1}{2} \sum_{y \in V(G)} \sum_{z \in V(G)} d(y, z). \quad (2)$$

It can be observed that the Wiener index is the first-order derivative of the Hosoya polynomial at $x = 1$.

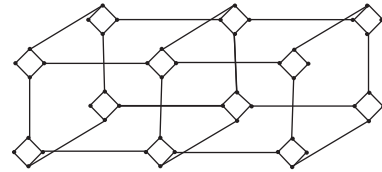


FIGURE 1: The hierarchical hypercube network $(\text{HHC} - 1)_{2 \times 2}$.

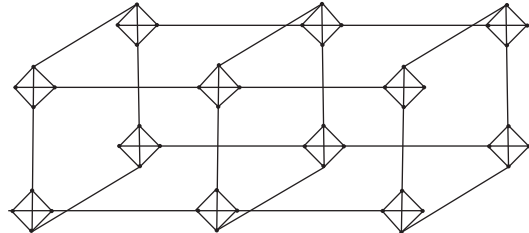


FIGURE 2: The hierarchical hypercube network $(\text{HHC} - 2)_{2 \times 2}$.

$$W(G) = \left. \frac{dH(G)}{dx} \right|_{x=1}. \quad (3)$$

Definition 3 (modified Wiener index). For a simple connected graph G , the modified Wiener index is denoted by $W_\lambda(G)$ and is defined as

$$W_{(\lambda G)} = \frac{1}{2} \sum_{y \in V(G)} \sum_{z \in V(G)} d(y, z)^\lambda, \quad (4)$$

where λ is any positive integer.

Definition 4 (hyper-Wiener index). For a simple connected graph G , the hyper-Wiener index is denoted by $WW(G)$ and is defined as

$$WW(G) = \frac{1}{2} \sum_{y \in V(G)} \sum_{z \in V(G)} (d(y, z) + d(y, z)^2). \quad (5)$$

The hyper-Wiener index (HWI) was introduced by Randić [38] and is used to forecast physical chemistry characteristics of organic compounds.

Definition 5 (modified hyper-Wiener index). Another variant of Wiener index is hyper-Wiener index (MHWI) which is denoted by $WW_\lambda(G)$. For a simple connected graph G , the modified Wiener index is defined as

$$WW_\lambda(G) = \frac{1}{2} \sum_{y \in V(G)} \sum_{z \in V(G)} (d(y, z)^\lambda + d(y, z)^{2\lambda}), \quad (6)$$

where λ is any positive integer.

Definition 6 (Harary polynomial). The Harary polynomial for a simple connected graph G is denoted by $h(G)$ and is defined as

$$h(G) = \sum_{y \in V(G)} \sum_{z \in V(G)} \frac{1}{d(y, z)} x^{d(y,z)}. \quad (7)$$

Definition 7 (generalized Harary index). The generalized Harary index for a simple connected graph G is denoted by $h_t(G)$ and is defined as

$$h_t(G) = \sum_{y \in V(G)} \sum_{z \in V(G)} \frac{1}{d(y, z) + t}, \tag{8}$$

where $t = 1, 2, 3, 4, \dots$

For detailed study on Harary polynomial and Harary index, we refer to the readers [39, 40] and references therein.

Definition 8 (multiplicative Wiener index). The multiplicative Wiener index for a simple connected graph G is denoted by $\pi(G)$ and is defined as

$$\pi(G) = \prod_{\{y,z\} \subseteq V(G)} d(y, z). \tag{9}$$

3. Methodology

With the aid of distance matrix of a graph G , we can evaluate Hosoya polynomial. To calculate the Hosoya polynomial, we

must calculate the number of pairs of vertices at distance $1, 2, 3, \dots, \text{dia}(G)$, where $\text{dia}(G) = \max\{d(u, v); u, v \in V(G)\}$. Mathematical induction will be used for the above cause. The usual vision of Hosoya polynomial is given below, where d represents the maximum distance in graph.

$$H(G; x) = a_0(n)x^0 + a_1(n)x^1 + a_2(n)x^2 + \dots + a_d(n)x^d. \tag{10}$$

4. Distance-Based Polynomials and Indices for Hierarchical Hypercube Networks

This section consists of two subsections. In Section 4.1, we present results about HHC-1, and in Section 4.2, we present results about HHC-2.

4.1. Distance-Based Polynomials and Indices for Hierarchical Hypercube Network HHC-1. In Theorem 1, we give Hosoya polynomial of HHC-1.

Theorem 1. For $n \geq 3$, the Hosoya polynomial of HHC – 1 is

$$H(\text{HHC} - 1; x) = (20 + 24n)x + (24 + 40n)x^2 + (24 + 64n)x^3 + (4 + 100n)x^4 + (-28 + 124n)x^5 + (-80 + 132n)x^6 + (-152 + 132n)x^7 + \sum_{8 \leq m \leq 2n+2} ((8(37 - 8m + 16n)))x^m + 108x^{2n+3} + 60x^{2n+4} + 20x^{2n+5}. \tag{11}$$

Proof. To prove this result, we need to calculate $|a_m(n)|$ = number of pair of vertices at distance m , where $m = 1, 2, 3, \dots, 2n + 5$. Using Figure 1, the number of pair of vertices at different distances is computed and is listed in Tables 1 and 2.

Now, by using Table 1, we have

$$\begin{aligned} |a_1(n)| &= 20 + 24n, \\ |a_2(n)| &= 24 + 40n, \\ |a_3(n)| &= 24 + 64n, \\ |a_4(n)| &= 4 + 100n, \\ |a_5(n)| &= -28 + 124n, \\ |a_6(n)| &= -80 + 132n, \\ |a_7(n)| &= -152 + 132n. \end{aligned} \tag{12}$$

The remaining proof is divided into the following two main cases.

Case 1. When $m \equiv 0 \pmod{2}$ and $8 < m \leq 2n + 2$.

It can be observed from Table 2 that

$$\begin{aligned} |a_8(3)| &= 168, \\ |a_8(4)| &= 296, \\ |a_8(5)| &= 424, \\ |a_8(6)| &= 552, \\ |a_8(7)| &= 680, \\ |a_8(8)| &= 808. \end{aligned} \tag{13}$$

Now, we can deduce that

$$|a_8(n)| = 40 + 128(n - 2). \tag{14}$$

In a similar fashion, we have

$$\begin{aligned} |a_{10}(4)| &= 168, \\ |a_{10}(5)| &= 296, \\ |a_{10}(6)| &= 424, \\ |a_{10}(7)| &= 552, \\ |a_{10}(8)| &= 680, \\ |a_{10}(9)| &= 808. \end{aligned} \tag{15}$$

TABLE 1: Pair of vertices in HHC-1 at different distances.

m	n						
	3	4	5	6	7	8	.
1	92	116	140	164	188	212	.
2	144	184	224	264	304	344	.
3	216	280	344	408	472	536	.
4	304	404	504	604	704	804	.
5	344	468	592	716	840	964	.
6	316	448	580	712	844	976	.
7	244	376	508	640	772	904	.

TABLE 2: Pair of vertices in HHC-1 at different distances.

m	n						
	3	4	5	6	7	8	.
8	168	296	424	552	680	808	.
9	—	232	360	488	616	744	.
10	—	168	296	424	552	680	.
11	—	—	232	360	488	616	.
12	—	—	168	296	424	552	.
13	—	—	—	232	360	488	.
14	—	—	—	168	296	424	.
15	—	—	—	—	232	360	.
16	—	—	—	—	168	296	.
17	—	—	—	—	—	232	.
18	—	—	—	—	—	168	.
19	—	—	—	—	—	—	.
20	—	—	—	—	—	—	.
21	—	—	—	—	—	—	.

It implies that

$$|a_{10}(n)| = 40 + 128(n - 3). \tag{16}$$

In a similar fashion, we infer

$$\begin{aligned} |a_{12}(n)| &= 40 + 128(n - 4), \\ |a_{14}(n)| &= 40 + 128(n - 5), \\ |a_{16}(n)| &= 40 + 128(n - 6), \\ &\dots \end{aligned} \tag{17}$$

Now, we have

$$|a_m(n)| = 40 + 128 \left(n - \frac{(m-4)}{2} \right) = 8(37 - 8m + 16n). \tag{18}$$

Case 2. When $m \equiv 1 \pmod{2}$ and $9 < m \leq 2n + 1$.

It can be observed from Table 2 that

$$\begin{aligned} |a_9(4)| &= 232, \\ |a_9(5)| &= 360, \\ |a_9(6)| &= 488, \\ |a_9(7)| &= 616, \\ |a_9(8)| &= 744, \\ |a_9(9)| &= 872. \end{aligned} \tag{19}$$

Now, we can deduce that

$$|a_9(n)| = 104 + 128(n - 3). \tag{20}$$

By means of the same trick, we obtain

$$\begin{aligned} |a_{11}(5)| &= 232, \\ |a_{11}(6)| &= 360, \\ |a_{11}(7)| &= 488, \\ |a_{11}(8)| &= 616, \\ |a_{11}(9)| &= 744, \\ |a_{11}(10)| &= 872, \end{aligned} \tag{21}$$

which reveal that

$$|a_{11}(n)| = 104 + 128(n - 4). \tag{22}$$

With a similar approach, we get

$$\begin{aligned} |a_{13}(n)| &= 104 + 128(n - 5), \\ |a_{15}(n)| &= 104 + 128(n - 6), \\ |a_{17}(n)| &= 104 + 128(n - 7), \\ &\dots \end{aligned} \tag{23}$$

Hence, we have

$$\begin{aligned} |a_m(n)| &= 104 + 128 \left(n - \frac{(m-3)}{2} \right) |a_m(n)| \\ &= 8(37 - 8m + 16n). \end{aligned} \tag{24}$$

One can see that in both cases, we get the same result, so we can write for $8 < m \leq 2n + 1$ as

$$|a_m(n)| = 8(37 - 8m + 16n), \quad (25)$$

and the remaining last three distances having fixed values are

$$\begin{aligned} |a_{2n+3}(n)| &= 108, \\ |a_{2n+4}(n)| &= 60, \\ |a_{2n+5}(n)| &= 20. \end{aligned} \quad (26)$$

By what have been mentioned above and using definition of Hosoya polynomial, we arrive at our desired result. \square

In Theorem 2, we give Harary polynomial for HHC-1.

Theorem 2. For $n \geq 3$, the Harary polynomial of HHC - 1 is

$$\begin{aligned} h(\text{HHC} - 1; x) &= (20 + 24n)x + \frac{(24 + 40n)}{2}x^2 + \frac{(24 + 64n)}{3}x^3 + \frac{(4 + 100n)}{4}x^4 + \frac{(-28 + 124n)}{5}x^5 \\ &+ \frac{(-80 + 132n)}{6}x^6 + \frac{(-152 + 132n)}{7}x^7 \\ &+ \sum_{8 \leq m \leq 2n+2} \frac{(8(37 - 8m + 16n))}{m}x^m + \frac{108}{2n+3}x^{2n+3} + \frac{60}{2n+4}x^{2n+4} + \frac{20}{2n+5}x^{2n+5}. \end{aligned} \quad (27)$$

Proof. The proof of this result is easy to follow by using information given in Theorem 1 and definition of Harary polynomial.

In Theorem 3, we give modified Wiener index, modified hyper-Wiener index, generalized Harary index, and multiplicative Wiener index of HHC-1. \square

Theorem 3. For HHC - 1, we have

(1) The modified Wiener index:

$$\begin{aligned} W_\lambda(\text{HHC} - 1) &= (20 + 24n)1^\lambda + (24 + 40n)2^\lambda + (24 + 64n)3^\lambda + (4 + 100n)4^\lambda + (-28 + 124n)5^\lambda \\ &+ (-80 + 132n)6^\lambda + (-152 + 132n)7^\lambda \\ &+ \sum_{8 \leq m \leq 2n+2} (8(37 - 8m + 16n))(m^\lambda) + (108)(2n + 3)^\lambda + (60)(2n + 4)^\lambda + (20)(2n + 5)^\lambda. \end{aligned} \quad (28)$$

(2) The modified hyper-Wiener index:

$$\begin{aligned} WW_\lambda(\text{HHC} - 1) &= (20 + 24n)(1^\lambda + 1^{2\lambda}) \\ &+ (24 + 40n)(2^\lambda + 2^{2\lambda}) + (24 + 64n)(3^\lambda + 3^{2\lambda}) \\ &+ (4 + 100n)(4^\lambda + 4^{2\lambda}) + (-28 + 124n)(5^\lambda + 5^{2\lambda}) + (-80 + 132n)(6^\lambda + 6^{2\lambda}) + (-152 + 132n)(7^\lambda + 7^{2\lambda}) \\ &+ \sum_{8 \leq m \leq 2n+2} (8(37 - 8m + 16n))(m^\lambda + m^{2\lambda}) + (108)((2n + 3)^\lambda + (2n + 3)^{2\lambda}) \\ &+ (60)((2n + 4)^\lambda + (2n + 4)^{2\lambda}) + (20)((2n + 5)^\lambda + (2n + 5)^{2\lambda}). \end{aligned} \quad (29)$$

(3) The generalized Harary index:

$$\begin{aligned}
 h_t(\text{HHC} - 1) &= \frac{(20 + 24n)}{1 + t} + \frac{(24 + 40n)}{2 + t} + \frac{(24 + 64n)}{3 + t} + \frac{(4 + 100n)}{4 + t} + \frac{(-28 + 124n)}{5 + t} \\
 &\quad + \frac{(-80 + 132n)}{6 + t} + \frac{(-152 + 132n)}{7 + t} \\
 &\quad + \sum_{8 \leq m \leq 2n+2} (8(37 - 8m + 16n)) \frac{1}{m + t} + \frac{108}{2n + 3 + t} + \frac{60}{2n + 4 + t} + \frac{20}{2n + 5 + t}.
 \end{aligned} \tag{30}$$

(4) The multiplicative Wiener index:

$$\begin{aligned}
 \pi(\text{HHC} - 1) &= 1^{(20+24n)} \times 2^{(24+40n)} \times 3^{(24+64n)} \times 4^{(4+100n)} \times 5^{(-28+124n)} \times 6^{(-80+132n)} \times 7^{(-152+132n)} \\
 &\quad \times \prod_{8 < m \leq 2n+2} m^{(8(37-8m+16n))} \times (2n + 3)^{108} \times (2n + 4)^{60} \times (2n + 5)^{20}.
 \end{aligned} \tag{31}$$

From Theorem 3, we get the following results immediately.

Corollary 1. For $\text{HHC} - 1$, we have

$$W(\text{HHC} - 1) = \frac{256n^3}{3} + 592n^2 + \frac{2696n}{3} + 376. \tag{32}$$

Proof. This result can be easily established by taking $\lambda = 1$ in (1) of Theorem 3. \square

Corollary 2. For $\text{HHC} - 1$, we have

$$\begin{aligned}
 \text{WW}(\text{HHC} - 1) &= \frac{256n^4}{3} + \frac{2624n^3}{3} + \frac{10544n^2}{3} \\
 &\quad + \frac{14056n}{3} + 1816.
 \end{aligned} \tag{33}$$

Proof. This result can be easily established by taking $\lambda = 1$ in (2) of Theorem 3. \square

Corollary 3. For $\text{HHC} - 1$, we have

$$\begin{aligned}
 H(\text{HHC} - 1) &= \frac{15599n}{100} + \frac{6347931761169771}{18014398509481984} \\
 &\quad + \sum_{8 \leq m \leq 2n+2} \frac{(8(37 - 8m + 16n))}{m} + \frac{108}{2n + 3} + \frac{20}{2n + 5} + \frac{30}{n + 2}.
 \end{aligned} \tag{34}$$

Proof. This result can be easily established by taking $t = 1$ in (3) of Theorem 3. \square

4.2. *Distance-Based Polynomials and Indices for Hierarchical Hypercube Network HHC-2.* In Theorem 4, we give Hosoya polynomial for HHC-2.

Theorem 4. For HHC – 2, the Hosoya polynomial is

$$\begin{aligned}
 H(\text{HHC} - 2; x) &= (28 + 32n)x + (24 + 48n)x^2 + (36 + 96n)x^3 + (-4 + 124n)x^4 + (-60 + 128n)x^5 \\
 &+ (-120 + 132n)x^6 + \sum_{m \equiv 0 \pmod{2}, 8 \leq m \leq 2n+2} (8(33 - 8m + 16n))x^m \\
 &+ \sum_{m \equiv 1 \pmod{2}, 7 \leq m \leq 2n+1} (-64(m - 2(2 + n)))x^m + 68x^{2n+3} + 32x^{2n+4} + 4x^{2n+5}.
 \end{aligned} \tag{35}$$

Proof. To prove this result, we have to calculate $|a_m(n)|$ where $m = 1, 2, 3, \dots, 2n + 5$. Here $|a_m(n)|$ is the same as in Theorem 1. From Figure 2, we can compute the number of pair of vertices in HHC-2 at different distances, which is given in Tables 3 and 4.

Now from Table 3, we have

$$\begin{aligned}
 |a_1(n)| &= 28 + 32n, \\
 |a_2(n)| &= 24 + 48n, \\
 |a_3(n)| &= 36 + 96n, \\
 |a_4(n)| &= -4 + 124n, \\
 |a_5(n)| &= -60 + 128n, \\
 |a_6(n)| &= -120 + 132n.
 \end{aligned} \tag{36}$$

The remaining proof is divided into the following two main cases.

Case 1. When $m \equiv 0 \pmod{2}$ and $8 < m \leq 2n + 2$.

It can be observed from Table 4 that

$$\begin{aligned}
 |a_8(3)| &= 136, \\
 |a_8(4)| &= 264, \\
 |a_8(5)| &= 392, \\
 |a_8(6)| &= 520, \\
 |a_8(7)| &= 648, \\
 |a_8(8)| &= 776.
 \end{aligned} \tag{37}$$

Now, we can deduce that

$$|a_8(n)| = 8 + 128(n - 2). \tag{38}$$

In a similar fashion, we have

$$\begin{aligned}
 |a_{10}(4)| &= 136, \\
 |a_{10}(5)| &= 264, \\
 |a_{10}(6)| &= 392, \\
 |a_{10}(7)| &= 520, \\
 |a_{10}(8)| &= 648, \\
 |a_{10}(9)| &= 776.
 \end{aligned} \tag{39}$$

It implies that

$$|a_{10}(n)| = 8 + 128(n - 3). \tag{40}$$

In a similar fashion, we infer

$$\begin{aligned}
 |a_{12}(n)| &= 8 + 128(n - 4), \\
 |a_{14}(n)| &= 8 + 128(n - 5), \\
 |a_{16}(n)| &= 8 + 128(n - 6), \\
 &\dots,
 \end{aligned} \tag{41}$$

which yield

$$|a_m(n)| = 8 + 128 \left(n - \frac{(m - 4)}{2} \right) = 8(33 - 8m + 16n). \tag{42}$$

Case 2. When $m \equiv 1 \pmod{2}$ and $7 < m \leq 2n + 1$.

It can be observed from Table 4 that

$$\begin{aligned}
 |a_7(3)| &= 192, \\
 |a_7(4)| &= 320, \\
 |a_7(5)| &= 448, \\
 |a_7(6)| &= 576, \\
 |a_7(7)| &= 704, \\
 |a_7(8)| &= 832.
 \end{aligned} \tag{43}$$

Now, we can deduce that

TABLE 3: Number of pair of vertices in HHC-2 at different distances.

m	n						
	2	3	4	5	6	7	.
1	92	124	156	188	220	252	.
2	120	168	216	264	312	360	.
3	228	324	420	516	612	708	.
4	244	368	492	616	740	864	.
5	196	324	452	580	708	836	.
6	144	276	408	540	672	804	.

TABLE 4: Number of pair of vertices of HHC-2 at different distances.

m	n						
	3	4	5	6	7	8	.
7	192	320	448	576	704	832	.
8	136	264	392	520	648	776	.
9	—	192	320	448	576	704	.
10	—	136	264	392	520	648	.
11	—	—	192	320	448	576	.
12	—	—	136	264	392	520	.
13	—	—	—	192	320	448	.
14	—	—	—	136	264	392	.
15	—	—	—	—	192	320	.
16	—	—	—	—	136	264	.
17	—	—	—	—	—	192	.
18	—	—	—	—	—	136	.
19	—	—	—	—	—	—	.
20	—	—	—	—	—	—	—
21	—	—	—	—	—	—	—

$$|a_7(n)| = 64 + 128(n - 2). \tag{44}$$

So, we obtain

$$\begin{aligned} |a_9(4)| &= 192, \\ |a_9(5)| &= 320, \\ |a_9(6)| &= 448, \\ |a_9(7)| &= 576, \\ |a_9(8)| &= 704, \\ |a_9(9)| &= 832, \end{aligned} \tag{45}$$

which reveal that

$$|a_9(n)| = 64 + 128(n - 3). \tag{46}$$

Also, we get

$$\begin{aligned} |a_{13}(n)| &= 64 + 128(n - 4), \\ |a_{15}(n)| &= 64 + 128(n - 5), \\ |a_{17}(n)| &= 64 + 128(n - 6), \\ &\dots \end{aligned} \tag{47}$$

Hence, we have

$$\begin{aligned} |a_m(n)| &= 64 + 128\left(n - \frac{(m - 3)}{2}\right) \\ &= -64(m - 2(2 + n)), \end{aligned} \tag{48}$$

and the remaining last three distances having fixed values are

$$\begin{aligned} |a_{2n+3}(n)| &= 68, \\ |a_{2n+4}(n)| &= 32, \\ |a_{2n+5}(n)| &= 4. \end{aligned} \tag{49}$$

By what have been mentioned above and using the definition of Hosoya polynomial, we arrive at our desired result. \square

In Theorem 5, we give Harary polynomial for HHC-2.

Theorem 5. For HHC - 2, the Harary polynomial is

$$\begin{aligned}
 h(\text{HHC} - 2; x) &= (28 + 32n)x + \frac{(24 + 48n)}{2}x^2 + \frac{(36 + 96n)}{3}x^3 + \frac{(36 + 96n)}{4}x^4 + \frac{(-60 + 128n)}{5}x^5 \\
 &+ \frac{(-120 + 132n)}{6}x^6 + \sum_{8 \leq m \leq 2n+2} \frac{(8(33 - 8m + 16n))}{m}x^m \\
 &+ \sum_{7 \leq m \leq 2n+1} \frac{(-64(m - 2(2 + n)))}{m}x^m + \frac{68}{2n + 3}x^{2n+3} + \frac{32}{2n + 4}x^{2n+4} + \frac{4}{2n + 5}x^{2n+5}.
 \end{aligned} \tag{50}$$

Proof. The proof of this theorem is straightforward from the facts specified in Theorem 4 and by definition of Harary polynomial. \square

Theorem 6. For HHC - 2, we have

(1) The modified Wiener index:

In Theorem 6, we give modified Wiener index, modified hyper-Wiener index, generalized Harary index, and multiplicative Wiener index for HHC-2.

$$\begin{aligned}
 W_\lambda(\text{HHC} - 2) &= (28 + 32n)1^\lambda + (24 + 48n)2^\lambda + (36 + 96n)3^\lambda + (36 + 96n)4^\lambda + (-60 + 128n)5^\lambda \\
 &+ (-120 + 132n)6^\lambda + \sum_{m \equiv 0 \pmod{2}, 8 \leq m \leq 2n+2} (8(33 - 8m + 16n))(m^\lambda) \\
 &+ \sum_{m \equiv 1 \pmod{2}, 7 \leq m \leq 2n+1} (-64(m - 2(2 + n)))(m^\lambda) + (68)(2n + 3)^\lambda + (32)(2n + 4)^\lambda + (4)(2n + 5)^\lambda.
 \end{aligned} \tag{51}$$

(2) The modified hyper-Wiener index:

$$\begin{aligned}
 WW_\lambda(\text{HHC} - 2) &= (28 + 32n)(1^\lambda + 1^{2\lambda}) + (24 + 48n)(2^\lambda + 2^{2\lambda}) + (36 + 96n)(3^\lambda + 3^{2\lambda}) \\
 &+ (36 + 96n)(4^\lambda + 4^{2\lambda}) + (-60 + 128n)(5^\lambda + 5^{2\lambda}) + (-120 + 132n)(6^\lambda + 6^{2\lambda}) \\
 &+ \sum_{m \equiv 0 \pmod{2}, 8 \leq m \leq 2n+2} (8(33 - 8m + 16n))(m^\lambda + m^{2\lambda}) \\
 &+ \sum_{m \equiv 1 \pmod{2}, 7 \leq m \leq 2n+1} (-64(m - 2(2 + n)))(m^\lambda + m^{2\lambda}) \\
 &+ (68)((2n + 3)^\lambda + (2n + 3)^{2\lambda}) + (32)((2n + 4)^\lambda + (2n + 4)^{2\lambda}) + (4)((2n + 5)^\lambda + (2n + 5)^{2\lambda}).
 \end{aligned} \tag{52}$$

(3) The generalized Harary index:

$$\begin{aligned}
 h_t(\text{HHC} - 2) &= \frac{(28 + 32n)}{1 + t} + \frac{(24 + 48n)}{2 + t} + \frac{(36 + 96n)}{3 + t} + \frac{(36 + 96n)}{4 + t} + \frac{(-60 + 128n)}{5 + t} + \frac{(-120 + 132n)}{6 + t} \\
 &+ \sum_{m \equiv 0 \pmod{2}, 8 \leq m \leq 2n+2} \frac{(8(33 - 8m + 16n))}{m + t} \\
 &+ \sum_{m \equiv 1 \pmod{2}, 7 \leq m \leq 2n+1} \frac{(-64(m - 2(2 + n)))}{m + t} + \frac{108}{2n + 3 + t} + \frac{60}{2n + 4 + t} + \frac{20}{2n + 5 + t}.
 \end{aligned} \tag{53}$$

(4) The multiplicative Wiener index:

$$\begin{aligned} \pi(\text{HHC} - 2) &= 1^{(28+32n)} \times 2^{(24+48n)} \times 3^{(36+96n)} \times 4^{(36+96n)} \times 5^{(-60+128n)} \times 6^{(-120+132n)} \\ &\times \prod_{m \equiv 0 \pmod{2}, 8 < m \leq 2n+2} m^{(8(33-8m+16n))} \times \prod_{m \equiv 1 \pmod{2}, 7 < m \leq 2n+1} m^{(-64(m-2(2+n)))} (2n+3)^{68} \\ &\times (2n+4)^{32} \times (2n+5)^4. \end{aligned} \quad (54)$$

From Theorem 6, we get the following results immediately.

Corollary 4. For $\text{HHC} - 2$, we have

$$W(\text{HHC} - 2) = \frac{256n^3}{3} + 520n^2 + \frac{2288n}{3} + 316. \quad (55)$$

Proof. This result can be easily established by taking $\lambda = 1$ in (1) of Theorem 6. \square

Corollary 5. For $\text{HHC} - 2$, we have

$$\begin{aligned} \text{WW}(\text{HHC} - 2) &= \frac{256n^4}{3} + \frac{2336n^3}{3} + \frac{8264n^2}{3} \\ &+ \frac{10480n}{3} + 1320. \end{aligned} \quad (56)$$

Proof. This result can be easily established by taking $\lambda = 1$ in (2) of Theorem 6. \square

Corollary 6. For $\text{HHC} - 2$, we have

$$\begin{aligned} H(\text{HHC} - 2) &= \frac{798n}{5} + 29 + \sum_{m \equiv 0 \pmod{2}, 8 \leq m \leq 2n+2} (8(33-8m+16n)) \frac{1}{m} \\ &+ \sum_{m \equiv 1 \pmod{2}, 7 \leq m \leq 2n+1} (-64(m-2(2+n))) \frac{1}{m} + \frac{108}{2n+3} + \frac{20}{2n+5} + \frac{30}{n+2}. \end{aligned} \quad (57)$$

Proof. This result can be easily established by taking $t = 1$ in (3) of Theorem 6. \square

5. Conclusion

Topological indices can be applied in different fields of science, such as material science, arithmetic, informatics, biology, and so on. However, the most critical use of topological indices to date is in the nonexact quantitative structure-property relationships and quantitative structure-activity relationships. In this paper, we studied hierarchical hypercube networks. We computed distance-based polynomials and distance-based indices for these networks. In fact, we computed Hosoya polynomials, Harary polynomials, Wiener index, and different variants of Wiener indices for the studied networks. Our results can help in understanding the topology of hierarchical hypercube networks and can be used to solve integral equations.

Data Availability

The data used to support the findings of this study are included within the article.

Conflicts of Interest

The authors declare that they have no conflicts of interest.

Authors' Contributions

Tingmei Gao wrote the final version of this paper, analyzed the results, and arranged funding for this study. Iftikhar Ahmed proved the results and wrote the first version of this paper.

References

- [1] S. C. Basak, D. Mills, B. D. Gute, G. D. Grunwald, and A. T. Balaban, "Applications of topological indices in the property/bioactivity/toxicity prediction of chemicals," in *Topology in Chemistry*, pp. 113–184, Woodhead Publishing, Sawston, UK, 2002.
- [2] M. P. Hanson and D. H. Rouvray, "Novel applications of topological indices. 2. Prediction of the threshold soot index for hydrocarbon fuels," *The Journal of Physical Chemistry*, vol. 91, no. 11, pp. 2981–2985, 1987.
- [3] P. J. Hansen and P. C. Jurs, "Chemical applications of graph theory. Part I. Fundamentals and topological indices," *Journal of Chemical Education*, vol. 65, no. 7, p. 574, 1988.

- [4] W. Gao, W. Wang, and M. R. Farahani, "Topological indices study of molecular structure in anticancer drugs," *Journal of Chemistry*, vol. 2016, Article ID 3216327, 8 pages, 2016.
- [5] S. Hayat and M. Imran, "Computation of topological indices of certain networks," *Applied Mathematics and Computation*, vol. 240, no. 23, pp. 213–228, 2014.
- [6] S. Hayat and M. Imran, "Computation of certain topological indices of nanotubes covered by C5 and C7," *Journal of Computational and Theoretical Nanoscience*, vol. 12, no. 4, pp. 533–541, 2015.
- [7] A. Q. Baig, M. Imran, and H. Ali, "On topological indices of poly oxide, poly silicate, DOX, and DSL networks," *Canadian Journal of Chemistry*, vol. 93, no. 7, pp. 730–739, 2015.
- [8] Y. Bashir, A. Aslam, M. Kamran et al., "On forgotten topological indices of some dendrimers structure," *Molecules*, vol. 22, no. 6, p. 867, 2017.
- [9] A. Aslam, J. L. G. Guirao, S. Ahmad, and W. Gao, "Topological indices of the line graph of subdivision graph of complete bipartite graphs," *Applied Mathematics & Information Sciences*, vol. 11, no. 6, pp. 1631–1636, 2017.
- [10] G. C. Marsden, P. J. Marchand, P. Harvey, and S. C. Esener, "Optical transpose interconnection system architectures," *Optics letters*, vol. 18, no. 13, pp. 1083–1085, 1993.
- [11] A. Al-Ayyoub, A. Awwad, K. Day, and M. Ould-Khaoua, "Generalized methods for algorithm development on optical systems," *The Journal of Supercomputing*, vol. 38, no. 2, pp. 111–125, 2006.
- [12] C. F. Wang and S. Sahni, "Matrix multiplication on the OTIS-mesh optoelectronic computer," *IEEE Transactions on Computers*, vol. 50, no. 7, pp. 635–646, 2001.
- [13] C. F. Wang and S. Sahni, "Image processing on the OTIS-mesh optoelectronic computer," *IEEE Transactions on Parallel and Distributed Systems*, vol. 11, no. 2, pp. 97–109, 2000.
- [14] C. F. Wang and S. Sahni, "Basic operations on the OTIS-mesh optoelectronic computer," *IEEE Transactions on Parallel and Distributed Systems*, vol. 9, no. 12, pp. 1226–1236, 1998.
- [15] S. Rajasekaran and S. Sahni, "Randomized routing, selection, and sorting on the OTIS-mesh," *IEEE Transactions on Parallel and Distributed Systems*, vol. 9, no. 9, pp. 833–840, 1998.
- [16] H. Hosoya, "On some counting polynomials in chemistry," *Discrete Applied Mathematics*, vol. 19, no. 1-3, pp. 239–257, 1988.
- [17] D. Stevanović, "Hosoya polynomial of composite graphs," *Discrete Mathematics*, vol. 235, no. 1-3, pp. 237–244, 2001.
- [18] M. R. Farahani, "On the Schultz polynomial and Hosoya polynomial of circumcoronene series of benzenoid," *Journal of Applied Mathematics & Informatics*, vol. 31, no. 5-6, pp. 595–608, 2013.
- [19] J. M. Kumar and L. M. Patnaik, "Extended hypercube: a hierarchical interconnection network of hypercubes," *IEEE Transactions on Parallel and Distributed Systems*, vol. 3, no. 1, pp. 45–57, 1992.
- [20] R.-Y. Wu, G.-H. Chen, Y.-L. Kuo, and G. J. Chang, "Node-disjoint paths in hierarchical hypercube networks," *Information Sciences*, vol. 177, no. 19, pp. 4200–4207, 2007.
- [21] Q. M. Malluhi and M. A. Bayoumi, "The hierarchical hypercube: a new interconnection topology for massively parallel systems," *IEEE Transactions on Parallel and Distributed Systems*, vol. 5, no. 1, pp. 17–30, 1994.
- [22] S. K. Yun and K. H. Park, "Comments on "Hierarchical cubic networks"," *IEEE Transactions on Parallel and Distributed Systems* vol. 9, no. 4, pp. 410–414, 1998.
- [23] M. Abd-El-Barr and T. F. Al-Somani, "Performance comparison of hierarchical interconnection networks," in *Proceedings of 2011 IEEE Pacific Rim Conference on Communications, Computers and Signal Processing*, pp. 191–196, IEEE, Victoria, British Columbia (BC), Canada, August 2011.
- [24] J.-S. Fu and G.-H. Chen, "Hamiltonicity of the hierarchical cubic network," *Theory of Computing Systems*, vol. 35, no. 1, pp. 59–79, 2002.
- [25] C. Chen and D. P. Agrawal, "dBCube: a new class of hierarchical multiprocessor interconnection networks with area efficient layout," *IEEE Transactions on Parallel and Distributed Systems*, vol. 4, no. 12, pp. 1332–1344, 1993.
- [26] S.-K. Yun and K. H. Park, "Hierarchical hypercube networks (HHN) for massively parallel computers," *Journal of Parallel and Distributed Computing*, vol. 37, no. 2, pp. 194–199, 1996.
- [27] S. P. Dandamudi and D. L. Eager, "On hypercube-based hierarchical interconnection network design," *Journal of Parallel and Distributed Computing*, vol. 12, no. 3, pp. 283–289, 1991.
- [28] C. H. Yeh and B. Parhami, "Swapped networks: unifying the architectures and algorithms of a wide class of hierarchical parallel processors," in *Proceedings of 1996 International Conference on Parallel and Distributed Systems*, pp. 230–237, IEEE, Tokyo, Japan, June 1996.
- [29] K. Ghose and K. R. Desai, "Hierarchical cubic networks," *IEEE Transactions on Parallel and Distributed Systems*, vol. 6, no. 4, pp. 427–435, 1995.
- [30] M. B. Galles and D. E. Lenoski, *U.S. Patent No. 5,669,008*, U.S. Patent and Trademark Office, Washington, USA, 1997.
- [31] C. H. Yeh and B. Parhami, "Hierarchical swapped networks: efficient low-degree alternatives to hypercubes and generalized hypercubes," in *Proceedings Second International Symposium on Parallel Architectures, Algorithms, and Networks (ISPAN'96)*, pp. 90–96, IEEE, Beijing, China, June 1996.
- [32] W.-K. Chiang and R.-J. Chen, "Topological properties of hierarchical cubic networks," *Journal of Systems Architecture*, vol. 42, no. 4, pp. 289–307, 1996.
- [33] M. Abd-El-Barr and T. F. Al-Somani, "Topological properties of hierarchical interconnection networks: a review and comparison," *Journal of Electrical and Computer Engineering*, vol. 2011, Article ID 189434, 12 pages, 2011.
- [34] S. P. Dandamudi and D. L. Eager, "Hierarchical interconnection networks for multicomputer systems," *IEEE Transactions on Computers*, vol. 39, no. 6, pp. 786–797, 1990.
- [35] M. Numan, S. I. Butt, S. I. Butt, and A. Taimur, "Super cyclic antimagic covering for some families of graphs," *Open Journal of Mathematical Sciences*, vol. 5, no. 1, pp. 27–33, 2021.
- [36] H. M. Nagesh and V. R. Girish, "On the entire Zagreb indices of the line graph and line cut-vertex graph of the subdivision graph," *Open Journal of Mathematical Sciences*, vol. 4, no. 1, pp. 470–475, 2020.
- [37] H. Wiener, "Structural determination of paraffin boiling points," *Journal of the American Chemical Society*, vol. 69, no. 1, pp. 17–20, 1947.
- [38] M. Randić, "Index," *Oral Cancer*, vol. 49, no. 3, pp. 483–496, 2002.
- [39] B. Lucic, A. Milicevic, S. Nikolic, and N. Trinajstić, "Harary index-twelve years later," *Croatica Chemica Acta*, vol. 75, no. 4, pp. 847–868, 2002.
- [40] B. Zhou, X. Cai, and N. Trinajstić, "On Harary index," *Journal of Mathematical Chemistry*, vol. 44, no. 2, pp. 611–618, 2008.

Research Article

Enumeration of the Edge Weights of Symmetrically Designed Graphs

Muhammad Javaid ¹, Hafiz Usman Afzal,¹ and Ebenezer Bonyah ²

¹Department of Mathematics, School of Science, University of Management and Technology, Lahore 54770, Pakistan

²Department of Mathematics Education, Akenten Appiah-Menka University of Skills Training and Entrepreneurial Development, Kumasi 00233, Ghana

Correspondence should be addressed to Ebenezer Bonyah; ebbonya@gmail.com

Received 16 July 2021; Accepted 21 August 2021; Published 9 September 2021

Academic Editor: Ali Ahmad

Copyright © 2021 Muhammad Javaid et al. This is an open access article distributed under the Creative Commons Attribution License, which permits unrestricted use, distribution, and reproduction in any medium, provided the original work is properly cited.

The idea of super $(a, 0)$ -edge-antimagic labeling of graphs had been introduced by Enomoto et al. in the late nineties. This article addresses super $(a, 0)$ -edge-antimagic labeling of a biparametric family of pancyclic graphs. We also present the aforesaid labeling on the disjoint union of graphs comprising upon copies of C_4 and different trees. Several problems shall also be addressed in this article.

1. Introduction

A graph $\Gamma(V, E)$ is a combination of two different sets, one is the set of vertices $V(\Gamma)$ and the other is the set of connections between these vertices, termed as set of edges $E(\Gamma)$. A graph Γ can either be connected or comprises upon connected parts known as graphs' components. The non-empty and simple graphs shall be considered here only all the way, consisting of $V(\Gamma)$, the set of vertices, and $E(\Gamma)$, the set of edges, having $|V(\Gamma)| = p$ and $|E(\Gamma)| = q$. In this case, the graph Γ is called a (p, q) -graph. Additionally, [1] can be cited for the comprehension of the graph theoretic terminologies.

A labeling is a function from the set of integers onto the components of a graph under certain constraints. The labeling is said to be total if it covers all components of the graph. If the labeling covers $V(\Gamma)$ or $E(\Gamma)$ only in the domain, then it is termed to be the vertex or edge labeling, respectively. The two important categories of labeling are magic and antimagic. The equal or unequal edge/vertex weights point towards, respectively, the magic and antimagic types of labeling.

Throughout the article, the abbreviations given in Table 1 are used.

Definition 1. On a (σ, ς) -graph $\Gamma = (V(\Gamma), E(\Gamma))$, a bijection γ from $V(\Gamma) \cup E(\Gamma) \xrightarrow{\text{onto}} \{1, 2, \dots, \sigma + \varsigma\}$ is the notion of (a, d) -EAMT labeling if we keep the restriction upon the edge weights $\gamma(u) + \gamma(uv) + \gamma(v)$, $\forall uv \in E(G)$, which generates a consecutive integer sequence, with a being the minimum edge weight and d being the common difference. Γ is notioned as an (a, d) -EAMT graph, with the existence of such labeling.

Definition 2. If the smallest labels $1, 2, \dots, \sigma$ are allocated to the points (vertices) of the (σ, ς) -graph Γ in an (a, d) -EAMT labeling, then this labeling is addressed as $S - (a, d)$ -EAMT labeling. And, Γ , in his scenario, is referred to be an $S - (a, d)$ -EAMT graph.

The edge weight (minimum) a (Definitions 1 and 2) becomes a constant at $d = 0, \forall uv \in E(\Gamma)$, and is called magic constant or magic sum of Γ .

Definition 3. A pancyclic graph $\Gamma(V, E)$ is a graph that contains the cycles of all orders up to $|V(\Gamma)|$.

The notion of magic labeling was highlighted by Sedlacek in the early sixties [2]. Later, Ringel and Hartsfield capitulated the idea of antimagic labeling with respect to vertex-

TABLE 1: Abbreviations being used onwards.

Terminology	Abbreviation
(a, d) -edge-antimagic total	(a, d) – EAMT
Super (a, d) -edge-antimagic total	$S - (a, d)$ – EAMT

sums of graphs in [3]. The idea of magic valuations of graphs had been brought by Kotzig and Rosa [4] which was indeed the graphs' $(a, 0)$ – EAMT labeling (introduced by Ringel et al. in the nineties [5]). Enomoto and Llado introduced the idea of $S - (a, 0)$ – EAMT labeling of graphs using the term super edge-magic labeling in [6]. In the early 21st century, Bertault and Simanjuntak brought out the graphs' (a, d) – EAMT labeling [7]. The following notable and handy conjectures are included in the vicinity of graphs' $(a, 0)$ – EAMT labeling.

Conjecture 1 (see [4]). *Every tree admits an $(a, 0)$ – EAMT labeling.*

Conjecture 2 (see [6]). *Every tree admits an $S - (a, 0)$ – EAMT labeling.*

In the support of Conjecture 2, certain classes of trees have been sorted out by scientists. For trees having maximum of seventeen vertices, in [8], this conjecture has been verified. For instance, the $S - (a, 0)$ – EAMT labeling on a class of trees termed as w -trees can be observed in [9]. Similarly, $S - (a, 0)$ – EAMT labeling on various classes consisting of subdivisions of trees can be seen in [10, 11]. Some derivations on vertex-antimagicness of regular graphs have been discussed in [12]. In [13], the same labeling for the union of unicyclic graphs and isolated vertices has been provided. Enomoto et al. proved [6] that if a (p, q) -graph Γ (simple) is $S - (a, 0)$ – EAMT, it implies $q \leq 2p - 3$. In addition, they derived that $K_{m,n}$ is $S - (a, 0)$ – EAMT only if either m or n is equal to 1. It is derived in [14] that the combination of graphs in the form of union of $K_{1,\theta}$ and $K_{1,\eta}$ is $S - (a, 0)$ – EAMT if $\theta = \chi(\eta + 1)$ or $\eta = \chi(\theta + 1)$. For only odd values of n , C_n is concentered to be $S - (a, 0)$ – EAMT [6]. The cycle of order 3 and cycle of order $n \geq 6$ are proven to be $S - (a, 0)$ – EAMT for even values of n . The generalized prism D_ξ is proven to be $S - (a, 0)$ – EAMT for all odd values of ξ in [15]. In [16, 17], $S - (a, 0)$ – EAMT labeling of maximum symmetric generalization of prism and special networks with magic constant $3p$ has been exhibited, respectively. An extremely important result on $S - (a, 0)$ – EAMT graphs is as follows.

Lemma 1 (see [15]). *A (p, q) -graph G is $S - (a, 0)$ – EAMT if and only if there exists a bijective function $\lambda: V(G) \rightarrow \{1, 2, \dots, p\}$ such that the set $S = \{\lambda(u) + \lambda(u) | uv \in E(G)\}$ consists of q consecutive integers. In such a case, λ*

extends to an $S - (a, 0)$ – EAMT labeling of G with magic constant $t = p + q + s$, where $s = \min(S)$ and $S = \{t - (p + 1), t - (p + 2), \dots, t - (p + q)\}$.

In Lemma 1, the sum $\zeta(u) + \zeta(v)$ is defined as edge sum for each edge $uv \in E(\Gamma)$. This lemma shall be used frequently in our findings, while it keeps this enough to allot the labels to merely the vertices of the network to capacitate the graph to be $S - (a, 0)$ – EAMT, where the edge-sums (consecutive) belong to \mathbb{N} . The given result is extremely relevant with regard to $S - (a, 0)$ – EAMT.

Lemma 2 (see [18]). *A simple graph Γ possesses an $S - (a, 0)$ – EAMT labeling $\Leftrightarrow \Gamma$ possesses an $S - (a - |E(G)| + 1, 2)$ – EAMT labeling.*

2. Main Results

In this section, we shall address our main findings. In Section 2.1, we define an $S - (a, 0)$ – EAMT labeling on a pancyclic family of graphs, namely, Usmanian pancyclic graph UP_n^t . In Section 2.2, we design $S - (a, 0)$ – EAMT labeling on various disjoint unions of graphs comprising upon copies of C_4 and various trees/forests. Throughout, $i \in [a, b]$ represents $a \leq i \leq b$, for $i, a, b \in \mathbb{N}$, whereas \mathbb{N}^{odd} and \mathbb{N}^{even} are the representations of odd and even natural numbers, respectively.

2.1. Usmanian Pancyclic Graph UP_n^t . In computer science, there is a similar importance of the networks having no cycles and networks having a range of cycles. The importance is similar for a network containing cycles of all lengths from one to the number of systems connected within. In this situation, the role of programmers becomes prominent to avoid hackers halting of data as there is a closed path between any two arbitrary computers corresponding to such networks. The first kind of network is termed as a tree (connected and acyclic) and later is known as pancyclic network (connected and containing every order's cycle). This section deals with a family of pancyclic graphs denoted by UP_n^t , which is biparametric, and reveals that such complex structures are $S - (a, 0)$ – EAMT. We shall first introduce this structure as Definition 4.

Definition 4. We are defining the Usmanian pancyclic graph, denoted by UP_n^t , being a graph with $|V(UP_n^t)| = tn$ and $|E(UP_n^t)| = 2tn - 3$, having the construction as follows ($n \geq 3$ being the order of the cycle C_n and $t \geq 2$ being the number of cycles):

- (1) For even n :
For $n \equiv 0 \pmod{4}$:
(i) For $n = 4$,

$$V(UP_4^t) = \{y_i, z_i: i \in [1, t]\} \cup \{x_i: i \in [1, 2t]\},$$

$$E(UP_4^t) = \{z_i z_{i+1}, y_i y_{i+1}: i \in [1, t - 1]\} \cup \{y_i x_{2i}, z_i x_{2i}: i \in [1, t]\} \cup \{z_i x_{2i-1}, y_i x_{2i-1}: i \in [1, t]\} \cup \{x_i x_{i+1}: i \in [1, 2t - 1]\}.$$

(1)

(ii) For $n = 8$,

$$\begin{aligned}
V(\text{UP}_8^t) &= \{x_i, v_i: i \in [1, t]\} \cup \{w_i, y_i, z_i: i \in [1, 2t]\} \\
E(\text{UP}_8^t) &= \{w_i w_{i+1}, y_i y_{i+1}, z_i z_{i+1}: i \in [2, 2t-2], i \in \mathbb{N}^{\text{even}}\} \cup \{z_i w_i, y_i z_i: i \in [1, 2t]\} \\
&\cup \{x_i y_{2i-1}, x_i y_{2i}, v_i w_{2i-1}, v_i w_{2i}: i \in [1, t]\} \\
&\cup \{y_i w_i: i \in [1, 2t]\} \cup \{x_i v_i: i \in [1, t]\} \cup \{z_i w_{i+1}, y_i z_{i+1}: i \in [1, 2t-1], i \in \mathbb{N}^{\text{odd}}\}.
\end{aligned} \tag{2}$$

(iii) For $n = 12$,

$$\begin{aligned}
V(\text{UP}_{12}^t) &= \{x_i^j: i \in [1, 2t], 2 \leq j \leq 6\} \cup \{x_i^j: i \in [1, t], j = 1, 7\}, \\
E(\text{UP}_{12}^t) &= \{x_i^j x_{i+1}^j: i \in [2, 2(t-1)], i \in \mathbb{N}^{\text{even}}, 3 \leq j \leq 5\} \cup \{x_i^j x_i^{j+1}: i \in [1, 2t], 2 \leq j \leq 5\} \\
&\cup \{x_i^1 x_{2i-1}^2, x_i^1 x_{2i}^2, x_i^7 x_{2i-1}^6, x_i^7 x_{2i}^6: i \in [1, t]\} \cup \{x_i^1 x_i^7: i \in [1, t]\} \cup \{x_i^j x_i^{8-j}: i \in [1, 2t], 2 \leq j \leq 6\} \\
&\cup \{x_i^4 x_i^7: i \in [1, 2t-1], i \in \mathbb{N}^{\text{odd}}\} \cup \{x_i^2 x_{i+1}^5, x_i^3 x_{i+1}^6: i \in [1, 2t-1], i \in \mathbb{N}^{\text{odd}}\} \cup \{x_i^1 x_{2i}^4: i \in [1, t]\}.
\end{aligned} \tag{3}$$

(iv) For $n \geq 16$,

$$\begin{aligned}
V(\text{UP}_n^t) &= \{x_i^j: i \in [1, 2t], 2 \leq j \leq \frac{n}{2}\} \cup \{x_i^j: i \in [1, t], j = 1, \frac{n+2}{2}\}, \\
E(\text{UP}_n^t) &= \{x_i^j x_{i+1}^j: i \in [2, 2(t-1)], i \in \mathbb{N}^{\text{even}}, \frac{n}{4} \leq j \leq \frac{n+8}{4}\} \cup \{x_i^j x_i^{j+1}: i \in [1, 2t], 2 \leq j \leq \frac{n-2}{2}\} \\
&\cup \{x_i^1 x_{2i-1}^2, x_i^1 x_{2i}^2, x_i^{(n+2)/2} x_{2i-1}^{n/2}, x_i^{(n+2)/2} x_{2i}^{n/2}: i \in [1, t]\} \cup \{x_i^1 x_i^{(n+2)/2}: i \in [1, t]\} \cup \{x_i^j x_i^{(n/2)+2-j}: i \in [1, 2t], 2 \leq j \leq \frac{n}{2}\} \\
&\cup \{x_i^j x_i^{(n/2)+5-j}: i \in [1, 2t-1], i \in \mathbb{N}^{\text{odd}}, 4 \leq j \leq \frac{n+4}{4}\} \cup \{x_i^2 x_{i+1}^{(n-2)/2}, x_i^3 x_{i+1}^{n/2}: i \in [1, 2t-1], i \in \mathbb{N}^{\text{odd}}\} \\
&\cup \{x_i^1 x_{2i}^{n-4/2}: i \in [1, t]\} \cup \{x_i^j x_i^{((n-2)/2)-j}: i \in [2, 2t], i \in \mathbb{N}^{\text{even}}, 2 \leq j \leq \frac{n-8}{4}\}.
\end{aligned} \tag{4}$$

For $n \equiv 2 \pmod{4}$:(i) For $n = 6$,

$$\begin{aligned}
V(\text{UP}_6^t) &= \{x_i, y_i, z_i: i \in [1, 2t]\}, \\
E(\text{UP}_6^t) &= \{z_i z_{i+1}, x_i x_{i+1}: i \in [1, 2t-1]\} \cup \{y_i z_i, x_i y_i: i \in [1, 2t]\} \cup \{y_i y_{i+1}: i \in [1, 2t-1]\} \cup \{x_i z_i: i \in [1, 2t]\}.
\end{aligned} \tag{5}$$

(ii) For $n = 10$,

$$\begin{aligned}
 V(\text{UP}_{10}^t) &= \{x_i^j : i \in [1, 2t], j \in [1, 5]\} \\
 E(\text{UP}_{10}^t) &= \{x_i^j x_i^{j+1} : i \in [1, 2t], 1 \leq j \leq 4\} \cup \{x_i^1 x_{i+1}^1, x_i^5 x_{i+1}^5 : i \in [1, 2t-1], i \in \mathbb{N}^{\text{odd}}\} \\
 &\quad \cup \{x_i^j x_{i+1}^j : i \in [2, 2(t-1)], i \in \mathbb{N}^{\text{even}}, 2 \leq j \leq 4\} \\
 &\quad \cup \{x_i^1 x_i^5, x_i^2 x_i^4 : i \in [1, 2t]\} \cup \{x_i^j x_{i+1}^{2+j} : i \in [1, 2t-1], i \in \mathbb{N}^{\text{odd}}, 1 \leq j \leq 3\}.
 \end{aligned} \tag{6}$$

(iii) For $n \geq 14$,

$$\begin{aligned}
 V(\text{UP}_n^t) &= \{x_i^j : i \in [1, 2t], 1 \leq j \leq \frac{n}{2}\}, \\
 E(\text{UP}_n^t) &= \{x_i^j x_i^{j+1} : i \in [1, 2t], 1 \leq j \leq \frac{n-2}{2}\} \cup \{x_i^1 x_{i+1}^1, x_i^{n/2} x_{i+1}^{n/2} : i \in [1, 2t-1], i \in \mathbb{N}^{\text{odd}}\} \\
 &\quad \cup \{x_i^j x_{i+1}^j : i \in [2, 2(t-1)], i \in \mathbb{N}^{\text{even}}, \frac{n-2}{4} \leq j \leq \frac{n+6}{4}\} \cup \{x_i^j x_i^{(n+2/2)-j} : i \in [1, 2t], 1 \leq j \leq \frac{n-2}{4}\} \\
 &\quad \cup \{x_i^j x_{i+1}^{(n-6/2)+j} : i \in [1, 2t-1], i \in \mathbb{N}^{\text{odd}}, 1 \leq j \leq 3\} \cup \{x_i^j x_i^{(n+8/2)-j} : i \in [1, 2t-1], i \in \mathbb{N}^{\text{odd}}, 4 \leq j \leq \frac{n+2}{4}\} \\
 &\quad \cup \{x_i^j x_i^{(n-4/2)-j} : i \in [2, 2t], i \in \mathbb{N}^{\text{even}}, 1 \leq j \leq \frac{n-10}{4}\}.
 \end{aligned} \tag{7}$$

(2) For odd n :

For $n \equiv 1 \pmod{4}$:

(i) For $n = 5$,

$$\begin{aligned}
 V(\text{UP}_5^t) &= \{z_i, y_i : i \in [1, 2t]\} \cup \{x_i : i \in [1, t]\}, \\
 E(\text{UP}_5^t) &= \{z_i z_{i+1} : i \in [1, 2t-1], i \in \mathbb{N}^{\text{odd}}\} \cup \{y_i z_i : i \in [1, 2t]\} \cup \{x_i y_{2i-1}, x_i y_{2i} : i \in [1, t]\} \\
 &\quad \cup \{y_i y_{i+1} : i \in [2, 2t-2], i \in \mathbb{N}^{\text{even}}\} \cup \{x_i z_{2i+1} : i \in [1, t-1]\} \cup \{x_i z_{2i-2} : i \in [2, t]\} \\
 &\quad \cup \{x_i z_{2i-1}, x_i z_{2i} : i \in [1, t]\}.
 \end{aligned} \tag{8}$$

(ii) For $n = 9$,

$$\begin{aligned}
 V(\text{UP}_9^t) &= \{w_i, v_i, y_i, z_i : i \in [1, 2t]\} \cup \{x_i : i \in [1, t]\}, \\
 E(\text{UP}_9^t) &= \{v_i v_{i+1} : i \in [1, 2t-1], i \in \mathbb{N}^{\text{odd}}\} \cup \{y_i z_i, z_i w_i, w_i v_i : i \in [1, 2t]\} \cup \{x_i y_{2i-1}, x_i y_{2i} : i \in [1, t]\} \\
 &\quad \cup \{y_i w_{i+1}, z_i z_{i+1}, w_i y_{i+1} : i \in [2, 2t-2], i \in \mathbb{N}^{\text{even}}\} \cup \{y_i w_i, y_i v_i : i \in [1, 2t]\} \cup \{x_i v_{2i-1}, x_i v_{2i} : i \in [1, t]\}.
 \end{aligned} \tag{9}$$

(iii) For $n \geq 13$,

$$\begin{aligned}
 V(\text{UP}_n^t) &= \left\{ x_i^j : i \in [1, 2t], j \in \left[2, \frac{n+1}{2}\right] \right\} \cup \left\{ x_i^1 : i \in [1, t] \right\}, \\
 E(\text{UP}_n^t) &= \left\{ x_i^j x_i^{j+1} : i \in [1, 2t], 2 \leq j \leq \frac{n-1}{2} \right\} \cup \left\{ x_i^1 x_{2i-1}^2, x_i^1 x_{2i}^2 : i \in [1, t] \right\} \\
 &\quad \cup \left\{ x_i^{n+1/2} x_{i+1}^{n+1/2} : 1 \leq i \leq 2t-1, i \in \mathbb{N}^{\text{odd}} \right\} \\
 &\quad \cup \left\{ x_i^{(n-1)/4} x_{i+1}^{(n+7)/4}, x_i^{(n+7)/4} x_{i+1}^{(n-1)/4}, x_i^{(n+3)/4} x_{i+1}^{(n+3)/4} : 2 \leq i \leq 2(t-1), i \in \mathbb{N}^{\text{even}} \right\} \\
 &\quad \cup \left\{ x_i^j x_i^{((n+3)/2)-j} : i \in [1, 2t], 2 \leq j \leq \frac{n-1}{4} \right\} \\
 &\quad \cup \left\{ x_i^j x_i^{(n+5/2)-j} : i \in [1, 2t], 2 \leq j \leq \frac{n-1}{4} \right\} \cup \left\{ x_i^1 x_{2i-1}^{(n+1)/2}, x_i^1 x_{2i}^{(n+1)/2} : i \in [1, t] \right\}.
 \end{aligned} \tag{10}$$

For $n \equiv 3 \pmod{4}$:

Define $\text{UP}_3^t \cong P_t \times C_3$ as follows:

(i) For $n = 3$:

$$\begin{aligned}
 V(\text{UP}_3^t) &= \{z_i, x_i, y_i : i \in [1, t]\}, \\
 E(\text{UP}_3^t) &= \{z_i z_{i+1}, x_i x_{i+1}, y_i y_{i+1} : i \in [1, t-1]\} \cup \{x_i z_i, x_i y_i, y_i z_i : i \in [1, t]\}.
 \end{aligned} \tag{11}$$

(ii) For $n = 7$,

$$\begin{aligned}
 V(\text{UP}_7^t) &= \{z_i, w_i, y_i : i \in [1, 2t]\} \cup \{x_i : i \in [1, t]\}, \\
 E(\text{UP}_7^t) &= \{w_i w_{i+1} : i \in [1, 2t-1], i \in \mathbb{N}^{\text{odd}}\} \cup \{z_i w_i, y_i z_i : i \in [1, 2t]\} \cup \{x_i y_{2i-1}, x_i y_{2i} : i \in [1, t]\} \\
 &\quad \cup \{z_i z_{i+1}, y_i w_{i+1}, w_i y_{i+1} : i \in [2, 2t-2], i \in \mathbb{N}^{\text{even}}\} \cup \{y_i w_i : i \in [1, 2t]\} \cup \{x_i w_{2i-1}, x_i w_{2i} : i \in [1, 2t]\}.
 \end{aligned} \tag{12}$$

(iii) For $n \geq 11$,

$$\begin{aligned}
 V(\text{UP}_n^t) &= \left\{ x_i^j : i \in [1, 2t], 2 \leq j \leq \frac{n+1}{2} \right\} \cup \left\{ x_i^1 : i \in [1, t] \right\}, \\
 E(\text{UP}_n^t) &= \left\{ x_i^j x_i^{j+1} : i \in [1, 2t], 2 \leq j \leq \frac{n-1}{2} \right\} \cup \left\{ x_i^1 x_{2i-1}^2, x_i^1 x_{2i}^2 : i \in [1, t] \right\} \cup \left\{ x_i^{(n+1)/2} x_{i+1}^{(n+1)/2} : i \in [1, 2t-1], i \in \mathbb{N}^{\text{odd}} \right\} \\
 &\quad \cup \left\{ x_i^{(n+1)/4} x_{i+1}^{(n+9)/4}, x_i^{(n+5)/4} x_{i+1}^{(n+5)/4}, x_i^{(n+9)/4} x_{i+1}^{(n+1)/4} : i \in [2, 2(t-1)], i \in \mathbb{N}^{\text{even}} \right\} \\
 &\quad \cup \left\{ x_i^j x_i^{((n+5)/2)-j} : i \in [1, 2t], 2 \leq j \leq \frac{n+1}{4} \right\} \cup \left\{ x_i^j x_i^{((n+3)/2)-j} : i \in [1, 2t], 2 \leq j \leq \frac{n-3}{4} \right\} \\
 &\quad \cup \left\{ x_i^1 x_{2i-1}^{(n+1)/2}, x_i^1 x_{2i}^{(n+1)/2} : i \in [1, t] \right\}.
 \end{aligned} \tag{13}$$

Theorem 1. *The pancyclic graph UP_n^t is $S - (a, 0) - \text{EAMT}$ admitting $a = 3tn, \forall t$ and $n \equiv 0 \pmod{2}$.*

Proof. We discuss here two cases as per Definition 4.

For $n \equiv 0 \pmod{4}$:

(i) For $n = 4$:

We define a labeling $\psi'_1: V(UP_4^t) \rightarrow \{1, 2, \dots, 4t\}$ as follows:

$$\psi'_1(x_i) = \begin{cases} 2i - 1: i \in [1, 2t - 1], & i \in \mathbb{N}^{\text{odd}}; \\ 2i: 2 \leq i \leq 2t, & i \in \mathbb{N}^{\text{even}}; \end{cases} \quad (14)$$

$$\psi'_1(y_i) = 4i - 2: i \in [1, t],$$

$$\psi'_1(z_i) = 4i - 1: i \in [1, t].$$

The edge-sums' set generated as per the labeling design constitutes a consecutive sequence of positive integers $3, 4, \dots, 8t - 1$. As per Lemma 1, ψ'_1 is extendable to an $S - (a, 0) - \text{EAMT}$ labeling of UP_4^t with magic constant $a = 12t$.

(ii) For $n = 8$:

We define a labeling $\psi''_1: V(UP_8^t) \rightarrow \{1, 2, \dots, 8t\}$ as follows:

$$\psi''_1(x_i) = 8i - 3: 1 \leq i \leq t,$$

$$\psi''_1(y_i) = 4i - 1: 1 \leq i \leq 2t,$$

$$\psi''_1(z_i) = \begin{cases} 4i - 3: i \in [1, 2t - 1], & i \in \mathbb{N}^{\text{odd}}; \\ 4i: 2 \leq i \leq 2t, & i \in \mathbb{N}^{\text{even}}; \end{cases} \quad (15)$$

$$\psi''_1(w_i) = 4i - 2: i \in [1, 2t],$$

$$\psi''_1(v_i) = 8i - 4: i \in [1, t].$$

The edge-sums' set generated as per the labeling design constitutes a consecutive sequence of positive integers $3, 4, \dots, 16t - 1$. In the light of Lemma 1, ψ''_1 constitutes an $S - (a, 0) - \text{EAMT}$ labeling of UP_8^t admitting $a = 24t$.

(iii) For $n \geq 12$:

We define a labeling $\psi_1: V(UP_n^t) \rightarrow \{1, 2, \dots, tn\}$ as follows:

$$\psi_1(x_i^j) = \begin{cases} \frac{2ni - n + 2}{2}: & i \in [1, t] \text{ and } j = 1; \\ \frac{ni - 4j + 6}{2}: & i \in [1, 2t - 1], j \in \left[2, \frac{n+4}{4}\right], i \in \mathbb{N}^{\text{odd}}; \\ \frac{ni + 4j - n - 2}{2}: & i \in [2, 2t], j \in \left[2, \frac{n}{4}\right], i \in \mathbb{N}^{\text{even}}; \\ \frac{ni + 4j - n - 4}{2}: & i \in [2, 2t], j = \frac{n+4}{4}, i \in \mathbb{N}^{\text{even}}; \\ \frac{ni + 4j - 2n - 4}{2}: & i \in [1, 2t - 1], j \in \left[\frac{n+8}{4}, \frac{n}{2}\right], i \in \mathbb{N}^{\text{odd}}; \\ \frac{ni - 4j + n + 4}{2}: & i \in [2, 2t], j \in \left[\frac{n+8}{4}, \frac{n}{2}\right], i \in \mathbb{N}^{\text{even}}; \\ \frac{2ni + 4j - 3n - 4}{2}: & i \in [1, t] \text{ and } j = \frac{n+2}{2}. \end{cases} \quad (16)$$

With the abovementioned scheme, the edge-sums being generated form a consecutive integer sequence set $\Delta = \{3, 4, \dots, 2tn - 1\}$. ψ_1 is extendible to $S - (a, 0) - \text{EAMT}$ labeling of $UP_n^t, n \geq 12$, according to Lemma 1, with $a = 3tn$.

For $n \equiv 2 \pmod{4}$:

(i) For $n = 6$:

The labeling $\psi'_2: V(UP_6^t) \rightarrow \{1, 2, \dots, 6t\}$ is being defined as follows:

$$\psi'_2(x_i) = \begin{cases} 3i: 1 \leq i \leq 2t - 1, & i \in \mathbb{N}^{\text{odd}}; \\ 3i - 1: 2 \leq i \leq 2t, & i \in \mathbb{N}^{\text{even}}; \end{cases}$$

$$\psi'_2(y_i) = \begin{cases} 3i - 2: 1 \leq i \leq 2t - 1, & i \in \mathbb{N}^{\text{odd}}; \\ 3i: 2 \leq i \leq 2t, & i \in \mathbb{N}^{\text{even}}; \end{cases} \quad (17)$$

$$\psi'_2(z_i) = \begin{cases} 3i - 1: 1 \leq i \leq 2t - 1, & i \in \mathbb{N}^{\text{odd}}; \\ 3i - 2: 2 \leq i \leq 2t, & i \in \mathbb{N}^{\text{even}}. \end{cases}$$

The edge-sums' set generated as per the labeling design constitutes a consecutive natural numbers' sequence $3, 4, \dots, 12t - 1$. As per Lemma 1, ψ'_2 is extendable towards $S - (a, 0)$ - EAMT labeling of UP^t_6 with $a = 18t$.

(ii) For $n \geq 10$:

Define a labeling $\psi_2: V(UP^n_t) \rightarrow \{1, 2, \dots, tn\}$ as the following function:

$$\psi_2(x^j_i) = \begin{cases} \frac{ni - 4j + 4}{2}: & i \in [1, 2t - 1], j \in \left[1, \frac{n+2}{4}\right], \quad i \in \mathbb{N}^{\text{odd}}; \\ \frac{ni + 4j - n}{2}: & i \in [2, 2t], j \in \left[1, \frac{n-2}{4}\right], \quad i \in \mathbb{N}^{\text{even}}; \\ \frac{ni + 4j - 2n - 2}{2}: & i \in [1, 2t - 1], j \in \left[\frac{n+6}{4}, \frac{n}{2}\right], \quad i \in \mathbb{N}^{\text{odd}}; \\ \frac{ni - 4j + n + 2}{2}: & i \in [2, 2t], j \in \left[\frac{n+2}{4}, \frac{n}{2}\right], \quad i \in \mathbb{N}^{\text{even}}. \end{cases} \quad (18)$$

With the abovementioned scheme, the edge-sums being generated form a consecutive integer sequence set $\{3, 4, \dots, 2tn - 1\}$. ψ_2 constitutes $S - (a, 0)$ - EAMT labeling of $UP^n_t, n \geq 10$, according to Lemma 1, admitting $a = 3tn$. \square

Theorem 2. *The pancyclic graph UP^n_t is $S - (a, 0)$ - EAMT with magic sum $a = 3tn$, for all t and $n \equiv 1 \pmod{2}$.*

Proof. We discuss here two cases.

For $n \equiv 1 \pmod{4}$:

(i) For $n = 5$:

Define a labeling $\psi'_3: V(UP^t_5) \rightarrow \{1, 2, \dots, 5t\}$ as follows:

$$\begin{aligned} \psi'_3(x_i) &= 5i - 2: i \in [1, t], \\ \psi'_3(y_i) &= \begin{cases} \frac{1}{2}(5i - 3): i \in [1, 2t - 1], & i \in \mathbb{N}^{\text{odd}}; \\ \frac{1}{2}(5i): i \in [2, 2t], & i \in \mathbb{N}^{\text{even}}; \end{cases} \\ \psi'_3(z_i) &= \begin{cases} \frac{1}{2}(5i - 1): i \in [1, 2t - 1], & i \in \mathbb{N}^{\text{odd}}; \\ \frac{1}{2}(5i - 2): i \in [2, 2t], & i \in \mathbb{N}^{\text{even}}. \end{cases} \end{aligned} \quad (19)$$

The edge-sums' set generated as per the labeling design constitutes a consecutive natural numbers' sequence $3, 4, \dots, 10t - 1$. ψ'_3 is extendable to $S - (a, 0)$ - EAMT labeling of UP^t_5 having $a = 15t$ (as per Lemma 1).

(ii) For $n = 9$:

We construct a labeling $\psi'_3: V(UP^t_9) \rightarrow \{1, 2, \dots, 9t\}$ as follows:

$$\psi''_3(x_i) = 9i - 4: 1 \leq i \leq t,$$

$$\psi''_3(y_i) = \begin{cases} \frac{1}{2}(9i - 3): i \in [1, 2t - 1], & i \in \mathbb{N}^{\text{odd}}; \\ \frac{1}{2}(9i - 4): i \in [2, 2t], & i \in \mathbb{N}^{\text{even}}; \end{cases}$$

$$\psi'_3(z_i) = \begin{cases} \frac{1}{2}(9i - 7): i \in [1, 2t - 1], & i \in \mathbb{N}^{\text{odd}}; \\ \frac{1}{2}(9i): i \in [2, 2t], & i \in \mathbb{N}^{\text{even}}; \end{cases}$$

$$\psi''_3(w_i) = \begin{cases} \frac{1}{2}(9i - 5): i \in [1, 2t - 1], & i \in \mathbb{N}^{\text{odd}}; \\ \frac{1}{2}(9i - 2): i \in [2, 2t], & i \in \mathbb{N}^{\text{even}}; \end{cases}$$

$$\psi''_3(v_i) = \begin{cases} \frac{1}{2}(9i - 1): i \in [1, 2t - 1], & i \in \mathbb{N}^{\text{odd}}; \\ \frac{1}{2}(9i - 6): i \in [2, 2t], & i \in \mathbb{N}^{\text{even}}. \end{cases} \quad (20)$$

The edge-sums' set generated as per the labeling design constitutes a natural numbers' sequence $3, 4, \dots, 18t - 1$. ψ''_3 is extendable to $S - (a, 0)$ - EAMT labeling of UP^t_9 , by Lemma 1, with the admittance of $a = 27t$.

(iii) For $n \geq 13$:

We are going to construct a labeling $\psi_3: V(UP^n_t) \rightarrow \{1, 2, \dots, tn\}$ as follows:

$$\psi_3(x_i^j) = \begin{cases} \frac{2ni - n + 1}{2}: & i \in [1, t], j = 1, \\ \frac{ni - 4j + 5}{2}: & i \in [1, 2t - 1], j \in \left[2, \frac{n+3}{4}\right], i \in \mathbb{N}^{\text{odd}}, \\ \frac{ni + 4j - n - 3}{2}: & i \in [2, 2t], j \in \left[2, \frac{n+3}{4}\right], i \in \mathbb{N}^{\text{even}}, \\ \frac{ni + 4j - 2n - 3}{2}: & i \in [1, 2t - 1], j \in \left[\frac{n+7}{4}, \frac{n+1}{2}\right], i \in \mathbb{N}^{\text{odd}}, \\ \frac{ni - 4j + n + 5}{2}: & i \in [2, 2t], j \in \left[\frac{n+7}{4}, \frac{n+1}{2}\right], i \in \mathbb{N}^{\text{even}}. \end{cases} \tag{21}$$

With the abovementioned scheme, the edge-sums being generated forms a consecutive integer sequence set $\{3, 4, \dots, 2tn - 1\}$. Once again, ψ_3 extends to a $S - (a, 0) - \text{EAMT}$ labeling of $\text{UP}_n^t, n \geq 13$ having $a = 3tn$ by Lemma 1.

For $n \equiv 3 \pmod{4}$:

(i) For $n = 3$:

We define a labeling $\psi_4': V(\text{UP}_3^t) \rightarrow \{1, 2, \dots, 3t\}$ as follows:

$$\begin{aligned} \psi_4'(x_i) &= \begin{cases} 3i - 2: 1 \leq i \leq t - 1, & i \in \mathbb{N}^{\text{odd}}, \\ 3i - 1: 2 \leq i \leq t, & i \in \mathbb{N}^{\text{even}}, \end{cases} \\ \psi_4'(y_i) &= \begin{cases} 3i: 1 \leq i \leq t - 1, & i \in \mathbb{N}^{\text{odd}}, \\ 3i - 2: 2 \leq i \leq t, & i \in \mathbb{N}^{\text{even}}, \end{cases} \tag{22} \\ \psi_4'(z_i) &= \begin{cases} 3i - 1: 1 \leq i \leq t - 1, & i \in \mathbb{N}^{\text{odd}}, \\ 3i: 2 \leq i \leq t, & i \in \mathbb{N}^{\text{even}}. \end{cases} \end{aligned}$$

The edge-sums' set generated as per the labeling design constitutes a consecutive sequence of positive integers $3, 4, \dots, 6t - 1$. Now, ψ_4' is extendable to $S - (a, 0) - \text{EAMT}$ labeling of $\text{UP}_3^t \cong P_t \times C_3$ [15] with $a = 9t$ according to Lemma 1.

(ii) For $n = 7$:

A labeling $\psi_4'': V(\text{UP}_7^t) \rightarrow \{1, 2, \dots, 7t\}$ is being defined as follows:

$$\psi_4''(x_i) = 7i - 3: 1 \leq i \leq t,$$

$$\begin{aligned} \psi_4''(y_i) &= \begin{cases} \frac{1}{2}(7i - 3): & i \in [1, 2t - 1], i \in \mathbb{N}^{\text{odd}}, \\ \frac{1}{2}(7i - 2): & i \in [2, 2t], i \in \mathbb{N}^{\text{even}}, \end{cases} \\ \psi_4''(z_i) &= \begin{cases} \frac{1}{2}(7i - 5): & i \in [1, 2t - 1], i \in \mathbb{N}^{\text{odd}}, \\ \frac{1}{2}(7i): & i \in [2, 2t], i \in \mathbb{N}^{\text{even}}, \end{cases} \tag{23} \\ \psi_4''(w_i) &= \begin{cases} \frac{1}{2}(7i - 1): & i \in [1, 2t - 1], i \in \mathbb{N}^{\text{odd}}, \\ \frac{1}{2}(7i - 4): & i \in [2, 2t], i \in \mathbb{N}^{\text{even}}. \end{cases} \end{aligned}$$

The edge-sums' set generated as per the labeling design constitutes a consecutive natural numbers' sequence $3, 4, \dots, 14t - 1$. Now, ψ_4'' is extendable to $S - (a, 0) - \text{EAMT}$ labeling of UP_7^t , according to Lemma 1 having $a = 21t$.

(iii) For $n \geq 11$:

The labeling $\psi_4: V(\text{UP}_n^t) \rightarrow \{1, 2, \dots, tn\}$ is constructed as follows:

$$\psi_4(x_i^j) = \begin{cases} \frac{2ni - n + 1}{2}: & i \in [1, t], j = 1, \\ \frac{ni - 4j + 5}{2}: & i \in [1, 2t - 1], j \in \left[2, \frac{n+1}{4}\right], i \in \mathbb{N}^{\text{odd}}, \\ \frac{ni + 4j - n - 3}{2}: & i \in [2, 2t], j \in \left[2, \frac{n+1}{4}\right], i \in \mathbb{N}^{\text{even}}, \\ \frac{ni + 4j - 2n - 3}{2}: & i \in [1, 2t - 1], j \in \left[\frac{n+5}{4}, \frac{n+1}{2}\right], i \in \mathbb{N}^{\text{odd}}, \\ \frac{ni - 4j + n + 5}{2}: & i \in [2, 2t], j \in \left[\frac{n+5}{4}, \frac{n+1}{2}\right], i \in \mathbb{N}^{\text{even}}. \end{cases} \tag{24}$$

With the abovementioned scheme, the edge-sums being generated form a consecutive integer sequence set $\{3, 4, \dots, 2tn - 1\}$. ψ_4 is extendable to an $S - (a, 0) - \text{EAMT}$ labeling of $UP_n^t, n \geq 11$, under the light of Lemma 1, admitting $a = 3tn$.

A direct outcome of Lemma 2 is as follows. \square

Theorem 3. *The pancyclic graph UP_n^t is $S - (tn + 4, 2) - \text{EAMT}$, for all t and n .*

2.2. $S - (a, 0) - \text{EAMT}$ Labeling of Disjoint Union of C_4 with Trees. It is a well-known fact that the graph C_4 is not $S - (a, 0) - \text{EAMT}$ [6], and work is still in progress in order to determine if its disjoint copies are $S - (a, 0) - \text{EAMT}$. In this section, we shall provide an $S - (a, 0) - \text{EAMT}$ labeling of disjoint copies of C_4 with various trees in the form of several results. This will give a support to researchers to carry out their work to determine the aforesaid labeling of the disjoint copies of C_4 . Throughout this section, the union will represent a disjoint union of graphs only.

Theorem 4. *For odd m , the graph $mC_4 \cup 2K_{1,m} \cup ((7m - 3)/2)K_1$ acquires an $S - (a, 0) - \text{EAMT}$ labeling admitting $a = 21m + 2$.*

Proof. Consider a graph $mC_4 \cup 2K_{1,m} \cup ((7m - 3)/2)K_1$ with vertex and edge sets:

$$\begin{aligned} V(\Lambda_1) &= \{x_1^i, x_2^i: i \in [1, m]\} \cup \{y_i, z_i: i \in [1, m]\} \\ &\cup \{k_i: 1 \leq i \leq 2m\} \cup \left\{l_i: 1 \leq i \leq \frac{7m-3}{2}\right\} \cup \{c_1, c_2\}, \\ E(\Lambda_1) &= \{y_i x_1^i, y_i x_2^i: 1 \leq i \leq m\} \cup \{z_i x_1^i, z_i x_2^i: 1 \leq i \leq m\} \\ &\cup \{c_1 k_i: 1 \leq i \leq m\} \cup \{c_2 k_i: m+1 \leq i \leq 2m\}. \end{aligned} \tag{25}$$

If $p = |V(\Lambda_1)| = (19m + 1)/2$ and $q = |E(\Lambda_1)| = 6m$, we sketch a labeling $f_1: V(\Lambda_1) \rightarrow \{1, 2, \dots, (19m + 1)/2\}$ as follows:

$$\begin{aligned} f_1(x_1^i) &= \begin{cases} \frac{1}{2}(7m+i), & 1 \leq i \leq m; i \equiv 1, \pmod{2}, \\ \frac{1}{2}(6m+i), & 2 \leq i \leq m-1; i \equiv 0, \pmod{2}, \end{cases} \\ f_1(x_2^i) &= 5m - (i - 1): 1 \leq i \leq m, \\ f_1(y_i) &= \begin{cases} \frac{i+4m+1}{2}, & 1 \leq i \leq m; i \equiv 1, \pmod{2}, \\ \frac{i+5m+1}{2}, & 2 \leq i \leq m-1; i \equiv 0, \pmod{2}, \end{cases} \end{aligned}$$

$$\begin{aligned} f_1(z_i) &= \begin{cases} \frac{1}{2}(i+10m+1), & i \in [1, m]; i \in \mathbb{N}^{\text{odd}}, \\ \frac{1}{2}(i+11m+1), & i \in [2, m-1]; i \in \mathbb{N}^{\text{even}}, \end{cases} \\ f_1(k_i) &= i: i \in [1, 2m], \\ f_1(c_1) &= \frac{15m+1}{2}, \\ f_1(c_2) &= \frac{19m+1}{2}, \\ f_1(l_i) &= \begin{cases} 6m+i, & 1 \leq i \leq \frac{3m-1}{2}, \\ i+6m+1, & i \in \left[\frac{3m+1}{2}, \frac{7m-3}{2}\right]. \end{cases} \end{aligned} \tag{26}$$

The edge-sums' sets constituted by the abovementioned design generates a consecutive sequence of integer $(11m + 3/2), (11m + 5/2), \dots, 23m + 1/2$. Under the shadow of Lemma 1, f_1 accredits an $S - (a, 0) - \text{EAMT}$ labeling of Λ_1 having $a = 21m + 2$. \square

Theorem 5. *For odd m , the graph $mC_4 \cup 2mK_2 \cup 2mK_1$ acquires an $S - (a, 0) - \text{EAMT}$ labeling having $a = (43m + 3)/2$.*

Proof. Consider the graph $\Lambda_2 \cong mC_4 \cup 2mK_2 \cup 2mK_1$, for odd m , with the following vertex-edge connections:

$$\begin{aligned} V(\Lambda_2) &= \{x_1^i, x_2^i: i \in [1, m]\} \cup \{z_i, y_i: 1 \leq i \leq m\} \\ &\cup \{q_i, p_i: i \in [1, 2m]\} \cup \{l_i: i \in [1, 2m]\}, \\ E(\Lambda_2) &= \{y_i x_1^i, y_i x_2^i: 1 \leq i \leq m\} \cup \{z_i x_1^i, z_i x_2^i: 1 \leq i \leq m\} \\ &\cup \{q_i p_i: i \in [1, 2m]\}. \end{aligned} \tag{27}$$

Here, order is $p = 10m$ and size is $q = 6m$. Now, we design a labeling $f_2: V(\Lambda_2) \rightarrow \{1, 2, \dots, 10m\}$ as follows:

$$\begin{aligned} f_2(x_1^i) &= \begin{cases} \frac{1}{2}(7m+i), & i \in [1, m]; i \in \mathbb{N}^{\text{odd}}, \\ \frac{1}{2}(6m+i), & i \in [2, m-1]; i \in \mathbb{N}^{\text{even}}, \end{cases} \\ f_2(x_2^i) &= 5m - (i - 1): i \in [1, m], \\ f_2(y_i) &= \begin{cases} \frac{1}{2}(i+4m+1), & i \in \{1, \dots, m\}; i \in \mathbb{N}^{\text{odd}}, \\ \frac{1}{2}(i+5m+1), & i \in \{2, \dots, m-1\}; i \in \mathbb{N}^{\text{even}}, \end{cases} \end{aligned}$$

$$\begin{aligned}
f_2(z_i) &= \begin{cases} \frac{1}{2}(i+10m+1), & i \in [1, m]; i \in \mathbb{N}^{\text{odd}}, \\ \frac{1}{2}(i+11m+1), & i \in [2, m-1]; i \in \mathbb{N}^{\text{even}}, \end{cases} \\
f_2(p_i) &= i: i \in [1, 2m], \\
f_2(q_i) &= \begin{cases} \frac{1}{2}(15m-i+2): i \in [1, m]; i \in \mathbb{N}^{\text{odd}}, \\ \frac{1}{2}(16m-i+2): i \in [2, m-1]; i \in \mathbb{N}^{\text{even}}, \\ \frac{1}{2}(21m-i+2): i \in [m+2, 2m-1]; i \in \mathbb{N}^{\text{odd}}, \\ \frac{1}{2}(20m-i+2): i \in [m+1, 2m]; i \in \mathbb{N}^{\text{even}}, \end{cases} \\
f_2(l_i) &= \begin{cases} i+6m: i \in [1, m], \\ i+7m: i \in [m+1, 2m]. \end{cases}
\end{aligned} \tag{28}$$

The edge-sums' set constituted by the scheme f_2 generates a sequence consisting of consecutive integer $(11m+3)/2, (11m+5)/2, \dots, (23m+1)/2$. Under the shadow of Lemma 1, f_2 constitutes an $S-(a, 0)$ -EAMT labeling of Λ_2 with magic sum $a = (43m+3)/2$. \square

Theorem 6. For odd m , the graph $mC_4 \cup 2P_{m+1} \cup ((5m-1)/2)K_1$ acquires an $S-(a, 0)$ -EAMT labeling having $a = 18m+5$.

Proof. Let $\Lambda_3 \cong mC_4 \cup 2P_{m+1} \cup ((5m-1)/2)K_1$, where m is odd, having vertex and edge sets interlinked:

$$\begin{aligned}
V(\Lambda_3) &= \{x_1^i, x_2^i: i \in [1, m]\} \cup \{z_i, y_i: i \in [1, m]\} \cup \{p_i: i \in [1, m+1]\} \\
&\quad \cup \{q_i: i \in [1, m+1]\} \cup \left\{l_i: i \in \left[1, \frac{5m-1}{2}\right]\right\}, \\
E(\Lambda_3) &= \{y_i x_1^i, y_i x_2^i: i \in [1, m]\} \cup \{z_i x_1^i, z_i x_2^i: i \in [1, m]\} \\
&\quad \cup \{p_i p_{i+1}: i \in [1, m]\} \cup \{q_i q_{i+1}: i \in [1, m]\}.
\end{aligned} \tag{29}$$

We have $p = (17m+3)/2$ and $q = 6m$. A labeling $f_3: V(\Lambda_3) \rightarrow \{1, 2, \dots, (17m+3)/2\}$ is being defined as follows:

$$\begin{aligned}
f_3(x_1^i) &= \begin{cases} \frac{1}{2}(5m+i+2), & i \in [1, m]; i \in \mathbb{N}^{\text{odd}}, \\ \frac{1}{2}(4m+i+2), & i \in [2, m-1]; i \in \mathbb{N}^{\text{even}}, \end{cases} \\
f_3(x_2^i) &= 4m-i+2: 1 \leq i \leq m, \\
f_3(y_i) &= \begin{cases} \frac{2m+i+3}{2}, & i \in [1, m]; i \in \mathbb{N}^{\text{odd}}, \\ \frac{3m+i+3}{2}, & i \in [2, m-1]; i \in \mathbb{N}^{\text{even}}, \end{cases} \\
f_3(z_i) &= \begin{cases} \frac{8m+i+3}{2}, & i \in \{1, \dots, m\}; i \in \mathbb{N}^{\text{odd}}, \\ \frac{9m+i+3}{2}, & i \in \{2, \dots, m-1\}; i \in \mathbb{N}^{\text{even}}, \end{cases}
\end{aligned}$$

$$\begin{aligned}
f_3(p_i) &= \begin{cases} \frac{i+1}{2}, & i \in [1, m]; i \in \mathbb{N}^{\text{odd}}, \\ \frac{11m+i+3}{2}, & i \in [2, m+1]; i \in \mathbb{N}^{\text{even}}, \end{cases} \\
f_3(q_i) &= \begin{cases} \frac{1}{2}(i+m+2), & i \in [1, m]; i \in \mathbb{N}^{\text{odd}}, \\ \frac{1}{2}(16m+i+2), & i \in [2, m+1]; i \in \mathbb{N}^{\text{even}}, \end{cases} \\
f_3(l_i) &= \begin{cases} i+5m+1: 1 \leq i \leq \frac{m+1}{2}, \\ \frac{2i+11m+3}{2}: \frac{m+3}{2} \leq i \leq \frac{5m-1}{2}. \end{cases}
\end{aligned} \tag{30}$$

The edge-sums' set constituted by the scheme f_3 generates a sequence consisting of consecutive integer $(7m+7)/2, (7m+9)/2, \dots, (19m+5)/2$. Under the shadow of Lemma 1, f_3 constitutes an $S-(a, 0)$ -EAMT of the graph Λ_3 with magic constant $a = 18m+5$. \square

Theorem 7. For odd m , $mC_4 \cup (2m - 2)K_2 \cup P_4 \cup 2mK_1$ possesses $S - (a, 0) - EAMT$ labeling having $a = (43m + 5)/2$.

Proof. With m taken odd, consider $\Lambda_4 \cong mC_4 \cup (2m - 2)K_2 \cup P_4 \cup 2mK_1$, having vertex-edge connections:

$$\begin{aligned} V(\Lambda_4) &= \{x_1^i, x_2^i; i \in [1, m]\} \cup \{y_i, z_i; i \in [1, m]\} \cup \{l_i; 1 \leq i \leq 2m\} \\ &\quad \cup \{q_i, p_i; i \in [1, 2(m - 1)]\} \cup \{t_i; i \in [1, 4]\}, \\ E(\Lambda_4) &= \{y_i x_1^i, y_i x_2^i; 1 \leq i \leq m\} \cup \{z_i x_1^i, z_i x_2^i; i \in [1, m]\} \\ &\quad \cup \{p_i q_i; i \in [1, 2(m - 1)]\} \cup \{t_i t_{i+1}; 1 \leq i \leq 3\}. \end{aligned} \tag{31}$$

Here, we have $p = 10m$ and $q = 6m + 1$. A labeling function $f: V(\Lambda_4) \rightarrow \{1, 2, \dots, 10m\}$ is being defined as follows:

$$\begin{aligned} f_4(x_1^i) &= \begin{cases} \frac{1}{2}(7m + i): & i \in [1, m]; i \in \mathbb{N}^{\text{odd}}, \\ \frac{1}{2}(6m + i): & i \in [2, m - 1]; i \in \mathbb{N}^{\text{even}}, \end{cases} \\ f_4(x_2^i) &= 5m - (i - 1); 1 \leq i \leq m, \\ f_4(y_i) &= \begin{cases} \frac{i + 4m + 1}{2}: & i \in \{1, \dots, m\}; i \in \mathbb{N}^{\text{odd}}, \\ \frac{i + 5m + 1}{2}: & i \in \{2, \dots, m - 1\}; i \in \mathbb{N}^{\text{even}}, \end{cases} \\ f_4(z_i) &= \begin{cases} \frac{i + 10m + 1}{2}: & i \in \{1, \dots, m\}; i \in \mathbb{N}^{\text{odd}}, \\ \frac{i + 11m + 1}{2}: & i \in \{2, \dots, m - 1\}; i \in \mathbb{N}^{\text{even}}, \end{cases} \\ f_4(p_i) &= i; i \in [1, 2(m - 1)], \\ f_4(q_i) &= \begin{cases} \frac{15m - i + 2}{2}: & i \in [1, m]; i \in \mathbb{N}^{\text{odd}}, \\ \frac{16m - i + 2}{2}: & i \in [2, m - 1]; i \in \mathbb{N}^{\text{even}}, \\ \frac{21m - i + 2}{2}: & i \in [m + 2, 2m - 3]; i \in \mathbb{N}^{\text{odd}}, \\ \frac{20m - i + 2}{2}: & \frac{i}{i\{m + 1, \dots, 2(m - 1)\}}; i \in \mathbb{N}^{\text{even}}, \end{cases} \end{aligned}$$

$$\begin{aligned} f_4(t_i) &= \begin{cases} 2m - 1: & i = 1; \\ \frac{19m + 3}{2}: & i = 2; \\ 2m: & i = 3; \\ 9m + 1: & i = 4; \end{cases} \\ f_4(l_i) &= \begin{cases} i + 6m: & 1 \leq i \leq m; \\ i + 7m: & i \in [m + 1, 2m]. \end{cases} \end{aligned} \tag{32}$$

The edge-sums' set constituted by the scheme f_4 generates a sequence consisting of consecutive integer $(11m + 3)/2, (11m + 5)/2, \dots, (23m + 3)/2$. Lemma 1 implies that f_4 extends to an $S - (a, 0) - EAMT$ labeling of Λ_4 with $a = (43m + 5)/2$. \square

Theorem 8. For odd m , $mC_4 \cup S_{m-1,m} \cup ((5m - 1)/2)K_1$ possesses an $S - (a, 0) - EAMT$ labeling with $a = 2(9m + 1)$.

Proof. Consider the graph $\Lambda_5 \cong mC_4 \cup S_{m-1,m} \cup ((5m - 1)/2)K_1$ with vertex-edge connections as follows:

$$\begin{aligned} V(\Lambda_5) &= \{x_1^i, x_2^i; i \in [1, m]\} \cup \{z_i, y_i; i \in [1, m]\} \\ &\quad \cup \{s_i, t_i; i \in [1, m]\} \cup \left\{l_i; i \in \left[1, \frac{5m - 1}{2}\right]\right\} \cup \{c\}, \\ E(\Lambda_5) &= \{y_i x_1^i, y_i x_2^i; i \in [1, m]\} \cup \{z_i x_1^i, z_i x_2^i; i \in [1, m]\} \\ &\quad \cup \{ct_i; i \in [1, m]\} \cup \{t_m s_i; i \in [1, m]\}. \end{aligned} \tag{33}$$

Then, $p = (17m + 1)/2$ and $q = 6m$. Again, a labeling function $f_5: V(\Lambda_5) \rightarrow \{1, 2, \dots, (17m + 1)/2\}$ is being defined as follows:

$$\begin{aligned} f_5(x_1^i) &= \begin{cases} \frac{1}{2}(5m + i): & i \in \{1, \dots, m\}; i \in \mathbb{N}^{\text{odd}}, \\ \frac{1}{2}(4m + i): & i \in [2, m - 1]; i \in \mathbb{N}^{\text{even}}, \end{cases} \\ f_5(x_2^i) &= 4m - (i - 1); i \in [1, m], \\ f_5(y_i) &= \begin{cases} \frac{i + 2m + 1}{2}: & i \in \{1, \dots, m\}; i \in \mathbb{N}^{\text{odd}}, \\ \frac{i + 3m + 1}{2}: & i \in \{2, \dots, m - 1\}; i \in \mathbb{N}^{\text{even}}, \end{cases} \\ f_5(z_i) &= \begin{cases} \frac{i + 8m + 1}{2}: & i \in [1, m]; i \in \mathbb{N}^{\text{odd}}, \\ \frac{i + 9m + 1}{2}: & i \in [2, m - 1]; i \in \mathbb{N}^{\text{even}}, \end{cases} \end{aligned}$$

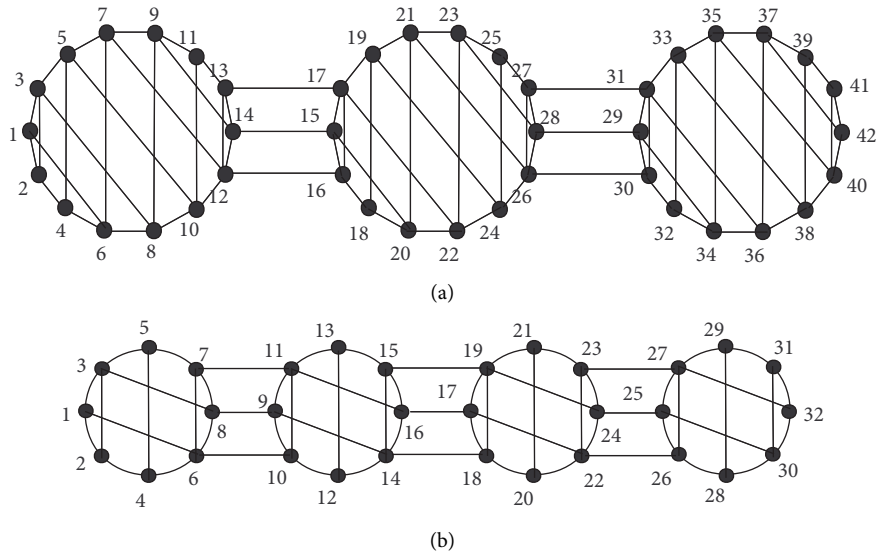


FIGURE 1: An $S - (126, 0) - EAMT$ and $S - (96, 0) - EAMT$ labeling of the pancyclic graphs (a) UP_{14}^3 and (b) UP_8^4 .

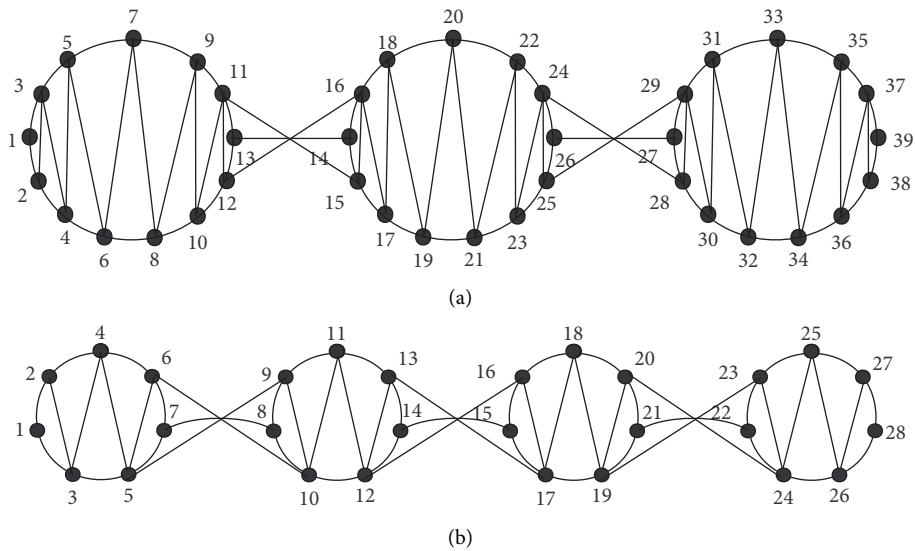


FIGURE 2: An $S - (117, 0) - EAMT$ and $S - (84, 0) - EAMT$ labeling of the pancyclic graphs (a) UP_{13}^3 and (b) UP_7^4 .

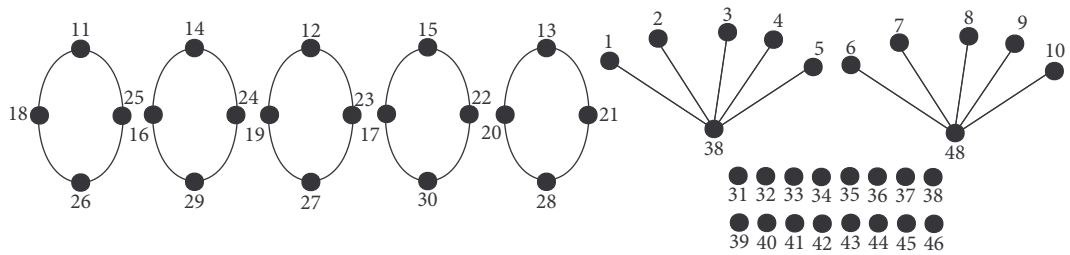


FIGURE 3: An $S - (107, 0) - EAMT$ labeling of the graph $5C_4 \cup 2K_{1,5} \cup 16K_1$.

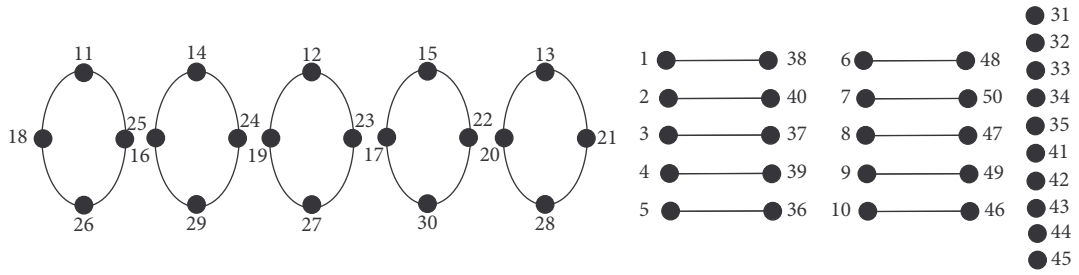


FIGURE 4: An $S - (109, 0)$ - EAMT labeling of the graph $5C_4 \cup 10K_2 \cup 10K_1$.

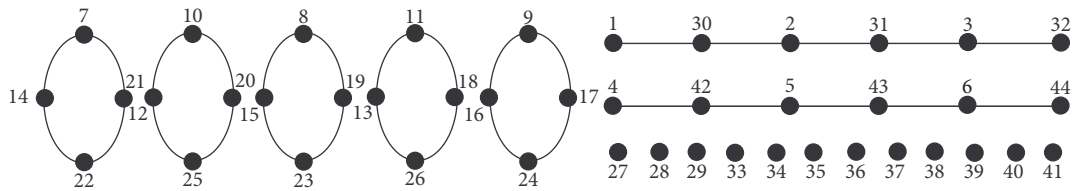


FIGURE 5: An $S - (95, 0)$ - EAMT labeling of the graph $5C_4 \cup 2P_6 \cup 12K_1$.

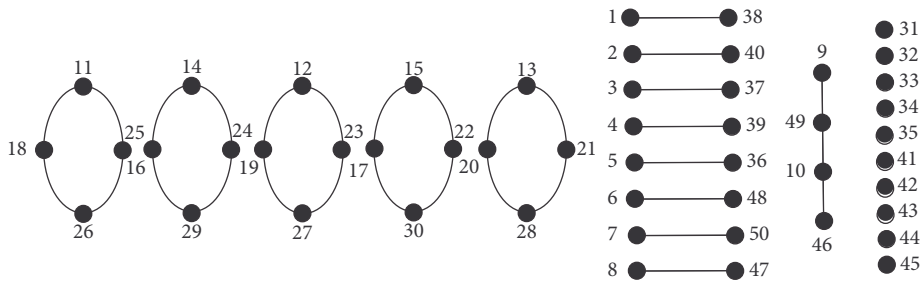


FIGURE 6: An $S - (109, 0)$ - EAMT labeling of the graph $5C_4 \cup 8K_2 \cup P_4 \cup 10K_1$.

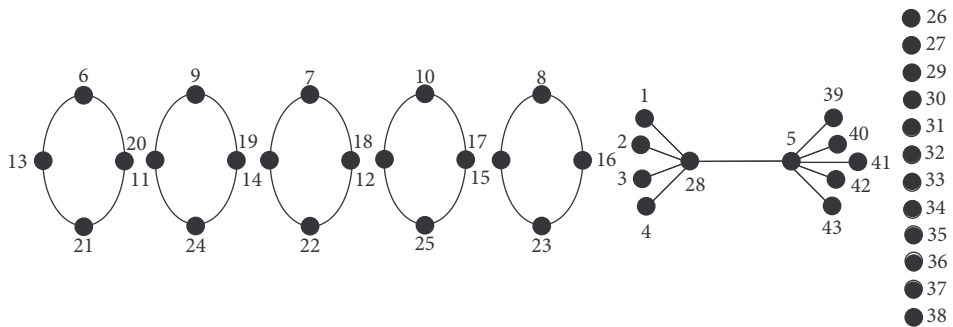


FIGURE 7: An $S - (92, 0)$ - EAMT labeling of the graph $5C_4 \cup S_{4,5} \cup 12K_1$.

$$\begin{aligned}
 f_5(t_i) &= i: 1 \leq i \leq m; \\
 f_5(s_i) &= \frac{2i + 15m + 1}{2}: 1 \leq i \leq m; \\
 f(c) &= \frac{11m + 1}{2}, \\
 f_5(l_i) &= \begin{cases} i + 5m: & i \in \left[1, \frac{m-1}{2}\right]; \\ i + 5m + 1: & i \in \left[\frac{m+1}{2}, \frac{5m-1}{2}\right]. \end{cases} \tag{34}
 \end{aligned}$$

The edge-sums' set constituted by the scheme f_2 generates a sequence consisting of consecutive integer $(7m + 3)/2, (7m + 5)/2, \dots, (19m + 1)/2$. Under the shadow of Lemma 1, f_5 constitutes to an $S - (a, 0) - \text{EAMT}$ labeling of Λ_1 admitting $a = 2(9m + 1)$.

The following results are direct consequences of Lemma 2, from Theorems 4–8. \square

Theorem 9. For odd m , the graph $mC_4 \cup 2K_{1,m} \cup ((7m - 3)/2)K_1$ admits an $S - (15m + 3, 2) - \text{EAMT}$ labeling.

Theorem 10. For odd m , the graph $mC_4 \cup 2mP_2 \cup 2mK_1$ admits an $S - ((31m + 5)/2, 2) - \text{EAMT}$ labeling.

Theorem 11. For odd m , the graph $mC_4 \cup 2P_{m+1} \cup ((5m - 1)/2)K_1$ admits an $S - (12m + 6, 2) - \text{EAMT}$ labeling.

Theorem 12. For odd m , $mC_4 \cup (2m - 2)P_2 \cup P_4 \cup 2mK_1$ admits an $S - ((31m + 5)/2, 2) - \text{EAMT}$ labeling.

Theorem 13. For odd m , $mC_4 \cup S_{m-1,m} \cup ((5m - 1)/2)K_1$ admits an $S - (12m + 3, 2) - \text{EAMT}$ labeling.

2.3. Examples and Proposed Open Problems. An $S - (126, 0) - \text{EAMT}$ labeling of the graph UP_n^t is being presented in Figure 1(a), corresponding to the parameters $t = 3$ and $n = 14$. Furthermore, Figure 1(b) presents an $S - (96, 0) - \text{EAMT}$ labeling of UP_n^t corresponding to $t = 4$ and $n = 8$. Here, it can be observed that the value of the magic constant is perfect as per our depiction in Theorem 1.

Figures 2(a) and 2(b) illustrate Theorem 2 by providing $S - (117, 0) - \text{EAMT}$ and $S - (84, 0) - \text{EAMT}$ labeling of the graph UP_n^t .

Figures 3–7 are the illustrations of Theorems 4–8, respectively, for particular values of the parameters involved.

The open problems related to Section 2.2 are as follows:

- (i) For even m , determine any $S - (a, 0) - \text{EAMT}$ labeling of $mC_4 \cup 2K_{1,m} \cup (7m - 3/2)K_1$
- (ii) For even m , determine any $S - (a, 0) - \text{EAMT}$ labeling of $mC_4 \cup 2mK_2 \cup 2mK_1$
- (iii) For even m , determine any $S - (a, 0) - \text{EAMT}$ labeling of $mC_4 \cup 2P_{m+1} \cup ((5m - 1)/2)K_1$
- (iv) For even m , determine any $S - (a, 0) - \text{EAMT}$ labeling of $mC_4 \cup (2m - 2)K_2 \cup P_4 \cup 2mK_1$

- (v) For even m , determine any $S - (a, 0) - \text{EAMT}$ labeling of $mC_4 \cup S_{m-1,m} \cup ((5m - 1)/2)K_1$

3. Conclusion

In this article,

- (i) We have obtained $S - (a, 0) - \text{EAMT}$ and $S - (a', 2) - \text{EAMT}$ labeling of a pancyclic class of graphs, namely, Usmanian pancyclic graph, denoted by UP_n^t .
- (ii) We have exhibited the existence of $S - (a, 0) - \text{EAMT}$ and $S - (a', 2) - \text{EAMT}$ labeling on disjoint copies of C_4 with various trees. Specifically, $mC_4 \cup 2K_{1,m} \cup (7m - 3/2)K_1$, $mC_4 \cup 2mK_2 \cup 2mK_1$, $mC_4 \cup 2P_{m+1} \cup (5m - 1/2)K_1$, $mC_4 \cup (2m - 2)K_2 \cup P_4 \cup 2mK_1$ and $mC_4 \cup S_{m-1,m} \cup (5m - 1/2)K_1$, whereas C_4 itself is not $S - (a, 0) - \text{EAMT}$. These obtained results open a new direction for researchers to derive $S - (a, 0) - \text{EAMT}$ labeling of disjoint copies of C_4 .
- (iii) A few open problems have also been proposed for future work in this area.

Data Availability

The whole data are included within this article. However, the reader may contact the corresponding author for more details on the data.

Conflicts of Interest

The authors declare no conflicts of interest.

References

- [1] D. B. West, *Introduction to Graph Theory*, Prentice Hall, Hoboken, NJ, USA, 2001.
- [2] J. Sedlacek, "Problem 27 in the theory of graphs and its applications," in *Proceedings of the Symposium Smolenice*, pp. 163–167, Smolenice, Slovakia, 1963.
- [3] N. Hartsfield and G. Ringel, *Pearls in Graph Theory*, Academia Press, Cambridge, MA, USA, 1990.
- [4] A. Kotzig and A. Rosa, "Magic valuations of finite graphs," *Canadian Mathematical Bulletin*, vol. 13, no. 4, pp. 451–461, 1970.
- [5] G. Ringel and A. S. Llado, "Another tree conjecture," *Bull ICA*, vol. 18, pp. 83–85, 1996.
- [6] H. Enomoto, A. Llado, T. Nakamigawa, and G. Ringel, "Super edge-magic graphs," *SUT Journal of Mathematics*, vol. 34, pp. 105–109, 1998.
- [7] R. Simanjuntak, F. Bertault, and M. Miller, "Two new (a, d) -EAT graph labelings," in *Proceedings of the Eleventh Australian Workshop of Combinatorial Algorithm*, pp. 179–189, Hunter Valley, Australia, 2000.
- [8] S. M. Lee and Q. X. Shan, *All Trees with at Most 17 Vertices Are Super Edge-Magic*, University Southern Illinois, in *Proceedings of the 16th MCCCC Conference*, 2002.
- [9] M. Javaid, M. Hussain, K. Ali, and K. H. Dar, "Super edge-magic total labeling on W -trees," *Utilitas Mathematica*, vol. 86, pp. 183–191, 2011.

- [10] M. Javaid, "On super edge-antimagic total labeling of subdivided stars," *Discussiones Mathematicae Graph Theory*, vol. 34, no. 4, pp. 691–705, 2014.
- [11] A. Raheem, A. Q. Baig, and M. Javaid, "On (a, d) -EAT labeling of subdivision of $K_{1,r}$," *Journal of Information and Optimization Sciences*, vol. 39, no. 3, pp. 643–650, 2018.
- [12] A. Ahmad, K. Ali, M. Bača, P. Kovář, and A. Semaničová-Feňovčíková, "Vertex-antimagic labelings of regular graphs," *Acta Mathematica Sinica, English Series*, vol. 28, no. 9, pp. 1865–1874, 2012.
- [13] A. Ahmad and F. A. Muntaner-Batle, "On super edge magic deficiency of unicyclic graphs," *Utilitas Mathematica*, vol. 98, pp. 379–386, 2015.
- [14] R. Figueroa-Centeno, R. Ichishima, and F. Muntaner-Batle, "On edge-magic labelings of certain disjoint unions of graphs," *Australasian Journal of Combinatorics*, vol. 32, pp. 225–242, 2005.
- [15] R. M. Figueroa-Centeno, R. Ichishima, and F. A. Muntaner-Batle, "The place of super edge-magic labelings among other classes of labelings," *Discrete Mathematics*, vol. 231, no. 1-3, pp. 153–168, 2001.
- [16] H. U. Afzal, "On super edge-magicness of two special families of graphs," *Utilitas Mathematica*, vol. 97, pp. 97–108, 2015.
- [17] A. Q. Baig and H. U. Afzal, "Super edge-magic (p, q) graphs with magic constant, $3p$," *Utilitas Mathematica*, vol. 98, pp. 53–63, 2015.
- [18] P. R. L. Pushpam and A. Saibulla, "Super (a, d) edge- antimagic total labeling of some classes of graphs," *SUT Journal of Mathematics*, vol. 48, no. 1, pp. 1–12, 2012.

Research Article

Sharp Lower Bounds of the Sum-Connectivity Index of Unicyclic Graphs

Maryam Atapour 

Department of Mathematics and Computer Science, Basic Science Faculty, University of Bonab, P.O. Box 55513-95133, Bonab, Iran

Correspondence should be addressed to Maryam Atapour; m.atapour@ubonab.ac.ir

Received 1 August 2021; Revised 17 August 2021; Accepted 23 August 2021; Published 2 September 2021

Academic Editor: Ali Ahmad

Copyright © 2021 Maryam Atapour. This is an open access article distributed under the Creative Commons Attribution License, which permits unrestricted use, distribution, and reproduction in any medium, provided the original work is properly cited.

The sum-connectivity index of a graph G is defined as the sum of weights $1/\sqrt{d_u + d_v}$ over all edges uv of G , where d_u and d_v are the degrees of the vertices u and v in graph G , respectively. In this paper, we give a sharp lower bound on the sum-connectivity index unicyclic graphs of order $n \geq 7$ and diameter $D(G) \geq 5$.

1. Introduction and Preliminaries

Let G be a simple graph with a vertex set $V = V(G)$ and edge set $E(G)$. The integers $n = n(G) = |V(G)|$ and $m = m(G) = |E(G)|$ are the order and the size of the graph G , respectively. The open neighborhood of vertex v is $N_G(v) = N(v) = \{u \in V(G) | uv \in E(G)\}$, and the degree of v is $d_G(v) = d_v = |N(v)|$. A pendant vertex is a vertex of degree one. The distance between two vertices is the number of edges in the shortest path connecting them, and the diameter $D(G)$ of G is the distance between any two furthest vertices in G . A diametral path is the shortest path in G connecting two vertices whose distance is $D(G)$. A unicyclic graph is a connected graph containing exactly one cycle. A subgraph G' of a graph G is a graph whose set of vertices is a subset of $V(G)$, and set of edges is a subset of $E(G)$.

A topological index is a numeric number associated with a molecular graph that correlates certain physicochemical properties of chemical compounds. The topological indices are useful in the prediction of physicochemical properties and the bioactivity of the chemical compounds [1–3]. Also, topological indices invariants are used for Quantitative Structure-Activity Relationship (QSAR) and Quantitative Structure-Property Relationship (QSPR) studies. It was demonstrated that the sum-connectivity index is well correlated with a variety of physicochemical properties of

alkanes, such as boiling point and enthalpy of formation. The sum-connectivity index is certainly the most widely applied in chemistry and pharmacology, in particular for designing quantitative structure-property and structure-activity relations. The sum-connectivity index is proposed to quantitatively characterize the degree of molecular branching.

Topological indices have been used and have been shown to give a high degree of predictability of pharmaceutical properties. The sum-connectivity index of a graph G was proposed in [4] defined as follows:

$$\text{SCI}(G) = \sum_{uv \in E(G)} \frac{1}{\sqrt{d_u + d_v}} \quad (1)$$

The applications of the sum-connectivity index have been investigated in [5, 6]. Some basic mathematical properties of the sum-connectivity index have been established in [4–8].

In [4], it was shown that for a graph G with $n \geq 5$ vertices and without isolated vertices, $\text{SCI}(G) \geq n - 1/\sqrt{n}$ with equality if and only if G is the star. For $n = 4$, this is not true since, for the union of two copies of the path on two vertices, its sum-connectivity index is $\sqrt{2}$, less than $3/2$. In [7], minimum sum-connectivity indices of trees and unicyclic graphs of a given matching number are characterized; in [8], sum-connectivity index of molecular trees are characterized;

and in [4], some of the lower and upper bounds for the sum-connectivity index of trees are obtained (see recent bounds [9–13]). We all know that the sum-connectivity index is one of the most important and practical indices and therefore has been considered by many researchers. In this paper, we will address one of the unresolved issues for the sum-connectivity index. In fact, we investigate the relationship between the sum-connectivity index and diameter of the graph, which is one of the important parameters in graph theory and we get new results. In other words, in this paper, we solve the problem of the relationship between the diameter of a graph and the sum-connectivity index for the unicyclic graph.

2. Main Results

We begin with the following lemma that we will need for obtaining our main results.

We denote $t(G)$ as the number of pendant vertices in a graph G .

Lemma 1. *Let G be any unicyclic graph and \mathbb{U} be a diametral path of G . If G contains a pendant vertex v not in \mathbb{U} , then there is a unicyclic graph $G' \subset G$ not containing v , such that $D(G) = D(G'), t(G') = t(G) - 1$, and $SCI(G') < SCI(G)$.*

Proof. Let \mathbb{U} be a diametral path of G and $v \in V(G)$ be a pendant vertex not in \mathbb{U} . We denote by u the closest vertex to v which is not of degree 2. Let G' be a subgraph of G obtained by the removal of the path connecting u and v from G . Let u' be the neighbor of u on the $u - v$ path (if the path has only one edge, then $u' = v$). Clearly, G' is a unicyclic graph, $D(G') = D(G)$, and $t(G') = t(G) - 1$. Furthermore,

$$SCI(G) - SCI(G') \geq \frac{1}{\sqrt{d(u) + 1}} + \sum_{w \in N(u) \setminus \{u'\}} \left(\frac{1}{\sqrt{d(u) + d(w)}} - \frac{1}{\sqrt{d(u) + d(w) - 1}} \right). \tag{2}$$

We know that the sum-connectivity index of the path uv is at least $1/\sqrt{d(u) + 1}$. Note that

$$\frac{1}{\sqrt{d(u) + d(w)}} - \frac{1}{\sqrt{d(u) + d(w) - 1}} \geq \frac{1}{\sqrt{d(u) + 1}} - \frac{1}{\sqrt{d(u)}}, \tag{3}$$

for every $w \in N(u) \setminus \{u'\}$; hence, we have

$$SCI(G) - SCI(G') \geq \frac{1}{\sqrt{d(u) + 1}} + (d(u) - 1) \left(\frac{1}{\sqrt{d(u) + 1}} - \frac{1}{\sqrt{d(u)}} \right). \tag{4}$$

Therefore, we get $SCI(G) > SCI(G')$. \square

By Lemma 1, it follows that for any unicyclic graph G , if \mathbb{U} is a diametral path of G , then there is a unicyclic graph $G' \subset G$ containing only pendant vertices of \mathbb{U} , where $D(G') = D(G)$ and $SCI(G') < SCI(G)$.

Here, we obtain a sharp bound on the sum-connectivity index of any unicyclic graph of diameter at least 5.

Theorem 2. *Let G be any unicyclic graph of diameter $D(G) \geq 5$. Then,*

$$SCI(G) \geq \frac{D(G)}{2} + \frac{5}{\sqrt{5}} + \frac{1}{\sqrt{3}} - 2. \tag{5}$$

Proof. We will complete the proof by considering the following four cases.

Case 1. If G does not contain any pendant vertex, then G is the cycle either with $2D(G)$ or $2D(G) + 1$ vertices, which implies that

$$SCI(G) \geq 2D(G) \left(\frac{1}{\sqrt{4}} \right) = D(G) > \frac{D(G)}{2} + \frac{5}{\sqrt{5}} + \frac{1}{\sqrt{3}} - 2. \tag{6}$$

Case 2. If G contains one pendant vertex, then G consists of the cycle C_r of length $r \geq 3$ and the path P having $s \geq 1$ edges, where $C_r \cap P$ consists of one vertex which has degree 3 in G . This degree will be included in the computation of $SCI(C_r)$ and $SCI(P)$. We have $SCI(G) = SCI(C_r) + SCI(P)$, where

$$SCI(C_r) = \sum_{uv \in E(C_r)} \frac{1}{\sqrt{d(u) + d(v)}} = (r - 2) \frac{1}{\sqrt{4}} + 2 \left(\frac{1}{\sqrt{5}} \right) = \frac{r}{2} + \frac{2\sqrt{5}}{5} - 1, \tag{7}$$

$$SCI(P) = \sum_{uv \in E(P)} \frac{1}{\sqrt{d(u) + d(v)}} = (s - 2) \frac{1}{\sqrt{4}} + \frac{1}{\sqrt{3}} + \frac{1}{\sqrt{5}} = \frac{s}{2} + \frac{\sqrt{3}}{3} + \frac{\sqrt{5}}{5} - 1.$$

If $s \geq 2$ and $\text{SCI}(P) = 1/2$ if $s = 1$. So, $\text{SCI}(P) \geq s/2$ for every $s \geq 1$, and the equality holds if $s = 1$.

If $r \geq 4$, then $D(G) \leq (r/2) + s$ and

$$\begin{aligned} \text{SCI}(G) &\geq \frac{r}{2} + \frac{2\sqrt{5}}{5} + \frac{s}{2} - 1 \\ &\geq \frac{r}{2} + \frac{2\sqrt{5}}{5} + \frac{D(G)}{2} - \frac{r}{4} - 1 \\ &= \frac{D(G)}{2} + \frac{r}{4} + \frac{2\sqrt{5}}{5} - 1 \\ &\geq \frac{D(G)}{2} + \frac{2\sqrt{5}}{5} \\ &> \frac{D(G)}{2} + \frac{5}{\sqrt{5}} + \frac{1}{\sqrt{3}} - 2. \end{aligned} \tag{8}$$

If $r = 3$, then $D(G) = s + 1$ and

$$\begin{aligned} \text{SCI}(G) &\geq \frac{3}{2} + \frac{2\sqrt{5}}{5} + \frac{s}{2} - 1, \\ &\geq \frac{3}{2} + \frac{2\sqrt{5}}{5} + \frac{D(G)}{2} - \frac{1}{2} - 1 \\ &= \frac{D(G)}{2} + \frac{2\sqrt{5}}{5} \\ &> \frac{D(G)}{2} + \frac{5}{\sqrt{5}} + \frac{1}{\sqrt{3}} - 2. \end{aligned} \tag{9}$$

Case 3. If G contains 2 pendant vertices, then G consists of the cycle C_r of length $r \geq 3$ and two paths X_1 and X_2 having $s_1 \geq 1$ and $s_2 \geq 1$ edges, respectively. We can assume that $C_r \cap X_1$ consists of one vertex and X_2 is attached either to an internal vertex of X_1 or to a vertex of C_r .

Case 3.1. If $X_1 \cap X_2 = \emptyset$, then we have $\text{SCI}(G) = \text{SCI}(C_r) + \text{SCI}(X_1) + \text{SCI}(X_2)$. For $i = 1, 2$,

$$\begin{aligned} \text{SCI}(X_i) &= \sum_{uv \in E(X_i)} \frac{1}{\sqrt{d(u) + d(v)}} \\ &= (s_i - 2) \frac{1}{\sqrt{4}} + \frac{1}{\sqrt{3}} + \frac{1}{\sqrt{5}} = \frac{s_i}{2} + \frac{\sqrt{3}}{3} + \frac{\sqrt{5}}{5} - 1. \end{aligned} \tag{10}$$

When $s_i \geq 2$ and $\text{SCI}(X_i) = 1/2$ if $s_i = 1$. If X_1 and X_2 are attached to nonadjacent vertices of C_r , then

$$\begin{aligned} \text{SCI}(C_r) &= \sum_{uv \in E(C_r)} \frac{1}{\sqrt{d(u) + d(v)}} \\ &= (r - 4) \frac{1}{\sqrt{4}} + 4 \left(\frac{1}{\sqrt{5}} \right) = \frac{r}{2} + \frac{4\sqrt{5}}{5} - 2. \end{aligned} \tag{11}$$

If X_1 and X_2 are attached to adjacent vertices of C_r , then

$$\begin{aligned} \text{SCI}(C_r) &= \sum_{uv \in E(C_r)} \frac{1}{\sqrt{d(u) + d(v)}}, \\ &= (r - 3) \frac{1}{\sqrt{4}} + 2 \left(\frac{1}{\sqrt{5}} \right) + \frac{1}{\sqrt{6}} \\ &= \frac{r}{2} + \frac{2\sqrt{5}}{5} + \frac{\sqrt{6}}{6} - \frac{3}{2} \\ &> \frac{r}{2} + \frac{4\sqrt{5}}{5} - 2. \end{aligned} \tag{12}$$

If $s_1 = s_2 = 1$, then $D(G) \leq (r/2) + 2$ and

$$\begin{aligned} \text{SCI}(G) &\geq \frac{r}{2} + \frac{4\sqrt{5}}{5} - 2 + \frac{1}{2} + \frac{1}{2}, \\ &\geq D(G) + \frac{4\sqrt{5}}{5} - 3 \\ &> \frac{D(G)}{2} + \frac{5}{\sqrt{5}} + \frac{1}{\sqrt{3}} - 2. \end{aligned} \tag{13}$$

So, we can assume that s_1 or s_2 is at least 2. We have $\text{SCI}(X_1) + \text{SCI}(X_2) \geq (s_1/2) + (s_2/2) + (\sqrt{3}/3) + (\sqrt{5}/5) - 1$ (the equality holds if s_1 or s_2 is 1).

If $r \geq 4$, then $D(G) \leq (r/2) + s_1 + s_2$ and

$$\begin{aligned} \text{SCI}(G) &\geq \frac{r}{2} + \frac{4\sqrt{5}}{5} - 2 + \frac{s_1}{2} + \frac{s_2}{2} + \frac{\sqrt{3}}{3} + \frac{\sqrt{5}}{5} - 1, \\ &\geq \frac{D(G)}{2} + \frac{r}{4} + \sqrt{5} + \frac{\sqrt{3}}{3} - 3 \\ &\geq \frac{D(G)}{2} + \sqrt{5} + \frac{\sqrt{3}}{3} - 2. \end{aligned} \tag{14}$$

If $r = 3$, then $D(G) \leq s_1 + s_2 + 1$ and

$$\begin{aligned} \text{SCI}(G) &\geq \frac{3}{2} + \frac{4\sqrt{5}}{5} - 2 + \frac{s_1}{2} + \frac{s_2}{2} + \frac{\sqrt{3}}{3} + \frac{\sqrt{5}}{5} - 1, \\ &\geq \frac{D(G)}{2} + \frac{4\sqrt{5}}{5} + \frac{\sqrt{3}}{3} + \frac{\sqrt{5}}{5} - 2 \\ &= \frac{D(G)}{2} + \sqrt{5} + \frac{\sqrt{3}}{3} - 2. \end{aligned} \tag{15}$$

Case 3.2. $X_1 \cap X_2$ is nonempty, and there is a diametral path containing both pendant vertices of G .

Let \mathbb{U} be the diametral path containing both pendant vertices of G . Then, $\mathbb{U} \subseteq X_1 \cup X_2$. One of the internal vertices, say x , of \mathbb{U} is of degree 3 or 4 in graph G . If x is adjacent to a pendant vertex of \mathbb{U} , then

$$\begin{aligned}
 \text{SCI}(\mathbb{U}) &= \sum_{uv \in E(\mathbb{U})} \frac{1}{\sqrt{d(u)} + d(v)} \\
 &= (D(G) - 3) \frac{1}{\sqrt{4}} + \frac{1}{\sqrt{3}} + \frac{1}{\sqrt{5}} + \frac{1}{\sqrt{6}} \quad (16) \\
 &= \frac{D(G)}{2} + \frac{\sqrt{3}}{3} + \frac{\sqrt{5}}{5} + \frac{\sqrt{6}}{6} - \frac{3}{2}
 \end{aligned}$$

If x is not adjacent to a pendant vertex of \mathbb{U} , then

$$\begin{aligned}
 \text{SCI}(\mathbb{U}) &\geq \frac{D(G) - 4}{2} + \frac{2\sqrt{3}}{3} + \frac{2\sqrt{6}}{6} \\
 &= \frac{D(G)}{2} + \frac{2\sqrt{3}}{3} + \frac{2\sqrt{6}}{6} - 2. \quad (17)
 \end{aligned}$$

Note that G contains also the cycle C_r , where one of the vertices is of degree 3 or 4 in G . We have

$$\begin{aligned}
 \text{SCI}(C_r) &= \sum_{uv \in E(C_r)} \frac{1}{\sqrt{d(u)} + d(v)} \\
 &= (r - 2) \frac{1}{\sqrt{4}} + 2 \left(\frac{1}{\sqrt{6}} \right) \geq \frac{3}{2} + \frac{2\sqrt{6}}{6} - 1 \quad (18) \\
 &= \frac{1}{2} + \frac{2\sqrt{6}}{6},
 \end{aligned}$$

which implies that

$$\begin{aligned}
 \text{SCI}(G) &\geq \text{SCI}(\mathbb{U}) + \text{SCI}(C_r) \\
 &\geq \frac{D(G)}{2} + \frac{\sqrt{3}}{3} + \frac{\sqrt{5}}{5} + \frac{\sqrt{6}}{6} - \frac{3}{2} + \frac{1}{2} + \frac{2\sqrt{6}}{6}, \\
 &= \frac{D(G)}{2} + \frac{\sqrt{3}}{3} + \frac{\sqrt{5}}{5} + \frac{\sqrt{6}}{2} - 1 \\
 &> \frac{D(G)}{2} + \frac{5}{\sqrt{5}} + \frac{1}{\sqrt{3}} - 2. \quad (19)
 \end{aligned}$$

Case 3.3. $X_1 \cap X_2$ is nonempty and there is a diametral path containing only one pendant vertex of G . Then, we denote this diametral path with \mathbb{U} containing only one pendant vertex of G . Since the other pendant vertex is not in \mathbb{U} , by Lemma 1, there is a unicyclic graph G' having one pendant vertex, such that $D(G') = D(G)$ and $\text{SCI}(G) > \text{SCI}(G')$, and we know that $\text{SCI}(G') > (D(G)/2) + (5/\sqrt{5}) + (1/\sqrt{3}) - 2$.

Case 4. If G contains at least 3 pendant vertices.

Let \mathbb{U} be a diametral path of G . Clearly, this path contains at most 2 pendant vertices of G . Since G contains $m \geq 3$ pendant vertices, we have at least $m - 2$ pendant vertices not in \mathbb{U} . By Lemma 1, there is a unicyclic graph $G' \subseteq G$ having only the pendant vertices of \mathbb{U} (at most 2 vertices), such that $D(G') = D(G)$, $t(G') = t(G) - 1$ and $\text{SCI}(G) > \text{SCI}(G')$.

From the previous cases, it follows that $\text{SCI}(G') > (D(G)/2) + (5/\sqrt{5}) + (1/\sqrt{3}) - 2$.

It is easy to show that the bound $\text{SCI}(G) \geq (D(G)/2) + (5/\sqrt{5}) + (1/\sqrt{3}) - 2$ is best possible because of the graph H , where $V(H) = \{u, v_0, v_1, v_2, \dots, v_{D(H)}\}$ and $E(H) = \{v_0v_1, v_1v_2, \dots, v_{D(H)-1}v_{D(H)}, uv_1, uv_3\}$ has the sum-connectivity index

$$\begin{aligned}
 \text{SCI}(H) &= (D(H) - 4) \frac{1}{\sqrt{4}} + 5 \left(\frac{1}{\sqrt{5}} \right) + \frac{1}{\sqrt{3}}, \quad (20) \\
 &= \frac{D(H)}{2} + \frac{5}{\sqrt{5}} + \frac{1}{\sqrt{3}} - 2.
 \end{aligned}$$

The proof is completed. \square

Now, we obtain lower bounds on the sum-connectivity index for unicyclic graphs of small diameter.

Theorem 3. Let G be an unicyclic graph of diameter $D(G)$. Then,

- (i) If $D(G) = 2$, then $\text{SCI}(G) \geq 1 + 2\sqrt{5}/5$
- (ii) If $D(G) = 3$, then $\text{SCI}(G) \geq 2\sqrt{5}/5 + \sqrt{6}/6 + 1$
- (iii) If $D(G) = 4$, then $\text{SCI}(G) \geq 1 + 4\sqrt{5}/5$

Proof. We can see that the proof of Theorem 2 holds for $D(G) = 3$ and $D(G) = 4$ except for Case 3.1, where $s_1 = s_2 = 1$.

Let $D(G) = 4$. We have $\text{SCI}(G) \geq D(G) + (1 + 4\sqrt{5}/5) - 3$ (as presented in the proof of Theorem 2), which is $(1 + 4\sqrt{5}/5)$. From the other cases, we obtain $\text{SCI}(G) \geq ((D(G)/2) + (5/\sqrt{5}) + (1/\sqrt{3}) - 2) = (\sqrt{5} + (1/\sqrt{3})) > (1 + 4\sqrt{5}/5)$, which implies that $\text{SCI}(G) \geq (1 + 4\sqrt{5}/5)$.

Let $D(G) = 3$. We have $\text{SCI}(G) \geq D(G) + 4\sqrt{5}/5 - 3$ (obtained in the proof of Theorem 2); Case 3.1 (if $s_1 = s_2 = 1$) is not sufficient now, so we give a better bound in this case. Since $s_1 = s_2 = 1$ and $D(G) = 3$, then P_1 and P_2 must be attached to adjacent vertices of C_r , which means that $\text{SCI}(C_r) = r/2 + 2\sqrt{5}/5 + \sqrt{6}/6 - 3/2$ in the proof of Theorem 2. Since $r \geq 3$, we obtain

$$\begin{aligned}
 \text{SCI}(G) &= \text{SCI}(C_r) + \text{SCI}(X_1) + \text{SCI}(X_2) \\
 &= \frac{r}{2} + \frac{2\sqrt{5}}{5} + \frac{\sqrt{6}}{6} - \frac{3}{2} + \frac{1}{2} + \frac{1}{2} \geq \frac{2\sqrt{5}}{5} + \frac{\sqrt{6}}{6} + 1. \quad (21)
 \end{aligned}$$

Let $D(G) = 2$. Except for C_5 and C_4 , the only unicyclic graphs H of diameter 2 are formed by the cycle C_3 , where $s \geq 1$ pendant vertices are adjacent to one of the vertices of C_3 . Let $V(C_3) = \{v_1, v_2, v_3\}$. We can assume that the pendant vertices u_1, u_2, \dots, u_p are adjacent to v_1 . Then, $\mathbb{U} = v_2v_1u_1$ is a diametral path of H , and from Lemma 1, it follows that there is a unicyclic graph $H' \subseteq H$, which contains only one pendant vertex u_1 (the pendant vertex (the pendant vertex in \mathbb{U})), where $\text{SCI}(H) \geq \text{SCI}(H')$. Since

$$\text{SCI}(H') = 2\left(\frac{1}{\sqrt{5}}\right) + 2\left(\frac{1}{\sqrt{4}}\right) = 1 + \frac{2\sqrt{5}}{5}, \quad (22)$$

$\text{SCI}(C_4) = 2$ and $\text{SCI}(C_5) = 5/2$, we obtain the bound $\text{SCI}(G) \geq 1 + 2\sqrt{5}/5$. \square

Corollary 4. *Let G be any unicyclic graph of order at least 7 and diameter $D(G) \geq 2$. Then,*

$$\text{SCI}(G) \geq \frac{D(G)}{2} + \frac{5}{\sqrt{5}} + \frac{1}{\sqrt{3}} - 2. \quad (23)$$

Proof. By Theorem 2, for $D(G) \geq 5$ and any n , we have $\text{SCI}(G) \geq ((D(G)/2) + (5/\sqrt{5}) + (1/\sqrt{3}) - 2)$. By Theorem 3, for $D(G) = 2$ and any n , we have $\text{SCI}(G) \geq 1 + 2\sqrt{5}/5$, which is greater than $((D(G)/2) + (5/\sqrt{5}) + (1/\sqrt{3}) - 2)$. It remains to prove Corollary 4 for $n \geq 7$ and $3 \leq D(G) \leq 4$. The proof of Theorem 2 holds also for $D(G) = 3$ and $D(G) = 4$ except for Case 3.1 where $s_1 = s_2 = 1$. We show that if $n \geq 7$, then $\text{SCI}(G) \geq ((D(G)/2) + (5/\sqrt{5}) + (1/\sqrt{3}) - 2)$ also in that case. If $n \geq 7$ and $p_1 = p_2 = 1$, then G contains the cycle C_k for $r \geq 5$ and $\text{SCI}(C_r) \geq r/2 + 4\sqrt{5}/5 - 2$ (given in Case 3.1 in the proof of Theorem 2). Since $\text{SCI}(X_1) = \text{SCI}(X_2) = 1/2$, we obtain

$$\text{SCI}(G) = \text{SCI}(C_r) + \text{SCI}(X_1) + \text{SCI}(X_2) \geq \frac{3}{2} + \frac{4\sqrt{5}}{5}, \quad (24)$$

which is greater than $\text{SCI}(G) \geq ((D(G)/2) + (5/\sqrt{5}) + (1/\sqrt{3}) - 2)$ for $D(G) = 3$ and $D(G) = 4$. \square

Corollary 5. *Let G be any unicyclic graph of order at least 7 and diameter $D(G) \geq 2$. Then,*

$$\frac{\text{SCI}(G)}{D(G)} \geq \frac{(\sqrt{3}/3) + \sqrt{5}}{n-2} - \frac{1}{2}, \quad (25)$$

$$\text{SCI}(G) - D(G) \geq \frac{\sqrt{3}}{3} + \sqrt{5} - \frac{n}{2} - 1.$$

Proof. By Theorem 2, we have $\text{SCI}(G) \geq (D(G)/2) + (5/\sqrt{5}) + 1/\sqrt{3} - 2$ and since $D(G) \leq n - 2$ for any graph G except for the path, hence, by the definition of sum-connectivity index, we have

$$\begin{aligned} \frac{\text{SCI}(G)}{D(G)} &\geq \frac{1}{2} + \frac{5}{\sqrt{5}D(G)} + \frac{1}{\sqrt{3}D(G)} - \frac{2}{D(G)}, \\ &\geq \frac{1}{2} + \frac{5}{\sqrt{5}(n-2)} + \frac{1}{\sqrt{3}(n-2)} - \frac{2}{D(G)} \\ &\geq \frac{1}{2} + \frac{5}{\sqrt{5}(n-2)} + \frac{1}{\sqrt{3}(n-2)} - 1 \\ &= \frac{(\sqrt{3}/3) + \sqrt{5}}{n-2} - \frac{1}{2}. \end{aligned} \quad (26)$$

Similarly, we obtain

$$\text{SCI}(G) - D(G) \geq \frac{\sqrt{3}}{3} + \sqrt{5} - \frac{D(G)}{2} - 2 \geq \frac{\sqrt{3}}{3} + \sqrt{5} - \frac{n}{2} - 1. \quad (27)$$

\square

3. Open Problem and Conclusion

In this paper, we investigate the relationship between the sum-connectivity index and the diameter of a graph and obtained a new lower bound for the sum-connectivity index of unicyclic graphs. However, there are still open and challenging problems for researchers, for example, the problem on the relationship between the sum-connectivity index and the diameter of bicyclic and tricyclic graphs. Moreover, the relationship between other topological indices such as F-index and GA-index with the diameter of unicyclic, bicyclic, and tricyclic graphs is still open.

Data Availability

The data used to support the findings of the study are included within the article.

Conflicts of Interest

The author declares that there are no conflicts of interest.

References

- [1] Z. Shao, M. Siddiqui, and M. Muhammad, "Computing zagreb indices and zagreb polynomials for symmetrical nanotubes," *Symmetry*, vol. 10, no. 7, p. 244, 2018.
- [2] Z. Shao, P. Wu, X. Zhang, D. Dimitrov, and J.-B. Liu, "On the maximum ABC index of graphs with prescribed size and without pendent vertices," *IEEE Access*, vol. 6, pp. 27604–27616, 2018.
- [3] Z. Shao, P. Wu, Y. Gao, I. Gutman, and X. Zhang, "On the maximum ABC index of graphs without pendent vertices," *Applied Mathematics and Computation*, vol. 315, pp. 298–312, 2017.
- [4] B. Zhou and N. Trinajstić, "On a novel connectivity index," *Journal of Mathematical Chemistry*, vol. 46, no. 4, pp. 1252–1270, 2009.
- [5] B. Lučić, S. Nikolić, N. Trinajstić, B. Zhou, and S. Ivaniš Turk, "Sum-Connectivity index," in *Novel Molecular Structure Descriptors - Theory and Applications I*, I. Gutman and B. Furtula, Eds., pp. 101–136, University of Kragujevac, Kragujevac, Serbia, 2010.
- [6] B. Lučić, N. Trinajstić, and B. Zhou, "Comparison between the sum-connectivity index and product-connectivity index for benzenoid hydrocarbons," *Chemical Physics Letters*, vol. 475, pp. 146–148, 2009.
- [7] Z. Du, B. Zhou, and N. Trinajstić, "Minimum sum-connectivity indices of trees and unicyclic graphs of a given matching number," *Journal of Mathematical Chemistry*, vol. 47, no. 2, pp. 842–855, 2010.
- [8] R. Xing, B. Zhou, and N. Trinajstić, "Sum-connectivity index of molecular trees," *Journal of Mathematical Chemistry*, vol. 48, no. 3, pp. 583–591, 2010.

- [9] S. Akram, M. Javaid, and M. Jamal, "Bounds on F-index of tricyclic graphs with fixed pendant vertices," *Open Mathematics*, vol. 18, no. 1, pp. 150–161, 2020.
- [10] A. Ali, L. Zhong, and I. Gutman, "Harmonic index and its generalizations: extremal results and bounds," *MATCH Communications in Mathematical and in Computer Chemistry*, vol. 81, no. 2, pp. 249–311, 2019.
- [11] W. Carballosa, D. Pestana, J. M. Sigarreta, and E. Tourís, "Relations between the general sum connectivity index and the line graph," *Journal of Mathematical Chemistry*, vol. 58, no. 10, pp. 2273–2290, 2020.
- [12] A. Jahanbani, "Two-tree graphs with minimum sum-connectivity index," *Discrete Mathematics, Algorithms and Applications*, vol. 13, Article ID 2150053, 2020.
- [13] M. Rizwan, A. A. Bhatti, M. Javaid, and F. Jarad, "Some bounds on bond incident degree indices with some parameters," *Mathematical Problems in Engineering*, vol. 2021, Article ID 8417486, 10 pages, 2021.

Research Article

Total Face Irregularity Strength of Grid and Wheel Graph under K-Labeling of Type (1, 1, 0)

Aleem Mughal and Noshad Jamil 

University of Management and Technology, Lahore, Pakistan

Correspondence should be addressed to Noshad Jamil; noshad.jamil@umt.edu.pk

Received 23 June 2021; Accepted 10 August 2021; Published 31 August 2021

Academic Editor: Muhammad Kamran Siddiqui

Copyright © 2021 Aleem Mughal and Noshad Jamil. This is an open access article distributed under the Creative Commons Attribution License, which permits unrestricted use, distribution, and reproduction in any medium, provided the original work is properly cited.

In this study, we used grids and wheel graphs $G = (V, E, F)$, which are simple, finite, plane, and undirected graphs with V as the vertex set, E as the edge set, and F as the face set. The article addresses the problem to find the face irregularity strength of some families of generalized plane graphs under k -labeling of type (α, β, γ) . In this labeling, a graph is assigning positive integers to graph vertices, graph edges, or graph faces. A minimum integer k for which a total label of all vertices and edges of a plane graph has distinct face weights is called k -labeling of a graph. The integer k is named as total face irregularity strength of the graph and denoted as $tfs(G)$. We also discussed a special case of total face irregularity strength of plane graphs under k -labeling of type (1, 1, 0). The results will be verified by using figures and examples.

1. Introduction

This article is based on simple, plane, finite, and undirected graphs $G = (V, E, F)$. Graph labeling is a mapping that maps graph elements (V, E, F) into positive integers, and we name these positive integers as labels. Suppose that $\alpha, \beta, \gamma \in \{0, 1\}$ and k is a positive integer, then a branch of labeling, named as, k -labeling of type (α, β, γ) , is a mapping ϕ from the set of graph elements (V, E, F) into the set of positive integers $\{1, 2, 3, \dots, k\}$. A labeling of type (1, 1, 0) of grid graph G_n^m means that vertices and edges are labeled but face is not labeled. We will work on labeling of type (1, 1, 0) for the grid graphs G_n^m , in which the vertices and edges will be labeled but our ultimate focus will be on calculating distinct face weights. A detailed review of graph labeling can be seen in [1].

If the domain of k -labeling of type (α, β, γ) is vertex set, edge set, face set, or vertex-edge set, then we name this as vertex k -labeling of type (1, 0, 0), edge k -labeling of type (0, 1, 0), face k -labeling of type (0, 0, 1), or total k -labeling of type (1, 1, 0), respectively. The other possible cases are vertex-face set, edge-face set, and vertex-edge-face set which we call as vertex-face k -labeling of type (1, 0, 1), edge-face

k -labeling of type (0, 1, 1), and entire k -labeling of type (1, 1, 1), respectively. The trivial case $(\alpha, \beta, \gamma) = (0, 0, 0)$ is not accepted. The weight of any vertex in a graph is the sum of labels of that particular vertex and its adjacent edges. The weight of any edge of a graph is the sum of labels of its adjacent vertices. The weight of any face in a graph is the sum of labels of that particular face and its surrounding vertices and edges. For a deep survey on weights of graph elements, reader can go through [2–4]. The weight of a face f of a plane graph G under k -labeling ϕ of type (α, β, γ) can be defined as follows:

$$Wt_{\phi_{(\alpha, \beta, \gamma)}}(f) = \alpha \sum_{v \sim f} \phi(v) + \beta \sum_{e \sim f} \phi(e) + \gamma \phi(f). \quad (1)$$

A k -labeling ϕ of type (α, β, γ) of the plane graph G is called face irregular k -labeling of type (α, β, γ) of the plane graph G if every two different faces have distinct weights; that is, for graph faces $f, g \in G$ and $f \neq g$, we have

$$Wt_{\phi_{(\alpha, \beta, \gamma)}}(f) \neq Wt_{\phi_{(\alpha, \beta, \gamma)}}(g). \quad (2)$$

Face irregularity strength of type (α, β, γ) of any plane graph G is the minimum integer k for which the graph G

admits a face irregular k -labeling of type (α, β, γ) . For a vertex-edge labeled graph G , the minimum integer k for which the graph G admits a face irregular k -labeling of type (α, β, γ) is called the total face irregularity strength of type (α, β, γ) of the plane graph G , and it is denoted by $\text{tfs}_{(\alpha, \beta, \gamma)}(G)$. A detailed work on irregularity strength of graphs can be seen in [4–12].

Gary Ebert et al. worked on the irregularity strength of $2 \times n$ grid in their research “Irregularity Strength for Certain Graphs,” [13]. Baca et al. determined total irregularity strength of graphs and calculated bounds and exact values for different families of graphs [14]. Baca et al. investigated face irregular evaluations of plane graphs and calculated face irregularity strength of type (α, β, γ) for ladder graphs [15].

By motivating from all abovementioned, we are working on grid graphs G_n^m with n rows and m columns. Labeling of a grid graph has many stages, depending on the size of graph, on the selection of rows and columns, and sometimes on the smaller and larger values of labeling. We will calculate the total face irregularity strength of grid graphs under labeling ϕ of type (α, β, γ) , and this work is a modification of abovementioned articles. Grid graphs are constructed by the graph Cartesian products of path graphs, that is, $G_n^m = P_{n+1} \square P_{m+1}$.

We will prove the exact value for the total face irregularity strength under k -labeling ϕ of type (α, β, γ) of grid graphs with the property $\lfloor (m+1)/3 \rfloor = m - 2 \lfloor (m+1)/3 \rfloor$ where $1 < m < n$.

We will prove the exact value for the total face irregularity strength under k -labeling ϕ of type (α, β, γ) of wheel graph W_n .

Baca et al. determined a lower bound for the face irregularity strength of type (α, β, γ) when a 2-connected plane graph G has more than one faces of the largest sizes [14, 16]. They presented the following theorem.

Theorem 1 (see [14, 16]). *Let $G = (V, E, F)$ be a 2-connected plane graph with n_i -sided faces, $i \geq 3$. Let $\alpha, \beta, \gamma \in \{0, 1\}$, $a = \min\{i: n_i \neq 0\}$, and $b = \max\{i: n_i \neq 0\}$. Then, the face irregularity strength of type (α, β, γ) of the plane graph G is*

$$\text{fs}_{(\alpha, \beta, \gamma)}(G) \geq \left\lceil \frac{(\alpha + \beta)a + \gamma + |F(G)| - 1}{(\alpha + \beta)b + \gamma} \right\rceil. \quad (3)$$

Proof. Suppose that face irregularity strength under a k -labeling ϕ of type α, β, γ of the plane graph G is k .

The smallest face weight under the face irregular k -labeling ϕ admits the value at least $(\alpha + \beta)a + \gamma$. Since $|F(G)| = \sum_{i=3}^b n_i$, it follows that the largest face weight attains the value at least $(\alpha + \beta)a + \gamma + |F(G)| - 1$ and at most $((\alpha + \beta)b + \gamma)k$. Hence,

$$(\alpha + \beta)a + \gamma + |F(G)| - 1 \leq ((\alpha + \beta)b + \gamma)k, \quad (4)$$

$$k \geq \left\lceil \frac{(\alpha + \beta)a + \gamma + |F(G)| - 1}{(\alpha + \beta)b + \gamma} \right\rceil. \quad \square$$

This lower bound can be improved when a 2-connected plane graph G contains only one face of the largest size, that is, $n_b = 1$ and $c = \max\{i: n_i \neq 0, i < b\}$. So, we present the following theorem to calculate the lower bounds for grid graphs G_n^m .

2. Main Results

In this research, we will demonstrate the tight lower bound for the total face irregular strength of type $(1; 1; 0)$ for the plan graph particularly grid and wheel graphs. It is sufficient to prove tight lower bound of grid graph that the exact value of $\text{tfs}(G_{mn})$ exists and differences in weights of the horizontal faces must be 1 and the differences in weights of the vertical faces is m .

Theorem 2. *Let $G = (V, E, F)$ be a 2-connected plane graph with n_i -sided faces, $i \geq 3$. Let $\alpha, \beta, \gamma \in \{0, 1\}$, $a = \min\{i: n_i \neq 0\}$ and $b = \max\{i: n_i \neq 0\}$, $n_b = 1$, and $c = \max\{i: n_i \neq 0, i \leq b\}$. Then, the total face irregularity strength of type (α, β, γ) of the plane graph G is*

$$\text{fs}_{(\alpha, \beta, \gamma)}(G) \geq \left\lceil \frac{(\alpha + \beta)a + \gamma + |F(G)| - 2}{(\alpha + \beta)c + \gamma} \right\rceil. \quad (5)$$

Proof. We suppose that total face irregularity strength of any 2-connected plane graph G under k -labeling ϕ of type α, β, γ is equal to k , that is,

$$\text{tfs}_{(\alpha, \beta, \gamma)}(G) = k. \quad (6)$$

Given that the largest face $n_b = 1$ for $i < b$. So, the smallest face weight under the face irregular k -labeling ϕ of type (α, β, γ) will have the minimum value $(\alpha + \beta)c + \gamma$. The total number of faces of the graph can be obtained by adding all the number of i -sided faces where $i \geq 3$. Hence, the largest face weight can have the minimum value $(\alpha + \beta)a + \gamma + |F(G)| - 2$ and maximum value $((\alpha + \beta)c + \gamma)k$. So, we can construct the following results:

$$(\alpha + \beta)a + \gamma + |F(G)| - 2 \leq ((\alpha + \beta)b + \gamma)k$$

$$\Rightarrow k \geq \left\lceil \frac{(\alpha + \beta)a + \gamma + |F(G)| - 2}{(\alpha + \beta)c + \gamma} \right\rceil. \quad (7)$$

Hence,

$$\text{tfs}_{(\alpha, \beta, \gamma)}(G) \geq \left\lceil \frac{(\alpha + \beta)a + \gamma + |F(G)| - 2}{(\alpha + \beta)c + \gamma} \right\rceil. \quad (8) \quad \square$$

From the above result, we see that if a 2-connected plane graph G contains only one largest face, then the lower bound for the face irregularity strength of type $(1, 1, 0)$ can be calculated as

$$\text{tfs}_{(1, 1, 0)}(G) \geq \left\lceil \frac{2a + |F(G)| - 2}{2c} \right\rceil. \quad (9)$$

In this research, we will prove the tight lower bound for the total face irregularity strength of type $(1, 1, 0)$ for the grid graph G_n^m and wheel graph W_n . To prove the tight lower bound of the grid graph, it will be sufficient to show that the exact value of $tfs(G_n^m)$ exists. The exact value of $tfs(G_n^m)$, that is, calculated from grid graph G_n^m under a graph k -labeling of

type $(1, 1, 0)$, exists if the differences in weights of the horizontal faces are 1 and the differences in weights of the vertical faces are m . Generalized grid graphs can be written as $G_n^m = P_{n+1} \square P_{m+1}$.

The vertex set and the edge set of the grid graph can be defined as follows:

$$V(P_{n+1} \square P_{m+1}) = \{v_i^j : i = 1, 2, \dots, n + 1, j = 1, 2, \dots, m + 1\},$$

$$E(P_{n+1} \square P_{m+1}) = \{v_i^j v_{i+1}^j : i = 1, 2, \dots, n, j = 1, 2, \dots, m + 1\} \cup \{v_i^j v_i^{j+1} : i = 1, 2, \dots, n + 1, j = 1, 2, \dots, m\}. \tag{10}$$

Theorem 3. Let $n, m \geq 2$ be positive integers and $G_n^m = P_{n+1} \square P_{m+1}$ be generalized grid graph, then

$$tfs_{(1,1,0)}(P_{n+1} \square P_{m+1}) = \left\lceil \frac{mn + 7}{8} \right\rceil. \tag{11}$$

In order to prove this, it will be sufficient to show that the exact value of $tfs(G_n^m)$ exists.

The vertices for the generalized graph G_n^m under a k -labeling ϕ of type $(1, 1, 0)$ in different intervals of i and j can be defined as follows:

$$\phi(v_i^j) = \begin{cases} 1 + \left\lfloor \frac{m+1}{3} \right\rfloor \left\lfloor \frac{i-1}{2} \right\rfloor, & \text{for } i = 1, 2, 3, \dots, 2 \left\lceil \frac{k}{\lfloor (m+1)/3 \rfloor} \right\rceil \text{ and } j = 1, 2, \dots, m + 1, \\ k, & \text{for } i = 2 \left\lceil \frac{k}{\lfloor (m+1)/3 \rfloor} \right\rceil + 1, \dots, n + 1 \text{ and } j = 1, 2, \dots, m + 1. \end{cases} \tag{12}$$

The horizontal edges for the generalized graph G_n^m under a k -labeling ϕ of type $(1, 1, 0)$ in different intervals of i and j can be defined as follows:

$$\phi(v_i^j v_{i+1}^j) = \begin{cases} 1 + \left\lfloor \frac{m+1}{3} \right\rfloor \left\lfloor \frac{i-1}{2} \right\rfloor, & \text{for } i = 1, 2, 3, \dots, 2 \left\lceil \frac{k}{\lfloor (m+1)/3 \rfloor} \right\rceil \text{ and } j = 1, 2, \dots, m, \\ k, & \text{for } i = 2 \left\lceil \frac{k}{\lfloor (m+1)/3 \rfloor} \right\rceil + 1, \dots, n + 1 \text{ and } j = 1, 2, \dots, m. \end{cases} \tag{13}$$

The vertical edges for the generalized graph G_n^m under a k -labeling ϕ of type $(1, 1, 0)$ in different intervals of i and j can be defined as follows:

$$\begin{aligned}
 \phi(v_i^j v_{i+1}^j) &= \left\{ \begin{aligned} &\left\lfloor \frac{j}{2} \right\rfloor, \quad \text{for } i = 1, 2, \dots, 2 \left\lfloor \frac{k}{\lfloor (m+1)/3 \rfloor} \right\rfloor - 1 \text{ and } j = 1, 2, \dots, m+1, \\ &\left\lfloor \frac{j}{2} \right\rfloor + \left\lfloor \frac{1}{2} \left(m - 3k + 3 + 3 \left\lfloor \frac{m+1}{3} \right\rfloor \left(\left\lfloor \frac{k}{\lfloor (m+1)/3 \rfloor} \right\rfloor - 1 \right) \right) \right\rfloor \left\lfloor \frac{1}{2} \left(i - 2 \left\lfloor \frac{k}{\lfloor (m+1)/3 \rfloor} \right\rfloor + 1 \right) \right\rfloor \\ &\quad \text{for } i = 2 \left\lfloor \frac{k}{\lfloor (m+1)/3 \rfloor} \right\rfloor, 2 \left\lfloor \frac{k}{\lfloor (m+1)/3 \rfloor} \right\rfloor + 1 \text{ and } j = 1, 3, \dots, m; m \equiv 1 \pmod{2} \\ &+ \left\lfloor \frac{1}{2} \left(m - 3k + 3 + 3 \left\lfloor \frac{m+1}{3} \right\rfloor \left(\left\lfloor \frac{k}{\lfloor (m+1)/3 \rfloor} \right\rfloor - 1 \right) \right) \right\rfloor \left\lfloor \frac{1}{2} \left(i - 2 \left\lfloor \frac{k}{\lfloor (m+1)/3 \rfloor} \right\rfloor + 1 \right) \right\rfloor \\ &\quad \text{or } j = 1, 3, \dots, m+1; m \equiv 0 \pmod{2}, \\ &\left\lfloor \frac{j}{2} \right\rfloor + \left\lfloor \frac{1}{2} \left(m - 3k + 3 + 3 \left\lfloor \frac{m+1}{3} \right\rfloor \left(\left\lfloor \frac{k}{\lfloor (m+1)/3 \rfloor} \right\rfloor - 1 \right) \right) \right\rfloor \left\lfloor \frac{1}{2} \left(i - 2 \left\lfloor \frac{k}{\lfloor (m+1)/3 \rfloor} \right\rfloor + 1 \right) \right\rfloor \\ &\quad \text{for } i = 2 \left\lfloor \frac{k}{\lfloor (m+1)/3 \rfloor} \right\rfloor, 2 \left\lfloor \frac{k}{\lfloor (m+1)/3 \rfloor} \right\rfloor + 1 \text{ and } j = 2, 4, \dots, m+1; m \equiv 1 \pmod{2} \\ &+ \left\lfloor \frac{1}{2} \left(m - 3k + 3 + 3 \left\lfloor \frac{m+1}{3} \right\rfloor \left(\left\lfloor \frac{k}{\lfloor (m+1)/3 \rfloor} \right\rfloor - 1 \right) \right) \right\rfloor \left\lfloor \frac{1}{2} \left(i - 2 \left\lfloor \frac{k}{\lfloor (m+1)/3 \rfloor} \right\rfloor + 1 \right) \right\rfloor \\ &\quad \text{or } j = 2, 4, \dots, m; m \equiv 0 \pmod{2}, \\ &\left\lfloor \frac{j}{2} \right\rfloor + \left(m - 3k + 3 + 3 \left\lfloor \frac{m+1}{3} \right\rfloor \left(\left\lfloor \frac{k}{\lfloor (m+1)/3 \rfloor} \right\rfloor - 1 \right) \right) \\ &\quad \text{for } i = 2 \left\lfloor \frac{k}{\lfloor (m+1)/3 \rfloor} \right\rfloor + 2, \dots, n \text{ and } j = 1, 3, \dots, m; m \equiv 1 \pmod{2} \\ &+ \left\lfloor \frac{m}{2} \right\rfloor \left\lfloor \frac{1}{2} \left(i - 2 \left\lfloor \frac{k}{\lfloor (m+1)/3 \rfloor} \right\rfloor - 1 \right) \right\rfloor + \left\lfloor \frac{m}{2} \right\rfloor \left\lfloor \frac{1}{2} \left(i - 2 \left\lfloor \frac{k}{\lfloor (m+1)/3 \rfloor} \right\rfloor - 1 \right) \right\rfloor, \\ &\quad \text{or } j = 1, 3, \dots, m+1; m \equiv 0 \pmod{2}, \\ &\left\lfloor \frac{j}{2} \right\rfloor + \left(m - 3k + 3 + 3 \left\lfloor \frac{m+1}{3} \right\rfloor \left(\left\lfloor \frac{k}{\lfloor (m+1)/3 \rfloor} \right\rfloor - 1 \right) \right) \\ &\quad \text{for } i = 2 \left\lfloor \frac{k}{\lfloor (m+1)/3 \rfloor} \right\rfloor + 2, \dots, n \text{ and } j = 2, 4, \dots, m+1; m \equiv 1 \pmod{2} \\ &+ \left\lfloor \frac{m}{2} \right\rfloor \left\lfloor \frac{1}{2} \left(i - 2 \left\lfloor \frac{k}{\lfloor (m+1)/3 \rfloor} \right\rfloor - 1 \right) \right\rfloor + \left\lfloor \frac{m}{2} \right\rfloor \left\lfloor \frac{1}{2} \left(i - 2 \left\lfloor \frac{k}{\lfloor (m+1)/3 \rfloor} \right\rfloor - 1 \right) \right\rfloor, \\ &\quad \text{or } j = 2, 4, \dots, m; m \equiv 0 \pmod{2}. \end{aligned} \right. \tag{14}
 \end{aligned}$$

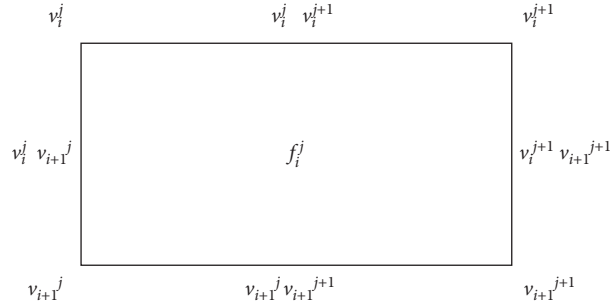
Figure 1 represents the generalized formula for face weights. The generalization of weights over the face f under

a k -labeling ϕ of type $(1, 1, 0)$ for the graph G_n^m can be defined as follows:

$$\begin{aligned}
 \text{Wt}_{(1,1,0)}(f_i^j) &= \sum_{v \sim f_i^j} f(v) + \sum_{e \sim f_i^j} f(e) = \phi(v_i^j) + \phi(v_i^{j+1}) + \phi(v_{i+1}^j) + \phi(v_{i+1}^{j+1}) + \phi(v_i^j v_{i+1}^{j+1}) \\ &\quad + \phi(v_i^j v_{i+1}^j) + \phi(v_{i+1}^j v_{i+1}^{j+1}) + \phi(v_i^{j+1} v_{i+1}^{j+1}). \tag{15}
 \end{aligned}$$

Horizontal differences in weights among different intervals of i and j can be calculated as follows:

$$\begin{aligned}
 &\text{For } i = 1, 2, 3, \dots, 2 \left\lfloor \frac{k}{\lfloor (m+1)/3 \rfloor} \right\rfloor - 2 \text{ and } j = 1, 2, \dots, m+1, \\
 \text{Wt}_{(1,1,0)}(f_i^{j+1}) - \text{Wt}_{(1,1,0)}(f_i^j) &= \phi(v_i^{j+1}) + \phi(v_i^{j+2}) + \phi(v_{i+1}^{j+1}) + \phi(v_{i+1}^{j+2}) + \phi(v_i^{j+1} v_{i+1}^{j+1}) \\ &\quad + \phi(v_{i+1}^{j+1} v_{i+1}^{j+2}) + \phi(v_i^{j+2} v_{i+1}^{j+2}) - \phi(v_i^j) - \phi(v_i^{j+1}) - \phi(v_{i+1}^j) - \phi(v_{i+1}^{j+1}) - \phi(v_i^j v_{i+1}^{j+1}) \\ &\quad - \phi(v_{i+1}^j v_{i+1}^{j+1}) - \phi(v_i^{j+1} v_{i+1}^{j+1}) \\ &= 1 + \left\lfloor \frac{m+1}{3} \right\rfloor \left\lfloor \frac{i-1}{2} \right\rfloor + 1 + \left\lfloor \frac{m+1}{3} \right\rfloor \left\lfloor \frac{i}{2} \right\rfloor + 1 + \left\lfloor \frac{m+1}{3} \right\rfloor \left\lfloor \frac{i-1}{2} \right\rfloor + 1 + \left\lfloor \frac{m+1}{3} \right\rfloor \left\lfloor \frac{i}{2} \right\rfloor + \left\lfloor \frac{j+2}{2} \right\rfloor - 1 \\ &\quad - \left\lfloor \frac{m+1}{3} \right\rfloor \left\lfloor \frac{i-1}{2} \right\rfloor - 1 - \left\lfloor \frac{m+1}{3} \right\rfloor \left\lfloor \frac{i}{2} \right\rfloor - 1 - \left\lfloor \frac{m+1}{3} \right\rfloor \left\lfloor \frac{i-1}{2} \right\rfloor - \left\lfloor \frac{j}{2} \right\rfloor - 1 - \left\lfloor \frac{m+1}{3} \right\rfloor \left\lfloor \frac{i}{2} \right\rfloor \\ &= \left\lfloor \frac{j+2}{2} \right\rfloor - \left\lfloor \frac{j}{2} \right\rfloor
 \end{aligned}$$

FIGURE 1: Construction of weights over the face f under k -labeling of type $(1, 1, 0)$.

$= 1$, for every value of j ,

For $i = 2 \left\lfloor \frac{k}{\lfloor (m+1)/3 \rfloor} \right\rfloor - 1$ and $j = 1, 2, \dots, m+1$,

$$\begin{aligned}
\text{Wt}_{(1,1,0)}(f_i^{j+1}) - \text{Wt}_{(1,1,0)}(f_i^j) &= \phi(v_i^{j+1}) + \phi(v_i^{j+2}) + \phi(v_{i+1}^{j+1}) + \phi(v_{i+1}^{j+2}) + \phi(v_i^{j+1} v_i^{j+2}) + \phi(v_i^{j+1} v_{i+1}^{j+1}) \\
&\quad + \phi(v_{i+1}^{j+1} v_{i+1}^{j+2}) + \phi(v_i^{j+2} v_{i+1}^{j+2}) - \phi(v_i^j) - \phi(v_i^{j+1}) - \phi(v_{i+1}^j) - \phi(v_{i+1}^{j+1}) - \phi(v_i^j v_{i+1}^j) \\
&\quad - \phi(v_{i+1}^j v_{i+1}^{j+1}) - \phi(v_i^{j+1} v_{i+1}^{j+1}) \\
&= 1 + \left\lfloor \frac{m+1}{3} \right\rfloor \left\lfloor \frac{i-1}{2} \right\rfloor + 1 + \left\lfloor \frac{m+1}{3} \right\rfloor \left\lfloor \frac{i}{2} \right\rfloor + 1 + \left\lfloor \frac{m+1}{3} \right\rfloor \left\lfloor \frac{i-1}{2} \right\rfloor + 1 + \left\lfloor \frac{m+1}{3} \right\rfloor \left\lfloor \frac{i}{2} \right\rfloor + \left\lfloor \frac{j+2}{2} \right\rfloor - 1 \\
&\quad - \left\lfloor \frac{m+1}{3} \right\rfloor \left\lfloor \frac{i-1}{2} \right\rfloor - 1 - \left\lfloor \frac{m+1}{3} \right\rfloor \left\lfloor \frac{i}{2} \right\rfloor - 1 - \left\lfloor \frac{m+1}{3} \right\rfloor \left\lfloor \frac{i-1}{2} \right\rfloor - \left\lfloor \frac{j}{2} \right\rfloor - 1 - \left\lfloor \frac{m+1}{3} \right\rfloor \left\lfloor \frac{i}{2} \right\rfloor \\
&= \left\lfloor \frac{j+2}{2} \right\rfloor - \left\lfloor \frac{j}{2} \right\rfloor \\
&= 1, \text{ for all values of } j,
\end{aligned}$$

For $i = 2 \left\lfloor \frac{k}{\lfloor (m+1)/3 \rfloor} \right\rfloor$ and $j = 1, 2, \dots, m+1$,

$$\begin{aligned}
\text{Wt}_{(1,1,0)}(f_i^{j+1}) - \text{Wt}_{(1,1,0)}(f_i^j) &= \phi(v_i^{j+1}) + \phi(v_i^{j+2}) + \phi(v_{i+1}^{j+1}) + \phi(v_{i+1}^{j+2}) + \phi(v_i^{j+1} v_i^{j+2}) + \phi(v_i^{j+1} v_{i+1}^{j+1}) \\
&\quad + \phi(v_{i+1}^{j+1} v_{i+1}^{j+2}) + \phi(v_i^{j+2} v_{i+1}^{j+2}) - \phi(v_i^j) - \phi(v_i^{j+1}) - \phi(v_{i+1}^j) - \phi(v_{i+1}^{j+1}) - \phi(v_i^j v_{i+1}^j) \\
&\quad - \phi(v_{i+1}^j v_{i+1}^{j+1}) - \phi(v_i^{j+1} v_{i+1}^{j+1}),
\end{aligned}$$

$$\begin{aligned}
\text{Wt}_{(1,1,0)}(f_i^{j+1}) - \text{Wt}_{(1,1,0)}(f_i^j) &= 1 + \left\lfloor \frac{m+1}{3} \right\rfloor \left\lfloor \frac{i-1}{2} \right\rfloor + k + 1 + \left\lfloor \frac{m+1}{3} \right\rfloor \left\lfloor \frac{i-1}{2} \right\rfloor + k + \left\lfloor \frac{j+2}{2} \right\rfloor \\
&\quad + \left[\frac{1}{2} \left(m - 3k + 3 + 3 \left\lfloor \frac{m+1}{3} \right\rfloor \right) \left(\left\lfloor \frac{k}{\lfloor (m+1)/3 \rfloor} \right\rfloor - 1 \right) \right] \left[\frac{1}{2} \left(i + 1 - 2 \left\lfloor \frac{k}{\lfloor (m+1)/3 \rfloor} \right\rfloor + 1 \right) \right] \\
&\quad + \left[\frac{1}{2} \left(m - 3k + 3 + 3 \left\lfloor \frac{m+1}{3} \right\rfloor \right) \left(\left\lfloor \frac{k}{\lfloor (m+1)/3 \rfloor} \right\rfloor - 1 \right) \right] \left[\frac{1}{2} \left(i + 1 - 2 \left\lfloor \frac{k}{\lfloor (m+1)/3 \rfloor} \right\rfloor + 1 \right) \right] \\
&\quad - 1 - \left\lfloor \frac{m+1}{3} \right\rfloor \left\lfloor \frac{i-1}{2} \right\rfloor - k - 1 - \left\lfloor \frac{m+1}{3} \right\rfloor \left\lfloor \frac{i-1}{2} \right\rfloor - \left\lfloor \frac{j}{2} \right\rfloor \\
&\quad - \left[\frac{1}{2} \left(m - 3k + 3 + 3 \left\lfloor \frac{m+1}{3} \right\rfloor \right) \left(\left\lfloor \frac{k}{\lfloor (m+1)/3 \rfloor} \right\rfloor - 1 \right) \right] \left[\frac{1}{2} \left(i - 2 \left\lfloor \frac{k}{\lfloor (m+1)/3 \rfloor} \right\rfloor + 1 \right) \right]
\end{aligned}$$

$$\begin{aligned}
& - \left\lceil \frac{1}{2} \left(m - 3k + 3 + 3 \left\lfloor \frac{m+1}{3} \right\rfloor \left(\left\lceil \frac{k}{\lfloor (m+1)/3 \rfloor} \right\rceil - 1 \right) \right) \right\rceil \left\lceil \frac{1}{2} \left(i - 2 \left\lfloor \frac{k}{\lfloor (m+1)/3 \rfloor} \right\rfloor + 1 \right) \right\rceil - k \\
& = \left\lceil \frac{j+2}{2} \right\rceil + \left\lceil \frac{1}{2} \left(m - 3k + 3 + 3 \left\lfloor \frac{m+1}{3} \right\rfloor \right) \left(\left\lceil \frac{k}{\lfloor (m+1)/3 \rfloor} \right\rceil - 1 \right) \right\rceil (1) + 0 - \left\lfloor \frac{j}{2} \right\rfloor \\
& \quad - \left\lceil \frac{1}{2} \left(m - 3k + 3 + 3 \left\lfloor \frac{m+1}{3} \right\rfloor \right) \left(\left\lceil \frac{k}{\lfloor (m+1)/3 \rfloor} \right\rceil - 1 \right) \right\rceil (1) - 0 \\
& = \left\lceil \frac{j+2}{2} \right\rceil - \left\lfloor \frac{j}{2} \right\rfloor \\
& = 1, \quad \text{for all } j = 1, 2, \dots, m+1,
\end{aligned}$$

For $i = 2 \left\lceil \frac{k}{\lfloor (m+1)/3 \rfloor} \right\rceil + 1$ and $j = 1, 3, \dots, m; m \equiv 1 \pmod{2}$ or $j = 1, 3, \dots, m+1; m \equiv 0 \pmod{2}$,

$$\begin{aligned}
\text{Wt}_{(1,1,0)}(f_i^{j+1}) - \text{Wt}_{(1,1,0)}(f_i^j) &= \phi(v_i^{j+1}) + \phi(v_i^{j+2}) + \phi(v_{i+1}^{j+1}) + \phi(v_{i+1}^{j+2}) + \phi(v_i^{j+1} v_{i+1}^{j+2}) + \phi(v_i^{j+1} v_{i+1}^{j+1}) \\
& \quad + \phi(v_{i+1}^{j+1} v_{i+1}^{j+2}) + \phi(v_i^{j+2} v_{i+1}^{j+2}) - \phi(v_i^j) - \phi(v_i^{j+1}) - \phi(v_{i+1}^j) - \phi(v_{i+1}^{j+1}) - \phi(v_i^j v_{i+1}^{j+1}) - \phi(v_i^j v_{i+1}^j) \\
& \quad - \phi(v_{i+1}^j v_{i+1}^{j+1}) - \phi(v_i^{j+1} v_{i+1}^{j+1}),
\end{aligned}$$

$$\begin{aligned}
\text{Wt}_{(1,1,0)}(f_i^{j+1}) - \text{Wt}_{(1,1,0)}(f_i^j) &= k + k + k + k + \left\lceil \frac{j+2}{2} \right\rceil \\
& \quad + \left\lceil \frac{1}{2} \left(m - 3k + 3 + 3 \left\lfloor \frac{m+1}{3} \right\rfloor \right) \left(\left\lceil \frac{k}{\lfloor (m+1)/3 \rfloor} \right\rceil - 1 \right) \right\rceil \left\lceil \frac{1}{2} \left(i - 2 \left\lfloor \frac{k}{\lfloor (m+1)/3 \rfloor} \right\rfloor + 1 \right) \right\rceil \\
& \quad + \left\lceil \frac{1}{2} \left(m - 3k + 3 + 3 \left\lfloor \frac{m+1}{3} \right\rfloor \right) \left(\left\lceil \frac{k}{\lfloor (m+1)/3 \rfloor} \right\rceil - 1 \right) \right\rceil \left\lceil \frac{1}{2} \left(i - 2 \left\lfloor \frac{k}{\lfloor (m+1)/3 \rfloor} \right\rfloor + 1 \right) \right\rceil \\
& \quad - k - k - k - k - \left\lfloor \frac{j}{2} \right\rfloor \\
& \quad - \left\lceil \frac{1}{2} \left(m - 3k + 3 + 3 \left\lfloor \frac{m+1}{3} \right\rfloor \right) \left(\left\lceil \frac{k}{\lfloor (m+1)/3 \rfloor} \right\rceil - 1 \right) \right\rceil \left\lceil \frac{1}{2} \left(i - 2 \left\lfloor \frac{k}{\lfloor (m+1)/3 \rfloor} \right\rfloor + 1 \right) \right\rceil \\
& \quad - \left\lceil \frac{1}{2} \left(m - 3k + 3 + 3 \left\lfloor \frac{m+1}{3} \right\rfloor \right) \left(\left\lceil \frac{k}{\lfloor (m+1)/3 \rfloor} \right\rceil - 1 \right) \right\rceil \left\lceil \frac{1}{2} \left(i - 2 \left\lfloor \frac{k}{\lfloor (m+1)/3 \rfloor} \right\rfloor + 1 \right) \right\rceil \\
& = \left\lceil \frac{j+2}{2} \right\rceil - \left\lfloor \frac{j}{2} \right\rfloor \\
& = 1, \quad \text{for every odd value of } j,
\end{aligned}$$

For $i = 2 \left\lceil \frac{k}{\lfloor (m+1)/3 \rfloor} \right\rceil + 1$ and $j = 2, 4, \dots, m+1; m \equiv 1 \pmod{2}$ or $j = 2, 4, \dots, m; m \equiv 0 \pmod{2}$,

$$\begin{aligned}
\text{Wt}_{(1,1,0)}(f_i^{j+1}) - \text{Wt}_{(1,1,0)}(f_i^j) &= \phi(v_i^{j+1}) + \phi(v_i^{j+2}) + \phi(v_{i+1}^{j+1}) + \phi(v_{i+1}^{j+2}) + \phi(v_i^{j+1} v_{i+1}^{j+2}) + \phi(v_i^{j+1} v_{i+1}^{j+1}) \\
& \quad + \phi(v_{i+1}^{j+1} v_{i+1}^{j+2}) + \phi(v_i^{j+2} v_{i+1}^{j+2}) - \phi(v_i^j) - \phi(v_i^{j+1}) - \phi(v_{i+1}^j) - \phi(v_{i+1}^{j+1}) - \phi(v_i^j v_{i+1}^{j+1}) - \phi(v_i^j v_{i+1}^j) \\
& \quad - \phi(v_{i+1}^j v_{i+1}^{j+1}) - \phi(v_i^{j+1} v_{i+1}^{j+1}),
\end{aligned}$$

$$\text{Wt}_{(1,1,0)}(f_i^{j+1}) - \text{Wt}_{(1,1,0)}(f_i^j) = k + k + k + k + \left\lceil \frac{j+2}{2} \right\rceil$$

$$\begin{aligned}
& + \left[\frac{1}{2} \left(m - 3k + 3 + 3 \left\lfloor \frac{m+1}{3} \right\rfloor \right) \left(\left\lfloor \frac{k}{\lfloor (m+1)/3 \rfloor} \right\rfloor - 1 \right) \right] \left[\frac{1}{2} \left(i - 2 \left\lfloor \frac{k}{\lfloor (m+1)/3 \rfloor} \right\rfloor + 1 \right) \right] \\
& + \left[\frac{1}{2} \left(m - 3k + 3 + 3 \left\lfloor \frac{m+1}{3} \right\rfloor \right) \left(\left\lfloor \frac{k}{\lfloor (m+1)/3 \rfloor} \right\rfloor - 1 \right) \right] \left[\frac{1}{2} \left(i - 2 \left\lfloor \frac{k}{\lfloor (m+1)/3 \rfloor} \right\rfloor + 1 \right) \right] \\
& - k - k - k - k - \left\lfloor \frac{j}{2} \right\rfloor \\
& - \left[\frac{1}{2} \left(m - 3k + 3 + 3 \left\lfloor \frac{m+1}{3} \right\rfloor \right) \left(\left\lfloor \frac{k}{\lfloor (m+1)/3 \rfloor} \right\rfloor - 1 \right) \right] \left[\frac{1}{2} \left(i - 2 \left\lfloor \frac{k}{\lfloor (m+1)/3 \rfloor} \right\rfloor + 1 \right) \right] \\
& - \left[\frac{1}{2} \left(m - 3k + 3 + 3 \left\lfloor \frac{m+1}{3} \right\rfloor \right) \left(\left\lfloor \frac{k}{\lfloor (m+1)/3 \rfloor} \right\rfloor - 1 \right) \right] \left[\frac{1}{2} \left(i - 2 \left\lfloor \frac{k}{\lfloor (m+1)/3 \rfloor} \right\rfloor + 1 \right) \right] \\
& = \left\lfloor \frac{j+2}{2} \right\rfloor - \left\lfloor \frac{j}{2} \right\rfloor \\
& = 1, \quad \text{for every even value of } j,
\end{aligned}$$

For $i = 2 \left\lfloor \frac{k}{\lfloor (m+1)/3 \rfloor} \right\rfloor + 2, \dots, n; j = 1, 3, \dots, m; m \equiv 1 \pmod{2}$ OR $j = 1, 3, \dots, m+1; m \equiv 0 \pmod{2}$,

$$\begin{aligned}
\text{Wt}_{(1,1,0)}(f_i^{j+1}) - \text{Wt}_{(1,1,0)}(f_i^j) &= \phi(v_i^{j+1}) + \phi(v_i^{j+2}) + \phi(v_{i+1}^{j+1}) + \phi(v_{i+1}^{j+2}) + \phi(v_i^{j+1} v_{i+1}^{j+2}) + \phi(v_i^{j+1} v_{i+1}^j) \\
&+ \phi(v_{i+1}^{j+1} v_{i+1}^{j+2}) + \phi(v_i^{j+2} v_{i+1}^{j+2}) - \phi(v_i^j) - \phi(v_i^{j+1}) - \phi(v_{i+1}^j) - \phi(v_{i+1}^{j+1}) - \phi(v_i^j v_{i+1}^{j+1}) - \phi(v_i^j v_{i+1}^j) \\
&- \phi(v_{i+1}^j v_{i+1}^{j+1}) - \phi(v_i^{j+1} v_{i+1}^{j+1}),
\end{aligned}$$

$$\begin{aligned}
\text{Wt}_{(1,1,0)}(f_i^{j+1}) - \text{Wt}_{(1,1,0)}(f_i^j) &= k + k + k + k + \left\lfloor \frac{j+2}{2} \right\rfloor + \left(m - 3k + 3 + 3 \left\lfloor \frac{m+1}{3} \right\rfloor \right) \left(\left\lfloor \frac{k}{\lfloor (m+1)/3 \rfloor} \right\rfloor - 1 \right) \\
&+ \left\lfloor \frac{m}{2} \right\rfloor \left[\frac{1}{2} \left(i - 2 \left\lfloor \frac{k}{\lfloor (m+1)/3 \rfloor} \right\rfloor - 1 \right) \right] + \left\lfloor \frac{m}{2} \right\rfloor \left[\frac{1}{2} \left(i - 2 \left\lfloor \frac{k}{\lfloor (m+1)/3 \rfloor} \right\rfloor - 1 \right) \right] - k - k - k - k - \left\lfloor \frac{j}{2} \right\rfloor \\
&- \left(m - 3k + 3 + 3 \left\lfloor \frac{m+1}{3} \right\rfloor \right) \left(\left\lfloor \frac{k}{\lfloor (m+1)/3 \rfloor} \right\rfloor - 1 \right) - \left\lfloor \frac{m}{2} \right\rfloor \left[\frac{1}{2} \left(i - 2 \left\lfloor \frac{k}{\lfloor (m+1)/3 \rfloor} \right\rfloor - 1 \right) \right] \\
&- \left\lfloor \frac{m}{2} \right\rfloor \left[\frac{1}{2} \left(i - 2 \left\lfloor \frac{k}{\lfloor (m+1)/3 \rfloor} \right\rfloor - 1 \right) \right] \\
&= \left\lfloor \frac{j+2}{2} \right\rfloor - \left\lfloor \frac{j}{2} \right\rfloor \\
&= 1, \quad \text{for all odd values of } j,
\end{aligned}$$

For $i = 2 \left\lfloor \frac{k}{\lfloor (m+1)/3 \rfloor} \right\rfloor + 2, \dots, n; j = 2, 4, \dots, m+1; m \equiv 1 \pmod{2}$ OR $j = 2, 4, \dots, m; m \equiv 0 \pmod{2}$,

$$\begin{aligned}
\text{Wt}_{(1,1,0)}(f_i^{j+1}) - \text{Wt}_{(1,1,0)}(f_i^j) &= \phi(v_i^{j+1}) + \phi(v_i^{j+2}) + \phi(v_{i+1}^{j+1}) + \phi(v_{i+1}^{j+2}) + \phi(v_i^{j+1} v_{i+1}^{j+2}) + \phi(v_i^{j+1} v_{i+1}^j) \\
&+ \phi(v_{i+1}^{j+1} v_{i+1}^{j+2}) + \phi(v_i^{j+2} v_{i+1}^{j+2}) - \phi(v_i^j) - \phi(v_i^{j+1}) - \phi(v_{i+1}^j) - \phi(v_{i+1}^{j+1}) - \phi(v_i^j v_{i+1}^{j+1}) - \phi(v_i^j v_{i+1}^j) \\
&- \phi(v_{i+1}^j v_{i+1}^{j+1}) - \phi(v_i^{j+1} v_{i+1}^{j+1}),
\end{aligned}$$

$$\text{Wt}_{(1,1,0)}(f_i^{j+1}) - \text{Wt}_{(1,1,0)}(f_i^j) = k + k + k + k + \left\lfloor \frac{j+2}{2} \right\rfloor + \left(m - 3k + 3 + 3 \left\lfloor \frac{m+1}{3} \right\rfloor \right) \left(\left\lfloor \frac{k}{\lfloor (m+1)/3 \rfloor} \right\rfloor - 1 \right)$$

$$\begin{aligned}
& + \left\lfloor \frac{m}{2} \right\rfloor \left\lfloor \frac{1}{2} \left(i - 2 \left\lfloor \frac{k}{\lfloor (m+1)/3 \rfloor} \right\rfloor - 1 \right) \right\rfloor + \left\lfloor \frac{m}{2} \right\rfloor \left\lfloor \frac{1}{2} \left(i - 2 \left\lfloor \frac{k}{\lfloor (m+1)/3 \rfloor} \right\rfloor - 1 \right) \right\rfloor - k - k - k - k - \left\lfloor \frac{j}{2} \right\rfloor \\
& - \left(m - 3k + 3 + 3 \left\lfloor \frac{m+1}{3} \right\rfloor \left(\left\lfloor \frac{k}{\lfloor (m+1)/3 \rfloor} \right\rfloor - 1 \right) \right) - \left\lfloor \frac{m}{2} \right\rfloor \left\lfloor \frac{1}{2} \left(i - 2 \left\lfloor \frac{k}{\lfloor (m+1)/3 \rfloor} \right\rfloor - 1 \right) \right\rfloor \\
& - \left\lfloor \frac{m}{2} \right\rfloor \left\lfloor \frac{1}{2} \left(i - 2 \left\lfloor \frac{k}{\lfloor (m+1)/3 \rfloor} \right\rfloor - 1 \right) \right\rfloor \\
& = \left\lfloor \frac{j+2}{2} \right\rfloor - \left\lfloor \frac{j}{2} \right\rfloor \\
& = 1, \quad \text{for all even values of } j.
\end{aligned}$$

(16)

Vertical differences in weights among different intervals of i and j can be calculated as follows:

$$\text{For } i = 1, 2, \dots, 2 \left\lfloor \frac{k}{\lfloor (m+1)/3 \rfloor} \right\rfloor - 2 \text{ and } j = 1, 2, \dots, m+1,$$

$$\begin{aligned}
\text{Wt}_{(1,1,0)}(f_{i+1}^j) - \text{Wt}_{(1,1,0)}(f_i^j) &= \phi(v_{i+1}^j) + \phi(v_{i+1}^{j+1}) + \phi(v_{i+2}^j) + \phi(v_{i+2}^{j+1}) + \phi(v_{i+1}^j v_{i+1}^{j+1}) + \phi(v_{i+1}^j v_{i+2}^j) \\
&+ \phi(v_{i+2}^j v_{i+2}^{j+1}) + \phi(v_{i+1}^{j+1} v_{i+2}^{j+1}) - \phi(v_i^j) - \phi(v_i^{j+1}) - \phi(v_{i+1}^j) - \phi(v_{i+1}^{j+1}) - \phi(v_i^j v_i^{j+1}) - \phi(v_i^j v_{i+1}^j) \\
&- \phi(v_{i+1}^j v_{i+1}^{j+1}) - \phi(v_i^{j+1} v_{i+1}^{j+1}),
\end{aligned}$$

$$\begin{aligned}
\text{Wt}_{(1,1,0)}(f_{i+1}^j) - \text{Wt}_{(1,1,0)}(f_i^j) &= 1 + \left\lfloor \frac{m+1}{3} \right\rfloor \left\lfloor \frac{i+1}{2} \right\rfloor + 1 + \left\lfloor \frac{m+1}{3} \right\rfloor \left\lfloor \frac{i+1}{2} \right\rfloor + \left\lfloor \frac{j}{2} \right\rfloor + \left\lfloor \frac{j+1}{2} \right\rfloor + 1 \\
&+ \left\lfloor \frac{m+1}{3} \right\rfloor \left\lfloor \frac{i+1}{2} \right\rfloor - 1 - \left\lfloor \frac{m+1}{3} \right\rfloor \left\lfloor \frac{i-1}{2} \right\rfloor - 1 - \left\lfloor \frac{m+1}{3} \right\rfloor \left\lfloor \frac{i-1}{2} \right\rfloor - 1 - \left\lfloor \frac{m+1}{3} \right\rfloor \left\lfloor \frac{i-1}{2} \right\rfloor \\
&- \left\lfloor \frac{j}{2} \right\rfloor - \left\lfloor \frac{j+1}{2} \right\rfloor \\
&= 3 \left\lfloor \frac{m+1}{3} \right\rfloor \left\lfloor \frac{i+1}{2} \right\rfloor - 3 \left\lfloor \frac{m+1}{3} \right\rfloor \left\lfloor \frac{i-1}{2} \right\rfloor \\
&= 3 \left\lfloor \frac{m+1}{3} \right\rfloor \left(\left\lfloor \frac{i+1}{2} \right\rfloor - \left\lfloor \frac{i-1}{2} \right\rfloor \right) \\
&= 3 \left\lfloor \frac{m+1}{3} \right\rfloor (1) \\
&= m,
\end{aligned}$$

$$\text{For } i = 2 \left\lfloor \frac{k}{\lfloor (m+1)/3 \rfloor} \right\rfloor - 1; j = 1, 2, \dots, m+1,$$

$$\begin{aligned}
\text{Wt}_{(1,1,0)}(f_{i+1}^j) - \text{Wt}_{(1,1,0)}(f_i^j) &= \phi(v_{i+1}^j) + \phi(v_{i+1}^{j+1}) + \phi(v_{i+2}^j) + \phi(v_{i+2}^{j+1}) + \phi(v_{i+1}^j v_{i+1}^{j+1}) + \phi(v_{i+1}^j v_{i+2}^j) \\
&+ \phi(v_{i+2}^j v_{i+2}^{j+1}) + \phi(v_{i+1}^{j+1} v_{i+2}^{j+1}) - \phi(v_i^j) - \phi(v_i^{j+1}) - \phi(v_{i+1}^j) - \phi(v_{i+1}^{j+1}) - \phi(v_i^j v_i^{j+1}) - \phi(v_i^j v_{i+1}^j)
\end{aligned}$$

$$\begin{aligned}
& -\phi(v_{i+1}^j v_{i+1}^{j+1}) - \phi(v_i^{j+1} v_{i+1}^{j+1}), \\
\text{Wt}_{(1,1,0)}(f_{i+1}^j) - \text{Wt}_{(1,1,0)}(f_i^j) &= k + k + k + \left\lfloor \frac{j}{2} \right\rfloor + \left\lfloor \frac{j+1}{2} \right\rfloor \\
& + \left\lfloor \frac{1}{2} \left(i + 1 - 2 \left\lfloor \frac{k}{\lfloor (m+1)/3 \rfloor} \right\rfloor + 1 \right) \right\rfloor \\
& \cdot \left(\left\lfloor \frac{1}{2} \left(m - 3k + 3 + 3 \left\lfloor \frac{m+1}{3} \right\rfloor \right) \left(\left\lfloor \frac{k}{\lfloor (m+1)/3 \rfloor} \right\rfloor - 1 \right) \right) \right\rfloor \\
& + \left\lfloor \frac{1}{2} \left(m - 3k + 3 + 3 \left\lfloor \frac{m+1}{3} \right\rfloor \right) \left(\left\lfloor \frac{k}{\lfloor (m+1)/3 \rfloor} \right\rfloor - 1 \right) \right\rfloor \\
& + \left\lfloor \frac{1}{2} \left(i + 1 - 2 \left\lfloor \frac{k}{\lfloor (m+1)/3 \rfloor} \right\rfloor + 1 \right) \right\rfloor \\
& \cdot \left(\left\lfloor \frac{1}{2} \left(m - 3k + 3 + 3 \left\lfloor \frac{m+1}{3} \right\rfloor \right) \left(\left\lfloor \frac{k}{\lfloor (m+1)/3 \rfloor} \right\rfloor - 1 \right) \right) \right\rfloor \\
& + \left\lfloor \frac{1}{2} \left(m - 3k + 3 + 3 \left\lfloor \frac{m+1}{3} \right\rfloor \right) \left(\left\lfloor \frac{k}{\lfloor (m+1)/3 \rfloor} \right\rfloor - 1 \right) \right\rfloor \\
& - 1 - \left\lfloor \frac{m+1}{3} \right\rfloor \left\lfloor \frac{i-1}{2} \right\rfloor - 1 - \left\lfloor \frac{m+1}{3} \right\rfloor \left\lfloor \frac{i-1}{2} \right\rfloor - 1 - \left\lfloor \frac{m+1}{3} \right\rfloor \left\lfloor \frac{i-1}{2} \right\rfloor - \left\lfloor \frac{j}{2} \right\rfloor - \left\lfloor \frac{j+1}{2} \right\rfloor \\
& = 3k + \left\lfloor \frac{1}{2} \left(i + 1 - 2 \left\lfloor \frac{k}{\lfloor (m+1)/3 \rfloor} \right\rfloor + 1 \right) \right\rfloor, \\
& \cdot \left(\left\lfloor \frac{(m - 3k + 3 + 3 \lfloor (m+1)/3 \rfloor) (\lfloor k/\lfloor (m+1)/3 \rfloor - 1)}{2} \right\rfloor \right) \\
& + \left\lfloor \frac{(m - 3k + 3 + 3 \lfloor (m+1)/3 \rfloor) (\lfloor k/\lfloor (m+1)/3 \rfloor - 1)}{2} \right\rfloor \\
& + \left\lfloor \frac{1}{2} (i + 1 - 2 \lfloor k/\lfloor (m+1)/3 \rfloor + 1) \right\rfloor \\
& \cdot \left(\left\lfloor \frac{(m - 3k + 3 + 3 \lfloor (m+1)/3 \rfloor) (\lfloor k/\lfloor (m+1)/3 \rfloor - 1)}{2} \right\rfloor \right) \\
& + \left\lfloor \frac{(m - 3k + 3 + 3 \lfloor (m+1)/3 \rfloor) (\lfloor k/\lfloor (m+1)/3 \rfloor - 1)}{2} \right\rfloor \\
& - 3 - 3 \left\lfloor \frac{m+1}{3} \right\rfloor \left\lfloor \frac{i-1}{2} \right\rfloor \\
& = 3k + (1) \left(m - 3k + 3 + 3 \left\lfloor \frac{m+1}{3} \right\rfloor \right) \left(\left\lfloor \frac{k}{\lfloor (m+1)/3 \rfloor} \right\rfloor - 1 \right) + 0 - 3 - 3 \left\lfloor \frac{m+1}{3} \right\rfloor \left\lfloor \frac{i-1}{2} \right\rfloor \\
& = 3k + m - 3k + 3 + 3 \left\lfloor \frac{m+1}{3} \right\rfloor \left\lfloor \frac{k}{\lfloor (m+1)/3 \rfloor} \right\rfloor - 3 \left\lfloor \frac{m+1}{3} \right\rfloor - 3 - 3 \left\lfloor \frac{m+1}{3} \right\rfloor \left\lfloor \frac{i-1}{2} \right\rfloor \\
& = m + 3 \left\lfloor \frac{m+1}{3} \right\rfloor \left(\left\lfloor \frac{k}{\lfloor (m+1)/3 \rfloor} \right\rfloor - 1 - \left\lfloor \frac{i-1}{2} \right\rfloor \right)
\end{aligned}$$

$$= m + 3 \left\lfloor \frac{m+1}{3} \right\rfloor \left(\left\lfloor \frac{k}{\lfloor (m+1)/3 \rfloor} \right\rfloor - 1 - \left\lfloor \left\lfloor \frac{k}{\lfloor (m+1)/3 \rfloor} \right\rfloor - 1 \right\rfloor \right) \\ = m,$$

$$\text{For } i = 2 \left\lfloor \frac{k}{\lfloor (m+1)/3 \rfloor} \right\rfloor; j = 1, 2, \dots, m+1,$$

$$\text{Wt}_{(1,1,0)}(f_{i+1}^j) - \text{Wt}_{(1,1,0)}(f_i^j) = \phi(v_{i+1}^j) + \phi(v_{i+1}^{j+1}) + \phi(v_{i+2}^j) + \phi(v_{i+2}^{j+1}) + \phi(v_{i+1}^j v_{i+1}^{j+1}) + \phi(v_{i+1}^j v_{i+2}^j) \\ + \phi(v_{i+2}^j v_{i+2}^{j+1}) + \phi(v_{i+1}^{j+1} v_{i+2}^{j+1}) - \phi(v_i^j) - \phi(v_i^{j+1}) - \phi(v_{i+1}^j) - \phi(v_{i+1}^{j+1}) - \phi(v_i^j v_{i+1}^j) - \phi(v_i^j v_{i+1}^{j+1}) \\ - \phi(v_{i+1}^j v_{i+1}^{j+1}) - \phi(v_i^{j+1} v_{i+1}^{j+1}),$$

$$\text{Wt}_{(1,1,0)}(f_{i+1}^j) - \text{Wt}_{(1,1,0)}(f_i^j) = k + k + k + \left\lfloor \frac{j}{2} \right\rfloor + \left\lfloor \frac{j+1}{2} \right\rfloor \\ + \left\lfloor \frac{1}{2} \left(i + 1 - 2 \left\lfloor \frac{k}{\lfloor (m+1)/3 \rfloor} \right\rfloor + 1 \right) \right\rfloor \\ \cdot \left(\left\lfloor \frac{1}{2} \left(m - 3k + 3 + 3 \left\lfloor \frac{m+1}{3} \right\rfloor \left(\left\lfloor \frac{k}{\lfloor (m+1)/3 \rfloor} \right\rfloor - 1 \right) \right) \right\rfloor \right) \\ + \left\lfloor \frac{1}{2} \left(m - 3k + 3 + 3 \left\lfloor \frac{m+1}{3} \right\rfloor \left(\left\lfloor \frac{k}{\lfloor (m+1)/3 \rfloor} \right\rfloor - 1 \right) \right) \right\rfloor \\ + \left\lfloor \frac{1}{2} \left(i + 1 - 2 \left\lfloor \frac{k}{\lfloor (m+1)/3 \rfloor} \right\rfloor + 1 \right) \right\rfloor \\ \cdot \left(\left\lfloor \frac{1}{2} \left(m - 3k + 3 + 3 \left\lfloor \frac{m+1}{3} \right\rfloor \left(\left\lfloor \frac{k}{\lfloor (m+1)/3 \rfloor} \right\rfloor - 1 \right) \right) \right\rfloor \right) \\ + \left\lfloor \frac{1}{2} \left(m - 3k + 3 + 3 \left\lfloor \frac{m+1}{3} \right\rfloor \left(\left\lfloor \frac{k}{\lfloor (m+1)/3 \rfloor} \right\rfloor - 1 \right) \right) \right\rfloor \\ - 1 - \left\lfloor \frac{m+1}{3} \right\rfloor \left\lfloor \frac{i-1}{2} \right\rfloor - 1 - \left\lfloor \frac{m+1}{3} \right\rfloor \left\lfloor \frac{i-1}{2} \right\rfloor - 1 - \left\lfloor \frac{m+1}{3} \right\rfloor \left\lfloor \frac{i-1}{2} \right\rfloor - \left\lfloor \frac{j}{2} \right\rfloor - \left\lfloor \frac{j+1}{2} \right\rfloor \\ - \left\lfloor \frac{1}{2} \left(i - 2 \left\lfloor \frac{k}{\lfloor (m+1)/3 \rfloor} \right\rfloor + 1 \right) \right\rfloor \\ \cdot \left(\left\lfloor \frac{1}{2} \left(m - 3k + 3 + 3 \left\lfloor \frac{m+1}{3} \right\rfloor \left(\left\lfloor \frac{k}{\lfloor (m+1)/3 \rfloor} \right\rfloor - 1 \right) \right) \right\rfloor \right) \\ + \left\lfloor \frac{1}{2} \left(m - 3k + 3 + 3 \left\lfloor \frac{m+1}{3} \right\rfloor \left(\left\lfloor \frac{k}{\lfloor (m+1)/3 \rfloor} \right\rfloor - 1 \right) \right) \right\rfloor \\ - \left\lfloor \frac{1}{2} \left(i - 2 \left\lfloor \frac{k}{\lfloor (m+1)/3 \rfloor} \right\rfloor + 1 \right) \right\rfloor \\ \cdot \left(\left\lfloor \frac{1}{2} \left(m - 3k + 3 + 3 \left\lfloor \frac{m+1}{3} \right\rfloor \left(\left\lfloor \frac{k}{\lfloor (m+1)/3 \rfloor} \right\rfloor - 1 \right) \right) \right\rfloor \right) \\ + \left\lfloor \frac{1}{2} \left(m - 3k + 3 + 3 \left\lfloor \frac{m+1}{3} \right\rfloor \left(\left\lfloor \frac{k}{\lfloor (m+1)/3 \rfloor} \right\rfloor - 1 \right) \right) \right\rfloor$$

$$\begin{aligned}
&= 3k \\
&+ \left(\left[\frac{1}{2} \left(m - 3k + 3 + 3 \left\lfloor \frac{m+1}{3} \right\rfloor \left(\left\lceil \frac{k}{\lfloor (m+1)/3 \rfloor} \right\rceil - 1 \right) \right) \right] \right) \\
&+ \left[\frac{1}{2} \left(m - 3k + 3 + 3 \left\lfloor \frac{m+1}{3} \right\rfloor \left(\left\lceil \frac{k}{\lfloor (m+1)/3 \rfloor} \right\rceil - 1 \right) \right) \right] \\
&+ \left(\left[\frac{1}{2} \left(m - 3k + 3 + 3 \left\lfloor \frac{m+1}{3} \right\rfloor \left(\left\lceil \frac{k}{\lfloor (m+1)/3 \rfloor} \right\rceil - 1 \right) \right) \right] \right) \\
&+ \left[\frac{1}{2} \left(m - 3k + 3 + 3 \left\lfloor \frac{m+1}{3} \right\rfloor \left(\left\lceil \frac{k}{\lfloor (m+1)/3 \rfloor} \right\rceil - 1 \right) \right) \right] \\
&- 3 - 3 \left\lfloor \frac{m+1}{3} \right\rfloor \left\lfloor \frac{i-1}{2} \right\rfloor \\
&- \left(\left[\frac{1}{2} \left(m - 3k + 3 + 3 \left\lfloor \frac{m+1}{3} \right\rfloor \left(\left\lceil \frac{k}{\lfloor (m+1)/3 \rfloor} \right\rceil - 1 \right) \right) \right] \right) \\
&+ \left[\frac{1}{2} \left(m - 3k + 3 + 3 \left\lfloor \frac{m+1}{3} \right\rfloor \left(\left\lceil \frac{k}{\lfloor (m+1)/3 \rfloor} \right\rceil - 1 \right) \right) \right] \\
&= 3k + \left(\left[\frac{(m - 3k + 3 + 3 \lfloor m + 1/3 \rfloor (\lceil k/\lfloor (m+1)/3 \rfloor - 1))}{2} \right] \right) \\
&+ \left[\frac{(m - 3k + 3 + 3 \lfloor m + 1/3 \rfloor (\lceil k/\lfloor (m+1)/3 \rfloor - 1))}{2} \right] \\
&- 3 - 3 \left\lfloor \frac{m+1}{3} \right\rfloor \left\lfloor \frac{i-1}{2} \right\rfloor \\
&= 3k + m - 3k + 3 + 3 \left\lfloor \frac{m+1}{3} \right\rfloor \left(\left\lceil \frac{k}{\lfloor (m+1)/3 \rfloor} \right\rceil - 1 \right) - 3 - 3 \left\lfloor \frac{m+1}{3} \right\rfloor \left\lfloor \frac{i-1}{2} \right\rfloor \\
&= m + 3 \left\lfloor \frac{m+1}{3} \right\rfloor \left(\left\lceil \frac{k}{\lfloor (m+1)/3 \rfloor} \right\rceil - 1 - \left\lfloor \frac{i-1}{2} \right\rfloor \right) \\
&= m + 3 \left\lfloor \frac{m+1}{3} \right\rfloor \left(\left\lceil \frac{k}{\lfloor (m+1)/3 \rfloor} \right\rceil - 1 - \left\lfloor \frac{i-1}{2} \right\rfloor \right) \\
&= m,
\end{aligned}$$

$$\text{For } i = 2 \left\lceil \frac{k}{\lfloor (m+1)/3 \rfloor} \right\rceil + 1; j = 1, 2, \dots, m+1,$$

$$\begin{aligned}
\text{Wt}_{(1,1,0)}(f_{i+1}^j) - \text{Wt}_{(1,1,0)}(f_i^j) &= \phi(v_{i+1}^j) + \phi(v_{i+1}^{j+1}) + \phi(v_{i+2}^j) + \phi(v_{i+2}^{j+1}) + \phi(v_{i+1}^j v_{i+1}^{j+1}) + \phi(v_{i+1}^j v_{i+2}^j) \\
&+ \phi(v_{i+2}^j v_{i+2}^{j+1}) + \phi(v_{i+1}^{j+1} v_{i+2}^{j+1}) - \phi(v_i^j) - \phi(v_i^{j+1}) - \phi(v_{i+1}^j) - \phi(v_{i+1}^{j+1}) - \phi(v_i^j v_i^{j+1}) - \phi(v_i^j v_{i+1}^j) \\
&- \phi(v_{i+1}^j v_{i+1}^{j+1}) - \phi(v_i^{j+1} v_{i+1}^{j+1}),
\end{aligned}$$

$$\text{Wt}_{(1,1,0)}(f_{i+1}^j) - \text{Wt}_{(1,1,0)}(f_i^j) = k + k + k + \left\lfloor \frac{j}{2} \right\rfloor + \left\lfloor \frac{j+1}{2} \right\rfloor + 2 \left(m - 3k + 3 + 3 \left\lfloor \frac{m+1}{3} \right\rfloor \left(\left\lceil \frac{k}{\lfloor (m+1)/3 \rfloor} \right\rceil - 1 \right) \right)$$

$$\begin{aligned}
 & + \left[\frac{1}{2} \left(i + 1 - 2 \left\lfloor \frac{k}{\lfloor (m+1)/3 \rfloor} \right\rfloor - 1 \right) \right] \left(\left\lfloor \frac{m}{2} \right\rfloor + \left\lfloor \frac{m}{2} \right\rfloor \right) \\
 & + \left[\frac{1}{2} \left(i + 1 - 2 \left\lfloor \frac{k}{\lfloor (m+1)/3 \rfloor} \right\rfloor - 1 \right) \right] \left(\left\lfloor \frac{m}{2} \right\rfloor + \left\lfloor \frac{m}{2} \right\rfloor \right) \\
 & - k - k - k - \left\lfloor \frac{j}{2} \right\rfloor - \left\lfloor \frac{j+1}{2} \right\rfloor - \left[\frac{1}{2} \left(i - 2 \left\lfloor \frac{k}{\lfloor (m+1)/3 \rfloor} \right\rfloor + 1 \right) \right] \\
 & \cdot \left(\left\lfloor \frac{(m-3k+3+3\lfloor (m+1)/3 \rfloor)(\lceil k/\lfloor (m+1)/3 \rceil - 1)}{2} \right\rfloor \right) \\
 & + \left[\frac{(m-3k+3+3\lfloor (m+1)/3 \rfloor)(\lceil k/\lfloor (m+1)/3 \rceil) - 1}{2} \right] \\
 & - \left[\frac{1}{2} \left(i - 2 \left\lfloor \frac{k}{\lfloor (m+1)/3 \rfloor} \right\rfloor + 1 \right) \right] \\
 & \cdot \left(\left\lfloor \frac{(m-3k+3+3\lfloor (m+1)/3 \rfloor)(\lceil k/\lfloor (m+1)/3 \rceil - 1)}{2} \right\rfloor \right) \\
 & + \left[\frac{(m-3k+3+3\lfloor (m+1)/3 \rfloor)(\lceil k/\lfloor (m+1)/3 \rceil) - 1}{2} \right] \\
 & = 2 \left(m - 3k + 3 + 3 \left\lfloor \frac{m+1}{3} \right\rfloor \left(\left\lfloor \frac{k}{\lfloor (m+1)/3 \rfloor} \right\rfloor - 1 \right) \right) \\
 & + (1)(m) - (1) \left(m - 3k + 3 + 3 \left\lfloor \frac{m+1}{3} \right\rfloor \left(\left\lfloor \frac{k}{\lfloor (m+1)/3 \rfloor} \right\rfloor - 1 \right) \right) \\
 & - (1) \left(m - 3k + 3 + 3 \left\lfloor \frac{m+1}{3} \right\rfloor \left(\left\lfloor \frac{k}{\lfloor (m+1)/3 \rfloor} \right\rfloor - 1 \right) \right) \\
 & = m,
 \end{aligned}$$

For $i = 2 \left\lfloor \frac{k}{\lfloor (m+1)/3 \rfloor} \right\rfloor + 2, \dots, n; j = 1, 2, \dots, m + 1,$

$$\begin{aligned}
 \text{Wt}_{(1,1,0)}(f_{i+1}^j) - \text{Wt}_{(1,1,0)}(f_i^j) &= \phi(v_{i+1}^j) + \phi(v_{i+1}^{j+1}) + \phi(v_{i+2}^j) + \phi(v_{i+2}^{j+1}) + \phi(v_{i+1}^j v_{i+1}^{j+1}) + \phi(v_{i+1}^j v_{i+2}^j) \\
 & + \phi(v_{i+2}^j v_{i+2}^{j+1}) + \phi(v_{i+1}^{j+1} v_{i+2}^{j+1}) - \phi(v_i^j) - \phi(v_i^{j+1}) \\
 & - \phi(v_{i+1}^j) - \phi(v_{i+1}^{j+1}) - \phi(v_i^j v_i^{j+1}) - \phi(v_i^j v_{i+1}^j) \\
 & - \phi(v_{i+1}^j v_{i+1}^{j+1}) - \phi(v_i^{j+1} v_{i+1}^{j+1}),
 \end{aligned}$$

$$\begin{aligned}
 \text{Wt}_{(1,1,0)}(f_{i+1}^j) - \text{Wt}_{(1,1,0)}(f_i^j) &= k + k + k + \left\lfloor \frac{j}{2} \right\rfloor + \left\lfloor \frac{j+1}{2} \right\rfloor + 2 \left(m - 3k + 3 + 3 \left\lfloor \frac{m+1}{3} \right\rfloor \left(\left\lfloor \frac{k}{\lfloor (m+1)/3 \rfloor} \right\rfloor - 1 \right) \right) \\
 & + \left[\frac{1}{2} \left(i + 1 - 2 \left\lfloor \frac{k}{\lfloor (m+1)/3 \rfloor} \right\rfloor - 1 \right) \right] \left(\left\lfloor \frac{m}{2} \right\rfloor + \left\lfloor \frac{m}{2} \right\rfloor \right) \\
 & + \left[\frac{1}{2} \left(i + 1 - 2 \left\lfloor \frac{k}{\lfloor (m+1)/3 \rfloor} \right\rfloor - 1 \right) \right] \left(\left\lfloor \frac{m}{2} \right\rfloor + \left\lfloor \frac{m}{2} \right\rfloor \right) - k - k
 \end{aligned}$$

$$\begin{aligned}
 & -k - \left\lfloor \frac{j}{2} \right\rfloor - \left\lfloor \frac{j+1}{2} \right\rfloor - 2 \left(m - 3k + 3 + 3 \left\lfloor \frac{m+1}{3} \right\rfloor \left(\left\lfloor \frac{k}{\lfloor (m+1)/3 \rfloor} \right\rfloor - 1 \right) \right) \\
 & - \left\lfloor \frac{1}{2} \left(i - 2 \left\lfloor \frac{k}{\lfloor (m+1)/3 \rfloor} \right\rfloor - 1 \right) \right\rfloor \left(\left\lfloor \frac{m}{2} \right\rfloor + \left\lfloor \frac{m}{2} \right\rfloor \right) - \left\lfloor \frac{1}{2} \left(i - 2 \left\lfloor \frac{k}{\lfloor (m+1)/3 \rfloor} \right\rfloor - 1 \right) \right\rfloor \left(\left\lfloor \frac{m}{2} \right\rfloor + \left\lfloor \frac{m}{2} \right\rfloor \right) \\
 & = m \left\lfloor \frac{1}{2} \left(i + 1 - 2 \left\lfloor \frac{k}{\lfloor (m+1)/3 \rfloor} \right\rfloor - 1 \right) \right\rfloor \\
 & + m \left\lfloor \frac{1}{2} \left(i + 1 - 2 \left\lfloor \frac{k}{\lfloor (m+1)/3 \rfloor} \right\rfloor - 1 \right) \right\rfloor - m \left\lfloor \frac{1}{2} \left(i - 2 \left\lfloor \frac{k}{\lfloor (m+1)/3 \rfloor} \right\rfloor - 1 \right) \right\rfloor \\
 & - m \left\lfloor \frac{1}{2} \left(i - 2 \left\lfloor \frac{k}{\lfloor (m+1)/3 \rfloor} \right\rfloor - 1 \right) \right\rfloor \\
 & = m \left(\left\lfloor \frac{(i+1 - 2\lfloor k/\lfloor (m+1)/3 \rfloor) - 1}{2} \right\rfloor + \left\lfloor \frac{(i+1 - 2\lfloor k/\lfloor (m+1)/3 \rfloor) - 1}{2} \right\rfloor \right) \\
 & - m \left(\left\lfloor \frac{(i - 2\lfloor k/\lfloor (m+1)/3 \rfloor) - 1}{2} \right\rfloor + \left\lfloor \frac{(i - 2\lfloor k/\lfloor (m+1)/3 \rfloor) - 1}{2} \right\rfloor \right) \\
 & = m \left(i + 1 - 2 \left\lfloor \frac{k}{\lfloor (m+1)/3 \rfloor} \right\rfloor - 1 \right) - m \left(i - 2 \left\lfloor \frac{k}{\lfloor (m+1)/3 \rfloor} \right\rfloor - 1 \right) \\
 & = m \left(i + 1 - 2 \left\lfloor \frac{k}{\lfloor (m+1)/3 \rfloor} \right\rfloor - 1 - i + 2 \left\lfloor \frac{k}{\lfloor (m+1)/3 \rfloor} \right\rfloor + 1 \right) \\
 & = m.
 \end{aligned} \tag{17}$$

Example 1. The total face irregularity strength of grid graph G_6^3 , under a k -labeling of type $(1, 1, 0)$ is 4.

Proof. The graph under consideration is $G_6^3 = P_7 \square P_4$. Figure 2 is a 4-labeling of type $(1, 1, 0)$ for the grid graph G_6^3 , and it will help us in calculating total face irregularity strength in different intervals of the grid graph.

Here, $k = \lceil (18 + 7)/8 \rceil = 4$, $\lfloor (m + 1)/3 \rfloor = 1$, $\lceil k/\lfloor (m + 1)/3 \rceil \rceil = 4$, and $m - 2\lfloor (m + 1)/3 \rfloor = 1$

In order to show that $tfs_{(1,1,0)}(G_6^3) = 4$, it is sufficient to prove that all the horizontal differences in face weights are 1 and all the vertical differences in face weights are 3. Now, we prove these results.

Horizontal differences in face weights can be calculated as follows:

For $i = 1, 2, 3, 4, 5, 6$ and $j = 1, 2, 3, 4$,

$$\begin{aligned}
 \text{Wt}_{(1,1,0)}(f_i^{j+1}) - \text{Wt}_{(1,1,0)}(f_i^j) &= \phi(v_i^{j+1}) + \phi(v_i^{j+2}) + \phi(v_{i+1}^{j+1}) + \phi(v_{i+1}^{j+2}) + \phi(v_i^{j+1} v_i^{j+2}) + \phi(v_i^{j+1} v_{i+1}^{j+1}) \\
 &+ \phi(v_{i+1}^{j+1} v_{i+1}^{j+2}) + \phi(v_i^{j+2} v_{i+1}^{j+2}) - \phi(v_i^j) - \phi(v_i^{j+1}) - \phi(v_{i+1}^j) - \phi(v_{i+1}^{j+1}) - \phi(v_i^j v_i^{j+1}) - \phi(v_i^j v_{i+1}^j) \\
 &- \phi(v_{i+1}^j v_{i+1}^{j+1}) - \phi(v_i^{j+1} v_{i+1}^{j+1}) \\
 &= \left\lfloor \frac{j+2}{2} \right\rfloor - \left\lfloor \frac{j}{2} \right\rfloor \\
 &= 1, \quad \text{for every value of } j,
 \end{aligned}$$

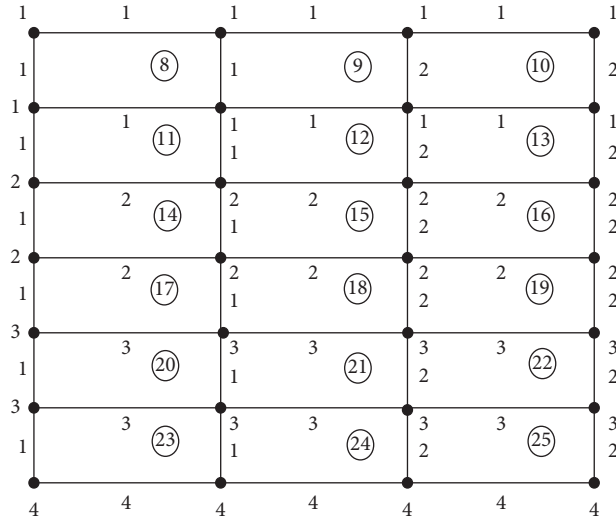


FIGURE 2: Total face irregular 4-labeling of the $(1, 1, 0)$ of grid graph G_6^3 .

For $i = 7$ and $j = 1, 2, \dots, m + 1$,

$$\begin{aligned}
 \text{Wt}_{(1,1,0)}(f_i^{j+1}) - \text{Wt}_{(1,1,0)}(f_i^j) &= \phi(v_i^{j+1}) + \phi(v_i^{j+2}) + \phi(v_{i+1}^{j+1}) + \phi(v_{i+1}^{j+2}) + \phi(v_i^{j+1}v_i^{j+2}) + \phi(v_i^{j+1}v_{i+1}^{j+1}) \\
 &\quad + \phi(v_{i+1}^{j+1}v_{i+1}^{j+2}) + \phi(v_i^{j+2}v_{i+1}^{j+2}) - \phi(v_i^j) - \phi(v_i^{j+1}) - \phi(v_{i+1}^j) - \phi(v_{i+1}^{j+1}) - \phi(v_i^jv_i^{j+1}) - \phi(v_i^jv_{i+1}^j) \\
 &\quad - \phi(v_{i+1}^jv_{i+1}^{j+1}) - \phi(v_i^{j+1}v_{i+1}^{j+1}) \\
 &= \left\lfloor \frac{j+2}{2} \right\rfloor - \left\lfloor \frac{j}{2} \right\rfloor \\
 &= 1, \text{ for all values of } j.
 \end{aligned} \tag{18}$$

Vertical differences in face weights can be calculated as follows:

For $i = 1, 2, 3, 4, 5, 6$ and $j = 1, 2, 3, 4$,

$$\begin{aligned}
 \text{Wt}_{(1,1,0)}(f_{i+1}^j) - \text{Wt}_{(1,1,0)}(f_i^j) &= \phi(v_{i+1}^j) + \phi(v_{i+1}^{j+1}) + \phi(v_{i+2}^j) + \phi(v_{i+2}^{j+1}) + \phi(v_{i+1}^jv_{i+1}^{j+1}) + \phi(v_{i+1}^jv_{i+2}^j) \\
 &\quad + \phi(v_{i+2}^jv_{i+2}^{j+1}) + \phi(v_{i+1}^{j+1}v_{i+2}^{j+1}) - \phi(v_i^j) - \phi(v_i^{j+1}) - \phi(v_{i+1}^j) - \phi(v_{i+1}^{j+1}) - \phi(v_i^jv_i^{j+1}) - \phi(v_i^jv_{i+1}^j) \\
 &\quad - \phi(v_{i+1}^jv_{i+1}^{j+1}) - \phi(v_i^{j+1}v_{i+1}^{j+1}) \\
 &= 3 \left\lfloor \frac{m+1}{3} \right\rfloor \\
 &= 3,
 \end{aligned}$$

For $i = 7; j = 1, 2, 3, 4$,

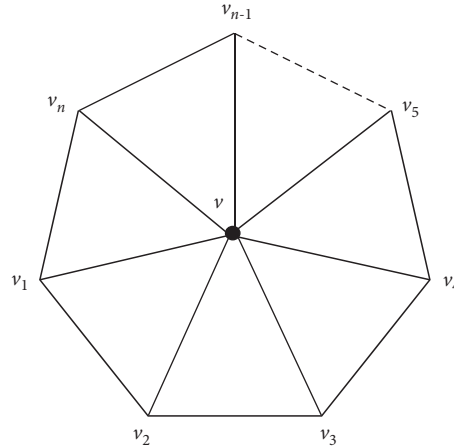


FIGURE 3: Wheel graph W_n .

$$\begin{aligned}
 \text{Wt}_{(1,1,0)}(f_{i+1}^j) - \text{Wt}_{(1,1,0)}(f_i^j) &= \phi(v_{i+1}^j) + \phi(v_{i+1}^{j+1}) + \phi(v_{i+2}^j) + \phi(v_{i+2}^{j+1}) + \phi(v_{i+1}^j v_{i+1}^{j+1}) + \phi(v_{i+1}^j v_{i+2}^j) \\
 &\quad + \phi(v_{i+2}^j v_{i+2}^{j+1}) + \phi(v_{i+1}^{j+1} v_{i+2}^{j+1}) - \phi(v_i^j) - \phi(v_i^{j+1}) - \phi(v_{i+1}^j) - \phi(v_{i+1}^{j+1}) - \phi(v_i^j v_i^{j+1}) - \phi(v_i^j v_{i+1}^j) \\
 &\quad - \phi(v_{i+1}^j v_{i+1}^{j+1}) - \phi(v_i^{j+1} v_{i+1}^{j+1}) \\
 &= m + 3 \left\lfloor \frac{m+1}{3} \right\rfloor \left(\left\lfloor \frac{k}{\lfloor (m+1)/3 \rfloor} \right\rfloor - 1 - \left\lfloor \frac{k}{\lfloor (m+1)/3 \rfloor} \right\rfloor - 1 \right) \\
 &= 3.
 \end{aligned}$$

(19)

It shows that all the differences of horizontal faces are equal to one and all the differences of vertical faces are equal to m . Hence, total face irregularity strength of grid graph G_6^3 is 4. \square

Theorem 4. . Let W_n be a wheel graph with $n + 1$ vertices, where $n \geq 3$. Then, under a total k -labeling of type $(1, 1, 0)$, we have

$$\text{tfs}(W_n) = \left\lceil \frac{n+4}{5} \right\rceil. \tag{20}$$

Proof. Let W_n be a wheel graph with $n + 1$ vertices, then by the definition of wheel graph, the total number of edges will be $2n$ and the total number of faces will be $n + 1$, that is,

$$\begin{aligned}
 |E(W_n)| &= 2n, \\
 |F(W_n)| &= n + 1.
 \end{aligned} \tag{21}$$

As we see that a wheel graph has 3-sided internal faces and external face, so by using Theorem 2, we have

$$\text{tfs}(W_n) \geq \left\lceil \frac{n+4}{5} \right\rceil. \tag{22}$$

In Figure 3, v is the vertex in the center of wheel graph W_n which is connecting to all the vertices v_i for $1 \leq i \leq n$. Similarly, for $1 \leq i \leq n - 1$, the edges of the wheel graph can

be constructed as $E(W_n) = \{vv_i, v_i v_{i+1}, vv_n, v_1 v_n\}$. Also for $1 \leq i \leq n - 1$, there will be exterior face, the n th interior face can be written as $f(W_n) = \{vv_1 v_n v\}$, and other all 3-sided interior faces can be written as $f(W_n) = \{vv_i v_{i+1} v\}$. Let us define a total k -labeling $\phi: V \cup E \rightarrow \{1, 2, 3, \dots, \lceil (n + 4)/5 \rceil\}$.

In Figure 4, we consider a finite wheel graph W_3 which is labeled under a 2-labeling of type $(1, 1, 0)$. So, for $1 \leq i \leq 3$, we have

$$\begin{aligned}
 \phi(v) &= \phi(v_2) = \phi(vv_i) = \phi(v_1 v_2) = 1, \\
 \phi(v_1) &= \phi(v_3) = \phi(v_1 v_3) = \phi(v_2 v_3) = 2.
 \end{aligned} \tag{23}$$

Weight of exterior face will be

$$\text{Wt}(f_{\text{exterior}}) = 10. \tag{24}$$

Weight of interior faces will be

$$\text{Wt}(f_i) = i + 6. \tag{25}$$

Now, let us talk about the graphs except W_3 for which we define the labeling as $\phi(v) = 1$:

- (i) For $1 \leq i \leq \lceil n/2 \rceil + 1$, we have $\phi(v_i) = \lceil 2i/5 \rceil$
- (ii) For $\lceil n/2 \rceil + 2 \leq i \leq n$, we have $\phi(v_i) = \lceil 2(n - i + 1)/5 \rceil + 1$
- (iii) For $1 \leq i \leq \lceil n/2 \rceil + 1$, we have $\phi(vv_i) = \lceil (2i - 1)/5 \rceil$

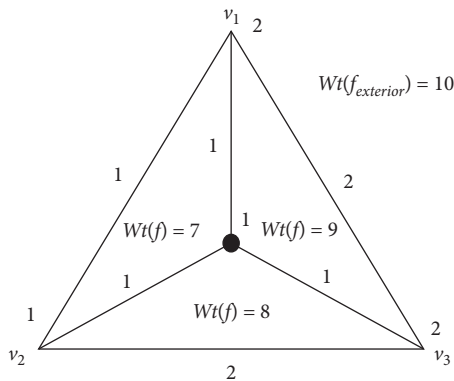


FIGURE 4: 2-labeling of a wheel graph W_3 .

- (iv) For $\lceil n/2 \rceil + 2 \leq i \leq n$, we have $\phi(vv_i) = \lceil (2(n-i) + 1)/5 \rceil + 1$
- (v) For $i = 1$, we have $\phi(v_1v_n) = 1$
- (vi) For $2 \leq i \leq \lceil n/2 \rceil$, we have $\phi(v_i v_{i+1}) = \lceil (2i - 2)/5 \rceil$
- (vii) For $i = \lceil n/2 \rceil + 1$, where $n \equiv m \pmod{6}$ in which $m = \{2, 3, 4, 5\}$, we have $\phi(v_i v_{i+1}) = \lceil (2i - 2)/5 \rceil$
- (viii) For $i = \lceil n/2 \rceil + 1$ where $n \equiv m \pmod{6}$ in which $m \in \{0, 1\}$, we have $\phi(v_i v_{i+1}) = \lceil (n + 4)/5 \rceil$
- (xi) For $i = \lceil n/2 \rceil + 2 \leq i \leq n - 1$, we have $\phi(v_i v_{i+1}) = \lceil (2(n-i) - 2)/5 \rceil + 1$

For weights of the wheel graph W_n , we proceed as follows:

- (i) For $i = 1$, we have $Wt(f_i) = 6$
- (ii) For $2 \leq i \leq \lceil (n+1)/2 \rceil$, we have $Wt(f_i) = 2i + 3$
- (iii) For $\lceil (n+1)/2 \rceil + 1 \leq i \leq n$, we have $Wt(f_i) = 2(n-i) + 8$
- (iv) For external weight, we will use $Wt(f_{\text{exterior}}) \geq 2n + 8$

We can easily observe that under the k -labeling ϕ of type $(1, 1, 0)$, the minimum k for which the wheel graph admits total face irregular strength is $\lceil (n+4)/5 \rceil$. Hence,

$$\text{tfs}(W_n) = \left\lceil \frac{n+4}{5} \right\rceil. \quad (26)$$

□

3. Conclusion

We investigated total face irregular strength of generalized plane grid graphs G_n^m and wheel graphs W_n under a graph k -labeling of type (α, β, γ) where $\alpha, \beta \in \{0, 1\}$. This work was based on the bright idea of finding face irregularity strength of ladder graphs by Martin Baca et al. [14]. In this article, we worked on the total face irregularity strength of grid and wheel graphs. We labeled graph vertices and graph edges but focussed on estimating face weights of graphs to prove the sharpness of k -labeling. We derived generalized formulas by considering graphs with different values of $n, m, \lfloor (m+1)/3 \rfloor$, and $m - 2\lfloor (m+1)/3 \rfloor$. Also, we verified the final results with example. In future, total and entire face

irregular strength of some more products of different plane graphs can be investigated under k -labeling of type (α, β, γ) .

Data Availability

No data were used to support this study.

Conflicts of Interest

The authors declare that they have no conflicts of interest.

References

- [1] G. Chartrand, M. S. Jacobson, J. Lehel, O. R. Oellermann, S. Ruiz, and F. Saba, "Irregular networks," *Congressus Numerantium*, vol. 64, pp. 187–192, 1988.
- [2] T. Nierhoff, "A tight bound on the irregularity strength of graphs," *SIAM Journal on Discrete Mathematics*, vol. 13, no. 3, pp. 313–323, 2000.
- [3] M. Kalkowski, M. Karoński, and F. Pfender, "A new upper bound for the irregularity strength of graphs," *SIAM Journal on Discrete Mathematics*, vol. 25, no. 3, pp. 1319–1321, 2011.
- [4] A. Ahmad, M. Bača, and M. K. Siddiqui, "On edge irregular total labeling of categorical product of two cycles," *Theory of Computing Systems*, vol. 54, no. 1, pp. 1–12, 2014.
- [5] D. Amar and O. Togni, "Irregularity strength of trees," *Discrete Mathematics*, vol. 190, no. 1-3, pp. 15–38, 1998.
- [6] J. H. Dimitz, D. K. Garnick, and A. Gyárfás, "On the irregularity strength of the $m \times n$ grid," *Journal of Graph Theory*, vol. 16, pp. 355–374, 1992.
- [7] A. Gyárfás, "The irregularity strength of $K_{m,m}$ is 4 for odd," *Discrete Mathematics*, vol. 71, pp. 273–274, 1998.
- [8] A. Frieze, R. J. Gould, M. Karoski, and F. Pfender, "On graph irregularity strength," *Journal of Graph Theory*, vol. 41, no. 2, pp. 120–137, 2002.
- [9] S. Jendrol', J. Miškuf, and R. Soták, "Total edge irregularity strength of complete graphs and complete bipartite graphs," *Discrete Mathematics*, vol. 310, pp. 400–407, 2010.
- [10] Nurdin, E. T. Baskoro, A. N. M. Salman, and N. N. Gaos, "On the total vertex irregularity strength of trees," *Discrete Mathematics*, vol. 310, no. 21, pp. 3043–3048, 2010.
- [11] M. Bača and M. K. Siddiqui, "Total edge irregularity strength of generalized prism," *Applied Mathematics and Computation*, vol. 235, pp. 168–173, 2014.
- [12] A. Ahmad, O. B. S. Al-Mushayt, and M. Bača, "On edge irregularity strength of graphs," *Applied Mathematics and Computation*, vol. 243, pp. 607–610, 2014.
- [13] G. Ebert, J. Hemmeter, F. Lazebnik, and A. Woldar, "Irregularity strengths of certain graphs," *Congressus Numerantium*, vol. 71, pp. 39–52, 1990.
- [14] M. Baca, S. Jendrol', M. Miller, and J. Ryan, "On irregular total labellings," *Discrete Mathematics*, vol. 307, pp. 1378–1388, 2007.
- [15] M. Bača, A. Ovais, A. Semaničová-Feňovčíková, and I. N. Suparta, "On face irregular evaluations of plane graphs," *Discussiones Mathematicae Graph Theory*, vol. 22, 2020.
- [16] M. Bača, S. Jendrol', K. Kathiresan, and K. Muthugurupackiam, "Entire labeling of plane graphs," *Applied Mathematics & Information Sciences*, vol. 9, no. 1, pp. 263–267, 2015.

Research Article

Minimum Partition of an r – Independence System

Zill-e-Shams,^{1,2} Muhammad Salman ,³ Zafar Ullah ,⁴ and Usman Ali ^{1,5}

¹Centre for Advanced Studies in Pure and Applied Mathematics (CASAPM), Bahauddin Zakariya University Multan, Multan 60800, Pakistan

²Department of Mathematics, The Women University, Multan, Pakistan

³Department of Mathematics, The Islamia University of Bahawalpur, Bahawalpur 63100, Pakistan

⁴Department of Mathematics, Division of Science and Technology, University of Education Lahore, Lahore 32200, Pakistan

⁵Institute de Mathematiques de Jussieu-Paris Rive Gauche-Paris, Paris, France

Correspondence should be addressed to Usman Ali; uali@bzu.edu.pk

Received 14 June 2021; Accepted 6 August 2021; Published 21 August 2021

Academic Editor: Ali Ahmad

Copyright © 2021 Zill-e-Shams et al. This is an open access article distributed under the Creative Commons Attribution License, which permits unrestricted use, distribution, and reproduction in any medium, provided the original work is properly cited.

Graph partitioning has been studied in the discipline between computer science and applied mathematics. It is a technique to distribute the whole graph data as a disjoint subset to a different device. The minimum graph partition problem with respect to an independence system of a graph has been studied in this paper. The considered independence system consists of one of the independent sets defined by Boutin. We solve the minimum partition problem in path graphs, cycle graphs, and wheel graphs. We supply a relation of twin vertices of a graph with its independence system. We see that a maximal independent set is not always a minimal set in some situations. We also provide realizations about the maximum cardinality of a minimum partition of the independence system. Furthermore, we study the comparison of the metric dimension problem of a graph with the minimum partition problem of that graph.

1. Introduction

An abstract idea of representing any objects which are connected to each other in a form of relation is a graph. In this representation, the object is called as a vertex and their relation denotes as an edge. Partition of a graph is the distribution of the whole graph data into disjoint subsets to different devices. The need of distributing huge graph data set is to process data efficiently and faster process of any graph related applications. Where graph partitioning is essential and applicable are given as follows:

- (1) Complex networks which include biological networks (in solving biological interaction problem in a huge biological network), social networks (Facebook, Twitter, and LinkedIn etc., and graph partitioning technology is used to process user query efficiently, as replying a query in a distributed manner is very handy and effective) [1], and transportation networks (graph partitioning can

speed up and could be effective in planning a route by using a GPS (global positioning system) tool in the digital era).

- (2) PageRank, which is an application used to compute the rank of web rank from web network.
- (3) VLSI design: Very large-scale integration (VLSI) system is one of the graph partitioning problems in order to reduce the connection between circuits in designing VLSI. The main objective of this partitioning is to reduce the VLSI design complexity by splitting them into a smaller component.
- (4) Image processing: Graph partitioning is one of the most attractive tools to split into several components of a picture, where pixels are denoted by vertices and if there are similarities between pixels are represented as edges [2].

Inspired by these interesting applications of graph partition, we consider a graph partition in the context of

resolving set of a graph, which is a well-known parameter in graph theory and having remarkable application in network discovery and verification.

A *set system* is a finite set S together with a family \mathcal{F} of subsets of S and is denoted by the pair (S, \mathcal{F}) . A set system (S, \mathcal{P}) is said to be an independence system if for every subset X of S possessing property \mathcal{P} , each proper subset of X also possesses the property \mathcal{P} , i.e., for each $X \subset S$ such that $X \in \mathcal{P}$, $Y \in \mathcal{P}$ for all $Y \subset X$. Actually, in an independence system (S, \mathcal{P}) , \mathcal{P} identified with the family of subsets of S possessing the property \mathcal{P} . A subset X of S which possess the property \mathcal{P} is said to be an *independent set* and *dependent set* otherwise. The *chromatic number* of (S, \mathcal{P}) is the smallest natural number n such that S can be partitioned into n independent sets and is denoted by $\chi(S, \mathcal{P})$. Clearly, a partition of S into n independent sets of (S, \mathcal{P}) can be identified by a coloring $\lambda: S \rightarrow \{1, 2, \dots, n\}$ of S such that for each color $c \in \{1, 2, \dots, n\}$, the color class $\{s \in S, \lambda(s) = c\}$ has the property \mathcal{P} , and vice versa. The coloring λ of S is called a \mathcal{P} -coloring of S . Thus, $\chi(S, \mathcal{P})$ is the least number of colors required by a \mathcal{P} -coloring of S and is also called the \mathcal{P} -chromatic number of S [3].

The \mathcal{P} -chromatic number $\chi(S, \mathcal{P})$ has been extensively studied by various graph theorists. Remarkable work has been done when S is V or E for a graph G having vertex set V and edge set E , and \mathcal{P} is a hereditary graphical property. For example, if \mathcal{P} is the property \mathcal{I} of being a vertex independent set, then $\chi(V, \mathcal{I})$ is the ordinary chromatic number of G ; if \mathcal{P} is the property \mathcal{E} of being an edge independent set, then $\chi(E, \mathcal{E})$ is the edge chromatic number of G ; if \mathcal{P} is the property \mathcal{F} of being a forest, then $\chi(E, \mathcal{F})$ is the arboricity of G . In the next section, we consider \mathcal{P} as the property \mathcal{R} of being a resolving set for G and define the \mathcal{R} -chromatic number of G associated with an r -independence system (V, \mathcal{R}) .

2. r – Independence System

Hereafter, we consider nontrivial, simple, and connected graph G with vertex set V and edge set E . We denote two adjacent vertices u and v in G by $u \sim v$ and nonadjacent vertices by $u \not\sim v$. The distance $d: V \times V \rightarrow \mathbb{Z}^+ \cup \{0\}$ is the length of a shortest path between two vertices in the pair $(u, v) \in V \times V$ and is denoted by $d(u, v)$. The maximum distance between the vertices of G is called the *diameter* of G , denoted by $\text{diam}(G)$. Two vertices u and v in G are *antipodal* or *diametral* if $d(u, v) = \text{diam}(G)$; otherwise, they are nonantipodal.

Let G be a graph. For any vertex v of G , the *metric code* or *code* of v with respect to an ordered k -subset $W = \{w_1, w_2, \dots, w_k\}$ of V is defined as

$$c_W(v) = (d(v, w_1), d(v, w_2), \dots, d(v, w_k)). \quad (1)$$

An ordered k -subset W of V is a *resolving set* for G if $c_W(u) \neq c_W(v)$ for every pair of vertices $(u, v) \in V \times V$. The cardinality of a minimum resolving set for G is called the *metric dimension* of G , denoted by $\text{dim}(G)$ or $\beta(G)$. A resolving set for G of cardinality $\text{dim}(G)$ is called a *metric basis*

or a *basis* of G [4–8]. In [9], it was found and, in [6], an explicit construction was given that finding the metric dimension of a graph is NP-hard. The concept of a resolving set, other than graph theory, is applied in many other areas such as coin-weighing problems [10], network discovery and verification [2], strategies for mastermind games [11], pharmaceutical chemistry [12], robot navigation [6], connected joins in graphs and combinatorial optimization [13], and sonar and coast guard Loran [8].

A subset S of the vertex set V of a graph G is an *r -independent set* if no proper subset of S is a resolving set for G . We denote \mathcal{R} as the property of being an r -independent set. That is, a subset S of V possesses the property \mathcal{R} if and only if S is an r -independent set. This concept was firstly introduced by Boutin and used the term *res-independent set* [14]. For simplicity, we use the term r -independent set rather than *res-independent set*. A family of subsets of V possessing the property \mathcal{R} is defined as

$$(V, \mathcal{R}) = \{S \subset V \mid S \text{ possesses the property } \mathcal{R}\}. \quad (2)$$

Thus, we have a set system (V, \mathcal{R}) consisting of those subsets of V which are possessing the property \mathcal{R} and is called the r -independence system. All the subsets possessing the property \mathcal{R} may or may not be resolving. This was an error made by Boutin in [14], and we rectified it in [15].

Remark 1. For a set $S \subset V$, the following assertions are equivalent:

- (1) $S \in (V, \mathcal{R})$
- (2) S possesses the property \mathcal{R}
- (3) S is an r -independent set

Remark 2. Let G be a graph with vertex set V of order n . Then,

- (1) $\{v\} \in (V, \mathcal{R})$ for each $v \in V$ obviously
- (2) $V \notin (V, \mathcal{R})$, because every $(n-1)$ -subset of V is a resolving set for G
- (3) a minimal resolving set for G is a maximal r -independent set, but converse is not always true [15]

2.1. Minimum Partition Problem. For a connected graph $G = (V, E)$ and the r -independence system (V, \mathcal{R}) , the minimum partition problem is to make a partition of V into the minimum number of subsets possessing the property \mathcal{R} .

The least natural number k , such that V can be partitioned into k subsets possessing the property \mathcal{R} , is called the *resolving chromatic number* of G associated with (V, \mathcal{R}) , denoted by $\chi_r(V, \mathcal{R})$. A coloring $\lambda: V \rightarrow \{1, 2, \dots, k\}$ of V such that for each color $c \in \{1, 2, \dots, k\}$, the color class $\{v \in V, \lambda(v) = c\}$ possesses the property \mathcal{R} is called an \mathcal{R} -coloring of V . Thus, $\chi_r(V, \mathcal{R})$ is the least number of colors required by an \mathcal{R} -coloring of V and is also called the \mathcal{R} -chromatic number of G .

Example 1. Let G be a graph with $V = \{v_1, v_2, v_3, v_4\}$ and $E = \{v_1 \sim v_2, v_2 \sim v_3, v_3 \sim v_4, v_4 \sim v_1\}$. Then only two colors are needed to properly color V , and it follows that the ordinary chromatic number $\chi(G) = 2$ with color classes

$\{v_1, v_3\}$ and $\{v_2, v_4\}$. The metric dimension of G is 2 and two nonantipodal vertices of G form a basis of G [4]. Accordingly, no 3–element subset of V possess the property \mathcal{R} and so the r –independence system is

$$(V, \mathcal{R}) = \{\{v_i\}, \{v_1, v_2\}, \{v_2, v_3\}, \{v_3, v_4\}, \{v_4, v_1\}, \{v_1, v_3\}, \{v_2, v_4\}; 1 \leq i \leq 4\}. \quad (3)$$

The minimum partition of V according to \mathcal{R} –coloring of V consists of two 2–element subsets of V from (V, \mathcal{R}) , and hence, $\chi_r(V, \mathcal{R}) = 2$.

In the above example, we obtained that the chromatic number and \mathcal{R} –chromatic number of a graph G are same. But, it is not necessary that these numbers are always same.

Example 2. Let G be a graph with $V = \{v_1, v_2, v_3, v_4\}$ and $E = \{v_1 \sim v_2, v_2 \sim v_3, v_3 \sim v_4\}$. Then only two colors are needed to properly color V , and it follows that the ordinary chromatic number $\chi(G) = 2$ with color classes $\{v_1, v_3\}$ and $\{v_2, v_4\}$. The metric dimension of G is 1, and $\{v_1\}, \{v_4\}$ are the only two bases of G [4, 6]. Accordingly, each 2–element subset of V is a resolving set for G , and so no 3–element subset of V possess the property \mathcal{R} . Thus, the r –independence system is

$$(V, \mathcal{R}) = \{\{v_i\}, \{v_2, v_3\}; 1 \leq i \leq 4\}. \quad (4)$$

The minimum partition of V according to \mathcal{R} –coloring of V consists of two bases sets and the set $\{v_2, v_3\}$ from (V, \mathcal{R}) . Hence, $\chi_r(V, \mathcal{R}) = 3$.

It is observed, from Examples 1 and 2, that $\chi(G) \leq \chi_r(V, \mathcal{R})$. But, it is not true generally as, in the next

example, we have a have a graph G such that $\chi(G) > \chi_r(V, \mathcal{R})$.

Example 3. Let G be a graph with $V = \{v_1, v_2, v_3\}$ and $E = \{v_1 \sim v_2, v_2 \sim v_3, v_3 \sim v_1\}$. Then, three colors are required to properly color V , and it follows that the ordinary chromatic number $\chi(G) = 3$ with color classes $\{v_1\}, \{v_2\}$ and $\{v_3\}$. The metric dimension of G is 2 and any two vertices of G can form a basis of G [4]. Accordingly, the 3–element set V does not possess the property \mathcal{R} and so the r –independence system is

$$(V, \mathcal{R}) = \{\{v_i\}, \{v_1, v_2\}, \{v_2, v_3\}, \{v_3, v_1\}; 1 \leq i \leq 3\}. \quad (5)$$

The minimum partition of V according to \mathcal{R} –coloring of V consists of one singleton set $\{v\}$ and one 2–element set $V - \{v\}$ from (V, \mathcal{R}) , and hence $\chi_r(V, \mathcal{R}) = 2$.

Example 4. Let G be a graph with $V = \{v_1, v_2, v_3, v_4, v_5\}$ and $E = \{v_1 \sim v_2, v_2 \sim v_3, v_3 \sim v_4, v_4 \sim v_5\}$. Then two colors are required to properly color V , and it follows that the ordinary chromatic number $\chi(G) = 2$ with color classes $\{v_2\}, \{v_4\}, \{v_5\}$ and $\{v_1\}, \{v_3\}$. The metric dimension of G is 2 and $\{v_4, v_5\}$ is a set of basis of G [4]. But the set of three elements $\{v_1, v_2, v_3\}$ which is not resolving set of G possess the property \mathcal{R} and so the r –independence system is

$$(V, \mathcal{R}) = \{\{v_i\}, \{v_1, v_2\}, \{v_1, v_3\}, \{v_1, v_4\}, \{v_1, v_5\}, \{v_2, v_3\}, \{v_2, v_4\}, \{v_2, v_5\}, \{v_1, v_2, v_3\}; 1 \leq i \leq 5\}. \quad (6)$$

The minimum partition of V according to \mathcal{R} –coloring of V consists of one 2–element set and one 3–element set $V - \{v\}$ from (V, \mathcal{R}) , and hence $\chi_r(V, \mathcal{R}) = 2$.

3. Three Well-Known Families

In this section, we consider families of path graphs, cycle graphs, and wheel graphs and solve the minimum partition problem for each family.

3.1. Path Graphs. A path graph P_n , for $n \geq 2$, has vertex set $V = \{v_1, v_2, \dots, v_n\}$ and edge set $E = \{v_i \sim v_{i+1}; 1 \leq i \leq n - 1\}$. The following result describes which subset of the vertex set of a path graph possesses the property \mathcal{R} .

Lemma 1. *No 3–element subset of the vertex set V of a path graph G possess the property \mathcal{R} .*

Proof. As $\dim(G) = 1$ and only each end vertex of G forms a basis of G [6], every 2–element subset of V is a resolving set for G . Consequently, no 3–element subset of V possess the property \mathcal{R} . \square

The next result investigates the number of subsets of the vertex set of a path graph possessing the property \mathcal{R} .

Lemma 2. *For all $n \geq 2$, if G is a path graph with vertex set V , then $|(V, \mathcal{R})| = (1/2)(n^2 - 3n + 6)$.*

Proof. According to Lemma 1, each singleton subset of V as well as each 2–element subset of $V - \{v_1, v_n\}$ possesses the property \mathcal{R} . It follows that for $n = 2, 3$, $(V, \mathcal{R}) = \{\{v_i\}; 1 \leq i \leq n\}$, and for all $n > 3$,

$$(V, \mathcal{R}) = \{\{v_i\}; 1 \leq i \leq n\} \cup V_2, \quad (7)$$

where V_2 denotes the collection of all the $\binom{n-2}{2}$ and 2-element subsets of $V - \{v_1, v_n\}$. Hence,

$$|(V, \mathcal{R})| = n + \binom{n-2}{2} = \frac{1}{2}(n^2 - 3n + 6). \quad (8)$$

□

The following result solves the minimum partition problem for a path graph.

Theorem 1. For all $n \geq 2$, the vertex set V of a path graph can be partitioned into $\lfloor (n+3)/2 \rfloor$ minimum number of subsets possessing the property \mathcal{R} .

Proof. Let the color classes, due to a coloring $\lambda: V \rightarrow \{1, 2, \dots, \lfloor (n+3)/2 \rfloor\}$ of V , are

When n is even, then $C_1 = \{v_1\}, C_2 = \{v_n\}$ and $C_{i+1} = \{v_i, v_{n-i+1}\}; 2 \leq i \leq ((n-2)/2)$

When n is odd, then $C_1 = \{v_1\}, C_2 = \{v_{\lfloor (n+1)/2 \rfloor}\}, C_3 = \{v_n\}$ and $C_{i+2} = \{v_i, v_{n-i+1}\}; 2 \leq i \leq ((n-3)/2)$

In both cases, all these color classes are lying in (V, \mathcal{R}) , by Lemma 2. It follows that λ is an \mathcal{R} -coloring of V , and these color classes define a partition of V into the sets possessing the property \mathcal{R} . Further, any partition of V of cardinality less than $\lfloor (n+3)/2 \rfloor$ contains at least one 2-element or 3-element subset S of V such that $S \in (V, \mathcal{R})$. Thus, a minimum partition of V has $\lfloor (n+3)/2 \rfloor$ subsets of V possessing the property \mathcal{R} . □

3.2. Cycle Graphs. A cycle graph C_n , for $n \geq 3$, has vertex set $V = \{v_1, v_2, \dots, v_n\}$ and edge set $E = \{v_i \sim v_{i+1}, v_n \sim v_1; 1 \leq i \leq n-1\}$. In the next result, we investigate which subset of the vertex set of a cycle graph possesses the property \mathcal{R} is.

Lemma 3. A subset of the vertex set V of a cycle graph G which possess the property \mathcal{R} is a singleton set or a 2-element set.

Proof. In [4, 5], it was shown that $\dim(G) = 2$ and any two nonantipodal vertices of G form a basis of G . Further note that, a 3-element subset S of V , whether containing two antipodal vertices or not, is not an r -independent set. It completes the proof. □

The number of subsets of the vertex set of a cycle graph possessing the property \mathcal{R} is counted in the following result.

Lemma 4. For all $n \geq 3$, if G is a cycle graph with vertex set V , then $|(V, \mathcal{R})| = (1/2)(n^2 + n)$.

Proof. Lemma 3 yields that each singleton subset of V as well as each 2-element subset of V possesses the property \mathcal{R} . It follows that for all $n \geq 3$,

$$(V, \mathcal{R}) = \{\{v_i\}; 1 \leq i \leq n\} \cup V_2, \quad (9)$$

where V_2 denotes the collection of all the $\binom{n}{2}$, 2-element subsets of V . Hence,

$$|(V, \mathcal{R})| = n + \binom{n}{2} = \left(\frac{1}{2}\right)(n^2 + n). \quad (10)$$

□

The minimum partition problem for a cycle graph is solved in the following result.

Theorem 2. For all $n \geq 3$, the vertex set V of a cycle graph can be partitioned into $\lceil n/2 \rceil$ minimum number of subsets possessing the property \mathcal{R} .

Proof. Let the color classes, due to a coloring $\lambda: V \rightarrow \{1, 2, \dots, \lceil n/2 \rceil\}$ of V , are as follows:

When n is even, then $C_i = \{v_i, v_{n-i+1}\}; 1 \leq i \leq (n/2)$.

When n is odd, then $C_1 = \{v_1\}$ and $C_i = \{v_i, v_{n-i+2}\}; 2 \leq i \leq ((n+1)/2)$.

In both the cases, all these color classes are lying in (V, \mathcal{R}) , by Lemma 4. It follows that λ is an \mathcal{R} -coloring of V , and these color classes define a partition of V into the sets possessing the property \mathcal{R} . Further, any partition of V of cardinality less than $\lceil n/2 \rceil$ contains at least one 3-element subset S of V such that $S \in (V, \mathcal{R})$. Thus, a minimum partition of V has $\lceil n/2 \rceil$ subsets of V possessing the property \mathcal{R} . □

3.3. Wheel Graphs. For $n \geq 3$, let $C_n: v_1 \sim v_2 \sim \dots \sim v_n \sim v_1$ be a cycle and K_1 be the trivial graph with vertex v . Then a wheel graph is the sum $W_n = K_1 + C_n$ with vertex set $V = \{v, v_i; 1 \leq i \leq n\}$ and edge set $E = \{v \sim v_i; 1 \leq i \leq n\} \cup E(C_n)$. For fixed $i; 1 \leq i \leq n$, let a path $P: v_i \sim v_{i+1} \sim \dots \sim v_{i+n-5}$ of order $n-4$ on the cycle C_n of W_n , where the indices greater than n or less than zero will be take modulo n . The following result describes the sets in W_n possessing the property \mathcal{R} for $n \geq 8$.

Remark 3. For $n \geq 8$, let W_n be a wheel graph with vertex set u . Let V be set of any $\{v_i, i = 1, \dots, n-4\}$ consecutive vertices of wheel graph, then V is a maximal independent set which is not a minimal resolving set.

Lemma 5. For $n \geq 8$, let W_n be a wheel graph with vertex set V . Then,

- (1) every k -element subset of the set $S = V(P) \cup \{v\}$ belongs to (V, \mathcal{R}) for $1 \leq k \leq n-3$
- (2) every k -element subset of the set $V - S$ belongs to (V, \mathcal{R}) for $1 \leq k \leq 4$

Proof

- (1) For fixed $i; 1 \leq i \leq n, S = \{v, v_j; i \leq j \leq i+n-5\}$. Since $d(v_{i+n-2}, v) = 1 = d(v_{i+n-3}, v)$ and $d(v_{i+n-2}, u) = 1 = d(v_{i+n-3}, u)$ for each $u \in V(P)$, $c_W(v_{i+n-2}) = c_W(v_{i+n-3})$ for any $W \subseteq S$. It follows the required result.

(2) Note that $V - S = \{v_{i+n-1}, v_{i+n-2}, v_{i+n-3}, v_{i+n-4}\}$. For any $x, y \in S - \{v, v_i, v_{i+n-5}\}$ and $d(x, w) = 2 = d(y, w)$ for each $w \in V - S$. This implies that $c_W(x) = c_W(y)$ for any $W \subseteq V - S$. Hence, the required result followed. \square

For wheel graphs, the following result solves the minimum partition problem.

Theorem 3. For $n \geq 3$, let W_n be a wheel graph with vertex set V . Then,

$$\chi_r(V, \mathcal{R}) = \begin{cases} 2, & \text{when } n \neq 5, 6, 7, \\ 3, & \text{when } n = 5, 6, 7. \end{cases} \quad (11)$$

Proof. It can be easily seen that a partition

- (i) $\{\{v_1, v_2\}, \{v_3, v\}\}$ is a minimum partition of V having sets possessing the property \mathcal{R} in W_3 ,
- (ii) $\{\{v_1, v_3, v\}, \{v_2, v_4\}\}$ is a minimum partition of V having sets possessing the property \mathcal{R} in W_4 ,
- (iii) $\{\{v_1, v_2\}, \{v_3, v_4\}, \{v_5, v\}\}$ is a minimum partition of V having sets possessing the property \mathcal{R} in W_5 ,
- (iv) $\{\{v\}, \{v_1, v_2, v_3\}, \{v_4, v_5, v_6\}\}$ is a minimum partition of V having sets possessing the property \mathcal{R} in W_6 , and
- (v) $\{\{v_1, v_2, v_3\}, \{v_4, v_5, v_6\}, \{v_7, v\}\}$ is a minimum partition of V having sets possessing the property \mathcal{R} in W_7 .

It follows that $\chi_r(V, \mathcal{R})$ is 2 when $n = 3, 4$ and is 3 when $n = 5, 6, 7$.

For all $n \geq 8$, let $\lambda: V \rightarrow \{1, 2\}$ be a coloring of V and let the corresponding color classes are $C_1 = V(P) \cup \{v\}$, where $P: v_i \sim v_{i+1} \sim \dots \sim v_{i+n-5}$ for any fixed $1 \leq i \leq n$, and $C_2 = V - C_1$. Then C_1 and C_2 define a partition of V . Also, Lemma 5 yields that both C_1 and C_2 possess the property \mathcal{R} . Therefore, λ is an \mathcal{R} -coloring of V , and hence $\chi_r(V, \mathcal{R}) = 2$. \square

4. Twins and r – Independence

Let v be a vertex of a graph G having vertex set V . Then the open neighborhood of v is $N(v) = \{u \in V: u \sim v \text{ in } G\}$ and the closed neighborhood of v is $N[v] = N(v) \cup \{v\}$. Two distinct vertices u and v of G are adjacent twins if $N[u] = N[v]$ and nonadjacent twins if $N(u) = N(v)$. Observe that if u, v are adjacent twins, then $u \sim v$ in G and if u, v are nonadjacent twins, then $u \not\sim v$ in G . Adjacent twins are called true twins and nonadjacent twins are called false twins. Either u, v are adjacent or nonadjacent twins, they are called twins. A vertex v is called self twin if neither $N(u) = N(v)$ nor $N[v] = N[u]$, for all $u \in V$. Each self twin in a graph makes a set of singleton twins. A set $T \subseteq V$ is called a twin set in G if u, v are twins in G for every pair of distinct vertices $u, v \in T$. The next lemma follows from the above definitions [16].

Lemma 6 (see [16]). If u and v are twins in a graph G , then $d(u, x) = d(v, x)$ for every vertex $x \in V - \{u, v\}$.

Due to Lemma 6, we have the following remark.

Remark 4

- (1) If u and v are twins in a graph G and W is a resolving set for G . Then either $u \in W$ or $v \in W$.
- (2) If T is a twin set in a graph G of order $t \geq 2$, then every resolving set for G contains at least $t - 1$ elements of T .

Removal of two twins from the vertex set makes it r -independent as given in the next result.

Lemma 7. Let T be a twin set of order $t \geq 2$ in a graph G having the vertex set V . Then, for any two elements $u, v \in T$, the set $V - \{u, v\}$ possesses the property \mathcal{R} .

Proof. Since $d(u, x) = d(v, x)$ for all $x \in V - \{u, v\}$, by Lemma 6, so no subset of $V - \{u, v\}$ is a resolving set for G . It follows the result. \square

Remarks 2 and 4 yield the following two results.

Lemma 8. Let T be a twin set of order $t \geq 2$ in a graph G . Then, for each $1 \leq k \leq t - 1$, any k -element subset S of T and the set $T - S$ both possess the property \mathcal{R} .

Proof. If $t = 2$, then each subset S of T of order less than $|T|$ as well as the set $T - S$ both are singleton, and so Remark 2(1) yields the result. If $t \geq 3$, then as $t - 1$ vertices of T must belong to any resolving set for G , by Remark 4(2), so no subset of T of order $\leq t - 2$ is not a resolving set, because there are at least two twins are remained in T form that one of them must belong to a resolving set for G , by Remark 4(1). It follows that any k -element subset S of T possesses the property \mathcal{R} for each $1 \leq k \leq t - 1$. Further, since the set $T - S$ is either singleton or contains at least more than one twins from T , no subset of $T - S$ is a resolving set for G . Thus, it must possess the property \mathcal{R} . \square

Lemma 8 can be generalized with the similar proof when a graph G has more than one twin sets of order at least two, and this generalization is stated in the following result.

Theorem 4. For $l \geq 2$, let T_1, T_2, \dots, T_l are twin sets in a graph G of orders t_1, t_2, \dots, t_l , respectively, where each $t_i \geq 2$. If S_i is a k_i -element subset of T_i for $1 \leq k_i \leq t_i - 1$, then

- (1) each S_i possesses the property \mathcal{R} ,
- (2) $\bigcup_{i=1}^l S_i$ possesses the property \mathcal{R} , and
- (3) $\bigcup_{i=1}^l T_i - \bigcup_{i=1}^l S_i$ possesses the property \mathcal{R} .

Remark 5. Let \mathcal{G} be a family of graph and $G \in \mathcal{G}$. For $l \geq 2$, let T_1, T_2, \dots, T_l are twin sets in a graph G of orders t_1, t_2, \dots, t_l , respectively, where each $t_i \geq 2$. Let a nonempty set S is union of singleton twin sets in G , and let $\{v_1, v_2\}$ belong to any one of T_1, T_2, \dots, T_l , then $S \cup T_i - \{v_1, v_2\}$ is a maximal independent set which is not minimal resolving set.

The following result states the relationship between twins and r -independence.

Theorem 5. *The \mathcal{R} -chromatic number of a graph G (except P_3) of order $n \geq 3$ having a nonsingleton twin set is two.*

Proof. Let G be a graph of order $n \geq 4$ with vertex set V , and let T be a twin set in G . Let $\lambda: V \rightarrow \{1, 2\}$ be a coloring of V , and let the corresponding color classes are $C_1 = V - \{u, v\}$ for any $u, v \in T$ and $C_2 = \{u, v\}$. Then C_1 and C_2 define a partition of V . Also, Lemma 7 implies that $C_1 \in (V, \mathcal{R})$. Further, since no path graph of order more than three has a twin set, so G is not a path graph. It follows that no singleton subset of C_2 is resolving, because a path graph only has a singleton resolving set [4]. Thus, $C_2 \in (V, \mathcal{R})$. Hence, λ is an \mathcal{R} -coloring of V , and so $\chi_r(V, \mathcal{R}) = 2$. \square

Remark 6

- (1) The converse of Theorem 5 is not true generally. Theorem 3 describes that the \mathcal{R} -chromatic number of a wheel graph W_n is two, but W_n has no twin class for any $n \geq 8$.
- (2) In Theorem 5, if G is P_3 , then G has one twin set containing two end vertices. But, the \mathcal{R} -chromatic number of G is three, by Theorem 1.

Next, we provide two well-known families of graphs as in the favor of Theorem 5.

4.1. Complete Multipartite Graphs. Let G be a complete multipartite graph with $k \geq 2$ partite sets V_1, V_2, \dots, V_k of cardinality m_1, m_2, \dots, m_k , respectively, where each $m_i \geq 1$.

- (i) If $m_i = 1$ for all $1 \leq i \leq k$, then G is a complete graph K_k having vertex as the twin set.
- (ii) If some of m_i is not equal to one. Let us suppose, without loss of generality, that $m_i = 1$ for $1 \leq i \leq l$ and $2 \leq l < k$. Then, G has $k - l + 1$ twin sets $V_{l+1}, V_{l+2}, \dots, V_k$ and $\bigcup_{i=1}^l V_i$.
- (iii) If $k = 2, m_1 = 1$ and $m_2 = 2$, then G is $K_{1,2} \cong P_3$.

As, the \mathcal{R} -chromatic number of P_3 is 3, by Theorem 1, so we receive the following consequence from Theorem 5.

Corollary 1. *The \mathcal{R} -chromatic number of a complete multipartite graph (which is not $K_{1,2}$) is two.*

Example 5 (Circulant networks).

The family of circulant networks is an important family of graphs, which is useful in the design of local area networks [17].

These networks are the special case of Cayley graphs $\text{Cay}(G; S)$ when the group G is Z_n (an additive group of integers modulo n) and $S \subseteq Z_n \setminus \{0\}$ [18]. These graphs are defined as follows: let n, m and a_1, a_2, \dots, a_m be positive integers, $1 \leq a_i \leq \lfloor n/2 \rfloor$ and $a_i \neq a_j$ for all $1 \leq i < j \leq m$. An undirected graph with the set of vertices $\{v_{i+1}; i \in Z_n\}$, and the set of edges $\{v_j \sim v_{j+a_i}; 1 \leq j \leq n, 1 \leq l \leq m\}$ is called a circulant graph, denoted by $C_n(a_1, a_2, \dots, a_m)$. The numbers a_1, a_2, \dots, a_m are called the generators, and we say that the edge $v_j \sim v_{j+a_i}$ is of type a_i . The indices after n will be taken modulo n . The cycle $v_1 \sim v_2 \sim \dots \sim v_n \sim v_1$ in $C_n(a_1, a_2, \dots, a_m)$ is called the principal cycle. Consider a class of circulant networks $C_{2n+2}(1, n)$, for $n \geq 1$. Then there are $n + 1$ twin sets $T_i = \{v_i, v_{i+n+1}\}$ for $1 \leq i \leq n + 1$. Thus, as a consequence of Theorem 5, the \mathcal{R} -chromatic number of $C_{2n+2}(1, n)$ is two.

5. Some Realizations

Remark 2(3) describes that there is no n -element r -independent set in a connected graph of order $n \geq 2$. Lemma 7 illustrates that a connected graph G of order $n \geq 3$ having twins (other than self twins) can have an $(n - 2)$ -element set as an r -independent set. In the result to follow, we characterize all the connected graphs of order $n \geq 2$ in which every $(n - 1)$ -element subset of the vertex set is r -independent.

Theorem 6. *Let G be a connected graph of order $n \geq 2$ with vertex set V . Then any $(n - 1)$ -element subset of V possesses the property \mathcal{R} if and only if G is a complete graph.*

Proof. Suppose that G is a complete graph. Then every two vertices of G are twins and V itself is the twin set in G . So Lemma 8 yields the required result.

Conversely, suppose that any $(n - 1)$ -element subset, say $S = \{s_1, s_2, \dots, s_{n-1}\}$, of V possesses the property \mathcal{R} . Then S is a resolving set for G , because for any $s_i \in S$, 0 lies at the i th position in the code $c_S(s_i)$, whereas the code $c_S(v)$ of the element $v \in V - S$ has all nonzero coordinates. Further, S is a minimum resolving set for G , because no k -element subset of S is a resolving set for any $1 \leq k \leq n - 2$, by our supposition. Thus, $\dim(G) = n - 1$. In [4, 6], it was shown that a graph G of order n has $\dim(G) = n - 1$ if and only if G is a complete graph. It completes the proof. \square

Since any singleton set is an r -independent, so we have the following consequences for a complete graphs.

Corollary 2. *The \mathcal{R} -chromatic number of a complete graph is two.*

If G is a connected graph of order $n \geq 2$ with vertex set V , then $2 \leq \chi_r(V, \mathcal{R}) \leq n$, by Remark 2(3). The next result characterizes all the connected graphs of order $n \geq 2$ having \mathcal{R} -chromatic number n .

Theorem 7. *Let G be a connected graph of order $n \geq 2$ with vertex set V . Then, $\chi_r(V, \mathcal{R}) = n$ if and only if G is either K_2 ($\cong P_2$) or P_3 ($\cong K_{1,2}$).*

Proof. If $G \cong K_2 (\cong P_2)$, then $\chi_r(V, \mathcal{R}) = 2$, by Corollary 2.

If $G \cong P_3 (\cong K_{1,2})$, then $\chi_r(V, \mathcal{R}) = 3$, by Theorem 1.

Conversely, suppose that for a connected graph G of order $n \geq 2$ with vertex set V , we have $\chi_r(V, \mathcal{R}) = n$. Then,

- (i) for $n = 2$, the only connected graph is $K_2 (\cong P_2)$ such that $\chi_r(V, \mathcal{R}) = 2 = n$, by Corollary 2,
- (ii) for $n = 3$, G is either $C_3 (\cong K_3)$ or $P_3 (\cong K_{1,2})$. Since the \mathcal{R} -chromatic number of C_3 is $2 = n - 1$, by Theorem 2, and the \mathcal{R} -chromatic number of P_3 is $3 = n$, by Theorem 1, so $G \cong P_3$ in this case.
- (iii) for $n \geq 4$, either G has a twin set or no twin set exists in G . In the former case, $\chi_r(V, \mathcal{R}) = 2 \neq n$, by Theorem 5. In the latter case, let $V = \{v_1, v_2, \dots, v_n\}$. Then, $\chi_r(V, \mathcal{R}) = n$ implies that the minimum partition of the r -independence system (V, \mathcal{R}) is $\{\{v_1\}, \{v_2\}, \dots, \{v_n\}\}$. It follows that no k -element subset of V belongs to (V, \mathcal{R}) for $k \geq 2$. Otherwise, $\chi_r(V, \mathcal{R}) \leq n - 1$. But, in every connected graph of order $n \geq 4$, at least one 2-element subset of V must possess the property \mathcal{R} , because singleton resolving sets exist in a path graph only (and in the case of path graph P_n , ($n \geq 4$), we have 2-element subsets of V in (V, \mathcal{R}) , by Lemma 2). Therefore, no connected graph G of order $n \geq 4$ exists such that $\chi_r(V, \mathcal{R}) = n$.

From the above three cases, we conclude that G is either $K_2 (\cong P_2)$ or $P_3 (\cong K_{1,2})$. □

From Theorem 7, it concludes that if G is a connected graph of order $n \geq 3$ with vertex set V and $G \cong P_3 (\cong K_{1,2})$, then $2 \leq \chi_r(V, \mathcal{R}) \leq n - 1$. All the connected graphs of order $n \geq 3$ having \mathcal{R} -chromatic number $n - 1$ are characterized in the following result.

Theorem 8. *Let G be a connected graph of order $n \geq 3$ with vertex set V . Then, $\chi_r(V, \mathcal{R}) = n - 1$ if and only if G is either $C_3 (\cong K_3)$ or P_4 or P_5 .*

Proof. If $G \cong C_3 (\cong K_3)$, then Theorem 2 yields that $\chi_r(V, \mathcal{R}) = n - 1$.

If $G \cong P_4$ or P_5 , then $\chi_r(V, \mathcal{R}) = n - 1$, by Theorem 1.

Conversely, suppose that for a connected graph G of order $n \geq 3$ with vertex set V , we have $\chi_r(V, \mathcal{R}) = n - 1$. Then,

- (i) for $n = 3$, G is either $P_3 (\cong K_{1,2})$ or $C_3 (\cong K_3)$. $G \cong P_3$ is not true, by Theorem 7. So $G \cong C_3$, by Theorem 2,
- (ii) for $n = 4$, $G \cong \{P_4, K_{1,3}, K_4 (\cong W_3), K_4 - e, K_4 - 2e (\cong P_4 \text{ and } C_4), C_4 (\cong K_{2,2})\}$, where $K_4 - e$ and $K_4 - 2e$ can be obtained by deleting one and two edges from K_4 , respectively. In this case, except P_4 , all the graphs has a twin set and so $\chi_r(V, \mathcal{R}) = 2 \neq n - 1$, by Theorem 5. Thus $G \cong P_4$, by Theorem 1.
- (iii) for $n \geq 5$, either G has no twin set or G has a twin set. $\chi_r(V, \mathcal{R}) = 2 \neq n - 1$ in the latter case, by Theorem 5. In the former case, except $G \cong P_n$, a minimum

resolving set for G is of at least two order, which implies that every 2-element subset of V belongs to (V, \mathcal{R}) . It follows that a minimum partition of V according to the r -independence system contains at least two 2-element subsets of V , which implies that $\chi_r(V, \mathcal{R}) \leq n - 2$, a contradiction. However, when $G \cong P_n$, then $\chi_r(V, \mathcal{R}) = 4 = n - 1$ only for $n = 5$ and $\chi_r(V, \mathcal{R}) \leq n - 2$ for $n \geq 6$, by Theorem 1.

From the above three case, we conclude that G is either $C_3 (\cong K_3)$ or P_4 or P_5 . □

Theorem 8 concludes that if G is a connected graph of order $n \geq 4$ with vertex set V and $G \cong \{P_4, P_5\}$, then $2 \leq \chi_r(V, \mathcal{R}) \leq n - 2$.

6. Metric Dimension and r - Independence

In this section, we develop a relationship between the metric dimension and \mathcal{R} -chromatic number of a connected graph by providing three existing type results.

There exists a connected graph whose metric dimension is different from its \mathcal{R} -chromatic number by one.

Theorem 9. *For even $n \geq 4$, there exists a connected graph G with vertex set V such that $\dim(G) - \chi_r(V, \mathcal{R}) = 1$.*

Proof. Let C_n be a cycle graph on even $n \geq 4$ vertices and a path P_2 . Then G is a graph obtained by taking the product of C_n and P_2 . Let the vertex set of G be $V = \{v_i, u_i; 1 \leq i \leq n\}$, and the edge set is $E = \{v_i \sim v_{i+1}, u_i \sim u_{i+1}, u_j \sim v_j; 1 \leq i \leq n - 1 \wedge 1 \leq j \leq n\}$. The resultant graph G consists of two n cycles: one is outer cycle $v_1 \sim v_2 \sim \dots \sim v_n \sim v_1$, and the other one is inner cycle $u_1 \sim u_2 \sim \dots \sim u_n \sim u_1$. It is shown, in [19], that $\dim(G) = 3$. Next, we investigate the \mathcal{R} -chromatic number of G with the help of the following five claims:

Claim 1. Every singleton, 2-element and 3-element subset of V possesses the property \mathcal{R} . Based on Remark 2(1) and due to $\dim(G) = 3$ [19], this claim is true, because a minimum resolving set for G is of cardinality 3, and so no singleton and 2-element subset of V is a resolving set for G .

Claim 2. For fixed $1 \leq i \leq n$, the sets $X = \{v_i, v_{i+(n/2)}, v\}$ and $Y = \{u_i, u_{i+(n/2)}, v\}$ are minimum resolving sets for G only when $v \in V - \{v_i, v_{i+(n/2)}, u_i, u_{i+(n/2)}\}$. Otherwise, $c_X(v_{i-1}) = c_X(v_{i+1})$ and $c_Y(v_{i-1}) = c_Y(v_{i+1})$.

Claim 3. For fixed $1 \leq i \leq n$, the set $Z = \{v_i, v_{i+(n/2)}, u_i, u_{i+(n/2)}\} \subset V$ possesses the property \mathcal{R} . By Claim 2, no subset of Z is a resolving set for G . It follows the required claim.

Claim 4. No r -independent set (other than Z) in G of cardinality greater than 3 contains any of the pairs $(v_i, v_{i+(n/2)})$ and $(u_i, u_{i+(n/2)})$.

Let S be an r -independent set in G of cardinality greater than 3. Suppose, without loss of

generality, S contains the pair $(v_i, v_{i+(n/2)})$. Then a subset $\{v_i, v_{i+(n/2)}, v\}$ of S for $v \in S - \{v_i, v_{i+(n/2)}\}$ is a resolving set for G , by Claim 2, which contradicts the r -independence of S . Thus, S cannot contain the pair $(v_i, v_{i+(n/2)})$. Similarly, the pair $(u_i, u_{i+(n/2)})$ will not contained in S .

Claim 5. For each $1 \leq k \leq n$, there is a k -element subset of V possessing the property \mathcal{R} . Claim 1 yields the result of $k = 1, 2, 3$. For $k = 4$, we have a set in (V, \mathcal{R}) , by Claim 3. Next, keeping Claim 4 in mind, let us consider two subset of V of cardinality n as follows: for fixed $1 \leq i \leq n$,

$$S_{1i} = \left\{ u_j, v_j; j = i + 1, i + 2, \dots, i + \frac{n}{2} \wedge l = i, i - 1, \dots, i - \frac{n}{2} + 1 \right\},$$

$$S_{2i} = \left\{ v_j, u_l; j = i + 1, i + 2, \dots, i + \frac{n}{2} \wedge l = i, i - 1, \dots, i - \frac{n}{2} + 1 \right\},$$

(12)

where the indices greater than n or less than or equal to zero will be taken modulo n . Then $d(u_i, x) = d(v_{i+1}, x)$ for all $x \in S_{1i}$ and $d(v_i, y) = d(u_{i+1}, y)$ for all $y \in S_{2i}$.

It follows that $c_W(u_i) = c_W(v_{i+1})$ for any $W \subseteq S_{1i}$ and $c_W(v_i) = c_W(u_{i+1})$ for any $W \subseteq S_{2i}$. Hence, both the S_{1i}, S_{2i} and each subset of any cardinality all are the subsets of V possessing the property \mathcal{R} , and of course, they are k -element subsets of V for $1 \leq k \leq n$.

Now, let $\lambda: V \rightarrow \{1, 2\}$ be a coloring of V , and let the corresponding color classes are, for fixed $1 \leq i \leq n$,

$$C_1 = \left\{ u_j, v_j; j = i + 1, i + 2, \dots, i + \frac{n}{2} \wedge l = i, i - 1, \dots, i - \frac{n}{2} + 1 \right\},$$

$$C_2 = \left\{ v_j, u_l; j = i + 1, i + 2, \dots, i + \frac{n}{2} \wedge l = i, i - 1, \dots, i - \frac{n}{2} + 1 \right\},$$

(13)

where the indices greater than n or less than or equal to zero will be taken modulo n . Then C_1 and C_2 define a partition of V . Also, Claim 5 yields that $C_1, C_2 \in (V, \mathcal{R})$. Hence, λ is an \mathcal{R} -coloring of V , and so $\chi_r(V, \mathcal{R}) = 2$. Therefore, $\dim(G) - \chi_r(V, \mathcal{R}) = 1$ for every even value of $n \geq 4$. \square

Remark 7. It is not necessary that the difference $\dim(G) - \chi_r(V, \mathcal{R})$ is constant (fixed) always. It can arbitrarily large depending upon the order of the graph. For instance, let G be a wheel graph of order $n \geq 8$, then $\dim(G) = \lfloor (2/5)(n + 1) \rfloor$ [20], and $\chi_r(V, \mathcal{R}) = 2$, by Theorem 3. So, it can be seen that the difference $\dim(G) - \chi_r(V, \mathcal{R}) = \lfloor (2/5)(n - 4) \rfloor$, which is depending upon n and is not fixed.

The next result shows that there exists a connected graph whose \mathcal{R} -chromatic number is different from its metric dimension by one.

Theorem 10. For odd $n \geq 3$, there exists a connected graph G with vertex set V such that $\chi_r(V, \mathcal{R}) - \dim(G) = 1$.

Proof. Let a cycle graph C_n on odd $n \geq 3$ vertices and a path P_2 . Then G is a graph obtained by taking the product of C_n and P_2 . Let the vertex set of G be $V = \{v_i, u_i; 1 \leq i \leq n\}$ and the edge set is $E = \{v_i \sim v_{i+1}, u_i \sim u_{i+1}, u_j \sim v_j; 1 \leq i \leq n - 1 \wedge 1 \leq j \leq n\}$. The resultant graph G consists of two n -cycles: one is outer cycle $v_1 \sim v_2 \sim \dots \sim v_n \sim v_1$, and the other one is inner cycle $u_1 \sim u_2 \sim \dots \sim u_n \sim u_1$. Note that $\text{diam}(G) = ((n + 1)/2)$, and it was show, in [19], that $\dim(G) = 2$, so a minimum resolving set for G consists of two vertices of G . Next, we investigate the \mathcal{R} -chromatic number of G on the base of the following six claims:

Claim 1. Every singleton and 2-element subset of V possesses the property \mathcal{R} . Based on Remark 2(1) and due to $\dim(G) = 2$ [19], this claim is true, because a minimum resolving set for G is of cardinality 2, and so no singleton subset of V is a resolving set for G .

Claim 2. A minimum resolving set for G contains both the vertices either from the outer cycle or from the inner cycle of G .

Let W be a minimum resolving set for G . For fixed $1 \leq i \leq n$, let $W = \{v_i, u_j\}$, where $1 \leq j \leq n$. Then,

$$c_W(v_{i+1}) = c_W(v_{i-1}) \text{ when } j = i,$$

$$c_W(v_{i+1}) = c_W(u_i) \text{ when } j = i + 1, i + 2, \dots, i + ((n - 1)/2), \text{ and}$$

$$c_W(v_j) = c_W(u_{j+1}) \text{ when } j = i + ((n - 1)/2) + 1, \dots, i + n,$$

where the indices greater than n or less than zero will be taken modulo n . It follows that W is not a resolving set for G , a contradiction.

Claim 3. For fixed $1 \leq i \leq n$, a minimum resolving set for G contains both the vertices:

$$x, y \in \{v_i, v_{i+(n-1)/2}, v_{i+(n-1)/2+1}, u_i, u_{i+(n-1)/2}, u_{i+(n-1)/2+1}\},$$

(14)

such that $d(x, y) = \text{diam}(G) - 1$.

Let W be a minimum resolving set for G , then W must contain both the vertices from the same cycle of G , by Claim 2. Let $W = \{v_i, v\}$ and $d(v_i, v) < \text{diam}(G) - 1$ (in G , no two vertices u, v belonging to a same cycle have $d(u, v) = \text{diam}(G)$). Then, $v \neq v_{i+((n-1)/2)}, v_{i+((n-1)/2)+1}$ and

$$c_W(u_{i+((n-1)/2)-1}) = c_W(v_{i+((n-1)/2)}) \text{ if } v \in \{v_{i+1}, \dots, v_{i+((n-1)/2)-1}\}, \text{ and}$$

$$c_W(v_{i+((n-1)/2)+1}) = c_W(u_{i+((n-1)/2)+2}) \text{ if } v \in \{v_{i+((n-1)/2)+2}, \dots, v_{i+n}\},$$

where the indices greater than n or less than or equal to zero will be taken modulo n . A

contradiction to the fact that W is a resolving set for G .

Claim 4. No r -independent set in G of cardinality greater than 2 contains two vertices x, y from a same cycle (outer or inner) of G such that $d(x, y) = \text{diam}(G) - 1$. Otherwise, the set $\{x, y\}$ is such a subset of that r -independent set which is resolving for G , by Claim 3.

Claim 5. For each $1 \leq k \leq n - 1$, there is a k -element subset of V possessing the property \mathcal{R} .

Claim 1 follows the claim for $k = 1, 2$. Next, keeping Claim 4 in mind, let us consider two subset of V of cardinality $n - 1$ as follows: for fixed $1 \leq i \leq n$,

$$S_{1i} = \left\{ u_j, v_l; j = i + 1, i + 2, \dots, i + \frac{n-1}{2} \wedge l = i, i - 1, \dots, i - \frac{n-1}{2} + 1 \right\},$$

$$S_{2i} = \left\{ v_j, u_l; j = i + 1, i + 2, \dots, i + \frac{n-1}{2} \wedge l = i, i - 1, \dots, i - \frac{n-1}{2} + 1 \right\},$$
(15)

where the indices greater than n or less than or equal to zero will be taken modulo n . Then, $d(u_i, x) = d(v_{i+1}, x)$ for all $x \in S_{1i}$ and $d(v_i, y) = d(u_{i+1}, y)$ for all $y \in S_{2i}$.

It follows that $c_W(u_i) = c_W(v_{i+1})$ for any $W \subseteq S_{1i}$ and $c_W(v_i) = c_W(u_{i+1})$ for any $W \subseteq S_{2i}$. Hence, both the set S_{1i}, S_{2i} and each subset of any cardinality all are the subsets of V

possessing the property \mathcal{R} , and of course, they are k -element subsets of V for $1 \leq k \leq n - 1$.

Claim 6. No r -independent set of cardinality greater than $n - 1$ exists in G . Otherwise, Claim 4 will be contradicted.

Now, let $\lambda: V \rightarrow \{1, 2, 3\}$ be a coloring of V , and let the corresponding color classes are: for fixed $1 \leq i \leq n$, $C_1 = \{v_{i+\text{diam}(G)}, u_{i+\text{diam}(G)}\}$,

$$C_2 = \left\{ u_j, v_l; j = i + 1, i + 2, \dots, i + \frac{n-1}{2} \wedge l = i, i - 1, \dots, i - \frac{n-1}{2} + 1 \right\},$$

$$C_3 = \left\{ v_j, u_l; j = i + 1, i + 2, \dots, i + \frac{n-1}{2} \wedge l = i, i - 1, \dots, i - \frac{n-1}{2} + 1 \right\},$$
(16)

where the indices greater than n or less than or equal to zero will be taken modulo n . Then C_1, C_2 , and C_3 define a partition of V . Also, Claims 1 and 5 yield that $C_1, C_2, C_3 \in (V, \mathcal{R})$. Hence, λ is an \mathcal{R} -coloring of V , and so $\chi_r(V, \mathcal{R}) = 3$. Therefore, $\chi_r(V, \mathcal{R}) - \dim(G) = 1$ for every odd value of $n \geq 3$. \square

Theorem 11. For odd $n \geq 3$, there exists a connected graph G with vertex set V such that $\chi_r(V, \mathcal{R}) = \dim(G)$.

Proof. Let G be a circulant network $C_{2n+1}(1, n)$ for odd $n \geq 3$ with vertex set $V = \{v_{i+1}; i \in Z_n\}$ (defined in Example 5), where the indices will be taken modulo n . The distance between v_i and v_j , ($j \neq i$) on the principal is denoted by $d^*(u_i, v_j)$ (for instance, in a circulant network $C_n(1, 3)$, $d(v_i, v_{i+3}) = 1$ where as $d^*(v_i, v_{i+3}) = 3$ for any $1 \leq i \leq n$). The metric dimension, $\dim(G)$, of G is 3 as shown in [21]. On the basis of the following three claims, we investigate the \mathcal{R} -chromatic number of G .

Remark 8. It is not necessary that the difference $\chi_r(V, \mathcal{R}) - \dim(G)$ is constant (fixed) always. It can arbitrarily large by depending upon the order of the graph. For instance, let G be a cycle graph of order $n \geq 3$, then $\dim(G) = 2$ [4] and $\chi_r(V, \mathcal{R}) = \lceil n/2 \rceil$, by Theorem 2. It can be seen that the difference $\chi_r(V, \mathcal{R}) - \dim(G) = \lfloor (n - 3)/2 \rfloor$, which is depending upon n and is not fixed.

Claim 1. Every k -element subset of V possesses the property \mathcal{R} for $1 \leq k \leq 3$.

As a minimum resolving set for G is of cardinality three, so no singleton and 2-element subset of V resolves G . It follows the claim.

Claim 2. No r -independent set in G of cardinality greater than three contains two vertices u and v such that $d^*(u, v) = n$.

The following result provides the existence of a connected graph whose metric dimension is equal to its \mathcal{R} -chromatic number.

If S is an r -independent set in G containing two vertices u and v such that $d^*(u, v) = n$, then the set $\{u, v, w\} \subset S$, for any $w \in S - \{u, v\}$, is a resolving set for G , a contradiction.

Claim 3. A maximum r -independent set in G consists of n consecutive vertices form the principal cycle.

Firstly, for fixed $1 \leq i \leq n$, we show that a set $S = \{v_i, v_{i+1}, \dots, v_{i+n-1}\} \subset V$ of n consecutive vertices form the principal cycle possesses the property \mathcal{R} . Note that, $d(v_{i+n}, s) = d(v_{i-1}, s)$ for all $s \in S$. It follows that $c_W(v_{i+n}) = c_W(v_{i-1})$ for each $W \subseteq S$. Hence, no subset of S is a resolving set for G . Secondly, if an r -independent set S either contains n non-consecutive vertices or contains more than n vertices (consecutive or nonconsecutive) form the principal cycle, then S must contradict Claim 2.

Now, let $\lambda: V \rightarrow \{1, 2, 3\}$ be a coloring of V , and let the corresponding color classes are: for fixed $1 \leq i \leq n$, $C_1 = \{v_{i+2n}\}$, $C_2 = \{v_i, v_{i+1}, \dots, v_{i+n-1}\}$, and $C_3 = \{v_{i+n}, v_{i+n+1}, \dots, v_{i+2n-1}\}$, where the indices will be taken modulo n . Then C_1, C_2 and C_3 define a partition of V . Also, Claims 1 and 3 yield that $C_1, C_2, C_3 \in (V, \mathcal{R})$. Hence, λ is an \mathcal{R} -coloring of V , and so $\chi_r(V, \mathcal{R}) = 3$. Therefore, $\chi_r(V, \mathcal{R}) = \dim(G)$ for every odd value of $n \geq 3$. \square

Data Availability

All the data and materials used to compute the results are provided in Section 1.

Conflicts of Interest

The authors declare that they have no conflicts of interest.

Acknowledgments

The first author, as a visiting researcher, is supported by the Punjab Higher Education Commission (PHEC) of Pakistan through International Research Support Fellowship (IRSF) Ref: PHEC/HRD/IRSF/1-20/2020/2674 at the University of Exeter, UK.

References

- [1] R. Trujillo-Rasua and I. Yero, "k-metric antidimension," *A privacy measure for social graphs*, *Information Sciences*, vol. 328, Article ID 403417, 2016.
- [2] Z. Beerliova, F. Eberhard, T. Erlebach et al., "Network discovery and verification," *IEEE Journal on Selected Areas in Communications*, vol. 24, no. 12, pp. 2168–2181, 2006.
- [3] S. Zhou, "Minimum partition of an independence system into independent sets," *Discrete Optimization*, vol. 6, no. 1, pp. 125–133, 2009.
- [4] G. Chartrand, L. Eroh, M. A. Johnson, and O. R. Oellermann, "Resolvability in graphs and the metric dimension of a graph," *Discrete Applied Mathematics*, vol. 105, no. 1–3, pp. 99–113, 2000.
- [5] F. Harary and R. A. Melter, "On the metric dimension of a graph," *Ars Combinatoria*, vol. 2, pp. 191–195, 1976.
- [6] S. Khuller, B. Raghavachari, and A. Rosenfeld, "Landmarks in graphs," *Discrete Applied Mathematics*, vol. 70, no. 3, pp. 217–229, 1996.
- [7] S. Li, J. B. Liu, and M. Munir, "On the metric dimension of generalized tensor product of interval with paths and cycles," *Journal of Mathematics*, vol. 2020, Article ID 2168713, 6 pages, 2020.
- [8] P. J. Slater, "Leaves of trees," *Congressus Numerantium*, vol. 14, pp. 549–559, 1975.
- [9] M. R. Garey and D. S. Johnson, *Computers and Intractability: A Guide to the Theory of NP-Completeness*, Freeman, New York, NY, USA, 1979.
- [10] N. Alon, D. N. Kozlov, and V. H. Vu, "The geometry of coin-weighting problems," in *Proceedings of the 37th Annual Symposium on Foundations of Computer Science*, vol. 96, pp. 524–532, Burlington, VT, USA, 1996.
- [11] V. Chvátal, "Mastermind," *Combinatorica*, vol. 3, no. 3–4, pp. 325–329, 1983.
- [12] M. A. Johnson, "Browseable structure-activity datasets," in *Advances in Molecular Similarity*, R. Carb-Dorca and P. Mezey, Eds., pp. 153–170, JAI Press, Greenwich, CT, USA, 1998.
- [13] A. Sebő and E. Tannier, "On metric generators of graph," *Mathematics of Operations Research*, vol. 29, no. 2, pp. 383–393, 2004.
- [14] D. L. Boutin, "Determining sets, resolving sets, and the exchange property," *Graphs and Combinatorics*, vol. 25, no. 6, pp. 789–806, 2009.
- [15] Z. E. Shams, M. Salman, and U. Ali, "On maximal det-independent (res-independent) sets in graphs (hal-03250074)," 2021.
- [16] C. Hernando, M. Mora, I. M. Pelayo, C. Seera, and D. R. Wood, "Extremal graph theory for metric dimension and diameter," *Electronic Journal of Combinatorics*, vol. 17, 2010.
- [17] J. C. Bermound, F. Comellas, and D. F. Hsu, "Distributed loop computer networks: survey," *Journal of Parallel and Distributed Computing*, vol. 24, pp. 2–10, 1995.
- [18] M. Salman, I. Javaid, and M. A. Chaudhry, "Resolvability in circulant graphs," *Acta Mathematica Sinica, English Series*, vol. 28, no. 9, pp. 1851–1864, 2012.
- [19] J. Cáceres, C. Hernando, M. Mora et al., "On the metric dimension of Cartesian products of graphs," *SIAM Journal on Discrete Mathematics*, vol. 21, no. 2, pp. 423–441, 2007.
- [20] P. S. Buczkowski, G. Chartrand, C. Poisson, and P. Zhang, "On k-dimensional graphs and their bases, periodica math," *Periodica Mathematica Hungarica*, vol. 46, no. 1, pp. 9–15, 2003.
- [21] I. Khalid, M. Salman, and F. Ali, "Metric index of circulant networks," 2013.

Research Article

On Constant Metric Dimension of Some Generalized Convex Polytopes

Xuewu Zuo ¹, Abid Ali ², Gohar Ali ², Muhammad Kamran Siddiqui ³,
Muhammad Tariq Rahim ⁴ and Anton Asare-Tuah ⁵

¹Department of General Education, Anhui Xinhua University, Hefei, China

²Department of Mathematics, Islamia College, Peshawar, Khyber Pakhtunkhwa, Pakistan

³Department of Mathematics, COMSATS University Islamabad, Lahore Campus, Pakistan

⁴Department of Mathematics, Abbottabad University of Science and Technology, Abbottabad, Khyber Pakhtunkhwa, Pakistan

⁵Department of Mathematics, University of Ghana, Legon, Ghana

Correspondence should be addressed to Anton Asare-Tuah; aasare-tuah@ug.edu.gh

Received 12 June 2021; Accepted 31 July 2021; Published 10 August 2021

Academic Editor: Antonio Di Crescenzo

Copyright © 2021 Xuewu Zuo et al. This is an open access article distributed under the Creative Commons Attribution License, which permits unrestricted use, distribution, and reproduction in any medium, provided the original work is properly cited.

Metric dimension is the extraction of the affine dimension (obtained from Euclidean space E^d) to the arbitrary metric space. A family $\mathcal{F} = (G_n)$ of connected graphs with $n \geq 3$ is a family of constant metric dimension if $\dim(G) = k$ (some constant) for all graphs in the family. Family \mathcal{F} has bounded metric dimension if $\dim(G_n) \leq M$, for all graphs in \mathcal{F} . Metric dimension is used to locate the position in the Global Positioning System (GPS), optimization, network theory, and image processing. It is also used for the location of hospitals and other places in big cities to trace these places. In this paper, we analyzed the features and metric dimension of generalized convex polytopes and showed that this family belongs to the family of bounded metric dimension.

1. Introduction

Let $G \in \mathcal{F}$ be a finite, simple, and undirected connected graph with vertex set $V = V(G) = \{v_1, v_2, \dots, v_n\}$ and edge set $E = E(G)$. The distance between two vertices is denoted by $d(v_s, v_j) = d_{s,j}$ where $d_{s,j}$ is the length of the shortest path between these vertices in G . Moreover, the distance $d_{s,j} = d_{j,s}$ because all graphs are undirected. An ordered subset $W = \{w_1, w_2, \dots, w_k\}$ of V is called a resolving set or locating set for G if for any two distinct vertices v_s and v_j , their codes are distinct with respect to Z , where $\text{code}(v_s) = (d(v_s, z_1), d(v_s, z_2), \dots, d(v_s, z_k)) \in \mathbb{W}^k$ is a vector [1]. $\min\{|W| : W \text{ is a resolving set of } G\} = \dim(G) = \beta(G)$ is called the metric dimension or locating number of G , and such a resolving set Z is called a basis set for G . To investigate Z is a basis set for G , it suffices to show that, for all different vertices $x, y \in V \setminus W$, their codes are also different because for any $w_j \in W$, $1 \leq j \leq k$, the j th component of the code is zero, while all other components are nonzero. For more details about $\beta(G)$ and resolving sets, one can read [1–4].

Lemma 1 (see [3]). *For a connected graph G with resolving set W , if $d(x_s, w) = d(x_j, w)$ for all $w \in V \setminus \{x_s, x_j\}$, then $W \cap \{x_s, x_j\} \neq \emptyset$.*

The join of two graphs G and H represented as $G + H$ is a graph with $V(G + H) = V(G) \cup V(H)$ and $E(G + H) = E(G) \cup E(H) \cup \{gh : g \in V(G) \text{ and } h \in V(H)\}$. $W_n = C_n + K_1$ is a wheel graph of order $n + 1$ for $n \geq 3$. $f_n = P_n + K_1$ is a fan graph obtained from the amalgamation of the path on n vertices with a single vertex graph K_n . Jahangir or gear graph J_{2n} is obtained from the wheel graph W_{2n} by deleting n -cycle edges alternatively; see in [4]. The following results appear in [5–7] for the graphs defined above.

Theorem 1. *For wheel graph W_n , fan graph f_n , and Jahangir graph J_{2n} , we have the following:*

- (i) $\beta(W_n) = \lfloor (2n + 2)/5 \rfloor$, for every $n \geq 7$
- (ii) $\beta(f_n) = \lfloor (2n + 2)/5 \rfloor$, for every $n \geq 7$

(iii) $\beta(J_{2n}) = \lfloor 2n/3 \rfloor$, for every $n \geq 4$

All the above three families of graphs are planar, and their metric dimension depends on the number of vertices in the graph, which shows that the metric dimension of these graphs is unbounded [8, 9]. Khuller et al. [10] clarified the properties of those graphs whose metric dimension is two.

Theorem 2 (see [10]). Let $\beta(G) = 2 = |W|$, where $W = \{x, y\} \subset V(G)$; then, the following holds:

- (i) There is a unique shortest path P between x and y
- (ii) $\deg(x) \leq 3$ or $\deg(y) \leq 3$
- (iii) For every other vertex z except x and y on P , $\deg(z) \leq 5$

Definition 1 (see [11]). A set $K \subset \mathbb{R}^d$ is said to be convex if the line segment \overline{xy} : $\lambda x + (1 - \lambda)y$, $0 \leq \lambda \leq 1$, lies inside K for all distinct pairs of point $x, y \in K$.

Definition 2 (see [11]). The smallest convex set containing K (the intersection of the family of all convex sets that contain K) is called the convex hull of K , denoted by $\text{Conv}(K) = \cap_{K \subset S_s} S_s$, where S_s is a convex set.

Definition 3 (see [11]). A convex polytope is a bounded convex linear combination of convex sets.

There are some families of graphs with constant metric dimension (see [2]); these families are generated by convex polytopes. The problem of finding $\beta(G)$ is NP-complete (see [2]).

Theorem 3 (see [12]). Let S_n^p be a convex polytope with p -pendent vertices; then, $\dim(S_n^p) = 3$ for all $n \geq 6$.

Theorem 4 (see [12]). The metric dimension of convex polytope T_n^p with p -pendent edges is 3 for every $n \geq 6$.

Theorem 5 (see [12]). $\beta(U_n^p) = 3$ for $n \geq 6$, where U_n^p is a convex polytope graph with p -pendents.

For more details about the metric dimension of certain families of graphs, see [13, 14]. Here, we will investigate

generalized convex polytopes with pendent edges for their metric dimensions.

2. Main Results

This section is devoted to the main results which we proved for the newly introduced generalized convex polytopes. The convex polytopes S_n , T_n , and U_n were examined by Muhammad et al. for their metric dimensions in [2] and proved that these families belong to the family of constant metric dimension.

Generalized convex polytope $S_{n,m}$ is the generalization of S_n , with one n -sided and infinite face each, 3-sided faces being $2n$, and 4-sided faces being $n(m - 2)$, so the total number of faces is $nm + 2$. The convex polytope $S_{n,m}^p$ is obtained from the generalized convex polytope graph by attached p -pendent vertices at the outer cycle of $S_{n,m}$, shown in Figure 1. The generalized convex polytope $S_{n,m}^p$ with p -pendents is a graph consisting of m cycles, with vertex and edge sets

$$\begin{aligned} V(S_{n,m}^p) &= \{X_s^j: 1 \leq s \leq n, 1 \leq j \leq m\}, \\ E(S_{n,m}^p) &= \{X_s^j X_{s+1}^j: 1 \leq s \leq n, 1 \leq j \leq m\} \\ &\cup \{X_s^j X_s^{j+1}: 1 \leq s \leq n, 1 \leq j \leq m\} \\ &\cup \{X_{s+1}^1 X_s^2: 1 \leq s \leq n\}. \end{aligned} \quad (1)$$

In the set of edges, indices are taken as modulo n and m .

In [2], it was shown that $\beta(S_n) = 3$, for $n \geq 6$. In the result below, we proved that the metric dimension for the generalized convex polytope of S_n is still 3, which implies that S_n , S_n^p , and $S_{n,m}^p$ belong to the same family of constant metric dimension.

Theorem 6. Let $G = S_{n,m}^p$ be the generalized convex polytope graph defined above; then, $\beta(G) = 3$ for $n \geq 6$ and $m \geq 5$.

Proof. Validating the mentioned theorem with the help of double inequalities, two cases are present:

Case (i): for n is even.

Let $n = 2\alpha'$ where $\alpha' \geq 3$ is an integer. As $|N_2(x)| \geq 6$ for all $x \in S_{n,m}$, it is guaranteed by [15] that $\beta(G) \geq 3$.

Consider $Z = \{X_1^1, X_2^1, X_{l+1}^1\}$ to be an ordered subset of $V(S_{n,m}^p)$; to show that Z is a basis set for G , codes of the elements of $V(S_{n,m}^p) \setminus Z$ with respect to Z are given in the following scheme:

$$\begin{aligned} r(X_s^1|Z) &= \begin{cases} (s-1, s-2, \alpha' - s + 1), & \alpha' \geq s \geq 3, \\ (2\alpha' - s + 1, 2\alpha' - s + 2, s - \alpha' - 1), & 2\alpha' \geq s \geq \alpha' + 2, \end{cases} \\ r(X_s^2|Z) &= \begin{cases} (1, 1, \alpha'), & s = 1, \\ (s, s - \alpha', \alpha' - s + 1), & \alpha' \geq s \geq 2, \\ (\alpha', \alpha', 1), & s = \alpha' + 1, \\ (2\alpha' - s + 1, 2\alpha' - s + 2, s - 1), & 2\alpha' \geq s \geq \alpha' + 2. \end{cases} \end{aligned} \quad (2)$$

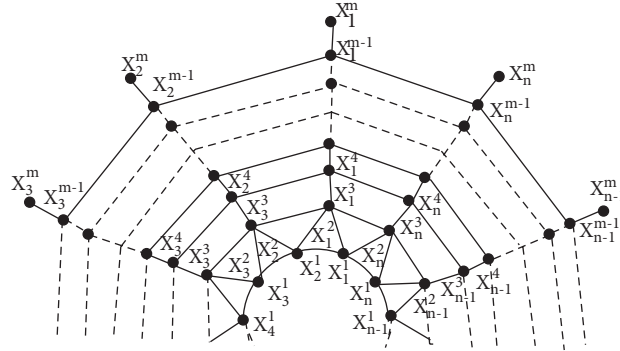


FIGURE 1: The generalized convex polytope graph $S_{n,m}^p$.

Codes for the vertices X_s^m for $1 \leq s \leq n$ and $m \geq 3$ are given in the following:

$$r(X_s^m|Z) = (m - 2, m - 2, m - 2) + r(X_s^2|Z). \quad (3)$$

It proves that $\beta(G) \leq 3$ implies that the metric dimension of $G = S_{n,m}^p$ is 3.

Case (ii): for n is an odd integer.

Let $n = 2\alpha' + 1$, where $\alpha' \geq 3$, and by [15], $\beta(G) \geq 3$; for reaching the conclusion, it remains to show that $\beta(G) \leq 3$.

Let $Z = \{X_1^1, X_2^1, X_{l+1}^1\}$ be an ordered subset of $S_{n,m}^p$; the formulation for the representation of nodes for $V(S_{n,m}^p) \setminus Z$ with respect to Z is given in the following:

$$r(X_s^1|Z) = \begin{cases} (s - 1, s - 2, \alpha' - s + 1), & \alpha' \geq s \geq 3, \\ (\alpha', \alpha', 1), & s = \alpha' + 2, \\ (2\alpha' - s + 2, 2\alpha' - s + 3, s - \alpha' - 1), & 2\alpha' + 1 \geq s \geq \alpha' + 3, \end{cases}$$

$$r(X_s^2|Z) = \begin{cases} (1, 1, \alpha'), & s = 1, \\ (s, s - \alpha', \alpha' - s, l - s + 1), & \alpha' \geq s \geq 2, \\ (\alpha' + 1, \alpha', 1), & s = \alpha' + 1, \\ (2\alpha' - s + 2, 2\alpha' - s + 3, s - \alpha'), & n \geq s \geq \alpha' + 2. \end{cases} \quad (4)$$

The representation of the vertices X_s^m , $1 \leq s \leq n$ and $m \geq 3$, is as follows:

$$r(X_s^m|Z) = (m - 2, m - 2, m - 2) + r(X_s^2|Z). \quad (5)$$

It shows that, for any two distinct vertices $x, y \in S_{n,m}^p$ for odd $n \geq 7$, $r(x|Z) \neq r(y|Z)$ implying that $\beta(G) \leq 3$; this completes the proof. \square

3. Generalized Convex Polytope Graph $T_{n,m}^p$

In [16], Imran et al. proved the metric dimension of convex polytope T_n . The general form of T_n is denoted by $T_{n,m}$ known as the generalized convex polytope (for short, GCP); this graph consists of one each n -sided and infinite face, respectively, and the number of 3-sided faces is $4n$ and 4-sided faces is $n(m - 3)$. The GCP graph $T_{n,m}^p$ is a graph with p -pendent edges. Vertex and edge sets for $G = T_{n,m}^p$ are given in the following:

$$V(T_{n,m}^p) = \{X_s^j : 1 \leq s \leq n, 1 \leq j \leq m\},$$

$$E(T_{n,m}^p) = \{X_s^j X_{s+1}^j : 1 \leq s \leq n, 1 \leq j \leq m\}$$

$$\cup \{X_s^j X_s^{j+1} : 1 \leq s \leq n, 1 \leq j \leq m - 3\}$$

$$\cup \{X_{s+1}^{m-2} X_s^{m-1} : 1 \leq s \leq n\} \cup \{X_s^{m-1} X_s^m : 1 \leq s \leq n\}. \quad (6)$$

In the set of edges, indices are taken as modulo n and m . In Figure 2, the graph $G = T_{n,m}^p$ is shown.

The result given below shows that $T_{n,m}^p$ belongs to the family of constant metric dimension.

Theorem 7. Let $T_{n,m}^p$ be a GCP graph with p -pendents for all $n \geq 6$; then, $\beta(T_{n,m}^p) = 3$.

Proof. As $|N_2(v)| \geq 6$ for all nonpendent vertices of $T_{n,m}^p$, $\beta(T_{n,m}^p) \geq 3$ for all $n \geq 6$ by [15]. To complete the proof, it suffices to show that any ordered subset of the vertices of this graph is a resolving set.

Case (i): for n is an even integer.

Let $n = 2\alpha'$ with $\alpha' \geq 3$; consider an ordered subset $Z = \{X_1^1, X_2^1, X_{l+1}^1\}$ of vertices of $T_{n,m}^p$. The representation of

vertices of $V(T_{n,m}^p) \setminus Z$ with respect to Z is formulated as follows:

$$r(X_s^1|Z) = \begin{cases} (s-1, s-2, \alpha' - s + 1), & \alpha' \geq s \geq 3, \\ (2\alpha' - s + \alpha', 2\alpha' - s + 2, s - \alpha' - 1), & 2\alpha' \geq s \geq \alpha' + 2, \end{cases}$$

$$r(X_s^2|Z) = \begin{cases} (1, 1, \alpha'), & s = 1, \\ (s, s - \alpha', \alpha' - s + 1), & \alpha' \geq s \geq 2, \\ (\alpha', \alpha', 1), & s = \alpha' + 1, \\ (2\alpha' - s + 1, 2\alpha' - s + 2, s - \alpha'), & 2 \geq s \geq \alpha' + 2. \end{cases} \quad (7)$$

For $3 \leq j \leq m - 2$,

$$r(X_s^j|Z) = (j-2, j-2, j-2) + s(X_s^2|Z). \quad (8)$$

$$r(X_s^{m-1}|Z) = \begin{cases} (2+1, 2+1, \alpha' + 1), & s = 1, \\ (s+2, s+1, \alpha' - s + 2), & \alpha' - 1 \geq s \geq 2, \\ (\alpha' + 2, \alpha' + 1, 3), & s = \alpha', \\ (\alpha' + 1, \alpha' + 2, 3), & s = \alpha' + 1, \\ (2\alpha' - s + 2, 2\alpha' - s + 3, s - \alpha' + 2), & \\ \alpha' + 2 \leq s \leq n - 1, & \\ (3, 3, \alpha' + 2), & s = n. \end{cases} \quad (9)$$

Codes of the pendent vertices are given as follows:

$$r(X_s^m|Z) = (1, 1, 1) + r(X_s^{m-1}|Z). \quad (10)$$

From the above formulation, it is obvious that no two distinct vertices of the GCP with pendants p have the same code with respect to Z , which implies that $\beta(T_{n,m}^p) = 3$.

Case (ii): for n is an odd integer.

Let $n = 2\alpha' + 1$ for $\alpha' \geq 3$; suppose an ordered subset $Z = \{x_1^1, X_2^1, X_{l+1}^1\}$ of vertices $V(T_{n,m}^p)$; to show that Z is a basis set for $T_{n,m}^p$, the formulation codes are given as follows:

$$r(X_s^1|Z) = \begin{cases} (s-1, s-2, \alpha' - s + 1), & \alpha' \geq s \geq 3, \\ (\alpha', \alpha', 1), & s = \alpha' + 2, \\ (2\alpha' - s + 2, 2\alpha' - s + 3, s - \alpha' - 1), & n \geq s \geq \alpha' + 3, \end{cases}$$

$$r(X_s^2|Z) = \begin{cases} (1, 1, \alpha'), & s = 1, \\ (s, s - 1, \alpha' - s + 1), & \alpha' \geq s \geq 2, \\ (\alpha' + 1, \alpha', 1), & s = \alpha' + 1, \\ (2\alpha' - s + 2, 2\alpha' - 3, s - \alpha' - 1), & n \geq s \geq \alpha' + 2. \end{cases} \quad (11)$$

Codes given to the vertices of other interior cycles are

$$r(X_s^j|Z) = (j - 2, j - 2, j - 2) + r(X_s^2|Z), \quad \text{for } 1 \leq j \leq m - 2. \quad (12)$$

Representation given to the second last cycle X_s^{m-1} is

$$r(X_s^{m-1}|Z) = \begin{cases} (2 + 1, 2 + 1, \alpha' + 1), & s = 1, \\ (s + 2, s + 1, \alpha' - s + 2), & \alpha' - 1 \geq s \geq 2, \\ (\alpha' + 2, \alpha' + 1, 3), & s = \alpha', \\ (\alpha' + 2, \alpha' + 2, 3), & s = \alpha' + 1, \\ (2\alpha' - s + 3, 2\alpha' - s + 4, s - \alpha' + 2), & \\ (n - 1 \geq s \geq \alpha' + 2), & \\ (3, 3, \alpha' + 2), & s = n. \end{cases} \quad (13)$$

The same representation is given to the pendent vertices:

$$r(X_s^m|Z) = (1, 1, 1) + r(X_s^{m-1}|Z). \quad (14)$$

It shows that Z is a resolving set for $T_{n,m}^p$ for n -odd and p -pendents, $\beta(T_{n,m}^p) = 3$, and this completes the proof. \square

4. Generalized Convex Polytope Graph $U_{n,m}^p$

In [2], the graph U_n is given, and a generalized graph $U_{n,m}^p$ of U_n is shown in Figure 3. The vertex and edge sets for this graph are given as follows:

$$\begin{aligned} V(U_{n,m}^p) &= \{X_s^j : 1 \leq s \leq n, s \leq j \leq m\}, \\ E(U_{n,m}^p) &= \{X_s^j X_{s+1}^j : 1 \leq s \leq n, 1 \leq j \leq m - 1\} \\ &\cup \{X_s^j X_s^{j+1} : 1 \leq s \leq n, 1 \leq j \leq m - 4\} \\ &\cup \{X_s^{m-3} X_s^{m-2} : 1 \leq s \leq n\} \\ &\cup \{X_s^{m-2} X_{s+1}^{m-3} : 1 \leq s \leq n\} \\ &\cup \{X_s^{m-2} X_s^{m-1} : 1 \leq s \leq n\} \\ &\cup \{X_s^{m-1} X_s^m : 1 \leq s \leq n\}. \end{aligned} \quad (15)$$

We will show that GCP graph $U_{n,m}^p$ with $n \geq 6$ along with p -pendent vertices belongs to the family of constant metric dimension and its locating number is 3.

Theorem 8. *Let $U_{n,m}^p$ be a GCP graph for $n \geq 6$; then, $\dim(U_{n,m}^p) = 3$.*

Proof. According to [15], $\dim(G) \geq 3$ if and only if $|N_2(x)| \geq 6$ or $|N_3(x)| \geq 8$ for all $x \in V(G)$ as $|N_2(x)| \geq 6$ for every nonpendent vertex x of $U_{n,m}^p$ implying that $\dim(U_{n,m}^p) \geq 3$. To reach the conclusion, it remains to show that there exists a resolving set for $U_{n,m}^p$ with exactly three elements. For this, consider the following two cases:

Case (i): for an integer n is even. Let $n = 2\alpha'$, where $\alpha' \geq 3$; take $Z = \{X_1^1, X_2^1, X_{\alpha'+1}^1\}$ to be an ordered subset of $V(U_{n,m}^p)$; to show that Z resolves vertices of the GCP, the representation of vertices of the GCP is shown as follows:

$$r(X_s^1|Z) = \begin{cases} (s - 1, s - 2, s - \alpha' + 1), & \alpha' \geq s \geq 3, \\ (2\alpha' - s + 1, 2\alpha' - s + 2, s - \alpha' - 1), & 2\alpha' \geq s \geq \alpha' + 2. \end{cases} \quad (16)$$

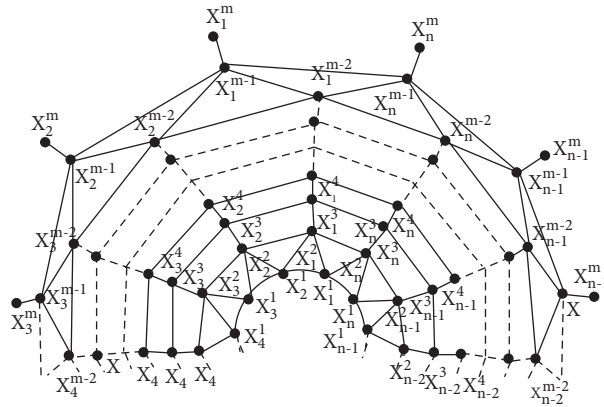


FIGURE 2: GCP graph $T_{n,m}^p$.

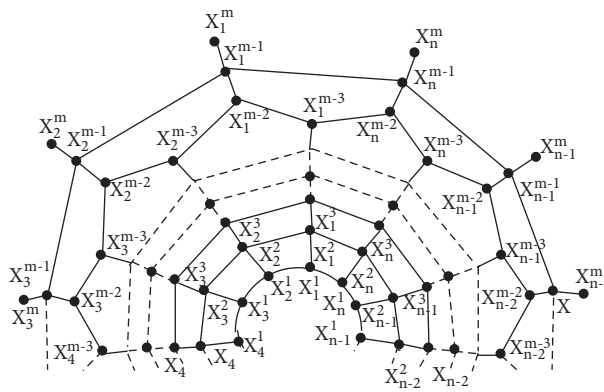


FIGURE 3: The generalized convex polytope graph $U_{n,m}^p$.

For $2 \leq j \leq m - 3$,

$$r(X_s^j|Z) = (j - 1, j - 1, j - 1) + r(X_s^1|Z). \quad (17)$$

Representation given to the X_i^{m-2} cycle is

$$r(X_s^{m-2}|Z) = \begin{cases} (3, 3, \alpha' + 2), & s = 1 \\ (s + 2, s + 1, \alpha' - s + 3), & \alpha' \geq s \geq 2, \\ (\alpha' + 2, \alpha' + 2, 3), & s = \alpha' + 1, \\ (2\alpha' - s + 3, 2\alpha' - s + 4, s - \alpha' + 2), & 2\alpha' \geq s \geq \alpha' + 2. \end{cases} \quad (18)$$

Representation of the vertices of the outer cycle is

$$r(X_s^{m-1}|Z) = (1, 1, 1) + r(X_s^{m-2}|Z), \quad 1 \leq s \leq n. \quad (19)$$

Representation of pendent vertices is

$$r(X_s^m|Z) = (2, 2, 2) + r(X_s^{m-2}|Z), \quad 1 \leq s \leq n. \quad (20)$$

It shows that Z is a resolving set for GCP $U_{n,m}^p$ implying that $\dim(U_{n,m}^p) = 3$.

Case (ii): when n is an odd integer. Let $n = 2\alpha' + 1$ for $\alpha' \geq 3$; let $Z = \{X_1^1, X_2^1, X_{\alpha'+1}^1\}$ be an ordered subset of the vertices of the GCP. To show that Z is a locating set for $U_{n,m}^p$, consider the codes' formulation of the vertices of the GCP with respect to Z as

$$r(X_1^1|Z) = \begin{cases} (s - 1, s - 2, \alpha' - s + 1), & \alpha' \geq s \geq 3, \\ (\alpha', \alpha', 1), & s = \alpha' + 2, \\ (2\alpha' - s + 2, 2\alpha' - s + 3, s - \alpha' - 1), & 2\alpha' + 1 \geq s \geq \alpha' + 3. \end{cases} \quad (21)$$

For $2 \leq j \leq m - 2$,

$$r(X_s^j|Z) = (j - 1, j - 1, j - 1) + r(X_s^1). \quad (22)$$

Representation given to the vertices of the interior cycle is

$$r(X_s^{m-2}|Z) = \begin{cases} (3, 3, \alpha' + 2), & s = 1, \\ (s + 2, s + 1, \alpha' - s + 3), & \alpha' \geq s \geq 2, \\ (\alpha' + 3, \alpha' + 2, 3), & s = \alpha' + 1, \\ (\alpha' + 2, \alpha' + 1, 4), & s = \alpha' + 2, \\ (\alpha' + 1, \alpha', 5), & s = \alpha' + 3, \\ (2\alpha' - s + 4, 2\alpha' - s + 5, s - \alpha' + 2), & \\ 2\alpha' + 1 \geq s \geq \alpha' + 3. \end{cases} \quad (23)$$

Representation given to the nodes of the outer cycle is

$$r(X_s^{m-1}|Z) = (1, 1, 1) + r(X_s^{m-2}|Z), \quad 1 \leq s \leq n. \quad (24)$$

Also, representation given to the nodes hanging is

$$(X_s^m|Z) = (2, 2, 2) + r(X_s^{m-2}|Z), \quad 1 \leq s \leq n. \quad (25)$$

It gives us that Z is a resolving set for GCP $U_{n,m}^p$, implying that the metric dimension of GCP $U_{n,m}^p$ is 3. \square

5. Concluding Remarks

In this paper, we focus to study those graphs obtained from convex polytopes and examine that generalized convex polytopes (GCPs) also belong to the family of constant metric dimension such as their parent graphs S_n, T_n , and U_n .

Data Availability

The data used to support the findings of this study are cited at relevant places within the text as references.

Conflicts of Interest

The authors declare that they have no conflicts of interest.

Authors' Contributions

All authors contributed equally to this work.

References

[1] J.-B. Liu, M. F. Nadeem, H. M. A. Siddiqui, and W. Nazir, "Computing metric dimension of certain families of toeplitz graphs," *IEEE Access*, vol. 7, pp. 126734–126741, 2019.

[2] I. Muhammad, A. Q. Baig, and A. Ali, "Families of plane graphs with constant metric dimension," *Utilitas Mathematica*, vol. 88, pp. 43–53, 2012.

[3] C. Gary, L. Eroh, M. A. Johnson, and O. R. Oellermann, "Resolvability in graphs and the metric dimension of a graph," *Discrete Applied Mathematics*, vol. 105, no. 1-3, pp. 99–113, 2000.

[4] I. Tomescu, J. Imran, and S. Imran, "On the partition and connected partition dimension of Wheels," *Ars Combinatoria*, vol. 84, pp. 311–318, 2007.

[5] B. Peter, C. Gary, C. Poisson, and P. Zhang, "On k -dimensional graphs and their bases," *Periodica Mathematica Hungarica*, vol. 46, no. 1, pp. 9–15, 2003.

[6] J. Cáceres, C. Hernando, M. Mora et al., "On the metric dimension of some families of graphs," *Electronic Notes in Discrete Mathematics*, vol. 22, no. 2, pp. 129–133, 2005.

[7] I. Tomescu and J. Imran, "On the metric dimension of the Jahangir graph," *Bulletin mathématique de la Société des Sciences Mathématiques de Roumanie*, vol. 7, pp. 371–376, 2007.

[8] I. Javaid, *On metric and partition dimension of some wheel related graphs*, PhD Thesis, GC University Lahore, Lahore, Pakistan, 2007.

[9] I. Javaid, M. T. Rahim, and K. Ali, "Families of regular graphs with constant metric dimension," *Utilitas Mathematica*, vol. 75, pp. 21–33, 2008.

[10] S. Khuller, B. Raghavachari, and A. Rosenfeld, "Landmarks in graphs," *Discrete Applied Mathematics*, vol. 70, no. 3, pp. 217–229, 1996.

[11] B. Grünbaum and G. C. Shephard, "Convex polytopes," *Bulletin of the London Mathematical Society*, vol. 1, no. 3, pp. 257–300, 1969.

[12] M. Imran, S. A. Ul Haq Bokhary, and A. Q. Baig, "On the metric dimension of convex polytopes," *AKCE International Journal of Graphs and Combinatorics*, vol. 10, no. 3, pp. 295–307, 2013.

[13] C. Gary, E. Salehi, and P. Zhang, "The partition dimension of a graph," *Aequationes Mathematicae*, vol. 59, pp. 45–54, 2000.

[14] I. Tomescu, "On the ratio between partition dimension and metric dimension of a connected graph," *Analele Universitatii Bucuresti. Matematica-Informatica*, vol. 55, pp. 3–10, 2006.

[15] Z. Shao, S. M. Sheikholeslami, Pu Wu, and J.-B. Liu, "The metric dimension of some generalized Petersen graphs," *Discrete Dynamics in Nature and Society*, vol. 8, pp. 19–29, 2018.

[16] M. Imran, S. A. Ul Haq Bokhary, and A. Q. Baig, "On families of convex polytopes with constant metric dimension," *Computers and Mathematics with Applications*, vol. 60, no. 9, pp. 2629–2638, 2010.

Research Article

Resistance Distance in Tensor and Strong Product of Path or Cycle Graphs Based on the Generalized Inverse Approach

Muhammad Shoaib Sardar ¹, Xiang-Feng Pan, ¹ Dalal Alrowaili ²,
and Imran Siddique ³

¹School of Mathematical Sciences, Anhui University, Hefei, Anhui 230601, China

²Department of Mathematics, College of Science, Jouf University, P.O. Box: 2014, Sakaka, Saudi Arabia

³Department of Mathematics, University of Management and Technology, Lahore 54770, Pakistan

Correspondence should be addressed to Imran Siddique; imransmsrazi@gmail.com

Received 11 June 2021; Accepted 22 July 2021; Published 9 August 2021

Academic Editor: Ali Ahmad

Copyright © 2021 Muhammad Shoaib Sardar et al. This is an open access article distributed under the Creative Commons Attribution License, which permits unrestricted use, distribution, and reproduction in any medium, provided the original work is properly cited.

Graph product plays a key role in many applications of graph theory because many large graphs can be constructed from small graphs by using graph products. Here, we discuss two of the most frequent graph-theoretical products. Let \mathcal{G}_1 and \mathcal{G}_2 be two graphs. The Cartesian product $\mathcal{G}_1 \square \mathcal{G}_2$ of any two graphs \mathcal{G}_1 and \mathcal{G}_2 is a graph whose vertex set is $V(\mathcal{G}_1 \square \mathcal{G}_2) = V(\mathcal{G}_1) \times V(\mathcal{G}_2)$ and $(a_1, a_2)(b_1, b_2) \in E(\mathcal{G}_1 \square \mathcal{G}_2)$ if either $a_1 = b_1$ and $a_2 b_2 \in E(\mathcal{G}_2)$ or $a_1 b_1 \in E(\mathcal{G}_1)$ and $a_2 = b_2$. The tensor product $\mathcal{G}_1 \times \mathcal{G}_2$ of \mathcal{G}_1 and \mathcal{G}_2 is a graph whose vertex set is $V(\mathcal{G}_1 \times \mathcal{G}_2) = V(\mathcal{G}_1) \times V(\mathcal{G}_2)$ and $(a_1, a_2)(b_1, b_2) \in E(\mathcal{G}_1 \times \mathcal{G}_2)$ if $a_1 b_1 \in E(\mathcal{G}_1)$ and $a_2 b_2 \in E(\mathcal{G}_2)$. The strong product $\mathcal{G}_1 \boxtimes \mathcal{G}_2$ of any two graphs \mathcal{G}_1 and \mathcal{G}_2 is a graph whose vertex set is defined by $V(\mathcal{G}_1 \boxtimes \mathcal{G}_2) = V(\mathcal{G}_1) \times V(\mathcal{G}_2)$ and edge set is defined by $E(\mathcal{G}_1 \boxtimes \mathcal{G}_2) = E(\mathcal{G}_1 \square \mathcal{G}_2) \cup E(\mathcal{G}_1 \times \mathcal{G}_2)$. The resistance distance among two vertices u and v of a graph \mathcal{G} is determined as the effective resistance among the two vertices when a unit resistor replaces each edge of \mathcal{G} . Let P_n and C_n denote a path and a cycle of order n , respectively. In this paper, the generalized inverse of Laplacian matrix for the graphs $P_{n_1} \times C_{n_2}$ and $P_{n_1} \boxtimes P_{n_2}$ was procured, based on which the resistance distances of any two vertices in $P_{n_1} \times C_{n_2}$ and $P_{n_1} \boxtimes P_{n_2}$ can be acquired. Also, we give some examples as applications, which elucidated the effectiveness of the suggested method.

1. Introduction

Graph products [1] became an interesting area of research, and different types of products have been worked out in graph theory and other fields. The Cartesian product $\mathcal{G}_1 \square \mathcal{G}_2$ of any two graphs \mathcal{G}_1 and \mathcal{G}_2 is a graph whose vertex set is $V(\mathcal{G}_1) \times V(\mathcal{G}_2)$ and two vertices (a_1, a_2) and (b_1, b_2) are adjacent in $\mathcal{G}_1 \square \mathcal{G}_2$ if and only if either $a_1 = b_1$ and a_2 is adjacent to b_2 in \mathcal{G}_2 , or $a_2 = b_2$ and a_1 is adjacent to b_1 in \mathcal{G}_1 . The tensor product $\mathcal{G}_1 \times \mathcal{G}_2$ of \mathcal{G}_1 and \mathcal{G}_2 is a graph whose vertex set is the Cartesian product of $V(\mathcal{G}_1) \times V(\mathcal{G}_2)$ and distinct vertices (a_1, a_2) and (b_1, b_2) are adjacent in $\mathcal{G}_1 \times \mathcal{G}_2$ if a_1 is adjacent to b_1 and a_2 is adjacent to b_2 . The strong product $\mathcal{G}_1 \boxtimes \mathcal{G}_2$ of graph \mathcal{G}_1 and \mathcal{G}_2 is a graph whose vertex set is $V(\mathcal{G}_1 \square \mathcal{G}_2)$ and distinct vertices (a_1, a_2) and (b_1, b_2) are adjacent in $\mathcal{G}_1 \boxtimes \mathcal{G}_2$ if either $a_1 = b_1$ and a_2 is adjacent to

b_2 , or $a_2 = b_2$ and a_1 is adjacent to b_1 , or a_1 is adjacent to b_1 and a_2 is adjacent to b_2 . It is the union of Cartesian product and tensor product. Sabidussi first proposed it in 1960 [2]. Let P_n and C_n be the path and the cycle graphs of order n , respectively. From the definition of tensor and strong product of graphs, the graphs $P_4 \times C_4$ and $P_4 \boxtimes P_4$ are depicted in Figure 1. The graph depicted in Figure 1(b) is also called a King's graph which is a strong product of two path graphs.

The resistance distance is a function of the distance in graphs, as suggested by Klein and Randić [3]. The resistance distance between any two vertices of a simple connected graph, G , is equal to the resistance between two equivalent points on an electrical network, constructed in such a way as (G) , of each of the edge to replace a load resistance of 1 ohm. It is symbolized by r_{ij} , where $i, j \in V$. The computation of

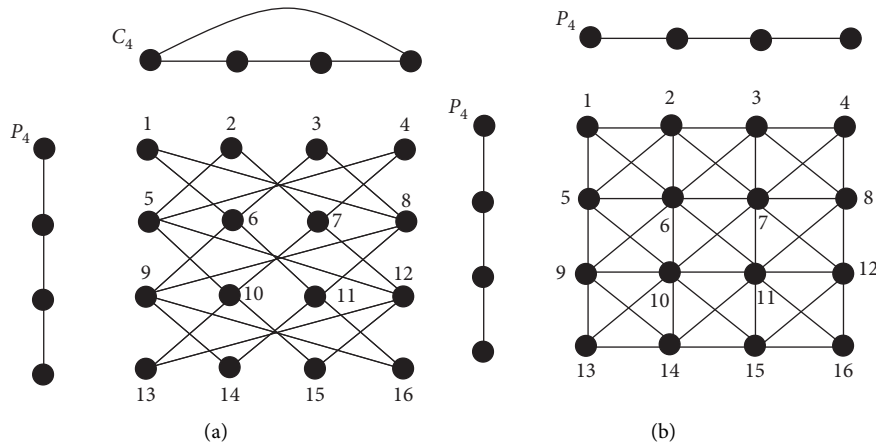


FIGURE 1: (a) $P_4 \times C_4$. (b) $P_4 \boxtimes P_4$.

resistance is relevant to a wide range of applications ranging from random walks [4], opinion formation [5], classical transport in disordered media [6], robustness of coupled oscillators network [7–9], first-passage processes [10], identifying the influential spreader node in a network [11], lattice Greens functions [12, 13], and resistance distance [3, 14] to graph theory [13, 15, 16]. At present, the resistance distance is a very suitable tool and internal graphic measurement to express the wave-like or fluid-like communication between two vertices [17]. It is also well studied in chemical and mathematical literature [3, 18–23].

Many kinds of formulae were attained for calculating the resistance distance, i.e., probabilistic formulae [4, 24], algebraic formulae [25–31], combinatorial formula [28], and so forth. Resistance distances have been procured for certain types of graphs, i.e., wheels and fans [18], cyclic graphs [32], some fullerene graphs [33], Cayley graphs [34], regular graphs [35, 36], pseudodistance regular graphs [37], and so forth. In recent years, the resistance distance of some graphic operations has been calculated (see [20, 38–41]).

In the present paper, we investigated the generalized inverse of Laplacian matrix for the graphs $P_{n_1} \times C_{n_2}$ and $P_{n_1} \boxtimes P_{n_2}$, based on which two-vertex resistances in $P_{n_1} \times C_{n_2}$ and $P_{n_1} \boxtimes P_{n_2}$ can be procured.

We ordered the paper in the following way. Section 2 covers some preliminary knowledge, i.e., basic definitions and necessary lemmas. In Section 3, we prove our main results, i.e., the generalized inverse of Laplacian matrix for tensor and strong product networks $P_{n_1} \times P_{n_2}$ and $P_{n_1} \boxtimes P_{n_2}$. In Section 4, as an application, we present a few examples. The final remarks are given in Section 5.

2. Preliminaries and Lemmas

Let \mathcal{G} be a simple graph, and the vertex and edge sets of \mathcal{G} are symbolized by $V(\mathcal{G}) = \{v_1, v_2, \dots, v_n\}$ and $E(\mathcal{G}) = \{e_1, e_2, \dots, e_m\}$, respectively. The adjacency matrix $A(\mathcal{G})$ of a graph \mathcal{G} is an $n \times n$ matrix, whose element a_{uv} is one when there is

an edge among vertex u and vertex v and zero when there is no edge between vertex u and vertex v . Let $D(\mathcal{G})$ be diagonal matrix with diagonal entries $d_{\mathcal{G}}(v_1), d_{\mathcal{G}}(v_2), \dots, d_{\mathcal{G}}(v_n)$. For a graph \mathcal{G} , let $L(\mathcal{G}) = D(\mathcal{G}) - A(\mathcal{G})$ be a Laplacian matrix of order $n \times n$. The incidence matrix $B(\mathcal{G})$ of a graph \mathcal{G} is an $n \times m$ matrix, where n and m are numbers of vertices and edges, respectively, such that $(B)_{ij}$ is 1 if the vertex v_i and edge e_j are incident and 0 otherwise. The identity matrix I_n is an $n \times n$ square matrix with 1s on main diagonal and 0s elsewhere.

Let $M = (m_{uv})_{i \times j}$ and $N = (n_{uv})_{i \times m}$ be the two matrices. The Kronecker product $M \otimes N$ is the $il \times jm$ matrix acquired from M by replacing each element m_{uv} by $m_{uv}N$ [42]. Let $M(1, 1)(\mathcal{G})$ be the matrix acquired by removing the 1st row and 1st column of a matrix $M(\mathcal{G})$ of a graph \mathcal{G} , and matrix $B(1)(\mathcal{G})$ is equal to the 1st row of an incidence matrix $B(\mathcal{G})$ of a graph \mathcal{G} . For example, considering a path graph P_3 , the

Laplacian matrix $L(P_3)$ is $\begin{pmatrix} 1 & -1 & 0 \\ -1 & 2 & -1 \\ 0 & -1 & 1 \end{pmatrix}$; then,

$L(1, 1)(P_3) = \begin{pmatrix} 2 & -1 \\ -1 & 1 \end{pmatrix}$. The incidence matrix $B(P_3)$ is

$\begin{pmatrix} 1 & 0 \\ 1 & 1 \\ 0 & 1 \end{pmatrix}$; then, $B(1)(P_3) = (1 \ 0)$.

Let M be a square matrix. A matrix \mathcal{Z} is called a $\{1\}$ -inverse of M if it satisfies $M\mathcal{Z}M = M$. $\{1\}$ -inverse of M is represented as $M^{(1)}$. A matrix \mathcal{Z} is a group inverse of a matrix M if it meets the following conditions [38]:

- (i) $M\mathcal{Z}M = M$
- (ii) $\mathcal{Z}M\mathcal{Z} = \mathcal{Z}$
- (iii) $\mathcal{Z}M = M\mathcal{Z}$

Let $M^\#$ symbolize a group inverse of M . If M is real symmetric, then $M^\#$ exists and $M^\#$ is a symmetric $\{1\}$ -inverse of M . Actually, $M^\#$ is equal to the Moore–Penrose inverse of M since M is symmetric [38].

The following lemma is used for computing the resistance distance.

Lemma 1 (see [38]). *Let L be a Laplacian matrix of a simple graph \mathcal{G} with vertex set $\{1, 2, \dots, n\}$. Then,*

$$r_{xy} = L_{xx}^\# + L_{yy}^\# - 2L_{xy}^\#. \quad (1)$$

Lemma 2 (see [38]). *For a nonsingular matrix $M = \begin{pmatrix} Q & N \\ R & P \end{pmatrix}$, if Q and P are nonsingular and $S = P - RQ^{-1}N$, then*

$$M^{-1} = \begin{pmatrix} Q^{-1} + Q^{-1}NS^{-1}RQ^{-1} & -Q^{-1}NS^{-1} \\ -S^{-1}RA^{-1} & S^{-1} \end{pmatrix} \quad (2)$$

is the Schur complement of Q in M .

C. Bu, in [38], stated the following expression.

Lemma 3 (see [38]). *Let $L = \begin{pmatrix} L_1 & L_2 \\ L_2^T & L_3 \end{pmatrix}$ be a Laplacian matrix of a graph \mathcal{G} and suppose each a column vector of L_2 is a zero vector or -1 ; then, the following matrix is a symmetric $\{1\}$ -inverse of L :*

$$X = \begin{pmatrix} L_1^{-1} & 0 \\ 0 & S^\# \end{pmatrix}, \quad (3)$$

where $S = L_3 - L_2^T L_1^{-1} L_2$.

The following expression, similar to Lemma 3, also holds for the Laplacian matrix of a simple graph. For more details, see [22, 39, 43].

Lemma 4. *If the Laplacian matrix of a simple graph \mathcal{G} is partitioned as $L = \begin{pmatrix} L_1 & L_2 \\ L_2^T & L_3 \end{pmatrix}$ and L_1 is nonsingular, then the following matrix is a symmetric $\{1\}$ -inverse of L :*

$$X = \begin{pmatrix} L_1^{-1} + L_1^{-1}L_2S^\#L_2^TL_1^{-1} & -L_1^{-1}L_2S^\# \\ -S^\#L_2^TL_1^{-1} & S^\# \end{pmatrix}, \quad (4)$$

where $S = L_3 - L_2^T L_1^{-1} L_2$.

3. Main Results

3.1. The Laplacian Generalized Inverse for Graph $P_{n_1} \times C_{n_2}$

Theorem 1 *Let \mathcal{G}_1 and \mathcal{G}_2 be a path graph and a cycle graph with vertices n_1 and n_2 , respectively. Then, the symmetric $\{1\}$ -inverse of $L(\mathcal{G}_1 \times \mathcal{G}_2)$ is*

$$\begin{bmatrix} L_1^{-1} + L_1^{-1}L_2S^\#L_2^TL_1^{-1} & -L_1^{-1}L_2S^\# \\ -S^\#L_2^TL_1^{-1} & S^\# \end{bmatrix}, \quad (5)$$

where

$$\begin{aligned} L_1 &= D(\mathcal{G}_2), \\ L_2 &= -B(1)(\mathcal{G}_1) \otimes A(\mathcal{G}_2), \\ L_3 &= 2D(1,1)(\mathcal{G}_1) \otimes I_{n_2} - A(1,1)(\mathcal{G}_1) \otimes A(\mathcal{G}_2), \\ S &= L_3 - [B(1)(\mathcal{G}_1)^T B(1)(\mathcal{G}_1)] \otimes [A(\mathcal{G}_2)(D(\mathcal{G}_2))^{-1} A(\mathcal{G}_2)]. \end{aligned} \quad (6)$$

Proof. Let $V(\mathcal{G}_1) = \{a_1, a_2, \dots, a_{n_1}\}$ and $V(\mathcal{G}_2) = \{b_1, b_2, \dots, b_{n_2}\}$. Then,

$$\{a_1, a_2, \dots, a_{n_1}\} \times \{b_1, b_2, \dots, b_{n_2}\} \quad (7)$$

is a partition of $V(\mathcal{G}_1 \times \mathcal{G}_2)$, where (a_1, b_1) and (a_2, b_2) are adjacent whenever (a_1, a_2) is an edge in \mathcal{G}_1 and (b_1, b_2) is an

edge in \mathcal{G}_2 . In $(\mathcal{G}_1 \times \mathcal{G}_2)$, $2n_2$ vertices are of degree 2 and $n_2(n_1 - 2)$ vertices are of degree 4. Label the vertices of $(\mathcal{G}_1 \times \mathcal{G}_2)$ like in Figure 1(a). According to partition (7), the Laplacian matrix of $\mathcal{G}_1 \times \mathcal{G}_2$ can be written as

$$\begin{bmatrix} D(\mathcal{G}_2) & -B(1)(\mathcal{G}_1) \otimes A(\mathcal{G}_2) \\ (-B(1)(\mathcal{G}_1)^T \otimes A(\mathcal{G}_2) & 2D(1,1)(\mathcal{G}_1) \otimes I_{n_2} - A(1,1)(\mathcal{G}_1) \otimes A(\mathcal{G}_2) \end{bmatrix}. \quad (8)$$

We start with the calculation of S . For simplicity, let

Due to Lemma 4, we have

$$\begin{aligned} L_1 &= D(\mathcal{G}_2), \\ L_2 &= -B(1)(\mathcal{G}_1) \otimes A(\mathcal{G}_2), \\ L_2^T &= (-B(1)(\mathcal{G}_1))^T \otimes A(\mathcal{G}_2), \\ L_3 &= 2 D(1, 1)(\mathcal{G}_1) \otimes I_{n_2} - A(1, 1)(\mathcal{G}_1) \otimes A(\mathcal{G}_2). \end{aligned} \tag{9}$$

$$\begin{aligned} S &= [2 D(1, 1)(\mathcal{G}_1) \otimes I_{n_2} - A(1, 1)(\mathcal{G}_1) \otimes A(\mathcal{G}_2)] \\ &\quad - [-B(1)(\mathcal{G}_1) \otimes A(\mathcal{G}_2)]^T [D(\mathcal{G}_2)]^{-1} [-B(1)(\mathcal{G}_1) \otimes A(\mathcal{G}_2)] \\ &= L_3 - [B(1)(\mathcal{G}_1)^T \otimes A(\mathcal{G}_2)] [D(\mathcal{G}_2)]^{-1} [B(1)(\mathcal{G}_1) \otimes A(\mathcal{G}_2)] \\ &= L_3 - [B(1)(\mathcal{G}_1)^T B(1)(\mathcal{G}_1)] \otimes [A(\mathcal{G}_2) [D(\mathcal{G}_2)]^{-1} A(\mathcal{G}_2)]. \end{aligned} \tag{10}$$

By using Lemma 4, the symmetric $\{1\}$ -inverse of $L(\mathcal{G}_1 \times \mathcal{G}_2)$ is

$$\begin{bmatrix} L_1^{-1} + L_1^{-1} L_2 S^\# L_2^T L_1^{-1} & -L_1^{-1} L_2 S^\# \\ -S^\# L_2^T L_1^{-1} & S^\# \end{bmatrix}, \tag{11}$$

where

$$\begin{aligned} L_1 &= D(\mathcal{G}_2), \\ L_2 &= -B(1)(\mathcal{G}_1) \otimes A(\mathcal{G}_2), \\ L_3 &= 2 D(1, 1)(\mathcal{G}_1) \otimes I_{n_2} - A(1, 1)(\mathcal{G}_1) \otimes A(\mathcal{G}_2), \\ S &= L_3 - [B(1)(\mathcal{G}_1)^T B(1)(\mathcal{G}_1)] \otimes [A(\mathcal{G}_2) (D(\mathcal{G}_2))^{-1} A(\mathcal{G}_2)]. \end{aligned} \tag{12}$$

$$D = \begin{pmatrix} 5 & 0 & \dots & 0 \\ 0 & 8 & & \\ \vdots & \ddots & & \\ 8 & & & \\ 5 & & & \\ 5 & & & \\ 8 & & & \\ \ddots & & & \\ 8 & & & \\ 5 & & & \\ 3 & & & \\ 5 & & & \\ \ddots & & & \\ 5 & & & \\ 0 & 3 & & \end{pmatrix}_{(n_1-1)(n_2) \times (n_1-1)(n_2)} \tag{13}$$

3.2. The Laplacian Generalized Inverse for Graph $P_{n_1} \boxtimes P_{n_2}$

Theorem 2. Let \mathcal{G}_1 and \mathcal{G}_2 be two paths with n_1 and n_2 vertices, respectively, and let

Then, the symmetric $\{1\}$ -inverse of $L(\mathcal{G}_1 \times \mathcal{G}_2)$ is

$$\begin{bmatrix} L_1^{-1} + L_1^{-1} L_2 S^\# L_2^T L_1^{-1} & -L_1^{-1} L_2 S^\# \\ -S^\# L_2^T L_1^{-1} & S^\# \end{bmatrix}, \tag{14}$$

where

$$\begin{aligned} L_1 &= 2 D(\mathcal{G}_2) + I_{n_2} - A(\mathcal{G}_2), \\ L_2 &= -B(1)(\mathcal{G}_1) \otimes [A(\mathcal{G}_2) + I_{n_2}], \\ L_3 &= D - [I_{n_1-1} \otimes A(\mathcal{G}_2) + A(1, 1)(\mathcal{G}_1) \otimes (A(\mathcal{G}_2) + I_{n_2})], \\ S &= L_3 - [B(1)(\mathcal{G}_1)^T B(1)(\mathcal{G}_1)] \otimes ([A(\mathcal{G}_2) + I_{n_2}] L_1^{-1} [A(\mathcal{G}_2) + I_{n_2}]). \end{aligned} \tag{15}$$

Proof. Let $V(\mathcal{G}_1) = \{a_1, a_2, \dots, a_{n_1}\}$ and $V(\mathcal{G}_2) = \{b_1, b_2, \dots, b_{n_2}\}$. Then,

$$V(\mathcal{G}_1 \boxtimes \mathcal{G}_2) = \{(a, b) | a \in V(\mathcal{G}_1), b \in V(\mathcal{G}_2)\} \quad (16)$$

and $E(\mathcal{G}_1 \boxtimes \mathcal{G}_2) = E(\mathcal{G}_1 \square \mathcal{G}_2) \cup E(\mathcal{G}_1 \times \mathcal{G}_2)$. The degree of vertices of $\mathcal{G}_1 \boxtimes \mathcal{G}_2$ is

$$\begin{aligned} d_{\mathcal{G}_1 \boxtimes \mathcal{G}_2}(a, b) &= d_{\mathcal{G}_1}(a) + d_{\mathcal{G}_2}(b) \\ &+ d_{\mathcal{G}_1}(a) \cdot d_{\mathcal{G}_2}(b), \quad (a, b) \in E(\mathcal{G}_1 \boxtimes \mathcal{G}_2). \end{aligned} \quad (17)$$

Label the vertices of $(\mathcal{G}_1 \boxtimes \mathcal{G}_2)$ like in Figure 1(b). According to partition (16), the Laplacian matrix of $\mathcal{G}_1 \boxtimes \mathcal{G}_2$ can be written as

$$\begin{bmatrix} 2D(\mathcal{G}_2) + I_{n_2} - A(\mathcal{G}_2) & -B(1)(\mathcal{G}_1) \otimes [A(\mathcal{G}_2) + I_{n_2}] \\ (-B(1)(\mathcal{G}_1))^T \otimes [A(\mathcal{G}_2) + I_{n_2}] & D - [I_{n_1-1} \otimes A(\mathcal{G}_2) + A(1, 1)(\mathcal{G}_1) \otimes (A(\mathcal{G}_2) + I_{n_2})] \end{bmatrix}. \quad (18)$$

We start with the calculation of S. For simplicity, let

$$\begin{aligned} L_1 &= 2D(\mathcal{G}_2) + I_{n_2} - A(\mathcal{G}_2), \\ L_2 &= -B(1)(\mathcal{G}_1) \otimes [A(\mathcal{G}_2) + I_{n_2}], \\ L_2^T &= (-B(1)(\mathcal{G}_1))^T \otimes [A(\mathcal{G}_2) + I_{n_2}], \\ L_3 &= D - [I_{n_1-1} \otimes A(\mathcal{G}_2) + A(1, 1)(\mathcal{G}_1) \otimes (A(\mathcal{G}_2) + I_{n_2})]. \end{aligned} \quad (19)$$

Due to Lemma 4, we have

$$\begin{aligned} S &= L_3 - (B(1)(\mathcal{G}_1)^T \otimes [A(\mathcal{G}_2) + I_{n_2}]) L_1^{-1} (B(1)(\mathcal{G}_1) \otimes [A(\mathcal{G}_2) + I_{n_2}]) \\ &= L_3 - [B(1)(\mathcal{G}_1)^T B(1)(\mathcal{G}_1)] \otimes ([A(\mathcal{G}_2) + I_{n_2}] L_1^{-1} [A(\mathcal{G}_2) + I_{n_2}]). \end{aligned} \quad (20)$$

By using Lemma 4, the symmetric {1}-inverse of $L(\mathcal{G}_1 \boxtimes \mathcal{G}_2)$ is

$$\begin{bmatrix} L_1^{-1} + L_1^{-1} L_2 S^\# L_2^T L_1^{-1} & -L_1^{-1} L_2 S^\# \\ -S^\# L_2^T L_1^{-1} & S^\# \end{bmatrix}, \quad (21)$$

where

$$\begin{aligned} L_1 &= 2D(\mathcal{G}_2) + I_{n_2} - A(\mathcal{G}_2), \\ L_2 &= -B(1)(\mathcal{G}_1) \otimes [A(\mathcal{G}_2) + I_{n_2}], \\ L_3 &= D - [I_{n_1-1} \otimes A(\mathcal{G}_2) + A(1, 1)(\mathcal{G}_1) \otimes (A(\mathcal{G}_2) + I_{n_2})], \\ S &= L_3 - [B(1)(\mathcal{G}_1)^T B(1)(\mathcal{G}_1)] \otimes ([A(\mathcal{G}_2) + I_{n_2}] L_1^{-1} [A(\mathcal{G}_2) + I_{n_2}]). \end{aligned} \quad (22)$$

□

4. Examples to Summarize the Main Results

Here, we discuss few examples to show that two-vertex resistances in graphs $P_{n_1} \times C_{n_2}$ and $P_{n_1} \times P_{n_2}$ can be procured by the proposed method.

Example 1. The resistance distance matrix for the graph $P_3 \times C_3$ (see Figure 2(a)).

The Laplacian matrix of $(P_3 \times C_3)$ is

$$\begin{bmatrix} D(C_3) & (-B(1)(P_3)) \otimes A(C_3) \\ (-B(1)(P_3))^T \otimes A(C_3) & 2D(1,1)(P_3) \otimes I_3 - A(1,1)(P_3) \otimes A(C_3) \end{bmatrix}. \quad (23)$$

From Theorem 1, we obtain

$$L^\#(P_3 \times C_3) = \begin{pmatrix} \frac{43}{72} & \frac{1}{72} & \frac{1}{72} & -\frac{5}{72} & \frac{7}{72} & \frac{7}{72} & \frac{1}{72} & -\frac{5}{72} & -\frac{5}{72} \\ \frac{1}{72} & \frac{43}{72} & \frac{1}{72} & \frac{7}{72} & -\frac{5}{72} & \frac{7}{72} & -\frac{5}{72} & \frac{1}{72} & -\frac{5}{72} \\ \frac{1}{72} & \frac{1}{72} & \frac{43}{72} & \frac{7}{72} & \frac{7}{72} & -\frac{5}{72} & -\frac{5}{72} & -\frac{5}{72} & \frac{1}{72} \\ -\frac{5}{72} & \frac{7}{72} & \frac{7}{72} & \frac{19}{72} & -\frac{5}{72} & -\frac{5}{72} & -\frac{11}{72} & \frac{1}{72} & \frac{1}{72} \\ \frac{7}{72} & -\frac{5}{72} & \frac{7}{72} & -\frac{5}{72} & \frac{19}{72} & -\frac{5}{72} & \frac{1}{72} & -\frac{11}{72} & \frac{1}{72} \\ \frac{7}{72} & \frac{7}{72} & -\frac{5}{72} & -\frac{5}{72} & -\frac{5}{72} & \frac{19}{72} & \frac{1}{72} & \frac{1}{72} & -\frac{11}{72} \\ \frac{1}{72} & -\frac{5}{72} & -\frac{5}{72} & -\frac{11}{72} & \frac{1}{72} & \frac{1}{72} & \frac{31}{72} & -\frac{11}{72} & -\frac{11}{72} \\ -\frac{5}{72} & \frac{1}{72} & -\frac{5}{72} & \frac{1}{72} & \frac{11}{72} & \frac{1}{72} & -\frac{11}{72} & \frac{31}{72} & -\frac{11}{72} \\ -\frac{5}{72} & -\frac{5}{72} & \frac{1}{72} & \frac{1}{72} & \frac{1}{72} & -\frac{11}{72} & -\frac{11}{72} & -\frac{11}{72} & \frac{31}{72} \end{pmatrix}. \quad (24)$$

By using Lemma 1 and $L^\#(P_3 \times C_3)$, the resistance distance matrix of $P_3 \times C_3$ is

$$R^\#(P_3 \times C_3) = \begin{pmatrix} 0 & \frac{7}{6} & \frac{7}{6} & 1 & \frac{2}{3} & \frac{2}{3} & 1 & \frac{7}{6} & \frac{7}{6} \\ \frac{7}{6} & 0 & \frac{7}{6} & \frac{2}{3} & 1 & \frac{2}{3} & \frac{7}{6} & 1 & \frac{7}{6} \\ \frac{7}{6} & \frac{7}{6} & 0 & \frac{2}{3} & \frac{2}{3} & 1 & \frac{7}{6} & \frac{7}{6} & 1 \\ 1 & \frac{2}{3} & \frac{2}{3} & 0 & \frac{2}{3} & \frac{2}{3} & 1 & \frac{2}{3} & \frac{2}{3} \\ \frac{2}{3} & 1 & \frac{2}{3} & \frac{2}{3} & 0 & \frac{2}{3} & \frac{2}{3} & 1 & \frac{2}{3} \\ \frac{2}{3} & \frac{2}{3} & 1 & \frac{2}{3} & \frac{2}{3} & 0 & \frac{2}{3} & \frac{2}{3} & 1 \\ 1 & \frac{7}{6} & \frac{7}{6} & 1 & \frac{2}{3} & \frac{2}{3} & 0 & \frac{7}{6} & \frac{7}{6} \\ \frac{7}{6} & 1 & \frac{7}{6} & \frac{2}{3} & 1 & \frac{2}{3} & \frac{7}{6} & 0 & \frac{7}{6} \\ \frac{7}{6} & \frac{7}{6} & 1 & \frac{2}{3} & \frac{2}{3} & 1 & \frac{7}{6} & \frac{7}{6} & 0 \end{pmatrix}, \tag{25}$$

where r_{ij} denotes the two-vertex resistance between vertices i and j .

Example 2. The resistance distance matrix for the graph $P_3 \boxtimes P_3$ (see Figure 2(b)).

The Laplacian matrix of $P_3 \boxtimes P_3$ is

$$\begin{bmatrix} 2D(P_3) + I_3 - A(P_3) & -B(1)(P_3) \times [A(P_3) + I_3] \\ (-B(1)(P_3))^T \times [A(P_3) + I_3] & D - [I_2 \otimes A(P_3) + A(1,1)(P_3) \otimes (A(P_3) + I_3)] \end{bmatrix}, \tag{26}$$

where $D = \begin{pmatrix} 5 & 0 & 0 & 0 & 0 & 0 \\ 0 & 8 & 0 & 0 & 0 & 0 \\ 0 & 0 & 5 & 0 & 0 & 0 \\ 0 & 0 & 0 & 3 & 0 & 0 \\ 0 & 0 & 0 & 0 & 5 & 0 \\ 0 & 0 & 0 & 0 & 0 & 3 \end{pmatrix}.$

Based on Theorem 2, we obtain that

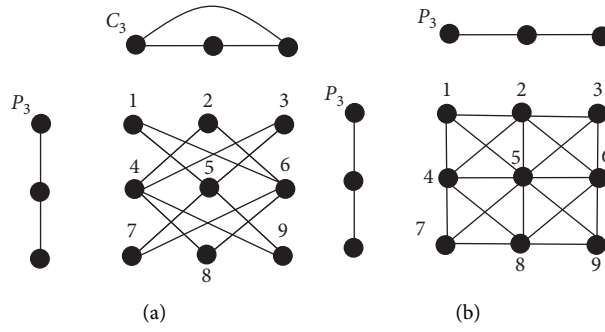


FIGURE 2: (a) $P_3 \times C_3$. (b) $P_3 \boxtimes P_3$.

$$L^\#(P_3 \boxtimes P_3) = \begin{pmatrix} \frac{728}{1779} & \frac{53}{468} & \frac{72}{1433} & \frac{227}{3276} & \frac{212}{4699} & \frac{25}{3276} & \frac{437}{16380} & \frac{1}{36} & \frac{857}{16380} \\ \frac{53}{468} & \frac{125}{468} & \frac{53}{468} & \frac{17}{468} & \frac{17}{468} & \frac{17}{468} & \frac{19}{468} & \frac{1}{36} & \frac{19}{468} \\ \frac{72}{1433} & \frac{53}{468} & \frac{728}{1779} & \frac{25}{3276} & \frac{212}{4699} & \frac{227}{3276} & \frac{857}{16380} & \frac{1}{36} & \frac{437}{16380} \\ \frac{227}{3276} & \frac{17}{468} & \frac{25}{3276} & \frac{346}{1931} & \frac{25}{3276} & \frac{13}{252} & \frac{25}{3276} & \frac{1}{36} & \frac{277}{3276} \\ \frac{212}{4699} & \frac{17}{468} & \frac{212}{4699} & \frac{25}{3276} & \frac{117}{1097} & \frac{25}{3276} & \frac{91}{2861} & \frac{1}{36} & \frac{91}{2861} \\ \frac{25}{3276} & \frac{17}{468} & \frac{227}{3276} & \frac{13}{252} & \frac{25}{3276} & \frac{587}{3276} & \frac{277}{3276} & \frac{1}{36} & \frac{25}{3276} \\ \frac{437}{16380} & \frac{19}{468} & \frac{857}{16380} & \frac{25}{3276} & \frac{91}{2861} & \frac{277}{3276} & \frac{511}{2001} & \frac{1}{36} & \frac{279}{2693} \\ \frac{1}{36} & \frac{1}{36} & \frac{1}{36} & \frac{1}{36} & \frac{1}{36} & \frac{1}{36} & \frac{1}{36} & \frac{5}{36} & \frac{1}{36} \\ \frac{857}{16380} & \frac{19}{468} & \frac{437}{16380} & \frac{277}{3276} & \frac{91}{2861} & \frac{25}{3276} & \frac{279}{2693} & \frac{1}{36} & \frac{511}{2001} \end{pmatrix}. \tag{27}$$

By using Lemma 1 and $L^\#(P_3 \boxtimes P_3)$, the resistance distance matrix of $P_3 \boxtimes P_3$

$$R^\#(P_3 \boxtimes P_3) = \begin{pmatrix} 0 & \frac{614}{1365} & \frac{28}{39} & \frac{614}{1365} & \frac{83}{195} & \frac{824}{1365} & \frac{28}{39} & \frac{824}{1365} & \frac{10}{13} \\ \frac{614}{1365} & 0 & \frac{614}{1365} & \frac{34}{91} & \frac{137}{455} & \frac{34}{91} & \frac{824}{1365} & \frac{6}{13} & \frac{824}{1365} \\ \frac{28}{39} & \frac{614}{1365} & 0 & \frac{824}{1365} & \frac{83}{195} & \frac{614}{1365} & \frac{10}{13} & \frac{824}{1365} & \frac{28}{39} \\ \frac{614}{1365} & \frac{34}{91} & \frac{824}{1365} & 0 & \frac{137}{455} & \frac{6}{13} & \frac{614}{1365} & \frac{34}{91} & \frac{824}{1365} \\ \frac{83}{195} & \frac{137}{455} & \frac{83}{195} & \frac{137}{455} & 0 & \frac{137}{455} & \frac{83}{195} & \frac{137}{455} & \frac{83}{195} \\ \frac{824}{1365} & \frac{34}{91} & \frac{614}{1365} & \frac{6}{13} & \frac{137}{455} & 0 & \frac{824}{1365} & \frac{34}{91} & \frac{614}{1365} \\ \frac{28}{39} & \frac{824}{1365} & \frac{10}{13} & \frac{614}{1365} & \frac{83}{195} & \frac{824}{1365} & 0 & \frac{614}{1365} & \frac{28}{39} \\ \frac{824}{1365} & \frac{6}{13} & \frac{824}{1365} & \frac{34}{91} & \frac{137}{455} & \frac{34}{91} & \frac{614}{1365} & 0 & \frac{614}{1365} \\ \frac{10}{13} & \frac{824}{1365} & \frac{28}{39} & \frac{824}{1365} & \frac{83}{195} & \frac{614}{1365} & \frac{28}{39} & \frac{614}{1365} & 0 \end{pmatrix}, \tag{28}$$

where r_{ij} denotes the two-vertex resistance between vertices i and j .

5. Conclusion

In this paper, we investigated the resistance distance in the tensor product of a path and a cycle as well as the strong product of two paths. First, we obtained the Laplacian matrix of these two kinds of product graphs. After calculation, we acquire the generalized inverse representations of the Laplacian matrices, and then, applying the generalized inverse theory of block matrices, we obtained the two-vertex resistances. Finally, we applied the above method to compute the resistance distance in graphs $P_3 \times C_3$ and $P_3 \boxtimes P_3$. We obtained the resistance distance between two pair of vertices in tensor and strong product of two classes of graphs. However, the resistance distance for some other graph products has not been solved yet. We recommend the readers to compute the resistance distance for other classes of graphs by using different graph products, i.e., zig zag product, modular product, co-normal product and lexicographical product.

Data Availability

No data were used in this study.

Conflicts of Interest

The authors declare that they have no conflicts of interest.

Acknowledgments

Xiang-Feng Pan was supported by the University Natural Science Research Project of Anhui Province under Grant no. KJ2020A0001.

References

- [1] R. Hammack, W. Imrich, and S. Klavzar, *Handbook of Product Graphs*, CRC Press, Boca Raton, FL, USA, 2016.
- [2] G. Sabidussi, "Graph multiplication," *Mathematische Zeitschrift*, vol. 72, pp. 446–457, 1960.
- [3] D. J. Klein and M. Randić, "Resistance distance," *Journal of Mathematical Chemistry*, vol. 12, no. 1, pp. 81–95, 1993.
- [4] P. G. Doyle and J. L. Snell, *Random Walks and Electric Networks*, Mathematical Association of America, Washington, DC, USA, 1984.
- [5] F. Baumann, I. M. Sokolov, and M. Tyloo, "A Laplacian approach to stubborn agents and their role in opinion formation on influence networks," *Physica A: Statistical Mechanics and Its Applications*, vol. 557, Article ID 124869, 2020.

- [6] S. Kirkpatrick, "Percolation and conduction," *Reviews of Modern Physics*, vol. 45, no. 4, pp. 574–588, 1973.
- [7] T. W. Grunberg and D. F. Gayme, "Performance measures for linear oscillator networks over arbitrary graphs," *IEEE Transactions on Control of Network Systems*, vol. 5, no. 1, pp. 456–468, 2018.
- [8] M. Tyloo, T. Coletta, and P. Jacquod, "Robustness of synchrony in complex networks and generalized Kirchhoff indices," *Physical Review Letters*, vol. 120, no. 8, Article ID 084101, 2018.
- [9] M. Tyloo, L. Pagnier, and P. Jacquod, "The key player problem in complex oscillator networks and electric power grids: resistance centralities identify local vulnerabilities," *Science Advances*, vol. 5, no. 11, Article ID eaaw8359, 2019.
- [10] S. Redner, *A Guide to First-Passage Processes*, Cambridge University Press, Cambridge, UK, 2001.
- [11] P. Van Mieghem, K. Devriendt, and H. Cetinay, "Pseudoinverse of the Laplacian and best spreader node in a network," *Physical Review E*, vol. 96, Article ID 032311, 2017.
- [12] S. Katsura and S. Inawashiro, "Lattice Green's functions for the rectangular and the square lattices at arbitrary points," *Journal of Mathematical Physics*, vol. 12, no. 8, pp. 1622–1630, 1971.
- [13] K. Woong, "Combinatorial Green's function of a graph and applications to networks," *Advances in Applied Mathematics*, vol. 46, pp. 417–423, 2011.
- [14] W. Xiao and I. Gutman, "Resistance distance and Laplacian spectrum," *Theoretical Chemistry Accounts: Theory, Computation, and Modeling (Theoretica Chimica Acta)*, vol. 110, no. 4, pp. 284–289, 2003.
- [15] L. Novak and A. Gibbons, *Hybrid Graph Theory and Network Analysis*, Cambridge University Press, Cambridge, UK, 2009.
- [16] K. Yenoke and M. K. A. Kaabar, "The bounds for the distance two labelling and radio labelling of nanostar tree dendrimer," *TELKOMNIKA Telecommunication Computing Electronics and Control*, vol. 19, no. 5, pp. 1–8, 2021.
- [17] D. J. Klein, "Resistance-distance sum rules," *Croatica Chemica Acta*, vol. 75, pp. 633–649, 2002.
- [18] R. B. Bapat and S. Gupta, "Resistance distance in wheels and fans," *Indian Journal of Pure and Applied Mathematics*, vol. 41, no. 1, pp. 1–13, 2010.
- [19] D. Babi?, D. J. Klein, I. Lukovits, S. Nikoli?, and N. Trinajsti?, "Resistance-distance matrix: a computational algorithm and its application," *International Journal of Quantum Chemistry*, vol. 90, no. 1, pp. 166–176, 2002.
- [20] J. Cao, J. B. Liu, and S. Wang, "Resistance distances in corona and neighborhood corona networks based on Laplacian generalized inverse approach," *Journal of Algebra and Its Applications*, vol. 18, no. 3, Article ID 1950053, 2019.
- [21] W. Fang, Y. Wang, J.-B. Liu, and G. Jing, "Maximum resistance-Harary index of cacti," *Discrete Applied Mathematics*, vol. 251, pp. 160–170, 2018.
- [22] J.-B. Liu and J. Cao, "The resistance distances of electrical networks based on Laplacian generalized inverse," *Neurocomputing*, vol. 167, no. 167, pp. 306–313, 2015.
- [23] V. G. Severino, "Resistance distance in complete n -partite graphs," *Discrete Appl. Math.* vol. 203, pp. 53–61, 2016.
- [24] C. St and J. A. Nash-Williams, "Random walks and electric currents in networks," *Mathematical Proceedings of the Cambridge Philosophical Society*, vol. 55, pp. 181–194, 1959.
- [25] H. Chen and F. Zhang, "Resistance distance and the normalized Laplacian spectrum," *Discrete Applied Mathematics*, vol. 155, no. 5, pp. 654–661, 2007.
- [26] D. J. Klein, "Graph geometry, graph metrics and Wiener," *MATCH Communications in Mathematical and in Computer Chemistry*, vol. 35, pp. 7–27, 1997.
- [27] C. R. Rao and S. K. Mitra, *Generalized Inverse of Matrices and its Applications*, Wiley, New York, NY, USA, 1971.
- [28] S. Seshu and M. B. Reed, *Linear Graphs and Electrical Networks*, Addison-Wesley, Reading, MA, USA, 1961.
- [29] G. E. Sharpe and G. P. H. Styan, "A note on equicofactor matrices," *Proceedings of the IEEE*, vol. 55, no. 7, pp. 1226–1227, 1967.
- [30] G. Sharpe and B. Spain, "On the solution of networks by means of the equicofactor matrix," *IRE Transactions on Circuit Theory*, vol. 7, no. 3, pp. 230–239, 1960.
- [31] G. Sharpe and G. Styan, "Circuit duality and the general network inverse," *IEEE Transactions on Circuit Theory*, vol. 12, no. 1, pp. 22–27, 1965.
- [32] H. Zhang and Y. Yang, "Resistance distance and Kirchhoff index in circulant graphs," *International Journal of Quantum Chemistry*, vol. 107, no. 2, pp. 330–339, 2007.
- [33] P. W. Fowler, "Resistance distances in Fullerene graphs," *Croatica Chemica Acta*, vol. 75, no. 2, pp. 401–408, 2002.
- [34] X. Gao, Y. Luo, and W. Liu, "Resistance distances and the Kirchhoff index in cayley graphs," *Discrete Applied Mathematics*, vol. 159, no. 17, pp. 2050–2057, 2011.
- [35] D. J. Klein, I. Lukovits, and I. Gutman, "On the definition of the hyper-wiener index for cycle-containing structures," *Journal of Chemical Information and Computer Sciences*, vol. 35, no. 1, pp. 50–52, 1995.
- [36] I. Lukovits and S. Nikoli?, N. Trinajsti?, Resistance distance in regular graphs," *International Journal of Quantum Chemistry*, vol. 3, no. 71, pp. 306–313, 1999.
- [37] S. Jafarizadeh, R. Sufiani, and M. A. Jafarizadeh, "Evaluation of effective resistances in pseudo-distance-regular resistor networks," *Journal of Statistical Physics*, vol. 1, no. 139, pp. 177–199, 2010.
- [38] C. Bu, B. Yan, X. Zhou, and J. Zhou, "Resistance distance in subdivision-vertex join and subdivision-edge join of graphs," *Linear Algebra and Its Applications*, vol. 458, pp. 454–462, 2014.
- [39] J.-B. Liu, X.-F. Pan, and F.-T. Hu, "The $\{1\}$ -inverse of the Laplacian of subdivision-vertex and subdivision-edge coronae with applications," *Linear and Multilinear Algebra*, vol. 65, no. 1, pp. 178–191, 2017.
- [40] X. Liu, J. Zhou, and C. Bu, "Resistance distance and Kirchhoff index of R-vertex join and R-edge join of two graphs," *Discrete Applied Mathematics*, vol. 187, pp. 130–139, 2015.
- [41] Z. Li, X. Zheng, J. Li, and Y. Pan, "Resistance distance-based graph invariants and spanning trees of graphs derived from the strong prism of a star," *Applied Mathematics and Computation*, vol. 382, 2020.
- [42] R. A. Horn and C. R. Johnson, *Topics in Matrix Analysis*, Cambridge University Press, Cambridge, UK, 1991.
- [43] L. Sun, W. Wang, J. Zhou, and C. Bu, "Some results on resistance distances and resistance matrices," *Linear and Multilinear Algebra*, vol. 63, no. 3, pp. 523–533, 2015.

Research Article

Super H -Antimagic Total Covering for Generalized Antiprism and Toroidal Octagonal Map

Amir Taimur,¹ Gohar Ali ,¹ Muhammad Numan,² Adnan Aslam ,³
and Kraidi Anoh Yannick ⁴

¹Department of Mathematics, Islamia College, Peshawar, Pakistan

²Department of Mathematics, COMSATS University Islamabad, Attock, Pakistan

³Department of Natural Sciences and Humanities, University of Engineering and Technology, Lahore (RCET), Lahore, Pakistan

⁴UFR of Mathematics and Computer Science, University Felix Houphouët Boigny of Coclody, Abidjan, Côte d'Ivoire

Correspondence should be addressed to Kraidi Anoh Yannick; kayanoh2000@yahoo.fr

Received 29 June 2021; Accepted 29 July 2021; Published 9 August 2021

Academic Editor: Ali Ahmad

Copyright © 2021 Amir Taimur et al. This is an open access article distributed under the Creative Commons Attribution License, which permits unrestricted use, distribution, and reproduction in any medium, provided the original work is properly cited.

Let G be a graph and $H \subseteq G$ be subgraph of G . The graph G is said to be (a, d) - H antimagic total graph if there exists a bijective function $f: V(H) \cup E(H) \rightarrow \{1, 2, 3, \dots, |V(H)| + |E(H)|\}$ such that, for all subgraphs isomorphic to H , the total H weights $W(H) = W(H) = \sum_{x \in V(H)} f(x) + \sum_{y \in E(H)} f(y)$ forms an arithmetic sequence $a, a + d, a + 2d, \dots, a + (n - 1)d$, where a and d are positive integers and n is the number of subgraphs isomorphic to H . An (a, d) - H antimagic total labeling f is said to be super if the vertex labels are from the set $\{1, 2, \dots, |V(G)|\}$. In this paper, we discuss super (a, d) - C_3 -antimagic total labeling for generalized antiprism and a super (a, d) - C_8 -antimagic total labeling for toroidal octagonal map.

1. Introduction

All the graphs that we consider in this works are finite, simple, and connected. Let G be a graph with vertex set and edge set denoted by $V(G)$ and $E(G)$, respectively. For the cardinality of vertex set and edge set, we use the notation $|V(G)|$ and $|E(G)|$, respectively. For basic definitions and terminology related to graph theory, the readers can see the book by Gross et al. [1].

A graph labeling is a map f that sends some of the graph elements (vertices or edges or both) to the set of positive integers. If the domain set of f is the set of vertices (edges), then f is called vertex (edge) labeling. If the domain set is $V(G) \cup E(G)$, then f is called total labeling. Let G be a graph and H_1, H_2, \dots, H_k be subgraphs of G . We say that the graph G has an H_1, H_2, \dots, H_k covering if each edge of G belongs to at least one of the subgraph H_i , where $1 \leq i \leq k$. If all $H_i, i = 1, 2, \dots, k$, are isomorphic to a graph H , then such a covering is called H covering of G . Suppose that a graph G admits an H covering. The graph G is called $(a, d)H$

antimagic if there exists a bijective function $f: V(H) \cup E(H) \rightarrow \{1, 2, 3, \dots, |V(H)| + |E(H)|\}$ such that, for all subgraphs isomorphic to H , the total H weights,

$$W(H) = W(K) = \sum_{x \in V(K)} f(x) + \sum_{y \in E(K)} f(y), \quad (1)$$

form an arithmetic sequence $a, a + d, a + 2d, \dots, a + (n - 1)d$, where a and d are positive integers and n is the number of subgraphs isomorphic to H . An (a, d) - H antimagic total labeling f is said to be super if the vertex labels are from the set $\{1, 2, \dots, |V(G)|\}$. If $d = 0$, then H is called (a, d) - H antimagic.

Kotzig and Rosa [2] and Enomoto et al. [3] introduced the concept of edge-magic and super edge-magic labeling. Gutierrez and Llado [4] first studied the H (super) magic coverings of a graph G . They proved that the cycle C_n and path P_n are P_m super magic for some m . The cycle (super) magic behavior of some classes of connected graphs is studied in Llado et al. [5]. They proved that prisms,

windmills, wheels, and books are C_m -magic for some m . Maryati et al. [6] investigated the G -supermagicness of a disjoint union of c copies of a graph G and showed that the disjoint union of any paths is cP_m -supermagic for some c and m . Maryati et al. [7] and Salman et al. [8] proved that certain families of trees are path-supermagic. Ngurah et al. [9] proved that triangles, chains, ladders, wheels, and grids are cycle-supermagic.

Inaya et al. [10] firstly introduced the concept of H -magic decomposition and H -antimagic decomposition. They showed that, for any graceful tree T with n edges, the complete graph K_{2n+1} admits $(a, d) - T$ antimagic decomposition for some a and all even differences $0 \leq d \leq n + 1$. They also proved that if any tree T with n edges admits α labeling, then the complete bipartite graph $K_{n,n}$ admits an $(a, d) - T$ antimagic decomposition for some a and d having same parity as n . The condition on the existence of C_{2k} super magic decomposition of complete n partite graph and its copies were given by Lian [11]. The H -supermagic decomposition of antiprisms is described by Hendy in [12] and the H -supermagic decompositions of the lexicographic product of graphs are discussed by Hendy et al. in [13]. In [14], Hendy et al. examined the existence of super $(a, d) - H$ magic labeling for toroidal grids and toroidal triangulations. Recently, Fenovcikova et al. [15] proved that wheels are cycle antimagic.

In this paper, we discuss the Super (a, d) - C_3 -antimagic total labeling for generalized antiprism and a Super (a, d) - C_8 -antimagic total labeling for toroidal octagonal map. We proved that the generalized antiprism \mathbb{A}_r^s admits (a, d) - C_3 -antimagic total labeling for $d = 0, 1$ and the toroidal octagonal map O_s^r admits a Super (a, d) - C_8 -antimagic total labeling, for $d = 1, 2, \dots, 7$.

2. Results on Super (a, d) - C_3 -Antimagic Total Covering of Generalized Antiprism \mathbb{A}_r^s

An r -sided generalized antiprism \mathbb{A}_r^s is defined as a polyhedron which is composed of s parallel copies of some particular r -sided polygon and connected by an alternating band of triangles. Figure 1 represents the labeled graph of generalized antiprism \mathbb{A}_r^s . We denote its vertex set and edge set by $V(\mathbb{A}_r^s)$ and $E(\mathbb{A}_r^s)$, respectively. The vertex set and the edge set of the generalized antiprism \mathbb{A}_r^s can be defined as follows:

$$\begin{aligned} V(\mathbb{A}_r^s) &= \{x_i^j, \text{ for } 0 \leq i \leq r-1, 0 \leq j \leq s-1\}, \\ E(\mathbb{A}_r^s) &= \{x_i^j x_{i+1}^j, \text{ for } 0 \leq i \leq r-1, 0 \leq j \leq s-1\} \\ &\cup \{x_i^j x_i^{j+1}, \text{ for } 0 \leq i \leq r-1, 0 \leq j \leq s-2\} \\ &\cup \{x_i^j x_{i+1}^{j+1}, \text{ for } 0 \leq i \leq r-1, 0 \leq j \leq s-2\}. \end{aligned} \tag{2}$$

The generalized antiprism \mathbb{A}_r^s admits a C_3 covering. Let z_i^j and f_i^j be the C_3 cycles which cover \mathbb{A}_r^s , where $0 \leq i \leq r-1$ and $0 \leq j \leq s-2$. The cycles z_i^j and f_i^j can be defined as

$$\begin{aligned} z_i^j &= x_i^j x_{i+1}^j x_{i+1}^{j+1} x_i^j, \text{ for } 0 \leq i \leq r-1, 0 \leq j \leq s-2, \\ f_i^j &= x_i^j x_{i+1}^{j+1} x_i^{j+1} x_i^j, \text{ for } 0 \leq i \leq r-1, 0 \leq j \leq s-2. \end{aligned} \tag{3}$$

It is easy to observe that $|V(\mathbb{A}_r^s)| = rs$ and $|E(\mathbb{A}_r^s)| = 3rs - 2r$. We first give an upper bound for d such that \mathbb{A}_r^s admits a super (a, d) - C_3 -antimagic covering.

Theorem 1. *Let $r, s \geq 3$ and \mathbb{A}_r^s be generalized antiprism graph. Then, there is no super (a, d) - C_3 -antimagic covering with $d \geq 6$.*

Proof. Suppose that \mathbb{A}_r^s has a super (a, d) - C_3 -antimagic covering. Let $f: V(\mathbb{A}_r^s) \cup E(\mathbb{A}_r^s) \rightarrow \{1, 2, 3, \dots, 4rs - 2r\}$ be a super (a, d) - C_3 -antimagic covering and $\{a_3, a_3 + d, a_3 + 2d, \dots, a_3 + (2rs - 2r - 1)d\}$ be the set of C_3 weights. The minimum weight on cycle C_3 is at least $12 + 3rs$ which is the sum of the smallest vertex labels $(1, 2, 3)$ and sum of smallest edge labels $(rs + 1, rs + 2, rs + 3)$. Thus,

$$a_3 \geq 12 + 3rs. \tag{4}$$

On the contrary, the maximum possible C_3 -weight is the sum of three largest possible vertex labels, namely, $rs - 2, rs - 1, rs$, and three the largest possible edge labels from the set, $\{4rs - 2r - 2, 4rs - 2r - 1, 4rs - 2r\}$. Hence, we have

$$a_3 + (2rs - 2r - 1)d \leq 15rs - 6r - 6. \tag{5}$$

From (4) and (5), an upper bound for the parameter d can be obtained as

$$\begin{aligned} d &\leq \frac{12rs - 16r - 18}{2rs - 2r - 1}, \\ d &\leq 6 - \frac{4r + 6}{2rs - 2r - 1}, \\ d &\leq 6. \end{aligned} \tag{6}$$

Thus, we have arrived at the desired result. \square

Theorem 2. *Let $r, s \geq 3$; then, the generalized antiprism \mathbb{A}_r^s admits a super $(9rs - 3r + 4, 0)$ - C_3 -antimagic total covering.*

Proof. Let $\phi: V(\mathbb{A}_r^s) \cup E(\mathbb{A}_r^s) \rightarrow \{1, 2, 3, \dots, 4rs - 2r\}$ be a total labeling of generalized antiprism \mathbb{A}_r^s defined as follows:

$$\begin{aligned} \phi(x_i^j) &= \{jr + 1 + i, \text{ for } 0 \leq i \leq r-1, 0 \leq j \leq s-1, \\ \phi(x_i^j x_{i+1}^j) &= \{(2s - j)r - i, \text{ for } 0 \leq i \leq r-1, 0 \leq j \leq s-1, \\ \phi(x_i^j x_i^{j+1}) &= \{(3s - 2 - j)r + r - i, \text{ for } 0 \leq i \leq r-1, 0 \leq j \leq s-2, \\ \phi(x_i^j x_{i+1}^{j+1}) &= \begin{cases} (4s - 3 - j)r + r - i, & \text{for } 0 \leq i \leq r-2, 0 \leq j \leq s-2, \\ (4s - 3 - j)r + 1, & \text{for } i = r-1, 0 \leq j \leq s-2. \end{cases} \end{aligned} \tag{7}$$

Under the labeling ϕ , the weights of 3- cycles z_i^j are

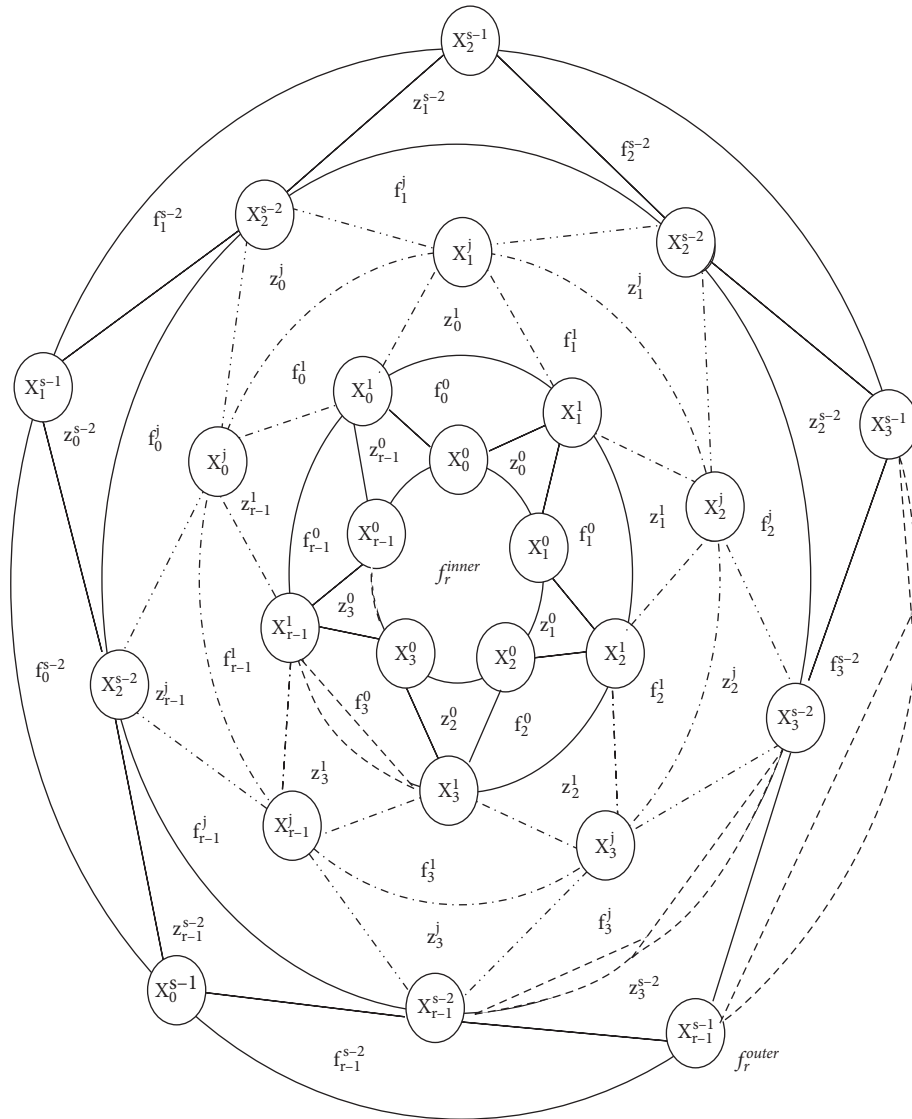


FIGURE 1: Generalized antiprism A_r^s .

$$\begin{aligned}
 W(z_i^j) &= \phi(x_i^j) + \phi(x_{i+1}^j) + \phi(x_{i+1}^{j+1}) + \phi(x_i^j x_{i+1}^j) + \phi(x_{i+1}^j x_{i+1}^{j+1}) + \phi(x_i^j x_{i+1}^{j+1}), \\
 W(z_i^j) &= \{9rs - 3r + 4, \quad \text{for } 0 \leq i \leq r-1, 0 \leq j \leq s-2
 \end{aligned}
 \tag{8}$$

And, the weights of 3-cycles f_i^j are

$$\begin{aligned}
 W(f_i^j) &= \phi(x_i^j) + \phi(x_{i+1}^{j+1}) + \phi(x_i^{j+1}) + \phi(x_i^j x_{i+1}^{j+1}) + \phi(x_{i+1}^{j+1} x_i^{j+1}) + \phi(x_i^{j+1} x_i^j), \\
 W(f_i^j) &= \{9rs - 3r + 4, \quad \text{for } 0 \leq i \leq r-1, 0 \leq j \leq s-2.
 \end{aligned}
 \tag{9}$$

Observe that the weights $W(z_i^j)$ and $W(f_i^j)$ of all cycles z_i^j and f_i^j are equal, and therefore, the resulting labeling is super $(9rs - 3r + 4, 0)\text{-}C_3$ total labeling. \square

Theorem 3. *Let $r, s \geq 3$; then, the generalized antiprism \mathbb{A}_r^s admits a super $(7rs + 4, 2)\text{-antimagic}$ total covering.*

Proof. Let $\chi: V(\mathbb{A}_r^s) \cup E(\mathbb{A}_r^s) \rightarrow \{1, 2, 3, \dots, 4rs - 2r\}$ be a total labeling of generalized antiprism \mathbb{A}_r^s defined as follows.

For $j = \text{even}$, the label on vertices x_i^j is defined as

$$\chi(x_i^j) = \begin{cases} 1 + i, & \text{for } 0 \leq i \leq r - 1, j = 0, \\ (j + 1)r, & \text{for } i = 0, 2 \leq j \leq s - 1, \\ jr + i, & \text{for } 1 \leq i \leq r - 1, 2 \leq j \leq s - 1. \end{cases} \quad (10)$$

For $j = \text{odd}$, the label on vertices x_i^j is defined as

$$\chi(x_i^j) = \begin{cases} jr + 1, & \text{for } i = 0, 1 \leq j \leq s - 1, \\ (j + 1)r + 1 - i, & \text{for } 1 \leq i \leq r - 1, 1 \leq j \leq s - 1. \end{cases} \quad (11)$$

For $j = \text{even}$, the label on edges $(x_i^j x_{i+1}^j)$ is defined as

$$\chi(x_i^j x_{i+1}^j) = \begin{cases} rs + 1 + i, & \text{for } 0 \leq i \leq r - 1, j = 0, \\ rs + (j + 1)r, & \text{for } i = 0, 2 \leq j \leq s - 1, \\ rs + jr + i, & \text{for } 1 \leq i \leq r - 1, 2 \leq j \leq s - 1. \end{cases} \quad (12)$$

For $j = \text{odd}$, the label on edges $(x_i^j x_{i+1}^j)$ is defined as

$$\chi(x_i^j x_{i+1}^j) = \begin{cases} rs + jr + 1, & \text{for } i = 0, 1 \leq j \leq s - 1, \\ rs + (j + 1)r + 1 - i, & \text{for } 1 \leq i \leq r - 1, 1 \leq j \leq s - 1. \end{cases} \quad (13)$$

The label on edges $(x_i^j x_i^{j+1})$ is defined as

$$\chi(x_i^j x_i^{j+1}) = \begin{cases} (3s - 2)r + 1 + i, & \text{for } 0 \leq i \leq r - 1, j = 0, \\ (3s - 1 - j)r, & \text{for } i = 0, 1 \leq j \leq s - 1, \\ (3s - 2 - j)r + i, & \text{for } 1 \leq i \leq r - 1, 1 \leq j \leq s - 1. \end{cases} \quad (14)$$

And, the label on edges $(x_i^j x_{i+1}^{j+1})$ is defined as

$$\chi(x_i^j x_{i+1}^{j+1}) = 3rs + jr - i, \quad \text{for } 0 \leq i \leq r - 1, 0 \leq j \leq s - 2. \quad (15)$$

Under the labeling χ , the weights of 3-cycle z_i^j are

$$W(z_i^j) = \chi(x_i^j) + \chi(x_{i+1}^j) + \chi(x_{i+1}^{j+1}) + \chi(x_i^j x_{i+1}^j) + \chi(x_{i+1}^j x_{i+1}^{j+1}) + \chi(x_i^j x_{i+1}^{j+1}). \quad (16)$$

For $j = \text{even}$, we have

$$W(z_i^j) = \begin{cases} 7rs + 8 + 2i, & \text{for } 0 \leq i \leq r - 2, j = 0, \\ 7rs + 4, & \text{for } i = r - 1, j = 0, \\ 7rs + 4jr + 2r + 2, & \text{for } i = 0, 2 \leq j \leq s - 2, \\ 7rs + 4jr + 2 + 2i, & \text{for } 1 \leq i \leq r - 1, 2 \leq j \leq s - 2. \end{cases} \quad (17)$$

For $j = \text{odd}$, we have

$$W(z_i^j) = \begin{cases} 7rs + 4jr + 4, & \text{for } i = 0, 1 \leq j \leq s - 2, \\ 7rs + 4jr + 2r + 4 - 2i, & \text{for } 1 \leq i \leq r - 1, 1 \leq j \leq s - 2. \end{cases} \quad (18)$$

The weight of 3-cycle f_i^j are

$$W(f_i^j) = \chi(x_i^j) + \chi(x_{i+1}^{j+1}) + \chi(x_i^{j+1}) + \chi(x_i^j x_{i+1}^{j+1}) + \chi(x_{i+1}^{j+1} x_i^{j+1}) + \chi(x_i^{j+1} x_i^j). \quad (19)$$

For $j = \text{even}$, we have

$$W(f_i^j) = \begin{cases} 7rs + 2r + 4, & \text{for } i = 0, j = 0, \\ 7rs + 4r + 4 - 2i, & \text{for } 1 \leq i \leq r - 1, j = 0, \\ 7rs + 4jr + 4r + 2 - 2i, & \text{for } 0 \leq i \leq r - 1, 2 \leq j \leq s - 2. \end{cases} \quad (20)$$

For $j = \text{odd}$, we have

$$W(f_i^j) = \begin{cases} 7rs + 4jr + 4r + 2, & \text{for } i = 0, 1 \leq j \leq s - 2, \\ 7rs + 4jr + 2r + 2 + 2i, & \text{for } 1 \leq i \leq r - 1, 1 \leq j \leq s - 2. \end{cases} \quad (21)$$

Observe that the weights $W(z_i^j)$ and $W(f_i^j)$ form an arithmetic progression with common difference 2 starting from $7rs + 4, 7rs + 6$ and ending at $11rs - 4r + 2$. This implies that the defined labeling is a super $(7rs + 4, 2)\text{-}C_3\text{-antimagic}$ total covering. \square

3. Results on Super $(a, d)\text{-}C_8\text{-Antimagic Total Covering of Toroidal Octagonal Planner Map } O_s^r$

A planar octagonal map is a graph obtained by joining octagons and squares in such a way that they cover the plane. To obtain the toroidal octagonal map, we apply torus identification on octagonal planner map. We denote the toroidal octagonal map with r rows and s column of octagons by O_s^r , where $s, r \geq 2$. The planar representation of O_s^r is depicted in Figure 2. The vertex set $V(O_s^r)$ and the edge set $E(O_s^r)$ of octagonal planner map O_s^r can be defined as follows:

$$\begin{aligned} V(O_s^r) &= \{u_i^j, v_i^j, w_i^j, x_i^j; 0 \leq i \leq r - 1 \text{ and } 0 \leq j \leq s - 1\}, \\ E(O_s^r) &= \{u_i^j v_i^j, w_i^j x_i^j; 0 \leq i \leq r - 1 \text{ and } 0 \leq j \leq s - 1\} \\ &\cup \{w_i^j u_i^{j-1}; 1 \leq i \leq s - 1 \text{ and } 0 \leq j \leq r - 1\} \\ &\cup \{w_i^0 u_i^{s-1}; 0 \leq i \leq r - 1\} \\ &\cup \{v_i^j w_{i+1}^{j+1}; 0 \leq i \leq r - 1 \text{ and } 0 \leq j \leq s - 2\} \\ &\cup \{v_i^{s-1} w_{i+1}^0; 0 \leq i \leq r - 1\} \\ &\cup \{v_i^j x_{i+1}^j; 0 \leq i \leq r - 1 \text{ and } 0 \leq j \leq s - 1\} \\ &\cup \{u_i^j x_i^j; 0 \leq i \leq r - 1 \text{ and } 0 \leq j \leq s - 1\}. \end{aligned} \quad (22)$$

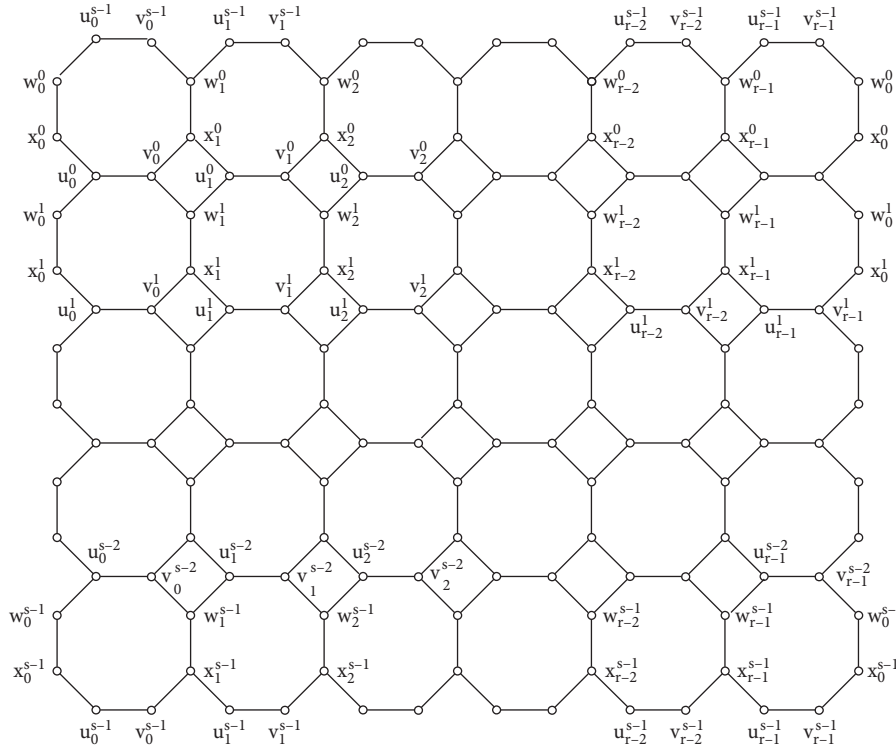


FIGURE 2: Toroidal octagonal map identification O_s^r

From the above sets, we have $|V(O_s^r)| = 4rs$ and $|E(O_s^r)| = 6rs$. We can cover the toroidal octagonal map O_s^r by the 8-sided cycles $C_{8,i}^j$. For $0 \leq j \leq s - 1$ and $0 \leq i \leq r - 1$,

the vertex set and edge set of 8-sided cycles $C_{8,i}^j$ can be defined as

$$\begin{aligned}
 V(C_{8,i}^j) &= \{w_i^j, u_i^{j-1}, v_i^{j-1}, w_{i+1}^j, x_{i+1}^j, v_i^j, u_i^j, x_i^j; 0 \leq i \leq r - 1, 1 \leq j \leq s - 1\}, \\
 E(C_{8,i}^j) &= \{w_i^j u_i^{j-1}, u_i^{j-1} v_i^{j-1}, v_i^{j-1} w_{i+1}^j, w_{i+1}^j x_{i+1}^j, v_i^j x_{i+1}^j, u_i^j v_i^j, x_i^j u_i^j, x_i^j w_i^j; 0 \leq i \leq r - 1, 1 \leq j \leq s - 1\}, \\
 V(C_{8,i}^0) &= \{w_i^0, u_i^{s-1}, v_i^{s-1}, w_{i+1}^0, x_{i+1}^0, v_i^0, u_i^0, x_i^0; 0 \leq i \leq r - 1\}, \\
 E(C_{8,i}^0) &= \{w_i^0 u_i^{s-1}, u_i^{s-1} v_i^{s-1}, v_i^{s-1} w_{i+1}^0, w_{i+1}^0 x_{i+1}^0, v_i^0 x_{i+1}^0, u_i^0 v_i^0, x_i^0 u_i^0, x_i^0 w_i^0; 0 \leq i \leq r - 1\}.
 \end{aligned} \tag{23}$$

We start by giving an upper bound for d such that O_s^r admits a super (a, d) - C_8 -antimagic covering.

Theorem 4. Suppose O_s^r admits a super (a, d) - C_8 -antimagic covering; then, $d \leq 80$.

Proof. Suppose O_s^r admits a super (a, d) - C_8 -antimagic covering. Then, the weight on cycle C_8 is atleast

$$\sum_{i=1}^8 i + \sum_{i=1}^8 (4rs + i) = 32rs + 72, \tag{24}$$

and the largest weight of C_8 is atmost

$$\sum_{i=1}^8 (4rs + 1 - i) + \sum_{i=1}^8 (10rs + 1 - i) = 112rs - 56. \tag{25}$$

Thus, we have

$$a + (rs - 1)d \leq 112rs - 56,$$

$$(rs - 1)d \leq 112rs - 56 - 32rs - 72,$$

$$d \leq \frac{80rs - 128}{rs - 1}, \tag{26}$$

$$d \leq 80.$$

□

In the next two theorems, we show that toroidal octagonal map O_s^r admits a super (a, d) - C_8 -antimagic covering for $d = 1, 2, \dots, 7$.

Theorem 5. Let $r, s \geq 2$; then, the toroidal octagonal map O_s^r is super (a, d) - C_8 -antimagic for $d \in \{1, 3, 5, 7\}$.

Proof. Define a total labeling $\varphi_d: V(O_s^r) \cup E(O_s^r) \longrightarrow \{1, 2, 3, \dots, |V(O_s^r)| + |E(O_s^r)|\}$, where $d \in \{1, 3, 5, 7\}$ as follows:

$$\begin{aligned}
 \varphi_d(u_i^j) &= jr + 1 + i, \quad 0 \leq i \leq r-1, 0 \leq j \leq s-1, \\
 \varphi_d(v_i^j) &= rs + jr + 1 + i, \quad 0 \leq i \leq r-1, 0 \leq j \leq s-1, \\
 \varphi_d(x_i^j) &= 3rs + (s-1-j)r + r - i, \quad 0 \leq i \leq r-1, 0 \leq j \leq s-1, \\
 \varphi_d(w_i^j) &= 2rs + jr + 1 + i, \quad 0 \leq i \leq r-1, 0 \leq j \leq s-1, \\
 \varphi_d(u_i^j v_i^j) &= 4rs + (s-1-j)r + r - i, \quad 0 \leq i \leq r-1, 0 \leq j \leq s-1, \\
 \varphi(x_i^j w_i^j) &= 5mn + 2jm + 1 + 2i, \quad 0 \leq i \leq r-1, 0 \leq j \leq s-1, \\
 \varphi_1(v_i^j x_{i+1}^j) &= \varphi_3(v_i^j x_{i+1}^j) = 8rs + (s-1-j)r + r - i, \quad 0 \leq i \leq r-1, 0 \leq j \leq s-1, \\
 \varphi_5(v_i^j x_{i+1}^j) &= \varphi_7(v_i^j x_{i+1}^j) = 8rs + jr + 1 + i, \quad 0 \leq i \leq r-1, 0 \leq j \leq s-1, \\
 \varphi_d(u_i^j w_i^{j+1}) &= 5rs + 2(s-1-j)r + 2r - 2i, \quad 0 \leq i \leq r-1, 0 \leq j \leq s-1, \\
 \varphi_1(v_i^j w_i^{j+1}) &= 7rs + (s-1-j)r + r - i, \quad 0 \leq i \leq r-1, 0 \leq j \leq s-1, \\
 \varphi_3(v_i^j w_i^{j+1}) &= \varphi_5(v_i^j w_i^{j+1}) = \varphi_7(v_i^j w_i^{j+1}) = 7rs + rj + 1 + i, \quad 0 \leq i \leq r-1, 0 \leq j \leq s-1, \\
 \varphi_1(x_i^j u_i^j) &= \varphi_3(x_i^j u_i^j) = \varphi_5(x_i^j u_i^j) = 9rs + (s-1-j)r + r - i, \quad 0 \leq i \leq r-1, 0 \leq j \leq s-1, \\
 \varphi_7(x_i^j u_i^j) &= 9rs + jr + 1 + i, \quad 0 \leq i \leq r-1, 0 \leq j \leq s-1.
 \end{aligned} \tag{27}$$

The total labeling φ_d labels the vertices $u_i^j, v_i^j, w_i^j, x_i^j$ from the set $\{1, 2, \dots, 4rs\}$ and the edges from the set $\{4rs + 1, 4rs + 2, \dots, 10rs\}$. For $0 \leq i \leq r-1$ and $0 \leq j \leq s-1$, the weight of cycles $C_{8,i}^j$ under φ_d is

$$\begin{aligned}
 W_d(C_{8,i}^j) &= \varphi_d(u_i^{j-1}) + \varphi_d(v_i^{j-1}) + \varphi_d(u_i^{j-1} v_i^{j-1}) + \varphi_d(w_{i+1}^j) + \varphi_d(w_i^j) + \varphi_d(w_{i+1}^j v_i^{j-1}) \\
 &\quad + \varphi_d(x_{i+1}^j) + \varphi_d(x_{i+1}^j w_{i+1}^j) + \varphi_d(v_i^j) + \varphi_d(v_i^j x_{i+1}^j) + \varphi_d(u_i^j) \\
 &\quad + \varphi_d(u_i^j v_i^j) + \varphi_d(x_i^j) + \varphi_d(x_i^j u_i^j) + \varphi_d(x_i^j w_i^j) + \varphi_d(w_i^j u_i^{j-1}), \\
 W_d(C_{8,i}^j) &= \begin{cases} 68rs + 2r + 10 + jr + i, & \text{for } d = 1, \\ 67rs + r + 11 + 3jr + 3i, & \text{for } d = 3, \\ 66rs + r + 12 + 5jr + 5i, & \text{for } d = 5, \\ 65rs + 13 + 7jr + 7i, & \text{for } d = 7. \end{cases} \tag{28}
 \end{aligned}$$

For the case $d = 1$, we have weights' set $\{68rs + 2r + 10, 68rs + 2r + 11, \dots, 69rs + 2r + 9\}$; similarly, for cases $d = 3, 5, 7$, we get the weights from the sets $\{67rs + r + 11, 67rs + r + 12, \dots, 70rs + r + 8\}$, $\{66rs + r + 12, 66rs + r + 17, \dots, 71rs + r + 7\}$, and $\{65rs + r + 13, 65rs + r + 20, \dots, 72rs + r + 5\}$, respectively. Hence, the weights of cycles $C_{8,i}^j$ form an arithmetic sequence with difference 1, 3, 5, and 7. \square

Theorem 6. Let $r, s \geq 2$; then, the toroidal map O_s^r is super (a, d) - C_8 -antimagic for $d \in \{2, 4, 6\}$.

Proof. Let $d \in \{2, 4, 6\}$ and $0 \leq i \leq r - 1, 0 \leq j \leq s - 1$. We define a total labeling ϕ_d of O_s^r as follows:

$$\begin{aligned}
 \phi_d(u_i^j) &= jr + 1 + i, \quad 0 \leq i \leq r - 1, 0 \leq j \leq s - 1, \\
 \phi_d(v_i^j) &= rs + jr + 1 + i, \quad 0 \leq i \leq r - 1, 0 \leq j \leq s - 1, \\
 \phi_d(x_i^j) &= 3rs + (s - 1 - j)r + r - i, \quad 0 \leq i \leq r - 1, 0 \leq j \leq s - 1, \\
 \phi_d(w_i^j) &= 2rs + jr + 1 + i, \quad 0 \leq i \leq r - 1, 0 \leq j \leq s - 1, \\
 \phi_d(u_i^j v_i^j) &= 8rs + (s - 1 - j)r + r - i, \quad 0 \leq i \leq r - 1, 0 \leq j \leq s - 1, \\
 \phi_2(x_i^j w_i^j) &= \phi_4(x_i^j w_i^j) = 9rs + (s - 1 - j)r + r - i, \quad 0 \leq i \leq r - 1, 0 \leq j \leq s - 1, \\
 \phi_6(x_i^j w_i^j) &= 9rs + jr + 1 + i, \quad 0 \leq i \leq r - 1, 0 \leq j \leq s - 1, \\
 \phi_2(v_i^j x_{i+1}^j) &= \phi_4(v_i^j x_{i+1}^j) = 6rs + jr + 1 + i, \quad 0 \leq i \leq r - 1, 0 \leq j \leq s - 1, \\
 \phi_6(v_i^j x_{i+1}^j) &= 6rs + (s - 1 - j)r + r - i, \quad 0 \leq i \leq r - 1, 0 \leq j \leq s - 1, \\
 \phi_d(u_i^j w_i^{j+1}) &= 4rs + jr + 1 + i, \quad 0 \leq i \leq r - 1, 0 \leq j \leq s - 1, \\
 \phi_d(v_i^j w_i^{j+1}) &= 5rs + rj + 1 + i, \quad 0 \leq i \leq r - 1, 0 \leq j \leq s - 1, \\
 \phi_2(x_i^j u_i^j) &= 7rs + (s - 1 - j)r + r - i, \quad 0 \leq i \leq r - 1, 0 \leq j \leq s - 1, \\
 \phi_4(x_i^j u_i^j) &= \phi_6(x_i^j u_i^j) = 7rs + jr + 1 + i, \quad 0 \leq i \leq r - 1, 0 \leq j \leq s - 1.
 \end{aligned} \tag{29}$$

The total labeling ϕ_d labels the vertices $u_i^j, v_i^j, w_i^j, x_i^j$ from the set $\{1, 2, \dots, 4rs\}$ and edges from the set $\{4rs + 1, 4rs + 2, \dots, 10rs\}$. This show that ϕ_d is a bijection

from set $V(O_s^r) \cup E(O_s^r)$ to set $\{1, 2, \dots, 10rs\}$. For $1 \geq i \geq l$ and $i \geq j \geq k$, the weights of $C_{8,i}^j$ under the labeling ϕ_d are

$$\begin{aligned}
 W_d(C_{8,i}^j) &= \phi_d(u_i^{j-1}) + \phi_d(v_i^{j-1}) + \phi_d(u_i^{j-1} v_i^{j-1}) + \phi_d(w_{i+1}^j) + \phi_d(w_i^j) + \phi_d(w_{i+1}^j v_i^{j-1}) \\
 &\quad + \phi_d(x_{i+1}^j) + \phi_d(x_{i+1}^j w_{i+1}^j) + \phi_d(v_i^j) + \phi_d(v_i^j x_{i+1}^j) + \phi_d(u_i^j) \\
 &\quad + \phi_d(u_i^j v_i^j) + \phi_d(x_i^j) + \phi_d(x_i^j u_i^j) + \phi_d(x_i^j w_i^j) + \phi_d(w_i^j u_i^{j-1}), \\
 W_d(C_{8,i}^j) &= \begin{cases} 75rs - 4r + 8 + 2jr + 2i, & \text{for } d = 2, \\ 74rs - 4r + 9 + 4jr + 4i, & \text{for } d = 4, \\ 73rs - 4r + 12 + 6jr + 6i, & \text{for } d = 6. \end{cases}
 \end{aligned} \tag{30}$$

For the case $d = 2$, we have weights from the set $\{75rs - 4r + 8, 75rs - 4r + 10, \dots, 77rs - 4r + 6\}$. Similarly, for cases $d = 4, 6$, we get weights from the sets $\{74rs - 4r + 9, 74rs - 4r + 13, \dots, 78rs - 4r + 5\}$ and $\{73rs - 4r + 12, 73rs - 4r + 18, \dots, 79rs - 4r + 6\}$, respectively. This showed that weights of the cycles $C_{8,i}^j$ form an arithmetic sequence with difference 2, 4, and 6. \square

4. Conclusion

In the present paper first, we constructed an upper bound for the parameter d for super (a, d) - C_3 -antimagic covering. Secondly, we examined the existence of super (a, d) - C_3 -antimagic labeling of generalized antiprism A_r^s . We showed that, for $r, s \geq 3$ the generalized antiprism A_r^s had

(a, d) - C_3 -antimagic covering for $d \in \{0, 2\}$. Thirdly, we constructed an upper bound for the parameter d for super (a, d) - C_8 -antimagic covering. Finally, we examined the existence of super (a, d) - C_8 -antimagic labeling of torodial map O_s^r . We showed that, for $m, n \geq 2$, the torodial octagonal map O_s^r had (a, d) - C_8 -antimagic covering for $d \in \{1, 2, 3, 4, 5, 6, 7\}$. We conclude the paper with the following open problems.

Open problem 1: find other possible bound for parameter d under (a, d) - C_3 -antimagic total covering and the corresponding remaining labeling of d for generalized antiprism A_r^s .

Open problem 2: find other possible bound for parameter d under (a, d) - C_8 -antimagic total covering and the corresponding remaining labeling of d for torodial octagonal map O_s^r .

Data Availability

No data were used to support the study.

Conflicts of Interest

The authors declare that they have no conflicts of interest.

References

- [1] J. L. Gross, J. Yellen, and P. Zhang, *Handbook of Graph Theory*, CRC Press, Taylor and Francis Group, Boca Raton, FL, USA, Second edition, 2014.
- [2] A. Kotzig and A. Rosa, "Magic valuations of finite graphs," *Canadian Mathematical Bulletin*, vol. 13, no. 4, pp. 451–461, 1970.
- [3] H. Enomoto, A. S. Llado, T. Nakamigawa, and G. Ringel, "Super edge-magic graphs," *SUT Journal of Mathematics*, vol. 34, pp. 105–109, 1998.
- [4] A. Gutierrez and A. Llado, "Magic coverings," *Journal of Combinatorial Mathematics and Combinatorial Computing*, vol. 55, pp. 43–46, 2005.
- [5] A. Llado and J. Moragas, "Cycle-magic graphs," *Discrete Mathematics*, vol. 307, no. 29–25, pp. 29–33, 2007.
- [6] T. K. Maryati, A. N. M. Salman, and E. T. Baskoro, "Supermagic coverings of the disjoint union of graphs and amalgamations," *Discrete Mathematics*, vol. 313, no. 4, pp. 397–405, 2013.
- [7] T. K. Maryati, A. N. M. Salman, E. T. Baskoro, J. Ryan, and M. Miller, "On H -supermagic labelings for certain shackles and amalgamations of a connected graph," *Utilitas Mathematica*, vol. 83, pp. 333–342, 2010.
- [8] A. N. M. Salman, A. A. G. Ngurah, and N. Izzati, "On (super)-edge-magic total labelings of subdivision of stars Sn ," *Utilitas Mathematica*, vol. 81, pp. 275–284, 2010.
- [9] A. A. G. Ngurah, A. N. M. Salman, and L. Susilowati, "H-supermagic labelings of graphs," *Discrete Mathematics*, vol. 310, no. 8, pp. 1293–1300, 2010.
- [10] N. Inayah, A. N. M. Salman, and R. Simanjuntak, "On (a, d) - H -antimagic coverings of graphs," *Journal of Combinatorial Mathematics and Combinatorial Computing*, vol. 71, pp. 273–281, 2009.
- [11] Z. Liang, "Cycle-supermagic decompositions of complete multipartite graphs," *Discrete Mathematics*, vol. 312, no. 22, pp. 3342–3348, 2012.
- [12] K. A. Hendy, "The H -super(anti)magic decomposition of antiprism graphs," *AIP Conference Proceedings*, vol. 1707, Article ID 020007, 2016.
- [13] K. A. Hendy, A. N. Sugeng, and M. Salman, "An H -super magic decompositions of the lexicographic product of graphs," *AIP Conference Proceedings*, vol. 2023, Article ID 020193, 2018.
- [14] K. A. Hendy, A. N. Mudholifah, K. A. Sugeng, M. Baca, and A. Semanicova-Fenovcikova, "On H -antimagic decomposition of toroidal grids and triangulations," *AKCE International Journal of Graphs and Combinatorics*, vol. 17, no. 3, 2019.
- [15] A. S. Fenovcikova, M. Baca, M. Lascakova, M. Miller, and J. Ryan, "Wheels are cycle-antimagic," *Electronic Notes in Discrete Mathematics*, vol. 48, pp. 11–18, 2015.

Research Article

New Results on the Geometric-Arithmetic Index

Akbar Jahanbani ¹, Maryam Atapour ², and Zhibin Du ³

¹Department of Mathematics, Azarbaijan Shahid Madani University, Tabriz, Iran

²Department of Mathematics and Computer Science, Basic Science Faculty, University of Bonab, P.O. Box 55513-95133, Bonab, Iran

³School of Software, South China Normal University, Foshan, Guangdong 528225, China

Correspondence should be addressed to Maryam Atapour; m.atapour@ubonab.ac.ir

Received 18 June 2021; Accepted 20 July 2021; Published 31 July 2021

Academic Editor: Ali Ahmad

Copyright © 2021 Akbar Jahanbani et al. This is an open access article distributed under the Creative Commons Attribution License, which permits unrestricted use, distribution, and reproduction in any medium, provided the original work is properly cited.

Let G be a graph with vertex set $V(G)$ and edge set $E(G)$. Let d_u denote the degree of vertex $u \in V(G)$. The geometric-arithmetic index of G is defined as $GA(G) = \sum_{uv \in E(G)} (2\sqrt{d_u d_v} / (d_u + d_v))$. In this paper, we obtain some new lower and upper bounds for the geometric-arithmetic index and improve some known bounds. Moreover, we investigate the relationships between geometric-arithmetic index and several other topological indices.

1. Introduction

Let G be a simple graph (i.e., graph without loops and multiple edges) with vertex set $V(G)$ and edge set $E(G)$. The integers $n = |V(G)|$ and $m = |E(G)|$ are the *order* and the *size* of the graph G , respectively. For $u \in V(G)$, we denote by d_u the degree of vertex u in G . The minimum and maximum degrees of a graph are denoted by δ and Δ , respectively.

Graph theory has provided chemists with a variety of useful tools, such as topological indices. A topological index $Top(G)$ of a graph G is a number with the property that, for every graph H isomorphic to G , $Top(H) = Top(G)$.

Molecular descriptors play a significant role in mathematical chemistry, especially in QSPR/QSAR investigations. Among them, special place is reserved for so-called topological descriptors. A topological index is a numeric quantity from the structural graph of a molecule.

Usage of topological indices in chemistry began in 1947 when Wiener [1] developed the most widely known topological descriptor, namely, the Wiener index, and used it to determine physical properties of types of alkanes known as paraffin (see, for instance, [2, 3]). The interest of topological indices lies in the fact that they synthesize some of the

properties of a molecule into a single number. With this in mind, hundreds of topological indices have been introduced and studied. Topological indices based on the vertex degree play a vital role in mathematical chemistry, and some of them are recognized as tools in chemical research.

Authors are studying various topological descriptors, such as Zagreb indices [4–6], general sum-connectivity index [7, 8], hyper-Zagreb index [9], and harmonic index [10, 11]. Besides the abovementioned ones, there are other topological descriptors based on end vertex degrees of edges of graphs that have found some applications in QSPR/QSAR research [2, 12, 13].

The geometric-arithmetic index of a graph is defined in [13] as

$$GA(G) = \sum_{uv \in E(G)} \frac{2\sqrt{d_u d_v}}{d_u + d_v} \quad (1)$$

The geometric-arithmetic index has a number of interesting properties, e.g., see [13]. The lower and upper bounds of the geometric-arithmetic index of connected graphs and the characterizations of graphs for which these bounds are best possible can be found in [13–16].

The aim of this paper is to investigate new relationships between the geometric-arithmic index and other topological indices. In particular, we obtain some lower and upper bounds for the geometric-arithmic index. Moreover, we improve some known bounds.

2. Preliminaries

Let us recall some remarkable lemmas which will be used in this paper.

The first one is a very straightforward observation.

$$\frac{n}{(1/x_1) + (1/x_2) + \dots + (1/x_n)} \leq \sqrt[n]{\prod_{i=1}^n x_i} \leq \frac{x_1 + x_2 + \dots + x_n}{n} \leq \sqrt{\frac{x_1^2 + x_2^2 + \dots + x_n^2}{n}}. \tag{3}$$

Lemma 3 (see [19]). *Let $a = (a_i)_{i=1}^n$ and $(b_i)_{i=1}^n$ be two sequences of positive numbers. For any $r \geq 0$,*

$$\sum_{i=1}^n \frac{a_i^{r+1}}{b^r} \geq \frac{(\sum_{i=1}^n a_i)^{r+1}}{(\sum_{i=1}^n b_i)^r}. \tag{4}$$

Lemma 4 (see [20]). *Let $r \leq a_i \leq R$ for $1 \leq i \leq m$ and r and R be some positive constants. Then,*

$$\sum_{i=1}^m a_i \sum_{i=1}^m \frac{1}{a_i} \leq m^2 \left(1 + \frac{1}{4} \left(1 - \frac{1 + (-1)^{m+1}}{2m^2} \left(\sqrt{\frac{R}{r}} - \sqrt{\frac{r}{R}} \right)^2 \right) \right). \tag{5}$$

Lemma 5 (see [21]). *If a_1, a_2, \dots, a_n and b_1, b_2, \dots, b_n are positive numbers, where $m_1 \leq a_i \leq N_1$ and $m_2 \leq b_i \leq N_2$ for each $1 \leq i \leq n$, then*

$$\sum_{i=1}^n a_i^2 \sum_{i=1}^n b_i^2 - \left(\sum_{i=1}^n a_i b_i \right)^2 \leq \frac{n^2}{4} (N_1 N_2 + m_1 m_2). \tag{6}$$

Lemma 6 (the Pólya–Szegő inequality, see p. 62 in [22]). *Let $a = (a_i)_{i=1}^n$ and $(b_i)_{i=1}^n$ be two sequences of positive numbers, where $0 < m_1 \leq a_i \leq M_1$ and $0 < m_2 \leq b_i \leq M_2$, for $i = 1, 2, \dots, n$. Then,*

$$\sum_{i=1}^n a_i^2 \sum_{i=1}^n b_i^2 \leq \frac{1}{4} \left(\sqrt{\frac{M_1 M_2}{m_1 m_2}} + \sqrt{\frac{m_1 m_2}{M_1 M_2}} \right)^2 \left(\sum_{i=1}^n a_i b_i \right)^2. \tag{7}$$

3. Upper Bounds for the Geometric-Arithmetic Index

In this section, we investigate the relationships between geometric-arithmic index and some topological indices. Moreover, we obtain some upper bounds for the geometric-arithmic index in terms of order, size, maximum degree, minimum degree, domination number, girth, number of cut edges, and number of pendent vertices.

Lemma 1 (see [17]). *Let x and y be two positive numbers. Then,*

$$\frac{2xy}{x+y} \leq \sqrt{xy} \leq \frac{((x+y)/2) + \sqrt{xy}}{2} \leq \frac{x+y}{2} \leq \sqrt{\frac{x^2+y^2}{2}}. \tag{2}$$

The following is the well-known inequality of arithmetic and geometric means.

Lemma 2 (inequality of arithmetic and geometric means, see [18]). *Let x_1, \dots, x_n be positive numbers. Then,*

The first and second Zagreb indices are vertex-degree-based graph invariants defined as

$$M_1(G) = \sum_{uv \in E(G)} (d_u + d_v), \tag{8}$$

$$M_2(G) = \sum_{uv \in E(G)} d_u d_v.$$

The quantity M_1 was first considered in 1972 [6], whereas M_2 in 1975 [5]. The general Randić index is defined as follows [23]:

$$R_\alpha(G) = \sum_{uv \in E(G)} (d_u d_v)^\alpha, \tag{9}$$

where α is a real number.

We begin with the establishment of an upper bound for the geometric-arithmic index in terms of the first Zagreb index and the general Randić index.

Theorem 1. *Let G be a graph. Then,*

$$GA(G) \leq \frac{M_1(G) + 2R_{1/2}(G)}{4}. \tag{10}$$

Proof. By Lemma 1, we have

$$GA(G) = \sum_{uv \in E(G)} \frac{2\sqrt{d_u d_v}}{d_u + d_v}$$

$$\leq \sum_{uv \in E(G)} \frac{2d_u d_v}{d_u + d_v}$$

$$\leq \sum_{uv \in E(G)} \frac{((d_u + d_v)/2) + \sqrt{d_u d_v}}{2} \tag{11}$$

$$= \sum_{uv \in E(G)} \frac{d_u + d_v + 2\sqrt{d_u d_v}}{4}$$

$$= \frac{M_1(G) + 2R_{1/2}(G)}{4},$$

as desired.

Using Lemma 1 and an argument similar to the proof of Theorem 1, we can obtain the next result. \square

Corollary 1. *Let G be a graph. Then,*

$$GA(G) \leq R_{1/2}(G). \tag{12}$$

From Lemma 1, we get

$$R_{1/2}(G) = \sum_{uv \in E(G)} \sqrt{d_u d_v} \leq \sum_{uv \in E(G)} \frac{d_u + d_v}{2} = \frac{M_1(G)}{2}. \tag{13}$$

Again by Lemma 1, we have

$$\begin{aligned} \frac{M_1(G) + 2R_{1/2}(G)}{4} &= \sum_{uv \in E(G)} \frac{d_u + d_v + 2\sqrt{d_u d_v}}{4} \\ &= \sum_{uv \in E(G)} \frac{((d_u + d_v)/2) + \sqrt{d_u d_v}}{2} \\ &\leq \sum_{uv \in E(G)} \frac{d_u + d_v}{2} = \frac{M_1(G)}{2}. \end{aligned} \tag{14}$$

Hence, we can see that the bounds in Theorem 1 and Corollary 1 improve the bound:

$$GA(G) \leq \frac{M_1(G)}{2}, \tag{15}$$

established in [15].

The proof of the following result can be found in [23].

Lemma 7 (see [23]). *Let G be a graph of size m . Then,*

$$R_\alpha(G) \leq m \left(\frac{\sqrt{8m+1} - 1}{2} \right)^{2\alpha}, \tag{16}$$

for $0 < \alpha \leq 1$.

Using Corollary 1 and Lemma 7, we can drive the next result.

Corollary 2. *Let G be a graph of size m . Then,*

$$GA(G) \leq \frac{m(\sqrt{8m+1} - 1)}{2}. \tag{17}$$

Lemma 8. *Let x and y be two positive numbers. Then,*

$$\begin{aligned} \frac{2\sqrt{xy}}{x+y} &\leq 1, \\ \frac{x+y}{\sqrt{xy}} &\geq 2. \end{aligned} \tag{18}$$

Now, we obtain an upper bound for the geometric-arithmetic index in terms of the first Zagreb index.

Theorem 2. *Let G be a graph of order $n \geq 2$, size m , and minimum degree δ . Then,*

$$GA(G) \leq m - n + \frac{M_1(G)}{\delta^2}. \tag{19}$$

Proof. Notice that

$$\sum_{uv \in E(G)} \frac{d_u + d_v}{d_u d_v} = \sum_{uv \in E(G)} \left(\frac{1}{d_u} + \frac{1}{d_v} \right) = n. \tag{20}$$

By Lemma 8, we have

$$\begin{aligned} GA(G) + n &= \sum_{uv \in E(G)} \left(\frac{2\sqrt{d_u d_v}}{d_u + d_v} + \frac{d_u + d_v}{d_u d_v} \right) \\ &\leq \sum_{uv \in E(G)} \left(1 + \frac{d_u + d_v}{d_u d_v} \right) \\ &= \sum_{uv \in E(G)} 1 + \sum_{uv \in E(G)} \frac{d_u + d_v}{d_u d_v} \\ &\leq m + \frac{M_1(G)}{\delta^2}, \end{aligned} \tag{21}$$

and this implies the desired bound.

A dominating set of a graph is a vertex subset whose closed neighborhood includes all vertices of the graph. The domination number of a graph G is the size of a minimum dominating set. \square

Theorem 3 (see [24]). *Let T be a tree of order n with domination number γ . Then,*

$$M_1(T) \leq (n - \gamma)(n - \gamma + 1) + 4(\gamma - 1). \tag{22}$$

By Theorems 2 and 3, we have the following result for trees with the given domination number.

Corollary 3. *Let T be a tree of order $n \geq 2$ with domination number γ . Then,*

$$GA(T) \leq (n - \gamma)(n - \gamma + 1) + 4(\gamma - 1) - 1. \tag{23}$$

Since for every two real numbers x, y , and $xy \leq ((x + y)^2/4)$, we have the next observation.

Lemma 9. *Let x and y be two real numbers, where $x + y \neq 0$. Then, $(xy/(x + y)^2) \leq (1/4)$.*

Next, we establish an upper bound for the geometric-arithmetic index in terms of the second Zagreb index.

Theorem 4. *Let G be a graph of size m with maximum degree Δ . Then,*

$$GA(G) \leq \frac{5m}{4} - \frac{M_2(G)}{4\Delta^2}. \tag{24}$$

Proof. By Lemmas 8 and 9, we have

$$\begin{aligned} \text{GA}(G) + \frac{M_2(G)}{4\Delta^2} &\leq \sum_{uv \in E(G)} \left(\frac{2\sqrt{d_u d_v}}{d_u + d_v} + \frac{d_u d_v}{(d_u + d_v)^2} \right) \\ &\leq \sum_{uv \in E(G)} \left(\frac{2\sqrt{d_u d_v}}{d_u + d_v} + \frac{1}{4} \right) \\ &\leq \sum_{uv \in E(G)} \left(1 + \frac{1}{4} \right) \\ &= \frac{5m}{4}, \end{aligned} \tag{25}$$

and this implies the desired bound. \square

In [25], it is proved that, for any tree T of order n , $M_2(T) \geq 4n - 8$. Using this and Theorem 4, we obtain the next result.

Corollary 4. *Let T be a tree of order n with maximum degree Δ . Then,*

$$\text{GA}(T) \leq \frac{5(n-1)}{4} - \frac{n-2}{\Delta^2}. \tag{26}$$

Here, we establish an upper bound for the geometric-arithmetic index in terms of the hyper-Zagreb index.

The hyper-Zagreb index is defined as follows [9]:

$$\text{HM}(G) = \sum_{uv \in E(G)} (d_u + d_v)^2. \tag{27}$$

Theorem 5. *Let G be a graph of order n , size m , and minimum degree δ . Then,*

$$\text{GA}(G) \leq m - n + \frac{\text{HM}(G)}{2\delta^2}. \tag{28}$$

Proof. By Inequality (21), we have

$$\begin{aligned} \text{GA}(G) + n &\leq \sum_{uv \in E(G)} 1 + \sum_{uv \in E(G)} \frac{d_u + d_v}{d_u d_v} \\ &\leq \sum_{uv \in E(G)} 1 + \sum_{uv \in E(G)} \frac{d_u + d_v}{(2d_u d_v / (d_u + d_v))} \\ &= \sum_{uv \in E(G)} 1 + \sum_{uv \in E(G)} \frac{(d_u + d_v)^2}{2d_u d_v} \\ &\leq m + \frac{\text{HM}(G)}{2\delta^2}. \end{aligned} \tag{29}$$

It leads to the desired bound. \square
The next result is proven in [26].

Theorem 6 (see [26]). *Let G be a graph with n vertices and m edges. Then,*

$$\text{HM}(G) \leq \frac{m^3(n+1)^6}{16n^2(n-1)^2}. \tag{30}$$

Theorems 5 and 6 lead to the desired result.

Corollary 5. *Let G be a graph of order n , size m , and minimum degree δ . Then,*

$$\text{GA}(G) \leq m - n + \frac{m^3(n+1)^6}{32\delta^2 n^2(n-1)^2}. \tag{31}$$

The redefined third Zagreb index is defined as follows [27]:

$$\text{ReZ}_3(G) = \sum_{uv \in E(G)} (d_u d_v)(d_u + d_v). \tag{32}$$

Now, we obtain an upper bound for the geometric-arithmetic index in terms of the second Zagreb index, the general Randić index, and the redefined third Zagreb index.

Theorem 7. *Let G be a graph with maximum degree Δ and minimum degree δ . Then,*

$$\text{GA}(G) \leq M_2(G) + \frac{R_{1/2}(G)}{\delta} - \frac{\text{ReZ}_3(G)}{2\Delta}. \tag{33}$$

Proof. It is easy to obtain

$$\begin{aligned} M_2(G) - \text{GA}(G) &= \sum_{uv \in E(G)} \left(d_u d_v - \frac{2\sqrt{d_u d_v}}{d_u + d_v} \right) \\ &= \sum_{uv \in E(G)} \left(\frac{(d_u + d_v)d_u d_v - 2\sqrt{d_u d_v}}{d_u + d_v} \right) \\ &= \sum_{uv \in E(G)} \frac{(d_u + d_v)d_u d_v}{d_u + d_v} - \sum_{uv \in E(G)} \frac{2\sqrt{d_u d_v}}{d_u + d_v} \\ &\geq \frac{\text{ReZ}_3(G)}{2\Delta} - \frac{R_{1/2}(G)}{\delta}. \end{aligned} \tag{34}$$

The desired bound follows. \square

Theorem 8. *Let G be a graph of order n , size m , maximum degree Δ , and minimum degree δ . Then,*

$$\text{GA}(G) \leq \frac{2m^2}{n} \left(1 + \frac{1}{4} \left(1 - \frac{1 + (-1)^{m+1}}{2m^2} \left(\frac{\Delta}{\delta} - \frac{\delta}{\Delta} \right)^2 \right) \right). \tag{35}$$

Proof. Now, putting $a_{uv} = (2\sqrt{d_u d_v} / (d_u + d_v))$ for each edge $uv \in E(G)$, $R = (\Delta/\delta)$, and $r = (\delta/\Delta)$ in Lemma 4, we have

$$\sum_{uv \in E(G)} \frac{2\sqrt{d_u d_v}}{d_u + d_v} \sum_{uv \in E(G)} \frac{d_u + d_v}{2\sqrt{d_u d_v}} \leq m^2 \left(1 + \frac{1}{4} \left(1 - \frac{1 + (-1)^{m+1} \left(\frac{\Delta}{\delta} - \frac{\delta}{\Delta} \right)^2}{2m^2} \right) \right). \tag{36}$$

On the contrary, we have

$$\frac{n}{2} = \sum_{uv \in E(G)} \frac{d_u + d_v}{2d_u d_v} \leq \sum_{uv \in E(G)} \frac{d_u + d_v}{2\sqrt{d_u d_v}} \tag{37}$$

Finally, we get the bound by using Inequalities (36) and (37).

The sigma index of G is defined in [28] as

$$\sigma(G) = \sum_{uv \in E(G)} (d_u - d_v)^2. \tag{38}$$

Here, we obtain an upper bound for the geometric-arithmetic index in terms of the first Zagreb index and the sigma index. \square

Theorem 9. *Let G be a nontrivial graph with maximum degree Δ . Then,*

$$GA(G) \leq \frac{M_1(G)}{2} - \frac{\sigma(G)}{4\Delta}. \tag{39}$$

Proof. For two real numbers x and y , we have that

$$xy = \frac{1}{4} \left((x + y)^2 - (x - y)^2 \right). \tag{40}$$

By (40), we obtain

$$\begin{aligned} GA(G) &= \sum_{uv \in E(G)} \frac{2\sqrt{d_u d_v}}{d_u + d_v} \leq \sum_{uv \in E(G)} \frac{2d_u d_v}{d_u + d_v} \\ &= \sum_{uv \in E(G)} \frac{(d_u + d_v)^2 - (d_u - d_v)^2}{2(d_u + d_v)} \\ &= \frac{1}{2} \sum_{uv \in E(G)} (d_u + d_v) - \sum_{uv \in E(G)} \frac{(d_u - d_v)^2}{2(d_u + d_v)} \tag{41} \\ &\leq \frac{1}{2} \sum_{uv \in E(G)} (d_u + d_v) - \sum_{uv \in E(G)} \frac{(d_u - d_v)^2}{4\Delta} \\ &= \frac{M_1(G)}{2} - \frac{\sigma(G)}{4\Delta}, \end{aligned}$$

and this implies the desired bound.

The general first F -index of a graph G is defined in [29] as

$$F_1^a(G) = \sum_{uv \in E(G)} (d_u^2 + d_v^2)^a, \tag{42}$$

where a is a real number. In particular, $F_1^1(G) = F(G)$.

Since for every two real numbers x and y , $(x - y)^2 \geq 0$, and we deduce that, for any graph G ,

$$\begin{aligned} F(G) &\geq 2M_2(G), \\ \sigma(G) &= F(G) - 2M_2(G). \end{aligned} \tag{43}$$

Using these and Theorem 9, we obtain the next result. \square

Corollary 6. *Let G be a nontrivial graph with maximum degree Δ . Then,*

$$GA(G) \leq \frac{M_1(G)}{2} - \frac{F(G) - 2M_2(G)}{4\Delta}. \tag{44}$$

From $F(G) \geq 2M_2(G)$, we would like to indicate that the above new bound improves the known bound:

$$GA(G) \leq \frac{M_1(G)}{2}, \tag{45}$$

which was established in [15].

Now, by using the following result, we want to obtain an upper bound for trees.

Theorem 10 (see [30]). *Let T be a tree of order n with independence number α . Then,*

$$M_1(T) \leq \alpha^2 - 3\alpha + 4n - 4. \tag{46}$$

Here, by Theorems 9 and 10, we obtain the next result.

Corollary 7. *Let T be a tree of order n with independence number α and maximum degree Δ . Then,*

$$GA(T) \leq \frac{\alpha^2 - 3\alpha + 4n - 4}{2} - \frac{\sigma(G)}{4\Delta}. \tag{47}$$

4. Lower Bounds for the Geometric-Arithmetic Index

In this section, we first investigate the relationships between the geometric-arithmetic index and some other topological indices, and then, we obtain some lower bounds for the geometric-arithmetic index which improve some well-known bounds.

Theorem 11. *Let G be a graph of size m with minimum degree δ . Then,*

$$GA(G) \geq \frac{4\delta^2 m^2}{HM(G)}. \tag{48}$$

Proof. By Lemmas 1 and 2, we have

$$\begin{aligned}
 \frac{m^2}{GA(G)} &= \frac{m^2}{\sum_{uv \in E(G)} \left(2\sqrt{d_u d_v} / (d_u + d_v) \right)} \\
 &\leq \sum_{uv \in E(G)} \frac{d_u + d_v}{2\sqrt{d_u d_v}} \\
 &\leq \sum_{uv \in E(G)} \frac{d_u + d_v}{(4d_u d_v / (d_u + d_v))} \\
 &= \sum_{uv \in E(G)} \frac{(d_u + d_v)^2}{4d_u d_v} \\
 &\leq \frac{1}{4\delta^2} \sum_{uv \in E(G)} (d_u + d_v)^2 \\
 &= \frac{HM(G)}{4\delta^2}.
 \end{aligned} \tag{49}$$

The result follows. \square

Here, by Theorems 11 and 6, we have the next result.

Corollary 8. *Let G be a graph of order n and size m , with minimum degree δ . Then,*

$$GA(G) \geq \frac{64n^2 \delta^2 (n-1)^2}{m(n+1)^6}. \tag{50}$$

Since for any real numbers x and y , it holds that $((x+y)^2/4) \leq ((x^2+y^2)/2)$; hence, by this fact and Inequality (49), we can obtain the following result.

Corollary 9. *Let G be a graph of size m with minimum degree δ . Then,*

$$GA(G) \geq \frac{2\delta^2 m^2}{F(G)}. \tag{51}$$

We start with a lower bound for the geometric-arithmetic index in terms of the general F -index.

Theorem 12. *Let G be a nontrivial graph of size m with minimum degree δ . Then,*

$$GA(G) \geq \frac{\sqrt{2}\delta m^2}{F_1^{1/2}(G)}. \tag{52}$$

Proof. Set $r = 1$, $a_{uv} = \sqrt[4]{2d_u d_v}$, and $b_{uv} = \sqrt{d_u^2 + d_v^2}$ for each $uv \in E(G)$. By Lemmas 1 and 3, we have

$$\begin{aligned}
 GA(G) &= \sum_{uv \in E(G)} \frac{2\sqrt{d_u d_v}}{d_u + d_v} \\
 &\geq \sum_{uv \in E(G)} \frac{2\sqrt{d_u d_v}}{2\sqrt{(d_u^2 + d_v^2)/2}} \\
 &= \sum_{uv \in E(G)} \frac{\sqrt{2d_u d_v}}{\sqrt{d_u^2 + d_v^2}} \\
 &= \sum_{uv \in E(G)} \frac{\left(\sqrt[4]{2d_u d_v} \right)^2}{\sqrt{d_u^2 + d_v^2}} \\
 &\geq \frac{\left(\sum_{uv \in E(G)} \sqrt[4]{2d_u d_v} \right)^2}{\sum_{uv \in E(G)} \sqrt{d_u^2 + d_v^2}} \\
 &\geq \frac{\sqrt{2}\delta m^2}{F_1^{1/2}(G)}.
 \end{aligned} \tag{53}$$

The proof is completed. \square

The harmonic index is defined as follows [11]:

$$H(G) = \sum_{uv \in E(G)} \frac{2}{d_u + d_v}. \tag{54}$$

Theorem 13. *Let G be a nontrivial graph of order n , size m , and minimum degree δ . Then,*

$$GA(G) \geq \delta(H(G) + n) - 2m. \tag{55}$$

Proof. Notice that

$$\begin{aligned}
 GA(G) + 2m &= \sum_{uv \in E(G)} \frac{2\sqrt{d_u d_v}}{d_u + d_v} + \sum_{u \in V(G)} d_u \\
 &\leq \sum_{uv \in E(G)} \frac{2\sqrt{d_u d_v}}{d_u + d_v} + \sum_{u \in V(G)} \delta \\
 &= \sum_{uv \in E(G)} \frac{2\sqrt{d_u d_v}}{d_u + d_v} + n\delta \\
 &\leq \delta H(G) + n\delta.
 \end{aligned} \tag{56}$$

The result follows. Applying (56), we obtain the next results. \square

Corollary 10. *Let G be a nontrivial graph of order n , size m , and minimum degree δ . Then,*

$$GA(G) \geq \frac{R_{1/2}(G)}{\Delta} + \delta n - 2m. \tag{57}$$

Corollary 11. Let G be a nontrivial graph of order n , size m , and minimum degree δ . Then,

$$GA(G) \geq \frac{\delta m}{\Delta} + \delta n - 2m. \tag{58}$$

Theorem 14 (see [31]). Let G be a connected graph of order $n \geq 3$. Then,

$$H(G) \geq \frac{2(n-1)}{n}. \tag{59}$$

A cut edge of a graph is an edge whose removal increases the number of connected components of the graph.

Lemma 10 (see [32]). Let G be a connected graph of order n and k' cut edges. Then,

$$m \leq \frac{(n-k')(n-k'-1)}{2} + k'. \tag{60}$$

Now, by Theorems 13 and 14, and Lemma 10, we can obtain the next result.

Corollary 12. Let G be a connected graph of order n , k' cut edges, and minimum degree δ . Then,

$$GA(G) \geq \delta \left(\frac{2(n-1)}{n} + n \right) - 2 \left(\frac{(n-k')(n-k'-1)}{2} + k' \right). \tag{61}$$

Here, we will use the following particular case of Jensen's inequality.

Lemma 11. Let $f(x)$ be a convex function defined in $x > 0$. For $x_1, x_2, \dots, x_m > 0$,

$$f\left(\frac{x_1 + x_2 + \dots + x_m}{m}\right) \leq \frac{1}{m} (f(x_1) + f(x_2) + \dots + f(x_m)). \tag{62}$$

The general sum-connectivity index is defined as follows [8]:

$$\chi_\alpha(G) = \sum_{uv \in E(G)} (d_u + d_v)^\alpha. \tag{63}$$

Now, we obtain a lower bound for the geometric-arithmetic index in terms of the general sum connectivity index.

Theorem 15. Let G be a graph of size m and minimum degree δ . Then,

$$GA(G) \geq \frac{4\delta^2 \sqrt{m^3}}{\sqrt{\chi_4(G)}}. \tag{64}$$

Proof. Since $f(x) = (1/x^2)$ is a convex function for $x > 0$, from Lemmas 1 and 11, we have

$$\begin{aligned} \left(\frac{m}{GA(G)}\right)^2 &= \left(\frac{m}{\sum_{uv \in E(G)} (2\sqrt{d_u d_v} / (d_u + d_v))}\right)^2 \\ &\leq \frac{1}{m} \sum_{uv \in E(G)} \left(\frac{d_u + d_v}{2\sqrt{d_u d_v}}\right)^2 \\ &\leq \frac{1}{m} \sum_{uv \in E(G)} \left(\frac{d_u + d_v}{(4d_u d_v / (d_u + d_v))}\right)^2 \\ &= \frac{1}{m} \sum_{uv \in E(G)} \left(\frac{(d_u + d_v)^2}{4d_u d_v}\right)^2 \\ &\leq \frac{1}{16m\delta^4} \sum_{uv \in E(G)} (d_u + d_v)^4 \\ &= \frac{\chi_4(G)}{16m\delta^4}, \end{aligned} \tag{65}$$

as desired. □

Now, we obtain an upper bound for the geometric-arithmetic index in terms of the sigma index.

Theorem 16. Let G be a simple connected graph of size m with maximum degree Δ , p pendent vertices, and minimum nonpendent vertex degree δ_1 . Then,

$$GA(G) \geq \frac{2p\sqrt{\Delta}}{1+\Delta} + \frac{\sqrt{4(m-p)^2 - (m-p/\delta_1^2)(\sigma(G) - p(\delta_1 - 1)^2)}}{\sqrt{(\Delta + \delta_1/2\sqrt{\Delta\delta_1}) + \sqrt{(2\sqrt{\Delta\delta_1}/\Delta + \delta_1)}}}. \tag{66}$$

Proof. We partition all the edges into two parts: pendent edges and nonpendent edges, so

$$GA(G) = \sum_{\substack{uv \in E(G) \\ d_u=1}} \frac{2\sqrt{d_v}}{1+d_v} + \sum_{\substack{uv \in E(G) \\ d_u, d_v \neq 1}} \frac{2\sqrt{d_u d_v}}{d_u + d_v}. \tag{67}$$

On one hand, for the pendent edges, it is not hard to check that $(2\sqrt{d_v}/(1+d_v))$ decreases in $2 \leq d_v \leq \Delta$; thus,

$$\sum_{\substack{uv \in E(G) \\ d_u=1}} \frac{2\sqrt{d_v}}{1+d_v} \geq \frac{2p\sqrt{\Delta}}{1+\Delta}. \tag{68}$$

Now, we consider the nonpendent edges. It is easy to see that the function $x + (1/x)$ gets its maximum value when x attains the maximum or minimum value. From $(\Delta/\delta) \geq (d_u/d_v) \geq (\delta/\Delta)$ for all u and $v \in V(G)$, we have

$$\sqrt{\frac{d_u}{d_v}} + \sqrt{\frac{d_v}{d_u}} \leq \sqrt{\frac{\Delta}{\delta}} + \sqrt{\frac{\delta}{\Delta}}, \tag{69}$$

which is equivalent to

$$\frac{2\sqrt{\Delta\delta_1}}{\Delta + \delta_1} \leq \frac{2\sqrt{d_u d_v}}{d_u + d_v} \leq 1. \tag{70}$$

Set $a_{uv} = 1$ and $b_{uv} = (2\sqrt{d_u d_v}/d_u + d_v)$ for each edge $uv \in E(G)$, $M_1 = m_1 = M_2 = 1$, and $m_2 = (2\sqrt{\Delta\delta_1}/\Delta + \delta_1)$ in Lemma 6, and we have

$$\begin{aligned} & \sum_{\substack{uv \in E(G) \\ d_v \neq 1}} 1^2 \sum_{\substack{uv \in E(G) \\ d_v \neq 1}} \left(\frac{2\sqrt{d_u d_v}}{d_u + d_v} \right)^2 \\ &= (m - p) \sum_{\substack{uv \in E(G) \\ d_v \neq 1}} \left(1 - \left(\frac{d_u - d_v}{d_u + d_v} \right)^2 \right) \\ &\leq \frac{1}{4} \left(\sqrt{\frac{1}{(2\sqrt{\Delta\delta_1}/\Delta + \delta_1)}} + \sqrt{\frac{2\sqrt{\Delta\delta_1}}{\Delta + \delta_1}} \right)^2 \left(\sum_{\substack{uv \in E(G) \\ d_v \neq 1}} \frac{2\sqrt{d_u d_v}}{d_u + d_v} \right)^2, \end{aligned} \tag{71}$$

which implies that

$$\begin{aligned} \sum_{\substack{uv \in E(G) \\ d_v \neq 1}} \frac{2\sqrt{d_u d_v}}{d_u + d_v} &\geq \frac{\sqrt{4(m - p) \sum_{\substack{uv \in E(G) \\ d_v \neq 1}} (1 - (d_u - d_v/d_u + d_v)^2)}}{\sqrt{(\Delta + \delta_1/2\sqrt{\Delta\delta_1})} + \sqrt{(2\sqrt{\Delta\delta_1}/\Delta + \delta_1)}} \\ &\geq \frac{\sqrt{4(m - p)^2 - (m - p/\delta_1^2) \sum_{\substack{uv \in E(G) \\ d_v \neq 1}} (d_u - d_v)^2}}{\sqrt{(\Delta + \delta_1/2\sqrt{\Delta\delta_1})} + \sqrt{(2\sqrt{\Delta\delta_1}/\Delta + \delta_1)}} \\ &= \frac{\sqrt{4(m - p)^2 - (m - p/\delta_1^2)(\sigma(G) - \sum_{uv \in E(G) d_u=1} (d_v - 1)^2)}}{\sqrt{(\Delta + \delta_1/2\sqrt{\Delta\delta_1})} + \sqrt{(2\sqrt{\Delta\delta_1}/\Delta + \delta_1)}} \\ &\geq \frac{\sqrt{4(m - p)^2 - (m - p/\delta_1^2)(\sigma(G) - p(\delta_1 - 1)^2)}}{\sqrt{(\Delta + \delta_1/2\sqrt{\Delta\delta_1})} + \sqrt{(2\sqrt{\Delta\delta_1}/\Delta + \delta_1)}}. \end{aligned} \tag{72}$$

Finally, the result follows from (67), (68), and (72).

Next, results are immediate consequences of Theorem 16 with the setting $p = 0$. \square

Corollary 13. For a graph G of size m with maximum degree Δ and minimum degree $\delta \geq 2$,

$$GA(G) \geq \frac{\sqrt{4m^2 - (m/\delta^2)\sigma(G)}}{\sqrt{(\Delta + \delta/2\sqrt{\Delta\delta})} + \sqrt{(2\sqrt{\Delta\delta}/\Delta + \delta)}} \tag{73}$$

Now, we obtain a lower bound for the geometric-arithmetic index in terms of the second Zagreb index and the general sum connectivity index.

Theorem 17. Let G be a graph of size m , maximum degree Δ , and minimum degree δ . Then,

$$GA(G) \geq \sqrt{4M_2(G)\chi_{-2}(G) - \frac{m^2}{4} \cdot \frac{\Delta^2 + \delta^2}{\Delta\delta}}. \tag{74}$$

Proof. By Lemma 5 and putting $a_{uv} = 2\sqrt{d_u d_v}$, $b_{uv} = (1/d_u + d_v)$, $m_1 = 2\delta$, $N_1 = 2\Delta$, $m_2 = (1/2\Delta)$, and $N_2 = (1/2\delta)$, we have

$$\sum_{i=1}^n 4d_u d_v \sum_{i=1}^n \frac{1}{(d_u + d_v)^2} - \left(\sum_{i=1}^n \frac{2\sqrt{d_u d_v}}{d_u + d_v} \right)^2 \leq \frac{m^2}{4} \cdot \frac{\Delta^2 + \delta^2}{\Delta\delta}. \tag{75}$$

This implies that

$$GA(G)^2 \geq 4M_2(G)\chi_{-2}(G) - \frac{m^2}{4} \cdot \frac{\Delta^2 + \delta^2}{\Delta\delta}. \tag{76}$$

The result follows.

Now, we obtain a lower bound for the geometric-arithmetic index in terms of the harmonic index. \square

Theorem 18. *Let G be a graph without isolated edges. Then,*

$$GA(G) \geq \sqrt{2}H(G). \tag{77}$$

Proof. Since for each $uv \in E(G)$, $d_u d_v \geq 2$, we obtain

$$GA(G) = \sum_{uv \in E(G)} \frac{2\sqrt{d_u d_v}}{d_u + d_v} \geq \sum_{uv \in E(G)} \frac{2\sqrt{2}}{d_u + d_v} = \sqrt{2}H(G), \tag{78}$$

as desired.

The proof of next results can be found in [33]. \square

Theorem 19 (see [33]). *Let G be a triangle-free graph of order n and the minimum degree $\delta \geq k$ ($k \leq (n/2)$). Then,*

$$H(G) \geq \frac{2k(n-k)}{n}. \tag{79}$$

Theorem 20 (see [33]). *Let G be a triangle-free graph of order n and size m . Then,*

$$H(G) \geq \frac{2m}{n}. \tag{80}$$

Applying Theorems 18–20, it leads to the next results.

Corollary 14. *Let G be a triangle-free graph of order n without isolated edges, and the minimum degree $\delta \geq k$ ($k \leq (n/2)$). Then,*

$$GA(G) \geq \frac{2\sqrt{2}k(n-k)}{n}, \tag{81}$$

$$GA(G) \geq \frac{2\sqrt{2}m}{n}. \tag{82}$$

We can see that Inequality (82) improves the next well-known result for triangle-free graphs [13]. Let G be a graph of order n and size m without isolated vertex. Then,

$$GA(G) \geq \frac{2m}{n}. \tag{83}$$

The eccentricity $\varepsilon(v)$ of v is defined as

$$\varepsilon(v) = \max\{d(v, w) : w \in V(G)\}, \tag{84}$$

where $d(v, w)$ is the length of a shortest path connecting v and w . The radius r and diameter D are defined as the minimum and maximum values among $\varepsilon(v)$ over all vertices $v \in V(G)$, respectively.

Xu [34] showed that, for any nontrivial connected graph G of order n , size m , and radius r , $H(G) \geq (m/n - r)$. Using this and Theorem 18, we obtain the next result.

Corollary 15. *Let G be a nontrivial connected graph of order n , size m , and radius r . Then,*

$$GA(G) \geq \frac{\sqrt{2}m}{n-r}. \tag{85}$$

Theorem 21. *Let G be a nontrivial connected graph of size m and radius r . Then,*

$$GA(G) \geq \frac{R_{1/2}(G)}{n-r}. \tag{86}$$

Proof. Note that, for each vertex $u \in V(G)$, we have $d_u \leq n - \varepsilon(u)$. Thus, for each edge $uv \in E(G)$,

$$\begin{aligned} GA(G) &= \sum_{uv \in E(G)} \frac{2\sqrt{d_u d_v}}{d_u + d_v} \geq \sum_{uv \in E(G)} \frac{2\sqrt{d_u d_v}}{2n - \varepsilon(u) - \varepsilon(v)} \\ &\geq \sum_{uv \in E(G)} \frac{2\sqrt{d_u d_v}}{2n - 2r} = \frac{R_{1/2}(G)}{n-r}, \end{aligned} \tag{87}$$

as desired. \square

Theorem 22. *Let G be a nontrivial graph of order n , size m , and p pendent edges without isolated vertex. Then,*

$$GA(G) \geq \frac{p}{\sqrt{n-1}} + \frac{m-p}{n-1-(p/2)}. \tag{88}$$

Proof. Since $0 < (1/d_u)$ and $(1/d_v) \leq 1$, therefore we deduce that

$$\begin{aligned} GA(G) &= \sum_{uv \in E(G)} \frac{2\sqrt{d_u d_v}}{d_u + d_v} \geq \sum_{uv \in E(G)} \frac{((1/d_u) + (1/d_v))\sqrt{d_u d_v}}{d_u + d_v} \\ &= \sum_{uv \in E(G)} \frac{1}{\sqrt{d_u d_v}} \end{aligned} \tag{89}$$

For each pendent edge $e = uv$, we clearly have $(1/\sqrt{d_u d_v}) \geq (1/\sqrt{n-1})$. If $e = uv$ is a nonpendent edge, then $d_u + d_v \leq 2(n-1) - p$, as any pendent vertex is adjacent to at most one of u and v . So, $\sqrt{d_u d_v} \leq (d_u + d_v/2) \leq n-1-(p/2)$; hence,

$$\frac{1}{\sqrt{d_u d_v}} \geq \frac{1}{n-1-(p/2)}. \tag{90}$$

Thus,

$$GA(G) \geq \frac{p}{\sqrt{n-1}} + \frac{m-p}{n-1-(p/2)}. \tag{91}$$

The desired result follows.

In [35], Kulli et al. defined the first and second generalized multiplicative Zagreb indices:

$$\begin{aligned} MZ_1^a(G) &= \prod_{uv \in E(G)} (d_u + d_v)^a, \\ MZ_2^a(G) &= \prod_{uv \in E(G)} (d_u d_v)^a. \end{aligned} \tag{92}$$

Here, we obtain a lower bound in terms of the first and second generalized multiplicative Zagreb indices. \square

Theorem 23. *Let G be a nontrivial graph of size m . Then,*

$$GA(G) \geq 2m \sqrt{\frac{MZ_2^{1/2}(G)}{MZ_1(G)}}. \tag{93}$$

Proof. By Lemma 2, we obtain

$$\begin{aligned} \frac{GA(G)}{2m} &= \frac{1}{m} \sum_{uv \in E(G)} \frac{\sqrt{d_u d_v}}{d_u + d_v} \\ &\geq \sqrt{\prod_{uv \in E(G)} \frac{\sqrt{d_u d_v}}{d_u + d_v}} \\ &= \sqrt[m]{\frac{\prod_{uv \in E(G)} \sqrt{d_u d_v}}{\prod_{uv \in E(G)} (d_u + d_v)}} = \sqrt[m]{\frac{MZ_2^{1/2}(G)}{MZ_1(G)}}, \end{aligned} \tag{94}$$

as desired. \square

Theorem 24. *Let G be a graph of size m and minimum degree δ . Then,*

$$GA(G) \geq \frac{4\delta^2 m^2}{HM(G)}. \tag{95}$$

Proof. By Lemma 1, we get

$$\begin{aligned} \frac{GA(G)}{2m} &= \frac{1}{m} \sum_{uv \in E(G)} \frac{\sqrt{d_u d_v}}{d_u + d_v} \\ &\geq \frac{1}{m} \sum_{uv \in E(G)} \frac{(2d_u d_v / (d_u + d_v))}{d_u + d_v} = \frac{1}{m} \sum_{uv \in E(G)} \frac{2d_u d_v}{(d_u + d_v)^2} \\ &\geq \frac{m}{\sum_{uv \in E(G)} ((d_u + d_v)^2 / 2d_u d_v)} \\ &\geq \frac{m}{(1/2\delta^2) \sum_{uv \in E(G)} (d_u + d_v)^2} \\ &= \frac{2\delta^2 m}{HM(G)}, \end{aligned} \tag{96}$$

as desired.

In the sequel, we obtain a lower bound in terms of the first Zagreb index. \square

Theorem 25. *Let G be a graph of size m , maximum degree Δ , and minimum degree δ . Then,*

$$GA(G) \geq \frac{\delta m}{\Delta} + 2m - \frac{M_1(G)}{\delta}. \tag{97}$$

Proof. By Lemma 8, we have

$$\begin{aligned} GA(G) + \frac{M_1(G)}{\delta} &\geq \sum_{uv \in E(G)} \left(\frac{2\sqrt{d_u d_v}}{d_u + d_v} + \frac{d_u + d_v}{\sqrt{d_u d_v}} \right) \\ &\geq \sum_{uv \in E(G)} \left(\frac{2\sqrt{d_u d_v}}{d_u + d_v} + 2 \right) \\ &= \sum_{uv \in E(G)} \frac{2\sqrt{d_u d_v}}{d_u + d_v} + \sum_{uv \in E(G)} 2 \\ &\geq \frac{\delta m}{\Delta} + 2m, \end{aligned} \tag{98}$$

and this implies the desired bound. \square

Zhou [36] proved that, for any triangle-free graph of order n and size m , $M_1(G) \leq mn$. Together with Theorem 25, we get the next result.

Corollary 16. *Let G be a triangle-free graph of order n , size m , maximum degree Δ , and minimum degree δ . Then,*

$$GA(G) \geq m \left(\frac{\delta}{\Delta} + 2 - \frac{n}{\delta} \right). \tag{99}$$

Inequality (98) leads to the following results.

Corollary 17. Let G be a graph of size m , maximum degree Δ , and minimum degree δ . Then,

$$GA(G) \geq \delta H(G) + 2m - \frac{M_1(G)}{\delta}, \tag{100}$$

$$GA(G) \geq \frac{R_{1/2}(G)}{\Delta} + 2m - \frac{M_1(G)}{\delta}.$$

Note that, for every two real numbers x and y , $((x + y)^2/xy) \geq 4$. Applying this, we obtain a lower bound for the geometric-arithmic index in terms of the hyper-Zagreb index.

Theorem 26. Let G be a graph of size m , maximum degree Δ , and minimum degree δ . Then,

$$GA(G) \geq \frac{\delta m}{\Delta} + 4m - \frac{HM(G)}{\delta^2}. \tag{101}$$

Proof. From the above inequality, we have

$$GA(G) + \frac{HM(G)}{\delta^2} \geq \sum_{uv \in E(G)} \left(\frac{2\sqrt{d_u d_v}}{d_u + d_v} + \frac{(d_u + d_v)^2}{d_u d_v} \right)$$

$$\geq \sum_{uv \in E(G)} \left(\frac{2\sqrt{d_u d_v}}{d_u + d_v} + 4 \right)$$

$$= \sum_{uv \in E(G)} \frac{2\sqrt{d_u d_v}}{d_u + d_v} + \sum_{uv \in E(G)} 4$$

$$\geq \frac{\delta m}{\Delta} + 4m, \tag{102}$$

and this implies the desired bound.

Here, we obtain a lower bound for the geometric-arithmic index in terms of the first Zagreb index. \square

Theorem 27. Let G be a graph of size m and minimum degree δ . Then,

$$GA(G) \geq 2m - \frac{M_1(G)}{2\delta}. \tag{103}$$

Proof. From the fact that $x + (1/x) \geq 2$ for any $x > 0$, we have

$$GA(G) + \frac{M_1(G)}{2\delta} \geq \sum_{uv \in E(G)} \left(\frac{2\sqrt{d_u d_v}}{d_u + d_v} + \frac{d_u + d_v}{2\sqrt{d_u d_v}} \right)$$

$$\geq \sum_{uv \in E(G)} 2 = 2m, \tag{104}$$

and this implies the desired bound. \square

Theorem 28 (see [37]). Let G be a graph of size m and diameter $D > 1$. Then,

$$M_1(G) \leq m^2 - m(D - 3) + (D - 2). \tag{105}$$

Now, by Theorems 27 and 28, we have the following result.

Corollary 18. Let G be a graph of size m , minimum degree δ , and diameter $D > 1$. Then,

$$GA(G) \geq 2m - \frac{m^2 - m(D - 3) + (D - 2)}{2\delta}. \tag{106}$$

Theorem 29 (see [38]). Let G be a graph of size m , with t triangles and pendent vertex p . Then,

$$M_1(G) \leq m(p + 2) + 3t. \tag{107}$$

Again, by Theorems 27 and 29, we have the following result.

Corollary 19. Let G be a graph of size m , with t triangles, leaf number L , and minimum degree δ . Then,

$$GA(G) \geq 2m - \frac{m(p + 2) + 3t}{2\delta}. \tag{108}$$

Theorem 30 (see [39]). Let G be a triangle- and quadrangle-free graph with $n > 1$ vertices. Then,

$$M_1(G) \leq n(n - 1). \tag{109}$$

Also, by Theorems 27 and 30, we have the following result.

Corollary 20. Let G be a triangle- and quadrangle-free graph of order n , size m , and minimum degree δ . Then,

$$GA(G) \geq 2m - \frac{n(n - 1)}{2\delta}. \tag{110}$$

Data Availability

The data used to support the findings of the study are provided within the article.

Conflicts of Interest

The authors declare that they have no conflicts of interests.

References

- [1] H. Wiener, "Structural determination of paraffin boiling points," *Journal of the American Chemical Society*, vol. 69, no. 1, pp. 17–20, 1947.
- [2] E. Estrada, L. Torres, L. Rodríguez, and I. Gutman, "An atom-bond connectivity index: modelling the enthalpy of formation of alkanes," *Indian Journal of Chemistry*, vol. 37A, pp. 849–855, 1998.

- [3] P. S. Ranjini, V. Loksha, M. Bindusree, and M. P. Raju, "New bounds on Zagreb indices and the Zagreb co-indices," *Boletim da Sociedade Paranaense de Matematica*, vol. 31, pp. 51–55, 2013.
- [4] H. Aram and N. Dehgardi, "Reformulated F -index of graph operations," *Communications in Combinatorics Optimization*, vol. 2, pp. 87–98, 2017.
- [5] I. Gutman, M. K. Jamil, and N. Akhter, "Graphs with fixed number of pendent vertices and minimal first Zagreb index," *Transactions on Combinatorics*, vol. 4, pp. 43–48, 2015.
- [6] I. Gutman and N. Trinajstić, "Graph theory and molecular orbitals. total π -electron energy of alternant hydrocarbons," *Chemical Physics Letters*, vol. 17, no. 4, pp. 535–538, 1972.
- [7] A. Ali, M. Javaid, M. Matejić, I. Milovanović, and E. Milovanović, "Some new bounds on the general sum-connectivity index," *Communications in Combinatorics and Optimization*, vol. 5, pp. 97–109, 2020.
- [8] B. Zhou and N. Trinajstić, "On general sum-connectivity index," *Journal of Mathematical Chemistry*, vol. 47, no. 1, pp. 210–218, 2010.
- [9] G. H. Shirdel, H. Rezapour, and A. M. Sayadi, "The hyper Zagreb index of graph operations," *Iranian Journal of Mathematical Chemistry*, vol. 4, pp. 213–220, 2013.
- [10] Z. Du, A. Jahanbai, and S. M. Sheikholeslami, "Relationships between randić index and other topological indices," *Communications in Combinatorics Optimization*, vol. 6, pp. 137–154, 2021.
- [11] S. Fajtlowicz, "On conjectures of grati-II," *Congruent Number*, vol. 60, pp. 187–197, 1987.
- [12] B. Furtula and I. Gutman, "A forgotten topological index," *Journal of Mathematical Chemistry*, vol. 53, no. 4, pp. 1184–1190, 2015.
- [13] D. Vukičević and B. Furtula, "Topological index based on the ratios of geometrical and arithmetical means of end-vertex degrees of edges," *Journal of Mathematical Chemistry*, vol. 46, pp. 1369–1376, 2009.
- [14] K. C. Das, I. Gutman, and B. Furtula, "Survey on geometric-arithmetic indices of graphs," *MATCH Communication in Mathematical and in Computer Chemistry*, vol. 65, pp. 595–644, 2011.
- [15] M. Mogharrab and G. H. Fath-Tabar, "Some bounds on GA_1 index of graph," *MATCH Communication in Mathematical and in Computer Chemistry*, vol. 65, pp. 33–38, 2011.
- [16] Y. Yuan, B. Zhou, and N. Trinajstić, "On geometric-arithmetic index," *Journal of Mathematical Chemistry*, vol. 47, no. 2, pp. 833–841, 2010.
- [17] I. J. Taneja, "Refinement of inequalities among means," *Journal of Combinatorics Information System Science*, vol. 31, pp. 343–364, 2006.
- [18] D. S. Bernstein, *Matrix Mathematics: Theory, Facts, and Formulas*, Princeton University Press, New Jersey, NY, USA, 2009.
- [19] J. Radon, "Theorie und anwendungen der absolut additiven mengenfunktionen," *Sitzungsber. Acad. Wissen. Wien*, vol. 122, pp. 1295–1438, 1913.
- [20] A. Lupas, "A remark on the schweitzer and kantorovich inequalities," *Univ. Beograd Publ. Elektrotehn. Fak. Ser. Mat. Fiz.*, vol. 381–409, pp. 13–15, 1972.
- [21] N. Ozeki, "On the estimation of inequalities by maximum and minimum values," *Journal College Arts Sciences*, vol. 5, pp. 199–203, 1968.
- [22] G. H. Hardy, J. E. Littlewood, and G. Pólya, *Inequalities*, Cambridge University Press, Cambridge, England, 1934.
- [23] B. Bollobás and P. Erdős, "Graphs of extremal weights," *Ars Combinatoria*, vol. 50, pp. 225–233, 1998.
- [24] B. Borovičanin and T. A. Lampert, "On the maximum and minimum Zagreb indices of trees with a given number of vertices of maximum degree," *MATCH Communication in Mathematical and in Computer Chemistry*, vol. 74, pp. 81–96, 2015.
- [25] K. C. Das and I. Gutman, "Some properties of the second Zagreb index," *MATCH Communication in Mathematical and in Computer Chemistry*, vol. 52, pp. 103–112, 2004.
- [26] S. Wang, W. Gao, M. K. Jamil, M. R. Farahani, and J. Liu, "Bounds of Zagreb indices and hyper Zagreb indices," *Mathematical Reports*, vol. 21, pp. 93–102, 2019.
- [27] P. S. Ranjini, V. Loksha, and A. Usha, "Relation between phenylene and hexagonal squeeze using harmonic index," *International Journal of Applied Graph Theory*, vol. 1, pp. 116–121, 2013.
- [28] I. Gutman, M. Togan, A. Yurttas, A. S. Cevik, and I. N. Cangul, "Inverse problem for sigma index," *MATCH Communication in Mathematical and in Computer Chemistry*, vol. 79, pp. 491–508, 2018.
- [29] V. R. Kulli, "F-indices of chemical networks," *International Journal of Mathematical Archive*, vol. 10, pp. 21–30, 2019.
- [30] K. C. Das, K. Xu, and I. Gutman, "On Zagreb and harary indices," *MATCH Communication in Mathematical and in Computer Chemistry*, vol. 70, pp. 301–314, 2013.
- [31] L. Zhong, "The harmonic index for graphs," *Applied Mathematics Letters*, vol. 25, no. 3, pp. 561–566, 2012.
- [32] A. Emanuela, T. Došlić, and A. Ali, "Two upper bounds on the weighted harary indices," *Discrete Mathematics Letters*, vol. 1, pp. 21–25, 2019.
- [33] J. Liu, "On the harmonic index of triangle-free graphs," *Applied Mathematics*, vol. 04, no. 08, pp. 1204–1206, 2013.
- [34] X. Xu, "Relationships between harmonic index and other topological indices," *Applied Mathematical Science*, vol. 6, pp. 2013–2018, 2012.
- [35] V. R. Kulli, B. Stone, S. Wang, and B. Wei, "Generalised multiplicative indices of polycyclic aromatic hydrocarbons and benzenoid systems," *Zeitschrift für Naturforschung A*, vol. 72, no. 6, pp. 573–576, 2017.
- [36] B. Zhou, "Zagreb indices," *MATCH Communication in Mathematical and in Computer Chemistry*, vol. 52, pp. 113–118, 2004.
- [37] B. Liu and I. Gutman, "Upper bounds for Zagreb indices of connected graphs," *MATCH Communication in Mathematical and in Computer Chemistry*, vol. 55, pp. 439–446, 2006.
- [38] M. J. Morgan and S. Mukwembi, "Bounds on the first Zagreb index, with applications," in *Topics in Chemical Graph Theory*, I. Gutman, Ed., pp. 215–228, University of Kragujevac, Kragujevac, Serbia, 2014.
- [39] B. Zhou and D. Stevanović, "A note on Zagreb indices," *MATCH Communication in Mathematical and in Computer Chemistry*, vol. 56, pp. 571–578, 2006.

Research Article

The Vertex-Edge Resolvability of Some Wheel-Related Graphs

Bao-Hua Xing,¹ Sunny Kumar Sharma ², Vijay Kumar Bhat ², Hassan Raza,³
and Jia-Bao Liu ⁴

¹School of Mathematics and Physics, Anqing Normal University, Anqing 246133, China

²School of Mathematics, Faculty of Sciences, Shri Mata Vaishno Devi University, Katra 182320, Jammu and Kashmir, India

³Business School, University of Shanghai for Science and Technology, Shanghai 200093, China

⁴School of Mathematics and Physics, Anhui Jianzhu University, Hefei 230601, China

Correspondence should be addressed to Vijay Kumar Bhat; vijaykumarbhat2000@yahoo.com

Received 22 May 2021; Accepted 27 June 2021; Published 14 July 2021

Academic Editor: Ali Ahmad

Copyright © 2021 Bao-Hua Xing et al. This is an open access article distributed under the Creative Commons Attribution License, which permits unrestricted use, distribution, and reproduction in any medium, provided the original work is properly cited.

A vertex $w \in V(H)$ distinguishes (or resolves) two elements (edges or vertices) $a, z \in V(H) \cup E(H)$ if $d(w, a) \neq d(w, z)$. A set W_m of vertices in a nontrivial connected graph H is said to be a mixed resolving set for H if every two different elements (edges and vertices) of H are distinguished by at least one vertex of W_m . The mixed resolving set with minimum cardinality in H is called the mixed metric dimension (vertex-edge resolvability) of H and denoted by $m \dim(H)$. The aim of this research is to determine the mixed metric dimension of some wheel graph subdivisions. We specifically analyze and compare the mixed metric, edge metric, and metric dimensions of the graphs obtained after the wheel graphs' spoke, cycle, and barycentric subdivisions. We also prove that the mixed resolving sets for some of these graphs are independent.

1. Introduction

Suppose $H = (V, E)$ is a nontrivial, simple, and connected graph, where E represents a set of edges and V represents a set of vertices. The distance between two vertices a and w in an undirected graph H , denoted by $d(a, w)$, is the length of a shortest $a - w$ path in H . In [1], Kelenc et al. introduced the concept of mixed metric dimension in graphs. This dimension of graph H is the mixture of metric and edge metric dimensions.

A vertex $w \in V$ is said to resolve two vertices v_1 and v_2 in H if $d(w, v_1) \neq d(w, v_2)$. Let w be a vertex and $W = \{v_1, v_2, v_3, \dots, v_p\}$ be an ordered subset of vertices in H . The metric coordinate (or metric representation) $r(w|W)$ of w with respect to W is the p -tuple $(d(w, v_1), d(w, v_2), d(w, v_3), \dots, d(w, v_p))$. Then, W is said to be a resolving set (or metric generator) for H if for every pair of vertices $v_1, v_2 \in V$ with $v_1 \neq v_2$, we have $r(v_1|W) \neq r(v_2|W)$. A resolving set with minimum cardinality is called the metric basis of H , and the cardinality of the metric basis set is the metric dimension $\dim(H)$ of H .

Slater introduced the idea of metric dimension in [2], where the metric generators were referred to as locating sets due to some relation with the problem of uniquely recognizing the location of intruders in networks. Harary and Melter, on the contrary, independently proposed the same concept of the metric dimension of a graph in [3], where metric generators were referred to as resolving sets. Several works on the applications and theoretical properties of this invariant have also been published. Metric dimension has various significant applications in computer science, mathematics, social sciences, chemical sciences, etc. [4–14]. There also exist some other variations of metric dimension in the literature: independent resolving sets [15], local metric dimension [16], solid metric dimension [11], fault-tolerant metric dimension [17], and so on.

The distance between an edge $e = ax$ and a vertex w is defined as $d(e, w) = d(ax, w) = \min\{d(a, w), d(x, w)\}$. A vertex $w \in V$ is said to resolve two edges e_1 and e_2 in H if $d(w, e_1) \neq d(w, e_2)$. Let e be an edge and $W_E = \{v_1, v_2, v_3, \dots, v_p\}$ be an ordered subset of vertices in H . The edge metric codes $r_E(e|W_E)$ of e with respect to W_E are the

p -tuple $(d(e, v_1), d(e, v_2), d(e, v_3), \dots, d(e, v_p))$. Then, W_E is said to be an edge resolving set for H if for every pair of edges $e_1, e_2 \in E$ with $e_1 \neq e_2$, we have $r_E(e_1|W_E) \neq r_E(e_2|W_E)$. An edge resolving set with minimum cardinality is called an edge metric basis for H , and the cardinality of this edge metric basis set is the edge metric dimension $\text{edim}(H)$ of H .

For a connected graph H , we see that every vertex of H is uniquely recognized by a resolving set W of H , and every edge of H is uniquely recognized by an edge resolving set W_E of H ; the natural question is as follows: whether every resolving set W is also an edge resolving set W_E for H and vice versa? Kelenc et al. in [18] proved that there exist some families of graphs for which the resolving set W is also an edge resolving set W_E , but in general, this is not true for every graph H . Similarly, for every graph H , the edge resolving set is not necessarily a resolving set for H .

Let us define a set of elements as $V \cup E$, i.e., each element is an edge or a vertex. A vertex $w \in V$ is said to resolve two elements a and z from $V \cup E$ if $d(w, a) \neq d(w, z)$. Let a be an element and $W_m = \{v_1, v_2, v_3, \dots, v_p\}$ be an ordered subset of vertices in H . The mixed metric codes $r_m(a|W_m)$ of a with respect to W_m are the p -tuple $(d(a, v_1), d(a, v_2), d(a, v_3), \dots, d(a, v_p))$. Then, W_m is said to be a mixed resolving set for H if for every pair of distinct elements $a_1, a_2 \in V \cup E$, we have $r_m(a_1|W_m) \neq r_m(a_2|W_m)$. A mixed resolving set with minimum cardinality is called a mixed metric basis for H , and the cardinality of this mixed metric basis set is the mixed metric dimension $\text{mdim}(H)$ of H . By the definition of the mixed metric dimension, it is clear that a mixed resolving set is both edge resolving set and a resolving set, so we have

$$\text{mdim}(H) \geq \max\{\text{edim}(H), \text{dim}(H)\}. \tag{1}$$

There are several studies [1, 19, 20] related to the mixed metric dimension of various graphs, for instance, cycle graphs, antiprism graphs, prism graphs, and convex polytopes, but there are many graphs for which the mixed metric dimension has not been found yet, such as the graphs obtained by some subdivisions of the wheel graph $W_{n,1}$. So, in this paper, we will compute the mixed metric dimension of the graphs obtained after the barycentric, spoke, and cycle subdivisions of the wheel graph $W_{n,1}$.

2. Preliminaries

In this section, we give the definition of a wheel and its related graphs, as well as recall some existing results on the edge metric dimension, and the metric dimension of wheel-related graphs.

2.1. Wheel Graph. A vertex u in an undirected graph G is said to be the universal vertex if it is adjacent to all other vertices of G . A wheel graph $W_{n,1}$ ($n \geq 3$) is a graph with $n + 1$ vertices obtained by joining a single universal vertex to all of the vertices of a cycle graph C_n . $W_{n,1}$ has a vertex set $V = \{v, k_1, k_2, k_3, \dots, k_n\}$ and an edge set $E = \{vk_j, k_jk_{j+1} \mid 1 \leq j \leq n\}$, where all of the indices are taken to be modulo n . The edges k_jk_{j+1} are called the cycle edges of $W_{n,1}$, and the edges vk_j are called as the spokes of the wheel graph.

We state that a family \mathcal{F} of nontrivial connected graphs has bounded mixed metric dimension if there exists a constant $L > 0$ for every graph H of \mathcal{F} such that $\text{mdim}(H) \leq L$; otherwise, \mathcal{F} has an unbounded mixed metric dimension. If all of the graphs in \mathcal{F} have the same mixed metric dimension, then \mathcal{F} is referred to as a family with a constant mixed metric dimension. Cycles C_n and paths P_n for $n \geq 3$ are the graph families with a constant mixed metric dimension.

2.2. Independent Mixed Resolving Set. A set W_m of vertices from H is said to be an independent mixed resolving set for H if W_m is an independent as well as mixed resolving set.

Let $WSS_{n,1}$, $WCS_{n,1}$, and $WBS_{n,1}$ be the graphs obtained from the wheel graph $W_{n,1}$ after spoke, cycle, and barycentric subdivisions of $W_{n,1}$, respectively. Recently, the metric and edge metric dimension for these three wheel-related graphs have been computed, and in [21], Raza and Bataineh made a comparison between the metric dimension and the edge metric dimension for these wheel-related graphs. The edge metric dimension and the metric dimension for these three graphs are as follows.

Proposition 1 (see [21]). $\text{edim}(WSS_{n,1}) = n - 1$, for $n \geq 6$.

Proposition 2 (see [21]). For $n \geq 6$, we have

$$\begin{aligned} \text{edim}(WCS_{n,1}) &= \text{edim}(WBS_{n,1}) \\ &= \begin{cases} 4h & \text{if } n = 6h \text{ or } n = 6h + 1, \\ 4h + 1 & \text{if } n = 6h + 2, \\ 4h + 2 & \text{if } n = 6h + 3 \text{ or } n = 6h + 4, \\ 4h + 3 & \text{if } n = 6h + 5. \end{cases} \end{aligned} \tag{2}$$

Proposition 3 (see [22]). $\text{dim}(WSS_{n,1}) = \lfloor 2n + 2/5 \rfloor$, for $n \geq 6$.

Proposition 4 (see [23, 22]). For $n \geq 6$, we have

$$\text{dim}(WCS_{n,1}) = \text{dim}(WBS_{n,1}) = \begin{cases} 4h & \text{if } n = 6h \text{ or } n = 6h + 1, \\ 4h + 1 & \text{if } n = 6h + 2, \\ 4h + 2 & \text{if } n = 6h + 3 \text{ or } n = 6h + 4, \\ 4h + 3 & \text{if } n = 6h + 5. \end{cases} \tag{3}$$

This article is organized as follows: in Section 3, we will study the mixed metric dimension of the spoke subdivision of the wheel graph $WSS_{n,1}$. In Sections 4 and 5, we will study the mixed metric dimension of the cycle and barycentric subdivision of the wheel graph, i.e., $WCS_{n,1}$ and $WBS_{n,1}$, respectively. We also give the comparative analysis for the mixed metric, edge metric, and metric dimension of the graphs obtained after the spoke, cycle, and barycentric subdivisions of the wheel graph. In Section 6, we conclude the obtained results.

3. Mixed Metric Dimension of the Spoke Subdivision of $W_{n,1}$

In this section, we determine the mixed metric dimension of the spoke subdivision of a wheel graph.

3.1. *Spoke Subdivision of $W_{n,1}$.* Suppose $W_{n,1}$ is a wheel graph with the vertex set $V(W_{n,1}) = \{k_1, k_2, k_3, \dots, k_n, v\}$ having a single universal vertex v . Now, each central spoke vk_j of $W_{n,1}$

is subdivided with a new vertex l_j . The resulting graph so obtained is known as the spoke subdivision wheel graph (SSWG) and is denoted by $WSS_{n,1}$. SSWG has $3n$ edges, $E(W_{n,1}) = \{vl_j, l_jk_j, k_jk_{j+1} | 1 \leq j \leq n\}$, and $2n + 1$ vertices, $V(W_{n,1}) = \{v, l_j, k_j | 1 \leq j \leq n\}$, where all indices are taken to be modulo n (see Figure 1). In this section, we obtain the mixed metric dimension of SSWG $WSS_{n,1}$.

Theorem 1. $mdim(WSS_{n,1}) = n$, for $n \geq 6$.

Proof. To prove that $mdim(WSS_{n,1}) \leq n$, we construct a mixed resolving set for $WSS_{n,1}$. Suppose $W_m = \{k_1, k_2, k_3, \dots, k_n\} \subseteq V(WSS_{n,1})$ having n cycle vertices from $WSS_{n,1}$. We claim that W_m is a mixed resolving set for $WSS_{n,1}$. Now, we can give mixed codes to each of the vertex and edge of $WSS_{n,1}$ with respect to W_m .

The sets of mixed metric codes for the vertices $\{v, l_j, k_j | 1 \leq j \leq n\}$ of $WSS_{n,1}$ are as follows:

$$\begin{aligned}
 A &= \left\{ r_m(v|W_m) = \underbrace{(2, 2, 2, \dots, 2)}_{n\text{-times}} \right\}, \\
 B &= \left\{ r_m(l_j|W_m) = \left(3, 3, \dots, 3, 2, \underbrace{1}_{j^{\text{th}}}, 2, 3, \dots, 3, 3 \right) | 1 \leq j \leq n \right\}, \\
 C &= \left\{ r_m(k_j|W_m) = \left(4, 4, \dots, 4, 3, 2, 1, \underbrace{0}_{j^{\text{th}}}, 1, 2, 3, 4, \dots, 4, 4 \right) | 1 \leq j \leq n \right\}.
 \end{aligned}
 \tag{4}$$

Next, the sets of mixed metric codes for the edges $\{vl_j, l_jk_j, k_jk_{j+1} | 1 \leq j \leq n\}$ of $WSS_{n,1}$ are as follows:

$$\begin{aligned}
 D &= \left\{ r_m(vl_j|W_m) = \left(2, 2, \dots, 2, \underbrace{1}_{j^{\text{th}}}, 2, \dots, 2, 2 \right) | 1 \leq j \leq n \right\}, \\
 E &= \left\{ r_m(l_jk_j|W_m) = \left(3, 3, \dots, 3, 2, 1, \underbrace{0}_{j^{\text{th}}}, 1, 2, 3, \dots, 3, 3 \right) | 1 \leq j \leq n \right\}, \\
 F &= \left\{ r_m(k_jk_{j+1}|W_m) = \left(4, 4, \dots, 4, 3, 2, 1, \underbrace{0}_{j^{\text{th}}}, 0, 1, 2, 3, 4, \dots, 4, 4 \right) | 1 \leq j \leq n \right\}.
 \end{aligned}
 \tag{5}$$

From these sets of mixed codes for $WSS_{n,1}$, we obtain that $|A| = 1$, $|B| = |C| = |D| = |E| = |F| = n$, and $A \cap B \cap C \cap D \cap E \cap F = \emptyset$, implying W_m to be a mixed resolving set for $WSS_{n,1}$, i.e., $mdim(WSS_{n,1}) \leq n$. Conversely, suppose, on the contrary, that there exists a mixed resolving set $W_m \subseteq WSS_{n,1}$ such that $|W_m| < n$. Then, we have the following cases to be considered:

Case (i): $v \notin W_m$. In this case, we further have two subcases:

Subcase (i): if $W_m \subset \{k_1, k_2, k_3, \dots, k_n\}$, then there exists at least one vertex k_j such that $k_j \notin W_m$. Then, for an edge vl_j and the vertex v , we have $r_m(vl_j|W_m) = r_m(v|W_m) = (2, 2, 2, \dots, 2)$, a contradiction. Therefore, the set W_m is not a mixed resolving set for $WSS_{n,1}$.

Subcase (ii): if $W_m \not\subseteq \{k_1, k_2, k_3, \dots, k_n\}$, then at least one vertex l_i belongs to the set W_m . Then, there exists one $k_j \notin W_m$, and the corresponding vertex $l_j \notin W_m$. Then, for an edge vl_j and the vertex v , we have

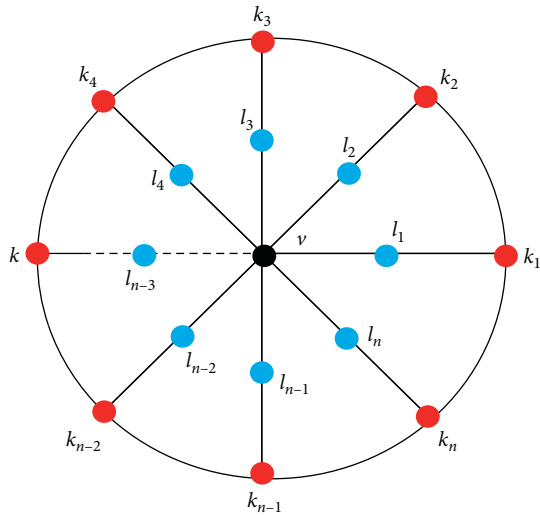


FIGURE 1: $WSS_{n,1}$.

$r_m(vl_j|W_m) = r_m(v|W_m)$, a contradiction. Therefore, again, in this case, the set W_m is not a mixed resolving set for $WSS_{n,1}$.

Case (ii): $v \in W_m$. In this case, we have two subcases:

Subcase (i): if $W_m \subset \{k_1, k_2, k_3, \dots, k_n\} \cup \{v\}$, then there exists at least one vertex k_j such that $k_j \notin W_m$. Then, clearly, for an edge vl_j and the vertex v , we have $r_m(vl_j|W_m) = r_m(v|W_m)$, a contradiction. Therefore, the set W_m is not a mixed resolving set for $WSS_{n,1}$.

Subcase (ii): if at least one l_j must belong to the set W_m , then there exists at least one vertex $k_j \notin W_m$, and the corresponding vertex $l_j \notin W_m$. Then, for an edge vl_j and a vertex v , we have $r_m(vl_j|W_m) = r_m(v|W_m)$, a contradiction. Therefore, again, in this case, the set W_m is not a mixed resolving set for $WSS_{n,1}$. Thus, in all the cases, we have $|W_m| \geq n$, implying $m\dim(WSS_{n,1}) = n$, which completes the proof of the theorem. $\square \square$

Remark 1. For the spoke subdivision wheel graph $H = WSS_{n,1}$, we find that $\dim(WSS_{n,1}) < edim(WSS_{n,1}) < m\dim(WSS_{n,1})$ (using Propositions 1 and 3 and Theorem 1). The comparison between these three dimensions of $WSS_{n,1}$ is clearly shown in Figure 2, and the value of each dimension depends on the number of vertices n in $WSS_{n,1}$.

4. Mixed Metric Dimension of the Cycle Subdivision of $W_{n,1}$

In this section, we determine the mixed metric dimension of the cycle subdivision of a wheel graph.

4.1. *Cycle Subdivision of $W_{n,1}$.* Suppose $W_{n,1}$ is a wheel graph with the vertex set $V(W_{n,1}) = \{k_1, k_2, k_3, \dots, k_n, v\}$ having a single universal vertex v . Now, each cycle edge k_jk_{j+1} of $W_{n,1}$ is subdivided with a new vertex l_j . The resulting graph so obtained is known as the cycle subdivision wheel graph (CSWG) and is denoted by $WCS_{n,1}$. CSWG has $3n$ edges, $E(WCS_{n,1}) = \{vk_j, k_jl_j, l_jk_{j+1} | 1 \leq j \leq n\}$, and $2n + 1$ vertices, $V(WCS_{n,1}) = \{v, l_j, k_j | 1 \leq j \leq n\}$, where all indices are taken to be modulo n (see Figure 3). In this section, we obtain the mixed metric dimension of CSWG $WCS_{n,1}$.

Theorem 2. For $n \geq 6$, we have

$$m\dim(WCS_{n,1}) = \begin{cases} 4h & \text{if } n = 6h, \\ 4h + 1 & \text{if } n = 6h + 1, \\ 4h + 2 & \text{if } n = 6h + 2, \\ 4h + 2 & \text{if } n = 6h + 3, \\ 4h + 3 & \text{if } n = 6h + 4, \\ 4h + 4 & \text{if } n = 6h + 5. \end{cases} \quad (6)$$

Proof. To prove this, we first generate the mixed resolving sets for all the cases, obtaining the upper bounds depending on the positive integer n . Then, in the end, we show that the lower bound (or reverse inequality) is the same as the upper bound to conclude the theorem.

Case (I): $n \equiv 0 \pmod{6}$. In this case, we have $n = 6h$, where $h \geq 2$ and $h \in \mathbb{N}$. Suppose an ordered subset $W_m = \{l_1, l_2, l_4, l_5, \dots, l_{n-2}, l_{n-1}\} = \{l_{3i+1}, l_{3i+2} | 0 \leq i \leq 2h - 1\}$ of vertices in $WCS_{n,1}$ with $|W_m| = 4h$. Next, we claim that W_m is the mixed resolving set for $WCS_{n,1}$. Now, we can give mixed codes to every vertex and edge of $WCS_{n,1}$ with respect to W_m . The sets of mixed metric codes for the vertices $\{u = v, l_j, k_j | 1 \leq j \leq n\}$ of $WCS_{n,1}$ are as follows:

$$A = \left\{ r_m(v|W_m) = \underbrace{(2, 2, 2, \dots, 2)}_{4h\text{-times}} \right\},$$

$$B = \left\{ \begin{aligned} & r_m(k_j|W_m) = (3, 3, 3, \dots, 3, d(l_{3i+2}, k_{3i+3}) = 1, 3, \dots, 3) \\ & j \equiv 0 \pmod{3} 0 \leq i \leq 2h - 1 \end{aligned} \right\} \cup$$

$$\left\{ \begin{aligned} & r_m(k_j|W_m) = (3, 3, 3, \dots, 3, d(l_{3i+1}, k_{3i+1}) = 1, 3, \dots, 3) \\ & j \equiv 1 \pmod{3} 0 \leq i \leq 2h - 1 \end{aligned} \right\} \cup$$

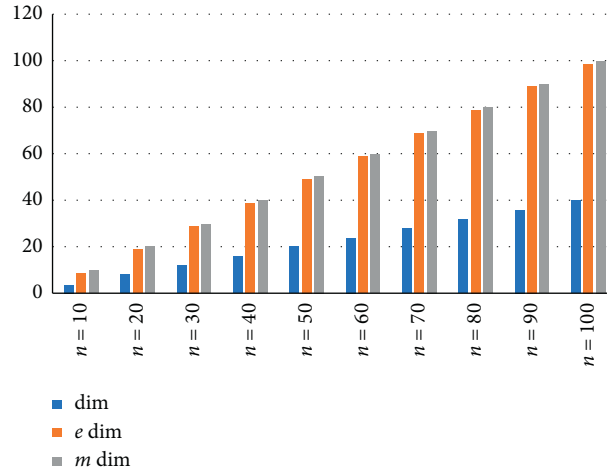
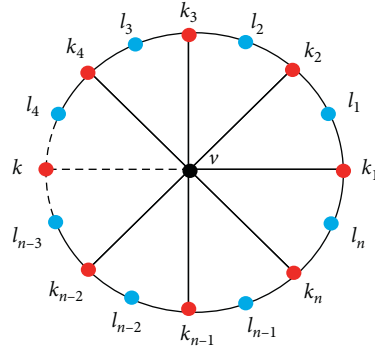


FIGURE 2: Comparison between $\dim(H)$, $\text{edim}(H)$, and $\text{mdim}(H)$.

$$C = \left\{ \begin{array}{l} r_m(k_j | W_m) = (3, 3, 3, \dots, 3, d(l_{3i+1}, k_{3i+2}) = 1, d(l_{3i+2}, k_{3i+2}) = 1, 3, \dots, 3) \mid \\ j \equiv 2 \pmod{3} 0 \leq i \leq 2h - 1 \end{array} \right\}, \\
 \left\{ \begin{array}{l} r_m(l_j | W_m) = (4, 4, 4, \dots, 4, d(l_{3i+2}, l_{3i+3}) = 2, d(l_{3i+4}, l_{3i+3}) = 2, 4, \dots, 4) \mid \\ j \equiv 0 \pmod{3} 0 \leq i \leq 2h - 1 \end{array} \right\} \cup \\
 \left\{ \begin{array}{l} r_m(l_j | W_m) = (4, 4, 4, \dots, 4, d(l_{3i+1}, l_{3i+1}) = 0, d(l_{3i+1}, l_{3i+2}) = 2, 4, \dots, 4) \mid \\ j \equiv 1 \pmod{3} 0 \leq i \leq 2h - 1 \end{array} \right\} \cup \\
 \left\{ \begin{array}{l} r_m(l_j | W_m) = (4, 4, 4, \dots, 4, d(l_{3i+1}, l_{3i+1}) = 2, d(l_{3i+1}, l_{3i+2}) = 0, 4, \dots, 4) \mid \\ j \equiv 2 \pmod{3} 0 \leq i \leq 2h - 1 \end{array} \right\}. \tag{7}$$

Next, the sets of mixed metric codes for the edges $\{vk_j, k_j l_j, l_j k_{j+1} \mid 1 \leq j \leq n\}$ of $\text{WCS}_{n,1}$ are as follows:

$$D = \{r_m(vk_j | W_m) = (2, 2, 2, \dots, 2, d(l_{3i+2}, vk_{3i+3}) = 1, 2, \dots, 2) \mid j \equiv 0 \pmod{3} \& 0 \leq i \leq 2h - 1\} \\
 \cup \{r_m(vk_j | W_m) = (2, 2, 2, \dots, 2, d(l_{3i+1}, vk_{3i+2}) = 1, 2, \dots, 2) \mid j \equiv 1 \pmod{3} \& 0 \leq i \leq 2h - 1\} \\
 \cup \{r_m(vk_j | W_m) = (2, 2, 2, \dots, 2, d(l_{3i+1}, vk_{3i+2}) = 1, d(l_{3i+2}, vk_{3i+2}) = 1, 2, \dots, 2) \mid j \equiv 2 \pmod{3} \& 0 \leq i \leq 2h - 1\}; \\
 E = \{r_m(k_j l_j | W_m) = (3, 3, 3, \dots, 3, d(l_{3i+2}, k_{3i+3} l_{3i+3}) = 1, d(l_{3i+4}, k_{3i+3} l_{3i+3}) = 2, 3, \dots, 3) \mid j \equiv 0 \pmod{3} \& 0 \leq i \leq 2h - 1\} \\
 \cup \{r_m(k_j l_j | W_m) = (3, 3, 3, \dots, 3, d(l_{3i+1}, k_{3i+1} l_{3i+1}) = 0, d(l_{3i+2}, k_{3i+1} l_{3i+1}) = 2, 3, \dots, 3) \mid j \equiv 1 \pmod{3} \& 0 \leq i \leq 2h - 1\} \\
 \cup \{r_m(k_j l_j | W_m) = (3, 3, 3, \dots, 3, d(l_{3i+1}, k_{3i+2} l_{3i+2}) = 1, d(l_{3i+2}, k_{3i+2} l_{3i+2}) = 0, 3, \dots, 3) \mid j \equiv 2 \pmod{3} \& 0 \leq i \leq 2h - 1\}; \\
 F = \{r_m(l_j k_{j+1} | W_m) = (3, 3, 3, \dots, 3, d(l_{3i+2}, l_{3i+3} k_{3i+4}) = 2, d(l_{3i+4}, l_{3i+3} k_{3i+4}) = 1, 3, \dots, 3) \mid j \equiv 0 \pmod{3} \& 0 \leq i \leq 2h - 1\} \\
 \cup \{r_m(l_j k_{j+1} | W_m) = (3, 3, 3, \dots, 3, d(l_{3i+1}, l_{3i+1} k_{3i+2}) = 0, d(l_{3i+2}, l_{3i+1} k_{3i+2}) = 1, 3, \dots, 3) \mid j \equiv 1 \pmod{3} \& 0 \leq i \leq 2h - 1\} \\
 \cup \{r_m(l_j k_{j+1} | W_m) = (3, 3, 3, \dots, 3, d(l_{3i+1}, l_{3i+2} k_{3i+3}) = 2, d(l_{3i+2}, l_{3i+2} k_{3i+3}) = 0, 3, \dots, 3) \mid j \equiv 2 \pmod{3} \& 0 \leq i \leq 2h - 1\}. \tag{8}$$

FIGURE 3: $WCS_{n,1}$.

From these sets of mixed codes for $WCS_{n,1}$, we obtain that $|A| = 1$, $|B| = |C| = |D| = |E| = |F| = n$, and $A \cap B \cap C \cap D \cap E \cap F = \emptyset$, implying W_m to be a mixed resolving set for $WCS_{n,1}$, i.e., $mdim(WCS_{n,1}) \leq 4h$. Next, using equation (1) and Proposition 2, we find that $mdim(WCS_{n,1}) = 4h$, in this case.

Case (II): $n \equiv 1 \pmod{6}$. In this case, we have $n = 6h + 1$, where $h \geq 2$ and $h \in \mathbb{N}$. Suppose an ordered

subset $W_m = \{l_1, l_2, l_4, l_5, \dots, l_{n-3}, l_{n-2}, l_n\} = \{l_{3i+1}, l_{3i+2} \mid 0 \leq i \leq 2h-1\} \cup \{l_n\}$ of vertices in $WCS_{n,1}$ with $|W_m| = 4h + 1$. Next, we claim that W_m is the mixed resolving set for $WCS_{n,1}$. Now, we can give mixed codes to every vertex and edge of $WCS_{n,1}$ with respect to W_m . The sets of mixed metric codes for the vertices $\{u = v, l_j, k_j \mid 1 \leq j \leq n\}$ of $WCS_{n,1}$ are as follows:

$$\begin{aligned}
 A &= \left\{ r_m(v|W_m) = \underbrace{(2, 2, 2, \dots, 2)}_{(4h+1)\text{-times}} \right\}; \\
 B &= \left\{ r_m(k_j|W_m) = (3, 3, 3, \dots, 3, d(l_{3i+2}, k_{3i+3}) = 1, 3, \dots, 3) \mid \right. \\
 &\quad \left. j \equiv 0 \pmod{3}, 0 \leq i \leq 2h-1 \right\} \cup \\
 &\quad \left\{ r_m(k_1|W_m) = \left(1, \underbrace{3, 3, \dots, 3}_{{(4h-1)\text{-times}}, 1} \right) \right\} \cup \\
 &\quad \left\{ r_m(k_j|W_m) = (3, 3, 3, \dots, 3, d(l_{3i+1}, k_{3i+1}) = 1, 3, \dots, 3) \mid \right. \\
 &\quad \left. j \equiv 1 \pmod{3}, 1 \leq i \leq 2h \right\} \cup \\
 &\quad \left\{ r_m(k_j|W_m) = (3, 3, 3, \dots, 3, d(l_{3i+1}, k_{3i+2}) = 1, d(l_{3i+2}, k_{3i+2}) = 1, 3, \dots, 3) \mid \right. \\
 &\quad \left. j \equiv 2 \pmod{3}, 0 \leq i \leq 2h-1 \right\}, \\
 C &= \left\{ r_m(l_j|W_m) = (4, 4, \dots, 4, d(l_{3i+2}, l_{3i+3}) = 2, d(l_{3i+4}, l_{3i+3}) = 2, 4, \dots, 4) \mid \right. \\
 &\quad \left. j \equiv 0 \pmod{3}, 0 \leq i \leq 2h-1 \right\} \cup
 \end{aligned}$$

$$\begin{aligned}
 & \left\{ r_m(l_1|W_m) = \left(0, 2, \underbrace{4, 4, 4, \dots, 4}_{(4h-2)\text{-times}}, 2 \right) \right\} \cup \\
 & \left\{ r_m(l_j|W_m) = (4, 4, 4, \dots, 4, d(l_{3i+1}, l_{3i+1}) = 0, d(l_{3i+1}, l_{3i+2}) = 2, 4, \dots, 4) \mid \right. \\
 & \qquad \qquad \qquad \left. j \equiv 1 \pmod{3} 1 \leq i \leq 2h \right\} \cup \\
 & \left\{ r_m(l_j|W_m) = (4, 4, 4, \dots, 4, d(l_{3i+1}, l_{3i+1}) = 2, d(l_{3i+1}, l_{3i+2}) = 0, 4, \dots, 4) \mid \right. \\
 & \qquad \qquad \qquad \left. j \equiv 2 \pmod{3} 0 \leq i \leq 2h - 1 \right\}. \tag{9}
 \end{aligned}$$

Next, the sets of mixed metric codes for the edges $\{vk_j, k_jl_j, l_jk_{j+1} \mid 1 \leq j \leq n\}$ of $WCS_{n,1}$ are as follows:

$$\begin{aligned}
 D = & \left\{ r_m(vk_j|W_m) = (2, 2, 2, \dots, 2, d(l_{3i+2}, vk_{3i+3}) = 1, 2, \dots, 2) \mid \right. \\
 & \qquad \qquad \qquad \left. j \equiv 0 \pmod{3} 0 \leq i \leq 2h - 1 \right\} \cup \\
 & \left\{ r_m(vk_1|W_m) = \left(1, \underbrace{2, 2, 2, \dots, 2}_{(4h-1)\text{-times}}, 1 \right) \right\} \cup \\
 & \left\{ r_m(vk_j|W_m) = (2, 2, 2, \dots, 2, d(l_{3i+1}, vk_{3i+1}) = 1, 2, \dots, 2) \mid \right. \\
 & \qquad \qquad \qquad \left. j \equiv 1 \pmod{3} 1 \leq i \leq 2h \right\} \cup \\
 & \left\{ r_m(vk_j|W_m) = (2, 2, 2, \dots, 2, d(l_{3i+1}, vk_{3i+2}) = 1, d(l_{3i+2}, vk_{3i+2}) = 1, 2, \dots, 2) \mid \right. \\
 & \qquad \qquad \qquad \left. j \equiv 2 \pmod{3} 0 \leq i \leq 2h - 1 \right\}, \\
 E = & \left\{ r_m(k_jl_j|W_m) = (3, 3, 3, \dots, 3, d(l_{3i+2}, k_{3i+3}l_{3i+3}) = 1, d(l_{3i+4}, k_{3i+3}l_{3i+3}) = 2, 3, \dots, 3) \mid \right. \\
 & \qquad \qquad \qquad \left. j \equiv 0 \pmod{3} 0 \leq i \leq 2h - 1 \right\} \cup \\
 & \left\{ r_m(k_1l_1|W_m) = \left(0, 2, \underbrace{3, 3, 3, \dots, 3}_{(4h-2)\text{-times}}, 1 \right) \right\} \cup \\
 & \left\{ r_m(k_jl_j|W_m) = (3, 3, 3, \dots, 3, d(l_{3i+1}, k_{3i+1}l_{3i+1}) = 0, d(l_{3i+2}, k_{3i+1}l_{3i+1}) = 2, 3, \dots, 3) \mid \right. \\
 & \qquad \qquad \qquad \left. j \equiv 1 \pmod{3} 1 \leq i \leq 2h \right\} \cup \\
 & \left\{ r_m(k_jl_j|W_m) = (3, 3, 3, \dots, 3, d(l_{3i+1}, k_{3i+2}l_{3i+2}) = 1, d(l_{3i+2}, k_{3i+2}l_{3i+2}) = 0, 3, \dots, 3) \mid \right. \\
 & \qquad \qquad \qquad \left. j \equiv 2 \pmod{3} 0 \leq i \leq 2h - 1 \right\}, \\
 F = & \left\{ r_m(l_jk_{j+1}|W_m) = (3, 3, 3, \dots, 3, d(l_{3i+2}, l_{3i+3}k_{3i+4}) = 2, d(l_{3i+4}, l_{3i+3}k_{3i+4}) = 1, 3, \dots, 3) \mid \right. \\
 & \qquad \qquad \qquad \left. j \equiv 0 \pmod{3} 0 \leq i \leq 2h - 1 \right\} \cup \\
 & \left\{ r_m(l_1k_2|W_m) = \left(0, 1, \underbrace{3, 3, 3, \dots, 3}_{(4h-2)\text{-times}}, 1 \right) \right\} \cup \\
 & \left\{ r_m(l_jk_{j+1}|W_m) = (3, 3, 3, \dots, 3, d(l_{3i+1}, l_{3i+1}k_{3i+2}) = 0, d(l_{3i+2}, l_{3i+1}k_{3i+2}) = 1, 3, \dots, 3) \mid \right. \\
 & \qquad \qquad \qquad \left. j \equiv 1 \pmod{3} 1 \leq i \leq 2h \right\} \cup \\
 & \left\{ r_m(l_jk_{j+1}|W_m) = (3, 3, 3, \dots, 3, d(l_{3i+1}, l_{3i+2}k_{3i+3}) = 2, d(l_{3i+2}, l_{3i+2}k_{3i+3}) = 0, 3, \dots, 3) \mid \right. \\
 & \qquad \qquad \qquad \left. j \equiv 2 \pmod{3} 0 \leq i \leq 2h - 1 \right\}. \tag{10}
 \end{aligned}$$

From these sets of mixed codes for $WCS_{n,1}$, we obtain that $|A| = 1$, $|B| = |C| = |D| = |E| = |F| = n$, and $A \cap B \cap C \cap D \cap E \cap F = \emptyset$, implying W_m to be a mixed resolving set for $WCS_{n,1}$, i.e., $m\dim(WCS_{n,1}) \leq 4h + 1$.
 Case (III): $n \equiv 2 \pmod{6}$. In this case, we have $n = 6h + 2$, where $h \geq 2$ and $h \in \mathbb{N}$. Suppose an ordered subset $W_m = \{l_1, l_2, l_4, l_5, l_7, \dots, l_{n-1}, l_n\} = \{l_{3i+1}, l_{3i+2} | 0$

$\leq i \leq 2h\}$ of vertices in $WCS_{n,1}$ with $|W_m| = 4h + 2$. Next, we claim that W_m is the mixed resolving set for $WCS_{n,1}$. Now, we can give mixed codes to every vertex and edge of $WCS_{n,1}$ with respect to W_m . The sets of mixed metric codes for the vertices $\{u = v, l_j, k_j | 1 \leq j \leq n\}$ of $WCS_{n,1}$ are as follows:

$$\begin{aligned}
 A &= \left\{ r_m(v|W_m) = \underbrace{(2, 2, 2, \dots, 2)}_{(4h+2)\text{-times}} \right\}, \\
 B &= \left\{ r_m(k_j|W_m) = (3, 3, 3, \dots, 3, d(l_{3i+2}, k_{3i+3}) = 1, 3, \dots, 3) \mid \right. \\
 &\quad \left. j \equiv 0 \pmod{3}, 0 \leq i \leq 2h - 1 \right\} \cup \\
 &\quad \left\{ r_m(k_1|W_m) = \left(1, \underbrace{3, 3, \dots, 3}_{(4h)\text{-times}}, 1 \right) \right\} \cup \\
 &\quad \left\{ r_m(k_j|W_m) = (3, 3, 3, \dots, 3, d(l_{3i+1}, k_{3i+1}) = 1, 3, \dots, 3) \mid \right. \\
 &\quad \left. j \equiv 1 \pmod{3}, 1 \leq i \leq 2h \right\} \cup \\
 &\quad \left\{ r_m(k_j|W_m) = (3, 3, 3, \dots, 3, d(l_{3i+1}, k_{3i+2}) = 1, d(l_{3i+2}, k_{3i+2}) = 1, 3, \dots, 3) \mid \right. \\
 &\quad \left. j \equiv 2 \pmod{3}, 0 \leq i \leq 2h \right\}, \tag{11} \\
 C &= \left\{ r_m(l_j|W_m) = (4, 4, 4, \dots, 4, d(l_{3i+2}, l_{3i+3}) = 2, d(l_{3i+4}, l_{3i+3}) = 2, 4, \dots, 4) \mid \right. \\
 &\quad \left. j \equiv 0 \pmod{3}, 0 \leq i \leq 2h - 1 \right\} \cup \\
 &\quad \left\{ r_m(l_1|W_m) = \left(0, 2, \underbrace{4, 4, 4, \dots, 4}_{(4h-1)\text{-times}}, 2 \right) \right\} \cup \\
 &\quad \left\{ r_m(l_j|W_m) = (4, 4, 4, \dots, 4, d(l_{3i+1}, l_{3i+1}) = 0, d(l_{3i+1}, l_{3i+2}) = 2, 4, \dots, 4) \mid \right. \\
 &\quad \left. j \equiv 1 \pmod{3}, 1 \leq i \leq 2h \right\} \cup \\
 &\quad \left\{ r_m(l_j|W_m) = (4, 4, 4, \dots, 4, d(l_{3i+1}, l_{3i+2}) = 2, d(l_{3i+2}, l_{3i+2}) = 0, 4, \dots, 4) \mid \right. \\
 &\quad \left. j \equiv 2 \pmod{3}, 0 \leq i \leq 2h \right\}.
 \end{aligned}$$

Next, the sets of mixed metric codes for the edges $\{vk_j, k_j l_j, l_j k_{j+1} | 1 \leq j \leq n\}$ of $WCS_{n,1}$ are as follows:

$$\begin{aligned}
 D &= \left\{ r_m(vk_j|W_m) = (2, 2, 2, \dots, 2, d(l_{3i+2}, vk_{3i+3}) = 1, 2, \dots, 2) \mid \right. \\
 &\quad \left. j \equiv 0 \pmod{3}, 0 \leq i \leq 2h - 1 \right\} \cup \\
 &\quad \left\{ r_m(vk_1|W_m) = \left(1, \underbrace{2, 2, 2, \dots, 2}_{(4h)\text{-times}}, 1 \right) \right\} \cup \\
 &\quad \left\{ r_m(vk_j|W_m) = (2, 2, 2, \dots, 2, d(l_{3i+1}, vk_{3i+1}) = 1, 2, \dots, 2) \mid \right. \\
 &\quad \left. j \equiv 1 \pmod{3}, 1 \leq i \leq 2h \right\} \cup
 \end{aligned}$$

$$\begin{aligned}
 E = & \left\{ r_m(vk_j|W_m) = (2, 2, 2, \dots, 2, d(l_{3i+1}, vk_{3i+2}) = 1, d(l_{3i+2}, vk_{3i+2}) = 1, 2, \dots, 2) \mid \right. \\
 & \left. j \equiv 2 \pmod{3} 0 \leq i \leq 2h \right\}, \\
 & \left\{ r_m(k_j l_j | W_m) = (3, 3, 3, \dots, 3, d(l_{3i+2}, k_{3i+3} l_{3i+3}) = 1, d(l_{3i+4}, k_{3i+3} l_{3i+3}) = 2, 3, \dots, 3) \mid \right. \\
 & \left. j \equiv 0 \pmod{3} 0 \leq i \leq 2h - 1 \right\} \cup \\
 & \left\{ r_m(k_1 l_1 | W_m) = \left(0, 2, \underbrace{3, 3, 3, \dots, 3}_{(4h-1)\text{-times}}, 1 \right) \right\} \cup \\
 & \left\{ r_m(k_j l_j | W_m) = (3, 3, 3, \dots, 3, d(l_{3i+1}, k_{3i+1} l_{3i+1}) = 0, d(l_{3i+2}, k_{3i+1} l_{3i+1}) = 2, 3, \dots, 3) \mid \right. \\
 & \left. j \equiv 1 \pmod{3} 1 \leq i \leq 2h \right\} \cup \\
 & \left\{ r_m(k_j l_j | W_m) = (3, 3, 3, \dots, 3, d(l_{3i+1}, k_{3i+2} l_{3i+2}) = 1, d(l_{3i+2}, k_{3i+2} l_{3i+2}) = 0, 3, \dots, 3) \mid \right. \\
 & \left. j \equiv 2 \pmod{3} 0 \leq i \leq 2h \right\}, \\
 F = & \left\{ r_m(l_j k_{j+1} | W_m) = (3, 3, 3, \dots, 3, d(l_{3i+2}, l_{3i+3} k_{3i+4}) = 2, d(l_{3i+4}, l_{3i+3} k_{3i+4}) = 1, 3, \dots, 3) \mid \right. \\
 & \left. j \equiv 0 \pmod{3} 0 \leq i \leq 2h - 1 \right\} \cup \\
 & \left\{ r_m(l_1 k_2 | W_m) = \left(0, 1, \underbrace{3, 3, 3, \dots, 3}_{(4h-1)\text{-times}}, 1 \right) \right\} \cup \\
 & \left\{ r_m(l_j k_{j+1} | W_m) = (3, 3, 3, \dots, 3, d(l_{3i+1}, l_{3i+1} k_{3i+2}) = 0, d(l_{3i+2}, l_{3i+1} k_{3i+2}) = 1, 3, \dots, 3) \mid \right. \\
 & \left. j \equiv 1 \pmod{3} 1 \leq i \leq 2h \right\} \cup \\
 & \left\{ r_m(l_j k_{j+1} | W_m) = (3, 3, 3, \dots, 3, d(l_{3i+1}, l_{3i+2} k_{3i+3}) = 2, d(l_{3i+2}, l_{3i+2} k_{3i+3}) = 0, 3, \dots, 3) \mid \right. \\
 & \left. j \equiv 2 \pmod{3} 0 \leq i \leq 2h \right\}. \tag{12}
 \end{aligned}$$

From these sets of mixed codes for $WCS_{n,1}$, we obtain that $|A| = 1$, $|B| = |C| = |D| = |E| = |F| = n$, and $A \cap B \cap C \cap D \cap E \cap F = \emptyset$, implying W_m to be a mixed resolving set for $WCS_{n,1}$, i.e., $mdim(WCS_{n,1}) \leq 4h + 2$. Case (IV): $n \equiv 3 \pmod{6}$. In this case, we have $n = 6h + 3$, where $h \geq 2$ and $h \in \mathbb{N}$. Suppose an ordered subset $W_m = \{l_1, l_2, l_4, l_5, l_7 \dots, l_{n-2}, l_{n-1}\} = \{l_{3i+1}, l_{3i+2}$

$0 \leq i \leq 2h\}$ of vertices in $WCS_{n,1}$ with $|W_m| = 4h + 2$. Next, we claim that W_m is the mixed resolving set for $WCS_{n,1}$. Now, we can give mixed codes to every vertex and edge of $WCS_{n,1}$ with respect to W_m . The sets of mixed metric codes for the vertices $\{u = v, l_j, k_j \mid 1 \leq j \leq n\}$ of $WCS_{n,1}$ are as follows:

$$\begin{aligned}
 A = & \left\{ r_m(v|W_m) = \underbrace{(2, 2, 2, \dots, 2)}_{(4h+2)\text{-times}} \right\}, \\
 B = & \left\{ r_m(k_j | W_m) = (3, 3, 3, \dots, 3, d(l_{3i+2}, k_{3i+3}) = 1, 3, \dots, 3) \mid \right. \\
 & \left. j \equiv 0 \pmod{3} 0 \leq i \leq 2h \right\} \cup \\
 & \left\{ r_m(k_j | W_m) = (3, 3, 3, \dots, 3, d(l_{3i+1}, k_{3i+1}) = 1, 3, \dots, 3) \mid \right. \\
 & \left. j \equiv 1 \pmod{3} 0 \leq i \leq 2h \right\} \cup \\
 & \left\{ r_m(k_j | W_m) = (3, 3, 3, \dots, 3, d(l_{3i+1}, k_{3i+2}) = 1, d(l_{3i+2}, k_{3i+2}) = 1, 3, \dots, 3) \mid \right. \\
 & \left. j \equiv 2 \pmod{3} 0 \leq i \leq 2h \right\}, \tag{13} \\
 C = & \left\{ r_m(l_j | W_m) = (4, 4, 4, \dots, 4, d(l_{3i+2}, l_{3i+3}) = 2, d(l_{3i+4}, l_{3i+3}) = 2, 4, \dots, 4) \mid \right. \\
 & \left. j \equiv 0 \pmod{3} 0 \leq i \leq 2h \right\} \cup \\
 & \left\{ r_m(l_j | W_m) = (4, 4, 4, \dots, 4, d(l_{3i+1}, l_{3i+1}) = 0, d(l_{3i+1}, l_{3i+2}) = 2, 4, \dots, 4) \mid \right. \\
 & \left. j \equiv 1 \pmod{3} 0 \leq i \leq 2h \right\} \cup \\
 & \left\{ r_m(l_j | W_m) = (4, 4, 4, \dots, 4, d(l_{3i+1}, l_{3i+2}) = 2, d(l_{3i+2}, l_{3i+2}) = 0, 4, \dots, 4) \mid \right. \\
 & \left. j \equiv 2 \pmod{3} 0 \leq i \leq 2h \right\}.
 \end{aligned}$$

Next, the sets of mixed metric codes for the edges $\{vk_j, k_jl_j, l_jk_{j+1} | 1 \leq j \leq n\}$ of $WCS_{n,1}$ are as follows:

$$\begin{aligned}
 D &= \{r_m(vk_j | W_m) = (2, 2, 2, \dots, 2, d(l_{3i+2}, vk_{3i+3}) = 1, 2, \dots, 2) | j \equiv 0 \pmod{3} \& 0 \leq i \leq 2h\} \\
 &\cup \{r_m(vk_j | W_m) = (2, 2, 2, \dots, 2, d(l_{3i+1}, vk_{3i+2}) = 1, 2, \dots, 2) | j \equiv 1 \pmod{3} \& 0 \leq i \leq 2h\} \\
 &\cup \{r_m(vk_j | W_m) = (2, 2, 2, \dots, 2, d(l_{3i+1}, vk_{3i+2}) = 1, d(l_{3i+2}, vk_{3i+2}) = 1, 2, \dots, 2) | j \equiv 2 \pmod{3} \& 0 \leq i \leq 2h\}; \\
 E &= \{r_m(k_jl_j | W_m) = (3, 3, 3, \dots, 3, d(l_{3i+2}, k_{3i+3}l_{3i+3}) = 1, d(l_{3i+4}, k_{3i+3}l_{3i+3}) = 2, 3, \dots, 3) | j \equiv 0 \pmod{3} \& 0 \leq i \leq 2h\} \\
 &\cup \{r_m(k_jl_j | W_m) = (3, 3, 3, \dots, 3, d(l_{3i+1}, k_{3i+1}l_{3i+1}) = 0, d(l_{3i+2}, k_{3i+1}l_{3i+1}) = 2, 3, \dots, 3) | j \equiv 1 \pmod{3} \& 0 \leq i \leq 2h\} \\
 &\cup \{r_m(k_jl_j | W_m) = (3, 3, 3, \dots, 3, d(l_{3i+1}, k_{3i+2}l_{3i+2}) = 1, d(l_{3i+2}, k_{3i+2}l_{3i+2}) = 0, 3, \dots, 3) | j \equiv 2 \pmod{3} \& 0 \leq i \leq 2h\}; \\
 F &= \{r_m(l_jk_{j+1} | W_m) = (3, 3, 3, \dots, 3, d(l_{3i+2}, l_{3i+3}k_{3i+4}) = 2, d(l_{3i+4}, l_{3i+3}k_{3i+4}) = 1, 3, \dots, 3) | j \equiv 0 \pmod{3} \& 0 \leq i \leq 2h\} \\
 &\cup \{r_m(l_jk_{j+1} | W_m) = (3, 3, 3, \dots, 3, d(l_{3i+1}, l_{3i+1}k_{3i+2}) = 0, d(l_{3i+2}, l_{3i+1}k_{3i+2}) = 1, 3, \dots, 3) | j \equiv 1 \pmod{3} \& 0 \leq i \leq 2h\}. \\
 &\cup \{r_m(l_jk_{j+1} | W_m) = (3, 3, 3, \dots, 3, d(l_{3i+1}, l_{3i+2}k_{3i+3}) = 2, d(l_{3i+2}, l_{3i+2}k_{3i+3}) = 0, 3, \dots, 3) | j \equiv 2 \pmod{3} \& 0 \leq i \leq 2h\};
 \end{aligned}
 \tag{14}$$

From these sets of mixed codes for $WCS_{n,1}$, we obtain that $|A| = 1$, $|B| = |C| = |D| = |E| = |F| = n$, and $A \cap B \cap C \cap D \cap E \cap F = \emptyset$, implying W_m to be a mixed resolving set for $WCS_{n,1}$, i.e., $mdim(WCS_{n,1}) \leq 4h + 2$. Next, using equation (1) and Proposition 2, we find that $mdim(WCS_{n,1}) = 4h + 2$, in this case.

Case (V): $n \equiv 4 \pmod{6}$. In this case, we have $n = 6h + 4$, where $h \geq 2$ and $h \in \mathbb{N}$. Suppose an ordered

subset $W_m = \{l_1, l_2, l_4, l_5, \dots, l_{n-3}, l_{n-2}, l_n\} = \{l_{3i+1}, l_{3i+2} | 0 \leq i \leq 2h\} \cup \{l_n\}$ of vertices in $WCS_{n,1}$ with $|W_m| = 4h + 3$. Next, we claim that W_m is the mixed resolving set for $WCS_{n,1}$. Now, we can give mixed codes to every vertex and edge of $WCS_{n,1}$ with respect to W_m . The sets of mixed metric codes for the vertices $\{u = v, l_j, k_j | 1 \leq j \leq n\}$ of $WCS_{n,1}$ are as follows:

$$\begin{aligned}
 A &= \left\{ r_m(v|W_m) = \underbrace{(2, 2, 2, \dots, 2)}_{(4h+3)\text{-times}} \right\}, \\
 B &= \left\{ r_m(k_j|W_m) = (3, 3, 3, \dots, 3, d(l_{3i+2}, k_{3i+3}) = 1, 3, \dots, 3) \mid \right. \\
 &\quad \left. j \equiv 0 \pmod{3} 0 \leq i \leq 2h \right\} \cup \\
 &\quad \left\{ r_m(k_1|W_m) = \left(1, \underbrace{3, 3, \dots, 3}_{{(4h+1)\text{-times}}, 1} \right) \right\} \cup \\
 &\quad \{r_m(k_j|W_m) = (3, 3, 3, \dots, 3, d(l_{3i+1}, k_{3i+1}) = 1, 3, \dots, 3) | j \equiv 1 \pmod{3} 1 \leq i \leq 2h + 1\} \cup \\
 &\quad \left\{ r_m(k_j|W_m) = (3, 3, 3, \dots, 3, d(l_{3i+1}, k_{3i+2}) = 1, d(l_{3i+2}, k_{3i+2}) = 1, 3, \dots, 3) \mid \right. \\
 &\quad \left. j \equiv 2 \pmod{3} 0 \leq i \leq 2h + 1 \right\},
 \end{aligned}$$

$$\begin{aligned}
C = & \left\{ r_m(l_j|W_m) = (4, 4, \dots, 4, d(l_{3i+2}, l_{3i+3}) = 2, d(l_{3i+4}, l_{3i+3}) = 2, 4, \dots, 4) \mid \right. \\
& \left. j \equiv 0 \pmod{3} 0 \leq i \leq 2h \right\} \\
\cup & \left\{ r_m(l_1|W_m) = \left(0, 2, \underbrace{4, 4, 4, \dots, 4}_{(4h)\text{-times}}, 2 \right) \right\} \cup \\
& \left\{ r_m(l_j|W_m) = (4, 4, 4, \dots, 4, d(l_{3i+1}, l_{3i+1}) = 0, d(l_{3i+1}, l_{3i+2}) = 2, 4, \dots, 4) \mid \right. \\
& \left. j \equiv 1 \pmod{3} 1 \leq i \leq 2h + 1 \right\} \cup \\
& \left\{ r_m(l_j|W_m) = (4, 4, 4, \dots, 4, d(l_{3i+1}, l_{3i+1}) = 2, d(l_{3i+1}, l_{3i+2}) = 0, 4, \dots, 4) \mid \right. \\
& \left. j \equiv 2 \pmod{3} 0 \leq i \leq 2h + 1 \right\}.
\end{aligned} \tag{15}$$

Next, the sets of mixed metric codes for the edges $\{vk_j, k_j l_j, l_j k_{j+1} \mid 1 \leq j \leq n\}$ of $WCS_{n,1}$ are as follows:

$$\begin{aligned}
D = & \left\{ r_m(vk_j|W_m) = (2, 2, 2, \dots, 2, d(l_{3i+2}, vk_{3i+3}) = 1, 2, \dots, 2) \mid \right. \\
& \left. j \equiv 0 \pmod{3} 0 \leq i \leq 2h \right\} \cup \\
& \left\{ r_m(vk_1|W_m) = \left(1, \underbrace{2, 2, 2, \dots, 2}_{(4h+1)\text{-times}}, 1 \right) \right\} \cup \\
& \left\{ r_m(vk_j|W_m) = (2, 2, 2, \dots, 2, d(l_{3i+1}, vk_{3i+1}) = 1, 2, \dots, 2) \mid \right. \\
& \left. j \equiv 1 \pmod{3} 1 \leq i \leq 2h + 1 \right\} \cup \\
& \left\{ r_m(vk_j|W_m) = (2, 2, 2, \dots, 2, d(l_{3i+1}, vk_{3i+2}) = 1, d(l_{3i+2}, vk_{3i+2}) = 1, 2, \dots, 2) \mid \right. \\
& \left. j \equiv 2 \pmod{3} 0 \leq i \leq 2h \right\}, \\
E = & \left\{ r_m(k_j l_j|W_m) = (3, 3, 3, \dots, 3, d(l_{3i+2}, k_{3i+3} l_{3i+3}) = 1, d(l_{3i+4}, k_{3i+3} l_{3i+3}) = 2, 3, \dots, 3) \mid \right. \\
& \left. j \equiv 0 \pmod{3} 0 \leq i \leq 2h \right\} \cup \\
& \left\{ r_m(k_1 l_1|W_m) = \left(0, 2, \underbrace{3, 3, 3, \dots, 3}_{(4h)\text{-times}}, 1 \right) \right\} \cup \\
& \left\{ r_m(k_j l_j|W_m) = (3, 3, 3, \dots, 3, d(l_{3i+1}, k_{3i+1} l_{3i+1}) = 0, d(l_{3i+2}, k_{3i+1} l_{3i+1}) = 2, 3, \dots, 3) \mid \right. \\
& \left. j \equiv 1 \pmod{3} 1 \leq i \leq 2h + 1 \right\} \cup \\
& \left\{ r_m(k_j l_j|W_m) = (3, 3, 3, \dots, 3, d(l_{3i+1}, k_{3i+2} l_{3i+2}) = 1, d(l_{3i+2}, k_{3i+2} l_{3i+2}) = 0, 3, \dots, 3) \mid \right. \\
& \left. j \equiv 2 \pmod{3} 0 \leq i \leq 2h + 1 \right\}, \\
F = & \left\{ r_m(l_j k_{j+1}|W_m) = (3, 3, 3, \dots, 3, d(l_{3i+2}, l_{3i+3} k_{3i+4}) = 2, d(l_{3i+4}, l_{3i+3} k_{3i+4}) = 1, 3, \dots, 3) \mid \right. \\
& \left. j \equiv 0 \pmod{3} 0 \leq i \leq 2h \right\} \cup \\
& \left\{ r_m(l_1 k_2|W_m) = \left(0, 1, \underbrace{3, 3, 3, \dots, 3}_{(4h)\text{-times}}, 1 \right) \right\} \cup \\
& \left\{ r_m(l_j k_{j+1}|W_m) = (3, 3, 3, \dots, 3, d(l_{3i+1}, l_{3i+1} k_{3i+2}) = 0, d(l_{3i+2}, l_{3i+1} k_{3i+2}) = 1, 3, \dots, 3) \mid \right. \\
& \left. j \equiv 1 \pmod{3} 1 \leq i \leq 2h + 1 \right\} \cup \\
& \left\{ r_m(l_j k_{j+1}|W_m) = (3, 3, 3, \dots, 3, d(l_{3i+1}, l_{3i+2} k_{3i+3}) = 2, d(l_{3i+2}, l_{3i+2} k_{3i+3}) = 0, 3, \dots, 3) \mid \right. \\
& \left. j \equiv 2 \pmod{3} 0 \leq i \leq 2h \right\}.
\end{aligned} \tag{16}$$

From these sets of mixed codes for $WCS_{n,1}$, we obtain that $|A| = 1, |B| = |C| = |D| = |E| = |F| = n$, and $A \cap B \cap C \cap D \cap E \cap F = \emptyset$, implying W_m to be a mixed resolving set for $WCS_{n,1}$, i.e., $mdim(WCS_{n,1}) \leq 4h + 3$.

Case (VI): $n \equiv 5 \pmod{6}$. In this case, we have $n = 6h + 5$, where $h \geq 1$ and $h \in \mathbb{N}$. Suppose an ordered

subset $W_m = \{l_1, l_2, l_4, l_5, \dots, l_{n-1}, l_n\} = \{l_{3i+1}, l_{3i+2} \mid 0 \leq i \leq 2h + 1\}$ of vertices in $WCS_{n,1}$ with $|W_m| = 4h + 4$. Next, we claim that W_m is the mixed resolving set for $WCS_{n,1}$. Now, we can give mixed codes to every vertex and edge of $WCS_{n,1}$ with respect to W_m . The sets of mixed metric codes for the vertices $\{u = v, l_j, k_j \mid 1 \leq j \leq n\}$ of $WCS_{n,1}$ are as follows:

$$\begin{aligned}
 A &= \left\{ r_m(v|W_m) = \underbrace{(2, 2, 2, \dots, 2)}_{(4h+4)\text{-times}} \right\}, \\
 B &= \left\{ r_m(k_j|W_m) = (3, 3, 3, \dots, 3, d(l_{3i+2}, k_{3i+3}) = 1, 3, \dots, 3) \mid \right. \\
 &\quad \left. j \equiv 0 \pmod{3} 0 \leq i \leq 2h \right\} \cup \\
 &\quad \left\{ r_m(k_1|W_m) = \left(\underbrace{1, 3, 3, \dots, 3, 1}_{(4h+2)\text{-times}} \right) \right\} \cup \\
 &\quad \left\{ r_m(k_j|W_m) = (3, 3, 3, \dots, 3, d(l_{3i+1}, k_{3i+1}) = 1, 3, \dots, 3) \mid \right. \\
 &\quad \left. j \equiv 1 \pmod{3} 1 \leq i \leq 2h + 1 \right\} \cup \\
 &\quad \left. \left\{ r_m(k_j|W_m) = (3, 3, 3, \dots, 3, d(l_{3i+1}, k_{3i+2}) = 1, d(l_{3i+2}, k_{3i+2}) = 1, 3, \dots, 3) \mid \right. \right. \\
 &\quad \left. \left. j \equiv 2 \pmod{3} 0 \leq i \leq 2h + 1 \right\} \right\}, \\
 C &= \left\{ r_m(l_j|W_m) = (4, 4, \dots, 4, d(l_{3i+2}, l_{3i+3}) = 2, d(l_{3i+4}, l_{3i+3}) = 2, 4, \dots, 4) \mid \right. \\
 &\quad \left. j \equiv 0 \pmod{3} 0 \leq i \leq 2h \right\} \cup \\
 &\quad \left\{ r_m(l_1|W_m) = \left(\underbrace{0, 2, 4, 4, 4, \dots, 4, 2}_{(4h+1)\text{-times}} \right) \right\} \cup \\
 &\quad \left\{ r_m(l_j|W_m) = (4, 4, 4, \dots, 4, d(l_{3i+1}, l_{3i+1}) = 0, d(l_{3i+1}, l_{3i+2}) = 2, 4, \dots, 4) \mid \right. \\
 &\quad \left. j \equiv 1 \pmod{3} 1 \leq i \leq 2h + 1 \right\} \cup \\
 &\quad \left. \left\{ r_m(l_j|W_m) = (4, 4, 4, \dots, 4, d(l_{3i+1}, l_{3i+2}) = 2, d(l_{3i+2}, l_{3i+2}) = 0, 4, \dots, 4) \mid \right. \right. \\
 &\quad \left. \left. j \equiv 2 \pmod{3} 0 \leq i \leq 2h + 1 \right\} \right\}.
 \end{aligned} \tag{17}$$

Next, the sets of mixed metric codes for the edges $\{vk_j, k_jl_j, l_jk_{j+1} \mid 1 \leq j \leq n\}$ of $WCS_{n,1}$ are as follows:

$$\begin{aligned}
 D &= \left\{ r_m(vk_j|W_m) = (2, 2, 2, \dots, 2, d(l_{3i+2}, vk_{3i+3}) = 1, 2, \dots, 2) \mid \right. \\
 &\quad \left. j \equiv 0 \pmod{3} 0 \leq i \leq 2h \right\} \cup \\
 &\quad \left\{ r_m(vk_1|W_m) = \left(\underbrace{1, 2, 2, 2, \dots, 2, 1}_{(4h+2)\text{-times}} \right) \right\} \cup \\
 &\quad \left\{ r_m(vk_j|W_m) = (2, 2, 2, \dots, 2, d(l_{3i+1}, vk_{3i+1}) = 1, 2, \dots, 2) \mid \right. \\
 &\quad \left. j \equiv 1 \pmod{3} 1 \leq i \leq 2h + 1 \right\} \cup \\
 &\quad \left\{ r_m(vk_j|W_m) = (2, 2, 2, \dots, 2, d(l_{3i+1}, vk_{3i+2}) = 1, d(l_{3i+2}, vk_{3i+2}) = 1, 2, \dots, 2) \mid \right. \\
 &\quad \left. j \equiv 2 \pmod{3} 0 \leq i \leq 2h + 1 \right\}, \\
 E &= \left\{ r_m(k_jl_j|W_m) = (3, 3, 3, \dots, 3, d(l_{3i+2}, k_{3i+3}l_{3i+3}) = 1, d(l_{3i+4}, k_{3i+3}l_{3i+3}) = 2, 3, \dots, 3) \mid \right. \\
 &\quad \left. j \equiv 0 \pmod{3} 0 \leq i \leq 2h \right\} \cup
 \end{aligned}$$

$$\begin{aligned}
 F = & \left\{ r_m(k_1 l_1 | W_m) = \left(0, 2, \underbrace{3, 3, 3, \dots, 3}_{(4h+1)\text{-times}}, 1 \right) \right\} \cup \\
 & \left\{ r_m(k_j l_j | W_m) = (3, 3, 3, \dots, 3, d(l_{3i+1}, k_{3i+1} l_{3i+1}) = 0, d(l_{3i+2}, k_{3i+1} l_{3i+1}) = 2, 3, \dots, 3) \mid \right. \\
 & \left. j \equiv 1 \pmod{3} 1 \leq i \leq 2h + 1 \right\} \cup \\
 & \left\{ r_m(k_j l_j | W_m) = (3, 3, 3, \dots, 3, d(l_{3i+1}, k_{3i+2} l_{3i+2}) = 1, d(l_{3i+2}, k_{3i+2} l_{3i+2}) = 0, 3, \dots, 3) \mid \right. \\
 & \left. j \equiv 2 \pmod{3} 0 \leq i \leq 2h + 1 \right\}, \\
 & \left\{ r_m(l_j k_{j+1} | W_m) = (3, 3, 3, \dots, 3, d(l_{3i+2}, l_{3i+3} k_{3i+4}) = 2, d(l_{3i+4}, l_{3i+3} k_{3i+4}) = 1, 3, \dots, 3) \mid \right. \\
 & \left. j \equiv 0 \pmod{3} 0 \leq i \leq 2h \right\} \cup \\
 & \left\{ r_m(l_1 k_2 | W_m) = \left(0, 1, \underbrace{3, 3, 3, \dots, 3}_{(4h+1)\text{-times}}, 2 \right) \right\} \cup \\
 & \left\{ r_m(l_j k_{j+1} | W_m) = (3, 3, 3, \dots, 3, d(l_{3i+1}, l_{3i+1} k_{3i+2}) = 0, d(l_{3i+2}, l_{3i+1} k_{3i+2}) = 1, 3, \dots, 3) \mid \right. \\
 & \left. j \equiv 1 \pmod{3} 1 \leq i \leq 2h + 1 \right\} \cup \\
 & \left\{ r_m(l_j k_{j+1} | W_m) = (3, 3, 3, \dots, 3, d(l_{3i+1}, l_{3i+2} k_{3i+3}) = 2, d(l_{3i+2}, l_{3i+2} k_{3i+3}) = 0, 3, \dots, 3) \mid \right. \\
 & \left. j \equiv 2 \pmod{3} 0 \leq i \leq 2h + 1 \right\}. \tag{18}
 \end{aligned}$$

From these sets of mixed codes for $WCS_{n,1}$, we obtain that $|A| = 1, |B| = |C| = |D| = |E| = |F| = n$, and $A \cap B \cap C \cap D \cap E \cap F = \emptyset$, implying W_m to be a mixed resolving set for $WCS_{n,1}$, i.e., $mdim(WCS_{n,1}) \leq 4h + 4$. Now, for the second, third, fifth, and sixth case, we obtain their lower bounds as follows.

For the second case, suppose that $W_m \subset V(WCS_{n,1})$ with $|W_m| < 4h + 1$ is a mixed resolving set for $WCS_{n,1}$. We have the following two cases to be considered:

Subcase (i): if $W_m \not\subset \{k_1, k_2, k_3, \dots, k_n\}$, then there must exist a vertex l_j such that $l_j \in W_m$. Then, there exists at least one vertex $l_i \in W_m$ such that $k_{i-1}, k_{i+1} \notin W_m$. Then, for the corresponding edges vk_{i-1} and vk_{i+1} , we have $r_m(vk_{i+1} | W_m) = r_m(vk_{i-1} | W_m)$, a contradiction. Therefore, W_m is not a mixed resolving set for $WCS_{n,1}$ in this case.

Subcase (ii): if $W_m \subset \{k_1, k_2, k_3, \dots, k_n\}$, then there exist at least two vertices k_i and k_j such that $k_i, k_j \notin W_m$. Then, for the edges vk_i and vk_j , we have $r_m(vk_i | W_m) = r_m(vk_j | W_m)$, a contradiction. Therefore, W_m is not a mixed resolving set for $WCS_{n,1}$ in this case as well. Thus, $|W_m| \geq 4h + 1$. This completes the proof for the second case.

For rest of the cases, the pattern is the same as that in Case (II). \square

5. Mixed Metric Dimension of the Barycentric Subdivision of $W_{n,1}$

In this section, we determine the mixed metric dimension of the barycentric subdivision of a wheel graph.

5.1. Barycentric Subdivision of $W_{n,1}$. Suppose $W_{n,1}$ is a wheel graph with the vertex set $V(W_{n,1}) = \{k_1, k_2, k_3, \dots, k_n, v\}$ having a single universal vertex v . Now, each of the edges $k_j k_{j+1}$ and vk_j ($1 \leq j \leq n$) of $W_{n,1}$ is subdivided with a new vertex. The resulting graph so obtained is known as the barycentric subdivision wheel graph (BSWG) and is denoted by $WBS_{n,1}$. BSWG has $4n$ edges, $E(WBS_{n,1}) = \{vl_j, l_j k_j, k_j m_j, m_j k_{j+1} \mid 1 \leq j \leq n\}$, and $3n + 1$ vertices, $V(WBS_{n,1}) = \{v, l_j, k_j, m_j \mid 1 \leq j \leq n\}$, where all indices are taken to be modulo n (see Figure 4). In this section, we obtain the mixed metric dimension of BSWG $WBS_{n,1}$.

Theorem 3. For $n \geq 6$, we have

$$mdim(WBS_{n,1}) = \begin{cases} 4h & \text{if } n = 6h, \\ 4h + 1 & \text{if } n = 6h + 1, \\ 4h + 2 & \text{if } n = 6h + 2, \\ 4h + 2 & \text{if } n = 6h + 3, \\ 4h + 3 & \text{if } n = 6h + 4, \\ 4h + 4 & \text{if } n = 6h + 5. \end{cases} \tag{19}$$

Proof. To prove this, we first generate the mixed resolving sets for all the cases, obtaining the upper bounds depending on the positive integer n . Then, in the end, we show that the lower bound (or reverse inequality) is the same as the upper bound to conclude the theorem.

Case (I): $n \equiv 0 \pmod{6}$. In this case, we have $n = 6h$, where $h \geq 2$ and $h \in \mathbb{N}$. Suppose an ordered subset $W_m = \{m_1, m_2, m_4, m_5, \dots, m_{n-2}, m_{n-1}\} = \{m_{3i+1}, m_{3i+2} \mid 0 \leq i \leq 2h - 1\}$ of vertices in $WBS_{n,1}$ with $|W_m| = 4h$. Next, we claim that W_m is the mixed resolving set for $WBS_{n,1}$. Now, we can give mixed codes to every vertex

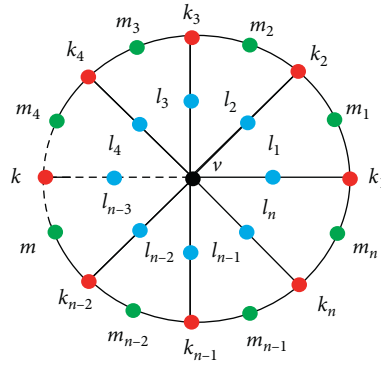


FIGURE 4: $WBS_{n,1}$.

and edge of $WBS_{n,1}$ with respect to W_m . The sets of mixed metric codes for the vertices $\{u = v, k_j, l_j, m_j | 1 \leq j \leq n\}$ of $WBS_{n,1}$ are as follows:

$$\begin{aligned}
 A &= \left\{ r_m(v|W_m) = \underbrace{(3, 3, 3, \dots, 3)}_{4h\text{-times}} \right\}, \\
 B &= \left\{ r_m(k_j|W_m) = \left(\begin{array}{l} 5, 5, 5, \dots, 5, d(m_{3i+1}, k_{3i+3}) = 3, d(m_{3i+2}, k_{3i+3}) = 1, \\ d(m_{3i+4}, k_{3i+3}) = 5, 5, \dots, 5 \end{array} \right) \middle| \right. \\
 &\quad \left. j \equiv 0 \pmod{3} 0 \leq i \leq 2h - 1 \right\} \cup \\
 &\quad \left\{ r_m(k_1|W_m) = \left(1, 3, \underbrace{5, \dots, 5}_{(4h-3)\text{-times}}, 3 \right) \right\} \cup \\
 &\quad \left\{ r_m(k_j|W_m) = \left(\begin{array}{l} 5, 5, 5, \dots, 5, d(m_{3i+2}, k_{3i+1}) = 3, d(m_{3i+4}, k_{3i+1}) = 1, \\ d(m_{3i+5}, k_{3i+1}) = 3, 5, \dots, 5 \end{array} \right) \middle| \right. \\
 &\quad \left. j \equiv 1 \pmod{3} 1 \leq i \leq 2h - 1 \right\} \cup \\
 &\quad \left\{ r_m(k_j|W_m) = (5, 5, 5, \dots, 5, d(m_{3i+1}, k_{3i+2}) = 1, d(m_{3i+2}, k_{3i+2}) = 1, 5, \dots, 5) \middle| \right. \\
 &\quad \left. j \equiv 2 \pmod{3} 0 \leq i \leq 2h - 1 \right\}, \\
 C &= \left\{ r_m(l_j|W_m) = (4, 4, 4, \dots, 4, d(m_{3i+2}, l_{3i+3}) = 2, 4, \dots, 4) \middle| \right. \\
 &\quad \left. j \equiv 0 \pmod{3} 0 \leq i \leq 2h - 1 \right\} \cup \\
 &\quad \left\{ r_m(l_j|W_m) = (4, 4, 4, \dots, 4, d(m_{3i+1}, l_{3i+1}) = 2, 4, \dots, 4) \middle| \right. \\
 &\quad \left. j \equiv 1 \pmod{3} 0 \leq i \leq 2h - 1 \right\} \cup \\
 &\quad \left\{ r_m(l_j|W_m) = (4, 4, 4, \dots, 4, d(m_{3i+1}, l_{3i+2}) = 2, d(m_{3i+2}, l_{3i+2}) = 2, 4, \dots, 4) \right\}, \\
 D &= \left\{ r_m(m_j|W_m) = \left(\begin{array}{l} 6, 6, \dots, 6, d(m_{3i+1}, m_{3i+3}) = 4, d(m_{3i+2}, m_{3i+3}) = 2, \\ d(m_{3i+4}, m_{3i+3}) = 2, d(m_{3i+5}, m_{3i+3}) = 4, 6, \dots, 6 \end{array} \right) \middle| \right. \\
 &\quad \left. j \equiv 0 \pmod{3} 0 \leq i \leq 2h - 1 \right\} \cup \\
 &\quad \left\{ r_m(m_1|W_m) = \left(0, 2, 6, 6, \dots, 6, 4 \right) \right\} \cup \\
 &\quad \left\{ r_m(m_j|W_m) = \left(\begin{array}{l} 6, 6, 6, \dots, 6, d(m_{3i+2}, m_{3i+1}) = 4, d(m_{3i+4}, m_{3i+1}) = 0, \\ d(m_{3i+5}, m_{3i+1}) = 2, 6, \dots, 6 \end{array} \right) \middle| \right. \\
 &\quad \left. j \equiv 1 \pmod{3} 0 \leq i \leq 2h - 1 \right\} \cup \\
 &\quad \left\{ r_m(l_j|W_m) = \left(\begin{array}{l} 6, 6, 6, \dots, 6, d(m_{3i+1}, m_{3i+2}) = 2, d(m_{3i+2}, m_{3i+2}) = 0, \\ d(m_{3i+4}, m_{3i+2}) = 4, 6, \dots, 6 \end{array} \right) \middle| \right. \\
 &\quad \left. j \equiv 2 \pmod{3} 0 \leq i \leq 2h - 1 \right\}.
 \end{aligned} \tag{20}$$

Next, the sets of mixed metric codes for the edges $\{vl_j, l_jk_j, k_jm_j, m_jk_{j+1} | 1 \leq j \leq n\}$ of $WBS_{n,1}$ are as follows:

$$\begin{aligned}
 E &= \left\{ r_m(vl_j|W_m) = (3, 3, 3, \dots, 3, d(m_{3i+2}, vl_{3i+3}) = 2, 3, \dots, 3) \mid \right. \\
 &\quad \left. j \equiv 0 \pmod{3} 0 \leq i \leq 2h-1 \right\} \cup \\
 &\left\{ r_m(vl_j|W_m) = (3, 3, 3, \dots, 3, d(m_{3i+1}, vl_{3i+1}) = 2, 3, \dots, 3) \mid \right. \\
 &\quad \left. j \equiv 1 \pmod{3} 0 \leq i \leq 2h-1 \right\} \cup \\
 &\left\{ r_m(vl_j|W_m) = (3, 3, 3, \dots, 3, d(m_{3i+1}, vl_{3i+2}) = 2, d(m_{3i+2}, vl_{3i+2}) = 2, 3, \dots, 3) \mid \right. \\
 &\quad \left. j \equiv 2 \pmod{3} 0 \leq i \leq 2h-1 \right\}, \\
 F &= \left\{ r_m(l_jk_j|W_m) = \left(4, 4, 4, \dots, 4, d(m_{3i+1}, l_{3i+3}k_{3i+3}) = 3, d(m_{3i+2}, l_{3i+3}k_{3i+3}) = 1, \right. \right. \\
 &\quad \left. \left. d(m_{3i+4}, l_{3i+3}k_{3i+3}) = 3, 4, \dots, 4 \right) \mid \right. \\
 &\quad \left. j \equiv 0 \pmod{3} 0 \leq i \leq 2h-1 \right\} \cup \\
 &\left\{ r_m(l_1k_1|W_m) = \left(1, 3, \underbrace{4, 4, \dots, 4}_{(4h-3)\text{-times}}, 3 \right) \right\} \cup \\
 &\left\{ r_m(l_jk_j|W_m) = \left(4, 4, 4, \dots, 4, d(m_{3i+2}, l_{3i+1}k_{3i+1}) = 3, d(m_{3i+4}, l_{3i+1}k_{3i+1}) = 1, \right. \right. \\
 &\quad \left. \left. d(m_{3i+5}, l_{3i+1}k_{3i+1}) = 3, 4, \dots, 4 \right) \mid \right. \\
 &\quad \left. j \equiv 1 \pmod{3} 1 \leq i \leq 2h-1 \right\} \cup \\
 &\left\{ r_m(l_jk_j|W_m) = (4, 4, 4, \dots, 4, d(m_{3i+1}, l_{3i+2}k_{3i+2}) = 1, d(m_{3i+2}, l_{3i+2}k_{3i+2}) = 1, 4, \dots, 4) \mid \right. \\
 &\quad \left. j \equiv 2 \pmod{3} 0 \leq i \leq 2h-1 \right\}, \\
 G &= \left\{ r_m(k_jm_j|W_m) = \left(5, 5, 5, \dots, 5, d(m_{3i+1}, k_{3i+3}m_{3i+3}) = 3, d(m_{3i+2}, k_{3i+3}m_{3i+3}) = 1, \right. \right. \\
 &\quad \left. \left. d(m_{3i+4}, k_{3i+3}m_{3i+3}) = 2, d(m_{3i+5}, k_{3i+3}m_{3i+3}) = 4, 5, \dots, 5 \right) \mid \right. \\
 &\quad \left. j \equiv 0 \pmod{3} 0 \leq i \leq 2h-1 \right\} \cup \\
 &\left\{ r_m(k_1m_1|W_m) = \left(0, 2, \underbrace{5, 5, \dots, 5}_{(4h-3)\text{-times}}, 3 \right) \right\} \cup \\
 &\left\{ r_m(k_jm_j|W_m) = \left(5, 5, 5, \dots, 5, d(m_{3i+2}, k_{3i+1}m_{3i+1}) = 3, d(m_{3i+4}, k_{3i+1}m_{3i+1}) = 0, \right. \right. \\
 &\quad \left. \left. d(m_{3i+5}, k_{3i+1}m_{3i+1}) = 2, 5, \dots, 5 \right) \mid \right. \\
 &\quad \left. j \equiv 1 \pmod{3} 1 \leq i \leq 2h-1 \right\} \cup \\
 &\left\{ r_m(k_jm_j|W_m) = \left(5, 5, 5, \dots, 5, d(m_{3i+1}, k_{3i+2}m_{3i+2}) = 1, d(m_{3i+2}, k_{3i+2}m_{3i+2}) = 0, \right. \right. \\
 &\quad \left. \left. d(m_{3i+4}, k_{3i+2}m_{3i+2}) = 4, 5, \dots, 5 \right) \mid \right. \\
 &\quad \left. j \equiv 2 \pmod{3} 0 \leq i \leq 2h-1 \right\}, \\
 H &= \left\{ r_m(m_jk_{j+1}|W_m) = \left(5, 5, 5, \dots, 5, d(m_{3i+1}, m_{3i+3}k_{3i+4}) = 4, d(m_{3i+2}, m_{3i+3}k_{3i+4}) = 2, \right. \right. \\
 &\quad \left. \left. d(m_{3i+4}, m_{3i+3}k_{3i+4}) = 1, d(m_{3i+5}, m_{3i+3}k_{3i+4}) = 3, 5, \dots, 5 \right) \mid \right. \\
 &\quad \left. j \equiv 0 \pmod{3} 0 \leq i \leq 2h-1 \right\} \cup \\
 &\left\{ r_m(m_1k_2|W_m) = \left(0, 1, \underbrace{5, 5, \dots, 5}_{(4h-3)\text{-times}}, 4 \right) \right\} \cup \\
 &\left\{ r_m(m_jk_{j+1}|W_m) = \left(5, 5, 5, \dots, 5, d(m_{3i+2}, m_{3i+1}k_{3i+2}) = 4, d(m_{3i+4}, m_{3i+1}k_{3i+2}) = 0, \right. \right. \\
 &\quad \left. \left. d(m_{3i+5}, m_{3i+1}k_{3i+2}) = 1, 5, \dots, 5 \right) \mid \right. \\
 &\quad \left. j \equiv 1 \pmod{3} 1 \leq i \leq 2h-1 \right\} \cup \\
 &\left\{ r_m(m_jk_{j+1}|W_m) = \left(5, 5, 5, \dots, 5, d(m_{3i+1}, m_{3i+2}k_{3i+3}) = 2, d(m_{3i+2}, m_{3i+2}k_{3i+3}) = 0, \right. \right. \\
 &\quad \left. \left. d(m_{3i+4}, m_{3i+2}k_{3i+3}) = 3, 5, \dots, 5 \right) \mid \right. \\
 &\quad \left. j \equiv 2 \pmod{3} 0 \leq i \leq 2h-1 \right\}.
 \end{aligned} \tag{21}$$

From these sets of mixed codes for $WBS_{n,1}$, we obtain that $|A| = 1, |B| = |C| = |D| = |E| = |F| = |G| = |H| = n$, and $A \cap B \cap C \cap D \cap E \cap F \cap G \cap H = \emptyset$, implying W_m to be a mixed resolving set for $WBS_{n,1}$, i.e., $mdim(WBS_{n,1}) \leq 4h$. Next, using equation (1) and Proposition 2, we find that $mdim(WBS_{n,1}) = 4h$, in this case.

Like the first case, the rest of the proof is similar to that of Theorem 2. \square

Remark 2. For the cycle and barycentric subdivision wheel graph, i.e., $H = WCS_{n,1}$ and $H = WBS_{n,1}$, we find that $\dim(H) = edim(H) = mdim(H)$ when $n = 6h$ and $n = 6h + 3$. For the rest of the values of the positive integer n , we have $\dim(H) = edim(H) < mdim(H)$ (using Propositions 2 and 4 and Theorems 2 and 3).

6. Conclusion

In this article, we have computed the mixed metric dimension for three families of graphs, namely, $WBS_{n,1}$, $WCS_{n,1}$, and $WSS_{n,1}$, obtained after the barycentric, cycle, and spoke subdivisions of the wheel graph $W_{n,1}$, respectively. We also observed that the mixed resolving sets for $WBS_{n,1}$ and $WCS_{n,1}$ are independent. For $WSS_{n,1}$, we found that $\dim(WSS_{n,1}) < edim(WSS_{n,1}) < mdim(WSS_{n,1})$, and for $H = WBS_{n,1}$ and $H = WCS_{n,1}$, we obtained the following relation: $\dim(H) = edim(H) \leq mdim(H)$ (partial answers to the questions raised in [1, 18]).

Data Availability

Data sharing is not applicable to this article as no datasets were generated or analyzed during the current study.

Conflicts of Interest

The authors declare no conflicts of interest.

Authors' Contributions

All the authors contributed equally to the final manuscript.

Acknowledgments

This research was supported by the Natural Science Foundation of China (11871077) and the NSF of Anhui Province (1808085MA04).

References

- [1] A. Kelenc, D. Kuziak, A. Taranenko, and I. G. Yero, "Mixed metric dimension of graphs," *Applied Mathematics and Computation*, vol. 314, pp. 429–438, 2017.
- [2] P. J. Slater, "Abstracts," *Stroke*, vol. 6, no. 5, pp. 549–559, 1975.
- [3] F. Harary and R. A. Melter, "On the metric dimension of a graph," *ARS Combinatoria*, vol. 2, pp. 191–195, 1976.
- [4] M. Azeem and M. F. Nadeem, "Metric-based resolvability of polycyclic aromatic hydrocarbons," *The European Physical Journal Plus*, vol. 136, no. 4, pp. 1–14, 2021.
- [5] G. Chartrand, L. Eroh, M. A. Johnson, and O. R. Oellermann, "Resolvability in graphs and the metric dimension of a graph," *Discrete Applied Mathematics*, vol. 105, no. 1-3, pp. 99–113, 2000.
- [6] Z. Hussain, M. Munir, A. Ahmad, M. Chaudhary, J. A. Khan, and I. Ahmed, "Metric basis and metric dimension of 1-pentagonal carbon nanocone networks," *Scientific Reports*, vol. 10, no. 1, pp. 1–7, 2020.
- [7] B. Deng, M. F. Nadeem, and M. Azeem, "On the edge metric dimension of different families of möbius networks," *Mathematical Problems in Engineering*, vol. 2021, Article ID 6623208, 9 pages, 2021.
- [8] S. Khuller, B. Raghavachari, and A. Rosenfeld, "Landmarks in graphs," *Discrete Applied Mathematics*, vol. 70, no. 3, pp. 217–229, 1996.
- [9] P. Singh, S. Sharma, S. K. Sharma, and V. K. Bhat, "Metric dimension and edge metric dimension of windmill graphs," *AIMS Mathematics*, vol. 6, no. 9, pp. 9138–9153, 2021.
- [10] H. Raza and Y. Ji, "Computing the mixed metric dimension of a generalized Petersen graph $P(n, 2)$," *Frontiers of Physics*, vol. 8211 pages, 2020.
- [11] A. Sebo and E. Tannier, "On metric generators of graphs," *Mathematics of Operations Research*, vol. 29, no. 2, pp. 383–393, 2004.
- [12] S. K. Sharma and V. K. Bhat, "Metric Dimension of heptagonal circular ladder," *Discrete Mathematics, Algorithms and Applications*, vol. 13, no. 1, Article ID 2050095, 2021.
- [13] S. K. Sharma and V. K. Bhat, "Fault-tolerant metric dimension of two-fold heptagonal-nonagonal circular ladder," *Discrete Mathematics, Algorithms and Applications*, Article ID 2150132, 2021.
- [14] M. F. Nadeem, M. Azeem, and A. Khalil, "The locating number of hexagonal Möbius ladder network," *Journal of Applied Mathematics and Computing*, vol. 66, no. 1, pp. 149–165, 2021.
- [15] G. Chartrand, V. Saenpholphat, and P. Zhang, "The independent resolving number of a graph," *Mathematica Bohemica*, vol. 128, no. 4, pp. 379–393, 2003.
- [16] F. Okamoto, B. Phinezy, and P. Zhang, "The local metric dimension of a graph," *Mathematica Bohemica*, vol. 135, no. 3, pp. 239–255, 2010.
- [17] C. Hernando, M. Mora, P. J. Slater, and D. R. Wood, "Fault-tolerant metric dimension of graphs," *Convexity in Discrete Structures*, vol. 5, pp. 81–85, 2008.
- [18] A. Kelenc, N. Tratnik, and I. G. Yero, "Uniquely identifying the edges of a graph: the edge metric dimension," *Discrete Applied Mathematics*, vol. 251, pp. 204–220, 2018.
- [19] H. Raza, J. B. Liu, and S. Qu, "On mixed metric dimension of rotationally symmetric graphs," *IEEE Access*, vol. 8, pp. 11560–11569, 2019.
- [20] H. Raza, Y. Ji, and S. Qu, "On mixed metric dimension of some path related graphs," *IEEE Access*, vol. 8, pp. 188146–188153, 2020.
- [21] Z. Raza and M. S. Bataineh, "The comparative analysis of metric and edge metric dimension of some subdivisions of the wheel graph," *Asian-European Journal of Mathematics*, vol. 14, no. 98, Article ID 2150062, 2020.
- [22] I. Tomescu and A. Riasat, "On metric dimension of uniform subdivisions of the wheel," *Utilitas Mathematica*, vol. 96, pp. 233–242, 2015.
- [23] I. Tomescu and I. Javaid, "On the metric dimension of the Jahangir graph," *Bulletin Mathématique de la Société des Sciences Mathématiques de Roumanie*, vol. 50, no. 98, pp. 371–376, 2007.

Research Article

Metric Dimension of Crystal Cubic Carbon Structure

Xiujun Zhang ¹ and Muhammad Naeem ²

¹School of Computer Science, Chengdu University, Chengdu, China

²Department of Mathematics and Statistics, Institute of Southern Punjab, Multan, Pakistan

Correspondence should be addressed to Muhammad Naeem; naempkn@gmail.com

Received 24 May 2021; Accepted 23 June 2021; Published 2 July 2021

Academic Editor: Ali Ahmad

Copyright © 2021 Xiujun Zhang and Muhammad Naeem. This is an open access article distributed under the Creative Commons Attribution License, which permits unrestricted use, distribution, and reproduction in any medium, provided the original work is properly cited.

For any given graph G , we say $W \subseteq V(G)$ is a resolving set or resolves the graph G if every vertex of G is uniquely determined by its vector of distances to the vertices in W . The metric dimension of G is the minimum cardinality of all the resolving sets. The study of metric dimension of chemical structures is increasing in recent times and it has application about the topology of such structures. The carbon atoms can bond together in various ways, called allotropes of carbon, one of which is crystal cubic carbon structure $CCC(n)$. The aim of this article is to find the metric dimension of $CCC(n)$.

1. Introduction

Let G be a simple connected graph and let $W = \{w_1, w_2, \dots, w_k\}$ be an ordered subset of the set of vertices $V(G)$ of G . The distance $d(u, v)$ of two vertices of G is the length of shortest path between u and v . The representation of a vertex u of G with respect to W is the k -vector $(d(u, w_1), d(u, w_2), \dots, d(u, w_k))$ and it is denoted as $r(u|W)$. The set W is called the resolving set or to resolve G if the representation of distinct vertices is distinct. That is, if u and v are two distinct vertices, then $r(u|W) \neq (v|W)$. The metric dimension of a graph is the cardinality of the minimal resolving set and it is denoted as $\beta(G)$. As there may be many different resolving subsets in $V(G)$ of different sizes, the study of the minimal one is important and it has been studied over the years. Some authors also use the term basis for G which is a resolving set with minimum cardinal number (see [1]). This work is about a study of resolving sets in chemical structural graphs.

The metric dimension of a general metric space was introduced in 1953 in [2], but at that time, it attracted little attention. Then, about twenty years later, it was applied to the distances between vertices of a graph [3–5]. Since then, it has been frequently used in graph theory, chemistry, biology, robotics, and many other disciplines. For some literature studies, see [6–9].

From many parameters for the study of graphs, the metric dimension is one of those that has many applications, and these applications are diverse like in pharmaceutical chemistry [10, 11], robot navigation [12], and combinatorial optimization [13]. A chemical compound or material can be represented by many graph structures, but only one of them may express its topological properties. The chemists require mathematical forms for a set of chemical compounds to give distinct representations to distinct compound structures. The structure of chemical compounds or materials can be represented by a labeled graph whose vertex and edge labels specify the atom and bond types, respectively. Thus, a graph theoretic interpretation of this problem is to provide representations for the vertices of a graph in such a way that distinct vertices have distinct representations.

At very high pressures of above 1000 GPa (gigapascal), one of the forms of carbon, namely, diamond, is predicted to transform into the so-called C_8 structure, a body-centered cubic structure with 8 atoms in the unit cell. This cubic carbon phase might have importance in astrophysics. Its structure is known in one of the metastable phases of silicon and is similar to cubane. The structure of this phase was proposed in 2012 as carbon sodalite [14]. In 2017, Baig et al. [15] modified and extended this structure and named it crystal cubic carbon $CCC(n)$. We are taking all the notations

as they were in [15]. The structure of crystal cubic carbon consists of cubes.

The molecular graph of crystal cubic carbon $CCC(n)$ for the second level is depicted in Figure 1. Its structure starts from one unit cube and then by attaching cubes at each vertex of the unit cube by an edge. For the third level, the $CCC(3)$ is constructed by attaching cube to each vertex of cubes of $CCC(2)$ having degree 3 or you can say by attaching cubes by an edge to all the white vertices of $CCC(2)$. So, at each level, a new set of cubes is attached by edges to the white vertices of cubes of the preceding level. The third level of $CCC(n)$ is displayed in Figure 2 which is constructed and

$$\begin{aligned} |V(CCC(n))| &= 2 \left\{ 24 \sum_{r=3}^n (2^3 - 1)^{r-3} + 31(2^3 - 1)^{n-2} + 2 \sum_{r=0}^{n-2} (2^3 - 1)^r + 3 \right\}, \\ |E(CCC(n))| &= 4 \left\{ 24 \sum_{r=3}^n (2^3 - 1)^{r-3} + 24(2^3 - 1)^{n-2} + 2 \sum_{r=0}^{n-2} (2^3 - 1)^r + 3 \right\}. \end{aligned} \quad (1)$$

There are some articles that describe the different topological properties of $CCC(n)$ structure, the famous of those topological indices are Randić, ABC, and Zagreb indices and other degree-based indices of $CCC(n)$ which are computed in [15–18]. In the articles [19, 20], the authors calculated eccentricity and Szeged-type topological indices of $CCC(n)$. The aim of this article is to compute the metric dimension of $CCC(n)$. Note that if $W = \{w_1, w_2, \dots, w_k\}$ is the ordered set of vertices of a graph G , then ξ^{th} component of $r(c|W)$ is $0 \iff c = w_\xi$. Thus, in order to show that W is a resolving set, it suffices to verify that $r(a|W) \neq r(b|W)$ for each pair of distinct vertices $a, b \in V(G) \setminus W$.

2. Main Result

In this section, we will present the main result about the $\beta(CCC(n))$. But before going further, let us discuss the very simple case of $CCC(1)$ which is just a cube. We claim that $\beta(CCC(1)) = 3$ indeed is true, let us see how.

Assume that $\beta(CCC(1)) = 1$, and because of symmetry, we can take any vertex of cube to be the resolving set as in Figure 3(a), say $W = \{a\}$, then $r(b|W) = r(c|W)$, which is a contradiction. So, $\beta(CCC(1)) > 1$. Assume that $\beta(CCC(1)) = 2$. Then, there are two possibilities for the elements of the resolving set W of $CCC(1)$ because of its symmetric shape. The possible cases are as follows:

- (I) The two elements of W are the vertices on the main diagonal of $CCC(1)$.
- (II) The two elements of W are on the same face of the cube. In this case, the both elements are either on the main diagonal of a face or on the same edge of a face.

Without loss of generality, we can assume that $W = \{a, f\}$ for case (I). For case (II) without loss of generality, we can assume $W = \{a, c\}$ and $W = \{b, c\}$, respectively. Then, Figures 3(b)–3(d) show that $\beta(CCC(1)) \neq 2$; the ordered pairs in these Figures denote the representations of the

presented in a most suitable manner to explain the structure of $CCC(n)$.

All the new attached cubes, at each level, will be called the outermost layer of cubes or outermost level of cubes, or you can say at each level, the cubes with white vertices will be called the outermost layer. As in $CCC(2)$, the outermost layer of cubes consists of 8 cubes. Because there are 7×8 vertices of degree 3, so in $CCC(3)$, the outermost layer of cubes will consist of 7×8 cubes. Similarly, this procedure is repeated to get the next level. The cardinality of vertices and edges in $CCC(n)$ is given below, respectively.

vertices. Thus, from Figure 3(e), it is proved that $\beta(CCC(1)) = 3$.

Now, we will prove the main result of this article.

Theorem 1. *The metric dimension of crystal cubic carbon structure $CCC(n)$ is $7^{n-2} \times 16$, for all $n \geq 2$, that is, $\beta(CCC(n)) = 7^{n-2} \times 16, \forall n \geq 2$.*

Proof. Let $G = CCC(n)$ be the crystal cubic carbon structure and $n \geq 2$. To show that the $\beta(CCC(n)) = 7^{n-2} \times 16$ firstly, we will show that $\beta(CCC(n)) \geq 7^{n-2} \times 16$. Let Q_n be a cube on the outermost layer of $CCC(n)$, as depicted in Figure 4 (note that there are no cubes attached to the vertices $b_1, b_2, b_3, c_1, c_2, c_3$, and u). In other words, all these vertices are of degree 3 and they belong to only one cube which is Q_n . Observe that the red vertex of cube Q_n is attached with red edge to a cube Q_{n-1} of the preceding level at its blue vertex. Also, note that $d(b_1, a) = 1 = d(b_2, a) = d(b_3, a)$ and $d(c_1, a) = 2 = d(c_2, a) = d(c_3, a)$ and $d(u, a) = 3$.

Let $W = \{w_1, w_2, \dots, w_k\}$ be a resolving set of $CCC(n)$. We claim that at least two vertices of Q_n belong to W . Suppose on contrary that no vertex of Q_n belongs to W and let $r(a|W)$ be a representation of vertex $a \in V(Q_n)$. Note that all the shortest paths from any vertex of Q_n to any vertex of W contain the vertex a of Q_n . So, we can say that all such paths pass through vertex a (path may end at it). Then,

$$\begin{aligned} r(b_1|W) &= (d(b_1, w_1), d(b_1, w_2), \dots, d(b_1, w_k)) \\ &= (d(a, w_1) + 1, d(a, w_2) + 1, \dots, d(a, w_k) + 1) \\ &= (d(b_2, w_1), d(b_2, w_2), \dots, d(b_2, w_k)) \\ &= r(b_2|W); \end{aligned} \quad (2)$$

this is a contradiction. Now, assume that exactly one vertex from the set $V(Q_n)$ belongs to W . Without loss of generality, we can assume that this common vertex is w_1 .

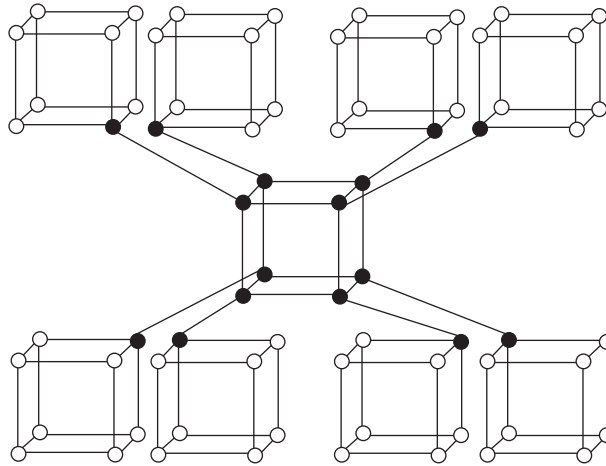


FIGURE 1: Crystal cubic carbon structure CCC(2).

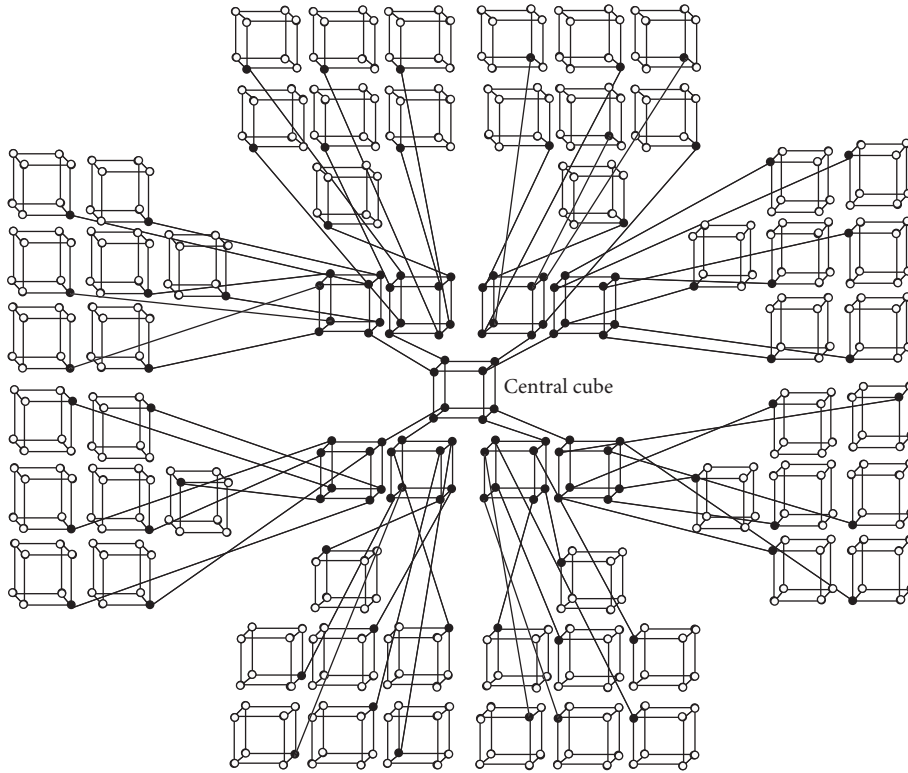


FIGURE 2: Crystal cubic carbon structure CCC(3), with CCC(1) as the central cube.

Case 1. If $w_1 = a$, then

$$\begin{aligned} r(b_1|W) &= (1, d(b_1, w_2), \dots, d(b_1, w_k)) \\ &= (1, d(b_2, w_2), \dots, d(b_2, w_k)) \quad (3) \\ &= r(b_2|W), \text{ a contradiction.} \end{aligned}$$

Case 2. If $w_1 = b_1$, then $d(c_1, w_1) = 1 = d(c_2, w_1)$

$$\begin{aligned} r(c_1|W) &= (1, d(c_1, w_2), \dots, d(c_1, w_k)) \\ &= (1, d(c_2, w_2), \dots, d(c_2, w_k)) \quad (4) \\ &= r(c_2|W), \text{ again a contradiction.} \end{aligned}$$

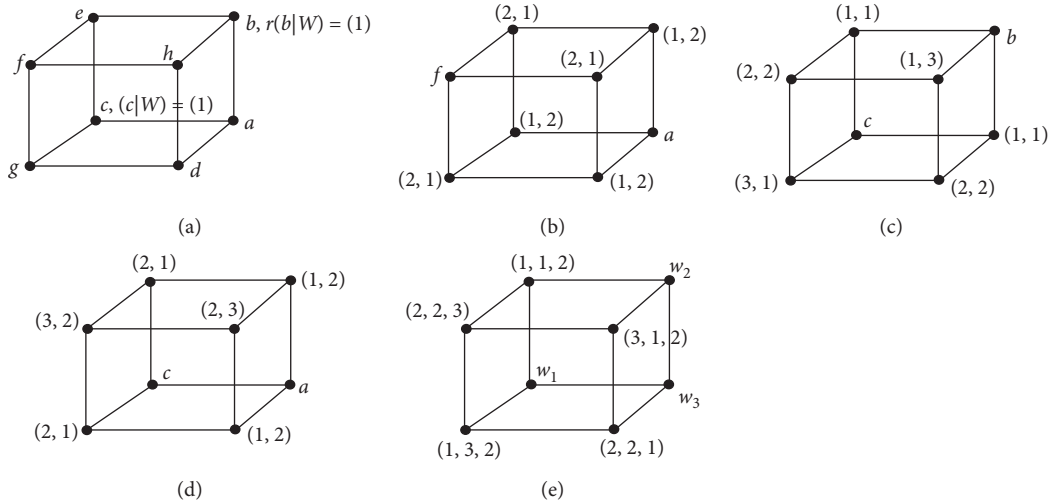


FIGURE 3: The graph of CCC(1) with all options of possible resolving sets.

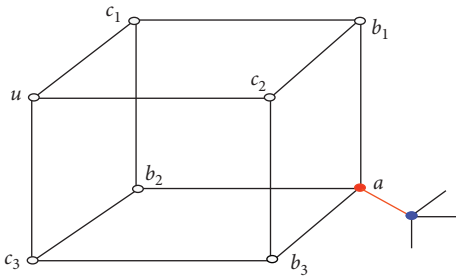


FIGURE 4: An arbitrary cube Q_n in the outermost layer of cubes of $CCC(n)$.

Similar contradictions appear for $w_1 = b_2$ and $w_1 = b_3$, let us look at it.

Case 3. If $w_1 = b_2$, then $d(c_1, w_1) = 1 = d(c_3, w_1)$

$$\begin{aligned} r(c_1|W) &= (1, d(c_1, w_2), \dots, d(c_1, w_k)) \\ &= (1, d(c_3, w_2), \dots, d(c_3, w_k)) \quad (5) \\ &= r(c_3|W), \text{ a contradiction.} \end{aligned}$$

Case 4. If $w_1 = b_3$, then $d(c_2, w_1) = 1 = d(c_3, w_1)$

$$\begin{aligned} r(c_2|W) &= (1, d(c_2, w_2), \dots, d(c_2, w_k)) \\ &= (1, d(c_3, w_2), \dots, d(c_3, w_k)) \quad (6) \\ &= r(c_3|W), \text{ a contradiction.} \end{aligned}$$

Case 5. If $w_1 = c_1$, then $d(b_1, w_1) = 1 = d(b_2, w_1)$

$$\begin{aligned} r(b_1|W) &= (1, d(b_1, w_2), \dots, d(b_1, w_k)) \\ &= (1, d(b_2, w_2), \dots, d(b_2, w_k)) \quad (7) \\ &= r(b_2|W), \text{ a contradiction.} \end{aligned}$$

Case 6. If $w_1 = c_2$, then $d(b_1, w_1) = 1 = d(b_3, w_1)$

$$\begin{aligned} r(b_1|W) &= (1, d(b_1, w_2), \dots, d(b_1, w_k)) \\ &= (1, d(b_3, w_2), \dots, d(b_3, w_k)) \quad (8) \\ &= r(b_3|W), \text{ a contradiction.} \end{aligned}$$

Case 7. If $w_1 = c_3$, then $d(b_2, w_1) = 1 = d(b_3, w_1)$

$$\begin{aligned} r(b_2|W) &= (1, d(b_2, w_2), \dots, d(b_2, w_k)) \\ &= (1, d(b_3, w_2), \dots, d(b_3, w_k)) \quad (9) \\ &= r(b_3|W), \text{ a contradiction.} \end{aligned}$$

Case 8. If $w_1 = u$, then $d(b_1, w_1) = 1 = d(b_3, w_1)$

$$\begin{aligned} r(b_1|W) &= (1, d(b_1, w_2), \dots, d(b_1, w_k)) \\ &= (1, d(b_3, w_2), \dots, d(b_3, w_k)) \quad (10) \\ &= r(b_3|W), \text{ a contradiction.} \end{aligned}$$

The contradiction in all the cases proved our claim. So, at least two vertices from the vertex set of Q_n are in the resolving set W of $CCC(n)$. Since Q_n was taken arbitrary, so W contains at least two vertices from each of the cube in the outermost layer of cubes of $CCC(n)$. By the construction of $CCC(n)$, we can see that at each step or at each level, the cubes in $CCC(n)$ are increased by a number equal to 7 multiplied by the number of cubes in the outermost layer of the previous level. For example, in $CCC(2)$, we have 8 cubes in the outer layer, and in $CCC(3)$, we have 7×8 cubes in the outermost layer. Thus, there are exactly $7^{n-2} \times 8$ cubes in the outermost layer of $CCC(n)$. Since from each such cube there are at least two vertices in W , so $\beta(CCC(n)) \geq 7^{n-2} \times 16$. \square

2.1. *Second Part of Proof.* In this part, we will show that $\beta(\text{CCC}(n)) \leq 7^{n-2} \times 16$. Let $W = \{w_1, w_2, \dots, w_k\}$ be the collection of all the vertices of type b_1 and b_2 just like we have discussed in part one of the proof and depicted in Figure 4. Then, $k = 7^{n-2} \times 16$. We claim that W is a resolving set of $\text{CCC}(n)$. The representations of the two arbitrary vertices of $\text{CCC}(n)$ can be compared in five different cases and they are discussed as follows:

- (1) The two arbitrary selected vertices are on the same cube in the outermost level of $\text{CCC}(n)$ (see Figure 4).
- (2) The two arbitrary selected vertices are on the same cube, but this cube is not the outer most cube and neither the central cube (i.e., $\text{CCC}(1)$), as depicted in Figure 5.
- (3) The two arbitrary selected vertices are on the central cube, as displayed in Figure 6.
- (4) The two arbitrary selected vertices are on a chain of cubes with one end being the cube of the outermost level (see Figure 7).
- (5) The two arbitrary selected vertices are on distinct chains of cubes and those chains are connecting at a cube which we can call a branching cube. As explained in Figure 8, in which B cube is the branching cube, S-cube and T-cube are on different chains each containing one of the selected vertices.

Case (1). This can be proved by a direct computation for the representation of all the vertices in this cube (Figure 4). Without loss of generality, we can assume that $w_1 = b_1, w_2 = b_2 \in W$, then $r(a|W) = (1, 1, d(a, w_3), \dots, d(a, w_k))$ and

$$\begin{aligned} r(b_3|W) &= (2, 2, d(a, w_3) + 1, \dots, d(a, w_k) + 1), \\ r(c_1|W) &= (1, 1, d(a, w_3) + 2, \dots, d(a, w_k) + 2), \\ r(c_2|W) &= (1, 3, d(a, w_3) + 2, \dots, d(a, w_k) + 2), \\ r(c_3|W) &= (3, 1, d(a, w_3) + 2, \dots, d(a, w_k) + 2), \\ r(u|W) &= (2, 2, d(a, w_3) + 3, \dots, d(a, w_k) + 3). \end{aligned} \tag{11}$$

We can see from the above that these representations are all distinct in this case.

Case (2). Let the two arbitrary selected vertices be on the same cube and this cube is not on the outermost cube and neither is it the central cube. A visualization of such cube is given in Figure 5. We can label the vertices of this cube Q_A , as shown in Figure 5. Without loss of generality, we can assume that w_1, w_2 are on the cube in the outermost layer of cubes and that cube is connected to cube Q_A at vertex u_1 by a chain of cubes. Similarly, we can assume that w_{2i-1}, w_{2i} are on the cube in the outermost layer of cubes and those cubes are connected to cube Q_A at vertices $u_i, i = 2, \dots, 7$, by a chain of cubes, respectively.

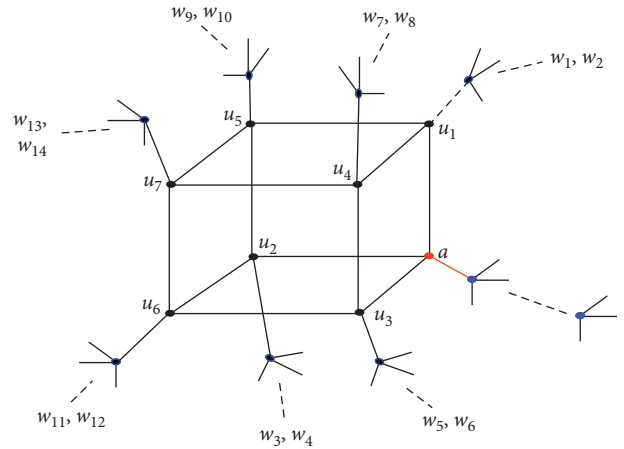


FIGURE 5: Arbitrary cube Q_A not in the outermost layer of cubes of $\text{CCC}(n)$ and nor the central cube. This cube is connected to the central cube by a chain of cubes at vertex a .

$$\begin{aligned} d(u_1, w_1) &\neq d(u_i, w_1), \quad i = 1, \dots, 7 \text{ and } i \neq 1, \\ d(u_2, w_3) &\neq d(u_i, w_3), \quad i = 1, \dots, 7 \text{ and } i \neq 2, \\ d(u_3, w_5) &\neq d(u_i, w_5), \quad i = 1, \dots, 7 \text{ and } i \neq 3, \\ d(u_4, w_7) &\neq d(u_i, w_7), \quad i = 1, \dots, 7 \text{ and } i \neq 4, \\ d(u_5, w_9) &\neq d(u_i, w_9), \quad i = 1, \dots, 7 \text{ and } i \neq 5, \\ d(u_6, w_{11}) &\neq d(u_i, w_{11}), \quad i = 1, \dots, 7 \text{ and } i \neq 6, \\ d(u_7, w_{13}) &\neq d(u_i, w_{13}), \quad i = 1, \dots, 7 \text{ and } i \neq 7. \end{aligned} \tag{12}$$

Also,

$$\begin{aligned} d(a, w_1) &= d(u_1, w_1) + 1, \\ d(a, w_3) &= d(u_2, w_3) + 1, \\ d(a, w_5) &= d(u_3, w_5) + 1, \\ d(a, w_7) &= d(u_4, w_7) + 2, \\ d(a, w_9) &= d(u_5, w_9) + 2, \\ d(a, w_{11}) &= d(u_6, w_{11}) + 2, \end{aligned} \tag{13}$$

and $d(a, w_{13}) = d(u_7, w_{13}) + 3$. All these computations show that $r(u_i|W) \neq r(u_j|W)$ for $i \neq j$ and $r(a|W) \neq r(u_i|W)$ for $i = 1, \dots, 7$. This completes the proof in this case.

Case (3). Assume that the two arbitrary selected vertices are on the central cube, as displayed in Figure 6, where just like in the previous case (2), we have labeled all 8 vertices with u_1, u_2, \dots, u_8 . Again, without loss of generality, we assume that $w_{2i-1}, w_{2i}, i = 1, \dots, 8$, are on the cube in the outermost layer of cubes and those outermost cubes containing w_{2i-1}, w_{2i} are connected to the central cube $\text{CCC}(1)$ at vertices $u_i, i = 1, 2, \dots, 8$, by a chain of cubes, respectively. These assumptions imply that

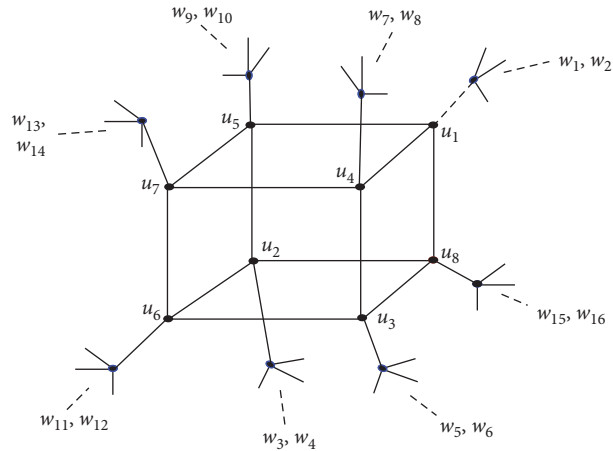


FIGURE 6: Central cube of $CCC(n)$, that is, the cube $CCC(1)$.

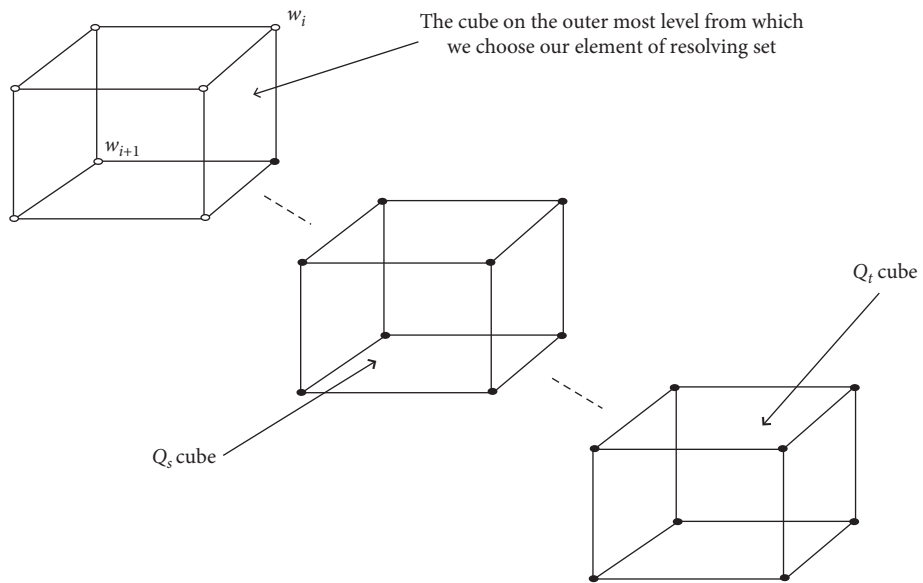


FIGURE 7: A chain of cubes with one end being the cube of the outermost level; Q_s and Q_t are arbitrary cubes on the chain but not the outermost cubes.

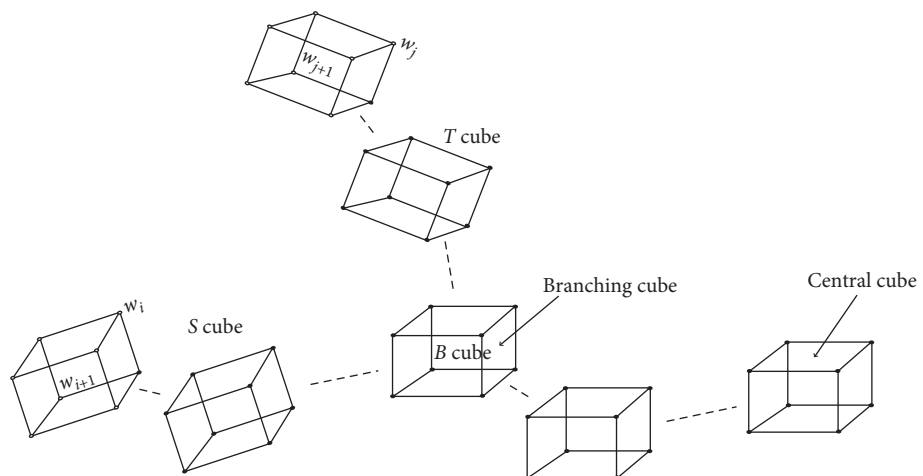


FIGURE 8: Branching cube and chain of cubes in $CCC(n)$.

$$\begin{aligned}
d(u_1, w_1) \neq d(u_i, w_1), & \quad 1 \leq i \leq 8 \text{ and } i \neq 1, \\
d(u_2, w_3) \neq d(u_i, w_3), & \quad 1 \leq i \leq 8 \text{ and } i \neq 2, \\
d(u_3, w_5) \neq d(u_i, w_5), & \quad 1 \leq i \leq 8 \text{ and } i \neq 3, \\
d(u_4, w_7) \neq d(u_i, w_7), & \quad 1 \leq i \leq 8 \text{ and } i \neq 4, \\
d(u_5, w_9) \neq d(u_i, w_9), & \quad 1 \leq i \leq 8 \text{ and } i \neq 5, \\
d(u_6, w_{11}) \neq d(u_i, w_{11}), & \quad 1 \leq i \leq 8 \text{ and } i \neq 6, \\
d(u_7, w_{13}) \neq d(u_i, w_{13}), & \quad 1 \leq i \leq 8 \text{ and } i \neq 7, \\
d(u_8, w_{15}) \neq d(u_i, w_{15}), & \quad 1 \leq i \leq 8 \text{ and } i \neq 8.
\end{aligned} \tag{14}$$

So, we get the conclusion that, in this case, again $r(u_i|W) \neq r(u_j|W)$ for $i \neq j$ and $1 \leq i \leq 8, 1 \leq j \leq 8$.

Case (4). Now, we are going to discuss case (4). Assume that the two arbitrary selected vertices s, t are on two distinct cubes and those cubes are on a chain of cubes, see Figure 7. Assume that one end of this chain is the outermost cube containing two arbitrary resolving elements, say w_1, w_2 (without loss of generality, we can assume that those vertices are w_1, w_2), and the other end is the central cube.

As depicted in Figure 7, let t be a vertex of cube Q_t and s be a vertex of cube Q_s , then $d(s, w_1) < d(t, w_1)$, and therefore, $r(s|W) \neq r(t|W)$. This completes the proof in this case.

Case (5). Finally, suppose that the two arbitrary selected vertices s, t are on distinct chains of cubes and those chains are connecting at a cube which we can call a branching cube; this branching cube can also be the central cube. As explained in Figure 8, in which B cube is the branching cube, S cube and T cube are on different chains each containing one of the selected vertices, that is, $s \in V(S)$ and $t \in V(T)$. Both of the two cubes S and T or any one of these cube can also be the cubes in the outermost level of cubes.

Note: in the idea of case (4), we can say that someone can select two vertices on different cubes such that there is chain of cube connecting them and both ends of this chain are the cubes on the outermost level of cubes. But then, there must be a cube (which we call branching cube) in this chain that connects to the central cube by the chain of cubes.) Without loss of generality, we can assume that $w_i = w_1, w_{i+1} = w_2$ and $w_j = w_3, w_{j+1} = w_4$. We can see that the length of the shortest path from vertex w_1 to vertex t of cube T is greater than the length of the shortest path from vertex w_1 to vertex s of cube S . Thus, $d(s, w_1) \neq d(t, w_1)$, so this implies that $r(s|W) \neq r(t|W)$.

All these five cases prove that $W = \{w_1, w_2, \dots, w_k\}$ is a resolving set. Since there are $7^{n-2} \times 16$ number of elements in W , therefore the proof of theorem concludes.

3. Conclusion

In this article, we have studied the metric dimension of the crystal cubic carbon structure and we gave a formula for its metric dimension. We have found that the metric dimension of CCC(n) is not constant and find its closed form.

Data Availability

All the proofs and exemplary data of this study are included in the article.

Conflicts of Interest

The authors declare that they have no conflicts of interest.

Acknowledgments

This work was supported by the National Key Research and Development Program under Grant 2018YFB0904205.

References

- [1] M. Baca, E. T. Baskoro, A. N. M. Salman, S. W. Saputro, and D. Suprijanto, "On metric dimension of regular bipartite graphs," *Bulletin mathématiques de la Société des sciences mathématiques de Roumanie*, vol. 54, pp. 15–28, 2011.
- [2] L. M. Blumenthal, *Theory and Applications of Distance Geometry*, Oxford University Press, Oxford, UK, 1953.
- [3] F. Harary and R. A. Melter, "On the metric dimension of a graph," *Ars Combinatoria*, vol. 2, pp. 191–195, 1976.
- [4] P. J. Slater, "Leaves of trees," *Congressus Numerantium*, vol. 14, pp. 549–559, 1975.
- [5] P. J. Slater, "Dominating and reference sets in a graph," *Journal of Mathematical and Physical Sciences*, vol. 22, no. 4, pp. 445–455, 1988.
- [6] J.-B. Liu, M. F. Nadeem, H. M. A. Siddiqui, and W. Nazir, "Computing metric dimension of certain families of toeplitz graphs," *IEEE Access*, vol. 7, pp. 126734–126741, 2019.
- [7] M. A. Mohammed, A. J. Munshid, H. M. A. Siddiqui, and M. R. Farahani, "Computing metric and partition dimension of tessellation of plane by boron nanosheets," *Eurasian Chemical Communications*, vol. 2, no. 10, pp. 1064–1071, 2020.
- [8] H. M. A. Siddiqui, S. Hayat, A. Khan, M. Imran, A. Razzaq, and J.-B. Liu, "Resolvability and fault-tolerant resolvability structures of convex polytopes," *Theoretical Computer Science*, vol. 796, pp. 114–128, 2019.
- [9] B. Yang, M. Rafiullah, H. M. A. Siddiqui, and S. Ahmad, "On resolvability parameters of some wheel-related graphs," *Journal of Chemistry*, vol. 2019, Article ID 9259032, 9 pages, 2019.
- [10] P. J. Cameron and J. H. VanLint, *Designs, Graphs, Codes and their Links in London Mathematical Society Student Texts*, Cambridge University Press, Cambridge, UK, 1991.
- [11] G. Chartrand, L. Eroh, M. A. Johnson, and O. R. Oellermann, "Resolvability in graphs and metric dimension of a graph," *Discrete Applied Mathematics*, vol. 105, pp. 99–113, 2000.
- [12] S. Khuller, B. Raghavachari, and A. Rosenfeld, "Localization in graphs," Technical Report CS-TR-3326, University of Maryland at College Park, College Park, MD, USA, 1994.
- [13] A. Sebo and E. Tannier, "On metric generators of graphs," *Mathematics of Operations Research*, vol. 29, pp. 383–393, 2004.
- [14] A. Pokropivny and S. Volz, "'C8" phase: supercubane, tetrahedral, BC-8 or carbon sodalite," *Physica Status Solidi B*, vol. 249, no. 9, pp. 1704–2170, 2012.
- [15] A. Q. Baig, M. Imran, W. Khalid, and M. Naeem, "Molecular description of carbon graphite and crystal cubic carbon structures," *Canadian Journal of Chemistry*, vol. 95, no. 6, pp. 674–686, 2017.

- [16] W. Gao, M. Siddiqui, M. Naeem, and N. Rehman, "Topological characterization of carbon graphite and crystal cubic carbon structures," *Molecules*, vol. 22, no. 9, p. 1496, 2017.
- [17] H. Yang, M. Naeem, and M. K. Siddiqui, "Molecular properties of carbon crystal cubic structures," *Open Chemistry*, vol. 18, no. 1, pp. 339–346, 2020.
- [18] M. A. Zahid, M. Naeem, A. Q. Baig, and W. Gao, "General fifth M-zagreb indices and fifth M-zagreb polynomials of crystal cubic carbon," *Utilitas Mathematica*, vol. 109, pp. 263–270, 2018.
- [19] M. Imran, M. Naeem, A. Q. Baig, M. K. Siddiqui, M. A. Zahid, and W. Gao, "Modified eccentric descriptors of crystal cubic carbon," *Journal of Discrete Mathematical Sciences & Cryptography*, vol. 22, no. 7, pp. 1215–1228, 2019.
- [20] H. Yang, M. Naeem, A. Q. Baig, H. Shaker, and M. K. Siddiqui, "Vertex Szeged index of crystal cubic carbon structure," *Journal of Discrete Mathematical Sciences & Cryptography*, vol. 22, no. 7, pp. 1177–1187, 2019.